AN INVESTIGATION OF THE APPLIED CHEMISTRY OF THE REACTIONS OF COAL AND NITROGEN DIOXIDE WITH A PARTICULAR EMPHASIS ON OXIDATIVE DESULFURIZATION

Thesis by

James Gregory Kralik

In Partial Fulfillment of the Requirements

for the Degree of

Doctor of Philosophy

California Institute of Technology

Pasadena, California

1982

(Submitted July 17, 1981)

Acknowledgements

It is with my deepest appreciation that I acknowledge my advisor, Professor William H. Corcoran, for his continuous support and encouragement during my stay at Caltech. I have found his comments and suggestions throughout this work to be insightful and helpful. The great degree of latitude he allowed me in conducting my research is especially appreciated. My continuing education has benefited substantially from my association with Dr. Corcoran.

Discussions with members of the Caltech community concerning various aspects of my research have proved to be very beneficial as well. In particular, I would like to acknowledge the contributions made by Dr. John J. Kalvinskas of the Jet Propulsion Laboratory through my conversations with him.

I would like to thank Zig Jenner and Erich Siegel of the Glassworking Shop for their expert construction of much of the experimental apparatus and George Griffith and Henry Smith of the Chemical Engineering Shop for their technical assistance on numerous occasions. I would also like to acknowledge the many contributions made by Hollis Reamer during the course of the experimental work. The prompt and courteous manner in which all of these people assisted me is greatly appreciated.

The financial support of the California Institute of Technology, the Jet Propulsion Laboratory and the Bechtel Corporation throughout this study is gratefully acknowledged.

The association I have had with my fellow graduate students helped to make my stay at Caltech very gratifying. My daily contact with Russ Bone, Nick Vasilakos, Gary Whatley and Samir Barudi was particularly enjoyable.

Special thanks go to my "second family", Ernie and Margaret Long, who

opened their home to me. They have made my stay in Southern California very pleasant.

I would also like to thank my brother for providing me periodic refuge in Las Vegas from the rigors of my studies.

Finally, I am greatly indebted to my parents for their constant love and support throughout my studies, which started with early research in pyrotechnics in their backyard. I humbly dedicate this thesis to them.

Abstract

The physical and chemical changes in coal resulting from mild oxidation at ambient conditions with NO_2 were studied. Various liquid phases were used as transport media for the NO_2. Subsequent to the oxidation, the coal was subjected to a wash with aqueous Na_2CO_3 at ambient conditions. Particular attention was given to the desulfurization of the coal. A mathematical model of the reactions between NO_2 and coal at temperatures less than 100°C and a pressure of 1 atm was developed from the experimental data. This model included the simultaneous diffusion and reaction of NO_2 in the solid-coal matrix and considered pore diffusion not to be controlling. The elemental composition and the energy content after processing were extensively examined. The effect of the NO_2 treatment on the pore structure was established.

Summary

Because of the increased interest in the exploitation of coal for energy and chemicals, many areas of coal chemistry are currently under investigation. The major motivation for the work discussed in this thesis was to investigate the applied chemistry of the reactions of coal and NO_2, with particular emphasis on oxidative desulfurization. A mathematical simulation of the reactions of NO_2 and coal at temperatures less than 100°C and at a pressure of 1 atm was developed from the experimental data. It was found that when the coal was exposed to NO_2 at concentrations of less than 2 F in CCl_4 at temperatures of 0 to 50°C, the rate of nitrogen uptake by the coal obeyed first order kinetics:

$$-\frac{dX}{dt} = k X, \quad \text{where}$$

$$X = 1 - \frac{m_N}{(m_N)_\infty}$$

m_N = the net increase in the nitrogen content of the coal (g N/100 g untreated coal),

$(m_N)_\infty$ = the net increase in the nitrogen content of the coal as the exposure time approaches infinity (g N/100g untreated coal),

k = the first order rate constant (min^{-1}), and

t = the time (min).

The values of k were found to be 0.0342, 0.0483 and 0.0466 min^{-1} at 0, 20 and 50°C, respectively, for the treatment of the PSOC 190 coal. The value of k determined for the treatment of the PSOC 276 coal with NO_2 in CCl_4 at 20°C was found to be 0.0183 min^{-1}. An analysis of the data also revealed that the rate of disappearance of NO_2 from the NO_2/CCl_4/coal system was governed by the rate of diffusion of NO_2 into the coal during the first 30 minutes of the NO_2 treatment. After 30 minutes, diffusion was found to no longer control the rate of NO_2

disappearance from the system. It was found that CCl_4 was the best liquid to use as a transport medium for NO_2 because it did not compete with the coal for NO_2 and was easily separated from the coal after the NO_2 treatment.

Because it was determined that NO_2 was soluble in the solid-coal matrix, the mathematical model incorporated both the diffusion of NO_2 in the solid-coal matrix and the chemical reaction of NO_2 with the coal. It was found that the nitrogen uptake by the PSOC 190 coal correlated best with a value of 10^{-15} cm^2/s for the coefficient of diffusion of NO_2 in the solid-coal matrix. The nitrogen uptake by the PSOC 276 coal, on the other hand, correlated best with a value of 5×10^{-14} cm^2/s for the NO_2 diffusion coefficient. Although the values obtained for the diffusion coefficient are several orders of magnitude less than those for the diffusion of other gases, such as N_2, O_2, CO_2 and CO in polymers (10^{-8} to 10^{-10} cm^2/s), the results indicated that diffusion of NO_2 in the solid-coal matrix was relatively slow and probably coupled with chemical bonding.

A study of the pore structure of the coal revealed that the rate of nitrogen uptake by the coal was governed by the pore structure of the coal particle. In particular, the specific surface area, pore volume, and pore-size distribution of the coal were determined as a function of the NO_2 exposure time, the NO_2 concentration, and the temperature. It was found that the first-order rate constants for nitrogen uptake by the two coals were proportional to their respective nitrogen-determined surface areas. It was found that the CO_2-determined surface areas did not correlate with the kinetic data at all. The results of the CO_2-adsorption study indicated that CO_2 was absorbed by the coal rather than just adsorbed on the surface of the coal.

A major result was developed from a study of the hydrogen, mineral matter and sulfur contents of the coal after treatment with NO_2 followed by washing in Na_2CO_3 (aq). The hydrogen content of the processed coal showed that up to 25 %

of the hydrogen in the untreated coal was replaced by oxygen donated by NO_2 to form a uniformly distributed, acidic precursor in the coal which imparted an ion-exchange characteristic to the treated coal. Upon exposure of the NO_2-treated coal to 0.1 M Na_2CO_3 (aq), the precursor bound the sodium ions, as evidenced by the qualitative elemental analysis of the mineral matter obtained with an energy-dispersive analyzer of x-rays. The PSOC 190 took up 0.03 g sodium/g coal, and the value for the PSOC 276 coal was 0.01 g sodium/g coal. The sodium ions exchanged with the hydrogen ions during the wash with Na_2CO_3 (aq). Upon combustion of the coal in an oxidizing atmosphere, this sodium-containing precursor trapped SO_2, which would have otherwise escaped in the flue gas, in the ash, probably in the form of Na_2SO_4. In particular, up to 96 % of the sulfur in a treated coal was retained in the ash upon combustion under fuel-lean conditions. The heating value of the coal was not decreased by more than 15 percent and averaged about 10 percent.

The work discussed in this thesis gave several important results which deserve continued investigation. Important areas for further study are suggested as follows:

1. The chemical structures formed in the coal by the oxidation with NO_2 should be established.
2. The use of oxidants other than NO_2 should be investigated.
3. The use of alkaline-earth and alkali metals other than sodium for trapping SO_2 during combustion of the processed coal should be studied further.
4. The effect of the pressure during the Na_2CO_3 (aq) wash should be investigated to determine if higher pressures can lead to greater penetration of the Na_2CO_3 (aq) solution into the oxidized coal.
5. The mathematical model should be modified so that it conforms more closely with the actual experimental conditions. In particular, the time dependence

of the bulk NO_2 concentration should be incorporated into the model. The solid void fraction should be replaced by using a Henry's law relationship which describes the concentration of NO_2 just inside the solid coal matrix relative to that in the solvent. Other pore geometries should be investigated as well.

TABLE OF CONTENTS

List of Figures

List of Tables

Nomenclature

A = the affinity of adsorption.

a = a pre-exponential constant.

A_a^T = the molecular cross-sectional area of the adsorbate at temperature T (cm^2/molecule).

a = the moles of adsorbate adsorbed at relative pressure $\frac{P}{P_0}$ (mol/g).

a_m = the moles of adsorbate adsorbed to form a monolayer (mol/g).

a_m = the external surface area of the coal particle (cm^2/g).

a_i = the activity of species i.

$C_i(t,X) = \frac{c_i}{(c_i)_0}$ = the dimensionless concentration of species i.

c_b = the bulk NO_2 concentration (mol/cm^3 void volume).

c_i = the concentration of species i (mol/cm^3).

c_s = the NO_2 concentration at the particle surface (mol/cm^3 void volume).

c_X^M = the coal species concentration (mol/cm^3 solid volume).

D = the diffusion coefficient (cm^2/s).

$D_{e,i}$ = the effective diffusivity of species i (cm^2/s).

D_i = the molecular diffusivity of species i (cm^2/s).

D_s = the NO_2 diffusivity in the solid coal matrix (cm^2/s).

E = the activation energy (cal/mol).

E = the electrode potential (V).

E_1 = the heat of adsorption of the monolayer (J/mol adsorbate).

E_L = the heat of liquefaction of the adsorbate (J/mol adsorbate).

E_0 = the reference potential (V).

F = the concentration in units of formality (mol/l).

f = the fraction of pore filling.

f_i = the fugacity of species i.

ΔG_a = the differential change in the molar free energy upon adsorption with the bulk liquid adsorbate at the same temperature as the standard (cal/mol).

ΔG^o_{298K} = the free energy of reaction at 298 K and 1 atm pressure (cal).

g = the acceleration of gravity (960 cm/s^2).

H_g = the heating value of the coal (Btu/lb$_m$).

ΔH^o_{298K} = the enthalpy of reaction at 298 K and 1 atm pressure (cal).

I = the ionic strength (mol/cm^3).

K_i = the dissociation constant of species i.

k = a first-order rate constant (s^{-1}).

k = a measure of the average pore size.

k_1 = a distribution characterization constant.

k_c = the mass transfer coefficient for NO_2 between the particle surface and the bulk solvent (cm/s).

k_j = a second-order rate constant (cm^3/mol/s).

L = the thickness of the solid slab comprising the idealized slit-pore geometry of the coal (cm).

L_i = the mass corrected mass loss of species i from the coal.

M_i = the molecular mass of species i.

$(MW)_i$ = the molecular mass of species i.

m_i = the molality of species i (mol/kg solvent).

m_i = the net mass increase of species i in the coal (g i/100g untreated coal).

N_0 = Avogadro's number (6.02 × 10^{23} molecules/mol).

P = the pressure (atm,torr).

$P_0 = P^0$ = the vapor pressure of the adsorbate (atm,torr).

$\frac{P}{P_0}$ = the relative pressure.

Q = the area of the pore cross-section (cm^2).

R = the gas constant (1.9872 cal/mol/K).

R = the potentiometric reading for the sample during HNO_2 analysis.

R_i = the net rate of formation of species i (mol/cm^3/s).

R_s = the potentiometric reading for the standard during the HNO_2 analysis.

r = the radial distance (cm).

r_k = the core radius (cm).

r_0 = the diffusion path length (cm).

S = the electrode slope.

S_a^i = the specific surface area determined with adsorbate i (cm^2/g adsorbent).

S_i = the specific entropy of phase i (cal/mol/K).

S_{micro} = the micropore surface area (cm^2/g adsorbent).

T = the temperature (K).

t = the time (s).

t = the film thickness (cm).

V = the average molar volume of the adsorbed phase (cm^3/mol).

V_a = the molar volume of an ideal gas at 273 K and 1 atm (22,414 cm^3/mol).

V_p = the total nitrogen-determined pore volume (cm^3 void/g solid).

V_s = the spherical shell volume (cm^3).

$\frac{dV}{dS}$ = the differential change in pore volume with respect to the pore surface area (cm).

W = the volume of the pore structure filled with adsorbate (cm^3).

W = the calorimeter constant (cal/g).

W_0 = the limiting adsorption volume in the micropores (cm^3/g adsorbent).

$X = \frac{x}{L}$ = a dimensionless thickness.

X_j = the solid coal species j.

x = the amount of adsorbate adsorbed (cm^3 at STP/g adsorbent).

x_M = the monolayer amount of adsorbate adsorbed (cm^3 at STP/g adsorbent).

z = a characteristic distance (cm).

z = the conversion.

z_i = the electric charge of species i.

Greek Symbols

α = a characteristic function of the pore environment.

α_j = the stoichiometric coefficient.

β = an affinity coefficient which allows the adsorption isotherms of different gases on the same solid to merge.

$\Gamma(n)$ = the gamma function evaluated at n.

γ_i = the activity coefficient of species i.

$(\gamma_{\pm})_i$ = the mean ion activity coefficient of species i.

γ_i^c = the activity coefficient of species i when molar concentrations are used.

$(\gamma_{\pm}^c)_i$ = the mean ion activity coefficient of species i when molar concentrations are used.

ε = the void fraction (cm^3 void/cm^3 total volume).

ε_s = the solid fraction (cm^3 solid/cm^3 total volume).

ϑ = the contact angle.

ϑ = the fraction of the monolayer occupied.

μ_i = the chemical potential of species i (cal/mol).

μ_l = the viscosity of species l (g/cm/s).

ρ_i = the density of species i (g/cm^3).

ρ_s = the solid density (g/cm^3).

σ = the surface tension (dyne/cm).

v_i = the molar volume of species i.

φ = the adsorption potential in the micropores.

τ = the particle tortuosity.

Special Characters

$\hat{x}$ = the quantity x in the solid coal matrix.

$\tilde{a}_i$, $\tilde{b}_i$, $\tilde{c}_i$ = the elements in the tridiagonal matrix.

(X) = the concentration of species X (mol/cm^3).

$(X)_0$ = the initial concentration of species X (mol/cm^3).

CHAPTER 1

Introduction

During the past decade, it has been generally recognized that the world supply of crude oil is being rapidly depleted. Indeed, a pervasive fear exists that mankind may not be capable of meeting its energy needs by the year 2000. As the United States has become increasingly dependent on foreign oil to supplement its own domestic production, the country has become more vulnerable to external political and economic manipulation. The recent escalation in world oil prices caused by the revolution in Iran and the concomitant interruption in the oil supply from the Persian Gulf states in 1979, however, has resulted in a decline in the amount of oil the United States now imports, which is due primarily to the increased efficiency in energy usage and to increased conservation. Nevertheless, the amount of oil the United States imports is still significant. This threat to national security can be countered by the aggressive development of domestic energy supplies. In any event, it will be necessary to switch from fossil fuels to some other energy source in the future.

There are predictions that by 2010, annual domestic oil production will decrease from 20 quads (1 quad = 10^{15} Btu) in 1975 to only 6 quads.[1] Even under the most favorable economic and regulatory conditions for oil exploration, annual production would still fall to 16 quads by 2010. Consequently, the annual level of oil production will decline. The level of natural gas production is projected to fall at an even faster rate, decreasing from an annual production of 19.7 quads in 1975 to only 5 quads in 2010.[2] Again, however, if quite favorable economic and regulatory conditions exist, production in 2010 is projected to fall only to 16 quads. In any event, natural gas production is expected to decline significantly in the future.

The situation with respect to coal, on the other hand, is not as bleak. Coal is the most abundant fossil fuel in the United States. Of the total domestic resource of 80,000 quads, only 6,000 quads are economically recoverable at this time. Nevertheless, the total annual consumption of coal is just 14 quads, or less than 0.3 percent of the recoverable reserves.[3] The nation uses about 10 percent of its recoverable oil and natural gas reserves each year, on the other hand. Although coal would seem to be the ideal panacea for the nation's energy ills, the rapid escalation in coal production and usage which would be required has many inherent problems. Primarily, the coal mining and utilization industry would experience a large expansion which would require the investment of hundreds of billions of dollars over the years. Furthermore, much effort must be expended to allow the combustion of coal to be conducted in an economically yet environmentally acceptable manner on such an expanded scale.

There are several other sources of energy which do not rely on the combustion of fossil fuels. Of these, the most important at this time is the production of electricity using the nuclear fission of uranium. The currently employed technology uses enriched uranium on a once-through basis without recycle. On this basis, only about 400 1,000 megawatt reactors, each of which have a 30-year lifespan, can be built before the entire domestic supply of recoverable uranium is committed. As of 1978, the equivalent of 46 such reactors were in operation in the United States. Therefore, even the prospects for nuclear power are somewhat limited, unless the uranium is recycled. Use of breeder reactors allows the uranium to be recycled up to one hundred times, however, which would greatly enhance the fuel supply for nuclear reactors. Environmental concerns, particularly after the incident at Three Mile Island, however, may prevent the expansion of the nuclear industry beyond its present day level. Consequently, reliance on nuclear fission to compensate for the continued decline in oil and gas supplies is

tenuous at best.

It does not appear likely that other alternatives for energy production will have a significant impact on the total energy picture for the balance of this century. Such processes as thermonuclear fusion and the conversion of solar energy are still in an incubative stage. Other processes, such as the conversion of geothermal and hydroelectric energy, have well established technologies but limited resources. And still other processes, such as the conversion of shale oil and tar sands to useful fuels, are being tested on a commercial scale but still face a myriad of environmental problems. A major breakthrough would be needed to advance any of these processes to the forefront in the fight to meet domestic energy needs with resources indigenous to the United States.

In view of the overall situation, it appears that in the case of oil and natural gas, the technology is extensive but the reserves are rapidly dwindling, whereas in the case of the more elegant schemes, the reserves appear to be inexhaustible but the technology has not been sufficiently developed. On the other hand, much of the technology needed for the commercial utilization of coal is already available, and the reserves of coal far exceed those of oil and natural gas. Consequently, it is not surprising that research in the area of coal utilization is extensive.

One area of particular interest involves pollution abatement. One particularly noxious pollutant is sulfur dioxide, which is evolved during coal combustion and is formed from the sulfur inherent in the coal. Current air quality standards require the removal of 70 to 90 % of all of the SO_2 which would otherwise enter the atmosphere upon combustion of the raw coal in a utility boiler. Consequently, the combustion of virtually any coal requires some degree of sulfur reduction, whether it is before or after combustion. Current technology employed on a commercial scale emphasizes the post-combustion treatment of

the flue gas with SO_2 scrubbers to meet air quality standards. This sort of treatment appears to be appropriate for large electric utility boilers. For smaller boilers and fuel burning equipment, however, desulfurization prior to combustion may be better.[4] The technology in this area is not as well developed as in the post-treatment case. Clearly, then, the incentive for developing techniques for pretreatment exists. If such techniques can lead to the formation of economically viable and commercially feasible processes, there will be time to develop other energy technologies without facing severe social, economic and political consequences.

References

1. National Research Council, Committee on Nuclear and Alternative Energy Systems, *Energy in Transition, 1985–2010*, (National Research Council, National Academy of Sciences, Washington, D.C., 1979) p. 18.

2. *Ibid.*

3. *Ibid.*, p. 19.

4. The United States Environmental Protection Agency, The Office of Energy, Minerals and Industry, Office of Research and Development, *Industrial Environmental Research Laboratory, Annual Report*, 1975, p. 2.

CHAPTER 2

BACKGROUND

2.1 Coal

Coal is the product resulting from the decomposition of plant material which lived millions of years ago. Thus, the composition of a particular seam of coal depends upon the composition of the flora and fauna from which it is derived and the environment in which the decompositon occurs.[1] Because the variation in the species of flora which lived even in previous epochs was quite extensive, the variation in coal composition is quite extensive as well. Indeed, samples of coal taken just feet apart from each other can show significant differences in elemental composition. Such variations lead to difficulties when designing processes employing coal, whether it be the combustion of coal to generate electricity or the chemical treatment of coal to obtain petrochemicals. Several methods of classifying the rank and petrographic constituents of coal have evolved as researchers attempt to gain a better understanding of coal.

The most widely used ranking system is probably the ASTM classification (ASTM D-338-66), which is based solely on the carbon content and the dry, mineral matter free (DMMF) heating value of the coal.[2] Anthracite has a carbon content of greater than 86 percent by mass. Anthracite is the oldest coal by rank since it has decomposed to the greatest degree by evolving almost all of its hydrogen. The next rank is bituminous, in which the coal has a DMMF heating value greater than 10,500 Btu/lb_m and a fixed carbon content less than 86 percent. Subbituminous coal has a DMMF heating value between 8,300 and 11,500 Btu/lb_m. The lowest rank is lignite, where the DMMF heat content is between 6,300 and 8,300 Btu/lb_m. Of the total proven coal reserves in the United States which are legally and economically recoverable, the proportion of anthracite:

bituminous:subbituminous:lignite is 2:52:38:8 .[3]

Several systems for classifying the petrography of coal exist. Thiessen[4] developed a method for classifying the macerals found in coal based on the transmittance and reflectance of light interacting with thin slices of coal. He found three basic macerals, namely anthraxylon, exinite and fusain. The Stopes-Heerlen[5] system also classifies the petrographic constituents of coal into three groups: vitrinite, exinite and inertinite. A more extensive system is used by the U.S. Bureau of Mines, which employs six classifications: vitrite, clarite, duroclarite, vitrinertite, clarodurite and durite. Knowledge of the petrographic constituents in a particular coal may enable a prediction of its extractibility with various solvents. For instance, recent research in this area by Vasilakos and Lawson[6] utilizing solubility parameter spectroscopy show that vitrinite in particular may be amenable to extraction with a 50:50 mixture of carbon tetrachloride and methanol.

2.2 Forms of Sulfur in Coal

Coal generally has a sulfur content of 1 to 4 mass percent, although it can be as high as 10 percent for coals mined from seams with large pyrite deposits.[7] Sulfur occurs in two basic forms in coal, either inorganic or organic. The ratio of inorganic to organic sulfur ranges from 4:1 to 1:3, with 2:1 being most common.[8] The major constituent of inorganic sulfur is iron disulfide, FeS_2, which occurs in various crystalline forms, namely pyrite, marcasite and troilite. These various crystalline forms are usually considered together as simply pyrite. The other major form of inorganic sulfur is sulfate, found as a salt with various metals, the most important being iron, calcium, magnesium and barium. Although the amount of sulfate sulfur in freshly mined coal is generally quite small relative to the amount of total sulfur, coal which has been exposed to oxygen in the presence of water can have virtually all of its inorganic sulfur in

sulfate form. The conversion of pyrite to ferric sulfate is due to the action of the thiobacillus ferroxidans bacterium, whose occurence is quite prolific in acid mine water.[9] Inorganic forms of sulfur generally occur as crystals or particles separate from the carbonaceous part of the coal. However, the size of the particles range anywhere from 1 μm to 1 mm in diameter.[10]

The other major form of sulfur found in coal is organic. In contrast to inorganic sulfur, organic sulfur is homogeneously distributed throughout the carbonaceous matrix of the coal.[11] The forms of organic sulfur are classified according to the functional group in which the sulfur occurs. The major forms are thiols, sulfides, disulfides and thiophenes. In the first three forms, the sulfur can be considered to be aliphatic, while in the thiophenic form, the sulfur is aromatic. The distribution of the various types of organic sulfur occurring in coal is not accurately known.

2.3 Coal Desulfurization

The sulfur in coal used for power generation can be removed either before or after combustion. Post-combustion desulfurization requires the use of large scrubbing towers where the flue gases from the boiler are contacted with an appropriate adsorber for SO_2, usually an aqueous lime solution. Although this method is the most widely used for desulfurization on an industrial scale, the costs encountered for incorporating flue gas scrubbing can be as high as 20 percent of the total capital outlay for a power plant.[12] Retrofitting an existing plant can be even more expensive. Furthermore, the scrubbers produce a large amount of sludge which poses a significant solid waste disposal problem. For instance, a typical lime scrubber generates 4.25 lb_m of dry sludge for every 1 lb_m of sulfur in the coal.[13]

Two basic methods exist for the removal of sulfur from coal prior to combus-

tion, namely physical and chemical. Physical desulfurization seeks to separate the sulfur from the coal without altering the sulfur or breaking chemical bonds in the process. The fact that no chemical bonds are broken implies that only the inorganic sulfur forms which, unlike the organic sulfur, are not intimately bound in the carbonaceous matrix can be physically removed. Several methods of physical cleaning of coal are currently in use.

One widely used process involves the separation of pyrite, which has a density of roughly 5.0 g/cm^3, from the rest of the coal, which has a density ranging from 1.0 to 1.6 g/cm^3, in a solvent with a density between 2.0 and 4.0 g/cm^3 .[14] Ideally, the pyrite sinks and the carbonaceous material floats. Good separation requires the coal to be milled to sufficiently small particle size so that the pyrite crystals are released from the rest of the coal. In cases where particle sizes are too small (on the order of 10^{-3} cm), electrostatic and dispersion forces predominate over buoyancy forces, resulting in separation difficulties.[15]

Another separation procedure employs a strong magnetic field (20,000 gauss vs. 0.57 gauss for the magnetic field of the earth) influencing a stream of ground coal.[16] Since pyrite has a dipole moment while the carbonaceous material does not, the pyrite particles, as well as any other inorganic material which has a dipole moment, is deflected from the stream. Other physical beneficiation methods include froth flotation, stage crushing, and microwave and electronic separation of pyrite.[17]

Although most physical beneficiation methods are relatively inexpensive, only inorganic sulfur forms are removed from the coal. Since current regulations regarding SO_2 emissions require 90 % sulfur removal for most coals,[18] removal of organic sulfur is necessary as well. Because organic sulfur is covalently bonded to carbon in the coal, processes energetically capable of breaking carbon-sulfur bonds are required. The sulfur is then removed in a form different than its form

in coal. Reductive desulfurization results in the removal of pyritic and organic sulfur as H_2S. The major disadvantages of the process include the high cost of maintaining the high temperature (450°C) and pressure (2500 psi) required for reaction and the high cost of hydrogen. For instance, FeS_2 does not react with H_2 below 450°C.[19] At that temperature, coal begins to thermally decompose and liquefy due to incorporation of H_2 into the organic structure. Organosulfur compounds also require temperatures greater that 400°C for H_2S evolution, even in the presence of catalysts such as CoO and MoO_3 supported on alumina.[20] Hydrodesulfurization is best suited for liquefaction and gasification processes where the coal is converted to a synthetic fuel.

Oxidative desulfurization schemes, on the other hand, seek to remove as much sulfur as possible while minimizing alterations in the rest of the coal structure. This is best accomplished by using cheap oxidants, such as air, under ambient conditions. The selectivity of the oxidant for sulfur with respect to the rest of the coal is of crucial importance in order to minimize the loss in heating value of the coal. Several oxidative desulfurization schemes have been developed. Most attain high inorganic sulfur removal without significant losses in heating value. Significant organic sulfur removal, however, is usually accompanied by a large amount of oxidation of the carbonaceous material.

The use of oxygen dissolved in an aqueous slurry of coal,[21] for instance, provides a good example. This scheme, sometimes referred to as the Ames process, attains 20 to 70 % pyrite removal at ambient pressure and 70°C, and up to 90 % pyrite removal at 300 psi of oxygen and 130°C. Under these conditions, however, some combustion occurs resulting in a 6 % mass loss. Both this process and the Meyer's process[21] rely on soluble sulfate as a chain carrier:

$$3\,Fe^{2+} + 1.5\,[O] \rightarrow 3\,Fe^{3+} + 1.5\,[O^{2-}], \qquad (2.3.1)$$

$$2\,Fe^{3+} + FeS_2 \rightarrow 3\,Fe^{2+} + 2\,S\,, \quad \text{or} \tag{2.3.2a}$$

$$14\,Fe^{3+} + FeS_2 + 8\,H_2O \rightarrow 15\,Fe^{2+} + 2\,SO_4^{2-} + 16\,H^+\,. \tag{2.3.2b}$$

Removal of organic sulfur involves the direct formation of sulfur-oxygen bonds, resulting in sulfoxides and sulfones which are then hydrolyzed:

$$R_2S \xrightarrow{[O]} \underset{sulfoxide}{R_2SO} \xrightarrow{[O]} \underset{sulfone}{R_2SO_2} \rightarrow 2RH + H_2SO_4$$

Utilizing temperatures from 150 to 200°C and pressures from 500 to 1500 psi, up to 50 % of the organic sulfur is removed. However, severe heating value losses of up to 50 % occur as well. Indeed, it is not clear if the organic sulfur removal is due solely to combustion or to a selective reaction of oxygen with organic sulfur.

Another process employs aqueous hydrogen peroxide under ambient conditions.[22] No appreciable pyrite removal occurs unless aqueous sulfuric acid is added. This requirement implies that soluble sulfate is needed as a chain carrier in this scheme as well. The overall reaction is:

$$2\,FeS_2 + 15\,H_2O_2 \rightarrow Fe_2(SO_4)_3 + H_2SO_4 + 14\,H_2O\,. \tag{2.3.3}$$

Complete pyrite removal can be attained without significant heating value losses. However, no organic sulfur removal occurs unless an excessive amount of H_2O_2 is added, which results in complete oxidation of the coal. This scheme is practical for pyrite removal only.

One promising oxidative desulfurization scheme is the chlorinolysis process developed by the Jet Propulsion Laboratory.[23] In this instance, chlorine gas is bubbled through a slurry of coal in an appropriate solvent such as water, methyl chloroform or carbon tetrachloride. The treated coal is thn stripped with N_2 to remove the chlorine. Once again, removal of pyrite is fairly complete. The pyrite is ultimately removed as $FeCl_3$ and H_2SO_4. The fact that Cl_2 is very selec-

tive for sulfur as opposed to carbon or hydrogen in model sulfur compounds implies that the selective attack of organic sulfur in coal should occur as well.[24] Research conducted to date, however, shows insignificant organic sulfur removal.[25] The problem may be the removal of the oxidized sulfur products, which may still be bound to the rest of the carbonaceous material. Although chlorine shows a high selectivity for sulfur oxidation, it does not have a propensity for simultaneous or subsequent carbon-sulfur bond scission. A major problem with the process involves the removal of chlorine from the desulfurized coal. The chlorinated coal generally has a high chlorine content of up to roughly 10-15 % by mass. Reducing the chlorine content to its pretreatment level (about 0.1 %) is quite difficult,although treatment of the coal with hydrogen at 450°C does lower the chlorine content to its pretreatment level. Coals with chlorine contents greater than a few tenths of one percent pose serious corrosion problems for combustion in utility boilers.

Aqueous nitric acid can also be used to remove sulfur from coal.[26] Indeed, 10 % aqueous nitric acid is used to wash coal in the standard procedure for the determination of the pyritic sulfur content of coal.[27] In this procedure, 1.0 g of coal is slurried in 50 ml of 10 % HNO_3 (aq) and stirred overnight. The amount of iron dissolved in solution is determined and is attributed to the pyrite in the coal. By definition, complete pyrite removal is obtained as follows:

$$FeS_2 + 14\ HNO_3 \rightarrow FeSO_4 + H_2SO_4 + 14\ NO_2 + 6\ H_2O\ . \qquad (2.3.4)$$

No organic sulfur removal occurs, however, when the coal is washed in 10 % HNO_3 (aq). Use of 35 % HNO_3 (aq) does result in substantial organic sulfur removal coupled with extensive oxidation of the coal. As in the case of aqueous oxygen, the organic sulfur removal may be due to non-selective oxidation of the coal. Treatment of anthracite and bituminous coals with mixtures of concentrated nitric and sulfuric acids indicate that coal is quite amenable to nitration,

the degree of which is independent of the rank and the temperature of the treatment.[28] All of the six coals examined, which had carbon contents ranging from 81 to 93 mass percent, show about a 27 ± 2 % mass increase due to the introduction of nitro groups alone, with the balance of the mass increase due to the creation of oxygenated groups in the aliphatic portion of the coal structure. Interestingly, there is no loss of carbon during nitration. Furthermore, there is an increase in the number of carboxyl, and to a much lesser extent, hydroxyl and carbonyl, groups in the coal after treatment. These two facts imply that carboxylic groups originate from the oxidation of methyl groups in the coal. The organic sulfur reduction for the bituminous coals ranges from 0 to 7 % while that of the anthracite is 44 %. The nitrogen contents increased from roughly 2 to 7 % as well. Since nitrogen in coal is ultimately converted to NO and NO_2 during combustion and are serious pollutants as well, nitric acid treatment compounds rather than alleviates the SO_2 emission problem. Whereas SO_2 can be scrubbed from the flue gas, oxides of nitrogen cannot be removed by stack gas scrubbing.

An analogous, but milder oxidizing agent is nitrogen dioxide. Pyrite reacts readily and exothermically with NO_2 under anhydrous and aqueous conditions:

$$FeS_2(s) + 6\ NO_2(g) \rightarrow FeSO_4(s) + SO_2(g) + 6\ NO(g)\ , \quad \text{where}$$

$$\Delta H^{\circ}_{298K} = -185 \text{ kcal and } \Delta G^{\circ}_{298K} = -222 \text{ kcal}\ , \quad \text{and} \qquad (2.3.5)$$

$$FeS_2(s) + 7\ NO_2(g,aq) + H_2O \rightarrow$$

$$FeSO_4(aq) + H_2SO_4(aq) + 7\ NO(g)\ , \quad \text{where}$$

$$\Delta H^{\circ}_{298K} = -260 \text{ kcal and } \Delta G^{\circ}_{298K} = -222 \text{ kcal}\ . \qquad (2.3.6)$$

Under anhydrous conditions, once a layer of $FeSO_4$ has formed on the surface of a pyrite particle, further reaction is inhibited due to the increased mass transfer limitations imposed on the NO_2. When reaction takes place in aqueous

solution, on the other hand, reaction is not inhibited because the $FeSO_4$ product is soluble. Therefore, complete conversion of pyrite to ferric sulfate and sulfuric acid is possible. The oxidation of organosulfur compounds proceeds as follows:

$$NO_2 + R{-}S{-}R' \rightarrow R{-}(SO){-}R' + NO\,, \quad \text{where}$$

$$\Delta H^{\circ}_{298K} = -12.2 \text{ kcal} \quad \text{and} \quad \Delta G^{\circ}_{298K} = -11.6 \text{ kcal}\,, \quad \text{and} \quad (2.3.7)$$

$$NO_2 + R{-}(SO){-}R' \rightarrow R{-}(SO_2){-}R' + NO\,, \quad \text{where}$$

$$\Delta H^{\circ}_{298K} = -41.6 \text{ kcal} \quad \text{and} \quad \Delta G^{\circ}_{298K} = -40.4 \text{ kcal}\,, \quad \text{and} \quad (2.3.8)$$

The thermodynamic data indicate that formation of the oxidized products is favored when no kinetic limitations exist. Mixtures of NO_2 and air are used commercially for the oxidation of dimethyl sulfide to dimethyl sulfoxide, for instance.[29] Di-n-butyl sulfide reacts readily with NO_2 at room temperature to form the corresponding sulfoxide and sulfone.[30] Reaction of NO_2 with dibenzothiophene, however, leads to products other than the sulfoxide or sulfone, which indicates that NO_2 does not demonstrate the selectivity for sulfur that Cl_2 does under similar conditions.[31] Some of the possible reactions of NO_2 with organic compounds are:

Ketone Formation: $R{-}CH_2{-}R' + 2\,NO_2 \rightarrow R{-}(C{=}O){-}R' +$

$$R{-}(C{=}O){-}R' + H_2O + 2\,NO\,, \quad \text{where}$$

$$\Delta H^{\circ}_{298K} = -59.6 \text{ kcal} \quad \text{and} \quad \Delta G^{\circ}_{298K} = -70.0 \text{ kcal}\,, \quad \text{and} \quad (2.3.9)$$

Carboxylic Acid Formation: $R{-}CH_3 + 3\,NO_2 \rightarrow$

$$R{-}COOH + H_2O + 3\,NO\,, \quad \text{where}$$

$$\Delta H^{\circ}_{298K} = -100.3 \text{ kcal and } \Delta G^{\circ}_{298K} = -111.2 \text{ kcal}\,, \text{ and } (2.3.10)$$

Phenol Formation: $C_6H_5{-}H + NO_2 \rightarrow C_6H_5{-}OH + NO\,, \quad \text{where}$

$$\Delta H^{\circ}_{298K} = -29.2 \text{ kcal} \quad \text{and} \quad \Delta G^{\circ}_{298K} = -30.3 \text{ kcal}\,, \quad \text{and } (2.3.11)$$

$$\textit{Substitution}:\ C_6H_5{-}H + 2\,NO_2 \rightarrow C_6H_5{-}NO_2 + HNO_2\,, \qquad (2.3.12)$$

where the thermodynamic quantities shown are for reactions in the gas phase. Values of ΔH^{o}_{298K} and ΔG^{o}_{298K} for the substitution reaction could not be estimated. It is apparent from comparison of the thermodynamic data for reaction of NO_2 and organosulfur compounds with that of NO_2 and simple organic compounds that NO_2 should show little or no selectivity for sulfur when kinetic limitations are nonexistent.

Recently, the reaction of NO_2 and coal in the gas phase has been investigated.[32] The treated coal is then washed in water to remove ferric sulfate. Further treatment with aqueous caustic is then claimed to remove organic sulfur. For example, a coal containing 3.6 % pyritic sulfur and 0.7 % organic sulfur is treated for three hours in a fixed bed at 100 ℃ with a gaseous mixture containing 5 to 10 % NO_2. The treated coal is then washed with water followed by a wash with 10 % NaOH (aq), leaving a coal with only 0.5 % total sulfur content. Unfortunately, there is no mention of mass or heating value losses, which makes it very difficult to verify the claims of high selectivity made by the authors. Furthermore, the coals examined were not predried to remove water. Thus, it is not clear whether NO_2 or nitric acid is the true oxidizing agent. Nitric acid results from the rapid reaction of NO_2 with water:

$$H_2O + 2\,NO_2 \rightarrow HNO_3 + HNO_2$$

$$3\,HNO_2 \rightarrow HNO_3 + NO$$

$$H_2O + 3\,NO_2 \rightarrow 2\,HNO_3 + NO \qquad (2.3.13)$$

Indeed, the presence of water can lead to the creation of many species, including not only nitrous (HNO_2) and nitric (HNO_3) acids, but nitrosonium (NO^+) and nitronium (NO_2^+) ions as well.[33] Any of these species are capable of reacting significantly with organic compounds. Indeed, overwhelming evidence exists that NO_2^+ is the active nitrating species in aromatic nitrations performed with

concentrated nitric acid or a mixture of concentrated nitric acid and concentrated sulfuric acid.[34] In more dilute solutions, however, the formation of NO_2^+ is greatly suppressed by water.[35] Therefore, participation of NO^+ and NO_2^+ in the reactions with coal would be possible if sufficient moisture exists in the pore structure of the coal. Once exposed to excess NO_2, the water can be quickly converted to concentrated nitric acid, allowing the formation of NO_2^+. On the other hand, NO_2 dissolved in organic solvents such as carbon tetrachloride does not ionize:

$$N_2O_4 \neq NO^+ + NO_3^- \qquad (2.3.14)$$

Although NO_2 can oxidize organosulfur compounds to the corresponding sulfones, removal of sulfur from these compounds is extremely difficult. The addition of oxygen atoms to a sulfur atom weakens the carbon-sulfur bonds by roughly 20 percent. Only aliphatic sulfones readily decompose, however, at room temperature in the presence of aqueous alkali:

$$R_2CH-CR_2-SO_2-R' + R''O^- \rightarrow$$

$$R_2C=CR_2 + R'SO_2^- + R''OH\ . \qquad (2.3.15)$$

The sulfonic acid ($R'SO_2^-$) is water soluble. If R' is still attached to the coal matrix, however, which is quite likely, there is no sulfur removal from the coal. Aromatic and thiophenic sulfones are extremely stable. Desulfurization requires extremely severe conditions before reaction will take place:

$$Ar-(SO_2)-Ar' \xrightarrow[300\,^\circ C]{NaOH} ArOH,\ Ar-Ar',\ Na_2SO_3\ ,\ \text{and} \qquad (2.3.16)$$

$$DBTO_2 \xrightarrow[300\,^\circ C]{NaOH} \textit{Dibenzofuran},\ \textit{Biphenyl},\ \text{and}\ Na_2SO_3 \qquad (2.3.17)$$

Coal would be severely oxidized under these conditions, resulting in high heating value losses. On the basis of these facts, one would not expect a significant degree of organic sulfur removal unless very severe conditions are employed.

2.4 Changes in Coal Structure Due to Reaction

During the reaction of NO_2 with coal, the structure of the coal itself changes. These changes can influence the course of the reaction. For instance, the addition of oxygen groups to the interior surfaces of the pores may inhibit further NO_2 mass transfer. All alterations occur on the atomic level. The best way to gauge these changes in the coal microstructure is by monitoring the variation in the appropriate macroscopic structural parameters. For instance, the specific surface area of the coal indicates the fraction of the solid material exposed. The total pore volume determines the void fraction of the solid. This parameter relates the degree of "openness" of the coal particle, which affects the rate of diffusion of molecular species into and out of the particle. More information is conveyed by the pore size distribution. Whereas the average pore size can be determined from the specific surface area and void fraction, the pore size distribution provides information concerning the pore volume as a function of the pore radius. The distribution serves as an indicator of the tortuosity of the particle, where the tortuosity is simply the reactant path length per unit thickness of the particle. Furthermore, coals with similar specific surface areas and void fractions may have vastly different pore size distributions. Thus, the rates of NO_2 transport may be quite different because the pore diameters of one coal may be smaller than those of another coal. Taken together, variations in these three parameters as a function of an appropriate reaction parameter can provide valuable information regarding the nature of the interaction of NO_2 and coal.

2.4.1 Measurement of the Specific Surface Area of Solids

The most common method of measuring the specific surface area of a solid involves the adsorption of a gas by the solid. Generally, the gas should not react chemically with the solid under the conditions of the measurement. The most

commonly used adsorbates are nitrogen, carbon dioxide and argon. Two theories are widely employed in obtaining the specific surface area from the adsorption data, namely that developed by Brunaeur, Emmett and Teller (BET), and that formulated by Dubinin and Polanyi (DP).

The BET theory is essentially an extension of Langmuir's one molecule to a site theory to encompass the formation of multilayers during adsorption.[37] The fundamental equation of the BET theory is:

$$\frac{P_2}{x\,(P_0 - P_2)} = \frac{1}{cx_m} + \frac{c-1}{cx_m} \times \frac{P_2}{P_0}, \quad \text{where} \tag{2.4.1}$$

P_2 = the system pressure,

P_0 = the adsorbate vapor pressure,

x = the amount of adsorbate adsorbed per unit adsorbent mass at pressure P_2 (cm^3 at STP /g adsorbent),

x_m = the monolayer amount of adsorbate adsorbed per unit adsorbent mass (cm^3 at STP /g adsorbent), and

$$C \approx e^{-\frac{E_1 - E_L}{RT}}, \quad \text{where} \tag{2.4.2}$$

E_1 = the heat of adsorption in the first layer (J /mol adsorbate), and

E_L = the heat of liquefaction of the adsorbate (J /mol adsorbate).

By plotting the adsorption data in the form $\frac{P_2}{x(P_0 - P_2)}$ vs. $\frac{P_2}{P_0}$ and performing a least squares fit to obtain the slope ($\frac{c-1}{cx_m}$) and the intercept ($\frac{1}{cx_m}$), one can determine the values of c and x_m. Application of this theory to a myriad of samples shows that the data are generally linear in the range $0.05 < \frac{P_2}{P_0} < 0.35$.[37] The specific surface area is then given by:

$$S_a = \frac{x_m N_0 A_a}{V_a}, \quad \text{where} \tag{2.4.3}$$

S_a = the specific surface area (cm^2 / g adsorbent),

N_0 = Avogadro's number = 6.02×10^{23} molecules / mole,

V_a = 22,414 cm^3 at STP / mol, and

A_a = the molecular cross–sectional area of the adsorbate (cm^2 / molecule).

The determination of the molecular cross-sectional area, A_a, is of crucial importance. The most common expression used for the calculation of A_a is based on the assumption of two dimensional close packing on the surface of the solid:[38]

$$A_a^T = 1.0911 \left(\frac{M_a}{N_0 \rho}\right)^{\frac{2}{3}}, \quad \text{where} \tag{2.4.4}$$

M_a = the molecular mass of the adsorbate (g / mol),

T = the temperature of the adsorbate (C), and

ρ = the density of the adsorbate at temperature T.

This formula yields the commonly used value for nitrogen adsorption at -196 °C of $A_{N_2}^{-196} = 16.2$ Å^2. Values ranging from 13 to 20 Å^2 have been reported, however.[39] It is postulated that the same adsorbate, in this case N_2, interacts differently with different surfaces. Furthermore, various adsorbates interact differently with the same solid. For instance, the expression above gives a value of 14.1 Å^2 for the molecular cross-sectional area of carbon dioxide at -80 °C. Comparison of surface areas determined from CO_2 adsorption data with those determined from N_2 adsorption data for the same solid, however, yield a range of values for $A_{CO_2}^{-77}$ of 15.4 to 44.2 Å^2.[40] It is obvious that some surfaces interact differently with CO_2, just as they do with N_2. In addition to the same forces accounting for N_2 adsorption, however, CO_2 possesses more potential modes of interaction. In the specific case of polymers, for instance, the permeabilities of

twenty different polymers to CO_2 are all roughly thirty times their permeablities to N_2.[41]

Another, less widely used theory for interpreting adsorption data is that of Dubinin's extension of the Polanyi adsorption potential theory.[42] The basic equation of the DP theory is:

$$W = a\,V = f(\Delta G_a), \quad \text{where} \tag{2.4.5}$$

W = the volume of the pore structure filled with adsorbate,

a = the moles of adsorbate adsorbed at the relative pressure $\frac{P}{P_0}$ defined above,

V = the average molar volume of the adsorbed phase, and

$f(\Delta G_a)$ = a function of ΔG_a, the molar free energy upon adsorption.

Dubinin derived the following equation for ΔG_a:

$$\Delta G_a = RT \ln \frac{P}{P_0}, \quad \text{where} \tag{2.4.6}$$

ΔG_a = the differential change in the molar free energy upon adsorption with the bulk liquid adsorbate at the same temperature as the standard,

R = the gas constant,

T = the absolute temperature (K), and

$\frac{P}{P_0}$ = the relative pressure.

Dubinin and Radushkevich modified the DP theory to account for micropore adsorption, where micropores are pores whose diameters are less than 15 Å. This modification is known as the Dubinin-Polanyi-Radushkevich (DPR) theory,[43] the fundamental postulate of which is:

$$W = f\left(\frac{\Delta G_a}{\beta}\right), \quad \text{where} \tag{2.4.7}$$

β = an affinity coefficient which allows the adsorption isotherms of different gases on the same solid to merge.

The basic result of the DPR theory is:

$$W = a\,V = W_0 \exp\left(-\frac{k\Delta G_a^2}{\beta^2}\right), \quad \text{where} \tag{2.4.8}$$

W_0 = the limiting adsorption volume in the micropores, and

k = a measure of the average pore size.

This equation can be rearranged to yield:

$$\ln a = \ln \frac{W_0}{V} - \frac{kR^2T^2}{\beta^2}\ln^2 \frac{P}{P_0}. \tag{2.4.9}$$

By plotting the adsorption data in the form of $\ln a$ vs. $\ln^2\left(\frac{P}{P_0}\right)$ and performing a least squares fit, the slope yields k and the intercept yields w_0, which is the micropore volume. This equation is particularly useful for obtaining the micropore volume from the low part of the adsorption isotherm. For instance, CO_2 has a vapor pressure at 298°K of 63.5 atm. If adsorption data is acquired in a glass apparatus where the system pressure cannot exceed 1 atm, then the relative pressure range available for examination is from 0 to 0.016. This range is not adequate for use of the BET theory, but it is satisfactory for application of the DPR theory.

The DPR theory has been modified by Kaganer to allow the calculation of the specific surface area.[44] The major assumption concerns the monolayer region where a Gaussian distribution of adsorption potential over the sites on the surface is postulated. The distribution is represented by:

$$\vartheta = \exp(-k_1 \Delta G_a^2) = \frac{a}{a_m}, \quad \text{where} \tag{2.4.10}$$

ϑ = the fraction of the monolayer occupied,

k_1 = a constant which characterizes the distribution,

a = the moles of adsorbate adsorbed at the relative pressure $\frac{P}{P_0}$, and

a_m = the moles of adsorbate adsorbed forming a monolayer.

After substituting the expression for ΔG_a and rearranging, one obtains:

$$\ln a = \ln a_m - k_1 R^2 T^2 \ln^2 \frac{P}{P_0}. \tag{2.4.11}$$

A plot of ln a vs. $\ln^2(\frac{P}{P_0})$ yields a straight line whose intercept gives a_m, from which the surface area can be obtained using the expression $S_a = a_m N_0 A_a$, where the quantities involved have been previously defined. Use of the Kaganer modification of the DPR theory gives values for a_m which agree within ± 3 % with those obtained for the same adsorbates by application of the BET theory, which is quite good, considering that the DPR theory usually uses relative pressures less than 0.1 while the BET theory requires relative pressures up to 0.35. It should be noted that the linearity of the DPR plot does not arise because of the generality with which log vs. log^2 plots can linearize data.[45] Indeed, nearly all DPR plots show significant deviation from linearity when the relative pressure exceeds 0.15.

2.4.2 The Adsorption of Nitrogen and Carbon Dioxide on Coal

Although N_2 is by far the most widely used adsorbate for obtaining adsorption isotherms, much of the work performed with coal utilizes CO_2.[46] Proponents of CO_2 claim that equilibrium between the bulk and adsorbed phases of the adsorbate occurs readily at 195°K when CO_2 is used while the same equilibrium may not occur at all at 77°K when N_2 is used. The fact that CO_2 possesses more

modes of interaction with the adsorbent, however, has negative implications regarding the validity of assuming solely physical adsorption of CO_2 on solid surfaces, especially on a surface of a polymer-like solid such as coal.

A study of the unsteady state diffusion of N_2 and CO_2 from coals with ultrafine pores ($d_p < 4$ Å) yields the following empirical expression for the diffusion coefficient:[47]

$$\frac{D^{\frac{1}{2}}}{r_0} = A\, e^{\frac{-E}{RT}}, \quad \text{where} \tag{2.4.12}$$

D = the diffusion coefficient (cm^2/s),

r_0 = the diffusion path length (cm),

A = the pre–exponential constant (cm /s), and

E = the activation energy for diffusion (kcal /mol).

The data yield values of E and A which are smaller for CO_2 than N_2. The data were obtained in the temperature range from 20 to 110°C. Extrapolation of these results to the appropriate adsorption temperatures indicate that $D_{CO_2}^{195^\circ K}$ is 10^6 to 10^7 times larger than $D_{N_2}^{77^\circ K}$. Although one might question the validity of extrapolating the results over such a large temperature range, the authors claim that since the pore radii are on the order of molecular dimensions, the diffusion process is analogous to conventional surface diffusion, except that two surfaces rather than one surface are involved. Therefore, neither E nor A is expected to be a function of temperature. The salient result, therefore, is that N_2 is not expected to diffuse into the micropores in a reasonable amount of time at 77°K. Indeed, even CO_2 is not expected to completely fill all of the micropores at 195°K within 30 minutes. Rather, the adsorption must be conducted at 295°K to insure complete pore filling.

More compelling evidence for favoring CO_2 over N_2 lies in the molecular sieve characteristics of coal. In a straightforward, yet elegant study, Medeiros and Petersen measured the surface areas of 4 Å and 5 Å molecular sieves using both the BET and DPR theories to interpret their data.[48] The results are shown in Table 2-1.

The N_2 adsorption was conducted at 77°K using a value of 16.2 Å^2 for the molecular cross-sectional area ($A_{N_2}^{77\,K}$), while the CO_2 adsorption was performed at 196°K using a value of 23.4 Å^2 for $A_{CO_2}^{196\,K}$. The results in the table imply that either N_2 or CO_2 is adequate for measuring the surface area of solids whose pores have diameters greater than or equal to 5 Å, but that only CO_2 is adequate when the pore diameters are less than 5 Å. The fact that the N_2 surface areas are about 20 % lower is probably due to the presence of a substantial minority of 4 Å pores in the 5 Å sieves. The N_2 determined areas of the 4 Å sieves, however, are roughly 40 to 50 times smaller than the CO_2 determined areas. The obvious implication is that CO_2 can penetrate 4 Å pores while N_2 cannot penetrate pores with diameters less than 5 Å. The fact that many coals show the same adsorption behavior as the 4 Å sieves indicates that the vast majority of the pore volume in most coals consists of micropores with diameters less than 5 Å.[49]

It should be noted, however, that most surface areas are used to determine the amount of solid exposed for reaction with some externally introduced reagent. If the reagent, such as NO_2, has molecular dimensions which do not allow penetration into micropores as small as those accessible to CO_2, then use of the CO_2 determined surface area could lead to wildly erroneous results. For this reason, the surface area of the solid, particularly in the case of catalysts, is determined with the reagent to be used whenever possible. In the case of NO_2 and coal, however, this is not possible since NO_2 reacts with coal at room temperature, which also happens to be the boiling point of NO_2. NO_2 should

TABLE 2-1

Surface Areas of 4A and 5A Molecular Sieves				
Sieve	BET Theory		DPR Theory	
	N_2	CO_2	N_2	CO_2
4A	11	480	12	540
5A	480	570	580	690

resemble N_2 more than CO_2, however, because NO_2 is a bent molecule while CO_2 is a linear molecule. Hence, N_2 determined surface areas should be better for use in the kinetic study of the NO_2-coal reaction.

As previously mentioned, other reasons exist for favoring N_2 over CO_2 for surface area determinations as well. Primarily, CO_2 is expected to interact with a solid surface, particularly that of coal, in more ways than N_2. For instance, a propensity of polar groups, such as -O or -NO_2, on the surface should lead to a stronger interaction with CO_2 than with N_2 due to the greater polarizability of CO_2. Furthermore, CO_2 can display much stronger quadrupole interactions with a polar surface than N_2. These reasons alone, however, cannot totally explain the large discrepancy between the N_2 and CO_2 determined surface areas. If one rejects the 4 Å molecular sieve characteristics of coal, the only other explanation is the absorption of CO_2 by the coal. If CO_2 absorption occurs, then the CO_2-determined surface area is really an indication of not only the exposed surface area but also the capacity of the solid to accept CO_2 as well. In the case of coal, the N_2 determined area could be taken as the true surface area component of the CO_2 determined "area", and the other roughly 98 % of the CO_2 "area" could be attributed to CO_2 uptake by the solid coal matrix.

More importantly, the validity of describing an organic structure as microporous with pore diameters of 4 Å is highly questionable since 4 Å is on the order of atomic dimensions. Indeed, such a description necessitates a distinction between the true interatomic voids which would comprise a pore and the interatomic voids encountered in loose bonds, such as hydrogen bonds (1.5 Å to 2.0 Å). It may be more appropriate to classify diffusion through such a structure as hindered molecular diffusion since the coal "molecules" are not free to counterdiffuse. There is no compelling evidence, however, to favor this theory over that of coal possessing pores mainly of diameters less than 5 Å.

2.4.3 The Measurement of Pore Volume

The pore volume of a solid is commonly expressed in terms of the void fraction:

$$\varepsilon = 1 - \frac{\rho}{\rho_s}, \quad \text{where} \tag{2.4.13}$$

ε = the void fraction (cm^3 void / cm^3 total volume),

ρ_s = the solid density (g solid / cm^3 solid), and

ρ = the total density (g solid / cm^3 total volume).

The solid density, ρ_s, is usually measured by helium displacement while the total density, ρ, is usually measured by mercury displacement. The helium fills the entire pore volume while the mercury cannot penetrate any of the pores. An alternative method for measuring the pore volume is by employing gas adsorption. If an entire gas adsorption-desorption isotherm is taken, the point closest to a relative pressure of unity corresponds to all of the pores being completely filled. The calculation of the total pore volume from the amount of gas adsorbed is straightforward:

$$V_p = \frac{x_T M}{\rho \upsilon}, \quad \text{where} \tag{2.4.14}$$

V_p = the total pore volume (cm^3 void / g solid),

x_T = the total amount of adsorbate adsorbed (cm^3 at STP / g solid),

M = the molecular mass of the adsorbate (g / mol),

ρ = the density of the adsorbate at the adsorption temperature (g adsorbate / cm^3 adsorbate), and

υ = 22,414 cm^3 / mol of ideal gas at 1 atm and 0°C (STP).

Since much more CO_2 is adsorbed for most coals than N_2, ostensibly because of the microporous structure of most coals, a substantial discrepancy between CO_2

and N_2 determined pore volumes exist. The same arguments regarding the molecular size of the reagent mentioned in the previous section still apply, however. An adsorbate which resembles as closely as possible the reagent should be employed if the solid surface area is to be used in conjunction with kinetic data.

2.4.4 The Determination of the Pore Size Distribution

Although the specific surface area and the void fraction can provide information about the pore volume of the solid, the pore size distribution conveys information concerning the pore *structure* of a solid. The development of the theory required to extract the pore size distribution from the adsorption-desorption isotherm began with the discovery of the phenomenon of capillary condensation in 1871 by Thomson.[50] Condensation of a vapor in a pore follows from the fact that the equilibrium pressure over a concave liquid surface is less than the saturated vapor pressure at the same temperature. The appropriate thermodynamic expression describing this phenomenon is the Kelvin equation:

$$\ln \frac{P}{P^0} = -\frac{\sigma v}{RT}\left(\frac{1}{r_1}+\frac{1}{r_2}\right) = -2\,\frac{\sigma v}{RT}\,\frac{1}{r}, \quad \text{where} \qquad (2.4.15)$$

P = the equilibrium pressure above a concave adsorbate meniscus,

P^0 = the saturated vapor pressure of the adsorbate,

σ = the surface tension of the liquid adsorbate,

v = the molar volume of the liquid adsorbate,

r_1, r_2 = the radii of curvature of the liquid surface, and

r = the radius of curvature of a hemispherical surface, i.e. $r_1 = r_2 = r$.

Zsigmondy then proposed that as the relative pressure, $\frac{P}{P^0}$, is increased that at first a layer of adsorbate is formed on the pore walls followed by capillary condensation in pores whose radii are less than or equal to the value of r

corresponding to $\frac{P}{P^0}$ given by the Kelvin equation.[51] In 1932, Foster realized that the thickness of the adsorbed layer must be accounted for when using the Kelvin equation to determine pore size distributions.[52] Development of the BET theory in 1932 allowed the calculation of the monolayer thickness, which then allowed the determination of the pore size distribution. In a further development in 1955, Dubinin and Pierce recognized the function of micropores in altering the mechanism of adsorption because of the increased force acting on the adsorbate molecules due to the proximity of the adsorbent walls.[53] The effect of this realization was to establish a lower limit on the domain of pore radii to which the Kelvin equation is validly applicable. Except for some slight modifications in the last twenty years, the theory as it existed in 1955 is still used today for the calculation of pore size distributions of solids.

2.4.4.1 The Derivation of the Kelvin Equation

In order to understand some of the limitations of the Kelvin equation and its applicability to adsorption-desorption isotherms, the full derivation of the Kelvin equation will be discussed. Referring to Figure 2-1, the difference in pressures on either side of the curved liquid surface is:

$$P_2 - P_1 = \sigma \left(\frac{1}{r_1} + \frac{1}{r_2}\right), \quad \text{where} \tag{2.4.16}$$

P_2 = the pressure on the concave side of the meniscus,

P_1 = the pressure on the convex side of the meniscus,

σ = the liquid surface tension, and

r_1, r_2 = the radii of curvature of the liquid surface.

At equilibrium, the chemical potentials, μ_i, in all phases are equal:

$$\mu_2 = \mu_{surface} = \mu_1, \tag{2.4.17}$$

Condensed Adsorbate in a Cylindrical Pore

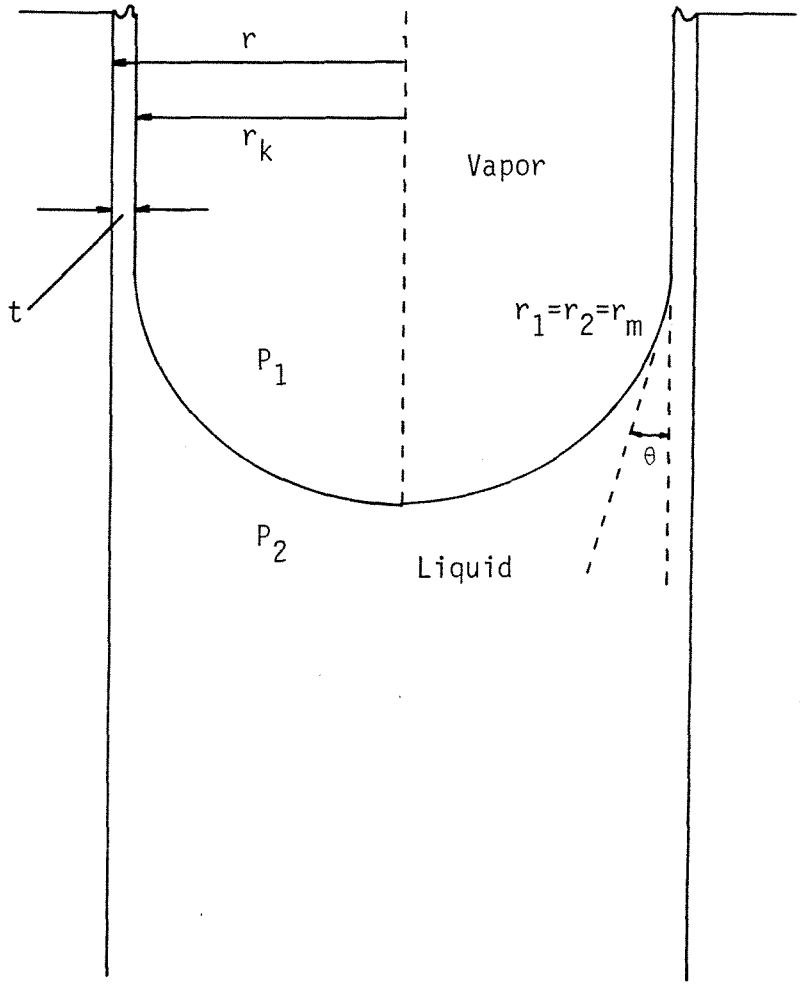

Figure 2-1

which implies that

$$dP_2 - dP_1 = 2\,d\left(\frac{\sigma}{r_m}\right) \quad \text{and} \quad d\mu_1 = d\mu_2. \tag{2.4.18}$$

where for a hemispherical meniscus $r_1 = r_2 = r_m$. Application of the Gibbs-Duhem equation to both phases results in:

$$S_1 dT + v_1 dP_1 + d\mu_1 = 0 \quad \text{and} \quad S_2 dT + v_2 dP_2 + d\mu_2 = 0, \quad \text{where} \tag{2.4.19}$$

S_i = the specific entropy of phase i (cal / mol / K),

T = the absolute temperature (K), and

v_i = the molar volume of phase i (cm^3 / mol).

If the vapor phase is on the convex side of the meniscus, then $v_2 << v_1$, which leads to

$$2\,d\left(\frac{\sigma}{r_m}\right) = -\frac{RT}{v_2 P_1} dP_1 = -\frac{RT}{v_2} d(\ln P_1) \tag{2.4.20}$$

at constant temperature ($dT = 0$). Integrating the left side from $r_m = r_m$ to $r_m = \infty$ and the right side from $P_2 = P$ to $P_2 = P^0$ while assuming that the liquid is incompressible in the range of P_2 from 0 to P^0 results in the Kelvin equation.

$$\ln\left(\frac{P}{P^0}\right) = -\frac{2\sigma v}{RT}\frac{1}{r_m}. \tag{2.4.21}$$

The major implication of the Kelvin equation is that capillary condensation will occur at some pressure less than the saturated vapor pressure if the condensed liquid forms a concave meniscus.

A model of the pore geometry must be adopted in order to calculate a pore size distribution. Generally, the pores are assumed to be cylindrical. If the meniscus has the contact angle ϑ with the adsorbed layer, the Kelvin equation is rewritten as:

$$\ln \frac{P}{P^0} = -\frac{2\sigma v}{RT}\frac{\cos \vartheta}{r_k}, \quad \text{where} \qquad (2.4.22)$$

ϑ = the contact angle, and

$r_k = r_m \cos \vartheta$ = the core radius.

Equation (2.4.22) forms the basis for the standard computational procedure described below for calculating the pore size distribution.

2.4.4.2 Hysteresis in the Adsorption-Desorption Isotherm

A common phenomenon observed in gas adsorption work is that the amount of adsorbate adsorbed will be higher in the desorption branch than in the adsorption branch of the isotherm at the same relative pressure. One hypothesis asserts that this phenomenon results from the difference between the advancing and receding contact angles which the adsorbate makes with the adsorbent surface.[51] This hypothesis is not accepted, however, mainly because there is no way to accurately measure the different contact angles. In fact, the contact angle for both capillary condensation and evaporation is assumed to be zero.

The most widely accepted theory accounting for hysteresis is the ink-bottle hypothesis.[55] The basic assumption concerns the pore structure which is assumed to contain large chambers connected by narrow passages. All pore segments will experience capillary condensation at the relative pressure corresponding to the pore radii given by the Kelvin equation as if the segments were totally independent. Evaporation, on the other hand, occurs in a different fashion. The Kelvin equation predicts that evaporation of the adsorbate occurs in pores of smaller radii at lower relative pressures due to the increased curvature of the meniscus. As a direct consequence, evaporation from the large chamber commences only when evaporation begins in the narrow neck to which the chamber is connected. Therefore, the chamber empties at a lower pressure

than that at which it fills, resulting in hysteresis. The ink-bottle hypothesis has a profound effect on the interpretation of the pore size distribution. If the pore volume of the adsorbent consists mainly of large chambers connected entirely with short segments of relatively narrow passages, the pore size distribution will indicate that the entire pore structure consists of pores with radii corresponding to the narrow passages.

2.4.4.3 The Range of Validity of the Kelvin Equation

It is important to establish the limits within which the Kelvin equation is applicable. Since the theory is based on thermodynamic arguments, it is valid only for the description of macroscopic systems. As a result, the Kelvin equation becomes inaccurate when the pore radius approaches molecular dimensions. Guggenheim concludes that surface tension becomes independent of pore radius only when the radius is greater than 500 Å,[56] while others contend that the equation is valid for radii as small as 15 Å.[57] An expression relating the surface tension of the liquid in the pore to the surface tension of the free liquid indicates that for a pore radius of 20 Å, the calculated values of the radii are high by a factor of 1.3.[58] Another study that uses partition functions to calculate the change in surface tension as a function of curvature indicates that the calculated values of pore radii are high by a factor of 1.41 for liquid N_2 at 77°K and a pore radius of 20 Å.[59]

Whereas the above treatments rely on the application of thermodynamics to systems containing a small number of molecules, Dubinin has developed an experimental method to determine the point of failure of the Kelvin equation by defining an affinity of adsorption, A:[60]

$$A = RT \ln \frac{P^0}{P} = \frac{2\sigma v}{r_m} \qquad (2.4.23)$$

At a given fraction of pore filling, f, r_m and $\frac{P}{P^0}$ have definite values so that

$$\left(\frac{\partial A}{\partial T}\right)_f = A\left[\frac{\partial \ln(\sigma v)}{\partial T}\right]_f. \qquad (2.4.24)$$

Over a short temperature range $\frac{\partial \ln(\sigma v)}{\partial T}$ is constant so that

$$\left(\frac{\partial A}{\partial T}\right)_f \propto A. \qquad (2.4.25)$$

By plotting the adsorption-desorption data for a variety of adsorbents in the form $\left(\frac{\partial A}{\partial T}\right)_f$ vs. A, Dubinin finds that the data are linear for pore radii greater than 15 Å. Significant deviation occurs for radii less than 15 Å. Based upon these experimental results, the Kelvin equation is usually assumed to hold for pore radii greater than 15 Å. For radii less than 15 Å, the results imply that a mechanism totally different than capillary condensation occurs.

Whereas a lower bound on the range of pore radii over which the Kelvin equation is valid exists because of the physical nature of pore filling, an upper bound exists because of experimental accuracy. According to the Kelvin equation, as the relative pressure approaches unity, the corresponding pore radius exponentially approaches infinity. Thus, the pore radius range from 300 Å to infinity corresponds to the relative pressure range from 0.969 to 1.000 for liquid N_2 at 77°K. Such a change in relative pressure usually corresponds to one step in the desorption branch of the isotherm. Therefore, application of the Kelvin equation is valid only in the pore radius range from 15 to 300 Å.

2.4.4.4 Application of the Kelvin Equation for Obtaining Pore Size Distributions

The most commonly used method for obtaining pore size distributions utilizes a correction which accounts for the changing thickness of the film of adsorbed gas on the pore walls as the relative pressure decreases.[61] This concept of film area is expressed mathematically as:

$$\Delta v = \Delta v_k + \Delta v_f = \Delta v_k + \Delta t \sum(\Delta S_p), \quad \text{where} \tag{2.4.26}$$

Δv = the total volume change measured at each point in the desorption branch of the isotherm,

Δv_k = the change in pore volume,

Δv_f = the volume of the adsorbate released from all exposed walls,

Δt = the reduction in film thickness, and

$\sum(\Delta S_p)$ = the area of pore walls for pores which have lost their capillary condensate.

For cylindrical pores,

$$\Delta S_p = \frac{2}{r_p}\Delta v_p, \quad \text{where} \tag{2.4.27}$$

$$\Delta v_p = \left(\frac{r_p}{r_k}\right)^2 \Delta v_k, \tag{2.4.28}$$

$r_p = r_k + t$ = the pore radius, and (2.4.29)

r_k = the core radius, where

the core refers to the void within the pore not encompassed by the condensate film (see Figure 2-1).

This formulation necessitates an expression relating the film thickness to the relative pressure. Wheeler has suggested that adsorption on the walls of fine pores is greater than on an open surface, particularly at low relative pressures.[62] Therefore, he proposes the use of the Halsey equation to determine the film thickness:[63]

$$t = \sigma \left[\frac{5}{\ln\left(\frac{P_0}{P}\right)}\right]^{\frac{1}{3}}, \quad \text{where} \tag{2.4.30}$$

σ = the thickness of a monolayer, and

$\frac{P_0}{P}$ = the relative pressure.

Several researchers have compared the adsorption data for various silicas and aluminas and for various non-porous solids and have found very good agreement with the Halsey equation in the relative pressure range from 0.2 to 1.0 using a value of 3.5 Å for the N_2 monolayer thickness, σ, at 77°K.[64] The Kelvin equation provides the expression for the core radius, r_k. Using the values of 34.6 cm^3/mol for the molar volume, 8.85 dyne/cm for the surface tension of liquid N_2 at 77°K, and zero for the contact angle, the Kelvin equation reduces to:

$$r_k = \frac{9.53}{\ln(\frac{P_0}{P})} \qquad (2.4.31)$$

The basic calculation scheme then becomes:

1. Calculate $(r_k)_i$, t_i, and $(r_p)_i = (r_k)_i + t_i$ for each desorption data point $(\frac{P_i}{P_0}, v_i)$ beginning with the highest relative pressure.
2. Interpolate between points to obtain $\overline{(r_p)_i} = \frac{1}{2}[(r_p)_{i+1} + (r_p)_i]$ and $\overline{(r_k)_i} = \frac{1}{2}[(r_k)_{i+1} + (r_k)_i]$.
3. Calculate $(\Delta t)_i = t_{i+1} - t_i$ and $(\Delta v)_i = v_{i+1} - v_i$.
4. Calculate $(\Delta v_f)_i = 0.064\ (\Delta t)_i \sum_{j=1}^{i-1} (\Delta S_p)_j$ and $(\Delta v_k)_i = (\Delta v)_i - (\Delta v_f)_i$.
5. Calculate $(\Delta v_p)_i = (\Delta v_i)\ [\frac{(r_p)_i}{(r_k)_i}]^2$ and $(\Delta S_p)_i = 2\ \frac{(\Delta v_p)_i}{(r_p)_i}$.
6. Repeat each step for the desired number of data points down to a relative pressure no less than 0.3.

2.4.4.5 Application of the DPR Theory to the Carbon Dioxide Isotherm for Micropore Analysis

Recently, Medek[65] has proposed a theory which allows the determination of

the micropore size distribution from the CO_2 isotherm using the DPR theory. Medek used Dubinin's equation in the form:

$$W = W_0 \exp\left[-\left(\frac{\Delta G_a}{E}\right)^n \right], \quad \text{where} \tag{2.4.32}$$

W = the volume of the pore structure filled with adsorbate at fugacity f ,

W_0 = the volume of the pore structure filled with adsorbate at fugacity f_s ,

$\Delta G_a = RT \ln(\frac{f_s}{f})$ = the differential molar work of adsorption,

E = a characteristic energy whose value increases with the fineness of the micropore structure, and

n = an exponent with a value near 2.0.

Basically, Medek transformed W as a function of $\ln \frac{f_s}{f}$ to a function of r, the micropore radius. The transformation required three assumptions, the first of which concerns the adsorption potential in the micropores, which is assumed to be adequately represented by:

$$\varphi = \alpha C N z^{-3} = k z^{-3}, \quad \text{where} \tag{2.4.33}$$

φ = the adsorption potential in the micropores,

α = a function of the pore environment,

C = a constant,

N = the number of adsorbed atoms per unit volume, and

z = the distance from the gas molecule to the solid surface.

DeBoer[66] has shown that α, and hence k, increase as the micropore radius decreases. This formulation neglects dipole-quadrupole and quadrupole-quadrupole interactions, which causes an error of roughly 10 %. This error is partially offset by the repulsion terms, however.

The second assumption treats the distance z as an average distance of the adsorbate molecule from all pertinent walls when several walls interact with the adsorbate molecule. In an enclosed environment, such an average z can be expressed as an equivalent radius:

$$z = r_e = \frac{2Q}{P}, \quad \text{where} \tag{2.4.34}$$

r_e = the equivalent radius,

Q = the area of the pore cross-section, and

P = the perimeter of the pore cross-section.

It is apparent that r_e does not depend upon any particular pore geometry.

The third assumption states that the dependence of φ on r_e described by equations (2.4.33) and (2.4.34) holds within the domain of micropore radii, namely 4 to 16 Å. Within this domain, adsorption proceeds by volume filling, that is, no adsorbed monolayer is first formed followed by condensation.

If there are no perturbations in the adsorbed phase, the following relationship holds:

$$\Delta G_a = \varphi = k r_e^{-3} . \tag{2.4.35}$$

Substitution of this expression into equation (2.4.32) yields

$$W = W_0 \exp\left[- \left(\frac{k}{E}\right)^n r_e^{-3n} \right] . \tag{2.4.36}$$

The micropore size distribution is then given by differentiation of W with respect to r_e, which gives

$$\frac{dW}{dr_e} = 3n W_0 \left(\frac{k}{E}\right)^n r_e^{-(3n+1)} \exp\left[- \left(\frac{k}{E}\right)^n r_e^{-3n} \right] . \tag{2.4.37}$$

An expression for the effective micropore surface area can be obtained by letting dh be an element of pore depth h, which when substituted in equation

(2.4.34) yields

$$r_e = \frac{2Q\,dh}{P\,dh} = 2\left(\frac{dW}{dS}\right)_{r_e}. \qquad (2.4.38)$$

Using the above expression in conjunction with equation (2.4.37) gives

$$\frac{dS}{dr_e} = 6nW_0\left(\frac{k}{E}\right)^n r_e^{-(3n+2)} \exp\left[-\left(\frac{k}{E}\right)^n r_e^{-3n}\right]. \qquad (2.4.39)$$

Integration of this equation yields

$$\int_0^{S_{micro}} dS = 2\,W_0\left(\frac{E}{k}\right)^{\frac{1}{3}} \int_0^{\infty} x^{\frac{1}{3n}} e^{-x} dx\,, \quad \text{where} \qquad (2.4.40)$$

$$x = \left(\frac{k}{E}\right)^n r_e^{-3n}.$$

After integration, one obtains

$$S_{micro} = 2\,W_0\left(\frac{E}{k}\right)^{\frac{1}{3}} \Gamma\left(\frac{3n+1}{3n}\right), \quad \text{where} \qquad (2.4.41)$$

$\Gamma(n)$ = the gamma function evaluated at n.

In order to utilize the equations above, values for some of the parameters are necessary. The best value for n is 2.0, which is based on optimal linearization for coke samples activated in CO_2.[65] The characteristic energy, E, is given by

$$E = 2.303\,RT\left[2.303\,\frac{d\,\log W}{d\,\log^n\left(\frac{f_s}{f}\right)}\right]^{-\frac{1}{n}}. \qquad (2.4.42)$$

It should be noted that the term in brackets is simply the slope of the DPR plot. The calculation of W_0 requires the density of the adsorbed phase, ρ_a. It is assumed that ρ_a at a given temperature T is the same as the bulk liquid density ρ_l at the temperature $(T - \Delta T)$. The empirically determined value of ΔT is 19°K. The resulting values for ρ_a as a function of temperature are

T (K)	252	273	287	298
ρ_a (g/cm^3)	1.111	1.023	0.955	0.889

The value of k is 3.145 kJ/nm^3 for CO_2,[67] which was determined empirically. With these values for n, E, ρ_a and k, it is now possible to calculate the micropore size distribution and effective micropore surface area.

2.5 Model of the Reaction System

A mathematical description of the physical and chemical nature of the NO_2/solvent/coal system is needed in order to quantify the experimental results. As a result, significant and trivial parameters can be identified. Of greatest significance, however, is the possibility to better predict the behavior of other coals under the same reaction conditions.

2.5.1 Derivation of the Pertinent Equations

For the sake of mathematical simplicity, the coal can be considered as a collection of spherical particles, all of which have the same radius. Within a spherical shell, the equation describing the transport and reaction of a given chemical species is:

$$\varepsilon V_s c_i \Big|_t^{t+\Delta t} = 4\pi \left[D_{e,i} (r+\Delta r)^2 \frac{\partial c_i}{\partial r}\Big|_{r+\Delta r} - D_{e,i}\, r^2 \frac{\partial c_i}{\partial r}\Big|_r \right] + V_s R_i \Delta t \,, \quad \text{where} \tag{2.5.1}$$

ε = the void fraction of the particle
(cm^3 void / cm^3 total solid volume),

V_s = the shell volume = $\frac{4\pi}{3}[\, 3r^2\Delta r + 3r(\Delta r)^2 + (\Delta r)^3 \,]$ (cm^3),

t = the time (sec),

Δt = the differential time element (sec),

r = the radial distance from the particle center to the inner shell surface (cm),

Δr = the shell thickness (cm),

c_i = the concentration of species i (mol / cm^3 void volume),

$D_{e,i}$ = the effective diffusivity = $\frac{\varepsilon D_i}{\tau}$ (cm^2/s),

τ = the tortuosity of the particle,

D_i = the molecular diffusivity of species i (cm^2 / s), and

R_i = the net rate of formation of species i within the shell (mol / cm^3 / s).

Dividing by $\Delta t\ \Delta r$ and taking the limit as $\Delta t \rightarrow 0$ and $\Delta r \rightarrow 0$ results in the partial differential equation:

$$\frac{\partial}{\partial t}(\varepsilon c_i) = \frac{\partial}{\partial r}\left[D_{e,i}\, r^2 \frac{\partial c_i}{\partial r} \right] + R_i \,. \qquad (2.5.2)$$

Generally, a rate expression corresponding to an appropriate reaction must be determined to proceed further. One possible reaction is:

$$\alpha_j NO_2 + X_j \xrightarrow{k_j} \alpha_j NO + (XO_{\alpha_j})_j \,, \quad \text{where} \qquad (2.5.3)$$

X_j = some coal species which reacts with NO_2,

(XO_{α_j}) = the oxidized coal species,

k_j = the second-order rate constant (cm^3 / mol / s), and

α_j = the stoichiometric coefficient.

The appropriate rate expression is:

$$R_i = -\sum_{j=1}^{N} k_j\, \varepsilon_s\, \rho_s\, S_a\, c^{\alpha_j}\, c_{X_j} \,, \quad \text{where} \qquad (2.5.4)$$

ε_s = the solid fraction of the particle (cm^3 solid / cm^3 total volume),

ρ_s = the solid density (g / cm^3 solid volume),

S_a = the specific surface area (cm^2 particle surface area / g),

c = the NO_2 concentration (mol NO_2 / cm^3 void volume),

c_{X_j} = the coal species concentration (mol X / cm^2 particle surface area), and

N = the total number of coal species.

The most logical selection for the coal surface species comprises the atomic elements which constitute the coal, namely C, H, N, O and S. In this case, then, $N = 5$. The appropriate boundary conditions are:

$$\varepsilon(t=0,r) = \varepsilon_0 \qquad (2.5.4a)$$

$$c(t=0,r) = c_0 \qquad (2.5.4b)$$

$$c_{X_j}(t=0,r) = (c_{X_j})_0 , \qquad (2.5.4c)$$

$$\frac{\partial}{\partial r} c(r,t) \,|_{r=0} = 0 , \qquad (2.5.4d)$$

$$D_e \frac{\partial}{\partial r} c(r,t) \,|_{r=R} = k_c (c_b - c_s) = 0 \text{ or } c(t,R) = c_b, \text{ where} \qquad (2.5.4e)$$

R = the particle radius (cm),

k_c = the mass transfer coefficient for NO_2 between the particle surface and the bulk solvent (cm/s),

c_b = the NO_2 concentration in the bulk solvent (mol/cm^3 void volume), and

c_s = the NO_2 concentration at the particle surface (mol/cm^3 void volume).

Equation (2.5.2) applies to those reactants not contained by the solid matrix of the coal. The appropriate equations for the coal species, X_j, are:

$$\frac{\partial}{\partial t}(\varepsilon_s \rho_s S_a c_{X_j}) = R_{X_j} = - \varepsilon_s \rho_s S_a k_j c^{\alpha_j} c_{X_j} . \qquad (2.5.5)$$

The corresponding boundary conditions are:

$$\varepsilon_s(t=0,r) = \varepsilon_{s0} , \qquad (2.5.5a)$$

$$c_{X_j}(t=0,r) = (c_{X_j})_0 , \qquad (2.5.5b)$$

$$c\ (t=0,r) = c_0. \qquad (2.5.5c)$$

The following assumptions are involved in this model:

1. The void fraction is a function of time only: $\varepsilon = \varepsilon(t)$ and $\varepsilon \neq \varepsilon(r)$.

2. There is no mass transfer resistance from the bulk phase to the particle surface.

3. The tortuosity factor, τ, is constant.

4. The solid density, ρ_s, is constant.

These assumptions are all subject to debate. The first assumption is highly questionable since ε changes presumably due to reaction, the rate of which is a function of the spatial dimension. Indeed, the porosity is commonly assumed to linearly depend on the solid reactant conversion:[68]

$$\varepsilon_s = \varepsilon_{s0} + c_{X0}^M (v_{s0} - v_s)(1 - \varepsilon_{s0})\left(1 - \frac{c_X^M}{c_{X0}^M}\right), \quad \text{where} \tag{2.5.6}$$

c_X^M = the molar surface site concentration (mol sites / cm^3 solid volume),

$c_{X0}^M = c_X^M (t=0)$,

v_{s0} = the reactant molar volume (cm^3 / mol),

v_s = the product molar volume (cm^3 / mol), and

$\varepsilon_{s0} = \varepsilon_s (t=0)$.

It is obvious that $\varepsilon_s = \varepsilon_{s0}$ if the solid reactant and product molar volumes are equal, namely $v_s = v_{s0}$. Since $\varepsilon = 1 - \varepsilon_s$ does change during reaction, however, it is only valid to consider ε in general terms as $\varepsilon(t,r)$. Inclusion of this refinement into the model poses no problem as long as an equation such as (2.5.6) is available.

The second assumption may also be suspect. Commonly, the boundary condition at the particle surface is expressed as:

$$D_e \left.\frac{\partial c}{\partial r}\right|_{r=R} = k_c (c_b - c_s) \neq 0. \tag{2.5.7}$$

In slurry reactors, the relative velocities of the solvent and the particles are essentially equal because the particles tend to move with the liquid. Agitation does not enhance the rate of mass transfer across the particle film when the

particles have diameters less than 200 microns.[69] A minimum value can be obtained for k_c by equating the settling velocity due to gravitational force to the relative velocity in the expression relating the Sherwood number to the Peclet number:[70]

$$(k_c)_{min} \left(\frac{\mu_l}{\rho_l D}\right)^{\frac{2}{3}} = 0.34 \left(\frac{\Delta\rho\, \mu_l\, g}{\rho_l^2}\right)^{\frac{1}{3}}, \quad \text{where} \tag{2.5.8}$$

μ_l = the viscosity of the liquid (g/cm/s),

ρ_l = the density of the liquid (g /cm^3),

$\Delta\rho = \rho_s - \rho_l$ = the density difference between the solid and liquid, and

g = the acceleration of gravity = 960 cm /s^2, and

At 25°C for the NO_2/CCl_4/Coal system, $(k_c)_{min} = 2.53\times10^{-3}$ cm/s. By equating the rate of reaction with the flux at $r = R$, one obtains:

$$r = a_m\, k_c\, (c_b - c_s), \quad \text{where} \tag{2.5.9}$$

$a_m = \frac{3}{\rho R}$ = the external surface area of the particle (cm^2 /g).

The initial rate of NO_2 disappearance is on the order of 3×10^{-5}mol NO_2/g coal/s. For a particle with a diameter of 100 microns, a_m = 462 cm^2/g. Using these figures results in:

$$c_{bulk} - c_{surface} = 3.2\times10^{-5} \text{ mol /cm}^3. \tag{2.5.10}$$

Under most reaction conditions, $c_b \approx 1.0\times10^{-3}$ mol/cm^3. Therefore, the change in NO_2 concentration from the bulk to the surface is only 3 % of the initial bulk concentration. After 15 minutes, the rate drops by a factor of ten, so that the difference between the bulk and surface concentrations becomes negligible. In the case of agitation, k_c would increase if it changes at all, resulting in even smaller differences between c_b and c_s. The second assumption is valid, therefore, unless very small NO_2 concentrations are encountered.

The third and fourth assumptions are more readily acceptable. Since previous work has shown that the pore size distribution of treated coal maintains the same character as the raw coal despite rather large decreases in pore volume, the tortuosity can be taken as constant. Such an assumption is valid because the tortuosity includes the effects of the altered diffusion path length as well as the changing cross-sectional area in the pores.[71]. Since the shape of the pore size distribution remains invariant, these effects are invariant. This conclusion does not mean, however, that the effective diffusivity, D_e, does not change. The decrease in D_e is accounted for by the decrease in the void fraction, ε. The fourth assumption is valid provided the solid does not react to a significant extent, which is the case in the experiments performed.

It should be noted that this model entails the numerical solution of the full unsteady-state equations. Most analyses of this sort, however, involve gas-solid noncatalytic systems where it is possible to neglect the time dependent terms by invoking the pseudo-steady-state approximation.[72] An analysis by Wen[73] has shown that the unsteady-state and pseudo-steady-state solutions converge if $\lambda << 1$, where λ is the root of the transcendental equation:

$$\varepsilon \frac{c_{NO_2}(t=0)}{c_X(t=0)} = \pi^{\frac{1}{2}} \lambda e^{\lambda^2} \operatorname{erf} \lambda . \qquad (2.5.11)$$

In gas-solid systems, $\lambda \approx 0.001$, which satisfies the condition. In the case of the NO_2/CCl_4/Coal system, however, this is not necessarily true. If the coal is considered as pure carbon with a specific gravity of 1.2, then $c_x(t=0) = 0.1$ mol/cm^3. Taking $\varepsilon = 0.1$ and $c_{NO_2}(t=0) = 0.001$ mol/ cm^3, then equation (2.5.11) gives a value of $\lambda \approx 0.04$, resulting in a 0.1% error in the pseudo-steady-state solution. This represents a best case scenario, however. If the NO_2 reacts only with 5 % of the coal material, on the other hand, then $c_x(t=0) = 0.005$ mol/cm^3 and $\lambda = 0.13$, which definitely does not satisfy the criterion. Thus, it appears that a

numerical solution of the full unsteady-state equations must be performed.

So far, only those equations concerning diffusion and reaction of NO_2 on exposed coal surfaces have been developed. The model assumes that only those atoms actually adjacent to the voids can react. The coal primarily used in this study has an initial nitrogen-determined surface area of 58 m^2/g. Assuming the coal is pure carbon with a density of 1.2 g/cm^3, only 1.7 % of the atoms comprising the solid are actually exposed. Since reactions of NO_2 and coal components occur to a greater extent, it is obvious that NO_2 penetrates beneath the exposed surface. Therefore, a set of equations describing the diffusion and reaction of NO_2 within the solid matrix of the coal are necessary as well.

In order to develop the appropriate equations, a pore structure must be assumed. The simplest geometry is the parallel slit pore model, which assumes the solid is comprised of slabs separated by voids, as depicted in Figure 2-2a. In this model, diffusion within the solid occurs in one linear dimension, as shown in Figure 2-2b. The same set of reactions in equation (2.5.3) can be used, namely

$$\alpha_j NO_2 + X_j \xrightarrow{k_j} \alpha_j NO + (XO_{\alpha_j})_j \,, \quad \text{where} \qquad (2.5.3)$$

X_j = some coal species which reacts with NO_2,

(XO_{α_j}) = the oxidized coal species,

k_j = the second-order rate constant (cm^3 /mol /s), and

α_j = the stoichiometric coefficient.

where now the reaction is understood to occur in the solid. Utilizing the same procedure used for deriving the earlier equations yields:

$$\frac{\partial}{\partial t}(\hat{\varepsilon}\hat{c}) = \frac{\partial}{\partial x}\left(\hat{D}_s \frac{\partial \hat{c}}{\partial x}\right) - \sum_{j=1}^{N} \nu_j \hat{\varepsilon}_s \hat{k}_j \hat{c}^{\alpha_j} \hat{c}_{X_j}^{\beta_j} \,, \quad \text{and} \qquad (2.5.12)$$

The Slab Model of the Solid With Slit Pores

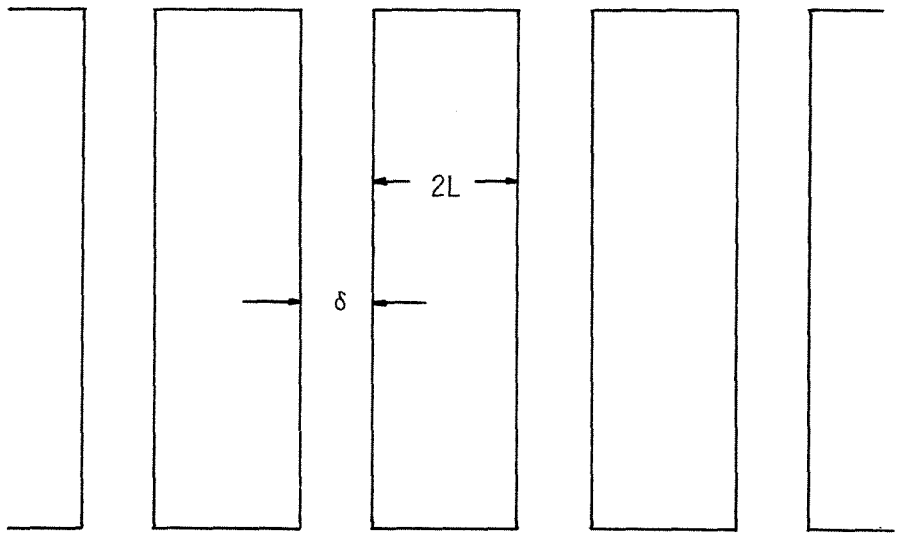

Figure 2-2a

Diffusion Into the Solid Slab of Thickness 2L With Reaction

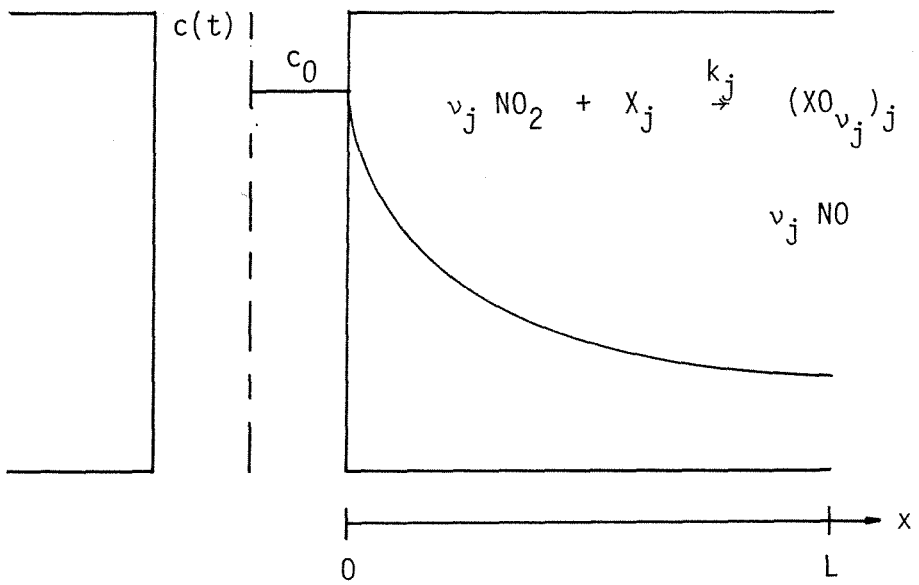

Figure 2-2b

$$\frac{\partial}{\partial t}(\hat{\varepsilon}_s \hat{c}_{X_j}) = -k_j \hat{\varepsilon}\hat{\varepsilon}_s \hat{c}^{\alpha_j} \hat{c}_{X_j}^{\beta_j} \text{ for } j=1,\ldots,N \text{ , where} \qquad (2.5.13)$$

$\hat{c}$ = the NO_2 concentration within the slab (mol /cm^3 void volume),

$\hat{c}_{X_j}$ = the X_j concentration within the slab (mol /cm^3 solid volume),

$\hat{\varepsilon}$ = the void fraction in the slab (cm^{3}void/cm^{3}total volume)

$\hat{\varepsilon}_s$ = the solid fraction in the slab (cm^{3}solid/cm^{3}total volume)

$\hat{D}_s$ = the effective diffusivity of NO_2 within the solid matrix (cm^2 /s),

$\hat{k}_j$ = the reaction rate coefficient for reaction j
[(cm^3 solid volume /mol)$^{\alpha_j}$ s^{-1}] , and

α_j, β_j = the reaction rate order in the NO_2 and substrate species, respectively.

The boundary conditions are:

$$\hat{c}(t,r,x=0) = c(t,r) , \qquad (2.5.13a)$$

$$\hat{c}(t=0,r,x) = 0 , \qquad (2.5.13b)$$

$$\frac{\partial \hat{c}(t,r,x)}{\partial x}\Big|_{x=L} = 0 , \text{ and} \qquad (2.5.13c)$$

$$\hat{c}_{X_j}(t=0,r,x) = (c_{X_j})_0, \qquad (2.5.13d)$$

assuming $\hat{\varepsilon}$ and $\hat{\varepsilon}_s$ are constant. In equation (2.5.12), $\hat{D}_s$ may be a function of $\hat{c}_{X_j}$, which is a function of x, although it is easier to assume that $\hat{D}_s$ is a constant. If the NO_2 reacts selectively with a minor component of the coal, such as sulfur, the structure will not be altered significantly, and $\hat{D}_s$ should remain relatively constant.

Ideally, the complete set of time dependent equations (2.5.2), (2.5.5), (2.5.12) and (2.5.13) which describe diffusion of NO_2 and reaction of NO_2 with the coal components should be solved simultaneously. Such a solution can be done in principle, but the computation time would be prohibitive. It is possible to

neglect equations (2.5.2) and (2.5.5), however. Since the coal used has a particle size distribution from 200 mesh (74 μm diameter) to 325 mesh (44 μm diameter), a value of R = 50 μm is a conservative estimate for computational purposes. Using a value of 1.0×10^{-5} cm^2/s for $\frac{D}{\tau}$ in the pores and a value of 0.10 for ε, a numerical solution of equations (2.5.2) with no reaction indicates that the concentration of NO_2 at the center of the particle attains 96 % of its bulk value within one second. Since significant reaction does not take place within this time span, assuming the NO_2 concentration initially in the pore structure to be equal to its bulk value should not introduce significant error. Therefore, penetration of NO_2 through the coal should be the only potentially significant mass transfer resistance.

2.5.2 The Reaction System

The mathematical model described in the previous section requires a set of chemical reactions, which must be proposed in order to calculate the rate terms in the diffusion and reaction equations. The major components of coal are carbon, hydrogen, nitrogen, inorganic and organic sulfur, oxygen and ash. Conceivably, NO_2 can react with all of the coal constituents. In order to keep the model mathematically tractable yet realistic, some assumptions concerning the types of reactions occurring can be made. For instance, NO_2 is assumed to oxidize methylene bridge ($-CH_2-$) groups and methyl ($-CH_3-$) groups to the corresponding ketones and carboxylic acids without any nitrogen substitution. On the other hand, NO_2 can not only oxidize aromatic $(C-H)_{ar}$ groups to the phenol $(C-OH)_{ar}$, but also replace hydrogen to form the corresponding nitro-aromatic $(C-NO_2)_{ar}$. Thus, the only mode of nitrogen uptake by the coal is assumed to be aromatic substitution. Furthermore, all aliphatic hydrogen is assumed to be indistinguishable. The same holds for all aromatic hydrogen.

These constraints result from the number of extents of reaction which can be determined from the elemental analysis of the coal, namely five. These concepts can be expressed as the following set of chemical reactions:

$$6\ NO_2\ (sol) + FeS_2\ (s) \xrightarrow{k_1} FeSO_4\ (s) + SO_2\ (sol) + 6\ NO\ (sol)\ , \quad (2.5.14a)$$

$$2\ NO_2\ (sol)\ +\ S_{org}\ (s)\ \xrightarrow{k_2}\ (SO_2)_{org}\ (sol)\ +\ 2\ NO\ (sol)\ , \quad (2.5.14b)$$

$$(CH_2)_{ali}(s) + 2\ NO_2(sol) \xrightarrow{k_3}\ (C{=}O)_{ali}(s) + H_2O(sol) + 2\ NO(sol), \quad (2.5.14c)$$

$$(CH)_{ar}\ (s)\ +\ NO_2\ (sol)\ \xrightarrow{k_4}\ (C{-}OH)_{ar}\ (s)\ +\ NO\ (sol)\ , \quad (2.5.14d)$$

$$(CH)_{ar}\ (s)\ +\ 2\ NO_2\ (sol)\ \xrightarrow{k_5} (C{-}NO_2)_{ar}\ (s)\ +\ HNO_2\ (sol). \quad (2.5.14e)$$

where *sol* implies that the species is solvated, *ali* refers to aliphatic and *ar* refers to aromatic. The extent of the first reaction is determined by the change in pyritic sulfur concentration, while the extent of the second reaction is determined by the change in organic sulfur concentration. The extent of the fifth reaction is determined from the change in nitrogen concentration, since only this reaction accounts for nitrogen uptake by the coal. The extent of the third reaction is given by the change in hydrogen concentration after correcting for hydrogen loss due to the fifth reaction. Finally, the extent of the fourth reaction is given by the change in oxygen concentration after correcting for the oxygen gain due to the other reactions.

2.5.3 Numerical Solution of the Modelling Equations

The most appropriate numerical method for solving equations (2.5.12) and (2.5.13) simultaneously employs implicit finite difference formulae. Although an explicit method would be much less time consuming computationally, severe

convergence problems are encountered using such a technique. These convergence problems are overcome through utilization of the more complicated implicit scheme. The finite difference equations are:

$$\frac{\partial c}{\partial t} \equiv \frac{1}{\Delta t}(c_i' - c_i)\,, \quad \text{and} \tag{2.5.15}$$

$$\frac{\partial^2 c}{\partial x^2} \equiv \frac{1}{(\Delta x)^2}(c_{i+1}' - 2c_i' + c_{i-1}')\,, \quad \text{where} \tag{2.5.16}$$

Δt = the time increment,

Δx = the spatial increment, where $L = N_x \Delta x$,

i = the index of the spatial increment, and

the prime indicates the variable is evaluated at the next time increment. The hats have been dropped for the sake of simplicity. Defining the dimensionless variables

$$C(t,X) = \frac{c(t,x)}{c(0,0)} = \frac{c}{c_0}$$

$$C_{X_j}(t,X) = \frac{c_{X_j}(t,x)}{c_{X_j}(0,0)} = \frac{c_{X_j}}{(c_{X_j})_0}, \quad \text{and}$$

$$X = \frac{x}{L},$$

the equations become:

$$\frac{\partial C}{\partial t} = \frac{D_s}{L^2}\frac{\partial^2 C}{\partial X^2} - \sum_{j=1}^{N} \nu_j k_j c_0^{\alpha_j - 1} [(c_{X_j})_0]^{\beta_j} C^{\alpha_j} C_{X_j}^{\beta_j}\,, \tag{2.5.17}$$

$$\frac{\partial C_{X_j}}{\partial t} = -k_j c_0^{\alpha_j} [(c_{X_j})_0]^{\beta_j - 1} C^{\alpha_j} C_{X_j}^{\beta_j}\,, \; j = 1,\ldots,N\,. \tag{2.5.18}$$

The boundary conditions become

$$C(t,X=0) = 1\,, \quad \text{and} \tag{2.5.18a}$$

$$\left.\frac{\partial C}{\partial X}\right|_{X=1} = 0\,, \tag{2.5.18b}$$

$$C_{X_j}(t=0,X) = 1\,, \quad j=1,\ldots,N\,. \tag{2.5.18c}$$

Application of the finite difference formulae yields:

$$\frac{1}{\Delta t}(C_i' - C_i) = \frac{D_s}{L^2}\frac{1}{(\Delta x)^2}(C_{i+1}' - 2C_i' + C_{i-1}')$$

$$- \sum_{j=1}^{N} \nu_j\, k_j\, c_0^{\alpha_j - 1}\, (c_{X_j})_0^{\beta_j}\, (C_i')^{\alpha_j}\, (C_{X_j}')_i^{\beta_j}\,, \tag{2.5.19}$$

$$\frac{1}{\Delta t}[(C_{X_j}')_i - (C_{X_j})_i] = -k_j\, c_0^{\alpha_j}\, (c_{X_j})_0^{\beta_j} (C_i')^{\alpha_j - 1}\, (C_{X_j}')_i^{\beta_j}\,, \quad j=1,\ldots N\,. \tag{2.5.20}$$

Rearrangement of equation (2.5.19) results in:

$$C_i = \tilde{a}_i C_{i-1}' + \tilde{b}_i C_i' + \tilde{c}_i C_{i+1}'\,, \quad \text{where} \tag{2.5.21}$$

$$\tilde{a}_i = \tilde{c}_i = -\frac{D_s}{L^2}\frac{\Delta t}{(\Delta x)^2}, \quad \text{and}$$

$$\tilde{b}_i = 1 + \Delta t \sum_{j=1}^{N} \nu_j\, k_j\, c_0^{\alpha_j - 1}\, (c_{X_j})_0^{\beta_j}\, (C_i')^{\alpha_j - 1}\, (C_{X_j}')_i^{\beta_j}\,.$$

Equation (2.5.21) gives the NO_2 concentration at each spatial point i as an implicit function of the NO_2 concentration at the previous time increment. Therefore, determination of the complete spatial concentration profile at a given time requires the simultaneous solution of the set of coupled equations generated by application of (2.5.21) at each point in the spatial dimension. If $\alpha_j = 1$ for all j, that is, if all the rate equations are linear in NO_2 concentration, then equation (2.5.21) is linear. Solution of the simultaneous equations is then easily accomplished using a Gaussian elimination procedure. If $\alpha_j \neq 1$ for any j, then (2.5.21) is no longer linear. The Gaussian elimination procedure can still be employed, however, by using an iterative scheme. The values for C_i determined

for the previous time step are used as initial guesses for the current time step and are used to calculate values for $\tilde{b}_i$. The set of equations is solved using the Gaussian elimination procedure and the new values of C_i are compared to the guesses. If all the values agree within a certain tolerance, usually about 0.01 % to minimize error propagation, then proceeding to the next time step is allowed. On the other hand, if any of the values do not agree within the set tolerance, then the new values of C_i are used as guesses and the procedure is repeated. If the time increment is small, the values of C_i do not change appreciably, and convergence is quite rapid, usually within four iterations.

Examination of the equation for $\tilde{b}_i$ also reveals a dependence upon $(C_{X_j})_i$ for the current time step. Once again, the values of $(C_{X_j})_i$ determined from the previous time step are used as initial guesses. Once satisfactory values for C_i are obtained using the procedure described above, new values for $(C_{X_j})_i$ are obtained using equation (2.5.20) in the form:

$$(C'_{X_j})_i - \Delta t\ k_j\ c_0^{\alpha_j}\ (c_{X_j})_0^{\beta_j - 1}\ (C'_i)^{\alpha_j}\ (C'_{X_j})_i^{\beta_j} = (C_{X_j})_i \ . \qquad (2.5.22)$$

If $\beta_j = 1$, then the equation for $(C'_{X_j})_i$ is linear, and is easily solved. If $\beta_j \neq 1$, then the equation must be solved by trial and error. If the values of $(C'_{X_j})_i$ given by (2.5.22) agree with the initial guesses within a given tolerance, proceeding to the subsequent time step is allowed. If any of the values do not agree, then the new values of $(C'_{X_j})_i$ are used as guesses, and the entire procedure is repeated. Again, if the time increment is small, convergence occurs quite rapidly.

The finite difference equations at the boundaries of the spatial domain are slightly different from the form given by (2.5.21), which results from the application of the boundary conditions. The condition that $C(t, 0) = 1$ yields

$$\tilde{b}_1 C_1' + \tilde{c}_1 C_2' = C_1 - \tilde{a}_1 C_0 , \qquad (2.5.23)$$

since C_0, the concentration at the surface, is constant for all time, i.e. $C_0' = C_0$. Application of the other boundary condition, $\left.\frac{\partial C}{\partial X}\right|_{X=1} = 0$, is a little more complicated. If there are M intervals in the spatial domain, expanding C_{M-1} in a Taylor series about $X = 1$ results in:

$$C_{M-1} = C_M + \left.\frac{\partial C}{\partial X}\right|_{X=1} \Delta x + \frac{(\Delta x)^2}{2} \left.\frac{\partial^2 C}{\partial X^2}\right|_{X=1} + \mathbf{O}[(\Delta x)^3] . \qquad (2.5.24)$$

The second term on the right side vanishes by application of the boundary condition. Rearrangement yields

$$\left.\frac{\partial^2 C}{\partial X^2}\right|_{X=1} = \frac{2}{(\Delta x)^2}(C_{M-1} - C_M) . \qquad (2.5.25)$$

Application of (2.5.25) to (2.5.17) followed by rearrangement yields

$$C_M = 2\tilde{a}_M C_{M-1}' + \tilde{b}_M C_M' . \qquad (2.5.26)$$

Therefore, the equations to be solved are

$$\tilde{b}_1 C_1' + \tilde{c}_1 C_2' = C_1 - \tilde{a}_1 C_0 , \qquad (2.5.27a)$$

$$\tilde{a}_i C_{i-1}' + \tilde{b}_i C_i' + \tilde{c}_i C_{i+1}' = C_i , \quad i=2,\ldots,M-1 \qquad (2.5.27b)$$

$$2\tilde{a}_M C_{M-1}' + \tilde{b}_M C_M' = C_M , \text{ where} \qquad (2.5.27c)$$

$$\tilde{a}_i = \tilde{c}_i = -\frac{D_s}{L^2}\frac{\Delta t}{(\Delta x)^2}, \quad i=1,\ldots,M \qquad (2.5.27d)$$

$$\tilde{b}_i = 1 + \Delta t \sum_{j=1}^{N} \nu_j k_j c_0^{\alpha_j - 1} (c_{X_j})_0^{\beta_j} (C_i')^{\alpha_j - 1} (C_{X_j}')_i^{\beta_j}, \; i=1,\ldots,M, \text{ and} \qquad (2.5.27e)$$

$$(C_{X_j}')_i - \Delta t \sum_{j=1}^{N} k_j c_0^{\alpha_j} (c_{X_j})_0^{\beta_j - 1} (C_i')^{\alpha_j} (C_{X_j}')_i^{\beta_j} = (C_{X_j})_i ,$$

$$i=1,\ldots M \; ; \; j=1,\ldots N . \qquad (2.5.28)$$

These equations were solved numerically on a PDP 11/34A computer. The solution for each set of parameters usually required 3 hours of CPU time for

diffusion with one chemical reaction. Incorporation of more chemical reactions would be expected to increase the CPU time required geometrically, due to the iterative nature of the numerical procedure.

References

1. Thiessen, R., U.S. Bur. Mines Inf. Circ. 7397, 1947, 53 pp.
2. Wen, C.Y., Lee, E. Stanley, eds., *Coal Conversion Technology*, (Addison-Wesley Publishing Company, Reading, Mass., 1979) pp.19-20.
3. U.S. Dept. of Energy, *Coal Data - A Reference*, Office of Energy Data and Interpretation, Energy Information Administration (Energy Information Administration Clearinghouse, Washington D.C., 1978), p. 2.
4. Thiessen, R., *Coal Age*, **18**, 1183-89,1223-28,1275-79 (1920); Thiessen, R., et. al., *Fuel*, **17**, 307-15 (1938).
5. Stopes, Marie D., *Proc. R. Soc.* (London), **B90**, 470-87 (1919).
6. Vasilakos, N.P., *Coal Desulfurization By Selective Chlorination*, PhD Thesis, California Institute of Technology, 1981.
7. Deurbruck, A.W., *Sulfur Reduction Potential of the Coals in the United States*, U.S. Bur. Mines RI7633, 1972.
8. Attar, A., Corcoran, W.H., *Ind. Eng. Chem. Prod. Res. Dev.*, **16**, 168 (1977).
9. Chandra, D., et. al., *Fuel*, **59**, 249 (1980); Silverman, M.P., et. al., *Fuel*, **42**, 113 (1963); Capes, C.E., et. al., *Canadian Mining and Metallurgical Bulletin*, November 1973, p. 88.
10. Greer, R.T., "Coal Microstructure and Pyrite Distribution", in *Coal Desulfurization*, T.D. Wheelock, ed., (ACS Symposium Series, No. 64, Am. Chem. Soc., 1977) pp. 3-15.
11. Bootent, D.A.D., Phillips, C.R., *Fuel*, **55**, 318 (1976).
12. National Research Council, *Energy in Transition 1985-2010*, (National Academy of Sciences, Washington, D.C., 1979) p. 166.
13. *Ibid.*, p. 165
14. Aplan, F.F., "Use of the Floatation Process for Desulfurization of Coal", in *Coal Desulfurization*, T.D. Wheelock, ed., (ACS Symposium Series, No. 64,

Am. Chem. Soc., 1977) pp. 70-82.

15. *Ibid.*

16. Lin, C.J., Liu, Y.A., "Desulfurization of Coals by High-Intensity High- Gradient Magnetic Separation: Conceptual Process Design and Cost Estimation", in *Coal Desulfurization*, T.D. Wheelock, ed., (ACS Symposium Series, No. 64, Am. Chem. Soc., 1977) pp. 121-142.

17. Wheelock, T.D., ed., *Coal Desulfurization*, (ACS Symposium Series, No. 64, Am. Chem. Soc., 1977) 332 pp.

18. Tabler, S.K., *Journal of the Air Pollution Control Association*, **29**, 803 (1979).

19. Meyers, R.A., *Coal Desulfurization*, (Marcel Dekker Inc., New York, New York, 1977) pp. 175-90.

20. Okamoto, Y., et. al., *J. Phys. Chem.*, **84**, 1833 (1980).

21. Friedman, S., "Oxidative Desulfurization of Coal", in *Coal Desulfurization*, Wheelock, T.D., ed., (ACS Symposium Series, No. 64, Am. Chem. Soc., 1977) pp. 164-72; Meyers, R.A., *op. cit.*

22. Meyers, R.A., *op. cit.*, pp. 216-19.

23. Hsu, G.C., et. al., "Coal Desulfurization by Low-Temperature Chlorinolysis", in *Coal Desulfurization*, Wheelock, T.D., ed., (ACS Symposium Series, No. 64, Am. Chem. Soc., 1977) pp. 206-17.

24. Vasilakos, N.P., *op. cit.*, pp. 69-86.

25. Kalvinskas, J.J., private communication.

26. Powell, A.R., Parr, S.W., *Univ. of Illinois Bull. No. 111*, 62 (1919).

27. Mott, R.A., *Fuel*, **29**, 53, (1950).

28. Mazumdar, B.K., et. al., *Fuel*, **46**, 379 (1967).

29. Smedslund, T.H., *U.S. Patent 2,581,050* (1948).

30. Kralik, J.G., private communication.

31. Kralik, J.G., Research Progress Report, February 6, 1979.

32. Diaz, A.F., Guth, E.D., *U.S. Patent 3,909,211* (1975); Diaz, A.F., "Oxidative Coal Desulfurization Using Nitrogen Oxides - The KVB Process", presented at the Symposium on Coal Cleaning to Achieve Energy and Environmental Goals, Hollywood, Florida, September 11-15, 1978.

33. Lynn, S., Mason, D.M., Corcoran, W.H., *J. Phys. Chem.*, **59**, 238 (1955); Robertson, G.D., Mason, D.M., Corcoran, W.H., *J. Phys. Chem.*, **59**, 683 (1955); England, C., Corcoran, W.H., *Ind. Eng. Chem. Fundam.*, **13**, 375 (1974).

34. March, J., *Advanced Organic Chemistry: Reactions, Mechanisms, and Structure*, (McGraw-Hill Book Company, New York, New York, 1968), pp. 396-99.

35. Lynn, S., Mason, D.M., Corcoran, W.H., *J. Phys. Chem.*, **59**, 238 (1955).

36. Benford, G.A., Ingold, C.K., *J. Chem. Soc.*, 929 (1938).

37. Langmuir, I., *J. Am. Chem. Soc.*, **38**, 2221 (1916); Brunauer, S., Emmett, P.H., Teller, E., *J. Am. Chem. Soc.*, **60**, 309 (1938)

38. Brunaeur, S., Emmett, P.H., *J. Am. Chem. Soc.*, **59**, 310 (1937)

39. Gregg, S.J., Sing, K.S.W.,*Adsorption, Surface Area and Porosity*, (Academic Press, New York, New York, 1967) pp. 67-75.

40. Walker, P.L., Kini, K.A., *Fuel*, **44**, 453 (1965); Aylmore, L.A.G., *Clays and Clay Minerals*, **22**, 175 (1974).

41. Crank, J., Park, G.S., *Diffusion in Polymers*, (Academic Press, New York, New York, 1968) p. 69.

42. Dubinin, M.M., *Quart. Rev. Chem. Soc.*, **9**, 101 (1959); *Chem. Rev.*, **60**, 235 (1960).

43. Dubinin, M.M., Radushkevich, L.V., *Proc. Acad. Sci USSR*, **55**, 331 (1947); Radushkevich, L.V., *Zhur. Fiz. Khim.*, **23**, 1410 (1949).

44. Kaganer, M.G., *Zhur. Fiz. Khim.*, **33**, 2202 (1959).

45. That is to say that the linearity of the log - $\log^2$ plot arises from the theory, and is not just the result of fortunate data manipulation.

46. Anderson, R.B., et. al., *J. Phys. Chem.*, **60**, 1548 (1960); *Fuel*, **41**, 559 (1962); Lamond, T.G., Marsh, H., *Carbon*, **1**, 281,293 (1964); Marsh, H., Wynne-Jones, W.F.K., *Carbon*, **1**, 269 (1964); Walker, P.L., Geller, I., *Nature*, **178**, 1001 (1956).

47. Nandi, S.P., Walker, P.L., *Fuel*, **43**, 385 (1964).

48. Medeiros, D.J., Petersen, E.E., *Changes in the Pore Structure of Coal with Progressive Extraction*, (Lawrence Berkeley Laboratory, University of California, Berkeley, 1975), 125 pp.

49. Gan, H., Nandi, S.P., Walker, P.L., *Fuel*, **51**, 272 (1972).

50. Thomson, W., *Phil. Mag.*, **42**(4), 448 (1871).

51. Zsigmondy, A., *Z. Anorg. Chem.*, **71**, 356 (1911).

52. Foster, A.G., *Trans. Faraday Soc.*, **28**, 645 (1932).

53. Dubinin, M.M., *Quart. Rev. Chem. Soc.*, **9**, 101 (1955); Pierce, C., *J. Phys. Chem.*, **57**, 64 (1953).

54. Defay, R., Prigonine, I., Bellemans, A., Everett, D.H., *Surface Tension and Adsorption*, (Longmans, London, 1966) p. 218.

55. Kraemer, E.O., in *Treatise on Physical Chemistry*, Taylor, H.S., ed., (Macmillan, New York, New York, 1931) p. 1661; McBain, J.W., *J. Am. Chem. Soc.*, **57**, 699 (1935).

56. Guggenheim, E.A., *Trans. Faraday Soc.*, **36**, 407 (1940).

57. Blackman, N., Lisgarten, N.D., Skinner, L.M., *Nature*, **217**, 1245 (1968).

58. Melrose, J.C., *AIChE J.*, **12**, 986 (1966).

59. Ahn, W.S., Jhon, M.S., Pak, H., Chang, S., *J. Colloid. Interface Sci.*, **38**, 605 (1972).

60. Dubinin, M.M., in *Surface Area Determination*, Proc. Intern. Symp., 1969, (Butterworths, London, 1970) p. 131; Bering, B.P., Dubinin, M.M., Serpinsky, V.V., *J. Colloid. Interface Sci.*, **21**, 378 (1968).

61. Orr, C., Dalla Valle, J.M., *Fine Particle Measurement*, (McMillan, London, 1959) p. 271.

62. Wheeler, A., *Catalysis*, **vol. II**, (Reinhold, New York, New York, 1955), p. 118.

63. Halsey, G.D., *J. Chem. Phys.*, **16**, 931 (1948).

64. Harris, M.R., Sing, K.S.W., *Chem. and Ind.*, 11 (1959); Lippens, B.C., Linsen, B.G., DeBoer, J.H., *J. Catal.*, **3**, 32 (1964); Cranston, R.W., Inkley, F.A., *Advances in Catalysis*, **vol. 9**, (Academic Press, New York, New York, 1957) p. 143.

65. Medek, J., *Fuel*, **56**, 131 (1977).

66. DeBoer, J.H., Custers, J.F., *Z. Phys. Chem.*, **B25**, 225 (1934).

67. Kadlec, O., *Pore Structure and Properties of Materials*, RILEM/IUPAC, Academia, Prague (1974), p. C-55.

68. Froment, G.F., Bischoff, K.B., *Chemical Reactor Analysis and Design*, (John Wiley and Sons, New York, New York, 1979) p. 243.

69. Smith, J.M., *Chemical Engineering Kinetics*, Second Edition, (McGraw-Hill Book Company, New York, New York, 1970) p. 243.

70. Friedlander, S.K., *AIChE J.*, **1**, 347 (1961).

71. Froment, G.F., *op. cit.*, p. 167.

72. *Ibid.*, p. 243.

73. Wen, C.Y., *Ind. Eng. Chem.*, **60**(9), 34 (1968).

CHAPTER 3

EXPERIMENTAL

The experiments were designed to obtain qualitative and quantitative information concerning the reaction of NO_2 and coal. The selectivity of NO_2 for sulfur and the extent of its removal, particularly the removal of organic sulfur, from the combustion gases of the coal was of primary interest. The alterations in the coal structure as a result of NO_2 treatment were also important. The experiments and analytical procedures were designed with these goals in mind.

3.1 Experimental Apparatus

3.1.1 The Experimental Apparatus for the Slurry Phase Reaction of Coal with Continuous Nitrogen Dioxide Flow

The reactor system is shown in Figure 3–1. The liquid NO_2 is heated in a stainless steel bomb to 50°C, at which temperature the vapor pressure of NO_2 is 3.4 atm. The lines and rotameter leading from the bomb to the reactor are heated to 70°C to prevent the condensation of NO_2. The heated NO_2 enters the bottom of the reactor and flows through a medium porosity (10-15 μm pores) fritted glass disc which allows the uniform formation of small gas bubbles (about 1 mm in diameter) in the slurry. The slurry is well stirred using a teflon coated magnetic stir bar and a magnetic stirrer. The effluent gases from the reactor then flow to a Perkin-Elmer 3920 gas chromatograph (GC) equipped with an automatic gas sampling valve. Alternatively, the effluent gases can be vented in the fume hood.

Treatments performed at room temperature are conducted in a glass reactor with a water jacket as depicted in Figure 3–2. Reactions at higher temperatures are performed in the reactor shown in Figure 3–3. This reactor is wrapped in

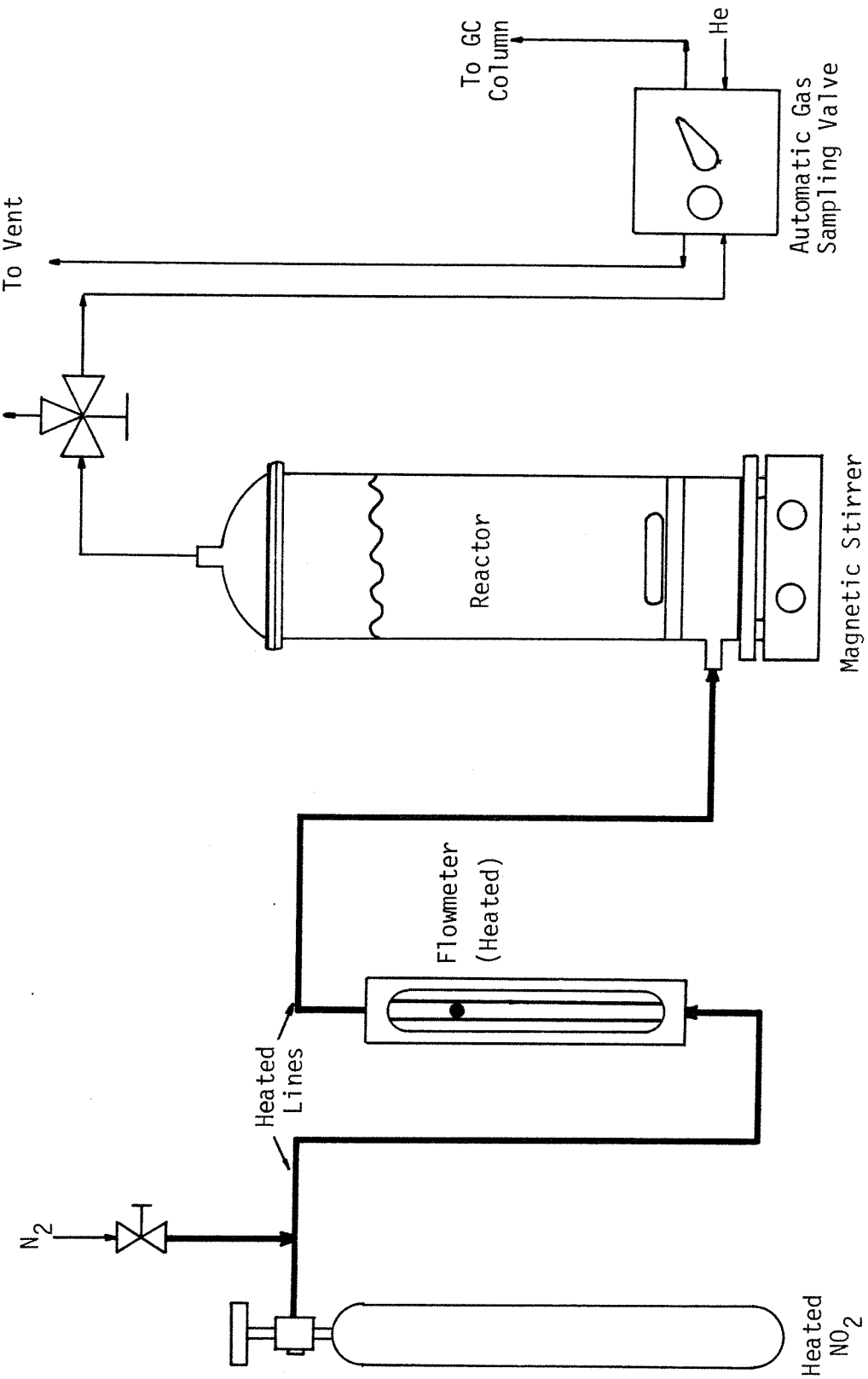

Schematic of the Reactor System

Figure 3-1

Coal Slurry Reactor With Water Jacket (Front View)

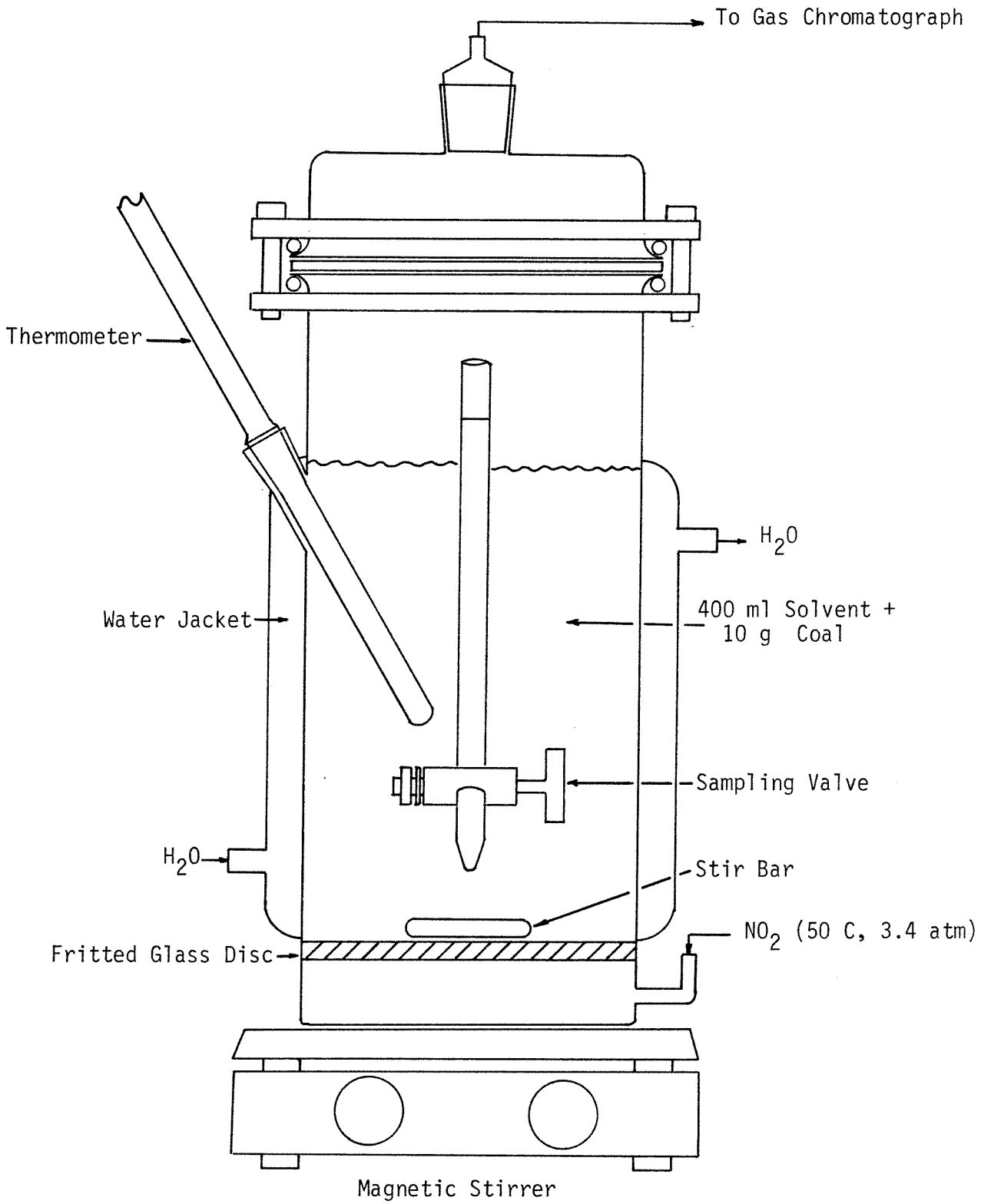

Figure 3-2a

Coal Slurry Reactor With Water Jacket (Side View)

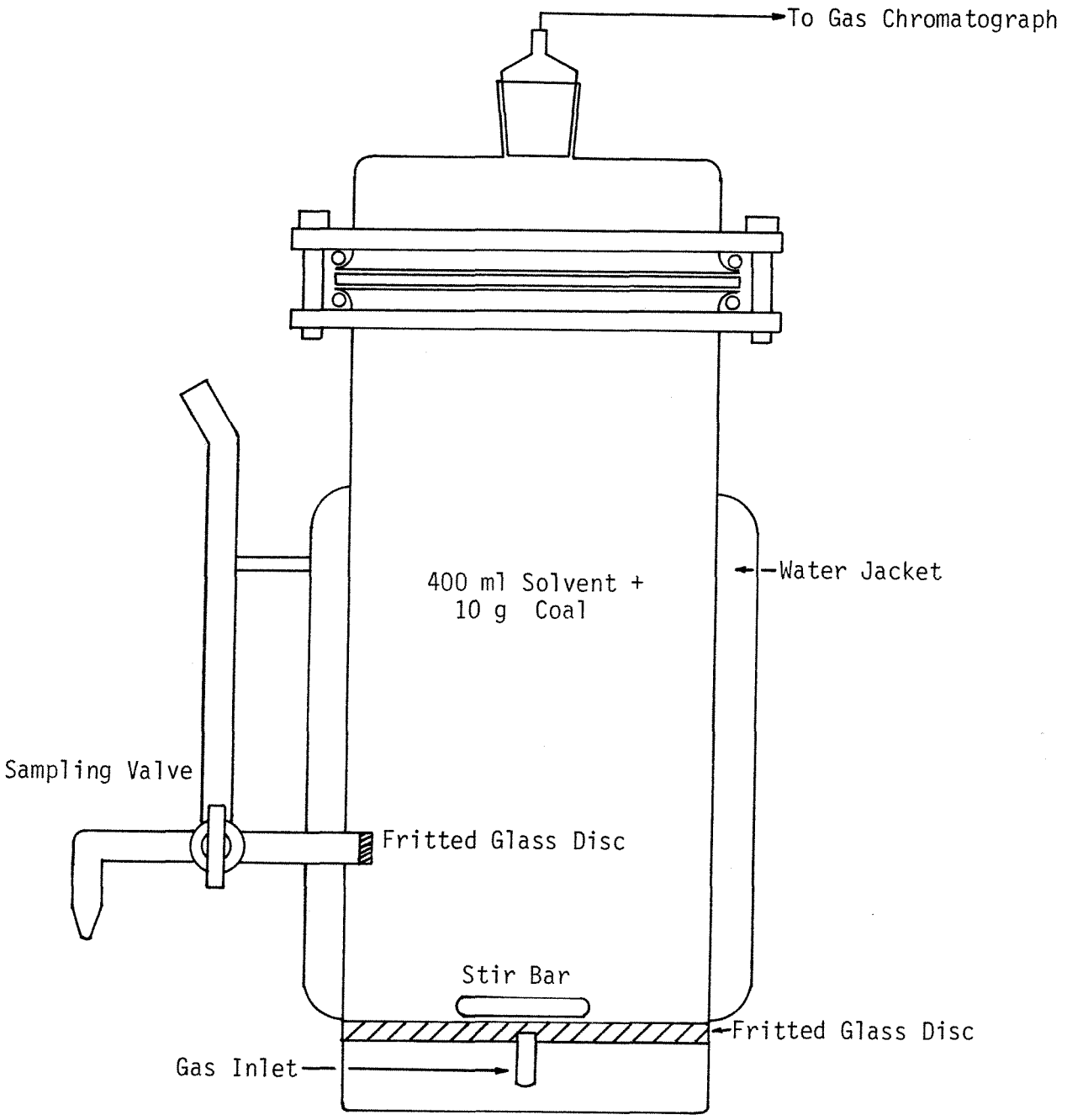

Figure 3-2b

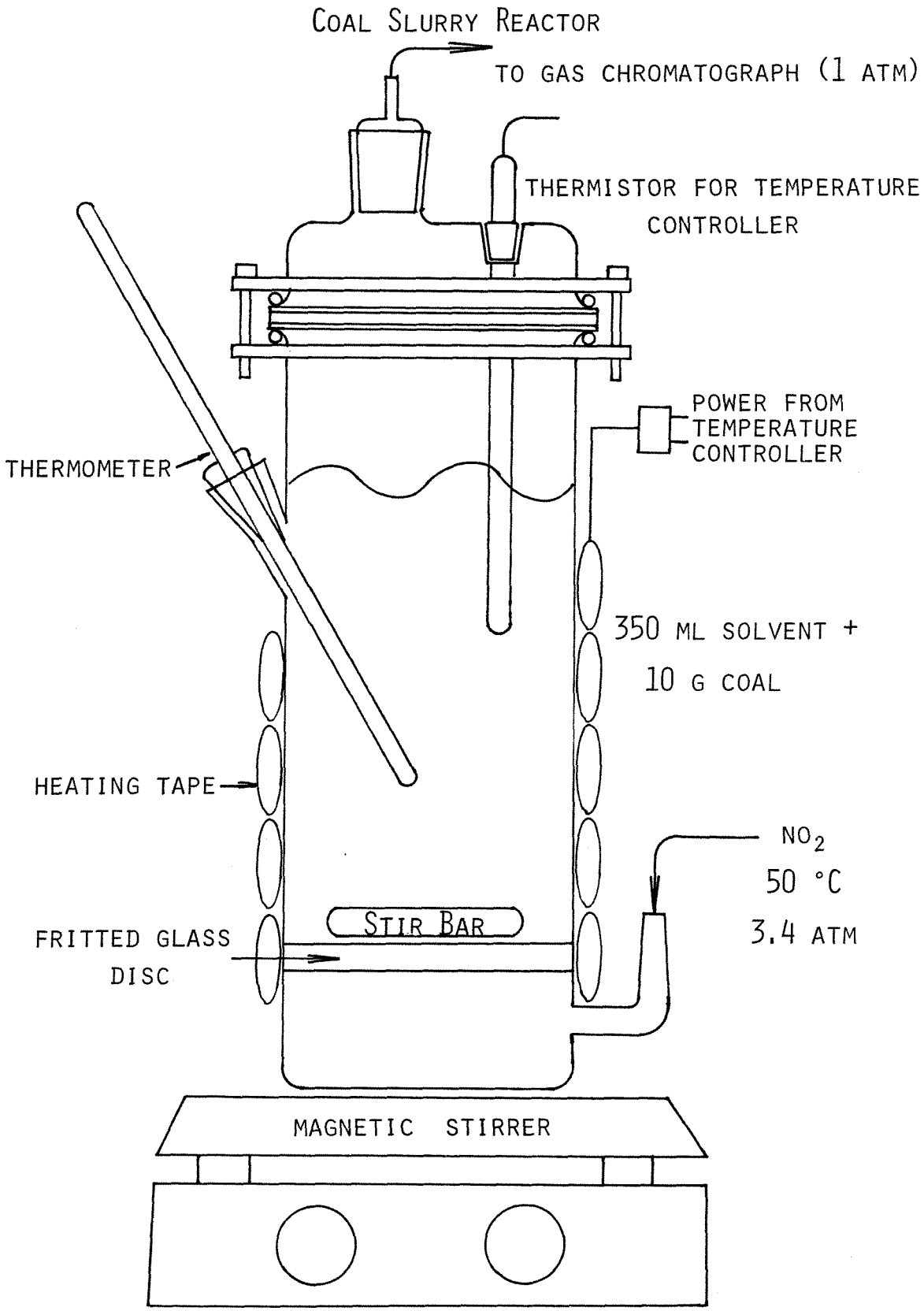
COAL SLURRY REACTOR
TO GAS CHROMATOGRAPH (1 ATM)
THERMISTOR FOR TEMPERATURE CONTROLLER
POWER FROM TEMPERATURE CONTROLLER
THERMOMETER
350 ML SOLVENT +
10 G COAL
HEATING TAPE
NO_2
50 °C
3.4 ATM
STIR BAR
FRITTED GLASS DISC
MAGNETIC STIRRER

Figure 3-3

heating tape connected to a temperature controller (Versa-Therm Proportional Electronic Temperature Controller- Model 2156). The controller uses a thermistor (Yellow Springs Instrument Company- Model 404). The slurry temperature is monitored independently with a mercury-in-glass thermometer. The sampling port allows the periodic removal of liquid samples for analysis. The fritted glass disc in the sampling line prevents the entrainment of coal particles during sampling.

The gas sampling valve on the GC allows the periodic injection of samples of the effluent gases into the GC column. Samples are injected every five to ten minutes, depending upon the length of time required for the separation of the various effluent components. The separation is performed on a 12 foot column (0.125 in. O.D.) packed with Porapak Q (80 to 100 mesh). The chromatograph is equipped with two detectors. The thermal conductivity detector (TCD) detects nitrogen, oxygen, oxides of nitrogen and any compound whose volume concentration exceeds roughly one percent. A flame photometric detector (FPD) is used to detect sulfur compounds whose volume concentration exceeds 0.1 ppm. The FPD utilizes a hydrogen flame to atomize the compounds which enter the detector. All of the sulfur is converted to an excited species, S_2^*, which immediately relaxes to the ground state while emitting a photon with a wavelength of 394 nm. An optical light pipe carries the photons to a 394 nm optical filter which screens out all photons except those in the 394 $\pm$ 2 nm wavelength range. These photons are then detected with a photomultiplier tube. The signal from either detector can be integrated electronically with a Perkin-Elmer Model 1 Integrator. Both signals are displayed graphically on a dual channel chart recorder (Linear Instruments Corporation).

3.1.2 The Apparatus for the Batch Slurry Phase Reaction

Some reactions were carried out in a batch system without continuous NO_2 flow. The reactor consists of a 500 ml three-neck round bottom boiling flask placed in a water bath as shown in Figure 3–4. The temperature of the slurry is monitored with a mercury-in-glass thermometer for all experiments except those conducted at 0°C, where a pentane-in-glass thermometer is used. The sampling tube consists of a 23 cm length of 6 mm O.D. glass tubing. The end of the tube which is immersed in the slurry is plugged with about 2 to 3 cm of pyrex wool to prevent the entrainment of the coal particles during sampling. Samples are withdrawn using a 10 cm^3 glass syringe equipped with a hypodermic needle, the base of which has been wrapped with a strip of paraffin film. The paraffin allows the formation of a tight seal between the base of the needle and the sampling tube. The slurry is maintained with magnetic stirring while the water bath is agitated with a variable speed stirrer (Talboys Engineering Corporation, Model 102).

3.2 Choice of Coal and Coal Pretreatment

Since the removal of organic sulfur in the form of SO_2 from the combustion gas of the coal is of primary concern, the ideal choice for study would be a coal with no pyritic sulfur. Furthermore, since changes in the pore structure of the coal are also of interest, a coal with a reasonably high surface area, say 100 m^2/g, would be desirable. The best choice from the extensive catalogue of coals available from the Pennsylvania State University Coal Bank is PSOC-190, an Illinois No. 6 bituminous coal. In order to mitigate intraparticle mass transfer effects, the coal particles should be as small as possible. The particles cannot be so small, however, as to create slurry suspension and filtration problems. The best particle size which satisfies these criteria appears to be in the range from 200 (74 μm diameter) to 325 (44 μm diameter) mesh. An analysis of the coal

Batch Reactor

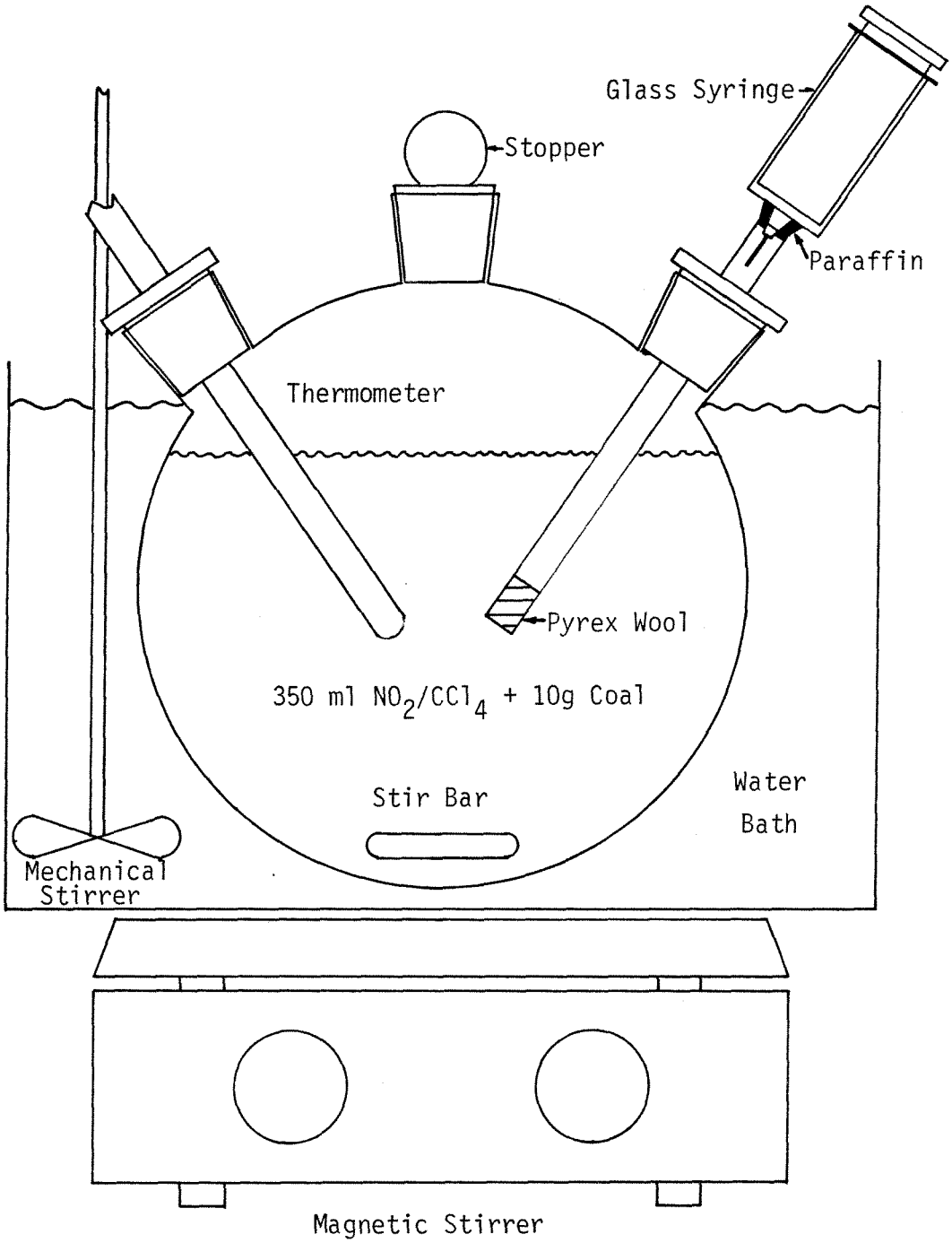

Figure 3-4

provided by the coal bank is shown in Table 3–1. An independent analysis of the particular mesh size of the ground coal used in the experiments is shown in Table 3–2. This analysis was performed using the various procedures described below. There is little difference between the analyses except for the sulfur content. The pyritic sulfur content is 80 % lower while the sulfate sulfur content is 440 % higher in the coal used than in the PSU Coal Bank Analysis. The carbon and hydrogen contents are slightly lower as well. These differences are caused by the weathering of the coal between the time of the coal bank analysis and the independent analysis. The time span is approximately 10 years. The difference in the particle size of the coal used in the analysis accounts for some of the discrepancy as well. Another set of runs was performed using another coal for purposes of comparison. The coal, PSOC 276 (Ohio No. 8), has the elemental composition shown in Table 3–3, as determined by the PSU Coal Bank. An independent analysis of the 200 to 325 mesh particle size fraction of the coal is given in Table 3–4.

The undried PSOC 190 contains 12.66 ± 0.17 % moisture by mass. The coal was not dried for those runs utilizing water as the solvent. Some preliminary runs employing pyridine and nitrobenzene as solvents used the undried coal as well. The coal was predried, however, when used for runs utilizing carbon tetrachloride as the solvent. The pretreatment consisted of vacuum drying the coal in 80 to 100 g quantities at approximately 180 to 200°C for several days. For some runs, the coal was first washed in deionized water, filtered, air dried and finally vacuum dried at 180 to 200°C for several days. The pretreatment conditions for the coals are shown in Table 3–5. The higher mass loss in the case of the washed and dried (W&D) PSOC 190 is due to the leaching of water soluble compounds from the coal.

TABLE 3-1

Elemental Analysis of PSOC 190 (Illinois No. 6) on a Dry Basis Provided by the PSU Coal Bank		
8.49 % Ash 69.15 % C 4.89 % H	1.00 % N 3.05 % S	0.10 % Sulfate Sulfur 1.05 % Pyritic Sulfur 1.90 % Organic Sulfur
Heating Value = 11,960 Btu/ lb_m		

TABLE 3-2

Elemental Analysis of PSOC 190 (+200-325 mesh) on a Dry Basis		
8.67 ± 0.08 % Ash 66.02 ± 0.19 % C 4.47 ± 0.07 % H	1.30 ± 0.03 % N 3.07 ± 0.01 % S	0.54 ± 0.02 % Sulfate Sulfur 0.21 ± 0.09 % Pyritic Sulfur 2.32 ± 0.06 % Organic Sulfur
Heating Value = 11,660 Btu/lb_m		

TABLE 3-3

Elemental Analysis of PSOC 276 (Ohio No. 8) on a Dry Basis Provided by the PSU Coal Bank		
11.19 % Ash 72.19 % C 4.96 % H	1.57 % N 3.47 % S	0.02 % Sulfate Sulfur 2.28 % Pyritic Sulfur 1.17 % Organic Sulfur
Heating Value = 12,990 Btu/lb_m		

TABLE 3-4

Elemental Analysis of PSOC 276 (+200-325 mesh) on a Dry Basis		
11.23 % Ash 71.00 % C 4.87 % H	1.37 % N 3.20 % S	0.14 % Sulfate Sulfur 2.12 % Pyritic Sulfur 0.94 % Organic Sulfur
Heating Value = 12,590 Btu/lb_m		

TABLE 3-5

Coal Pretreatment Conditions

Designation	Initial Mass (g)	Final Mass (g)	Volume H_2O (ml)	Wash T (C)	Wash Time Time (min)	Drying T (C)	Drying Time (da)	Mass Loss Loss (%)
Predried PSOC 190 -Batch 1	70.61	61.55				200	7	12.83
Predried PSOC 190 -Batch 2	87.76	76.80				190	2	12.49
Washed & Dried PSOC 190 -Batch 1	103.74	85.38	1000	25	120	200	7	17.69
Washed & Dried PSOC 190 -Batch 2	94.68	77.83	1000	25	120	195	2	17.80
Washed & Dried PSOC 276	74.74	70.31	1000	25	150	175	4	5.93

3.3 Experimental Procedure

3.3.1 Procedure for the Slurry Phase Reaction with Continuous Nitrogen Dioxide Flow

3.3.1.1 Preliminary

The set of preliminary runs consists of six experiments using three different solvents, namely water, pyridine and nitrobenzene, at room temperature and 80°C. The coal used in each experiment was the PSOC 190 (+100-200 mesh) coal. Although the NO_2 flowrate was not monitored, there was sufficient flow to cause agitation even without magnetic stirring. Approximately 10g of raw, undried coal were slurried with 250 to 300 ml of the solvent in the reactor while purging with N_2. The slurry was heated for those runs at 80°C while purging with N_2. NO_2 was then bubbled through the slurry for two hours. Magnetic stirring was used to maintain the slurry and to aid in heat transfer. The slurry was then filtered and the solid coal left was washed with water until the filtrate was neutral to litmus paper. In the case of nitrobenzene, however, the filter tended to clog, so that the coal left over was not washed further. The filtered coal was then dried under vacuum at 100°C until a pressure of less than 0.001 torr could be maintained. Such drying usually required several days, particularly for the coal samples treated in nitrobenzene. After drying, the samples were weighed to determine the coal mass loss for each experiment.

Extraction of the coal occurred when pyridine and nitrobenzene were used. Therefore, these solvents were distilled from the filtrates. The pyridine filtrate was distilled up to 116°C (pyridine b.p. 115.5 C). Pyridine forms an azeotrope with water(57.0% pyridine/ 43.0% water), however, which boils at 92.6°C. Thus, most of the distillate was in the 92-96°C range. There was not very much residue left. Distillation of the nitrobenzene filtrate, on the other hand, yielded large amounts of extract which were saved for analysis. The experimental conditions

for this set of runs are found in Table 3–6.

3.3.1.2 Runs Using Water as the Solvent

A set of exploratory runs using water as a solvent was conducted. Approximately 10g of the undried PSOC 190 coal (+200-325 mesh) were slurried with 300 ml of deionized water in the reactor. While maintaining the slurry with magnetic stirring, NO_2 was admitted at a constant flowrate as indicated by the flowmeter. Although the actual NO_2 mass flowrate was never determined, the NO_2 flowrates were essentially equal throughout the series of runs. These experiments were conducted in the reactor without the water jacket at room temperature. There was a temperature rise of a few degrees due to the exothermicity of the reaction. At the end of the reaction, the slurry was filtered and the coal was washed six times with 250 ml of deionized water. The coal was allowed to air dry and was then dried under vacuum for 6 hours at 100 to 110°C. A blank run using N_2 instead of NO_2 was performed as well. After drying, the samples were weighed to determine the mass loss and saved for further analysis. The pertinent experimental conditions are tabulated in Table 3–7.

Approximately 1g samples of the NO_2 treated coals were then washed with an aqueous solution of 0.5g anhydrous Na_2CO_3 dissolved in 50 ml deionized water. The slurry was stirred for two hours at room temperature. The slurry was then filtered and washed five times with 75 ml of deionized water. The coal was allowed to air dry and was then vacuum dried for 1 day at 110 to 120°C. The samples were then weighed to determine the mass loss and saved for further analysis. The overall mass loss due to treatment with NO_2 followed by washing with Na_2CO_3 (aq) are also tabulated in Table 3–7.

Another set of experiments using water as a solvent under more controlled conditions was done as well. The weighed coal was loaded into the reactor with

TABLE 3-6

Experimental Conditions for Preliminary Runs Using PSOC 190 (+100-325 mesh) and NO_2 for 120 min

Run #	Sample	Coal Mass (g)	Solvent Volume (ml)	Temperature (C)			Mass Loss (%)
				High	Low	Average	
1	H_2O/NO_2/Coal	9.5039	300	28	23	26	14.4
2	H_2O/NO_2/Coal	9.4284	300	80	23[1]	78[1]	13.2
3	Pyridine/NO_2/Coal	9.2551	250	30	25	26	22.8
4	Pyridine/NO_2/Coal	10.2647	300	95	79	83	16.2
5	Nitrobenzene/NO_2/Coal	10.7623	250	38	24	34	37.6
	Extract						−54.1[2]
6	Nitrobenzene/NO_2/Coal	10.3873	250	88	78	81	54.6
	Extract						−38.6[2]

[1] The NO_2 was bubbled in while the slurry was being heated. The slurry was 72 C after 30 min and 82 C after 45 min. The temperature was maintained at roughly 80 C after that time.

[2] Represents the extract mass as a percentage of the initial coal mass.

TABLE 3-7

Experimental Conditions for Exploratory Runs Using Water As A Solvent for the Treatment of PSOC 190 (+200-325 mesh) with NO_2

Run #	Reaction Time (min)	Initial Coal Mass (g)	Temperature Range (C)	Relative NO_2 Flow Rate	Mass Loss Due to NO_2 Treatment (%)	Mass Loss Due to Na_2CO_3(aq) Wash (%)	Overall Mass Loss (%)[1]
7 (Blank)	120	11.7094	26.5	0.00	15.84	10.04	24.29
8	30	10.9133	26-28	1.33	14.48	8.17	21.47
9	60	10.8578	26-29	1.24	13.89	10.50	22.93
10	90	10.4977	25-29	1.27	12.66	10.01[2]	21.40[2]
11	120	11.1770	26-29	1.22	11.79	16.88	26.68
12	240	10.6012	24-31	-[3]	10.33	6.12	15.82
13	480	10.2654	24-31	-[3]	12.71	7.74	19.47

[1] Represents percent mass loss relative to initial mass of coal. Let f = the fractional mass loss due to NO_2 treatment, m_i = the initial mass of NO_2 treated coal used for the Na_2CO_3 (aq) washand m_f = the final mass of washed coal. Then

$$\text{Overall Mass Loss} = \frac{m_i - m_f(1-f)}{m_i}.$$

[2] Stopcock grease melted and contaminated this sample during drying because the temperature rose to 140 C. Thus, the mass loss figures are low.

[3] NO_2 flow rate not monitored.

350 ml of deionized water to form a slurry. The slurry was purged with N_2 for at least 30 minutes to eliminate dissolved O_2 while stirring magnetically. Then NO_2 was admitted at a constant flowrate as indicated by the flowmeter. For these runs, the NO_2 mass flowrate was determined by weighing the NO_2 bomb before and after the experiment and dividing the mass difference by the reaction time. Liquid samples were withdrawn every 15 minutes for analysis of HNO_3 (aq) and HNO_2 (aq). At the end of the run, the slurry was filtered and the coal was washed six times with 100 ml of deionized water. The coal was allowed to air dry and was then vacuum dried for several hours at 100 to 120°C. The samples were then weighed to determine the mass loss and saved for analysis. The experimental conditions are shown in Table 3–8. It should be noted that the NO_2 flowrates for the experiments run for various reaction times are not the same. This variation is symptomatic of the extreme difficulty encountered when attempting to keep a constant flow rate of NO_2. Because NO_2 dimerizes to N_2O_4 to a different extent depending on temperature and pressure, minor fluctuations in these parameters in the NO_2 lines and the flowmeter can cause problems, including condensation of NO_2 in the lines. Heating the lines and the flowmeter to a temperature higher than the bomb temperature helps to alleviate these problems to a great extent. Nevertheless, averaging the flowrates for runs 14, 15, 19 and 20 yields a value of 0.774 ± 0.039 g NO_2/min. Clearly, it would be desirable to obtain better flow rate control. Such control, however, would necessitate extremely fine temperature (± 0.1°C) and pressure (± 5 torr) controlling capability. Of course, the whole problem can be circumvented by using a batch reactor, which will be discussed later. Samples of the NO_2 treated coals were also washed with aqueous Na_2CO_3 using the procedure discussed above.

TABLE 3-8

Experimental Conditions for Runs Using Water As A Solvent for the Treatment of PSOC 190 (+200-325 mesh) with NO_2

Run #	Reaction Time (min)	Initial Coal Mass (g)	Temperature Range (C)	Average NO_2 Flow Rate (g/min)	Mass Loss Due to NO_2 Treatment (%)	Mass Loss Due to Na_2CO_3(aq) Wash (%)	Overall Mass Loss (%)[1]
14 (No Coal)	240		25 -37	0.778			
15	60	10.0015	23.0 -23.8	0.697	17.56	3.83	20.72
16	120	10.0011	22.6 -24.0	0.269	17.43	4.26	20.95
17	120	10.0025	24.6 -25.6	0.483	15.52	4.86	19.63
18	120	10.0013	23.0 -24.0	1.039	14.47	3.60	17.55
19	180	10.0029	23.6 -26.0	0.862	13.86	4.55	17.78
20	240	10.0066	23.2 -25.0	0.759	13.70	5.73	18.64

[1] Represents percent mass loss relative to initial mass of coal. Let f = the fractional mass loss due to NO_2 treatment, m_i = the initial mass of NO_2 treated coal used for the Na_2CO_3 (aq) wash and m_f = the final mass of washed coal. Then

$$\text{Overall Mass Loss} = \frac{m_i - m_f(1-f)}{m_i}.$$

3.3.1.3 Runs Using Carbon Tetrachloride as the Solvent

Carbon tetrachloride was chosen as a solvent in order to avoid the reactions which take place between NO_2 and water when water is the solvent. Therefore, the only species capable of attacking the coal in a coal/CCl_4 slurry is NO_2, rendering the evaluation of the kinetic data much easier. Two sets of experiments were conducted using carbon tetrachloride as a solvent in the continuous flow reactor.

The first set of experiments consisted of seven runs at room temperature. Approximately five grams of predried PSOC 190 coal (+200-325 mesh) - Batch 1 were placed in the vacuum assembly shown in Figure 3–5. The assembly was placed on a vacuum rack and evacuated at room temperature for two hours. The vacuum rack was then isolated from the vacuum pump and the valve isolating a flask containing degassed CCl_4 was opened. The coal was allowed to adsorb CCl_4 at room temperature for one hour. The tube containing the coal was then placed in an ice bath. After approximately one more hour, enough CCl_4 had condensed in the tube to form a thick slurry. This procedure was adopted to ensure that the pores of the coal particles filled completely with CCl_4, because it is not known if CCl_4 could wet the entire coal particle. The assembly was then connected to a flask containing CCl_4. The valve was opened and the assembly flooded with liquid CCl_4. The slurry was then mixed with enough CCl_4 which was dried over anhydrous $MgSO_4$ to make 400 ml of slurry. The slurry was placed in the reactor with the water jacket and purged for one hour with N_2 while being stirred magnetically. Then NO_2 was admitted at a constant flowrate as indicated by the flowmeter for various reaction times. The average NO_2 mass flowrate was determined by dividing the difference in the bomb mass before and after the run by the reaction time. Liquid samples were withdrawn every 15 minutes to determine the NO_2 concentration. At the end of the run, the slurry was filtered and

CCl_4 Saturation Assembly

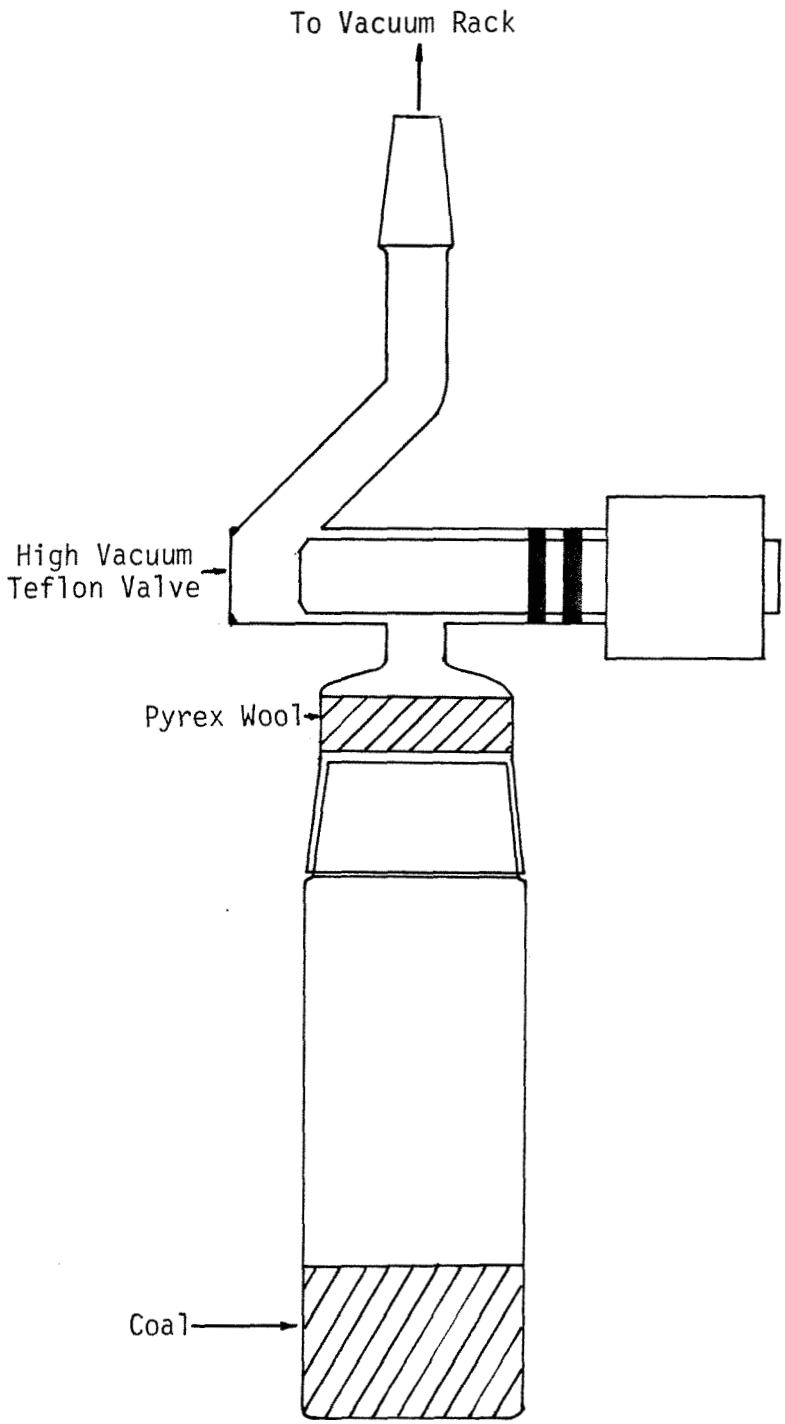

Figure 3-5

the coal was placed immediately in a 200 ml round bottom boiling flask and connected to the vacuum rack. The samples were dried under vacuum for 12 hours at roughly 160°C. The samples were then weighed to determine the mass loss. Samples of the treated coals were also washed with aqueous Na_2CO_3 using the procedure discussed in the previous section. The experimental conditions are shown in Table 3–9. Referring to the table, it should be noted that the coal from Run 26 was vacuum dried for 12 hours at room temperature rather than 160°C in order to determine the effect of the drying temperature. As expected, a significant amount of otherwise volatile material is not removed at room temperature.

The second set of experiments consisted of five runs conducted at 50°C. The major advantage in conducting the experiment at 50°C is that it is possible to saturate the CCl_4 with NO_2. By using a flowrate of roughly 1 g NO_2/min, it is possible to saturate 400 ml of CCl_4 in 30 minutes. As in the previous set of experiments, approximately five grams of predried PSOC 190 coal (+200-325 mesh) - Batch 2 were used. The coal was not presaturated with CCl_4, however, since such pretreatment did not seem to alter the reaction to any discernible extent. The coal was added to the reactor wrapped in heating tape after 400 ml reagent grade CCl_4 were saturated for 45 minutes with NO_2. The same NO_2 flowrate as indicated by the flowmeter was used throughout this set of experiments. The slurry was stirred with a magnetic stirrer at all times and liquid samples were withdrawn every fifteen minutes. At the end of the run, the slurry was filtered and the coal was placed immediately in a 200 ml round bottom boiling flask and connected to the vacuum rack. The coal was vacuum dried for 6 hours at temperatures ranging from 100 to 120°C. The samples were then weighed to determine the mass loss. Samples of the treated coals were also washed with aqueous Na_2CO_3 using the procedure described in section 3.3.1.2. The experimental con-

TABLE 3-9

Experimental Conditions for Runs Using CCl_4 As A Solvent for the Treatment of PSOC 190 (+200-325 mesh) with NO_2 in the Continuous Flow Reactor

Run #	Reaction Time (min)	Initial Coal Mass (g)	Temperature Range (C)	Average NO_2 Flow Rate (g/min)	Mass Loss Due to NO_2 Treatment (%)	Mass Loss Due to Na_2CO_3(aq) Wash (%)	Overall Mass Loss (%)[1]
21	30	5.0131	25 -27	1.233	-9.69	9.70	0.01
22	60	5.0305	26 -27	1.203	-11.56	9.43	-1.04
23	90	5.0380	25 -28	1.224	-16.53	11.33	-3.33
24	120	5.0245	24 -28	1.153	-14.95	15.05	2.35
25	120	5.0125	25 -28	1.195	-17.23	13.57	-1.32
26	120	5.0054	25 -27	1.420	-33.51[2]	-[2]	-[2]
27	180	5.0175	25 -28	1.246	-17.27	13.86	-1.01

[1] Represents percent mass loss relative to initial mass of coal. Let f = the fractional mass loss due to NO_2 treatment, m_i = the initial mass of NO_2 treated coal used for the Na_2CO_3 (aq) wash and m_f = the final mass of washed coal. Then

$$\text{Overall Mass Loss} = \frac{m_i - m_f(1-f)}{m_i}.$$

[2] After treatment with NO_2, this coal was vacuum dried for 12 hours at room temperature.

ditions are shown in Table 3–10. It should be noted that a minimum of coal should be used in order to avoid a significant decrease in NO_2 concentration when the coal is initially added. Enough coal must be used, however, to provide a sufficient amount of sample for analysis. The best compromise is five grams, which is the amount used. Of much greater importance is the fact that the treated coals could not be washed in 0.1 M Na_2CO_3 (aq) and then filtered. The coals treated with NO_2 at 50°C appeared to dissolve completely in 0.1 M Na_2CO_3 (aq) while coals treated with NO_2 at lower temperatures (25°C) do not dissolve. Rather, these coals treated at 50°C seem to form an emulsion which cannot be filtered.

3.3.2 Procedure for the Slurry Phase Reaction in the Batch Reactor

Due to the difficulty in maintaining a reproducible NO_2 flowrate to the continuous-flow reactor within a set of runs, several experiments were run in the batch reactor shown in Figure 3–4. Four sets of experiments were conducted. For each set of runs, approximately 800 to 900 ml of reagent grade CCl_4 were exposed to a stream of NO_2 until the NO_2 concentration was approximately 2.5 F, which served as a stock solution. This solution was stored in a dark bottle and kept in a closed cabinet to prevent any photolysis of NO_2. Furthermore, the solution was used within a week to ensure that the NO_2 concentration was relatively constant.

For each run, enough stock solution was added to reagent grade CCl_4 to make 350 ml of solution with $[NO_2] \approx$ 1.0 to 1.1 F. The solution was placed in the reactor and then sealed to prevent the escape of NO_2. The reactor and its contents were then allowed to equilibrate thermally with the water bath. The bath temperature was maintained by adding small amounts of ice or by heating slightly with the combination magnetic stirrer/heater unit. After thermal equilibrium was attained, approximately ten grams of coal were added to the reactor while

TABLE 3-10

Experimental Conditions for Runs Using CCl_4 As A Solvent for the Treatment of PSOC 190 (+200-325 mesh) with NO_2 in the Continuous Flow Reactor at 50 C

Run #	Reaction Time Time	Initial Coal Mass (g)	Temperature Range (C)	NO_2 Concentration (mol/l)			Mass Gain (%)	Drying Temperature (C)
				High	Low	Average[1]		
28	30	5.0067	50.0± 0.2	1.299	1.088	1.196± 0.086	21.06	115
29	60	5.0083	50.0± 0.2	1.233	1.067	1.159± 0.053	21.55	118
30	90	5.0041	50.0± 0.2	1.276	1.073	1.184± 0.057	26.93	97[2]
31	120	5.0123	50.0± 0.2	1.212	0.974	1.152± 0.077	25.80	109
32	180	5.0140	50.0± 0.2	1.305	1.063	1.179± 0.069	28.93	113

[1] The average shown was obtained by simple averaging of the values obtained for $[NO_2]$ while the error shown is the standard deviation of the average.

[2] For some unknown reason, the heating mantle did not raise the temperature as high as it did in other runs, even though the voltage supplied in all five runs was the same.

the CCl_4/NO_2 solution was stirred. Initially, the slurry temperature rose 1 to 2°C within the first minute, but then fell back within the next few minutes as the slurry thermally equilibrated with the water bath. Liquid samples were withdrawn every 15 minutes for determination of the NO_2 concentration. At the end of the run, the slurry was filtered and the coal was placed immediately in a 200 ml round bottom boiling flask and connected to the vacuum rack. The coal was vacuum dried for 3 hours at 120°C. The samples were then weighed to determine the mass loss. Samples of the treated coals were also washed in aqueous Na_2CO_3. The procedure used for the wash was the same as that discussed in section 3.3.1.2, except five grams of the NO_2 treated coal were slurried with 250 ml Na_2CO_3 (aq: 10g Na_2CO_3 (anhydrous)/l). After stirring for two hours at room temperature, the slurry was filtered and the coal was washed five times with 100 ml of deionized water. After air drying overnight, the coal was vacuum dried for four hours at 130°C. These samples were then weighed to determine the overall mass loss.

The experiments in the first set of runs were run for different lengths of time to generate kinetic data. The experimental conditions are shown in Table 3–11. The washed and dried (W&D) PSOC 190 (+200-325 mesh) - Batch 1 coal was used in this set of experiments. All of the experiments were conducted at 20°C. The experiments in the second set of runs were run at different initial concentrations of NO_2 in order to obtain data regarding the effect of $[NO_2]$ on the kinetics of the various reactions between NO_2 and coal. The experimental conditions can be found in Table 3–12. All of these experiments were run at 20°C as well. It should be noted that Run 36 appears in Table 3–12 as well as Table 3–11 for purposes of comparison. The experiments in the third set of runs were conducted for various lengths of time at 0°C in order to generate kinetic data at another temperature. The pertinent experimental conditions have been tabu-

TABLE 3-11

Experimental Conditions for Runs Using CCl_4 As A Solvent for the Treatment of W&D PSOC 190 (+200-325 mesh) -Batch 1 with NO_2 in the Batch Reactor at 20 C

Run #	Reaction Time (min)	Initial Coal Mass (g)	Average Temperature (C)[1]	$[NO_2]_0$ (mol/l)	Mass Gain Due to NO_2 Treatment (%)	Mass Loss Due to Na_2CO_3(aq) Wash (%)	Overall Mass Gain (%)[2]
33	30	10.0043	20.3± 0.2	1.122	13.02	3.99	8.52
34	60	10.0064	20.1± 0.1	1.058	14.55	4.67	9.20
35	90	10.0118	20.0± 0.1	1.081	16.67	5.60	10.14
36	120	10.0164	20.2± 0.1	1.087	16.86	5.08	10.92
37	180	10.0107	20.0± 0.1	1.091	15.63	4.67	10.22

[1] Deviation is the standard deviation of the average of the slurry temperatures, which were taken every 15 minutes.

[2] Represents percent mass loss relative to initial mass of coal. Let f = the fractional mass loss due to NO_2 treatment, m_i = the initial mass of NO_2 treated coal used for the Na_2CO_3 (aq) wash and m_f = the final mass of washed coal. Then

Overall Mass Loss = $\frac{m_i - m_f(1-f)}{m_i}$.

TABLE 3-12

Experimental Conditions for Runs Using CCl_4 As A Solvent for the Treatment of W&D PSOC 190 (+200-325 mesh) -Batch 1 with NO_2 in the Batch Reactor at 20 C For Different Initial NO_2 Concentrations

Run #	Reaction Time (min)	Initial Coal Mass (g)	Average Temperature (C)[1]	$[NO_2]_0$ (mol/l)	Mass Gain Due to NO_2 Treatment (%)	Mass Loss Due to Na_2CO_3(aq) Wash (%)	Overall Mass Gain (%)[2]
38	120	10.0162	20.2± 0.1	0.097	5.69	2.27	3.29
39	120	10.0187	20.2± 0.1	0.488	12.72	4.27	7.90
36	120	10.0164	20.2± 0.1	1.087	16.86	5.08	10.92
40	120	10.0060	20.0± 0.1	1.713	20.74	8.11	10.95
41	120	9.9933	20.2± 0.1	1.874	22.81	9.25	11.45

[1] Deviation is the standard deviation of the average of the slurry temperatures, which were taken every 15 minutes.

[2] Represents percent mass loss relative to initial mass of coal. Let f = the *fractional mass loss* due to NO_2 treatment, m_i = the initial mass of NO_2 treated coal used for the Na_2CO_3 (aq) wash and m_f = the final mass of washed coal. Then

$$\text{Overall Mass Loss} = \frac{m_i - m_f(1-f)}{m_i}.$$

lated in Table 3–13. The second batch of washed and dried PSOC 190 coal was used in these runs. Examination of Table 3–5, however, indicates that there is no discernible difference between the two batches of washed and dried coal. The experiments in the fourth and final set of runs were run using washed and dried (W&D) PSOC 276 (+200-325 mesh) coal at 20°C in order to generate kinetic data which can be compared with the data from the data set using the PSOC 190 coal. Furthermore, the two coals have very different pore structures ($S_a^{N_2}$ = 55 m^2/g for PSOC 190 vs. $S_a^{N_2}$ = 9 m^2/g for PSOC 276). Since the PSOC 276 coal has a much smaller void fraction than the PSOC 190 coal, comparison of the kinetic data should provide an insight into intraparticle mass transfer effects. The experimental conditions are shown in Table 3–14. It should be noted that Run 47 is a blank run in which the coal was slurried in pure CCl_4 and stirred for two hours at room temperature, filtered, vacuum dried and weighed. A sample from this run was then treated with aqueous Na_2CO_3 in the manner described above, filtered, vacuum dried and weighed.

TABLE 3-13

Experimental Conditions for Runs Using CCl_4 As A Solvent for the Treatment of W&D PSOC 190 (+200-325 mesh) -Batch 2 with NO_2 in the Batch Reactor at 0 C

Run #	Reaction Time (min)	Initial Coal Mass (g)	Average Temperature (C)[1]	$[NO_2]_0$ (mol/l)	Mass Gain Due to NO_2 Treatment (%)	Mass Loss Due to Na_2CO_3(aq) Wash (%)	Overall Mass Gain (%)[2]
42	30	10.0114	0.9± 0.1	0.985	11.54	4.27	6.78
43	60	10.0138	0.5± 0.1	1.040	14.12	5.21	8.17
44	90	10.0054	0.6± 0.2	1.008	14.40	4.97	8.72
45	120	10.0079	0.5± 0.1	1.048	15.82	5.54	9.41
46	180	10.0136	0.5± 0.1	1.028	16.20	5.03	10.36

[1] Deviation is the standard deviation of the average of the slurry temperatures, which were taken every 15 minutes.

[2] Represents percent mass loss relative to initial mass of coal. Let f = the fractional mass loss due to NO_2 treatment, m_i = the initial mass of NO_2 treated coal used for the Na_2CO_3 (aq) wash and m_f = the final mass of washed coal. Then

Overall Mass Loss = $\frac{m_i - m_f(1-f)}{m_i}$.

TABLE 3-14

Experimental Conditions for Runs Using CCl_4 As A Solvent for the Treatment of W&D PSOC 278 (+200-325 mesh) with NO_2 in the Batch Reactor at 20 C

Run #	Reaction Time (min)	Initial Coal Mass (g)	Average Temperature (C)[1]	$[NO_2]_0$ (mol/l)	Mass Gain Due to NO_2 Treatment (%)	Mass Loss Due to Na_2CO_3(aq) Wash (%)	Overall Mass Gain (%)[2]
47[1]	120	10.0098	20.2± 0.1	0.000	-2.08	3.95	-5.94
48	30	10.0038	20.0± 0.1	1.044	7.79	3.62	3.89
49	60	10.0086	20.0± 0.1	1.048	10.63	4.26	5.92
50	90	10.0013	19.8± 0.1	1.097	12.13	4.51	7.07
51	120	10.0062	19.8± 0.1	1.090	14.33	4.99	8.63
52	180	10.0046	19.9± 0.1	1.074	15.67	4.05	10.98

[1] A blank run.

[2] Deviation is the standard deviation of the average of the slurry temperatures, which were taken every 15 minutes.

[3] Represents percent mass loss relative to initial mass of coal. Let f = the fractional mass loss due to NO_2 treatment, m_i = the initial mass of NO_2 treated coal used for the Na_2CO_3 (aq) wash and m_f = the final mass of washed coal. Then

Overall Mass Loss = $\frac{m_i - m_f(1-f)}{m_i}$.

3.4 Chemical Analysis

3.4.1 Analysis of Nitrogen Dioxide and Related Species

3.4.1.1 Analysis of Nitric and Nitrous Acid in the Liquid Phase When Water Was the Solvent

Samples of the liquid phase were withdrawn every 15 minutes from the reactor during a run. When water was the solvent, the predominant liquid phase species derived from NO_2 were HNO_3 and HNO_2. Since the reaction between NO_2 and H_2O is so rapid, very little solvated NO_2 can exist unless the concentration of HNO_3 is quite high (about 16 M). Since the concentration of HNO_3 never exceeded 10 M in any of the experiments, it was assumed that only HNO_3 and HNO_2 were present in the bulk liquid phase. Reaction of HNO_3 (aq) with coal, however, leads to the formation of NO_2 in situ as evidenced by the presence of NO_2 in the vapor space in the reactor.

3.4.1.1.1 Analysis of Nitric Acid

Exactly 100.00± 0.05 ml of deionized water were pipetted into a 200 ml beaker. The pH of the H_2O was measured using a Radiometer Model 26 pH meter to determine the initial pH of the water, pH_0. Then 1.00± 0.05 ml of the liquid sample was pipetted into the H_2O, which was then magnetically stirred for 1 minute. The pH was then measured to determine pH_1. Since $pH = -\log a_{H^+}$, where a_{H^+} is the activity of H^+, $a_{H^+} = \gamma_{H^+} m_{H^+}$, where γ_{H^+} is the activity coefficient of H^+ and m_{H^+} is the molality of H^+, and $c_{H^+} = \frac{m_{H^+} \rho_s}{1 + m_{H^+} M_{H^+}}$, where c_{H^+} is the molar concentration of H^+, ρ_s is the solution density and M_{H^+} is the molecular mass of H^+,

$$m_{H^+} = (m_{H^+})_1 - (m_{H^+})_0 = (\frac{10^{-pH_1}}{\gamma_{H^+}})_1 - (\frac{10^{-pH_0}}{\gamma_{H^+}})_0 . \qquad (3.4.1)$$

The H^+ present is due to the dissociation of both HNO_3 and HNO_2. Since pH_1 is usually between 0.0 and 3.0, the HNO_3 may not be completely dissociated. Furthermore, HNO_2 has a pK_a of 3.37. Therefore, a substantial fraction of the H^+ present can be attributed to the dissociation of HNO_2, particularly at higher pH values. Therefore, two simultaneous mass action equations must be solved, namely

$$\frac{a_{H^+}\, a_{NO_3^-}}{a_{HNO_3}} = K_1 , \quad \text{and} \qquad (3.4.2)$$

$$\frac{a_{H^+}\, a_{NO_2^-}}{a_{HNO_2}} = K_2 , \quad \text{where} \qquad (3.4.3)$$

a_i = the activity of species i,

K_1 = the dissociation constant of HNO_3, and

K_2 = the dissociation constant of HNO_2.

These equations can be expressed in terms of activity coefficients as

$$\frac{(\gamma_\pm)^2_{HNO_3}\, m_{H^+}\, m_{NO_3^-}}{\gamma_{HNO_3} m_{HNO_3}} = K_1 , \text{ and} \qquad (3.4.4)$$

$$\frac{(\gamma_\pm)^2_{HNO_2}\, m_{H^+}\, m_{NO_2^-}}{\gamma_{HNO_2} m_{HNO_2}} = K_2 , \text{ where} \qquad (3.4.5)$$

$(\gamma_\pm)_i$ = the mean ion activity coefficient of species i, and

γ_i = the activity coefficient of undissociated species i.

Letting the extent of HNO_3 dissociation be x and the extent of HNO_2 dissociation be y, then

$$m_{H^+} = x(m_{HNO_3})_0 + y(m_{HNO_2})_0 .$$

$m_{NO_3^-} = x\,(m_{HNO_3})_0$,

$m_{NO_2^-} = y\,(m_{HNO_2})_0$,

$m_{HNO_3} = (1-x)\,(m_{HNO_3})_0$, and

$m_{HNO_2} = (1-y)\,(m_{HNO_2})_0$, where

$(m_i)_0$ = the total concentration of species i, expressed as undissociated i.

Substitution of these expressions into equations (3.4.4) and (3.5.5) yields

$$\frac{x}{1-x}\left[\frac{(\gamma_\pm)^2_{HNO_3}}{\gamma_{HNO_3}}\right]\left[x\,(m_{HNO_3})_0 + y\,(m_{HNO_2})_0\right] = K_1 , \quad \text{and} \tag{3.4.6}$$

$$\frac{y}{1-y}\left[\frac{(\gamma_\pm)^2_{HNO_2}}{\gamma_{HNO_2}}\right]\left[x\,(m_{HNO_3})_0 + y\,(m_{HNO_2})_0\right] = K_2 . \tag{3.4.7}$$

The value of $(m_{HNO_2})_0$ is known from the determination of HNO_2 discussed in the next section. Furthermore, m_{H^+} can be determined if values for γ_{H^+} are known:

$$a_{H^+} = \gamma_{H^+}\, m_{H^+} = \gamma^c_{H^+}\, c_{H^+} , \quad \text{where} \tag{3.4.8}$$

γ_i^c = the activity coefficient when molar concentrations are used.

Although values for γ_{H^+} cannot be determined directly by experiment, determination of $\gamma_{NO_3^-}$ and $(\gamma_\pm)_{HNO_3}$ allows the calculation of γ_{H^+}:

$$\gamma_{H^+} = \frac{(\gamma_\pm)^2_{HNO_3}}{\gamma_{NO_3^-}} \quad \text{or} \quad \gamma^c_{H^+} = \frac{(\gamma^c_\pm)^2_{HNO_3}}{\gamma^c_{NO_3^-}}, \tag{3.4.9}$$

where the superscript c denotes that molar concentrations are to be used. It should be noted that the conversion from molal to molar units is easily accomplished using the following formula:

$$c_i = \frac{m_i}{1 + \sum_{i=1}^{N} m_i (MW)_i} \rho_s \,, \quad \text{where} \tag{3.4.10}$$

N = the total number of solute species,

$(MW)_i$ = the molecular mass of species i (g/mol),

ρ_s = the solution density (g / cm^3),

m_i = the molality of species i (mol/kg solvent), and

c_i = the molarity of species i (mol/l solution).

Equations (3.4.6) and (3.4.7) can be rewritten as:

$$\frac{x}{1-x}\left[\frac{(\gamma_{\pm}^{c})^2_{HNO_3}}{\gamma_{HNO_3}{}^{c}}\right]\left[\, x(c_{HNO_3})_0 + y(c_{HNO_2})_0\right] = K_1^c \,, \quad \text{and} \tag{3.4.11}$$

$$\frac{y}{1-y}\left[\frac{(\gamma_{\pm}^{c})^2_{HNO_2}}{\gamma_{HNO_2}{}^{c}}\right]\left[\, x(c_{HNO_3})_0 + y(c_{HNO_2})_0\right] = K_2^c \,, \quad \text{where} \tag{3.4.12}$$

$c_{H^+} = x(c_{HNO_3})_0 + y(c_{HNO_2})_0$,

$c_{NO_3^-} = x(c_{HNO_3})_0$,

$c_{NO_2^-} = y(c_{HNO_2})_0$,

$c_{HNO_3} = (1-x)\,(c_{HNO_3})_0$, and

$c_{HNO_2} = (1-y)\,(c_{HNO_2})_0$.

The determination of $(c_{HNO_3})_0$ is now relatively straightforward since c_{H^+} and $(c_{HNO_2})_0$ are known. First, equation (3.4.12) is used to determine y in the form:

$$y = \left[\, 1 + \frac{(\gamma_{\pm}^{c})^2_{HNO_2}}{\gamma^c_{HNO_2}} \frac{c_{H^+}}{K_2^c}\right]^{-1} . \tag{3.4.13}$$

It is important to recall that the activity coefficients must be evaluated at the appropriate ionic strength, which in this case is given by:

$$I = x(c_{HNO_3})_0 + y(c_{HNO_2})_0 = c_{H^+} . \qquad (3.4.14)$$

The value for x is now determined by equation (3.4.11) recast as:

$$x = [\, 1 + \frac{(\gamma_{\pm}^c)^2_{HNO_3}}{\gamma^c_{HNO_3}} \frac{c_{H^+}}{K_1^c}]^{-1} . \qquad (3.4.15)$$

Finally, $(c_{HNO_3})_0$ is given by equation (3.4.14) rewritten as:

$$(c_{HNO_3})_0 = \frac{1}{x}[\, c_{H^+} - y\,(c_{HNO_2})_0 \,] . \qquad (3.4.16)$$

The values for $(\gamma_{\pm}^c)_{HNO_3}$ and $\gamma^c_{HNO_3}$ determined by Davis and deBruin[1] were used in the calculations and are shown in Table 3–15. It should be noted that the values for the ionic strength, I, given in Table 3–15 were obtained by multiplying $(c_{HNO_3})_0$ by the degree of dissociation, α. Therefore, $(\gamma_{\pm}^c)_{HNO_3}$ and $\gamma^c_{HNO_3}$ are now given as a function of the ionic strength. Linear interpolation was used between the appropriate points to obtain the necessary values for the calculation. The authors determined a value of 15.4± 2.1 for K_1^c. The values given for $\gamma^c_{NO_3^-}$ in Table 3–15 were obtained using the method proposed by Bates and Alfenar as described by O'Brien and Bautista.[2] By using the Cl^- ion in aqueous NaCl solutions as a standard, the mean ionic activity coefficient of any simple ionic species can be obtained. In this case,

$$\log \gamma^c_{NO_3^-} = \log \gamma^c_{a^-} + 2 \log [\, \frac{(\gamma_{\pm}^c)_{HNO_3}}{(\gamma_{\pm}^c)_{HCl}}] . \qquad (3.4.17)$$

The value for $\gamma^c_{a^-}$ is given by

$$-\log \gamma^c_{a^-} = \frac{0.509\, I^{\frac{1}{2}}}{1.0 + 1.5\, I^{\frac{1}{2}}} , \qquad (3.4.18)$$

where I is the ionic strength, which in general is given by

TABLE 3-15

Values for the Activity Coefficients of HNO_3, H^+, and NO_3^-

$(c_{HNO_3})_0$ (mol/l soln)	α Degree of Dissociation	I (mol/l soln)	$(\gamma_{\pm}^{c})_{HNO_3}$	$\gamma_{HNO_3}^{c}$	$\gamma_{NO_3^-}^{c}$	$\gamma_{H^+}^{c}$
0.000	1.0000	0.00000	1.000	1.000	1.000	1.000
0.001	0.99994	0.00100	0.996	1.001	0.965	1.028
0.002	0.99988	0.00200	0.953	1.001	0.954	0.952
0.005	0.99972	0.00500	0.929	1.002	0.930	0.928
0.01	0.99947	0.0100	0.906	1.003	0.907	0.905
0.02	0.9990	0.0200	0.877	1.006	0.876	0.878
0.05	0.9978	0.0499	0.831	1.015	0.824	0.838
0.1	0.9960	0.100	0.796	1.031	0.778	0.815
0.2	0.9930	0.199	0.763	1.063	0.723	0.805
0.5	0.9852	0.493	0.741	1.165	0.641	0.857
0.7	0.980	0.686	0.746	1.24	0.604	0.921
1.0	0.973	0.973	0.766	1.36	0.561	1.046
1.5	0.961	1.442	0.825	1.58	0.500	1.361

$$I = \frac{1}{2}\sum_{i=1}^{N} z_i^2 c_i \,, \quad \text{where} \tag{3.4.19}$$

z_i = the charge on species i, (eg. $z_{H^+} = +1$, $z_{NO_3^-} = -1$ and $z_{HNO_3} = 0$), and

c_i = the molar concentration of species i (mol/l solution).

Values for $\gamma^c_{H^+}$ were then calculated using the definition of the mean ionic activity coefficient, namely

$$\gamma^c_{H^+} = \frac{(\gamma^c_{\pm})^2_{HNO_3}}{\gamma^c_{NO_3^-}}. \tag{3.4.20}$$

Values for $\gamma^c_{HNO_2}$ are available, but values for $(\gamma^c_{\pm})_{HNO_2}$ have not been determined. Lumme and Tummavuori, however, have determined K^c_2 as a function of the ionic strength.[3] Thus, the activity coefficients are implicitly included in the expression for K^c_2:

$$K^c_2\,(I) = \frac{\gamma^c_{HNO_2}}{(\gamma^c_{\pm})_{HNO_2}} K^c_2 \,. \tag{3.4.21}$$

The authors obtained the following expression for $K^c_2\,(I)$:

$$-\log\,[K^c_2(I)] = 3.148 - 1.023\, I^{\frac{1}{2}}\,(1 + 1.622\, I^{\frac{1}{2}})^{-1} + 0.261\, I \,. \tag{3.4.22}$$

Equation (3.4.13) is then simplified to

$$y = [\,1 + \frac{c_{H^+}}{K^c_2(I)}\,]^{-1} \,. \tag{3.4.23}$$

Therefore, using the values for c_{H^+} and $(c_{HNO_2})_0$, equation (3.4.23) was used to calculate y, equation (3.4.15) was used to calculate x and equation (3.4.16) was used to calculate $(c_{HNO_3})_0$.

3.4.1.1.2 Analysis of Nitrous Acid

The concentration of HNO_2 (aq) was determined using an Orion Research Model 95-46 nitrogen oxide electrode and Model 407 meter. The electrode utilizes a hydrophobic gas permeable membrane to separate the sample solution from the internal electrode solution. The gaseous anhydrides of nitrous acid, generated by acidifying an aqueous nitrite sample, diffuse through the membrane until the partial pressures of the nitrogen oxides, namely NO, NO_2, N_2O_3 and N_2O_4, are the same on both sides of the membrane. The nitrogen oxides affect the HNO_2 concentration in the internal filling solution through the following equilibria:

$$H^+ (aq) + NO_2^- (aq) = HNO_2 (aq)$$

$$2\, HNO_2 (aq) = NO (aq) + NO_2 (aq) + H_2O$$

$$NO (aq) = NO (g)$$

$$NO_2 (aq) = NO_2 (g)$$

$$NO (g) + NO_2 (g) = N_2O_3 (g)$$

$$N_2O_3 (g) = N_2O_3 (aq)$$

Once the nitrogen oxides have equilibrated across the membrane, the following expression describes the relationship among H^+, NO_2^- and HNO_2:

$$\frac{a_{H^+}\, a_{NO_2^-}}{a_{HNO_2}} = K = \text{constant}. \qquad (3.4.24)$$

The concentration of NO_2^- in the internal filling solution is sufficiently high relative to the concentrations of H^+ and HNO_2 so that $c_{NO_2^-}$ can be considered constant. Thus, the H^+ concentration becomes proportional to the HNO_2 concentration. It is the H^+ activity that is actually determined. The relationship between the electrode potential and the H^+ activity, a_{H^+}, is given by the Nernst equation:

$$E = E_0 + S \log a_{H^+}, \quad \text{where} \qquad (3.4.25)$$

E = the electrode potential,

E_0 = a reference potential,

S = a constant, commonly referred to as the electrode slope, and

a_{H^+} = the H^+ activity.

Because a_{H^+} is proportional to a_{HNO_2}, however, equation (3.4.25) can be rewritten as

$$E = E_1 + S \log a_{HNO_2} . \qquad (3.4.26)$$

Therefore, the electrode potential is proportional to log a_{HNO_2}.

The measurement of a_{HNO_2} involves adding an appropriate volume of the sample taken from the reactor to a solution containing 100.00 ml deionized water and 10.00 ml of an acid buffer. The buffer is present to ensure that a pH of 1.7 is maintained during the measurement. At this pH, virtually all of the nitrite will be in the form of HNO_2. The use of an acidic medium also inhibits the decomposition of HNO_2 via

$$3\, HNO_2\,(aq) \rightleftarrows H^+ + NO_3^-\,(aq) + 2\, NO\,(g) + H_2O .$$

Furthermore, the adsorption of CO_2, which can interfere in the measurement, from the atmosphere is not appreciable when the pH is less than 6.2. The buffer consists of 190 g of anhydrous Na_2SO_4 in roughly 800 ml of deionized water in a one liter volumetric flask. After the Na_2SO_4 has dissolved, 53 ml of concentrated H_2SO_4 are added and mixed. The buffer solution is then diluted to one liter total volume and stored in a dark bottle. The amount of sample added to the solution was chosen so that the electrode response would be within the linear range of the meter. This range was determined by calibrating the meter using samples of known NO_2^- concentration. The standardizing solutions were made by weighing

out to 0.1 mg roughly 0.7 g of reagent grade $NaNO_2$ and dissolving it in deionized water in a 100.00 ml volumetric flask to form a 0.10 M $NaNO_2$ (aq) solution. Then 10.00 ml of this solution were diluted to 100.00 ml to form a 0.010 M $NaNO_2$ (aq) solution. In a similar manner, 10^{-3} M and 10^{-4} M $NaNO_2$ (aq) solutions were made. Using these solutions, the linear range of the meter was established to be between 10^{-5} M and 5×10^{-3} M $NaNO_2$ (aq). It should be noted that the solution to which the sample is added has an ionic strength of roughly 6.4 M. Thus, addition of the sample should not change the ionic strength to any appreciable degree. Therefore, the activity coefficients for NO_2^-, H^+ and HNO_2 should not change. Therefore, the activities in equations (3.4.25) and (3.4.26) can be replaced with their corresponding concentrations.

Since the concentration of HNO_2 in the reactor was on the order of 0.1 M, rather small samples were added to the buffer solution. A Hamilton 50 μl syringe calibrated to 1 μl was used to add the appropriate amount of sample to the solution. The solution was slowly stirred using a magnetic stirrer during the reading. Equilibration with the electrode usually occurred within one minute. The HNO_2 concentration in the reactor is given by

$$(c_{HNO_2})_0 = (c_{HNO_2})_S \frac{R}{R_S}\left(\frac{110.00 + V}{V}\right), \quad \text{where} \tag{3.4.27}$$

$(c_{HNO_2})_0$ = the concentration of HNO_2 in the reactor,

$(c_{HNO_2})_S$ = the concentration of HNO_2 in the standard,

R = the meter reading,

R_S = the meter reading for the standard, and

V = the volume of the sample (ml).

The concentration of HNO_3 as a function of time for those runs using water as the solvent is shown in Table 3–16, while the concentration of HNO_2 as a func-

TABLE 3-16

Concentrations of HNO_3 for Runs Using Water as the Solvent							
Reaction Time (min)	Run Number						
	14	15	16	17	18	19	20
0	0.0002	.0028	0.0024	0.0027	0.0023	0.0028	0.0036
15	0.212	0.280	0.049	0.187	0.364	0.316	0.249
30	0.709	0.726	0.182	0.572	0.781	0.923	0.761
45	1.292	1.292	0.267	0.946	1.356	1.495	1.495
60	2.102	1.749	0.381	1.324	2.876	2.102	2.313
90	3.951		0.676	2.258	4.476	3.579	3.856
120	4.956		0.940	3.169	6.166	4.475	5.078
150	6.632					5.733	6.473
180	8.077					8.490	7.684
210	9.889						9.382
240	12.297						11.416
Mean NO_2 Flowrate (g/min)	0.778	0.697	0.269	0.483	1.039	0.862	0.759

All concentrations are in units of (mol/l)

TABLE 3-17

Concentrations of HNO_2 for Runs Using Water as the Solvent							
Reaction Time (min)	Run Number						
	14	15	16	17	18	19	20
0	0.0	0.0	0.0	0.0	0.0	0.0	0.0
15	0.092	0.098	0.021	0.065	0.100	0.082	0.093
30	0.169	0.218	0.068	0.176	0.203	0.188	0.150
45	0.243	0.338	0.101	0.250	0.298	0.248	0.200
60	0.318	0.349	0.125	0.249	0.356	0.368	0.318
90	0.370		0.185	0.235	0.250	0.368	0.222
120	0.388		0.229	0.293	0.412	0.438	0.124
150	0.430					0.302	0.233
180	0.447					0.456	0.283
210	0.450						0.103
240	-						0.199
Mean NO_2 Flowrate (g/min)	0.778	0.697	0.269	0.483	1.039	0.862	0.759

All concentrations are in units of (mol/l)

tion of time for those same runs is tabulated in Table 3–17. It should be noted that neither the HNO_3 concentration nor the HNO_2 concentration was determined for the exploratory runs using water as the solvent (Runs 7-13).

3.4.1.2 Analysis of Nitrogen Dioxide in the Liquid Phase When Carbon Tetrachloride Was Used as a Solvent

As mentioned earlier, CCl_4 was chosen as a solvent in order to avoid any reaction between NO_2 and the solvent. Thus, the only dissolved NO_2 species should have been NO_2 or the dimer N_2O_4. Analysis of the NO_2/CCl_4 stock solution one week after it was made on the gas chromatograph indicated that only NO_2 and/or N_2O_4 were present. The relative amounts of NO_2 and N_2O_4 depend on temperature and pressure. Although the equilibrium constant for NO_2 dimerization in the gas phase is known, its value in the solvated state is unknown. Consequently, for the purposes of further discussion, N_2O_4 and/or NO_2 will be referred to as simply NO_2. Since only one solvated species predominantly exists, the determination of the NO_2 concentration is rather easy.

A 1.00 ml liquid sample from the reactor was pipetted into an excess amount of NaOH (aq) which had been standardized with $KHC_8H_4O_4$. The concentration of the NaOH (aq) stock solution was roughly 0.1 M. The solution was stirred vigorously with a magnetic stirrer which resulted in the formation of a fine emulsion of CCl_4 droplets. The fine emulsion facilitated the mass transfer of NO_2 from the CCl_4 phase to the aqueous phase. The solution was stirred for one minute, since this period was determined to be sufficient for complete transfer of NO_2 from the CCl_4 phase to the aqueous phase. Once the NO_2 enters the aqueous phase, it rapidly reacts with the excess base:

$$2\,NO_2\,(aq) + 2\,NaOH\,(aq) \rightarrow NaNO_2\,(aq) + NaNO_3\,(aq) + H_2O\,.$$

The excess NaOH was titrated with standardized HCl (aq) of approximately 0.1 M

concentration using phenolphthalein as an indicator. The NO_2 concentration is then given by

$$c_{NO_2} = 1000.0\,(V_0 c_{NaOH} - V c_{HCl}), \quad \text{where} \tag{3.4.28}$$

c_i = the concentration of species i (mol/l),

V_0 = the volume of $NaOH\ (aq)$ initially used (ml), and

V = the volume of $HCl\ (aq)$ needed to neutralize the excess NaOH (aq).

The concentration of NO_2 in the solvent as a function of time for those runs utilizing CCl_4 as the solvent is tabulated in Table 3–16.

3.4.2 Analysis of the Gaseous Species

As shown in Figure 3–1, the gaseous species produced in the runs with continuous NO_2 flow were conducted to the gas chromatograph equipped with the automatic gas sampling valve. The samples were injected every 10 minutes. The samples were separated on a 12 foot by 0.125 inch column packed with Porapak Q (80 to 100 mesh) at 25°C. As expected, the major component for those runs using water as the solvent was NO, although NO_2 did begin to appear after the concentration of HNO_3 approached roughly 12 M. The primary purpose of the GC analysis, however, was to detect any volatile sulfur compounds. The flame photometric detector did not detect any gaseous sulfur species when either water or CCl_4 was the solvent. Therefore, the GC analysis was discontinued after the first run using CCl_4 as the solvent. The fundamental conclusion is that any sulfur removed from the coal must reside in the solvent, which is really not surprising since even if all of the sulfur were removed from the coal, the sulfur content of the solvent would be only about 0.05 % by mass.

TABLE 3-18

Concentrations of NO_2 for Runs Using CCl_4 as the Solvent							
Reaction Time (min)	Run Number						
	21	22	23	24	25	26	27
0	0.0	0.0	0.0	0.0	0.0	0.0	0.0
15	0.519	0.404	0.367	0.526	0.399	0.258	0.359
30	1.206	1.046	1.054	1.164	1.077	0.858	1.134
45		1.824	1.617	1.671	1.945	2.152	1.904
60		2.824	2.619	2.507	2.654	3.140	2.956
75			3.310	-	3.496	4.004	3.555
90			4.058	3.880	4.203	4.830	4.304
105				-	4.998	5.526	4.959
120				4.998	5.610	6.120	-
135							6.314
150							6.837
165							7.661
180							8.221
Mean NO_2 Flowrate (g/min)	1.233	1.203	1.224	1.153	1.195	1.420	1.246

All concentrations are in units of (mol/l)

TABLE 3-18 (continued)

Concentrations of NO_2 for Runs Using CCl_4 as the Solvent					
Reaction Time (min)	Run Number				
	28	29	30	31	32
0	1.299	1.233	1.276	1.212	1.305
15	1.088	1.067	1.073	0.974	-
30	1.200	1.154	1.158	1.133	1.063
45		-	1.181	1.160	-
60		1.177	1.192	1.187	1.179
75			1.208	-	-
90			1.202	1.206	1.131
105				-	-
120				1.189	1.171
135					-
150					1.200
165					-
180					1.204

All concentrations are in units of (mol/l)

TABLE 3-18 (continued)

Concentrations of NO_2 for Runs Using CCl_4 as the Solvent					
Reaction Time (min)	Run Number				
	33	34	35	36	37
0	1.122	1.058	1.081	1.087	1.091
15	0.880	0.843	0.876	0.849	0.911
30	0.763	0.763	0.810	0.837	0.861
45		0.792	0.808	0.802	0.835
60		0.714	0.792	0.798	0.802
75			0.792	0.748	0.794
90			0.769	0.752	0.771
105				0.738	0.732
120			0.683	-	
135				0.722	
150				0.705	
165				0.701	
180				0.705	

All concentrations are in units of (mol/l)

TABLE 3-18 (continued)

Concentrations of NO_2 for Runs Using CCl_4 as the Solvent					
Reaction Time (min)	Run Number				
	38	39	36	40	41
0	0.0972[1]	0.488	1.087	1.713	1.874
15	0.0317	0.369	0.849	1.433	1.568
30	0.0219	0.336	0.837	1.318	1.519
45	0.0206	0.319	0.802	1.285	1.490
60	0.0151	0.301	0.798	1.274	1.471
75	-	0.301	0.748	1.240	1.428
90	0.0110	0.273	0.752	1.246	1.465
105	0.0106	0.280	0.738	1.238	1.443
120	0.0124	0.280	0.683	1.234	1.434

All concentrations are in units of (mol/l)

[1] For this run, both the HCl(aq) and NaOH(aq) were diluted to about 0.01 M.

TABLE 3-18 (continued)

Concentrations of NO_2 for Runs Using CCl_4 as the Solvent					
Reaction Time (min)	Run Number				
	42	43	44	45	46
0	0.985	1.040	1.008	1.048	1.028
15	0.783	0.857	0.811	0.886	0.876
30	0.746	0.798	0.764	0.842	0.800
45		0.796	0.767	0.815	0.788
60		0.760	0.741	0.800	0.788
75			0.693	0.794	0.769
90			0.718	0.788	0.759
105				0.764	0.742
120				0.773	0.746
135					0.730
150					0.738
165					0.703
180					0.728

All concentrations are in units of (mol/l)

TABLE 3-18 (continued)

Concentrations of NO_2 for Runs Using CCl_4 as the Solvent					
Reaction Time (min)	Run Number				
	48	49	50	51	52
0	1.044	1.048	1.097	1.090	1.074
15	0.892	0.904	0.913	0.967	0.891
30	0.791	0.818	0.894	0.906	0.891
45		0.766	0.871	0.868	0.857
60		0.719	0.839	0.852	0.830
75			0.812	0.841	0.794
90			0.761	0.816	0.788
105				0.789	0.783
120				0.755	0.761
135					0.757
150					0.766
165					0.766
180					0.723

All concentrations are in units of (mol/l)

Run 47 was a blank run and is therefore not listed in the table.

3.4.3 Analysis of the Coal

3.4.3.1 Carbon, Hydrogen and Nitrogen Analysis of the Coal

The coal from Runs 1-6 was not analyzed for C, H or N. The coal from Runs 7-27 was analyzed for C, H and N by the Caltech Microanalytical Laboratory. A 2-3 mg sample of coal was combusted in a stream of oxygen. The amount of CO_2 and H_2O produced was determined. The NO_x produced was converted to N_2 by passing the NO_x over a bed of copper metal. Duplicate analyses were performed on the NO_2 treated coal samples. The fact that the duplicate analyses usually agreed within 1 percent indicates that even 2 to 3 mg samples are representative of the bulk coal, which is not unexpected because the coal consists of particles between 200 and 325 mesh. If the particles are assumed to be spherical with a radius of 50 μm and a density of 1.3 g/cm^3, then 1 mg consists of roughly 2500 particles, which should provide a fairly representative sampling of the bulk coal.

The C and H contents of the coal from Runs 28-52 were determined by the Analytical Services Laboratory of the Colorado School of Mines Research Institute. In this case, approximately 0.1 g of the coal was combusted in a stream of oxygen and the amount of CO_2 and H_2O produced was measured. The N content of the coal from Runs 28-52 was determined by Galbraith Laboratories, Inc. Approximately 15 mg of coal were used in the N determination using the Dumas method. The Dumas method is necessary because much of the nitrogen in the NO_2 treated coal is in the form of -NO and/or -NO_2 groups. The Kjeldahl method suffers from the inability to convert all organic -NO_x groups to NH_3. Therefore, a Kjeldahl analysis grossly underestimates the nitrogen content of the NO_2 treated coals. On the other hand, the Dumas method is ideally suited to the determination of the nitrogen content of NO_2 treated coals because this method relies on the easy and complete conversion of coal nitrogen to NO_x via combustion. The

TABLE 3-19

Elemental Analysis of the Treated Coal Samples

Run #	Mass Gain (%)	Ash (%)	C (%)	H (%)	N (%)	Cl (%)	S_{LECO} (%)	S_{BOMB} (%)	Heating Value Btu/lb_m
1	- 14.4						1.75± 0.02		11,800
2	- 13.2						1.62± 0.01		12,000
3	- 22.8						1.75± 0.02		12,200
4	- 16.2						1.26± 0.06		10,500
5 Coal	- 37.6						1.38± 0.01		9,200
5 Extract	54.1						0.59± 0.01		9,200
6 Coal	- 54.6						1.63± 0.01		8,500
6 Extract	38.6						1.73± 0.02		8,600
7	- 15.84	6.76± 0.27	67.89	4.69	1.21		2.52± 0.01		12,200
8	- 14.48						2.30± 0.02		11,860
9	- 13.89						2.12± 0.02		11,420
10	- 12.66						2.06± 0.01		11,580
11	- 11.79						2.00± 0.01		11,320
12	- 10.33		62.52	3.83	3.91		1.75± 0.01		10,850
13	- 12.71						1.55± 0.01		10,070
7C	- 24.29						2.24± 0.02		12,910
8C	- 21.47						1.91± 0.03		12,360
9C	- 22.93						1.59± 0.02		11,370
10C	- 21.40						1.46± 0.03		11,660
11C	- 26.68						1.12± 0.00		11,150
12C	- 15.82						0.51± 0.03		11,160
13C	- 19.47						0.13± 0.02		9,860
15	- 17.56	6.74± 0.13					2.07± 0.02		12,210
16	- 17.43	6.58± 0.25					2.13± 0.02		11,780
17	- 15.52	6.04± 0.28					1.94± 0.01		11,230
18	- 14.47	5.48± 0.21					1.84± 0.02		11,220
19	- 13.86	5.51± 0.21					1.73± 0.00		9,970
20	- 13.70	5.04± 0.17					1.68± 0.02		10,670

TABLE 3-19 (continued)

Elemental Analysis of the Treated Coal Samples									
Run #	Mass Gain (%)	Ash (%)	C (%)	H (%)	N (%)	Cl (%)	S_{LECO} (%)	S_{BOMB} (%)	Heating Value Btu/lb_m
15C	- 20.72						1.48± 0.06		
16C	- 20.95						1.53± 0.05		12,100
17C	- 19.63						0.98± 0.03		11,310
18C	- 17.55						0.62± 0.01		10,730
19C	- 17.78						0.41± 0.04		
20C	- 18.64						0.40± 0.02		
21	9.69	5.95	55.98	3.50	3.77	1.58	2.48± 0.01	2.41	9,430
22	11.56	5.69	53.62	3.28	4.26	2.74	2.26± 0.04	2.41	9,420
23	16.53	4.79	52.36	3.08	4.40	3.95	2.10± 0.04	2.57	8,740
24	14.95	6.00					2.07± 0.04		9,020
25	17.23	5.93	51.64	2.97	4.38	4.36	2.11± 0.02	2.19	8,500
26	33.51	6.02					1.75± 0.03	2.10	7,700
27	17.27	5.80	51.17	3.02	4.58	4.42	2.13± 0.04	2.21	8,410
21C	1.19	14.14	54.71	3.56	3.42	0.34	0.70± 0.01	1.72	9,620
22C	1.04	15.94	51.65	3.14	3.76	0.53	0.47± 0.04	1.64	9,250
23C	3.33	15.97	51.00	3.38	4.00	0.47	0.33± 0.01	1.64	9,040
24C	-2.35						0.30± 0.01		9,020
25C	1.32	15.04	48.81	3.21	3.96	0.32	0.11± 0.02	1.61	8,860
27C	1.01	15.22	48.99	3.25	4.11	0.55	0.11± 0.01	1.59	8,780
28	21.06	7.15	53.9	3.46	4.61	3.16	2.04± 0.02	2.28	8,780
29	21.55	7.19	53.2	3.34	4.84	3.77	2.02± 0.03	2.11	8,590
30	26.93	6.53	51.2	3.45	5.11	4.78	1.85± 0.08	2.18	8,140
31	25.80	5.59	50.8	3.43	4.81	4.40	1.85± 0.05	2.16	8,200
32	28.93	8.19	49.6	3.30	5.02	4.95	1.78± 0.05	2.14	7,610

TABLE 3-19 (continued)

Elemental Analysis of the Treated Coal Samples

Run #	Mass Gain (%)	Ash (%)	C (%)	H (%)	N (%)	Cl (%)	S_{LECO} (%)	S_{BOMB} (%)	Heating Value Btu/lb_m
28C	4.14	4.54	57.5	3.88		0.45	1.461± 0.011	1.57	9,220
29C	4.72	5.01				0.62	1.467± 0.008		8,950
30C	7.94	4.41	54.8	3.85		0.59	1.380± 0.015	1.44	8,800
31C	5.04	3.76	56.7	3.83		0.51	1.405± 0.032	1.48	8,670
32C	5.42	3.60	54.6	3.62		0.60	1.299± 0.036	1.44	8,530
33	13.02	6.35	61.0	3.74	3.91	1.34		2.01	9,750
34	14.55	6.40	59.4	3.52	4.15	1.70		2.01	9,590
35	16.67	6.19	58.3	3.44	4.33	2.18		2.02	9,250
36	16.86	6.29	58.1	3.33	4.35	2.10		1.99	9,290
37	15.63	6.39	58.4	3.17	4.21	2.47		2.01	9,160
33C	8.52	14.95	59.9	3.65	3.56	0.074	0.204± 0.008	1.74	9,650
34C	9.20	15.63	59.6	3.46	3.76	0.038	0.196± 0.032	1.73	9,560
35C	10.14	15.97	58.4	3.44	3.85	0.048	0.133± 0.024	1.66	9,510
36C	10.92	15.74	58.2	3.52	4.05	0.078	0.096± 0.038	1.68	9,520
37C	10.22	16.30	57.3	3.34	4.08	0.114	0.096± 0.075	1.62	9,380
38	5.69	6.52	64.3	4.12	2.88	0.25		2.10	11,470
39	12.72	6.17	60.8	3.82	3.95	1.03		2.04	9,690
36	16.86	6.29	58.1	3.33	4.35	2.10		1.99	9,290
40	22.81	6.17	57.1	3.58	4.74	3.87		1.89	8,910
41	20.74	5.96	57.3	3.63	4.68	3.10		1.91	8,920
38C	3.29	11.81	63.8	3.80	2.60	0.080	1.202± 0.055	1.62	10,770
39C	7.90	15.09	59.7	3.61	3.60	0.074	0.355± 0.055	1.74	9,830
36C	10.92	15.74	58.2	3.52	4.05	0.078	0.096± 0.038	1.68	9,520
40C	11.45	21.46	58.2	3.23	4.30	0.029	0.146± 0.047	1.55	9,080
41C	10.95	18.54	57.4	3.34	4.18	0.022	0.132± 0.042	1.64	9,160

TABLE 3-19 (continued)

Elemental Analysis of the Treated Coal Samples									
Run #	Mass Gain (%)	Ash (%)	C (%)	H (%)	N (%)	Cl (%)	S_{LECO} (%)	S_{BOMB} (%)	Heating Value Btu/lb_m
42	11.54	7.08	64.6	4.68	3.51	1.42		2.12	10,310
43	14.12	6.63	61.1	4.69	3.83	1.87		2.07	10,020
44	14.40	6.45	58.4	3.30	4.00	1.84		2.02	10,140
45	15.82	6.42	57.4	2.76	4.07	2.35		2.06	10,040
46	16.20	6.44	60.7	4.19	4.13	2.59		2.02	9,700
42C	6.78	14.26	62.0	3.91	3.22	0.114	0.883± 0.008	1.69	10,220
43C	8.17	14.86	60.9	3.92	3.62	0.168	0.529± 0.010	1.62	9,920
44C	8.72	15.23	61.3	3.82	3.58	0.145	0.535± 0.014	1.63	9,900
45C	9.41	15.95	60.2	3.77	3.65	0.188	0.437± 0.006	1.76	9,860
46C	10.36	9.61	61.0	3.54	3.76	0.168	0.337± 0.043	1.62	9,980
47	-2.08	10.79	70.8	4.87	1.40	0.098		3.27	12,530
48	7.79	9.47	64.9	4.33	3.27	0.788		2.80	11,060
49	10.63	9.67	63.2	4.31	3.71	1.030		2.78	10,730
50	12.13	9.63	62.2	4.16	3.92	1.202		2.77	10,570
51	14.33	9.22	60.8	4.13	4.02	1.634		2.77	10,340
52	15.67	9.50	59.2	3.92	4.50	2.025		2.73	10,070
47C	-5.94	11.37	71.1	4.94	1.47	0.050	3.591± 0.029	3.21	
48C	3.89	13.11	65.7	4.31	2.96	0.077	2.760± 0.044	2.84	11,420
49C	5.92	14.41	63.9	4.18	3.39	0.106	2.575± 0.024	2.60	11,060
50C	7.07	14.98	62.7	3.90	3.71	0.102	2.496± 0.002	2.85	10,670
51C	8.63	14.26	62.2	3.89	3.69	0.114	2.163± 0.016	2.45	10,460
52C	10.98	14.47	60.8	3.88	3.97	0.264	2.014± 0.004	2.38	10,310

NO_x is then converted to N_2 and the amount of N_2 produced is then determined. The C, H and N contents of all of the runs can be found in Table 3–19.

3.4.3.2 Determination of the Ash Content of the Coal

Approximately 50 mg of coal were placed in a tared porcelain boat. The boat had been predried at 750°C and placed in a dessicator to cool. The boat and coal were placed in the combustion tube of the Leco Resistance Furnace shown in Figure 3–6. The temperature used for the determination was 750°C. A stream of oxygen (0.5 l/min) was passed through the tube for 10 minutes, then the boat was removed and allowed to cool in a dessicator. It had been determined that 10 minutes was more than adequate for the complete combustion of the coal sample. After the boat had cooled, it was weighed. The ash content is given by the following formula:

$$Mass\ \%\ Ash \equiv 100\ \frac{m_i - m_f}{m_s}, \quad \text{where} \tag{3.4.29}$$

m_f = the mass of the boat and ash (g),

m_i = the mass of the boat and uncombusted coal (g), and

m_s = the sample mass (g).

The ash contents of the coal from all of the runs can be found in Table 3–19.

3.4.3.3 The Sulfur Analysis of the Coal

There are two methods commonly used to determine the total sulfur content of coal. One method involves the combustion of coal in a stream of oxygen. The combustion gases then pass through an aqueous HCl solution which absorbs the SO_2 produced via combustion. The amount of SO_2 absorbed is determined by titration with KIO_3 (aq). This method (ASTM E30-47) will be referred to as the Leco method because a Leco Sulfur Analyzer based on this procedure was used. The second method (ASTM D 3177-73) involves mixing the coal with a mixture of

MgO and Na_2CO_3, which is called the Eschka mixture, and igniting the mixture in a bomb under 30 atm of oxygen. The SO_2 produced by combustion is absorbed by the Eschka mixture and converted to sulfate. The residue in the bomb is leached with hot water and the sulfate is precipitated as $BaSO_4$. After the $BaSO_4$ is filtered and dried, it is weighed to give the sulfur content gravimetrically. This second method will be referred to as the Bomb method. Both methods are discussed in more detail below.

3.4.3.3.1 The Leco Method

Approximately 50 mg of coal were burned in a stream of oxygen (1.0 l/min) at 1200°C in a Leco Resistance Furnace, Model 571-018 equipped with a titrator as shown in Figure 3–6. The combustion gases were then bubbled through an aqueous HCl solution (15 ml concentrated HCl/l solution) to which approximately 2 ml of starch indicator (2 g starch + 6 g KI + 150 ml H_2O) were added. The reactions which occur in the solution are:

$$KIO_3 + 5\,KI + 6\,HCl = 6\,KCl + 3\,I_2$$

$$SO_2 + I_2 + H_2O = H_2SO_4 + 2\,HI$$

$$I_2 + Starch = Blue\ Color$$

The solution is titrated with 0.001 M KIO_3 (aq) in a manner such that the solution stays a light blue which corresponds to a slight excess of KIO_3 (aq). It should be noted that at 1200°C, about 1 % of the sulfur in the coal is oxidized to SO_3 rather than SO_2. Therefore, the system was calibrated at least once a day using a coal (NBS-1631-C) with a sulfur content of 3.02 % by mass. Four sulfur determinations were made on the NO_2-treated coals while three sulfur determinations were made on the NO_2-treated coals washed with Na_2CO_3 (aq). The results are shown in Table 3–19 in the column headed S_{LECO}. Since the coals treated with NO_2 in CCl_4 had up to 5 % chlorine by mass, the modification suggested by Bremanis was used.[4] The author claims that the addition of roughly

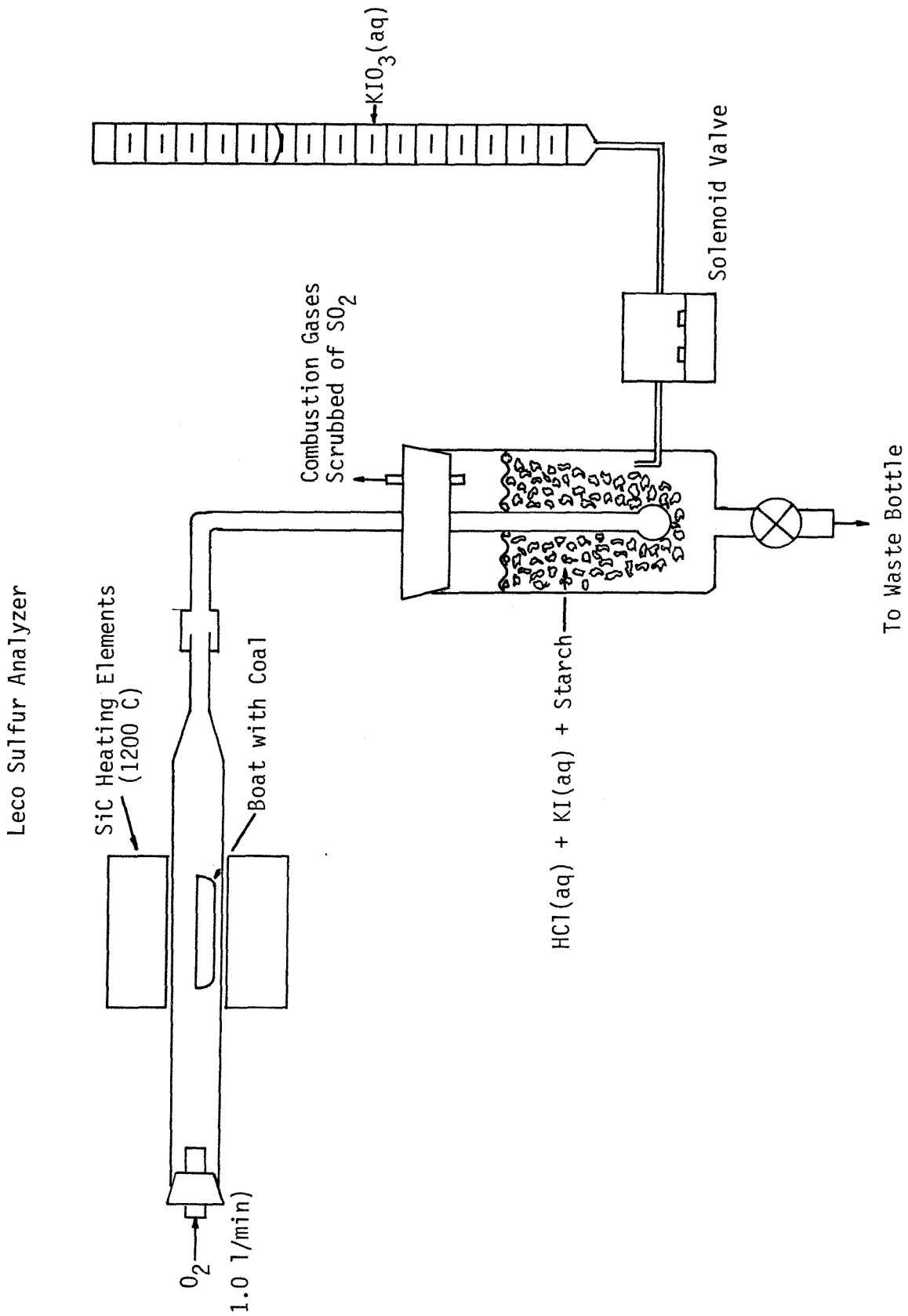
Leco Sulfur Analyzer
SiC Heating Elements (1200 C)
Boat with Coal
O_2 (1.0 l/min)
KIO_3(aq)
Combustion Gases Scrubbed of SO_2
Solenoid Valve
HCl(aq) + KI(aq) + Starch
To Waste Bottle

Figure 3-6

1 g NaN_3 to the titration vessel eliminates both chlorine and nitrogen interferences. Therefore, NaN_3 was added to the titration vessel when the coal from Runs 21-52 was analyzed. There was little difference in the sulfur determinations, however, whether or not NaN_3 was used, even though the levels of nitrogen and chlorine in the treated coals are substantial.

3.4.3.3.2 The Bomb Method

Because chlorine can cause an interference in the Leco method, the sulfur contents of the coal from Runs 21-52 were determined using the Bomb method. These analyses were performed by the Analytical Services Laboratory of the Colorado School of Mines Research Institute. The results are tabulated in Table 3–19 under the column headed S_{BOMB}. The basic procedure involves mixing about 1 g of coal with 3 g of Eschka mixture (2 g calcined MgO + 1 g anhydrous Na_2CO_3). Approximately 1 g of this mixture is then placed in a bomb calorimeter, which is then filled to 30 atm with oxygen. The bomb is placed in a water bath, the mixture is ignited and the bomb is allowed to cool for at least 10 minutes. The pressure is then slowly released and the bomb and the residue are washed thoroughly with hot water. The residue is allowed to digest with hot water for about one hour. The solution is filtered and the insoluble residue is washed at least five times with hot water. After further treatment, excess $BaCl_2$ (aq) is added to precipitate $BaSO_4$, which is then filtered, dried and weighed. It is important to note that in the Leco method, some of the sulfur may potentially be trapped by the ash, whereas in the Bomb method, all of the sulfur is trapped by the Eschka mixture as water soluble sulfate.

3.4.3.3.3 Analysis for Forms of Sulfur

Since the washed and dried PSOC 190 coal contains mainly organic sulfur and only about 0.25 % pyritic sulfur, only total sulfur analyses of the treated coal

were performed. The PSOC 276 coal, however, contains roughly 2.3 % pyritic and 1.2 % organic sulfur, it was necessary to determine the amount of sulfate, pyritic and organic sulfur in the treated coals (ASTM D2492-68).

The determination of sulfate requires the leaching of the coal with boiling HCl (aq) (2 parts concentrated HCl + 3 parts H_2O) for 30 minutes. The coal is filtered and washed six more times with hot, dilute HCl (aq) (1 part concentrated HCl + 23 parts H_2O). The ASTM procedure dictates that the sulfate-sulfur content is determined by measuring the iron content of the leach solution and assuming that all of the sulfate is in the form of ferric sulfate. It is doubtful that all of the sulfate exists as ferric sulfate, however. Therefore, this procedure was modified so that the sulfate sulfur is determined by precipitating the sulfate in the leach solution as $BaSO_4$, using the procedure described in the determination of the total sulfur content. This procedure is obviously superior to the ASTM procedure because the sulfur is determined directly.

The residual coal from the sulfate determination is then leached with HNO_3 (aq) (1 part concentrated HNO_3 + 7 parts H_2O) overnight at room temperature. The coal is then filtered and washed six times with more HNO_3 (aq). Once again, the ASTM procedure determines the pyritic sulfur by measuring the amount of iron in the leach solution. The procedure was again modified, however, so that the pyritic sulfur content of the coal was given by $BaSO_4$ precipitation. It is possible that the pyrite may react during NO_2 treatment resulting in sulfur removal. The iron may remain in the coal, however, and then be leached during the pyrite determination, which would lead to a high pyrite determination if the ASTM procedure is used.

The organic sulfur content of the coal is then given by the difference between the total sulfur content and the sum of the pyritic and sulfate sulfur contents. These analyses were performed by the Analytical Services Laboratory of the

Colorado School of Mines Research Institute. The results of the forms of sulfur analyses can be found in Table 3–20.

3.4.3.4 The Chlorine Analysis of the Coal

As mentioned above, Runs 21-52 employed CCl_4 as the solvent during the NO_2 treatment. In order to determine whether all of the solvent was being removed by the vacuum drying, these coals were analyzed for their chlorine content. The procedure used (ASTM D2361-66) is quite straightforward. Approximately 0.5 g of coal was mixed with 0.5 g of Eschka mixture (2 parts calcined MgO + 1 part anhydrous Na_2CO_3) and placed in a bomb whose interior was coated with 5 ml of $(NH_4)_2CO_3$ (aq) (10 g $(NH_4)_2CO_3$–H_2O/100 ml H_2O). The bomb was filled to 30 atm with oxygen and placed in a water bath. The mixture was ignited and the bomb was allowed to cool for at least 10 minutes. The pressure was slowly released and the interior of the bomb was thoroughly washed with hot water. The washings were transferred to a 250 ml beaker and acidified by adding 3 ml concentrated nitric acid. Then 25.00 ml of 0.025 N $AgNO_3$ (aq) were added. The Cl^- present then precipitated as AgCl (s). The $AgNO_3$ (aq) solution was made by weighing about 4.25 g of $AgNO_3$, which had been dried overnight at 125°C, to 0.1 mg and mixing with H_2O in a one liter volumetric flask. After the $AgNO_3$ (aq) was added, the solution was stirred and allowed to stand for 15 minutes. Then 5 to 10 ml of nitrobenzene were added and the solution was stirred vigorously to form an emulsion. The excess $AgNO_3$ was titrated with 0.025 N KCNS (aq) using 8 to 10 drops of $FeNH_4(SO_4)_2$ (aq) as an indicator. The KCNS (aq) titrant was standardized with the $AgNO_3$ (aq) solution. The surface of the nitrobenzene droplets serves as a sink for the AgCNS as it is formed. It is possible to form an $(AgCNS)^+$ species which could then accept another CNS^- to form $Ag(CNS)_2$. The presence of the nitrobenzene surface, however, inhibits the formation of the $Ag(CNS)^+$ species, thus ensuring a one-to-one correspondence between CNS^- and

TABLE 3-20

Analysis for Forms of Sulfur for Treated PSOC 276 Coal					
Run #	Time (min)	Mass Percent Sulfur			
		Pyritic	Sulfate	Organic	Total
Raw PSOC 276		2.12	0.14	0.94	3.20
47	0	2.28	0.13	0.86	3.27
48	30	1.88	0.19	0.73	2.80
49	60	1.77	0.20	0.81	2.78
50	90	1.74	0.21	0.82	2.77
51	120	1.80	0.21	0.76	2.77
52	180	1.64	0.25	0.84	2.73
47C		1.92	0.12	1.17	3.21
48C		1.97	0.08	0.79	2.84
49C		1.82	0.07	0.71	2.60
50C		1.75	0.06	1.04	2.85
51C		1.60	0.06	0.79	2.45
52C		1.72	0.07	0.59	2.38

Ag^+. The chlorine content of the coal is given by

$$Mass\ \%\ Cl = \frac{3.5453}{m}(V_0\, c_{AgNO_3} - V\, c_{KCNS}), \quad \text{where} \qquad (3.4.30)$$

m = the sample mass (g),

c_{KCNS} = the $KCNS$ concentration (mol/l),

c_{AgNO_3} = the $AgNO_3$ concentration (mol/l),

V_0 = the volume of $AgNO_3\,(aq)$ used (ml), and

V = the volume of $KCNS\,(aq)$ needed to titrate the excess $AgNO_3\,(aq)$ (ml).

The results of the chlorine analyses can be found in Table 3–19.

3.4.3.5 The Analysis of the Heating Value of the Coal

The procedure used for determining the heating value of the coal follows the ASTM D 2015-66 procedure. An adiabatic bomb calorimeter manufactured by the Parr Instrument Company was used. Approximately 0.5 g of coal was weighed to the nearest 0.1 mg and placed in a metal crucible. The crucible was then placed in the bomb which contained 1.0 ml of water. The bomb was sealed and filled to 30 atm with oxygen. The electrical leads to the ignition system were connected and the bomb was carefully placed in the water bath which contained 2000.0 g of water. The top of the jacket was put in place and the mechanical stirrer was connected. The system was allowed to thermally equilibrate for at least five minutes. As the run commenced (t = 0), the temperature was read every minute to an accuracy of ± 0.001°C. The coal was ignited at t = 5 minutes and the temperature was read 45, 60, 75, 90, 105 and 120 seconds after ignition to an accuracy of ± 0.005°C. After t = 7 minutes, the temperature was again read every minute to an accuracy of ± 0.001°C. Such reading continued until the temperature was constant or changed at a constant rate, which usually

occured at about t = 15 minutes. After the run was completed, the mechanical stirrer was disconnected and the jacket top was removed. The bomb was removed from the water bath and the bomb pressure was released over a three minute period. The bomb interior was washed with water thoroughly. The washings were collected in a beaker and titrated with Na_2CO_3 (aq) (20.9 g anhydrous Na_2CO_3/l) using methyl orange as an indicator to determine the correction for the formation of HNO_3. The length of unburned fuse was measured to determine the fuse correction. The heating value of the coal is given by:

$$H_g = \frac{1.8}{m}[W(\Delta T) - e_1 - e_2 - e_3], \quad \text{where} \tag{3.4.31}$$

H_g = the heating value of the coal (Btu/lb_m),

m = the sample mass (g),

e_1 = $23.0 - x(2.3)$ = the fuse correction (cal), where

x = the length of the unburned fuse (cm),

e_2 = $14.00\, m\, S$ = the correction for H_2SO_4 formation, where

S = the mass % sulfur in the coal,

e_3 = $0.2658\, c_{Na_2CO_3}\, V$ = the correction for HNO_3 formation, where

$c_{Na_2CO_3}$ = the Na_2CO_3 (aq) concentration (g Na_2CO_3/l), and

V = the volume of $Na_2CO_3(aq)$ required in the titration (ml),

W = a system constant (cal/g), and

ΔT = $T_f - T_i - r_f(t_f - t_{60}) - r_i(t_{60} - t_i)$ = the temperature change (C), where

T_f = the temperature at $t = t_f$ (C),

T_i = the temperature at $t = t_i$ (C),

r_f = the final, constant rate of change in the temperature (C/min),

r_i = the initial, constant rate of change in the temperature (C/min),

t_f = the time at which the final, constant rate of change in temperature begins (min),

t_i = the time at which the coal is ignited (min), and

t_{60} = the time at which the temperature rise is 60% of the total temperature rise (min).

The results of the heating value determinations are given in Table 3–19. The system constant W was determined by calibrating the calorimeter with benzoic acid, which has a heating value of 11,373 Btu/lb_m.

3.4.4 Analysis of the Surface Area and Pore Size Distribution of the Coal

The apparatus used for the surface area analysis is shown in Figure 3–7. It consists of two dosing chambers, a gas reservoir, a sample chamber and various outlets. The various gas pressures were measured with a Wallace and Tiernan Model FA 145 mechanical gauge, which measured from 0 to 1 atm with an accuracy of 0.01 in Hg. During the course of a run, the gauge case was continually evacuated to ensure as complete a vacuum as possible. The pressure was also monitored with an Edwards Model 8/2 Pirani gauge. This gauge had an effective range from 0.0001 to 1 torr. This gauge was used primarily to monitor the pressure during sample preparation and the mechanical gauge case pressure during the run. During the run, the gauge case pressure was maintained below 0.05 torr, which is well within the accuracy of the mechanical gauge (about 0.25 torr).

The volume of the primary dosing chamber, which is adjacent to the sample chamber, was determined by gas exchange with the secondary dosing chamber, whose volume was determined by gas exchange with a bulb of known volume. The bulb consisted of a 100 ml round bottom boiling flask joined to a high vacuum stopcock. The bulb volume was measured by first evacuating it on the

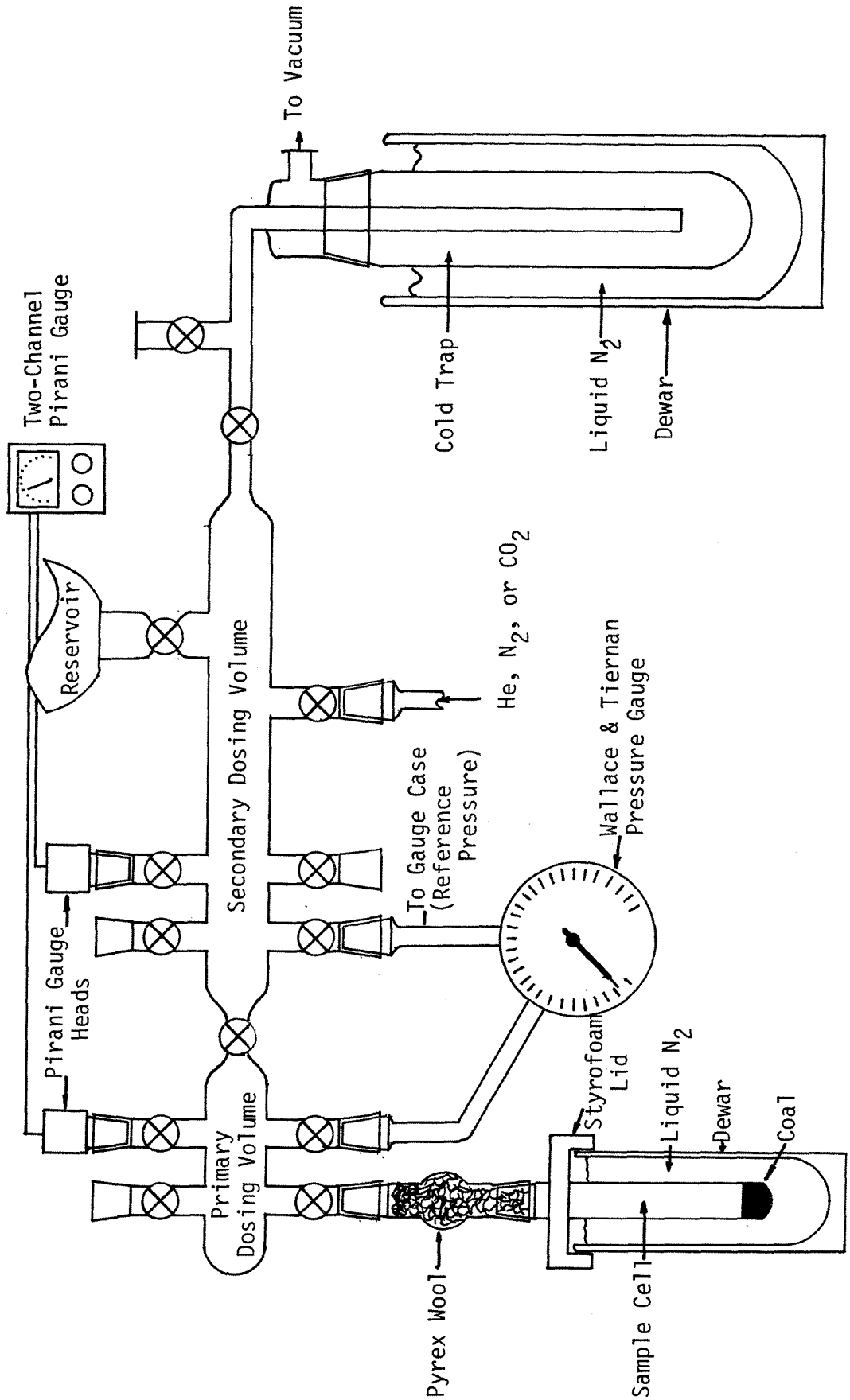
Gas Adsorption Apparatus
To Vacuum
Two-Channel Pirani Gauge
Cold Trap
Liquid N_2
Dewar
Reservoir
Secondary Dosing Volume
He, N_2, or CO_2
To Gauge Case (Reference Pressure)
Wallace & Tiernan Pressure Gauge
Pirani Gauge Heads
Primary Dosing Volume
Styrofoam Lid
Liquid N_2
Dewar
Coal
Pyrex Wool
Sample Cell

Figure 3-7

vacuum rack and then weighing it. The bulb was then placed in a water bath at 29.55°C. The stopcock was opened and the bulb was allowed to fill with reagent grade acetone. The filled bulb was allowed to thermally equilibrate for ten minutes. The stopcock was then closed and all surfaces of the bulb exposed to the exterior were dried. The bulb was then weighed. Since the density of acetone at 29.55°C is 0.77928 g/cm^3,[5] the volume of the bulb was determined to be 97.528 ± 0.008 g/cm^3. Once the bulb volume was known, determination of the volume of any portion of the vacuum rack was quite simple. In this case, the bulb was connected to the secondary dosing volume and filled with nitrogen to some pressure determined with the mechanical gauge. The bulb stopcock was then closed and the rest of the system was evacuated. The primary and secondary dosing volumes were then isolated from the vacuum pump and the bulb stopcock was then opened. Assuming ideal gas behavior,

$$V_{ps} = \frac{P_b}{P_{ps}} V_b \,, \quad \text{where} \tag{3.4.32}$$

V_{ps} = the total volume of the bulb and primary and secondary dosing volumes (cm^3),

P_b = the pressure of N_2 in the bulb initially (in Hg),

P_{ps} = the final pressure in the system (in Hg), and,

V_b = 97.528 cm^3 = the bulb volume (cm^3).

The average of three determinations yielded a value for V_{ps} of 614.43 ± 0.56 cm^3. Following a similar procedure, the volume of the primary dosing volume was determined to be 205.29 ± 0.62 cm^3.

Although the coal samples were previously dried, they were vacuum dried before a surface area determination at 110 to 120°C overnight. Generally, 0.3 to 0.4 g of sample were used in the determination. Typically, a pressure less than 0.010 torr could be maintained over the sample after such drying, which

indicates the removal of virtually all of the light volatile material in the coal samples. The dead volume of the sample cell containing the coal was determined using helium and employing the gas exchange procedure described above with the primary dosing volume. Generally two determinations of the dead volume were made. The atmospheric pressure, which was equal to the vapor pressure of the liquid nitrogen in the dewar in which the sample cell was immersed, was measured by simply filling the two dosing volumes with nitrogen in excess of 1 atm and then opening the system to the atmosphere and reading the mechanical gauge pressure. The system was then purged with nitrogen, closed to the atmosphere and evacuated to less than 0.01 torr in order to eliminate any atmospheric contamination.

The general procedure for nitrogen adsorption involved obtaining roughly 7 to 10 adsorption points between the relative pressures of 0.0 and 0.4. These points were used in the BET calculations. Usually another 7 to 10 points were needed to obtain the final adsorption point which was generally between a relative pressure of 0.98 to 1.00. Finally, about 12 to 18 desorption points were obtained down to a relative pressure of roughly 0.3. These desorption points were used to obtain the pore size distribution. In order to complete the determination of the adsorption-desorption isotherms in a reasonable amount of time (about 12 hrs), 15 minutes were allowed for equilibrium to be attained. At the beginning of each point determination, the sample dewar was refilled to overflowing with liquid nitrogen in order to ensure that the sample cell was immersed to the same depth of liquid nitrogen for each measurement.

The accuracy of this procedure was examined by applying it to two samples of known surface area. The first standard examined was a porous rubber (SCI-IUPAC-NPL Vulcan 3-G(2700), Code No. 2A/32/1) which had a predetermined surface area of 71.3 ± 2.7 m^2/g. The procedure described above gave a valu

73.2 ± 0.5 m^2/g, which is within the range quoted. The second standard was a silica (SCI-IUPAC-NPL Gasil Silica (1), Code No. 8A/31/32) which had a predetermined surface area of 286.1 ± 3.5 m^2/g. The procedure described above yielded values of 238.0 ± 0.3 m^2/g and 240.5 ± 0.3 m^2/g. Although the values obtained are lower than the quoted value, previous workers have obtained values around 240 m^2/g.[6] It may be that this standard has been contaminated with water, the removal of which would be quite difficult due to the fine pore structure of the silica coupled with the highly polar surface. Therefore, results obtained with this standard should probably be used only for approximate comparisons. The fact that the surface area obtained for the Vulcan standard agrees so well with the quoted value indicates that the procedure is acceptable.

The results of the nitrogen adsorption studies can be found in Appendix A. The data are presented graphically in the form of adsorption-desorption isotherms. The plots of the BET parameters ($\frac{P}{P_0}$ and $\frac{P}{V(P_0 - P)}$) as well as the pore size distributions are in Appendix A as well.

The CO_2 adsorption studies were conducted at room temperature. As mentioned in the previous chapter, higher temperatures should favor faster equilibration between the bulk and adsorbed CO_2 phases. Since the vapor pressure of CO_2 at room temperature is roughly 63.5 atm, the relative pressure range which could be examined was 0.000 to 0.016. Although this range is inadequate for the application of the BET theory, it is ideal for the application of the DPR theory.

The procedure employed for the CO_2 adsorption studies is essentially that described for the N_2 adsorption studies. A CO_2 adsorption run was made the day after the N_2 adsorption run for the same sample. After the N_2 run, the sample was evacuated overnight at room temperature. This procedure was adequate to allow the maintenance of a pressure less than 0.01 torr in the system after it

was isolated from the vacuum pump. The dead volume of the sample cell was again determined with helium, but this time at room temperature. Approximately 10 CO_2 adsorption points were taken. Initially, the first two points were spaced about 1 in Hg apart. The pressure spacing between subsequent points was increased by roughly 0.5 in Hg each time so that the final points were roughly 4.0 to 4.5 in Hg apart. This procedure was adopted because the abscissa of the DPR plot is $\log^2 \frac{P}{P_0}$. Therefore, the spacing of the adsorption points on the DPR plot was more even. Five minutes were allowed for equilibration, although no discernible change in pressure could be detected after 2 minutes. The results of the CO_2 adsorption experiments are in Appendix A. The data are presented in the form of DPR plots $\left(\log^2 \frac{P}{P_0} \text{ vs. } \log V\right)$.

3.5 The Examination of the Coal and Ash Using Scanning Electron Microscopy

Examination of the coal particles before and after treatment with NO_2 using the scanning electron microscope (SEM) can reveal the structural changes which occur. Although the nature of the surface of the coal particles precludes any precise quantitative measurements with the SEM, qualitative conclusions can be drawn regarding the effect of the various experimental parameters (e.g., reaction time, temperature, solvent, etc.) on the gross structural properties of the coal.

The SEM used for the examinations was manufactured by International Scientific Instruments, Inc. (Model Super-II) which was equipped with an energy dispersive analyzer of x-rays (EDAX) manufactured by Tracor Northern, Inc. (Model TN-1700). The images of the particles were obtained using secondary electrons. Although the SEM was capable of achieving up to 160,000 magnification, in practice, magnifications above roughly 10,000 could not be attained when coal was being examined. Because coal is mainly carbon and because carbon is such a light element, the electrons in the impinging beam interact more diffusely with coal than with a metal, such as copper. Therefore, obtaining a sharp image is much harder at higher magnifications. Consequently, the best resolution obtainable was about 1000 Å. Since most of the pore structure in coal is composed of micropores (d_p < 15 Å), it was impossible to detect any of the pore openings in the particles.

In addition to the production of backscattered electrons, the interaction of the impinging electron beam also yields x-rays. There are two electron beam-solid interactions which lead to the production of x-rays. They are core scattering, which results in the emission of a continuous spectrum, and inner shell ionization, which yields the characteristic spectrum. The characteristic spectrum allows the qualitative identification of the elements present in the sample. The

basic function of the EDAX is to collect all of the x-rays produced and analyze their energies and present the results in convenient form on a cathode ray tube. A facsimile of a typical EDAX spectrum is shown in Figure 3–8. The EDAX is calibrated using the x-rays generated by aluminum and zirconium or zirconium and gold to fix the energy scale. Once calibrated, the element corresponding to any peak can be readily identified. The interested reader is referred to the excellent text by Goldstein, et.al., for a more detailed discussion of the concepts presented above.[7]

The method of mounting the samples depended upon the size of the coal particles. Particles larger than 100 mesh were mounted on aluminum discs using silver paint as a mortar. Smaller particles were mounted on aluminum discs using two sided Scotch tape. Because particle charging was a problem, particularly with smaller particles, the mounted samples were coated with gold (40 mA for 5 min), which provided a conduction path from the particles to the electrical ground of the SEM. The coating of gold was on the order of 100 Å thick.

For any given sample, usually 15 to 25 separate particles were examined with pictures taken of the most representative. The EDAX spectra usually required 100 to 1000 seconds of data acquisition to yield an acceptable signal to noise ratio. The SEM photographs and EDAX spectra can be found in the appropriate portion of the results and discussion section.

A Typical EDAX Spectrum for a Highly Chlorinated Coal

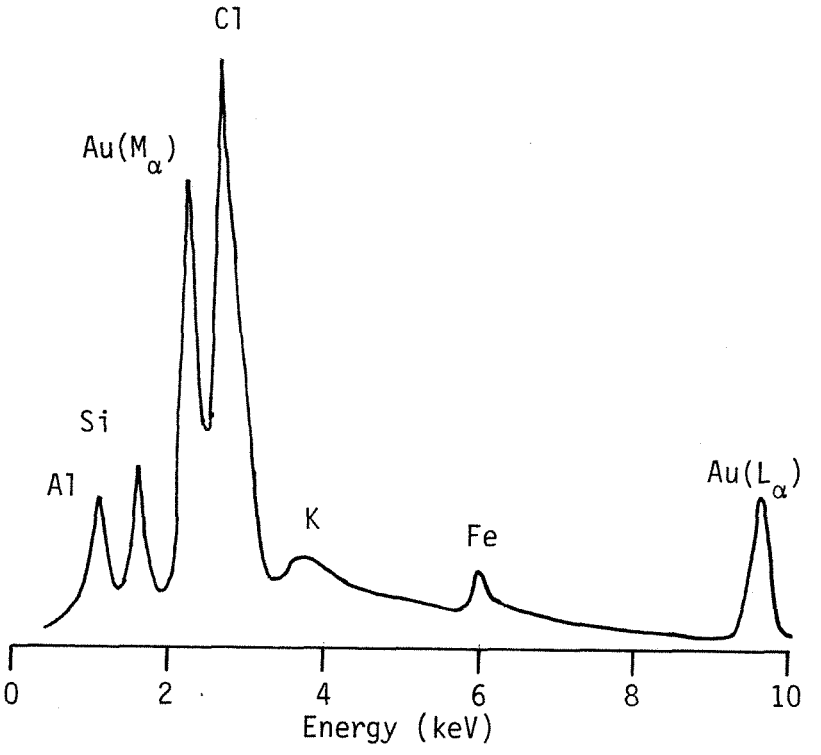

Figure 3-8

References

1. Davis, W., deBruin, H.J., *J. Inorg. Nucl. Chem.*, **26,** 1069 (1964).

2. O'Brien, W.G., Bautista, R.G., 'The Activity Behavior of the $NdNO_3$–HNO_3–H_2O–HDEHP–AMSCO System" in *Thermodynamic Behavior of Electrolytes in Mixed Solvents - II*, Furter, W.F., ed., (Adv. Chem. Ser. 177, Am. Chem. Soc, Washington, D.C., 1979) pp. 323-45.

3. Lumme, P., Tummavuori, J., *Acta. Chem. Scand.*, **19,** 617 (1965).

4. Bremanis, E., et. al., *Materials Research and Standards*, October 1967, 459.

5. Washburn, E.W., ed., *International Critical Tables*, **3,** (McGraw- Hill Book Company, New York, New York, 1928) p. 28.

6. Duncan, T.M., private communication.

7. Goldstein, J.I., Yakowitz, H., eds., *Practical Scanning Electron Microscopy*, (Plenum Press, New York, New York, 1975) 582 pp.

CHAPTER 4

RESULTS AND DISCUSSION

This chapter is divided into three main sections. The first section is concerned with the general aspects of the time histories of the various species of interest in the system. The first section has two subsections, the first of which deals with the concentration histories of the liquid phase components derived from NO_2. For instance, for those runs using H_2O as the solvent, the primary liquid phase species of interest are HNO_3 (aq) and HNO_2 (aq). In those runs using CCl_4 as the solvent, however, the only significant liquid phase species is solvated NO_2. The second subsection discusses the fate of the elements comprising the coal, namely C, H, N, O, Cl, mineral matter and S. The change in the heating value of the coal as a function of the various reaction parameters is also discussed. Particular attention is paid to the change in the sulfur content of the coal relative to the changes in the contents of the other coal components. An appropriate macroscopic parameter with which to compare the extent of desulfurization is the heating value retention of the treated coal, which is an indicator of the selectivity of the process for sulfur removal. The desulfurization and the heating value retention are lumped together in a parameter labelled the beneficiation coefficient, which serves as the final topic in the first section.

The second section is also divided into two subsections which both deal with alterations in the coal surface. The first subsection discusses qualitative physical changes in the coal particles as revealed by use of the scanning electron microscope. The physical nature of the ash particles remaining after combustion of the treated coal is discussed as well. Furthermore, qualitative chemical changes on the particle surface deduced from spectra obtained with the energy

dispersive analyzer of x-rays are discussed as well. The spectra of the ash particles in particular provide cogent supporting evidence for the interpretation of the results discussed in the first section in regard to desulfurization. The second subsection deals with the results of the N_2 and CO_2 adsorption studies of the treated coals. In particular, changes in the specific surface area, whether obtained with N_2 or CO_2, are correlated with the reaction parameters and changes in the chemical composition of the coal. Variations in the pore and micropore size distribution induced by chemical treatment of the coal are discussed as well. Furthermore, qualitative conclusions regarding the effect of the porosity of the coal particles on the kinetics of the coal-NO_2 reaction can be deduced from the adsorption studies. When the results of this section are coupled with those of the previous section, a general mechanism which describes the NO_2-coal system can be postulated.

In order to quantify the mechanism obtained on the basis of the results of the first two sections, the third section deals with the results of the mathematical modelling of the reaction system. This section first deals with the applicabilty of the pseudo-steady-state approximation to the equations which describe the system. The selection of the appropriate reaction parameters, such as reaction rate constants and diffusion lengths, which are consistent with the premises of the model, are then discussed. The effect of the assumptions inherent in the model upon the correlation of the conversions predicted by the model with the actually observed conversions is treated as well. The main goal in employing the model is to estimate the reaction rate constants and the diffusion coefficient of NO_2 in the solid coal matrix. The results of the application of the model to the kinetic data to this end form the final topic of discussion in this section.

Ultimately, the results from the three sections are combined to arrive at an overall mechanism which describes the NO_2-coal reaction system qualitatively

and quantitatively. The assimilation of the information discussed in this section to arrive at such a mechanism is the subject of the next chapter.

4.2 Chemical Changes in the System

4.2.1 Liquid Phase Species

4.2.1.1 Runs Using Water as the Solvent

All of the runs using water as the solvent employed the flow reactor for the NO_2 treatment. Therefore, the concentrations of the primary species in the liquid phase derived from NO_2, namely HNO_3 and HNO_2, would be expected to demonstrate a roughly linear increase as a function of time. Referring to Figure 4–1, such a linear increase for (HNO_3) is indeed found to occur. The figure shows two curves. The top curve corresponds to the situation where the reactor has been charged with 350 ml H_2O but no coal, while the curve just below represents the case where 10 g of coal have been slurried with 350 ml of H_2O. It should be noted that the NO_2 mass flowrates are virtually identical (within 2.5%), but the temperatures are different. The run with no coal was conducted in an uncooled reactor, while the reaction with the coal was run in the water-cooled reactor. Reactions of NO_2 and coal conducted at different NO_2 flowrates in the uncooled reactor show similar temperature increases, however. Despite this difference, the major implication of Figure 4–1 is that the coal does not compete with H_2O for NO_2 to any discernible extent. This effect may be due to one of two causes. First, the rate of formation of HNO_3 may be kinetically limited at the NO_2 flowrate used resulting in an excess amount of unreacted NO_2 dissolved in the aqueous phase. Thus, if the coal were to serve as an NO_2 sink, it still would not affect the rate of HNO_3 formation. Most studies of the NO_2/H_2O system indicate that once the NO_2 is solvated, however, it quickly reacts with H_2O to form HNO_3 and HNO_2. Therefore, since the coal particles are completely encompassed by solvent, it is not likely that any portion of the coal will encounter NO_2 (aq). The second, and more plausible, explanation is that the rate of reaction of HNO_3 with coal is much slower than the rate of HNO_3 formation. This

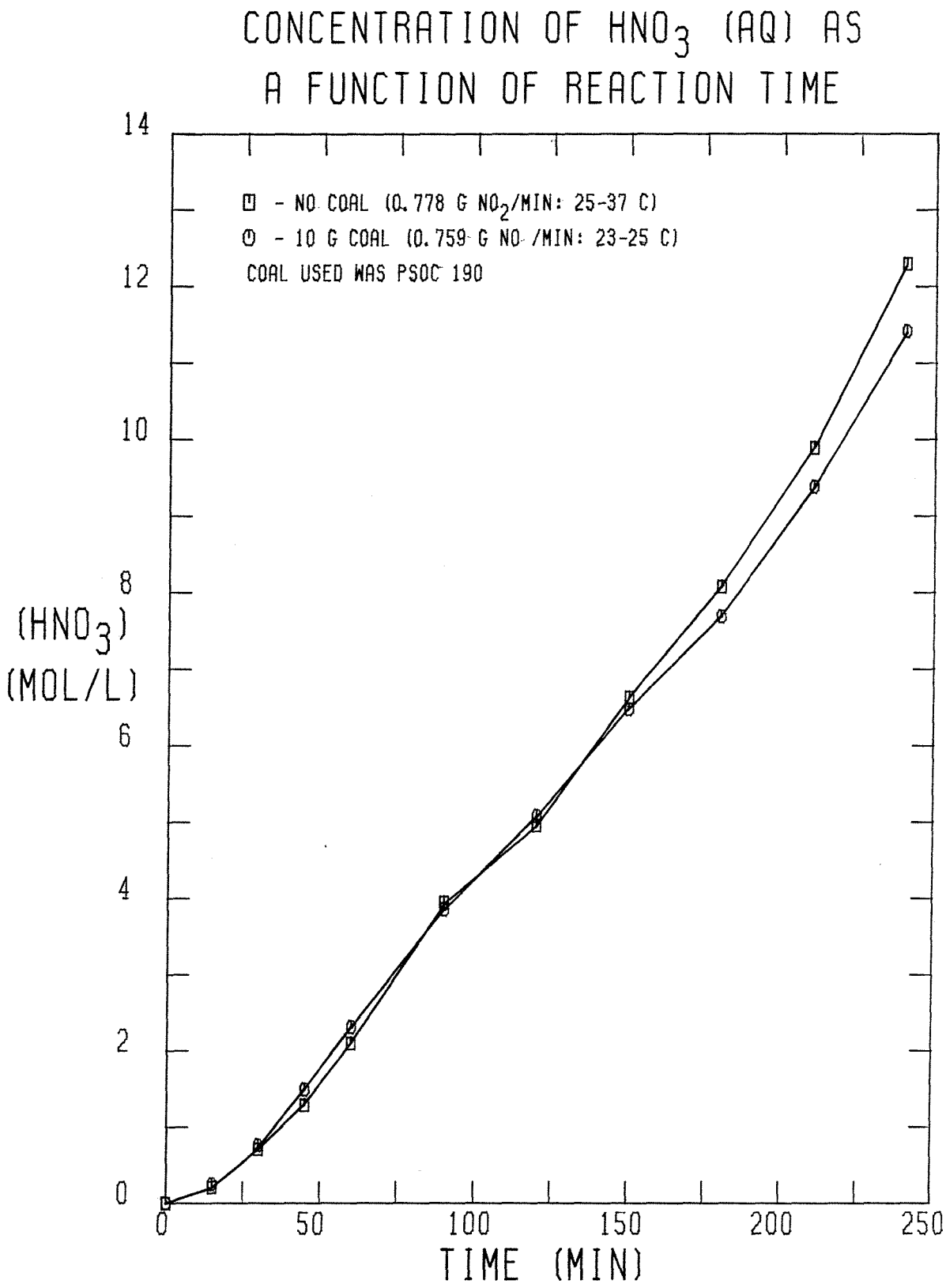
CONCENTRATION OF HNO_3 (AQ) AS A FUNCTION OF REACTION TIME
□ - NO COAL (0.778 G NO_2/MIN: 25-37 C)
⏲ - 10 G COAL (0.759 G NO /MIN: 23-25 C)
COAL USED WAS PSOC 190
(HNO_3) (MOL/L)
0
2
4
6
8
10
12
14
0
50
100
150
200
250
TIME (MIN)

FIGURE 4-1

difference could be a consequence of a low stoichiometric requirement of the coal for HNO_3. Indeed, in a separate experiment, 10 g of coal were slurried in 250 ml of H_2O previously saturated with NO_2. Initially, (HNO_3) = 10.61 M and (HNO_2) = 0.496 M. After 120 minutes, (HNO_3) = 9.63 M and (HNO_2) = 0.371 M. Based on the temperature during the reaction, which rose to a maximum after 15 minutes and then decreased, the reaction was essentially complete after 120 minutes. Therefore, the stoichiometric requirement of the coal for HNO_3 is approximately 0.025 mol HNO_3/g coal, which correlates with the slight divergence of the two curves in Figure 4–1 quite well; that is, HNO_3 is formed much faster than it can be depleted by reaction with the coal.

The presence of coal drastically affects the concentration history of HNO_2, however, as shown in Figure 4–2. When no coal is present, (HNO_2) approaches 0.45 M in a smooth, asymptotic fashion. This behavior is exactly what is expected on the basis of the kinetic studies performed by other workers on the decomposition of HNO_2 (aq), which was found to be fourth order in (HNO_2).[1] Incorporation of the expression for the rate of HNO_2 decomposition into this system yields the following equation:

$$\frac{dc}{dt} = k_1 - k_0 \frac{c^4}{p_{NO}^2}, \quad \text{where} \tag{4.2.1}$$

$c = \dfrac{(HNO_2)}{(HNO_2)_\infty}$ = a dimensionless concentration,

$(HNO_2)_\infty$ = the HNO_2 concentration as $t \to \infty$, (mol/ l),

k_1 = the rate of formation of HNO_2 (mol/l/s),

k_0 = the rate constant for the decomposition of HNO_2 (atm^2/s), and

p_{NO} = the partial pressure of NO (atm).

The first term on the right hand side of equation (4.2.1) was chosen on the basis

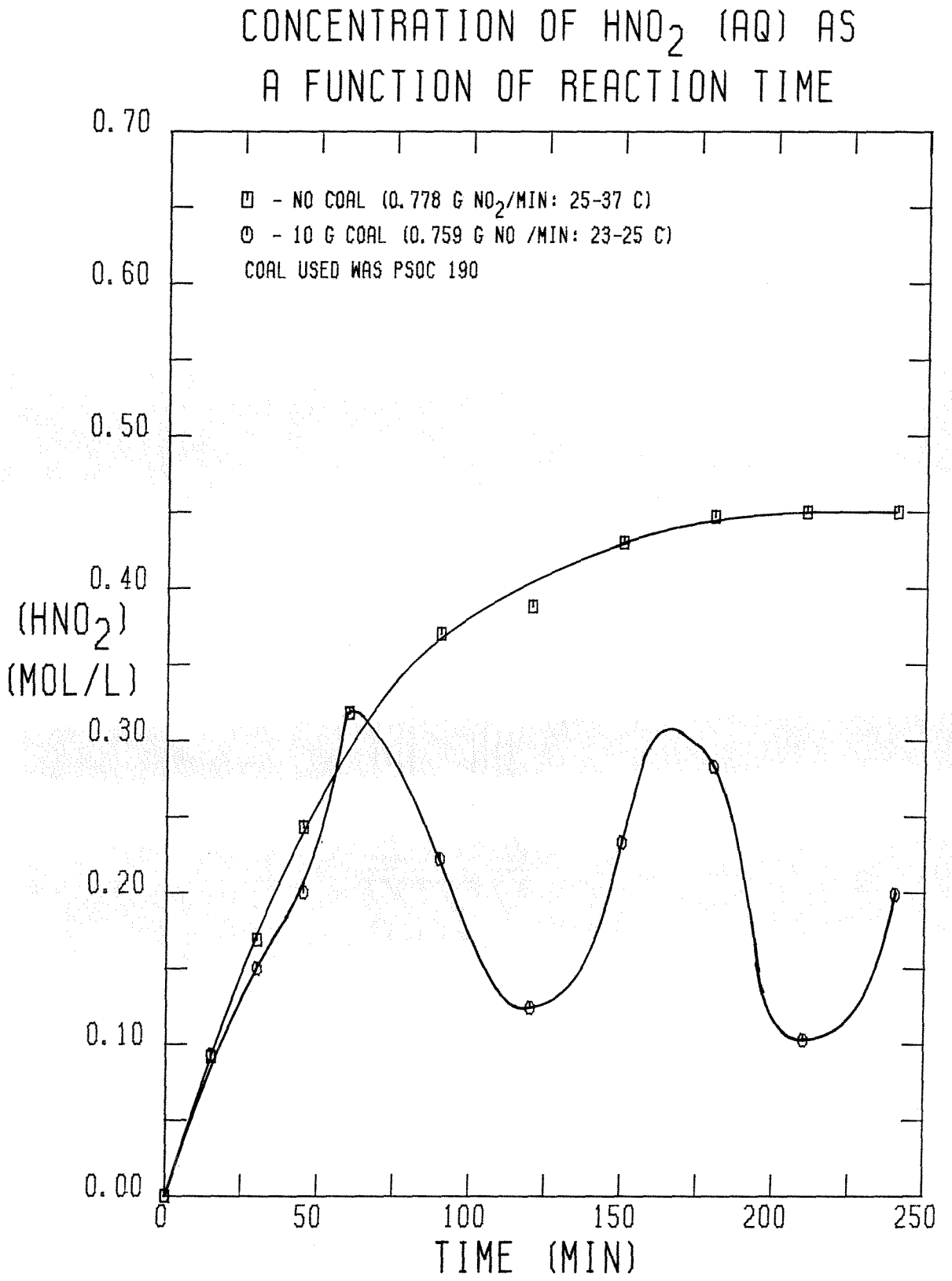
CONCENTRATION OF HNO_2 (AQ) AS A FUNCTION OF REACTION TIME
□ - NO COAL (0.778 G NO_2/MIN: 25-37 C)
⊙ - 10 G COAL (0.759 G NO /MIN: 23-25 C)
COAL USED WAS PSOC 190
0.70
0.60
0.50
0.40
0.30
0.20
0.10
0.00
(HNO_2) (MOL/L)
0
50
100
150
200
250
TIME (MIN)

FIGURE 4-2

of the linear time dependence of (HNO_3) which is simply the consequence of the constant NO_2 flowrate. Assuming that the only reaction of importance accounting for the formation of HNO_2 is

$$2\,NO_2 + H_2O = HNO_3 + HNO_2\,,$$

one obtains a value for $k_1 = 8.95\times10^{-4}\ s^{-1}$ based upon the NO_2 flowrate of 0.778 g NO_2/min, a value of 0.45 M for $(HNO_2)_\infty$, and a solvent volume of 350 ml. Furthermore, examination of equation (4.2.1) indicates that if c approaches a constant value, namely unity, as $t \to \infty$, then

$$\frac{dc}{dt} = 0 = k_1 - \frac{k_0}{p_{NO}^2}, \quad \text{or} \tag{4.2.2}$$

$$p_{NO} = \left(\frac{k_0}{k_1}\right)^{\frac{1}{2}}. \tag{4.2.3}$$

Therefore, if k_0 and k_1 are known, then p_{NO} is determined as well.

The second term of equation (4.2.1) accounts for the rate of decomposition of HNO_2 due to the reaction

$$3\,HNO_2\,(aq) = HNO_3\,(aq) + H_2O + 2\,NO\,(g)\,,$$

with the rate equation

$$-\frac{d(HNO_2)}{dt} = k\,\frac{(HNO_2)^4}{p_{NO}^2}, \quad \text{where} \tag{4.2.4}$$

$$k = \frac{k_0}{(HNO_2)_\infty^3}.$$

Abel and Schmid[1] determined a value for k_0 of 0.767 $l^3/mol^3/s$ at 25°C and 8.75 $l^3/mol^3/s$ at 40°C. The integral average temperature of the run was 34°C. Assuming that the rate constant follows an Arrhenius form, namely $k = A\,e^{\frac{-E}{RT}}$,

an interpolated value for k at 34°C of 3.40 $l^3/mol^3/s$ is obtained. Using equation (4.2.3), a value of p_{NO} = 18.6 atm is obtained, which is obviously much too high, since the system is run at atmospheric pressure. The value for k_1 cannot be too wrong since it is based on the actual data for this system. In order for equation (4.2.3) to predict a value of p_{NO} between 0 and 1 atm, k_1 would have to be at least 350 times greater, which is not possible because the NO_2 is simply not supplied that rapidly. Therefore, the error must lie in the term accounting for the decomposition of HNO_2. It is most likely that under the rather concentrated conditions which exist in the system that the kinetics of the decomposition do not follow those in equation (4.2.4), which were deduced from the study of more dilute solutions. Another possibility is that the large increase in the ionic strength of the solution affects the rate of decomposition of HNO_2, which results in a further increase in the ionic strength. Thus, an increase in the ionic strength of the aqueous solution may inhibit the decomposition reaction, resulting in a lower rate.

If one assumes that equation (4.2.1) accurately describes the kinetics for the reactor flow system, an implicit solution for c can be obtained analytically as

$$t = \frac{p_{NO}^{\frac{1}{2}}}{4(k_0 k_1^3)^{\frac{1}{4}}}\left[2 \tan^{-1} c + \ln \frac{1+c}{1-c} \right], \qquad (4.2.5)$$

where it is assumed that p_{NO} is constant throughout the time domain. Using the value of $8.95\times10^{-4}\, s^{-1}$ for k_1, a value of $8.95\times10^{-4}\, s^{-1}$ is obtained for $\frac{k_0}{p_{NO}^2}$ according to equation (4.2.3). A comparison of the time history of (HNO_2) with that predicted by equation (4.2.5) is shown in Figure 4–3. The values of c for the data and the prediction match at $t = 0$ and as $t \to \infty$ by virtue of the boundary conditions. The prediction for c rises much more slowly than the data show, although the predicted values for c show the same general trend as the data. As

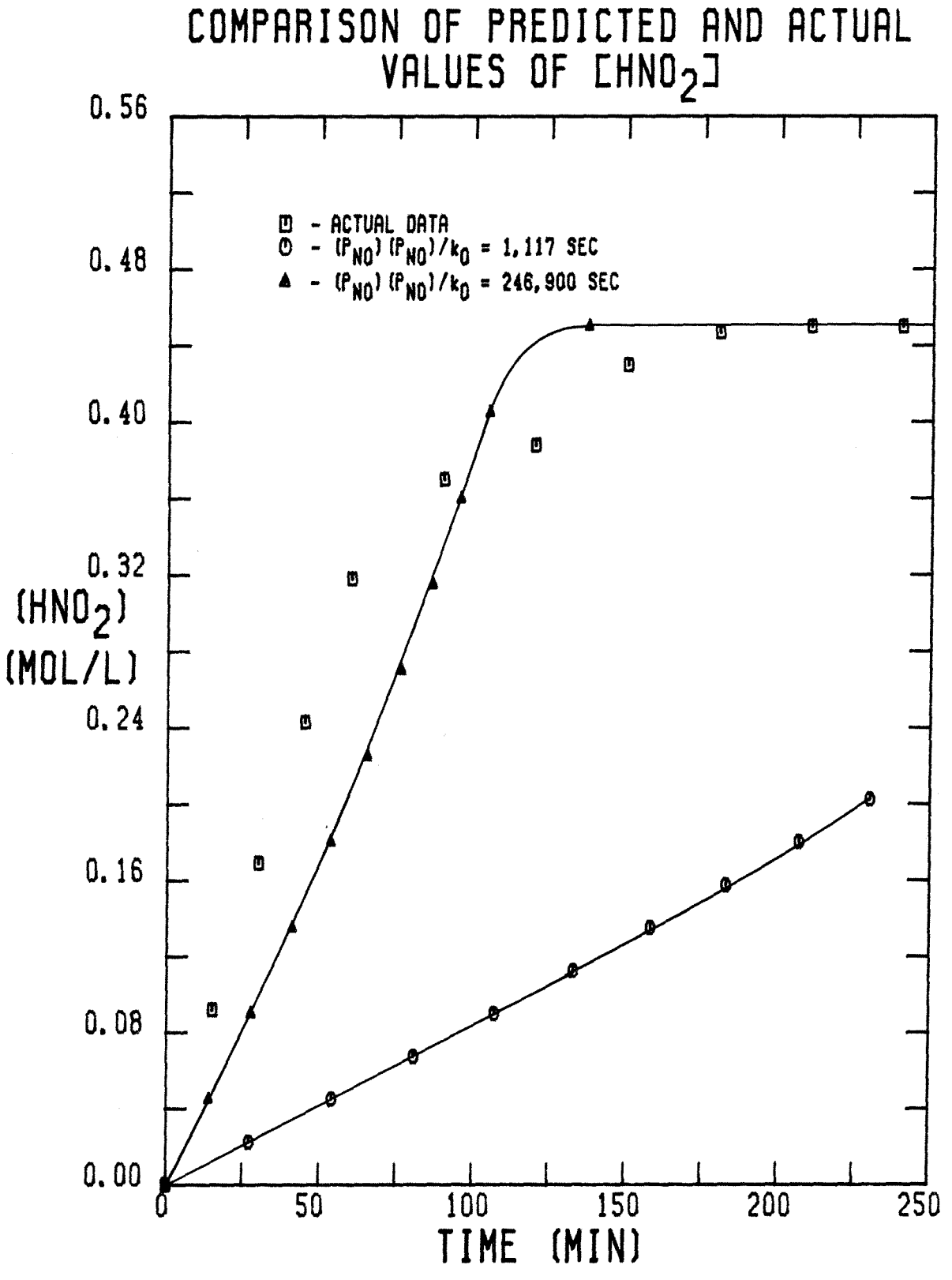
COMPARISON OF PREDICTED AND ACTUAL VALUES OF [HNO2]
0.56
0.48
0.40
0.32
0.24
0.16
0.08
0.00
(HNO2) (MOL/L)
- ACTUAL DATA
- (PNO) (PNO)/k0 = 1,117 SEC
- (PNO) (PNO)/k0 = 246,900 SEC
0
50
100
150
200
250
TIME (MIN)

FIGURE 4-3

the upper curve in Figure 4–3 shows, a much better fit of the data is obtained by letting $4(\frac{k_0 k_1^3}{p_{NO}^2})^{\frac{1}{4}} = 9.28\times10^{-4}\ s^{-1}$, which yields a value of $4.05\times10^{-6}\ s^{-1}$ for $\frac{k_0}{p_{NO}^2}$. This result would imply that the rate constant for HNO_2 decomposition according to equation (4.2.4) is at least 10^5 times smaller than the value for k obtained for dilute solutions, implying a rather severe inhibiting effect by the ionic strength. Such inhibition, however, is not outside the realm of possibility. Indeed, in a study of HNO_2 decomposition conducted as part of this series of experiments, in a solution which initially had $(HNO_2)_0 = 0.684$ M and $(HNO_3)_0 = 9.88$ M, (HNO_2) dropped asymptotically to 0.500 M and (HNO_3) rose to 10.12 M within 90 minutes. Furthermore, 12 hours later, (HNO_2) was 0.496 M, indicating that further HNO_2 decomposition had ceased, whereas the kinetics indicated by equation (4.2.4) would predict that the HNO_2 would ultimately vanish. The salient feature of this discussion is that when no coal is present, the time history of (HNO_2) is what would be qualitatively expected.

The time history of (HNO_2) when coal is present is radically different from the (HNO_2) time history when coal is absent. Indeed, examination of Figure 4–2 reveals an oscillatory behavior displayed by (HNO_2) when coal is present. Such behavior indicates that coal greatly complicates the kinetics of HNO_2 formation and decomposition. The peaks in the curves must be caused by a reaction between HNO_2, or some species derived from HNO_2, and coal whose rate is a strong function of the concentration of HNO_2 or the species derived from HNO_2. The oscillatory nature of (HNO_2) as a function of time indicates that HNO_2 is involved in a series of reactions which allows the HNO_2 concentration to decrease before the rate of the reaction begins to decrease as well. On the other hand, if HNO_2 were reacting directly with the coal, one would expect (HNO_2) to just approach a limiting value asymptotically which corresponds to the situation

where the rate of formation of HNO_2 balances the sum of the rates of decomposition and reaction with coal; that is, there would be no oscillatory behavior. Unfortunately, not enough information is available from which to deduce the mechanism for this unusual kinetic behavior. In any event, the addition of coal to the H_2O/NO_2 system greatly modifies the kinetics.

Another parameter of importance is the mass flowrate of NO_2 because it dictates the concentrations of HNO_3 and HNO_2 in the aqueous phase. Figure 4–4 depicts the concentration of HNO_3 as a function of reaction time for three NO_2 mass flowrates, namely 0.269, 0.483 and 1.039 g NO_2 /min. The curves corresponding to the lower two flowrates display a linear dependence of (HNO_3) on time, which is in accordance with the previous discussion concerning Figure 4–1. The curve corresponding to the highest flowrate, however, has an interesting "kink" between 45 and 60 minutes. Between 0 and 45 minutes, the (HNO_3) curve is linear in reaction time with a slope of roughly 1.8 mol/l/hr, while the curve between 60 and 120 minutes is also linear with an approximate slope of 3.3 mol/l/hr. The most logical explanation for this behavior is that as the flowrate approaches 1 g NO_2/min, the coal begins to compete with H_2O for available NO_2 because NO_2 is now supplied at a rate greater than that of its conversion to HNO_3 immediately upon absorption. Rather, the NO_2 now has the opportunity to diffuse into the aqueous phase and encounter the coal before it reacts with H_2O. The kink occurs when the coal-NO_2 (aq) reaction is completed, after which time all of the absorbed NO_2 reacts with H_2O to form HNO_3 and HNO_2. Furthermore, the higher flowrates should alter the physical nature of the NO_2 bubble–coal slurry system, the effects of which on the kinetics can be significant. For example, after 120 minutes of reaction, 46.4, 87.5 and 80.1 % of the total amount of NO_2 admitted to the reactor was converted to HNO_3 at flowrates of 0.269, 0.483 and 1.039 g NO_2/min, respectively. This variation in NO_2

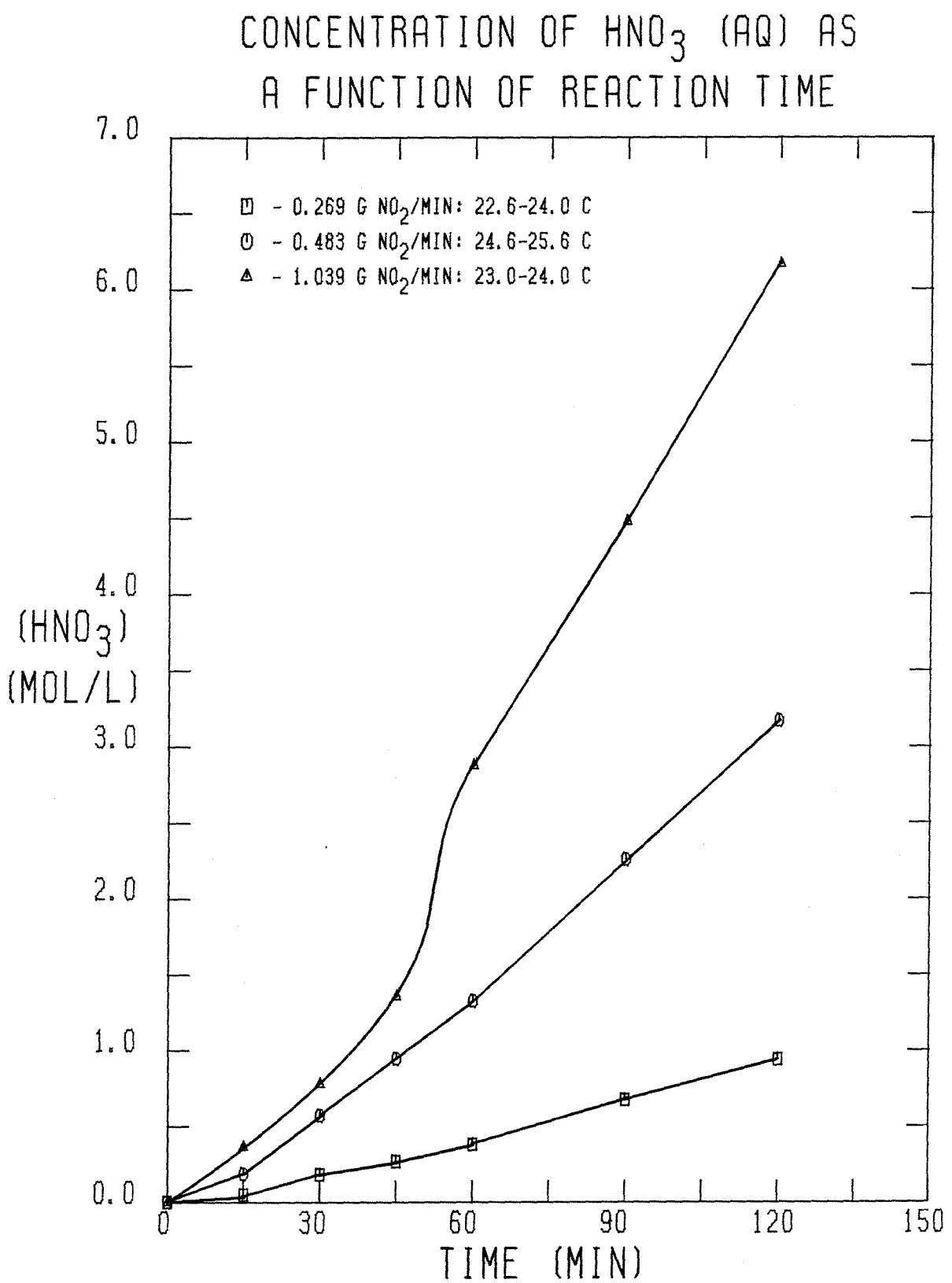
CONCENTRATION OF HNO_3 (AQ) AS A FUNCTION OF REACTION TIME
□ - 0.269 G NO_2/MIN: 22.6-24.0 C
◎ - 0.483 G NO_2/MIN: 24.6-25.6 C
△ - 1.039 G NO_2/MIN: 23.0-24.0 C
7.0
6.0
5.0
4.0
3.0
2.0
1.0
0.0
(HNO_3)
(MOL/L)
0
30
60
90
120
150
TIME (MIN)

FIGURE 4-4

conversion can be attributed to both changes in the physical nature of the system as the flowrate increases and changes in the kinetics as (HNO_3) increases.

The dependence of (HNO_2) as a function of reaction time upon the NO_2 flowrate is shown in Figure 4–5. The curve corresponding to the lowest flowrate shows nothing unusual. The behavior of (HNO_2) at this flowrate is that predicted by equation (4.2.5) with $4(\frac{k_0 k_1^3}{p_{NO}^2})^{\frac{1}{4}} = 2.88\times10^{-3}\ s^{-1}$ if $(HNO_2)_\infty = 0.45$ M. The curve corresponding to a flowrate of 0.483 g NO_2/min shows a slight peak between 45 and 60 minutes, drops a little at 90 minutes, then begins to increase again at 120 minutes. This trend is even more pronounced for the curve corresponding to the highest NO_2 flowrate. The implication of this plot is that once (HNO_2) exceeds roughly 0.24 M, the coal begins to react with some species derived from HNO_2 at a rate faster than that at which HNO_2 can be formed. Furthermore, it appears that after 90 minutes, either the reaction with coal slows down enough so that HNO_2 can be formed faster than it is depleted, or that the coal has completely reacted. In any event, the presence of coal greatly modifies the kinetics of HNO_2 formation, reaction and decomposition.

Indeed, much controversy surrounds the exact mechanism responsible for the absorption of NO_2 in water to form HNO_3. In particular, some workers[2] claim that the mass transfer resistance in the gas film separating a bubble from the liquid determines the rate while other workers[3] claim that the reaction of NO_2 once it is absorbed determines the overall rate of HNO_3 formation. Furthermore, the occurrence of a "mist" seems to confuse everyone attempting a mechanistic explanation for the system. Despite these differences of opinion, the widely accepted mechanism for the NO_2 absorption process is:

$$2\,NO_2\,(g) + H_2O = HNO_3\,(aq) + HNO_2\,(aq)$$

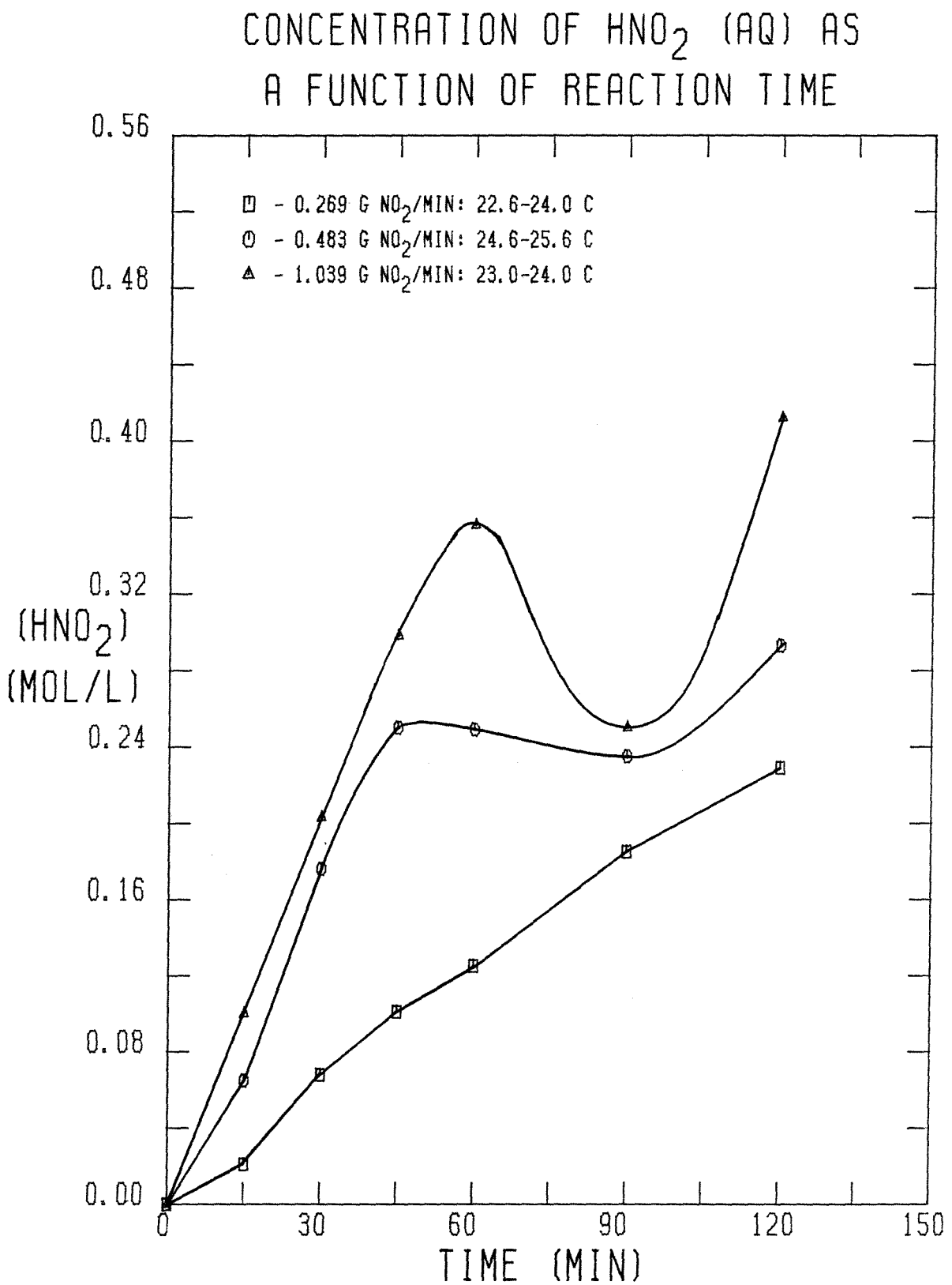
CONCENTRATION OF HNO_2 (AQ) AS A FUNCTION OF REACTION TIME
□ - 0.269 G NO_2/MIN: 22.6-24.0 C
○ - 0.483 G NO_2/MIN: 24.6-25.6 C
△ - 1.039 G NO_2/MIN: 23.0-24.0 C
0.56
0.48
0.40
0.32
0.24
0.16
0.08
0.00
(HNO_2) (MOL/L)
0
30
60
90
120
150
TIME (MIN)

FIGURE 4-5

$$3\,HNO_2\,(aq) = HNO_3\,(aq) + H_2O + 2\,NO\,(g)$$

The overall reaction is:

$$3\,NO_2\,(g) + H_2O = 2\,HNO_3\,(aq) + NO\,(g)$$

Examination of this equation reveals that only two moles of HNO_3 should be formed for every three moles of NO_2 adsorbed.

In keeping with the tradition of confusion surrounding this system, the results of this study are at variance with the commonly accepted mechanism. In particular, an examination of the (HNO_3) data shows that at an NO_2 flowrate of 0.483 g NO_2/min, 87.5 % of the NO_2 is converted to HNO_3 while at a flowrate of 1.039 g NO_2/min, 80.1 % of the NO_2 ends up as HNO_3. In both cases, the NO_2 conversion exceeds the 66.7 % predicted by the commonly accepted mechanism. Furthermore, the amount of NO coming off the top of the reactor is well below that predicted on the basis of the mechanism. These facts suggest that another mechanism is occurring in this situation. At a flowrate of 0.269 g NO_2/min, however, only 46.4 % of the NO_2 is converted to HNO_3, which is within the bounds of the commonly accepted model.

A rather plausible scheme accounting for these discrepancies suggests itself. First, it should be noted that in those studies whose data were employed to arrive at the commonly accepted mechanism, the NO_2 was absorbed from a stream consisting primarily of an inert carrier, usually N_2. Thus, the NO byproduct can be effectively purged from the system. In this study, on the other hand, pure NO_2 was admitted to the system. Therefore, any gas flow from the top of the reactor, which was virtually 100 % NO as determined by GC analysis, had to be generated by the system itself, assuming of course that all of the NO_2 was absorbed by the system. A very important reaction under these conditions

involves NO and NO_2:

$$NO\,(g) + NO_2\,(g) \rightleftharpoons N_2O_3\,(g)$$

Although the amount of N_2O_3 which exists at equilibrium is quite small (≈ 1 % by volume), N_2O_3 is rapidly absorbed by water. Since equilibrium is rapidly achieved as well, if excess NO_2 is present in the gas phase, the overall rate of conversion of NO to N_2O_3 followed by adsorption can be quite high. The reaction between N_2O_3 and H_2O yields more HNO_2:

$$N_2O_3\,(g) + H_2O \rightarrow 2\,HNO_2\,(aq)$$

Therefore, it is conceptually possible to recirculate the NO as it is produced to form nitric acid via the HNO_2 decomposition reaction:

$$3\,HNO_2\,(aq) \rightleftharpoons HNO_3\,(aq) + H_2O + 2\,NO\,(g)$$

It should be noted that for every three moles of NO recirculated, two moles of HNO_3 and one mole of NO are produced. Therefore, recirculation should allow NO_2 conversions to HNO_3 in excess of 66.7 %.

The crucial criterion for this scheme is that once the NO is formed and enters the gas phase, it encounters an NO_2 molecule with which to react. Furthermore, this reaction must occur in an environment where the N_2O_3 has access to the bulk aqueous phase. In the case of conventional NO_2 absorbers, this may not be possible by virtue of the purging action of the inert carrier gas. That is, once the NO molecule leaves the aqueous phase, there may be insufficient time for the NO molecule to react with an NO_2 molecule to form an N_2O_3 molecule, which can then be absorbed by the bulk liquid phase. The major limitation may simply be the low concentration of NO_2 in the gas phase. In this study, however, the only possible gas phase species are NO, NO_2, H_2O and smaller amounts of HNO_3

and HNO_2. Thus, when the NO enters the gas phase, it has a very high probability of encountering an NO_2 molecule. Furthermore, since no inert carrier gas is purging the system, the time allowed for the sequence of steps mentioned above for NO recirculation is greatly increased. Thus, the possibility of successful NO recirculation is greatly enhanced when pure NO_2 is admitted to the reactor.

The fact that the NO_2 conversion at the low flowrate is smaller than that at the higher flowrates can readily be explained. At the lower NO_2 flowrates, the NO_2 may be absorbed as soon as it enters the reactor. Thus, no NO_2 is left to combine with the NO as it escapes the liquid phase. Consequently, the amount of NO recirculation is greatly reduced. Furthermore, the interfacial area between the gas and aqueous phases will be less when the flowrate is lower. Thus, it is more likely that the NO will escape the aqueous phase into the gas phase at the top of the reactor. As the flowrate increases, the residence time of the NO_2 molecules in the gas phase of the reactor increases, which means that the concentration of NO_2 in the gas phase increases. The interfacial area increases as well. Hence, the NO produced is more likely to encounter NO_2 in the gas phase and react to form N_2O_3, which is then recirculated to form more HNO_3, as the flowrate increases. Finally, if the flowrate is too high, the residence time of the NO_2 bubbles in the liquid will be too short to allow complete absorption. Therefore, the conversion of NO_2 to HNO_3 should begin to decrease after the flowrate exceeds the value corresponding to complete NO_2 absorption at the top of the liquid phase. The range of flowrates used in this study seems to cover the entire spectrum of cases discussed above since conversions of NO_2 to HNO_3 of 46.4, 87.5, 89.8 and 80.1 % were obtained at flowrates of 0.269, 0.483, 0.759 and 1.039 g NO_2/min, respectively.

Although the mechanism discussed above is quite plausible, uncertainties about the effect of coal on the nature of NO_2 absorption remain. Furthermore,

it is the interaction of the oxidant with the coal which is of primary interest. In an aqueous slurry through which NO_2 is bubbled, several potential oxidizing species, such as HNO_3, HNO_2, NO_2 (aq) and perhaps even NO^+ and NO_2^+, may be available to react with the coal. The quantitative determination of the relative reactivities of these species with coal would be a major study in itself, and was not attempted in this work. In order to gain a better understanding of the relationship between the kinetics of the NO_2–coal reaction and desulfurization, a system where only the coal reacts with NO_2 was needed. Such a system exists if the NO_2 cannot react with the solvent, as it does with H_2O. For this reason, CCl_4 was deemed the best solvent for the system because it does not react with NO_2. The fate of NO_2 in CCl_4 is the basis of the next section.

4.2.1.2 Runs Using Carbon Tetrachloride as the Solvent

Although the majority of the runs using CCl_4 as the solvent was conducted in the batch reactor, the first two sets of runs were conducted in the flow reactor. The first set of runs (Runs 21–27) was conducted at 25°C with an NO_2 flowrate of roughly 1.2 g NO_2/min. A composite (NO_2) history which can be applied to each run individually can be obtained by averaging the values of (NO_2) of each reaction in the set at each reaction time. For instance, the values of (NO_2) at t = 30 minutes for Runs 21–27 are averaged to obtain the composite value of (NO_2) at t = 30 minutes. As t increases, the number of values to be averaged decreases since the reactions within the set are run for times from 30 to 180 minutes. Consequently, the composite value of (NO_2) from t = 135 to t = 180 minutes will be equal to the value of (NO_2) for the corresponding 180 minute run within the set. Such a composite (NO_2) history for Runs 21–27 is shown in Figure 4–6. The size of the error bars is determined by the standard deviation of the average and serves as an indication of the degree of variation between the runs. Considering the difficulty in reproducing the NO_2 flowrates, the degree of variation in (NO_2) between runs is not that extensive. Furthermore, a straight line can be drawn through all of the points which indicates that (NO_2) is a linear function of t. Such a result is expected because the amount of NO_2 being admitted to the reactor is far in excess of the amount which ultimately reacts with the coal. Interestingly, however, not all of the NO_2 admitted to the reactor is absorbed by the solvent. For instance, after 180 minutes only about 65 % of the NO_2 admitted to the reactor is retained by the CCl_4. This observation is not surprising because although CCl_4 shows a high affinity for NO_2, the high NO_2 flowrate does not allow sufficient contact time between the bubbles and solvent for complete absorption.

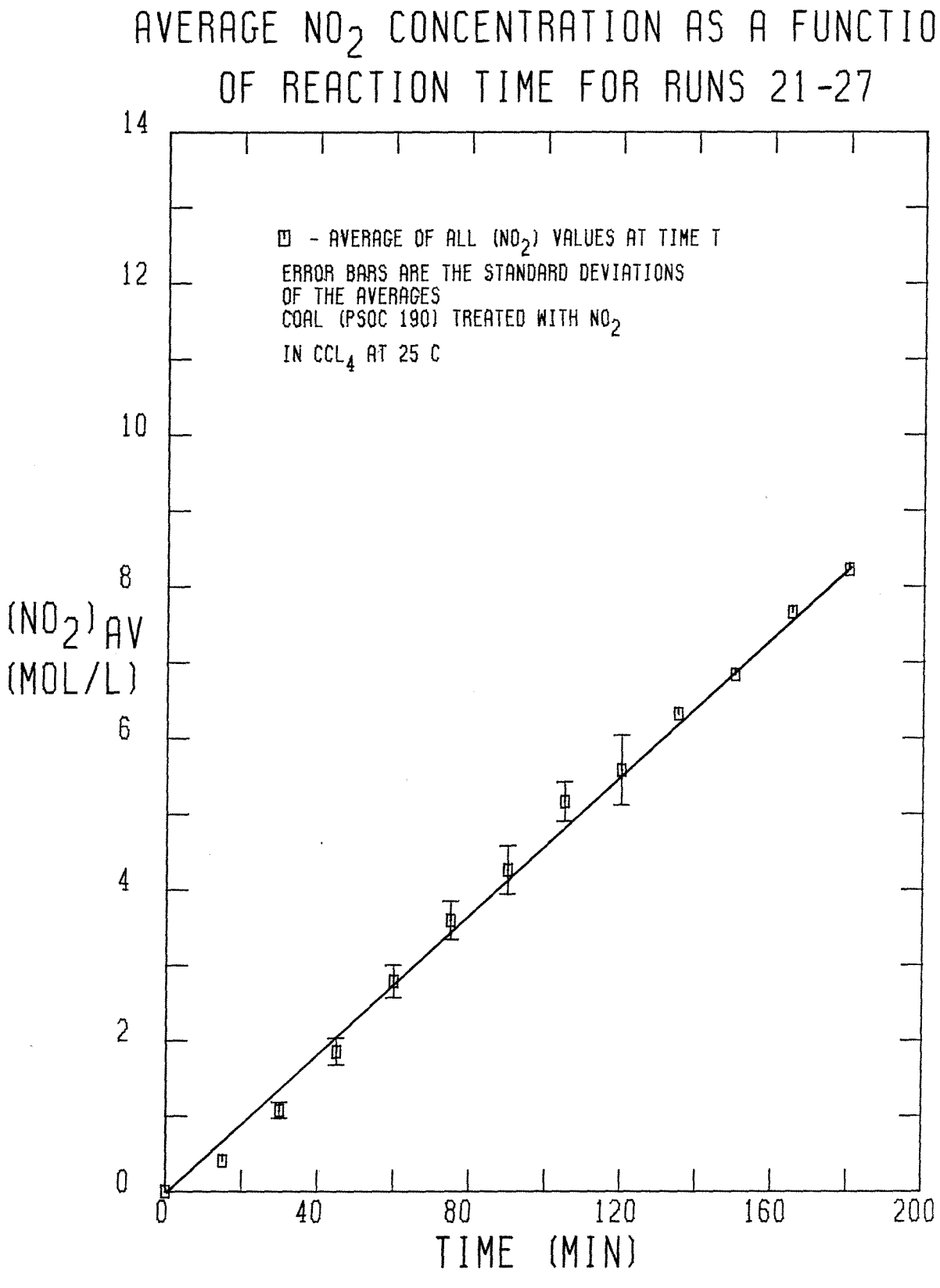
AVERAGE NO_2 CONCENTRATION AS A FUNCTION OF REACTION TIME FOR RUNS 21-27
□ - AVERAGE OF ALL (NO_2) VALUES AT TIME T
ERROR BARS ARE THE STANDARD DEVIATIONS OF THE AVERAGES
COAL (PSOC 190) TREATED WITH NO_2 IN CCL_4 AT 25 C
$(NO_2)_{AV}$ (MOL/L)
0
2
4
6
8
10
12
14
0
40
80
120
160
200
TIME (MIN)

FIGURE 4-6

The second set of experiments conducted in the flow reactor (Runs 28–32) was performed at 50°C. At this temperature, it was possible to saturate the CCl_4 with NO_2. The saturation concentration was roughly 1.27 F NO_2. The composite (NO_2) history is shown in Figure 4–7. A very interesting feature is immediately noticeable, namely the rapid decrease in (NO_2) at the beginning of the reaction. This phenomenon is readily explained. Before the reaction is begun, the CCl_4 is saturated with NO_2 at a flow rate of roughly 1.3 g NO_2/min. Saturation usually takes about 30 minutes, although the NO_2 is allowed to flow for 45 minutes to insure complete saturation. Once saturation is achieved, the ten grams of coal are dumped into the reactor. Obviously, the coal reacts with the NO_2 at a rate which initially is much greater than the rate at which the NO_2 is supplied to the reactor. According to the plot, this quick reaction is near completion after just 15 minutes because (NO_2) has begun to rise again. It is interesting to note, however, that the concentration of NO_2 does not reach its initial value as the reaction time increases, but remains about 5 % lower. This observation could be attributed to a second, much slower reaction which is taking place. Another possibility is that the presence of solid particles suspended in the CCl_4 affects the NO_2 residence time in the reactor and its mass transfer from the gas to the liquid phase so that the (NO_2) saturation concentration is lowered. Evidence based upon the elemental analysis of the coal discussed in the next section indicates that a second, much slower reaction may indeed be occurring. The possibility that the coal is affecting the NO_2 equilibrium between the gas and liquid phases, however, cannot be ignored either.

The next set of reactions (Runs 33–37) was conducted in the batch reactor at 20°C. The primary purpose in using the batch reactor was to avoid the problems created by fluctuations in the NO_2 flowrate from one run to the next. The composite (NO_2) history for this set of experiments is shown in Figure 4–8. An

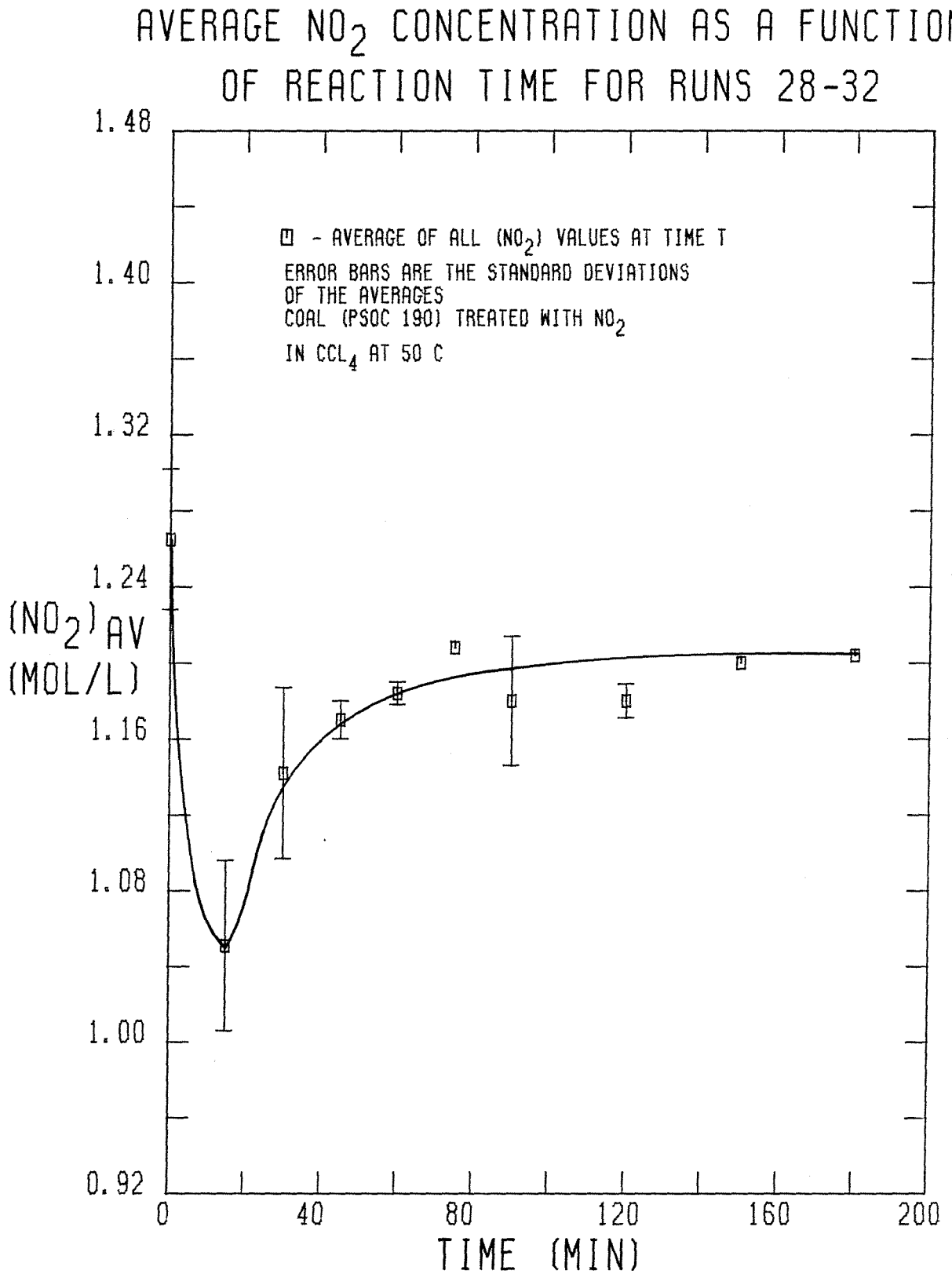
AVERAGE NO_2 CONCENTRATION AS A FUNCTION OF REACTION TIME FOR RUNS 28-32
□ - AVERAGE OF ALL (NO_2) VALUES AT TIME T
ERROR BARS ARE THE STANDARD DEVIATIONS OF THE AVERAGES
COAL (PSOC 190) TREATED WITH NO_2 IN CCL_4 AT 50 C
$(NO_2)_{AV}$ (MOL/L)
1.48
1.40
1.32
1.24
1.16
1.08
1.00
0.92
0
40
80
120
160
200
TIME (MIN)

FIGURE 4-7

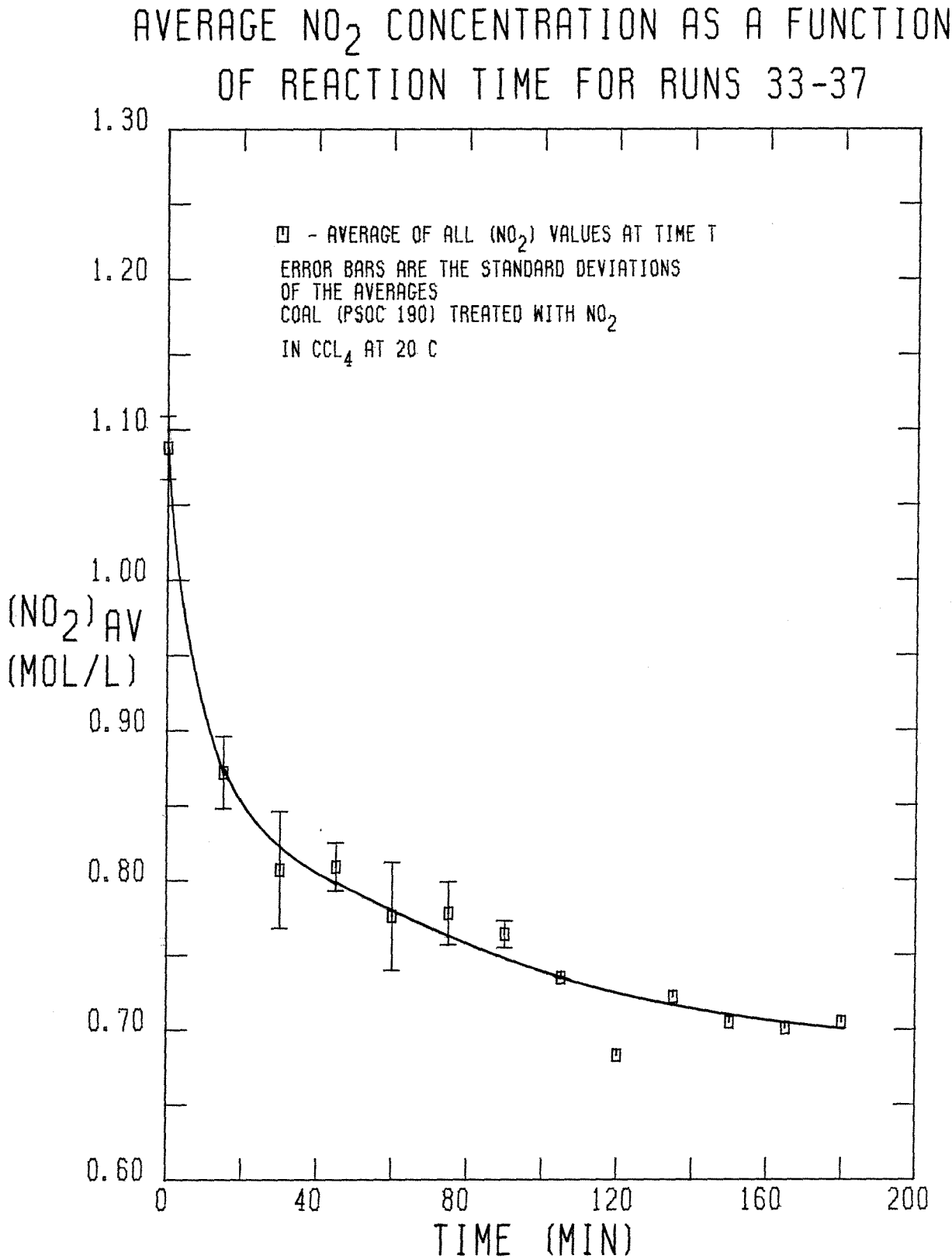
AVERAGE NO_2 CONCENTRATION AS A FUNCTION OF REACTION TIME FOR RUNS 33-37
□ - AVERAGE OF ALL (NO_2) VALUES AT TIME T
ERROR BARS ARE THE STANDARD DEVIATIONS OF THE AVERAGES
COAL (PSOC 190) TREATED WITH NO_2 IN CCL_4 AT 20 C
1.30
1.20
1.10
1.00
0.90
0.80
0.70
0.60
$(NO_2)_{AV}$ (MOL/L)
0
40
80
120
160
200
TIME (MIN)

FIGURE 4-8

examination of this figure reveals that (NO_2) drops quite rapidly within the first 30 minutes and then decays at a much slower rate thereafter. Once again, these trends suggest that two processes involving NO_2 consumption, one of which proceeds at a much slower rate than the other, are occurring. Another possibility is that just a single reaction whose rate depends on (NO_2) and the nitrogen content in the coal is taking place. Such a dependence would account for the very rapid, then more gradual decline in (NO_2) as t increases and the number of coal sites decreases.

The composite (NO_2) history for the set of experiments conducted at 0°C (Runs 42–46) shown in Figure 4–9 displays the same trends as in the previous set, namely the rapid then more gradual decline in (NO_2). It should be noted, however, that the rate of NO_2 consumption, particularly for times greater than 60 minutes, is lower at 0°C than at 20°C. This fact simply implies that the rate of NO_2 consumption is dependent upon the reaction temperature to a discernible extent. The effect of temperature on (NO_2) is shown graphically in Figure 4–10, which shows the relative composite NO_2 concentration at 0 and 20°C as a function of reaction time. The plot plainly shows that NO_2 is depleted at a slower rate at 0°C than at 20°C. The temperature can affect the reaction rate in two ways. First, the rate constant is probably a function of temperature, and a decrease in temperature would be expected to decrease the rate of NO_2 consumption. A second, and more subtle, effect of the temperature concerns the relative amounts of NO_2 and the dimer N_2O_4 and whether the rate depends on (NO_2), (N_2O_4) or [(NO_2) + (N_2O_4)]. Although the equilibrium distribution between NO_2 and N_2O_4 in the gas phase is well known, no equilibrium data in a solvated state such as $NO_2(CCl_4)$ are available. If one assumes that the gas phase equilibrium data hold for the solvated state as well, however, then at 20°C, 27.4 % of the amount of NO_2 + N_2O_4 should be NO_2, while at 0°C, only 12.7 % should be in

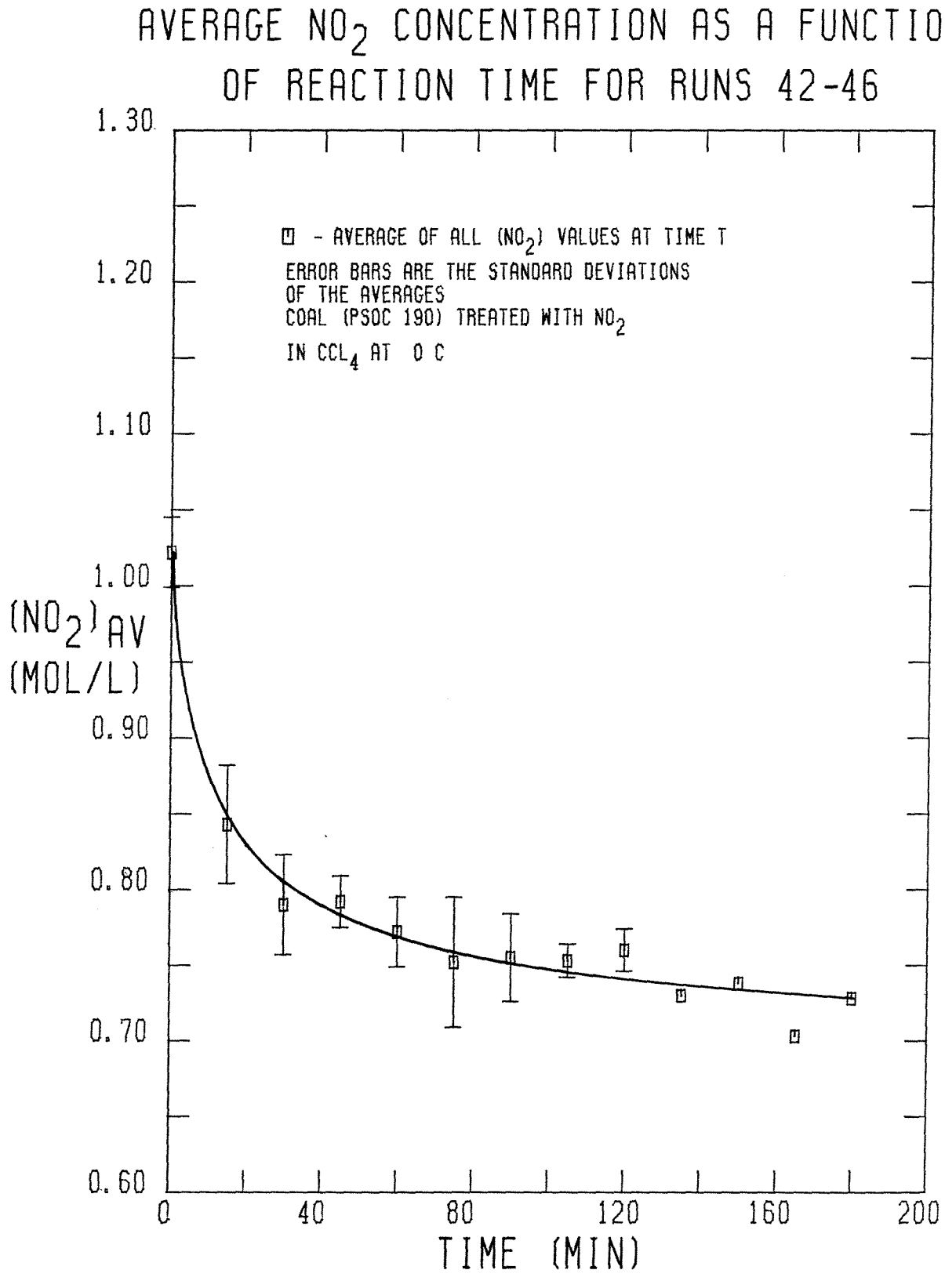
AVERAGE NO_2 CONCENTRATION AS A FUNCTION OF REACTION TIME FOR RUNS 42-46
- AVERAGE OF ALL (NO_2) VALUES AT TIME T
ERROR BARS ARE THE STANDARD DEVIATIONS OF THE AVERAGES
COAL (PSOC 190) TREATED WITH NO_2 IN CCL_4 AT 0 C
$(NO_2)_{AV}$ (MOL/L)
1.30
1.20
1.10
1.00
0.90
0.80
0.70
0.60
0
40
80
120
160
200
TIME (MIN)

FIGURE 4-9

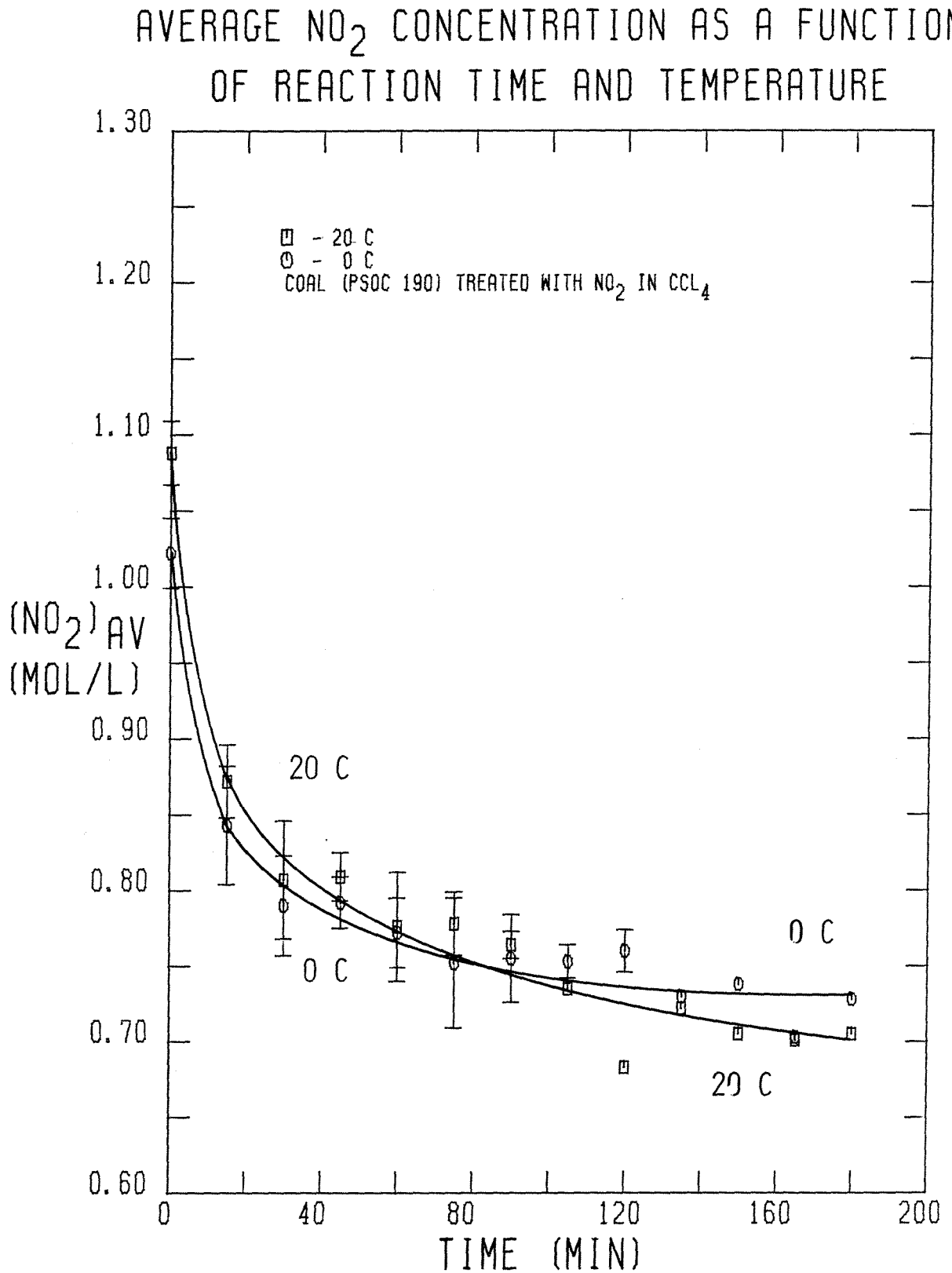
AVERAGE NO_2 CONCENTRATION AS A FUNCTION OF REACTION TIME AND TEMPERATURE
□ - 20 C
○ - 0 C
COAL (PSOC 190) TREATED WITH NO_2 IN CCL_4
$(NO_2)_{AV}$ (MOL/L)
1.30
1.20
1.10
1.00
0.90
0.80
0.70
0.60
0
40
80
120
160
200
TIME (MIN)
20 C
0 C
0 C
20 C

FIGURE 4-10

the form of NO_2. Thus, the ratio of (NO_2) at 20°C to that at 0°C is greater than 2, yet the ratio of the initial rates is only about 1.15 while the ratio of the initial values of $[(NO_2) + (N_2O_4)]$ is 1.065, which would then imply a very weak dependence of the initial rate on just (NO_2). Obviously the rate cannot depend in a simple manner on (N_2O_4) exclusively because (N_2O_4) increases as the temperature decreases. Consequently, if the rate constant is not a function of temperature, the ratio of initial rates should be proportional to some power of 0.832 (the ratio of (N_2O_4) at 20°C to that at 0°C), which is less than unity. The use of initial rates eliminates any effect of a dependence of the rate on the concentration of species in the coal. It would appear, then, that the rate probably is proportional to $[(NO_2) + (N_2O_4)]^n$. For the sake of simplicity, the quantity in brackets will be referred to as simply (NO_2) in the future with the understanding that it corresponds to the total amount of NO_2 and N_2O_4 expressed as moles of NO_2.

It is interesting to note that at t = 75 minutes, the ratio of the rates at the two temperatures is about 1.8 and at t = 165 minutes, the ratio is roughly 1.6. These ratios were adjusted to differences in (NO_2) by assuming a first order dependence of the rate on (NO_2). These facts are consistent with the occurrence of two different processes, because if only one process were occurring, the ratio of the rates would be constant for all reaction times. It should be kept in mind that if the rate also depends upon the concentration of coal species in a simple and straightforward manner (i.e., Rate $\propto$ $(\text{sites})^n$), the ratio of the rates will be affected because the coal species concentration at a given reaction time should be higher at the lower temperature than at the higher temperature because of the difference in their rates. Thus, a coal substrate concentration dependence should offset the temperature and (NO_2) effects to some degree, with the consequence that the ratio of rates approaches unity. In this case, however, the ratio actually becomes larger than the ratio of initial rates and

then decreases slightly as the reaction time increases, which implies that two independent processes are probably occurring and that some coal-species concentration-dependence of the rates may exist as well.

Certainly, it may be argued that a 20°C temperature difference is not large enough to reveal unambiguous temperature effects. On the basis of the facts discussed above, however, some qualitative conclusions may be drawn, primarily that the temperature does affect the rate of NO_2 consumption to a discernible extent. Furthermore, it appears that the rate does not depend on the relative concentrations of the NO_2 monomer or N_2O_4 dimer, but may depend on the total concentration of NO_2 and N_2O_4. Also, the reaction rate may depend on the concentration of species in the coal.

The composite (NO_2) history for the set of runs using the PSOC 276 coal (Runs 47–52) is displayed in Figure 4–11. In this case, the initial rate of NO_2 consumption is not as great as in the corresponding set using the PSOC 190 coal. Nevertheless, the comments pertaining to the consumption of NO_2 by the PSOC 190 coal apply to the PSOC 276 coal as well. The slight difference between the curves can be attributed to several factors. First, whereas the PSOC 190 coal has an initial N_2 determined specific surface area ($S_a^{N_2}$) of 55 m^2/g, the PSOC 276 coal has a N_2 determined specific surface area of only 8.6 m^2/g. On this basis, it is surprising that the difference in rates is not much greater. Consequently, even if the rate of NO_2 consumption by the coal is a weak function of $S_a^{N_2}$, this effect alone could account for the difference in rates. A second possible cause of the difference in rates may be attributed to a difference in the nature and number of reactive species between the two coals. Although this point is treated in the section dealing with the coal analysis, it appears that that difference cannot be too great. Only a small difference would be needed, however, to account for the small difference in the reaction rates of the coals. A comparison of the

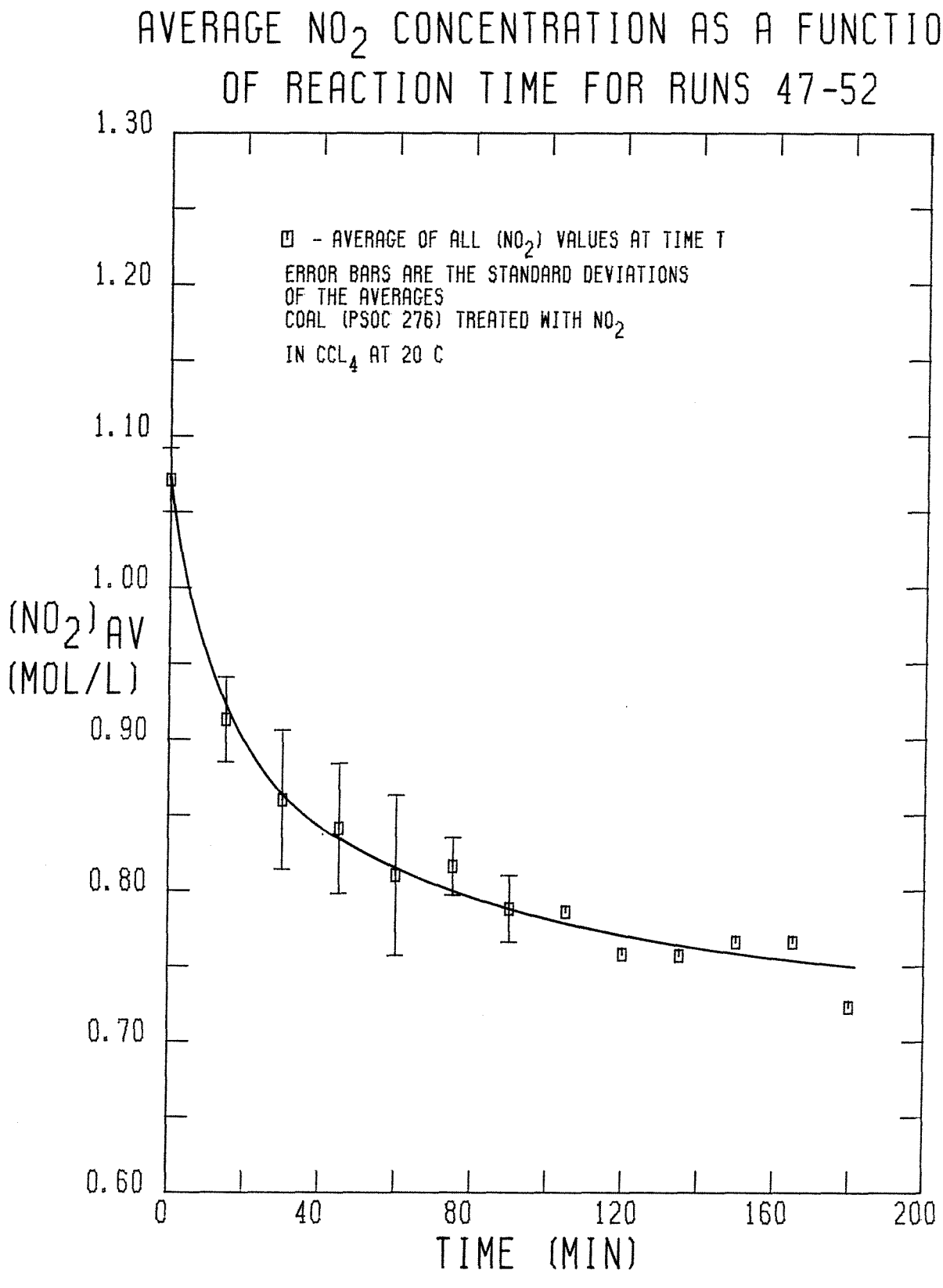
AVERAGE NO_2 CONCENTRATION AS A FUNCTION OF REACTION TIME FOR RUNS 47-52
□ - AVERAGE OF ALL (NO_2) VALUES AT TIME T
ERROR BARS ARE THE STANDARD DEVIATIONS OF THE AVERAGES
COAL (PSOC 276) TREATED WITH NO_2 IN CCL_4 AT 20 C
1.30
1.20
1.10
1.00
0.90
0.80
0.70
0.60
$(NO_2)_{AV}$ (MOL/L)
0
40
80
120
160
200
TIME (MIN)

FIGURE 4-11

composite (NO_2) histories for the two coals is shown graphically in Figure 4–12. Referring to this figure, it is interesting to note that after the initial drop in (NO_2), both curves are basically parallel. This behavior occurs after about 45 minutes of reaction time. On this basis, it seems that initially the rate of the reaction of NO_2 with the coal is affected by the pore structure and/or the nature of the species in the coal while at later times, the rate is independent of the physical nature of the coal.

Finally, a set of experiments was conducted at various initial concentrations of NO_2 (Runs 38–41). The composite (NO_2) history for these runs is shown in Figure 4–13. The concentrations are plotted on a relative basis for ease of comparison. One obvious feature is that the relative consumption of NO_2 increases as the initial NO_2 concentration, $(NO_2)_0$, decreases. Furthermore, the curve tends to level off at earlier times as $(NO_2)_0$ increases. Both of these features result from the dependence of the reaction rate on (NO_2). Indeed, graphical differentiation yields some interesting results. For instance, an evaluation of the rate at $t = 0$ should reveal the dependence of the initial rate on NO_2. Unfortunately, graphical differentiation at the endpoint of a locus is rather difficult because it is quite hard to accurately determine the tangent at the endpoint. The initial rate can be approximated, however, as $\frac{[c_0 - c_{15}]}{15}$(mol/l/min), where c_{15} is the value of (NO_2) at t = 15 minutes. A visual inspection of Figure 4–13 shows that this approximation should provide a good first order estimate of the initial rate, particularly at the higher values of $(NO_2)_0$. If the initial rate for the run where $(NO_2)_0$ = 0.097 F is defined as unity, the following results are obtained for the relative initial rates:

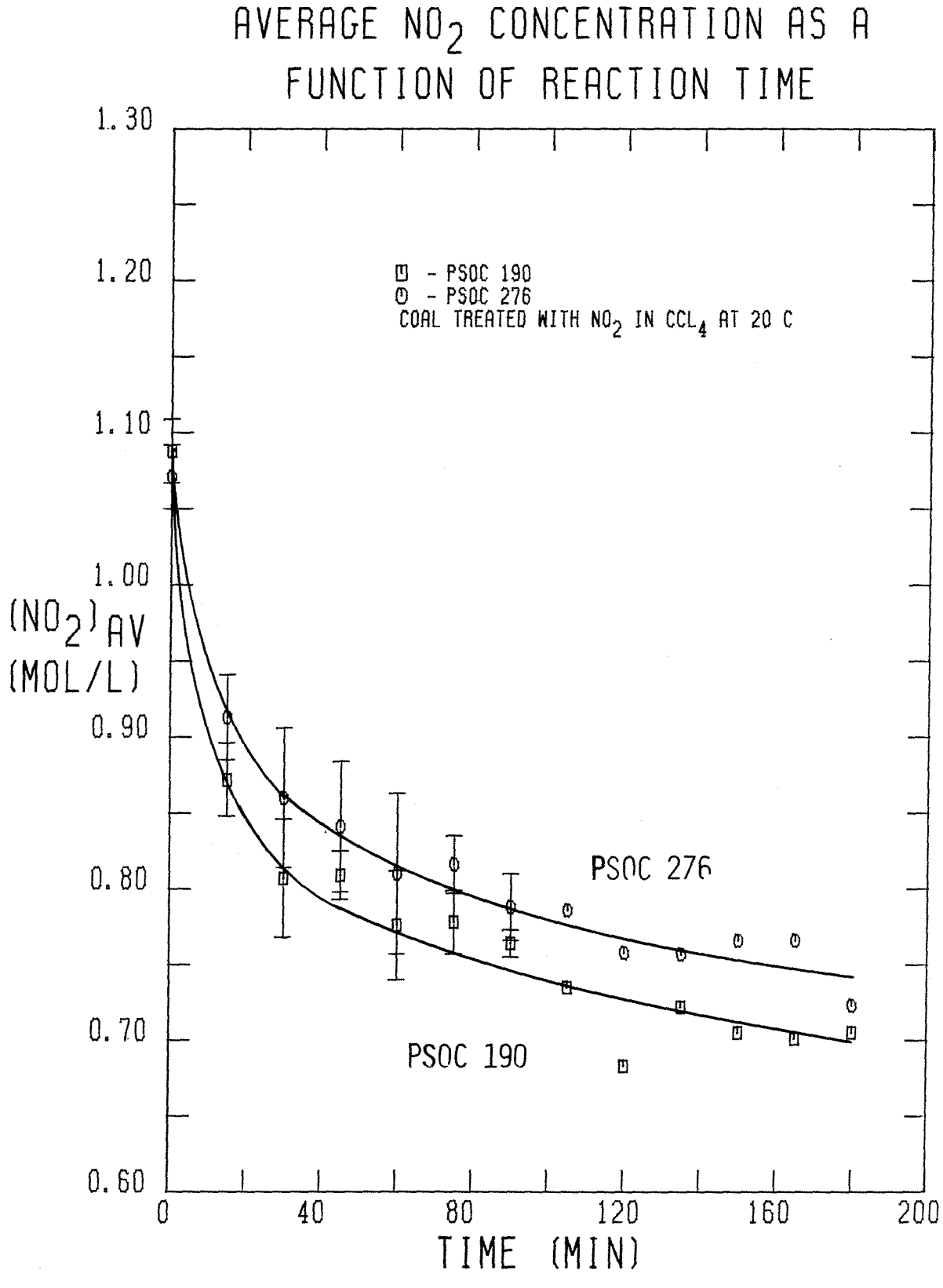
AVERAGE NO_2 CONCENTRATION AS A FUNCTION OF REACTION TIME
1.30
1.20
1.10
1.00
0.90
0.80
0.70
0.60
$(NO_2)_{AV}$ (MOL/L)
□ - PSOC 190
○ - PSOC 276
COAL TREATED WITH NO_2 IN CCL_4 AT 20 C
PSOC 276
PSOC 190
0
40
80
120
160
200
TIME (MIN)

FIGURE 4-12

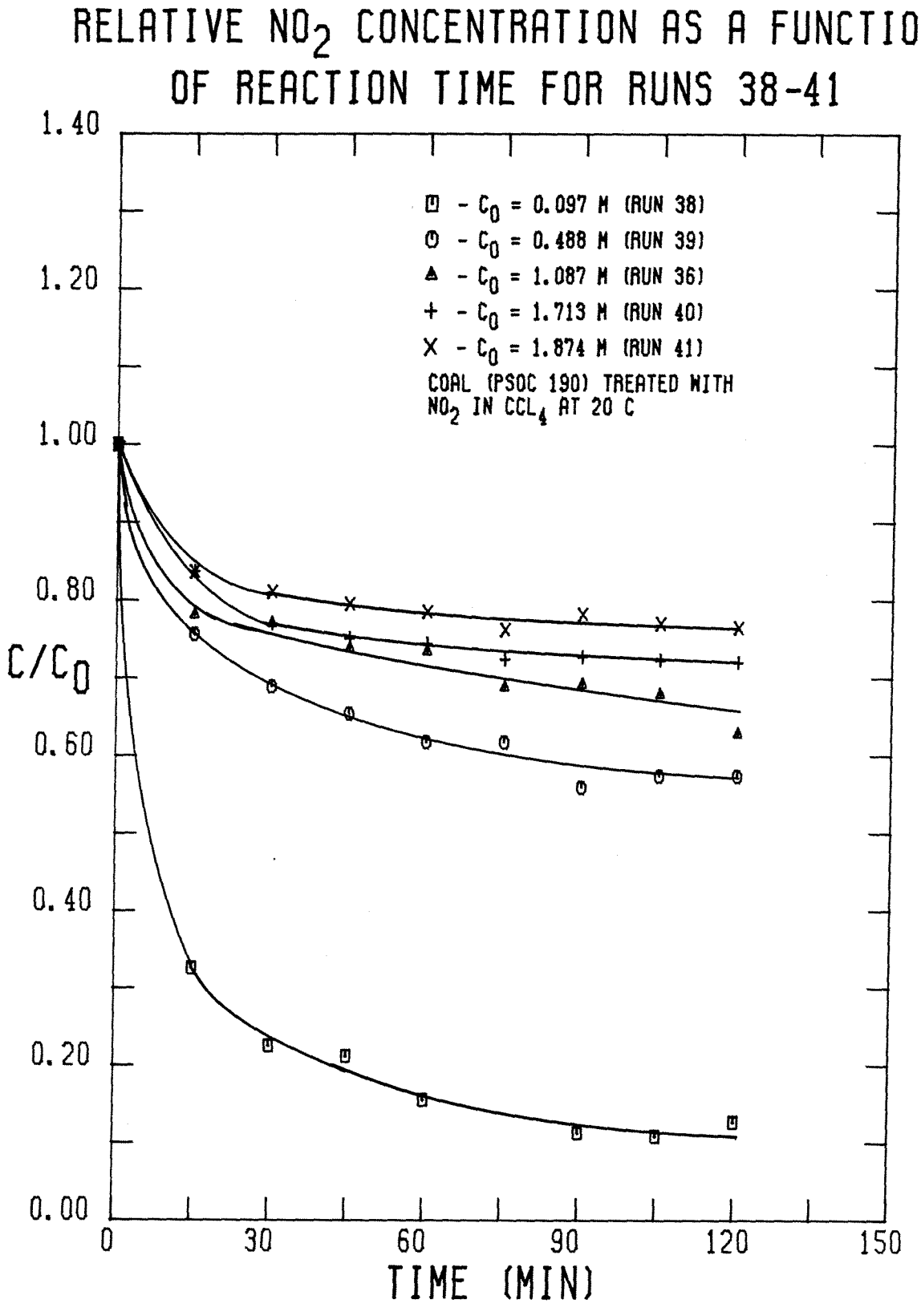
RELATIVE NO_2 CONCENTRATION AS A FUNCTION OF REACTION TIME FOR RUNS 38-41
□ - C_0 = 0.097 M (RUN 38)
○ - C_0 = 0.488 M (RUN 39)
△ - C_0 = 1.087 M (RUN 36)
+ - C_0 = 1.713 M (RUN 40)
X - C_0 = 1.874 M (RUN 41)
COAL (PSOC 190) TREATED WITH NO_2 IN CCL_4 AT 20 C
C/C0
TIME (MIN)
1.40
1.20
1.00
0.80
0.60
0.40
0.20
0.00
0
30
60
90
120
150

FIGURE 4-13

$\frac{c_0}{0.097}$	1	5.03	11.21	17.66	19.32
Initial Rate	1	1.82	3.64	4.28	4.68
$(\frac{c_0}{0.097})^{0.5}$	1	2.24	3.35	4.20	4.40

These results indicate that the initial rate is proportional to $(NO_2)^{0.5}$. A determination of the rate of (NO_2) decay at t = 15 minutes helps to confirm the dependence of the rate on $(NO_2)^{0.5}$. A graphical differentiation at t = 15 minutes is much more accurate because the accurate determination of the tangent to the locus is easier. If the curve corresponding to $(NO_2)_0$ = 0.097 F is taken as the reference with NO_2 concentration c' and rate r', the following results are obtained:

$(\frac{c}{c'})$	1	11.66	26.84	45.31	49.54
$(\frac{r}{r'})$	1	3.77	5.85	8.76	8.09
$(\frac{c}{c'})^{0.5}$	1	3.41	5.18	6.73	7.04
$[\frac{r/r'}{(c/c')^{0.5}}]$	1	1.10	1.13	1.30	1.15

These results indicate that the rate of NO_2 consumption by the coal depends on $(NO_2)^{0.5}$. Furthermore, the fact that the ratio of the relative rate to the square root of the relative NO_2 concentration tends to change slightly implies that perhaps there is a discernible dependence of the rate at t = 15 minutes on the concentration of reactive species in the coal because the extent of reaction of NO_2 with coal would be different for the various values of $(NO_2)_0$ at t = 15 minutes. If the rate did depend on the coal-species concentration, then $[\frac{r/r'}{(c/c')^{0.5}}]$ would not be constant, as appears to be the case. A graphical differentiation of the plots at t = 60 minutes, using the results obtained for the

curve corresponding to $(NO_2)_0$ = 0.097 F as the reference yields the following results:

$(\frac{C}{C'})_{t=60}$	1	19.98	52.97	84.59	97.66
$(\frac{r}{r'})_{t=60}$	1	4.70	8.29	7.92	8.20
$(\frac{C}{C'})^{0.5}_{t=60}$	1	4.47	7.28	9.20	9.88
$[\frac{r/r'}{(c/c')^{0.5}}]_{t=60}$	1	1.05	1.14	0.861	0.830

It is interesting to note that at the higher NO_2 concentrations the relative rates are essentially equal, which implies that the rate of NO_2 consumption is becoming independent of (NO_2). This feature is consistent with the concept of two different processes which account for the decay of (NO_2) because the rate expression is changing as t increases. Furthermore, the rates of the reactions with the three lowest initial values of (NO_2) still obey a rate dependence of $(NO_2)^{0.5}$. This apparent paradox is easily resolved because the extent of reaction of NO_2 with the species in the coal is not as great for the low values of $(NO_2)_0$ as for the higher values. Stated another way, the upper curves of Figure 4–13 at t = 60 minutes correspond to the situation where the first process (Rate $\propto$ $(NO_2)^{0.5}$) is already completed and the second process (Rate does not depend on (NO_2)) predominates. On the other hand, the lower curves at t = 60 minutes correspond to the situation where the first process still predominates.

Further evidence in support of the two process theory can be obtained by determining the rate constants assuming the rate can be expressed as

$$Rate = k\,(NO_2)^{0.5}. \qquad (4.2.6)$$

The values determined for k are:

c_0 (M)	$k_{t=0}$ ($M^{-0.5}$ min^{-1})	$k_{t=15}$ ($M^{-0.5}$ min^{-1})	$k_{t=60}$ ($M^{-0.5}$ min^{-1})
0.097	0.0140	0.00574	0.00134
0.488	0.0114	0.00631	0.00140
1.087	0.0152	0.00648	0.00152
1.713	0.0143	0.00746	0.00115
1.874	0.0149	0.00660	0.00110
	k_{avg} = 0.0140 ± 0.0013	k_{avg} = 0.00652 ± 0.00056	k_{avg} = 0.00130 ± 0.00015

Obviously, some change in the kinetics must account for the large drop in k from t = 0 to t = 60 minutes, or k must depend upon some other parameter. It would seem that as the extent of conversion of the coal species approaches unity, the scarcity of the remaining reactive species could affect the rate. Indeed, the amount of NO_2 far exceeds the uptake capacity of the coal. Thus, once the coal is saturated, the reaction for this mode of NO_2 consumption must cease. The coal-species concentration may affect the rate of NO_2 consumption, however, only towards the end of the reaction. Therefore, the two processes referred to above may actually correspond to the same reaction; that is, the rate law may actually be more complex than that given in equation (4.2.6). Rather, the rate may be better expressed empirically as

$$Rate = \frac{k_1 (NO_2)^{0.5} (S)}{(NO_2)^{0.5} + k_2(S)}, \quad \text{where} \qquad (4.2.7)$$

(S) = the coal-species concentration (mol/ g coal), and

k_1, k_2 = the appropriate rate constants.

Thus, at the beginning of the reaction, $k_2(S) >> (NO_2)^{0.5}$, so that the rate is of the form given in equation (4.2.6). As (S) approaches zero, however, $(NO_2)^{0.5} >> k_2(S)$ so that the rate is now proportional to (S). Such a rate

expression would then qualitatively explain the results.

There is a very interesting relationship between the global rate expression given in equation (4.2.7) and the rate expression obtained when the resistance to diffusion of NO_2 controls the reaction rate.[4] If the specific rate of reaction between NO_2 and the coal species is given by

$$r_s = k_s\,(NO_2)^n\,, \quad \text{where} \tag{4.2.8}$$

r_s = the specific rate of NO_2 consumption (M/min),

k_s = the specific rate constant (min^{-1}–M^{1-n}),

(NO_2) = the NO_2 concentration at any point within the particle (M), and

n = the order of the rate dependence on (NO_2),

then the global rate of NO_2 consumption is given by

$$R_{NO_2} = \eta\, k_s\,(NO_2)_b^n\,, \quad \text{where} \tag{4.2.9}$$

R_{NO_2} = the global rate of NO_2 consumption (M/min),

η = the effectiveness factor, and

$(NO_2)_b$ = the bulk NO_2 concentration.

In the region of strong pore diffusion resistance, the effectiveness factor is given by:

$$\eta = \frac{1}{\varphi} = \frac{1}{L}\left[\frac{2\,D_e}{(n+1)\,k_s\,(NO_2)_b^{n-1}}\right]^{0.5}\,, \quad \text{where} \tag{4.2.10}$$

φ = the Thiele modulus,

L = the appropriate diffusion length, which for spherical particles would be equal to the particle radius, R (cm), and

D_e = the effective diffusivity of NO_2 in the particle (cm^2/min).

Substituting equation (4.2.10) into (4.2.9) yields the following expression for the global rate of NO_2 consumption:

$$R_{NO_2} = \left(\frac{2}{n+1}\frac{k_s D_e}{R_2}\right)^{0.5} (NO_2)^{\frac{n+1}{2}} . \qquad (4.2.11)$$

Applying this expression to the results of this study reveals that $n = 0$ if pore diffusion resistance is rate controlling. If the rate of the NO_2/coal reaction controlled the global rate of NO_2 consumption during the first 60 minutes of the reaction, on the other hand, then the specific rate would have to be a function of $(NO_2)^{0.5}$. No simple mechanism can result in such a dependence. Therefore, the dependence of the global rate of NO_2 consumption during the initial stage of the reaction on $(NO_2)^{0.5}$ is due simply to the domination of the resistance to diffusion of NO_2 in the solid coal matrix. That this is the case is not surprising. During the initial stage of the reaction, the NO_2 is reacting as soon as it diffuses into the coal, which implies that the specific rate does not depend on (NO_2) but may or may not depend on (S).

The kinetic behavior at later reaction times readily follows from the discussion above. As (S) approaches zero, the rate of consumption of NO_2 declines so that the resistance to diffusion of NO_2 no longer controls the rate. Rather, the rate is now controlled by the chemical reaction, the rate of which is dependent on (S) by virtue of the scarcity of reactive species in the coal. The dependence of the global rate on (NO_2) vanishes, however, which is in accord with the results obtained at later reaction times. Therefore, the kinetic data derived from the experiments using different initial (NO_2) concentrations is entirely consistent with a model where the resistance to diffusion of NO_2 in the solid coal matrix controls the global rate of NO_2 consumption during the initial stage of the NO_2-coal reaction and when at later times in the reaction, the specific rate of chemical reaction controls the global rate of NO_2 consumption. Furthermore, the specific rate of chemical reaction does not depend on (NO_2), but it may or may not depend on (S). The fact that the rate constant, k, given by equation (4.2.6)

varies with $(NO_2)_0$ in the later stages of the reaction indicates that the specific rate probably does depend on (S).

4.2.2 Solid Phase Species

4.2.2.1 Overall Mass Gain

An examination of the limited data for Runs 1–6 in Table 3–6 concerning the effect of the solvent on the mass loss of the coal due to the NO_2 treatment allows some qualitative conclusions to be made. First, the mass loss of the coal decreases as the treatment temperature increases where water and pyridine are used as the solvents. The reverse is true, however, when nitrobenzene is the solvent. These trends can readily be explained on the basis of the solubility of NO_2 in the various solvents coupled with the ability of the solvent to extract coal. The solubility of NO_2 in all three solvents should decrease as the temperature increases, but the amount of the solubility change may vary from one solvent to the other. Offsetting the decrease in solubility as the temperature increases is the rate of the reaction between NO_2 and coal, which should increase with the temperature. Since NO_2 is very soluble in nitrobenzene, the solubility effect may not be as pronounced as in the case when water and pyridine are used as the solvents. Furthermore, the extraction of portions of the coal into the solvent render the extracted coal more susceptible to attack by NO_2. Whereas neither pyridine nor water extract an appreciable amount of the coal, nitrobenzene extracts 37.6 and 54.6 % of the coal at 34 and 81°C, respectively.

It should be noted that just drying the coal used in these runs results in a 12.29 % mass loss while washing the raw coal in water at 25°C for two hours, filtering the coal and then drying it results in a 15.84 % mass loss. Thus, the mass loss of 14.4 and 13.2 % when the coal was treated with NO_2 in H_2O at 26 and 78°C, respectively, actually represents a net mass increase, which can be attributed to the uptake by the coal of nitrogen and oxygen. If the raw coal is just washed in pyridine, filtered and dried, there is a 15.84 % mass loss, which can be attributed to the removal of water plus a minor amount of extraction.

Treatment of the coal slurried in pyridine with NO_2 at 26 and 83°C results in a 22.8 and 16.2 % mass loss, respectively. Thus, a net mass loss occurs due to NO_2 treatment when pyridine is the solvent. Most likely, the NO_2-treated coal is extracted to a slightly greater extent by pyridine than the raw coal. If the raw coal is just slurried in nitrobenzene, filtered and dried, only a 7 % mass loss occurs, which implies a net mass gain of about 6 %, which can be attributed to the incomplete removal of the nitrobenzene by vacuum drying. When the coal slurried in nitrobenzene is exposed to NO_2, however, 37.6 and 54.6 % of the coal is extracted at 34 and 81°C, respectively. When the recovered extract is included, the overall mass losses are - 16.5 and 16.0 % at 34 and 81°C, respectively. Obviously the reaction of the coal with NO_2 yields coal derived products which are quite soluble in nitrobenzene. Furthermore, the large increase in the overall mass loss as the temperature increases may be attributed to the faster rate of oxidation of the coal at the higher temperature. Therefore, the predominance of the decrease in NO_2 solubility in water and pyridine over the increase in the rate of the oxidation of the coal as the temperature increases accounts for the decrease in mass loss when these two solvents are used, while the predominance of the increase in the rate of the coal oxidation rate over the NO_2 solubility decrease as the temperature increases accounts for the increase in mass loss when nitrobenzene is the solvent.

The mass loss of the coal due to NO_2 treatment in water at 25°C (Runs 7–11) and due to the wash of the NO_2-treated coal in 0.1 M Na_2CO_3 (aq) is displayed graphically as a function of NO_2 treatment time in Figure 4–14. As noted above, just washing the coal in water, filtering and vacuum drying results in a 15.84 % mass loss, which is due mainly to the removal of the moisture in the raw coal. Washing the washed and dried coal in 0.1 M Na_2CO_3 (aq) for two hours at 25°C results in an additional 10.04 % mass loss so that the overall mass loss with

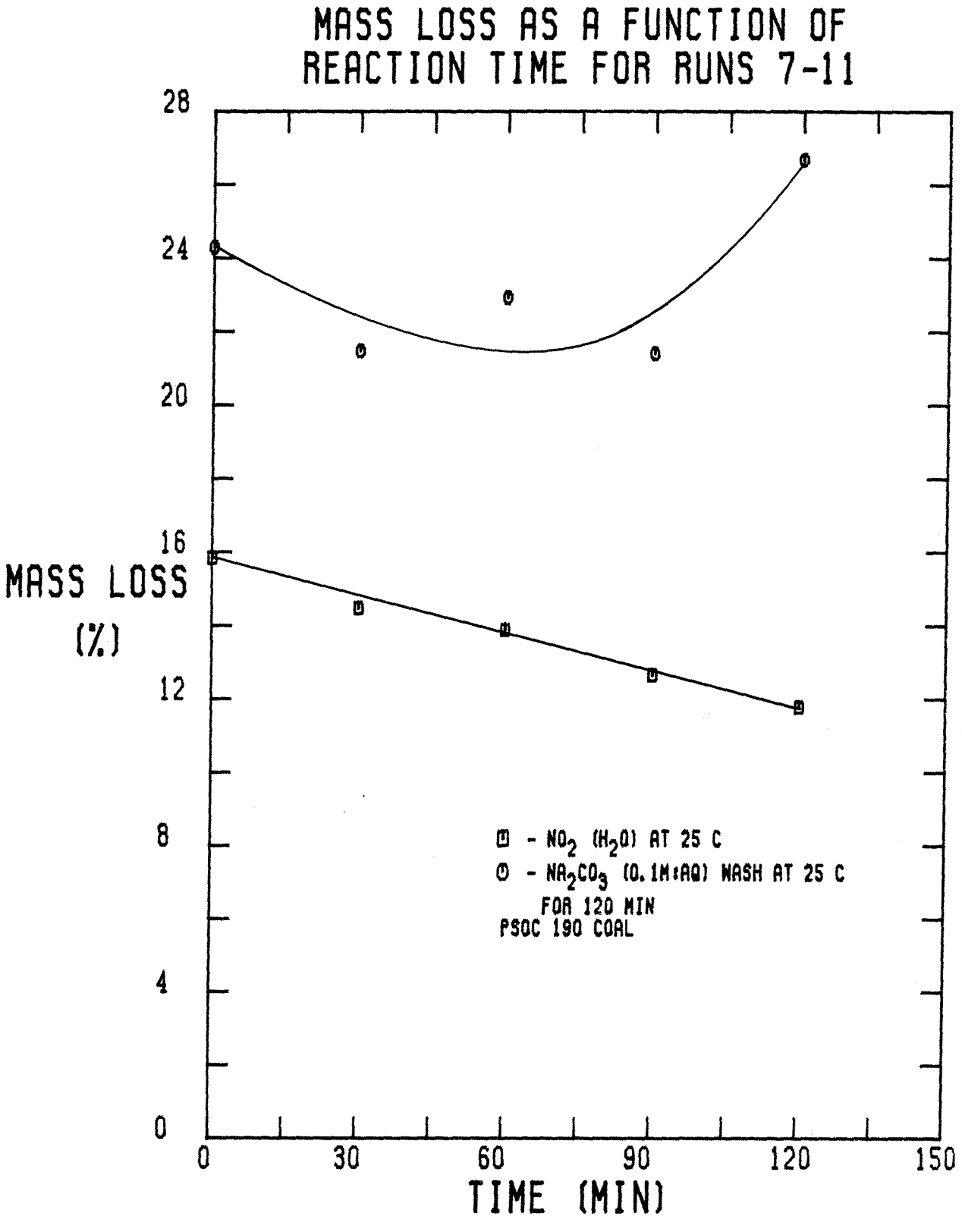
MASS LOSS AS A FUNCTION OF
REACTION TIME FOR RUNS 7-11
MASS LOSS
(%)
28
24
20
16
12
8
4
0
0
30
60
90
120
150
TIME (MIN)
- NO2 (H2O) AT 25 C
- NA2CO3 (0.1M:AQ) WASH AT 25 C
FOR 120 MIN
PSOC 190 COAL

FIGURE 4-14

respect to the raw coal is 24.29 %. It is interesting to note that the mass loss due to NO_2 treatment decreases as the reaction time increases. This decrease is the result of the nitrogen and oxygen uptake by the coal increasing with the NO_2 exposure time. The overall mass loss after washing the NO_2-treated coal in 0.1 M Na_2CO_3 (aq), on the other hand, increases with NO_2-exposure time after an initial decrease. This increase in mass loss may be attributed to the removal of oxidized coal products, the quantity of which should increase with NO_2-treatment time. The initial decrease in overall mass loss is due to the very rapid uptake of nitrogen and oxygen by the coal without sufficient oxidation to render a significant amount of the coal soluble in 0.1 M Na_2CO_3 (aq). Continued exposure of the coal to NO_2, however, eventually results in a larger portion of the coal becoming soluble in 0.1 M Na_2CO_3 (aq), which then accounts for the increase in the mass loss. It should be noted that the overall mass loss at t = 90 minutes (21.40 %) is not included in the plot because of contamination during drying. Furthermore, the results for Runs 12 and 13 have not been included because the NO_2 flowrates during treatment were not monitored.

The mass loss results for the second set of experiments (Runs 15–20) using water as the solvent can be found in Table 3–8. As expected, the mass loss due to NO_2 treatment decreases as the exposure time or NO_2 flowrate increases. Interestingly, in this set of runs the mass loss due to NO_2 treatment initially increases from 15.84 % (no NO_2) to 17.56 % (NO_2 for 60 min), which implies that some water soluble products from the coal-NO_2 reaction are leached into solution. This extraction only occurs to a small extent (1.72 % of the total mass) and must occur in the initial stage of the reaction since the mass loss begins to decrease after t = 60 minutes. The additional mass loss due to the Na_2CO_3 (aq) wash is much less in this set than the previous set of runs. The overall mass loss decreases from 24.29 % (t=0) to 17.55 % (t=120) and then begins to increase

after t = 120 minutes. This minimum at t = 120 minutes contrasts with the minimum at t = 60 minutes in the previous set. The shift in the minimum is probably due to the lower NO_2 flowrates used in this set than in the previous set of runs. The same argument concerning the two-stage mechanism discussed above, however, pertains in this set of runs as well.

In the runs conducted with CCl_4 as the solvent, the coal was dried before treatment with NO_2 in order to mitigate the effects of water on the reaction. Thus, the NO_2-treated coals always gain mass relative to the untreated, predried coal. For instance, the mass gain results of the set of experiments conducted at 25°C in the flow reactor are shown in Figure 4–15. The mass gain due to the uptake of O and N during the NO_2 treatment approaches 18 %. Furthermore, there is no change in the mass gain after 120 minutes of NO_2 treatment, which implies that the process accounting for N and O uptake is complete within 120 minutes. An examination of the curve depicting the overall mass gain after the NO_2-treated coals are washed in 0.1 M Na_2CO_3 (aq) reveals that the overall mass gain is essentially zero, which implies that roughly the same amount of material taken up by the coal during NO_2 treatment is removed by the aqueous Na_2CO_3 wash. It is not necessarily true, however, that the *same* material taken up by the coal during NO_2 treatment is removed by the Na_2CO_3 (aq) wash.

The mass gain results of the set of experiments (Runs 28–32) conducted at 50°C in the flow reactor are shown in Figure 4–16. In this case, the mass gain due to NO_2 treatment approaches 30 % at 180 minutes and shows no signs of levelling off, which contrasts with the 18 % limit of the previous set. Obviously the increase in temperature has increased the rate of the coal-NO_2 reaction. The coal treated at 50°C could not be washed in 0.1 M Na_2CO_3 (aq) because the treated coal completely emulsified and could not be filtered. Therefore, the coal samples were washed in 2 M HNO_3 (aq). The overall mass gain after the

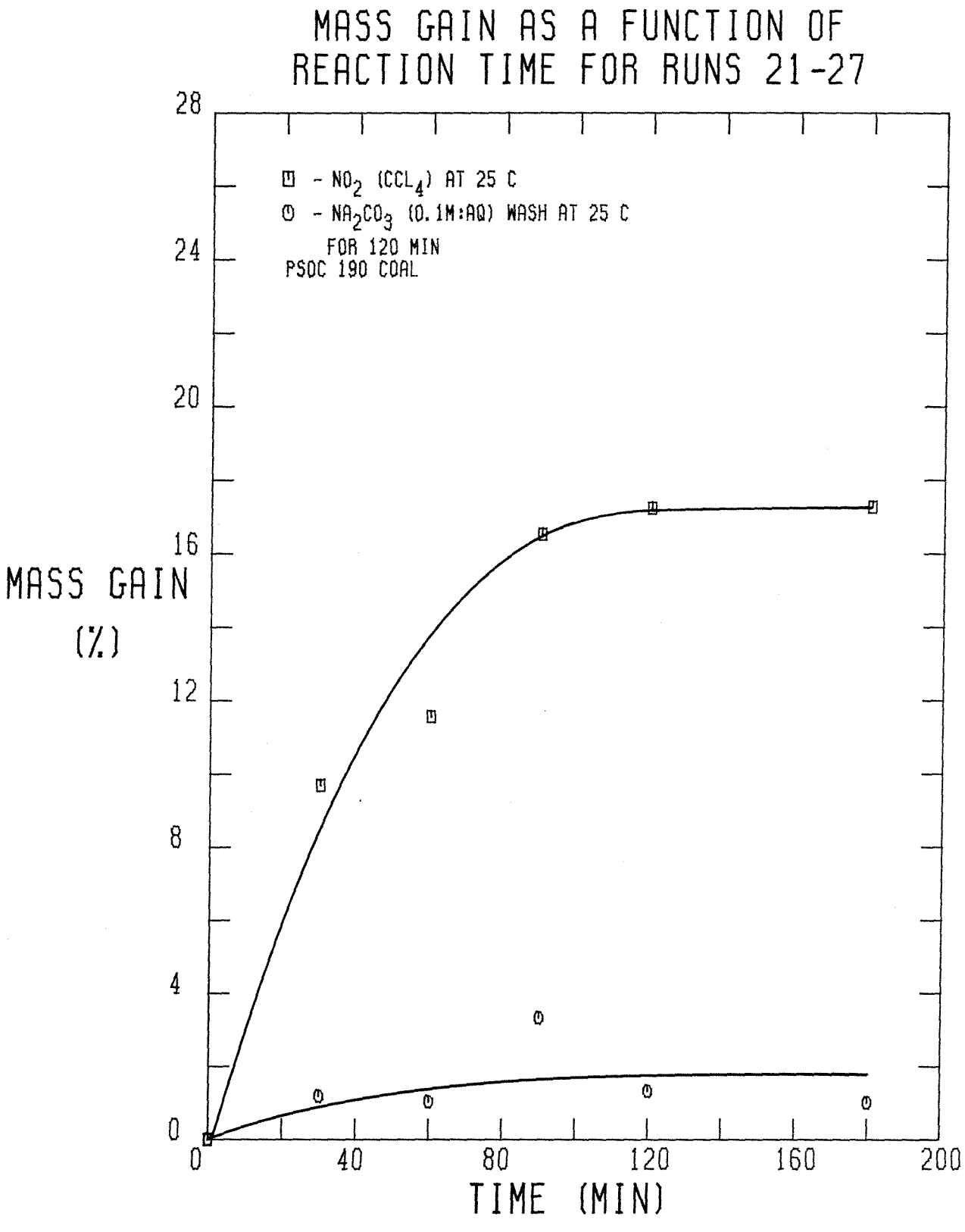
MASS GAIN AS A FUNCTION OF
REACTION TIME FOR RUNS 21-27
□ - NO2 (CCL4) AT 25 C
○ - NA2CO3 (0.1M:AQ) WASH AT 25 C
FOR 120 MIN
PSOC 190 COAL
MASS GAIN
(%)
0
4
8
12
16
20
24
28
0
40
80
120
160
200
TIME (MIN)

FIGURE 4-15

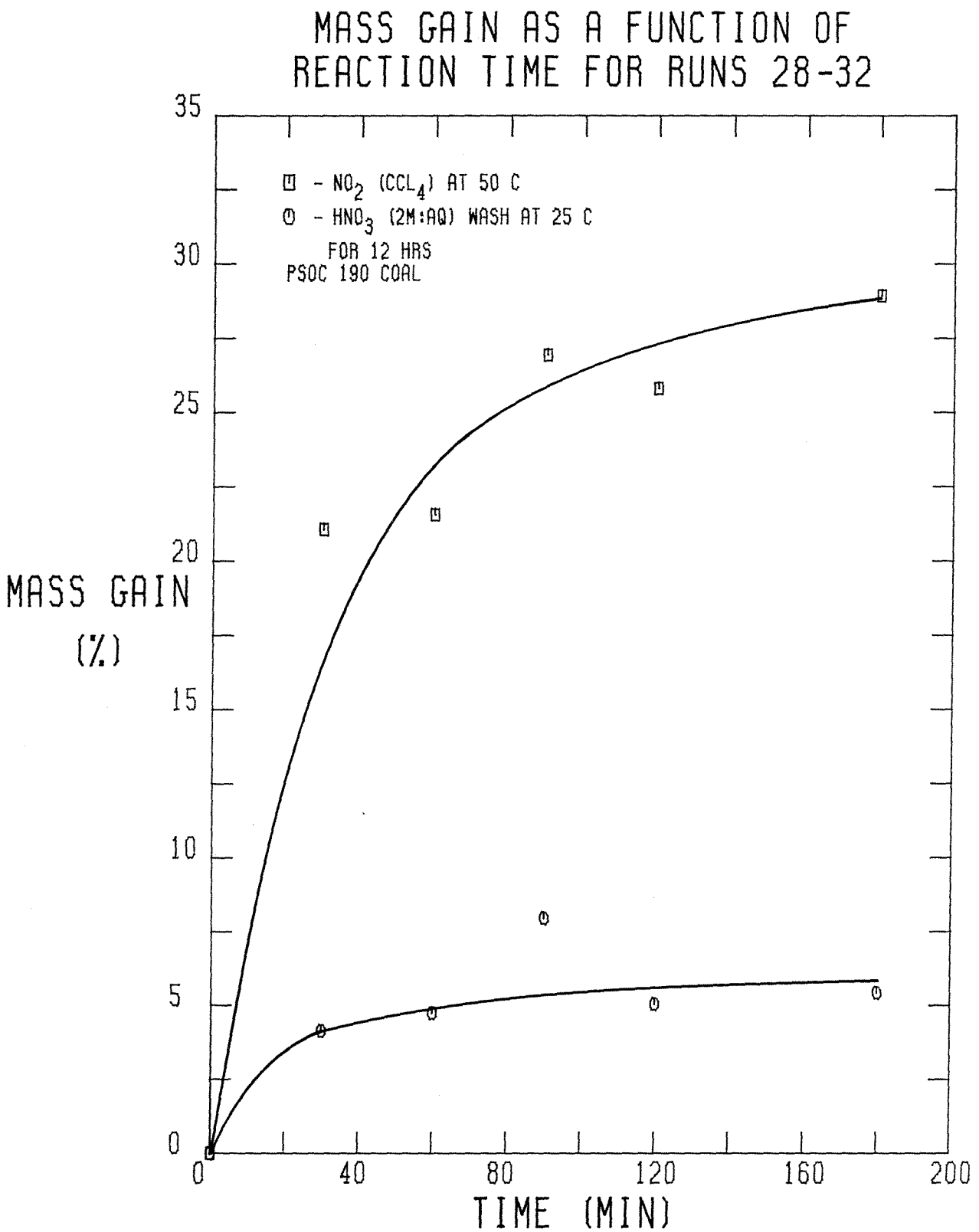
MASS GAIN AS A FUNCTION OF
REACTION TIME FOR RUNS 28-32
□ - NO2 (CCL4) AT 50 C
○ - HNO3 (2M:AQ) WASH AT 25 C
FOR 12 HRS
PSOC 190 COAL
MASS GAIN
(%)
0
5
10
15
20
25
30
35
0
40
80
120
160
200
TIME (MIN)

FIGURE 4-16

HNO_3 (aq) wash is about 6 % at t = 180 minutes and continues to rise slightly, which indicates that HNO_3 (aq) does not extract as much material from the NO_2-treated coal as Na_2CO_3 (aq).

The coal used in the runs conducted in the batch reactor was washed in H_2O at 25°C for two hours, filtered and vacuum dried before being treated with NO_2. While just drying the coal removed 12.49 % of the mass, washing the coal before drying in H_2O resulted in mass losses of 17.69 and 17.80 % for the two batches. Therefore, about 5.25 % of the coal mass is soluble in H_2O. Although this difference should not affect the mass gain results for the NO_2 treatment of the washed and dried or just predried coal to an appreciable extent, it does influence the overall mass gain results. During the NO_2 treatment, presumably all portions of the coal are attacked by NO_2 and there is no extraction of the coal products by the CCl_4. The overall mass gain results, however, will be based on two different bases. The Na_2CO_3 (aq) wash of the predried coal treated with NO_2 should remove the 5.25 mass percent water soluble material already removed in the washed and dried coal. Therefore, with all other things being equal, the overall mass gain for the predried coal treated with NO_2 and washed with 0.1 M Na_2CO_3 (aq) should be about 5.25 % lower than the overall mass gain for the washed and dried coal treated in the same manner. Consequently, comparison of the results from experiments in which the predried coal is used in one and the washed and dried coal is used in the other must take this difference into account. As it turns out, however, other circumstances preclude the comparison of results for the Na_2CO_3 (aq) wash of the two different pretreated coals treated with NO_2. Since all of the runs discussed below (Runs 33–52) used washed and dried coal, the problem discussed above does not pertain, which is fortunate because it is precisely these runs which provide the basis of many of the comparisons which are made.

The mass gain results for the set of the experiments conducted at 20°C in the batch reactor (Runs 33-37) are displayed in Figure 4–17. It appears that the mass gain for both the NO_2-treated and Na_2CO_3 (aq)-washed coals reaches a maximum at 120 minutes of NO_2 exposure, although it is difficult to determine if the drop at t = 180 minutes is simply due to an inadvertent deviation from the standard drying procedure. It is also possible, however, that after prolonged exposure ($t >$ 120 minutes), the solvent begins to slowly extract some of the reacted coal, which would account for the drop of about 1 % from t = 120 to t = 180 minutes. The drop in the overall mass curve is not as noticeable, which suggests that the maximum removal of coal derived products of the NO_2-coal reaction is about 6 % by mass. It should be noted that the overall mass gain is roughly 11 % at t = 120 minutes while the overall mass gain for the set of runs conducted at 25°C, in which the NO_2 concentration, (NO_2), was much greater, is only about 6 %, even after adjustment for the difference in the coal pretreatment. The mass gain curves for the NO_2-treated coals are basically identical, however, with both approaching 17 % as the exposure time increases. These results indicate that the mass gain due to NO_2 treatment does not depend upon the (NO_2) history to a discernible extent while the overall mass gain does show such a dependence. These trends are consistent with a two-process reaction theory for NO_2 consumption. The first process, whose rate is independent of the (NO_2) history, accounts for the uptake of material by the coal during NO_2 treatment while the second process, whose rate does depend on the (NO_2) history, accounts for the formation of coal derived products soluble in 0.1 M Na_2CO_3 (aq).

The mass gain results for the series of experiments conducted at 0°C (Runs 42–46) are plotted in Figure 4–18. The results are basically the same as in the previous series of runs, except the mass gain due to NO_2 treatment approaches 16 % instead of 17 % and the overall mass gain approaches 10 % instead of 11 %.

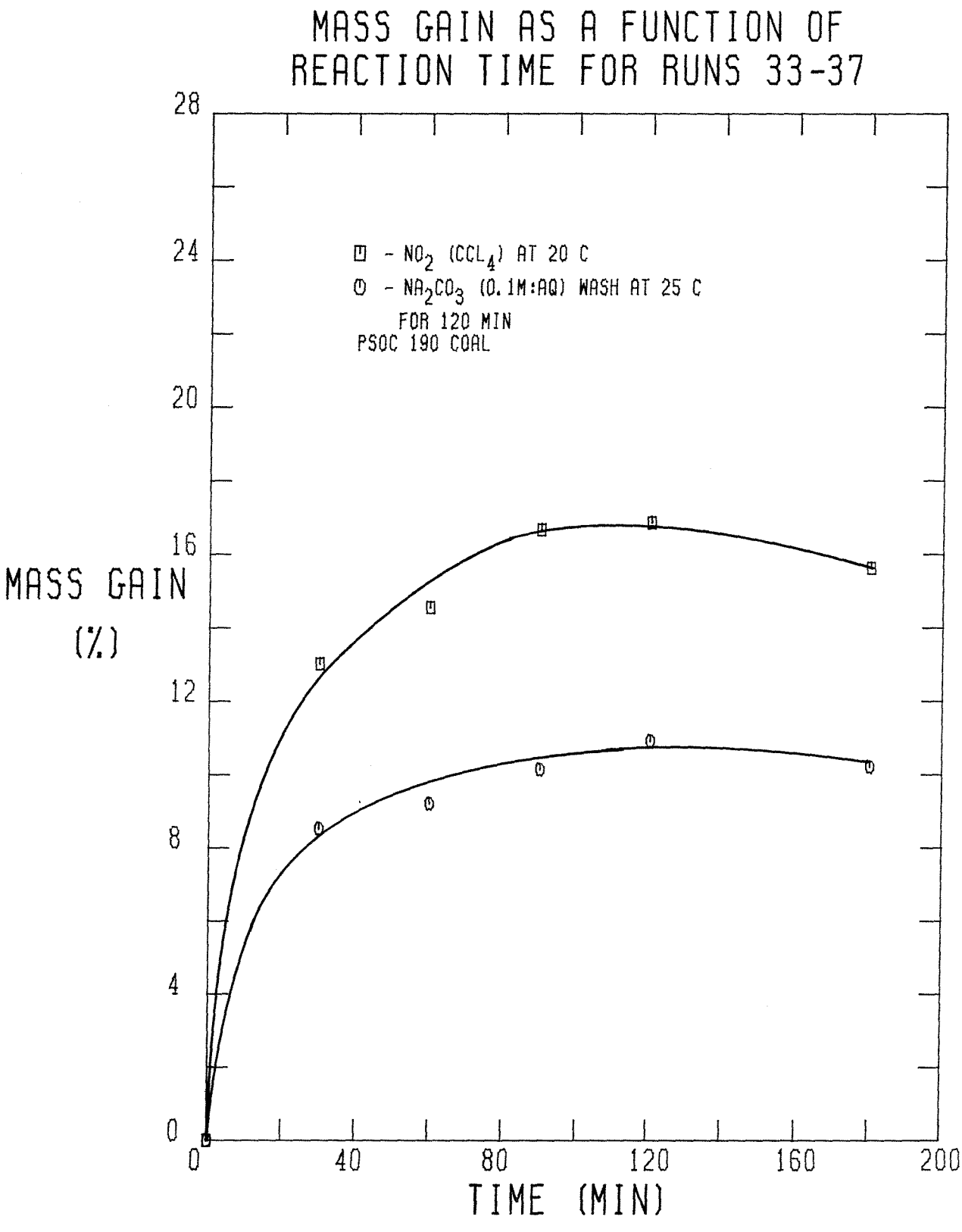
MASS GAIN AS A FUNCTION OF
REACTION TIME FOR RUNS 33-37
□ - NO2 (CCL4) AT 20 C
○ - NA2CO3 (0.1M:AQ) WASH AT 25 C
FOR 120 MIN
PSOC 190 COAL
MASS GAIN
(%)
0
4
8
12
16
20
24
28
0
40
80
120
160
200
TIME (MIN)

FIGURE 4-17

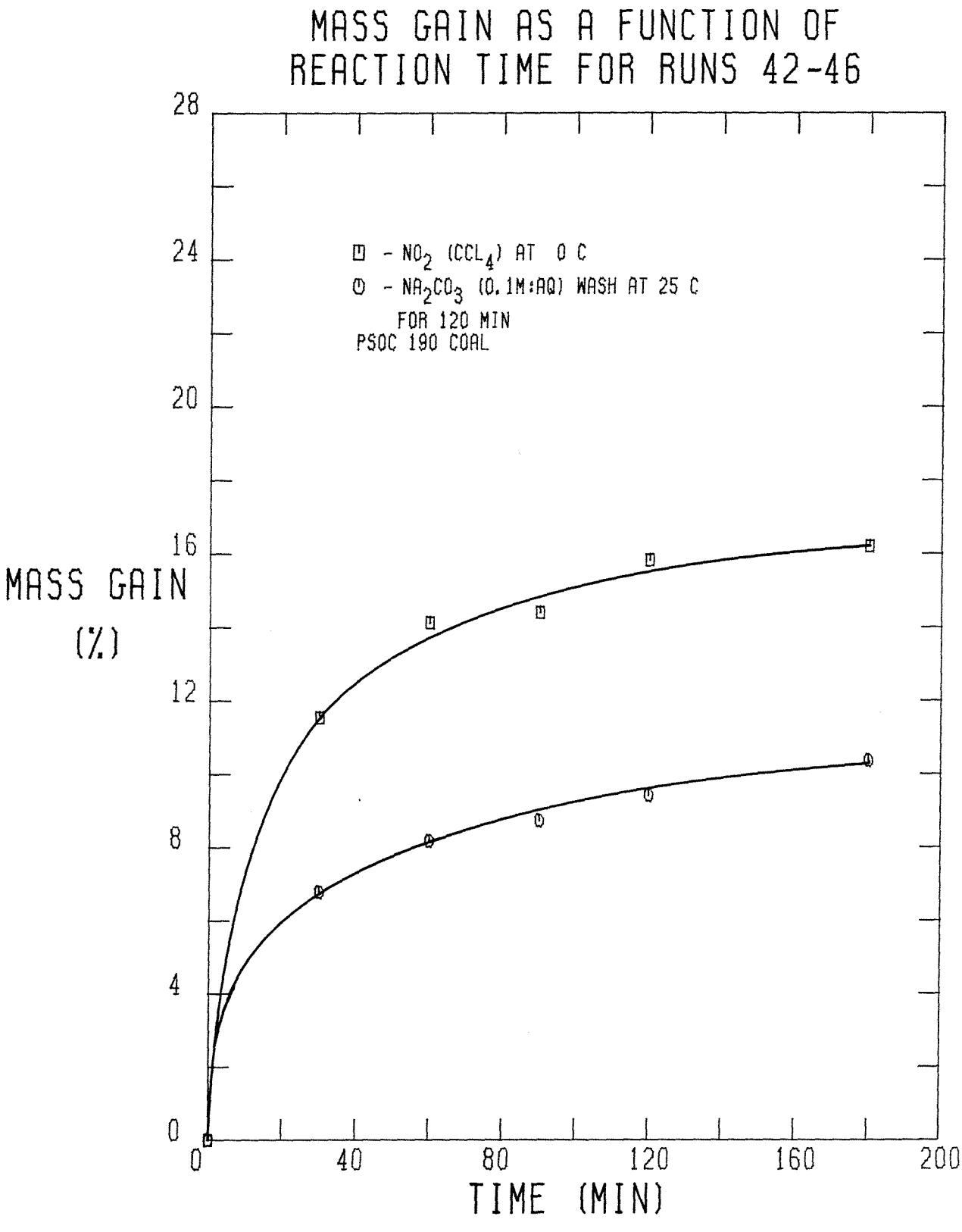
MASS GAIN AS A FUNCTION OF
REACTION TIME FOR RUNS 42-46
□ - NO2 (CCL4) AT 0 C
○ - NA2CO3 (0.1M:AQ) WASH AT 25 C
FOR 120 MIN
PSOC 190 COAL
MASS GAIN
(%)
TIME (MIN)
0
4
8
12
16
20
24
28
0
40
80
120
160
200

FIGURE 4-18

The rate of increase in the mass gain curves, however, is roughly equal to that in the previous set of runs.

The dependence of the mass gain due to NO_2 treatment on temperature is shown graphically in Figure 4–19. This plot clearly shows that running the NO_2 treatment at 0°C or 20°C has little effect on the mass gain while conducting the treatment at 50°C almost doubles the mass gain. When this latter fact is considered in light of the complete emulsification of the coal treated with NO_2 at 50°C in 0.1 M Na_2CO_3 (aq), it appears that the rate of the reaction which produces compounds which are soluble in aqueous Na_2CO_3 is much greater at 50°C than at either 20°C or 0°C. The effect of temperature on the overall mass gain is shown in Figure 4–20. Since the amount of material leached from the coals treated with NO_2 at both 20°C and 0°C by the 0.1 M Na_2CO_3 (aq) wash is equal, it follows that the reaction which produces the soluble coal compounds proceeds to the same extent at both 20 and 0°C. Therefore, the difference between the two mass gain curves can be attributed to a mild temperature dependence of the other, independent reaction which contributes to the mass gain.

The effect of the initial concentration of NO_2, $(NO_2)_0$, on the mass gain is displayed graphically in Figure 4–21. A very interesting feature concerning the mass gain due to NO_2 treatment is evident. The curve shows two linear regions of different slopes which implies that more than one process is occurring, which is consistent with the two-stage reaction theory. At low values of $(NO_2)_0$, there is an insufficient amount of NO_2 available to complete the coal-NO_2 reaction. As $(NO_2)_0$ is increased so that NO_2 is in excess, the quick process accounting for the uptake of nitrogen and oxygen is complete within two hours. The additional mass gain for higher values of $(NO_2)_0$ may be attributed to the mass gain associated with the reaction which generates the coal derived products soluble in aqueous Na_2CO_3. The overall mass gain curve provides direct confirmatory

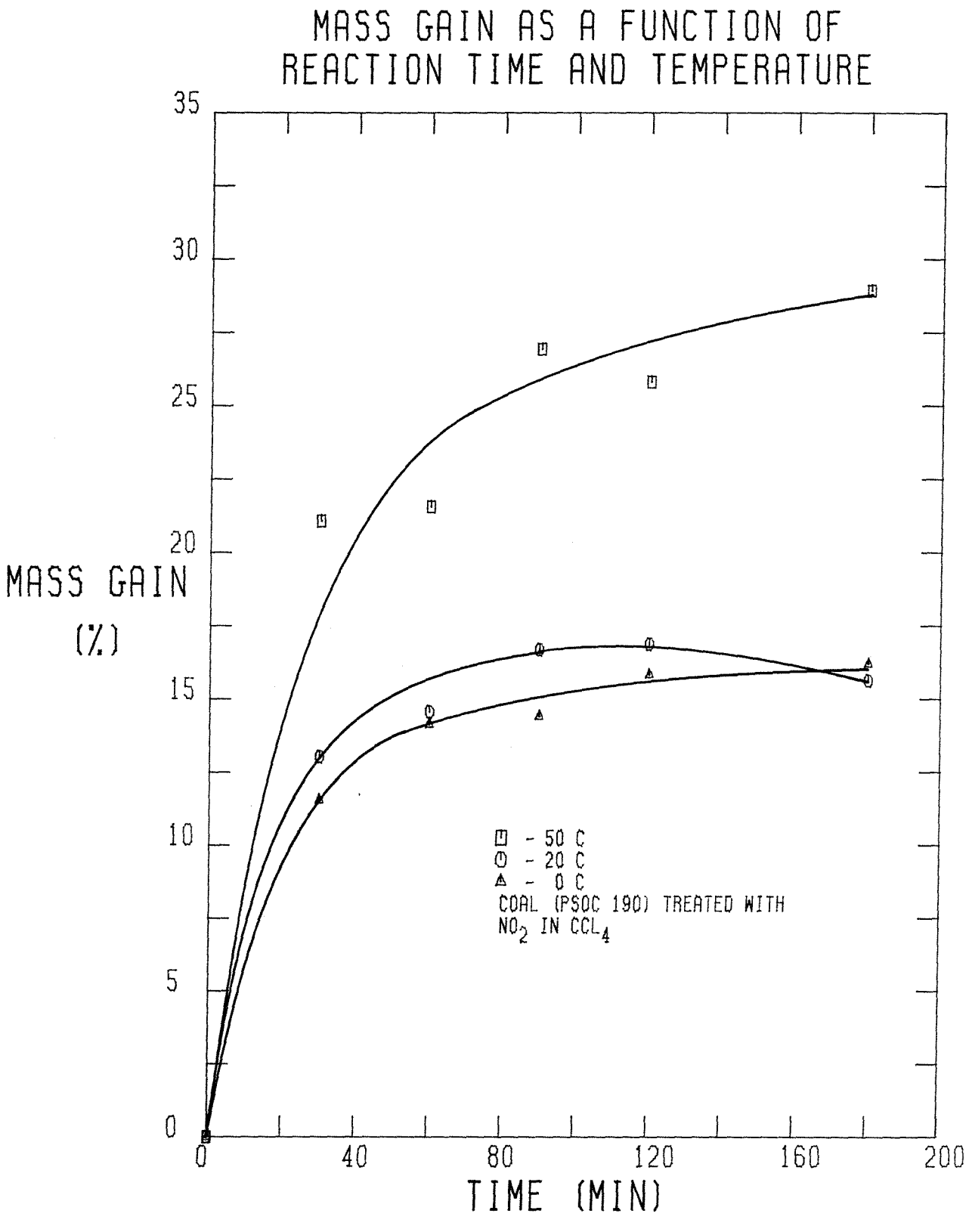
MASS GAIN AS A FUNCTION OF
REACTION TIME AND TEMPERATURE
MASS GAIN
(%)
35
30
25
20
15
10
5
0
0
40
80
120
160
200
TIME (MIN)
- 50 C
- 20 C
- 0 C
COAL (PSOC 190) TREATED WITH
NO2 IN CCL4

FIGURE 4-19

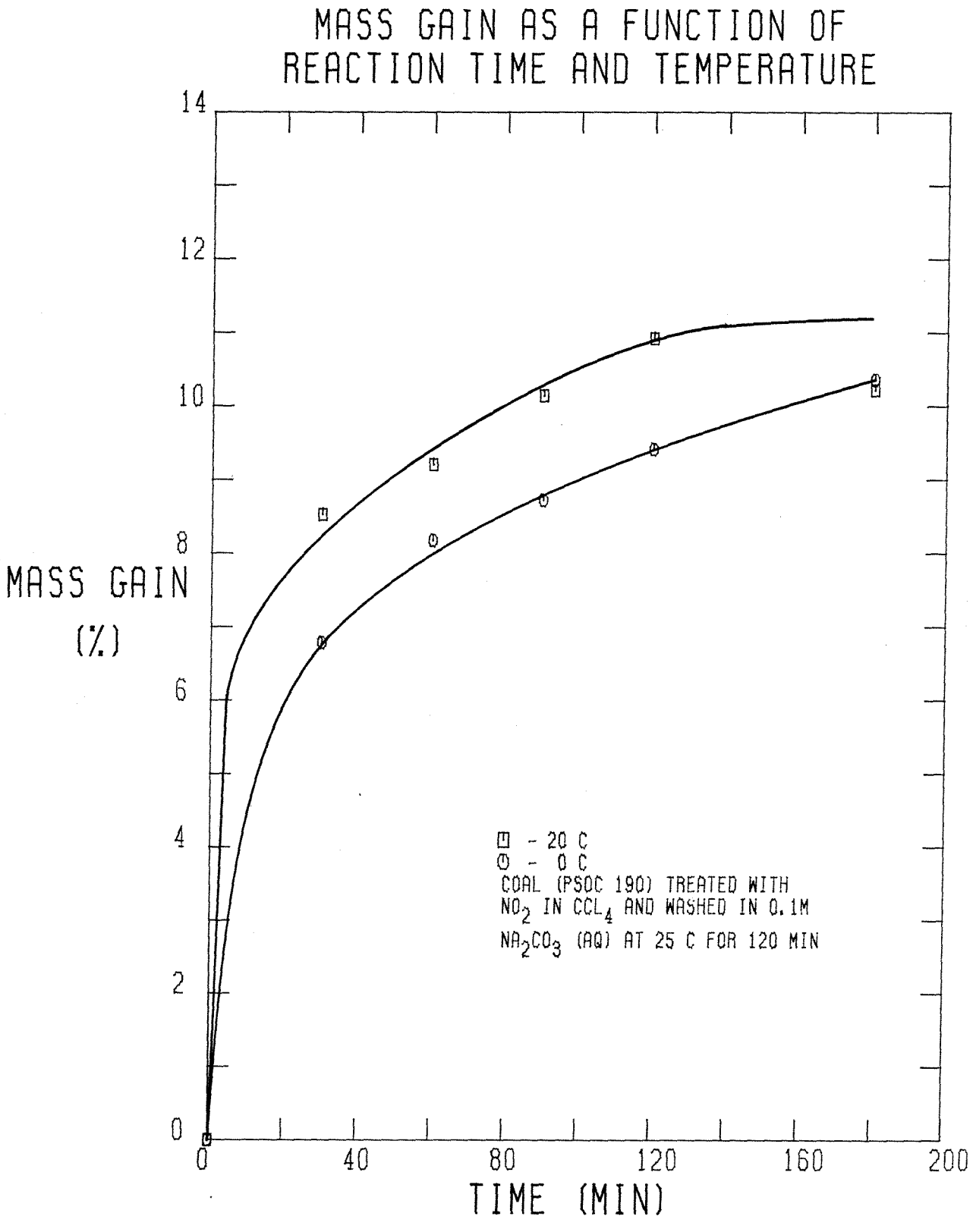
MASS GAIN AS A FUNCTION OF
REACTION TIME AND TEMPERATURE
MASS GAIN
(%)
TIME (MIN)
0
2
4
6
8
10
12
14
0
40
80
120
160
200
□ - 20 C
Ⓞ - 0 C
COAL (PSOC 190) TREATED WITH
NO_2 IN CCL_4 AND WASHED IN 0.1M
NA_2CO_3 (AQ) AT 25 C FOR 120 MIN

FIGURE 4-20

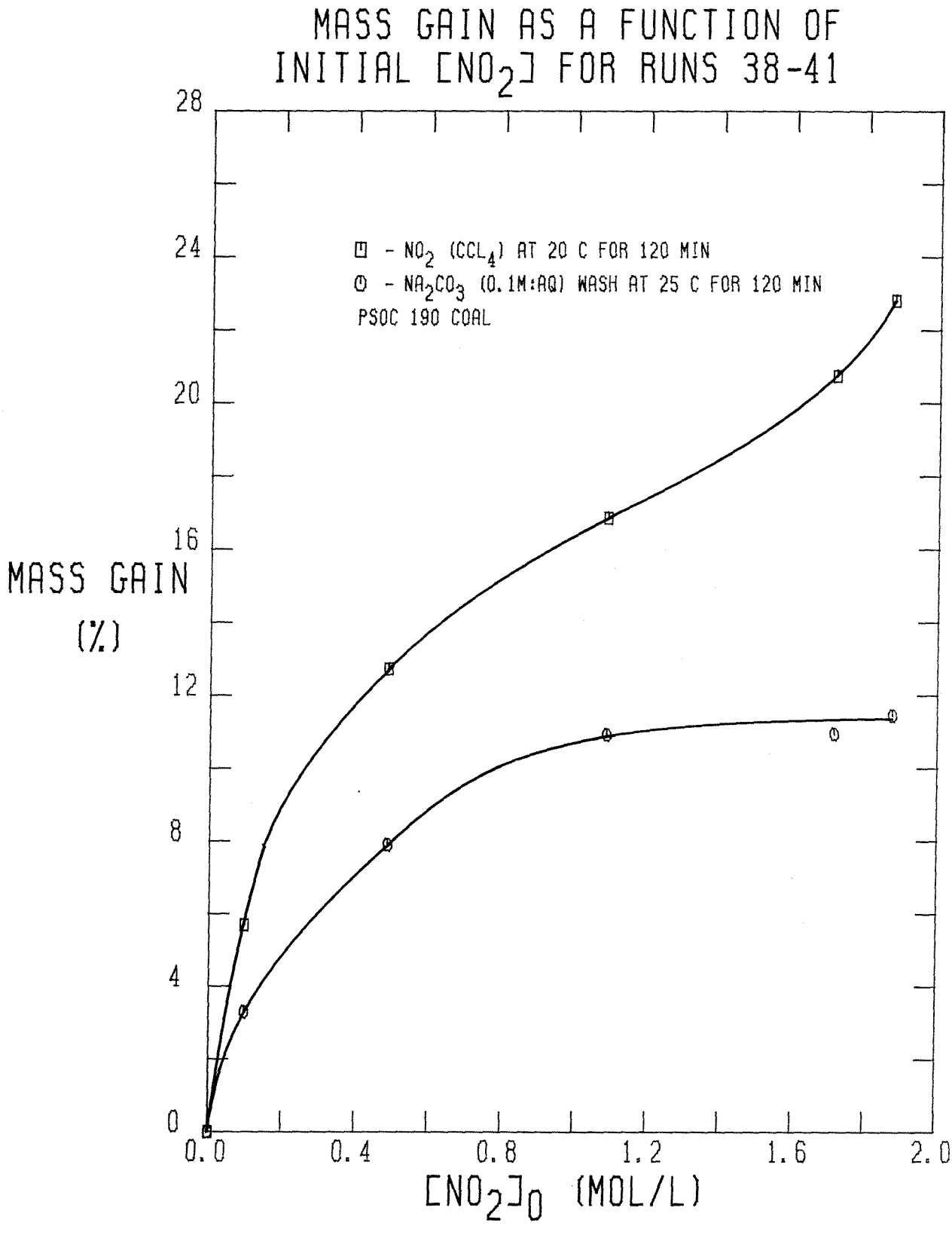
MASS GAIN AS A FUNCTION OF
INITIAL [NO2] FOR RUNS 38-41
□ - NO2 (CCL4) AT 20 C FOR 120 MIN
Ø - NA2CO3 (0.1M:AQ) WASH AT 25 C FOR 120 MIN
PSOC 190 COAL
MASS GAIN
(%)
28
24
20
16
12
8
4
0
0.0
0.4
0.8
1.2
1.6
2.0
[NO2]0 (MOL/L)

FIGURE 4-21

evidence of this interpretation. Once $(NO_2)_0$ exceeds 1.0 F, the overall mass gain remains constant at about 11 %. Therefore, the process which accounts for the uptake of material not leached by Na_2CO_3 (aq) is complete within 120 minutes provided $(NO_2)_0$ exceeds 1.0 F. Any additional mass the coal takes up at higher values of $(NO_2)_0$ due to the NO_2 treatment is leached by the Na_2CO_3 (aq) wash.

The mass gain results for the PSOC 276 coal treated at 20°C (Runs 47–52) are shown in Figure 4–22. In this instance, both curves continue to rise after 180 minutes, which implies that neither of the two reactions discussed above are completed within three hours of NO_2 treatment. This behavior is a result of the resistance to pore diffusion by NO_2 in this coal. A comparison of the mass gain results due to NO_2 treatment for the PSOC 190 and PSOC 276 coals is displayed in Figure 4–23, which clearly demonstrates the behavioral difference. Whereas the mass gain for the PSOC 190 levels off after 90 minutes at about 17 %, the mass gain for the PSOC 276 has reached only 16 % after 180 minutes, but is still rising. Indeed, if these curves were extrapolated, they would converge at about 180 minutes. The obvious implication is that the difference in the pore structures of the two coals (the specific surface area of the PSOC 190 is 58 m^2/g while that of the PSOC 276 is only 8.6 m^2/g) is affecting the rate of the NO_2-coal reaction. Given that the difference in pore structures is so great, it is surprising that the mass gain curves do not show a greater amount of deviation. A comparison of the overall mass gain curves after the NO_2-treated coal is washed in 0.1 M Na_2CO_3 (aq) for the two coals is depicted in Figure 4–24. In this instance, if the two curves are extrapolated, they would also intersect at about 240 minutes, provided that the point at 180 minutes for the PSOC 190 coal is neglected. The rejection of this point seems reasonable in view of the previous discussion concerning the anomalous nature of the mass gain results for this run. Since the overall mass gains differ as well as the mass gains of the NO_2-

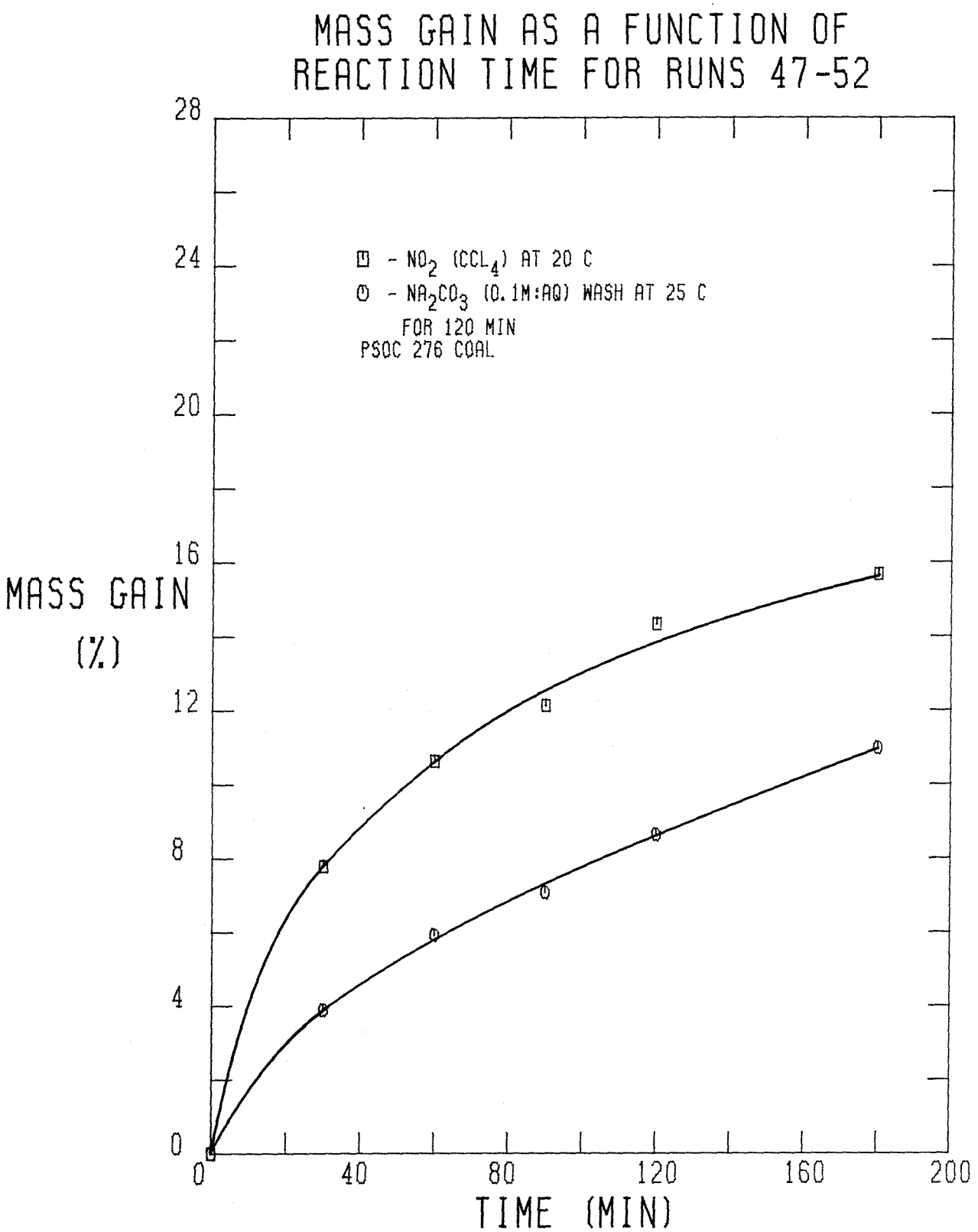
MASS GAIN AS A FUNCTION OF
REACTION TIME FOR RUNS 47-52
□ - NO2 (CCL4) AT 20 C
○ - NA2CO3 (0.1M:AQ) WASH AT 25 C
FOR 120 MIN
PSOC 276 COAL
MASS GAIN
(%)
0
4
8
12
16
20
24
28
0
40
80
120
160
200
TIME (MIN)

FIGURE 4-22

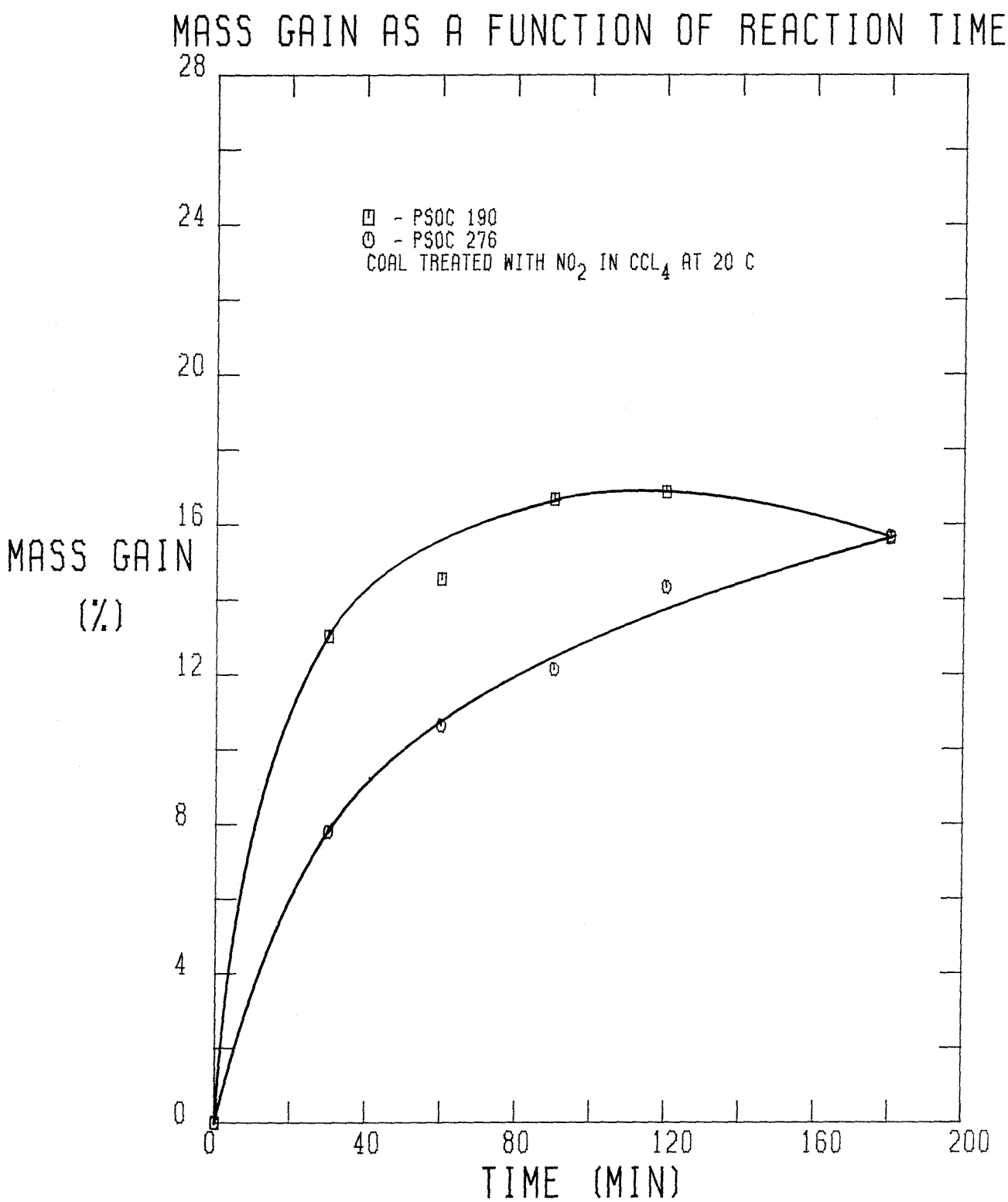
MASS GAIN AS A FUNCTION OF REACTION TIME
□ - PSOC 190
○ - PSOC 276
COAL TREATED WITH NO_2 IN CCL_4 AT 20 C
MASS GAIN (%)
TIME (MIN)
0
4
8
12
16
20
24
28
0
40
80
120
160
200

FIGURE 4-23

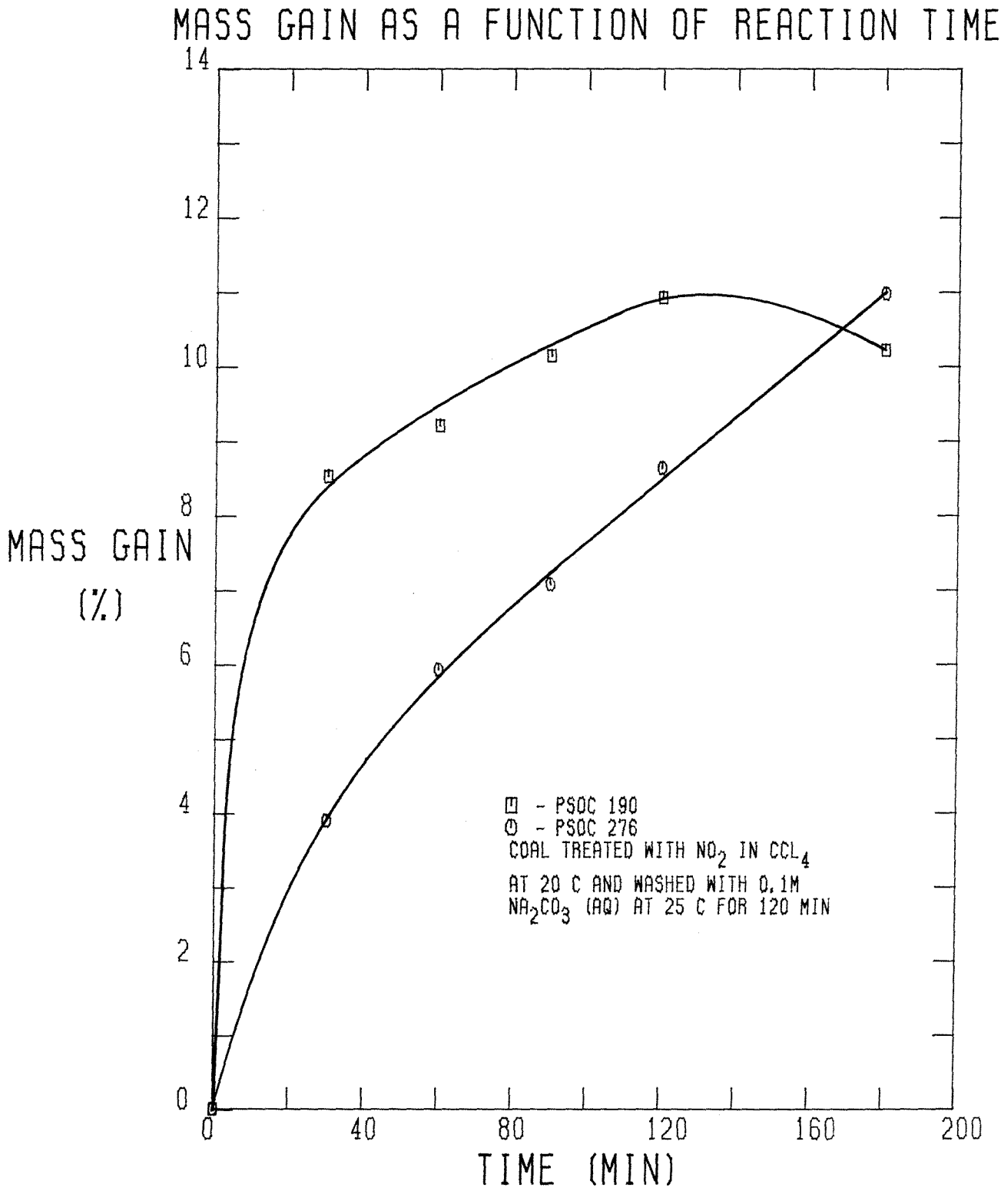
MASS GAIN AS A FUNCTION OF REACTION TIME
MASS GAIN (%)
TIME (MIN)
0
2
4
6
8
10
12
14
0
40
80
120
160
200
□ - PSOC 190
Ⓣ - PSOC 276
COAL TREATED WITH NO_2 IN CCL_4
AT 20 C AND WASHED WITH 0.1M
NA_2CO_3 (AQ) AT 25 C FOR 120 MIN

FIGURE 4-24

treated coals, it is apparent that the pore structure affects both processes which account for the mass gain.

On the basis of the features of the mass gain results discussed in this section, several conclusions can be made. First, the choice of solvent affects the mass gain due to NO_2 treatment because of the solubility of NO_2 in the solvent and the ability of the solvent to remove coal derived reaction products. For instance, the use of water as the solvent for NO_2 treatment results in a very small mass gain after NO_2 treatment and an overall mass loss of roughly 10 % after washing the NO_2-treated coal in Na_2CO_3 (aq). On the other hand, the use of nitrobenzene as the solvent results in the extraction of up to 55 % of the coal during NO_2 treatment, which is due to the chemical alteration of a large portion of the coal by NO_2 which is rendered soluble in nitrobenzene. At the other end of the spectrum, the use of CCl_4 as the solvent results in large mass gains, both for NO_2 treatment (17 % to 29 %) and for the Na_2CO_3 (aq) wash of the NO_2-treated coals (11 %), which is a consequence of the inability of CCl_4 to extract any portion of the coal, whether or not it has been treated with NO_2. Thus, the solvent plays a crucial role in the reaction system by virtue of its interaction with both NO_2 and the coal.

The effect of temperature and $(NO_2)_0$ on the mass gain results is basically that which is expected. An increase in temperature increases the mass gain under the same reaction conditions. The mass gain for NO_2 treatment continually increases as $(NO_2)_0$ is increased as well. The overall mass gain after the NO_2-treated coal is washed in 0.1 M Na_2CO_3 (aq), however, levels off once $(NO_2)_0$ exceeds 1.0 F.

Most importantly, all of these facts are consistent with the concept of a two stage process which accounts for NO_2 consumption and the mass gain of the solid. The first stage is responsible for adding mass derived from NO_2 and/or

the solvent to the coal in a manner such that the altered coal is still not soluble in 0.1 M Na_2CO_3 (aq). This process is generally quite rapid and is completed within 60 to 180 minutes depending on the temperature and $(NO_2)_0$. The second stage is responsible for the further addition of mass to the coal during the NO_2 treatment. This additional mass, however, is incorporated into the coal in a manner which allows the altered portions of the coal to be leached by 0.1 M Na_2CO_3 (aq). This process is slower than the first process.

4.2.2.2 The Carbon Content of the Coal

The coal samples generated by the NO_2 treatment and the subsequent wash in 0.1 M Na_2CO_3 (aq) were analyzed for their carbon content as part of the kinetic study of the NO_2-coal reaction system. Because the use of water as the solvent renders such a kinetic study so intractable, no analysis of the carbon content of the coal samples from those experiments were performed, namely Runs 1 to 20. In the remaining experiments in which CCl_4 was employed as the solvent, there is no reaction between the NO_2 and the solvent, which renders the interpretation of the kinetic data much easier.

Because the treatment of the coal slurried in CCl_4 with NO_2 resulted in an increase in the chlorine content of the coal from virtually zero to several mass percent and because evidence discussed later indicates that this increase is due to adsorbed CCl_4, the carbon contents of coals listed in Table 3–19 have been corrected for the amount of carbon in the adsorbed CCl_4. This correction, however, generally amounts to only a few tenths of one percent in the uncorrected carbon contents. Carbon contents which have been corrected for the amount of adsorbed chlorine will be referred to as "mass corrected carbon contents". These carbon contents, however, are carbon concentrations. Therefore, they have not been adjusted for the mass gain due to NO_2 treatment.

The mass corrected carbon contents of the experiments run at 25 ℃ (Runs 21–27) are shown in Figure 4–25. The curves for both the NO_2-treated coal and the NO_2-treated coal washed in 0.1 M Na_2CO_3 (aq) (hereinafter referred to simply as the "washed coal") show the same general trend. Initially, the carbon content drops rather quickly and then falls at a slower rate. This behavior seems to correlate quite well with the mass gain data obtained for this set of experiments. If the carbon content, however, is adjusted for the mass gain to obtain the absolute amount of carbon lost relative to the pretreated coal (expressed as the

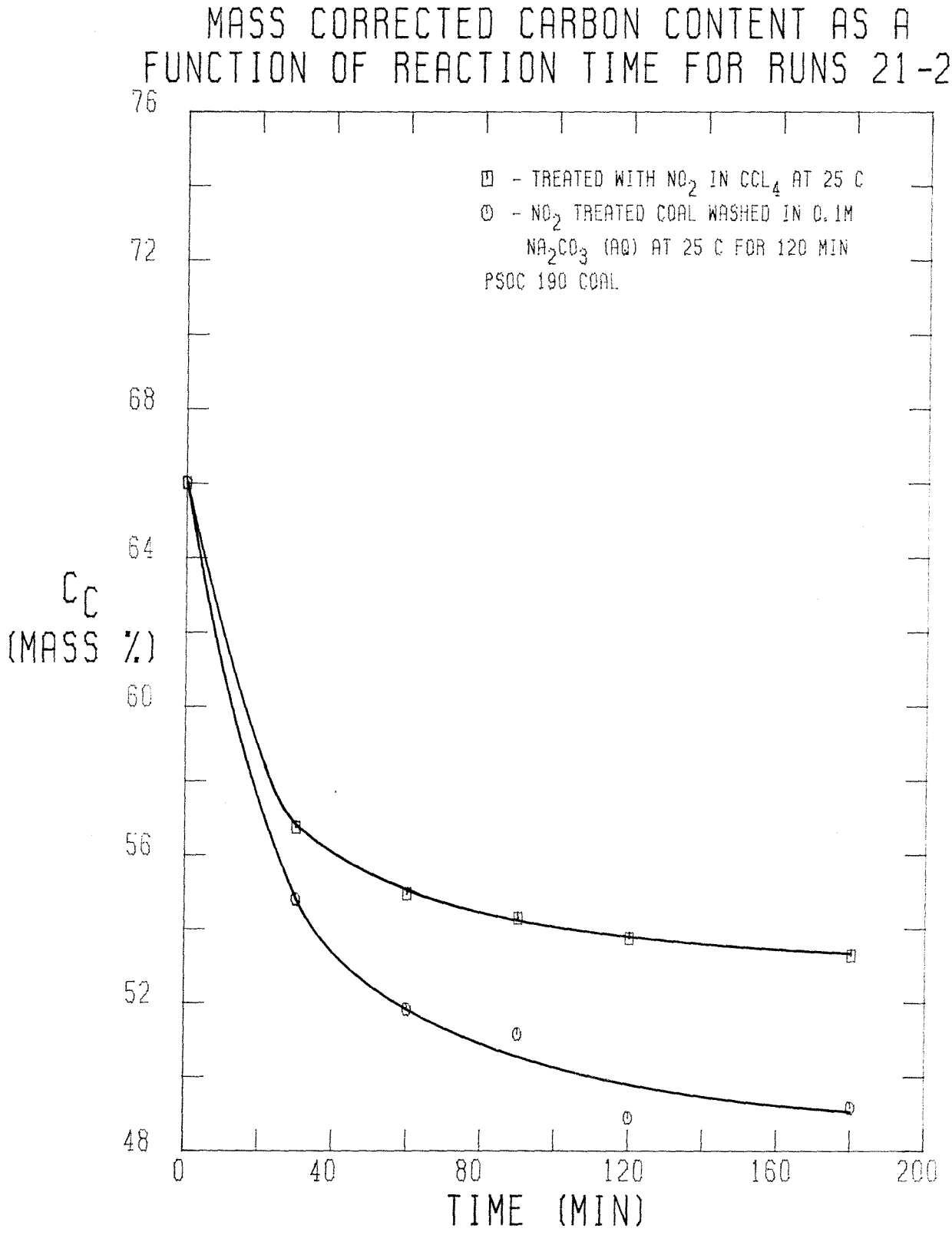
MASS CORRECTED CARBON CONTENT AS A FUNCTION OF REACTION TIME FOR RUNS 21-27
□ - TREATED WITH NO_2 IN CCL_4 AT 25 C
① - NO_2 TREATED COAL WASHED IN 0.1M NA_2CO_3 (AQ) AT 25 C FOR 120 MIN
PSOC 190 COAL
C_C (MASS %)
76
72
68
64
60
56
52
48
0
40
80
120
160
200
TIME (MIN)

FIGURE 4-25

"mass corrected carbon loss," L_C), the results appear as shown in Figure 4–26. An examination of this figure reveals that treatment with NO_2 at 25°C in the flow reactor results in the very rapid removal of substances from the coal which contain roughly 10 % of the total carbon in the pretreated coal. This process appears to be complete within about 60 minutes. This process probably involves the NO_2 attack of the lighter volatile material in the coal, which in its unaltered state is insoluble in CCl_4. The attack by NO_2, however, could render this material soluble in CCl_4. The results of the carbon loss due to the Na_2CO_3 (aq) wash indicate that the process which generates coal material soluble in Na_2CO_3 (aq) is continuing even at 180 minutes. This process accounts for another 14 to 15 % loss in carbon so that the total carbon loss after the Na_2CO_3 (aq) wash is 25 % of the original carbon in the pretreated coal after treatment with NO_2 for 180 minutes. Once again, these results mesh quite well with the two-stage process postulated for NO_2 consumption.

The mass corrected carbon contents of the coal samples from the experiments conducted at 20°C in the batch reactor (Runs 33–37) are depicted graphically in Figure 4–27. It would appear that during the NO_2 treatment, the carbon content of the coal begins to increase after 120 minutes. The carbon content at 180 minutes, however, reflects the anomaly in the mass gain for this run discussed in the section dealing with the mass gain results. Otherwise, the curves demonstrate the same behavior as in the previous section, although the decrease in carbon content is not as great. This difference is revealed in the carbon loss results shown in Figure 4–28. In this instance, the carbon loss due to NO_2 treatment is essentially zero, which implies that no coal substances which contain carbon are being extracted during the NO_2 treatment. This result is in stark contrast with the loss of up to 10 % of the carbon during NO_2 treatment in the previous set of runs. The explanation lies in the fact that in the

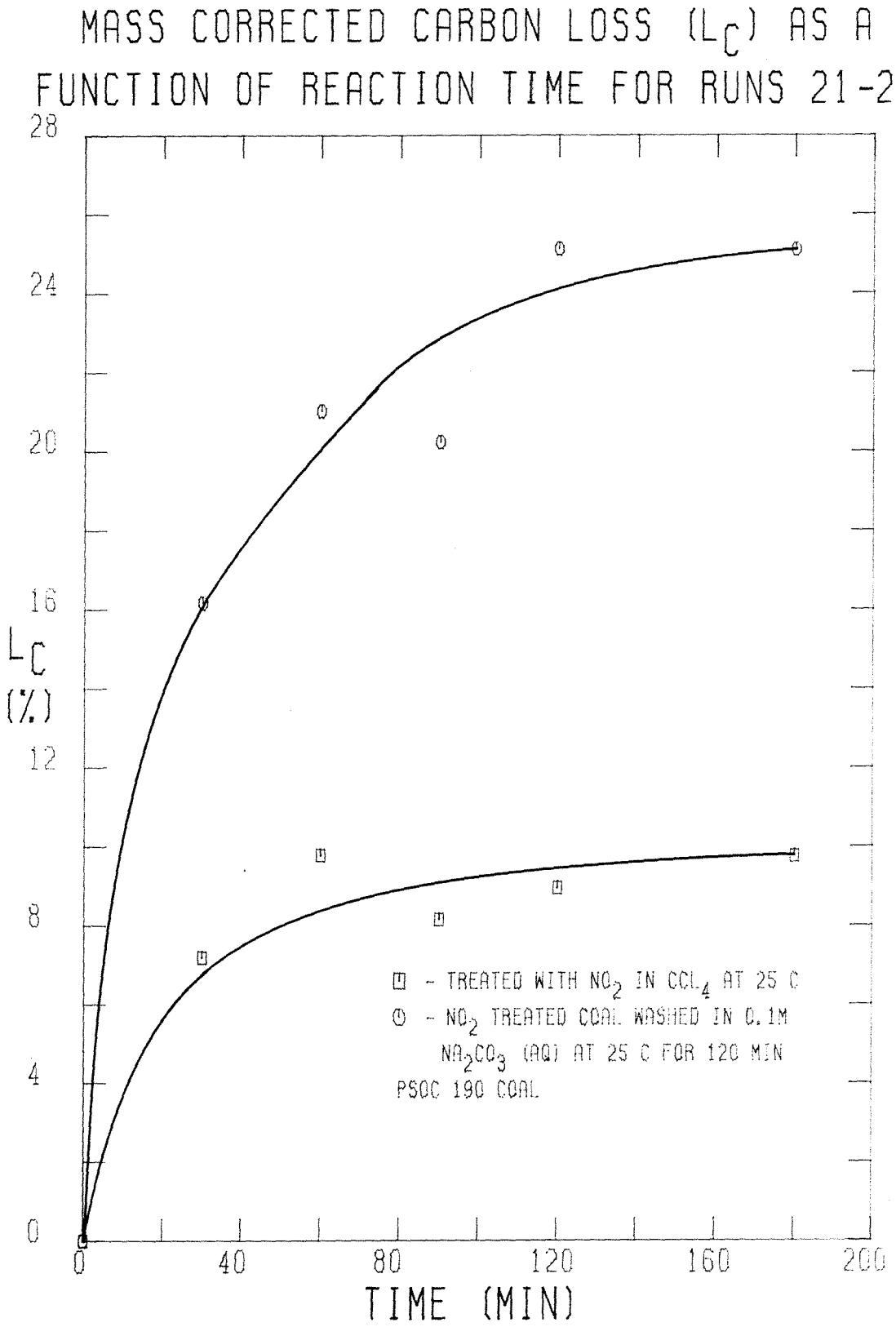
MASS CORRECTED CARBON LOSS (L_C) AS A FUNCTION OF REACTION TIME FOR RUNS 21-27
28
24
20
16
12
8
4
0
L_C (%)
0
40
80
120
160
200
TIME (MIN)
- TREATED WITH NO_2 IN CCL_4 AT 25 C
- NO_2 TREATED COAL WASHED IN 0.1M NA_2CO_3 (AQ) AT 25 C FOR 120 MIN
PSOC 190 COAL

FIGURE 4-26

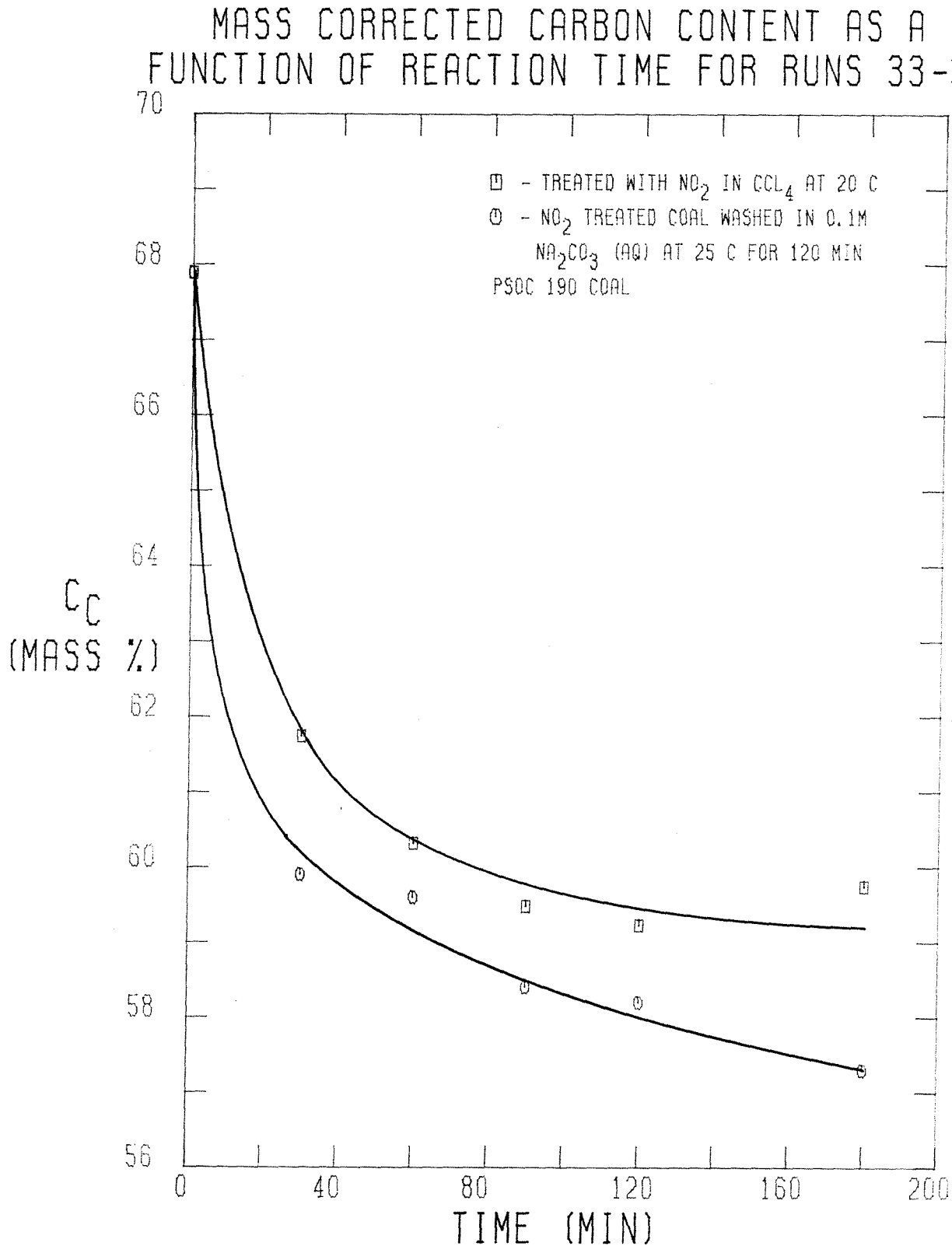
MASS CORRECTED CARBON CONTENT AS A FUNCTION OF REACTION TIME FOR RUNS 33-37
□ - TREATED WITH NO_2 IN CCL_4 AT 20 C
① - NO_2 TREATED COAL WASHED IN 0.1M NA_2CO_3 (AQ) AT 25 C FOR 120 MIN
PSOC 190 COAL
C_C (MASS %)
70
68
66
64
62
60
58
56
0
40
80
120
160
200
TIME (MIN)

FIGURE 4-27

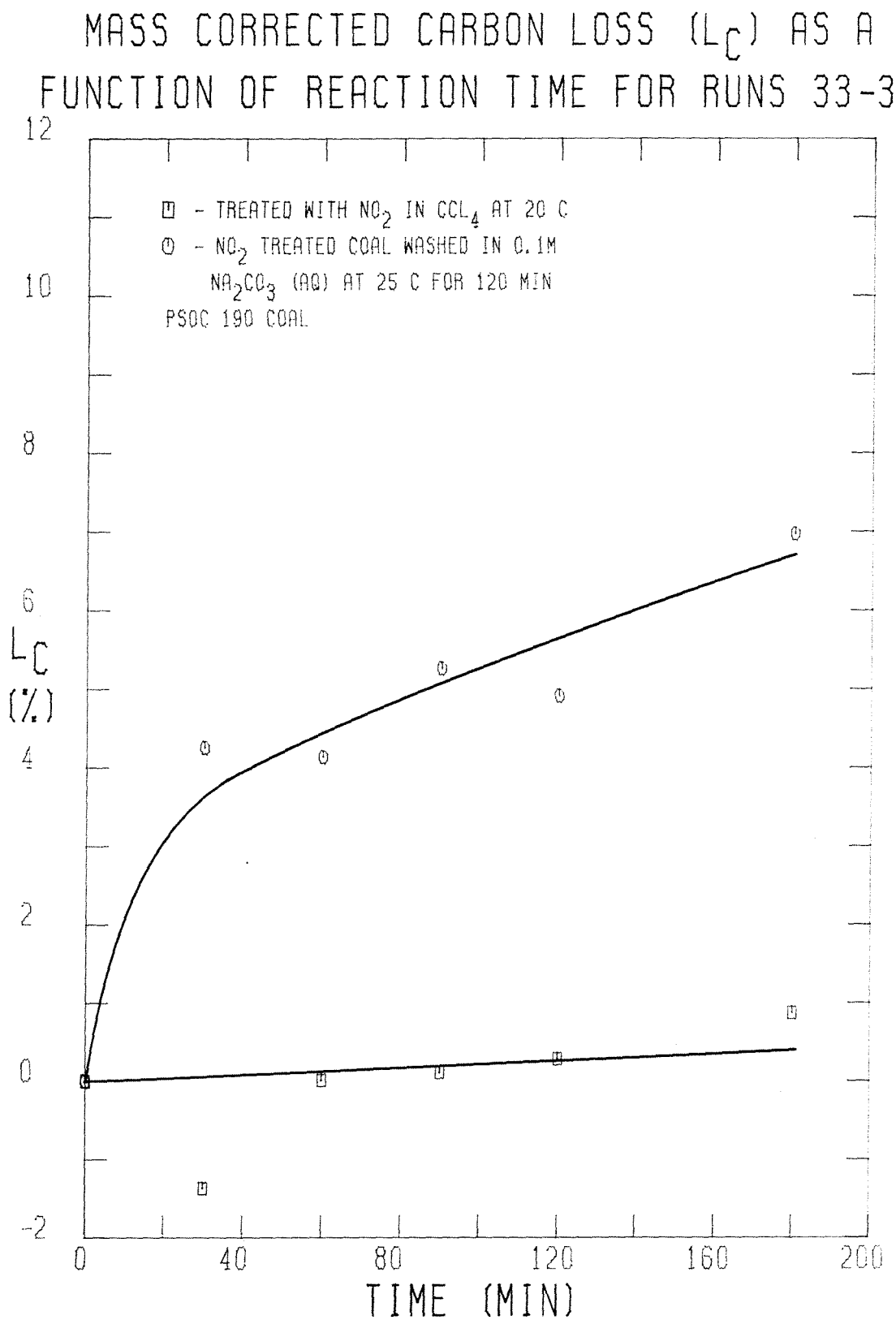
MASS CORRECTED CARBON LOSS (L_C) AS A FUNCTION OF REACTION TIME FOR RUNS 33-37
□ - TREATED WITH NO_2 IN CCL_4 AT 20 C
① - NO_2 TREATED COAL WASHED IN 0.1M NA_2CO_3 (AQ) AT 25 C FOR 120 MIN
PSOC 190 COAL
L_C (%)
12
10
8
6
4
2
0
-2
0
40
80
120
160
200
TIME (MIN)

FIGURE 4-28

previous set of experiments, (NO_2) is a linear function of time, starting at zero and reaching roughly 8 F at t = 180 minutes. In this set of experiments, on the other hand, (NO_2) is initially 1.1 F and drops to 0.75 F at t = 180 minutes. Therefore, a very large increase in (NO_2) will result in some extraction of carbon containing compounds. Furthermore, the carbon loss after the Na_2CO_3 (aq) wash is much smaller in this set than in the previous set, which is also a consequence of the large difference in (NO_2). In this instance, L_C rises rapidly to 4 % within 30 minutes, and then rises at a slower rate to 7 % at t = 180 minutes. This trend contrasts with the 25 % carbon loss after washing in Na_2CO_3 (aq) in the previous set. Thus, (NO_2) affects the extent of both processes responsible for the loss of carbon.

Figure 4–29 shows the mass corrected carbon content of the coal samples from the set of experiments conducted at 0°C in the batch reactor (Runs 42–46). It appears that the slight increase in the carbon content curve at 180 minutes in the previous set is more pronounced in this set. Furthermore, the points at 90 and 120 minutes for the NO_2-treated coal are below those of the washed coal, which is unusual. Whether this increase is a true effect or simply the result of bad carbon analyses is not clear. It should be noted that the curve corresponding to the Na_2CO_3 (aq)-washed coal demonstrates the usual unimodal decrease as the reaction time increases, levelling off at about 60 to 61 %. The absolute carbon loss results displayed in Figure 4–30 can shed some light on the problem. The values of L_C for the NO_2-treated coal show a large amount of scatter from −3.5 % to +2.5 %. It should be noted that negative values of L_C imply an increase in the absolute carbon content, which is impossible unless carbon derived from CCl_4, but no longer associated with chlorine, is taken up by the coal. Since the behavior shown here does not occur at higher temperatures, and since there is no evidence that NO_2 reacts with CCl_4, even in the presence of

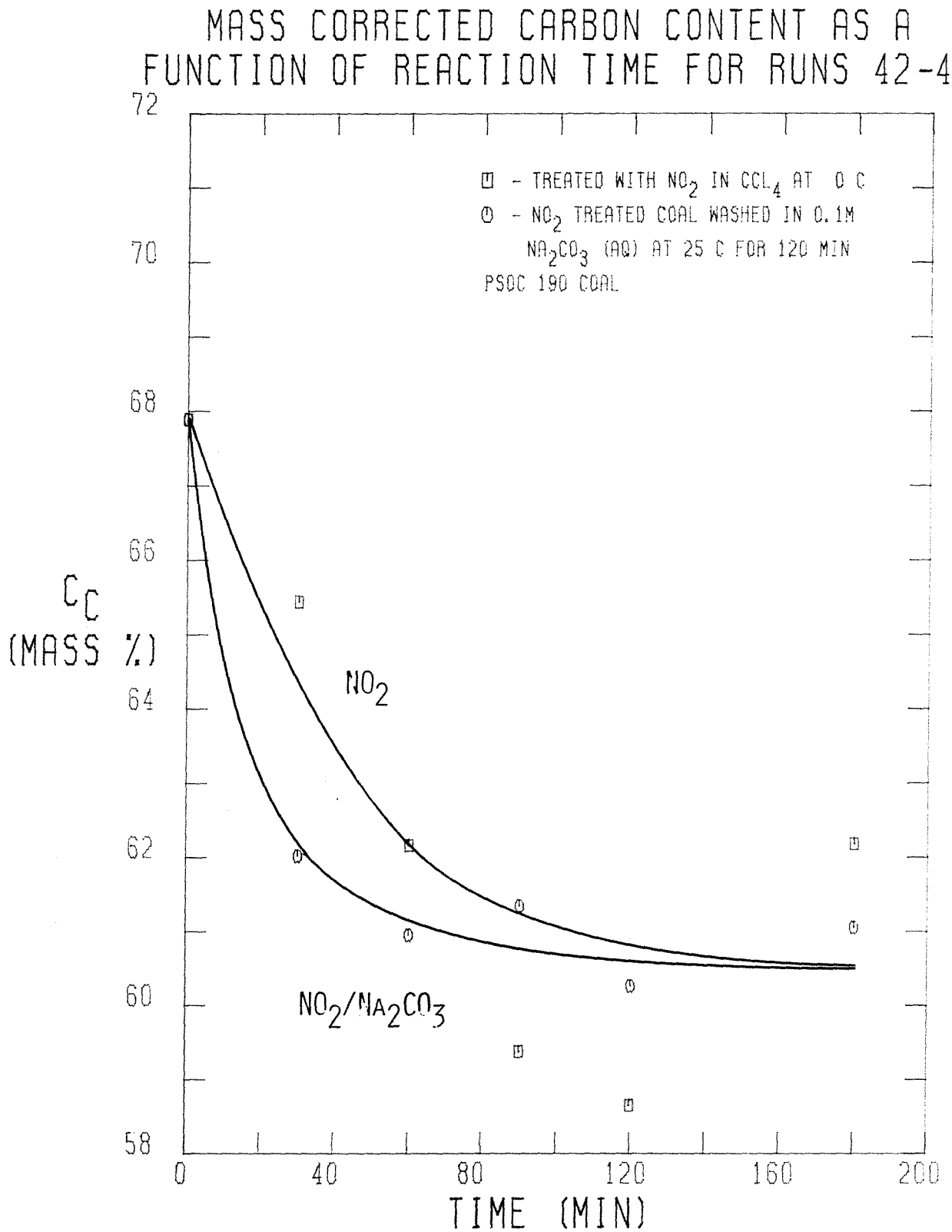
MASS CORRECTED CARBON CONTENT AS A FUNCTION OF REACTION TIME FOR RUNS 42-46
72
70
68
66
64
62
60
58
C_C (MASS %)
0
40
80
120
160
200
TIME (MIN)
- TREATED WITH NO_2 IN CCL_4 AT 0 C
- NO_2 TREATED COAL WASHED IN 0.1M NA_2CO_3 (AQ) AT 25 C FOR 120 MIN
PSOC 190 COAL
NO_2
NO_2/NA_2CO_3

FIGURE 4-29

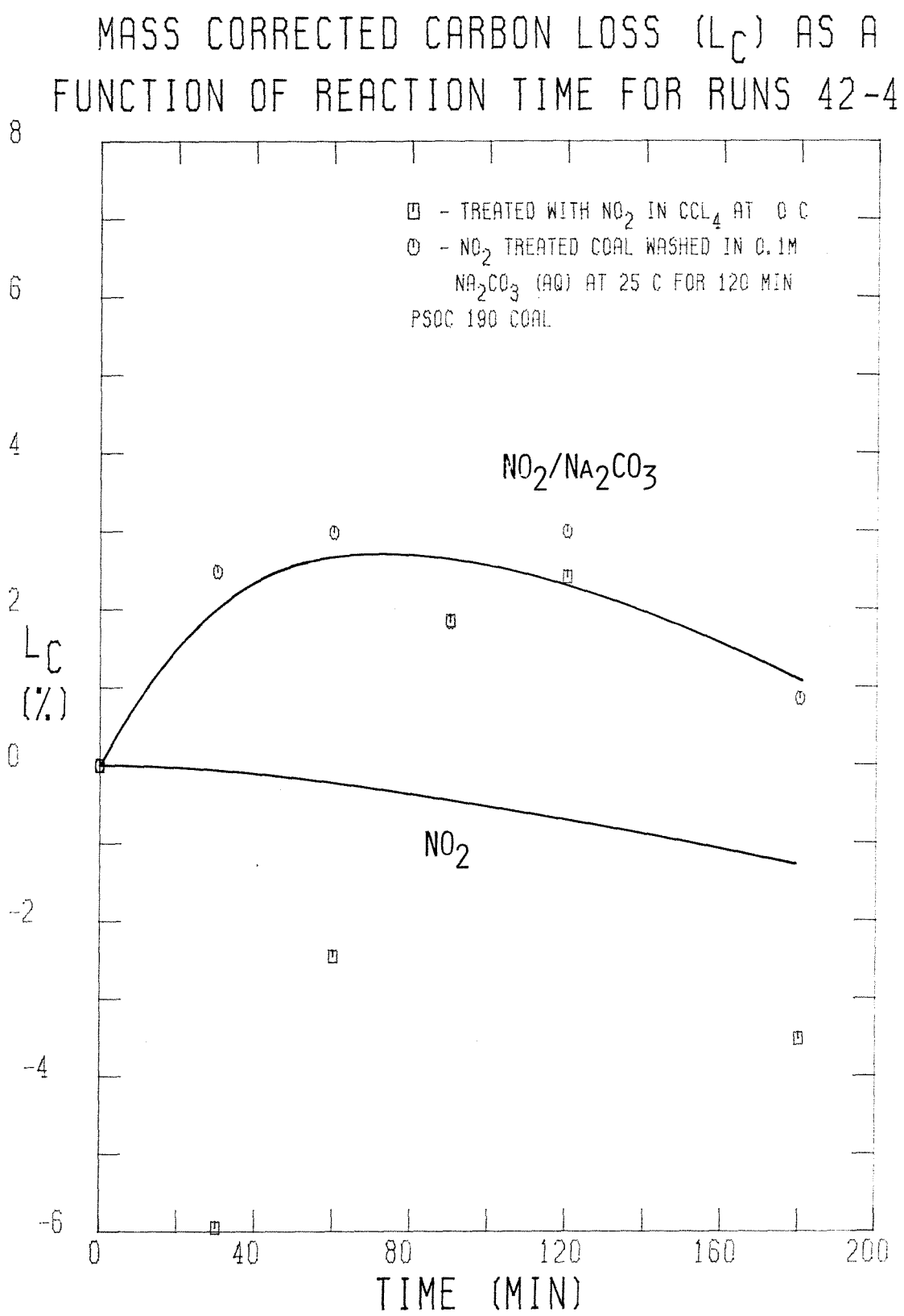
MASS CORRECTED CARBON LOSS (L_C) AS A FUNCTION OF REACTION TIME FOR RUNS 42-46
□ - TREATED WITH NO_2 IN CCL_4 AT 0 C
① - NO_2 TREATED COAL WASHED IN 0.1M NA_2CO_3 (AQ) AT 25 C FOR 120 MIN
PSOC 190 COAL
NO_2/NA_2CO_3
NO_2
L_C (%)
8
6
4
2
0
-2
-4
-6
0
40
80
120
160
200
TIME (MIN)

FIGURE 4-30

coal, such an explanation is virtually impossible. Therefore, the scatter must be due to either an inconsistent drying procedure or bad carbon analyses or both. The curve for the Na_2CO_3 (aq) washed coal shows a broad maximum of about 3 % from t = 60 minutes to t = 120 minutes before dropping back down to 1 % at t = 180 minutes. Such behavior is also unexpected, which implies that the carbon results for this entire set are suspect. Despite the data scatter, however, the results do imply that there is very little change in the absolute carbon content of the processed coal relative to the pretreated coal. For instance, whereas L_C at 20°C approaches 7 % for the washed coals, at 0°C L_C is not greater than 3 %, which would be qualitatively expected if the rate of the process responsible for generating Na_2CO_3 (aq) soluble compounds has a typical temperature dependence.

The effect of the temperature of the NO_2 treatment on the mass corrected carbon content of the NO_2-treated coals is shown in Figure 4–31. It should be noted that only predried coal was used in the 50°C runs while washed and dried coal was used in the other runs. Thus, the initial carbon contents differ by about 2 %, as reflected in the figure. Despite this difference, it is obvious that the magnitude of the decrease in carbon content increases as a function of temperature. It should be noted that the intersection of the two curves corresponding to 20 and 0°C is probably due to the large amount of scatter in the carbon analyses for the runs done at 0°C. Nevertheless, the basic trend exhibited in terms of the temperature dependence of the carbon contents is quite clear and is that which is expected. The mass corrected carbon loss as a function of temperature and reaction time is shown in Figure 4–32. Despite the scatter in the points, the basic conclusion is that treatment of coal with NO_2 under mild conditions does not result in significant losses of carbon, even at 50°C, where L_C is roughly 4 %.

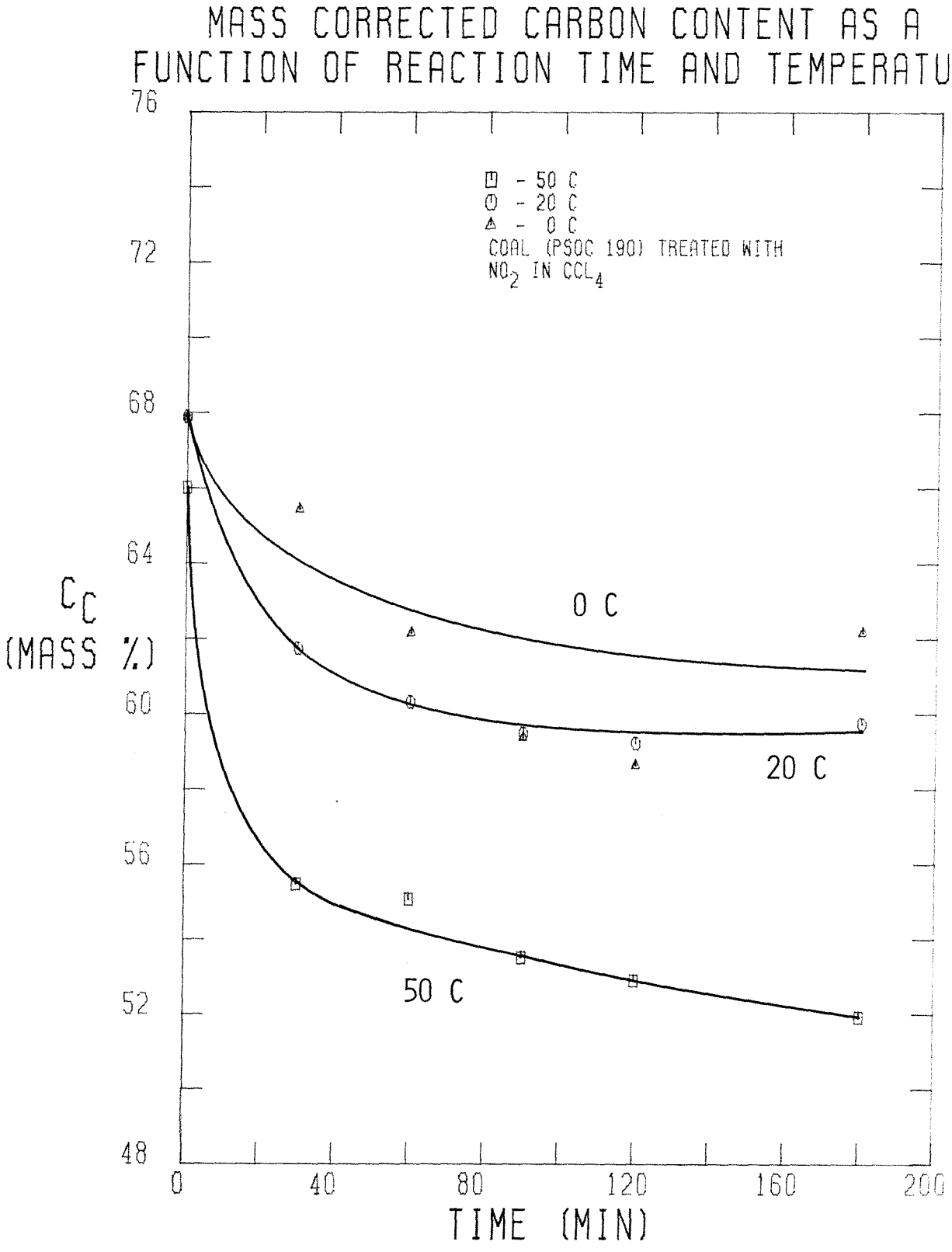
MASS CORRECTED CARBON CONTENT AS A FUNCTION OF REACTION TIME AND TEMPERATURE
□ - 50 C
○ - 20 C
△ - 0 C
COAL (PSOC 190) TREATED WITH
NO2 IN CCL4
0 C
20 C
50 C
CC (MASS %)
TIME (MIN)
76
72
68
64
60
56
52
48
0
40
80
120
160
200

FIGURE 4-31

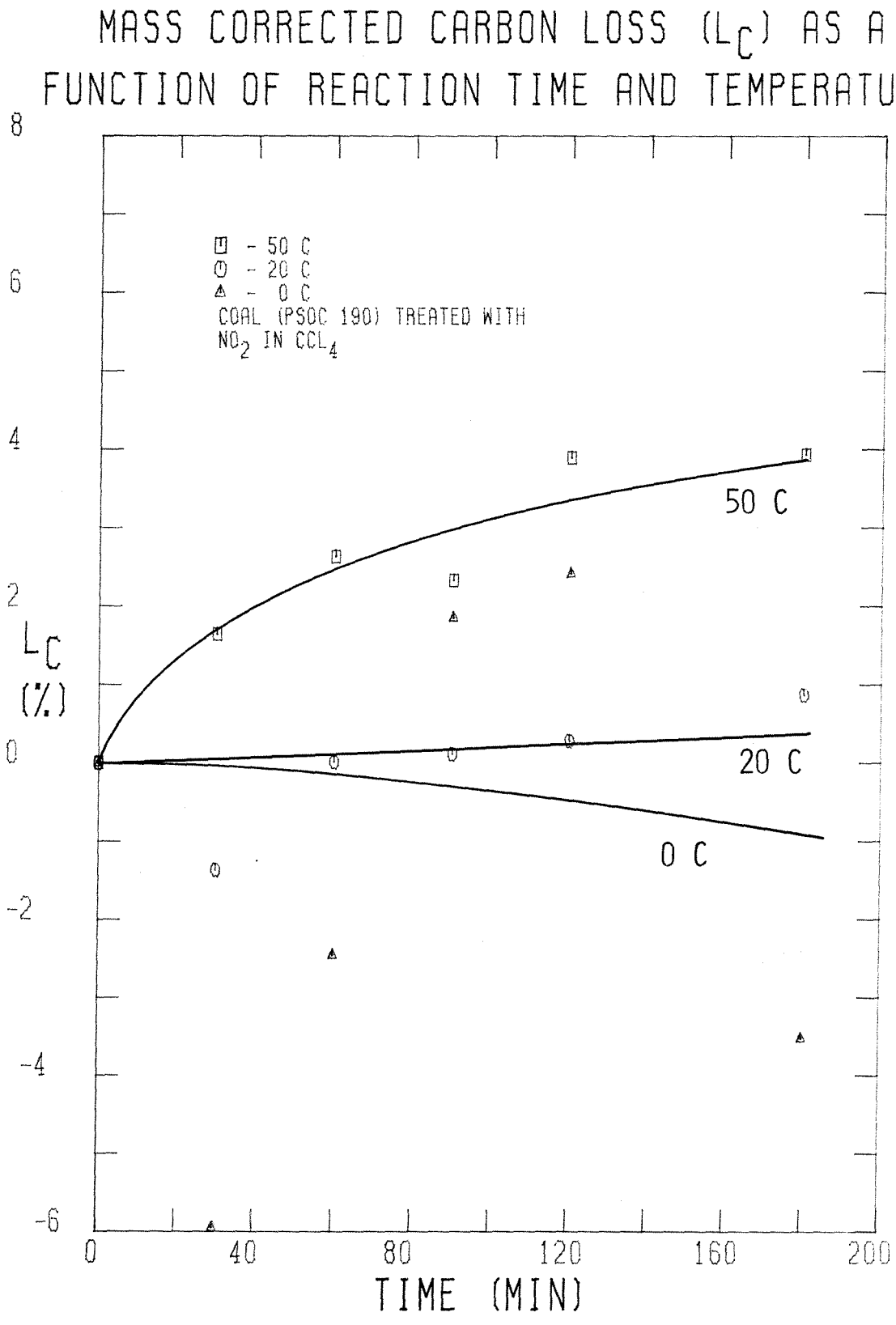
MASS CORRECTED CARBON LOSS (L_C) AS A FUNCTION OF REACTION TIME AND TEMPERATURE
□ - 50 C
○ - 20 C
△ - 0 C
COAL (PSOC 190) TREATED WITH NO_2 IN CCL_4
50 C
20 C
0 C
L_C (%)
8
6
4
2
0
-2
-4
-6
0
40
80
120
160
200
TIME (MIN)

FIGURE 4-32

Figure 4–33 depicts the effect of the NO_2 treatment temperature on the mass corrected carbon contents of Na_2CO_3 (aq) washed coal samples. Once again, the higher the temperature, the larger the decrease in carbon content. Both curves demonstrate the same trend as the corresponding mass gain curves, namely a very rapid initial change followed by a more gradual change. Adjustment of the carbon contents for the mass gain results in the values of the mass corrected carbon loss shown in Figure 4–34. Whereas NO_2 treatment at 20°C for 180 minutes results in an overall carbon loss of 7 %, the same treatment at 0°C results in only about a 3 % overall carbon loss. Furthermore, the overall carbon loss due to NO_2 treatment at 20°C increases almost linearly as a function of reaction time between 30 and 180 minutes, and shows no sign of beginning to level off. On the other hand, the overall carbon loss due to NO_2 treatment at 0°C seems to level off after 60 minutes, and if the point at 180 minutes is included, it actually decreases after 120 minutes. Such a decrease might be explained if the extent of the reaction which produces the Na_2CO_3 (aq) soluble coal derived products is quite limited and basically complete within 60 minutes at 0°C, but the reaction which accounts for the mass gain in the coal continues. The continuation of the second process could conceivably increase the degree of pore blocking so that as the NO_2 treatment continues, the accessibility of Na_2CO_3 (aq) to the soluble coal derived products is diminished. The amount of variation in the values of L_C, however, is rather small for the 0°C runs, and the trend shown by the data may be caused simply by problems in the carbon analysis. Nevertheless, conducting the experiments at 0 or 20°C has a discernible and significant effect on the overall carbon loss.

The effect of the initial NO_2 concentration, $(NO_2)_0$, on the mass corrected carbon content for NO_2 treatment at 20°C (Runs 38–41) is shown in Figure 4–35. The curves for both the NO_2–treated coal and the Na_2CO_3 (aq)-washed coal show

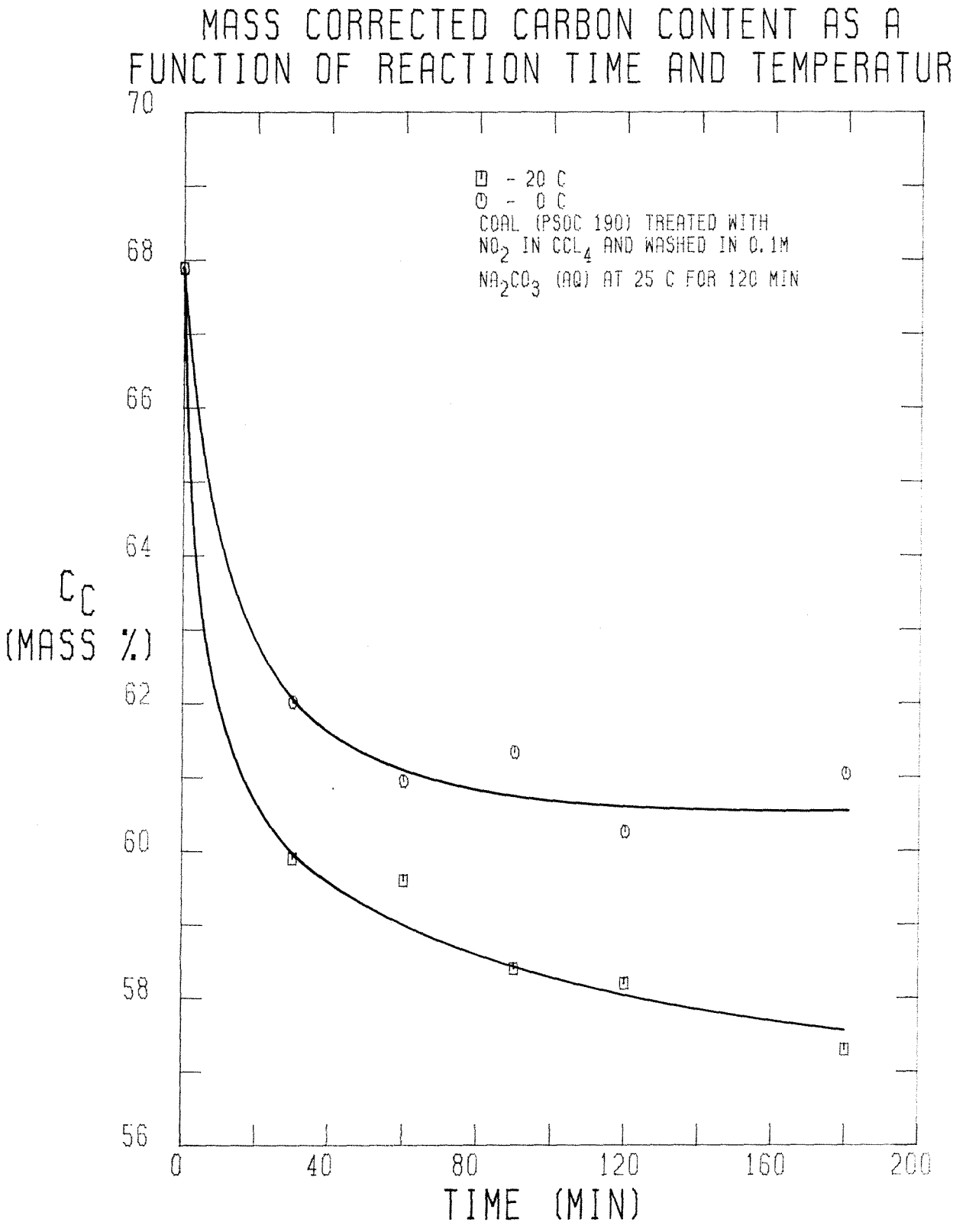
MASS CORRECTED CARBON CONTENT AS A FUNCTION OF REACTION TIME AND TEMPERATURE
□ - 20 C
○ - 0 C
COAL (PSOC 190) TREATED WITH
NO_2 IN CCL_4 AND WASHED IN 0.1M
NA_2CO_3 (AQ) AT 25 C FOR 120 MIN
C_C
(MASS %)
70
68
66
64
62
60
58
56
0
40
80
120
160
200
TIME (MIN)

FIGURE 4-33

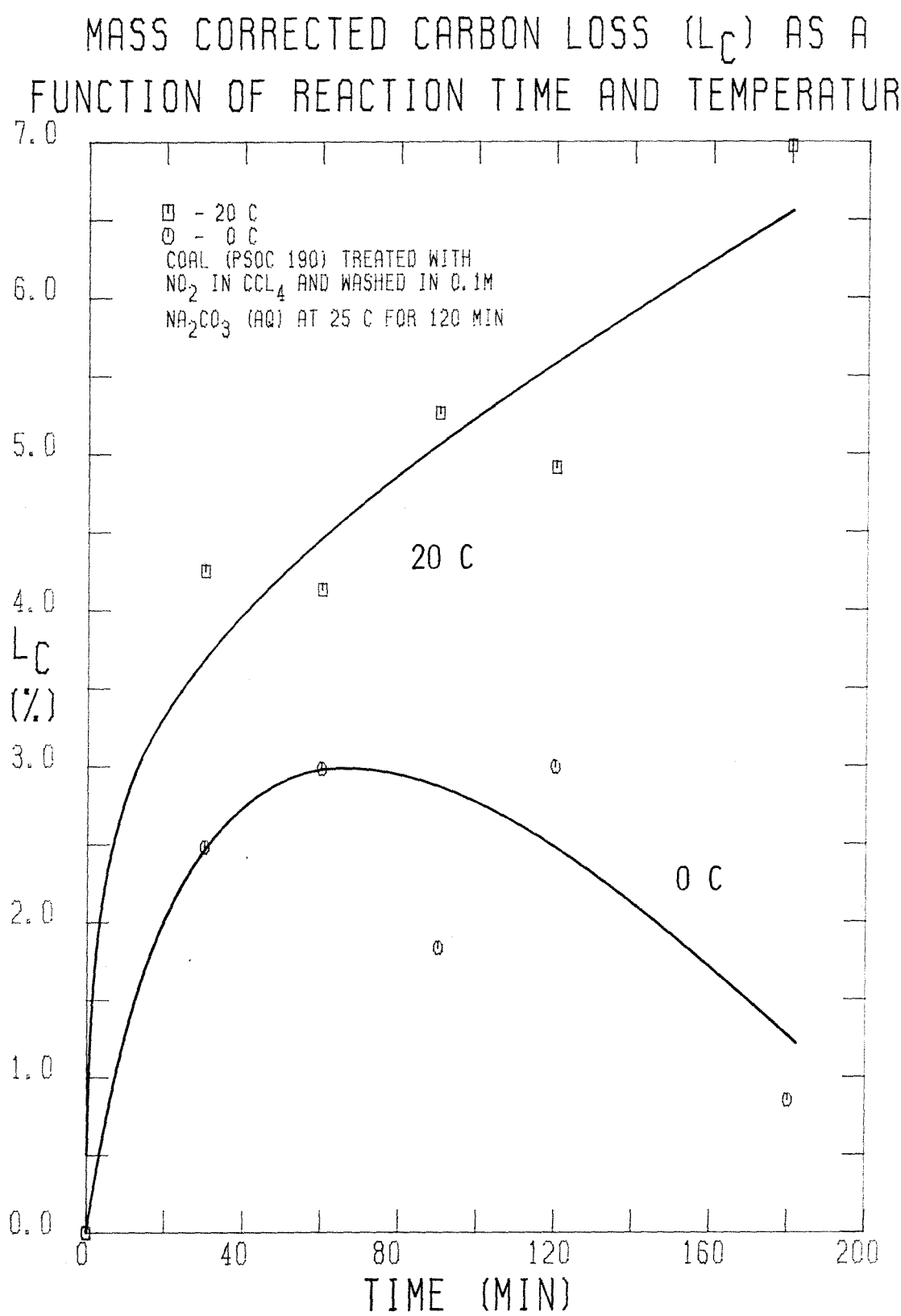
MASS CORRECTED CARBON LOSS (L_C) AS A FUNCTION OF REACTION TIME AND TEMPERATURE
□ - 20 C
○ - 0 C
COAL (PSOC 190) TREATED WITH
NO_2 IN CCL_4 AND WASHED IN 0.1M
NA_2CO_3 (AQ) AT 25 C FOR 120 MIN
20 C
0 C
L_C (%)
7.0
6.0
5.0
4.0
3.0
2.0
1.0
0.0
0
40
80
120
160
200
TIME (MIN)

FIGURE 4-34

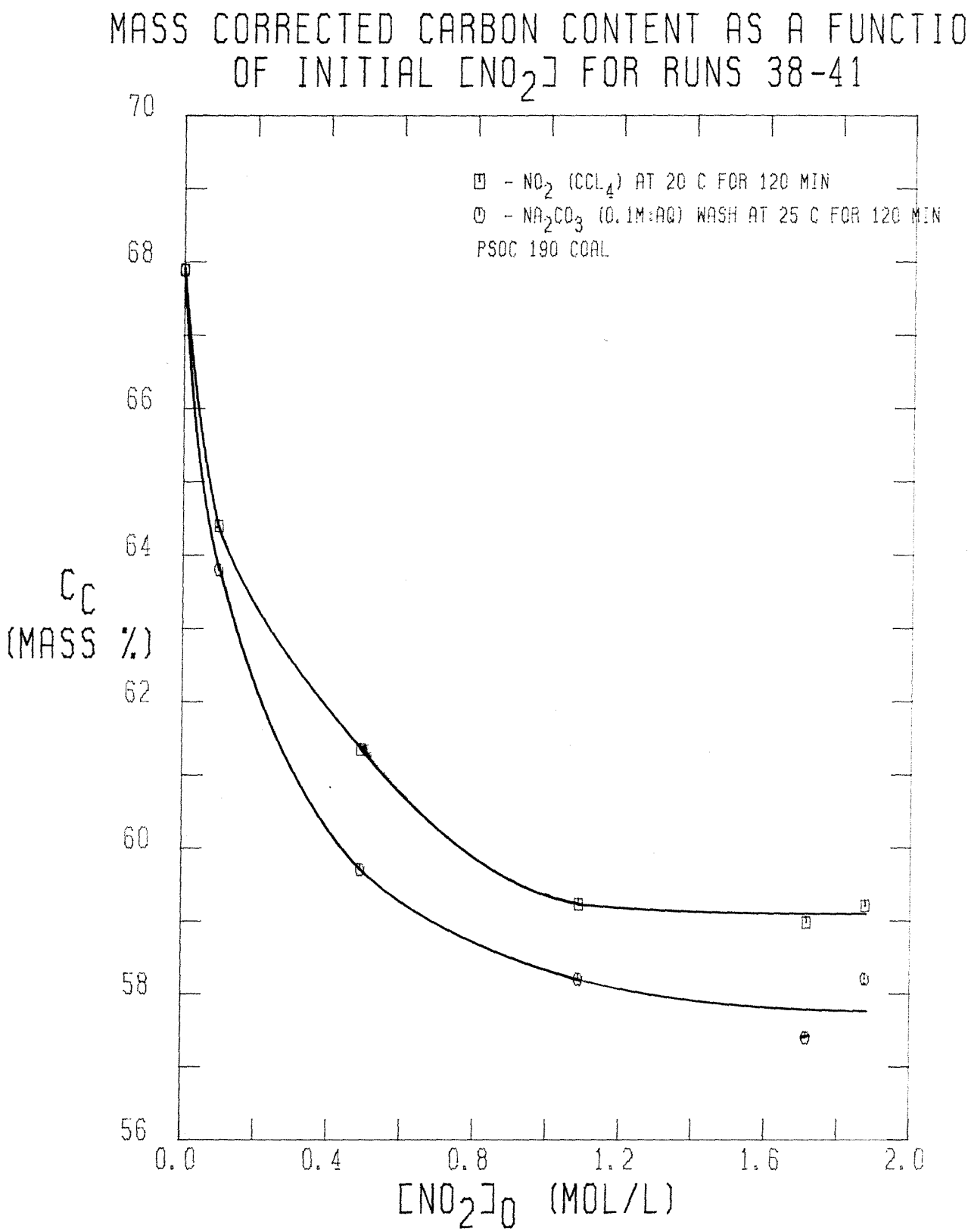
MASS CORRECTED CARBON CONTENT AS A FUNCTION OF INITIAL [NO2] FOR RUNS 38-41
□ - NO2 (CCL4) AT 20 C FOR 120 MIN
○ - NA2CO3 (0.1M:AQ) WASH AT 25 C FOR 120 MIN
PSOC 190 COAL
70
68
66
64
62
60
58
56
CC (MASS %)
0.0
0.4
0.8
1.2
1.6
2.0
[NO2]0 (MOL/L)

FIGURE 4-35

the same trends, including the slight increase in carbon content at the end of the reaction, which lends credibility to the postulated phenomenon of diminished accessibility of Na_2CO_3 (aq) to the coal derived products as the NO_2-exposure time is increased. An examination of the mass corrected carbon loss shown in Figure 4–36, however, reveals that the NO_2 treatment does not result in the loss of any carbon from the pretreated coal, which is in accord with previous observations. As mentioned earlier, negative values of L_C are physically impossible, so that the error must lie in the accuracy of the carbon analysis. The curve for the overall carbon loss shows a maximum for L_C of about 6 % when $(NO_2)_0$ = 1.7 F. Interestingly, the rise in L_C after the Na_2CO_3 (aq) wash is quite rapid as $(NO_2)_0$ increases, which implies that the production of the Na_2CO_3 (aq) soluble coal derived products is essentially complete in 120 minutes if $(NO_2)_0$ is greater than about 0.5 F. As $(NO_2)_0$ is increased beyond 1.7 F, however, the process responsible for diminishing the accessibility to the Na_2CO_3 (aq) soluble coal derived products begins to predominate, so that L_C begins to fall. Thus, the use of an initial NO_2 concentration of about 1.0 F seems to insure complete production of the Na_2CO_3 (aq) soluble compounds in 120 minutes at 20°C without allowing their accessibility for extraction to be unduly diminished by excessive reaction of the coal with NO_2.

The results of the mass corrected carbon analyses of the PSOC 276 coal treated with NO_2 at 20°C (Runs 47–52) are displayed graphically in Figure 4–37. In this case, the curves practically coincide, which suggests that the Na_2CO_3 (aq) wash does not alter the NO_2–treated coal. Indeed, the curve for the NO_2–treated coal is actually below that of the washed coal, which implies that the Na_2CO_3 (aq) wash is removing material from the NO_2–treated coal which does not contain coal-derived carbon. This phenomenon is exactly the opposite of that of the PSOC 190 coal treated with NO_2. An inspection of Figure 4–38,

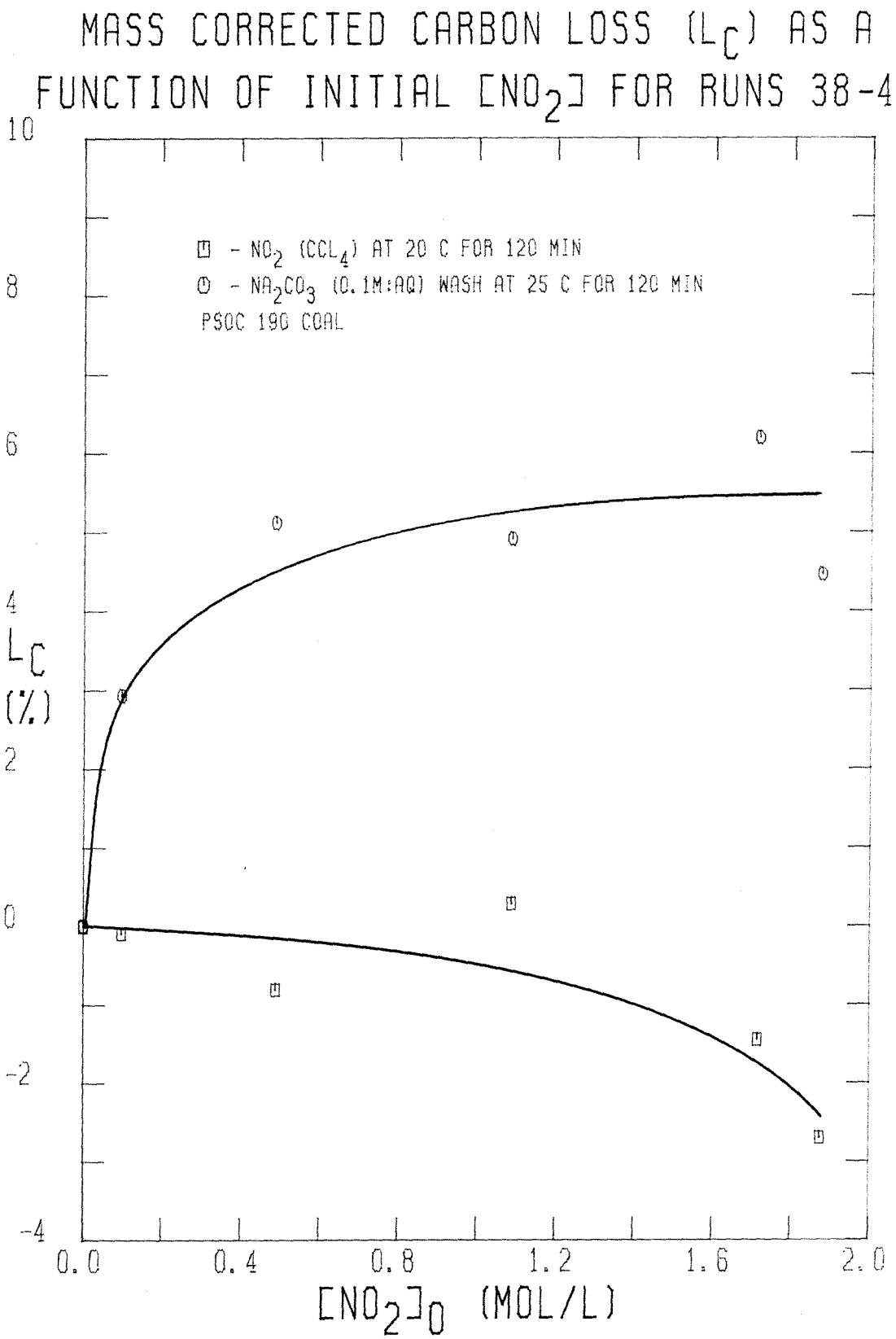
MASS CORRECTED CARBON LOSS (L_C) AS A FUNCTION OF INITIAL [NO_2] FOR RUNS 38-41
□ - NO_2 (CCL_4) AT 20 C FOR 120 MIN
Ⓘ - NA_2CO_3 (0.1M:AQ) WASH AT 25 C FOR 120 MIN
PSOC 190 COAL
10
8
6
4
2
0
-2
-4
L_C (%)
0.0
0.4
0.8
1.2
1.6
2.0
$[NO_2]_0$ (MOL/L)

FIGURE 4-36

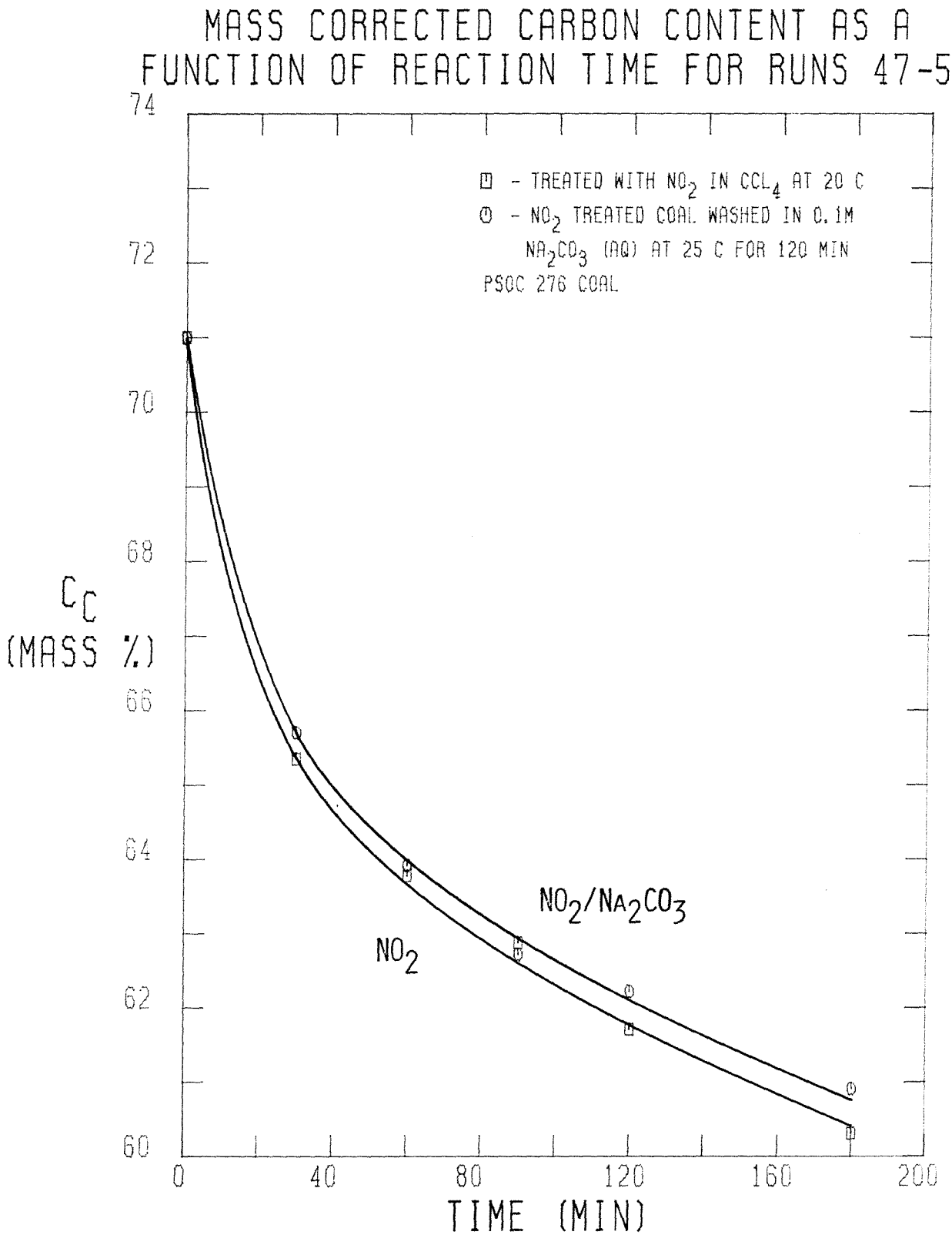
MASS CORRECTED CARBON CONTENT AS A FUNCTION OF REACTION TIME FOR RUNS 47-52
□ - TREATED WITH NO2 IN CCL4 AT 20 C
⊙ - NO2 TREATED COAL WASHED IN 0.1M NA2CO3 (AQ) AT 25 C FOR 120 MIN
PSOC 276 COAL
NO2/NA2CO3
NO2
CC (MASS %)
TIME (MIN)
74
72
70
68
66
64
62
60
0
40
80
120
160
200

FIGURE 4-37

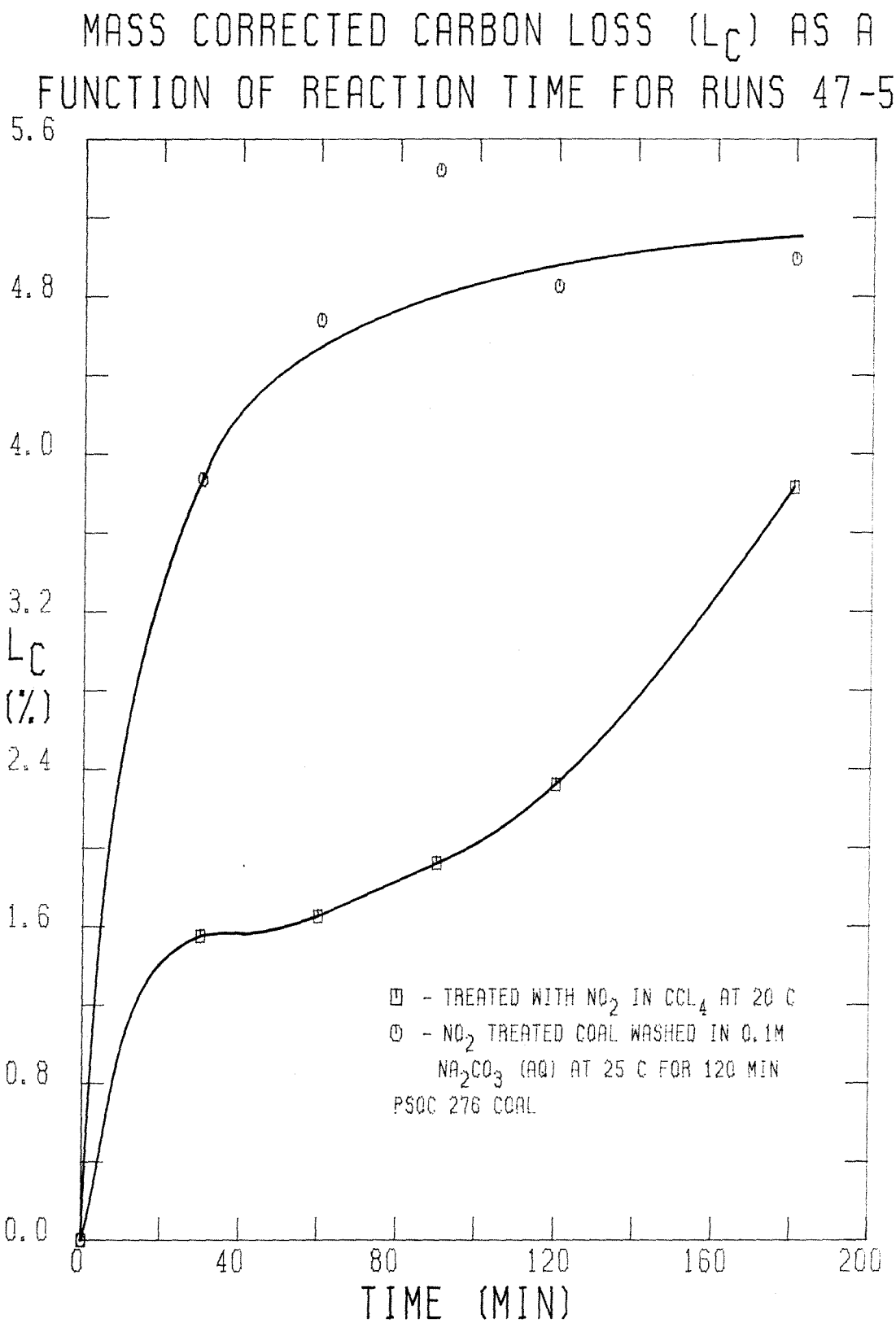
MASS CORRECTED CARBON LOSS (L_C) AS A FUNCTION OF REACTION TIME FOR RUNS 47-52
5.6
4.8
4.0
3.2
2.4
1.6
0.8
0.0
L_C (%)
0
40
80
120
160
200
TIME (MIN)
- TREATED WITH NO_2 IN CCL_4 AT 20 C
- NO_2 TREATED COAL WASHED IN 0.1M NA_2CO_3 (AQ) AT 25 C FOR 120 MIN
PSOC 276 COAL

FIGURE 4-38

which contains the mass corrected carbon loss for the processed PSOC 276, reveals that the NO_2–treated coal suffers a carbon loss which approaches 4 % at 180 minutes. The fact that there is any carbon removal from the PSOC 276 coal during the NO_2 treatment in the batch reactor contrasts with the fact that no carbon removal occurs when the PSOC 190 coal is treated with NO_2. In the case of the PSOC 276 coal, apparently there is a component which is rapidly extracted by the NO_2/CCl_4 solution within 30 minutes. Further exposure results in even more extraction. Furthermore, the rate of this second process seems to increase with exposure time. On the other hand, the carbon loss due to the Na_2CO_3 (aq) wash seems to rise quickly and level off at about 5 % after about 60 minutes of treatment with NO_2. It would be interesting to know if the two curves would meet at longer NO_2-treatment times. Theoretically, the value of L_C for the Na_2CO_3 (aq) wash must always be greater than or equal to the value of L_C for the NO_2–treated coal, unless there is an uptake of carbonate by the NO_2–treated coal. In any event, L_C for the washed coal is greater than L_C for the NO_2–treated coal within the domain of NO_2-exposure times used.

The difference between the mass corrected carbon contents of the NO_2-treated PSOC 190 and PSOC 276 coals is shown in Figure 4–39. It should be noted that the initial carbon content of the pretreated PSOC 276 coal is about 3 % higher than that of the pretreated PSOC 190. Therefore, both coals show a similar absolute drop in carbon content during the first 90 minutes of treatment. Beyond that time, however, the carbon content of the PSOC 276 coal continues to drop at a fairly constant rate while that of the PSOC 190 coal levels off. A comparison of the mass corrected carbon loss of the NO_2-treated PSOC 190 and PSOC 276 coals is displayed graphically in Figure 4–40. Whereas the treated PSOC 276 shows a very rapid initial rise in L_C, the treated PSOC 190 does not. Both curves, however, display the same accelerating increase in L_C after t = 60

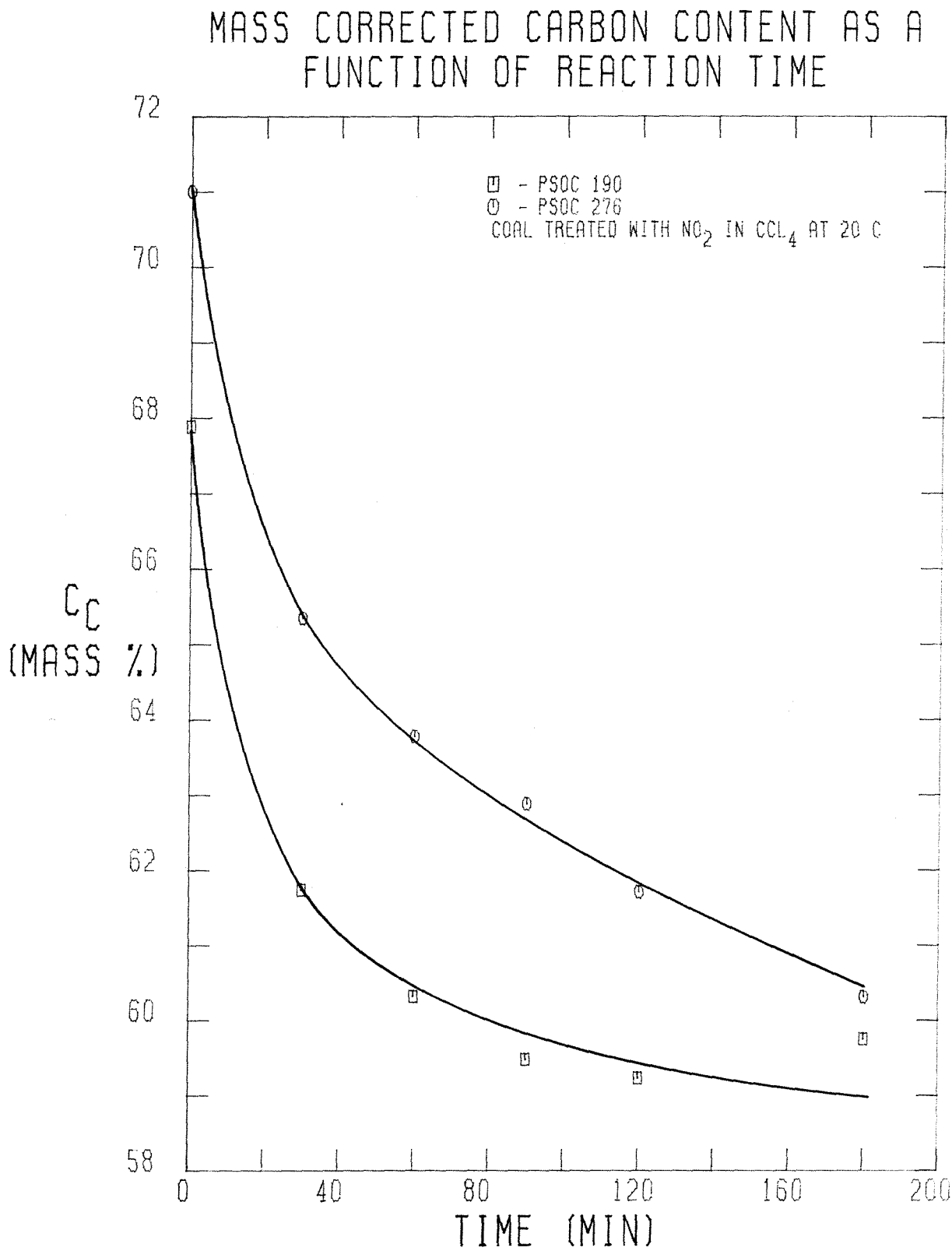
MASS CORRECTED CARBON CONTENT AS A FUNCTION OF REACTION TIME
□ - PSOC 190
○ - PSOC 276
COAL TREATED WITH NO_2 IN CCL_4 AT 20 C
C_C (MASS %)
72
70
68
66
64
62
60
58
0
40
80
120
160
200
TIME (MIN)

FIGURE 4-39

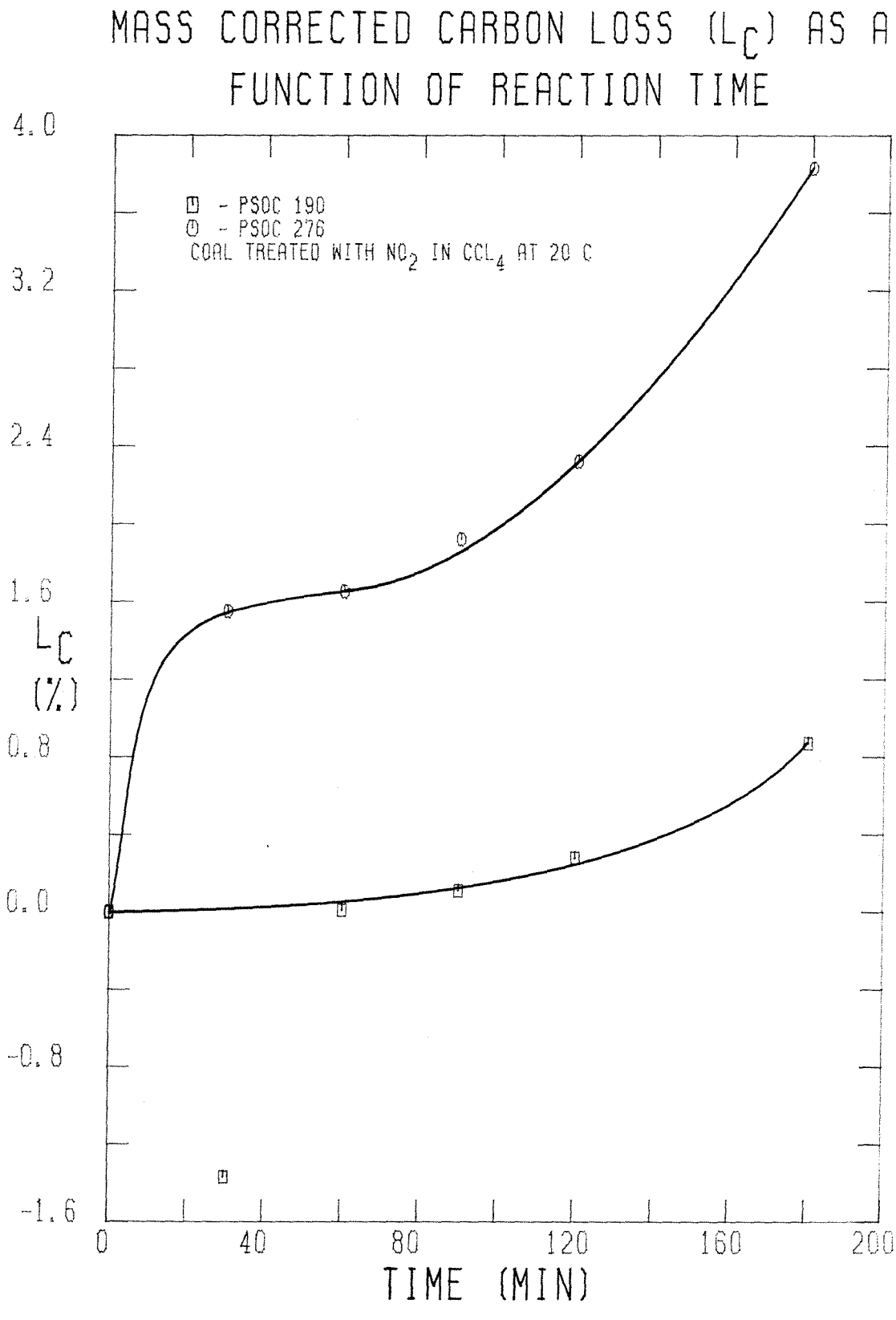
MASS CORRECTED CARBON LOSS (L_C) AS A FUNCTION OF REACTION TIME
- PSOC 190
- PSOC 276
COAL TREATED WITH NO_2 IN CCL_4 AT 20 C
4.0
3.2
2.4
1.6
0.8
0.0
-0.8
-1.6
L_C (%)
0
40
80
120
160
200
TIME (MIN)

FIGURE 4-40

minutes, which implies that the process responsible for this behavior is common to both coals. What is indeed surprising is that although the PSOC 276 coal has roughly four times less pore volume than the PSOC 190 coal, it is the treated PSOC 276 which shows a much greater carbon loss. Obviously the difference in the chemical nature of the carbon in the two coals must account for the difference in the carbon losses. In particular, the PSOC 276 coal has a carbon containing component which is readily extracted by the NO_2/CCl_4 solution while the PSOC 190 coal does not. Furthermore, the remaining carbon in the PSOC 276 coal is attacked and extracted by the NO_2/CCl_4 solution to a greater extent than the carbon in the PSOC 190 coal.

A comparison of the mass corrected carbon content of the NO_2–treated coal washed in Na_2CO_3 (aq) when either PSOC 190 or PSOC 276 coals are used is shown in Figure 4–41. Again, the carbon content of the PSOC 190 coal drops more than that of the PSOC 276 coal, even after adjusting for the difference in initial carbon contents. The carbon content of the washed PSOC 276 coal, however, continues to fall at a greater rate than that of the PSOC 190 coal after 180 minutes. A better idea of the overall carbon loss for the two coals can be obtained by referring to Figure 4–42, in which are plotted the mass corrected carbon losses. Both coals show a very rapid increase in L_C of about 4 %. After 30 minutes of NO_2 exposure, L_C for the PSOC 190 coal then continues to increase at a slower, yet constant rate, reaching a value of 7 % at t = 180 minutes. On the other hand, L_C for the PSOC 276 coal gradually levels off at about 5 % after roughly 90 minutes of NO_2 treatment. This behavior of the Na_2CO_3 (aq) washed coals is exactly the opposite of that of the NO_2–treated coals, in which L_C for the PSOC 276 exceeded that of the PSOC 190 by a factor of almost five. Thus, while the porosity of the coal does not affect the limited amount of attack and extraction of carbon containing compounds in coal by the NO_2/CCl_4 solution, it does

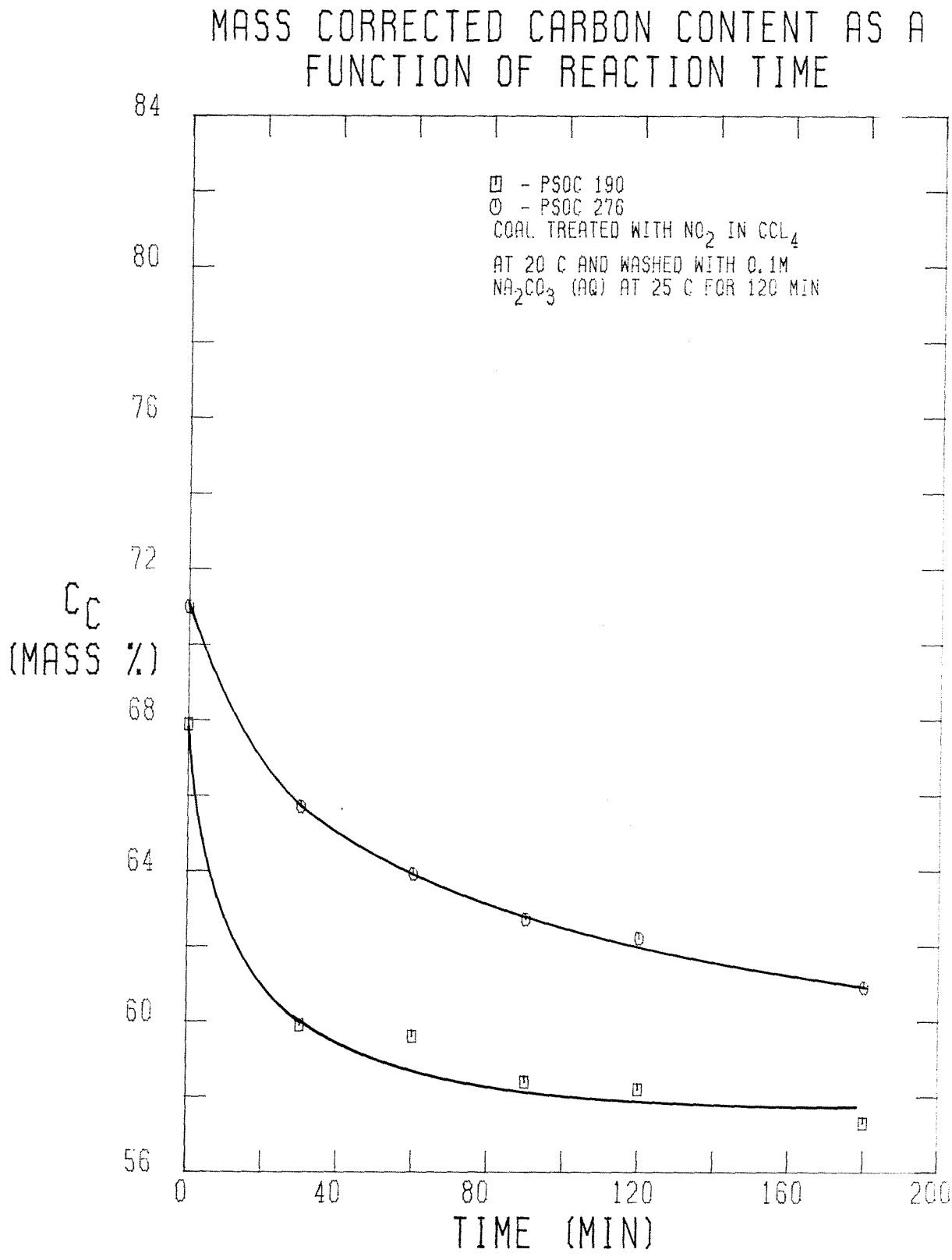
MASS CORRECTED CARBON CONTENT AS A FUNCTION OF REACTION TIME
84
80
76
72
68
64
60
56
C_C (MASS %)
0
40
80
120
160
200
TIME (MIN)
- PSOC 190
- PSOC 276
COAL TREATED WITH NO_2 IN CCL_4
AT 20 C AND WASHED WITH 0.1M
NA_2CO_3 (AQ) AT 25 C FOR 120 MIN

FIGURE 4-41

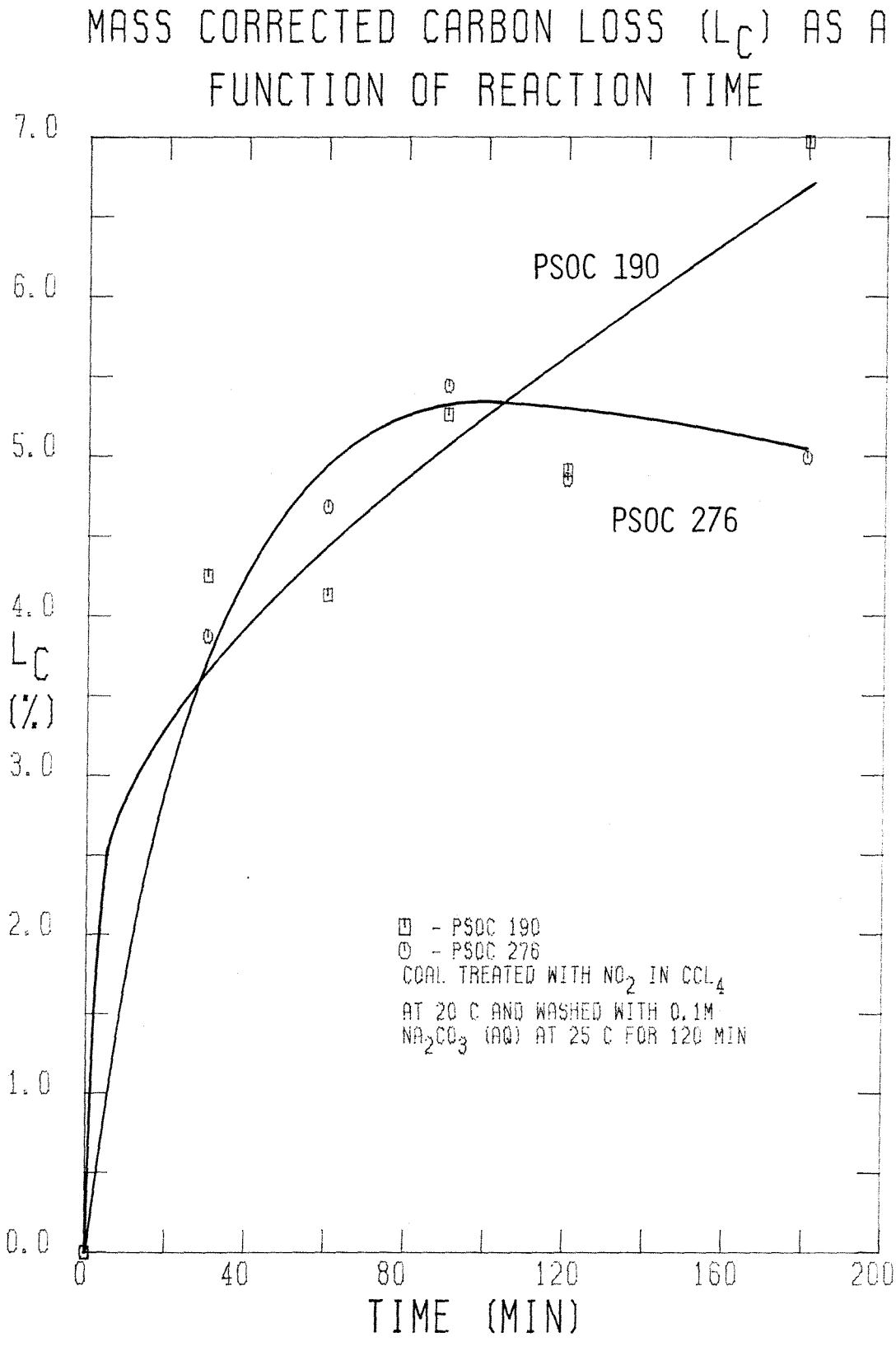
MASS CORRECTED CARBON LOSS (L_C) AS A FUNCTION OF REACTION TIME
7.0
6.0
5.0
4.0
3.0
2.0
1.0
0.0
L_C (%)
PSOC 190
PSOC 276
□ - PSOC 190
○ - PSOC 276
COAL TREATED WITH NO_2 IN CCL_4
AT 20 C AND WASHED WITH 0.1M
NA_2CO_3 (AQ) AT 25 C FOR 120 MIN
0
40
80
120
160
200
TIME (MIN)

FIGURE 4-42

affect the overall carbon loss after the Na_2CO_3 (aq) wash.

On the basis of the points discussed above, several generalizations concerning the effect of the NO_2 treatment conditions on the carbon content of the coal can be made. Of primary importance is the fact that the NO_2 treatment of the coal slurried in CCl_4 does not lead to any significant carbon losses, provided that (NO_2) does not exceed roughly 2 F. Furthermore, treating the coal in the temperature range from 0 to 50°C does not significantly affect the minimal amount of carbon loss that does occur. Of the experiments conducted, the maximum carbon loss was 4 % when the PSOC 190 coal was treated at 50°C for 180 minutes and was 4 % when the PSOC 276 coal was treated at 20°C for 180 minutes. Furthermore, the porosity of the coal does not seem to affect the attack and extraction of carbon compounds in the coal by the NO_2/CCl_4 solution.

The other parameters mentioned above, however, namely the NO_2-treatment time and temperature, (NO_2) and the porosity of the coal do affect the overall carbon loss when the NO_2–treated coals are washed in 0.1 M Na_2CO_3 (aq). In particular, longer NO_2-treatment times and higher treatment temperatures result in the production of a greater amount of coal-derived carbon containing compounds which are soluble in aqueous Na_2CO_3. Also, higher values of (NO_2) result in a faster rate of production of these compounds. Finally, the porosity of the coal may affect the removal of these compounds since they must be removed from the interior of the coal particle. This last conclusion follows from the fact that other evidence, in particular the nitrogen content data, suggests that the extent of reaction of NO_2 with the two coals is equal, from which it follows that the porosity of the coal does not affect the extent of the NO_2-coal reaction. Since both coals possess approximately the same elemental composition, one would expect approximately the same distribution of NO_2-coal reaction products. Thus, if their removal from the two different coals is different, then any

physical differences in the coal which might cause variations in their accessibility during the wash with Na_2CO_3 (aq) must be responsible. The obvious difference in this case is the porosity.

4.2.2.3 The Hydrogen Content of the Coal

One of the most likely elemental compositions of the coal to be affected by NO_2 treatment is that of hydrogen because in the oxidation of hydrocarbons, the C–H bonds are generally more susceptible to cleavage than C–C bonds. Therefore, a knowledge of the variations in the hydrogen content induced by treatment with NO_2 under various conditions is essential for a clear understanding of the kinetics. Because the use of water as a solvent greatly complicates the kinetics of the coal-NO_2 reaction, the hydrogen contents of those coal samples generated by experiments utilizing water as a solvent (Runs 1–20) were not determined. Thus, the effect of the various reaction parameters on the change in hydrogen content to be discussed below is concerned exclusively with those runs using CCl_4 as the solvent, which does not chemically react with NO_2.

The mass corrected hydrogen content of the coal samples generated by treatment with NO_2 at 25°C in the flow reactor (Runs 21–27) are shown in Figure 4–43. Once again, the phrase "mass corrected" refers to the fact that the hydrogen contents listed in Table 3–19 have been adjusted for the adsorption of CCl_4. In this case, the effect is only indirect in that the mass gain results must be adjusted while the absolute amount of hydrogen remains invariant, which results in a change in hydrogen content expressed on a mass percentage basis. The curves show the same basic behavior as those of the carbon content, namely a very rapid decrease in the hydrogen content, c_H, followed by a more gradual decline. In the case of hydrogen, however, c_H is slightly higher after the Na_2CO_3 (aq) wash than after the NO_2 treatment, which implies that the wash is removing compounds with a lower hydrogen concentration than the remaining coal. The Na_2CO_3 (aq) wash does remove some hydrogen containing compounds, however, which is demonstrated by the mass corrected hydrogen loss, L_H, of the treated coal samples shown in Figure 4–44. The mass corrected hydrogen loss is

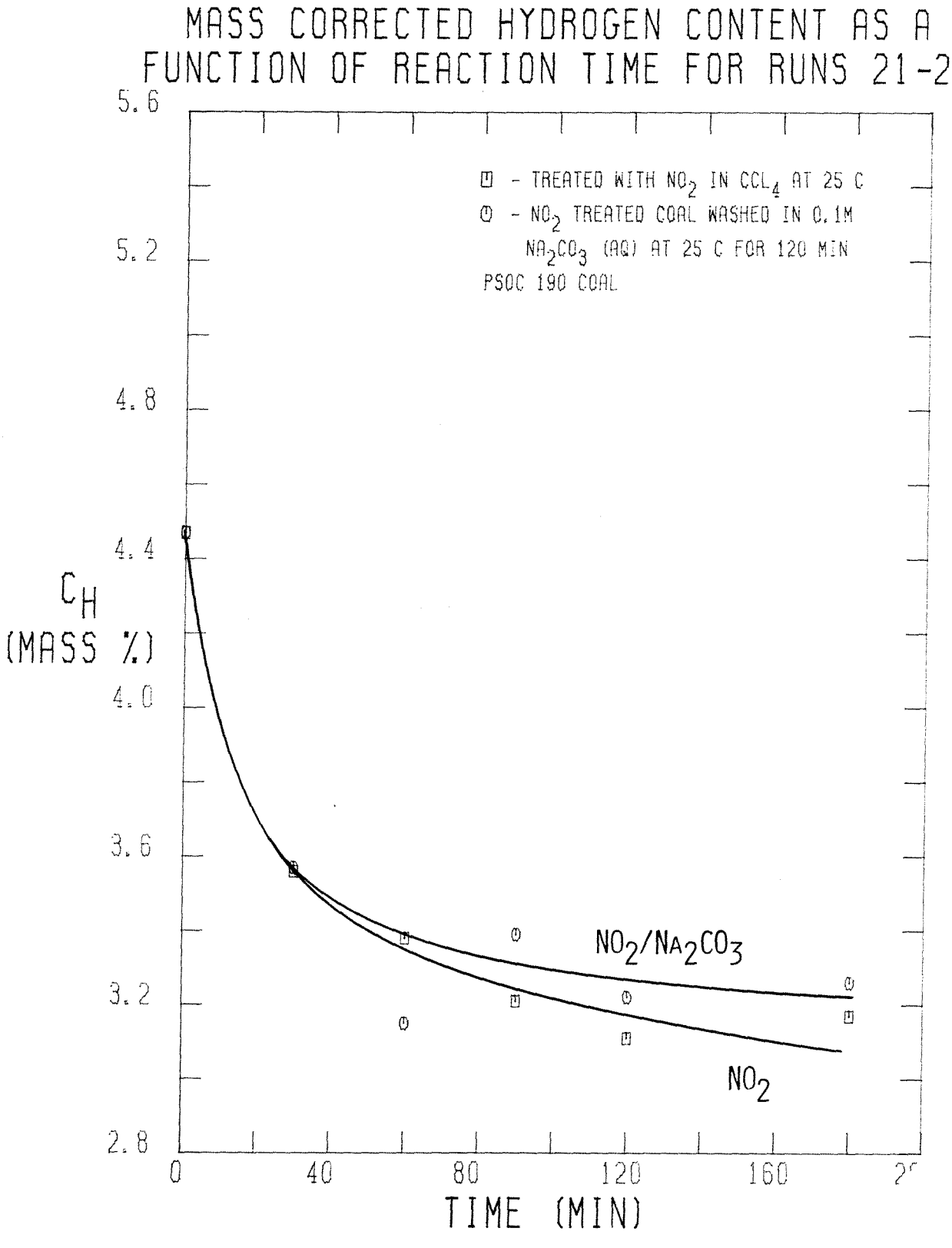
MASS CORRECTED HYDROGEN CONTENT AS A FUNCTION OF REACTION TIME FOR RUNS 21-27
5.6
5.2
4.8
4.4
4.0
3.6
3.2
2.8
C_H (MASS %)
0
40
80
120
160
TIME (MIN)
- TREATED WITH NO2 IN CCL4 AT 25 C
- NO2 TREATED COAL WASHED IN 0.1M NA2CO3 (AQ) AT 25 C FOR 120 MIN
PSOC 190 COAL
NO2/NA2CO3
NO2

FIGURE 4-43

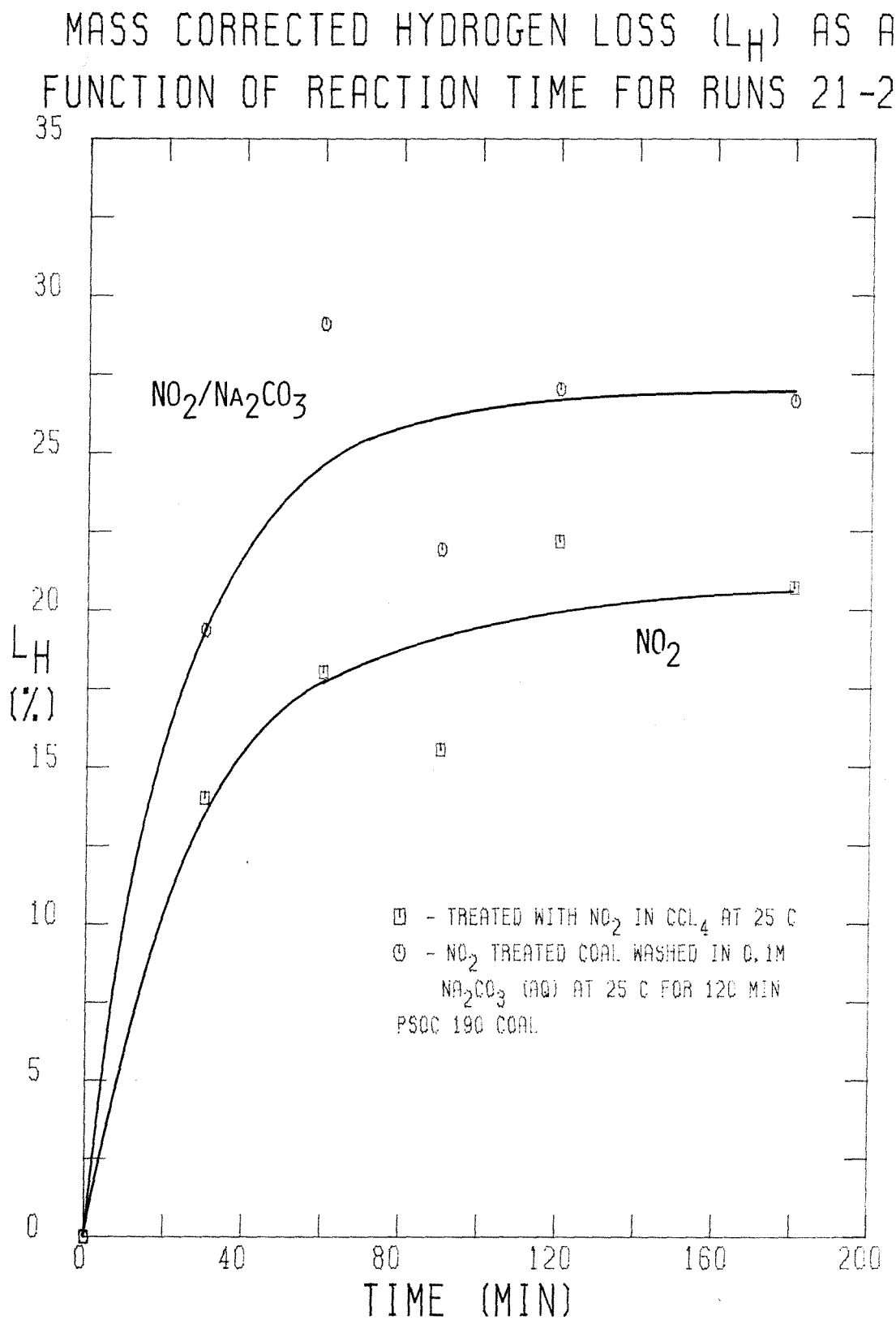
MASS CORRECTED HYDROGEN LOSS (L_H) AS A FUNCTION OF REACTION TIME FOR RUNS 21-27
35
30
25
20
15
10
5
0
L_H (%)
NO_2/NA_2CO_3
NO_2
- TREATED WITH NO_2 IN CCL_4 AT 25 C
- NO_2 TREATED COAL WASHED IN 0.1M NA_2CO_3 (AQ) AT 25 C FOR 120 MIN
PSOC 190 COAL
0
40
80
120
160
200
TIME (MIN)

FIGURE 4-44

obtained by simply adjusting the values of c_H for the mass gain to obtain the absolute hydrogen mass, subtracting the result from the initial absolute hydrogen mass and dividing the difference by the initial absolute hydrogen mass; that is

$$L_H\,(\%) \;=\; 100\;\frac{m_0(c_H)_0 - mc_H}{m_0(c_H)_0}, \quad \text{where} \tag{4.2.12}$$

m_0 = the initial mass of coal used in the run (g),

m = the final mass recovered after treatment (g),

$(c_H)_0$ = the initial hydrogen content (mass %), and

c_H = the hydrogen content of the treated coal (mass %).

Figure 4–44 clearly demonstrates that a significant amount of hydrogen is lost during the NO_2 treatment. Furthermore, the Na_2CO_3 (aq) wash removes an additional, but smaller amount of the original hydrogen in the coal. It should be remembered that in this series of runs, (NO_2) rose linearly from zero to 8 F at t = 180 minutes and resulted in a 10 % carbon loss after NO_2 treatment for 180 minutes and a 26 % carbon loss after the corresponding Na_2CO_3 (aq) wash. If the results for L_H and L_C for this set of runs are combined, it appears that the NO_2 treatment removes carbon and hydrogen in a molar ratio of 1.0 to 1.8. On the other hand, the Na_2CO_3 (aq) wash results in the overall removal of carbon and hydrogen in a molar ratio of 1.1 to 1.0. The original pretreated coal has a molar ratio of carbon to hydrogen of 1.23 to 1.00. These results indicate that the hydrogen is lost mainly in the NO_2 treatment while the carbon is lost mainly in the Na_2CO_3 (aq) wash under the conditions employed for Runs 21–27.

The dependence of the mass corrected hydrogen contents of the coal samples treated with NO_2 at 20℃ in the batch reactor (Runs 33–37) as a function of NO_2-exposure time are depicted graphically in Figure 4–45. Both curves show a

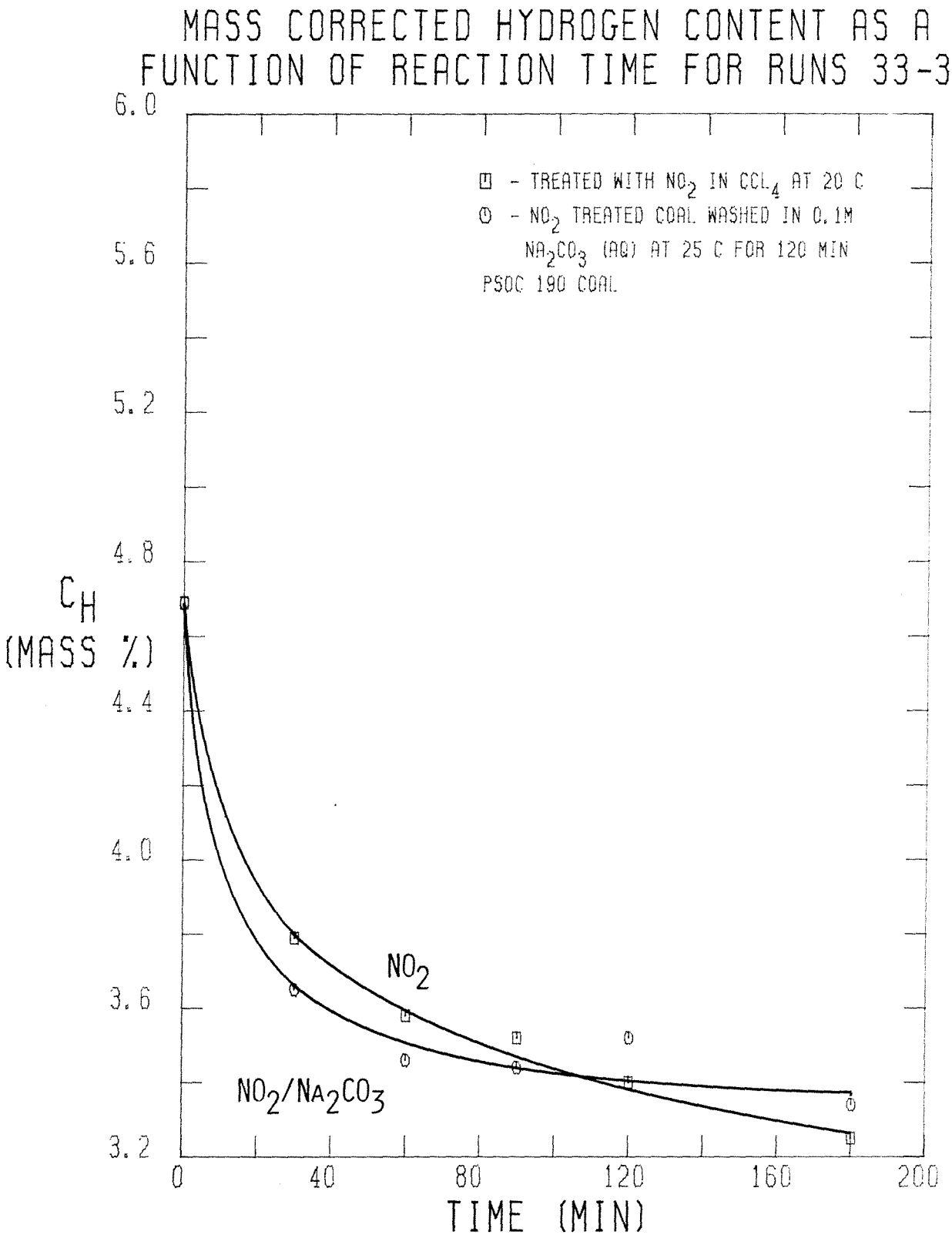
MASS CORRECTED HYDROGEN CONTENT AS A FUNCTION OF REACTION TIME FOR RUNS 33-37
□ - TREATED WITH NO2 IN CCL4 AT 20 C
⊙ - NO2 TREATED COAL WASHED IN 0.1M NA2CO3 (AQ) AT 25 C FOR 120 MIN
PSOC 190 COAL
NO2
NO2/NA2CO3
CH (MASS %)
TIME (MIN)
6.0
5.6
5.2
4.8
4.4
4.0
3.6
3.2
0
40
80
120
160
200

FIGURE 4-45

rapid drop in c_H followed by a more gradual decline, just as in the previous set, even though the NO_2-treatment conditions were vastly different. In this case, both curves are virtually identical, which implies that the Na_2CO_3 (aq) wash removes compounds with the same c_H as the remaining coal. The values of the mass corrected hydrogen loss for this set of runs are plotted in Figure 4–46. In contrast to the previous set of runs, L_H for NO_2 treatment rises rapidly within 30 minutes and then continues to rise linearly at about one-fourth the initial rate thereafter, reaching a value of roughly 22.5 % after 180 minutes. Washing the NO_2–treated coal with 0.1 M Na_2CO_3 (aq) results in an additional hydrogen loss at NO_2-reaction times less than 90 minutes. As the NO_2–exposure time approaches 180 minutes, however, the additional hydrogen loss vanishes, which implies that a sufficiently long exposure to NO_2 at 20°C (i.e., $t >$ 180 minutes) accounts for all of the hydrogen removal. Thus, the coal-derived compounds leached by Na_2CO_3 (aq) contain no hydrogen, which is in direct contrast to the carbon loss results which show that NO_2 treatment results in no carbon removal and that all of the carbon loss is attributable to the Na_2CO_3 (aq) wash.

The mass corrected hydrogen contents of the coal samples treated with NO_2 at 0°C in the batch reactor (Runs 42–46) are shown in Figure 4–47. The values of c_H for the NO_2 treatment are quite scattered, which is also true for the corresponding values of c_C. The corresponding mass gain curve, however, shows quite normal behavior, which precludes inconsistencies in the drying procedure as the cause of the scatter. Despite the scatter, however, the values of c_H show a very gradual decline on the whole. The values of c_H after washing the NO_2–treated coal in 0.1 M Na_2CO_3 (aq), on the other hand, are much more consistent. Indeed, c_H drops rapidly during the first 30 minutes and then falls linearly at a reduced rate thereafter, which is similar to the trend in the previous set. An examination of the corresponding values of L_H in Figure 4–48

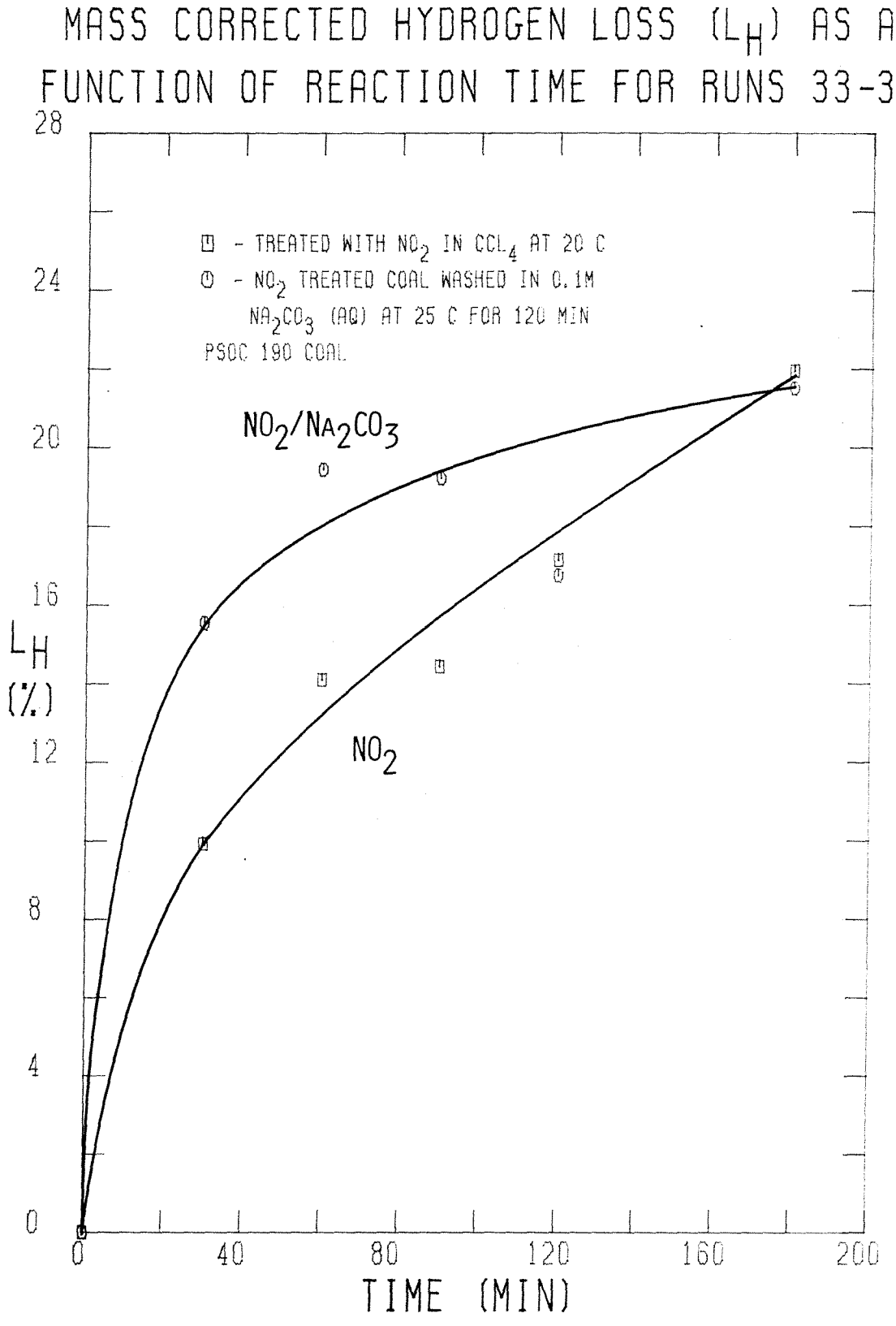
MASS CORRECTED HYDROGEN LOSS (L_H) AS A FUNCTION OF REACTION TIME FOR RUNS 33-37
□ - TREATED WITH NO_2 IN CCL_4 AT 20 C
⊙ - NO_2 TREATED COAL WASHED IN 0.1M NA_2CO_3 (AQ) AT 25 C FOR 120 MIN
PSOC 190 COAL
NO_2/NA_2CO_3
NO_2
L_H (%)
TIME (MIN)
0
4
8
12
16
20
24
28
0
40
80
120
160
200

FIGURE 4-46

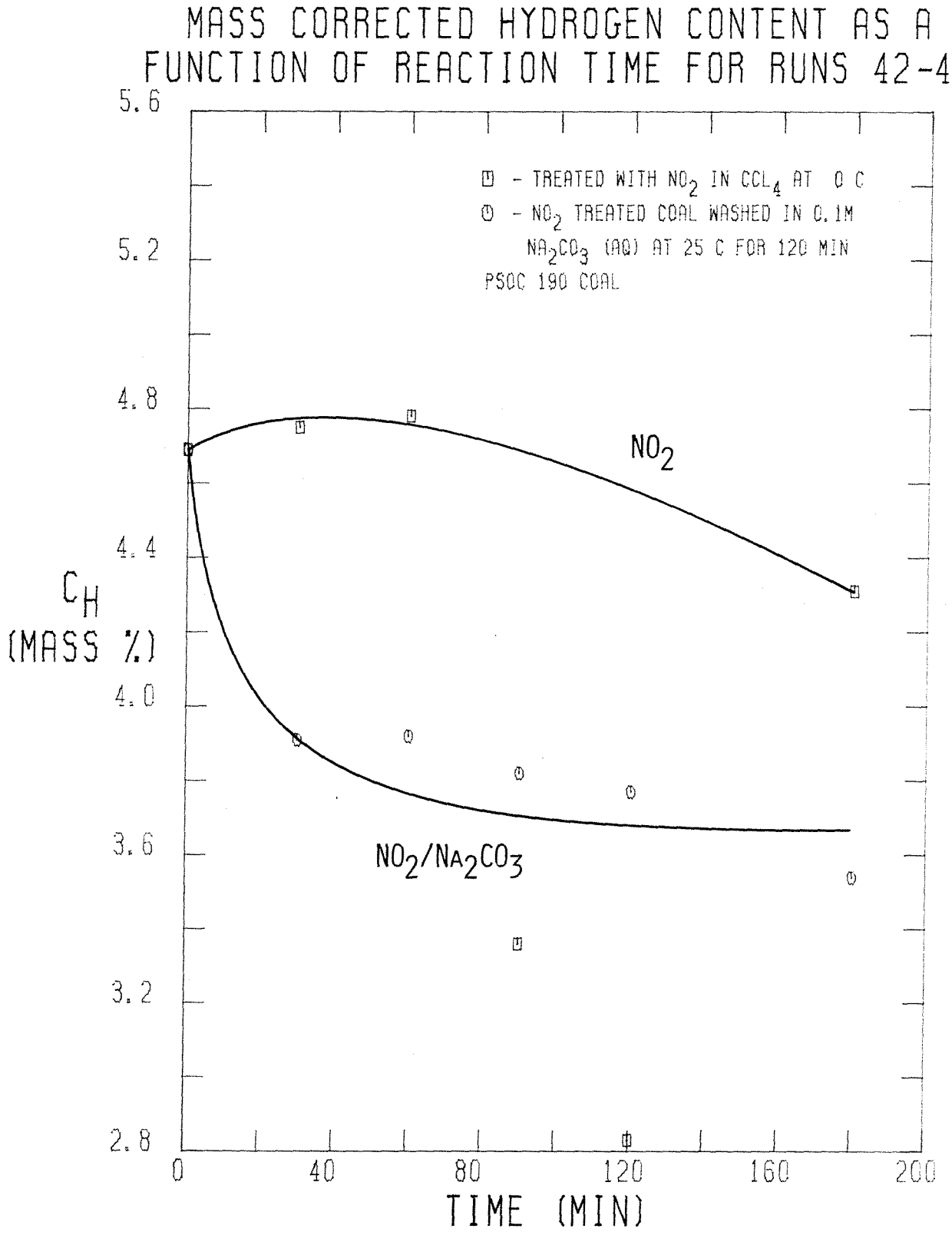
MASS CORRECTED HYDROGEN CONTENT AS A FUNCTION OF REACTION TIME FOR RUNS 42-46
□ - TREATED WITH NO2 IN CCL4 AT 0 C
① - NO2 TREATED COAL WASHED IN 0.1M NA2CO3 (AQ) AT 25 C FOR 120 MIN
PSOC 190 COAL
NO2
NO2/NA2CO3
CH (MASS %)
TIME (MIN)
5.6
5.2
4.8
4.4
4.0
3.6
3.2
2.8
0
40
80
120
160
200

FIGURE 4-47

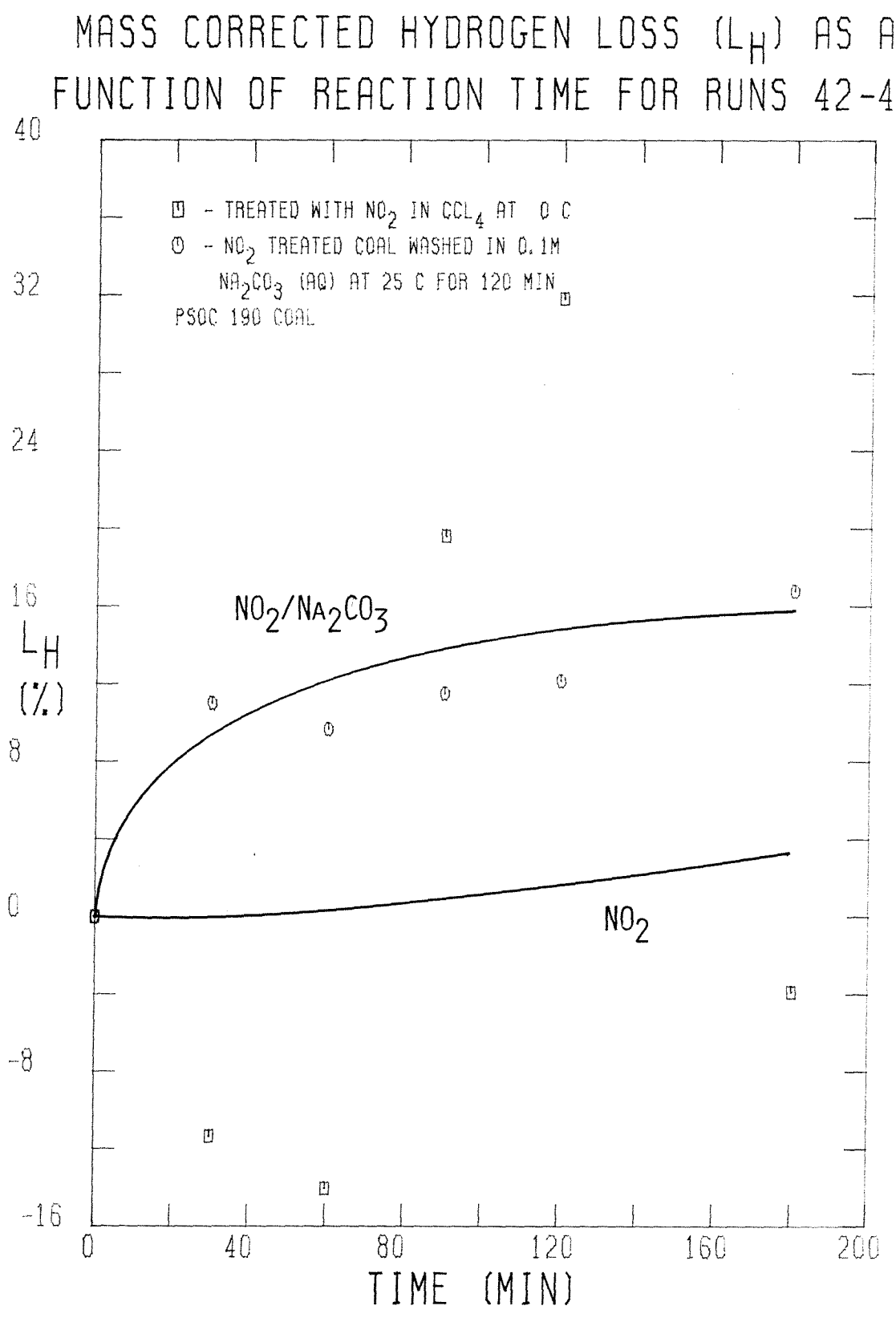
MASS CORRECTED HYDROGEN LOSS (L_H) AS A FUNCTION OF REACTION TIME FOR RUNS 42-46
□ - TREATED WITH NO_2 IN CCL_4 AT 0 C
① - NO_2 TREATED COAL WASHED IN 0.1M NA_2CO_3 (AQ) AT 25 C FOR 120 MIN
PSOC 190 COAL
NO_2/NA_2CO_3
NO_2
L_H (%)
40
32
24
16
8
0
-8
-16
0
40
80
120
160
200
TIME (MIN)

FIGURE 4-48

reveals the serious nature of the inconsistencies in the hydrogen analysis for the NO_2–treated coals, since there is absolutely no process by which the absolute amount of hydrogen in the coal can increase (negative value of L_H) during the NO_2 treatment in the CCl_4 solvent. Furthermore, it is highly unlikely that the value of L_H for the NO_2–treated coal can exceed that of the coal washed in Na_2CO_3 (aq). On this basis, none of the hydrogen analyses of the NO_2–treated coals are correct. The values of L_H for the Na_2CO_3 (aq)-washed coal samples are much more consistent, however. During the first 30 minutes of NO_2 exposure, L_H of the washed coal rises rapidly to 11 %. For longer NO_2–reaction times, L_H increases at a much slower rate, reaching about 17 % after 180 minutes. It is interesting to note that the corresponding carbon loss after the NO_2–treated coal is washed in 0.1 M Na_2CO_3 (aq) reaches a maximum of only 3 % of the original carbon in the coal. Therefore, hydrogen removal is much easier than carbon removal when the coal is treated at 0°C with NO_2 and washed in 0.1 M Na_2CO_3 (aq).

The effect of the NO_2-treatment temperature on the values of c_H for the NO_2–treated coal is illustrated in Figure 4–49. The curves for c_H corresponding to NO_2 treatment at 50°C and 20°C are virtually identical, while that at 0°C has been omitted because of the scatter in the analyses mentioned above. An examination of the absolute hydrogen loss shown in Figure 4–50, however, reveals that more hydrogen is lost at 20°C than at 50°C during the NO_2 treatment. Furthermore, L_H at 20°C seems to continually increase with NO_2–exposure time while L_H at 50°C rises at a slower rate and tends to level off at longer exposure times. It should be noted that the curve for L_H at 50°C has been drawn in a unimodal fashion despite the apparent drop between 60 and 90 minutes because there is no possible physical explanation why L_H should drop in such a fashion. Rather, the drop must be attributed to the uncertainty in the hydrogen analysis.

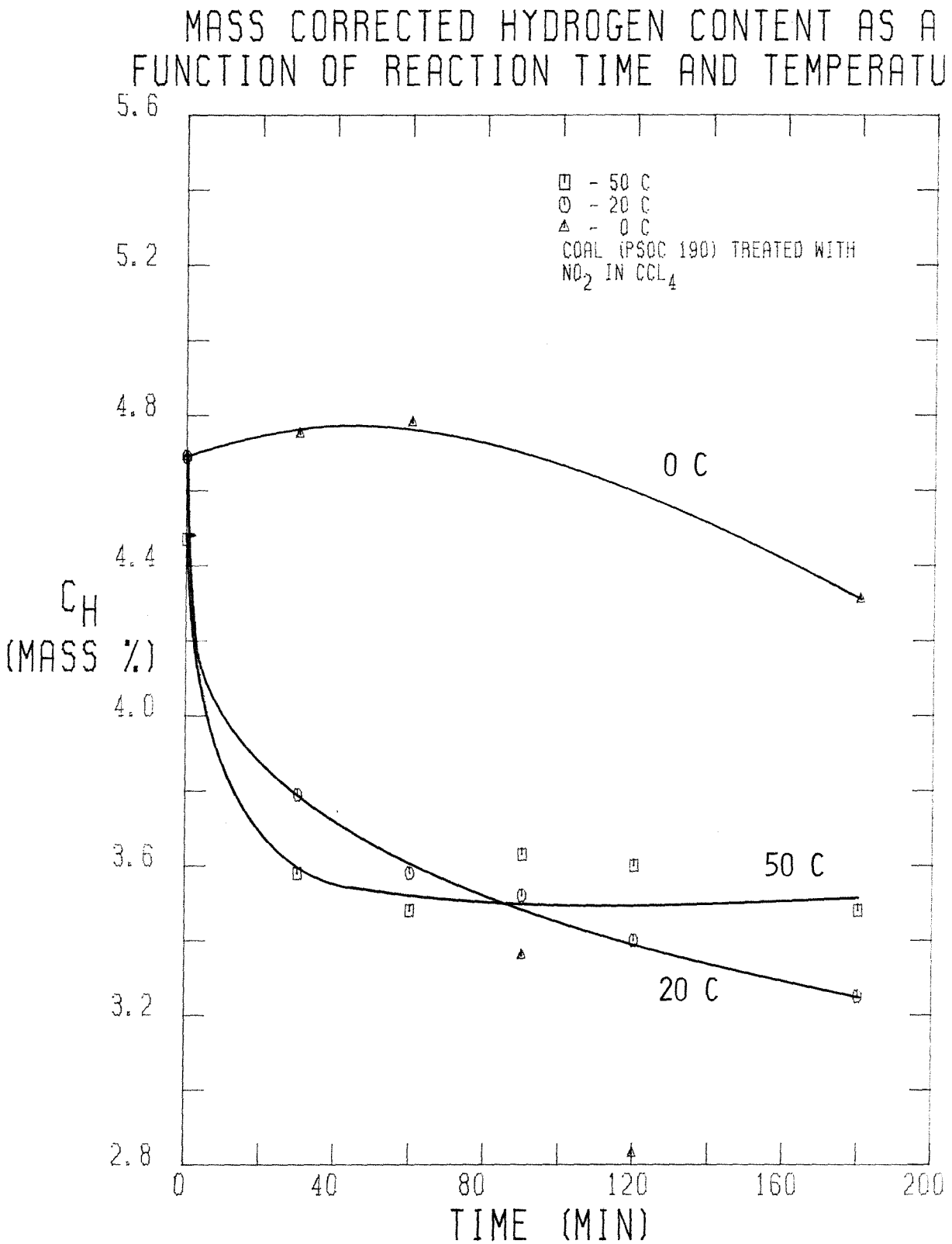
MASS CORRECTED HYDROGEN CONTENT AS A FUNCTION OF REACTION TIME AND TEMPERATURE
□ - 50 C
○ - 20 C
△ - 0 C
COAL (PSOC 190) TREATED WITH NO_2 IN CCL_4
0 C
50 C
20 C
C_H (MASS %)
5.6
5.2
4.8
4.4
4.0
3.6
3.2
2.8
0
40
80
120
160
200
TIME (MIN)

FIGURE 4-49

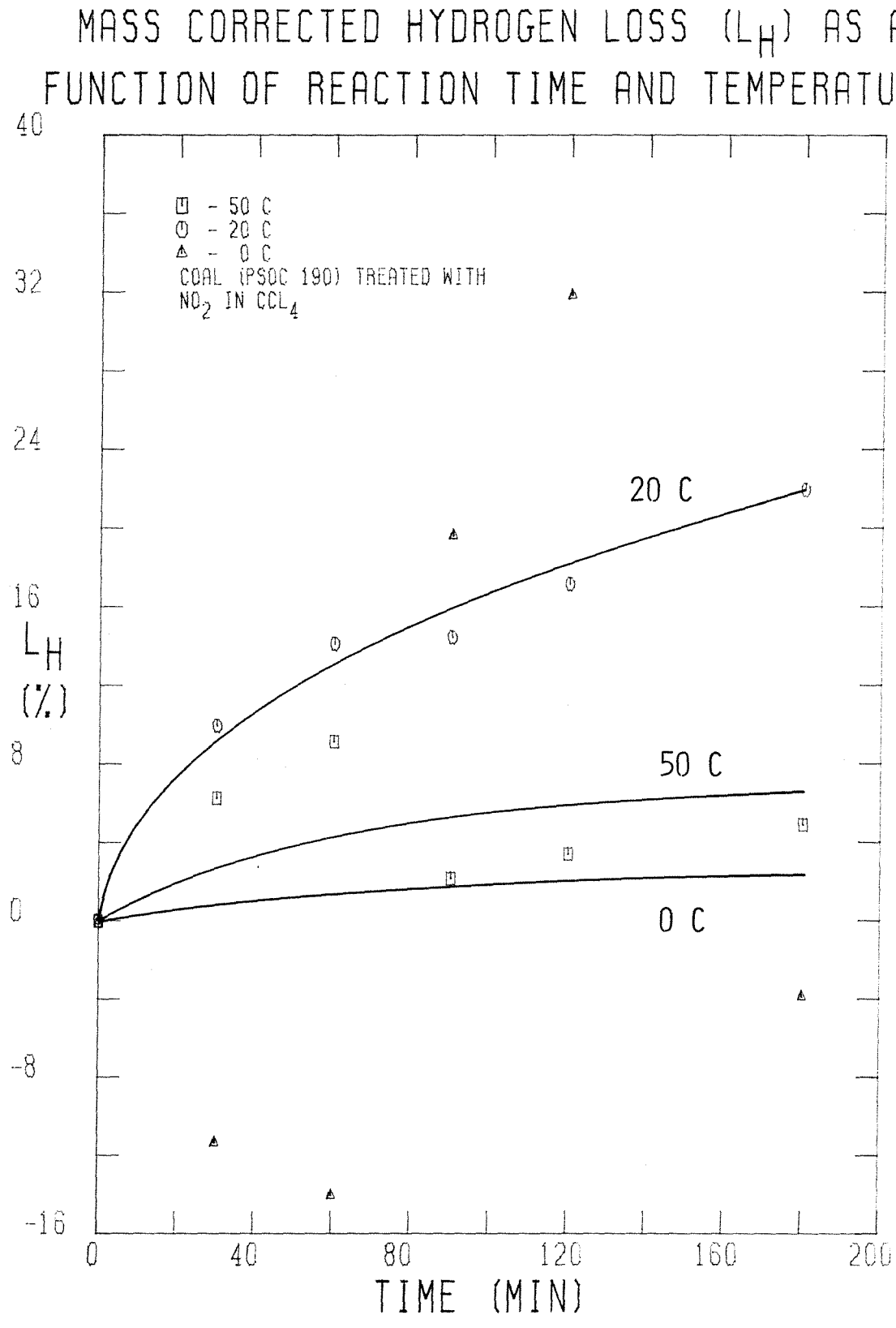
MASS CORRECTED HYDROGEN LOSS (L_H) AS A FUNCTION OF REACTION TIME AND TEMPERATURE
50 C
20 C
0 C
COAL (PSOC 190) TREATED WITH NO_2 IN CCL_4
20 C
50 C
0 C
L_H (%)
40
32
24
16
8
0
-8
-16
0
40
80
120
160
200
TIME (MIN)

FIGURE 4-50

Nevertheless, all of the values of L_H at 50°C are smaller than those at 20°C. This trend is exactly the opposite of that for the carbon loss. The carbon loss at 50°C is greater than that at 20°C during NO_2 treatment, which is expected. The only explanations for the temperature behavior of L_H are that the rate of hydrogen removal decreases with increasing temperature due to an increase in the resistance to mass transfer out of the particle or that the hydrogen containing products from the NO_2-coal reaction are reincorporated into the coal at a rate which increases with increasing temperature.

Unfortunately, the coal treated at 50°C with NO_2 could not be washed in 0.1 M Na_2CO_3 (aq) and recovered successfully so that a comparison of the hydrogen content of the washed coals as a function of temperature could not be made. Nevertheless, the values of c_H for coals treated at 20°C and 0°C with NO_2 and then washed with 0.1 M Na_2CO_3 (aq) are shown in Figure 4–51. Both curves show the same trend with the 20°C curve possessing a larger initial drop than the 0°C curve. After adjusting the values of c_H for the overall mass gains, the values of L_H shown in Figure 4–52 are obtained. Once again, the amount of hydrogen removed due to NO_2 treatment at 20°C is greater than that due to NO_2 treatment at 0°C. Both L_H curves show an initially rapid rise followed by a more gradual increase with NO_2–exposure time. At 30 minutes, the molar ratio of C to H loss is 1.0 to 3.6 at 0°C and 1.0 to 3.0 at 20°C. At 180 minutes, the molar ratio of C to H loss is 1.0 to 5.0 at 0°C and 1.0 to 2.5 at 20°C. Since the coal initially has a molar C to H ratio of 1.21 to 1.00, these results imply that hydrogen is much more readily removed than carbon by treatment with NO_2 followed by washing with 0.1 M Na_2CO_3 (aq). Furthermore, the rate of the reaction responsible for the ultimate removal of hydrogen is much less affected by temperature than the rate of the process responsible for the ultimate removal of carbon.

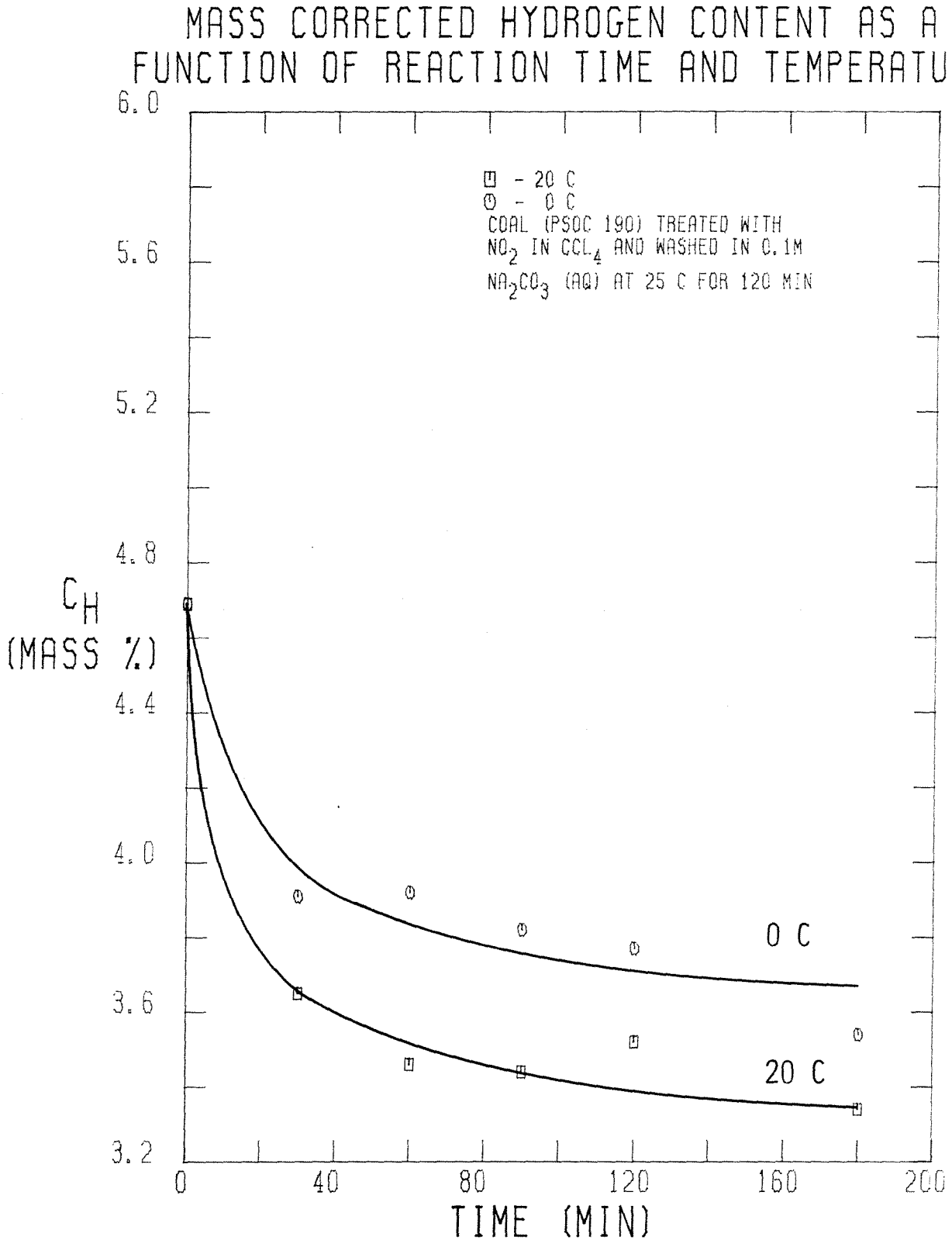
MASS CORRECTED HYDROGEN CONTENT AS A FUNCTION OF REACTION TIME AND TEMPERATURE
□ - 20 C
Ⓤ - 0 C
COAL (PSOC 190) TREATED WITH NO_2 IN CCL_4 AND WASHED IN 0.1M NA_2CO_3 (AQ) AT 25 C FOR 120 MIN
C_H (MASS %)
6.0
5.6
5.2
4.8
4.4
4.0
3.6
3.2
0 C
20 C
0
40
80
120
160
200
TIME (MIN)

FIGURE 4-51

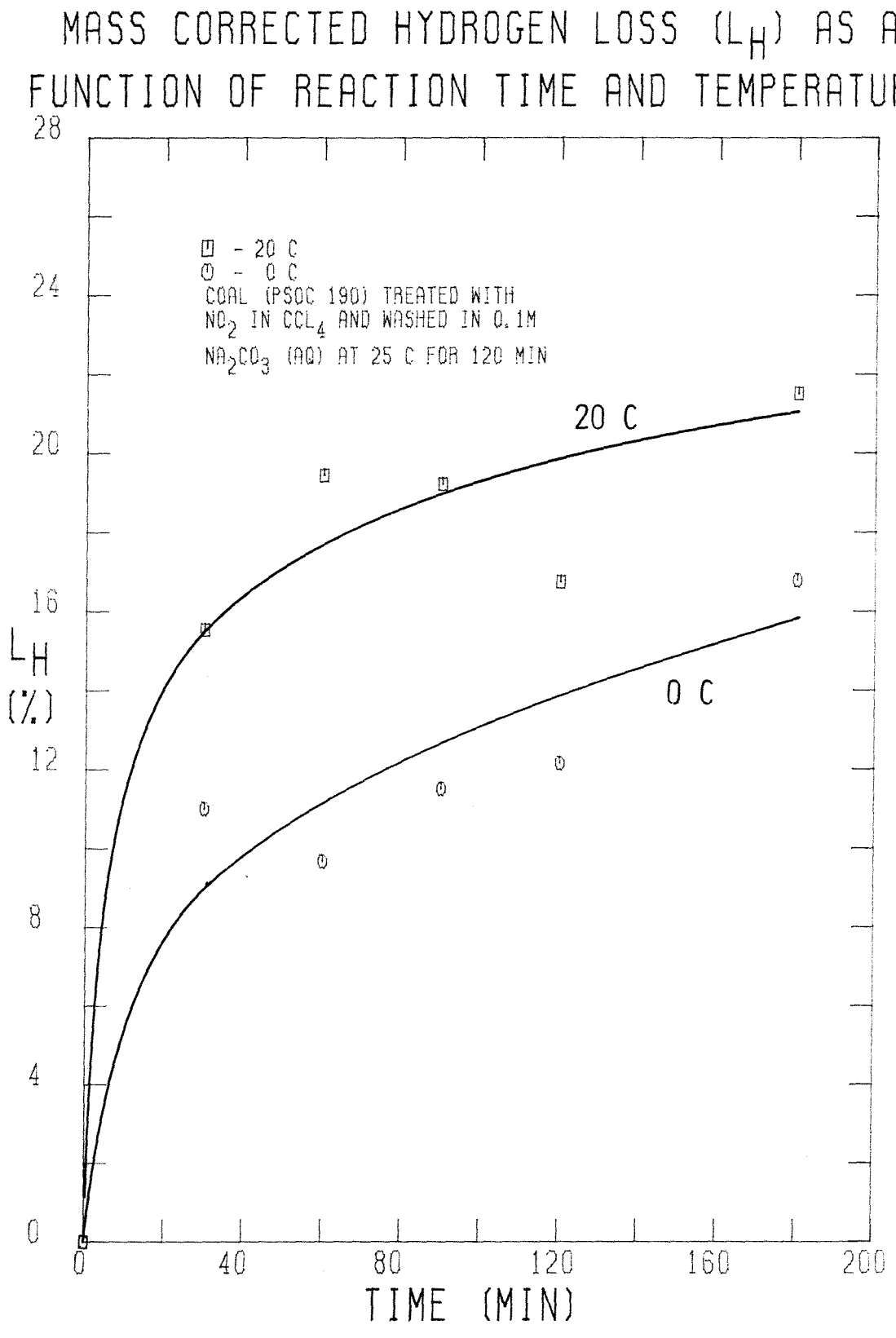
MASS CORRECTED HYDROGEN LOSS (L_H) AS A FUNCTION OF REACTION TIME AND TEMPERATURE
□ - 20 C
○ - 0 C
COAL (PSOC 190) TREATED WITH
NO_2 IN CCL_4 AND WASHED IN 0.1M
NA_2CO_3 (AQ) AT 25 C FOR 120 MIN
20 C
0 C
L_H (%)
TIME (MIN)
0
4
8
12
16
20
24
28
0
40
80
120
160
200

FIGURE 4-52

The influence of the initial NO_2 concentration, $(NO_2)_0$, on the mass corrected hydrogen content of the coal after 120 minutes of NO_2 treatment at 20°C and subsequent washing in Na_2CO_3 (aq) (Runs 38–41) is shown in Figure 4–53. During the NO_2 treatment, once $(NO_2)_0$ is greater than about 0.5 F, c_H no longer decreases after 120 minutes of exposure to NO_2. The initial NO_2 concentration does affect the value of c_H after the Na_2CO_3 (aq) wash, however. Not only is c_H further reduced after the wash, but it continues to decrease as $(NO_2)_0$ increases. The values of the hydrogen loss, L_H, for this set of runs shown in Figure 4–54 clearly demonstrate the effect of $(NO_2)_0$ on the removal of hydrogen during the NO_2 treatment and during the wash. During the NO_2 treatment, L_H does not seem to depend on $(NO_2)_0$. Rather, the presence of a sufficient amount of NO_2 results in the facile removal of roughly 8 % of the hydrogen within 120 minutes. The further removal of hydrogen by the Na_2CO_3 (aq) wash, however, does seem to depend on $(NO_2)_0$. Values of $(NO_2)_0$ between 0.1 and 1.1 F all result in the removal of about 16 % of the original hydrogen by washing. Once $(NO_2)_0$ exceeds 1.1 F, however, the value of L_H due to washing in Na_2CO_3 (aq) begins to rapidly increase. This increase is a consequence of the greater extent of oxidation of the coal which occurs when (NO_2) is increased. It is interesting to note that the values for the carbon loss after the Na_2CO_3 (aq) wash for this set of experiments levels off at approximately 5.5 % after $(NO_2)_0$ exceeds 0.5 F. Thus, values of $(NO_2)_0$ greater than 1.0 F result in the formation of additional Na_2CO_3 (aq) soluble compounds which contain hydrogen but no carbon. The most obvious explanation is that additional H_2O is formed during the two hour NO_2 treatment. This H_2O is trapped in the NO_2-treated coal, but is removed by the Na_2CO_3 (aq) wash.

The treatment of PSOC 276 coal with NO_2 at 20°C in the batch reactor (Runs 47–52) results in the mass corrected hydrogen contents displayed graphically in Figure 4–55. The values for c_H after the NO_2 treatment show an initially rapid

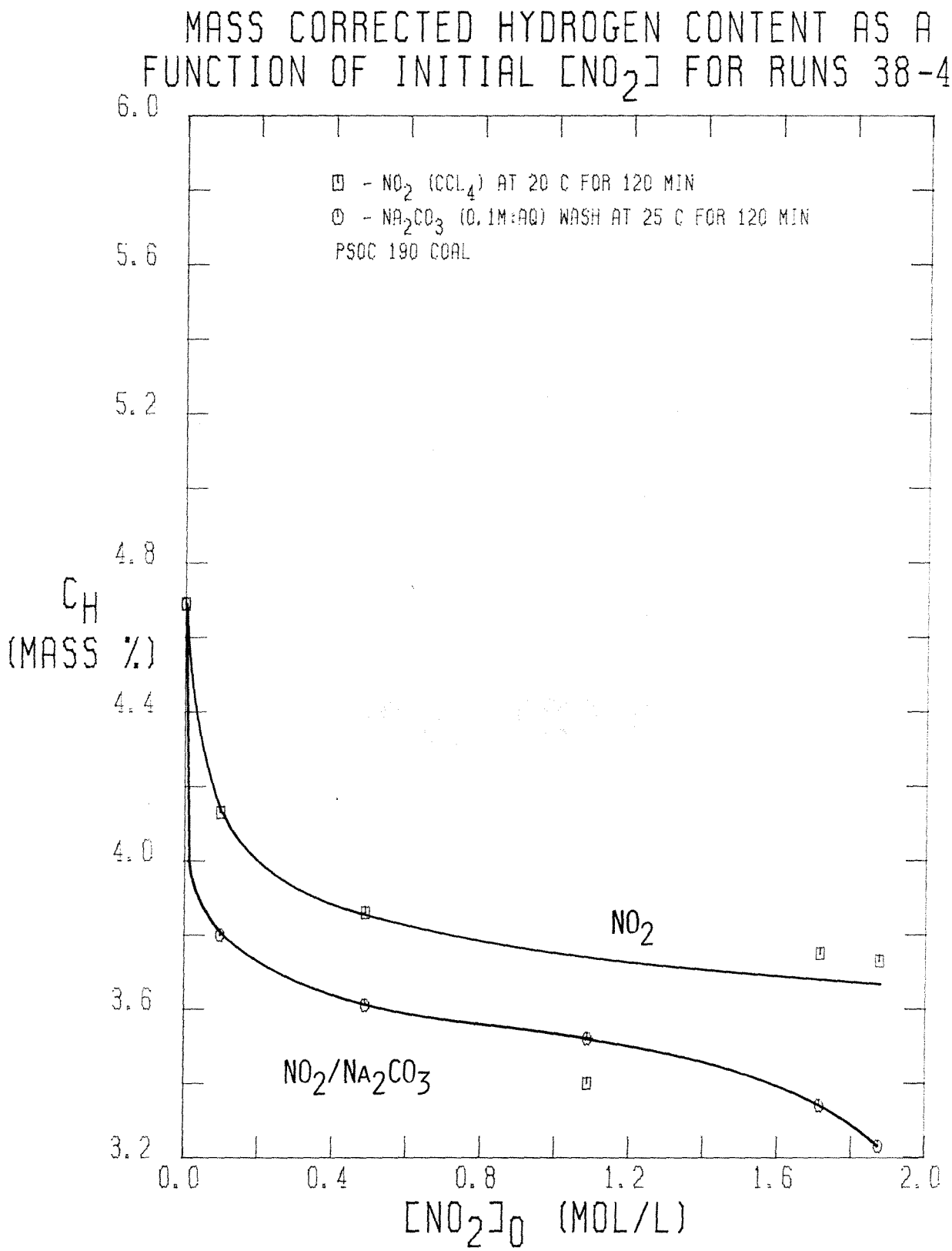
MASS CORRECTED HYDROGEN CONTENT AS A FUNCTION OF INITIAL [NO2] FOR RUNS 38-41
□ - NO2 (CCL4) AT 20 C FOR 120 MIN
○ - NA2CO3 (0.1M:AQ) WASH AT 25 C FOR 120 MIN
PSOC 190 COAL
NO2
NO2/NA2CO3
CH (MASS %)
[NO2]0 (MOL/L)
6.0
5.6
5.2
4.8
4.4
4.0
3.6
3.2
0.0
0.4
0.8
1.2
1.6
2.0

FIGURE 4-53

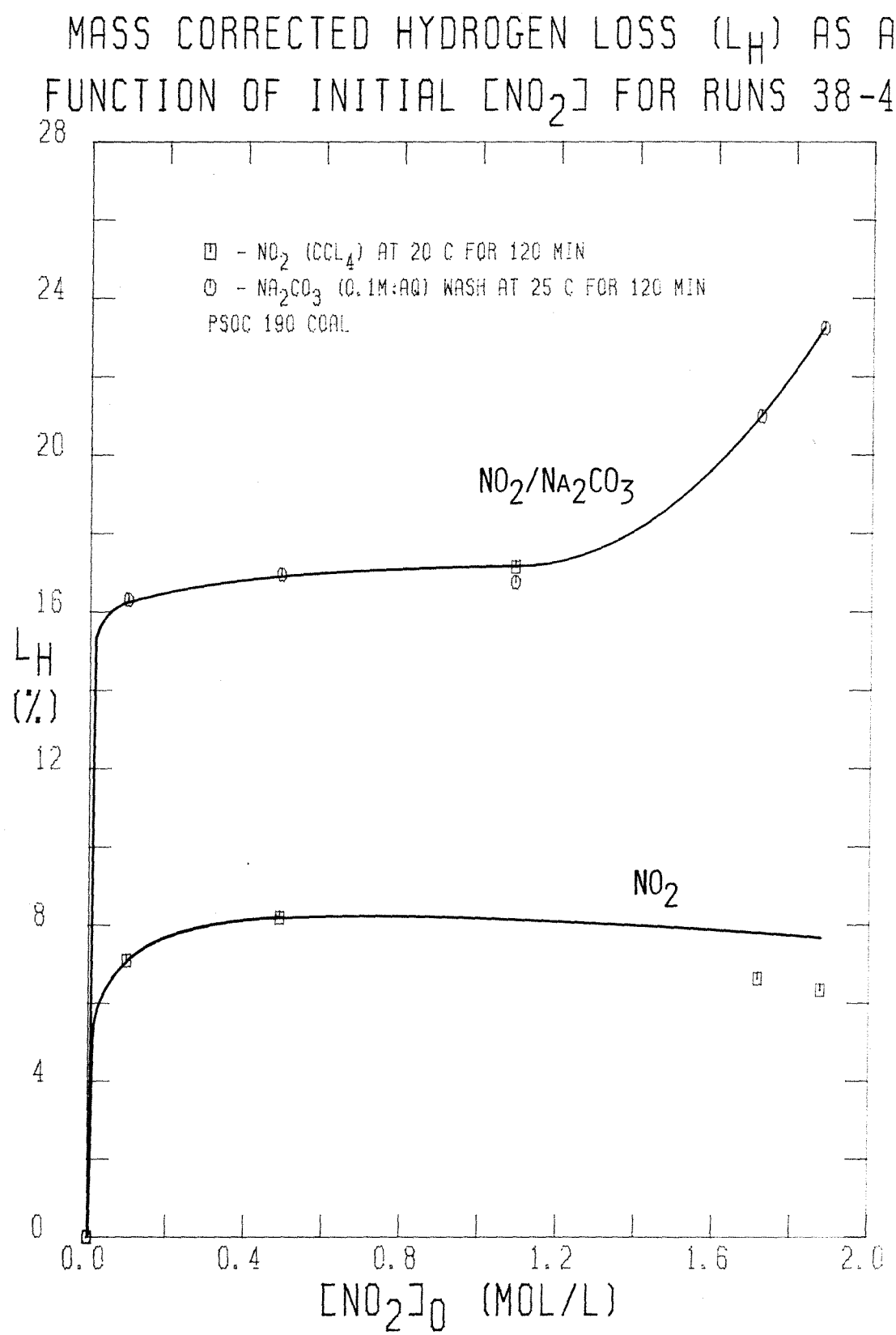
MASS CORRECTED HYDROGEN LOSS (L_H) AS A FUNCTION OF INITIAL $[NO_2]$ FOR RUNS 38-41
□ - NO_2 (CCL_4) AT 20 C FOR 120 MIN
○ - NA_2CO_3 (0.1M:AQ) WASH AT 25 C FOR 120 MIN
PSOC 190 COAL
NO_2/NA_2CO_3
NO_2
L_H (%)
$[NO_2]_0$ (MOL/L)
0
4
8
12
16
20
24
28
0.0
0.4
0.8
1.2
1.6
2.0

FIGURE 4-54

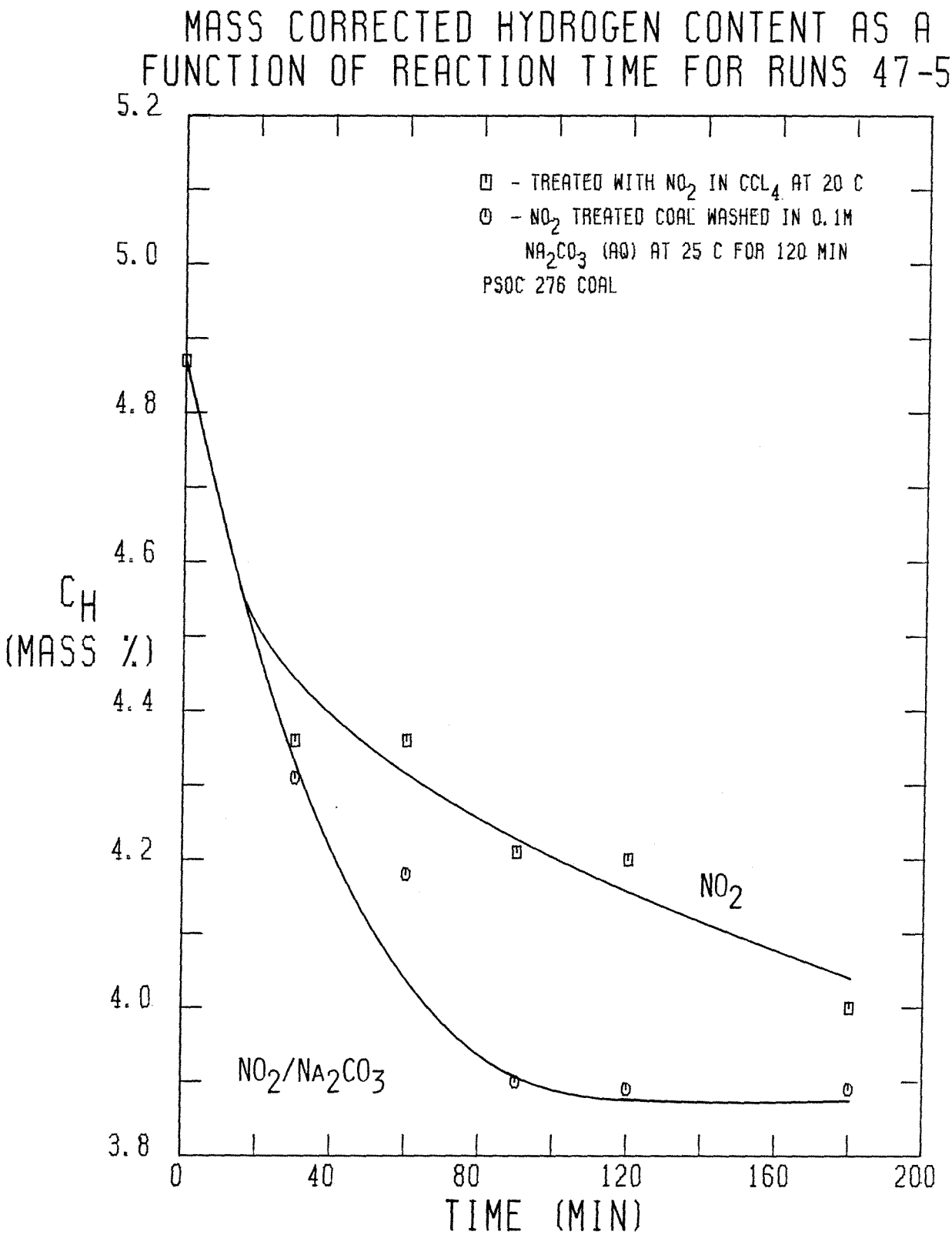
MASS CORRECTED HYDROGEN CONTENT AS A FUNCTION OF REACTION TIME FOR RUNS 47-52
□ - TREATED WITH NO2 IN CCL4 AT 20 C
⊙ - NO2 TREATED COAL WASHED IN 0.1M NA2CO3 (AQ) AT 25 C FOR 120 MIN
PSOC 276 COAL
NO2
NO2/NA2CO3
CH (MASS %)
TIME (MIN)
5.2
5.0
4.8
4.6
4.4
4.2
4.0
3.8
0
40
80
120
160
200

FIGURE 4-55

decline followed by a more gradual decrease thereafter. Washing the NO_2–treated coals in 0.1 M Na_2CO_3 (aq) results in a further reduction in c_H, although c_H seems to level off after 90 minutes of NO_2 exposure. The values of the mass corrected hydrogen loss of the NO_2-treated PSOC 276 coal, L_H, are shown in Figure 4–56. The hydrogen loss during the NO_2 treatment seems to be a linear function of time, reaching a value of about 7 % after 180 minutes. The values of L_H after the Na_2CO_3 (aq) wash, however, indicate that an ultimate hydrogen removal of roughly 14 % occurs at 90 minutes of NO_2 treatment. As with the PSOC 190 coal, the water is trapped in the NO_2-treated PSOC 276 coal. The Na_2CO_3 (aq) wash, however, does not remove the water from the NO_2-treated PSOC 276 coal.

A comparison of the values for c_H of the PSOC 190 and PSOC 276 coals after treatment with NO_2 is shown in Figure 4–57. The figure plainly shows that a much larger drop in the hydrogen content of the PSOC 190 coal occurs during the NO_2 treatment than in the PSOC 276 coal. Furthermore, the rate of decrease in c_H is greater for the PSOC 190 coal than the PSOC 276 coal. A comparison of the respective hydrogen losses, which can be found in Figure 4–58, confirms that the extent and rate of hydrogen removal during the NO_2-coal reaction is much greater for the PSOC 190 than PSOC 276. This difference in hydrogen loss can be attributed to the difference in the pore volumes of the two coals. Based on the nitrogen content data to be discussed in the next section, the accessibility of the hydrogen in the two coals to NO_2 is basically the same. Therefore, the difference in hydrogen loss must be due to the difference in the resistance to mass transfer of the oxidized hydrogen compounds out of the particle.

Figure 4–59 contains, in graphical form, the values of c_H for the two coals which had been treated with NO_2 and subsequently washed in 0.1 M Na_2CO_3 (aq).

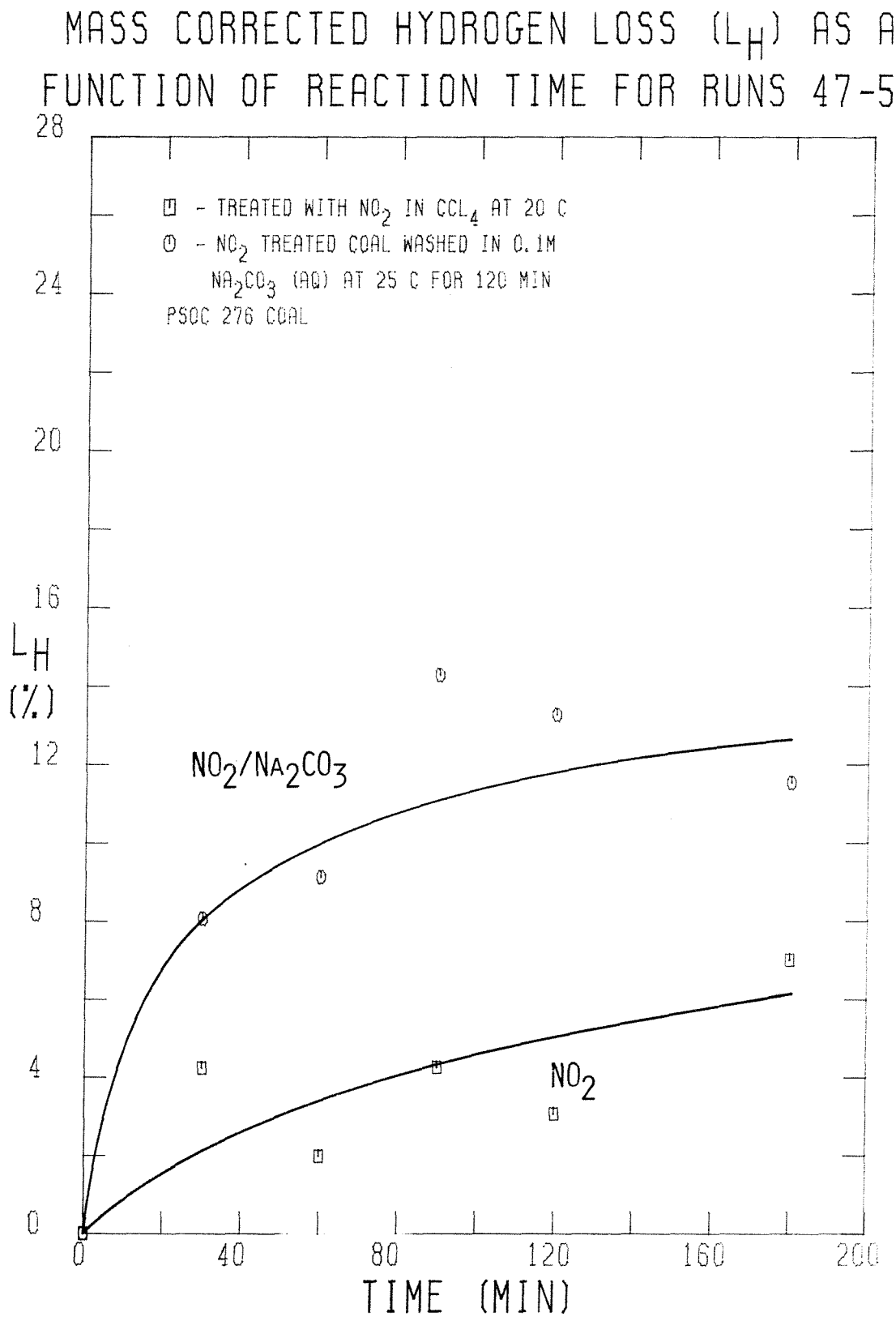
MASS CORRECTED HYDROGEN LOSS (L_H) AS A FUNCTION OF REACTION TIME FOR RUNS 47-52
□ - TREATED WITH NO_2 IN CCL_4 AT 20 C
⊙ - NO_2 TREATED COAL WASHED IN 0.1M NA_2CO_3 (AQ) AT 25 C FOR 120 MIN
PSOC 276 COAL
NO_2/NA_2CO_3
NO_2
L_H (%)
TIME (MIN)
0
4
8
12
16
20
24
28
0
40
80
120
160
200

FIGURE 4-56

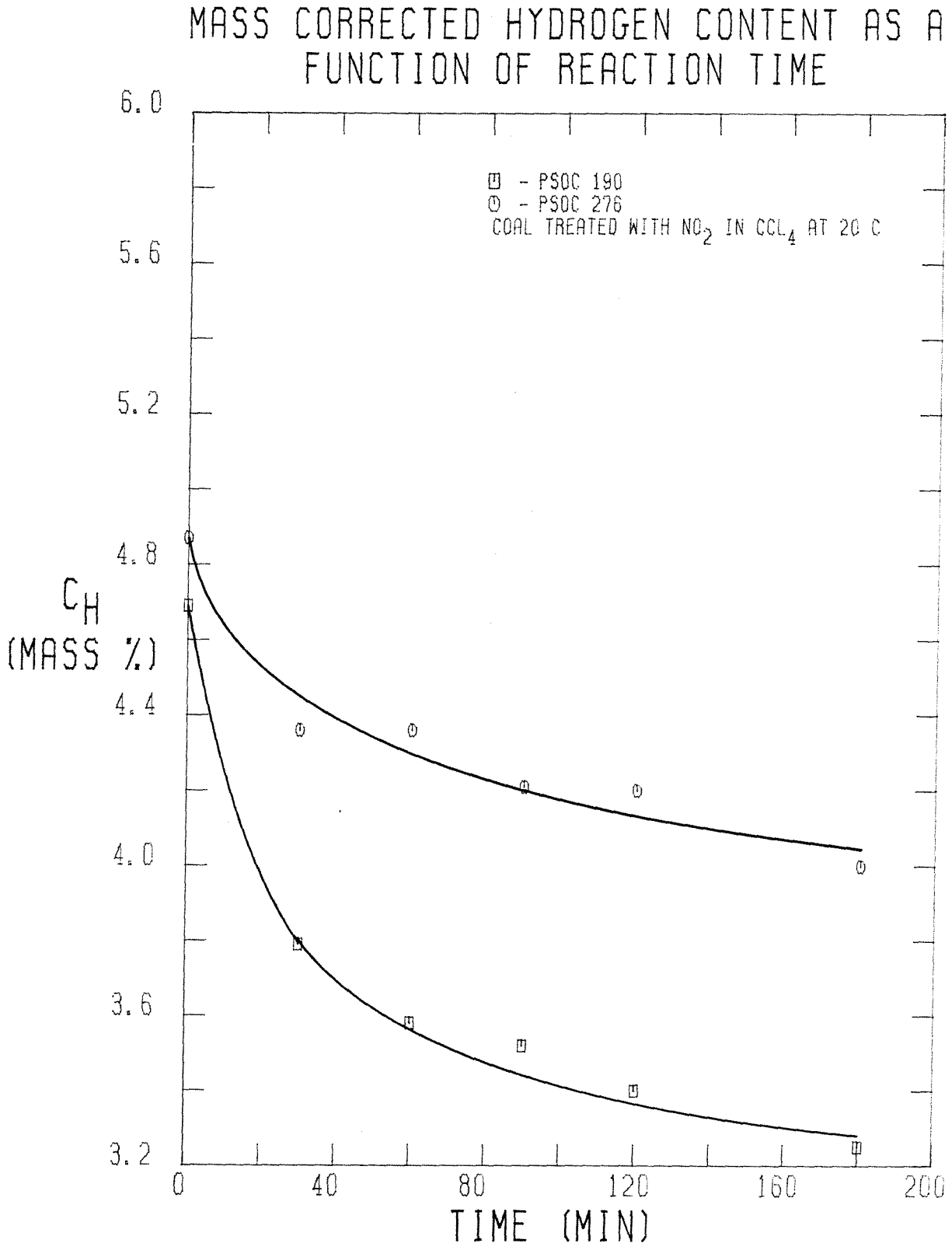
MASS CORRECTED HYDROGEN CONTENT AS A FUNCTION OF REACTION TIME
6.0
5.6
5.2
4.8
4.4
4.0
3.6
3.2
C_H (MASS %)
- PSOC 190
- PSOC 276
COAL TREATED WITH NO_2 IN CCL_4 AT 20 C
0
40
80
120
160
200
TIME (MIN)

FIGURE 4-57

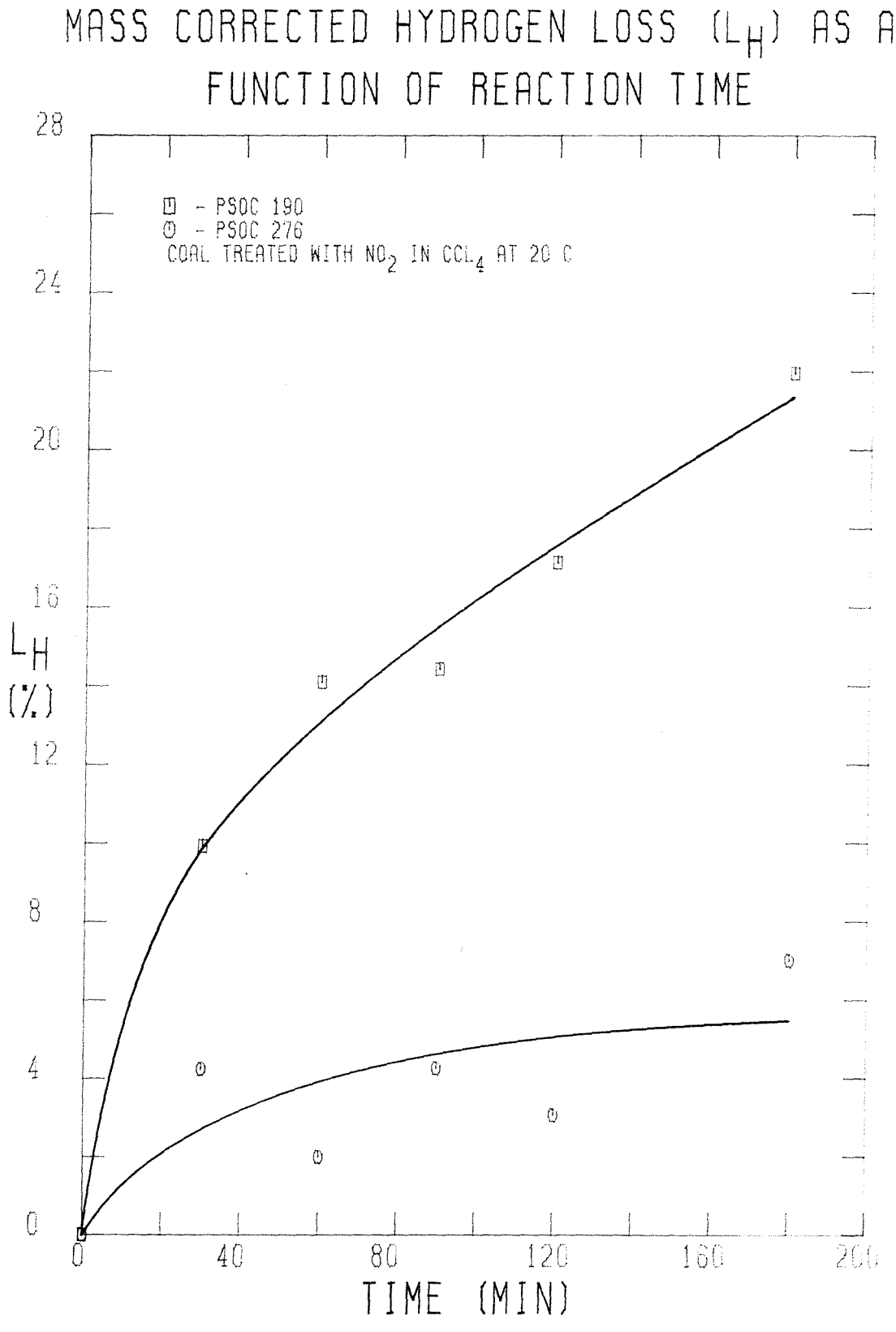
MASS CORRECTED HYDROGEN LOSS (L_H) AS A FUNCTION OF REACTION TIME
□ - PSOC 190
○ - PSOC 276
COAL TREATED WITH NO_2 IN CCL_4 AT 20 C
L_H (%)
28
24
20
16
12
8
4
0
0
40
80
120
160
200
TIME (MIN)

FIGURE 4-58

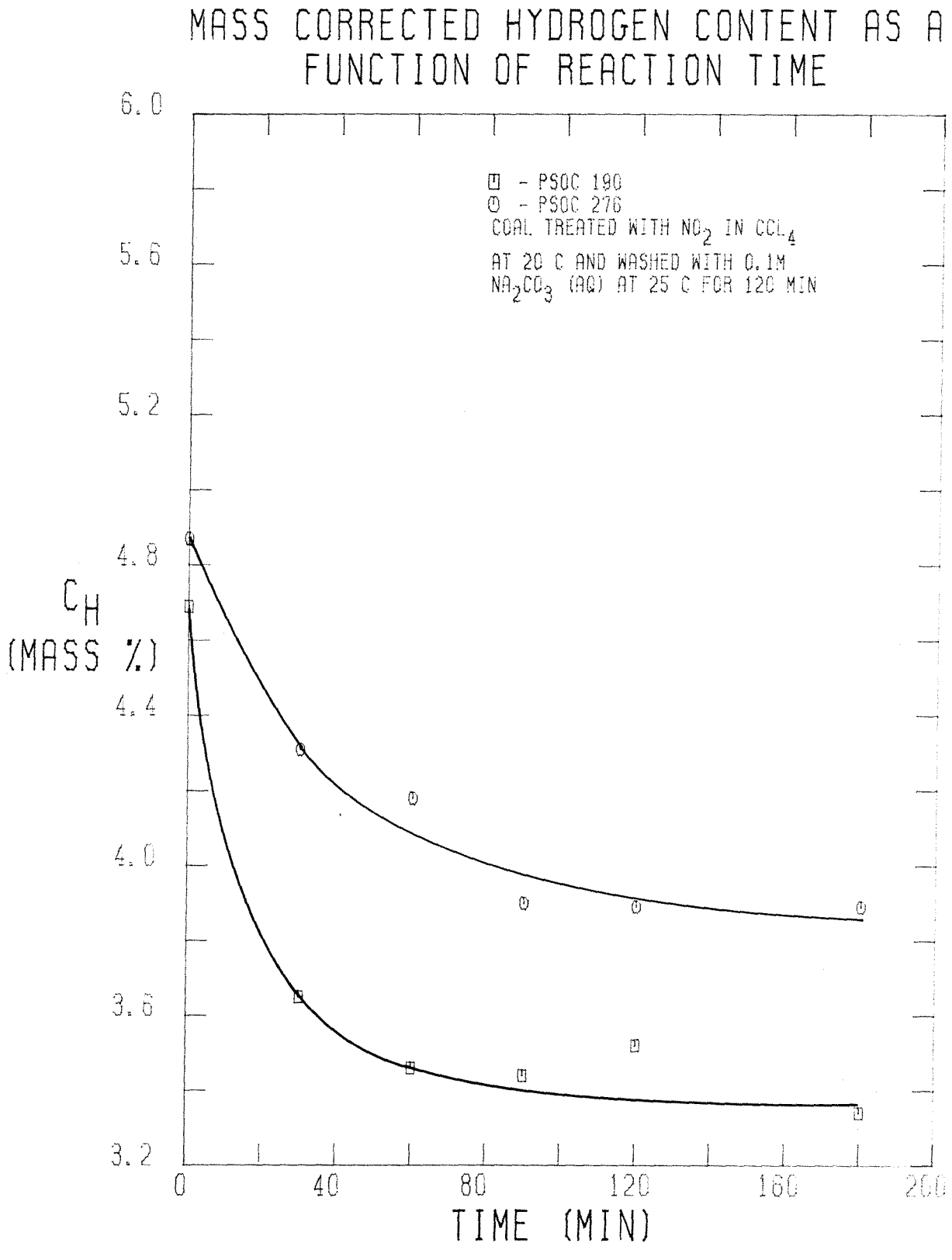
MASS CORRECTED HYDROGEN CONTENT AS A FUNCTION OF REACTION TIME
□ - PSOC 190
○ - PSOC 276
COAL TREATED WITH NO_2 IN CCL_4
AT 20 C AND WASHED WITH 0.1M
NA_2CO_3 (AQ) AT 25 C FOR 120 MIN
C_H (MASS %)
6.0
5.6
5.2
4.8
4.4
4.0
3.6
3.2
0
40
80
120
160
200
TIME (MIN)

FIGURE 4-59

Once again, c_H is lower for the processed PSOC 190 than the processed PSOC 276. Furthermore, the values of c_H for the two coals seem to level off after 90 minutes of NO_2 treatment. The values of the mass corrected hydrogen loss for the processed coals are shown in Figure 4–60. Once again, more hydrogen is removed from the PSOC 190 than from the PSOC 276. The difference in L_H after the wash, however, is not nearly as large as the difference in L_H after the NO_2 treatment. Thus, the Na_2CO_3 (aq) wash removes more soluble coal-derived hydrogen-containing compounds from the PSOC 276 than from the PSOC 190, both of which have been treated with NO_2. It is interesting to note that L_H for the PSOC 190 continues to increase with NO_2–exposure time while L_H for the PSOC 276 reaches a maximum at 90 minutes and then declines. This behavioral difference is caused by the differences in the pore structures of the two coals. For instance, it appears that more extensive oxidation of PSOC 190 does not inhibit the removal of coal-derived products by Na_2CO_3 (aq), while excessive oxidation of PSOC 276 does inhibit such removal. It is interesting to note that the carbon loss results roughly parallel the hydrogen loss results of the coals treated with NO_2 which are then washed with 0.1 M Na_2CO_3 (aq). The difference in the carbon loss ($\approx$ 0.2 %), however, is much less than the difference in the hydrogen loss ($\approx$ 6 to 8 %), which implies that the molar ratio of carbon to hydrogen removal is greater for the treated PSOC 276 than for the treated PSOC 190. For instance, the molar ratio of carbon to hydrogen loss after washing the coal treated with NO_2 for 30 minutes in 0.1 M Na_2CO_3 (aq) is 1.0 to 3.0 for the PSOC 190 and 1.0 to 1.7 for the PSOC 276. After treatment with NO_2 for 180 minutes, the molar ratio of carbon to hydrogen removal for the washed coals is 1.0 to 2.5 for the PSOC 190 and 1.0 to 1.9 for the PSOC 276. It should be noted that both pretreated coals had a molar carbon to hydrogen ratio of 1.21 to 1.00. Therefore, both coals suffer more hydrogen than carbon loss on a molar basis.

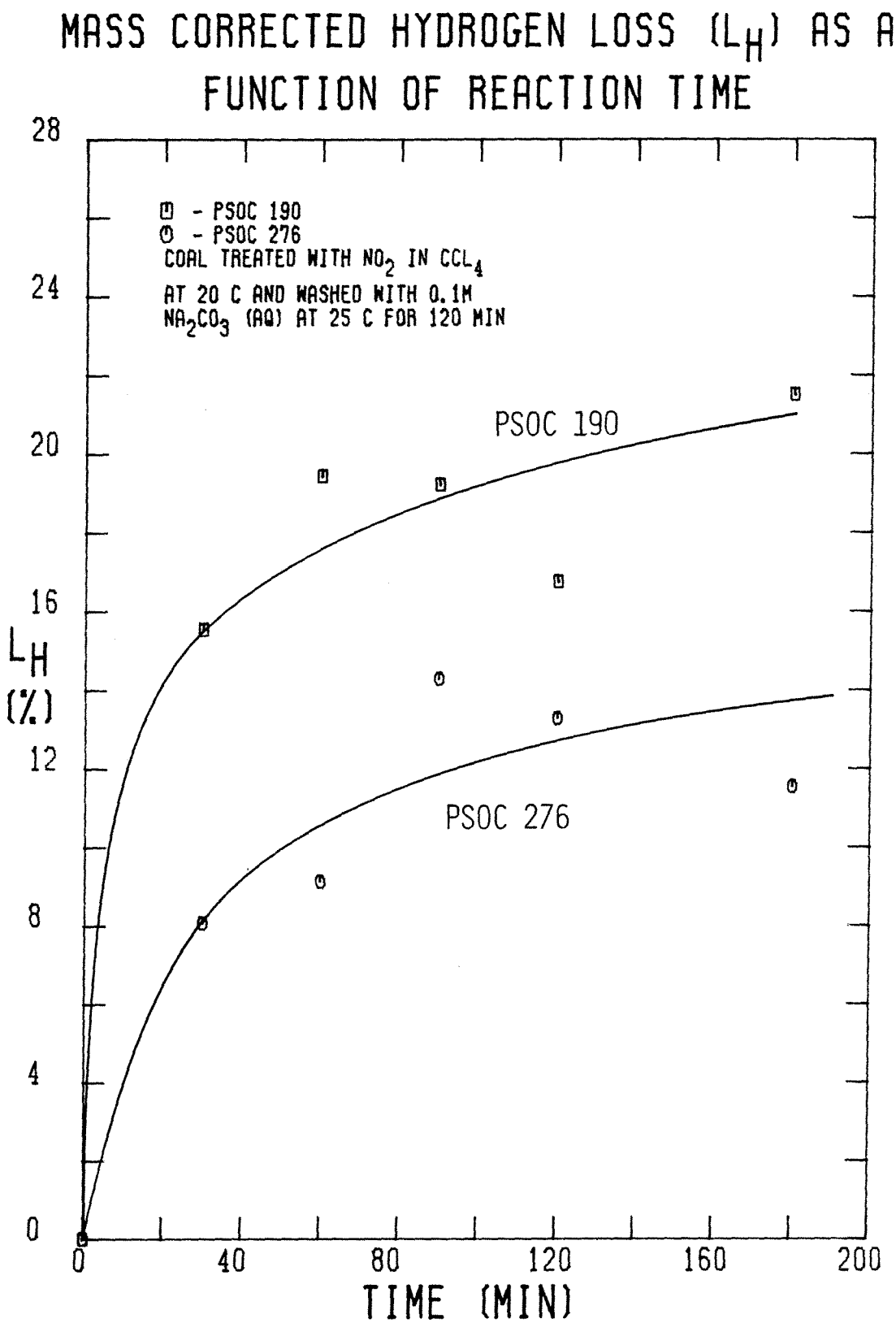
MASS CORRECTED HYDROGEN LOSS (L_H) AS A FUNCTION OF REACTION TIME
□ - PSOC 190
○ - PSOC 276
COAL TREATED WITH NO_2 IN CCL_4
AT 20 C AND WASHED WITH 0.1M
NA_2CO_3 (AQ) AT 25 C FOR 120 MIN
PSOC 190
PSOC 276
L_H (%)
TIME (MIN)
0
4
8
12
16
20
24
28
0
40
80
120
160
200

FIGURE 4-60

On the basis of the discussion of the effect of the various reaction parameters on the fate of the hydrogen in the coal, several general conclusions can be made. For instance, because most of the hydrogen loss during the NO_2 treatment occurs within the first 30 minutes, the hydrogen which is accessible to NO_2 is rapidly attacked. Furthermore, the values of c_H for the PSOC 190 treatment with NO_2 are roughly equal to those of the subsequently washed coals, which implies that the wash removes compounds with the same hydrogen content as the remaining coal. Such is not the case, however, with the processed PSOC 276, mainly because not all of the reacted hydrogen is removed during the NO_2 treatment. Washing the coal in Na_2CO_3 (aq), however, results in the removal of the oxidized hydrogen.

The effect of the NO_2 concentration on the extent and rate of hydrogen removal appears to be minimal. As long as NO_2 is in stoichiometric excess, the hydrogen readily reacts and is ultimately removed, which implies that mass transfer resistances control the extent and rate of the hydrogen loss. The temperature of the NO_2 treatment affects the extent of the hydrogen removal. The fact that the hydrogen loss is greater at 20°C than at 50°C implies that the oxidized hydrogen-containing compounds are more easily trapped in the coal when the NO_2-treatment temperature is increased. On the other hand, as the temperature is lowered from 20 to 0°C, the hydrogen loss decreases as well. In this case, the extent of the oxidation of hydrogen by NO_2 is diminished by the lower rate at 0 than at 20°C. It appears, therefore, that the maximum hydrogen removal during NO_2 treatment occurs at about 20 to 25°C, at which temperature the rate of the NO_2-coal reaction is at its maximum value before the rate of the process which causes the entrapment of the oxidized hydrogen begins to dominate the overall extent of the hydrogen removal.

The most general statement which can be made about the nature of the interaction between NO_2 and the coal hydrogen is that the hydrogen is very susceptible to attack by NO_2. Furthermore, the removal of the oxidized hydrogen depends exclusively on the resistance to mass transfer presented by the pore structure of the coal. Alterations in the pore structure which occur during the NO_2-coal reaction, therefore, affect the extent of subsequent hydrogen removal during the Na_2CO_3 (aq) wash. In general, however, a smaller pore volume in the pretreated coal results in a smaller extent of hydrogen removal during the processing.

4.2.2.4 The Nitrogen Content of the Coal

During the course of the reaction of NO_2 with coal slurried in CCl_4, it is possible that the NO_2 may become chemically and physically incorporated into the solid coal matrix. Fortunately, the extent of such incorporation can be measured by determining the change in nitrogen content of the coal during treatment because the only source of additional nitrogen is NO_2 when CCl_4 is the solvent. When water is used as the solvent, on the other hand, several forms of nitrogen exist in solution, including HNO_3 and HNO_2. Thus, the determination of the relative amounts of nitrogen donated by these species to the coal is quite difficult. Consequently, no systematic nitrogen analyses were made of the coals which were treated with NO_2 in water (Runs 1–20). The following discussion pertains exclusively to the treatment of coal slurried in CCl_4 with NO_2 and subsequently washed in 0.1 M Na_2CO_3 (aq).

The mass corrected nitrogen content, c_N, of the coal samples treated with NO_2 at 25°C in the flow reactor (Runs 21–27) is shown as a function of reaction time in Figure 4–61. The curves for the NO_2-treated coal and the subsequently washed coal both display a smooth unimodal rise. As expected, the wash does remove some of the added nitrogen, but certainly not all of it. The net increase in the nitrogen mass, m_N, of the treated coal relative to the initial mass of the pretreated coal is shown in Figure 4–62 as a function of NO_2-reaction time. The net increase is expressed in terms of grams of nitrogen per 100 grams of the initial pretreated coal. The curves in this figure also show a smooth unimodal rise in the nitrogen content of the treated coal. Furthermore, the curve for the washed coal indicates the removal of about one gram of the nitrogen added to 100 grams of the pretreated coal for all of the NO_2-treatment times even though the total amount of nitrogen added to the coal continues to increase. This constant amount of removal indicates that about one gram of the added nitrogen is

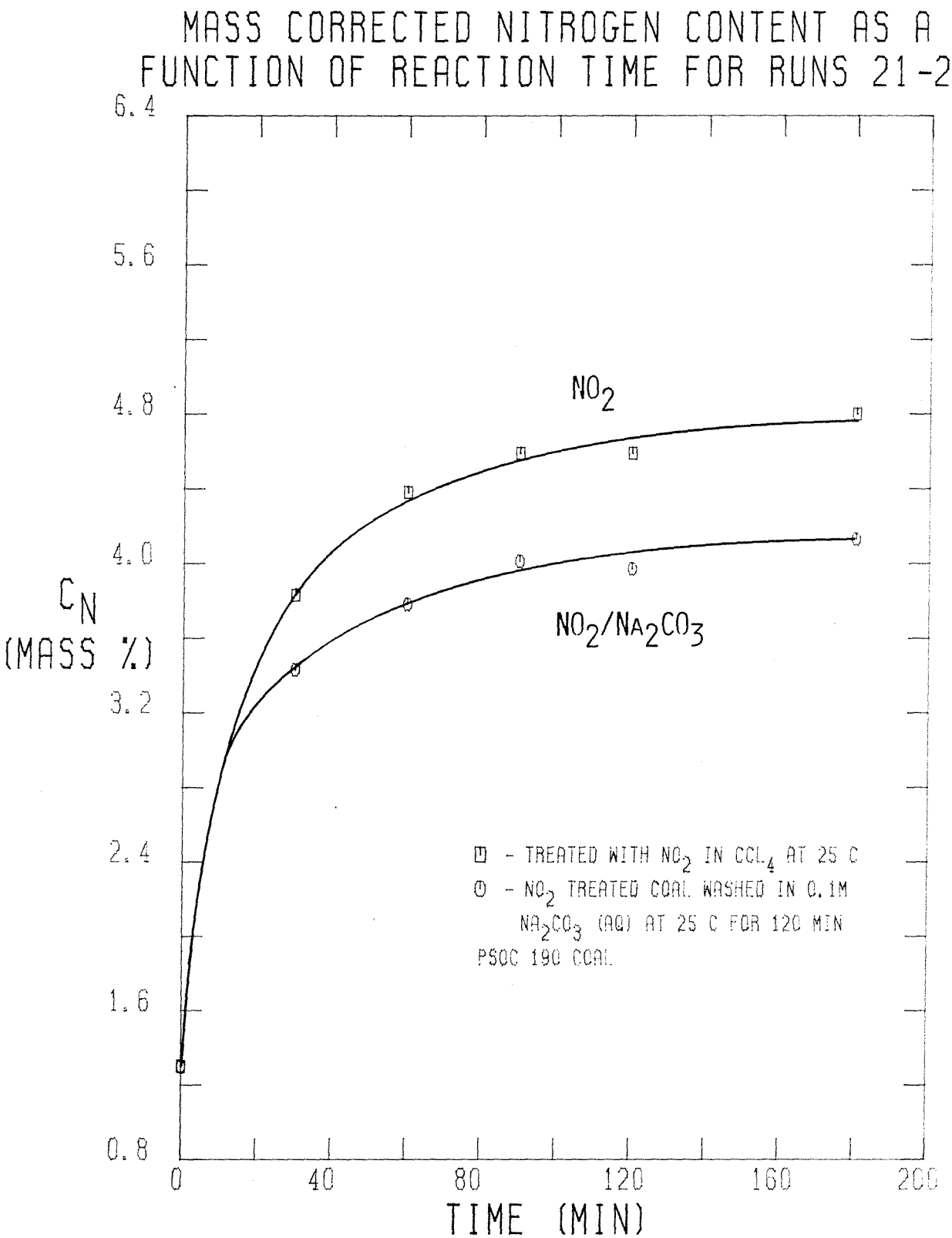
MASS CORRECTED NITROGEN CONTENT AS A FUNCTION OF REACTION TIME FOR RUNS 21-27
6.4
5.6
4.8
4.0
3.2
2.4
1.6
0.8
C_N (MASS %)
NO_2
NO_2/NA_2CO_3
0
40
80
120
160
200
TIME (MIN)
- TREATED WITH NO_2 IN CCL_4 AT 25 C
- NO_2 TREATED COAL WASHED IN 0.1M NA_2CO_3 (AQ) AT 25 C FOR 120 MIN
PSOC 190 COAL

FIGURE 4-61

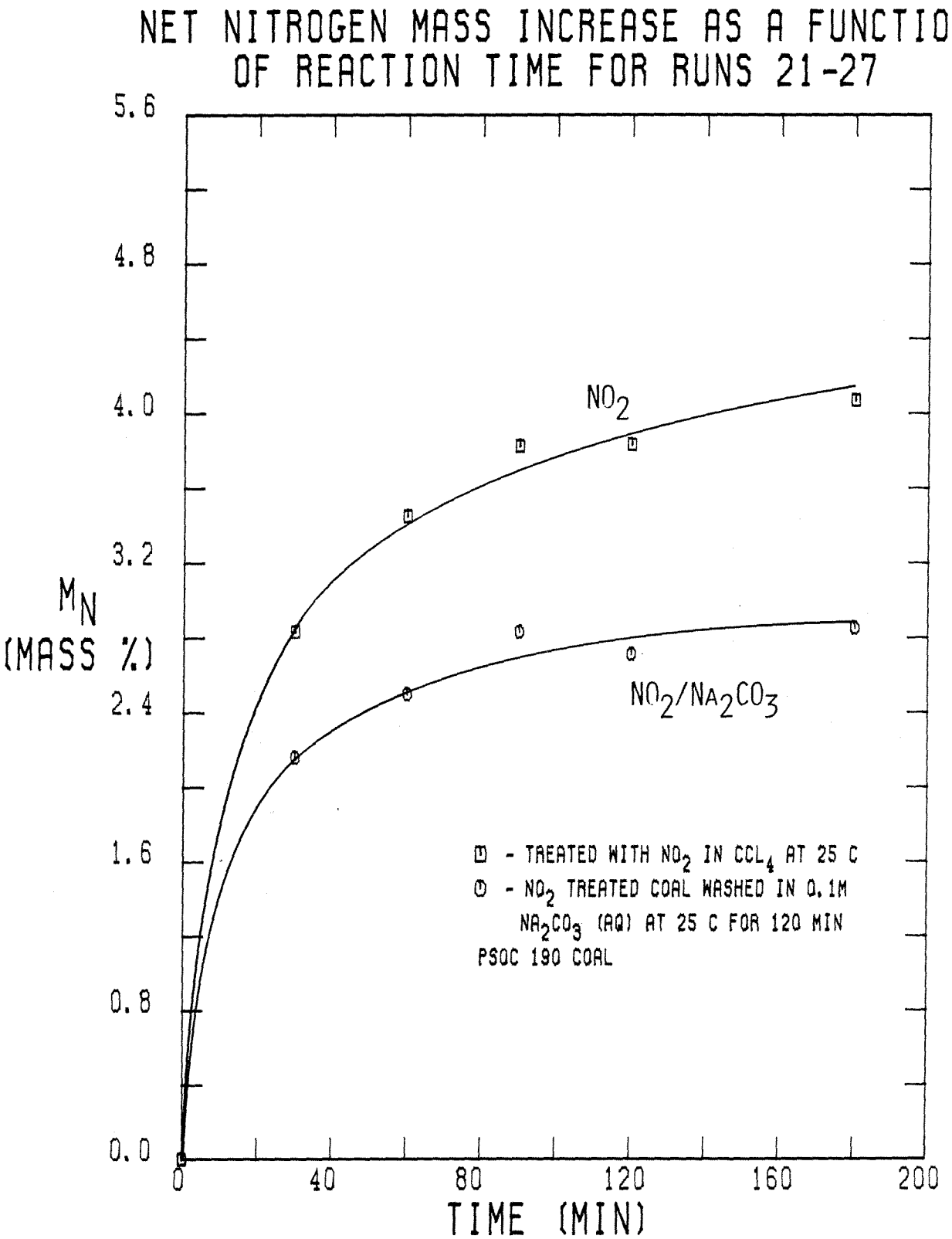
NET NITROGEN MASS INCREASE AS A FUNCTION OF REACTION TIME FOR RUNS 21-27
5.6
4.8
4.0
3.2
2.4
1.6
0.8
0.0
M_N (MASS %)
NO_2
NO_2/NA_2CO_3
□ - TREATED WITH NO_2 IN CCL_4 AT 25 C
① - NO_2 TREATED COAL WASHED IN 0.1M NA_2CO_3 (AQ) AT 25 C FOR 120 MIN
PSOC 190 COAL
0
40
80
120
160
200
TIME (MIN)

FIGURE 4-62

easily displaced during the Na_2CO_3 (aq) wash. Furthermore, the NO_2-coal process which accounts for this portion of the added nitrogen is quite rapid. It is likely that this portion is simply NO_2 adsorbed on the coal surface and possibly trapped in the pores. Once the coal is washed in 0.1 M Na_2CO_3 (aq), however, the adsorbed NO_2 would be displaced by the more strongly adsorbed aqueous species. The displaced NO_2 can then react quickly with the Na_2CO_3 (aq) to form $NaNO_2$ and $NaNO_3$:

$$2\ NO_2\ +\ Na_2CO_3\ \rightarrow\ NaNO_2\ +\ NaNO_3\ +\ CO_2\ .$$

Furthermore, if NO_2 is trapped in the pore structure, treatment with aqueous Na_2CO_3 may dilate the pore structure enough to allow the trapped NO_2 to be displaced as well.

Some useful kinetic results can be extracted from the data as it is presented in Figure 4–62. If it is assumed that the rate of nitrogen uptake by the coal depends only on the availability of sites in the coal, the following rate expression results:

$$\frac{dm_N^s}{dt} = -k\ m_N^s\ , \quad \text{where} \tag{4.2.13}$$

m_N^s = the residual capacity in the coal for nitrogen uptake (gN/ 100g initial coal), and

k = the first order rate constant

In order to use equation (4.2.13), the initial value for m_N^s is needed. Because the top curve in Figure 4–62 seems to asymptotically approach 4.10 mass % N, which implies the exhaustion of sites, this would seem a good first guess for the initial value of m_N^s, m_{N0}^s. In general, the integration of equation (4.2.13) results in

$$\ln \frac{m_N^s}{m_{N0}^s} = -kt \qquad (4.2.14)$$

Furthermore, m_N^s is equal to $m_{N0}^s - m_N$, where m_N is the net increase in the mass of nitrogen in the coal, that is, the values plotted in Figure 4–62. Thus, equation (4.2.14) can be rewritten as

$$\ln(m_{N0}^s - m_N) = \ln m_{N0}^s - kt. \qquad (4.2.15)$$

Therefore, if the data are converted to the form of $\ln(m_{N0}^s - m_N)$ vs. t and fitted using a least squares procedure, the slope will be simply $-k$. The value of m_{N0}^s can be varied until the least squares fit gives an intercept which equals $\ln m_{N0}^s$. The closeness of the fit is given by the correlation coefficient, r^2. A perfect fit of the data to a straight line gives a value of r^2 of unity. A range of values for m_{N0}^s from 4.08 to 4.30 were used, and the results are shown in Table 4–1. It is immediately obvious that the convergence between the guessed and calculated values of m_{N0}^s is very rapid. An examination of Table 4–1 reveals that the best agreement is obtained using a value of 4.082 for m_{N0}^s, which yields a value of 0.0302 min^{-1} for k. It should be noted, however, that the best value of r^2 is obtained using a value of 4.11 for m_{N0}^s, which gives a value of k of 0.0241 min^{-1}. Further examination of Table 4–1 discloses that while the range of values chosen for m_{N0}^s does not strongly affect r^2, the variation in k is quite significant. Nevertheless, the value obtained for k should be a good estimate.

It should be noted that if the rate depended on the concentration of NO_2, the rate expression would be

$$\frac{dm_N^s}{dt} = -k\, m_N^s (NO_2)^n, \quad \text{where} \qquad (4.2.16)$$

k = the rate constant (l^n–mol^{-n}–min^{-1}),

(NO_2) = the NO_2 concentration in the liquid phase (mol–l^{-1}), and

TABLE 4-1

Results of the Least-Squares Fit of the Nitrogen Uptake Data for Runs 21-27 to Equation (4.2.15) Using Various Values of m_{N0}^{S}

m_{N0}^{S} (g N/100 g untreated coal)		r^2	k (min^{-1})
Chosen	Calculated		
4.08	4.23	0.9457	0.0312
4.082	4.06	0.9512	0.0302
4.09	3.65	0.9635	0.0276
4.095	3.50	0.9670	0.0265
4.10	3.38	0.9689	0.0255
4.11	3.21	0.9697	0.0241
4.12	3.10	0.9683	0.0230
4.15	2.90	0.9587	0.0206
4.30	2.70	0.9034	0.0152

n = the order of the NO_2 dependence.

Because (NO_2) is known as a function of time, the integration of (4.2.16) yields

$$\ln \frac{m_N^s}{m_{N0}^s} = -k \int_0^t (NO_2)^n \, dt \ , \qquad (4.2.17)$$

where the integration is performed numerically. The best least squares fit of the data for n=1 gives a value of r^2=0.9250 for m_{N0}^s=4.08 and a value for k of 0.00706 l–mol^{-1}–min^{-1}. For the case where n=0.5, the best value for r^2 is 0.9458 when m_{N0}^s=4.08. The corresponding value for k is 0.0159 l$^{0.5}$–mol$^{-0.5}$–min^{-1}. Furthermore, as n is increased, the best value for r^2 decreases. Therefore, the best fit occurs when n=0, which implies that the rate of nitrogen uptake does not depend on (NO_2). This conclusion is consistent with the results obtained with the (NO_2) data, namely that the specific rate of the coal-NO_2 reaction is independent of (NO_2). This result is not surprising because the amount of NO_2 in the flow reactor is rapidly in excess.

The values of the mass corrected nitrogen content of the coal samples treated with NO_2 at 20°C in the batch reactor and subsequently washed in 0.1 M Na_2CO_3 (aq) (Runs 33–37) are displayed graphically in Figure 4–63. The curves clearly demonstrate that nitrogen is quickly assimilated by the coal, with over 85 % of the maximum value of c_N attained within 30 minutes. Once again, the curve corresponding to the washed coal indicates that only a small portion of the added nitrogen is removed by the wash in 0.1 M Na_2CO_3 (aq). The net increase in the mass of nitrogen per 100 grams of initial coal is shown as a function of NO_2-treatment time in Figure 4–64. In general, the curves show a smooth unimodal rise. The Na_2CO_3 (aq) wash removes between 15 and 21 % of the added nitrogen, except at t = 180 minutes, when only 10 % is removed. However, the value of c_N at t = 180 minutes for the NO_2-treated coal appears to be low, which would account for the relatively low removal of added nitrogen.

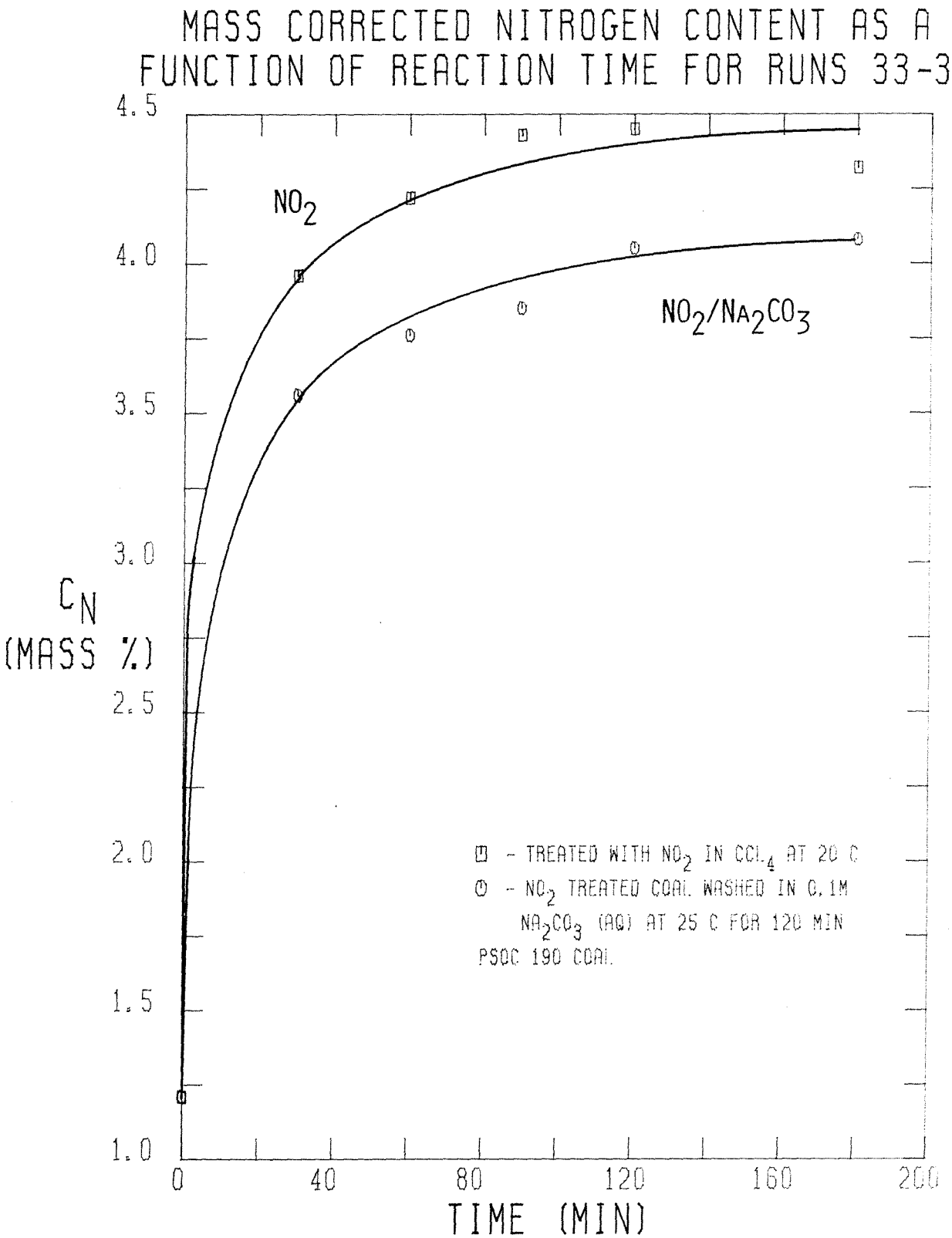
MASS CORRECTED NITROGEN CONTENT AS A FUNCTION OF REACTION TIME FOR RUNS 33-37
4.5
4.0
3.5
3.0
2.5
2.0
1.5
1.0
C_N (MASS %)
NO_2
NO_2/NA_2CO_3
0
40
80
120
160
200
TIME (MIN)
- TREATED WITH NO_2 IN CCL_4 AT 20 C
- NO_2 TREATED COAL WASHED IN 0.1M NA_2CO_3 (AQ) AT 25 C FOR 120 MIN
PSOC 190 COAL

FIGURE 4-63

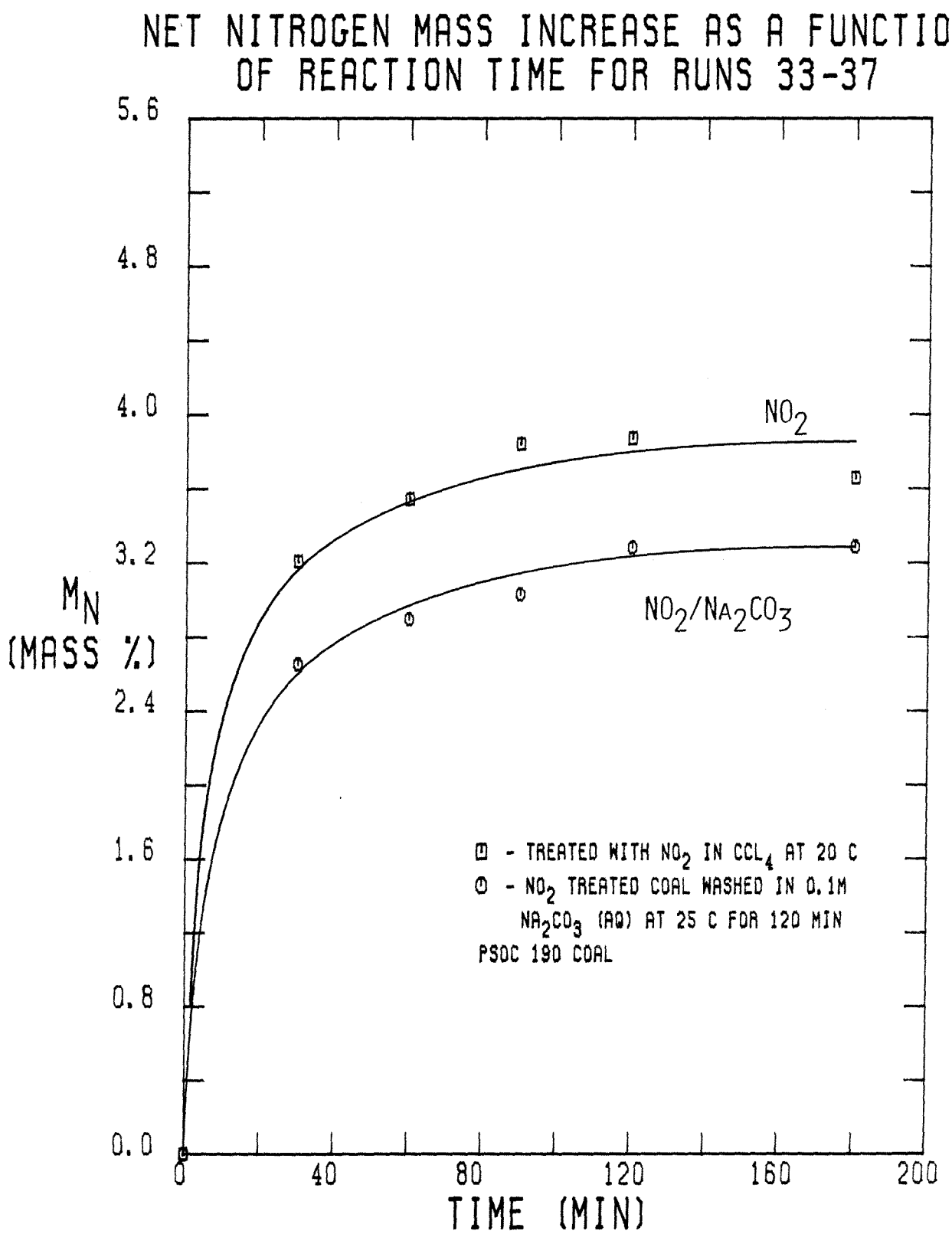
NET NITROGEN MASS INCREASE AS A FUNCTION OF REACTION TIME FOR RUNS 33-37
5.6
4.8
4.0
3.2
2.4
1.6
0.8
0.0
M_N (MASS %)
0
40
80
120
160
200
TIME (MIN)
NO_2
NO_2/Na_2CO_3
- TREATED WITH NO_2 IN CCL_4 AT 20 C
- NO_2 TREATED COAL WASHED IN 0.1M NA_2CO_3 (AQ) AT 25 C FOR 120 MIN
PSOC 190 COAL

FIGURE 4-64

Because the removal is essentially constant, the rate of the process which accounts for the uptake of permanent nitrogen is essentially equal to the rate of the process which accounts for the uptake of nitrogen which is removed by the wash. This conclusion is consistent with the notion that the features of the coal which account for the uptake of the easily displaced nitrogen are themselves a consequence of the NO_2-coal reaction. That is, the NO_2 adsorbed on the surface of the coal, which is displaced by the wash, is held by polar oxygen atoms which are themselves introduced into the coal as a result of the NO_2-coal reaction.

If the procedure adopted for the previous set of runs for obtaining kinetic rate constants is applied to this set of runs, the results are quite ambiguous. The value of m_{N0}^s which gives the best correlation of the data and the resulting rate constants are:

	m_{N0}^s (g N/100 g coal)			
n	Chosen	Calculated	r^2	k
0	3.89	3.90	0.9842	0.0483 min^{-1}
0.5	3.89	3.92	0.9847	0.0519 $l^{0.5}$–$mol^{-0.5}$–min^{-1}
1	3.90	3.90	0.9850	0.0550 l–mol^{-1}–min^{-1}

It should be noted that the data point for t = 180 minutes was discarded because it represented a decrease in m_N from t = 120 minutes, an unlikely possibility. An examination of the values given above reveals that all choices of n yield the same value for r^2, although they yield different values for k. This puzzling trend is readily explained, however, because both $\int (NO_2)^{0.5} dt$ and $\int (NO_2) dt$ are themselves linear functions of t with correlation coefficients of 0.9996 and 0.9984, respectively. Therefore, the inclusion of a rate dependence on $(NO_2)^n$ only serves to alter the time scale. Consequently, a determination of the rate dependence is not possible in this set of runs.. Since the previous set of runs as well as the (NO_2) data indicate that the specific rate of nitrogen uptake

is independent of (NO_2), however, it is probably true in this case as well. Even though (NO_2) is only in the range from 0.7 to 1.1 F in this set and rose uniformly from 0 to 8 F in the previous set, the NO_2 is still in excess in both sets. Therefore, a dependence of the rate on (NO_2) would be expected to be weak at best.

Figure 4–65 contains the values of the mass corrected nitrogen content of the coal treated with NO_2 at 0°C and subsequently washed in 0.1 M Na_2CO_3 (aq) (Runs 42–46) in graphical form. Once again, both curves show a smooth unimodal rise. Furthermore, the wash removes a small portion of the added nitrogen. The net increase in the nitrogen mass of the processed coal is shown in Figure 4–66 as a function of NO_2-exposure time. The shape of the loci in this figure are the same as those in the previous figure, which implies that much of the mass gain occurs as a consequence of the same process which accounts for the uptake of nitrogen by the coal. Just as in the previous set of experiments, about 17 to 21 % of the total added nitrogen mass is removed by the Na_2CO_3 (aq) wash, even though the amount of added nitrogen is about 15 % less at 0°C than at 20°C. The fact that the same proportion of the added nitrogen is removed provides further evidence in support of the notion that the amount of nitrogen eventually displaced by aqueous Na_2CO_3 is proportional to the amount of added nitrogen which remains after the wash. Consequently, the features introduced into the coal which account for the uptake of the displaced nitrogen result from the uptake of the nitrogen which remains after the wash.

An analysis of the kinetic data for this set of experiments using the procedure discussed earlier provides rate constants which can be compared with those of the previous set of experiments. Furthermore, the problem which occurred in the previous set regarding the inability to determine the dependence of the rate on (NO_2) occurs in this set as well. For instance, if n in equation (4.2.17) is zero, the data should be correlated in the form of $\ln \frac{m_N^s}{m_{N0}^s}$ vs. t. If

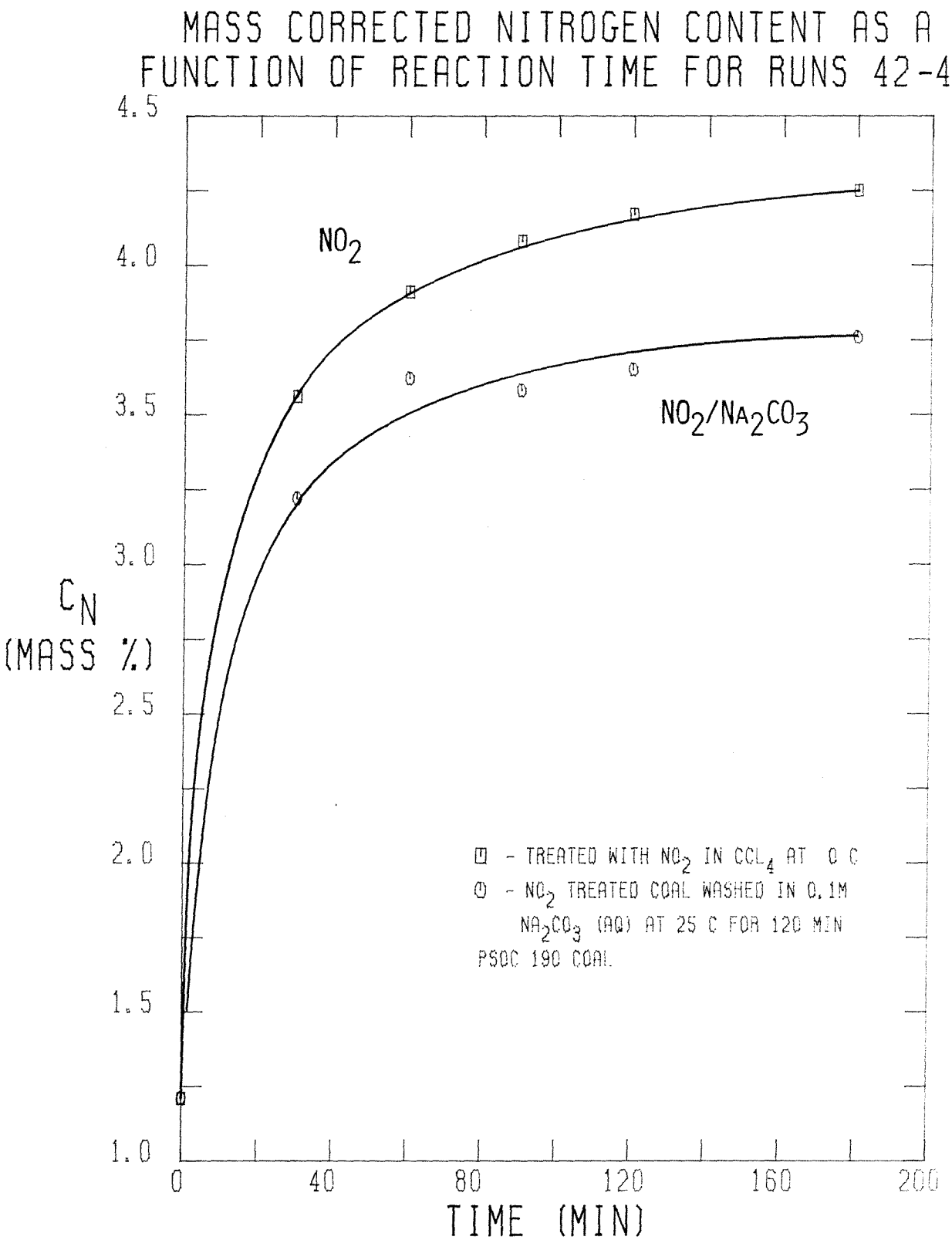
MASS CORRECTED NITROGEN CONTENT AS A FUNCTION OF REACTION TIME FOR RUNS 42-46
4.5
4.0
3.5
3.0
2.5
2.0
1.5
1.0
C_N (MASS %)
NO_2
NO_2/NA_2CO_3
0
40
80
120
160
200
TIME (MIN)
- TREATED WITH NO_2 IN CCL_4 AT 0 C
- NO_2 TREATED COAL WASHED IN 0.1M NA_2CO_3 (AQ) AT 25 C FOR 120 MIN
PSOC 190 COAL

FIGURE 4-65

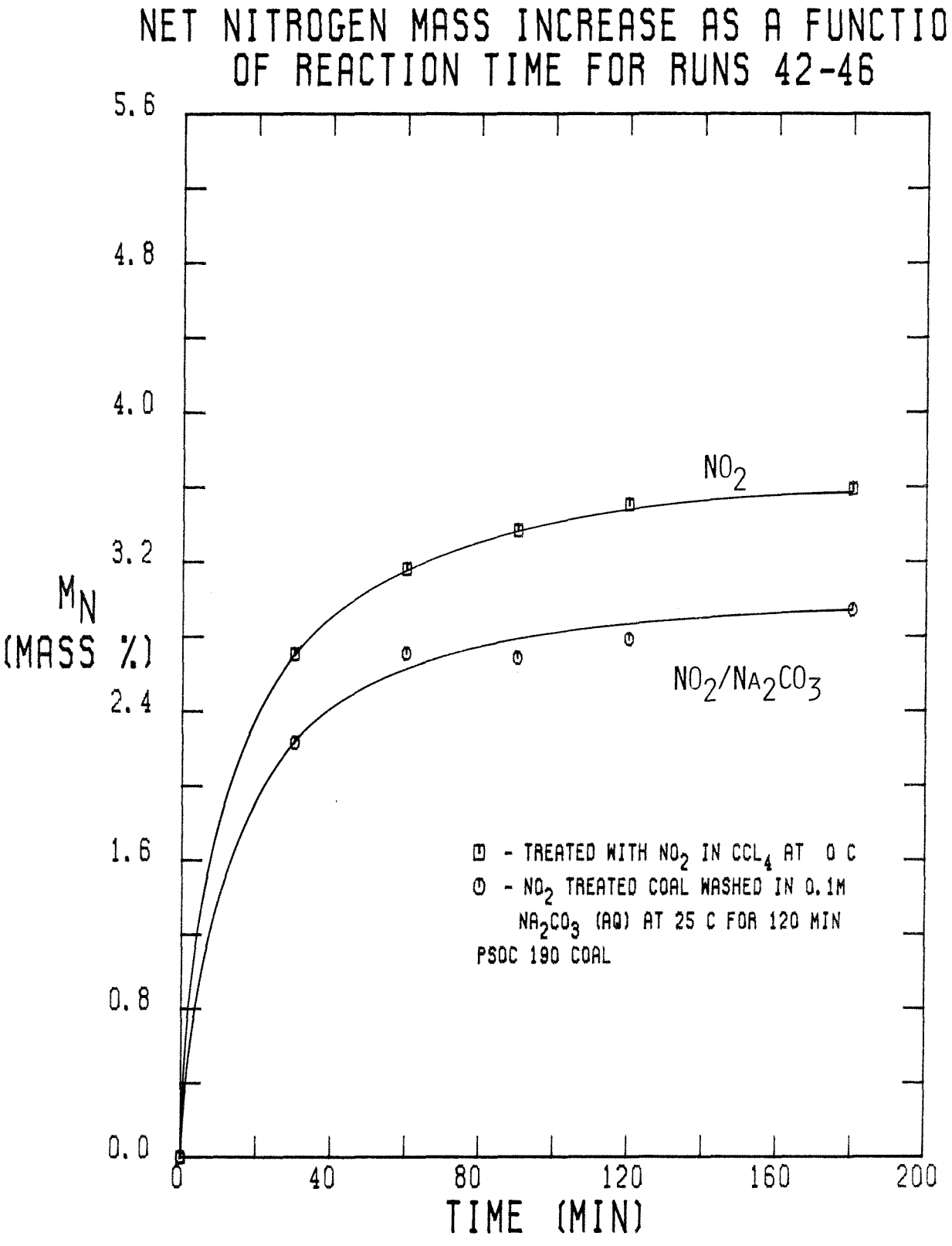
NET NITROGEN MASS INCREASE AS A FUNCTION OF REACTION TIME FOR RUNS 42-46
5.6
4.8
4.0
3.2
2.4
1.6
0.8
0.0
M_N (MASS %)
0
40
80
120
160
200
TIME (MIN)
NO_2
NO_2/NA_2CO_3
- TREATED WITH NO_2 IN CCL_4 AT 0 C
- NO_2 TREATED COAL WASHED IN 0.1M NA_2CO_3 (AQ) AT 25 C FOR 120 MIN
PSOC 190 COAL

FIGURE 4-66

n is equal to unity, then the data should be correlated in the form of $\ln \frac{m_N^s}{m_{N0}^s}$ vs. $\int_0^t (NO_2)\, dt$. A least squares fit of t vs. $\int_0^t (NO_2)\, dt$ yields a value for the correlation coefficient of 0.9990. The fit of t vs. $\int_0^t (NO_2)^{0.5}\, dt$ yields a value for r^2 of 0.9998 as well. The results of the fit of the data from this set are:

	m_{N0}^s (g N/100 g coal)			
n	Chosen	Calculated	r^2	k
0	3.60	3.58	0.9730	0.0342 min^{-1}
0.5	3.60	3.62	0.9754	0.0380 $l^{0.5}$–$mol^{-0.5}$–min^{-1}
1	3.60	3.58	0.9802	0.0415 l–mol^{-1}–min^{-1}

The values for k given here are about 30 % lower than those from the previous set, which indicates an important temperature effect. It is also interesting to note that while the best value for m_{N0}^s at 20°C is 3.90, at 0°C the best value is 3.60, which implies that the initial capacity of the coal for nitrogen uptake is temperature dependent. Indeed, the curves for m_N at the two temperatures definitely indicate different limiting values for m_N of roughly 3.9 and 3.6 at 20 and 0°C respectively. The difference cannot be due to the thermal contraction of the coal because it has been determined that coal generally contracts in volume by only 4 % when the temperature is lowered from 25°C to -196°C.[4] The only apparent explanation is that a small fraction (10 %) of the capacity which was available for nitrogen uptake at 20°C is no longer available at 0°C due to energy requirements.

The mass corrected nitrogen contents of the NO_2-treated coals are shown as functions of NO_2-exposure time and temperature in Figure 4–67. Included in this figure are the data from the NO_2 treatment at 50°C which have yet to be discussed. The data from the runs at 20°C and 0°C have been discussed above. When these curves are considered together, the effect of the temperature can be

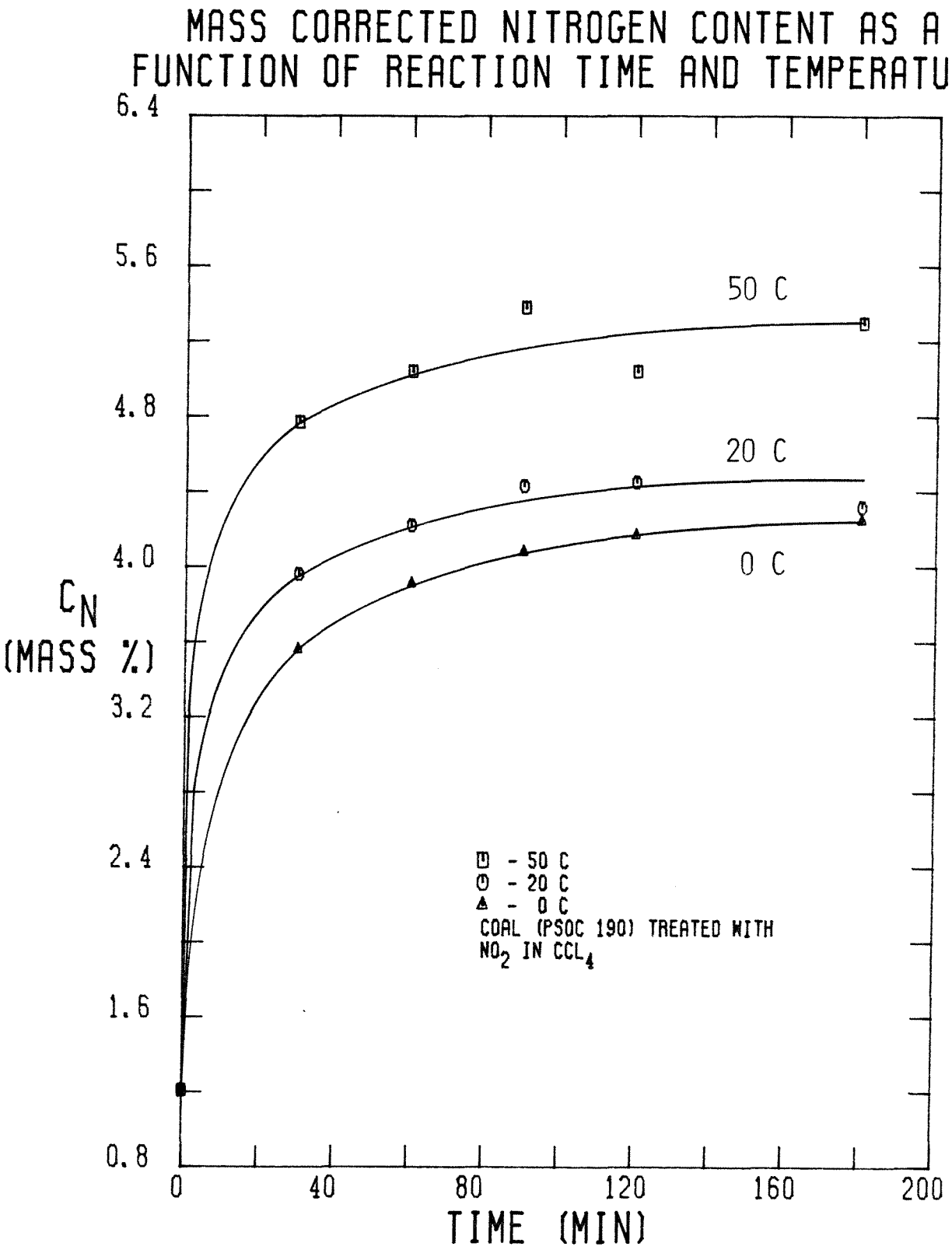
MASS CORRECTED NITROGEN CONTENT AS A FUNCTION OF REACTION TIME AND TEMPERATURE
6.4
5.6
4.8
4.0
3.2
2.4
1.6
0.8
C_N (MASS %)
50 C
20 C
0 C
□ - 50 C
○ - 20 C
△ - 0 C
COAL (PSOC 190) TREATED WITH NO_2 IN CCL_4
0
40
80
120
160
200
TIME (MIN)

FIGURE 4-67

plainly seen. As mentioned above, not only does c_N increase to a greater degree as the temperature is increased, but the limiting value of c_N as the exposure time approaches infinity rises with the temperature as well. Figure 4–68 contains the net increase in the mass of nitrogen of the NO_2-treated coal as a function of NO_2-exposure time and temperature. The curves in this figure have the same smooth unimodal shape as in the previous figure.

It should be noted that the apparent fluctuation in the values of m_N for the 50°C treatment at 90 and 120 minutes leads to two possible interpretations of the data when attempting to obtain kinetic information. One interpretation is given by the manner in which the 50°C curve is drawn in Figure 4–68, that is, it is assumed that m_N smoothly rises from 60 to 180 minutes with the points at 90 and 120 minutes significantly removed from the curve. Because the runs performed at 50°C were conducted in the flow reactor, (NO_2) was essentially constant at 1.18 F throughout the course of the reaction. Therefore, the dependence of the rate on (NO_2) cannot be determined, just as in the runs done at 20 and 0°C. If the smoothed values of m_N are used at 90 and 120 minutes, the best value for m^s_{N0} at 50°C is 5.27 (g N/100 g initial coal) which yields a least squares fit value for m^s_{N0} of 5.32 (g N/100 g initial coal). The corresponding value for k is 0.0376 min^{-1} and the correlation coefficient is 0.9404. Thus, the values of k at the various temperatures are:

T(°C)	0	20	50
k(min^{-1})	0.0342	0.0483	0.0376

These results indicate a very unusual temperature effect which cannot be explained. The second interpretation of the 50°C data, however, alters this trend somewhat. Recalling that the nitrogen uptake reaction appeared to be complete within 120 minutes at 20°C, it would not be unreasonable to expect that the reaction would be complete within an even shorter amount of time at 50°C. If

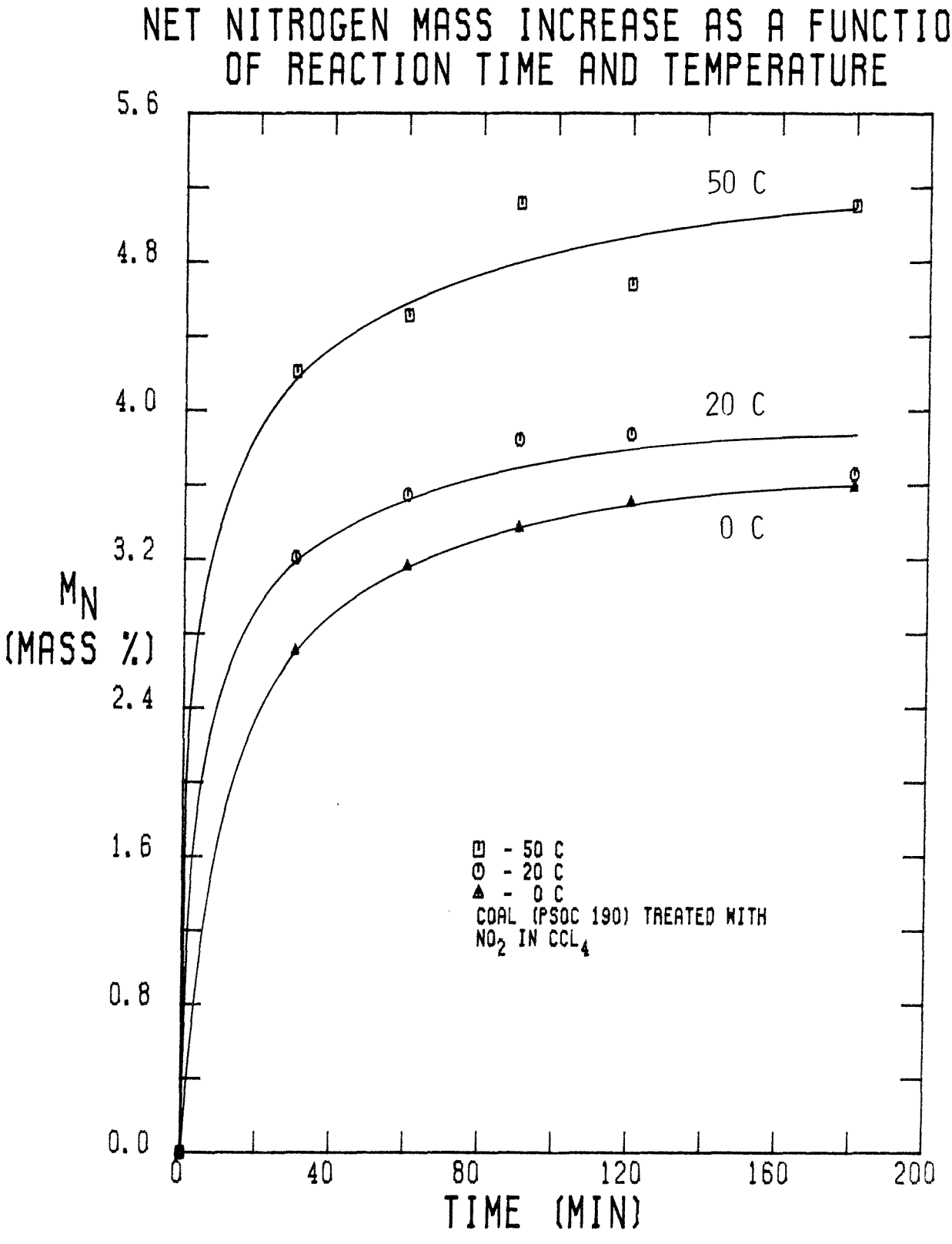
NET NITROGEN MASS INCREASE AS A FUNCTION OF REACTION TIME AND TEMPERATURE
5.6
4.8
4.0
3.2
2.4
1.6
0.8
0.0
M_N (MASS %)
50 C
20 C
0 C
□ - 50 C
○ - 20 C
▲ - 0 C
COAL (PSOC 190) TREATED WITH NO_2 IN CCL_4
0
40
80
120
160
200
TIME (MIN)

FIGURE 4-68

the point at 120 minutes is discarded, such would be precisely the case, since the points at 90 and 180 minutes are essentially equal. Therefore, the reaction appears to be complete within 90 minutes at 50°C. By using only the data points at 0, 30, 60 and 90 minutes, the best value for m^s_{N0} is 5.33 (g N/100 g initial coal). The least squares fit yields a value for m^s_{N0} of 5.39 g N/100 g initial coal and a value for k of 0.0466 min^{-1}. The value of the correlation coefficient is 0.9320. Thus, the second interpretation of the data yields the following values for the rate constant:

T(C)	0	20	50
k(min^{-1})	0.0342	0.0483	0.0466

These results imply that the rate constant is roughly equal at 20 and 50°C, but less at 0°C. There is no simple explanation for this behavior because a smooth temperature dependence is expected. One possibility is that the rate constant at 50°C represents rate control by diffusional resistances rather than by kinetic limitations. It should be noted that the kinetic data for (NO_2) indicate that diffusional resistances control the global rate of NO_2 consumption for the first 30 to 60 minutes. Since the reaction at 50°C is roughly 90 % complete within 60 minutes, one might expect diffusional resistances to play a more predominant role than in experiments conducted at lower temperatures where the time required for complete reaction is longer. Indeed, the value of k at 20°C may also be the result of diffusional limitations on the rate, when only 120 minutes are required for completion of the reaction. At 0°C, however, the reaction is not complete within 180 minutes, which indicates that the kinetics of the nitrogen uptake reaction may be rate controlling. In any case, the values of k obtained provide good estimates for further kinetic interpretation in the mathematical modelling of the reaction system.

Another interesting feature mentioned above concerns the limiting value of

m_N as the reaction time approaches infinity, $(m_N)_\infty$. Based on the kinetic analysis, $(m_N)_\infty = m^s_{N0}$, which yields the following values for $(m_N)_\infty$:

T(C)	0	20	50
$(m_N)_\infty$ (g N/100 g coal)	3.60	3.89	5.33

There is a definite increase in $(m_N)_\infty$ with temperature which implies that the capacity of the coal for the uptake of nitrogen is a function of temperature. As previously mentioned, the thermal expansion of the coal is too slight to account for such a large increase in $(m_N)_\infty$ with temperature. Rather, the explanation must reside in the energetics of the reaction. That is, the activation energy for nitrogen uptake varies from one site to another, rather than being the same for all sites. Thus, as the temperature is increased, more sites are available for the uptake of nitrogen.

The values of the mass corrected nitrogen content of the coals treated with NO_2 at 20 and 0°C which were subsequently washed in 0.1 M Na_2CO_3 (aq) are shown graphically in Figure 4–69 as a function of NO_2-exposure time. Basically, both loci have the same general shape with the 0°C curve being slightly below the 20°C curve. Furthermore, both curves parallel the curves corresponding to the NO_2-treated coal. Figure 4–70 contains the corresponding values for m_N, which demonstrates that the net nitrogen mass increase of the washed coal follows the same trend as that of the NO_2-treated coal. In particular, m_N decreases between 15 and 20 % due to the wash at both temperatures, which emphasizes the high degree of correlation between the uptake of nitrogen which is displaced during the wash and the uptake of nitrogen which remains after the wash.

The effect of the initial concentration of NO_2, $(NO_2)_0$, on the nitrogen content of the coal treated with NO_2 for 120 minutes is demonstrated graphically in Figure 4–71. Both curves show the same general trends, namely an initially rapid rate of increase in c_N which gradually decreases at higher values of $(NO_2)_0$. Once

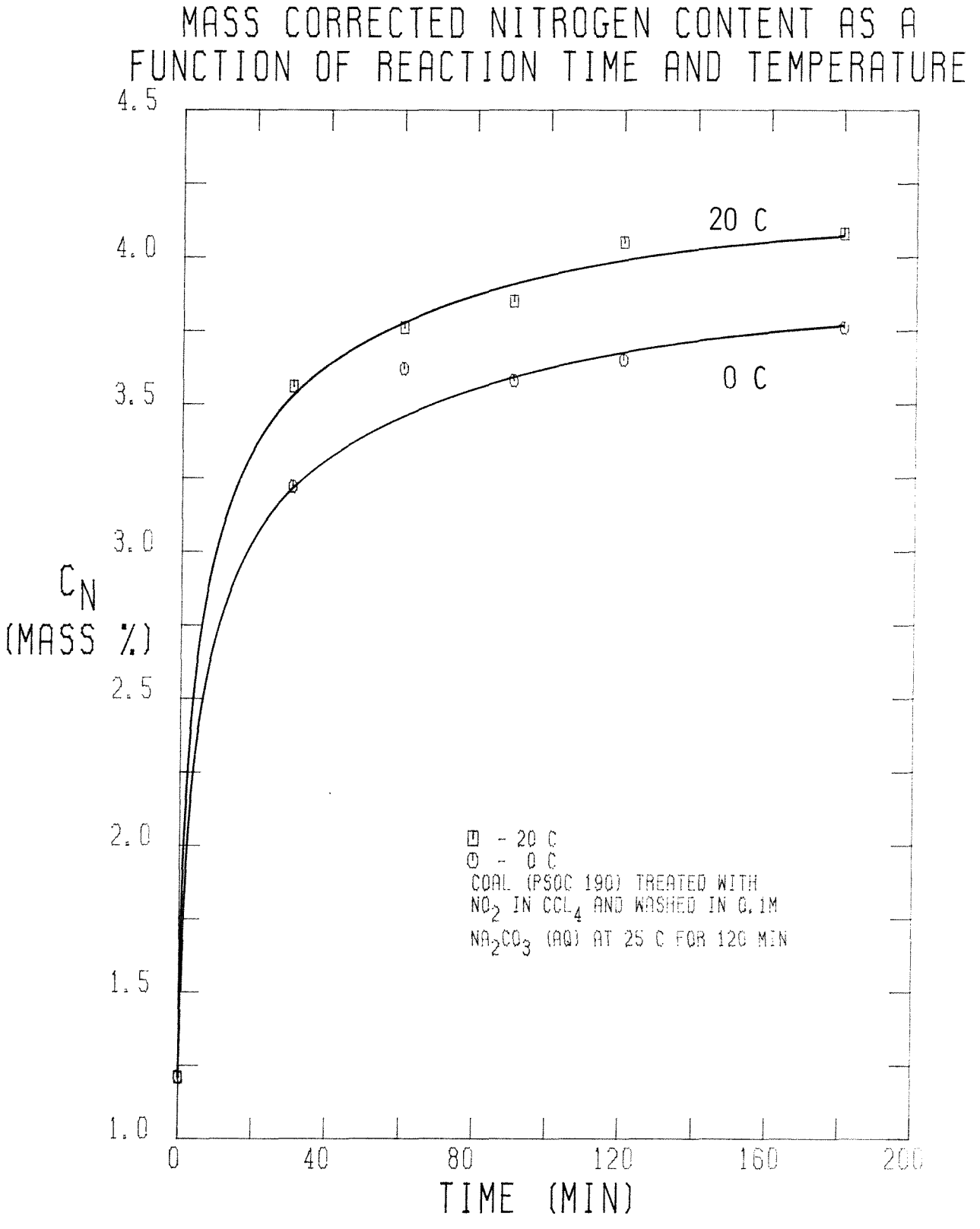
MASS CORRECTED NITROGEN CONTENT AS A FUNCTION OF REACTION TIME AND TEMPERATURE
4.5
4.0
3.5
3.0
2.5
2.0
1.5
1.0
C_N (MASS %)
20 C
0 C
□ - 20 C
○ - 0 C
COAL (PSOC 190) TREATED WITH NO_2 IN CCL_4 AND WASHED IN 0.1M NA_2CO_3 (AQ) AT 25 C FOR 120 MIN
0
40
80
120
160
200
TIME (MIN)

FIGURE 4-69

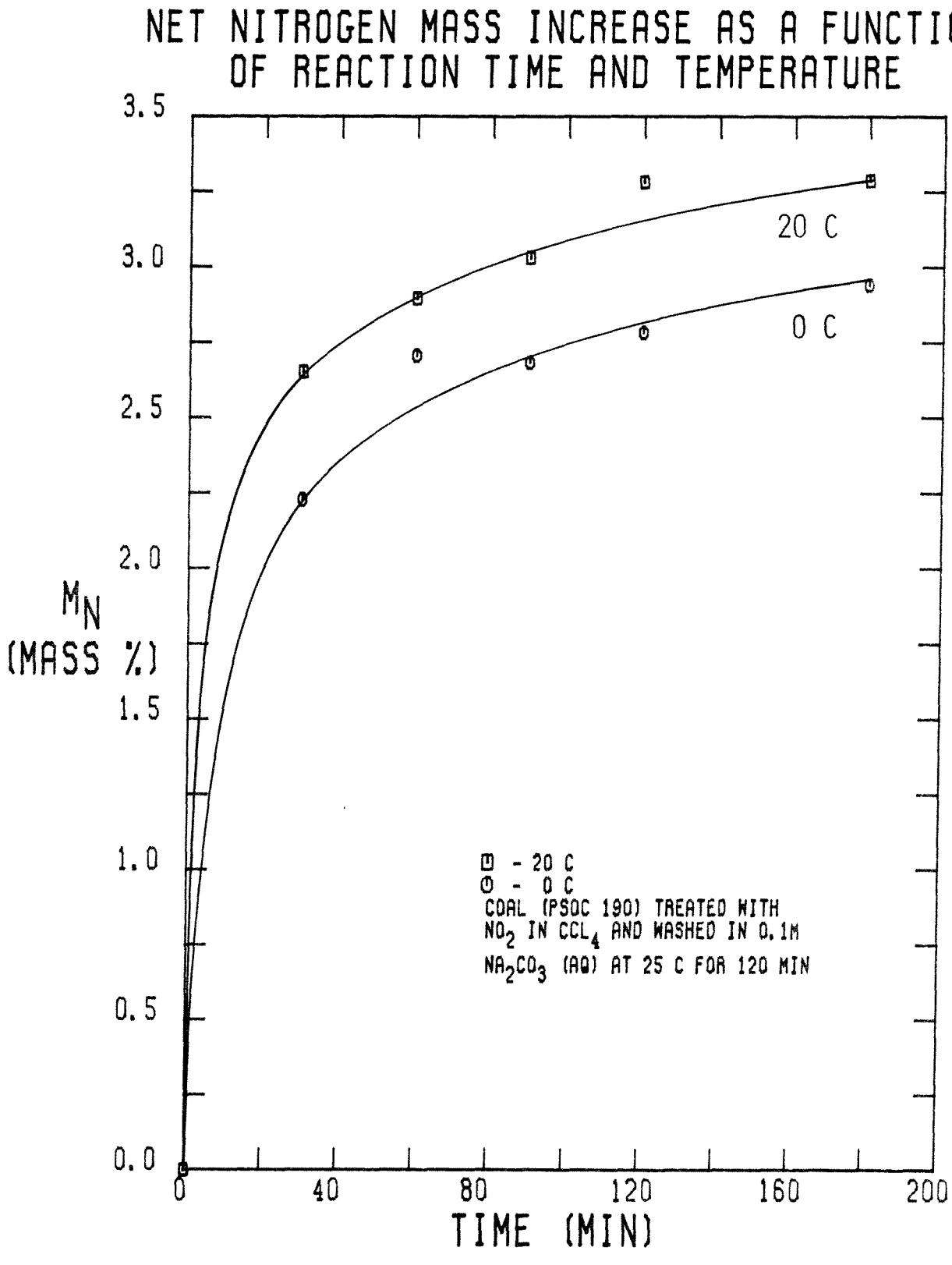
NET NITROGEN MASS INCREASE AS A FUNCTION OF REACTION TIME AND TEMPERATURE
3.5
3.0
2.5
2.0
1.5
1.0
0.5
0.0
M_N (MASS %)
20 C
0 C
□ - 20 C
◷ - 0 C
COAL (PSOC 190) TREATED WITH NO_2 IN CCL_4 AND WASHED IN 0.1M NA_2CO_3 (AQ) AT 25 C FOR 120 MIN
0
40
80
120
160
200
TIME (MIN)

FIGURE 4-70

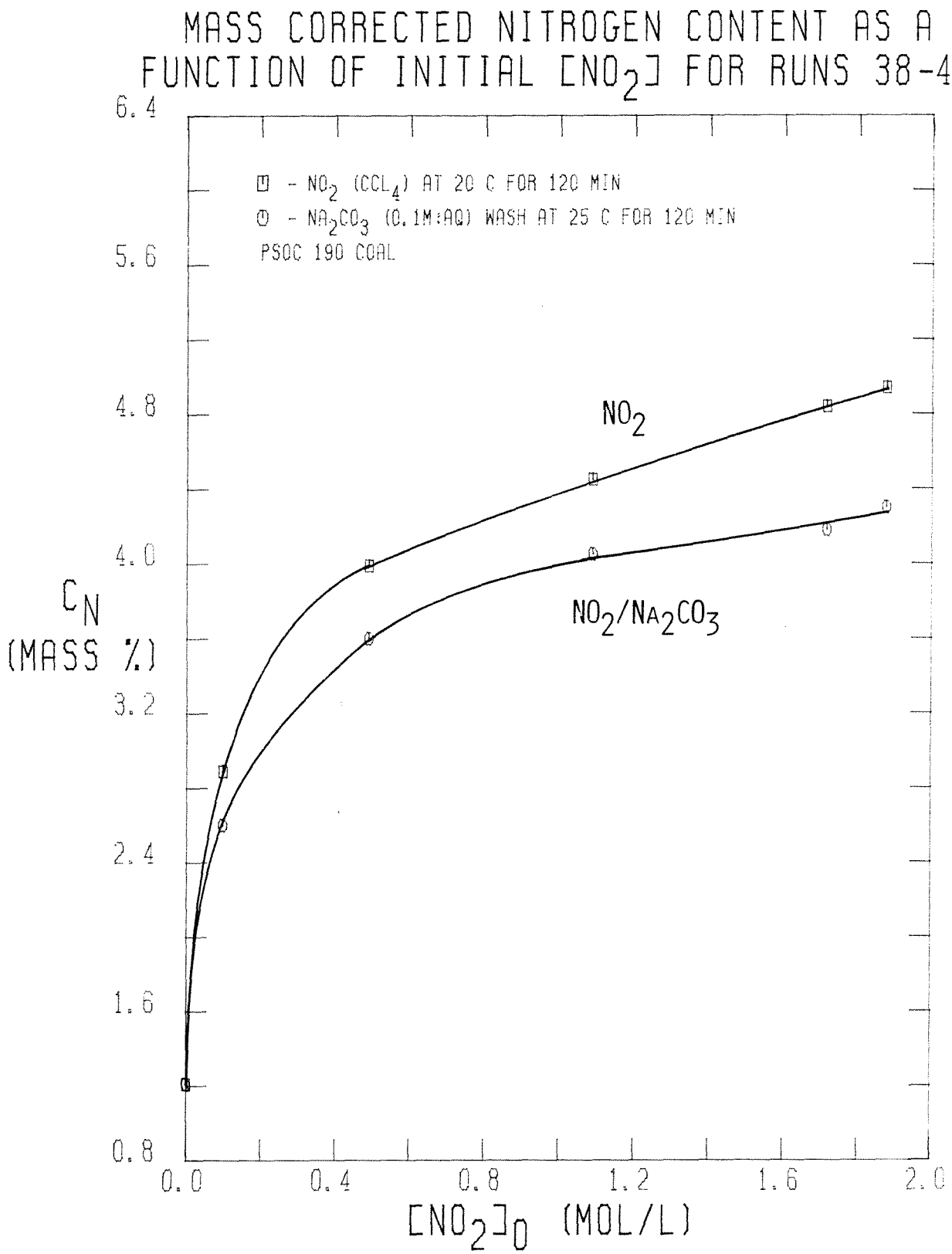
MASS CORRECTED NITROGEN CONTENT AS A FUNCTION OF INITIAL [NO2] FOR RUNS 38-41
□ - NO2 (CCL4) AT 20 C FOR 120 MIN
○ - NA2CO3 (0.1M:AQ) WASH AT 25 C FOR 120 MIN
PSOC 190 COAL
NO2
NO2/NA2CO3
CN (MASS %)
6.4
5.6
4.8
4.0
3.2
2.4
1.6
0.8
0.0
0.4
0.8
1.2
1.6
2.0
[NO2]0 (MOL/L)

FIGURE 4-71

$(NO_2)_0$ exceeds roughly 0.5 F, however, the rate of increase in c_N is constant. Such behavior is indicative of systems where a solute is distributed between two different phases in a simple manner. That is, the NO_2 is distributed between the CCl_4 and coal in a manner such that the quantity $\frac{c_N - c_N^*}{(NO_2)}$ is constant, where c_N^* is the value of c_N as (NO_2) approaches zero. The quantity $\frac{c_N - c_N^*}{(NO_2)}$ is commonly referred to as the partition coefficient. In this case, a least squares fit of the points at (NO_2) = 0.49, 1.08, 1.71 and 1.87 F yields values of 3.816 mass percent for c_N^* and 0.8137 l/mol/(mass %) for the partition coefficient. The correlation coefficient for the fit is 0.9799. In any case, it is evident that c_N does depend on (NO_2).

In order to incorporate the data shown in Figure 4–71 into the kinetic analysis, it is necessary to convert c_N to m_N. Thus, the values of the net nitrogen mass increase for the processed coal are displayed graphically in Figure 4–72, which shows that the same trends which apply to c_N apply to m_N as well. The corresponding partition coefficient is 1.1711 (g N)-l/mol/(100g initial coal) with a value for m_N^* of 2.979 g N/100g coal. The correlation coefficient of the fit is 0.9864. This behavior implies that the limiting value for m_N as the exposure time approaches infinity, $(m_N)_\infty$, is determined by (NO_2) in the liquid phase. Thus, the rate of nitrogen uptake must depend on (NO_2) as well. It should be noted that when $(NO_2)_0$ is less than 0.5 F, there is insufficient NO_2 to complete the uptake of nitrogen within 120 minutes. For higher values of $(NO_2)_0$, however, the reaction is probably complete because the set of experiments run at 20°C (Runs 33–37), where $(NO_2)_0$ = 1.087 F, indicates that the reaction is complete within 120 minutes. Unfortunately, these data do not allow the determination of the rate dependence on (NO_2). Indeed, it is quite interesting to note that while the analysis of the (NO_2) data indicates the

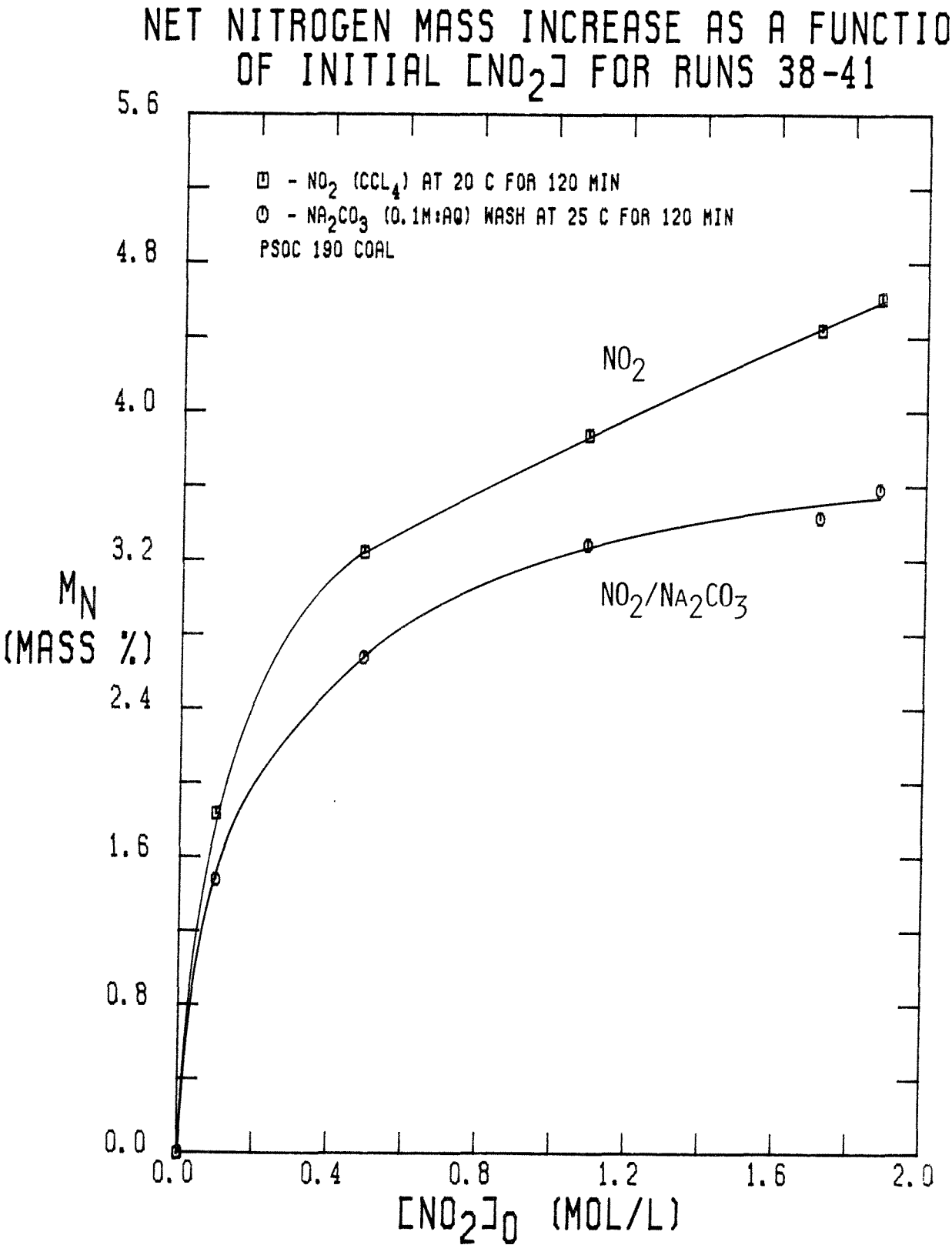
NET NITROGEN MASS INCREASE AS A FUNCTION OF INITIAL [NO2] FOR RUNS 38-41
□ - NO2 (CCL4) AT 20 C FOR 120 MIN
○ - NA2CO3 (0.1M:AQ) WASH AT 25 C FOR 120 MIN
PSOC 190 COAL
NO2
NO2/NA2CO3
MN (MASS %)
[NO2]0 (MOL/L)
5.6
4.8
4.0
3.2
2.4
1.6
0.8
0.0
0.0
0.4
0.8
1.2
1.6
2.0

FIGURE 4-72

specific rate does not depend on (NO_2) and the analysis of the nitrogen uptake data from Runs 33–37 seems to confirm no (NO_2) dependence, the analysis of the nitrogen uptake data for various values of $(NO_2)_0$ does indicate a dependence of the rate on (NO_2). This apparent dilemma can be resolved by noting that (NO_2) seems only to dictate the number of available sites in the coal for nitrogen uptake, m^s_{N0}. There may still be no dependence of the rate on (NO_2), however. Rather, the value of the rate changes with (NO_2) because m^s_{N0} changes (Rate = $k\ m^s_N$). These conclusions are consistent with the notion that the nitrogen uptake of the coal is the result of the establishment of an equilibrium distribution of NO_2 between the solvent and the coal. Furthermore, attainment of this distribution must be irreversible, otherwise the added nitrogen would be removed during the vacuum drying. Thus, by incorporating the results from the experiments conducted at different temperatures, (NO_2) does affect m^s_{N0}, but the rate of nitrogen uptake does not depend explicitly on (NO_2).

The effect of the pore structure on the nitrogen uptake by the coal can be determined by examining the values of c_N and m_N for the treated PSOC 276 coal. The values for c_N of the PSOC 276 treated with NO_2 and subsequently washed in 0.1 M Na_2CO_3 (aq) are shown in Figure 4–73. It should be noted that c_N in both cases is still rising after 180 minutes of NO_2 exposure. Furthermore, the Na_2CO_3 (aq) wash does not remove very much of the added nitrogen. The corresponding values for m_N of the treated PSOC 276 are depicted graphically in Figure 4–74. As with c_N, the values of m_N continue to rise in both cases even after 180 minutes of NO_2 exposure, which implies that the uptake of nitrogen by the PSOC 276 coal at 20℃ is not complete within 180 minutes. The Na_2CO_3 (aq) wash removes between 18 and 21 % of the added nitrogen, which is exactly the same range of relative nitrogen removal from the NO_2-treated PSOC 190 coal. Because the pore volumes of the two coals differ by a factor of four, this con-

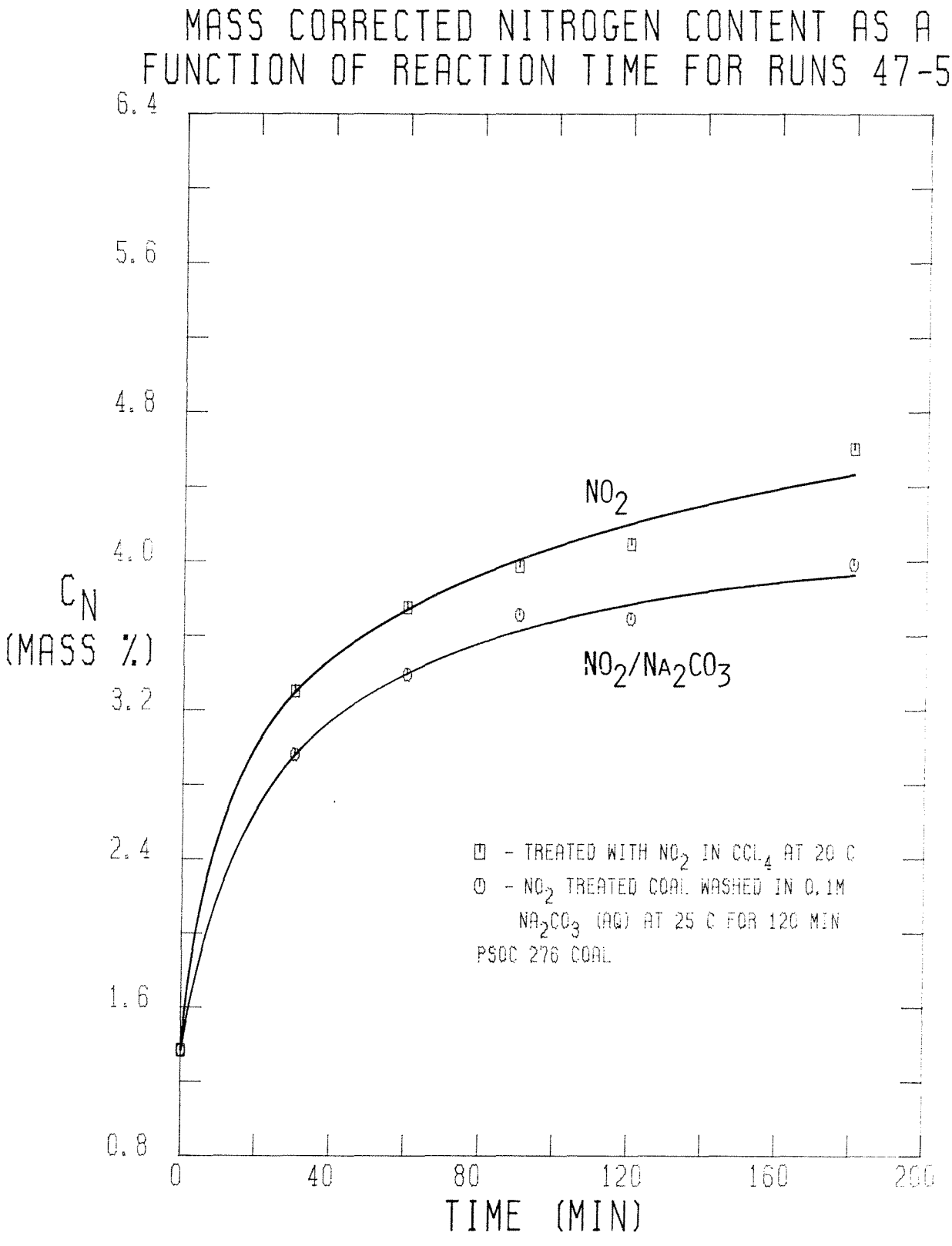
MASS CORRECTED NITROGEN CONTENT AS A FUNCTION OF REACTION TIME FOR RUNS 47-52
6.4
5.6
4.8
4.0
3.2
2.4
1.6
0.8
C_N (MASS %)
NO_2
NO_2/NA_2CO_3
□ - TREATED WITH NO_2 IN CCL_4 AT 20 C
Ⓓ - NO_2 TREATED COAL WASHED IN 0.1M NA_2CO_3 (AQ) AT 25 C FOR 120 MIN
PSOC 276 COAL
0
40
80
120
160
200
TIME (MIN)

FIGURE 4-73

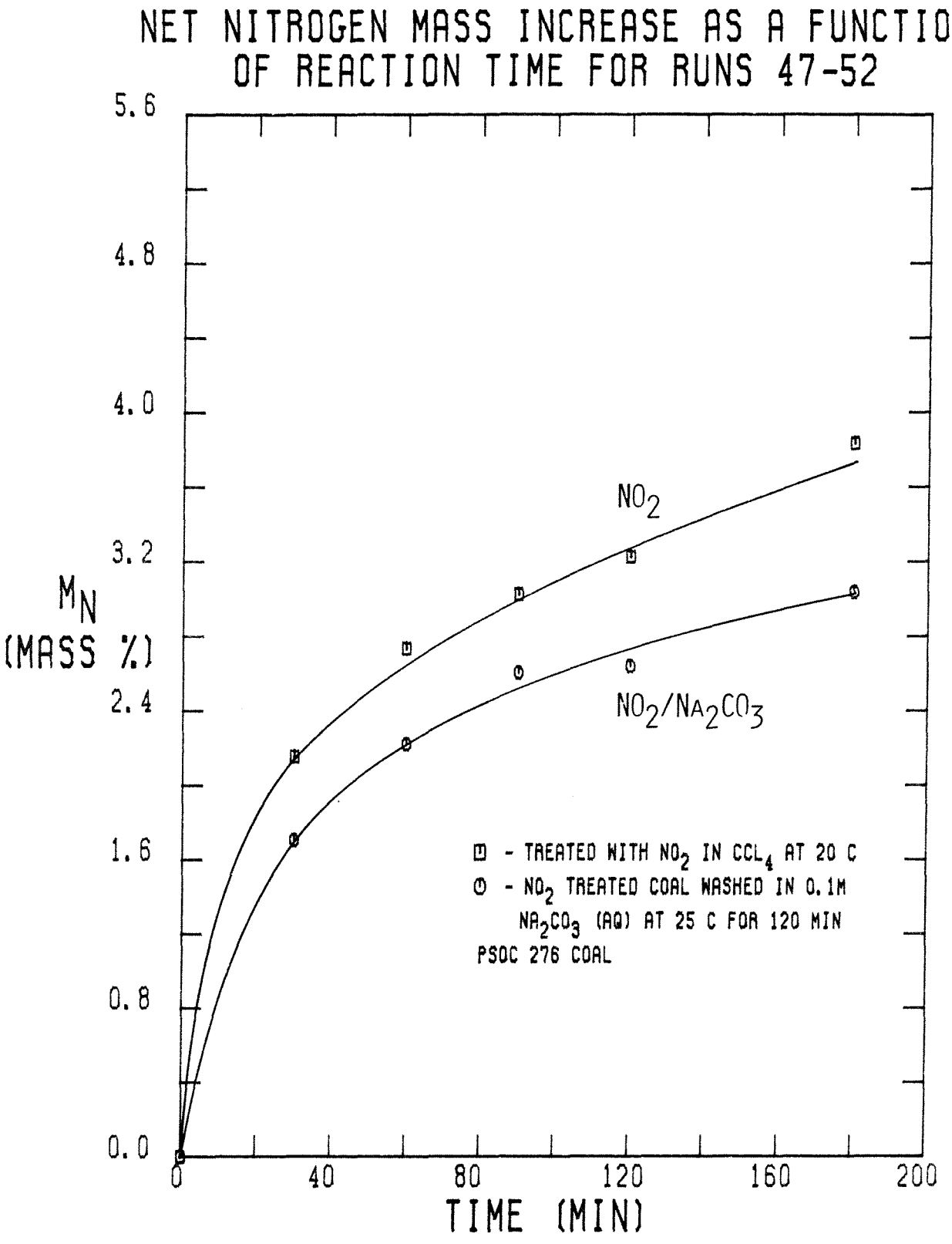
NET NITROGEN MASS INCREASE AS A FUNCTION OF REACTION TIME FOR RUNS 47-52
5.6
4.8
4.0
3.2
2.4
1.6
0.8
0.0
M_N (MASS %)
0
40
80
120
160
200
TIME (MIN)
NO_2
NO_2/NA_2CO_3
- TREATED WITH NO_2 IN CCL_4 AT 20 C
- NO_2 TREATED COAL WASHED IN 0.1M NA_2CO_3 (AQ) AT 25 C FOR 120 MIN
PSOC 276 COAL

FIGURE 4-74

stant partial removal of added nitrogen indicates that no matter how much nitrogen is added to the coal, roughly 18 to 20 % of it will be displaced during the Na_2CO_3 (aq) wash. This constant relative nitrogen removal serves as very strong confirmatory evidence that the process which accounts for the eventually displaced nitrogen uptake and the process which accounts for the uptake of the nitrogen which remains after the wash are the same; that is, the alterations in the coal which account for the uptake of the displaced nitrogen are themselves a consequence of the uptake of the remaining nitrogen.

A comparison of the values of the mass corrected nitrogen content, c_N, of the two coals treated with NO_2 at 20°C is provided in Figure 4–75. The curve for the treated PSOC 190 rises sharply and levels off after about 90 minutes. On the other hand, the curve for the treated PSOC 276 rises less rapidly but eventually crosses the other curve at about 150 minutes. The corresponding values for the net nitrogen mass increase, m_N, are shown graphically in Figure 4–76 and demonstrate the same trends as the values of c_N. The values of m_N for the NO_2 treated PSOC 190 rise rapidly and level off at about 3.9 g N/100 g initial coal, while those of m_N for the treated PSOC 276 rise more gradually to about 3.8 g N/100 g initial coal after 180 minutes of NO_2 treatment. The value of m_N for the PSOC 276, however, continues to rise at 180 minutes while that of m_N for the PSOC 190 has levelled off. Therefore, the mass of added nitrogen should be higher in the PSOC 276 than in the PSOC 190 at longer NO_2-exposure times. This result is indeed striking because the initial pore volume of the PSOC 276 is roughly four times smaller than that of the PSOC 190. Therefore, there is no correlation between the amount of nitrogen uptake and the pore structure of the coal, which implies that penetration of the NO_2 into the solid coal structure must occur. The plausibility of solid penetration is enhanced by the fact that even if the entire pore structure of the PSOC 190 were filled with liquid NO_2 after

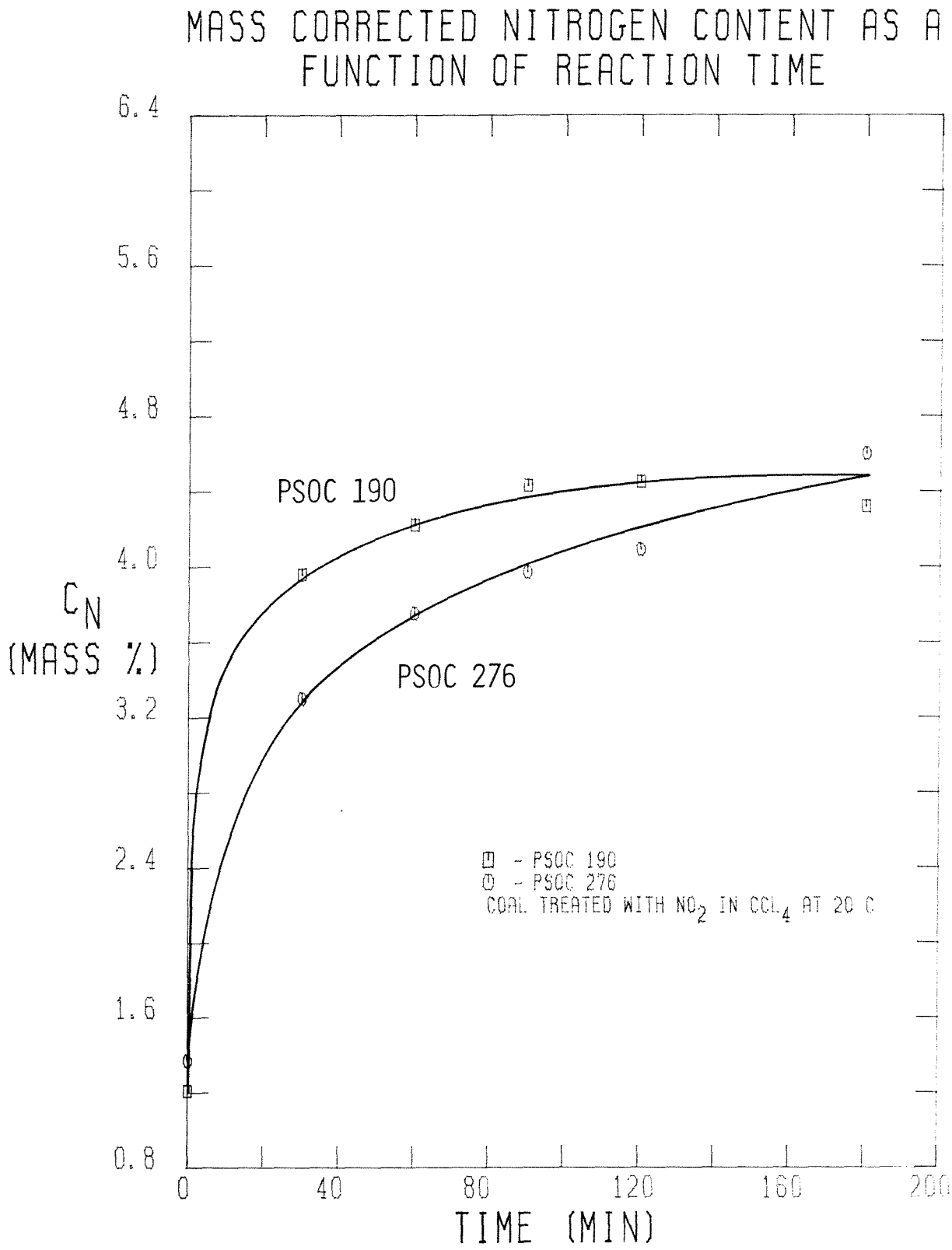
MASS CORRECTED NITROGEN CONTENT AS A FUNCTION OF REACTION TIME
6.4
5.6
4.8
4.0
3.2
2.4
1.6
0.8
C_N (MASS %)
PSOC 190
PSOC 276
- PSOC 190
- PSOC 276
COAL TREATED WITH NO_2 IN CCL_4 AT 20 C
0
40
80
120
160
200
TIME (MIN)

FIGURE 4-75

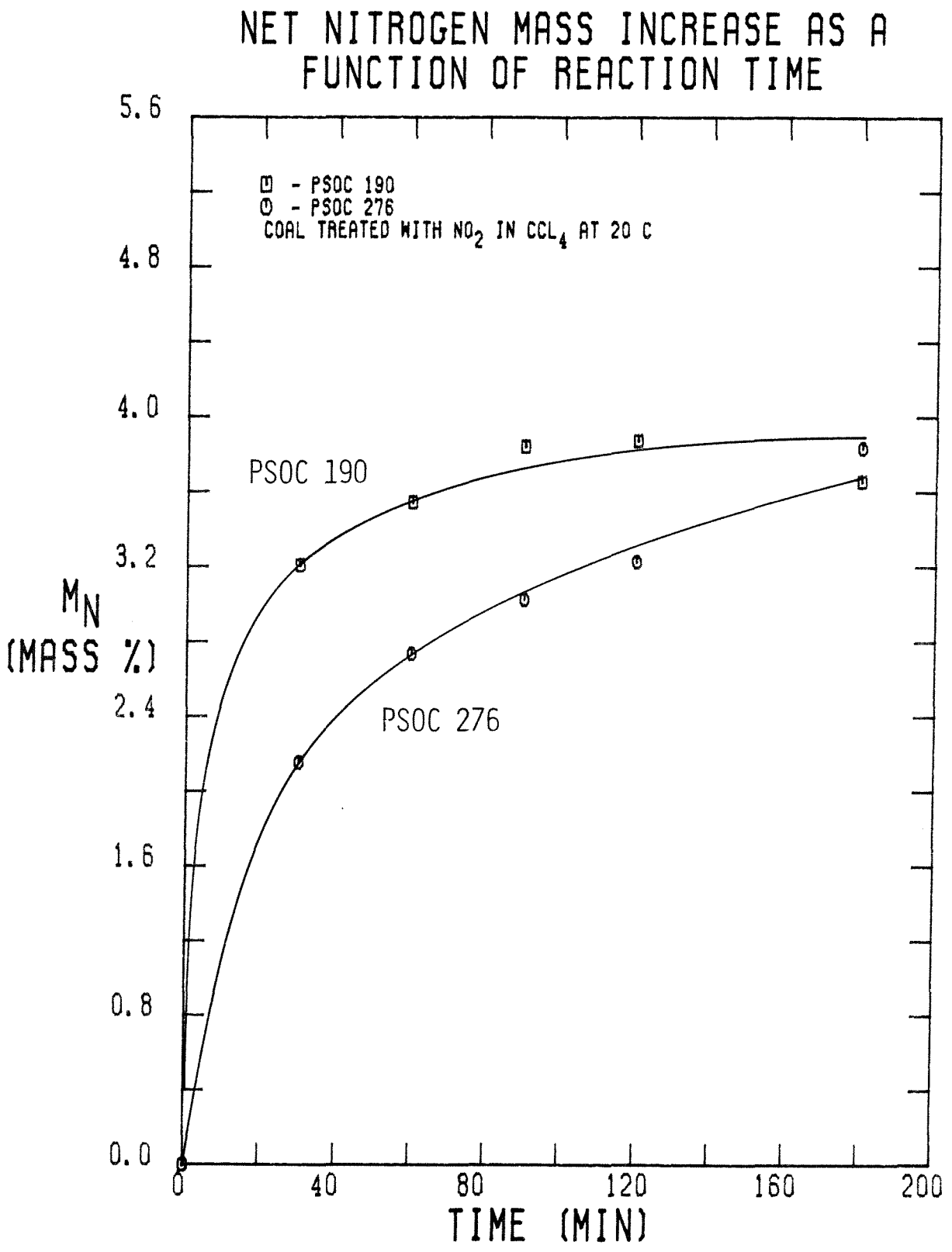
NET NITROGEN MASS INCREASE AS A FUNCTION OF REACTION TIME
- PSOC 190
- PSOC 276
COAL TREATED WITH NO_2 IN CCL_4 AT 20 C
PSOC 190
PSOC 276
M_N (MASS %)
TIME (MIN)
5.6
4.8
4.0
3.2
2.4
1.6
0.8
0.0
0
40
80
120
160
200

FIGURE 4-76

the vacuum drying, it could contain only 40 % off the total nitrogen uptake. In the case of the PSOC 276, no more than 7 % of the total nitrogen uptake could be accommodated by the pore structure alone.

A graphical comparison of the values of the mass corrected nitrogen content, c_N, of the two NO_2-treated coals subsequently washed in 0.1 M Na_2CO_3 (aq) is shown in Figure 4–77. The corresponding values of the net nitrogen mass increase, m_N, are displayed in Figure 4–78. In both cases, for both coals, the values of c_N and m_N parallel those of the respective unwashed coals, even to the extent of being roughly 15 to 21 % lower in value. Because the values of m_N for both coals are roughly equal, this result implies that the absolute amount of nitrogen removed may depend on the length of time of the wash rather than the accessibility of the aqueous Na_2CO_3 solution to the interior of the coal particle. Indeed, if the nitrogen uptake is the result of the establishment of an equilibrium between NO_2 in the liquid and solid phases, it is reasonable to expect that once the concentration of NO_2 in the liquid phase is lowered, the NO_2 should diffuse out of the coal. The diffusion of NO_2 out of the coal, however, must be inhibited, perhaps through some weak bonding of the NO_2 to the oxidized coal, otherwise the vacuum drying at 120°C for 180 minutes would be expected to be sufficient for the removal of the NO_2 taken up by the coal. In any case, such a mechanism requires no distinction between the "displaced" and "remaining" nitrogen. Rather, all of the added nitrogen is the result of a single diffusion process. The "displaced" nitrogen is just the portion of the added nitrogen which has sufficient time to diffuse out of the coal during the Na_2CO_3 (aq) wash. Therefore, the nitrogen removal is simply the result of the establishment of an equilibrium of NO_2 in the coal and Na_2CO_3 (aq) phases, just as in the NO_2 treatment. Unfortunately, it is impossible to determine whether that equilibrium is established within the 120 minutes of the Na_2CO_3 (aq) wash because all of the NO_2-

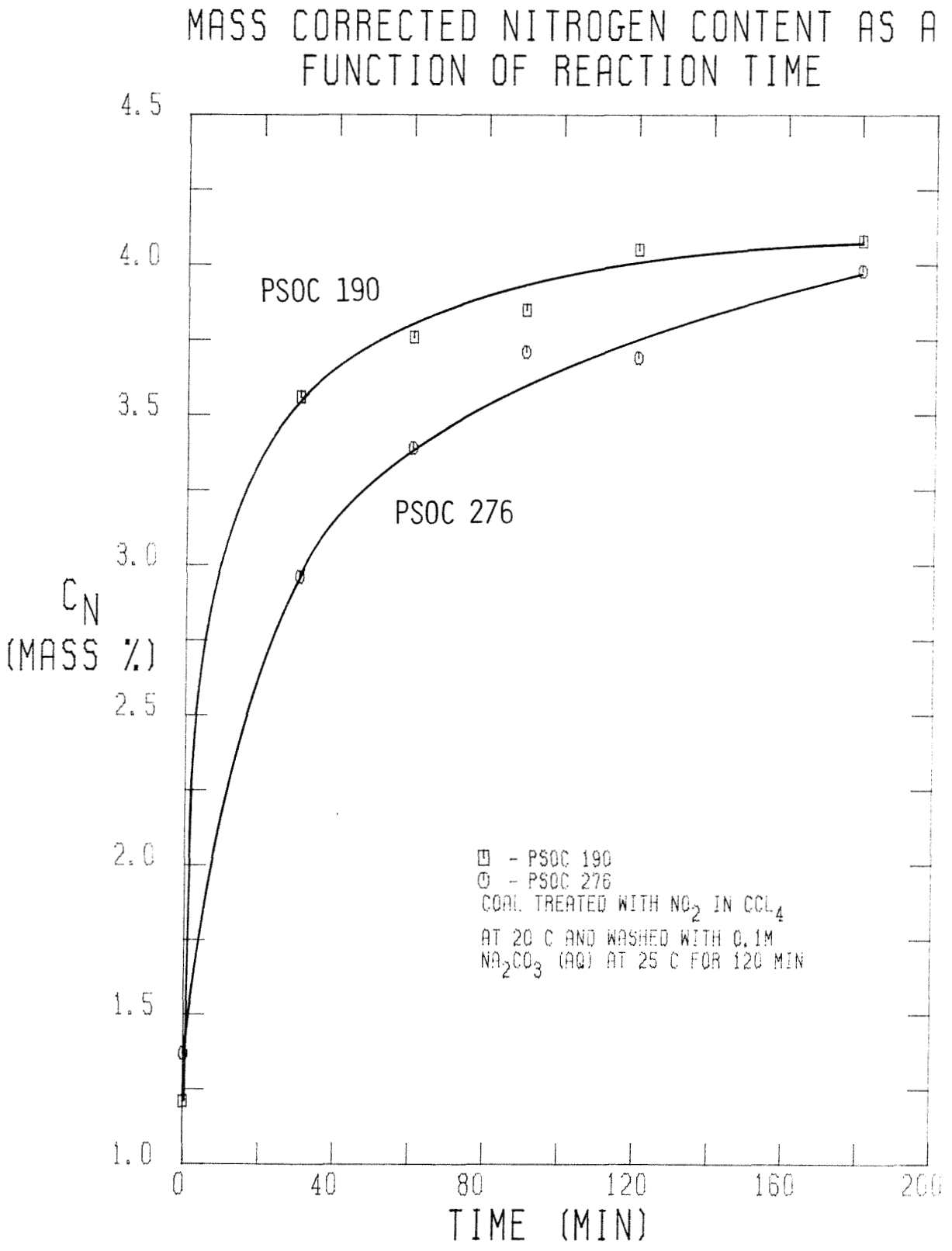
MASS CORRECTED NITROGEN CONTENT AS A FUNCTION OF REACTION TIME
4.5
4.0
3.5
3.0
2.5
2.0
1.5
1.0
C_N (MASS %)
PSOC 190
PSOC 276
□ - PSOC 190
○ - PSOC 276
COAL TREATED WITH NO_2 IN CCL_4
AT 20 C AND WASHED WITH 0.1M
NA_2CO_3 (AQ) AT 25 C FOR 120 MIN
0
40
80
120
160
200
TIME (MIN)

FIGURE 4-77

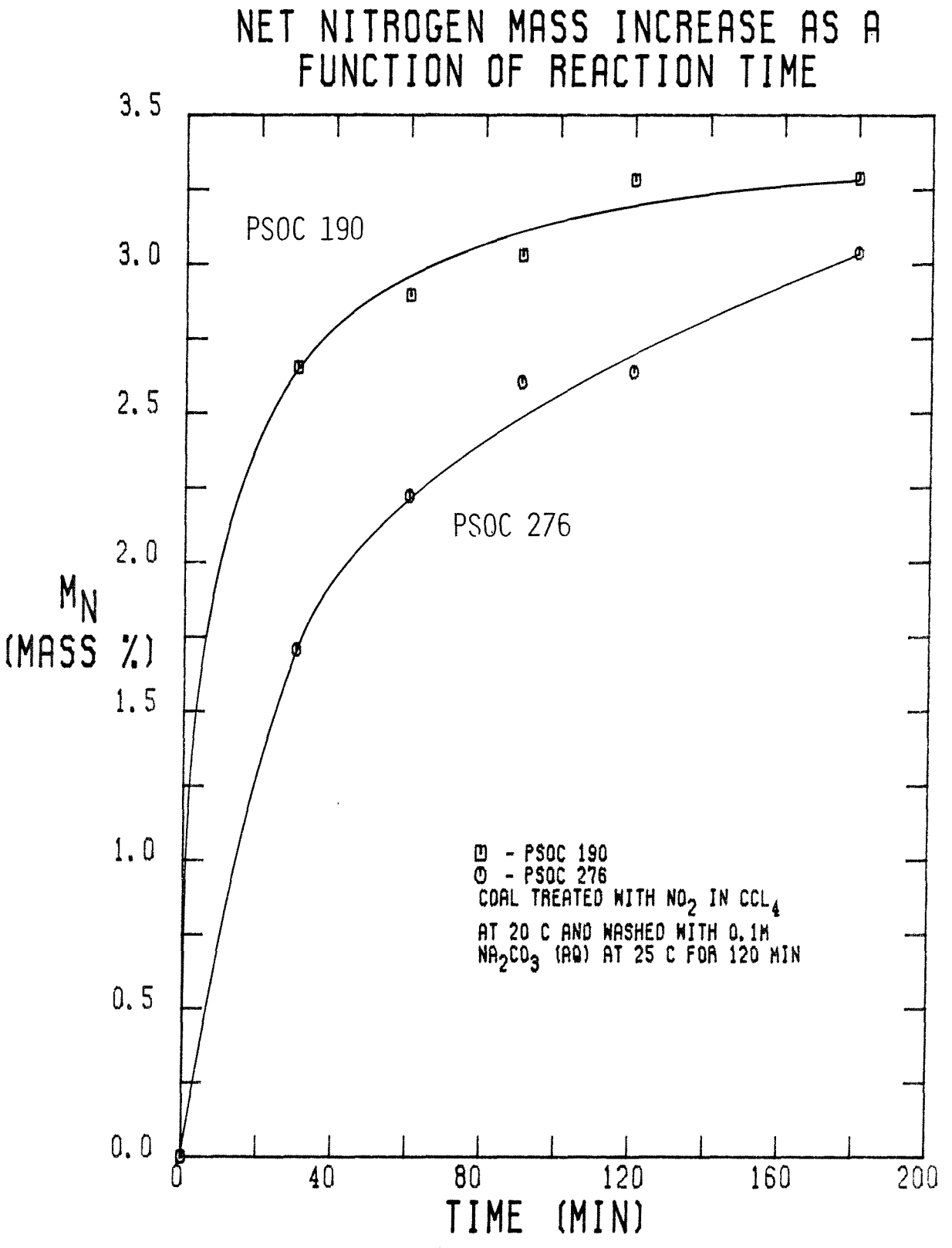
NET NITROGEN MASS INCREASE AS A FUNCTION OF REACTION TIME
PSOC 190
PSOC 276
M_N (MASS %)
TIME (MIN)
0.0
0.5
1.0
1.5
2.0
2.5
3.0
3.5
0
40
80
120
160
200
- PSOC 190
- PSOC 276
COAL TREATED WITH NO_2 IN CCL_4
AT 20 C AND WASHED WITH 0.1M
NA_2CO_3 (AQ) AT 25 C FOR 120 MIN

FIGURE 4-78

treated coal samples were washed in the same manner.

If the data for m_N of the NO_2-treated PSOC 276 are fit to equation (4.2.17) in the manner described above for the various values of n, the following values for the rate constant, k, are obtained:

	m_{N0}^s (g N/100 g coal)			
n	Chosen	Calculated	r^2	k
0	3.94	3.94	0.9378	0.0183 min^{-1}
0.5	3.96	3.95	0.9415	0.0194 $l^{0.5}$–$mol^{-0.5}$–min^{-1}
1	3.98	3.99	0.9443	0.0207 l–mol^{-1}–min^{-1}

Once again, $\int_0^t (NO_2)^n \, dt$ correlates with t almost perfectly, so that it is not possible to use this procedure to determine the dependence of the rate on (NO_2). Nevertheless, it seems reasonable to expect the notion of the NO_2 uptake being the result of an equilibrium process between the liquid phase and the coal to apply to the PSOC 276 as well as the PSOC 190. Indeed, a comparison of the results for the case when n = 0 for the PSOC 190 treated with NO_2 at 20°C with the PSOC 276 treated under the same conditions lends support to this theory. The values of m_{N0}^s, r^2 and k are:

	m_{N0}^s (g N/100 g coal)			
Coal	Chosen	Calculated	r^2	k (min^{-1})
PSOC 190	3.89	3.90	0.9842	0.0483
PSOC 276	3.94	3.94	0.9378	0.0183

It is quite striking that although the values of k differ by a factor of almost three, the values of m_{N0}^s differ by only 1 %. Therefore, the rate of nitrogen uptake by the two coals differs discernibly, but the ultimate amount of added nitrogen is the same for both coals, which implies that the partition coefficient of NO_2 between CCl_4 and the coal is independent of the pore structure of the coal. In particular, if the value of m_N^* of 2.979 g N/100 g initial coal obtained

from the fit of the partition coefficient expression $K = \frac{m_N - m_N^*}{(NO_2)}$ to the PSOC 190 data is used for the PSOC 276 data at 180 minutes as well, the value obtained for K is 1.188 l-(g N)-mol^{-1}-(g N/100 g initial coal)$^{-1}$, which compares quite favorably with the value of 1.171 l-(g N)-mol^{-1}-(g N/100 g initial coal)$^{-1}$ obtained for the PSOC 190 coal. The pore structure does affect the rate at which equilibrium is established, however, as evidenced by the different values of k.

On the basis of the analysis of the nitrogen uptake by the coal, several generalizations regarding the interaction of NO_2 and coal may be made. Probably the most important conclusion is that the increase in nitrogen content of the coal is the result of the establishment of an equilibrium distribution of NO_2 between the liquid CCl_4 phase and the coal, rather than the result of an irreversible chemical reaction. Furthermore, the value of the partition coefficient, which describes the equilibrium distribution, does not depend on the pore structure of the coal, as evidenced by the virtually identical net increase in nitrogen mass of the treated PSOC 190 and PSOC 276 coals, which possess quite different pore structures yet similar elemental compositions. The pore structure does affect the rate at which NO_2 attains equilibrium, however. In particular, the initial pore volume of the PSOC 190 is roughly four times that of the PSOC 276 and the rate constants for the process differ by a factor of three.

Certain other factors affect the rate of nitrogen uptake as well. In particular, the rate depends on the capacity of the coal for accommodating the NO_2. The rate does not depend explicitly on the NO_2 concentration, however. Rather, the capacity for nitrogen uptake, m_{N0}^s, is determined by (NO_2), as expressed by the equation for the partition coefficient. Thus, the "capacity for nitrogen uptake" is really just a measure of the extent of the deviation of the system from equilibrium. Thus, the rate can be expressed as

$$\frac{dm_N^s}{dt} = -k\, m_N^s\,, \quad \text{where} \tag{4.2.18}$$

m_N^s = $m_{NO}^s[(NO_2)] - m_N$ = the capacity for nitrogen uptake,

$m_{NO}^s[(NO_2)]$ = the initial capacity for nitrogen uptake, which is a function of (NO_2),

m_N = the net nitrogen mass increase, and

k = the first order rate constant.

If the expression for the partition coefficient is incorporated, equation (4.2.18) becomes

$$\frac{dm_N^s}{dt} = -k\,[K\,(NO_2)_\infty + m_N^* - m_N(t)]\,, \quad \text{where} \tag{4.2.19}$$

K = the partition coefficient (g N–l–mol^{-1}–(100g initial coal)$^{-1}$),

$(NO_2)_\infty$ = the final equilibrium value of (NO_2) in the liquid phase (F),

m_N^* = the value of m_N as (NO_2) → 0 (g N/100g initial coal),

$m_N(t)$ = the nitrogen mass increase in the coal (g N/100g initial coal), and

k = the rate constant (min^{-1}).

Thus, only the equilibrium value of (NO_2) affects the rate, at least for the range of values of (NO_2) used in this study, where NO_2 is always in excess.

The effect of temperature on the kinetics occurs not only in the rate constant, k, but also in the partition coefficient, K, as reflected in m_{N0}^s. The change in K with temperature is not unexpected, as evidenced by the values obtained for m_{N0}^s for the NO_2-treated PSOC 190:

T(C)	0	20	50
m_{N0}^s (g N/100g initial coal)	3.60	3.89	5.33

Therefore, the nitrogen uptake by the coal increases with temperature. This increase is probably due to the ability of the coal to adsorb more NO_2 when its

thermal enery is increased. The effect of the temperature on k is not completely expected, however. The values obtained for k are:

T(C)	0	20	50
k (min^{-1})	0.0342	0.0483	0.0466

The change in k from 0 to 20°C is not unusual and probably reflects the normally expected effect of temperature on the kinetics. On the other hand, the values of k at 20 and 50°C are about equal. It should be noted, however, that the 50°C treatment was done in the flow reactor, while the treatments at 0 and 20°C were done in the batch reactor. Evidence that the type of reactor used can influence the rate is provided by the value of k for the NO_2 treatment in the flow reactor at 25°C which is 0.0302 min^{-1} contrasted with a value of 0.0483 min^{-1} for the experiments conducted at 20°C in the batch reactor. Nevertheless, the overall value of the rate constant under all of the conditions examined is 0.04 ± 0.01 min^{-1}.

Finally, it should be noted that the nitrogen removed during the Na_2CO_3 (aq) wash also seems to be the result of an equilibrium process. This conclusion is based on the fact that the amount of nitrogen removed from all of the treated coal samples is consistently between 15 and 21 % of the added nitrogen. The difference in the pore structures of the treated PSOC 190 and PSOC 276 has absolutely no effect on the amount of nitrogen removed. Thus, it appears that the entire change in the nitrogen content of the coal through the course of the treatment is simply the result of equilibrium processes.

4.2.2.5 The Oxygen Content of the Coal

When coal is treated with NO_2, the oxygen content of the coal should increase due not only to oxidation of various aliphatic portions of the coal but also to the incorporation of NO_2 into the coal as well. Fortunately, when CCl_4 is the solvent, the only source of additional oxygen is NO_2. When water is the solvent, on the other hand, various potential oxygen donors to the coal are formed, mainly HNO_3 (aq), HNO_2 (aq) and NO_2 (aq), which render the determination of the extent to which each of these species donate oxygen to the coal virtually impossible. Therefore, the following discussion concerning the changes in oxygen content of the coal during treatment with NO_2 and subsequent washing in 0.1 M Na_2CO_3 (aq) is limited exclusively to those experiments in which CCl_4 is the solvent (Runs 21–52).

Before the results of the oxygen determinations are discussed, one important point must be made. The oxygen contents are obtained by adding the carbon, hydrogen, nitrogen, chlorine, sulfur and mineral matter contents and subtracting the sum from 100 percent. Consequently, the error in the oxygen content is the sum of the errors for all of the other analyses. In general, the relative errors in the other analyses are less than three percent, which implies that the relative error in the oxygen content can be as high as 20 percent, although it is generally on the order of 5 to 10 percent. Therefore, the likelihood of unexplainable deviations of single oxygen determinations from general trends is greatly enhanced. Indeed, the degree of scatter in the data can be sufficiently large to render the determination of definite trends virtually impossible. Having made this point, the results of the oxygen determinations will now be discussed.

The mass corrected oxygen content, c_O, of the coal treated with NO_2 at 25 °C in the flow reactor and subsequently washed in 0.1 M Na_2CO_3 (aq) (Runs 21–27) is shown as a function of NO_2-reaction time in Figure 4–79. The data indicate that

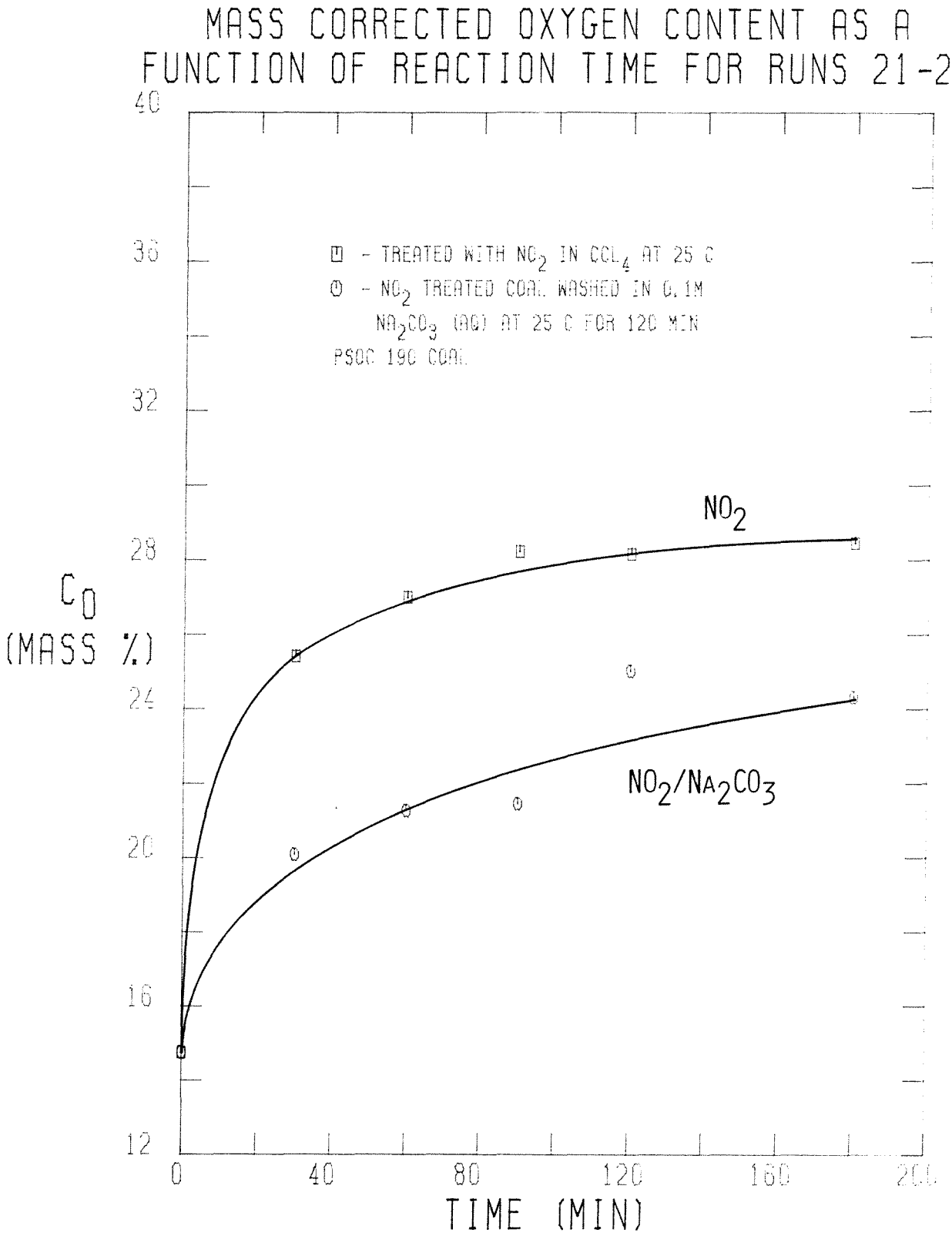
MASS CORRECTED OXYGEN CONTENT AS A FUNCTION OF REACTION TIME FOR RUNS 21-27
40
36
32
28
24
20
16
12
0
40
80
120
160
200
TIME (MIN)
C0 (MASS %)
⊡ - TREATED WITH NO2 IN CCL4 AT 25 C
⊙ - NO2 TREATED COAL WASHED IN 0.1M NA2CO3 (AQ) AT 25 C FOR 120 MIN
PSOC 190 COAL
NO2
NO2/NA2CO3

FIGURE 4-79

after 90 minutes of NO_2 treatment, c_O no longer increases, which implies that the processes which account for oxygen uptake by the coal are completed. This behavior is identical with that shown by the nitrogen and overall mass uptakes of the treated coals. The oxygen content of the washed coal basically parallels that of the NO_2-treated coal, but at much lower values. If the values of c_O are adjusted for the mass gain, the values of the net oxygen mass increase, m_O, are obtained as displayed in Figure 4–80. The upper curve in the figure, which corresponds to the NO_2-treated coal, also indicates that oxygen uptake is complete within 90 minutes, attaining a limiting value of roughly 17 (g O/100g initial coal) after 180 minutes of NO_2 exposure. If it is assumed that all of the hydrogen removal is the result of conversion of $-CH_2-$ and $-CH_3$ groups to $>C=O$ and $-COOH$ groups and that the nitrogen uptake consists exclusively of NO_2 uptake (i.e., no chemical incorporation of any nitrogen containing species except NO_2), it is possible to determine if these two processes alone can account for the oxygen uptake by the coal. The results for the NO_2-treated coal are:

Time(min)		0	30	60	90	120	180
m_O (g O/100g coal)	Determined	0.0	12.68	14.50	16.76	16.72	17.05
	Calculated	0.0	11.49	14.34	14.31	16.70	16.71

Except for the point at 90 minutes, the values are quite close, which, in view of the potential error in m_O of up to 10 %, indicates that the oxygen uptake by the coal can indeed be accounted for by these two processes alone.

Such a comparison for the washed coals, however, yields a different result, as might be expected since the wash removes oxidized portions of the NO_2-treated coal, which contain most of the oxidized $-CH_2-$ groups. Theoretically, if all of the $>C=O$ and $-COOH$ groups are removed during the wash, then the oxygen uptake can be accounted for solely by the residual nitrogen uptake. The results obtained are:

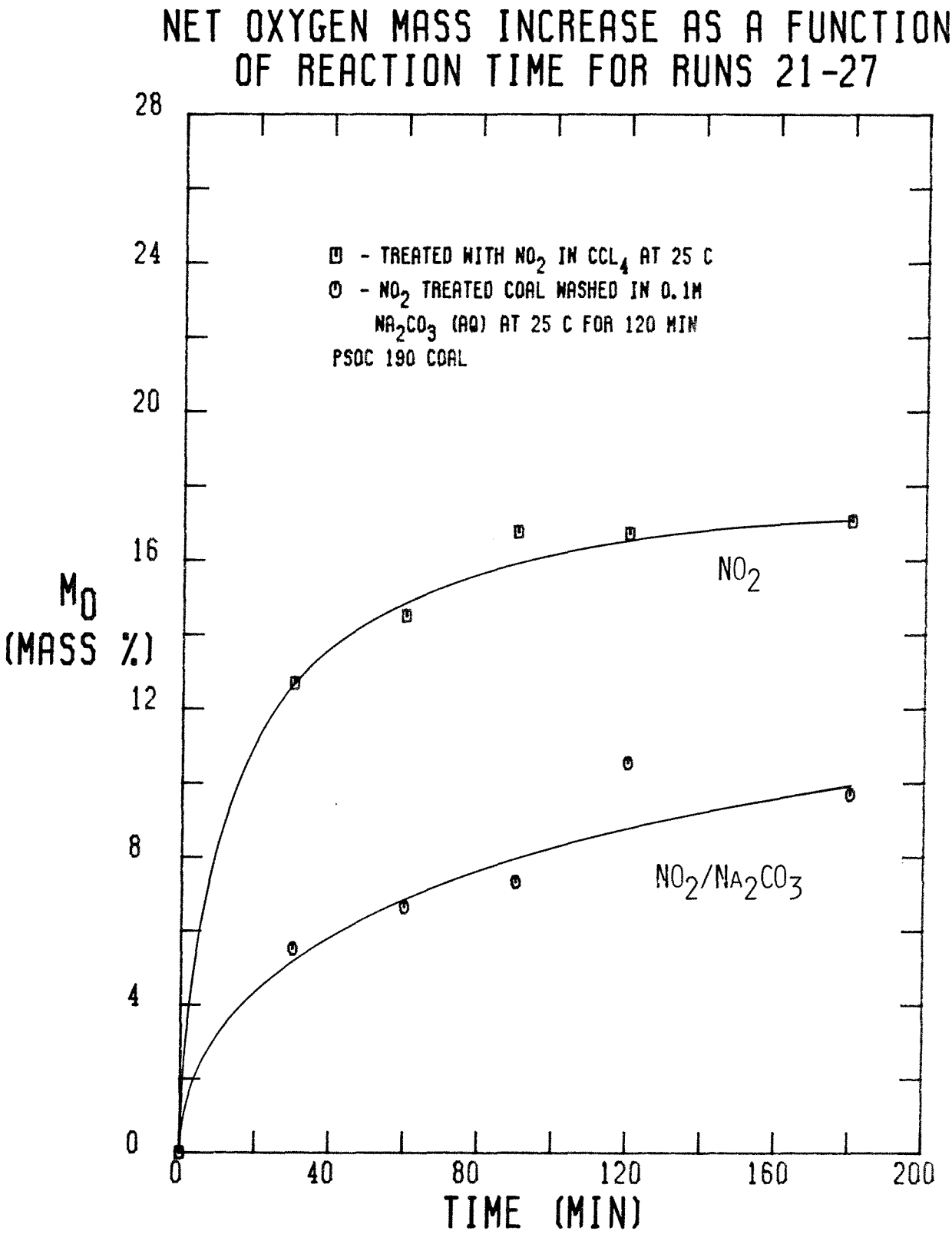
NET OXYGEN MASS INCREASE AS A FUNCTION OF REACTION TIME FOR RUNS 21-27
□ - TREATED WITH NO2 IN CCL4 AT 25 C
⊙ - NO2 TREATED COAL WASHED IN 0.1M NA2CO3 (AQ) AT 25 C FOR 120 MIN
PSOC 190 COAL
NO2
NO2/NA2CO3
MO (MASS %)
TIME (MIN)
0
4
8
12
16
20
24
28
0
40
80
120
160
200

FIGURE 4-80

Time(min)		0	30	60	90	120	180
m_O	Determined	0.0	5.51	6.63	7.31	10.53	9.69
(g O/100g coal)	H loss + N gain	0.0	11.86	16.12	14.33	15.87	16.05
	N gain only	0.0	4.94	5.71	6.48	6.20	6.52

The results indicate that removal of the oxidized $-CH_2-$ and $-CH_3$ groups does occur to a significant extent by virtue of the higher oxygen uptakes predicted on the basis of the hydrogen loss and residual nitrogen uptake taken together (i.e., no removal of oxidized $-CH_2-$ or $-CH_3$ groups). On the other hand, the residual nitrogen uptake, if taken as NO_2, cannot account for all of the increase in the oxygen content. This result simply implies that not all of the oxidized $-CH_2-$ and $-CH_3$ groups are removed during the wash.

The values of c_O for the coal treated with NO_2 at 20°C in the batch reactor and subsequently washed in 0.1 M Na_2CO_3 (aq) (Runs 33–37) are displayed graphically in Figure 4–81. Once again, the data for the NO_2-treated coal indicate that the process accounting for the oxygen uptake is essentially complete within 90 to 120 minutes with a rather large increase in c_O. On the other hand, the data for the washed coal show virtually no change in c_O during the processing, which implies that all of the oxygen added during the NO_2 processing is removed during the wash. These conclusions are supported by the values for the net oxygen mass increase, m_O, displayed in Figure 4–82. Whereas there is an uptake of roughly 12 g O/100g coal during the NO_2 treatment, the uptake drops to only 3 g O/100g coal after the wash.

A comparison of these values of m_O for the NO_2-treated coal with the values predicted on the basis of the nitrogen uptake and hydrogen loss yields:

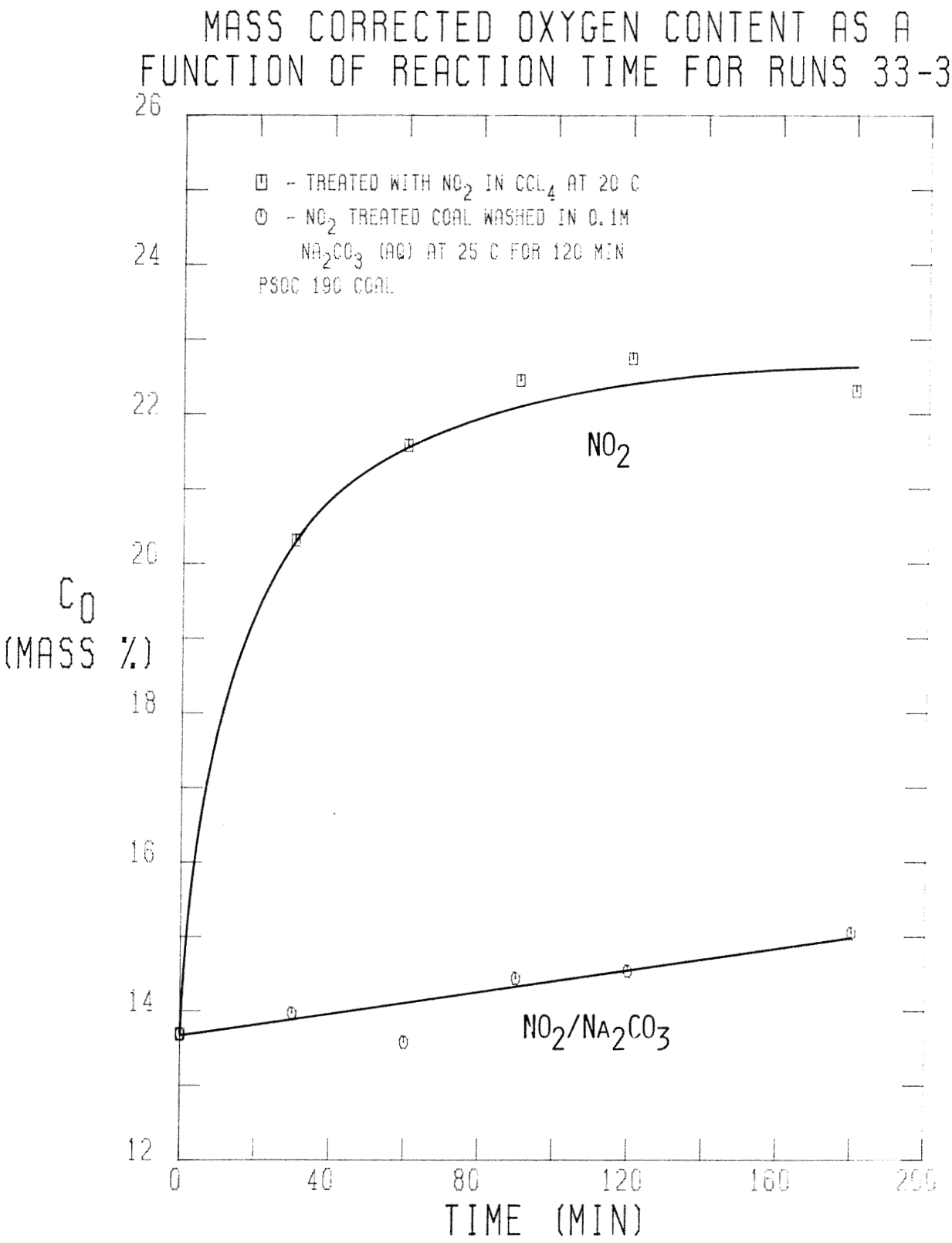
MASS CORRECTED OXYGEN CONTENT AS A FUNCTION OF REACTION TIME FOR RUNS 33-37
□ - TREATED WITH NO2 IN CCL4 AT 20 C
Ⓘ - NO2 TREATED COAL WASHED IN 0.1M NA2CO3 (AQ) AT 25 C FOR 120 MIN
PSOC 190 COAL
NO2
NO2/NA2CO3
CO (MASS %)
TIME (MIN)
26
24
22
20
18
16
14
12
0
40
80
120
160
200

FIGURE 4-81

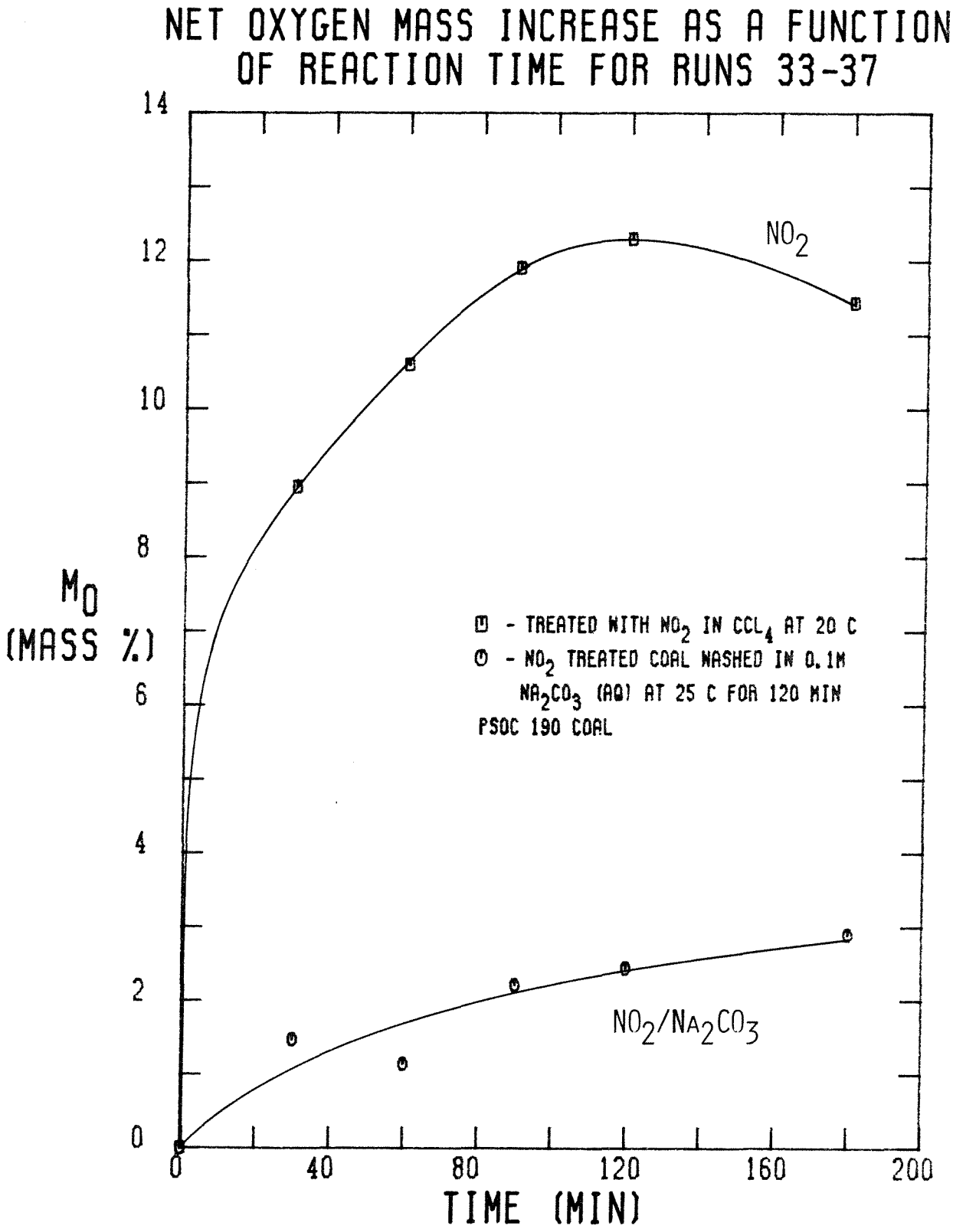
NET OXYGEN MASS INCREASE AS A FUNCTION OF REACTION TIME FOR RUNS 33-37
14
12
10
8
6
4
2
0
M_O (MASS %)
NO_2
□ - TREATED WITH NO_2 IN CCL_4 AT 20 C
○ - NO_2 TREATED COAL WASHED IN 0.1M NA_2CO_3 (AQ) AT 25 C FOR 120 MIN
PSOC 190 COAL
NO_2/NA_2CO_3
0
40
80
120
160
200
TIME (MIN)

FIGURE 4-82

	Time(min)	0	30	60	90	120	180
m_O	Determined	0.0	8.95	10.60	11.91	12.30	11.44
	H loss + N gain	0.0	11.06	13.39	14.20	15.28	16.60
(g O/100g coal)	N gain only	0.0	7.34	8.10	8.78	8.85	8.36

The values predicted by the nitrogen uptake (as NO_2) and hydrogen loss taken together yield values which are about 25 % too high, while the values predicted on the basis of nitrogen uptake alone are about 25 to 30 % too low. On this basis, it would appear that only about half of the oxidized $-CH_2-$ and $-CH_3$ groups are converted to $>C=O$ and $-COOH$ groups during the NO_2 treatment, while the other half lose their hydrogen without any oxygen uptake. For instance, the $-CH_2-$ group could be converted to $>C(NO_2)_2$ or $>C(NO)_2$ groups, where the oxygen uptake is included in the nitrogen uptake as NO_2. In any case, it should be remembered that the relative error in the oxygen determinations can be quite high, so that either set of predicted values of m_O probably agree within this relative error with the determined values of m_O. Thus, it would appear that the oxygen uptake can be accounted for by the hydrogen loss and nitrogen uptake during the NO_2 treatment. The problem of the accumulation of errors in the oxygen determinations is illustrated by the contrast between the determined values of m_O for the washed coal with those predicted on the basis of nitrogen uptake alone:

	Time(min)	0	30	60	90	120	180
m_O	Determined	0.0	1.47	1.14	2.21	2.44	2.90
(g O/100g coal)	Calculated	0.0	6.06	6.62	6.93	7.50	7.51

Indeed, the calculated values are roughly 3 to 5 times greater than the determined values. On this basis, only 20 to 35 % of the nitrogen uptake is in the form of NO_2, the rest being in the form of unoxidized nitrogen, which is highly unlikely. Rather, the cumulative errors in the oxygen determinations probably

account for the discrepancy, although another possibility suggests itself. If most of the added oxygen in the coal is due to NO_2, much of the sodium uptake may be by the NO_2 incorporated into the coal. As a result, oxygen which is coupled with sodium will be determined as mineral matter in the form of Na_2O rather than as organic oxygen in the coal. In this particular case, however, the sodium uptake can potentially trap only 2.2 g O/100g coal, which is still not enough to make the experimental and calculated values of m_O agree.

Figure 4–83 contains the values for the mass corrected oxygen content of the coal treated with NO_2 at 0°C in the batch reactor and subsequently washed in 0.1 M Na_2CO_3 (aq) (Runs 42–46) as a function of NO_2-exposure time. It should be noted that the data points for t = 180 minutes both deviate drastically from the trends set by the other points. Therefore, they were not considered when the curves were drawn, but are included in the plot for the sake of completeness. As in the previous set of runs, the rise in c_O is substantial for the NO_2-treated coal, but a little more gradual. Because c_O has not levelled off after 120 minutes of NO_2 treatment, it can be concluded that the process accounting for the oxygen uptake is not yet complete. It is interesting to note that c_O for the washed coal actually drops relative to c_O for the pretreated coal, which implies that the wash removes portions of the pretreated coal with oxygen contents greater than the overall oxygen content of the raw coal. These conclusions are supported by the values of m_O for this same set of runs shown in Figure 4–84. Indeed, the wash of the NO_2-treated coal does actually result in a small net loss of oxygen, which would result if the oxygen were not uniformly distributed in the coal and those portions with the higher oxygen contents were removed during the wash. Such a non-uniform distribution would occur if the coal had been exposed to air for long periods of time which would allow the coal surface to have become oxidized. In view of the large errors in the oxygen determinations, however, it is probably

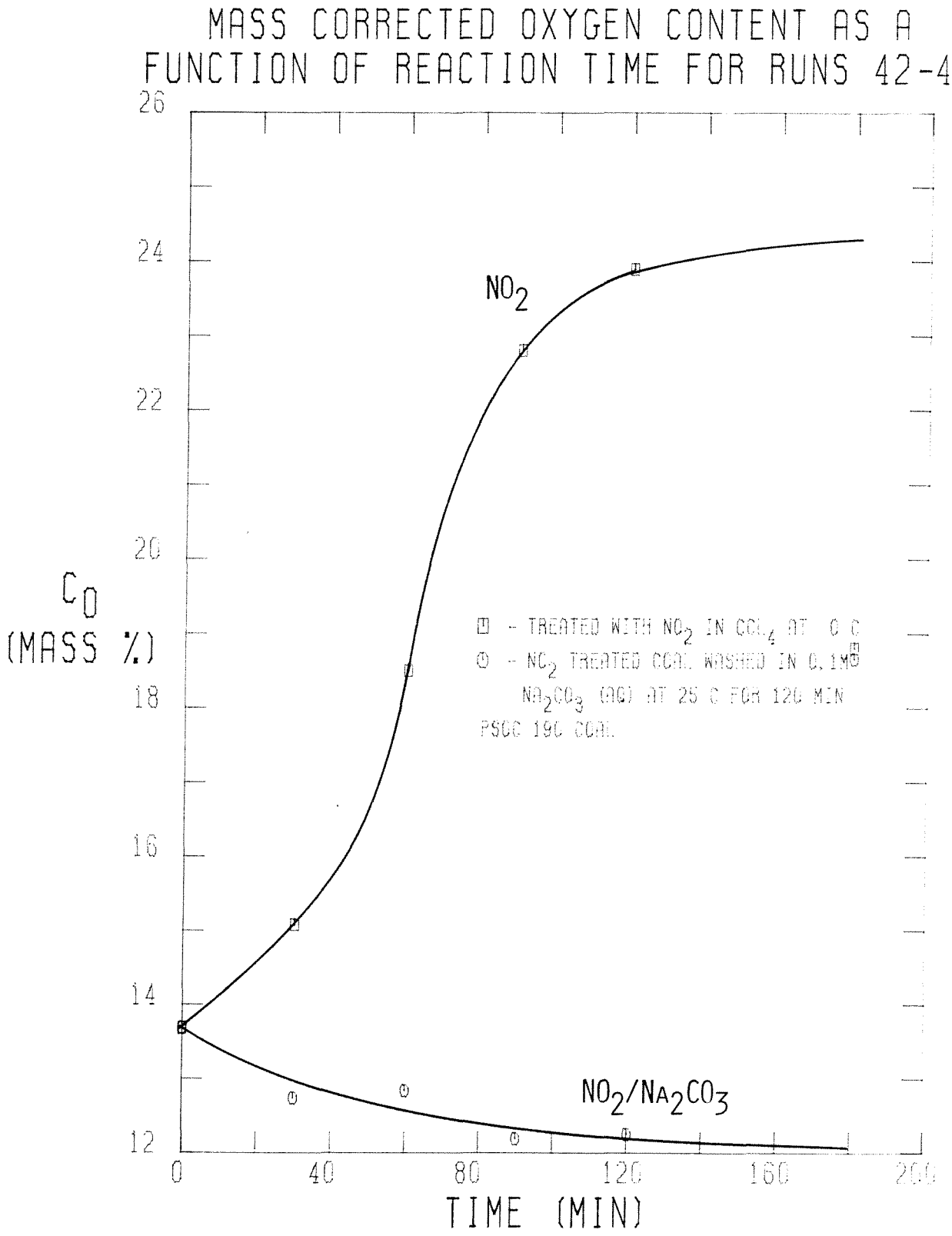
MASS CORRECTED OXYGEN CONTENT AS A FUNCTION OF REACTION TIME FOR RUNS 42-46
26
24
22
20
18
16
14
12
C_O (MASS %)
NO_2
NO_2/NA_2CO_3
0
40
80
120
160
200
TIME (MIN)

FIGURE 4-83

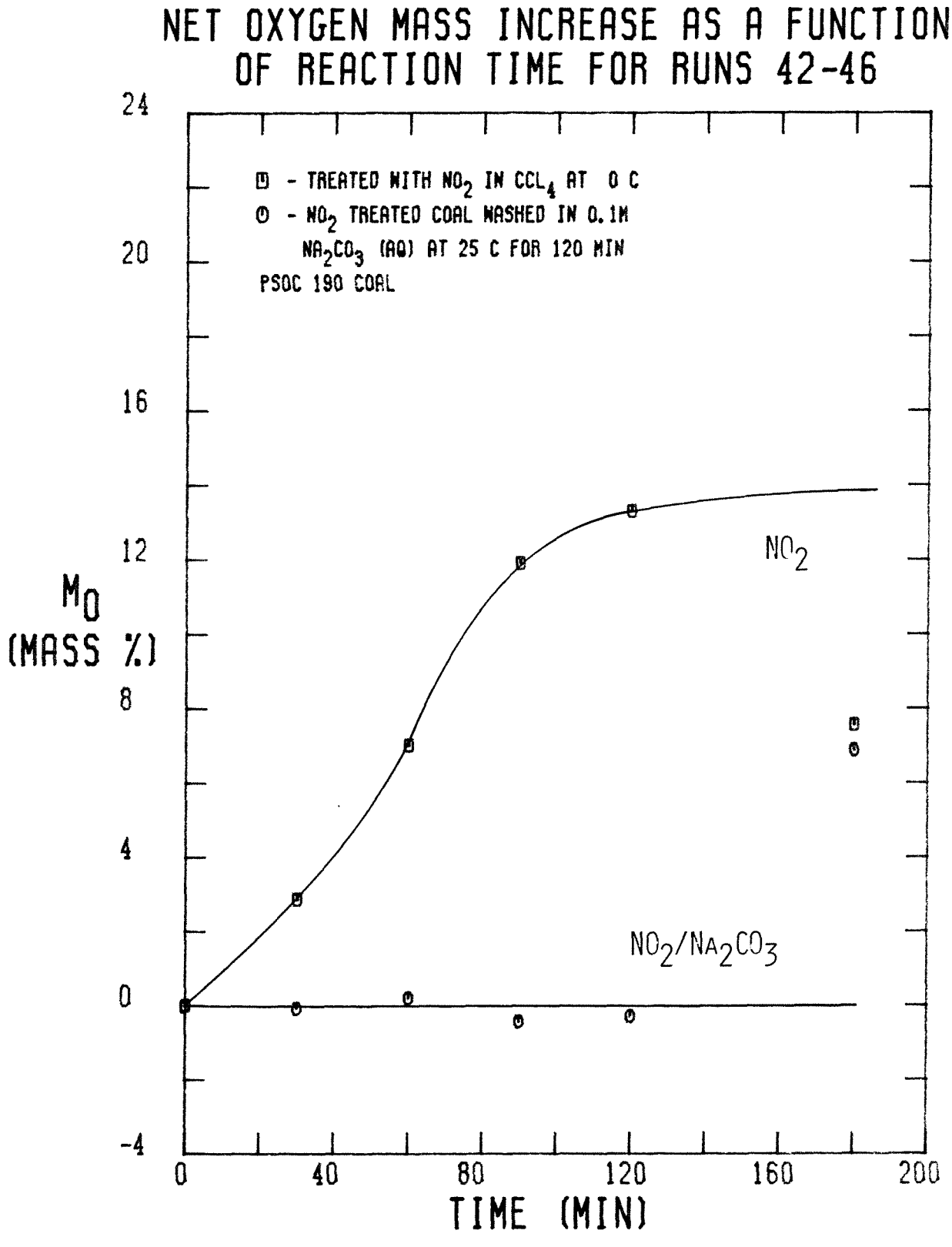
NET OXYGEN MASS INCREASE AS A FUNCTION OF REACTION TIME FOR RUNS 42-46
□ - TREATED WITH NO2 IN CCL4 AT 0 C
○ - NO2 TREATED COAL WASHED IN 0.1M NA2CO3 (AQ) AT 25 C FOR 120 MIN
PSOC 190 COAL
NO2
NO2/NA2CO3
MO (MASS %)
TIME (MIN)
24
20
16
12
8
4
0
-4
0
40
80
120
160
200

FIGURE 4-84

safer to conclude that there is no net oxygen uptake after the NO_2-treated coal is washed in 0.1 M Na_2CO_3 (aq).

A comparison of the determined and calculated values of m_O for the NO_2 treated coals can be based on the following results:

Time(min)		0	30	60	90	120	180
m_O	Determined	0.0	2.86	7.01	11.90	12.30	7.57
(g O/100g coal)	Calculated	0.0	6.18	7.22	7.69	8.01	8.20

These values show that not all of the oxygen uptake can be attributed to the uptake of NO_2 alone. Unfortunately, the hydrogen analyses for these runs cannot be trusted because some of them indicate a net hydrogen increase during the NO_2 treatment, which cannot be correct. When the cumulative errors in the determined values of m_O are taken into account, however, it is probably safe to conclude that the oxygen uptake is the result of nitrogen uptake as NO_2 and conversion of $-CH_2-$ and $-CH_3$ groups to $>C=O$ and $-COOH$ groups. The determined and calculated values of m_O for the washed coal are:

Time(min)		0	30	60	90	120	180
m_O	Determined	0.0	-0.09	0.19	-0.45	-0.30	6.88
(g O/100g coal)	Calculated	0.0	5.09	6.18	6.13	6.36	6.72

There are two explanations for the gross disparity between these sets of values of m_O. The first is that the error in the determined values of m_O is on the order of 6 g O/100g coal, which is high, but not outside the realm of possibility. Even if sodium trapping of oxygen is considered, the error is still on the order of 4 g O/100g coal. The other possibility is that most of the oxygen in the pretreated coal is on the coal surface. Because the Na_2CO_3 (aq) wash probably removes most of the coal derived products of the NO_2 treatment from the coal surface, a net loss of the original oxygen in the coal would occur. This loss could then be offset by the increase in oxygen content due to NO_2 uptake to a certain

degree. In this case, the loss in original oxygen is just matched by the uptake in NO_2. Because the PSOC 190 was exposed to weather for five years after it was mined, this explanation would seem viable, if it is assumed that the pretreatment does not remove the surface oxygen. Yet, the results for the PSOC 190 treated at 20°C seem to correlate very well with the calculated values, so the disparity must be attributed to errors in the hydrogen analyses. It is unfortunate that the oxygen determinations could not be done directly in order to mitigate the error.

The effect of temperature on the change in c_O for the coal treated with NO_2 is shown graphically in Figure 4–85. The loci demonstrate that c_O increases at a faster rate at higher temperatures during the initial 60 minutes of the NO_2 treatment. At about 90 minutes, c_O for the coals treated with NO_2 at 50°C and 20°C seems to level off, while c_O for the coal treated with NO_2 at 0°C continues to increase beyond that of the 20°C coal. If the point at 180 minutes for the coal treated at 0°C is neglected, then the value of c_O for the coal treated at 0°C actually exceeds that of the coal treated at 20°C. There is no logical explanation for this behavior, although it should be remembered that the cumulative error in the oxygen determinations may account for the observed temperature effect. The corresponding values of m_O are displayed in Figure 4–86, where they basically show the same behavior as the values of c_O, including the crossing of the 0 and 20°C curves at 90 minutes. It is interesting to note that not all of the oxygen uptake at 50°C can be accounted for by the nitrogen uptake and hydrogen loss after 90 minutes. The determined and calculated values for m_O are:

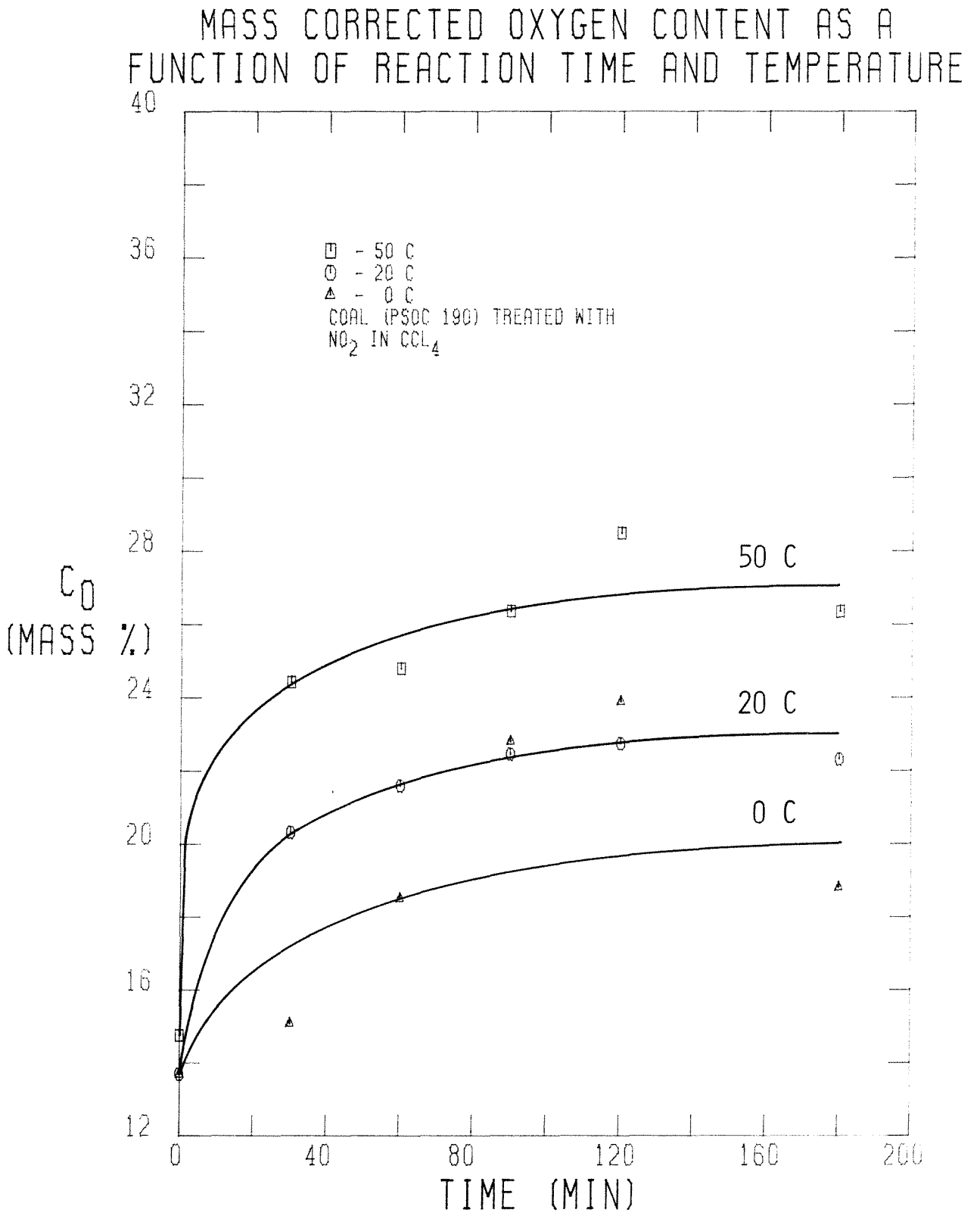
MASS CORRECTED OXYGEN CONTENT AS A FUNCTION OF REACTION TIME AND TEMPERATURE
□ - 50 C
○ - 20 C
△ - 0 C
COAL (PSOC 190) TREATED WITH NO_2 IN CCL_4
50 C
20 C
0 C
C_O (MASS %)
TIME (MIN)
40
36
32
28
24
20
16
12
0
40
80
120
160
200

FIGURE 4-85

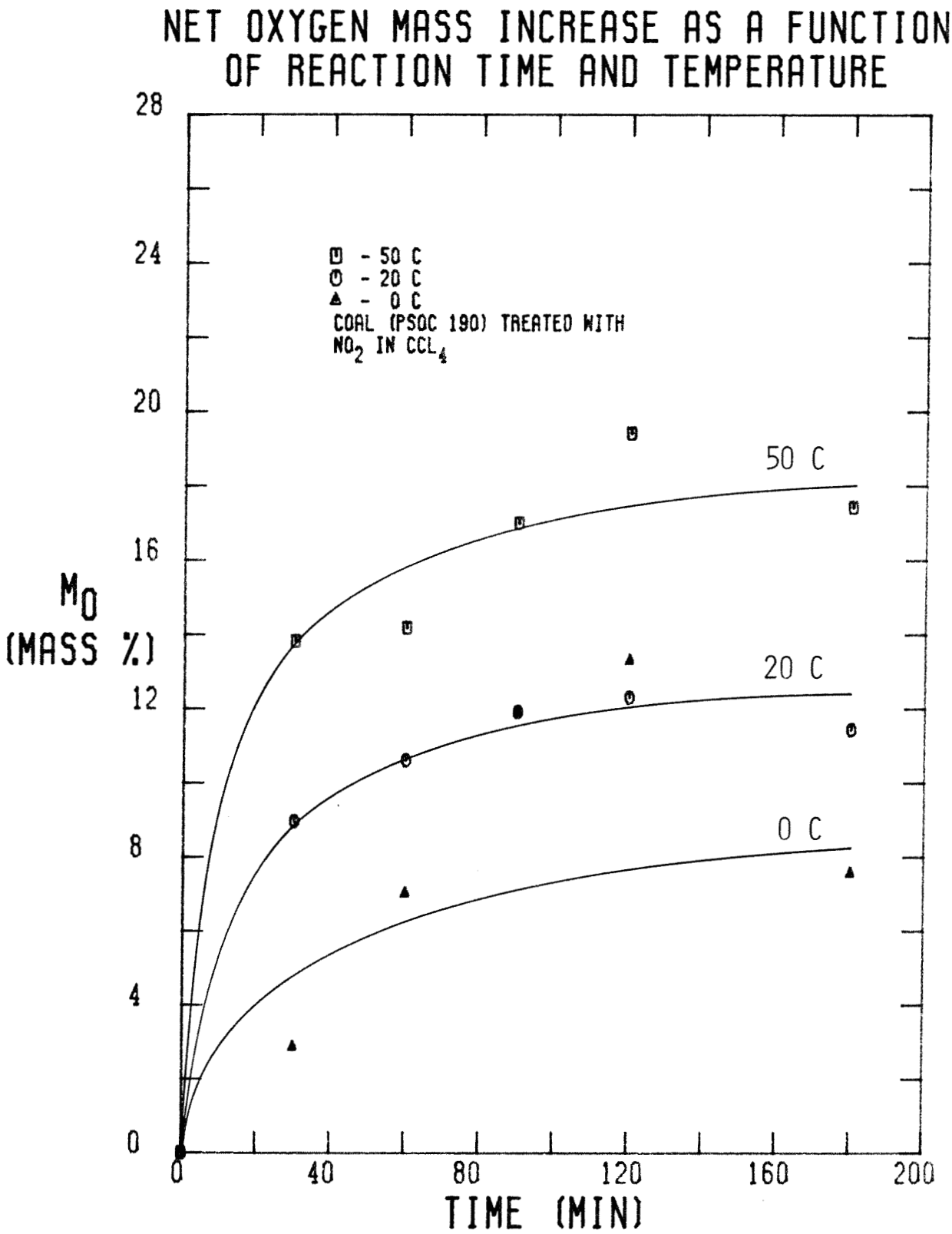
NET OXYGEN MASS INCREASE AS A FUNCTION OF REACTION TIME AND TEMPERATURE
50 C - 50 C
20 C - 20 C
0 C - 0 C
COAL (PSOC 190) TREATED WITH NO_2 IN CCL_4
50 C
20 C
0 C
M_O (MASS %)
TIME (MIN)
0
4
8
12
16
20
24
28
0
40
80
120
160
200

FIGURE 4-86

Time(min)		0	30	60	90	120	180
m_O	Determined	0.0	13.82	14.18	17.00	19.42	17.43
(g O/100g coal)	Calculated	0.0	11.86	13.58	12.46	11.92	13.36

These results contrast with those for the 20°C runs, where the values calculated for m_O on the basis of nitrogen uptake and hydrogen loss exceeded the determined values. Thus, at 50°C, another process may account for oxygen uptake, such as the formation of alcohols or phenols, which do not result in any hydrogen loss. In any event, more extensive oxygen uptake at 50°C during the NO_2 treatment correlates well with the much greater dissolution of the coal in 0.1 M Na_2CO_3 (aq) than the coals treated with NO_2 at 20 and 0°C.

Figure 4–87 demonstrates the effect of the NO_2-treatment temperature on the value of c_O for the subsequently washed coal. The primary feature of the plot is that the NO_2 treatment at 20°C results in a net increase of roughly 1.5 mass percent in c_O while the NO_2 treatment at 0°C results in a net loss of about 1.5 mass percent in c_O. The difference can be attributed to the lower nitrogen uptake at 0°C than at 20°C. It is also obvious that the value determined for c_O after 180 minutes of NO_2 exposure at 0°C is probably in error, and has consequently been ignored. The corresponding values of m_O are shown in Figure 4–88, where they display the same trends as the values of c_O. In both curves, however, the net amount of added oxygen never exceeds 3 g O/100g coal. Thus, in view of the potential error in m_O, it would be safe to conclude that after the wash of the NO_2-treated coal, there is essentially no net oxygen mass increase in the coal. The added sodium, however, should trap some oxygen (up to 2.2 g O/100g coal). The oxygen then appears as mineral matter and not organic oxygen.

The effect of the initial concentration of NO_2, $(NO_2)_0$, on c_O after 120 minutes of exposure is displayed graphically in Figure 4–89. The curve which

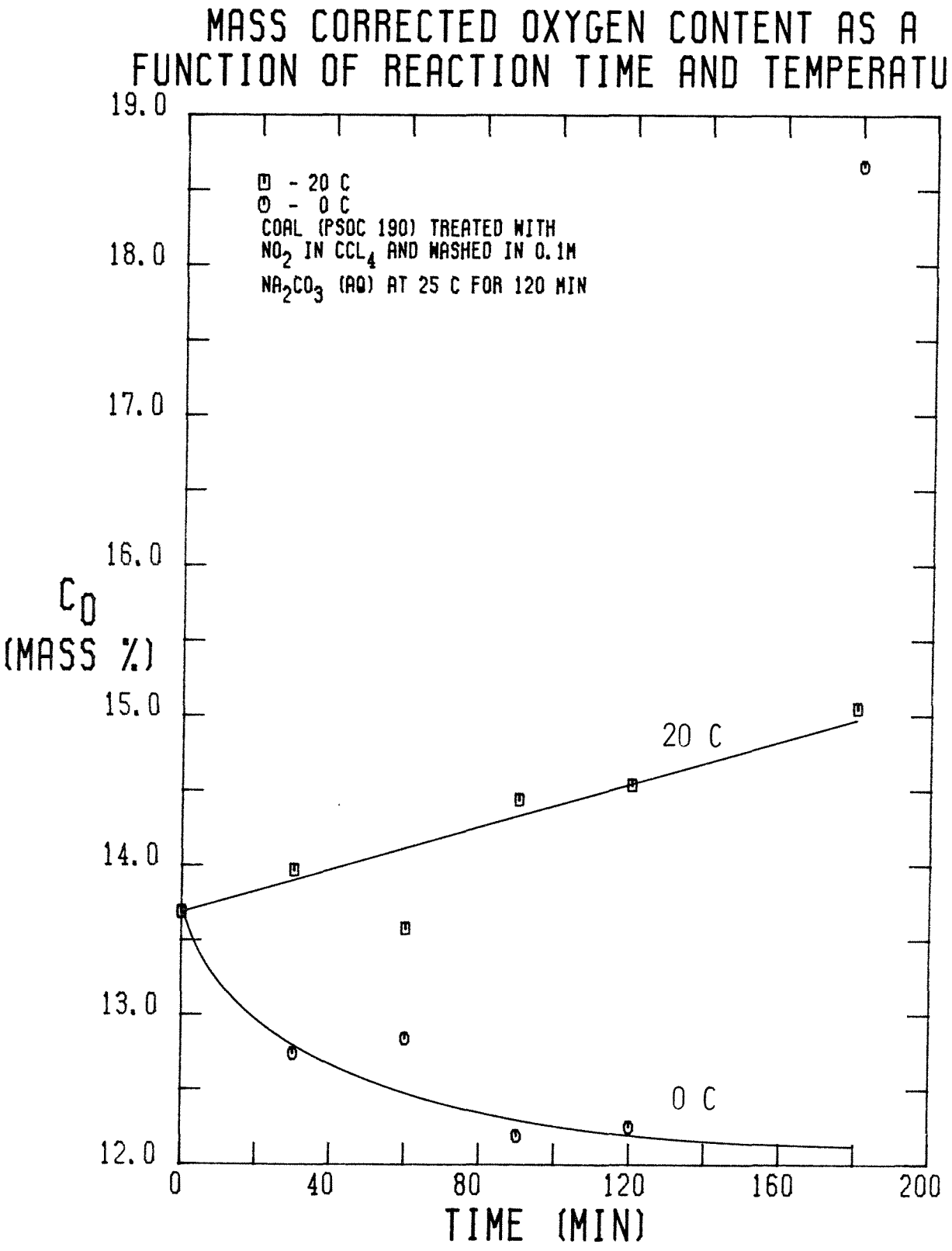
MASS CORRECTED OXYGEN CONTENT AS A FUNCTION OF REACTION TIME AND TEMPERATURE
□ - 20 C
○ - 0 C
COAL (PSOC 190) TREATED WITH
NO_2 IN CCL_4 AND WASHED IN 0.1M
NA_2CO_3 (AQ) AT 25 C FOR 120 MIN
20 C
0 C
C_O
(MASS %)
19.0
18.0
17.0
16.0
15.0
14.0
13.0
12.0
0
40
80
120
160
200
TIME (MIN)

FIGURE 4-87

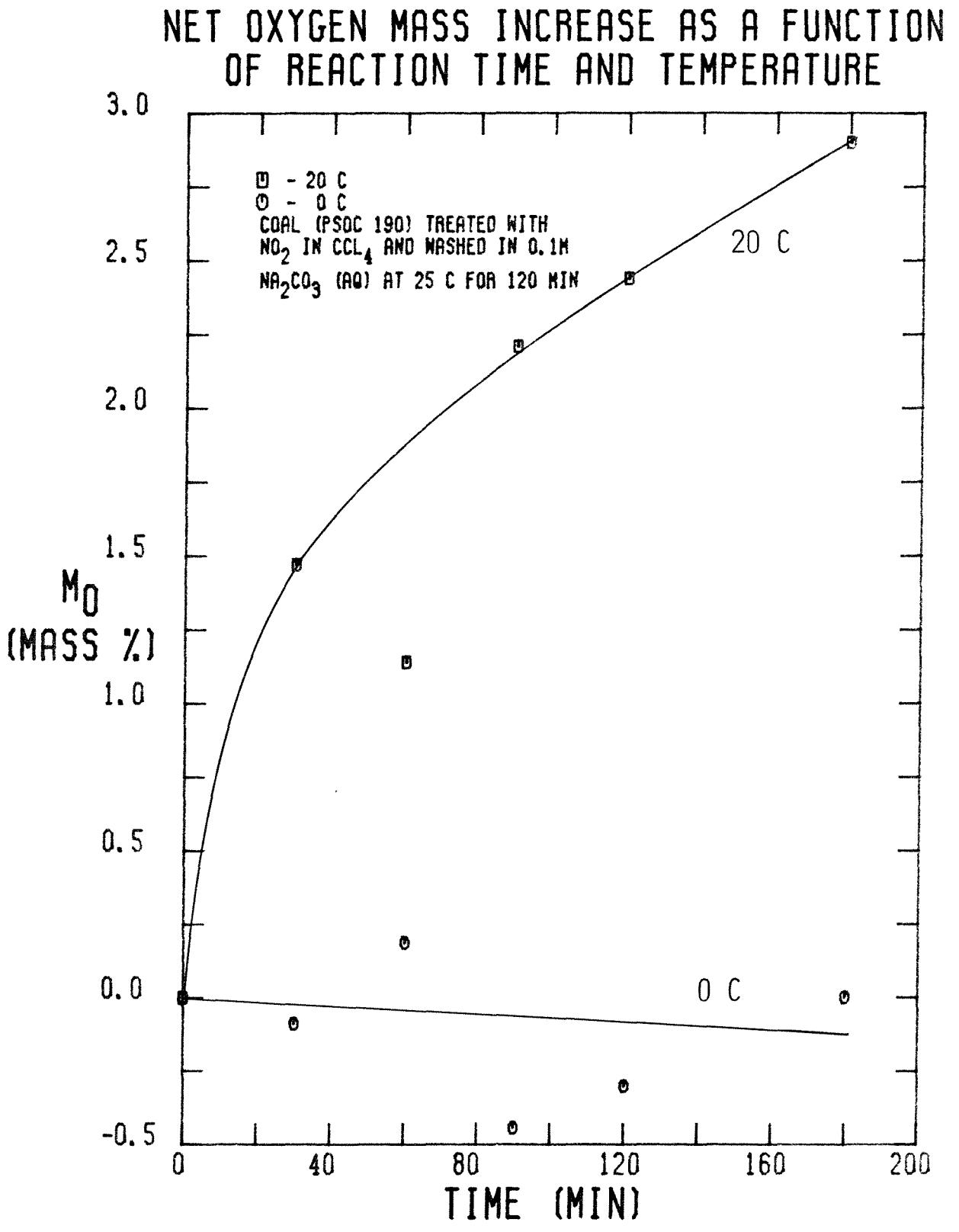
NET OXYGEN MASS INCREASE AS A FUNCTION OF REACTION TIME AND TEMPERATURE
□ - 20 C
○ - 0 C
COAL (PSOC 190) TREATED WITH NO2 IN CCL4 AND WASHED IN 0.1M NA2CO3 (AQ) AT 25 C FOR 120 MIN
20 C
0 C
MO (MASS %)
TIME (MIN)
3.0
2.5
2.0
1.5
1.0
0.5
0.0
-0.5
0
40
80
120
160
200

FIGURE 4-88

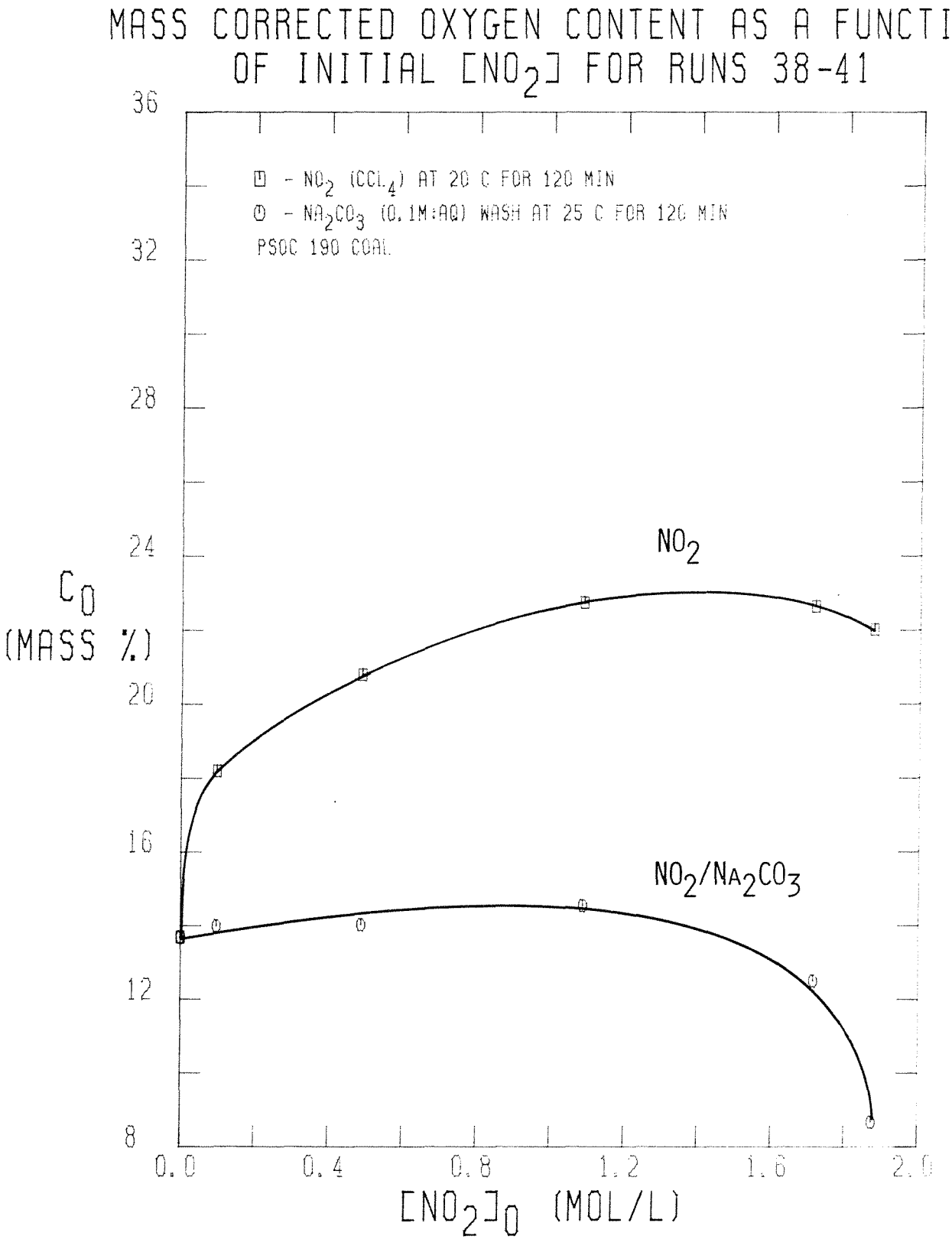
MASS CORRECTED OXYGEN CONTENT AS A FUNCTION OF INITIAL [NO2] FOR RUNS 38-41
□ - NO2 (CCl4) AT 20 C FOR 120 MIN
Ⓘ - NA2CO3 (0.1M:AQ) WASH AT 25 C FOR 120 MIN
PSOC 190 COAL
NO2
NO2/NA2CO3
C0 (MASS %)
[NO2]0 (MOL/L)
36
32
28
24
20
16
12
8
0.0
0.4
0.8
1.2
1.6
2.0

FIGURE 4-89

corresponds to the NO_2-treated coal shows a unique feature, namely a maximum at roughly $(NO_2)_0$ = 1.4 F. The decrease in c_O at greater values of $(NO_2)_0$ could be caused by the increased uptake of material by the coal which does not contain oxygen relative to the uptake of material which does contain oxygen. In this particular system, the only possibility is the CCl_4 solvent, but the values of c_O have already been corrected for the CCl_4 uptake. Another possibility is that the amount of oxidized coal material removed is higher at larger values of $(NO_2)_0$. This possibility is supported somewhat by the carbon content data which show a slight increase in c_C once $(NO_2)_0$ exceeds 1.7 F. In any case, the decrease in c_O at high values of $(NO_2)_0$ is slight and may be due simply to errors in the oxygen determination. The curve for the washed coal actually shows a decrease in c_O as $(NO_2)_0$ increases. This behavior supplies further evidence to support the theory that the sodium is trapping the added oxygen. As $(NO_2)_0$ is increased, so is the extent of the oxidation in the coal, which should result in more uptake of sodium during the Na_2CO_3 (aq) wash. Indeed, the corresponding values of the net increase in the mass of the mineral matter (Figure 4–109) are quite consistent with the values of m_O in this respect.

The corresponding values of m_O are shown in Figure 4–90 as a function of $(NO_2)_0$. The behavior of m_O parallels that of c_O for both the NO_2-treated coal and the subsequently washed coal, for the same reasons as cited above for the trends in c_O. In the case of the NO_2-treated coal, the values of m_O calculated on the basis of the nitrogen uptake and the hydrogen loss can be compared with the determined values of m_O:

Time(min)		0	30	60	90	120	180
m_O	Determined	0.0	5.50	9.50	12.30	12.75	12.24
(g O/100g coal)	Calculated	0.0	6.85	10.48	15.28	12.64	12.92

In every case, the calculated value of m_O slightly exceeds the determined value,

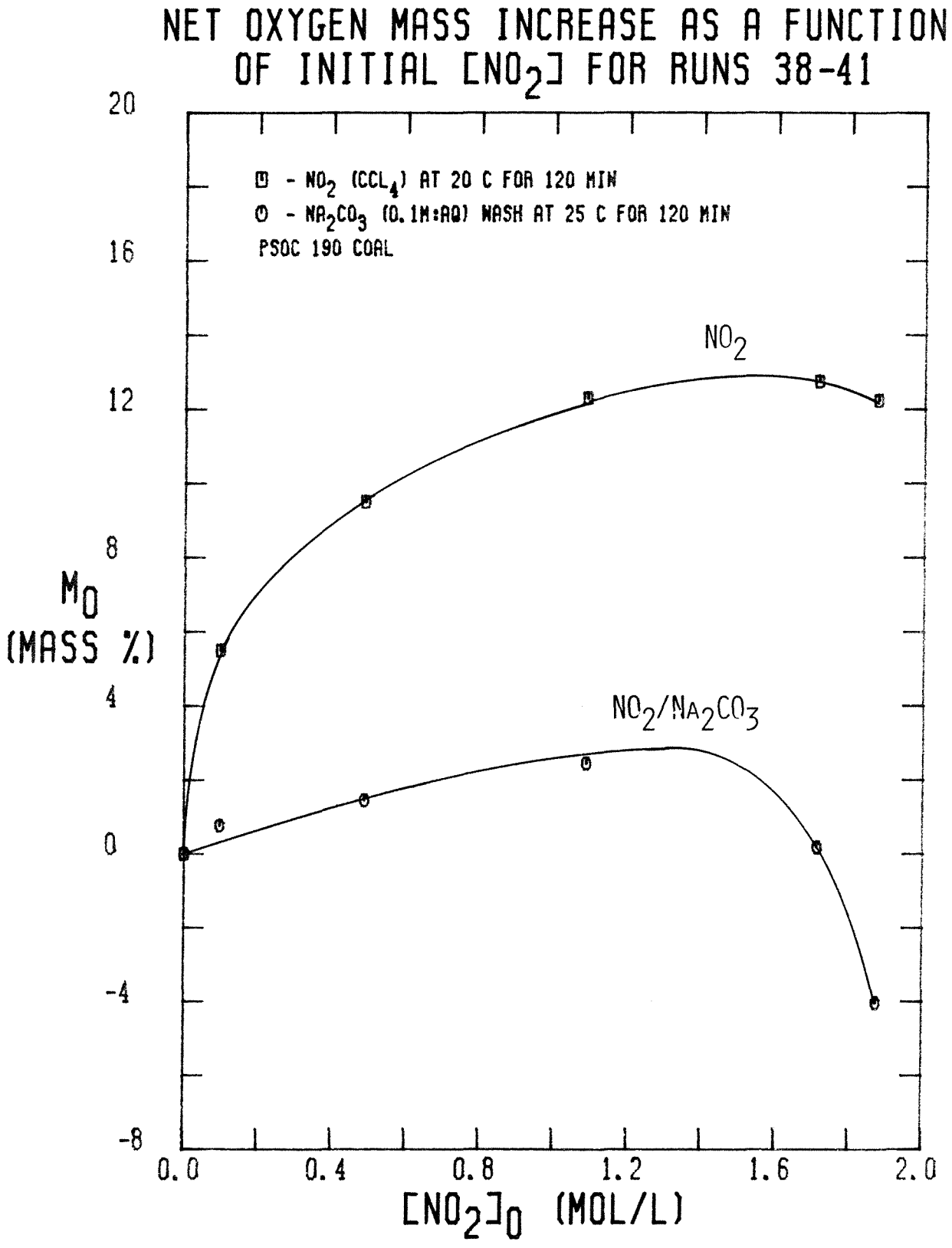
NET OXYGEN MASS INCREASE AS A FUNCTION OF INITIAL [NO2] FOR RUNS 38-41
□ - NO2 (CCL4) AT 20 C FOR 120 MIN
○ - NA2CO3 (0.1M:AQ) WASH AT 25 C FOR 120 MIN
PSOC 190 COAL
NO2
NO2/NA2CO3
MO (MASS %)
[NO2]O (MOL/L)
20
16
12
8
4
0
-4
-8
0.0
0.4
0.8
1.2
1.6
2.0

FIGURE 4-90

but they agree within the potential error for the determined value of m_O. Thus, the oxygen uptake during the NO_2 treatment is the result of the uptake of NO_2 by the coal and the conversion of $-CH_2-$ and $-CH_3$ groups to $>C=O$ and $-COOH$ groups in the coal. The values of m_O for the washed coal indicate again that the net oxygen mass increase due to NO_2 uptake is offset to a varying degree by the preferential removal of portions of the coal rich in oxygen and the trapping of oxygen by sodium.

The effect of the coal particle porosity can be determined if coals with similar elemental compositions but different pore volumes are treated in an identical manner. In this study, the PSOC 276 has a pore volume about four times smaller than that of the PSOC 190, yet both coals have approximately the same elemental composition. The values of c_O for the PSOC 276 treated with NO_2 at 20°C in the batch reactor and subsequently washed in 0.1 M Na_2CO_3 (aq) are shown in Figure 4–91 as a function of NO_2-exposure time. During the NO_2 treatment, c_O rises rapidly within the first 30 minutes, and then rises more gradually. Even after 180 minutes of NO_2 exposure, c_O still shows no sign of beginning to level off. The trend in c_O is quite similar to that in the nitrogen content as well. The curve for the washed coal is essentially parallel to, but lower than, that of the unwashed coal, demonstrating that the wash removes material from the coal which is rich in oxygen and that the added sodium traps oxygen as well. Ostensibly, the material removed is the portion of the coal which is heavily oxidized by the NO_2.

The corresponding net oxygen mass increase, m_O, of the processed coal is shown as a function of NO_2-reaction time in Figure 4–92. The basic trend in m_O is the same as in c_O, namely a very rapid increase followed by a more gradual increase which appears to be linear with respect to the NO_2-exposure time. Thus, the process which accounts for the uptake of oxygen is not complete

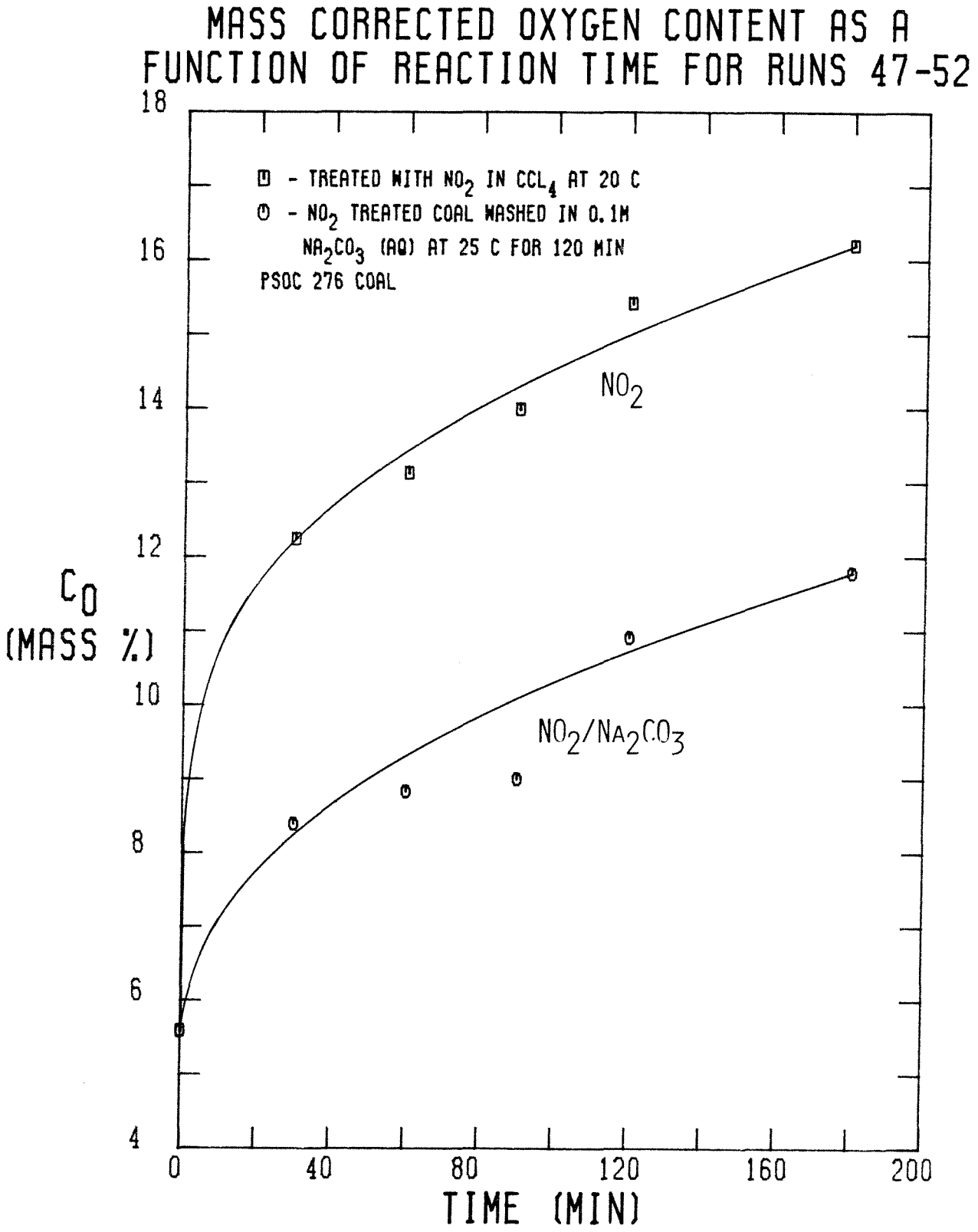
MASS CORRECTED OXYGEN CONTENT AS A FUNCTION OF REACTION TIME FOR RUNS 47-52
□ - TREATED WITH NO2 IN CCL4 AT 20 C
⊙ - NO2 TREATED COAL WASHED IN 0.1M NA2CO3 (AQ) AT 25 C FOR 120 MIN
PSOC 276 COAL
NO2
NO2/NA2CO3
CO (MASS %)
TIME (MIN)
18
16
14
12
10
8
6
4
0
40
80
120
160
200

FIGURE 4-91

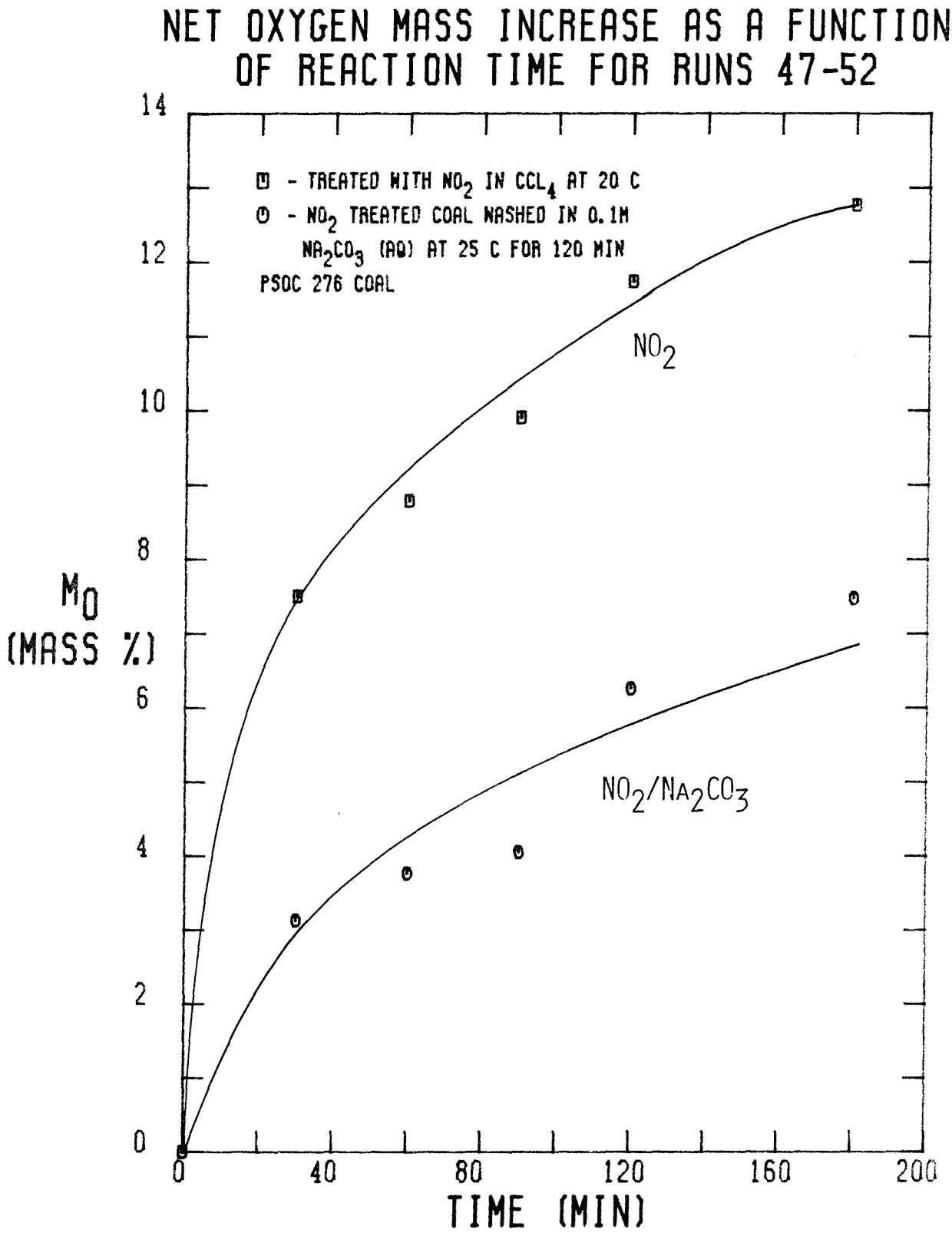
NET OXYGEN MASS INCREASE AS A FUNCTION OF REACTION TIME FOR RUNS 47-52
□ - TREATED WITH NO2 IN CCL4 AT 20 C
○ - NO2 TREATED COAL WASHED IN 0.1M NA2CO3 (AQ) AT 25 C FOR 120 MIN
PSOC 276 COAL
NO2
NO2/NA2CO3
MO (MASS %)
TIME (MIN)
0
2
4
6
8
10
12
14
0
40
80
120
160
200

FIGURE 4-92

within 180 minutes. The value of m_O calculated on the basis of nitrogen uptake and hydrogen loss, together with the determined values of m_O are:

Time(min)		0	30	60	90	120	180
m_O	Determined	0.0	7.50	8.78	9.90	11.74	12.76
(g O/100g coal)	Calculated	0.0	6.58	7.02	8.57	8.57	11.50

In this instance, the calculated values are about 10 to 20 % lower than the determined values. If the determined values are assumed to be accurate, then the difference could be attributed to the formation of alcohols, in which no nitrogen is taken up or hydrogen is lost by the coal. Thus, in the case of the NO_2 treatment of the PSOC 276 coal, the data are consistent with three processes responsible for oxygen uptake; ketone and carboxylic acid formation with hydrogen loss, alcohol formation with no hydrogen loss, and NO_2 uptake.

The curve for the values of m_O for the washed coal has the same shape as that for the unwashed coal, but the value of m_O is about 50 % lower. The values imply that roughly half of the net amount of added oxygen is either removed by the wash or trapped by added sodium. The values of m_O calculated on the basis of nitrogen uptake alone can be compared with the actually determined values:

Time(min)		0	30	60	90	120	180
m_O	Determined	0.0	3.13	3.76	4.04	6.26	7.47
(g O/100g coal)	Calculated	0.0	3.90	5.08	5.95	6.03	6.94

In this case, the calculated values exceed the determined values when the NO_2 exposure is less than 120 minutes, but then fall below at longer NO_2-treatment times, which implies that the net oxygen increase due to NO_2 uptake is offset by the removal of the oxygen rich portions of the NO_2-treated coal, which is consistent with the earlier interpretation of the determined values of m_O for the washed coals. The amount of sodium added to the PSOC 276 can only account for the trapping of a maximum of 1.0 g O/100g coal. Consequently, most of the

oxygen removal by the Na_2CO_3 (aq) wash of the NO_2-treated PSOC 276 can be attributed to the removal of oxidized portions of the coal.

The values of c_O for the two coals treated with NO_2 at 20°C in the batch reactor are shown graphically in Figure 4–93 as a function of reaction time for the purpose of comparison. Although the initial oxygen contents differ by 8 mass percent, both show a rise of roughly 6 mass percent within the first 30 minutes. The value of c_O for the NO_2-treated PSOC 190 rises only another 2.5 mass percent, however, before levelling off at 90 minutes, while the value of c_O for the NO_2-treated PSOC 276 continues to rise linearly with increasing reaction time by another 4 mass percent at 180 minutes. The corresponding values of m_O for the two NO_2-treated coals are shown in Figure 4–94. This plot clearly shows that during the first 120 minutes of treatment, about 15 % less oxygen is taken up by the PSOC 276 than by the PSOC 190. Therefore, the pore structure of the coal has little or no effect on the uptake of oxygen. This is not surprising, since roughly 80 % of the oxygen uptake may be attributed to the uptake of NO_2, the extent of which is not affected by the coal porosity.

Figure 4–95 contains the values of c_O for the two NO_2-treated coals washed in 0.1 M Na_2CO_3 (aq) in graphical form. It is immediately obvious that while there is hardly any change in the oxygen content of the washed PSOC 190, there is a significant increase in c_O in the washed PSOC 276. These results imply that while essentially all of the added oxygen is either removed from the NO_2-treated PSOC 190, presumably in the form of oxidized coal components, or trapped by the added sodium to form Na_2O, quite a large amount of the oxidized PSOC 276 remains after the wash. The values of m_O for the washed coals shown in Figure 4–96 demonstrate this difference more clearly. In particular, the net oxygen mass increase of the washed PSOC 276 is about three times as great as that of the washed PSOC 190. The results of this comparison are consistent with the

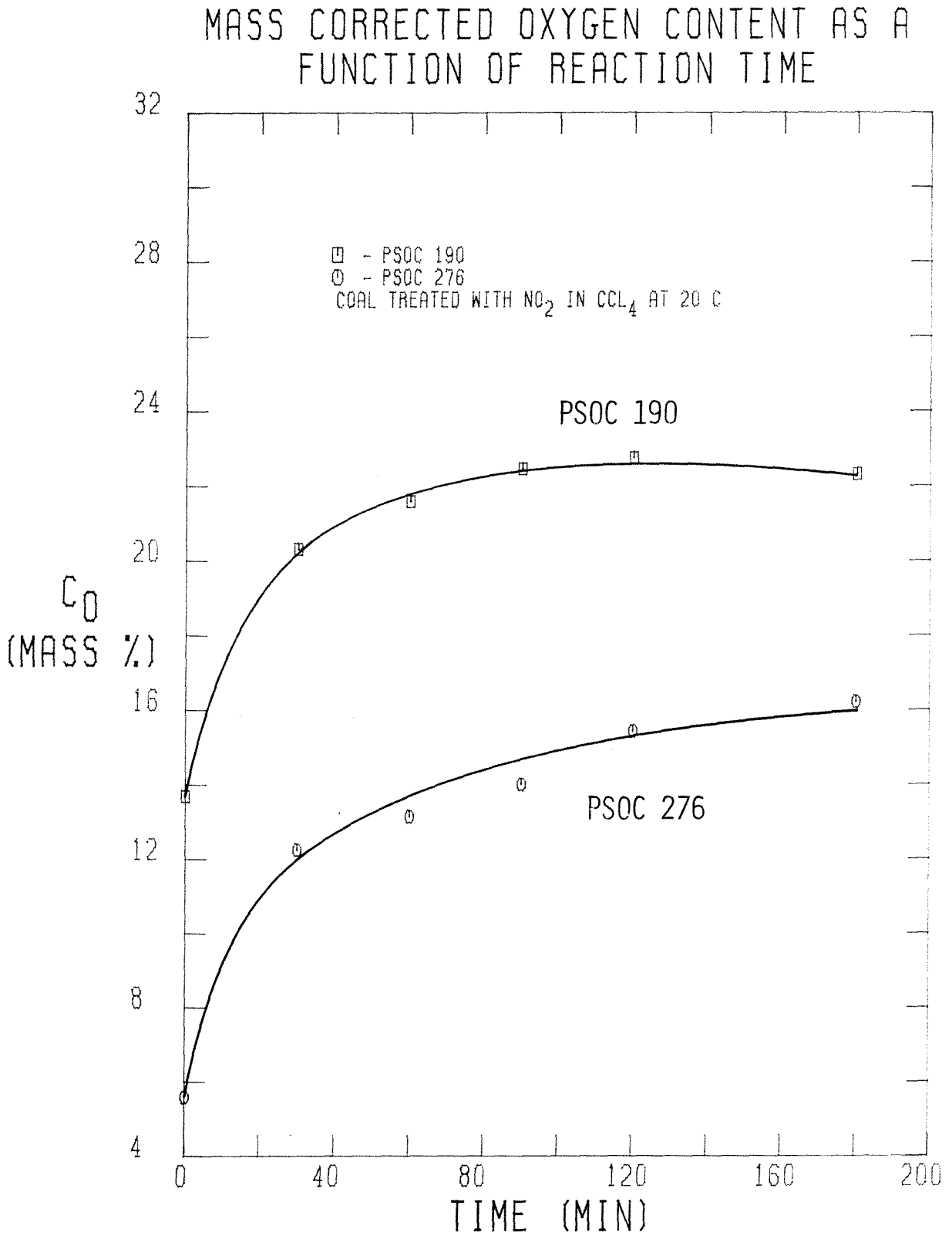
MASS CORRECTED OXYGEN CONTENT AS A FUNCTION OF REACTION TIME
□ - PSOC 190
○ - PSOC 276
COAL TREATED WITH NO_2 IN CCL_4 AT 20 C
PSOC 190
PSOC 276
C_O (MASS %)
TIME (MIN)
32
28
24
20
16
12
8
4
0
40
80
120
160
200

FIGURE 4-93

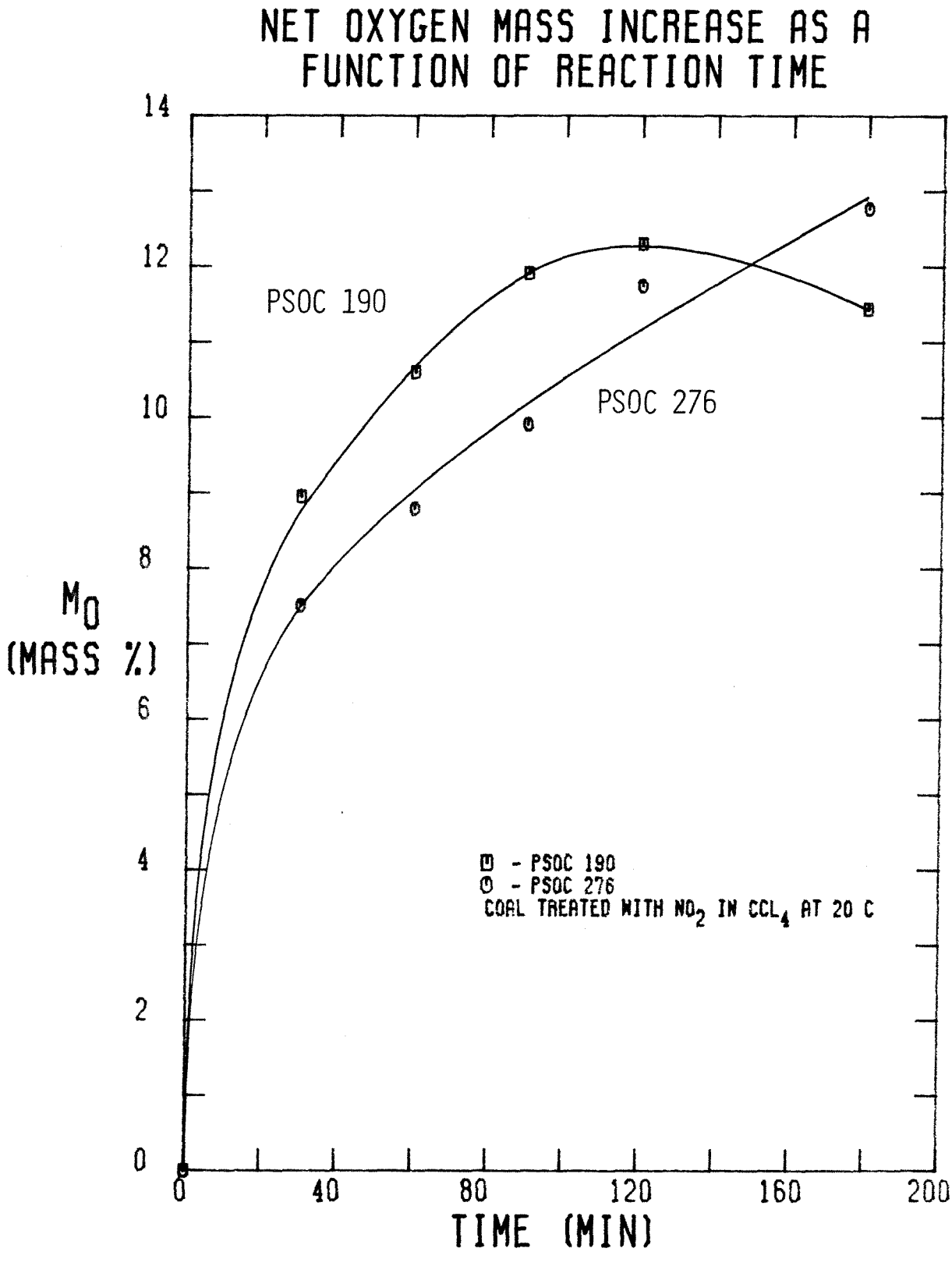
NET OXYGEN MASS INCREASE AS A FUNCTION OF REACTION TIME
14
12
10
8
6
4
2
0
M_O (MASS %)
PSOC 190
PSOC 276
□ - PSOC 190
○ - PSOC 276
COAL TREATED WITH NO_2 IN CCL_4 AT 20 C
0
40
80
120
160
200
TIME (MIN)

FIGURE 4-94

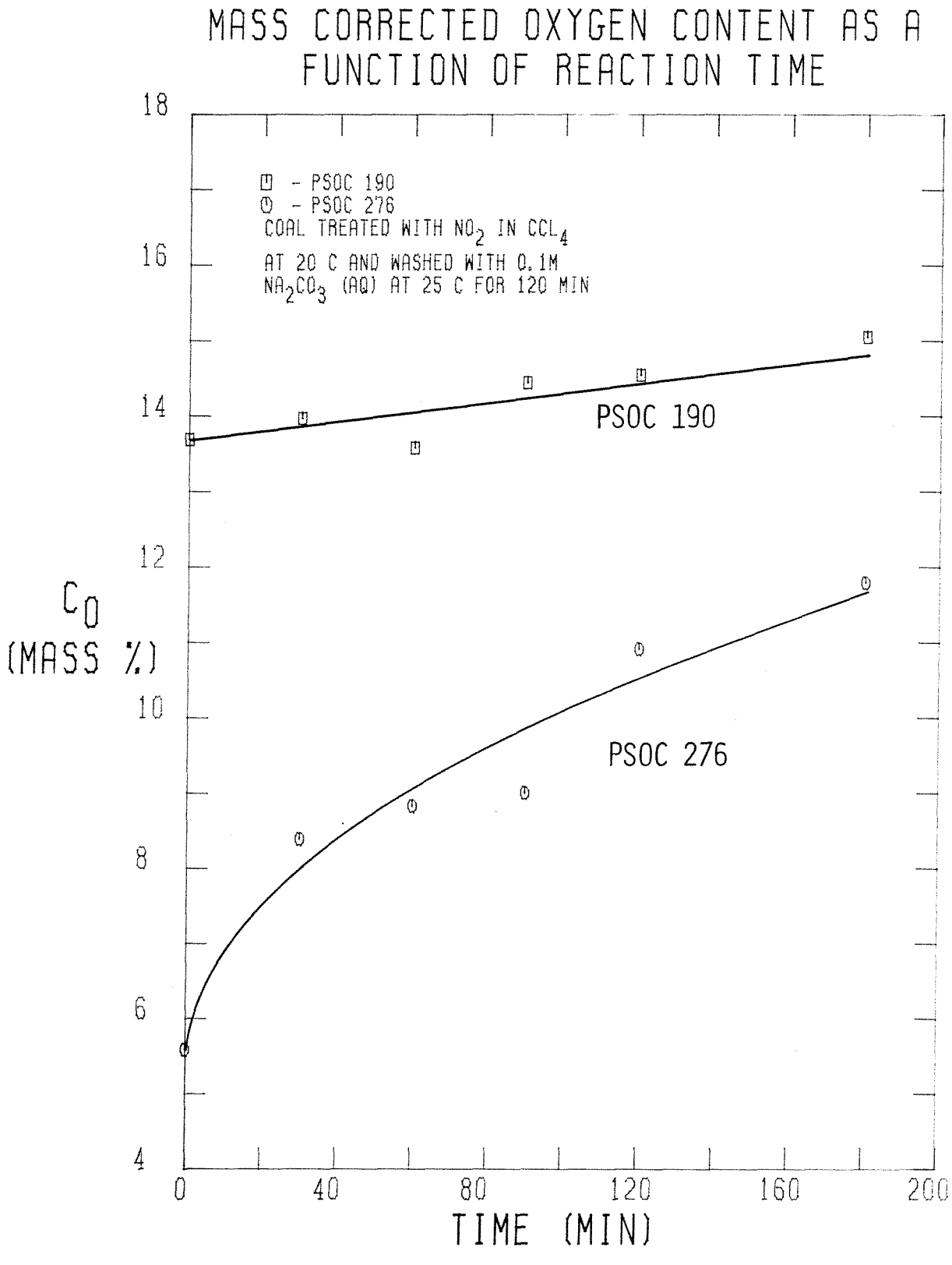
MASS CORRECTED OXYGEN CONTENT AS A FUNCTION OF REACTION TIME
□ - PSOC 190
Ⓘ - PSOC 276
COAL TREATED WITH NO_2 IN CCL_4
AT 20 C AND WASHED WITH 0.1M
NA_2CO_3 (AQ) AT 25 C FOR 120 MIN
PSOC 190
PSOC 276
C_O (MASS %)
TIME (MIN)
18
16
14
12
10
8
6
4
0
40
80
120
160
200

FIGURE 4-95

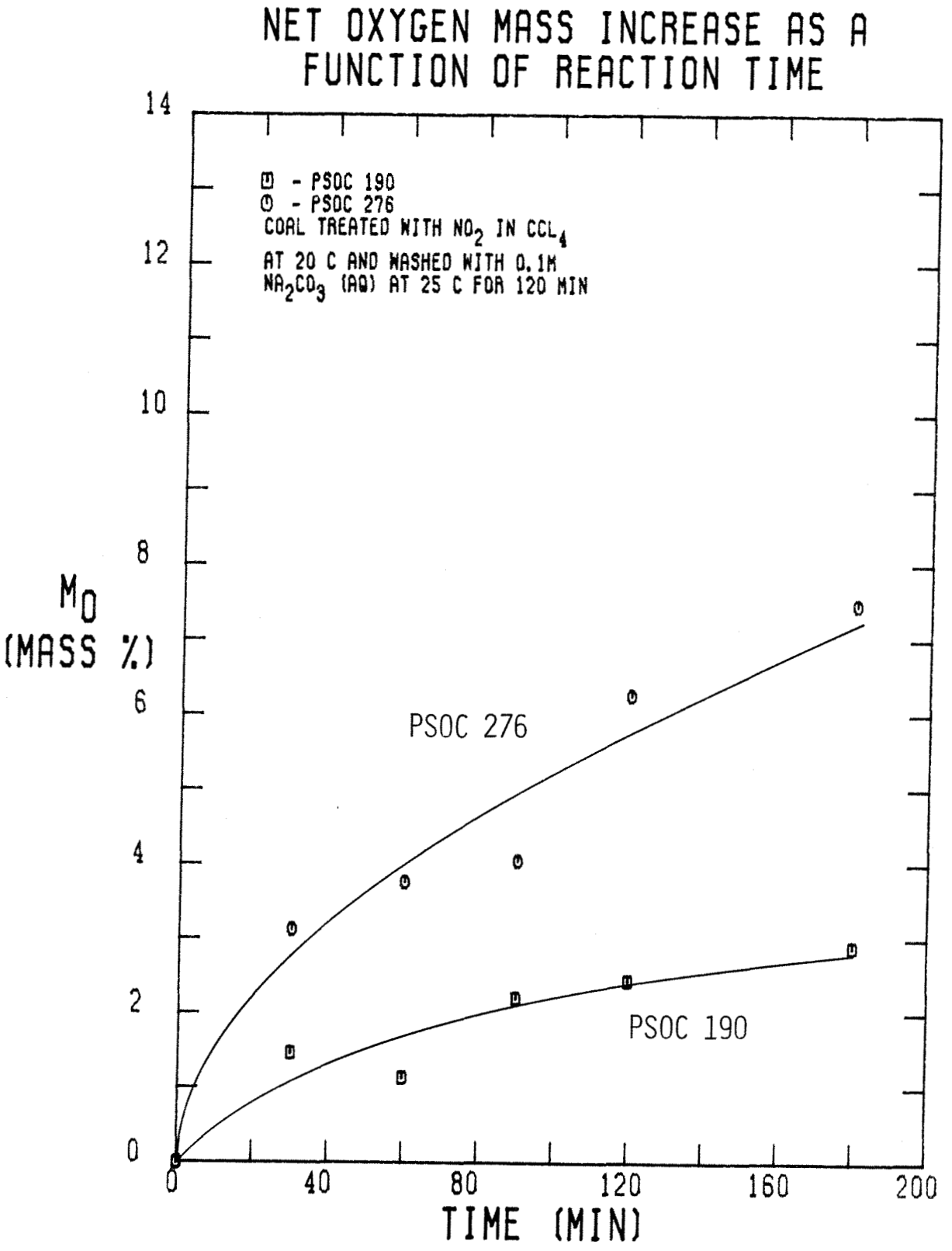
NET OXYGEN MASS INCREASE AS A FUNCTION OF REACTION TIME
□ - PSOC 190
○ - PSOC 276
COAL TREATED WITH NO2 IN CCL4
AT 20 C AND WASHED WITH 0.1M
NA2CO3 (AQ) AT 25 C FOR 120 MIN
PSOC 276
PSOC 190
MO (MASS %)
TIME (MIN)
0
2
4
6
8
10
12
14
0
40
80
120
160
200

FIGURE 4-96

previously mentioned mechanism in which the particle porosity has no effect on the extent of the NO_2-coal reaction, but does influence the removal of the coal derived products and the transport of Na_2CO_3 (aq) into the coal particle. That is, NO_2 experiences no resistance to transport into the particle, but the subsequent removal of the resulting products is affected by the porosity. This difference is simply the result of the relative size of the species involved; that is, NO_2 is small enough so that it is not affected by the pore structure during transport while the Na_2CO_3 (aq) and the reaction products are larger and more polar than NO_2, due to the added oxygen groups, and are therefore influenced during transport by the pore structure to a greater degree. Furthermore, more of the oxygen may be trapped by sodium in the PSOC 190 than in the PSOC 276. According to the previously mentioned theory regarding sodium uptake, the sodium is adsorbed by anionic oxygen groups introduced into the coal by the NO_2 treatment. Thus, any oxygen which is coupled with sodium appears as Na_2O in the mineral matter. Consequently, oxygen which adsorbs sodium is analyzed as mineral matter rather than organic oxygen. Since the sodium uptake by the PSOC 190 is roughly three times that by the PSOC 276, proportionately more of the oxygen in the PSOC 190 is classified as mineral matter than that of the PSOC 276.

Based on the discussion of the data presented above, several conclusions regarding the mechanism of oxygen uptake by the coal can be made. In general, the uptake of oxygen during the NO_2 treatment can be accounted for mainly by the uptake of nitrogen as NO_2 and the oxidation of $-CH_2-$ groups to $>C=O$ groups and $-CH_3-$ groups to $-C(=O)OH$ groups. The NO_2 uptake accounts for roughly 80 % of the total oxygen uptake and as a consequence, the values of c_O and m_O roughly parallel the values of c_N and m_N. On the other hand, the Na_2CO_3 (aq) wash of the NO_2-treated PSOC 190 results in values of m_O much less than those

predicted on the basis of the net nitrogen mass increase. One possible explanation is that the oxygen increase due to the residual NO_2 uptake is offset by the removal of initially oxygen rich portions of the PSOC 190, which are the result of the surface oxidation of the coal through weathering. Such weathering establishes a nonuniform oxygen distribution in the coal, with the oxygen rich surface of the coal being the most susceptible to NO_2 attack and subsequent removal during the Na_2CO_3 (aq) wash. It should be noted that the PSOC 276 has not been exposed to air oxidation as long as the PSOC 190. Furthermore, the net oxygen mass increase of the washed PSOC 276 can be accounted for by the residual nitrogen uptake taken as NO_2, which provides further evidence in support of the oxygen uptake being due mainly to NO_2 uptake.

The effect of temperature on the uptake of oxygen is negligible from 0 to 20°C, with the uptake of NO_2 and the hydrogen loss accounting for virtually all of the oxygen uptake. At 50 C, however, an additional process apparently occurs, namely alcohol formation. The net amount of oxygen uptake after the Na_2CO_3 (aq) wash is essentially zero for the coal treated at 0°C with NO_2 and about 3 g O/100g initial coal for the coal treated at 20°C with NO_2. This slight difference may be attributed to the difference in the NO_2 uptakes, which is slightly lower at 0°C than at 20°C.

As expected, the initial concentration of NO_2 affects the oxygen uptake during the NO_2 treatment. In general, the oxygen uptake during the NO_2 treatment can be attributed to the uptake of nitrogen as NO_2 and the hydrogen loss within the range of values of $(NO_2)_0$ from 0 to 2 F. The values determined for m_O of the Na_2CO_3 (aq) washed coal, however, are well below those calculated on the basis of just the residual amount of NO_2 uptake, which supports the theory of the removal of initially oxygen rich portions of the coal, which are created by the NO_2 treatment, during the Na_2CO_3 (aq) wash.

Finally, the porosity of the coal does not affect the amount of oxygen uptake during the NO_2 treatment. The net amount of oxygen remaining after the Na_2CO_3 (aq) wash, however, does depend on the coal particle porosity. This behavior is the consequence of the fact that the transport of NO_2 through the particle is not affected by the pore structure, while the transport of the Na_2CO_3 (aq) solution into and the coal derived products out of the coal is influenced by the porosity, mainly because these species are larger in size and more polar than NO_2. Hence, these compounds interact with the coal surface more than NO_2, both from a steric and an electrostatic standpoint.

4.2.2.6 The Chlorine Content of the Coal

Although chlorine is generally a minor component in coal rarely exceeding a few tenths of one mass percent in content, its presence can lead to serious corrosion problems in boilers, particularly with the heat exchangers. The treatment of the coal with NO_2 does not directly affect the chlorine content, except perhaps to lower it. When CCl_4 is used as the solvent, however, a potential source of chlorine exists for coal if all of the solvent is not removed during the vacuum drying. As mentioned in the previous sections, total CCl_4 removal is in fact not achieved, resulting in an increase in the chlorine content of several mass percent. Because concentrated solutions of NO_2 and CCl_4 are stable for weeks and gas chromatographic analysis of liquid phase samples still show only the NO_2 and CCl_4 peaks, it is fairly certain that the chlorine uptake is due to adsorbed CCl_4 and not some reactive chlorine species derived from CCl_4. Furthermore, the Na_2CO_3 (aq) wash generally removes all of the added chlorine, which would correspond to a relatively weakly adsorbed species such as CCl_4 being displaced by a more strongly adsorbed species such as Na^+ or CO_3^{2-} or even H_2O. Thus, the remainder of this section will discuss the change in chlorine content during the NO_2-coal reaction when CCl_4 is the solvent and during the subsequent wash in the context of the mechanism just discussed.

The values of the chlorine content for the coal treated with NO_2 at 25°C in the flow reactor and subsequently washed in 0.1 M Na_2CO_3 (aq) (Runs 21–27) are shown as a function of NO_2-exposure time in Figure 4–97. Obviously, the values of c_{CL} are based on the coal as obtained after the reaction and have not been corrected for CCl_4 uptake as for all of the other elemental compositions. The curve for the NO_2-treated coal follows the same trend as that of the hydrogen loss and nitrogen uptake curves, which implies that the alterations induced in the coal by the NO_2 attack on the coal are responsible for the CCl_4 uptake. It

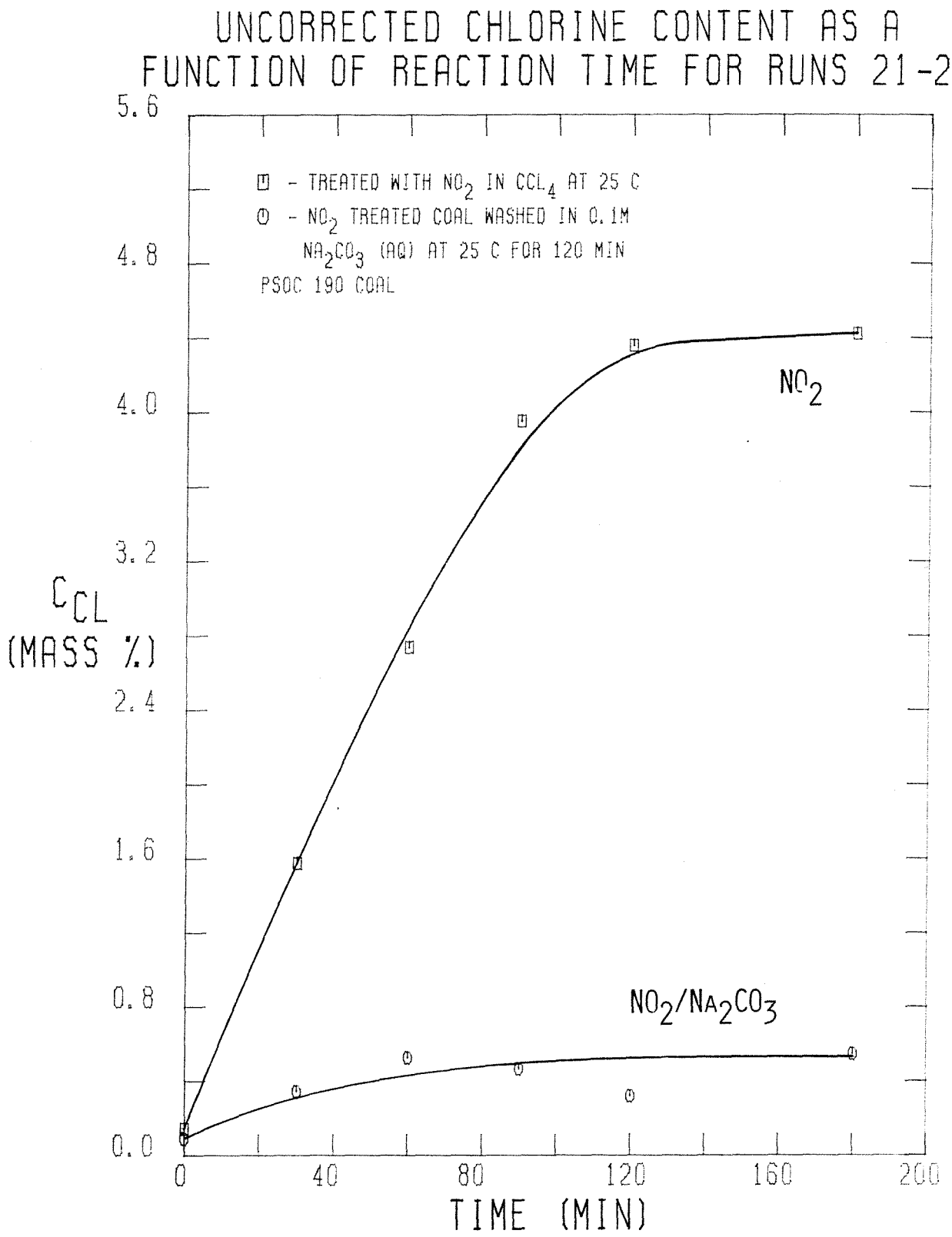
UNCORRECTED CHLORINE CONTENT AS A FUNCTION OF REACTION TIME FOR RUNS 21-27
- TREATED WITH NO2 IN CCL4 AT 25 C
- NO2 TREATED COAL WASHED IN 0.1M NA2CO3 (AQ) AT 25 C FOR 120 MIN
PSOC 190 COAL
NO2
NO2/NA2CO3
C CL (MASS %)
TIME (MIN)
5.6
4.8
4.0
3.2
2.4
1.6
0.8
0.0
0
40
80
120
160
200

FIGURE 4-97

should be noted that the points at $t = 0$ correspond to raw coal washed with CCl_4 for 120 minutes at 25°C and subsequently washed in 0.1 M Na_2CO_3 (aq). Therefore, the raw coal does not adsorb CCl_4, but the NO_2-treated coal does adsorb CCl_4. The NO_2 attack introduces polar groups into the coal which then interact more strongly with the CCl_4 than the unaltered coal. As mentioned previously, the Na_2CO_3 (aq) wash then removes virtually all of the added chlorine as evidenced by the lower curve in the figure. It is entirely reasonable to expect that the aqueous solution interacts more strongly with the polar groups in the coal and hence displaces the CCl_4. It should be noted that whereas the removal of the oxidized portions of the coal seems to depend upon the degree of coal oxidation, the removal of the adsorbed CCl_4 is quite rapid, which implies that the adsorbed CCl_4 is readily accessible to the aqueous Na_2CO_3 solution.

The values of c_{CL} for the coal treated with NO_2 at 20°C in the batch reactor and subsequently washed with 0.1 M Na_2CO_3 (aq) (Runs 33–37) are displayed graphically in Figure 4–98. In this instance, the rise in c_{CL} is more gradual, reaching a value of about 2.5 mass percent after 180 minutes of exposure to NO_2, whereas in the previous set of experiments, c_{CL} reached a limiting value of 4.4 mass percent after 120 minutes of NO_2 treatment in the flow reactor. The difference is due to the disparity in the NO_2 concentration, (NO_2), which is roughly 1 F in this set and 0 to 8 F as a linear function of time in the previous set. The c_{CL} curve parallels that of the hydrogen loss and nitrogen uptake, which supports the notion that the NO_2 attack on the coal hydrogen yields a species capable of adsorbing CCl_4. As well, the Na_2CO_3 (aq) wash removes all of the chlorine added during the NO_2 treatment, which implies that the adsorbed CCl_4 is easily displaced by the more polar aqueous species. The values of c_{CL} for the coal treated at 0°C in the batch reactor and subsequently washed in 0.1 M Na_2CO_3 (aq) (Runs 42–46) are shown in Figure 4–99 and they possess the

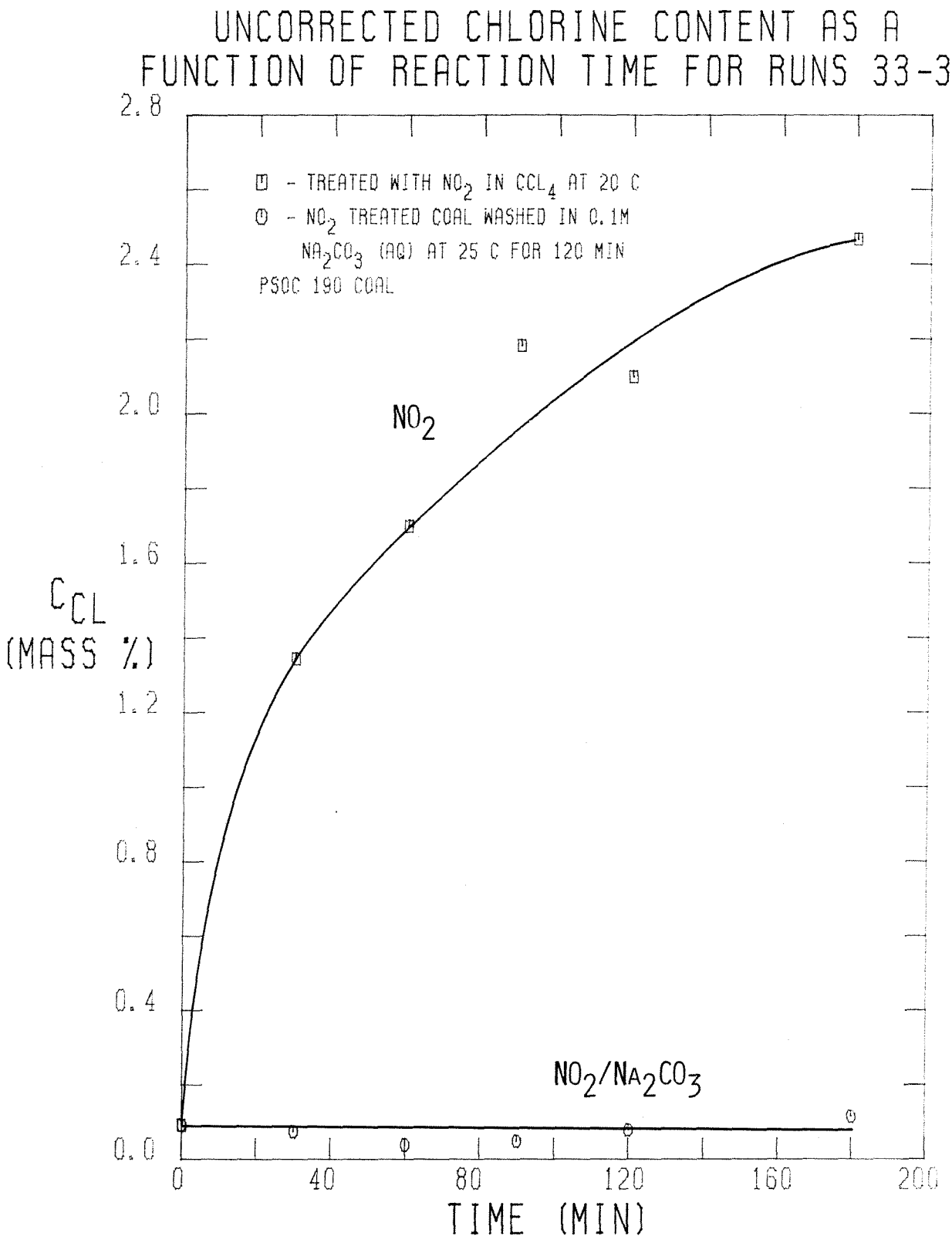
UNCORRECTED CHLORINE CONTENT AS A FUNCTION OF REACTION TIME FOR RUNS 33-37
□ - TREATED WITH NO2 IN CCL4 AT 20 C
⊙ - NO2 TREATED COAL WASHED IN 0.1M NA2CO3 (AQ) AT 25 C FOR 120 MIN
PSOC 190 COAL
NO2
NO2/NA2CO3
CCL (MASS %)
TIME (MIN)
2.8
2.4
2.0
1.6
1.2
0.8
0.4
0.0
0
40
80
120
160
200

FIGURE 4-98

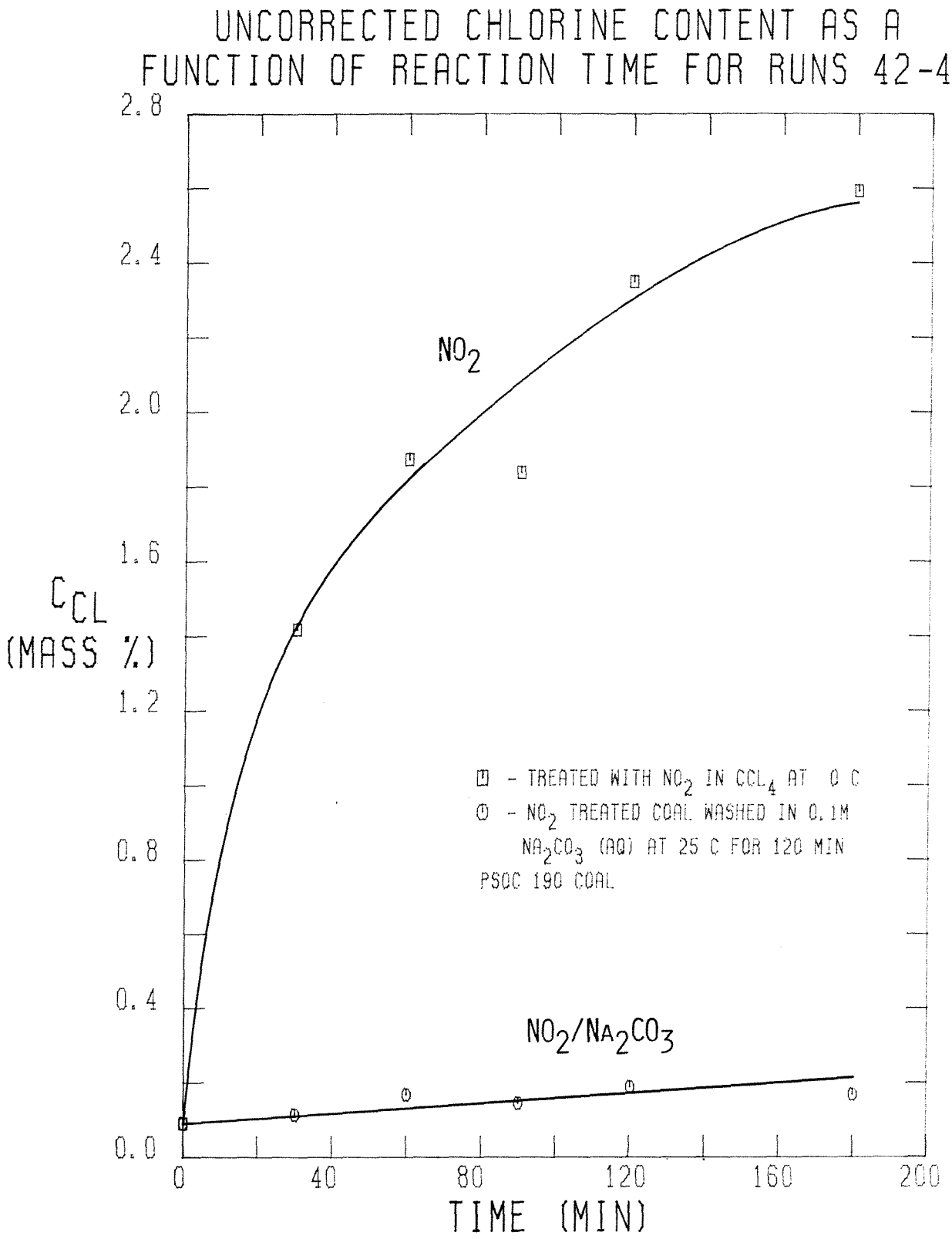
UNCORRECTED CHLORINE CONTENT AS A FUNCTION OF REACTION TIME FOR RUNS 42-46
2.8
2.4
2.0
1.6
1.2
0.8
0.4
0.0
C_{CL} (MASS %)
NO_2
NO_2/NA_2CO_3
- TREATED WITH NO_2 IN CCL_4 AT 0 C
- NO_2 TREATED COAL WASHED IN 0.1M NA_2CO_3 (AQ) AT 25 C FOR 120 MIN
PSOC 190 COAL
0
40
80
120
160
200
TIME (MIN)

FIGURE 4-99

same basic trends as discussed in regard to the previous set of experiments.

The effect of temperature on the uptake of chlorine during the NO_2 treatment is more clearly demonstrated in Figure 4–100, in which the values of c_{CL} for the coal treated at 0, 20 and 50°C are plotted. As mentioned above, the curves for the coal treated at 0 and 20°C are virtually identical. Both curves correlate well with the respective hydrogen loss results. At 50°C, however, the amount of chlorine uptake almost doubles. Furthermore, the amount of chlorine uptake does not correlate with the hydrogen loss at 50°C during NO_2 treatment. As mentioned in the discussion of the hydrogen loss, however, trapping of the oxidized hydrogen compounds (mainly water) within the coal may occur to a larger extent at 50°C than at 20°C. It should be noted that the values of c_{CL} do parallel those of c_N and c_O with respect to temperature. Indeed, one would expect that if the amount of CCl_4 adsorbed is proportional to the degree of oxidation of the coal, which produces the polar groups and which increases with temperature, then the chlorine content should increase with increasing NO_2-treatment temperature. Because the coal treated at 50°C could not be washed in 0.1 M Na_2CO_3 (aq), the extent of the removal of added chlorine by the aqueous solution could not be determined. Nevertheless, in view of the facile removal of the added chlorine in the other coal samples, it seems likely that the chlorine added during the NO_2 treatment at 50°C should also be readily removed.

The effect of the initial NO_2 concentration, $(NO_2)_0$, on the amount of chlorine uptake is shown in Figure 4–101. The amount of chlorine added during the NO_2 treatment at 20°C for 120 minutes increases linearly with $(NO_2)_0$ up to 1.7 F, where c_{CL} reaches a value of 3.1 mass percent. At higher values of $(NO_2)_0$, c_{CL} increases at a faster rate. In this case, the amount of added chlorine does not parallel the amount of hydrogen lost during the NO_2 treatment, but does parallel the amount of added nitrogen and oxygen. It should be noted that the molar

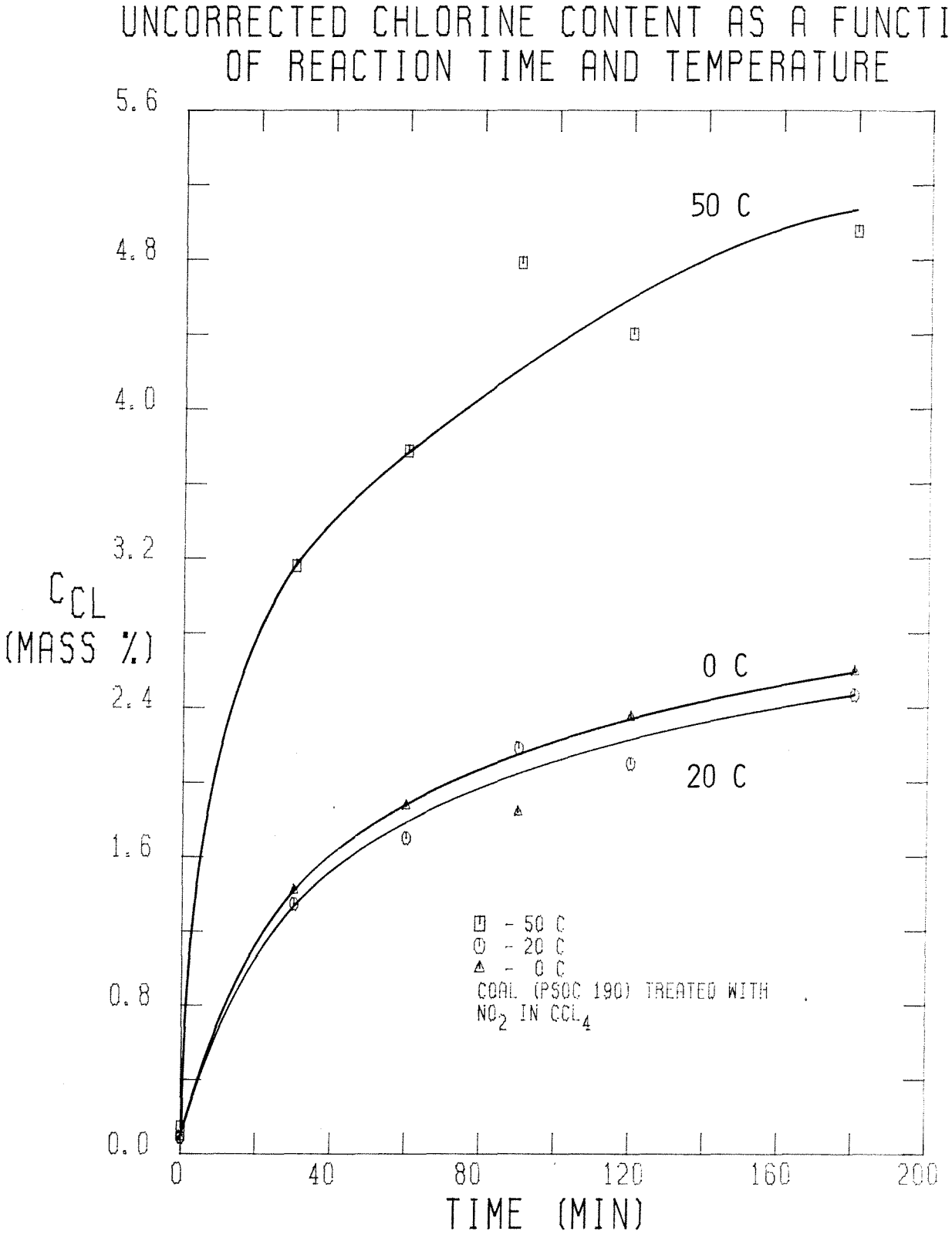
UNCORRECTED CHLORINE CONTENT AS A FUNCTION OF REACTION TIME AND TEMPERATURE
5.6
4.8
4.0
3.2
2.4
1.6
0.8
0.0
C_{CL} (MASS %)
50 C
0 C
20 C
0
40
80
120
160
200
TIME (MIN)
- 50 C
- 20 C
- 0 C
COAL (PSOC 190) TREATED WITH NO_2 IN CCL_4

FIGURE 4-100

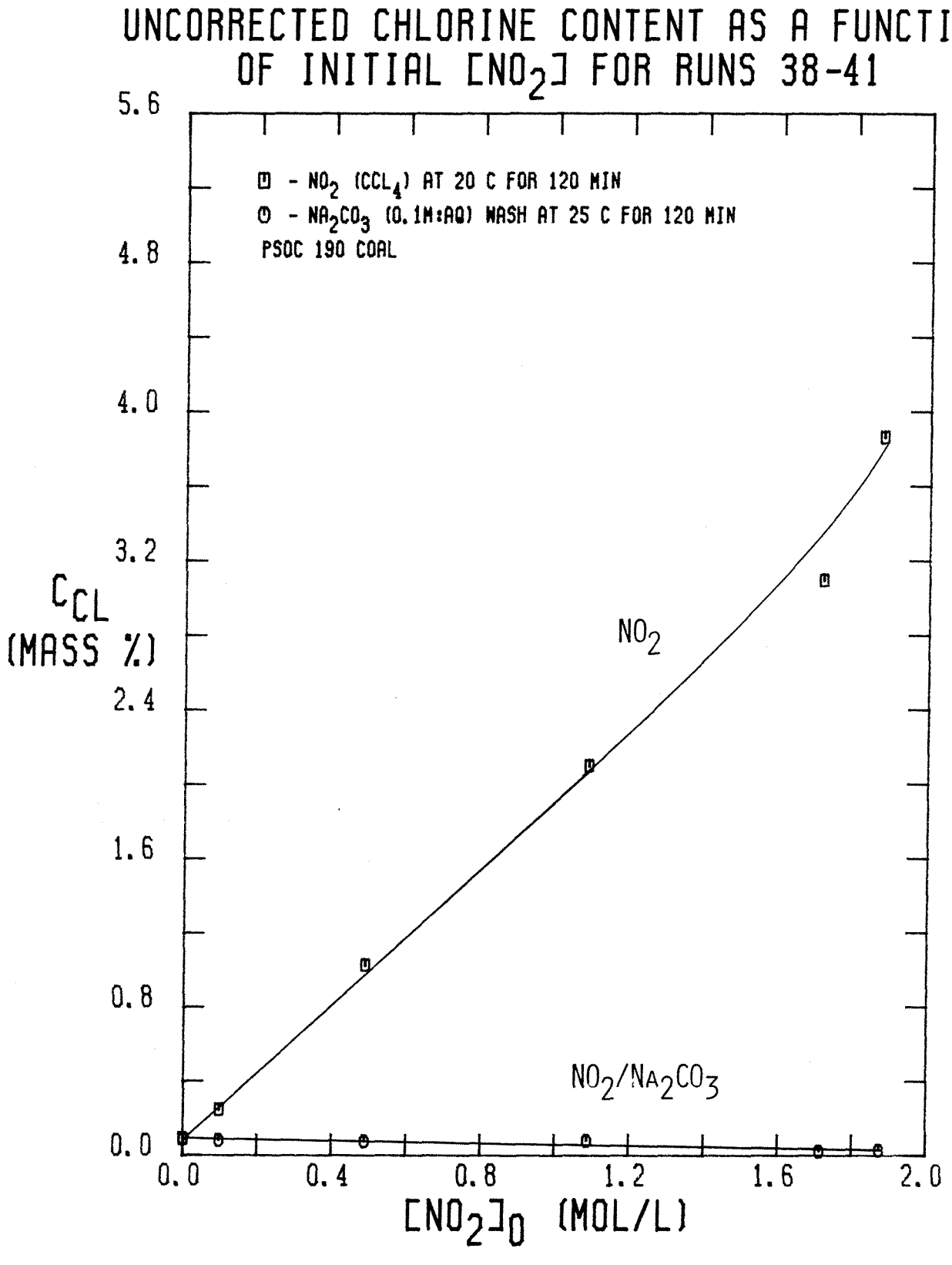
UNCORRECTED CHLORINE CONTENT AS A FUNCTION OF INITIAL [NO2] FOR RUNS 38-41
□ - NO2 (CCL4) AT 20 C FOR 120 MIN
○ - NA2CO3 (0.1M:AQ) WASH AT 25 C FOR 120 MIN
PSOC 190 COAL
NO2
NO2/NA2CO3
CCL (MASS %)
[NO2]0 (MOL/L)
5.6
4.8
4.0
3.2
2.4
1.6
0.8
0.0
0.0
0.4
0.8
1.2
1.6
2.0

FIGURE 4-101

ratio of added chlorine taken as CCl_4 to oxidized hydrogen is less than one percent for all values of $(NO_2)_0$, which implies that only a small portion of the oxidized sites actually adsorb CCl_4. Thus, it seems reasonable that due to the size of the CCl_4 molecule, it is adsorbed only at sites easily accessed by Na_2CO_3 (aq), which is supported by the values of c_{CL} for the washed coals which indicate the complete removal of the added chlorine.

The values of c_{CL} for the PSOC 276 treated with NO_2 at 20°C in the batch reactor and susequently washed in 0.1 M Na_2CO_3 (aq) (Runs 47–52) are depicted graphically in Figure 4–102. Once again, c_{CL} during NO_2 treatment rises with increased NO_2-exposure time, reaching a value of roughly 2.0 mass percent after 180 minutes of treatment. The behavior of c_{CL} is similar to that of c_N and c_O as well, being linearly proportional to the NO_2-exposure time after 30 minutes. Interestingly, all of the added chlorine is displaced during the Na_2CO_3 (aq) wash, even though the PSOC 276 has an initial pore volume which is four times smaller than that of the PSOC 190. Thus, not only does the pore structure not affect the uptake of NO_2 and CCl_4 during the NO_2 treatment, it also does not affect the removal of the adsorbed CCl_4 during the Na_2CO_3 (aq) wash, which seems reasonable in view of the molecular size of CCl_4 relative to those of the aqueous species in the Na_2CO_3 (aq) solution. That is, any location within the coal particle to which CCl_4 can penetrate is also accessible to the Na_2CO_3 (aq) solution, in which the molecular sizes are smaller than that of CCl_4.

A graphical comparison of the values of c_{CL} for the PSOC 190 and PSOC 276 treated with NO_2 at 20°C in the batch reactor is provided in Figure 4–103. The curves for the two coals are basically parallel after the initial 30 minutes, with the PSOC 190 acquiring about 0.5 mass percent more chlorine than the PSOC 276. This behavior is in accord with the nitrogen and oxygen uptake data as well as the hydrogen loss data.

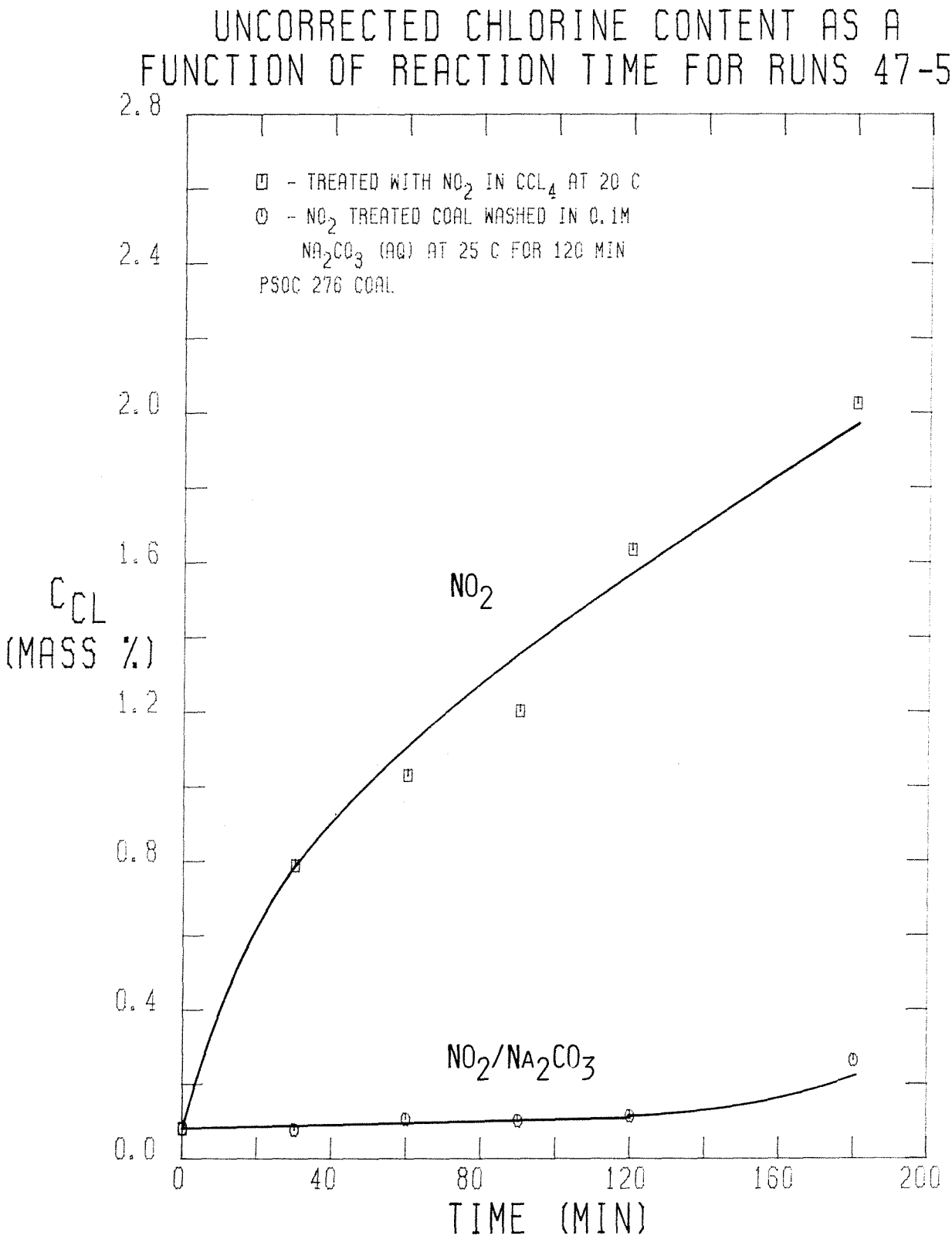
UNCORRECTED CHLORINE CONTENT AS A FUNCTION OF REACTION TIME FOR RUNS 47-52
□ - TREATED WITH NO2 IN CCL4 AT 20 C
⊙ - NO2 TREATED COAL WASHED IN 0.1M NA2CO3 (AQ) AT 25 C FOR 120 MIN
PSOC 276 COAL
NO2
NO2/NA2CO3
CCL (MASS %)
TIME (MIN)
0.0
0.4
0.8
1.2
1.6
2.0
2.4
2.8
0
40
80
120
160
200

FIGURE 4-102

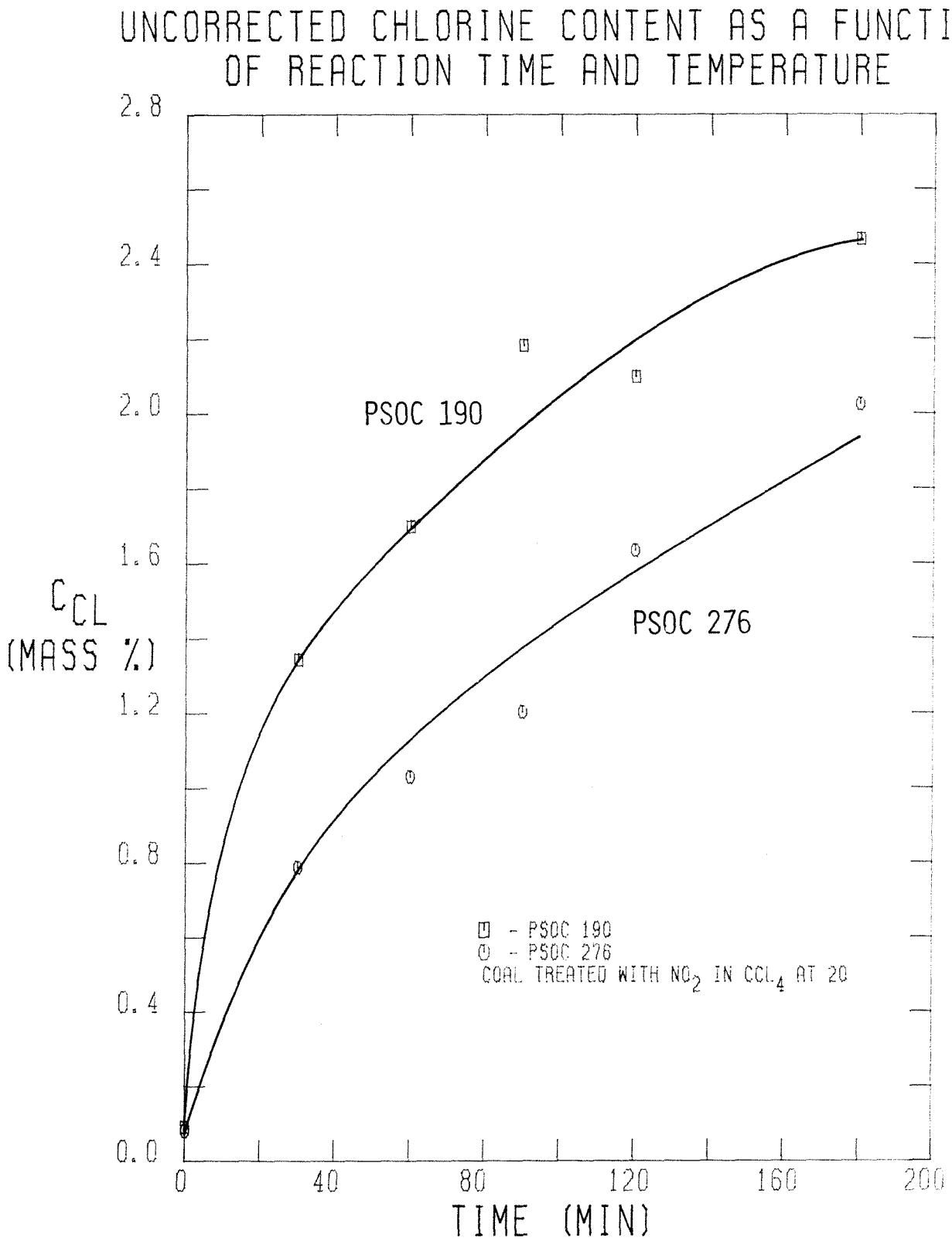
UNCORRECTED CHLORINE CONTENT AS A FUNCTION OF REACTION TIME AND TEMPERATURE
2.8
2.4
2.0
1.6
1.2
0.8
0.4
0.0
C_{CL} (MASS %)
PSOC 190
PSOC 276
□ - PSOC 190
○ - PSOC 276
COAL TREATED WITH NO_2 IN CCL_4 AT 20
0
40
80
120
160
200
TIME (MIN)

FIGURE 4-103

On the basis of the consistent chlorine data discusssed in this section, a probable mechanism which accounts for the chlorine uptake can be formulated. Quite simply, the attack of NO_2 on the coal produces polar groups which then adsorb the CCl_4 solvent. The adsorbed CCl_4 is not removed by vacuum drying at 120°C. The polar groups introduced into the coal consist primarily of anionic oxygen, which replaces roughly 25 % of the coal hydrogen, and adsorbed NO_2 . Either of these groups is sufficiently polar to adsorb CCl_4. Once the NO_2-treated coal is exposed to 0.1 M Na_2CO_3 (aq), however, the adsorbed CCl_4 is readily displaced by Na^+ (aq) and/or H_2O. Because the aqueous species are smaller in size than CCl_4, they should penetrate to any location in the coal particle which is accessible to CCl_4, resulting in the total displacement of all the adsorbed CCl_4.

4.2.2.7 The Mineral Matter Content of the Coal

One of the major constituents of coal is the various forms of inorganic material, generally metal oxides and sulfides, conveniently lumped together as mineral matter. The mineral matter does not contribute to the heating value of the coal, yet it is quite difficult and costly to remove it from the coal before combustion. Rather, the ash resulting from combustion is removed from the boiler, which contributes to the cost of operating the combustion process. Therefore, if portions of the mineral matter are removed during the NO_2 treatment, this would be an added benefit. As the discussion of the mineral matter determinations in this section will reveal, however, the NO_2 treatment results in a slight decrease in mineral matter content, but the Na_2CO_3 (aq) wash results in a two-fold increase in the mineral matter content.

The net mineral matter mass increase, m_{MM}, is shown as a function of NO_2-exposure time in Figure 4–104 for coal that was treated with NO_2 at 25°C in the flow reactor and that was then washed in 0.1 M Na_2CO_3 (aq) (Runs 21–27). The data indicate that roughly 12 to 24 mass percent of the mineral matter is removed during the NO_2 treatment. In view of the fact that CCl_4 is the solvent, it is hard to imagine how such a significant portion of the metal oxides which comprise the mineral matter can be removed. The scatter in the data suggests that the relative error in m_{MM} is substantial. Nevertheless, the removal of mineral matter is clearly indicated. The NO_2 is not expected to react with the metal oxides further, since they are already oxidized. Rather, the NO_2 must form a sort of metal oxide complex which is soluble in the NO_2-CCl_4 solution.

In any case, the amount of mineral matter removed during the NO_2 treatment pales when compared to the extremely large increase in mineral matter content after the Na_2CO_3 (aq) wash. This increase is due to the uptake of Na^+ cations by the coal during the wash, as will be demonstrated when the x–ray analysis of the

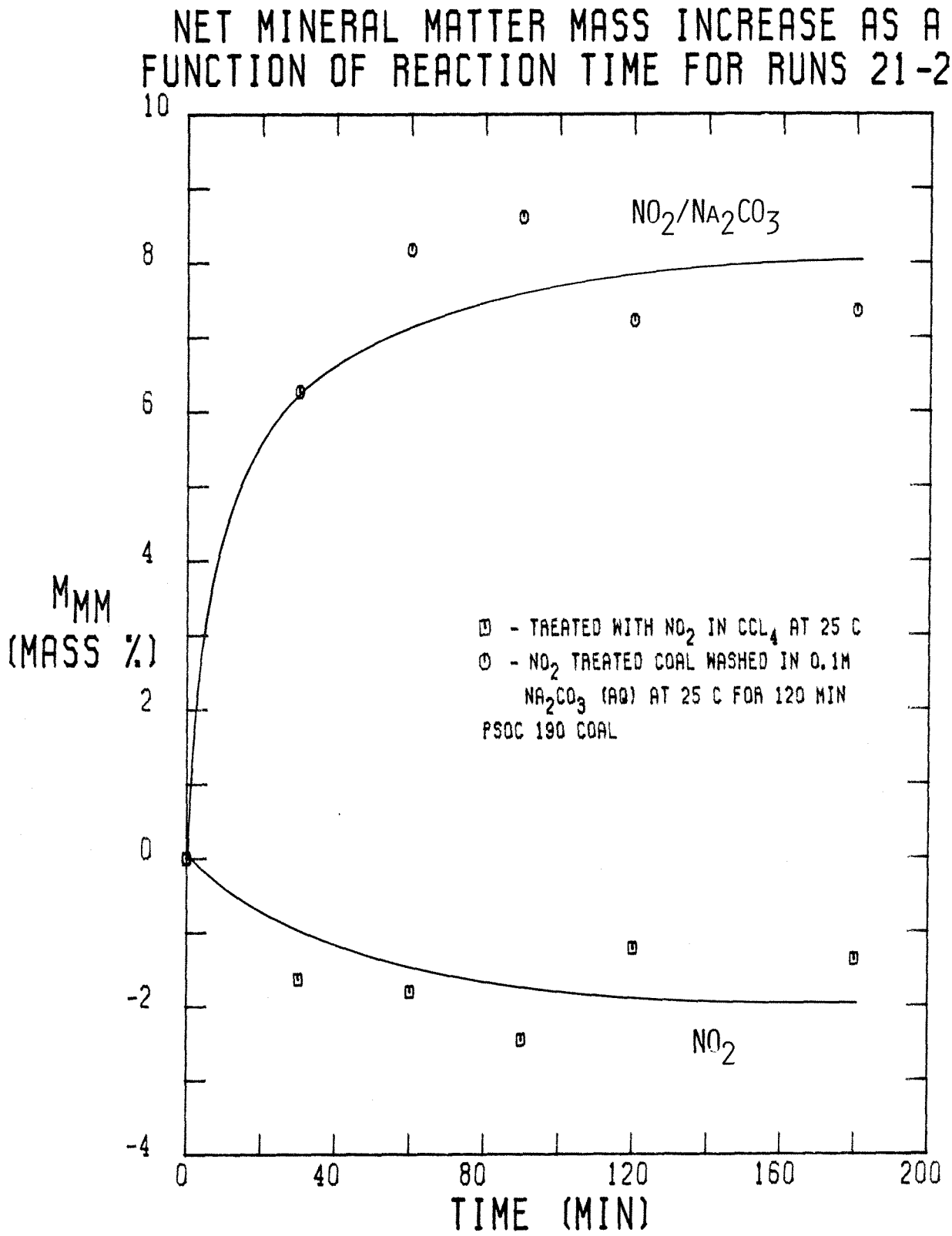
NET MINERAL MATTER MASS INCREASE AS A FUNCTION OF REACTION TIME FOR RUNS 21-27
10
8
6
4
2
0
-2
-4
M_{MM} (MASS %)
0
40
80
120
160
200
TIME (MIN)
NO_2/NA_2CO_3
NO_2
- TREATED WITH NO_2 IN CCL_4 AT 25 C
- NO_2 TREATED COAL WASHED IN 0.1M NA_2CO_3 (AQ) AT 25 C FOR 120 MIN
PSOC 190 COAL

FIGURE 4-104

ash is discussed in the section dealing with the surface analysis of the coal. Furthermore, it is the large sodium content of the coal which accounts for the large removal of SO_2 from the combustion gases. It is the Na^+ which is ultimately adsorbed by the oxygenated groups which are introduced into the coal during the NO_2 treatment. Indeed, it is the Na^+ which displaces the adsorbed CCl_4 due to its stronger interaction with the ionic groups on the coal surface. In this particular set of experiments, the mineral matter content almost doubles after 90 minutes of NO_2 treatment followed by the Na_2CO_3 (aq) wash. The decrease in the amount of added mineral matter at higher reaction times could be due to more extensive pore blocking, which would inhibit the transport of Na_2CO_3 (aq) into the interior of the coal particle. These results indicate that the NO_2 treatment allows the coal to accept roughly 0.3 g Na/10g coal, a significant amount. It should be noted that while just Na^+ is probably taken up by the coal, the mineral matter content is determined on the basis of the ash, in which all sodium is converted to Na_2O or Na_2SO_4 . The rapid rise in m_{MM} after the wash correlates quite well with the rapid loss in hydrogen, which lends credence to the notion that the anionic oxygen atoms which replace the coal hydrogen do in fact adsorb the CCl_4 and the Na^+ cations. It should be noted that the molar ratio of sodium uptake to hydrogen loss is about 1 to 8 after converting the amount of Na_2O and Na_2SO_4 in the ash to sodium. Furthermore, it is also possible that any adsorbed NO_2 binds Na^+ as well.

The values of m_{MM} obtained for the coal treated with NO_2 at 20°C in the batch reactor and subsequently washed in 0.1 M Na_2CO_3 (aq) (Runs 33–37) are shown graphically in Figure 4–105. In this set of experiments, only 6 to 9 % of the mineral matter is removed during the NO_2 treatment as opposed to 12 to 24 % in the previous set. This difference is probably due to the different NO_2 concentrations in the set of experiments, namely about 1 F in this set and 0 to 8 F as a

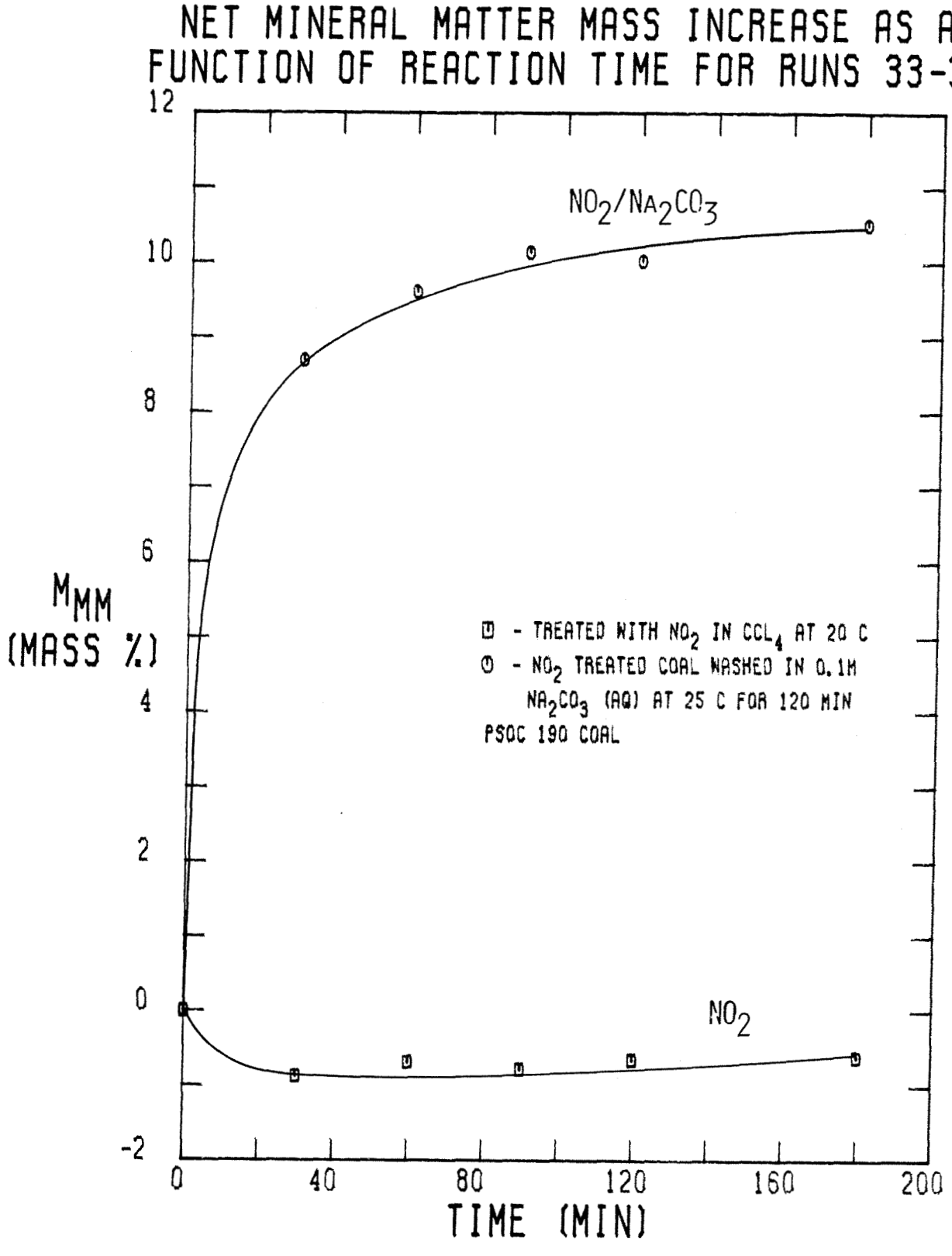
NET MINERAL MATTER MASS INCREASE AS A FUNCTION OF REACTION TIME FOR RUNS 33-37
NO_2/NA_2CO_3
NO_2
M_{MM} (MASS %)
TIME (MIN)
12
10
8
6
4
2
0
-2
0
40
80
120
160
200
- TREATED WITH NO_2 IN CCL_4 AT 20 C
- NO_2 TREATED COAL WASHED IN 0.1M NA_2CO_3 (AQ) AT 25 C FOR 120 MIN
PSOC 190 COAL

FIGURE 4-105

linear function of exposure time in the previous set. Once again, however, the Na_2CO_3 (aq) wash results in a doubling of the original mineral matter content of the coal. Furthermore, the mass increase in mineral matter parallels the hydrogen loss in that roughly 90 % of the change occurs within the first 30 minutes of NO_2 exposure, which agrees with the theory that the removal of hydrogen during the NO_2 treatment creates sites capable of adsorbing Na^+ during the wash. The values of m_{MM} for the coal treated with NO_2 at 0°C in the batch reactor and subsequently washed in 0.1 M Na_2CO_3 (aq) (Runs 42–46) demonstrate the same behavior as in the previous set of runs, as illustrated in Figure 4–106. The amount of mineral matter removed during the NO_2 treatment is only about 4 to 6 % of the original mineral matter content. The amount of mineral matter doubles, however, after the Na_2CO_3 (aq) wash, which indicates a substantial amount of Na^+ adsorption. It should be noted that the point at 180 minutes has been neglected in drawing the curve because it deviates so much from the rest of the data.

The effect of the temperature on the removal of mineral matter during the NO_2 treatment is shown in Figure 4–107. It it interesting to note that at 50°C, there is actually a small increase in the mineral matter content. Perhaps some further oxidation of the mineral matter occurs at 50°C that does not occur at 20 or 0°C, at which temperatures a slight decrease in the mineral matter content occurs. It should be noted that the values obtained for m_{MM} at 120 and 180 minutes of NO_2 treatment at 50°C deviate significantly from their corresponding curve, which only serves as an indication of the potential error in the determination. The curves corresponding to NO_2 treatment at 20 and 0°C are much smoother. Indeed, the m_{MM} curve for the 20°C NO_2 treatment virtually levels off after 30 minutes at about an 0.8 % loss, while the curve for the 0°C NO_2 treatment approaches a loss of roughly 0.6 % in a more gradual fashion. This

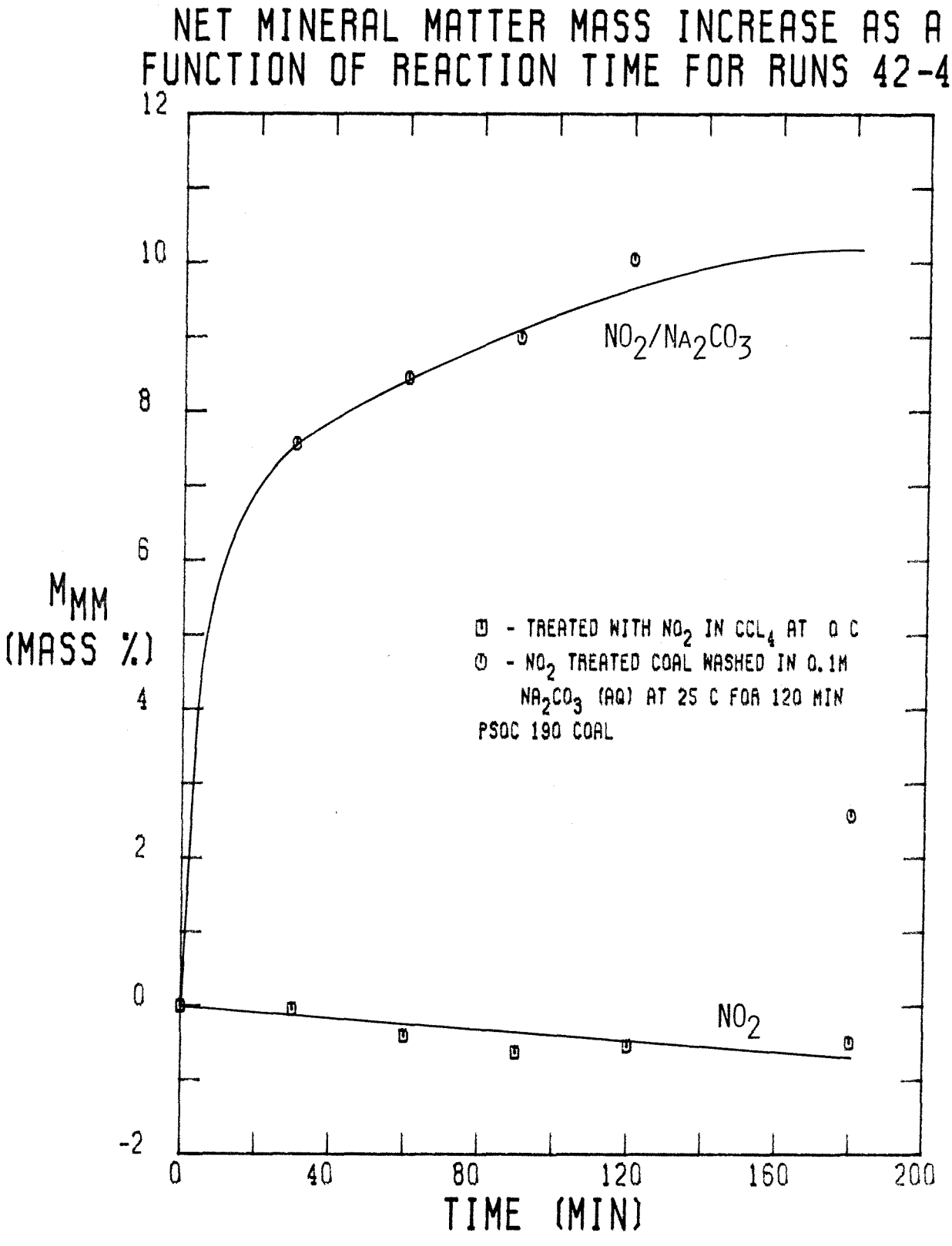
NET MINERAL MATTER MASS INCREASE AS A FUNCTION OF REACTION TIME FOR RUNS 42-46
12
10
8
6
4
2
0
-2
M_{MM} (MASS %)
0
40
80
120
160
200
TIME (MIN)
NO_2/NA_2CO_3
NO_2
- TREATED WITH NO_2 IN CCL_4 AT 0 C
- NO_2 TREATED COAL WASHED IN 0.1M NA_2CO_3 (AQ) AT 25 C FOR 120 MIN
PSOC 190 COAL

FIGURE 4-106

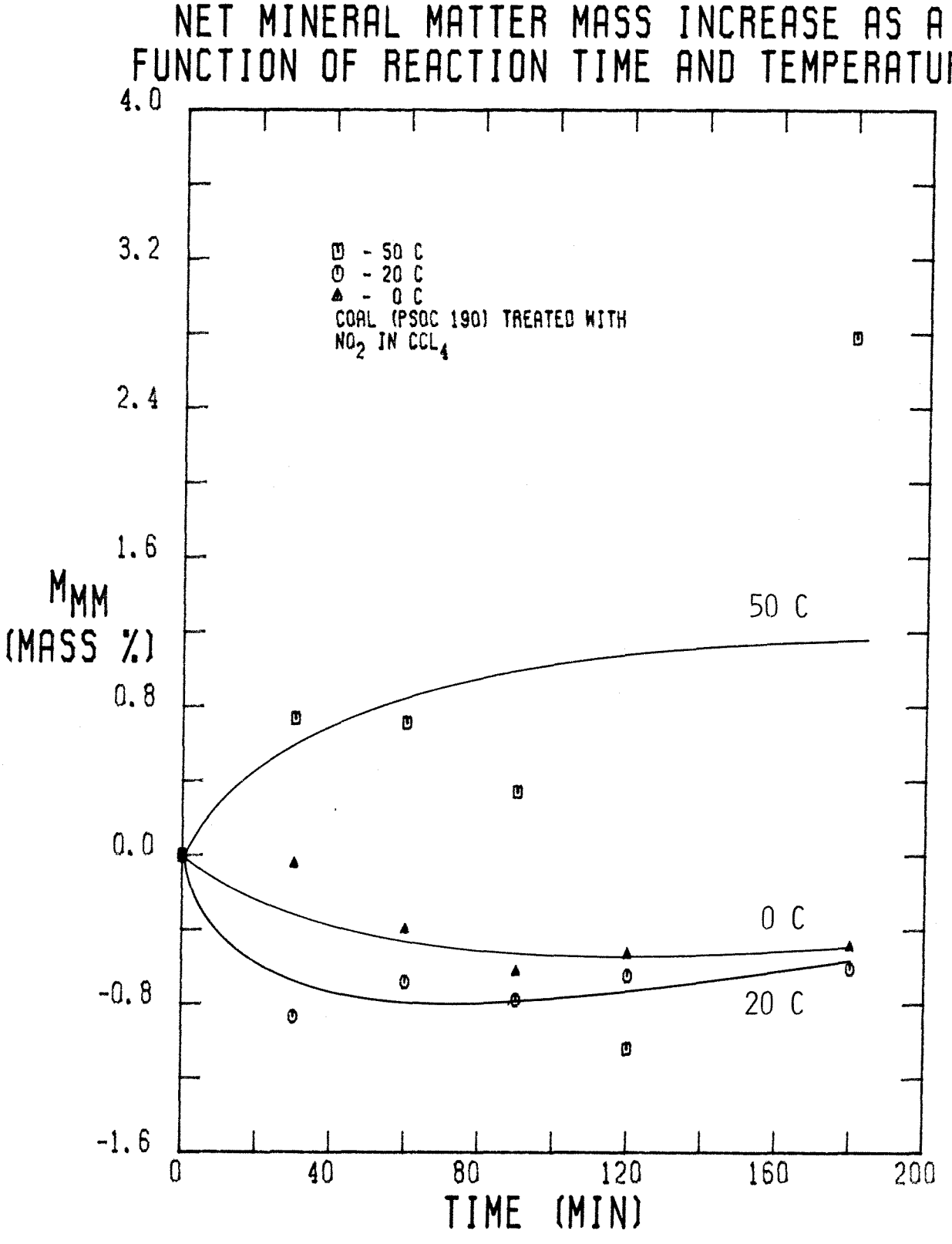
NET MINERAL MATTER MASS INCREASE AS A FUNCTION OF REACTION TIME AND TEMPERATURE
4.0
3.2
2.4
1.6
0.8
0.0
-0.8
-1.6
0
40
80
120
160
200
TIME (MIN)
M_MM (MASS %)
- 50 C
- 20 C
- 0 C
COAL (PSOC 190) TREATED WITH NO2 IN CCL4
50 C
0 C
20 C

FIGURE 4-107

behavior is consistent with the other data which suggests a slower NO_2-coal reaction at 0 than 20°C.

The net mineral matter mass increase in the coals treated with NO_2 at 20 and 0°C and subsequently washed in 0.1 M Na_2CO_3 (aq) is plotted as a function of NO_2-exposure time in Figure 4–108. As expected, the rise in m_{MM} is a little more rapid at 20 than at 0°C, with both curves eventually converging at 120 minutes, which is consistent with the nitrogen uptake and hydrogen loss data. Thus, whether the NO_2 treatment is performed at 20 or 0°C does not seem to make much difference in the increase in m_{MM} after the Na_2CO_3 (aq) wash. There is no curve for the 50°C treatment because the treated coal could not be filtered from the Na_2CO_3 (aq) solution.

The effect of the initial NO_2 concentration, $(NO_2)_0$, on the mineral matter content after treatment with NO_2 at 20°C for 120 minutes followed by the Na_2CO_3 (aq) wash (Runs 38–41) is illustrated in Figure 4–109. It is interesting to note that 12 % of the mineral matter is lost when $(NO_2)_0$ = 0.097 F and that the loss then decreases with increasing $(NO_2)_0$, which implies that lower concentrations of NO_2 favor mineral matter removal. This trend is probably the result of more extensive pore blocking at higher values of (NO_2) which inhibits mineral matter removal. The amount of Na^+ uptake during the wash as indicated by the net mineral matter mass increase closely follows the nitrogen uptake and hydrogen loss data. There is a gradual increase in m_{MM} as the value of (NO_2) rises to about 1 F. As (NO_2) becomes greater, m_{MM} begins to increase at an accelerating rate, which gives an overall sigmoidal shape to the curve, much as in the case of the corresponding nitrogen uptake and hydrogen loss curves. Therefore, the variation in the extent of oxidation of the coal as $(NO_2)_0$ changes correlates quite well with the variation in m_{MM} as $(NO_2)_0$ changes, which implies that the alterations introduced into the coal through oxidation are responsible

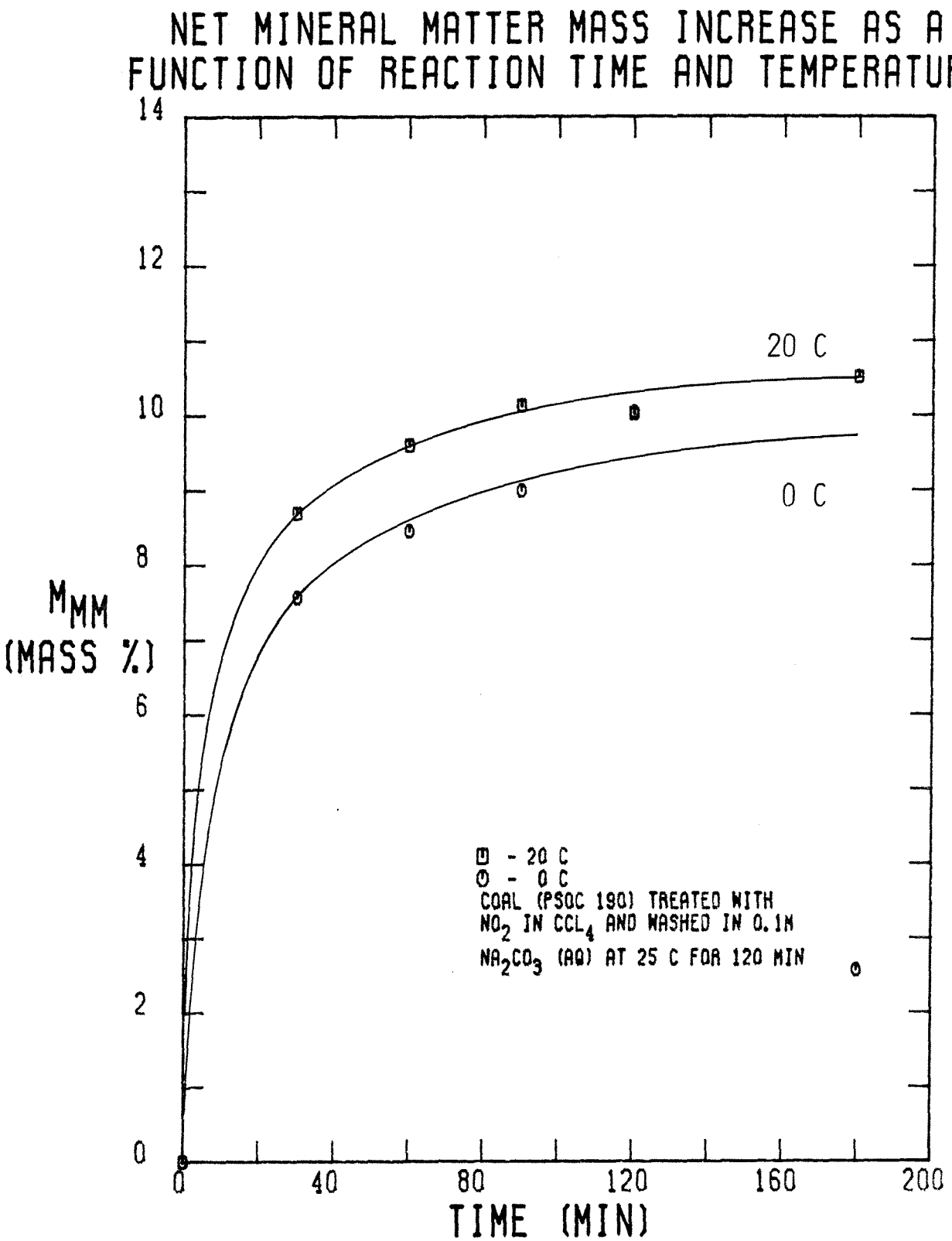
NET MINERAL MATTER MASS INCREASE AS A FUNCTION OF REACTION TIME AND TEMPERATURE
14
12
10
8
6
4
2
0
M_{MM} (MASS %)
20 C
0 C
□ - 20 C
○ - 0 C
COAL (PSOC 190) TREATED WITH NO_2 IN CCL_4 AND WASHED IN 0.1M NA_2CO_3 (AQ) AT 25 C FOR 120 MIN
0
40
80
120
160
200
TIME (MIN)

FIGURE 4-103

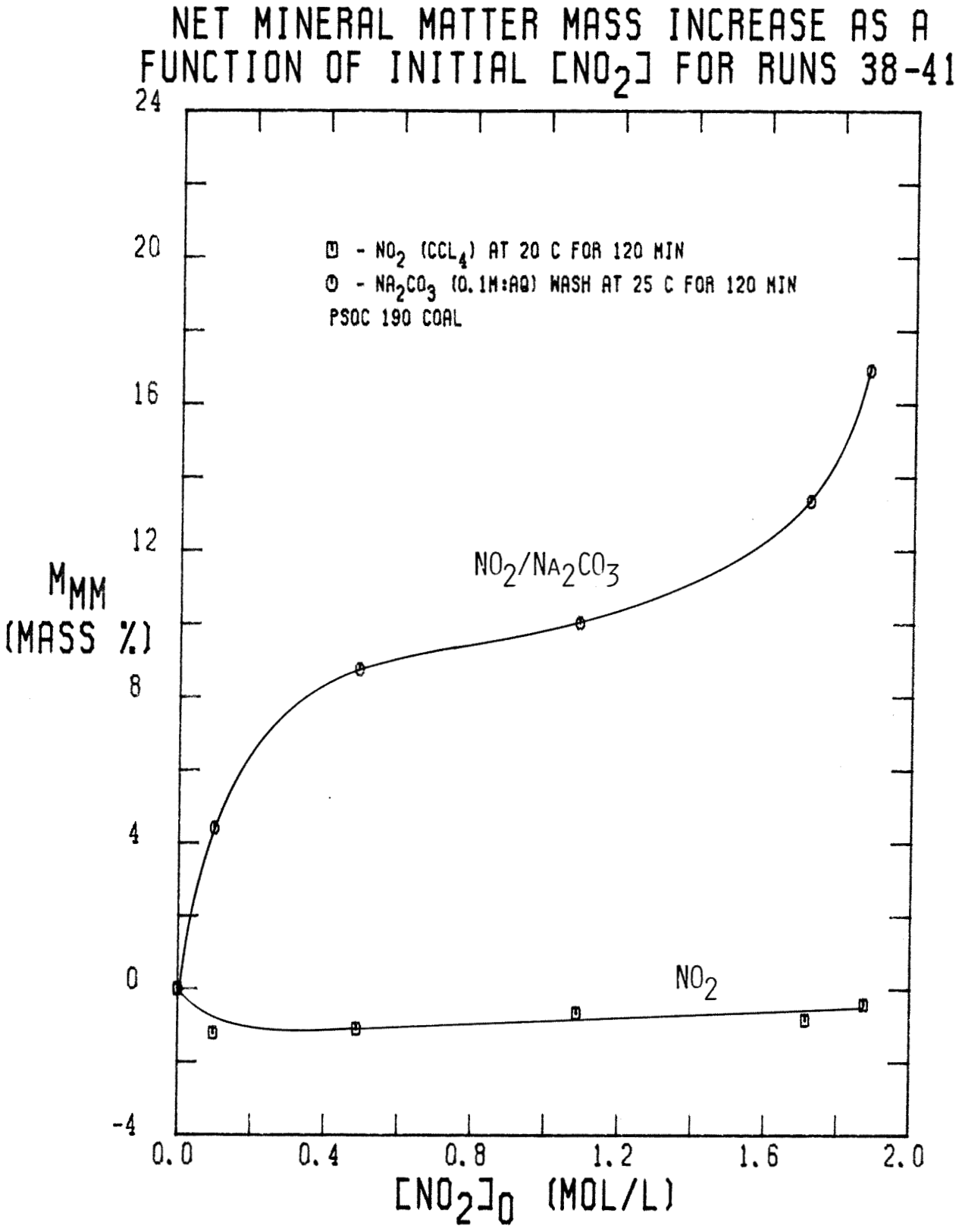
NET MINERAL MATTER MASS INCREASE AS A FUNCTION OF INITIAL [NO2] FOR RUNS 38-41
□ - NO2 (CCL4) AT 20 C FOR 120 MIN
○ - NA2CO3 (0.1M:AQ) WASH AT 25 C FOR 120 MIN
PSOC 190 COAL
NO2/NA2CO3
NO2
MMM (MASS %)
[NO2]0 (MOL/L)
24
20
16
12
8
4
0
-4
0.0
0.4
0.8
1.2
1.6
2.0

FIGURE 4-109

for the uptake of sodium.

The values of m_{MM} of the PSOC 276 treated with NO_2 at 20°C in the batch reactor and subsequently washed in 0.1 M Na_2CO_3 (aq) (Runs 47–52) are shown as a function of NO_2-exposure time in Figure 4–110. As before, the NO_2 treatment results in the removal of some of the mineral matter. Once again, there is a rapid drop in m_{MM} followed by a gradual increase after 30 minutes, which implies that a certain portion of the mineral matter is rapidly removed. Again, this result is puzzling because none of the mineral matter is expected to be soluble in the NO_2/CCl_4 solution. The Na_2CO_3 (aq) wash then results in an increase in m_{MM}. Again, the rise in m_{MM} is quite rapid and seems to level off at about 3.5 % after roughly 90 minutes of NO_2 exposure. The extent of the rise in the treated PSOC 276 is not nearly as great as in the treated PSOC 190, however, as demonstrated in Figure 4–111. The increase in m_{MM} for the treated PSOC 190 is three times as great as the increase in m_{MM} for the treated PSOC 276, which seems to be due to the difference in pore volume of the two coals. Whereas NO_2 can penetrate either coal with virtually identical ease, the transport of aqueous Na_2CO_3 into the coal particle is indeed affected by the pore structure. In fact, the fourfold difference in the pore volumes of the two coals correlates with the threefold difference in the increase of m_{MM} for the two coals. Nevertheless, the difference in the amount of sodium uptake by the two coals accounts for a significant disparity in the amount of SO_2 trapped during combustion. Whereas 95 % of the sulfur in the treated PSOC 190 is trapped, only about 38 % of the sulfur in the treated PSOC 276 is trapped during combustion.

On the basis of the trends displayed by the mineral matter content during the course of treatment, a mechanism for the ultimate uptake of sodium can be proposed. The exposure of the coal to NO_2 results in the loss of roughly 25 % of the original hydrogen content in the coal as well as the uptake of NO_2 by the

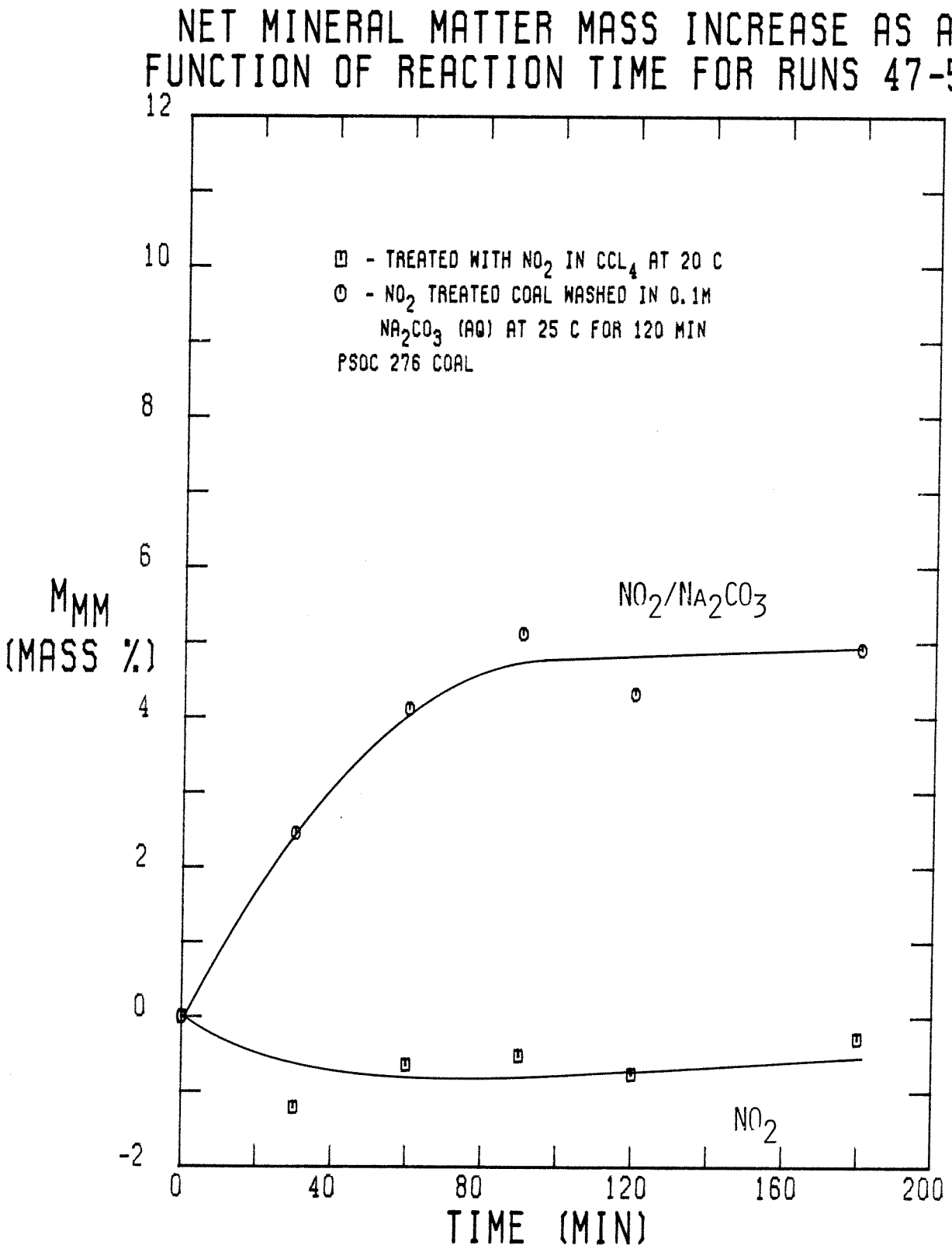
NET MINERAL MATTER MASS INCREASE AS A FUNCTION OF REACTION TIME FOR RUNS 47-52
□ - TREATED WITH NO2 IN CCL4 AT 20 C
○ - NO2 TREATED COAL WASHED IN 0.1M NA2CO3 (AQ) AT 25 C FOR 120 MIN
PSOC 276 COAL
NO2/NA2CO3
NO2
MMM (MASS %)
TIME (MIN)
12
10
8
6
4
2
0
-2
0
40
80
120
160
200

FIGURE 4-110

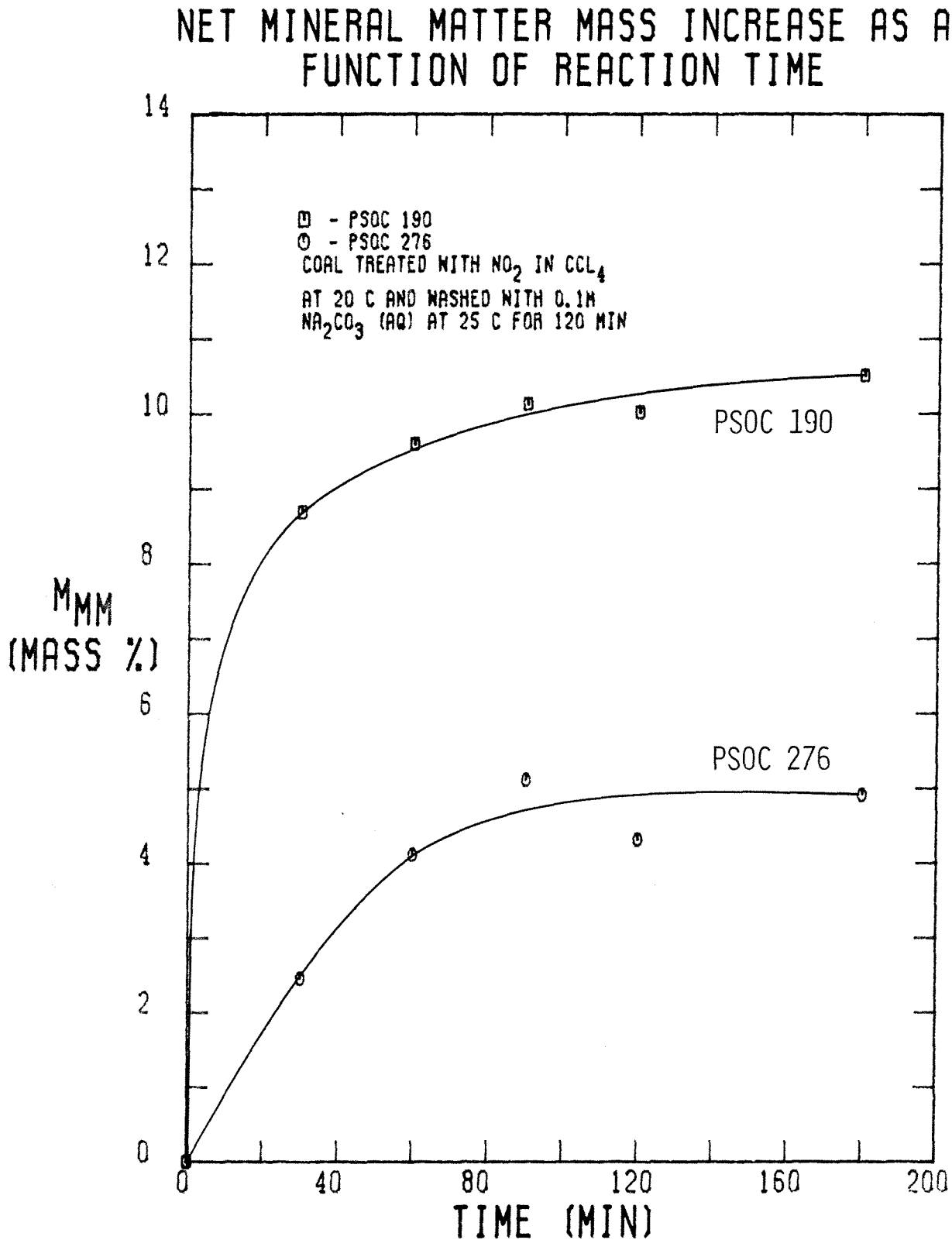
NET MINERAL MATTER MASS INCREASE AS A FUNCTION OF REACTION TIME
□ - PSOC 190
○ - PSOC 276
COAL TREATED WITH NO_2 IN CCL_4
AT 20 C AND WASHED WITH 0.1M
NA_2CO_3 (AQ) AT 25 C FOR 120 MIN
PSOC 190
PSOC 276
M_{MM} (MASS %)
TIME (MIN)
0
2
4
6
8
10
12
14
0
40
80
120
160
200

FIGURE 4-111

coal. Consequently, a large number of anionic oxygen atoms are introduced into the coal where the hydrogen is displaced as well as polar oxygen atoms where NO_2 resides in the coal. It is these oxygen atoms which account for the adsorption of CCl_4 during the NO_2 treatment which is not removed by vacuum drying at 120°C for three hours. Once the NO_2-treated coal is exposed to Na_2CO_3 (aq), the weakly adsorbed CCl_4 is displaced by the more strongly interacting aqueous species, in particular Na^+. Furthermore, many of the anionic oxygen sites which do not contain adsorbed CCl_4 do adsorb Na^+, mainly because Na^+ is smaller than CCl_4 and can therefore migrate into smaller pores. The overall pore structure, however, does influence the amount of sodium ultimately taken up by the coal, as evidenced by the different results obtained with the PSOC 190 and PSOC 276 coals.

4.2.2.8 The Sulfur Content of the Coal

The ultimate goal of this work is to determine if the sulfur can be removed from the coal through treatment with NO_2 followed by a Na_2CO_3 (aq) wash without altering the remainder of the coal to any great extent. So far, the discussion of the results has centered on the alterations in the remainder of the coal introduced by the treatment. In this section, the discussion will focus exclusively on the effect of the treatment on the sulfur content of the coal. In particular, the effect of the NO_2-treatment time, temperature and NO_2 concentration on the ultimate sulfur removal will be examined. Furthermore, the difference between the sulfur determinations using the Bomb and Leco methods of analysis, which were discussed in the experimental section, will play a crucial role in the interpretation of the results.

The values of the sulfur content of the PSOC 190 treated in the various solvents in the flow reactor (Runs 1–6) which are tabulated in Table 3–19 indicate some interesting effects by the solvent on the overall desulfurization. All of the sulfur determinations done for this set of experiments utilized the Leco method. When water is the solvent, temperature seems to have little effect, because at 25°C, 43 % of the sulfur is removed while at 80°C, 47 % of the sulfur is removed. Since only 24 % of the initial sulfur is inorganic (raw, undried PSOC 190 was used in the experiments), some removal of organic sulfur must occur during the NO_2 treatment. Unfortunately, it is impossible to determine what type of organic sulfur groups are attacked by the NO_2-H_2O system, although it is probable that any aliphatic sulfur groups are more easily attacked than thiophenic sulfur groups. Temperature seems to have a more pronounced effect on sulfur removal when pyridine is used as the solvent. When the coal is treated at 25°C, 43 % of the sulfur is removed, the same amount as when H_2O is the solvent. When the coal is treated at 80°C, however, 59 % of the sulfur is removed, which is greater

than the corresponding removal when H_2O is the solvent. Perhaps the ability of the pyridine to extract a small amount of the coal allows NO_2 greater access to the particle interior. Another possible explanation is that while NO_2 reacts with water to form HNO_3 and HNO_2, NO_2 does not react with the pyridine. Thus, two different mechanisms occur in the two solvents. The use of nitrobenzene as the solvent poses another problem in that in the presence of NO_2 it extracts up to 50 % of the coal. Because of its high affinity for coal and its high boiling point, nitrobenzene is virtually impossible to separate from the coal, even with vacuum drying at 150°C. Therefore, it is hard to determine an exact mass loss or gain for the treated coal. Nevertheless, on the basis of the residual coal and the recovered extract, NO_2 treatment at 33°C of the nitrobenzene-coal slurry results in about a 61 % sulfur removal after adjustment for the 16.5 % overall mass gain, while treatment at 80°C yields only a 45 % sulfur removal. It should be noted that at 80°C, there is an overall mass loss of 16 %, which implies that the extent of oxidation at 80°C is much greater than at 33°C. Because of the difficulties in separating aromatic solvents from the coal, they were no longer used in this study. The extent of the sulfur removal, however, is rather impressive and seems to be greater than when H_2O is the solvent. It should be noted, however, that the potential interference of the nitrogen added to the coal, by both NO_2 uptake and incompletely removed pyridine or nitrobenzene, may be the reason for the high desulfurizations indicated by the Leco analysis. Hence, these results must be viewed with some suspicion.

The values of the sulfur conversion, X_s, as a function of NO_2-exposure time for the PSOC 190 coal treated with NO_2 in water at 25 to 30°C in the flow reactor and subsequently washed with 0.1 M Na_2CO_3 (aq) (Runs 7–13) are shown graphically in Figure 4–112. The sulfur conversion is just the fraction of the initial sulfur which is removed during processing. Values of X_s are obtained from c_S by

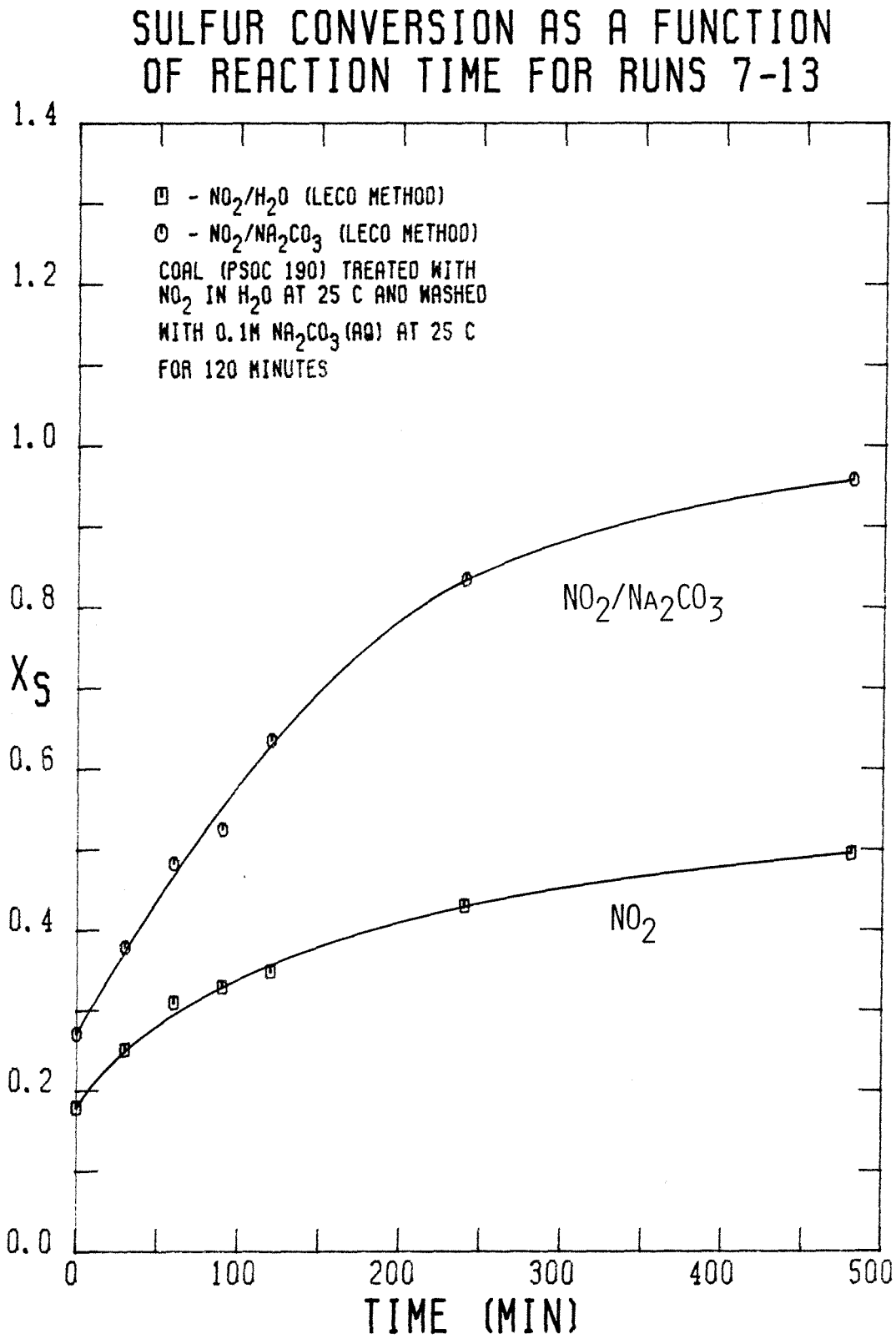
SULFUR CONVERSION AS A FUNCTION OF REACTION TIME FOR RUNS 7-13
□ - NO2/H2O (LECO METHOD)
○ - NO2/NA2CO3 (LECO METHOD)
COAL (PSOC 190) TREATED WITH NO2 IN H2O AT 25 C AND WASHED WITH 0.1M NA2CO3 (AQ) AT 25 C FOR 120 MINUTES
NO2/NA2CO3
NO2
XS
TIME (MIN)
1.4
1.2
1.0
0.8
0.6
0.4
0.2
0.0
0
100
200
300
400
500

FIGURE 4-112

adjusting for any mass gain which occurs. It should be noted that just washing the coal in water removes 18 % of the total sulfur in the raw coal, and subsequent washing in 0.1 M Na_2CO_3 (aq) results in an overall sulfur removal of 27 %. The form of sulfur removed by this washing is sulfate sulfur. Thus, the values for X_s in the figure at t = 0 are 0.18 for the NO_2-treated coal and 0.27 for the NO_2-treated coal washed in 0.1 M Na_2CO_3 (aq). It should be noted that the coal treated with NO_2 in water experiences a mass loss of several percent relative to the dried raw coal. A further mass loss occurs after washing in Na_2CO_3 (aq). Consequently, no mass adjustments were made in X_s as they would be if a mass gain were to occur. If a mass gain occurs, it is assumed that some material such as solvent is adsorbed by the coal, thereby diluting the sulfur and causing a decrease in the sulfur content. The conversion, however, is based on the absolute mass of sulfur removed. Thus, when the sulfur content, c_S, is used to calculate the conversion, the decrease in c_S due to dilution must be taken into account. On the other hand, when a mass loss occurs, it is assumed that the material lost has the same composition as the remaining coal. Therefore, no mass adjustment is made in X_s when a mass loss occurs. The curve for the NO_2-treated coal shows that X_s rises from 0.18 initially to 0.50 after 8 hours of NO_2 treatment in a fairly smooth manner. Because the sulfur analyses were done using the Leco method, all that can be said is that roughly 50 % of the original sulfur in the coal does not appear as SO_2 in the combustion gases. Whether the SO_2 was trapped by the ash during combustion is not known, although it seems unlikely since sodium seems to account for the SO_2 trapping. Rather, it is more likely that the sulfur is actually removed from the coal during the NO_2/H_2O/coal treatment in the form of water soluble sulfate. The curve for the NO_2-treated coal washed in 0.1 M Na_2CO_3 (aq) indicates that X_s rises from 0.27 initially to 0.96 after 8 hours of NO_2 treatment. Thus, virtually all of the sulfur in the raw

coal which would be converted to SO_2 during combustion can be removed from the flue gases. Although the ash of the Na_2CO_3 (aq) washed coal was not examined, it seems reasonable to expect that the uptake of sodium occurs because the NO_2 treatment still introduces anionic oxygen into the coal whether H_2O or CCl_4 is the solvent. Indeed, the increase in X_s due to the Na_2CO_3 (aq) wash can probably be attributed to the trapping of SO_2 by adsorbed sodium to produce Na_2SO_4 during combustion.

The next set of experiments (Runs 15–20) was performed under more controlled conditions. The values of the sulfur conversion, X_s, are given in Table 4-2 along with the pertinent reaction conditions. Several trends are established by the data. After an initial jump in X_s during the first 30 minutes of NO_2 exposure, X_s rises more gradually, reaching a value of 0.45 after 4 hours, which implies that a certain portion of the sulfur is rapidly removed by the aqueous NO_2 solution while the remaining sulfur is removed at a much slower pace. The same trend occurs for values of X_s corresponding to the Na_2CO_3 (aq) washed coal as well. Furthermore, it appears that under these reaction conditions a limiting value of 87 % of the potential SO_2 can be prevented from entering the flue gas during combustion. As mentioned above, the value for X_s after the NO_2 treatment actually represents the amount of sulfur removed from the coal while the additional sulfur removal resulting from the Na_2CO_3 (aq) wash probably represents the sulfur which is trapped as SO_2 during combustion by the adsorbed sodium.

The remainder of this section will be concerned with the change in sulfur content due to NO_2 treatment when CCl_4 is the solvent. Because NO_2 does not react with CCl_4, the only important oxidant is NO_2, whereas when H_2O is the solvent, several important oxidants exist, namely HNO_3 (aq), HNO_2 (aq) and NO_2 (aq). Therefore, in the remaining experiments, the oxidation of the various species in

TABLE 4-2

Sulfur Conversion (X_S) for Runs Using Water as a Solvent for the Treatment of PSOC 190 Coal (+200-325 mesh) with NO_2

Run #	Reaction Time (min)	T (C)	Mean NO_2 Flowrate (g NO_2/min)	$X_S = 1 - \frac{C_S}{(C_S)_0}$	
				After NO_2 Treatment	After Wash Na_2CO_3 (aq)
Blank				0.1681	0.2710
15	60	23.0-23.8	0.697	0.3257	0.5179
16	120	22.6-24.0	0.269	0.3062	0.5016
17	120	24.6-25.6	0.483	0.3681	0.6800
18	120	23.0-24.0	1.039	0.4007	0.7980
19	180	23.6-26.0	0.962	0.4365	0.8664
20	240	23.2-25.0	0.759	0.4528	0.8697

the coal can be attributed to NO_2, which will simplify the interpretation of the effect of the various reaction parameters on the sulfur removal.

The first set of experiments using CCl_4 as the solvent (Runs 21–27) was conducted in the flow reactor at roughly 25°C. The values for the mass corrected sulfur content, c_S, are shown as a function of NO_2-reaction time in Figure 4–113 for both the NO_2-treated coal and the coal subsequently washed in 0.1 M Na_2CO_3 (aq). It should be noted that the phrase "mass corrected" means that the sulfur content has been adjusted to account for the adsorbed CCl_4. The initial sulfur content of the predried PSOC 190 is 3.167 mass percent. Basically, c_S for the NO_2-treated coal undergoes an initial drop of about 0.7 % after 180 minutes, which is due partially to the dilution effect of the mass gain and also to the removal of some sulfur. Any sulfur removed is probably in the form of SO_2, which is produced by the reaction of NO_2 with the pyrite, which exists to the small extent of 0.21 mass percent in the PSOC 190 coal, and with easily oxidized organic sulfur structures in the coal. The curve corresponding to the sulfur content of the washed coal determined by the Bomb method, c_S^B, shows an initial drop and then levels off at about 1.6 %, which indicates that a portion of the sulfur in the coal reacts rapidly with NO_2 and is easily removed during the Na_2CO_3 (aq) wash. That is, just exposing the coal to a small amount of NO_2 (less than 0.25 F) for a short time (30 minutes or less) results in the complete conversion of about half of the sulfur into forms which are leached out of the coal by the Na_2CO_3 (aq) wash. More severe NO_2 treatment does not enhance the removal of sulfur from the coal. The curve corresponding to the values of the amount of sulfur converted to SO_2 during combustion by the Leco method, c_S^L, indicates that under the reaction conditions employed, NO_2-exposure times greater than 30 minutes do result in greater sulfur removal. Because the difference between c_S^B and c_S^L represents the amount of sulfur trapped as Na_2SO_4

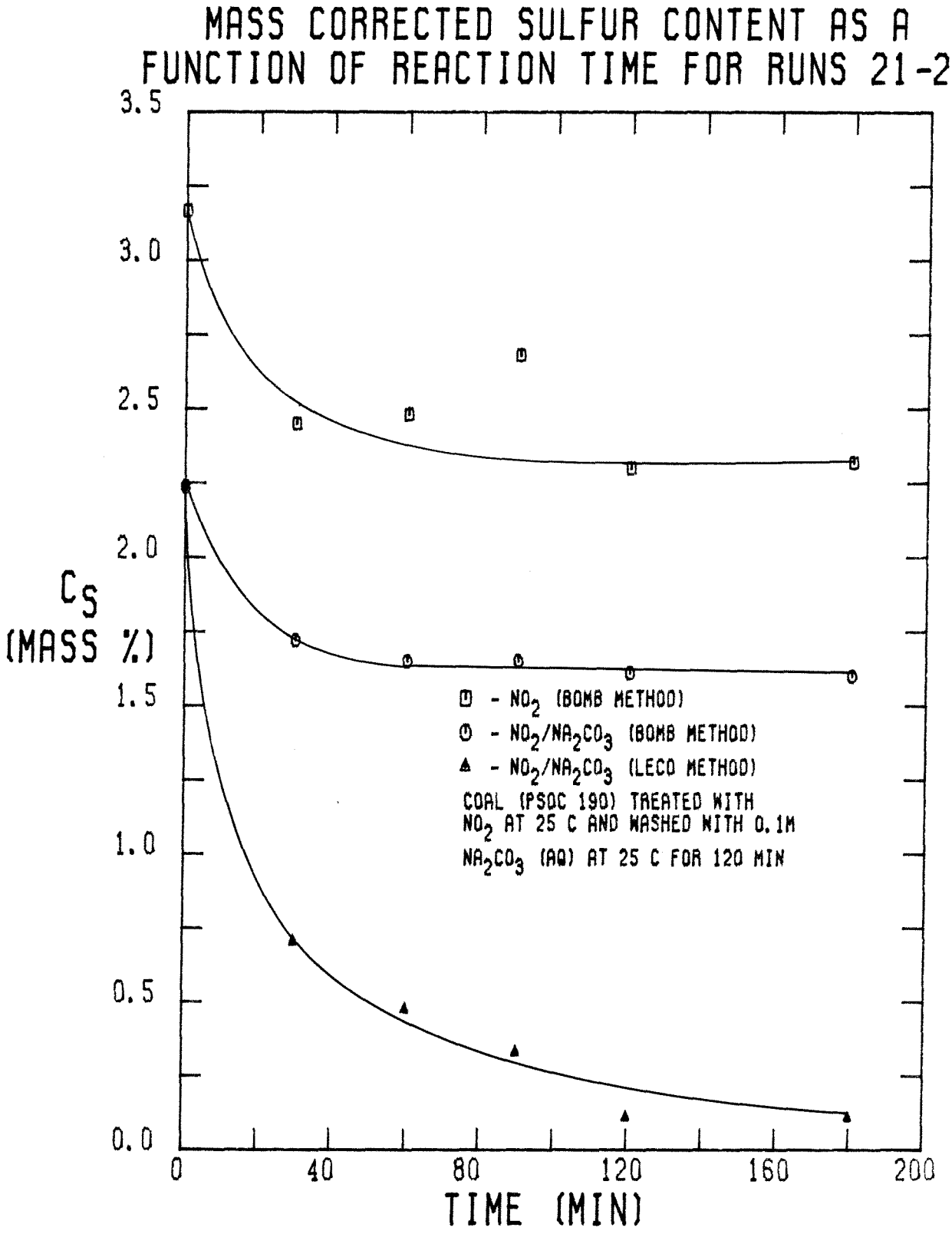
MASS CORRECTED SULFUR CONTENT AS A FUNCTION OF REACTION TIME FOR RUNS 21-27
3.5
3.0
2.5
2.0
1.5
1.0
0.5
0.0
C_S (MASS %)
0
40
80
120
160
200
TIME (MIN)
- NO_2 (BOMB METHOD)
- NO_2/NA_2CO_3 (BOMB METHOD)
- NO_2/NA_2CO_3 (LECO METHOD)
COAL (PSOC 190) TREATED WITH NO_2 AT 25 C AND WASHED WITH 0.1M NA_2CO_3 (AQ) AT 25 C FOR 120 MIN

FIGURE 4-113

by the adsorbed sodium during combustion, these results imply that the rate of the process which accounts for the ultimate uptake of sodium is much slower than the rate of the process which accounts for the removal of the portion of the sulfur which is easily attacked by NO_2 and extracted by Na_2CO_3 (aq).

If the values of c_S are adjusted for the net mass gain, the values for the sulfur conversion, X_s, can be obtained by using the following expression:

$$X_S = 1 - \frac{(f + 1)\, c_s}{c_0}, \quad \text{where} \tag{4.2.19}$$

f = the fractional mass gain,

c_S = the mass corrected sulfur content (mass %), and

c_0 = the initial sulfur content (mass %).

The values for X_s corresponding to the values of c_S discussed above are shown graphically in Figure 4–114. The values of X_s for the NO_2-treated coal indicate the facile removal of roughly 20 % of the initial sulfur in the coal. As mentioned above, the removal is the result of SO_2 production from the reaction of NO_2 with pyrite and aliphatic sulfur structures in the coal. It should be noted that complete conversion of pyrite to ferric sulfate and SO_2 by the NO_2 attack can account for only about 3 % of the sulfur removal. The values of the conversion for the subsequently washed coal based on the Bomb determination, X_S^B, indicate a removal of an additional 30 % of the sulfur. Initially, the coal contains 19.4 % of its sulfur in the form of sulfate, which accounts for the majority of the sulfur removal during the Na_2CO_3 (aq) wash. The remaining sulfur removal can be attributed to the leaching of other sulfates formed by the reaction of NO_2 with the coal. In total, this two step process removes 50 % of the sulfur initially in the coal, although just washing the predried coal in 0.1 M Na_2CO_3 (aq) removes 30 % of the sulfur. During the Na_2CO_3 (aq) wash, however, the coal also takes up Na^+, which is adsorbed by the anionic oxygen introduced into the coal during

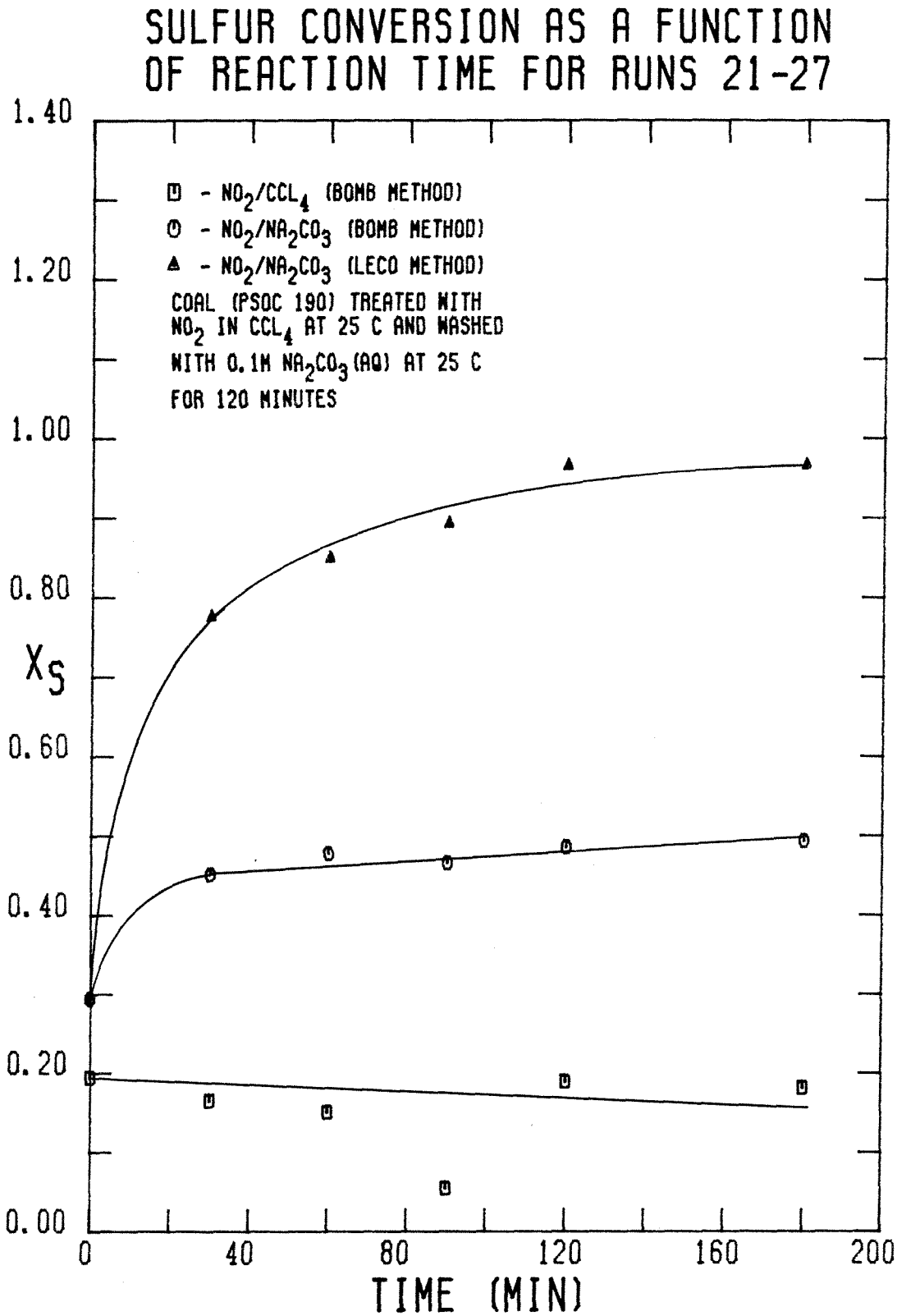
SULFUR CONVERSION AS A FUNCTION OF REACTION TIME FOR RUNS 21-27
□ - NO2/CCL4 (BOMB METHOD)
○ - NO2/NA2CO3 (BOMB METHOD)
△ - NO2/NA2CO3 (LECO METHOD)
COAL (PSOC 190) TREATED WITH NO2 IN CCL4 AT 25 C AND WASHED WITH 0.1M NA2CO3(AQ) AT 25 C FOR 120 MINUTES
XS
1.40
1.20
1.00
0.80
0.60
0.40
0.20
0.00
0
40
80
120
160
200
TIME (MIN)

FIGURE 4-114

the NO_2 treatment. This uptake of sodium results in virtually complete removal of SO_2 from the flue gases during combustion, as indicated by the curve corresponding to the values of X_S^L, which are based on the Leco determination of the sulfur content. Even after just 30 minutes of NO_2 exposure, 78 % of the normally produced amount of SO_2 is removed from the combustion gas. More extensive NO_2 treatment results in the eventual removal of 97 % of the potential SO_2 emissions.

The second set of experiments conducted in the flow reactor using CCl_4 as the solvent was performed at 50°C, at which temperature the saturation concentration of NO_2 is about 1.2 F. The mass corrected sulfur content of the NO_2-treated coal and the coal subsequently washed in 2 M HNO_3 (aq) for 12 hours is displayed as a function of NO_2-exposure time in Figure 4–115. It should be noted that a wash of the NO_2-treated coal in 0.1 M Na_2CO_3 (aq) could not be performed because the coal completely emulsified, rendering filtration impossible. This problem did not occur when the coal was treated with NO_2 at 20 and 0°C, which implies that the extent of oxidation of the coal is immensely enhanced at 50°C. Once again, the NO_2 treatment causes a rapid drop initially in c_S, which was determined by the Bomb method, after which c_S is constant at about 2.30 mass percent for longer exposure times. This decrease is caused partially by the dilution effect of the mass gain and partially by the removal of a portion of the initial sulfur which is susceptible to rapid attack by NO_2 to form SO_2, which then diffuses into the bulk liquid phase. The sulfur content of the washed coal was determined by both the Bomb and the Leco methods. The values of the sulfur content determined by the Bomb method, c_S^B, define the middle curve of Figure 4–115, in which c_S^B drops to 1.57 % after 30 minutes of NO_2 treatment and then levels off at about 1.45 % thereafter. Thus, the HNO_3 (aq) wash removes additional sulfur, primarily sulfates and any unreacted pyrite. It should be noted

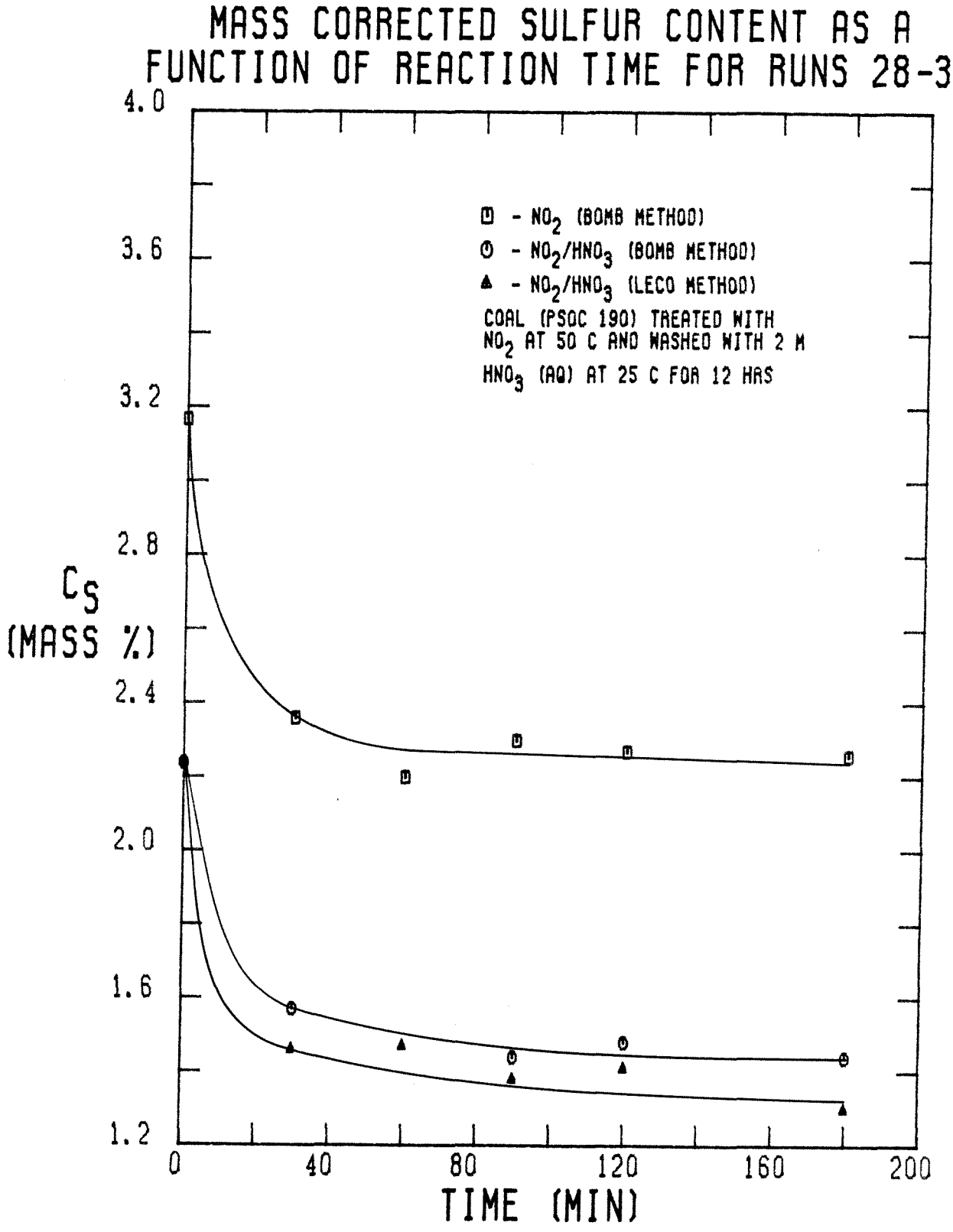
MASS CORRECTED SULFUR CONTENT AS A FUNCTION OF REACTION TIME FOR RUNS 28-32
□ - NO2 (BOMB METHOD)
⊙ - NO2/HNO3 (BOMB METHOD)
▲ - NO2/HNO3 (LECO METHOD)
COAL (PSOC 190) TREATED WITH NO2 AT 50 C AND WASHED WITH 2 M HNO3 (AQ) AT 25 C FOR 12 HRS
Cs (MASS %)
4.0
3.6
3.2
2.8
2.4
2.0
1.6
1.2
0
40
80
120
160
200
TIME (MIN)

FIGURE 4-115

that just washing the coal in 2 M HNO_3 (aq), which is the standard ASTM procedure for the determination of the inorganic sulfur content, results in a drop in c_S from 3.17 % to 2.24 %. Therefore, the NO_2 treatment does cause additional sulfur removal. The most interesting part of Figure 4–115, however, is the bottom curve, which is defined by the values of the sulfur content of the HNO_3 (aq) washed coal determined by the Leco method, c_S^L. What is so important is that c_S^L is essentially equal to c_S^B, which indicates that all of the residual sulfur in the washed coal is converted to SO_2 during combustion and enters the flue gas stream and is not trapped by the ash. This result provides unequivocal evidence that the uptake of Na^+ during the Na_2CO_3 (aq) wash is responsible for the trapping of SO_2 during combustion in the ash.

Figure 4–116 contains the values of the sulfur conversion, X_s, corresponding to the values of c_S in Figure 4–115. Basically, after an adjustment for the mass gain is made, it appears that the NO_2 treatment results in a sulfur removal of only about 13 to 14 %. Washing the NO_2-treated coal in 2 M HNO_3 (aq) results in an overall sulfur removal of about 50 %, which is about the same removal obtained when coal treated with NO_2 at 25°C is washed in 0.1 M Na_2CO_3 (aq). This similarity in sulfur removals implies that the wash is just removing water soluble sulfates. The pH of the aqueous solution determines to what extent the oxidized coal emulsifies. Finally, the sulfur conversion based on c_S^L is essentially equal to that based on c_S^B, as stated previously. Therefore, it is the added sodium which is responsible for trapping the sulfur as Na_2SO_4 in the ash during combustion, and not some error in the Leco method which accounts for the difference in c_S^B and c_S^L of the NO_2-treated coals washed in 0.1 M Na_2CO_3 (aq).

The values of c_S for the PSOC 190 coal treated with NO_2 at 20°C in the batch reactor and subsequently washed with 0.1 M Na_2CO_3 (aq) (Runs 33–37) are plotted as a function of NO_2-exposure time in Figure 4–117. The PSOC 190 coal used

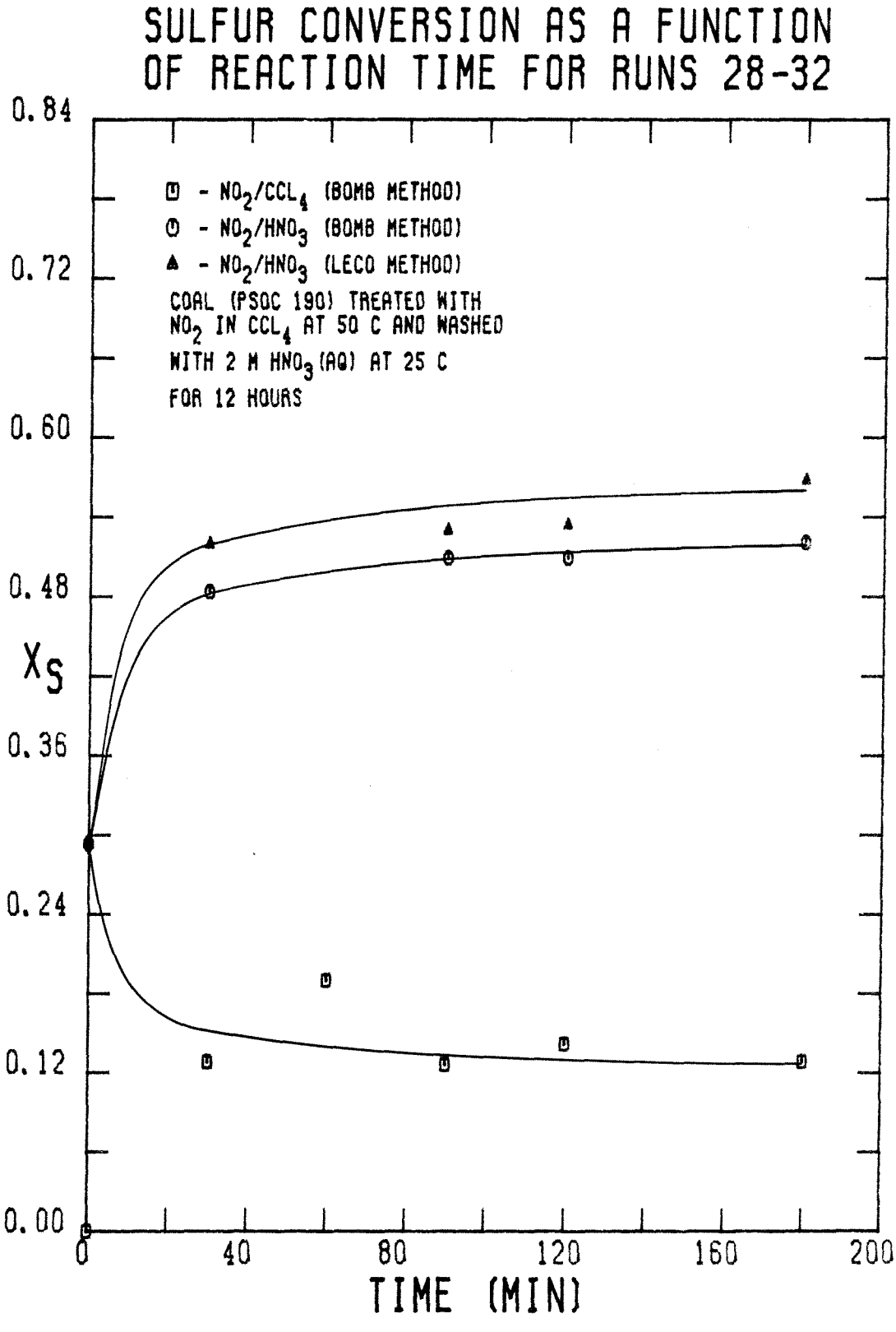
SULFUR CONVERSION AS A FUNCTION OF REACTION TIME FOR RUNS 28-32
0.84
0.72
0.60
0.48
0.36
0.24
0.12
0.00
X_S
□ - NO_2/CCL_4 (BOMB METHOD)
○ - NO_2/HNO_3 (BOMB METHOD)
▲ - NO_2/HNO_3 (LECO METHOD)
COAL (PSOC 190) TREATED WITH NO_2 IN CCL_4 AT 50 C AND WASHED WITH 2 M HNO_3(AQ) AT 25 C FOR 12 HOURS
0
40
80
120
160
200
TIME (MIN)

FIGURE 4-116

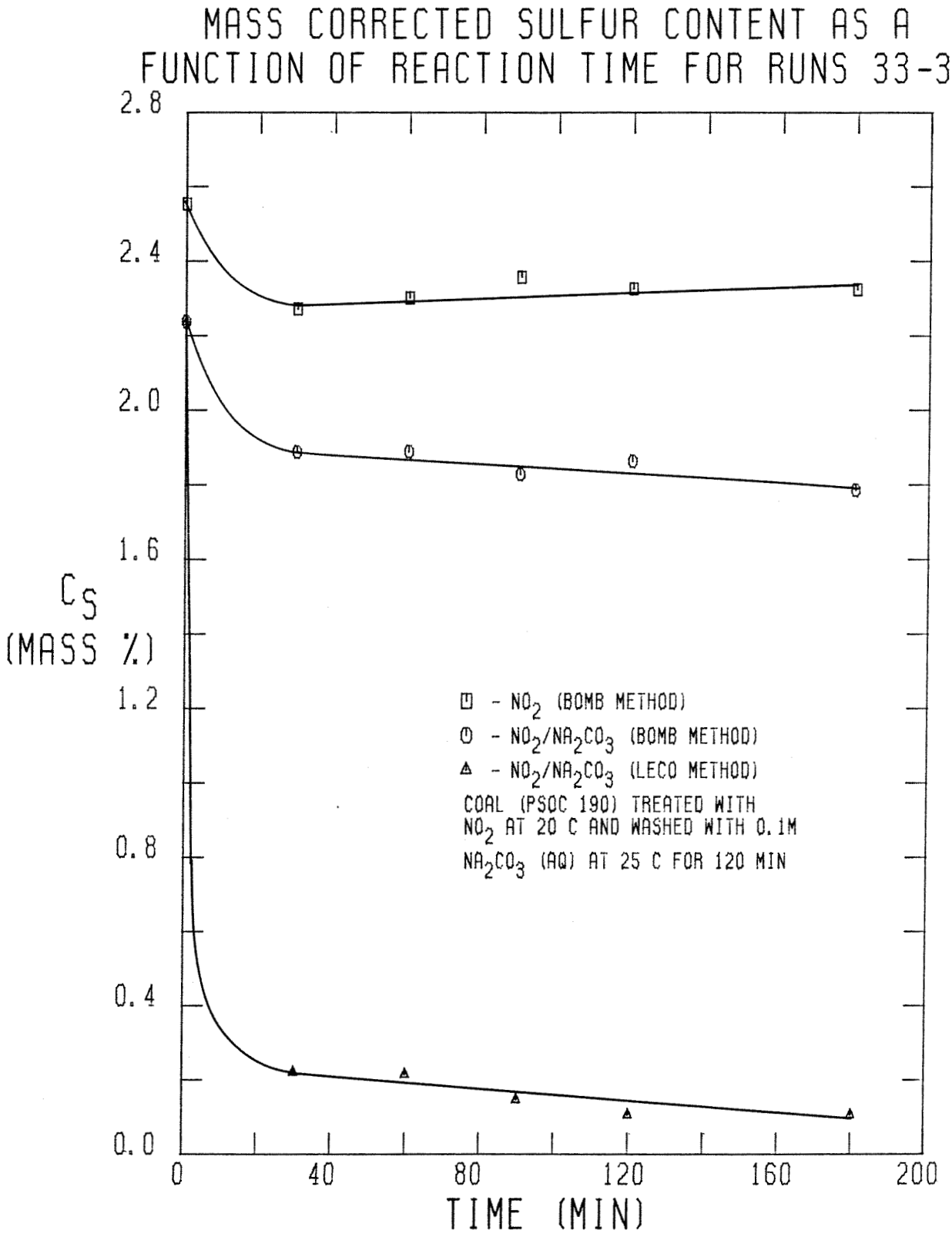
MASS CORRECTED SULFUR CONTENT AS A FUNCTION OF REACTION TIME FOR RUNS 33-37
2.8
2.4
2.0
1.6
1.2
0.8
0.4
0.0
C_S (MASS %)
0
40
80
120
160
200
TIME (MIN)
□ - NO_2 (BOMB METHOD)
⊙ - NO_2/NA_2CO_3 (BOMB METHOD)
△ - NO_2/NA_2CO_3 (LECO METHOD)
COAL (PSOC 190) TREATED WITH NO_2 AT 20 C AND WASHED WITH 0.1M NA_2CO_3 (AQ) AT 25 C FOR 120 MIN

FIGURE 4-117

in this study was washed in water and vacuum dried. The coal has an initial sulfur content of 2.554 mass percent. As before, there is an initial drop in c_S after 30 minutes of NO_2 exposure, after which time no further change in c_S seems to occur. In particular, the NO_2 treatment results in a drop in c_S from 2.55 to roughly 2.30 mass percent. The Na_2CO_3 (aq) wash results in additional sulfur removal, with c_S^B being about 1.8 to 1.9 mass percent. As usual, the value of c_S^I for the washed coal is quite low, reaching a value of roughly 0.1 mass percent after 180 minutes of NO_2 exposure.

The corresponding values of the sulfur conversion for Runs 33–37 are displayed graphically in Figure 4–118 as a function of NO_2-exposure time. The NO_2 treatment results in only a 10 percent removal of sulfur. Still, some organic sulfur must be removed since the only inorganic sulfur present is pyrite, which comprises only 0.21 mass percent of the coal. Complete conversion of the pyrite to ferric sulfate and SO_2 would result in only a 3 % sulfur conversion. Thus, aliphatic sulfur structures in the coal are probably oxidized by the NO_2 as well. Washing the treated coal in 0.1 M Na_2CO_3 (aq) results in additional sulfur removal which gives an overall sulfur conversion based on the Bomb analysis, X_S^B, of about 30 %. The amount of sulfur removed from the combustion gas, X_S^I, by the adsorbed Na^+ rapidly exceeds 90 % and levels off at 96 %. Thus, the majority of the desulfurization in terms of reduction of SO_2 levels in the combustion gas is due to trapping of SO_2 by sodium in the form of Na_2SO_4 in the ash.

The effect of NO_2-exposure time on the mass corrected sulfur content of the coal treated at 0 °C in the batch reactor and subsequently washed in 0.1 M Na_2CO_3 (aq) (Runs 42–46) is illustrated in Figure 4–119. The NO_2 treatment results in a rapid, yet small drop in c_S from 2.55 mass percent to about 2.36 mass percent. Likewise, the Na_2CO_3 (aq) wash of the NO_2-treated coal results in a decrease in c_S to about 1.8 mass percent after 30 minutes of NO_2

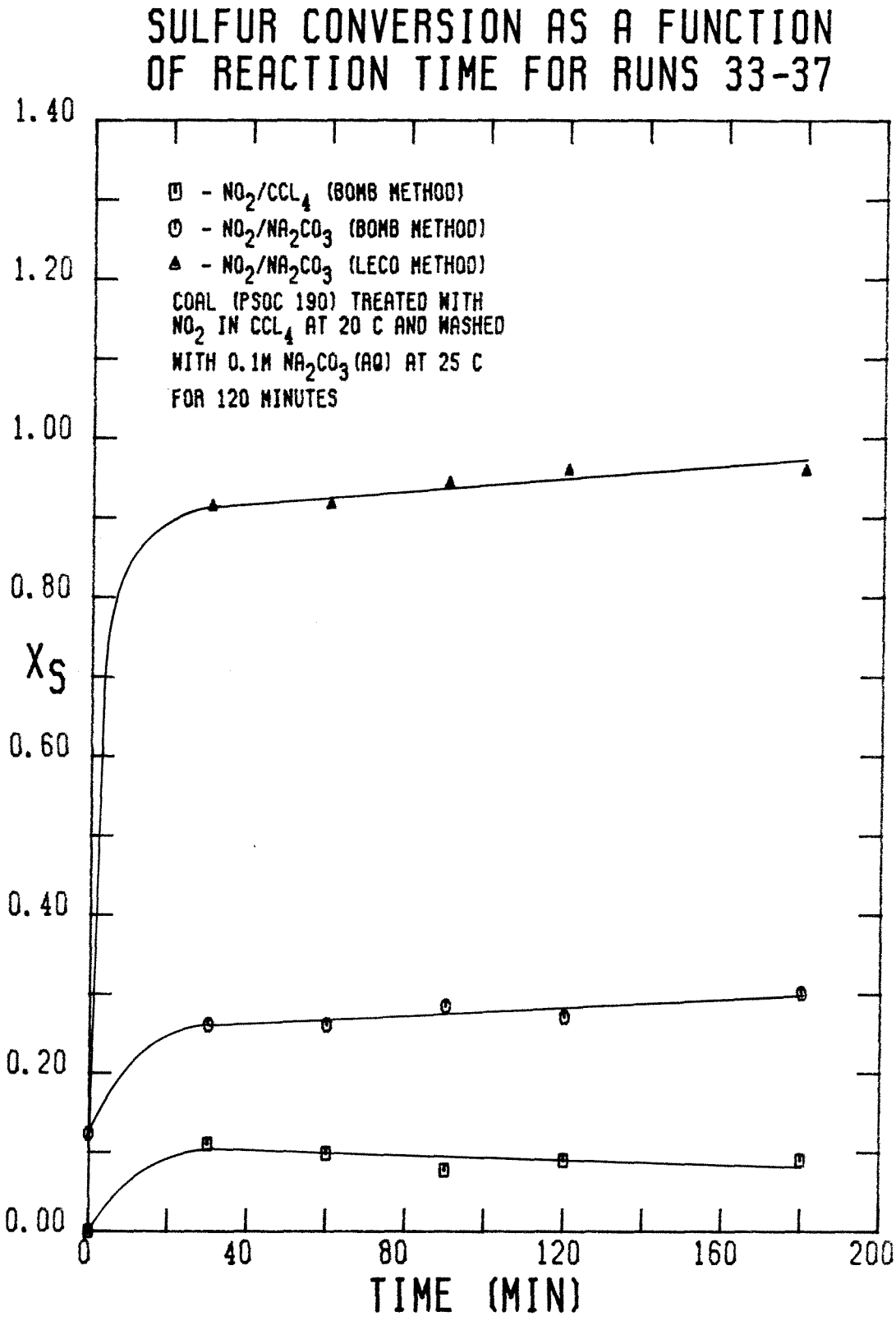
SULFUR CONVERSION AS A FUNCTION OF REACTION TIME FOR RUNS 33-37
□ - NO2/CCL4 (BOMB METHOD)
○ - NO2/NA2CO3 (BOMB METHOD)
△ - NO2/NA2CO3 (LECO METHOD)
COAL (PSOC 190) TREATED WITH NO2 IN CCL4 AT 20 C AND WASHED WITH 0.1M NA2CO3(AQ) AT 25 C FOR 120 MINUTES
1.40
1.20
1.00
0.80
XS
0.60
0.40
0.20
0.00
0
40
80
120
160
200
TIME (MIN)

FIGURE 4-118

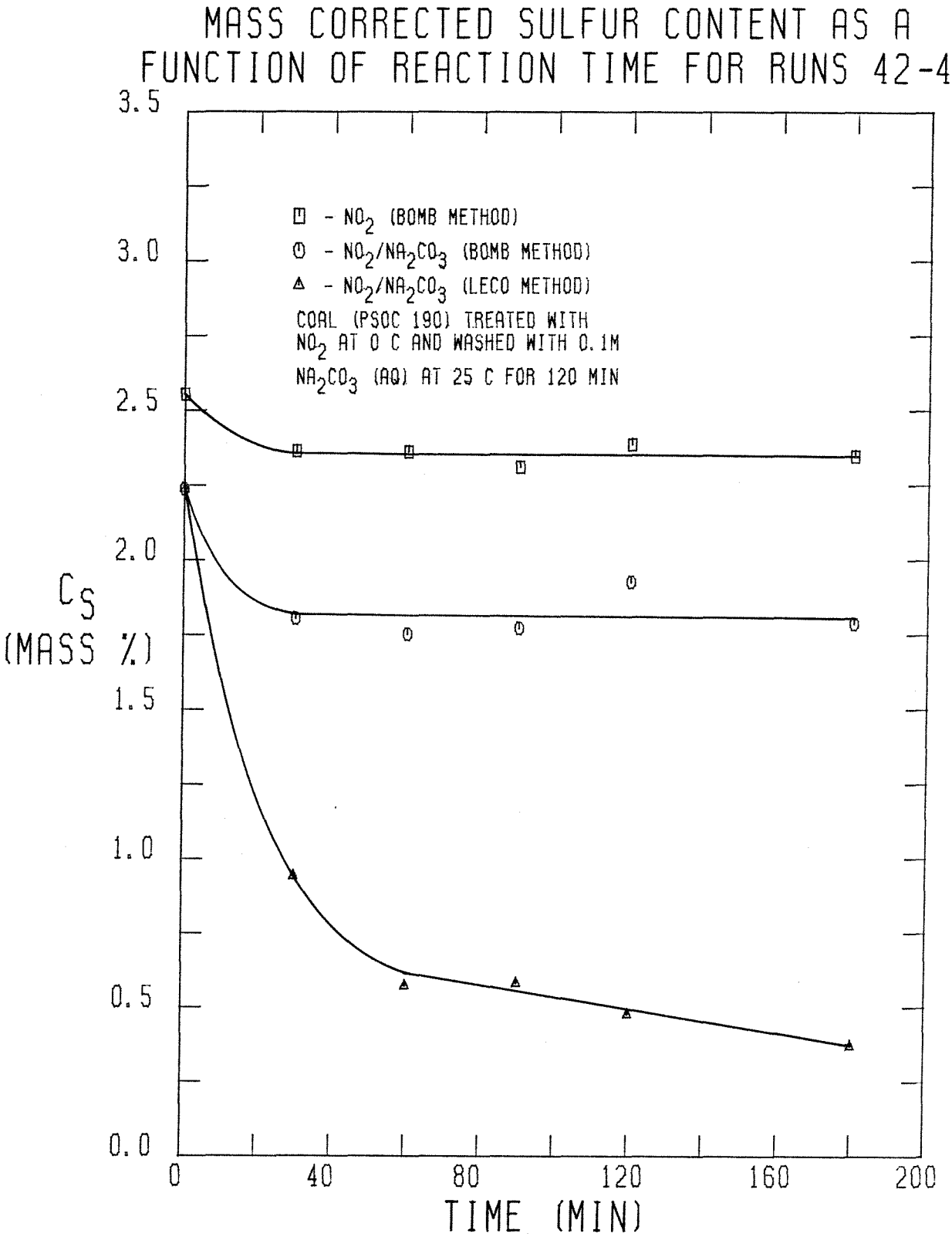
MASS CORRECTED SULFUR CONTENT AS A FUNCTION OF REACTION TIME FOR RUNS 42-46
□ - NO2 (BOMB METHOD)
① - NO2/NA2CO3 (BOMB METHOD)
△ - NO2/NA2CO3 (LECO METHOD)
COAL (PSOC 190) TREATED WITH NO2 AT 0 C AND WASHED WITH 0.1M NA2CO3 (AQ) AT 25 C FOR 120 MIN
CS (MASS %)
TIME (MIN)
3.5
3.0
2.5
2.0
1.5
1.0
0.5
0.0
0
40
80
120
160
200

FIGURE 4-119

exposure, after which time c_S^B is essentially constant. The concentration of sulfur which ultimately appears as SO_2, however, decreases more gradually, which implies that the NO_2-coal reaction proceeds at a discernible rate at 0°C. The values of the sulfur conversion, X_s, corresponding to the values of c_S for Runs 42–46 are displayed graphically in Figure 4–120. As expected, the NO_2 treatment yields a small sulfur conversion of only about 8 %. Washing the NO_2-treated coal in 0.1 M Na_2CO_3 (aq) results in an overall sulfur removal of about 30 %, which seems to be the case for all of the runs discussed so far in which PSOC 190 coal was used. The values of X_S^L, which are based on the sulfur content determined by the Leco method, however, rise at a slower rate, reaching a value of 0.85 after 180 minutes of NO_2 exposure. Therefore, the rate of introduction of the anionic oxygen atoms into the coal during the NO_2-coal reaction is slower at 0°C than at higher temperatures. This behavior is consistent with the nitrogen and oxygen uptake data as well as the hydrogen loss data.

The effect of temperature on the removal of sulfur during the NO_2 treatment is illustrated in Figure 4–121, where X_s is plotted as a function of NO_2-exposure time. Although there is extensive scatter in the data, a general dependence of X_s on the temperature can be seen. In particular, X_s increases with increasing temperature, ranging from about 8 % sulfur removal at 0°C to 16 % sulfur removal at 50°C. A very interesting feature of this plot is the pronounced peak in X_s at t = 60 minutes when the coal is treated with NO_2 at 50°C. There are several possible explanations for this behavior. First, it is possible that once the SO_2 enters the liquid phase, it may react with the coal at a rate which is slower than its rate of formation to form more stable sulfur compounds in the coal. The second possibility is that most of the SO_2 is removed during the vacuum drying at 120°C, when the high temperature permits the evolution of SO_2. Because the pore volume continues to decrease with increasing NO_2-exposure time, less SO_2

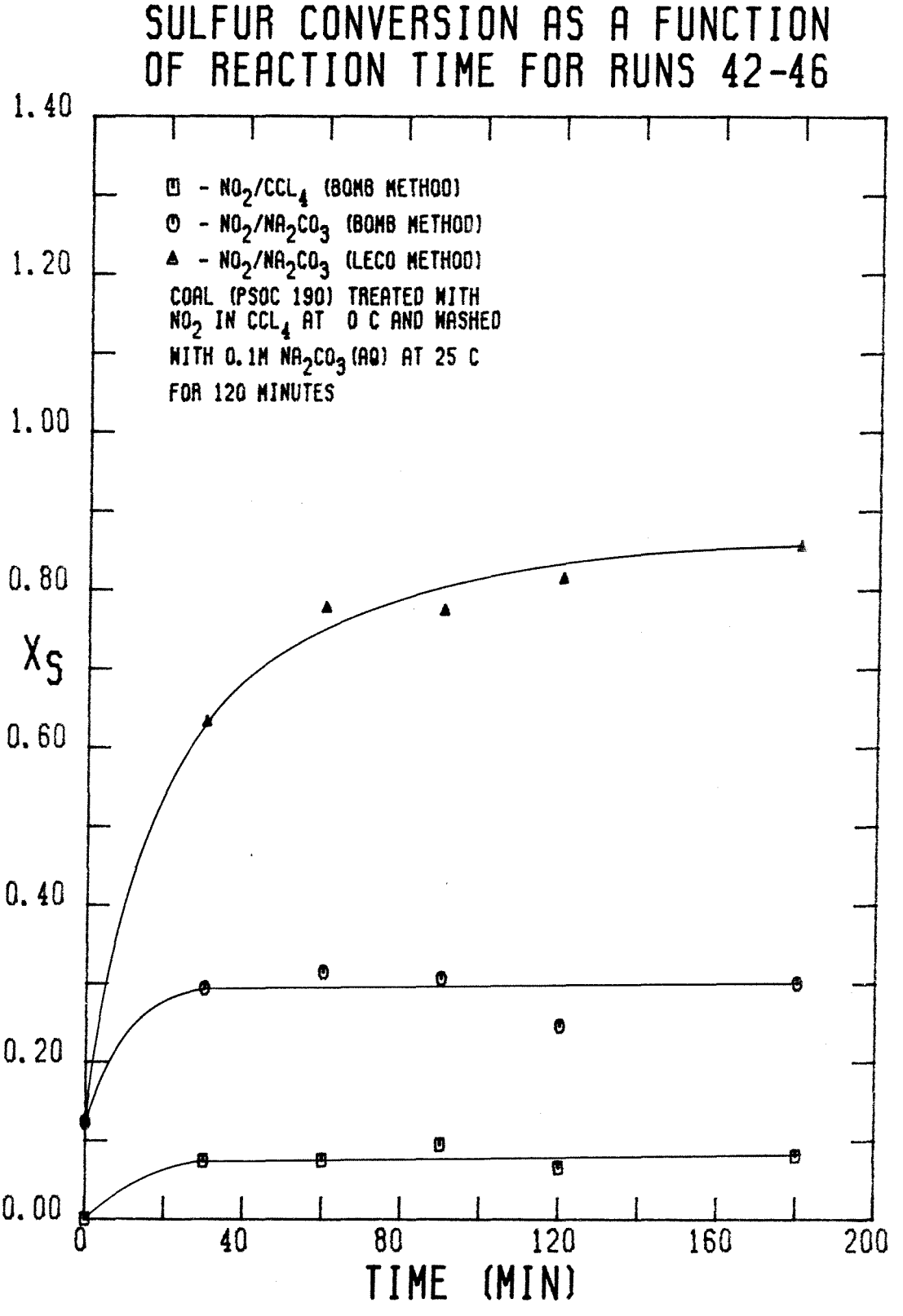
SULFUR CONVERSION AS A FUNCTION
OF REACTION TIME FOR RUNS 42-46
□ - NO2/CCL4 (BOMB METHOD)
⊙ - NO2/NA2CO3 (BOMB METHOD)
▲ - NO2/NA2CO3 (LECO METHOD)
COAL (PSOC 190) TREATED WITH
NO2 IN CCL4 AT 0 C AND WASHED
WITH 0.1M NA2CO3 (AQ) AT 25 C
FOR 120 MINUTES
1.40
1.20
1.00
0.80
0.60
0.40
0.20
0.00
XS
0
40
80
120
160
200
TIME (MIN)

FIGURE 4-120

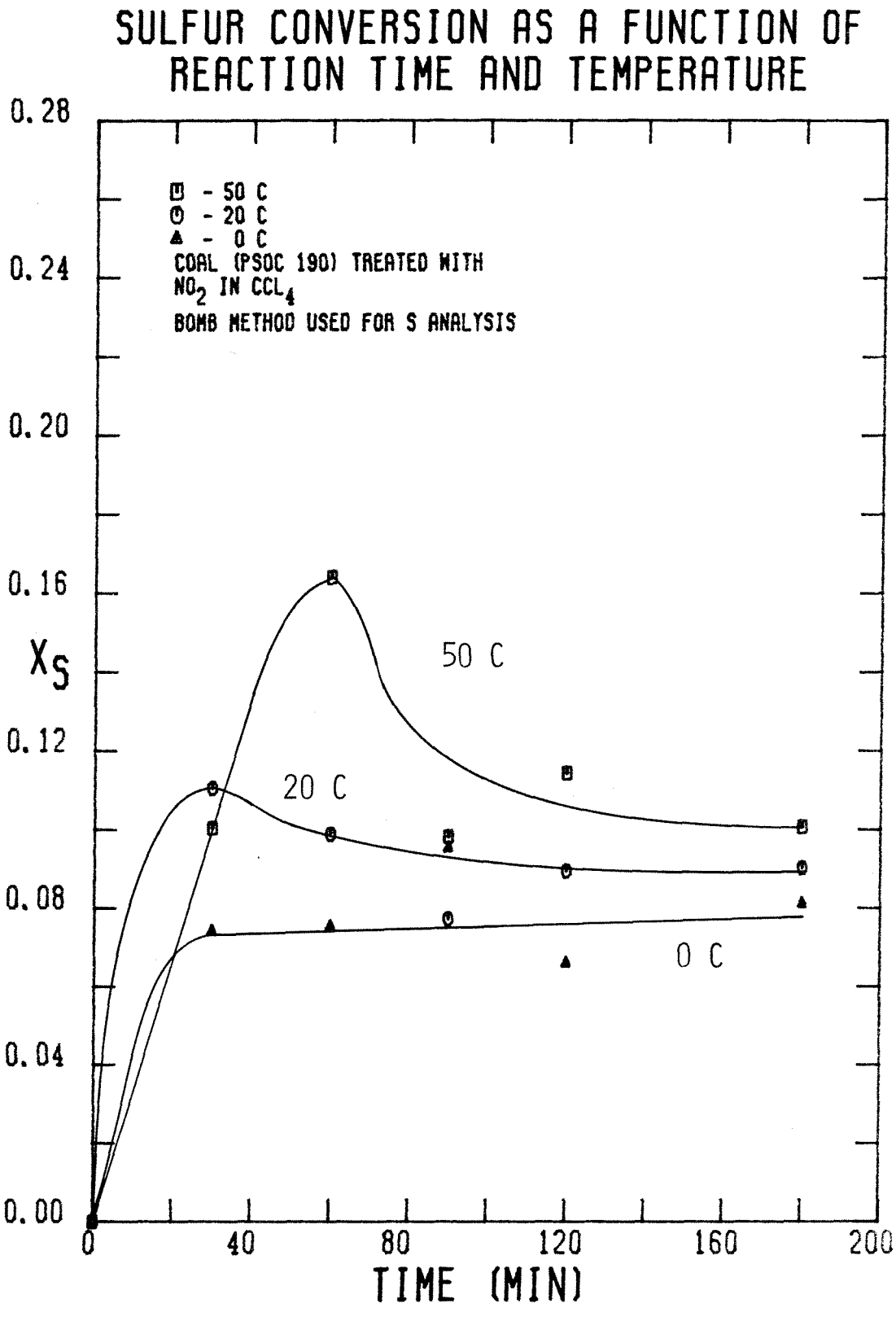
SULFUR CONVERSION AS A FUNCTION OF REACTION TIME AND TEMPERATURE
0.28
0.24
0.20
0.16
0.12
0.08
0.04
0.00
X_S
- 50 C
- 20 C
- 0 C
COAL (PSOC 190) TREATED WITH
NO_2 IN CCL_4
BOMB METHOD USED FOR S ANALYSIS
50 C
20 C
0 C
0
40
80
120
160
200
TIME (MIN)

FIGURE 4-121

can evolve from the coals treated for longer times since it becomes increasingly trapped in the solid. It should be noted that a slight peak occurs in the X_s curve at t = 30 minutes for the coal treated at 20°C while the curve for X_s at 0°C resembles a simple step function. Because the extent of coal oxidation, and hence the degree of pore blocking, increases with temperature, the curves for X_s at 20°C and 0°C indicate less SO_2 formation, but also less effect of any pore blocking on the ultimate removal of the SO_2. In any case, the amount of sulfur removed during the NO_2 treatment is minimal, regardless of the treatment temperature.

Figure 4–122 contains the values for the sulfur conversion based on the Bomb method, X_S^B, as a function of NO_2-exposure time for the Na_2CO_3 (aq) washed coal which was treated with NO_2 at 20 and 0°C. It is interesting to note that X_S^B is slightly higher for the coal treated with NO_2 at 0 than at 20°C, which may be the result of more pore blocking at the higher treatment temperature. The two curves converge at t = 180 minutes, however, indicating that 30 % of the original sulfur content is physically removed from the coal. Such an amount of sulfur removal necessitates the removal of organic sulfur since only 13 % of the initial sulfur content consists of inorganic sulfur. Nevertheless, the amounts of sulfur removed from the washed coals which were treated at both temperatures are roughly equal and the results indicate that the reaction which produces the sulfur species which are leached by the Na_2CO_3 (aq) solution is complete within 30 minutes of NO_2 exposure. Therefore, about 30 % of the original sulfur in the washed and dried PSOC 190 is rapidly attacked by NO_2 and removed from the coal either as SO_2 during the NO_2 treatment and subsequent vacuum drying or as water soluble sulfur-containing compounds during the Na_2CO_3 (aq) wash, regardless of the NO_2 treatment temperature.

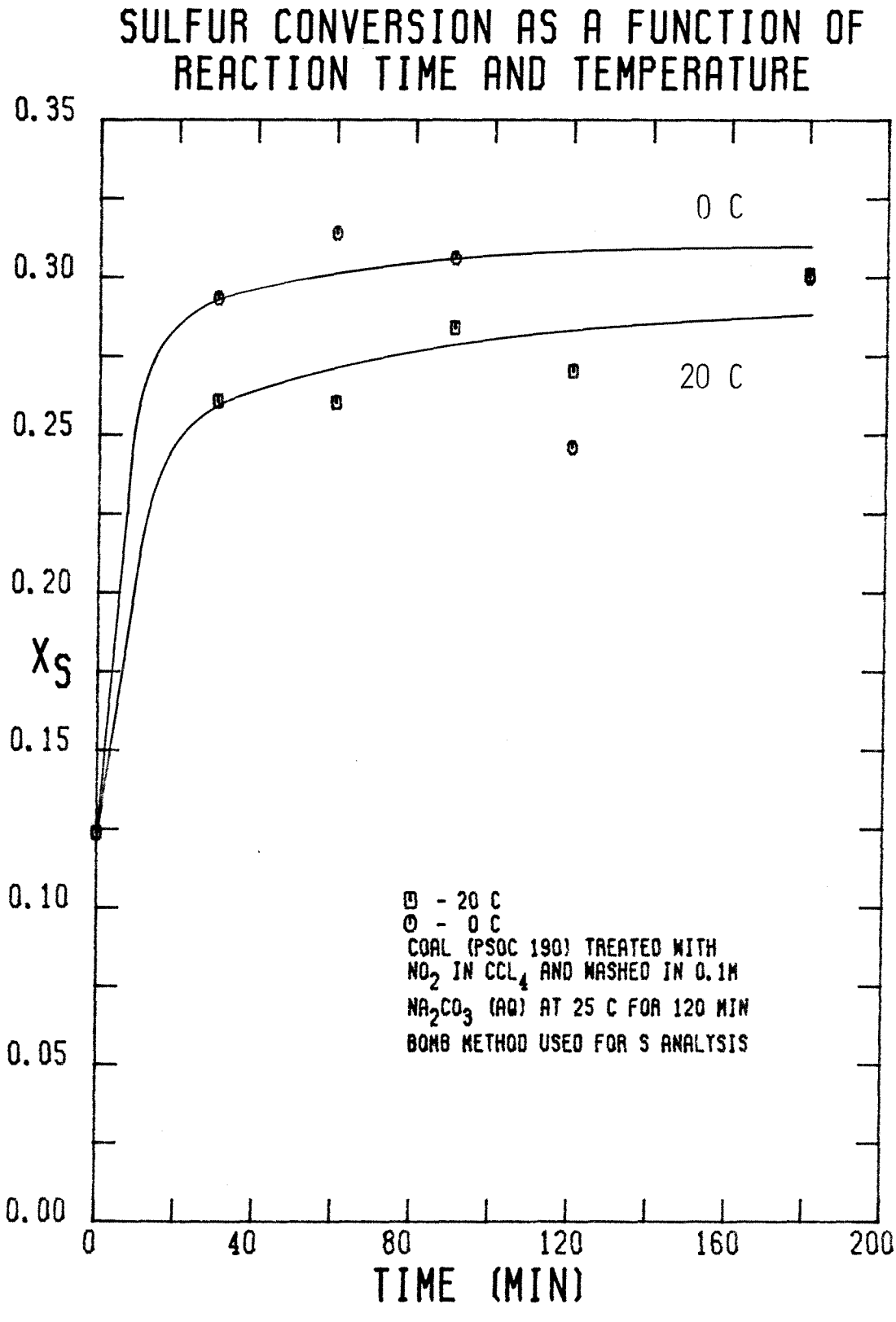
SULFUR CONVERSION AS A FUNCTION OF
REACTION TIME AND TEMPERATURE
0.35
0.30
0.25
0.20
0.15
0.10
0.05
0.00
X_S
0 C
20 C
□ - 20 C
○ - 0 C
COAL (PSOC 190) TREATED WITH
NO_2 IN CCL_4 AND WASHED IN 0.1M
NA_2CO_3 (AQ) AT 25 C FOR 120 MIN
BOMB METHOD USED FOR S ANALYSIS
0
40
80
120
160
200
TIME (MIN)

FIGURE 4-122

The temperature of the NO_2 treatment does affect the ultimate removal of SO_2 from the combustion gas, as Figure 4–123 clearly demonstrates. If the coal is treated with NO_2 at 20°C, after just 30 minutes, the Na_2CO_3 (aq) washed coal has a sulfur conversion based on the Leco method, X_S^L, of 0.91. Thus, only 9 % of the sulfur in the unprocessed coal evolves as SO_2 during combustion of the washed coal. After 180 minutes of NO_2 treatment, the washed coal evolves SO_2 to the extent of only 4 % of that of the untreated coal. Treatment of the coal at the same concentration of NO_2 but at 0°C instead of 20°C, however, results in lower levels of SO_2 removal during combustion. For instance, X_S^L of the Na_2CO_3 (aq) washed coal after 30 minutes of NO_2 treatment is only 0.63 and after 180 minutes of NO_2 treatment, X_S^L of the washed coal is still only 0.85. This behavior parallels that of the nitrogen and oxygen uptake data, which simply implies that the amount of sodium taken up by the coal during the Na_2CO_3 (aq) wash is proportional to the amount of anionic oxygen introduced into the coal during the NO_2 treatment. The rate of the NO_2-coal reaction is demonstrably slower at 0°C than at 20°C, as indicated by the nitrogen and oxygen uptake data. Perhaps the most important point to stress is that even after 180 minutes of NO_2 treatment at 20°C, the amount of sodium taken up by the coal during the subsequent Na_2CO_3 (aq) wash does not exceed the amount required for the quantitative trapping of SO_2. For example, if the additional amount of mineral matter taken up by the NO_2-treated coal during the Na_2CO_3 (aq) wash is attributed exclusively to sodium, then the washed coal contains 0.0027 moles Na/g coal and 0.00056 moles S/g coal, of which 0.00051 moles S/g coal are trapped as SO_2. Thus, the coal contains 5.4 times as much sodium as sulfur. Because two moles of sodium and one mole of sulfur are needed to produce one mole of Na_2SO_4, then 2.7 times the stoichiometric amount of sodium is needed to insure complete SO_2 trapping. Stated another way, the efficiency of sodium for captur-

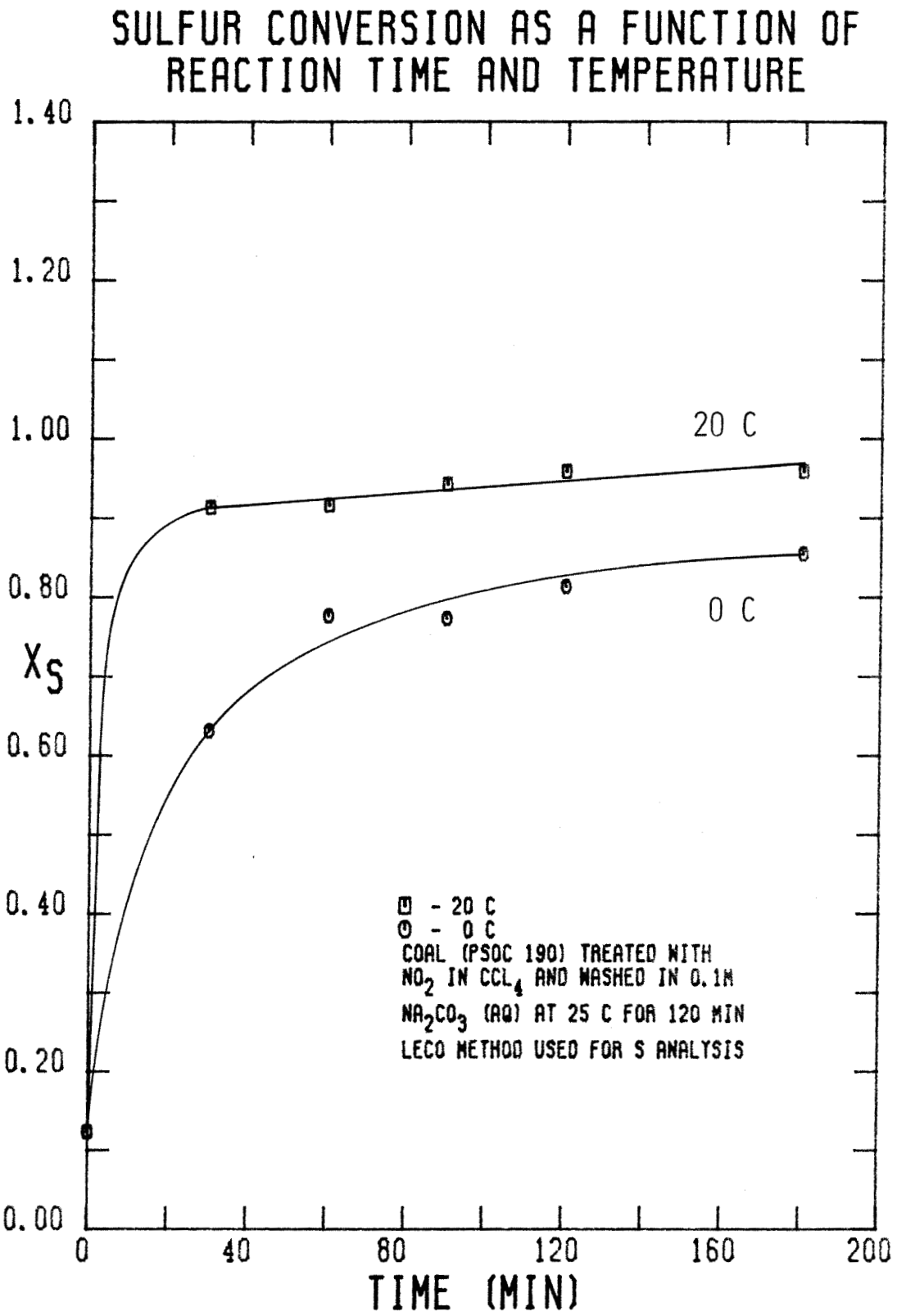
SULFUR CONVERSION AS A FUNCTION OF REACTION TIME AND TEMPERATURE
1.40
1.20
1.00
0.80
0.60
0.40
0.20
0.00
X_S
20 C
0 C
□ - 20 C
○ - 0 C
COAL (PSOC 190) TREATED WITH NO_2 IN CCL_4 AND WASHED IN 0.1M NA_2CO_3 (AQ) AT 25 C FOR 120 MIN
LECO METHOD USED FOR S ANALYSIS
0
40
80
120
160
200
TIME (MIN)

FIGURE 4-123

ing SO_2 is only about 37 %. Consequently, 180 minutes of NO_2 treatment at 20°C seems to introduce enough anionic oxygen to result in the uptake of just enough Na^+ during the wash for SO_2 trapping. On the other hand, if the NO_2 treatment is conducted at 0°C, 180 minutes is not a sufficient amount of time for the introduction of the required amount of anionic oxygen. Hence, not enough sodium is taken up during the wash for the complete trapping of SO_2 during combustion if the coal is treated with NO_2 at 0°C for only 180 minutes.

The effect of the initial NO_2 concentration, $(NO_2)_0$, on the mass corrected sulfur content is displayed graphically in Figure 4–124. As usual, the NO_2 treatment results in a sudden drop in c_S at the smallest value of $(NO_2)_0$ used. At higher values of $(NO_2)_0$, c_S is essentially constant. This behavior confirms the notion that a small portion of the sulfur is easily removed from the coal even when (NO_2) is quite small. The removal of sulfur from the NO_2-treated coal during the Na_2CO_3 (aq) wash shows some dependence on $(NO_2)_0$. For instance, when $(NO_2)_0$ = 0.1 F, c_S^B, the sulfur content based on the Bomb analysis, does not decrease as much as when $(NO_2)_0$ = 0.5 F, which implies that the rate of the reaction responsible for producing the Na_2CO_3 (aq) soluble sulfur species does depend on (NO_2). When $(NO_2)_0$ is in the range from 0.5 F and 1.7 F, c_S^B is almost constant. Once $(NO_2)_0$ exceeds 1.7 F, c_S^B begins to decline again. It should be noted that the hydrogen content displays the same type of behavior. Thus, the higher rate of decline in c_S at high values of $(NO_2)_0$ may be the result of the dependence of the rate of the NO_2-coal reaction, which produces the water soluble sulfur compounds, on (NO_2). The value of the sulfur content based on the Leco method, c_S^L, also depends on $(NO_2)_0$. Once $(NO_2)_0$ exceeds 1.1 F, however, c_S^L is constant at about 0.1 mass percent when the coal is treated for 120 minutes with NO_2. In fact, c_S^L actually begins to increase a little at higher values of $(NO_2)_0$. In any case, treating the coal for 120 minutes with NO_2 at a concentra-

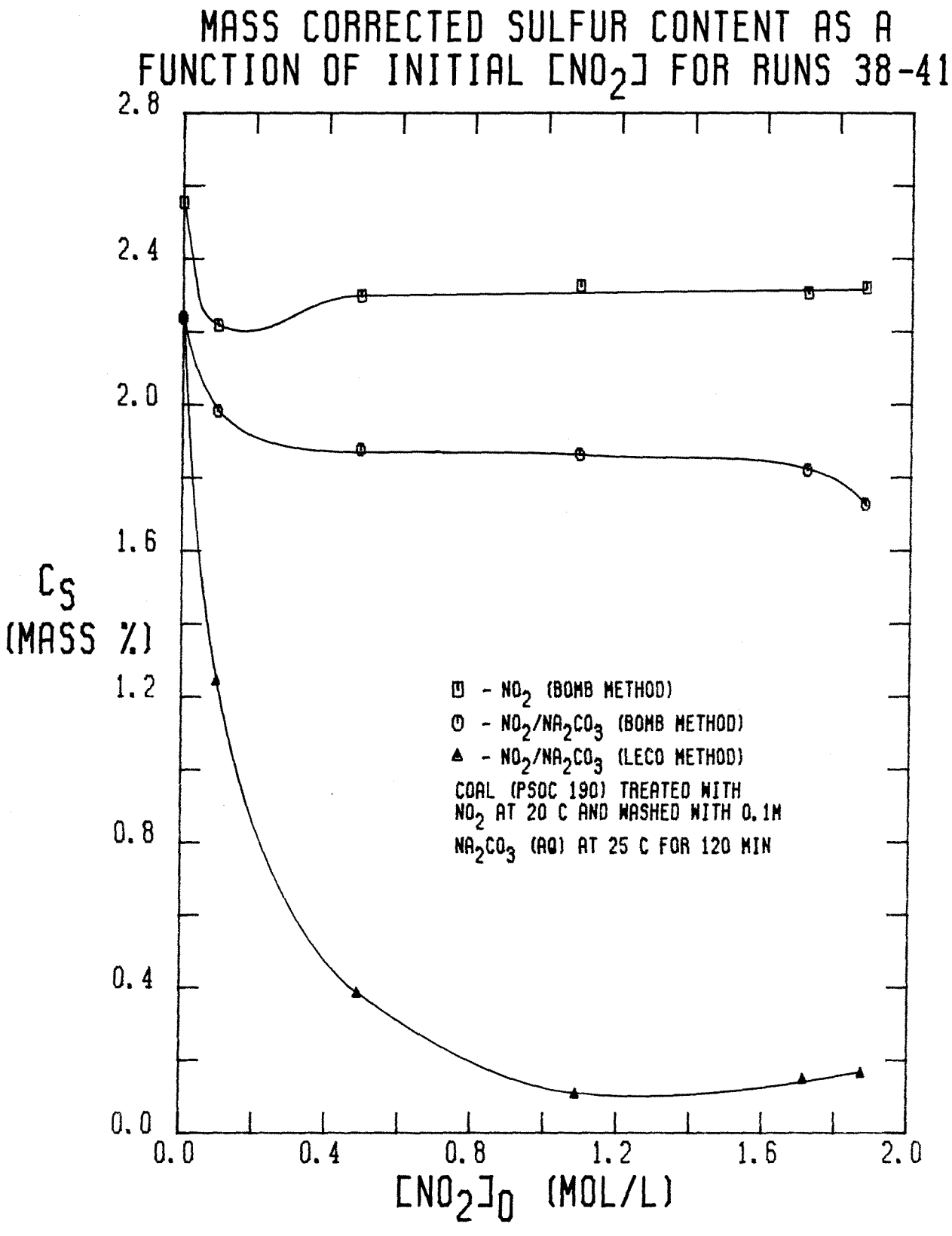
MASS CORRECTED SULFUR CONTENT AS A FUNCTION OF INITIAL [NO2] FOR RUNS 38-41
2.8
2.4
2.0
1.6
1.2
0.8
0.4
0.0
CS (MASS %)
0.0
0.4
0.8
1.2
1.6
2.0
[NO2]0 (MOL/L)
- NO2 (BOMB METHOD)
- NO2/NA2CO3 (BOMB METHOD)
- NO2/NA2CO3 (LECO METHOD)
COAL (PSOC 190) TREATED WITH NO2 AT 20 C AND WASHED WITH 0.1M NA2CO3 (AQ) AT 25 C FOR 120 MIN

FIGURE 4-124

tion exceeding 1.1 F at 20°C insures the introduction of enough anionic oxygen for the uptake of enough sodium to trap virtually all of the SO_2 produced during combustion.

Figure 4—125 contains the values of the sulfur conversion, X_s, as a function of $(NO_2)_0$ for NO_2 treatment at 20°C for 120 minutes followed by a wash in 0.1 M Na_2CO_3 (aq) at 25°C for 120 minutes. As $(NO_2)_0$ increases, the amount of sulfur removed during the NO_2 treatment goes through a maximum of 13 % at the lowest initial NO_2 concentration, before dropping to about 9 % at the higher values of $(NO_2)_0$. More oxidation of the coal occurs as (NO_2) increases, which results in more pore blocking. Thus, the decrease in X_s at higher values of $(NO_2)_0$ is caused by some trapping of SO_2 in blocked pores which would otherwise be removed from the coal. The middle curve in the figure indicates that the yield of sulfur compounds soluble in 0.1 M Na_2CO_3 (aq) which are produced by the NO_2 treatment depends on $(NO_2)_0$ in a unique way. If $(NO_2)_0$ is too low (< 0.1 F), not all of the potentially soluble sulfur compounds are formed. When $(NO_2)_0$ is in the range from 0.5 F to about 1.5 F, X_s is constant at about 0.27. At higher values of $(NO_2)_0$, X_s begins to rise at an accelerating pace, which implies that the rate of the NO_2-coal reaction responsible for sulfur removal during the Na_2CO_3 (aq) wash does not have a simple dependence on (NO_2). It should be noted that the decrease in X_s is small enough that experiments at even higher values of $(NO_2)_0$ need to be conducted in order to establish a definite trend. In any case, any residual sulfur is essentially trapped during combustion provided $(NO_2)_0$ exceeds roughly 1.1 F. If $(NO_2)_0$ is less than 1.1 F, not enough anionic oxygen can be introduced into the coal within 120 minutes to insure the uptake of a sufficient amount of sodium during the Na_2CO_3 (aq) wash to trap all of the SO_2 produced by the residual sulfur during combustion. Provided enough NO_2 is present and a sufficient amount of time is provided for the NO_2-coal system to

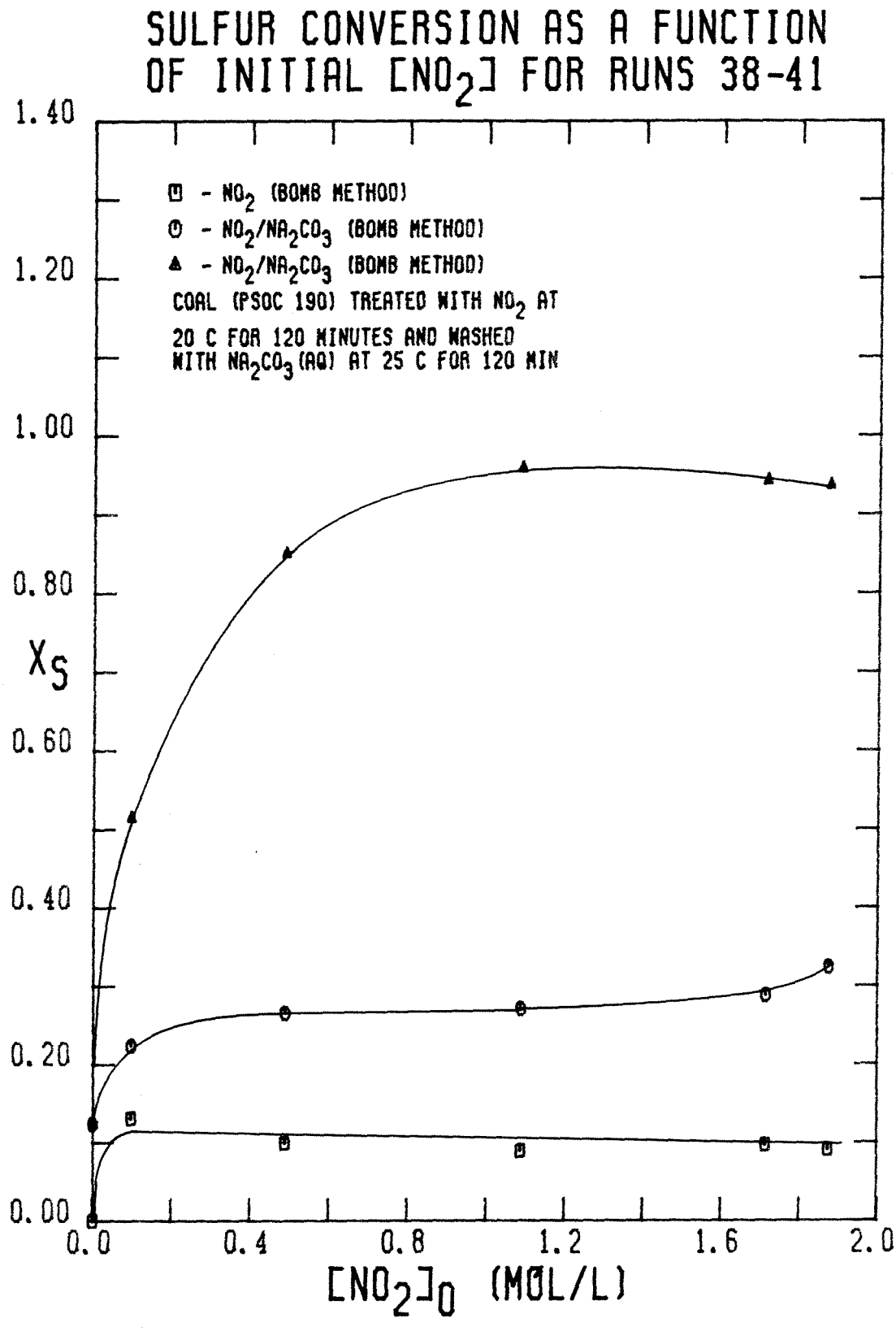
SULFUR CONVERSION AS A FUNCTION OF INITIAL [NO2] FOR RUNS 38-41
□ - NO2 (BOMB METHOD)
○ - NO2/NA2CO3 (BOMB METHOD)
▲ - NO2/NA2CO3 (BOMB METHOD)
COAL (PSOC 190) TREATED WITH NO2 AT 20 C FOR 120 MINUTES AND WASHED WITH NA2CO3(AQ) AT 25 C FOR 120 MIN
1.40
1.20
1.00
0.80
0.60
0.40
0.20
0.00
XS
0.0
0.4
0.8
1.2
1.6
2.0
[NO2]0 (MOL/L)

FIGURE 4-125

react, roughly 95 % of the SO_2 which would be produced by the combustion of the untreated coal is prevented from entering the flue gas. It should be noted that as (NO_2) increases, the amount of carbonaceous material in the coal which is oxidized increases, as evidenced by the carbon and hydrogen loss data, which results in a decrease in the heating value of the coal. Therefore, $(NO_2)_0$ should not exceed 1.1 F because X_S^L, the sulfur conversion based on the Leco method, does not increase but the heating value does continue to decrease.

In order to determine the effect of the porosity of the coal particle on the extent of the sulfur removal, a set of experiments was conducted in which the PSOC 276 coal, which initially had about 25 % of the pore volume of the PSOC 190 coal used in the previous experiments, was treated with NO_2 at 20°C for various times in the batch reactor (Runs 47–52). The mass corrected sulfur content, c_S, of the processed coal is shown in Figure 4–126. During the NO_2 treatment, c_S goes through a minimum at 30 minutes and then increases. On the other hand, c_S decreases smoothly during the Na_2CO_3 (aq) wash as the length of the NO_2-treatment time increases. Based on the Bomb analysis for sulfur, c_S^B of the washed coal seems to level off at about 2.6 mass percent. On the basis of the Leco analysis for sulfur, however, c_S^L of the washed coal appears to be continually decreasing even after 180 minutes of NO_2 treatment. It should be noted that the Bomb and Leco sulfur determinations of the PSOC 276 coal washed in 0.1 M Na_2CO_3 (aq) after being washed in CCl_4 (Run 47C) do not agree, but differ by 0.4 mass percent. The Leco analysis is more in agreement with the original PSOC analysis of the raw coal, however.

The behavior demonstrated by c_S is paralleled by the sulfur conversion, X_s, as shown in Figure 4–127. In particular, the sulfur removed during the NO_2 treatment reaches a maximum of 5.7 % after 30 minutes before dropping back to about 1.2 % after 180 minutes. These data are consistent with the theory that

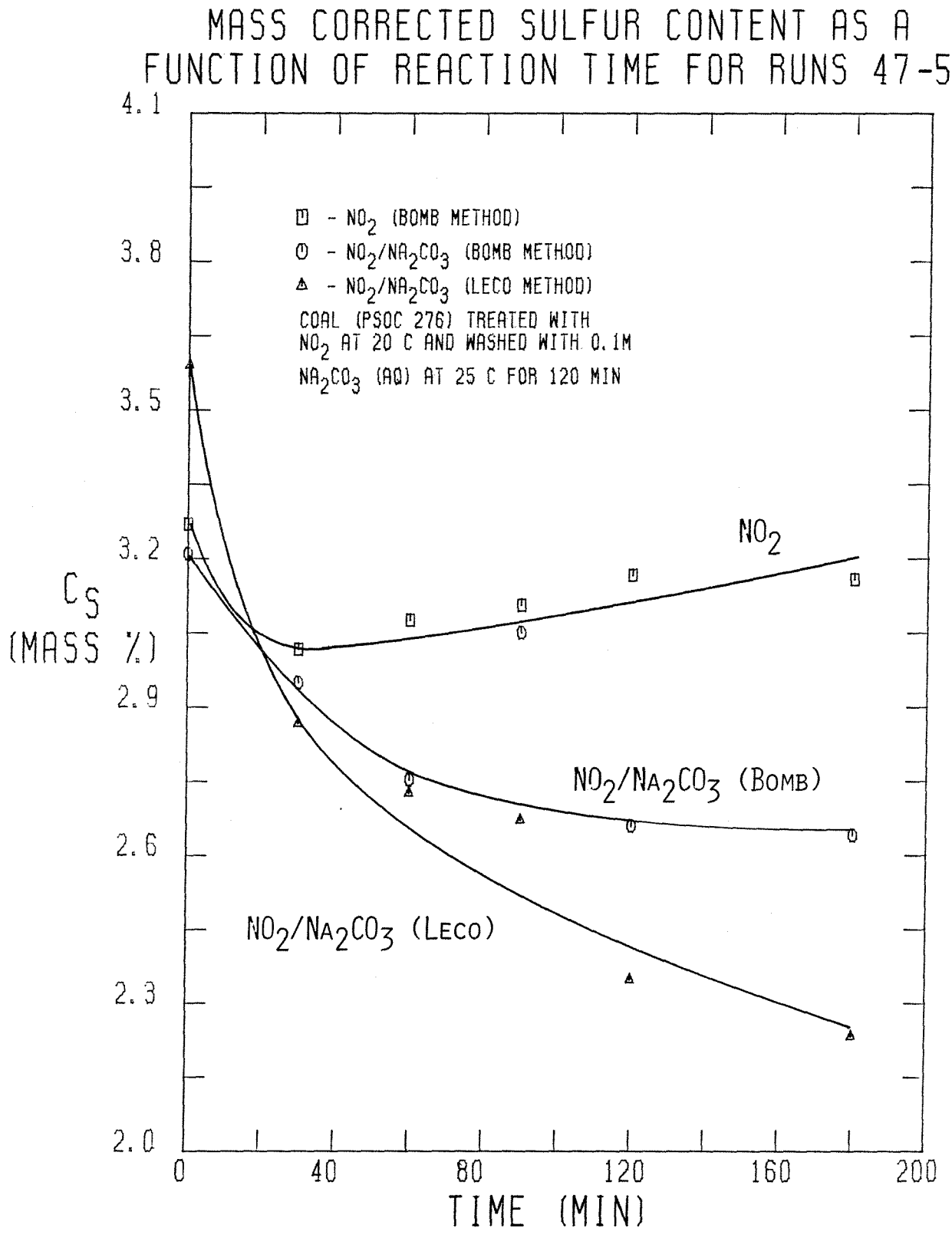
MASS CORRECTED SULFUR CONTENT AS A FUNCTION OF REACTION TIME FOR RUNS 47-52
□ - NO2 (BOMB METHOD)
○ - NO2/NA2CO3 (BOMB METHOD)
△ - NO2/NA2CO3 (LECO METHOD)
COAL (PSOC 276) TREATED WITH NO2 AT 20 C AND WASHED WITH 0.1M NA2CO3 (AQ) AT 25 C FOR 120 MIN
NO2
NO2/NA2CO3 (BOMB)
NO2/NA2CO3 (LECO)
CS (MASS %)
TIME (MIN)
4.1
3.8
3.5
3.2
2.9
2.6
2.3
2.0
0
40
80
120
160
200

FIGURE 4-126

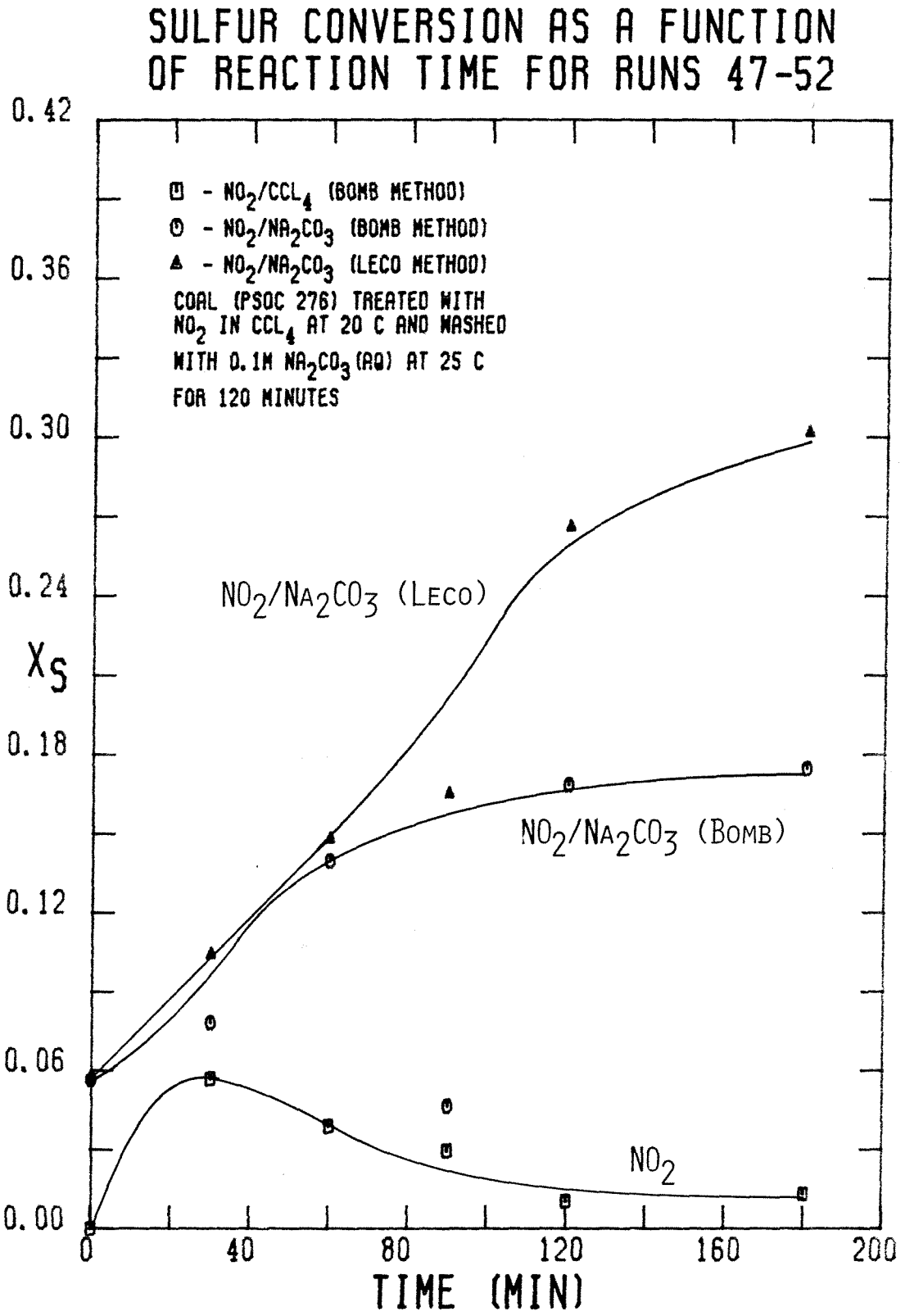
SULFUR CONVERSION AS A FUNCTION OF REACTION TIME FOR RUNS 47-52
□ - NO2/CCL4 (BOMB METHOD)
○ - NO2/NA2CO3 (BOMB METHOD)
△ - NO2/NA2CO3 (LECO METHOD)
COAL (PSOC 276) TREATED WITH NO2 IN CCL4 AT 20 C AND WASHED WITH 0.1M NA2CO3 (AQ) AT 25 C FOR 120 MINUTES
NO2/NA2CO3 (LECO)
NO2/NA2CO3 (BOMB)
NO2
XS
TIME (MIN)
0.42
0.36
0.30
0.24
0.18
0.12
0.06
0.00
0
40
80
120
160
200

FIGURE 4-127

most of the SO_2 formed during the NO_2 treatment is removed by the vacuum drying after the reaction is terminated. Because the extent of pore blocking increases as the NO_2-treatment time increases, less of the SO_2 is removed during the post-treatment vacuum drying. The total sulfur removal after the Na_2CO_3 (aq) wash based on the Bomb method appears to level off at about 17.5 % after 180 minutes of NO_2 treatment. It should be noted that the value of X_S^B at 90 minutes was disregarded when the curve for X_S^B was drawn because of its large deviation from the trend established by the remainder of the points. The total amount of sulfur prevented from appearing as SO_2 in the flue gas is given by X_S^I, which is based on the Leco method. After 180 minutes of NO_2 treatment, only 40 % of the original sulfur content is effectively removed from the combustion gas, although X_S^I still seems to be increasing.

It is important to note that 66 % of the sulfur in the PSOC 276 is pyritic, while there is virtually none in the PSOC 190 coal. As the analysis of the forms of sulfur in the treated PSOC 276 coal shown in Table 3–20 indicates, very little of the pyritic sulfur is removed by the processing. This is not surprising when CCl_4 is the solvent, since once the surface of a FeS_2 crystal is oxidized, no further oxidation can occur because of the layer of $FeSO_4$ formed, which is insoluble in CCl_4. If H_2O were used as the solvent, however, then the surface of the crystal would be continually renewed because of the high solubility of $FeSO_4$ in aqueous solutions. Because the pyritic sulfur occurs as crystals in the coal, it represents concentrated sources of SO_2 during combustion. Consequently, very little of the SO_2 produced from the pyrite can be trapped by sodium since it is dispersed throughout the carbonaceous material of the coal. Indeed, after 180 minutes of NO_2 treatment and being washed in 0.1 M Na_2CO_3 (aq), only about 10 % of the pyrite is removed. If it is assumed that the difference between the Leco and Bomb determinations of the sulfur content can be attributed to the trapping of

the organic sulfur, the following values of the conversion of organic sulfur, $X_{S,O}$, are obtained:

NO_2 Exposure Time (min)	0	30	60	90	120	180
$X_{S,O}$	0.0	0.127	0.200	0.150	0.349	0.653

Therefore, the true efficiency of sodium for trapping sulfur is enhanced. The extent of the SO_2 trapping, however, is not as great as in the treated PSOC 190, probably because not enough sodium is adsorbed by the treated PSOC 276, which is caused by its smaller pore volume.

A comparison of the total amount of sulfur removed from the PSOC 190 and PSOC 276 during the NO_2 treatment is depicted in Figure 4–128 in the form of sulfur conversion, X_s, as a function of NO_2-exposure time. In both cases, a maximum in X_s occurs at 30 minutes of 0.11 for the PSOC 190 and of 0.06 for the PSOC 276. As the amount of exposure increases, X_s declines to 0.09 for the PSOC 190 and to 0.01 for the PSOC 276. This behavior is best explained by the theory that the sulfur is removed primarily as SO_2 during the vacuum drying of the coal after the coal is filtered from the NO_2-CCl_4 solution. Because the extent of oxidation of the coal increases with increasing NO_2-exposure time, the amount of pore blocking increases as well. As the pore structure is increasingly isolated from the particle exterior, less of the SO_2 that would otherwise evolve during the vacuum drying actually does manage to escape from the coal particles. This theory presupposes that the reaction of NO_2 with the portion of the sulfur in the coal which produces the SO_2 is complete within a very short time (< 30 minutes). Based on the fact that simple aliphatic sulfides, such as n–butyl sulfide, are instantaneously oxidized to yield SO_2 upon exposure to NO_2, this supposition is not unreasonable. Thus, although the pore structure does not seem to affect the transport of NO_2 into the coal particle, it does affect the transport of SO_2 out of the coal particle. It is also interesting to note that

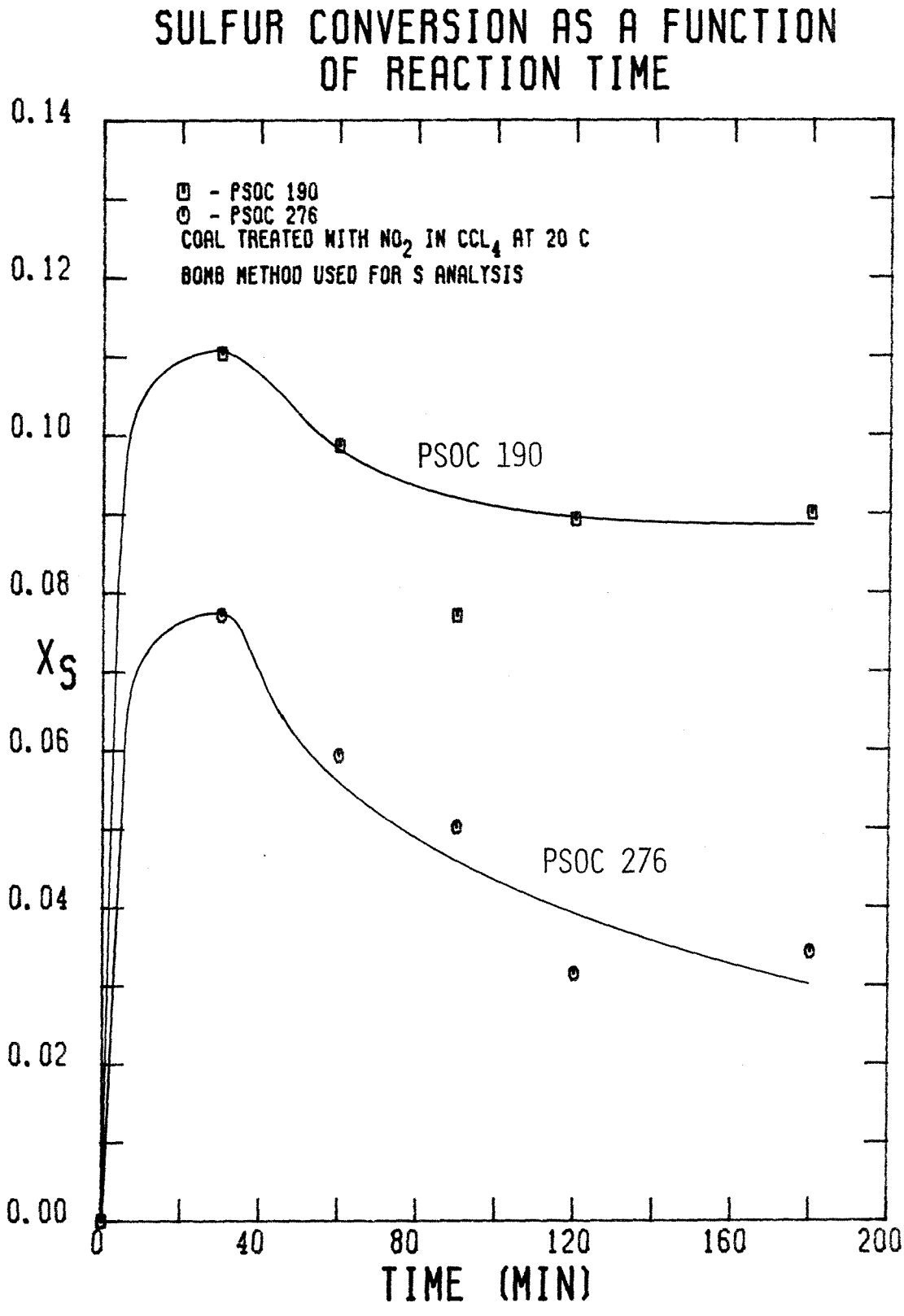
SULFUR CONVERSION AS A FUNCTION OF REACTION TIME
□ - PSOC 190
○ - PSOC 276
COAL TREATED WITH NO_2 IN CCL_4 AT 20 C
BOMB METHOD USED FOR S ANALYSIS
PSOC 190
PSOC 276
X_S
0.14
0.12
0.10
0.08
0.06
0.04
0.02
0.00
0
40
80
120
160
200
TIME (MIN)

FIGURE 4-128

although the PSOC 276 coal initially has more sulfur than the PSOC 190 coal, particularly in the form of pyrite, whose crystal surface is readily oxidized by NO_2, the amount of sulfur removed from the PSOC 276 coal is less than that removed from the PSOC 190 coal. This difference can also be attributed to the different pore structures of the two coals. That is, the amount of SO_2 formed as the result of the NO_2-coal reaction may be greater in the PSOC 276 than in the PSOC 190, but the extent of SO_2 removal is much less in the PSOC 276 than in the PSOC 190.

The total amount of sulfur removed from the two coals during the Na_2CO_3 (aq) wash of the NO_2-treated coal is shown graphically in Figure 4–129 in the form of X_S^B as a function of NO_2-exposure time. The rise in X_S^B for the PSOC 190 coal is quite rapid within the first 30 minutes of NO_2 treatment, reaching a value of 0.26. After 30 minutes, X_S^B changes very little, attaining a value of only 0.30 after 180 minutes of NO_2 treatment. On the other hand, the value of X_S^B for the washed PSOC 276 rises more gradually, attaining a value of 0.17 after 180 minutes of NO_2 treatment. It should be noted that the values of X_S^B at $t = 0$ differ for the two coals, which results from the fact that there is less sulfate initially in the PSOC 276 than in the PSOC 190. Nevertheless, the amount of sulfur removed by the NO_2 treatment and Na_2CO_3 (aq) wash is about 40 % lower in the PSOC 276 than in the PSOC 190. Once again, the disparity in the amount of sulfur removal is due to the different pore structures of the two coals. Just as in the case of SO_2 removal, more water soluble sulfur forms may be formed in the PSOC 276 than in the PSOC 190 during the NO_2 treatment. The accessibility of these oxidized sulfur species to Na_2CO_3 (aq), however, is greatly diminished in the PSOC 276 relative to the PSOC 190, resulting in less sulfur removal.

The pore structure also affects the amount of SO_2 trapped during combustion, as evidenced by Figure 4–130, which contains the values of the sulfur

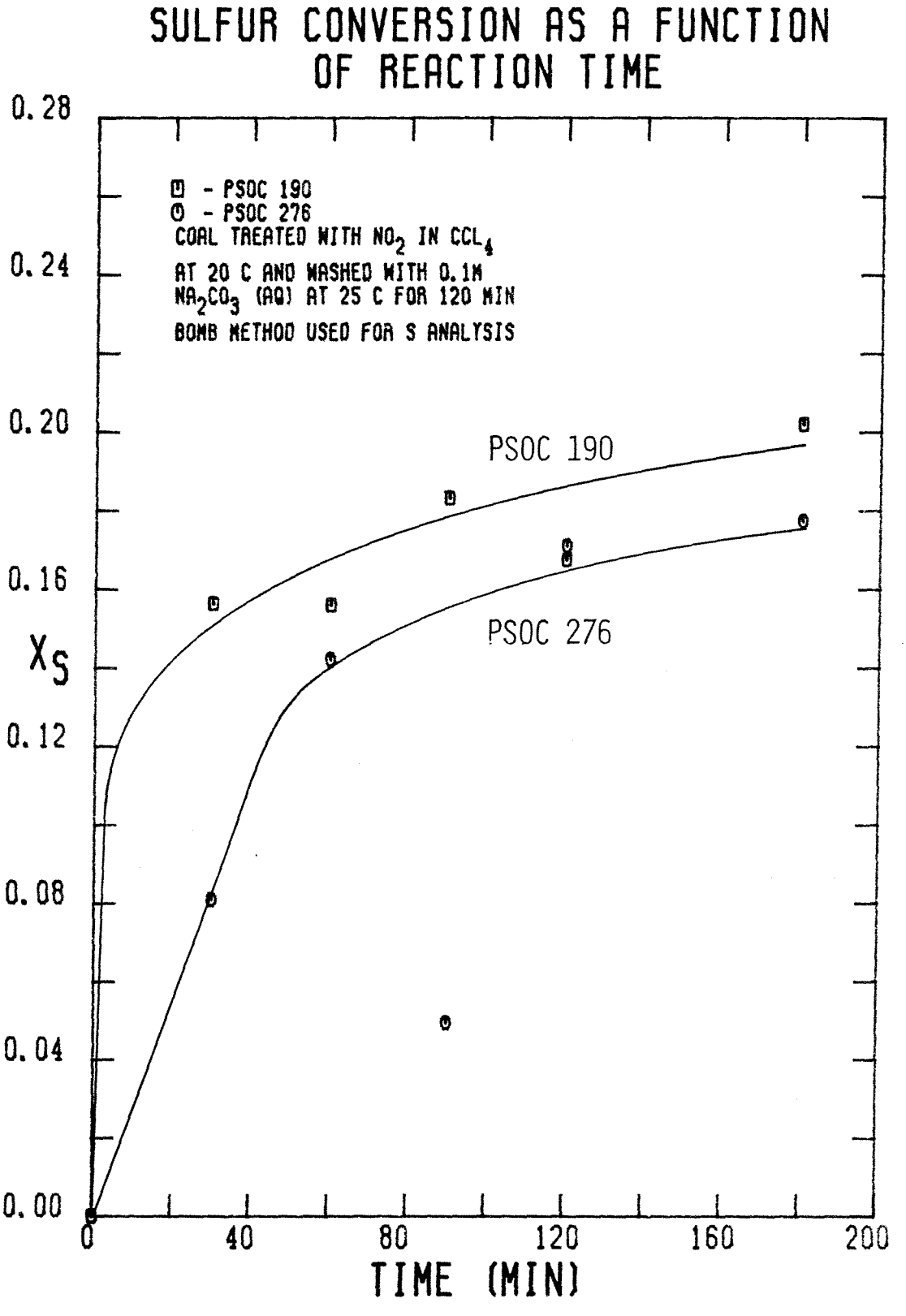
SULFUR CONVERSION AS A FUNCTION OF REACTION TIME
□ - PSOC 190
○ - PSOC 276
COAL TREATED WITH NO2 IN CCL4
AT 20 C AND WASHED WITH 0.1M
NA2CO3 (AQ) AT 25 C FOR 120 MIN
BOMB METHOD USED FOR S ANALYSIS
PSOC 190
PSOC 276
Xs
0.28
0.24
0.20
0.16
0.12
0.08
0.04
0.00
0
40
80
120
160
200
TIME (MIN)

FIGURE 4-129

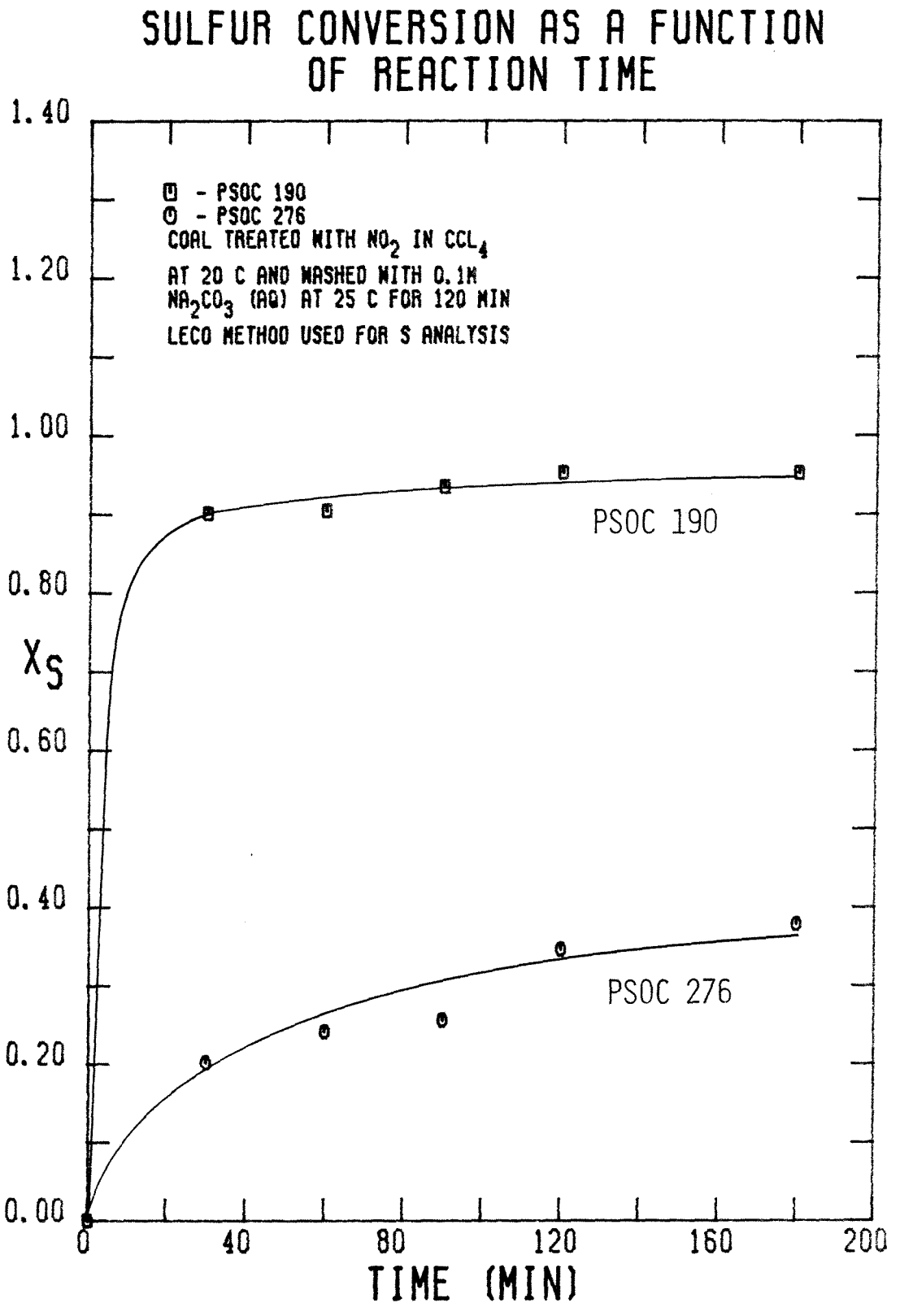
SULFUR CONVERSION AS A FUNCTION OF REACTION TIME
1.40
1.20
1.00
0.80
0.60
0.40
0.20
0.00
X_S
- PSOC 190
- PSOC 276
COAL TREATED WITH NO_2 IN CCL_4
AT 20 C AND WASHED WITH 0.1M
NA_2CO_3 (AQ) AT 25 C FOR 120 MIN
LECO METHOD USED FOR S ANALYSIS
PSOC 190
PSOC 276
0
40
80
120
160
200
TIME (MIN)

FIGURE 4-130

conversion based on the Leco method for sulfur analysis, X_S^L, for the two processed coals. It is immediately obvious that while virtually all of the sulfur in the PSOC 190 is prevented from entering the combustion gas as SO_2, only about 40 % of the sulfur in the PSOC 276 is so prevented. Furthermore, X_S^L for the processed PSOC 190 reaches a value of 0.91 within just 30 minutes of NO_2 treatment and rises more slowly thereafter, ultimately reaching a value of 0.96 after 180 minutes of NO_2 treatment. On the other hand, X_S^L for the processed PSOC 276 rises more slowly, reaching a value of only 0.40 after 180 minutes of NO_2 exposure. If the added mineral matter to the PSOC 276 is assumed to be derived solely from sodium, then the washed coal has 0.0014 mol Na/g coal and 0.00013 mol S/g coal which is trapped as SO_2. Thus, the efficiency of sodium for trapping SO_2 is only 18 % in the PSOC 276 as opposed to 37 % in the PSOC 190. The difference in the amount of sulfur removed from the two coals can again be attributed to their different pore structures. Because the accessibility of the interior of the treated PSOC 276 coal particles is less than that of the PSOC 190 coal particles, a smaller portion of the sites for potential uptake of sodium are available, which explains the difference in the sodium uptake by the two coals. Hence, the amount of SO_2 trapped during combustion of the processed PSOC 276 is smaller by virtue of the smaller amount of sodium in the PSOC 276. The difference in the trapping efficiencies of sodium in the two coals may be attributed to the proximity of sodium to the sulfur in the coal. That is, the greater amount of sodium taken up by the PSOC 190 than by the PSOC 276 implies that the Na_2CO_3 (aq) solution has penetrated further into the NO_2 treated PSOC 190 coal particles. If the residual sulfur is uniformly distributed throughout the particle, then the sodium is closer to the sulfur in the PSOC 190 than in the PSOC 276. Such proximity is important, because during combustion, the SO_2 which is formed must encounter the sodium containing flux before it is carried

away by the rest of the combustion gases to be successfully trapped in the ash. Obviously, a greater degree of penetration of the coal particle by the Na_2CO_3 (aq) solution results in a closer proximity of sodium to sulfur. Thus, the pore structure has a compound effect on the amount of SO_2 trapped as Na_2SO_4. Not only does a smaller pore volume result in less sodium uptake, but it also reduces the efficiency of the sodium for trapping SO_2.

Based on the results discussed in this section, the mechanism of sulfur removal during the NO_2 treatment and subsequent Na_2CO_3 (aq) wash can be described. During the NO_2 treatment, a small portion of the sulfur is readily attacked by NO_2 to form SO_2, which is removed primarily during the post-reaction drying. Although the pore structure does not seem to hinder the transport of NO_2 into the particle interior, it does affect the transport of SO_2 out of the particle during the vacuum drying. In particular, the extent of pore blocking increases with NO_2-exposure time while the SO_2 formation is essentially complete upon exposure of the coal to NO_2. The effect of (NO_2) is also consistent with the notion of SO_2 removal during the vacuum drying, because X_s is greatest at the lowest value of $(NO_2)_0$ used, although the decline in X_s at higher values of $(NO_2)_0$ is not great. Nevertheless, less pore blocking occurs when (NO_2) is lower. Thus, more SO_2 should be removed when $(NO_2)_0$ is lower, which is indeed the case.

The reaction of NO_2 with coal also results in the formation of sulfur compounds which are leached from the coal during the Na_2CO_3 (aq) wash. The accessibility of these species to the Na_2CO_3 (aq) solution is dictated by the pore structure as well. The smaller the pore volume, the less sulfur which is removed by the leaching action of the Na_2CO_3 (aq) solution. The temperature of the NO_2 treatment has a slight inverse effect on the sulfur removal, with slightly more sulfur removal occurring during the wash of the coal treated with NO_2 at 20 °C.

This effect is due to the greater extent of pore blocking which occurs at 20°C than at 0°C. Also, the effect of (NO_2) on the amount of sulfur leached from the coal is not great, which implies that the reaction which produces the soluble sulfur species is essentially complete upon exposure of the coal to NO_2.

The third effect of the NO_2 treatment on the coal is to introduce anionic oxygen atoms into the particle which then adsorb Na^+ during the Na_2CO_3 (aq) wash. It is the sodium which accounts for the difference in the determination of the sulfur content of the washed coal by the Bomb and Leco methods. The pore structure of the NO_2-treated coal has a profound effect on the amount of SO_2 trapped by sodium to form a Na_2SO_4 flux during combustion of the washed coal. Not only does the accessibility of the Na^+ adsorption sites determine the amount of sodium taken up by the coal, but it also dictates the proximity of the sodium to the sulfur in the coal. Thus, as the pore volume decreases, not only is an increasingly insufficient amount of sodium taken up for complete SO_2 trapping, but the distance between the sodium and the sulfur increases, which causes a decrease in the SO_2 trapping efficiency of the sodium. The temperature of the NO_2 treatment also affects the amount of sulfur trapped during combustion because the rate of anionic oxygen uptake during the NO_2 treatment depends on the temperature, which dictates the amount of sodium taken up by the coal during the Na_2CO_3 (aq) wash. Furthermore, since (NO_2) also affects the rate of uptake of anionic oxygen, and hence, that of sodium, by the coal, the amount of SO_2 trapped during combustion depends on (NO_2) as well.

Therefore, the most important parameter which influences the amount of sulfur which is ultimately prevented from entering the combustion gas is the pore structure. Although the transport of NO_2 into the coal is not affected by the pore structure, the removal of SO_2 during the NO_2 treatment and subsequent vacuum drying and the removal of water soluble sulfur compounds during

the Na_2CO_3 (aq) wash are governed by the pore structure. The most critical aspect of the process, however, is the accessibility of the Na_2CO_3 (aq) solution to the anionic oxygen introduced into the coal, because the majority of the sulfur removal occurs as SO_2 trapping by sodium during combustion. Therefore, if a coal has a low pore volume, such as that of the PSOC 276, it is important to enhance the accessibility of the particle interior to the Na_2CO_3 (aq) solution during the processing to insure the maximum amount of sodium uptake, and hence, SO_2 trapping in the ash.

4.2.2.9 The Heat Content of the Coal

The best macroscopic indicator of the extent of oxidation of the coal due to processing is the loss in the heat content of the coal. The coal loses some of its heating value whenever a C–H or C–C bond is broken, due to the reaction of the NO_2 with the coal, to produce H_2O, CO_2, ketone, alcohol and carboxylic acid groups in the coal. A comparison of the loss in heating value with the sulfur removal is an indication of the selectivity of the process for the elimination of SO_2 emissions relative to the oxidation of the rest of the coal. In this section, however, only the change in the heat content of the coal as a function of the various reaction parameters will be discussed.

The values of the corrected heat content, H_g, of the coal after treatment with NO_2 in water, pyridine and nitrobenzene (Runs 1–6) can be found in Table 3–19. H_g is the energy content of the treated coal after adjustment for the mass loss or gain so that the units are Btu per lb_m of coal initially used. When the PSOC 190 coal is treated with NO_2 in H_2O at 26 and 78°C, the overall loss in H_g is 13.4 and 10.7 %, respectively. The overall loss in the heat content, L_{H_g}, represents the total amount of energy lost by the coal due to the treatment:

$$L_{Hg} = 1 - \frac{mH}{m_0 H_0}, \quad \text{where} \tag{4.2.20}$$

m = the mass of coal recovered after treatment (lb_m),

m_0 = the initial mass of coal used (lb_m),

H = the heat content of the coal after treatment (Btu/lb_m), and

H_0 = the initial heat content of the coal (Btu/lb_m).

It is interesting to note that L_{H_g} is higher at 26°C than at 78°C, which is probably caused by the decrease in NO_2 solubility in water as the temperature increases. When the coal is slurried in pyridine and treated with NO_2 at 26°C and 83°C, the

overall loss in heat content is 19.2 % and 24.5 % respectively, which is higher than when H_2O is the solvent. The higher values of L_{H_g} are due to the greater solubility of NO_2 in pyridine than in H_2O and to the fact that NO_2 does not react with pyridine but does react with H_2O, which competes with coal for NO_2. When nitrobenzene is used as the solvent for the slurry, the overall heating value loss is only 8.1 % when the coal is treated with NO_2 at 34°C, but rises to 38.4 % when the treatment temperature is 84 %. It should be noted that the removal of aromatic solvents, particularly nitrobenzene, from the coal is extremely difficult even when vacuum drying is employed. Because any residual pyridine or nitrobenzene would add to the heat content of the coal, the values of L_{H_g} must be considered as suspicious and taken only as minimum values of the real loss in the heat content.

The values of the corrected heat content of the PSOC 190 coal treated with NO_2 in the uncooled flow reactor using water as the solvent and subsequently washed in 0.1 M Na_2CO_3 (aq) (Runs 7–13) are shown in Figure 4–131 as a function of NO_2-exposure time. It is immediately obvious that very little of the heat content is lost during the NO_2 treatment, with L_{H_g} reaching a value of only 2.8 % after 180 minutes. The Na_2CO_3 (aq) wash results in more substantial losses in H_g, however, which get as high as 20 % after 180 minutes of NO_2 treatment. Thus, the NO_2 treatment renders the otherwise insoluble portions of the coal soluble in 0.1 M Na_2CO_3 (aq) with a minimal amount of oxidation. During the NO_2 treatment, the coal is exposed to rather high concentrations of HNO_3 (aq) and HNO_2 (aq), which are the primary oxidants present. Apparently oxygen is introduced into the coal in such a manner that the oxidized portions of the coal are not soluble in water under acidic conditions. Upon exposure to 0.1 M Na_2CO_3 (aq), however, which has a pH of 11.6 at 25°C, the oxidized portions of the coal dissolve in the aqueous solution, as evidenced by the dark brown

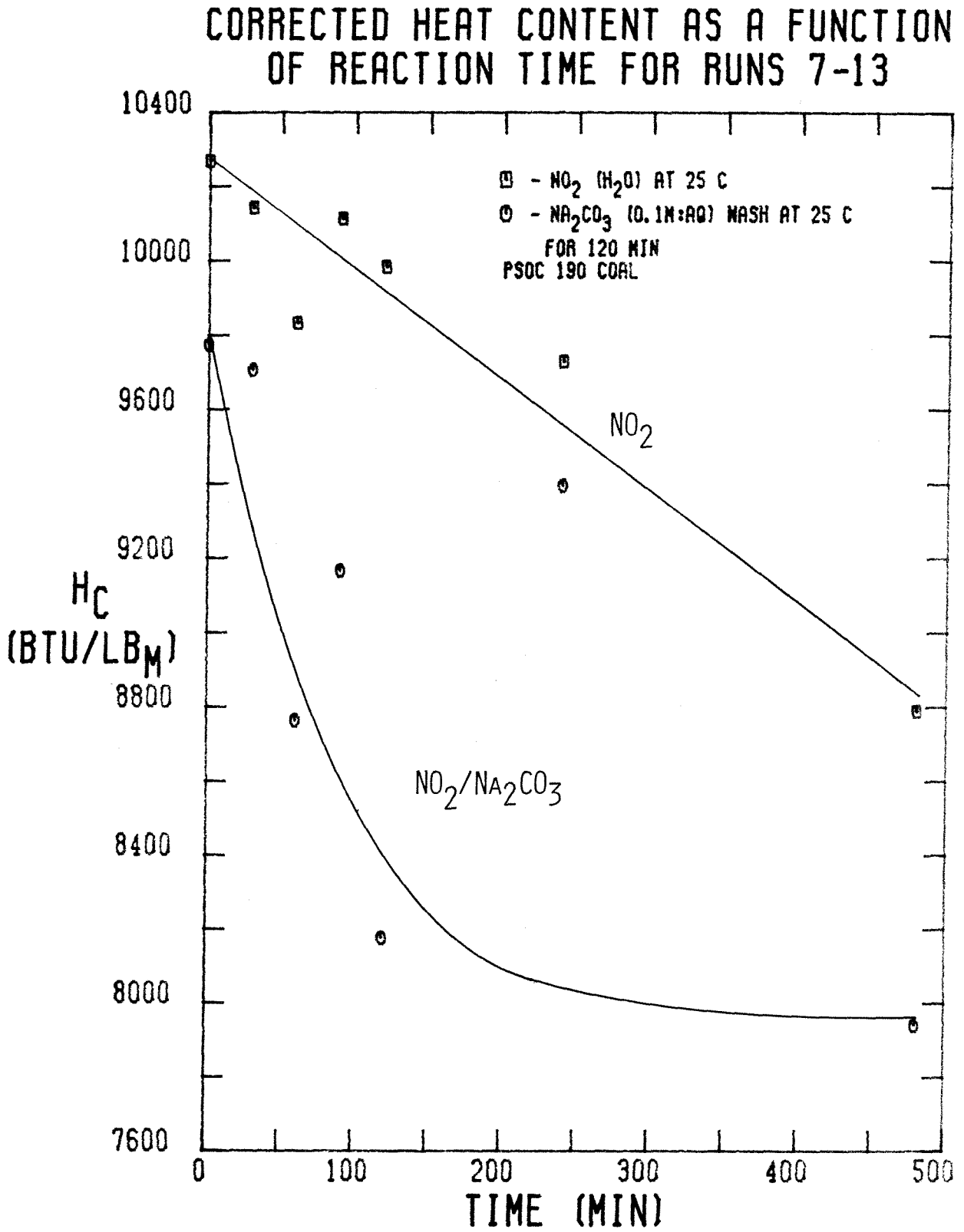
CORRECTED HEAT CONTENT AS A FUNCTION OF REACTION TIME FOR RUNS 7-13
□ - NO2 (H2O) AT 25 C
○ - NA2CO3 (0.1M:AQ) WASH AT 25 C FOR 120 MIN
PSOC 190 COAL
NO2
NO2/NA2CO3
HC (BTU/LBM)
10400
10000
9600
9200
8800
8400
8000
7600
0
100
200
300
400
500
TIME (MIN)

FIGURE 4-131

color of the filtrate, and are removed from the coal. This sequence suggests that the oxidized portions of the coal are organic acids with a pK_a somewhere between 0 and 12, which are insoluble in acidic media but quite soluble in basic media. These acids derived from the oxidation of coal are commonly referred to collectively as humic acids. On the basis of the loss in heat content of the coal, there is no reason that continued exposure to NO_2 would not eventually lead to the total oxidation of the coal.

The change in the heating value of the coal due to NO_2 treatment in water and the subsequent Na_2CO_3 (aq) wash (Runs 15–20) can be determined from the values of H_g given in Table 4–3. These values of H_g are basically consistent with those of the previous set. Most of the loss in H_g occurs during the NO_2 treatment rather than during the Na_2CO_3 (aq) wash, however, which may be the result of the lower concentrations of HNO_3 (aq) and HNO_2 (aq) in Runs 16, 17 and 18 than in the previously discussed experiments when the NO_2 flowrate was not monitored. It should be noted that at all three flowrates, the loss in H_g after 120 minutes of NO_2 treatment is 7 %, which implies that a small portion of the carbonaceous material in the coal is removed from the coal by the NO_2-H_2O solution system, regardless of the concentrations of the oxidizing species and the pH of the solution. The amount of NO_2 admitted to the reactor does affect the heat content loss as expected, due to the greater oxidation which occurs at higher oxidant concentrations. In this set of experiments, roughly 15 % or less of the heating value was lost in those runs in which the heat content of the washed coal was determined, which is about the same as the heat content loss suffered in the previous set of experiments.

The values of H_g determined for the predried PSOC 190 coal treated with NO_2 when slurried with CCl_4 and subsequently washed with 0.1 M Na_2CO_3 (aq) (Runs 21–27) are displayed graphically in Figure 4–132. Whenever CCl_4 is used as the

TABLE 4-3

The Corrected Heat Content of the PSOC 190 Coal Treated With NO_2 in Water at 25 C in the Flow Reactor (Runs 15-20)

Run #	Reaction Time (min)	Mean NO_2 Flowrate (g NO_2/min)	H_g (Btu/lb_m)	
			After NO_2 Treatment	After Wash With Na_2CO_3 (aq)
Raw	120	0.0	10,269	10,269
15	60	0.697	10,066	
16	120	0.269	9,727	9,565
17	120	0.483	9,487	9,090
18	120	1.039	9,596	8,847
19	180	0.862	8,588	
20	240	0.759	9,208	

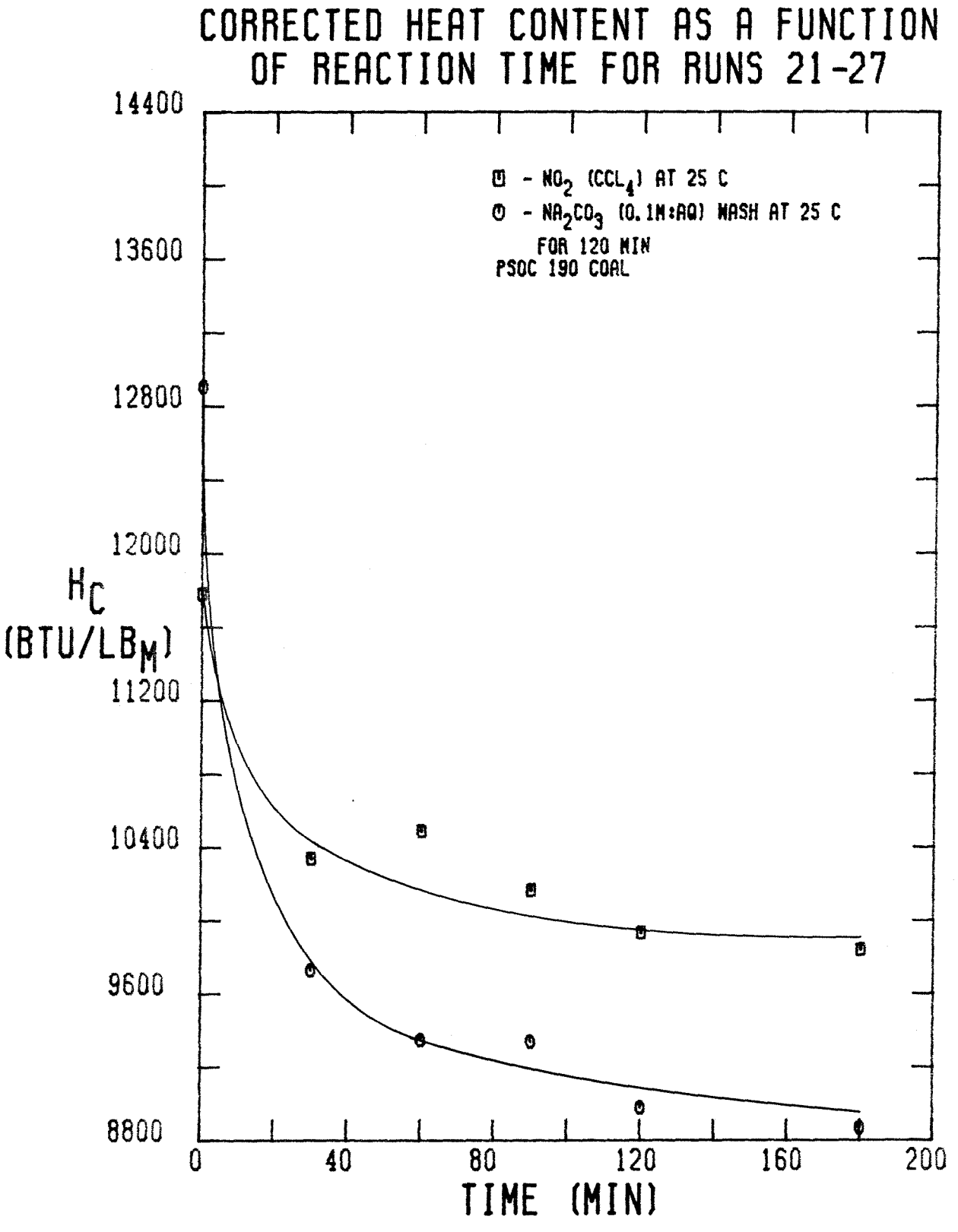
CORRECTED HEAT CONTENT AS A FUNCTION OF REACTION TIME FOR RUNS 21-27
14400
13600
12800
12000
11200
10400
9600
8800
H_C (BTU/LB$_M$)
0
40
80
120
160
200
TIME (MIN)
- NO_2 (CCL_4) AT 25 C
- NA_2CO_3 (0.1M:AQ) WASH AT 25 C
FOR 120 MIN
PSOC 190 COAL

FIGURE 4-132

solvent, the heat content of the treated coal must be adjusted for the amount of adsorbed CCl_4, which has a heating value of 436.5 Btu/lb_m. As the plot clearly shows, H_g drops in an exponentially decaying manner. The decline in H_g corresponds to the loss in carbon and hydrogen for these runs during the NO_2 treatment. The curve seems to level off at about 9800 Btu/lb_m, however, which corresponds to a 16 % heating value loss. The lower curve in the figure corresponds to the value of H_g for the washed coal after treatment with NO_2 and parallels the upper curve, levelling off at about 8800 Btu/lb_m after 180 minutes of exposure to NO_2, which corresponds to a 25 % loss in heating value. These results imply that a substantial portion of the oxidized coal is soluble in the NO_2-CCl_4 solution and that a smaller amount is removed by the Na_2CO_3 (aq) wash. Although the loss in H_g in this set of runs is greater than when H_2O is the NO_2-treatment solvent, it should be noted that NO_2 reacts with H_2O while it does not react with CCl_4. Consequently, the NO_2 concentration is much higher in CCl_4 than in H_2O, and more oxidation of the coal is not unexpected when CCl_4 is the solvent.

The values of H_g for the PSOC 190 coal treated with NO_2 at 20°C in the batch reactor and subsequently washed with 0.1 M Na_2CO_3 (aq) (Runs 33–37) are displayed in Figure 4–133 as a function of the NO_2-exposure time. Once again, H_g shows a very rapid drop within the first 30 minutes of NO_2 exposure followed by a more gradual decline. This behavior confirms the notion that a portion of the coal which accounts for roughly 9 % of the heating value is rapidly extracted by the NO_2-CCl_4 solution. Further oxidation of the coal results in a 12 % loss of heating value during the NO_2 treatment after 180 minutes of exposure. A more interesting feature is revealed by the lower curve in the plot, which shows that after the initial exposure of the coal to NO_2, no more oxidation which results in heating value losses after the wash occurs. For all of the NO_2-treatment times

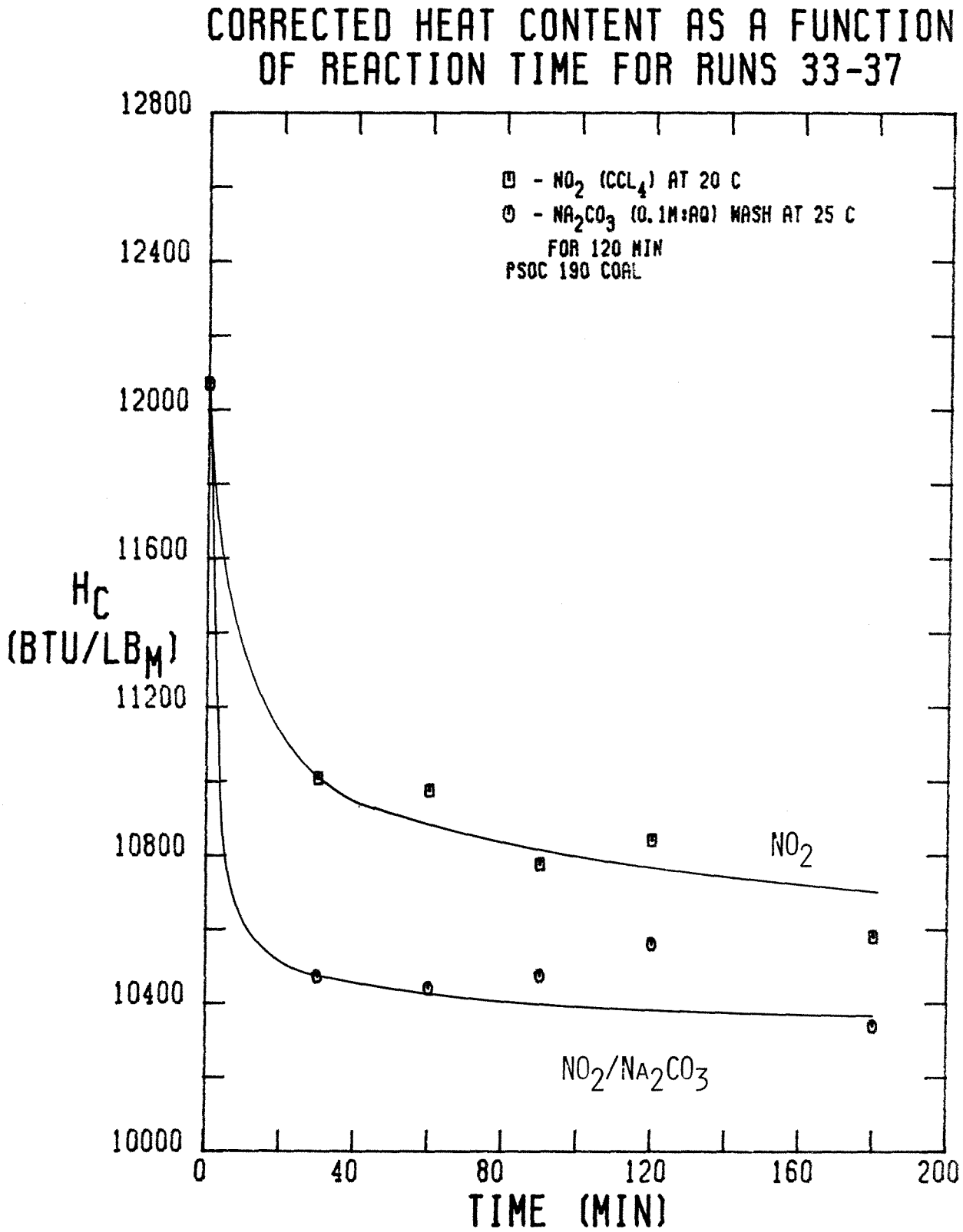
CORRECTED HEAT CONTENT AS A FUNCTION OF REACTION TIME FOR RUNS 33-37
□ - NO2 (CCL4) AT 20 C
⊙ - NA2CO3 (0.1M:AQ) WASH AT 25 C FOR 120 MIN
PSOC 190 COAL
HC (BTU/LBM)
12800
12400
12000
11600
11200
10800
10400
10000
0
40
80
120
160
200
TIME (MIN)
NO2
NO2/NA2CO3

FIGURE 4-133

used, the loss in H_g of the washed coal is about 15 %. These results agree with the carbon and hydrogen loss data and indicate that any portion of the coal which is ultimately oxidized is rapidly attacked and extracted from the coal by the NO_2-CCl_4 solution.

The values of H_g for the PSOC 190 coal treated with the NO_2-CCl_4 solution at 0°C in the batch reactor and subsequently washed in 0.1 M Na_2CO_3 (aq) (Runs 42–46) are depicted graphically in Figure 4–134. Once again, the major portion of the loss in H_g during the NO_2 treatment occurs within the first 30 minutes, resulting in a 5 % decline in H_g. After an additional 150 minutes of NO_2 exposure, H_g declines another 2 %. The loss in H_g due to the Na_2CO_3 (aq) wash occurs as a result of the first 30 minutes of the NO_2 treatment as well. The overall heating value loss is roughly 9 %. The speed with which the heating value loss occurs suggests that a portion of the coal is rapidly attacked and extracted by the NO_2-CCl_4 solution. This conclusion is also supported by the carbon and hydrogen loss data.

The effect of temperature on the loss in H_g during the NO_2 treatment is shown in Figure 4–135, where the corrected heat content of the coal relative to the initial heat content of the pretreated coal, $\frac{H_g}{(H_g)_0}$, is plotted as a function of the NO_2-exposure time. As anticipated, a higher NO_2-treatment temperature results in a larger heating value loss. In each set of runs, the major portion of the decline in H_g occurs during the first 30 minutes of NO_2 treatment, with heating value losses of 5, 9 and 11 % at 0, 20 and 50°C, respectively. Furthermore, the rate of the decline in H_g after the initial 30 minutes increases with increasing temperature. For example, after 180 minutes of NO_2 treatment, the heating value losses are 7, 12 and 18 % at 0, 20 and 50°C, respectively. These results are in accord with the carbon and hydrogen loss data, as well as the nitrogen uptake

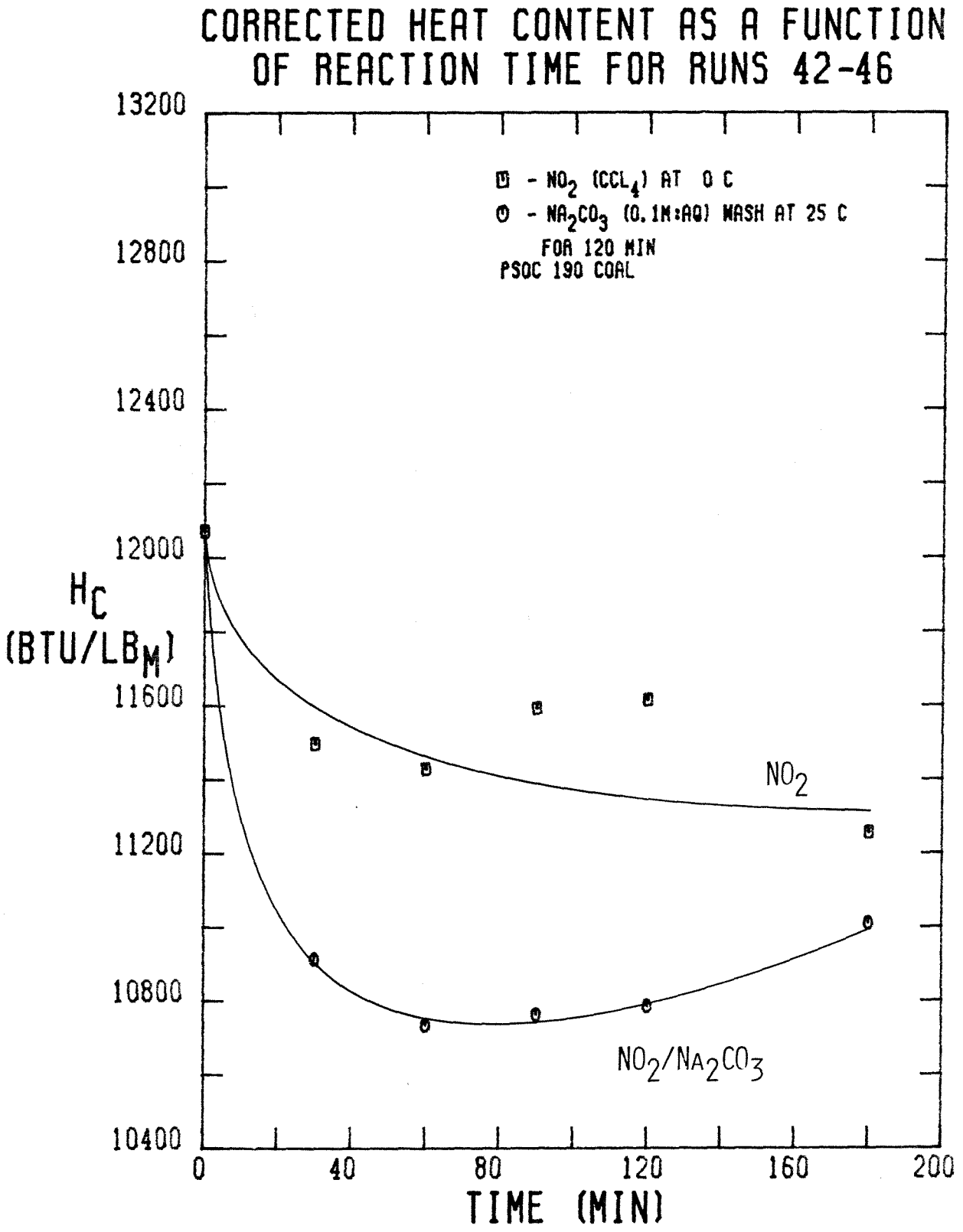
CORRECTED HEAT CONTENT AS A FUNCTION OF REACTION TIME FOR RUNS 42-46
□ - NO2 (CCL4) AT 0 C
○ - NA2CO3 (0.1M:AQ) WASH AT 25 C FOR 120 MIN
PSOC 190 COAL
NO2
NO2/NA2CO3
HC (BTU/LBM)
TIME (MIN)
13200
12800
12400
12000
11600
11200
10800
10400
0
40
80
120
160
200

FIGURE 4-134

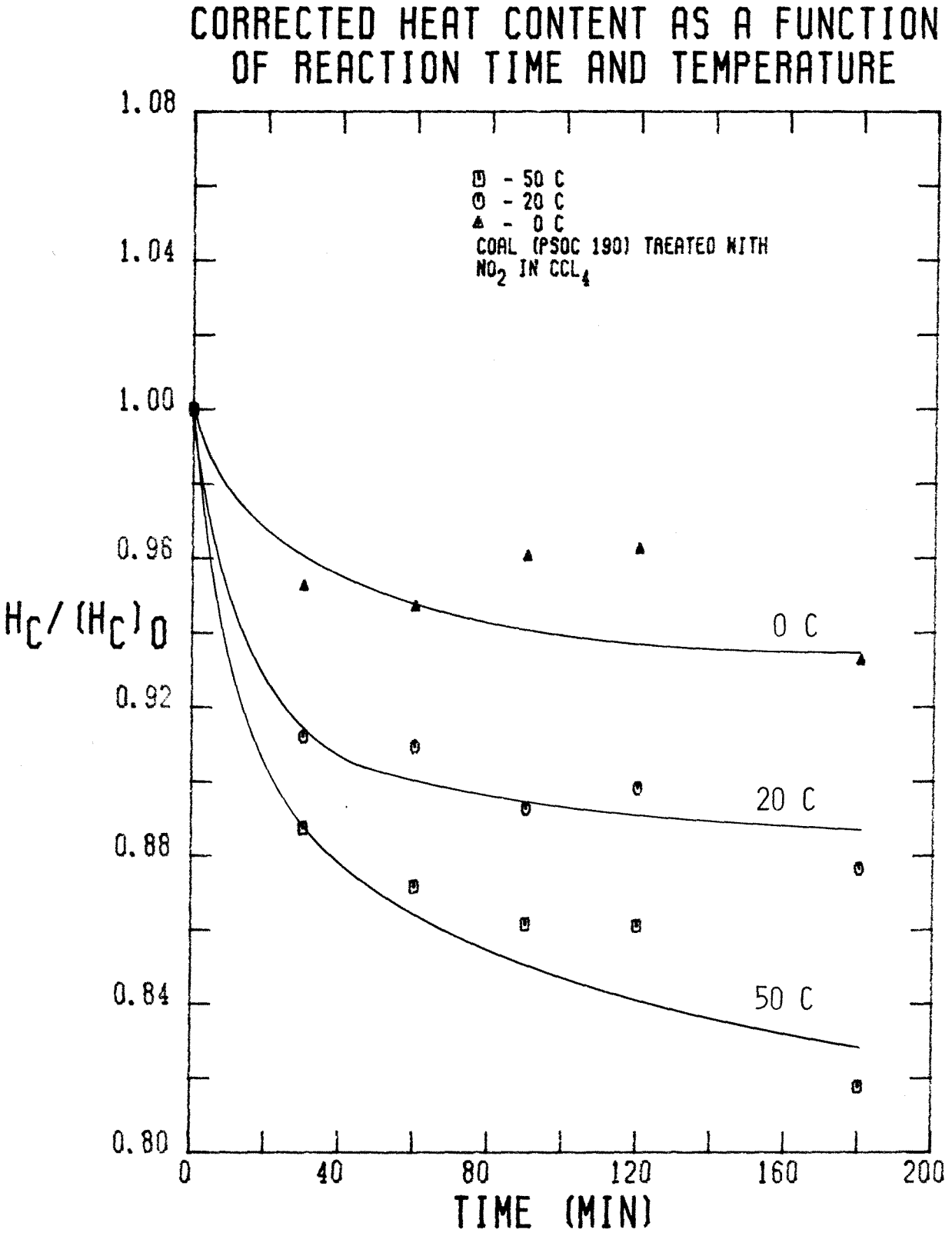
CORRECTED HEAT CONTENT AS A FUNCTION OF REACTION TIME AND TEMPERATURE
50 C
20 C
0 C
COAL (PSOC 190) TREATED WITH NO2 IN CCL4
1.08
1.04
1.00
0.96
0.92
0.88
0.84
0.80
HC/(HC)0
0
40
80
120
160
200
TIME (MIN)

FIGURE 4-135

data, all of which indicate that the rate of the NO_2-coal oxidation reaction increases with increasing temperature. Furthermore, the results support the theory that some portion of the coal, such as easily accessed volatile material, is readily attacked and extracted by the NO_2-CCl_4 solution, regardless of the treatment temperature.

The effect of the NO_2-treatment temperature on the heat content of the coal after the Na_2CO_3 (aq) wash is illustrated in Figure 4—136. Once again, the loss in H_g is greater when the NO_2-treatment temperature is higher. The most interesting feature of the plot, however, is that virtually all of the decline in H_g is due to the oxidation of the coal within the first 30 minutes of its exposure to NO_2. Treatment of the coal with NO_2 at 0°C results in a roughly 10 % loss in heating value, while treatment at 20°C results in an approximately 14 % loss in heating value. These results suggest that any oxidation of the coal which occurs under the conditions employed in the batch reactor and which result in the extraction of carbonaceous material or the formation of compounds soluble in Na_2CO_3 (aq) is quickly completed. This interpretation of the heating value data is basically consistent with the carbon and hydrogen loss data in that the latter also demonstrate that the major portion of their rise for the washed coal occurs within the first 30 minutes of the NO_2 treatment. The loss in carbon and hydrogen continues to rise for longer NO_2-exposure times, albeit at a much slower rate, while the heating value remains constant. This apparent paradox is easily resolved, however. The slow removal of carbon and hydrogen from the coal during the Na_2CO_3 (aq) wash may correspond to the leaching of oxidized carbon and hydrogen containing species which have little or no heating value. Such species may include H_2O, CO_2 and heavily oxidized humic acids. In other words, these oxidized species are formed within the first 30 minutes of the NO_2 treatment, but they may also be trapped within the coal particle, due perhaps to

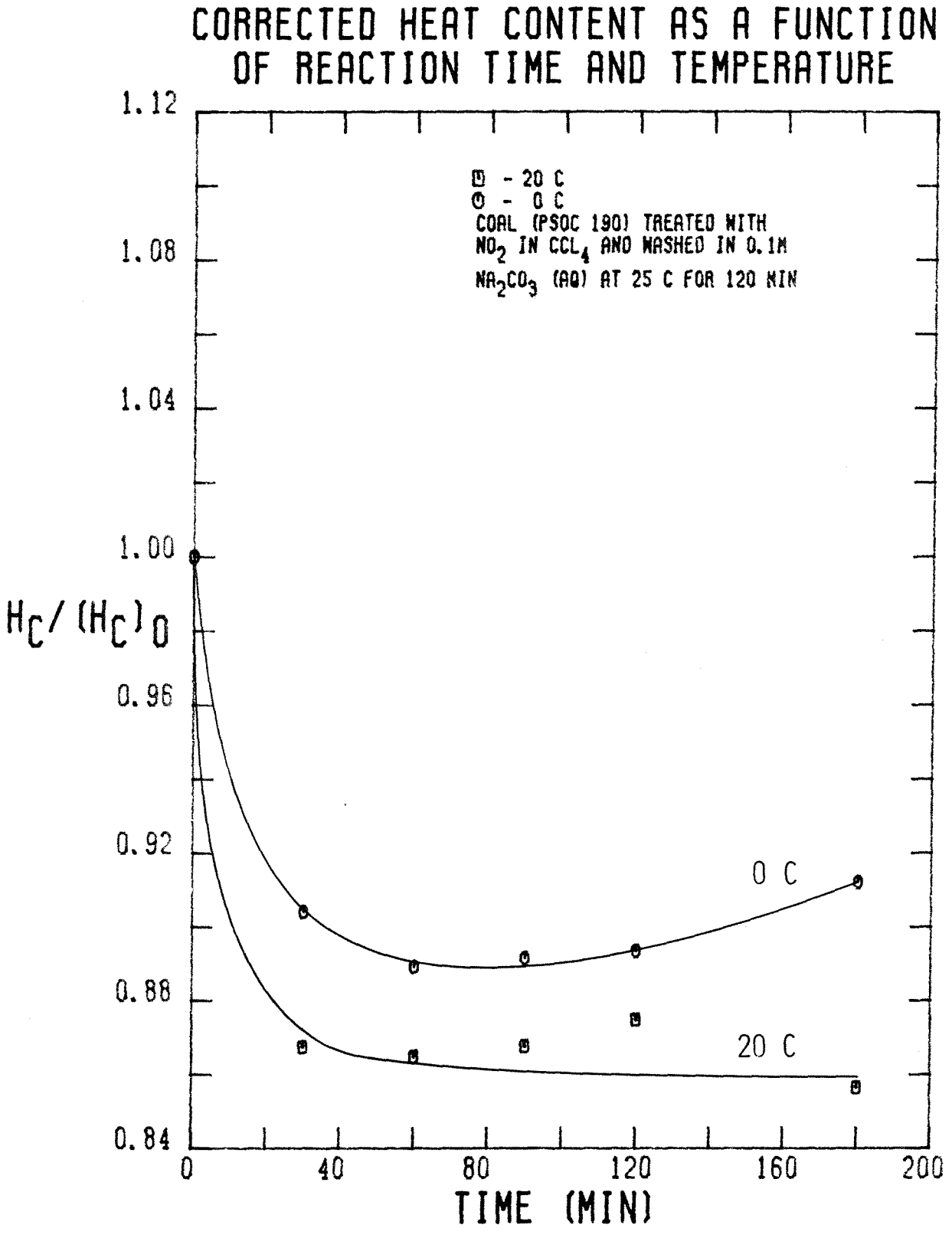
CORRECTED HEAT CONTENT AS A FUNCTION OF REACTION TIME AND TEMPERATURE
1.12
1.08
1.04
1.00
0.96
0.92
0.88
0.84
$H_C/(H_C)_0$
- 20 C
- 0 C
COAL (PSOC 190) TREATED WITH NO_2 IN CCL_4 AND WASHED IN 0.1M NA_2CO_3 (AQ) AT 25 C FOR 120 MIN
0 C
20 C
0
40
80
120
160
200
TIME (MIN)

FIGURE 4-136

pore blocking. Longer exposure to NO_2, however, renders these species more easily extracted by the Na_2CO_3 (aq) solution, perhaps because additional NO_2 exposure and NO_2 uptake by the coal enhances the accessibility of the Na_2CO_3 (aq) solution to these species. For instance, the uptake of NO_2 may increase the solubility of water in the coal, thereby allowing greater penetration of the coal particle by the Na_2CO_3 (aq) solution. In any case, the heat content data indicate that the oxidation of the coal is complete within 30 minutes, while the carbon and hydrogen loss data suggest that the removal of the oxidized species by the Na_2CO_3 (aq) wash is a much slower process.

The effect of the initial concentration of NO_2, $(NO_2)_0$, on the corrected heat content, H_g, of the PSOC 190 coal after 120 minutes of exposure to NO_2 is illustrated in Figure 4–137. The upper curve depicts the value of H_g for the coal after treatment with NO_2 as a function of reaction time. When $(NO_2)_0$ is small (0.01 F), very little oxidation occurs as evidenced by the fact that the heat content determined after the NO_2 treatment is actually greater than that of the pretreated coal. Once $(NO_2)_0$ exceeds 0.5 F, however, H_g seems to level off at 10,800 Btu/lb_m, which represents a loss of about 10 % in the heating value. On the other hand, the bottom curve demonstrates how the heating value of the Na_2CO_3 (aq) washed coal varies with $(NO_2)_0$. Initially, the curve drops sharply, and then begins to decline at a more gradual rate once $(NO_2)_0$ exceeds 0.5 F. This trend is consistent with the previously discussed mechanism in which a portion of the carbonaceous material in the coal is rapidly attacked and extracted by the Na_2CO_3 (aq) solution. In addition, further oxidation of the rest of the coal occurs, the extent of which depends on $(NO_2)_0$ in an almost linear fashion. Since more of the original coal material is removed by the Na_2CO_3 (aq) wash as $(NO_2)_0$ increases, it is possible that the oxidized species have larger heating values. That is, a higher concentration of NO_2 leads to the formation of

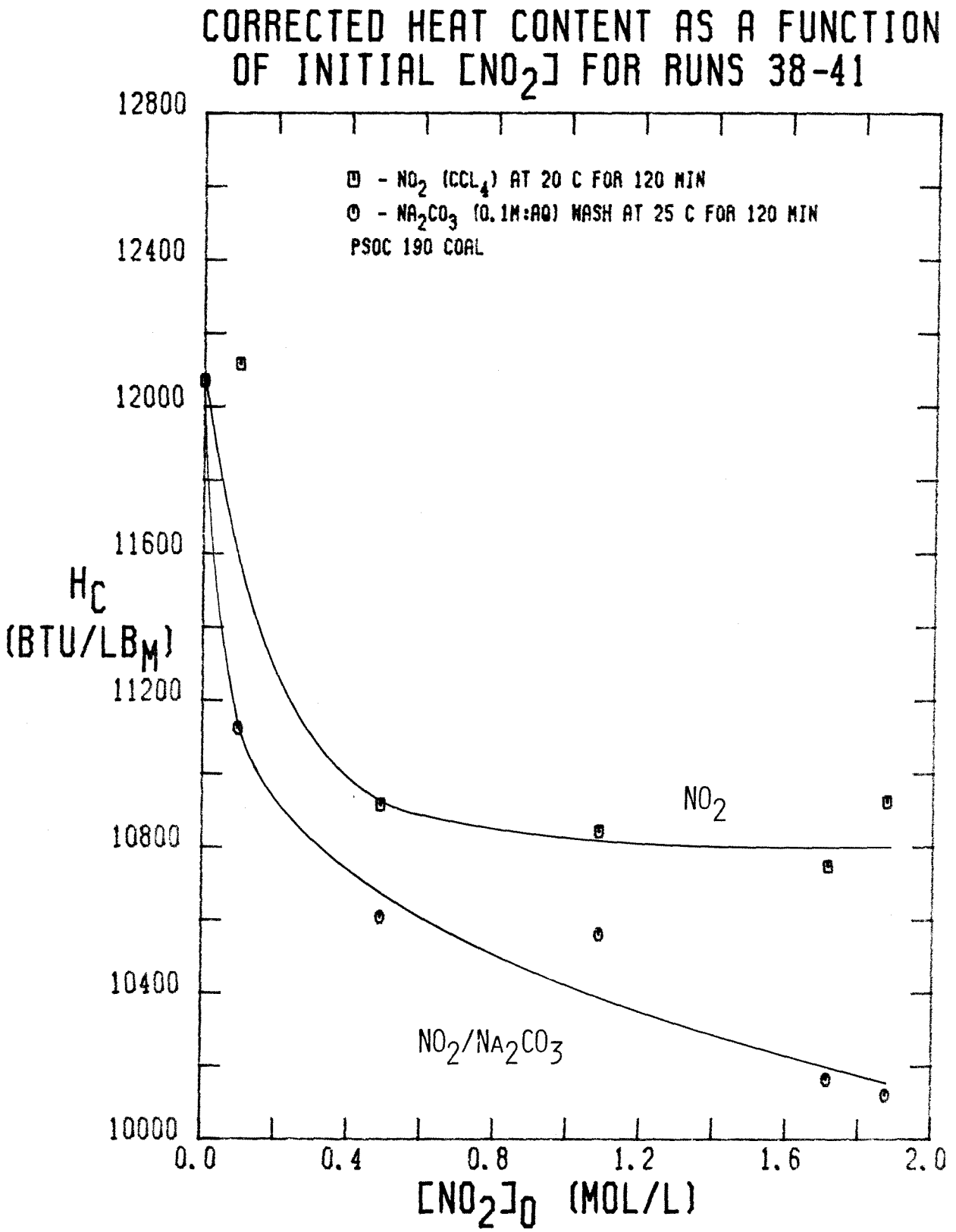
CORRECTED HEAT CONTENT AS A FUNCTION OF INITIAL [NO2] FOR RUNS 38-41
□ - NO2 (CCL4) AT 20 C FOR 120 MIN
⊙ - NA2CO3 (0.1M:AQ) WASH AT 25 C FOR 120 MIN
PSOC 190 COAL
12800
12400
12000
11600
11200
10800
10400
10000
HC (BTU/LBM)
NO2
NO2/NA2CO3
0.0
0.4
0.8
1.2
1.6
2.0
[NO2]0 (MOL/L)

FIGURE 4-137

coal-derived species that are soluble in Na_2CO_3 (aq) which are not as extensively oxidized as when (NO_2) is lower. It is interesting to note that the sigmoidal shape of the lower curve in this figure parallels that of the corresponding hydrogen loss curve exactly, which supports the notion that less oxidized species are removed by the Na_2CO_3 (aq) wash from the coal treated at higher NO_2 concentrations.

In order to determine the effect of the pore structure of the coal on the NO_2-coal reaction, another coal, PSOC 276, which has an initial pore volume four times less than that of the PSOC 190 coal, was treated with NO_2 at 20°C for various exposure times in the batch reactor and subsequently washed in 0.1 M Na_2CO_3 (aq) (Runs 47–52). The values of the corrected heat content are displayed as a function of the NO_2-exposure time in Figure 4–138. During the NO_2 treatment, H_g falls rapidly within the first 30 minutes, and then more slowly thereafter, so that after 180 minutes, there is a 7.5 % loss in the heat content. The coal, when subsequently washed in 0.1 M Na_2CO_3 (aq), also displays a rapid decline in H_g within the first 30 minutes of the NO_2 treatment. After 90 minutes of NO_2 treatment, however, the Na_2CO_3 (aq) wash does not result in any further decline in H_g, which levels off at about 11,400 Btu/lb_m, a 9 % loss in the heat content. Therefore, the same interpretation applied to the processed PSOC 190 coal applies to this set of runs as well. That is, a portion of the coal, such as some of the light volatile matter, is rapidly attacked and oxidized by the NO_2-CCl_4 solution. Of this oxidized coal material, that which is not extracted from the coal during the NO_2 treatment is removed by the Na_2CO_3 (aq) wash.

A comparison of the change in the heat content of the PSOC 190 and PSOC 276 coals during NO_2 treatment at 20°C in the batch reactor is provided in Figure 4–139. Both coals show a rapid decline in H_g during the first 30 minutes followed by a more gradual decline thereafter. The rate of decline in H_g for the

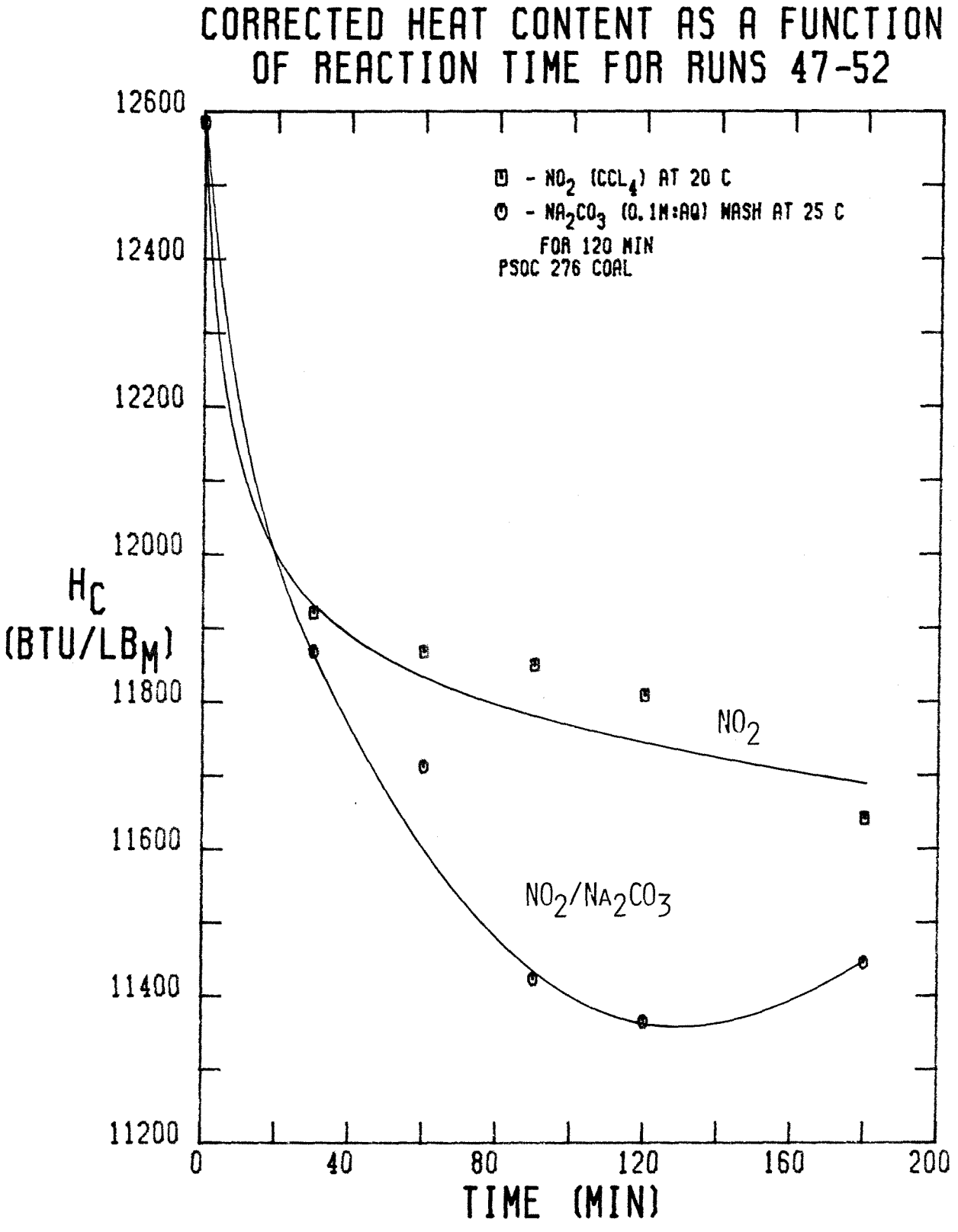
CORRECTED HEAT CONTENT AS A FUNCTION OF REACTION TIME FOR RUNS 47-52
□ - NO2 (CCL4) AT 20 C
⊙ - NA2CO3 (0.1M:AQ) WASH AT 25 C FOR 120 MIN
PSOC 276 COAL
NO2
NO2/NA2CO3
HC (BTU/LBM)
TIME (MIN)
12600
12400
12200
12000
11800
11600
11400
11200
0
40
80
120
160
200

FIGURE 4-138

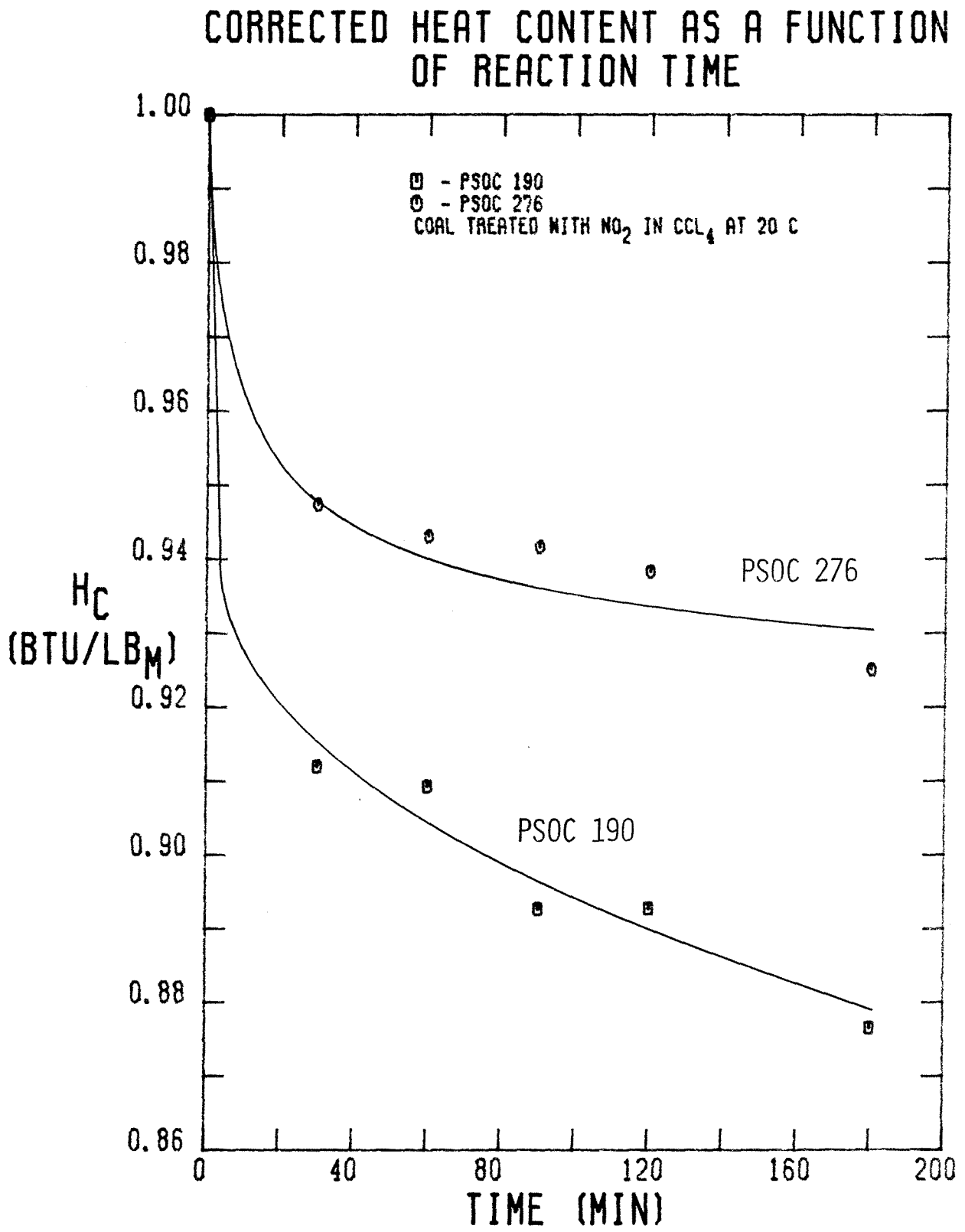
CORRECTED HEAT CONTENT AS A FUNCTION OF REACTION TIME
1.00
0.98
0.96
0.94
0.92
0.90
0.88
0.86
H_C (BTU/LB$_M$)
PSOC 190
PSOC 276
COAL TREATED WITH NO_2 IN CCL_4 AT 20 C
PSOC 276
PSOC 190
0
40
80
120
160
200
TIME (MIN)

FIGURE 4-139

PSOC 190 coal is greater than that in the PSOC 276 coal, however. Indeed, the decline in H_g for the PSOC 190 coal is approximately 1.7 times that of the PSOC 276 at all NO_2-exposure times. Furthermore, the decrease in H_g after the first 30 minutes is a linear function of the exposure time for both coals, which is also indicative of the nitrogen uptake data. In any case, it is obvious that the differences between the two coals cause disparate losses in H_g. Conceivably, the difference could be in the chemical composition of the two coals, with fewer species available for oxidation in the PSOC 276 than in the PSOC 190. This scenario is unlikely, however, because the chemical compositions of the two coals are virtually identical. Indeed, the carbon to hydrogen ratio, which serves as an indicator of the relative amounts of aliphatic and aromatic hydrogen, differs by only 1.2 % between the two coals. Thus, the concentration of reactive species in the two coals should be about the same. Furthermore, the accessibility of the NO_2 to these species is independent of the pore structure of the coal. Nevertheless, the difference in the pore structures of the two coals would lead one to expect that less conversion of hydrogen should occur in the PSOC 276 than in the PSOC 190, due to a greater degree of steric hindrance in the solid coal matrix. That is, even though the total nitrogen uptake by the two coals are equal, the relative amounts of physical and chemical incorporation of nitrogen in the two coals may be different.

A comparison of the change in the heat content of the two NO_2-treated coals after being washed in 0.1 M Na_2CO_3 (aq) for 120 minutes at 25 °C is shown in Figure 4–140. In this case, a distinct difference in the change in H_g for the two coals can be detected. Whereas the first 30 minutes of NO_2 exposure accounts for essentially all of the 14 % loss in H_g after the Na_2CO_3 (aq) wash of the PSOC 190 coal, longer exposure of the PSOC 276 to NO_2 results in additional oxidation and loss in the heat content, which reaches about 10 % after 120 minutes of

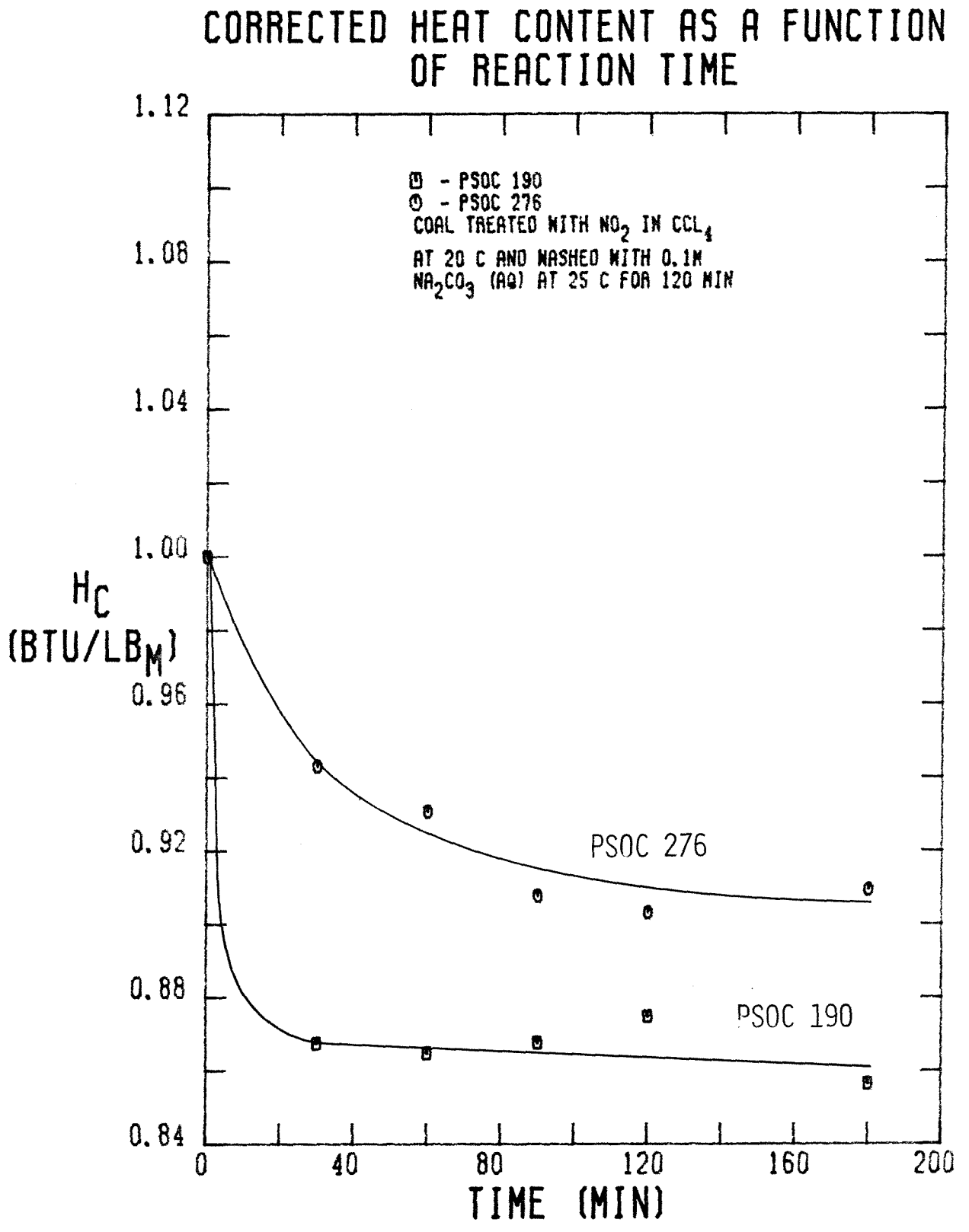
CORRECTED HEAT CONTENT AS A FUNCTION OF REACTION TIME
- PSOC 190
- PSOC 276
COAL TREATED WITH NO_2 IN CCL_4
AT 20 C AND WASHED WITH 0.1M
NA_2CO_3 (AQ) AT 25 C FOR 120 MIN
PSOC 276
PSOC 190
H_C
(BTU/LB_M)
1.12
1.08
1.04
1.00
0.96
0.92
0.88
0.84
0
40
80
120
160
200
TIME (MIN)

FIGURE 4-140

reaction. The fact that the value of H_g for the washed PSOC 276 continues to decrease for longer NO_2-exposure times can be attributed to the increased resistance to mass transfer of the soluble oxidized coal species out of the PSOC 276 coal. Once again, this behavioral difference can be attributed to the influence of the pore structure on the rate and extent of oxidation. This same influence of the pore structure accounts for the similar difference in the rate of nitrogen uptake by the two coals as well. Thus, the pore structure of the coal does affect the extent of the heating value loss to a small degree, although it seems to possess a much stronger influence on the extent of desulfurization through SO_2 trapping by adsorbed sodium.

Based on this discussion of the changes which occur in the heat content of the processed coal, several conclusions regarding the effect of the reaction parameters on the extent of oxidation of the coal may be made. It should be noted that the heat content data support the conclusions made in earlier sections regarding the oxidation of the coal, as it should, since the change in heating value is really a composite of the changes in the elemental composition of the coal.

The effect of the solvent on the extent of the oxidation of the coal depends upon the amount of competition there is between the solvent and coal for NO_2. For instance, when H_2O is the solvent, virtually all of the NO_2 reacts with the solvent to form HNO_3 (aq) and HNO_2 (aq), which then become the primary coal oxidants. When CCl_4 is the solvent, however, only the coal reacts with NO_2. Because NO_2 can penetrate the solid coal matrix more readily than HNO_3 (aq) or HNO_2 (aq), more oxidation occurs when CCl_4 is the solvent than when H_2O is the solvent, under the same reaction conditions.

The effect of temperature on the overall rate of the oxidation of the coal by NO_2 is important. At 50°C, the extent of oxidation is so large that once the

treated coal is exposed to 0.1 M Na_2CO_3 (aq), it completely emulsifies and cannot be filtered. If the coal is treated with NO_2 at 20°C, the oxidation reaction which produces the coal-derived species which are soluble in 0.1 M Na_2CO_3 (aq) is complete within the first 30 minutes. The same is true if the coal is treated with NO_2 at 0°C as well, although the extent of the oxidation is somewhat less. Thus, it appears that a portion of the coal, such as part of the light volatile matter, is readily attacked by the NO_2-CCl_4 solution and either extracted during the NO_2 treatment or leached during the Na_2CO_3 (aq) wash. The extent of the oxidation of the coal increases dramatically with temperature, however, which implies that more of the coal structure is susceptible to oxidation as the temperature rises. For instance, certain bonds which cannot be broken by NO_2 at 0°C or 20°C may be broken at 50°C, which is exactly the interpretation given for the effect of the temperature of the NO_2 treatment on the uptake of nitrogen by the coal, in that the accessibility to the reactive species in the coal is determined by the temperature. Furthermore, the effect of $(NO_2)_0$ on the extent of the oxidation is similar to that on the nitrogen uptake, both of which increase with increasing $(NO_2)_0$. Because an increase in the bulk concentration of NO_2 results in more NO_2 uptake by the coal, more oxidation of the coal occurs, which results in higher losses in the heating value.

Finally, the pore structure influences the extent of the loss in the heating value of the coal. The pore structure has very little effect upon the penetration of NO_2 into the coal but apparently does influence the subsequent oxidation which occurs. The pore structure also influences the removal of the oxidized coal species, especially during the Na_2CO_3 (aq) wash. The pore structure seems to primarily affect the extent of the oxidation reactions of NO_2 with the reactive species in the solid coal matrix, perhaps because the degree of steric hindrance in the NO_2-coal reaction increases as the pore volume decreases.

4.2.2.10 The Selectivity of the Desulfurization Process

The results of the last two sections can be combined to determine the selectivity of the NO_2 treatment and the Na_2CO_3 (aq) wash for the removal of sulfur relative to the oxidation of the rest of the coal. The selectivity is defined by the beneficiation coefficient, B, which is given by:

$$B = \left[1 - \frac{(1 + f)\, c_S}{(c_S)_0} \right] \left[\frac{H_g}{(H_g)_0} \right], \quad \text{where} \tag{4.2.21}$$

f = the fractional mass gain of the treated coal relative to the initial mass of coal used. (If a mass loss occurs, $f = 0$),

c_S = the sulfur content of the treated coal corrected for any CCl_4 adsorption (mass %),

$(c_S)_0$ = the sulfur content of the coal before processing (mass %),

H_g = the heat content of the treated coal corrected for any mass change (Btu/lb_m of initial coal used), and

$(H_g)_0$ = the heat content of the pretreated coal before processing (Btu/lb_m coal)

Thus, B can range from 0 to 1. A value of 0 corresponds to either no sulfur removal or the complete oxidation of the coal while a value of 1 corresponds to the complete removal of sulfur with no loss in the heating value of the coal. Basically, the equation for B contains a penalty for the desulfurization which is based on the extent of the oxidation of the rest of the coal as reflected by the heating value loss. As will be seen, values of B above 0.85 are quite hard to attain due to the small amount of oxidation of the coal which occurs under even the most mild NO_2-treatment conditions.

Because the coal treated with NO_2 in Runs 1–6 was not subsequently washed in 0.1 M Na_2CO_3 (aq), values of the ultimate beneficiation cannot be determined. Furthermore, the amount of pyridine and nitrobenzene adsorption makes it impossible to determine the actual heating value loss of the treated coal.

Therefore, the beneficiation results will deal exclusively with those runs in which H_2O or CCl_4 is the solvent.

The values of *B* obtained for the first set of runs conducted at 25°C in the flow reactor with H_2O as the solvent (Runs 7–13) are displayed graphically in Figure 4–141 as a function of the NO_2-exposure time. Only the Leco method was used in the sulfur determinations, so just two sets of values were obtained, one of which corresponds to the washed coal. The bottom curve, which is defined by the values of *B* for the NO_2 treated coal, rises from about 0.18 at $t = 0$ to roughly 0.42 at $t = 480$ minutes, where the curve begins to level off. The value of 0.18 at $t = 0$ is due to the removal of sulfate sulfur by washing the raw coal in H_2O without any NO_2 being admitted. The curve begins to level off after long exposure times because oxidation of the coal continues but the removal of sulfur begins to stop. The top curve corresponds to the beneficiation of the NO_2-treated coal after the Na_2CO_3 (aq) wash, which reaches a maximum of 0.76 at $t = 240$ minutes. Even though more sulfur is removed after 480 minutes of NO_2 treatment, the increased desulfurization is more than offset by the increased loss in heat content, so *B* declines. Thus, under the conditions employed in this set of experiments, the coal should not be treated with NO_2 for more than 240 minutes.

Table 4–4 contains the values of *B* obtained when the coal was treated with NO_2 for varying lengths of time and at varying NO_2 flowrates at 25°C in the flow reactor (Runs 15–20). It should be noted that 27 % of the initial sulfur content can be removed simply by washing the coal first in water and then in 0.1 M Na_2CO_3 (aq), which results in no oxidation of the coal. As expected, the beneficiation of the NO_2-treated coal increases when the HNO_3 (aq) and HNO_2 (aq) concentrations are increased due to higher NO_2 flowrates or when the exposure time is increased. In the wide range of NO_2 flowrates and reaction

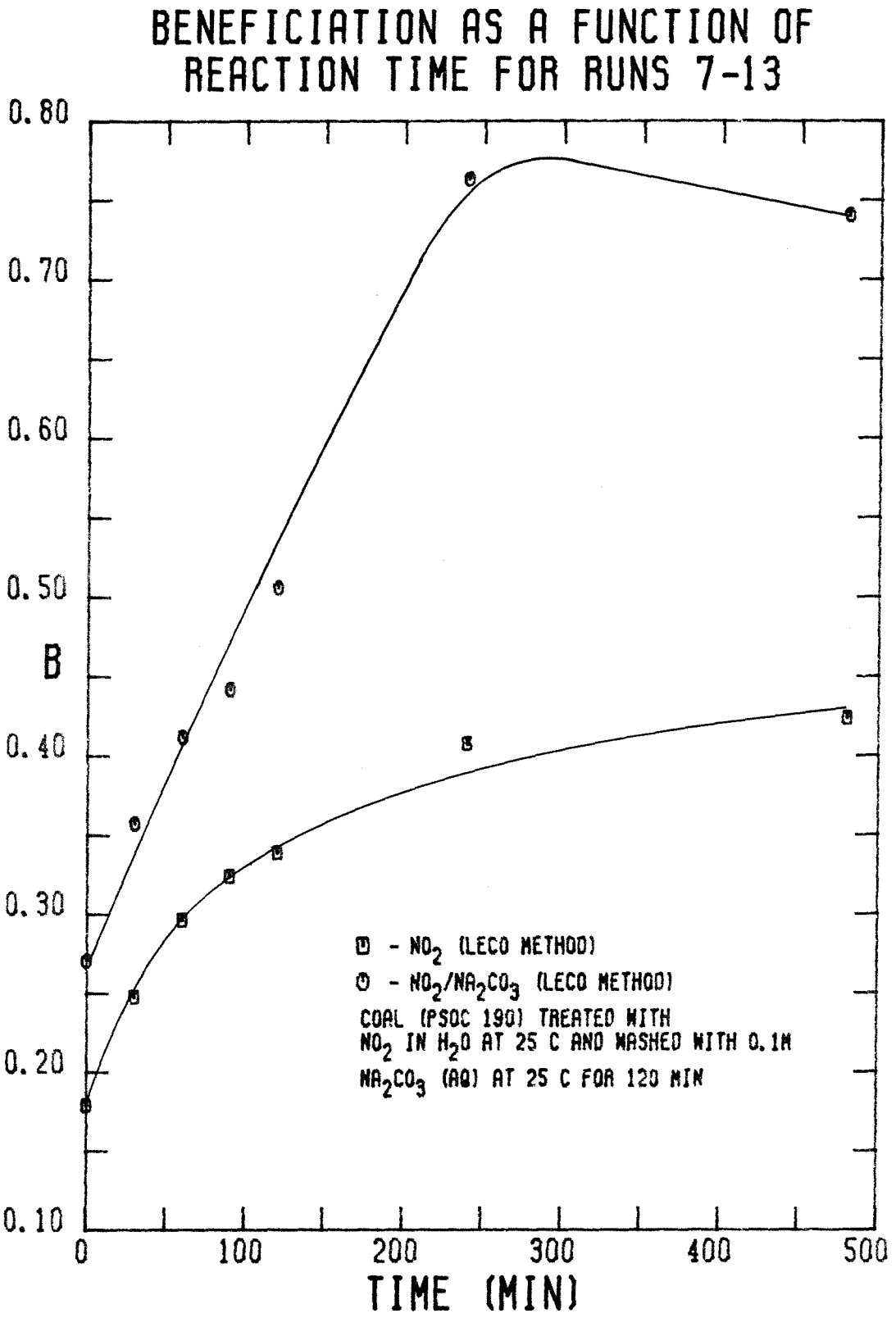
BENEFICIATION AS A FUNCTION OF REACTION TIME FOR RUNS 7-13
0.80
0.70
0.60
0.50
B
0.40
0.30
0.20
0.10
0
100
200
300
400
500
TIME (MIN)
- NO_2 (LECO METHOD)
- NO_2/NA_2CO_3 (LECO METHOD)
COAL (PSOC 190) TREATED WITH
NO_2 IN H_2O AT 25 C AND WASHED WITH 0.1M
NA_2CO_3 (AQ) AT 25 C FOR 120 MIN

FIGURE 4-141

TABLE 4-4

The Beneficiation of the Processed PSOC 190 Coal (Runs 15-20)				
Run #	Reaction Time (min)	Mean NO_2 Flowrate (g NO_2/min)	*B*	
			After NO_2 Treatment	After Wash With Na_2CO_3 (aq)
Raw	120	0	0.1681	0.2710
15	60	0.697	0.3193	
16	120	0.269	0.2900	0.4672
17	120	0.483	0.3401	0.6026
18	120	1.039	0.3745	0.6875
19	180	0.862	0.3650	
20	240	0.759	0.4060	

times used, B is between 0.3 and 0.4, which results from the fact that most of the sulfur which is removed during the NO_2 treatment is rapidly attacked and extracted by the NO_2-H_2O solution. The notion of a rapid attack of NO_2 on the coal also correlates quite well with the heating value loss data.

Only the values of H_g for the Na_2CO_3 (aq) washed coal from Runs 16, 17 and 18 were obtained, so values of B for the washed coal are available only for those runs. These values of B demonstrate, however, that the larger HNO_3 (aq) and HNO_2 (aq) concentrations obtained at higher flowrates do lead to a greater amount of SO_2 trapping, ostensibly due to greater sodium uptake by the NO_2-treated coal during the Na_2CO_3 (aq) wash, without a great increase in the oxidation of the rest of the coal. That is, the small amount of oxidation which occurs after the initial attack and extraction of the coal accounts for the introduction into the coal of the anionic oxygen which ultimately adsorbs Na^+ during the subsequent wash. If the oxidation conditions are too severe, however, the increased loss in heat content more than offsets the enhanced amount of SO_2 trapping, as evidenced by the previous set of experiments. In all of the experiments discussed so far, H_2O has been the solvent for the NO_2 treatment. The rest of this section will deal with the beneficiation of the coal when CCl_4 is used as the solvent for the NO_2 treatment.

The values of B for the PSOC 190 coal slurried in CCl_4 and treated with NO_2 at 25°C in the flow reactor and subsequently washed in 0.1 M Na_2CO_3 (aq) are given as a function of NO_2-exposure time in Figure 4–142. The bottom curve corresponds to the beneficiation of the NO_2-treated coal. It is obvious that all of the beneficiation occurs within the first 30 minutes, which is the result of the rapid reaction of NO_2 and coal alluded to in the previous sections. Washing the NO_2-treated coal in 0.1 M Na_2CO_3 (aq), although it does raise B, does not really result in any additional beneficiation over that obtained by washing the

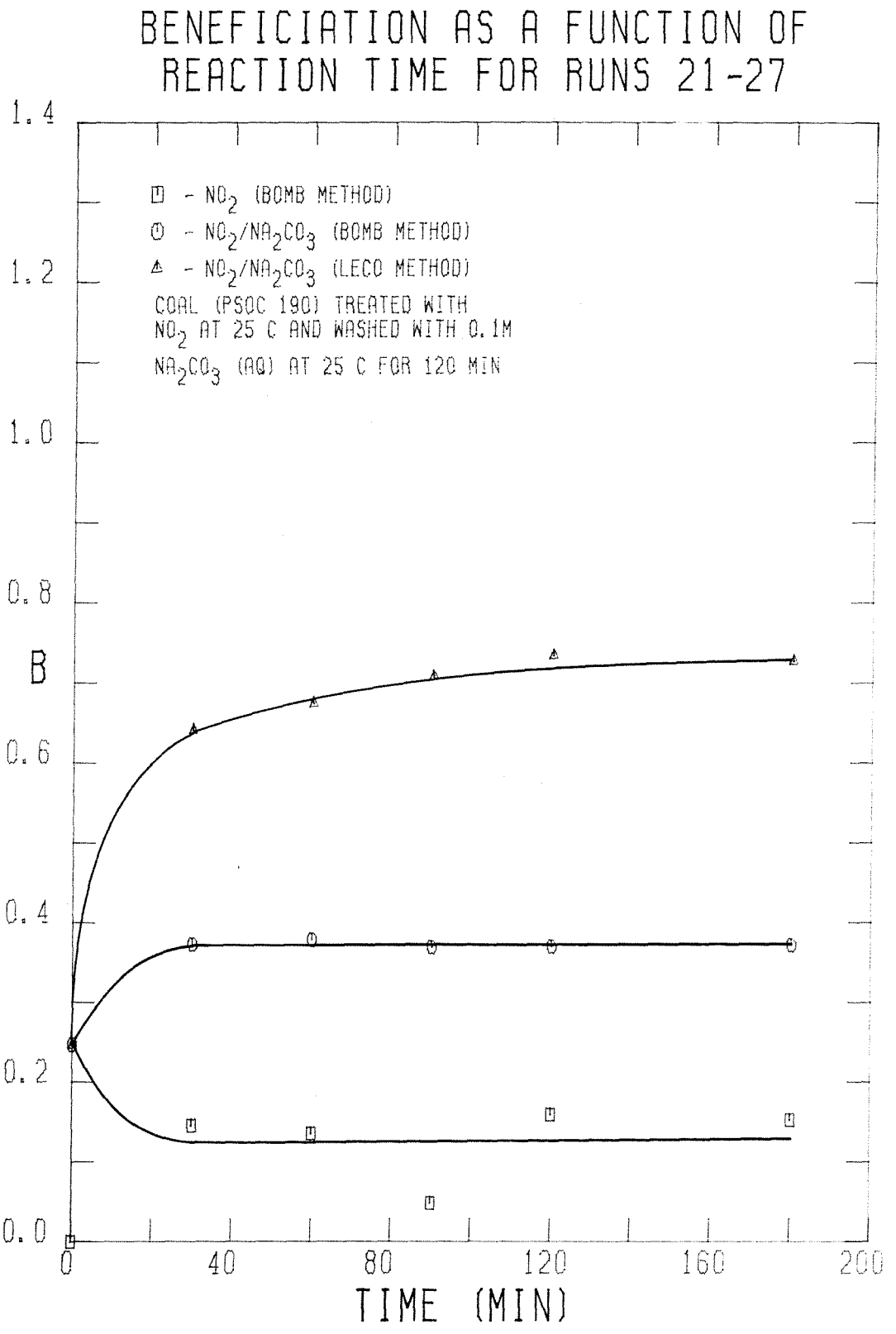
BENEFICIATION AS A FUNCTION OF REACTION TIME FOR RUNS 21-27
1.4
1.2
1.0
0.8
0.6
0.4
0.2
0.0
B
□ - NO2 (BOMB METHOD)
○ - NO2/NA2CO3 (BOMB METHOD)
△ - NO2/NA2CO3 (LECO METHOD)
COAL (PSOC 190) TREATED WITH NO2 AT 25 C AND WASHED WITH 0.1M NA2CO3 (AQ) AT 25 C FOR 120 MIN
0
40
80
120
160
200
TIME (MIN)

FIGURE 4-142

untreated coal in Na_2CO_3 (aq). That is, the increase in *B* for the washed coal over the treated coal can be attributed to the removal of sulfur compounds which would be removed by the Na_2CO_3 (aq) wash even if the coal had not been treated with NO_2. The wash of the NO_2-treated coal does result in the uptake of Na^+, however, which has been demonstrated to be responsible for the trapping of SO_2 during combustion. Once again, the upper curve in the plot indicates that the major fraction of the beneficiation occurs because of the anionic oxygen introduced into the coal within the first 30 minutes of reaction. Due to the rather substantial loss in heating value, however, the maximum value attained for *B* is only about 0.73, even though 97 % of the SO_2 has been removed from the combustion gas.

The beneficiation of the coal treated with NO_2 at 20°C when slurried in CCl_4 in the batch reactor and subsequently washed in 0.1 M Na_2CO_3 (aq) (Runs 33–37) is plotted as a function of the NO_2-exposure time in Figure 4–143. The trends in the values of *B* for the coal are the same as those in the previous set of experiments, namely that virtually all of the beneficiation is the result of the first 30 minutes of the NO_2 treatment. Thus, for longer NO_2-exposure times, any additional sulfur removal is balanced by an additional loss in heating value. The ultimate beneficiation reaches a maximum value of 0.84, however, as compared to only 0.73 in the previous set, which is the result of less loss in the heating value of the coal with the same sulfur removal of 96 %. Less oxidation occurs because the NO_2 concentration in this set of runs is about 1 F while in the previous set of runs, the NO_2 concentration rises linearly from 0 to 8 F during the total exposure time of 180 minutes. Nevertheless, even these milder NO_2-treatment conditions result in a 15 % loss in heating value, which is significant, but not drastic.

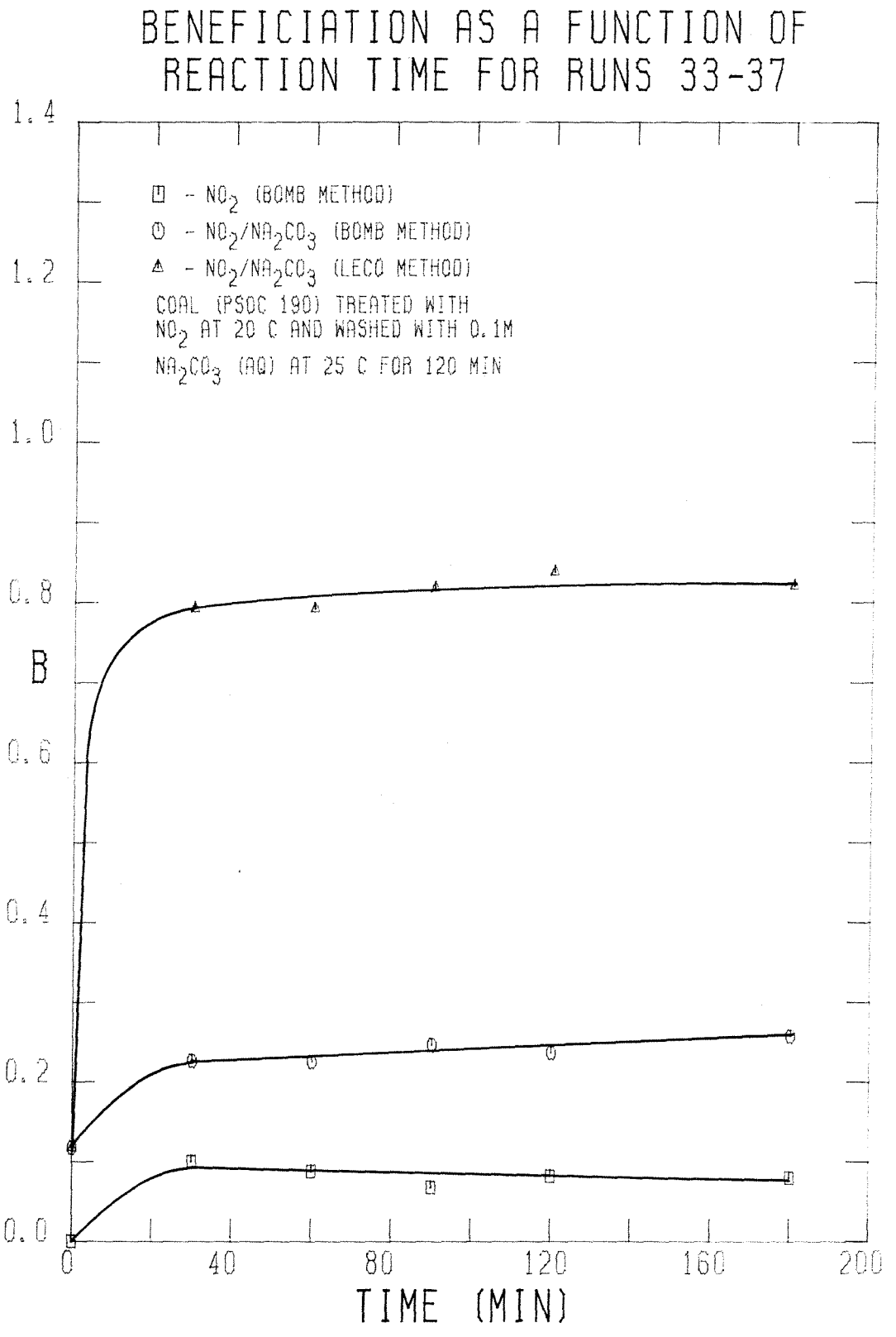
BENEFICIATION AS A FUNCTION OF
REACTION TIME FOR RUNS 33-37
1.4
1.2
1.0
0.8
0.6
0.4
0.2
0.0
B
□ - NO2 (BOMB METHOD)
⊙ - NO2/NA2CO3 (BOMB METHOD)
△ - NO2/NA2CO3 (LECO METHOD)
COAL (PSOC 190) TREATED WITH
NO2 AT 20 C AND WASHED WITH 0.1M
NA2CO3 (AQ) AT 25 C FOR 120 MIN
0
40
80
120
160
200
TIME (MIN)

FIGURE 4-143

The values of *B* for the coal treated with the NO_2-CCl_4 solution at 0°C in the batch reactor and subsequently washed in 0.1 M Na_2CO_3 (aq) (Runs 42–46) are displayed graphically in Figure 4–144 as a function of NO_2-exposure time. The beneficiation of the coal due to the NO_2 treatment never exceeds 0.10, which is the result of the diminished extent of the removal of oxidized matter from the coal under these conditions. The Na_2CO_3 (aq) wash of the coal, however, reveals that the extent of the NO_2-coal reaction is slightly less than that at 20°C. Although the middle curve in the figure is level after 30 minutes of NO_2 treatment, the top curve actually increases after 30 minutes, reaching a value of *B* of 0.78 after 180 minutes of NO_2 treatment. Furthermore, the shape of the top curve suggests that further NO_2 treatment at 0°C would yield an even greater beneficiation of the coal.

The effect of the NO_2-treatment temperature on the beneficiation of the coal due to the NO_2 treatment is illustrated in Figure 4–145. As expected, the value of *B* increases with temperature, although the difference between the corresponding curves is quite slight. All of the curves seem to level off after the first 30 minutes at values of *B* of 0.07, 0.09 and 0.11 at 0, 20 and 50°C, respectively. It should be noted that the value of *B* at 60 minutes for the 50°C NO_2 treatment results from a spuriously low sulfur determination, and was therefore disregarded when the locus was drawn. In any case, the temperature of the NO_2 treatment has very little effect on the beneficiation of the coal due just to the NO_2 treatment.

The beneficiation of the coal due to the Na_2CO_3 (aq) wash of the coal treated with NO_2 at 0 and 20°C, based on the sulfur determinations made by the Bomb method, is plotted as a function of the NO_2-exposure time in Figure 4–146. It is very interesting to note that the NO_2 treatment at 0°C results in a beneficiation for the washed coal which is about 15 % greater than that for the coal treated

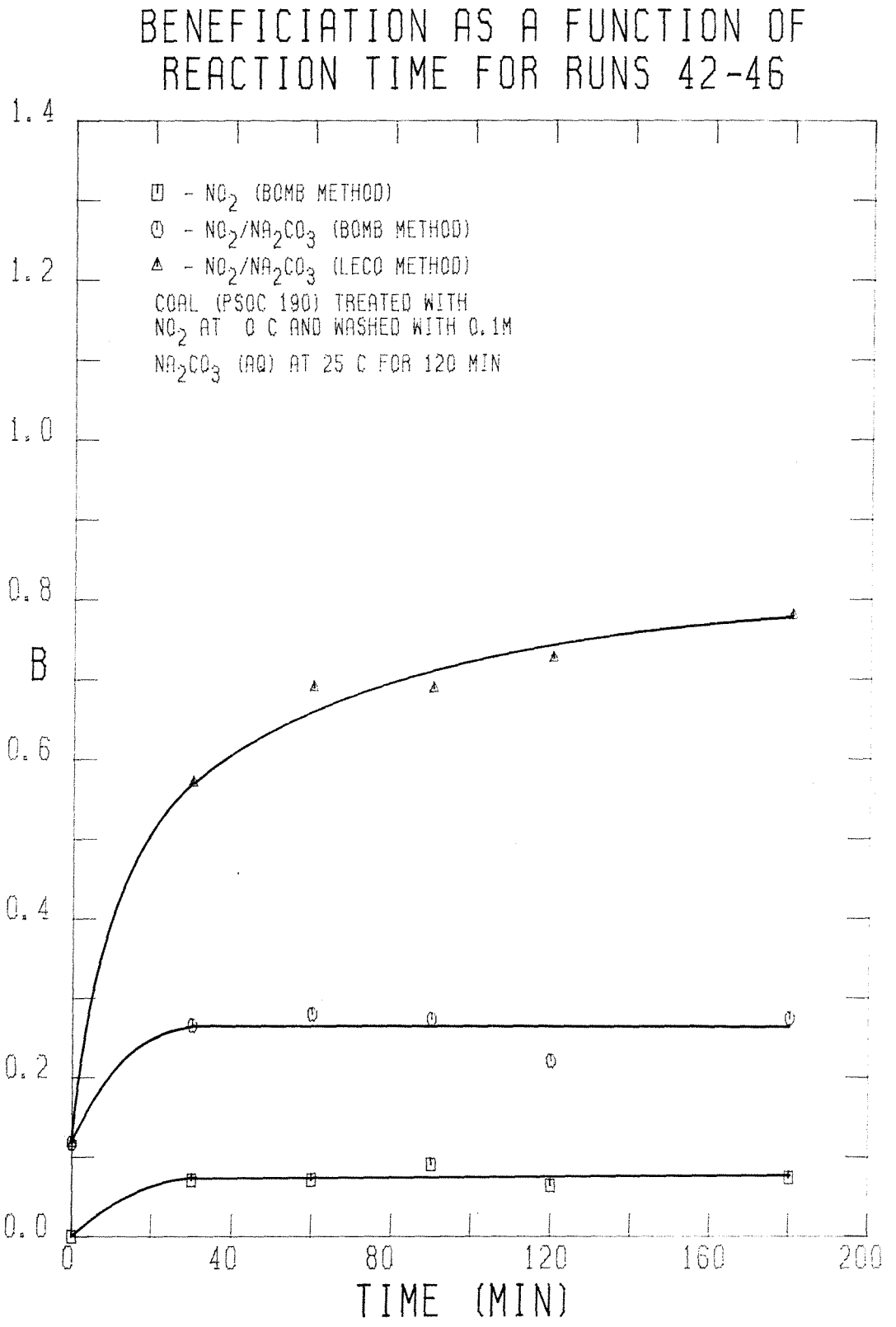
BENEFICIATION AS A FUNCTION OF
REACTION TIME FOR RUNS 42-46
1.4
1.2
1.0
0.8
0.6
0.4
0.2
0.0
B
□ - NO2 (BOMB METHOD)
⏀ - NO2/NA2CO3 (BOMB METHOD)
△ - NO2/NA2CO3 (LECO METHOD)
COAL (PSOC 190) TREATED WITH
NO2 AT 0 C AND WASHED WITH 0.1M
NA2CO3 (AQ) AT 25 C FOR 120 MIN
0
40
80
120
160
200
TIME (MIN)

FIGURE 4-144

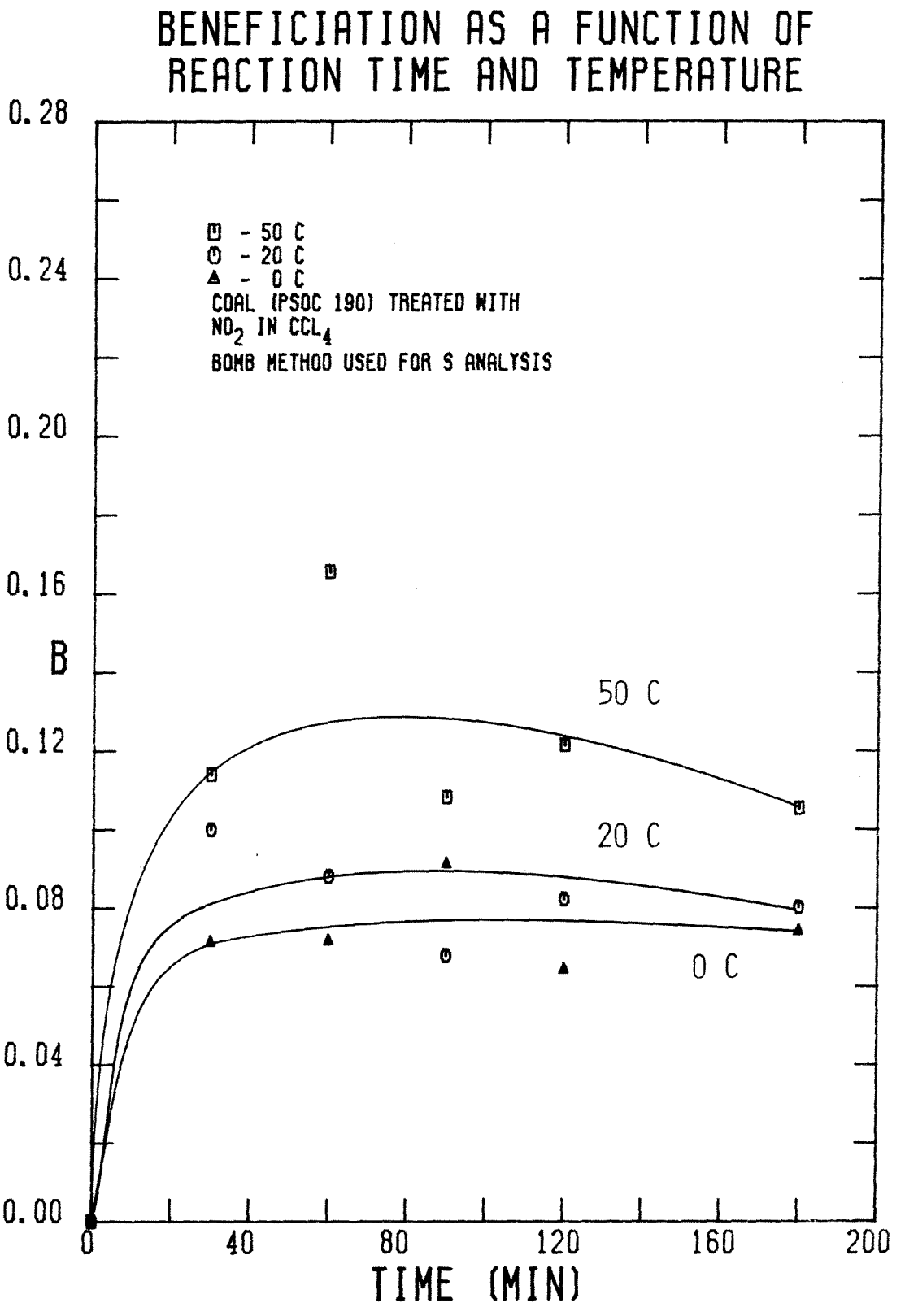
BENEFICIATION AS A FUNCTION OF
REACTION TIME AND TEMPERATURE
0.28
0.24
0.20
0.16
0.12
0.08
0.04
0.00
B
□ - 50 C
○ - 20 C
△ - 0 C
COAL (PSOC 190) TREATED WITH
NO2 IN CCL4
BOMB METHOD USED FOR S ANALYSIS
50 C
20 C
0 C
0
40
80
120
160
200
TIME (MIN)

FIGURE 4-145

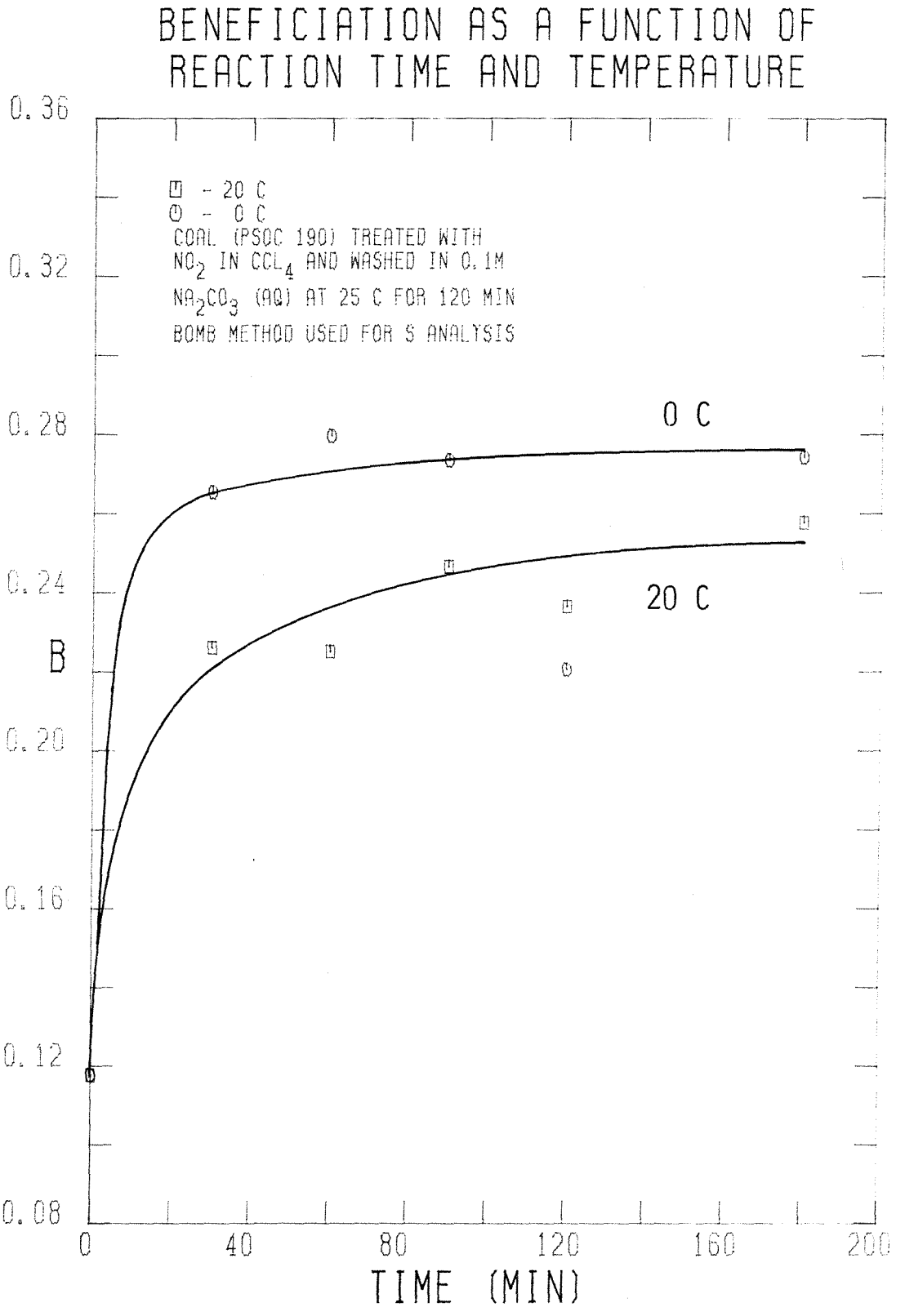
BENEFICIATION AS A FUNCTION OF
REACTION TIME AND TEMPERATURE
0.36
0.32
0.28
0.24
0.20
0.16
0.12
0.08
B
- 20 C
- 0 C
COAL (PSOC 190) TREATED WITH
NO2 IN CCL4 AND WASHED IN 0.1M
NA2CO3 (AQ) AT 25 C FOR 120 MIN
BOMB METHOD USED FOR S ANALYSIS
0 C
20 C
0
40
80
120
160
200
TIME (MIN)

FIGURE 4-146

with NO_2 at 20°C. This feature can be explained on the basis of the greater extent of oxidation, and hence, pore blocking of the coal which occurs at the higher temperature. Therefore, there is less resistance to the mass transfer of the oxidized material out of the particle for the coal treated with NO_2 at 0°C than 20°C. Consequently, there is more sulfur removal and beneficiation of the coal treated with NO_2 at the lower temperature.

When the beneficiation is based on the amount of SO_2 removed from the combustion gas, however, an increase in the temperature of the NO_2 treatment from 0 to 20°C results in a greater beneficiation, as illustrated by Figure 4–147. Because the rate of the NO_2-coal reaction is greater at higher temperatures, more anionic oxygen is introduced into the coal. Hence, there is more sodium uptake and a greater extent of SO_2 trapping, which results in greater beneficiation. It is interesting to note that the two curves seem to converge as the NO_2-treatment time increases, which implies that, given enough time, treatment with NO_2 at 0°C will give as a high a degree of beneficiation of the coal as treatment at 20°C. The temperature effect demonstrated by the curves in this figure are consistent with the effect implied by the other elemental analyses, all of which indicate a slower NO_2-coal reaction at 0°C than at 20°C.

The effect of the initial NO_2 concentration, $(NO_2)_0$, on the beneficiation of the processed coal (Runs 38–41) is illustrated in Figure 4–148. The beneficiation due to the NO_2 treatment does not depend on $(NO_2)_0$, as demonstrated by the lower curve in the plot. Apparently, exposure of the coal to a very small amount of NO_2 is all that is required for the removal of all the sulfur that can be removed during the NO_2 treatment. The middle curve, which corresponds to the beneficiation of the treated coal after washing in 0.1 M Na_2CO_3 (aq), demonstrates the same behavior as the lower curve. Thus, only small amounts of NO_2 are needed for the oxidation and removal of all the sulfur which can be removed

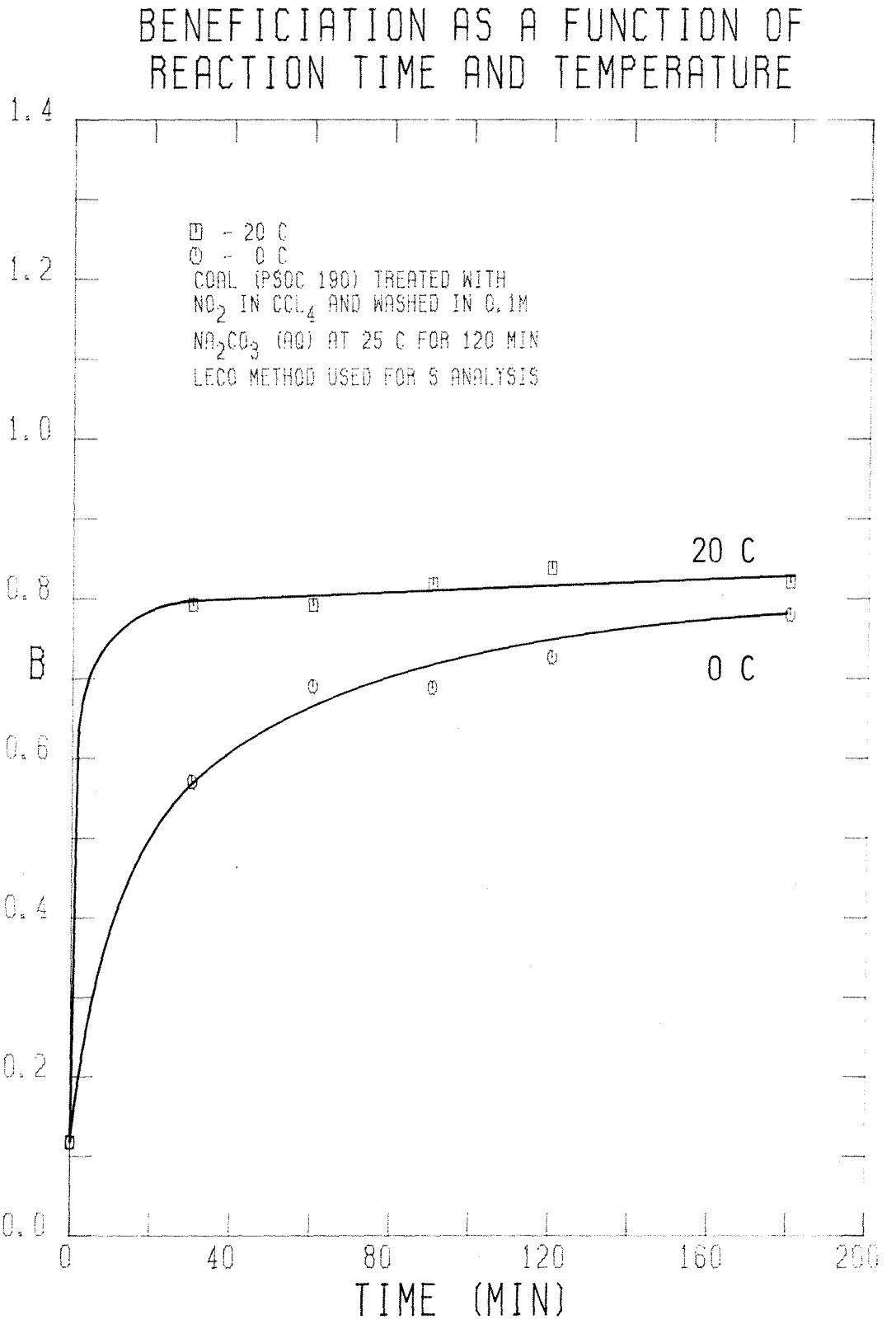
BENEFICIATION AS A FUNCTION OF
REACTION TIME AND TEMPERATURE
□ - 20 C
○ - 0 C
COAL (PSOC 190) TREATED WITH
NO_2 IN CCL_4 AND WASHED IN 0.1M
NA_2CO_3 (AQ) AT 25 C FOR 120 MIN
LECO METHOD USED FOR S ANALYSIS
20 C
0 C
B
1.4
1.2
1.0
0.8
0.6
0.4
0.2
0.0
0
40
80
120
160
200
TIME (MIN)

FIGURE 4-147

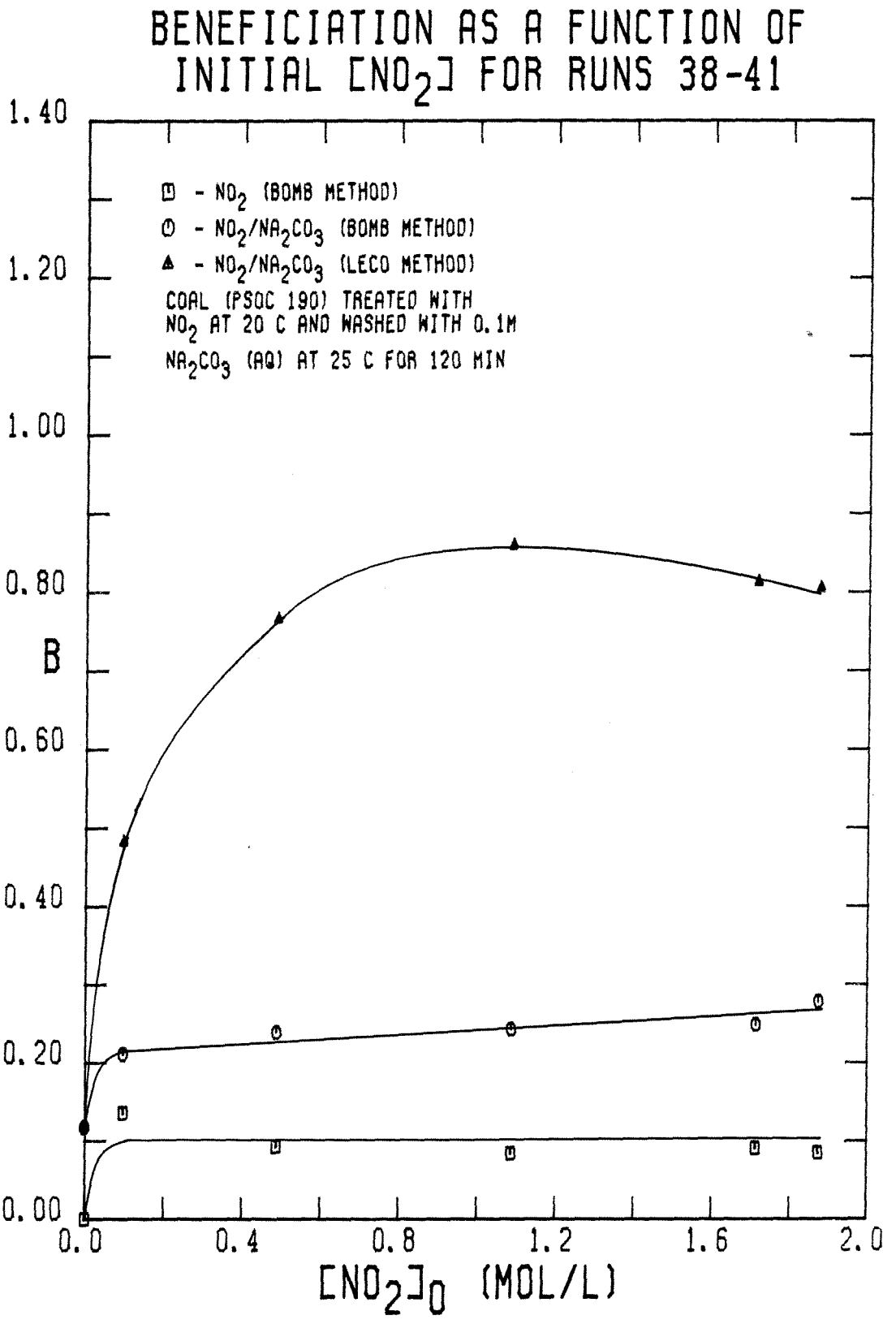
BENEFICIATION AS A FUNCTION OF INITIAL [NO2] FOR RUNS 38-41
1.40
1.20
1.00
0.80
0.60
0.40
0.20
0.00
B
0.0
0.4
0.8
1.2
1.6
2.0
[NO2]0 (MOL/L)
□ - NO2 (BOMB METHOD)
○ - NO2/NA2CO3 (BOMB METHOD)
△ - NO2/NA2CO3 (LECO METHOD)
COAL (PSOC 190) TREATED WITH NO2 AT 20 C AND WASHED WITH 0.1M NA2CO3 (AQ) AT 25 C FOR 120 MIN

FIGURE 4-148

from the coal. The initial NO_2 concentration, however, does affect the beneficiation of the coal from the standpoint of the reduction of SO_2 in the combustion gas, as illustrated by the top curve. In particular, the curve shows a maximum in B of 0.86 when the coal is treated for 120 minutes with an initial NO_2 concentration of 1.1 F. For higher values of $(NO_2)_0$, more oxidation of the coal occurs without any additional sulfur removal. Consequently, B decreases. Thus, more extensive oxidation is required for sufficient sodium uptake than is required for the maximum physical removal of sulfur from the processed coal.

The effect of the porosity of the coal particle on the beneficiation was determined by running a set of experiments in which PSOC 276 coal, which has a pore volume about four times smaller than the PSOC 190 coal, was treated with NO_2 at 20°C in the batch reactor and subsequently washed in 0.1 M Na_2CO_3 (aq) (Runs 47–52). The values of B from these runs are plotted in Figure 4–149 as a function of NO_2-exposure time. The lower curve in the figure shows the beneficiation of the PSOC 276 after the NO_2 treatment. The highest value of B of roughly 0.05 is obtained after the shortest exposure time, which implies that longer exposure times lead to less SO_2 removal from the coal during this stage of the processing. The middle curve, which corresponds to the beneficiation of the coal during the Na_2CO_3 (aq) wash, shows a rapid rise and then levels off at a value of about 0.16 after 180 minutes of NO_2 exposure. Thus, all of the sulfur which can possibly be removed from the NO_2 treated coal during the Na_2CO_3 (aq) wash is removed after 180 minutes of NO_2 treatment. Additional sulfur removal, and hence beneficiation, may be prevented by pore blocking, which inhibits the further extraction of otherwise soluble sulfur species by the Na_2CO_3 (aq) solution. The top curve, however, shows that additional NO_2 exposure beyond 180 minutes would lead to greater beneficiation of the coal from the standpoint of SO_2 emissions. Furthermore, it should be noted that 66 % of the sulfur in the coal is

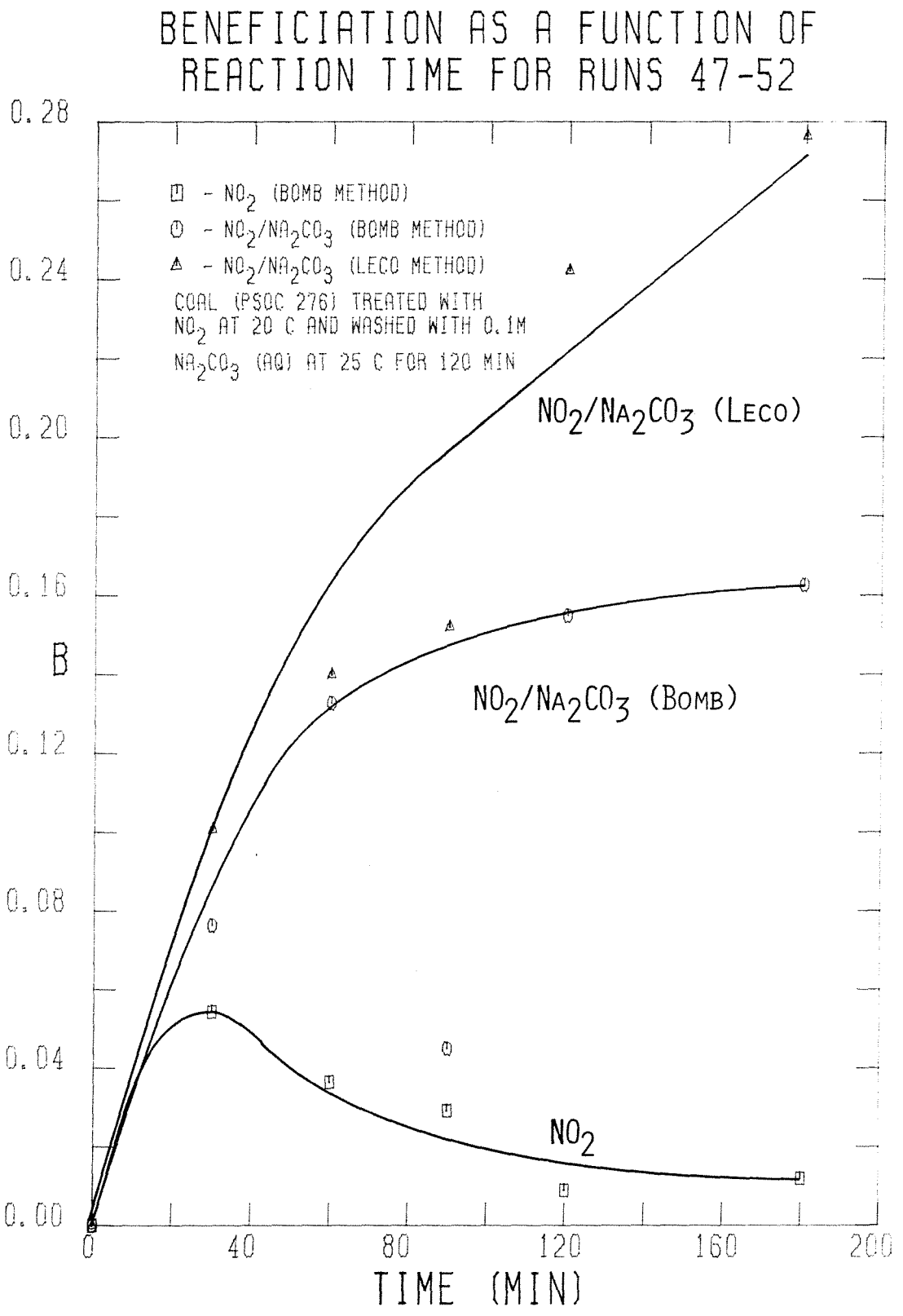
BENEFICIATION AS A FUNCTION OF
REACTION TIME FOR RUNS 47-52
0.28
0.24
0.20
0.16
0.12
0.08
0.04
0.00
B
0
40
80
120
160
200
TIME (MIN)
□ - NO2 (BOMB METHOD)
○ - NO2/NA2CO3 (BOMB METHOD)
△ - NO2/NA2CO3 (LECO METHOD)
COAL (PSOC 276) TREATED WITH
NO2 AT 20 C AND WASHED WITH 0.1M
NA2CO3 (AQ) AT 25 C FOR 120 MIN
NO2/NA2CO3 (LECO)
NO2/NA2CO3 (BOMB)
NO2

FIGURE 4-149

pyritic, of which only about 10 % is removed from the coal by the processing. Consequently, about 65 % of the SO_2 derived from the organic sulfur during combustion is trapped by the sodium, which is adsorbed during the Na_2CO_3 (aq) wash after the coal has been treated for 180 minutes with NO_2. The data also indicate that further NO_2 exposure would result in more sodium uptake and beneficiation in terms of organic sulfur removal as well. Therefore, the pore structure of the PSOC 276 dictates that NO_2-exposure times greater than 180 minutes are needed at 20°C for the maximum beneficiation of the coal.

A comparison of the beneficiation of the PSOC 190 and PSOC 276 coals by the NO_2 treatment is provided in Figure 4–150. The curves for both coals demonstrate the same behavior, namely that the maximum beneficiation occurs after only 30 minutes of NO_2 treatment. This behavior is consistent with the notion that most of the sulfur removed in this stage of the process is removed as SO_2 during the vacuum drying. It may be that as more oxidation of the coal occurs at longer NO_2-exposure times, more trapping of SO_2, which would otherwise evolve during the post-reaction vacuum drying, occurs. Although the smaller pore volume of the PSOC 276 accounts for the smaller amount of beneficiation, the problem of pore blocking occurs in both coals. Indeed, the problem is more severe in the PSOC 276, which is a consequence of its smaller initial pore volume. That is, the interior of the PSOC 276 coal particles is easier to isolate than that of the PSOC 190 coal particles because less oxidation is needed for pore blocking.

The values of B for the two NO_2-treated coals after being washed in 0.1 M Na_2CO_3 (aq), based on the Bomb method of sulfur analysis, are plotted in Figure 4–151 as a function of NO_2-exposure time. It is immediately obvious that virtually all of the beneficiation which occurs for the PSOC 190 coal is due to the first 30 minutes of the NO_2 treatment. On the other hand, the value of B for the

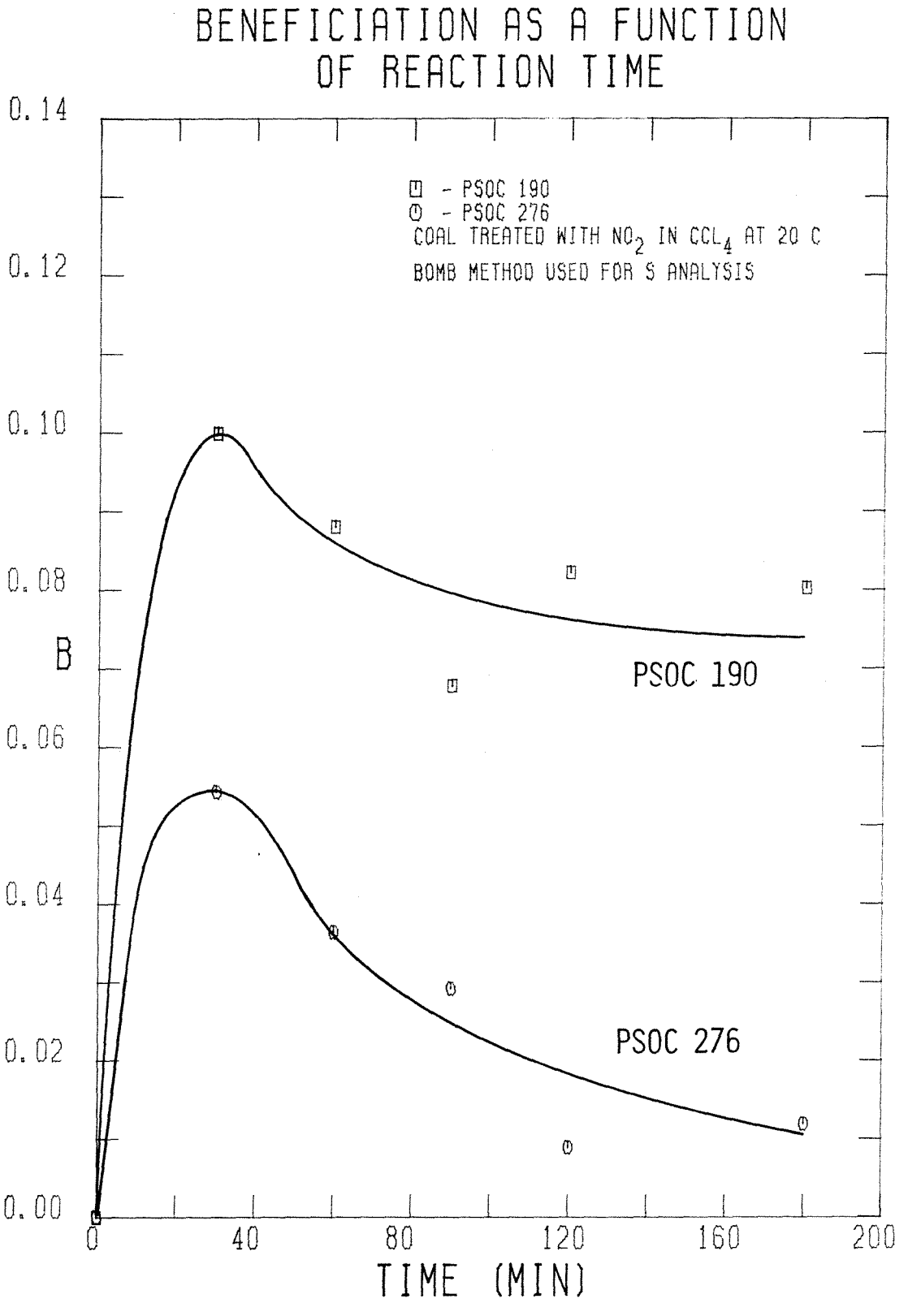
BENEFICIATION AS A FUNCTION
OF REACTION TIME
0.14
0.12
0.10
0.08
0.06
0.04
0.02
0.00
B
- PSOC 190
- PSOC 276
COAL TREATED WITH NO_2 IN CCL_4 AT 20 C
BOMB METHOD USED FOR S ANALYSIS
PSOC 190
PSOC 276
0
40
80
120
160
200
TIME (MIN)

FIGURE 4-150

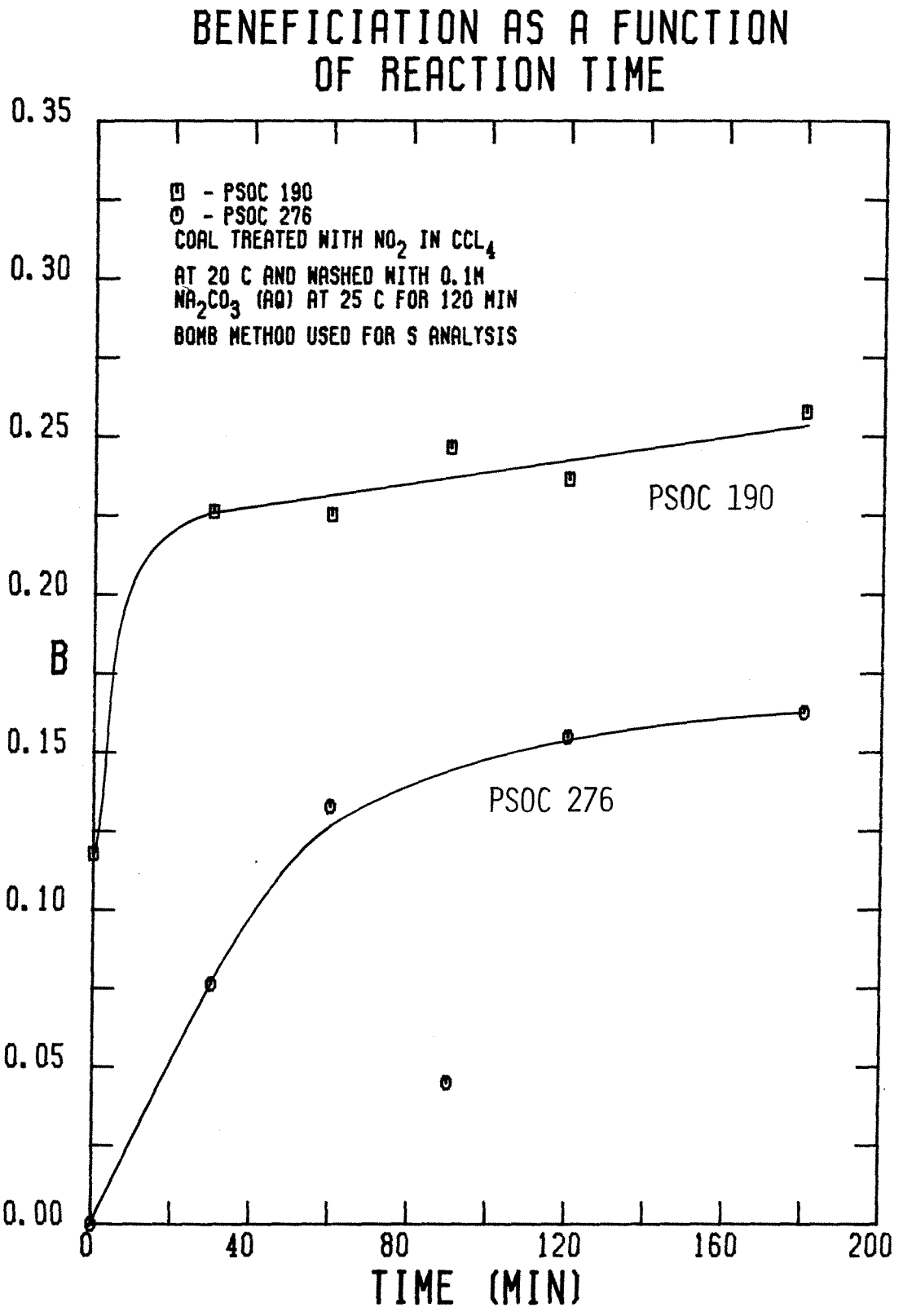
BENEFICIATION AS A FUNCTION
OF REACTION TIME
0.35
0.30
0.25
0.20
0.15
0.10
0.05
0.00
B
- PSOC 190
- PSOC 276
COAL TREATED WITH NO_2 IN CCL_4
AT 20 C AND WASHED WITH 0.1M
NA_2CO_3 (AQ) AT 25 C FOR 120 MIN
BOMB METHOD USED FOR S ANALYSIS
PSOC 190
PSOC 276
0
40
80
120
160
200
TIME (MIN)

FIGURE 4-151

PSOC 276 coal rises at a more gradual rate, which is the result of the slower rate of the reaction of NO_2 with the PSOC 276 than with the PSOC 190. As the discussion of the data in the previous sections indicates, this slower rate is caused by the smaller surface area in the PSOC 276 coal. It is interesting to note that the net beneficiation relative to just washing the untreated coal in 0.1 M Na_2CO_3 (aq) is actually greater for the PSOC 276 than the PSOC 190, which is due to the presence of more $FeSO_4$, which is easily leached from the NO_2-treated coal during the wash, in the PSOC 276 than in the PSOC 190.

In terms of the removal of SO_2 from the combustion gas, however, the beneficiation of the PSOC 190 is much greater than that of the PSOC 276, as illustrated in Figure 4–152. Whereas the value of *B* for the processed PSOC 190 is between 0.80 and 0.85 for all of the NO_2-treatment times used, that of the PSOC 276 only reaches 0.28 after 180 minutes of NO_2 exposure. It should be noted, however, that 66 % of the initial sulfur content of the PSOC 276 consists of pyrite, of which only a maximum of 10 % is removed by the processing. Consequently, up to 65 % of the organic sulfur is trapped in the ash of the treated PSOC 276 during combustion. Thus, if the PSOC 276 were treated with NO_2 when slurried in water for 180 minutes, so that all of the pyrite were removed, the actual sulfur removal would be about 88 %. If the loss in heating value due to the treatment remained at about 10 %, then the beneficiation of the treated PSOC 276 would be 0.79, which is quite comprable to that of the PSOC 190 coal, which has virtually no pyritic sulfur. Consequently, the pore structure of the coal does not have as strong an influence on the beneficiation as the figure might suggest. Rather, it is the difference in the relative amounts of pyritic and organic sulfur in the coals which causes most of the disparity in the extents of the beneficiation of the two coals. Nevertheless, the pore structure does affect the rate of the NO_2-coal reaction, which is slower in the PSOC 276 than in the

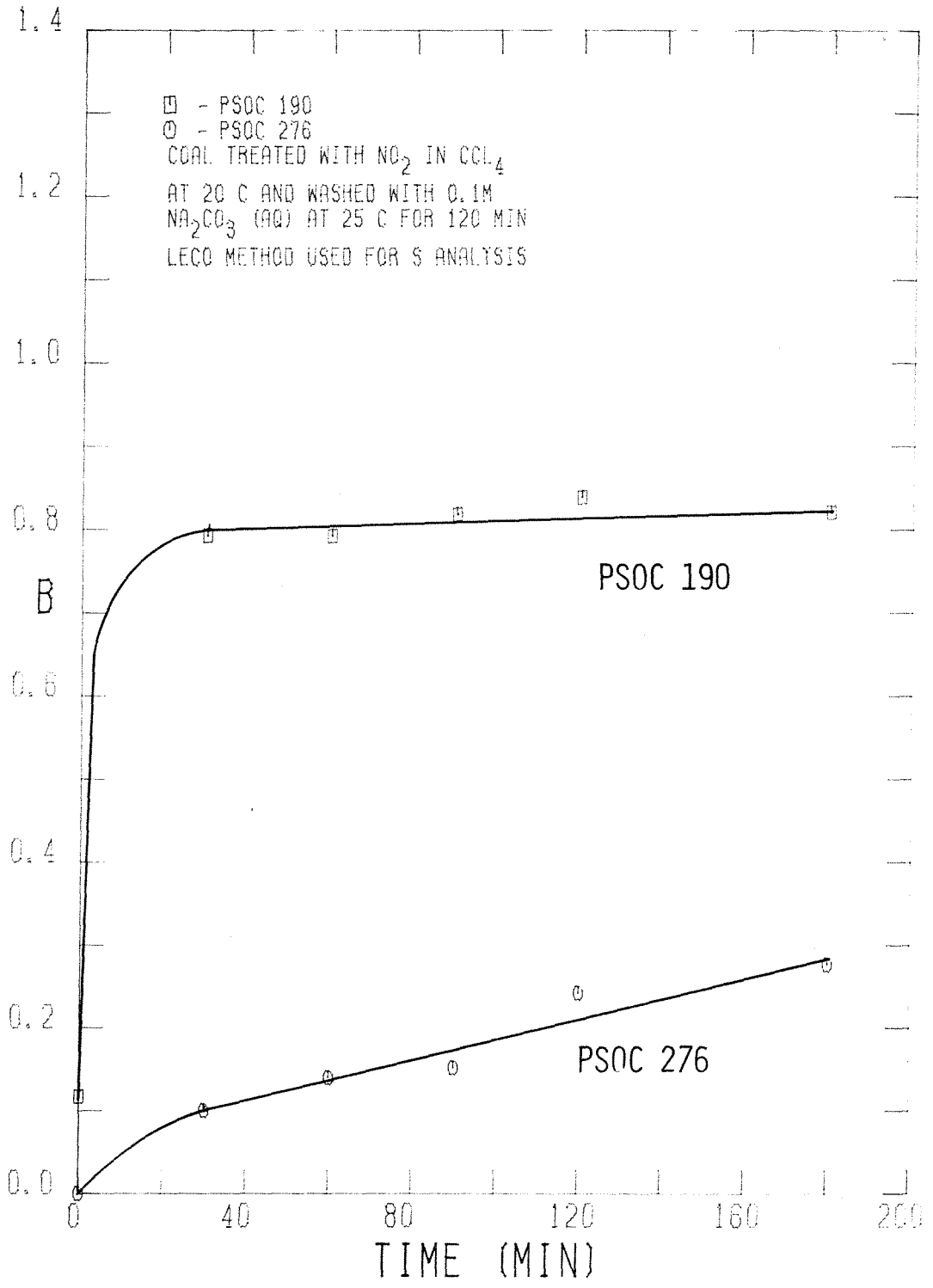
BENEFICIATION AS A FUNCTION
OF REACTION TIME
1.4
1.2
1.0
0.8
0.6
0.4
0.2
0.0
B
□ - PSOC 190
○ - PSOC 276
COAL TREATED WITH NO_2 IN CCL_4
AT 20 C AND WASHED WITH 0.1M
NA_2CO_3 (AQ) AT 25 C FOR 120 MIN
LECO METHOD USED FOR S ANALYSIS
PSOC 190
PSOC 276
0
40
80
120
160
200
TIME (MIN)

FIGURE 4-152

PSOC 190, as exemplified by the fact that virtually all of the beneficiation of the PSOC 190 occurs within the first 30 minutes of the NO_2 exposure, while the data for the PSOC 276 indicate that NO_2 exposures beyond 180 minutes would increase the beneficiation.

The major purpose of this section has been to identify the effects of the various reaction parameters on the selectivity of the NO_2 reaction and Na_2CO_3 (aq) wash for desulfurization of the coal relative to the oxidation of the rest of the coal, as expressed by the beneficiation coefficient, *B*. It should now be apparent that these effects are interdependent, which is primarily the consequence of the fact that the uptake of sodium by the NO_2-treated coal, which is responsible for trapping SO_2 during combustion, depends upon the amount of anionic sodium introduced into the coal, which is proportional to the extent of oxidation of the coal. Nevertheless, a point is reached in the oxidation which corresponds to the minimum amount of sodium required for the maximum extent of SO_2 trapping. At this point, the maximum beneficiation is achieved. Further oxidation only continues to deplete the heat content of the coal, which results in a decline in the beneficiation.

The point at which the maximum beneficiation occurs in terms of the NO_2-exposure time depends on the pore structure of the coal. For example, the maximum beneficiation of the PSOC 190 coal occurs within the first 30 minutes of the NO_2 treatment, while the maximum beneficiation of the PSOC 276 coal cannot be achieved, even after 180 minutes of NO_2 exposure. The pore structure also determines the accessibility of the interior of the coal particle to sodium. Thus, a sufficient amount of anionic oxygen may be introduced into the coal, but it may not adsorb much Na^+ if the pores are of a sufficiently small diameter to preclude the transport of Na^+. Because the proximity of the sodium to the sources of SO_2 also affects the efficiency of SO_2 trapping, the effect of the

porosity on the beneficiation is compounded. Indeed, if the pore volume of the coal is sufficiently small, the maximum attainable beneficiation may be dictated solely by the porosity of the coal. Some semblance of this effect is demonstrated by the PSOC 276 coal relative to the PSOC 190 coal, although the small pore volume of the PSOC 276 coal is not sufficiently small to be the limiting factor in the beneficiation.

The maximum beneficiation attained depends on the type of sulfur in the coal and the solvent used for the NO_2 treatment. For instance, the maximum value of B for the PSOC 190 coal, in which virtually all of the sulfur is organic, is 0.85, while that for the PSOC 276 coal, in which 67 % of the sulfur is pyritic, is only 0.28. If water is used as the solvent for the NO_2 treatment, however, complete pyritic sulfur removal should be obtained for the PSOC 276 coal, which would then yield a value of B of about 0.8, provided the loss in the heating value of the coal did not change. On the other hand, the beneficiation of the PSOC 190 does not differ when either CCl_4 or H_2O is used, because the pretreated PSOC 190 contains no inorganic sulfur.

The effect of the temperature and the concentration of NO_2 during the NO_2 treatment seems to affect the beneficiation of all coals in the same general manner. Of course, the effect of the treatment conditions on B relative to the optimum value of B will depend on the coal as well. For instance, an increase in the temperature of the NO_2 treatment results in a higher rate of oxidation of the coal. For example, if the PSOC 190 is treated at 50°C with NO_2, the coal cannot be subsequently washed in 0.1 M Na_2CO_3 (aq) and filtered because the oxidation of the coal is so severe. On the other hand, if the PSOC 190 is treated at 20°C, a very high beneficiation is achieved. If the NO_2 treatment is conducted at 0°C, however, the beneficiation begins to decline because of insufficient sodium uptake. Thus, 20°C seems to be the best NO_2-treatment temperature for the

PSOC 190. A temperature greater than 20°C may be better for the treatment of the PSOC 276 coal with NO_2, however, because the NO_2-PSOC 276 coal reaction at 20°C is not complete even after 180 minutes. The effect of the NO_2 concentration is quite similar. For example, the optimum NO_2 concentration for the beneficiation of the PSOC 190 is 1.1 F for 120 minutes of NO_2 treatment. Higher concentrations result in excessive oxidation while lower concentrations result in the introduction of an insufficient amount of anionic oxygen for Na^+ uptake. On the other hand, higher NO_2 concentrations might yield greater beneficiation of the PSOC 276 coal. Hence, the optimal NO_2-treatment conditions which yield the greatest beneficiation are dictated by the physical structure and chemical composition of the coal.

4.3 Physical Changes in the Coal

4.3.1 Qualitative Changes in the Exterior Coal Surface

During the course of the NO_2 treatment and subsequent wash, various chemical changes occur in the coal, as were discussed in the previous section. Consequently, it seems reasonable to expect that these chemical changes result in alterations in the physical structure of the coal as well. One tool which can be used to gauge the extent of the physical change in the coal is the scanning electron microscope, hereinafter referred to with the acronym SEM. Due to the imaging process inherent in the SEM, coal particles can be examined at magnifications of up to 10,000 times while maintaining a sufficiently large depth of field to render a three dimensional quality to the image. Unfortunately, only the exterior surface of the particle can be examined. Nevertheless, alterations should occur on the exterior surface at least as readily as on the interior surfaces. Therefore, an examination of the exterior of the particle should provide a good qualitative indication of the changes induced throughout the particle by the processing. Coal samples from representative runs were examined with the SEM. Photographs of some of the particles examined form the basis for the rest of this section.

Photographs of the images obtained by the SEM of the raw PSOC 190 coal are shown in Figure 4–153. All four photographs show the same general features for the coal particles. In particular, all of the particles are covered with much smaller particles, which is a result of the grinding process. These smaller particles adhere to the larger particles and are not removed during the sieving. The dimensions of all of the large particles in the pictures range from roughly 40 to 150 μm. As photo d) shows, however, there is a multitude of smaller particles as well, which have dimensions ranging from roughly 20 to 50 μm.

Just washing the coal in water for 120 minutes at 25°C (Run 7) does not seem to clean the exterior coal surface to any discernible extent, as the photos in Figure 4–154 demonstrate. In each photo, all of the particles are still covered with a multitude of smaller particles. Thus, the removal of the water soluble material from the coal (≈ 4 % by mass of the raw coal) has not affected the coal appreciably. Washing the coal subsequently in 0.1 M Na_2CO_3 (aq) for 120 minutes at 25°C (Run 7C), however, results in the removal of a substantial amount of the smaller particles from the exterior of the large particles, as Figure 4–155 clearly shows. Because this wash removed an additional 10 % of the original coal mass without reducing the mass corrected heating value of the coal, the material removed must consist of soluble mineral matter. Therefore, the small particles on the surface of the larger coal particles consist of mineral matter, which has no heating value. The spectrum obtained with the energy-dispersive-analyxer of x–rays, hereinafter referred to by the acronym EDAX, in photo d) still shows the presence of Al, Si and sulfur, however. The sulfur peak is virtually masked by the largest peak in the spectrum, which is due to the M_α x–ray emission peak produced by the gold coating on the particle surface, referred to in the figure as Au(M). The tip of the peak due to S, however, is just discernible as a shoulder on the right side of the Au peak. Therefore, although a large amount of mineral matter has been removed by the Na_2CO_3 (aq) wash, a substantial amount still remains in the coal.

Run 18 was chosen as the most representative experiment which used water as the solvent for the NO_2 treatment. The run was conducted for 120 minutes at 25°C. The SEM photographs are shown in Figure 4–156. It can be seen that the NO_2/H_2O treatment does result in the removal of some of the smaller mineral matter particles from the external surface of the larger coal particles. Otherwise, the coal particles seem to be unaltered by the treatment.

SEM photographs of the NO_2-treated coal subsequently washed in 0.1 M Na_2CO_3 (aq) for 120 minutes at 25°C (Run 18C) are shown in Figure 4–157. As photo a) shows, the processing with NO_2 results in a rather large amount of surface cleaning, just as the processing without NO_2 does. Most of the coal particles have an additional feature, however, as demonstrated by photos b), c) and d). Not only are most of the small particles removed from the coal surface, but the surface also shows a large amount of etching. Whereas the untreated coal particles show rather smooth surfaces after the Na_2CO_3 (aq) wash, the coal particles treated with NO_2 have very rough surfaces after the Na_2CO_3 (aq) wash. Such etching can be attributed to the removal of the oxidized portions of the coal by the wash. In addition, some particles have very extensive fissures which are absent in the untreated coal particles. Such fissuring is indicative of the breakdown of the integral structure of the coal particle. While the fissuring is discernible, its occurrence is quite infrequent, which implies the coal particle seems to maintain most of its overall structure during processing.

When CCl_4 is the solvent used during the NO_2 treatment, no alterations in the external particle surface are apparent, as shown in Figure 4–158, which contains the SEM photographs of coal particles from Run 37, in which the coal was treated for 180 minutes at 20°C. These photos contain no indication that the particles are any different from untreated coal particles, primarily because no mineral matter is removed, which is expected because CCl_4 is the solvent. Even though the coal is oxidized by the NO_2 treatment, none of the resulting material is soluble in CCl_4, as the photos plainly demonstrate. Once the coal treated with NO_2 in CCl_4 is washed in 0.1 M Na_2CO_3 (aq), however, the etching, fissuring and mineral matter removal which resulted when the coal treated with NO_2 in H_2O was washed in Na_2CO_3 (aq) occurs in this case as well. The SEM photographs in Figure 4–159 clearly demonstrate this fact.

The other coal used in this study is the PSOC 276 coal. SEM photographs of the coal after washing in CCl_4 for 120 minutes at 20°C (Run 47) are shown in Figure 4–160. The particles are quite similar in appearance to those of the PSOC 190 coal, although there is not as much mineral matter dispersed on the external surface of the particle. The subsequent wash of the untreated coal in 0.1 M Na_2CO_3 (aq) at 25°C for 120 minutes (Run 47C) does not result in any discernible cleaning of the particle surfaces, in contrast to the Na_2CO_3 (aq) wash of the untreated PSOC 190 coal. The SEM photographs in Figure 4–161 support this claim.

In contrast to the PSOC 190 coal, however, treatment of the PSOC 276 coal with NO_2 in CCl_4 for 180 minutes (Run 52) and subsequent washing in 0.1 M Na_2CO_3 (aq) for 120 minutes at 25°C (Run 52C) does not result in any noticeable etching or fissuring of the coal particles, as demonstrated by the SEM photographs in Figure 4–162. The NO_2 treatment does not lead to any visible change in the external particle surface, which is also the case with the PSOC 190 coal. On the other hand, the Na_2CO_3 (aq) wash of the NO_2-treated PSOC 276 only leads to the removal of mineral matter from the external particle surface without any of the etching or fissuring which occurs in the washed PSOC 190 coal. This result is consistent with the smaller extent of reaction which occurred when the PSOC 276 coal was treated with NO_2 than when the PSOC 190 was similarly treated.

The examination of the coal particles with the SEM, therefore, has revealed some interesting qualitative effects of the NO_2-Na_2CO_3 treatment on the particle structure. Initially, the coal particles have a large amount of smaller particles consisting of mineral matter adhering to them. Oxidation of the coal with NO_2 allows these smaller particles to be removed from the coal particle surface by the Na_2CO_3 (aq) wash. Just washing the raw coal in Na_2CO_3 (aq) does not remove

all of these smaller particles. Therefore, oxidation prior to the wash is necessary for complete removal. Furthermore, the surface of the NO_2-treated PSOC 190 coal is etched by the Na_2CO_3 (aq) wash and a small amount of fissuring in the particles occurs as well. The etching results from the removal of oxidized portions of the coal from the particle surface. The fissuring is caused by the breakdown of the internal structure of the particle which is probably induced by the penetration of the Na_2CO_3 (aq) solution into the interior of the NO_2-treated coal particles. In the case of the PSOC 276 coal, however, where the extent of the NO_2-coal reaction is not as great as when the PSOC 190 coal is used, no such etching or fissuring occurs. Consequently, the degree of the alterations introduced into the surface of the particles depends on the extent of the reaction of NO_2 with the coal.

RAW PSOC 190 COAL (+200 - 325 MESH)

A) x700

B) x700

FIGURE 4-153

RAW PSOC 190 COAL (+200 - 325 MESH)

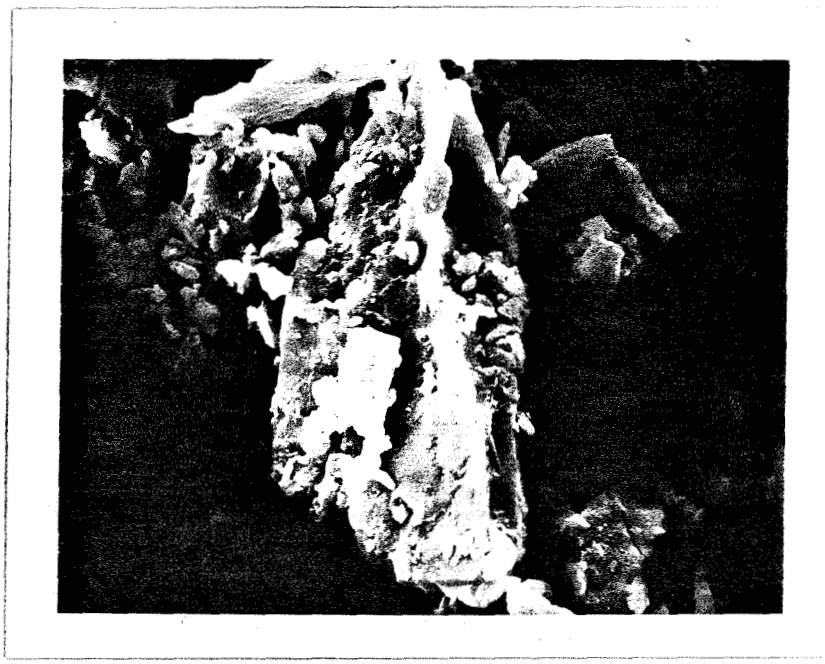

c) x700

D) x280

FIGURE 4-153

RUN 7 (N_2/H_2O - 120 MIN) PSOC 190 (+200 - 325 MESH)

A) x700

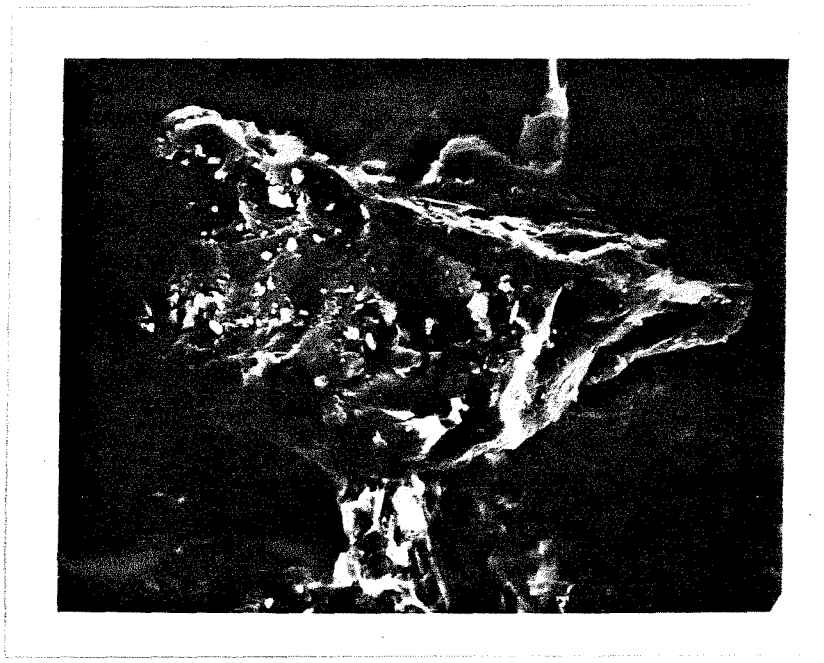

B) x700

FIGURE 4-154

RUN 7 (N_2/H_2O - 120 MIN) PSOC 190 (+200 - 325 MESH)

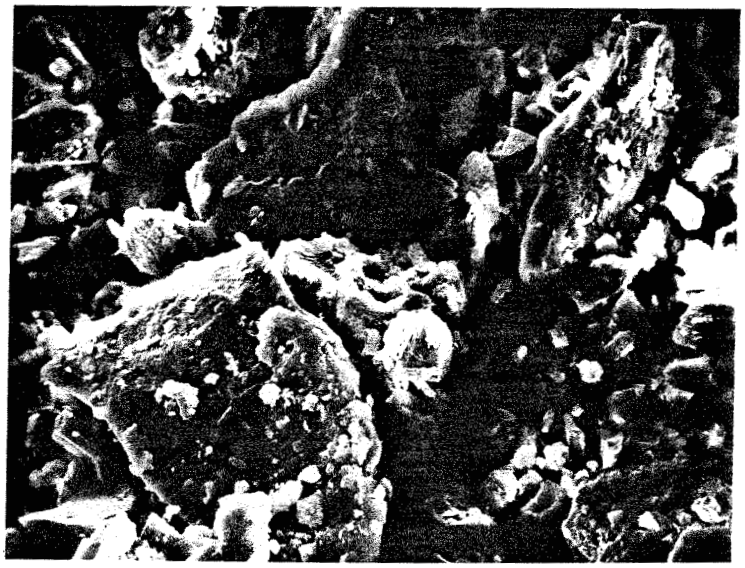

c) x490

D) x490

FIGURE 4-154

RUN 7C (N_2/H_2O - 120 MIN, Na_2CO_3(AQ) - 120 MIN)
PSOC 190 (+200 - 325 MESH)

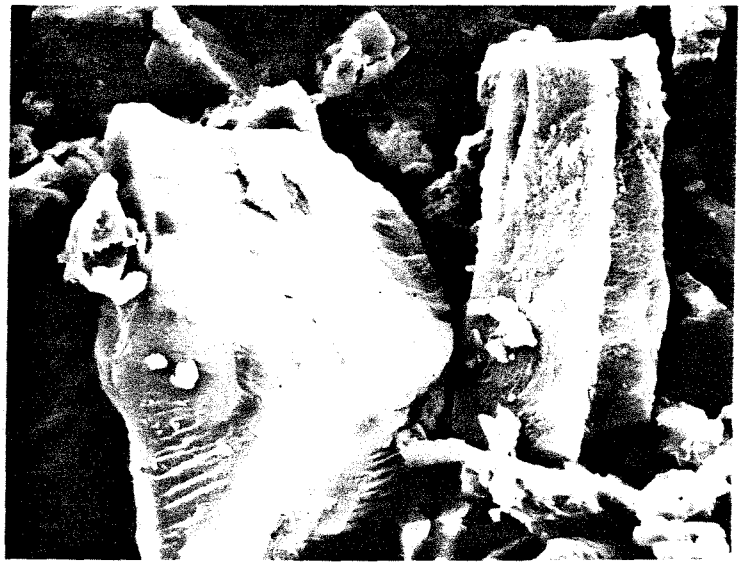

A) X700

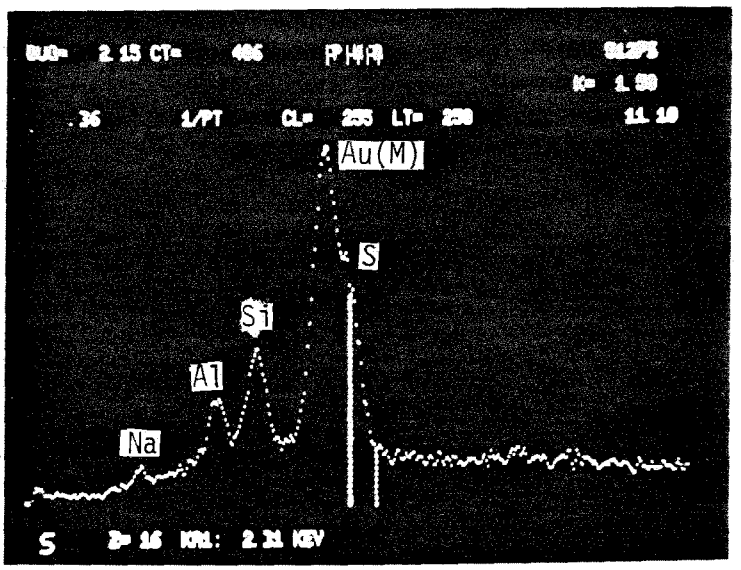

B) EDAX - PEAKS FOR NA, AL, SI, AU(M) AND S

FIGURE 4-155

RUN 7C (N_2/H_2O - 120 MIN, NA_2CO_3(AQ) - 120 MIN)
PSOC 190 (+200 - 325 MESH)

C) x700

D) x490

FIGURE 4-155

RUN 18 (NO_2/H_2O - 120 MIN) PSOC 190 (+200 - 325 MESH)

A) X490

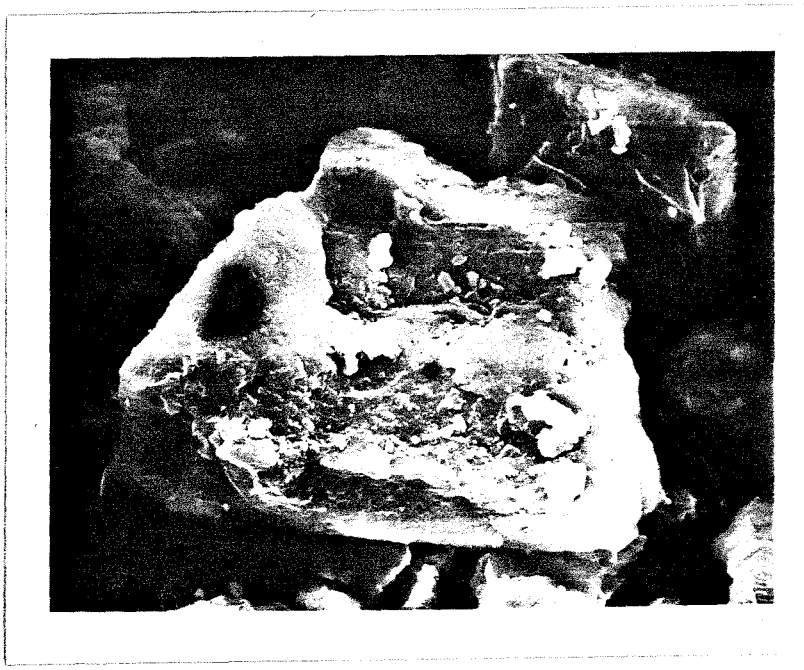

B) X700

FIGURE 4-156

RUN 18C (NO_2/H_2O - 120 MIN, Na_2CO_3(AQ) - 120 MIN)
PSOC 190 (+200 - 325 MESH)

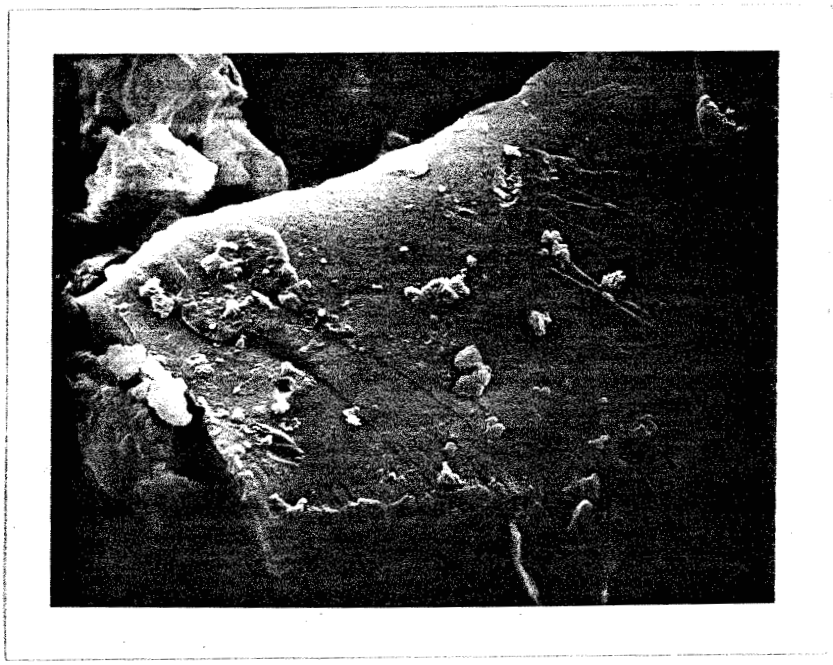

A) X960

B) X830

FIGURE 4-157

RUN 18C (NO_2/H_2O - 120 MIN, Na_2CO_3(AQ) - 120 MIN)
PSOC 190 (+200 - 325 MESH)

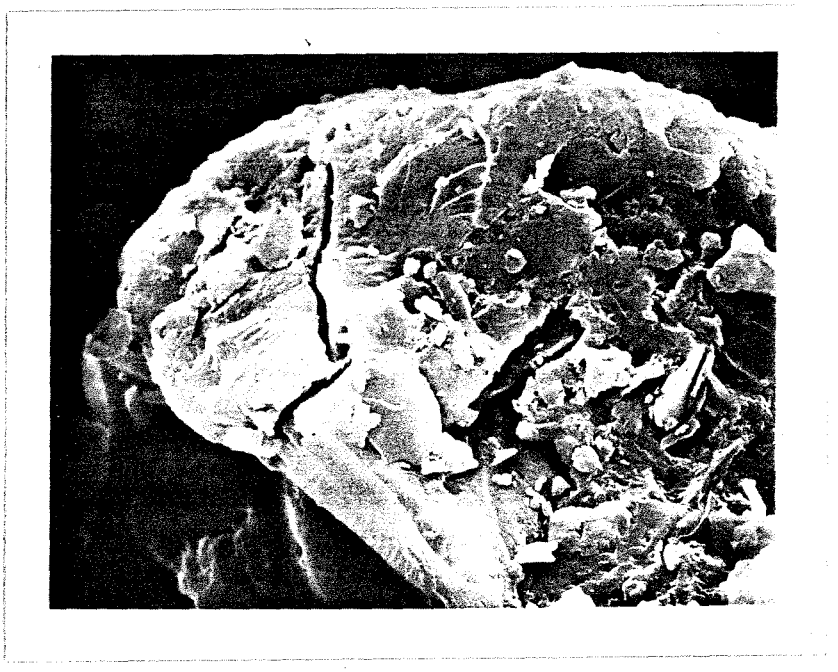

c) x1330

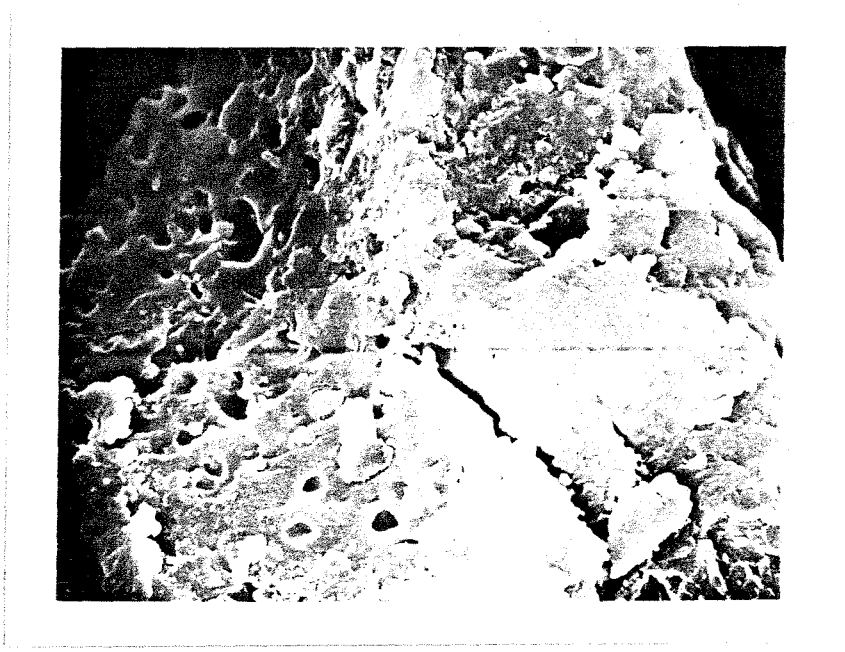

D) x2400

FIGURE 4-157

RUN 37 (NO_2/CCL_4 - 180 MIN) PSOC 190 (+200 - 325 MESH)

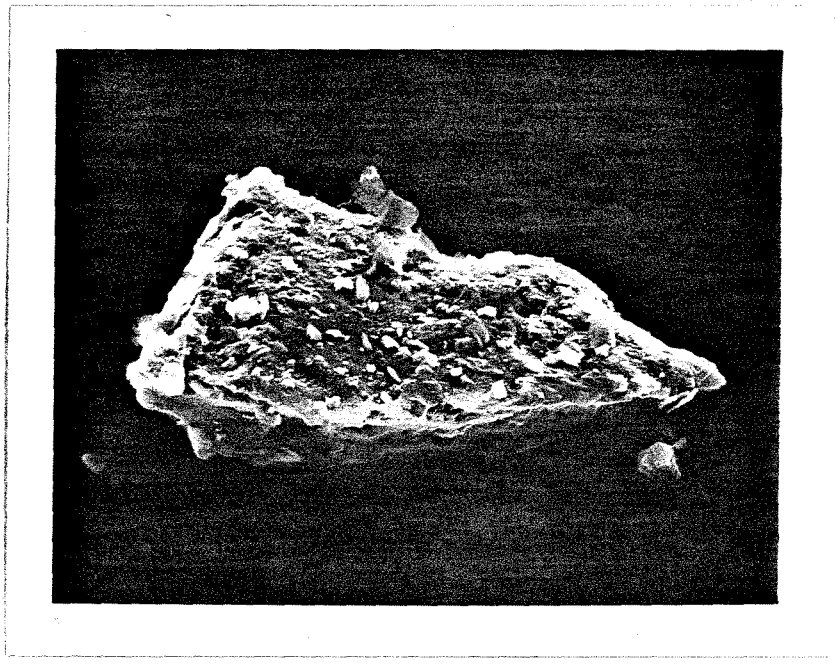

A) x750

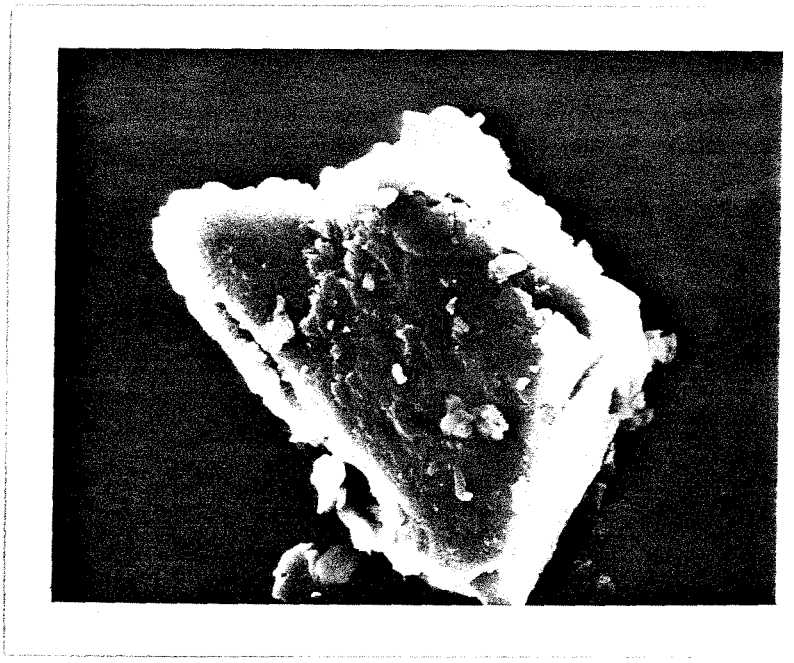

B) x1400

FIGURE 4-158

RUN 37C (NO_2/CCL_4 - 120 MIN, NA_2CO_3(AQ) - 120 MIN)
PSOC 190 (+200 - 325 MESH)

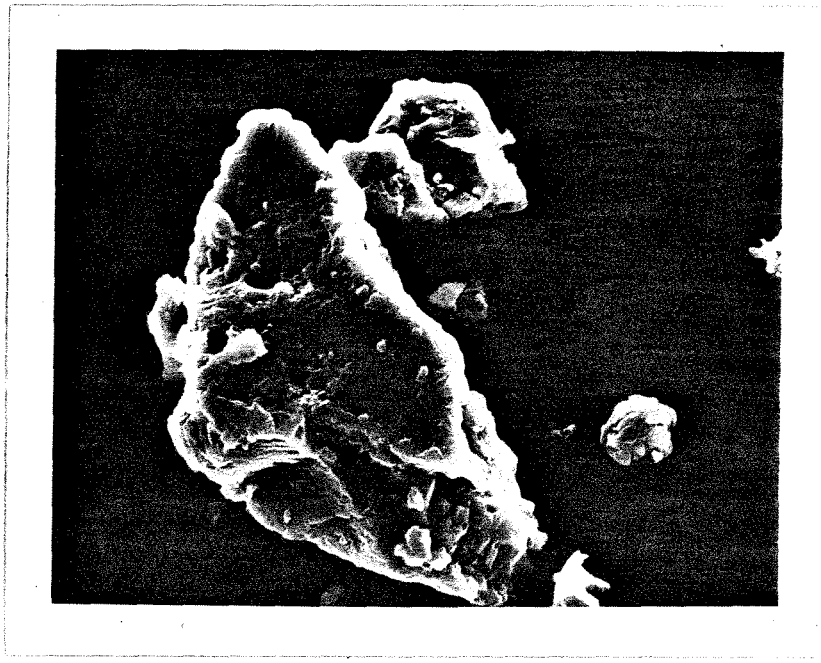

A) x950

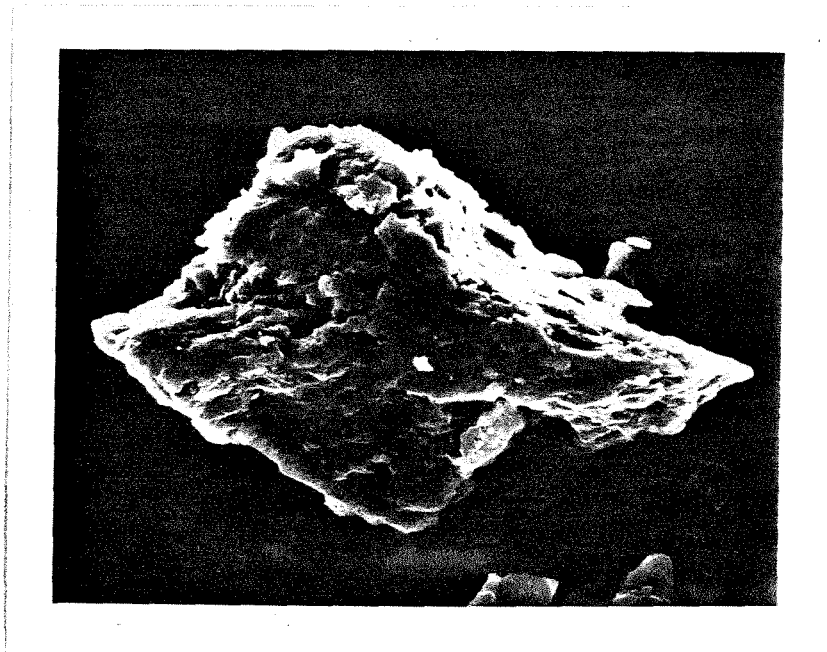

B) x750

FIGURE 4-159

RUN 47 (CCL_4 WASH - 120 MIN) PSOC 276 (+200 - 325 MESH)

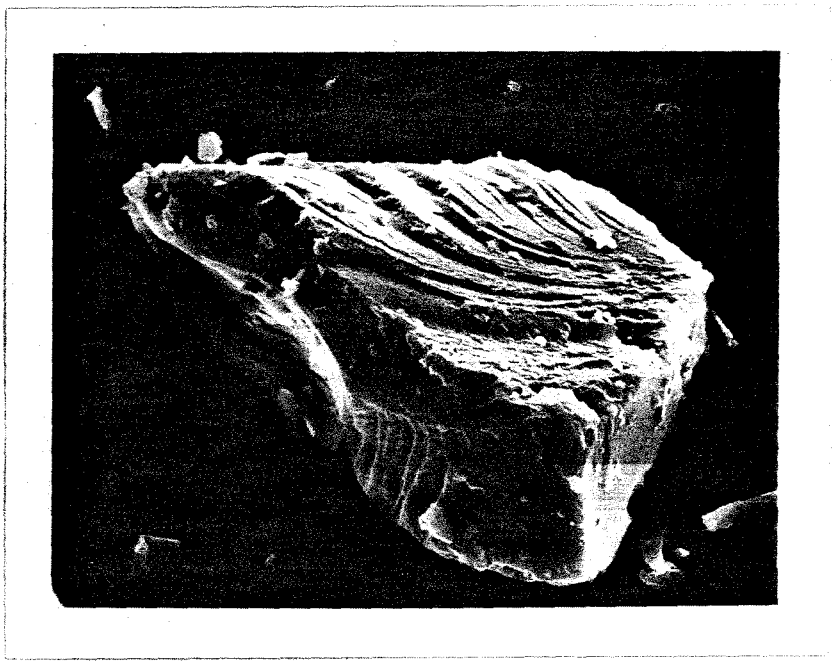

A) x950

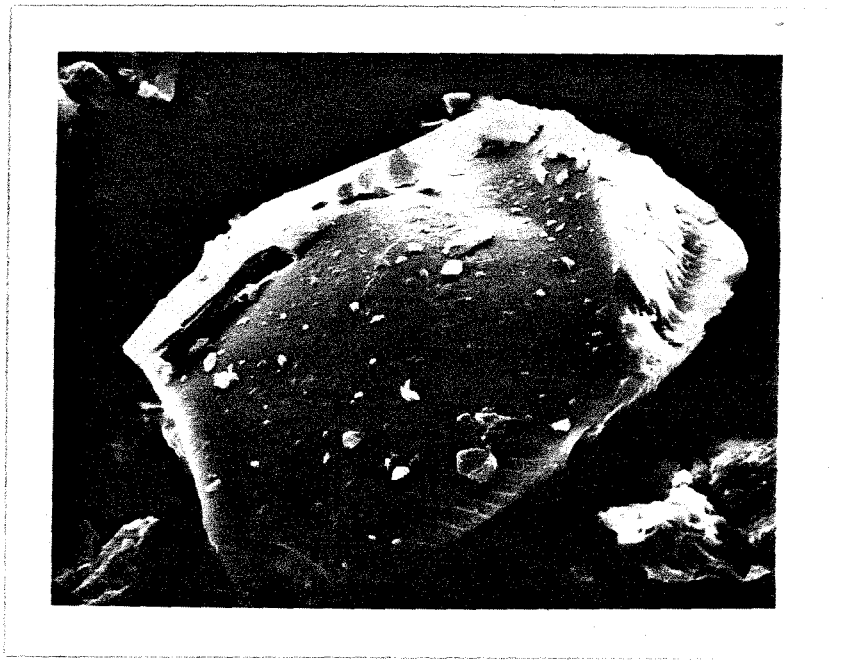

B) x950

FIGURE 4-160

RUN 47C (CCL_4 WASH - 120 MIN, NA_2CO_3(AQ) - 120 MIN)
PSOC 276 (+200 - 325 MESH)

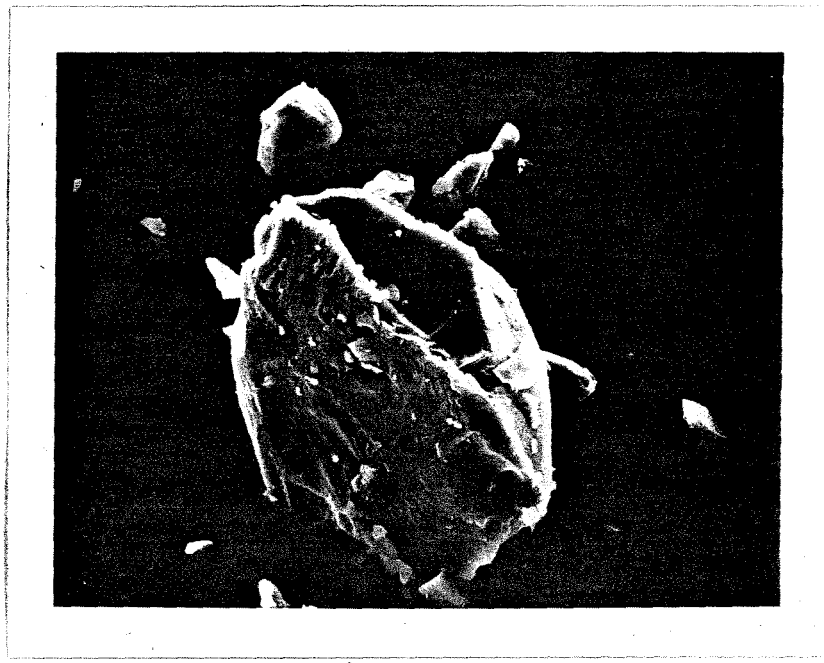

A) X470

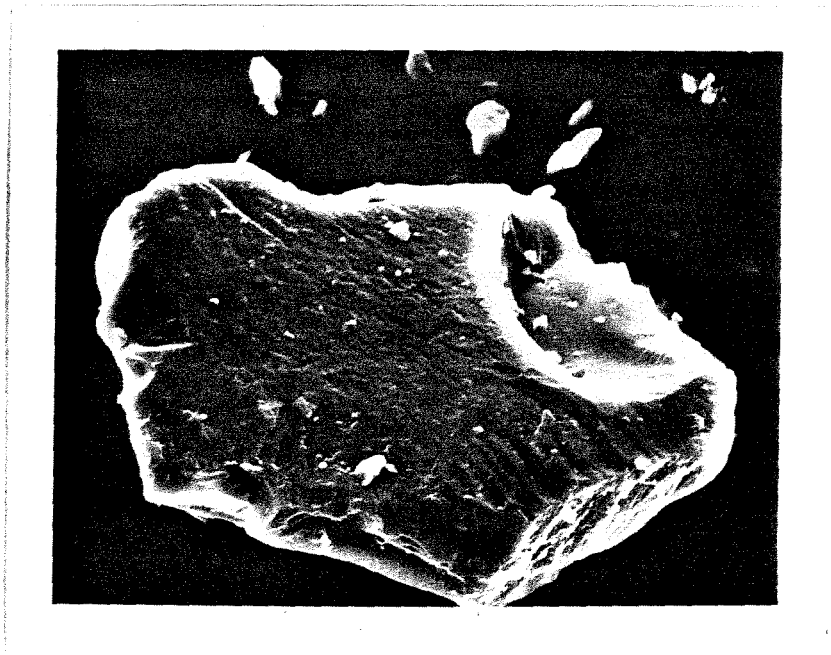

B) X750

FIGURE 4-161

RUN 52 PSOC 276 (+200 - 325 MESH)

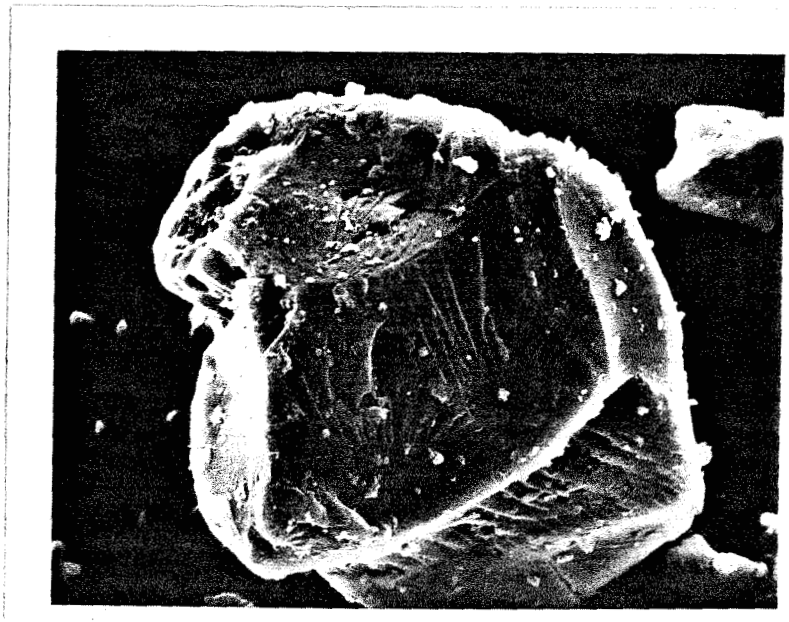

A) NO_2/CCL_4 - 180 MIN, X950

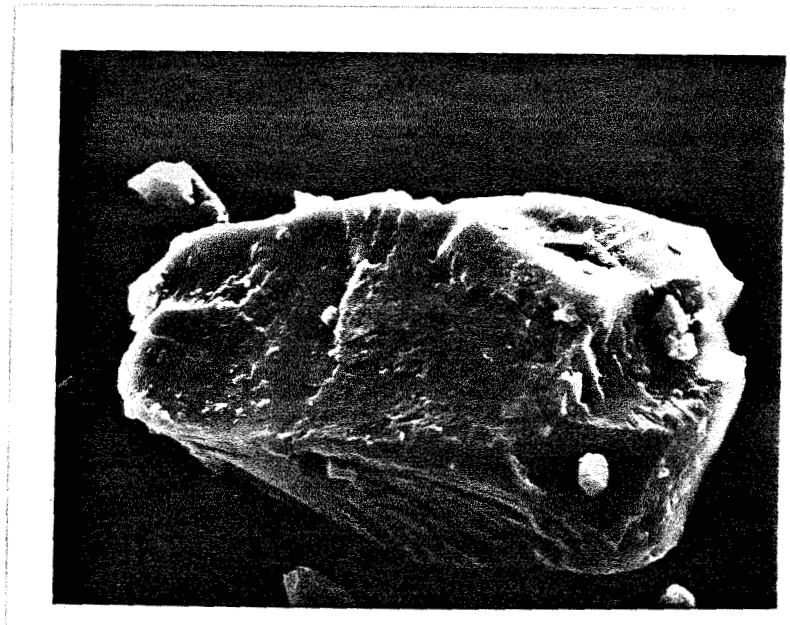

B) NO_2/CCL_4 - 180 MIN, NA_2CO_3(AQ) - 120 MIN, X950

FIGURE 4-162

4.3.2 Qualitative Changes in the Chemical and Physical Nature of the Ash

Throughout the previous discussion, reference has been made to the uptake of sodium by the NO_2-treated coal during the Na_2CO_3 (aq) wash and the trapping of SO_2 during combustion by the added sodium. This section will discuss the evidence for this claim, which is provided by the EDAX spectra of the ash particles remaining after the combustion of the processed coal. These spectra provide unequivocal evidence that the intimate addition of sodium to the coal results in the retention of sulfur in the ash.

A photograph obtained with the SEM of some of the ash obtained from the combustion of raw PSOC 190 coal along with the corresponding EDAX spectrum is shown in Figure 4–163. The photo clearly shows that the ash particles are quite small with dimensions on the order of about 10 μm. The EDAX spectrum reveals that the ash consists primarily of Al and Si, probably in the form of Al_2O_3 and SiO_2. In addition to Al and Si, the ash also consists of Fe and smaller amounts of K, Ca, and Ti. The ash of the coal treated with NO_2 in CCl_4 for 180 minutes (Run 37) has the same characteristics as that of the raw coal, as the SEM photograph and EDAX spectrum in Figure 4–164 clearly demonstrates. The ash still consists of rather small particles and contains Al, Si, K, Ca, Ti and Fe. In addition, the ash of the NO_2-treated coal has a minute amount of sulfur, probably in the form of $Fe_2(SO_4)_3$, which is formed by the oxidation of the small amount of pyrite in the coal.

Figure 4–165 contains an SEM photo and EDAX spectrum of the ash obtained from the combustion at 750°C of NO_2-treated coal after washing in 0.1 M Na_2CO_3 (aq) (Run 37C). The photo clearly shows that the ash now consists of relatively large, spherical, porous globules with diameters on the order of 1 to 2 mm. The globular nature of the ash is due to the fluxing of the ash during combustion, which does not occur when the untreated coal is burned. The EDAX

spectrum shows a large amount of Na and S in the ash, in addition to the other elements present in the ash of the untreated coal. The small group of peaks to the right of the S peak are due to the M_α x-rays of the silver paint used to mount the ash particles on the aluminum disc. The sodium in the ash is the result of the uptake of Na^+ by the oxidized coal during the Na_2CO_3 (aq) wash since the sodium compounds formed during combustion are not volatile at 750 °C. Because only the addition of sodium to the coal results in the retention of sulfur by the ash, it is reasonable to expect that the sulfur is retained as Na_2SO_4 in the ash, particularly in view of the fact that the combustion occurs under highly oxygen rich conditions. In any case, this EDAX spectrum provides the explanation for the disparity in the Bomb and Leco sulfur analyses of the coal. The oxidative treatment followed by the uptake of sodium in the coal allows the sulfur to be trapped in the ash during combustion rather than to escape as SO_2.

In order to determine if the ash structure containing Na_2SO_4 is stable under conditions employed in coal-fired boilers, the coal from Run 37C was also combusted at 1200 °C. The resulting ash was examined with the SEM. Photographs of representative ash particles are shown in Figure 4-166. Once again, the ash consists of relatively large, porous, globular particles, with dimensions on the order of 1 mm. The globular nature can be attributed to the fluxing of the mineral matter in the coal during combustion. Since globules are not formed during the combustion of the untreated coal, the added sodium must account for the ability of the ash to flux during the combustion of the processed coal. The porous nature of the ash globules is due to the escape of gases during the combustion of the treated coal. Figure 4-167 contains some typical EDAX spectra. The top spectrum indicates the presence of sodium, but very little sulfur. Rather, the point on the surface of the ash particle corresponding to this spec-

trum consists mainly of Al, Si and Fe. The bottom spectrum, however, is more typical. It indicates the presence of large amounts of Na and S, as well as Al, Si and Fe. Because virtually all of the sulfur in the coal from Run 37C is trapped in the ash, these spectra indicate that the ash particles are not a homogeneous mixture of Na, Al, Si, S and Fe. Rather, the ash particles consist of regions rich in Na_2SO_4 and poor in Al_2O_3 and SiO_2 and other regions poor in Na_2SO_4 and rich in Al_2O_3 and SiO_2. This heterogeneous mixture is expected because Na_2SO_4 melts at 884°C, but Al_2O_3 and SiO_2 melt at much higher temperatures, 2015°C and 1710°C, respectively. Therefore, not all of the ash components are expected to melt at the combustion temperature of 1200°C, leading to the formation of globules consisting of SiO_2, Al_2O_3 and some Fe_2O_3 crystals embedded in a glassy matrix of sodium salts, including Na_2SO_4.

In contrast to the PSOC 190 coal, treatment of the PSOC 276 coal with NO_2 followed by washing in Na_2CO_3 (aq) leads to much less sodium uptake by the coal. Consequently, there is less sulfur trapping by the ash during combustion. Figure 4–168 contains an SEM photo and EDAX spectrum of the ash remaining after combustion of the raw PSOC 276 coal. The photo shows that the ash consists of very small particles with dimensions on the order of several microns, just as in the case with the ash from the PSOC 190 coal. The spectrum indicates that the elemental compositions of the two ashes are quite similar as well. In particular, the ash consists primarily of Al_2O_3 and SiO_2, with smaller amounts of K_2O, CaO, TiO_2 and Fe_2O_3.

Exposure of the PSOC 276 coal to NO_2 in CCl_4 for 180 minutes at 20°C (Run 52) does not seem to alter the nature of the ash, as the SEM photograph and EDAX spectrum in Figure 4–169 demonstrate. The ash is still comprised of small, jagged particles of relatively small size. The EDAX spectrum indicates that the ash still consists primarily of Al_2O_3, SiO_2 and Fe_2O_3. The fact that the Fe

peak in this spectrum is larger than that in the spectrum of the ash from the raw PSOC 276 just serves as an indication of the heterogeneity of the chemical composition of the ash particles.

Washing the NO_2-treated PSOC 276 coal in Na_2CO_3 (aq) (Run 52C) does result in some sodium uptake, but only to about one third the extent of that of the NO_2-treated PSOC 190 coal. Figure 4–170 consists of an SEM photograph and EDAX spectrum of the ash obtained from the combustion of the coal from Run 52C at 750°C. In contrast to the ash from Run 37C, the ash particles from this run are much smaller and are still jagged, which is the result of less sodium uptake. Nevertheless, the EDAX spectrum shows that some sodium uptake and sulfur trapping has occurred. The fact that the Al and Si peaks are larger, however, indicates that the uptake of sodium is not as great in the treated PSOC 276 coal as in the treated PSOC 190 coal.

If the processed PSOC 276 is burned at 1200°C, however, the ash particles contain a sufficient amount of sodium to acquire the globular nature of the processed PSOC 190. Indeed, the SEM photographs in Figure 4–171 demonstrate that the ash now consists of very porous, roughly spherical particles with diameters on the order of about 0.5 mm. As the EDAX spectra in Figure 4–172 show, however, the amount of sodium in the ash is relatively small. Consequently, the amount of sulfur trapped in the ash during combustion is relatively small as well. The implications of these spectra are consistent with the results discussed previously, namely that not as much sulfur is trapped by the processed PSOC 276 coal as by the processed PSOC 190 coal during combustion. It is interesting to note that the size of the Fe peak in the spectra of the PSOC 276 ash is much greater than that of the PSOC 190 ash, which is due to the large amount of pyrite in the PSOC 276 coal (2.1 mass %) than in the PSOC 190 coal (0.1 mass %).

The SEM photographs and EDAX spectra of the ash obtained from the combustion of the processed coal discussed in this section provide unequivocal evidence that the treatment of the coal with NO_2 followed by a Na_2CO_3 (aq) wash results in the significant reduction of SO_2 emissions during combustion. In particular, the sodium taken up by the oxidized coal forms a well distributed precursor for the trapping of sulfur during combustion of the coal. During combustion, this precursor forms a flux which traps the SO_2 produced from the sulfur in the coal in the form of Na_2SO_4 in the ash. In the case of the processed PSOC 190 coal, 96 % of the SO_2 is removed from the combustion gases, while in the case of the PSOC 276 coal, only about 40 % of the SO_2 is eliminated from the combustion gases.

Finally, it should be noted that the stability of the sulfate-containing flux during combustion is not in doubt, particularly from a commercial standpoint. When the coal was burned at both 750 and 1200°C, the ash was left in the Leco furnace for six minutes with a steady stream of oxygen (0.5 l/min) passing over it. This amount of time is sufficient for any decomposition of the ash which may occur. Furthermore, in a coal-fired utility boiler, the residence time of the ash is only on the order of a few seconds. Consequently, if the Na_2SO_4-flux structure does not decompose in six minutes, it should be stable for a few seconds. Therefore, SO_2 which would otherwise escape in the flue gas is trapped as Na_2SO_4, which is removed from the boiler along with the rest of the ash.

ASH (1200 C) FROM RAW PSOC 190 (+200 - 325 MESH)

A) x480

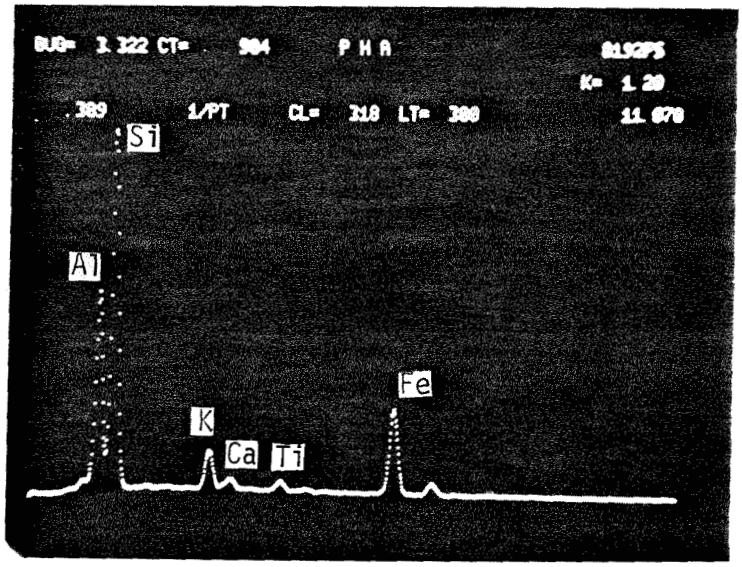

B) EDAX - PEAKS FOR AL, SI, K, CA, TI AND FE

FIGURE 4-163

ASH (750 C) FROM RUN 37 (NO_2/CCL_4 - 180 MIN)
PSOC 190 (+200 - 325 MESH)

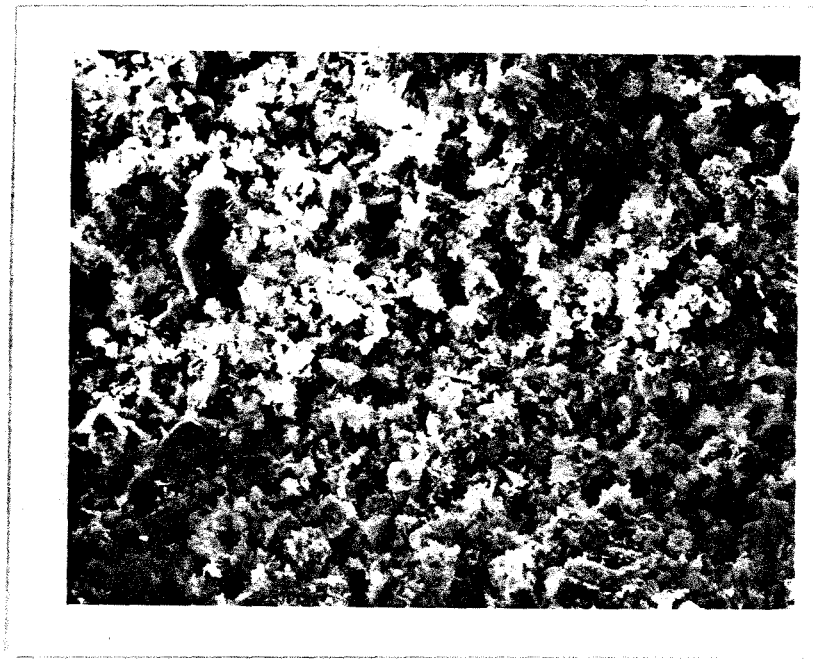

A) X 480

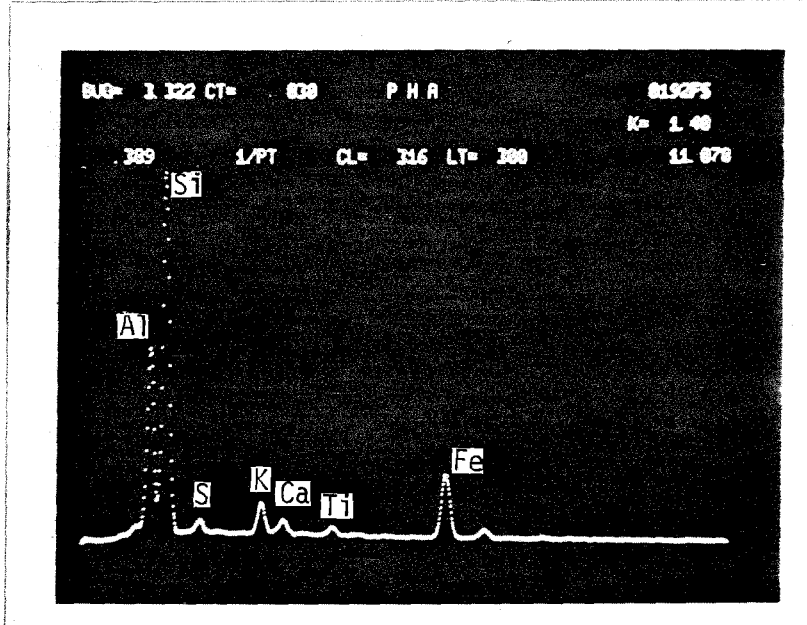

B) EDAX - PEAKS FOR AL, SI, S, K, CA, TI, AND FE

FIGURE 4-164

ASH (750 C) FROM RUN 37C (NO_2/CCL_4 - 180 MIN, Na_2CO_3(AQ) - 120 MIN) PSOC 190 (+200 - 325 MESH)

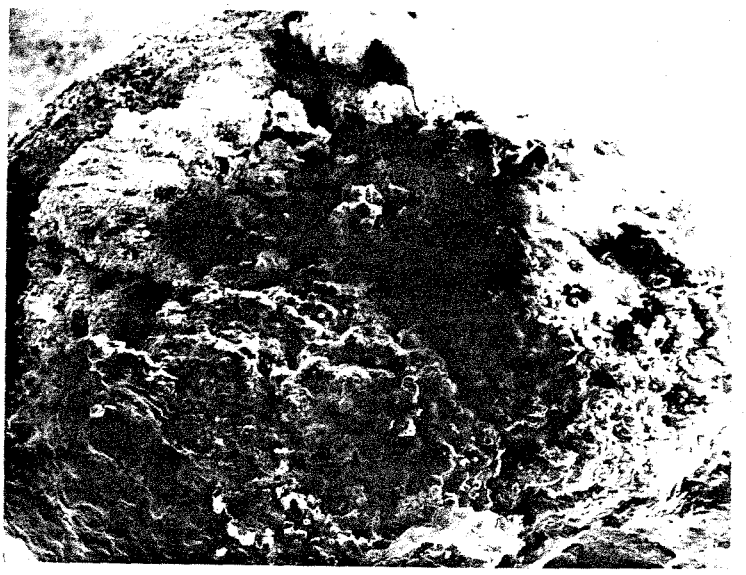

A) X 48

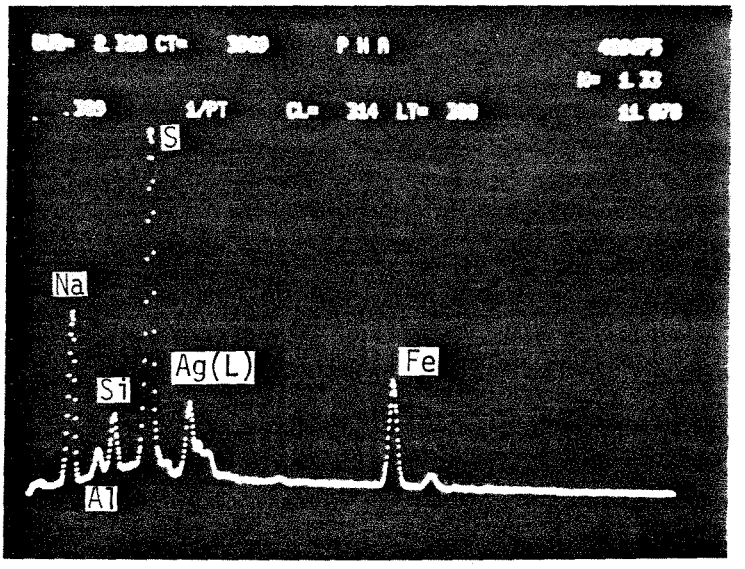

B) EDAX - PEAKS FOR NA, AL, SI, S, AG(L) AND FE

FIGURE 4-165

ASH (1200 C) FROM RUN 37C (NO_2/CCL_4 - 180 MIN, NA_2CO_3(AQ) - 120 MIN) PSOC 190 (+200 - 325 MESH)

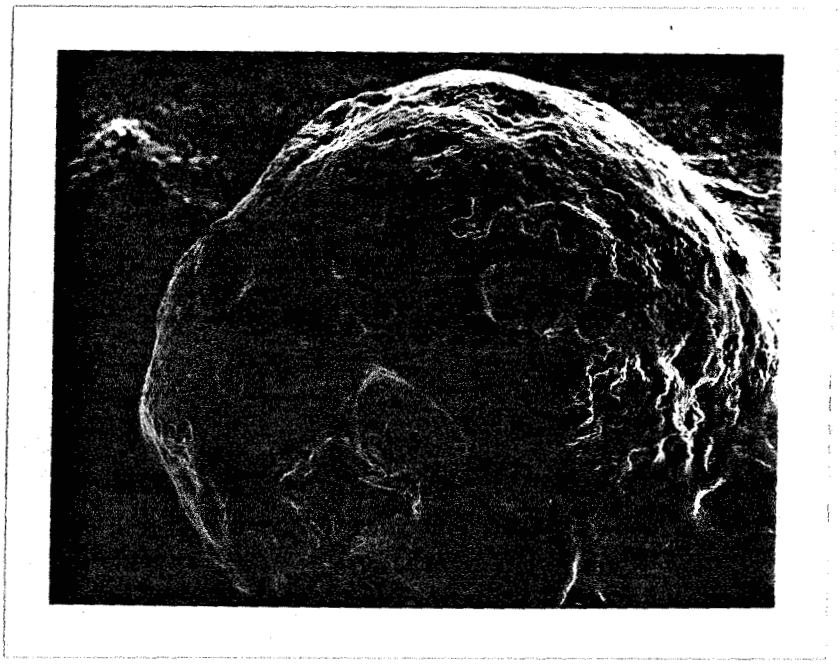

A) X 100

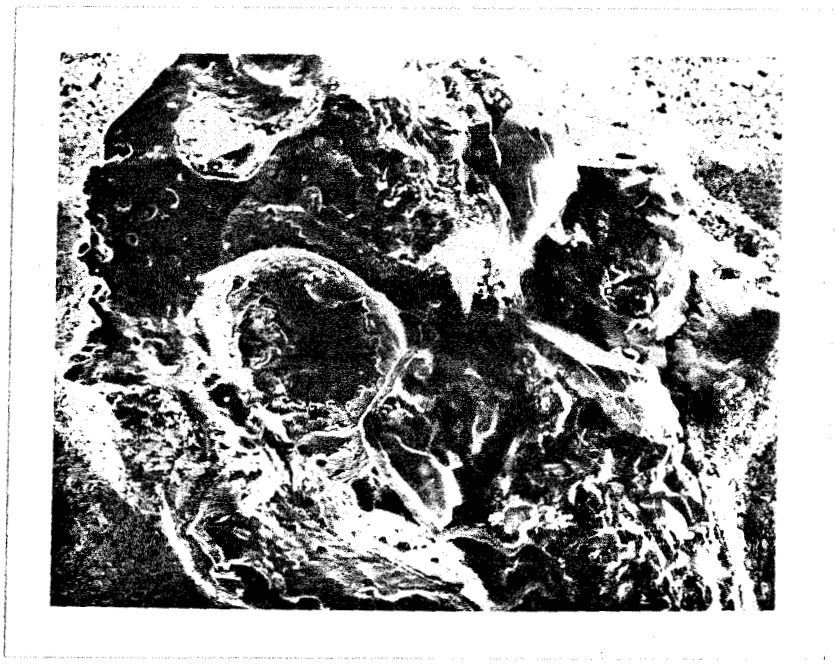

B) X 200

FIGURE 4-166

EDAX SPECTRA FOR ASH (1200 C) FROM RUN 37C (NO_2/CCL_4 - 180 MIN, NA_2CO_3(AQ) - 120 MIN) PSOC 190 (+200-325 MESH)

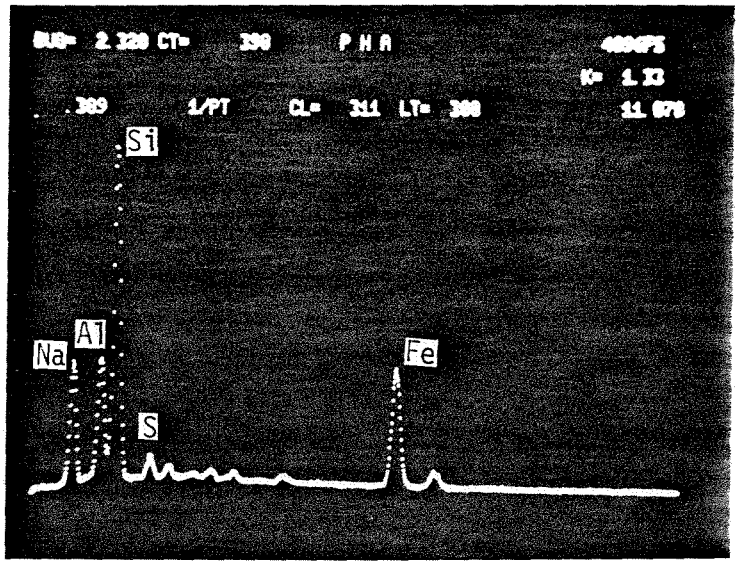

A) PEAKS FOR NA, AL, SI, S AND FE

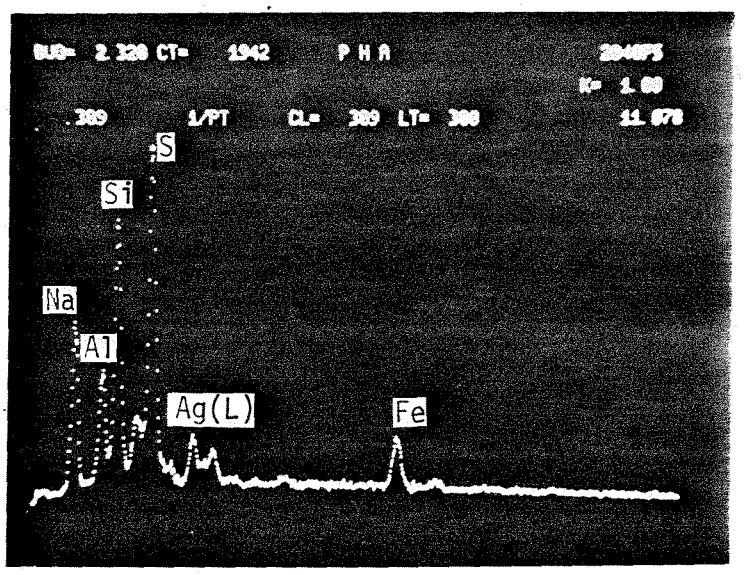

B) PEAKS FOR NA, AL, SI, S, AG(L) AND FE

FIGURE 4-167

ASH (1200 C) FROM RAW PSOC 276 (+200 - 325 MESH)

A) X 470

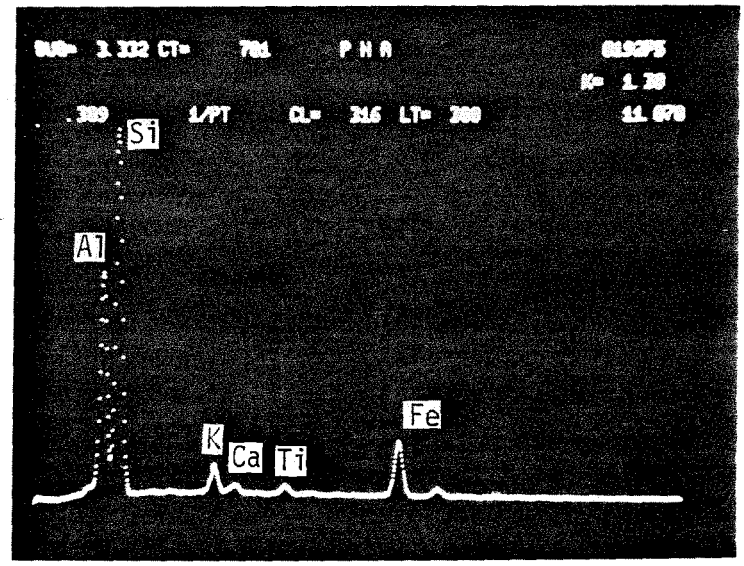

B) EDAX - PEAKS FOR AL, SI, K, CA, TI AND FE

FIGURE 4-168

ASH (750 C) FROM RUN 52 (NO_2/CCL_4 - 180 MIN)
PSOC 276 (+200 - 325 MESH)

A) X 900

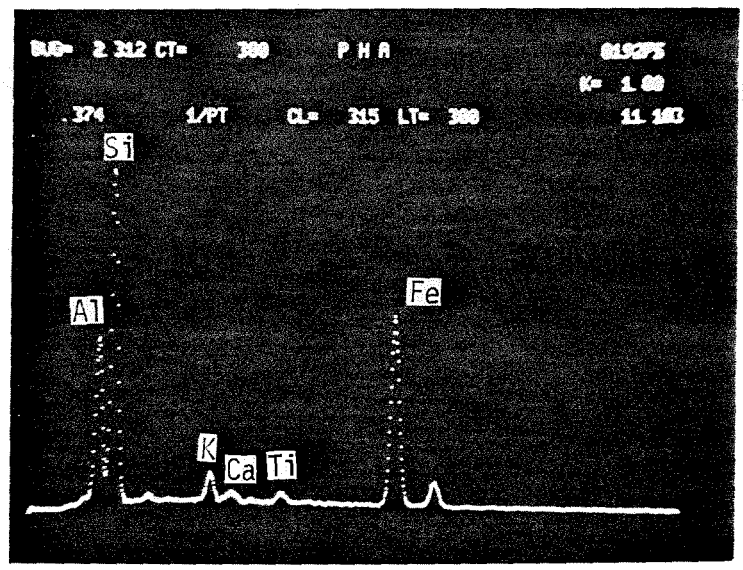

B) EDAX - PEAKS FOR AL, SI, K, CA, TI AND FE

FIGURE 4-169

ASH (750 C) FROM RUN 52C (NO_2/CCL_4 - 180 MIN, NA_2CO_3(AQ) - 120 MIN) PSOC 276 (+200-325 MESH)

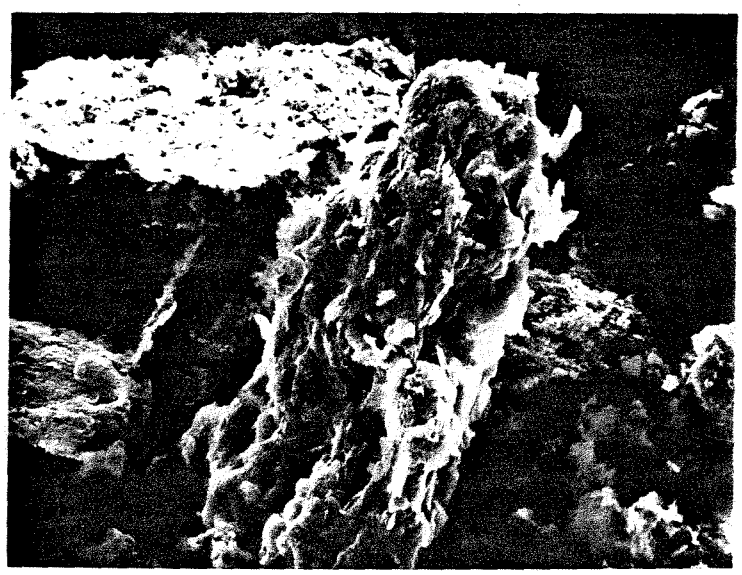

A) X 950

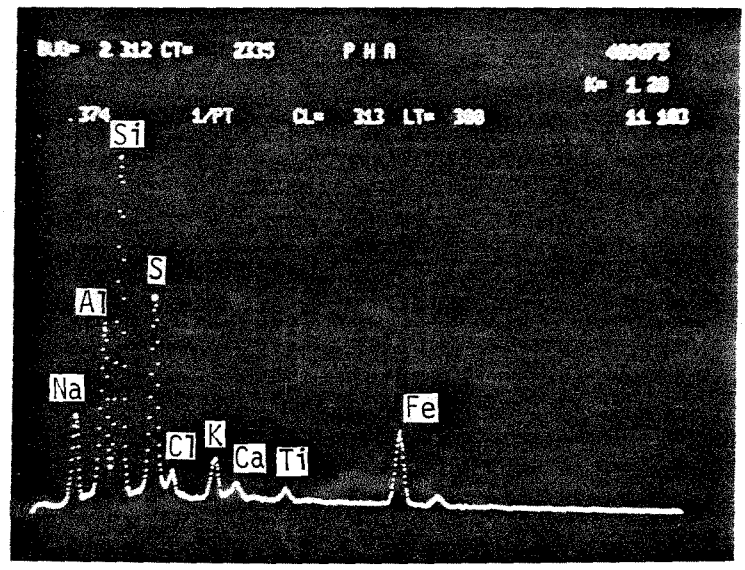

B) EDAX - PEAKS FOR NA, AL, SI, S, CL, K, CA, TI AND FE

FIGURE 4-170

ASH (1200 C) FROM RUN 52C (NO_2/CCL_4 - 180 MIN, NA_2CO_3(AQ) - 120 MIN) PSOC 276 (+200-325 MESH)

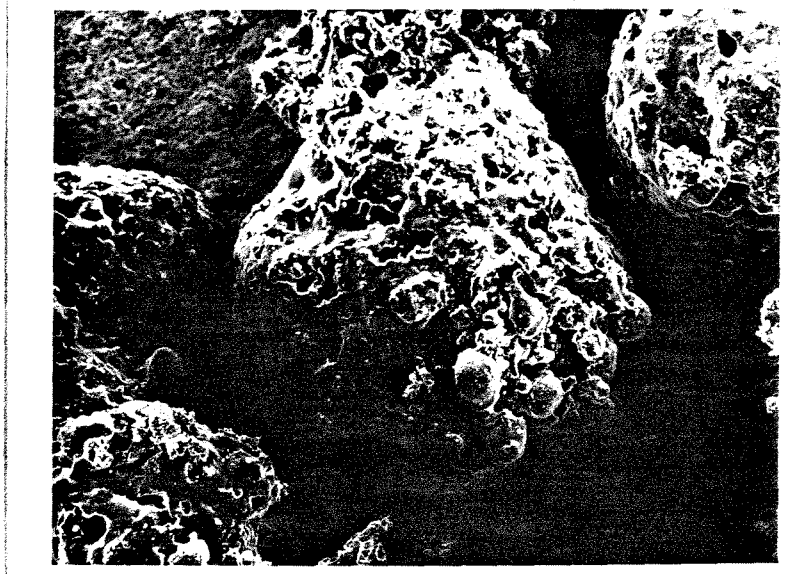

A) X 95

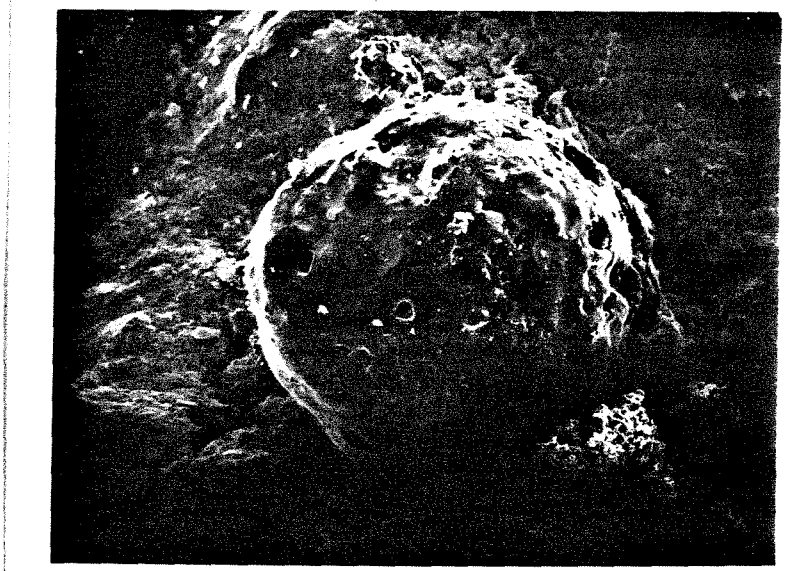

B) X 95

FIGURE 4-171

EDAX SPECTRA FOR ASH (1200 C) FROM
RUN 52C (NO_2/CCL_4 - 180 MIN, NA_2CO_3(AQ) - 120 MIN)
PSOC 276 (+200-325 MESH)

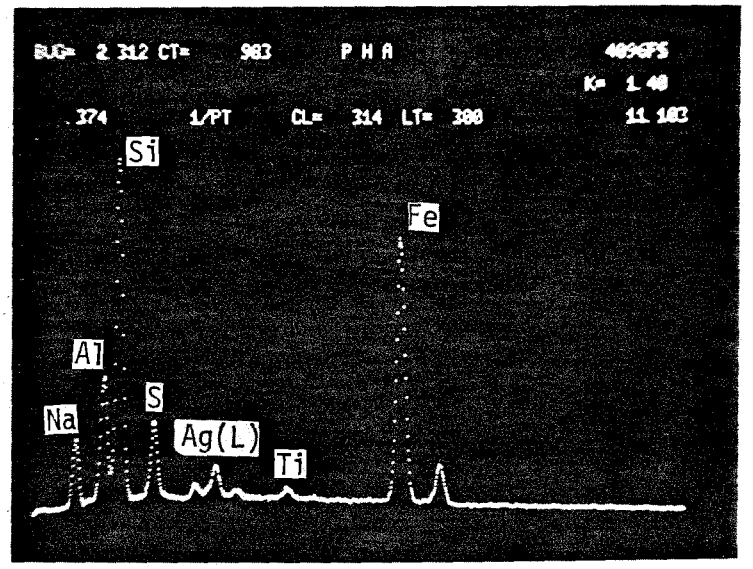

A) PEAKS FOR NA, AL, SI, S, AG(L), TI AND FE

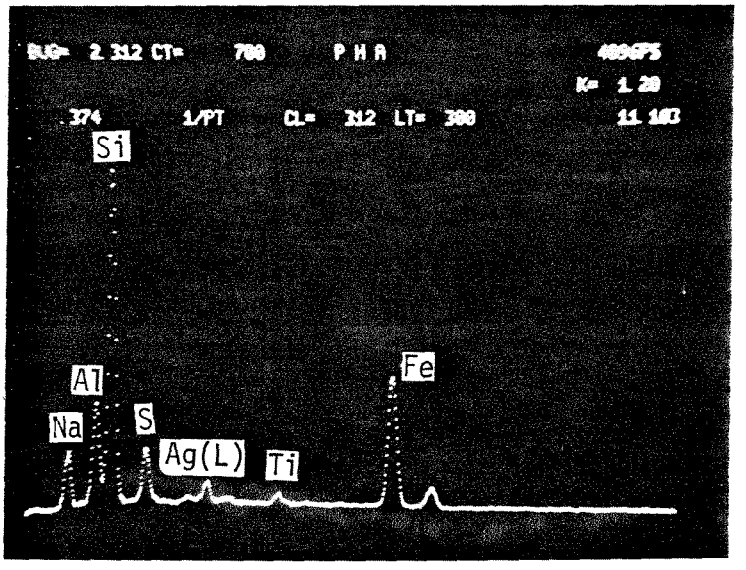

B) PEAKS FOR NA, AL, SI, S, AG(L), TI AND FE

FIGURE 4-172

4.3.3 Changes in the Surface Area, Pore volume and Pore Size Distribution of the Coal

The previous discussion in this section dealt exclusively with the qualitative changes induced in the physical structure of the coal by the NO_2 and Na_2CO_3 (aq) treatment. This section will discuss these changes in a more quantitative manner. In particular, the specific surface area (S_a), the pore volume (V_p) and the pore size distribution of some of the treated coals were determined. Changes in these three parameters due to the coal treatment provide a good macroscopic indication of the alterations introduced into the particle structure. Knowledge of the variations in S_a, V_p and the pore size distribution due to the processing then allows the determination of the effect of the reaction parameters, such as NO_2-exposure time and temperature, on the particle structure of the coal. Furthermore, the effect of the particle structure on the extent of reaction with the coal can also be determined.

4.3.3.1 Standardization of the Procedure

As mentioned in the experimental discussion, the surface area of the two standards were measured in order to check the experimental procedure. The first standard examined was the Vulcan rubber, which gave a value for S_a of 74.57 ± 0.35 m^2/g, which agrees with the quoted value of 71.3 ± 2.7 m^2/g within experimental error. It is interesting to note that the pore size distribution, which can be found in Appendix A (Figure A–2), shows a broad peak at a pore radius of about 100 Å. Furthermore, the N_2 adsorption-desorption isotherm (Figure A–1) shows that 70 % of the pore volume is encompassed by pores with radii greater than 15 Å. The volume of N_2 still adsorbed during desorption at a relative pressure of 0.35 corresponds to the pore volume encompassed by pores with radii less than 15 Å. The other 30 % of the pore volume occurs in micropores, the structure of which cannot be determined using N_2 adsorption.

The other standard examined was the silica, which gave a value of S_a of 242.8 ± 0.2 m^2/g, which is slightly lower than the quoted value of 286.1 ± 3.5 m^2/g. As previously mentioned, however, other workers have also obtained low values of S_a for this standard, which suggests that this standard may be contaminated. The pore size distribution for this sample, which can be found in Appendix A (Figure A–5), also shows a broad peak with a maximum at a pore radius of about 50 Å. Furthermore, the N_2 adsorption-desorption isotherm indicates that 86 % of the pore volume is encompassed by pores with radii greater than 15 Å, and that only 14 % of the pore volume consists of micropores.

An N_2 adsorption-desorption isotherm (Figure A–7) was also obtained for another solid, namely activated coconut charcoal, which consisted of particles in the range from 80 to 90 mesh. The value obtained for S_a is 979.1 ± 1.9 m^2/g, which is rather high, but quite reasonable for an activated charcoal. In this instance, the pore size distribution (Figure A–8) shows more distinctive features than those of the two previous samples, with a sharp peak at a value for r_p of 19 Å. Another peak is shown at 11 Å, but due to the invalidity of the Kelvin equation for values of r_p below 15 Å, this peak should not be considered too seriously. The more interesting fact, however, is that the N_2 adsorption-desorption isotherm indicates that roughly 96 % of the pore volume is enclosed in pores with radii less than 15 Å. Consequently, the pore size distribution shown in Figure A–8 only corresponds to 4 % of the total pore volume.

In any event, the acquisition of the N_2 adsorption-desorption isotherms for these three samples has served two useful purposes. Primarily, the determination of the surface areas provided a means by which to check the experimental procedure. The results indicate that the experimental procedure is satisfactory. Furthermore, the difference in the results for the three samples, particularly with regard to the pore size distributions, demonstrates the additional

information regarding the pore structure which can be extracted from the isotherm. In particular, not only can the total pore volume be measured, but its distribution among micro and macro pores can be determined as well. Furthermore, the pore size distribution obtained from the isotherm yields more precise information regarding those pores with radii between 15 and roughly 200 Å.

4.3.3.2 The Reproducibility of the Procedure

In order to determine the accuracy of the surface area measurement and pore size distribution determination, the N_2 adsorption-desorption isotherms for several samples were acquired more than once. In particular, the reproducibility of peaks in the pore size distribution is of primary concern. By obtaining more than one isotherm, the sensitivity of the results to the experimental procedure can be determined.

For instance, two determinations of the surface area on the same sample of raw PSOC 190 (+100-200 mesh) yielded values of 70.0 ± 0.3 and 72.6 ± 0.3 m^2/g. These values, although they do not agree within experimental error, still indicate a reasonably good reproducibility. More importantly, however, the pore size distributions obtained from the isotherms are virtually identical. Both distributions show a single peak at 19 Å, although the peak heights differ by 15 %. Such a relatively large discrepancy is not unexpected since the pore size distribution is essentially a numerical differentiation of the isotherm. Consequently, small errors in the isotherm are amplified in the pore size distribution. Nevertheless, the agreement between the two pore size distributions is quite good, as demonstrated in Figure 4–173, in which both pore size distributions are plotted together.

Although the +100-200 mesh PSOC 190 was used in Runs 1–6, the finer +200-325 mesh PSOC 190 coal was used in the remainder of the runs. As it turns out,

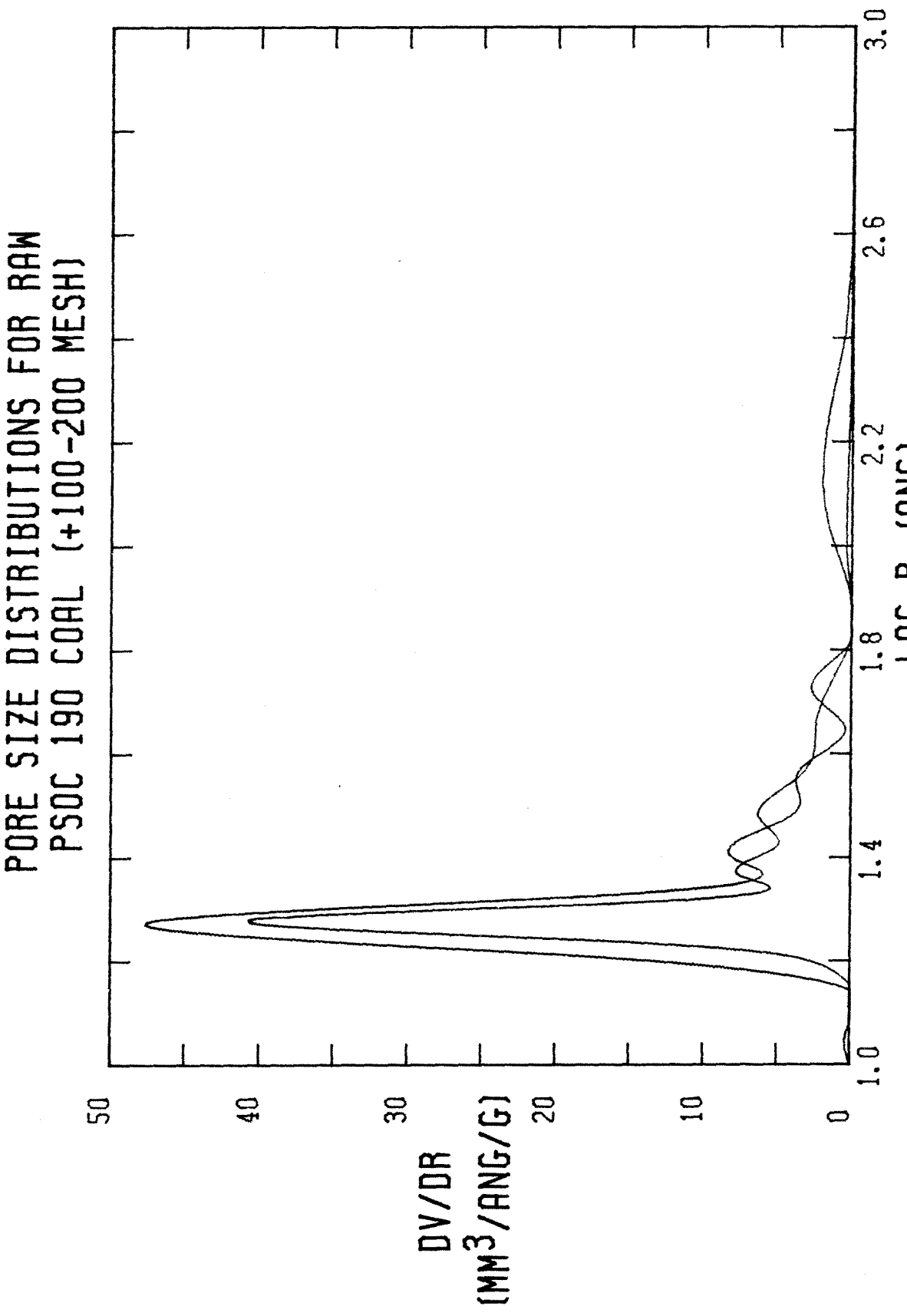
PORE SIZE DISTRIBUTIONS FOR RAW
PSOC 190 COAL (+100-200 MESH)
DV/DR
(MM3/ANG/G)
0
10
20
30
40
50
1.0
1.4
1.8
2.2
2.6
3.0
LOG R (ANG)

FIGURE 4-173

the particle size has a profound effect on the specific surface area and total pore volume. Six N_2 adsorption-desorption isotherms were obtained for the same sample of the raw PSOC 190 (+200-325 mesh), which yielded values of 43.4 ± 0.3, 44.4 ± 0.2, 46.1 ± 0.3, 45.3 ± 0.2, 46.0 ± 0.2 and 43.4 ± 0.2 m^2/g for $S_a^{N_2}$, which are about 40 % lower than the values obtained for the +100-200 mesh coal. Such loss in the surface area and pore volume as the particle size decreases is typically observed for most coals. Once again, the pore size distributions obtained from the isotherms are virtually the same. As in the case of the larger particle size coal, the pore size distributions have a single peak at a value of r_p of 19 Å. Furthermore, the peak heights are just about equal, as demonstrated by Figure 4–174, which contains the six pore size distributions plotted together.

Because many of the runs used the washed and dried PSOC 190 (+200-325 mesh) coal, five N_2 adsorption-desorption isotherms for the same sample of this coal were obtained as well. The calculated values of $S_a^{N_2}$ are 55.0 ± 0.3, 59.5 ± 0.3, 59.5 ± 0.3, 57.7 ± 0.3 and 58.6 ± 0.3 m^2/g. Once again, the reproducibility is excellent, particularly if the first value is discarded. It is interesting to note that just washing the raw coal in water for 120 minutes at 25°C increases the surface area by 30 % over that of the unwashed coal. Since the water wash does not remove any of the organic matter in the coal, which follows from the fact that the mass corrected heat content of the washed coal is the same as that of the unwashed coal, the increase in the surface area, and hence pore volume, must be attributed to the removal of water soluble inorganic material contained within the pore structure of the coal. Once this material is removed, more of the pore structure can be accessed by nitrogen during the BET run.

The pore size distributions based on isotherms of the washed PSOC 190 are once again virtually identical. As in the case of the unwashed coal, all of the

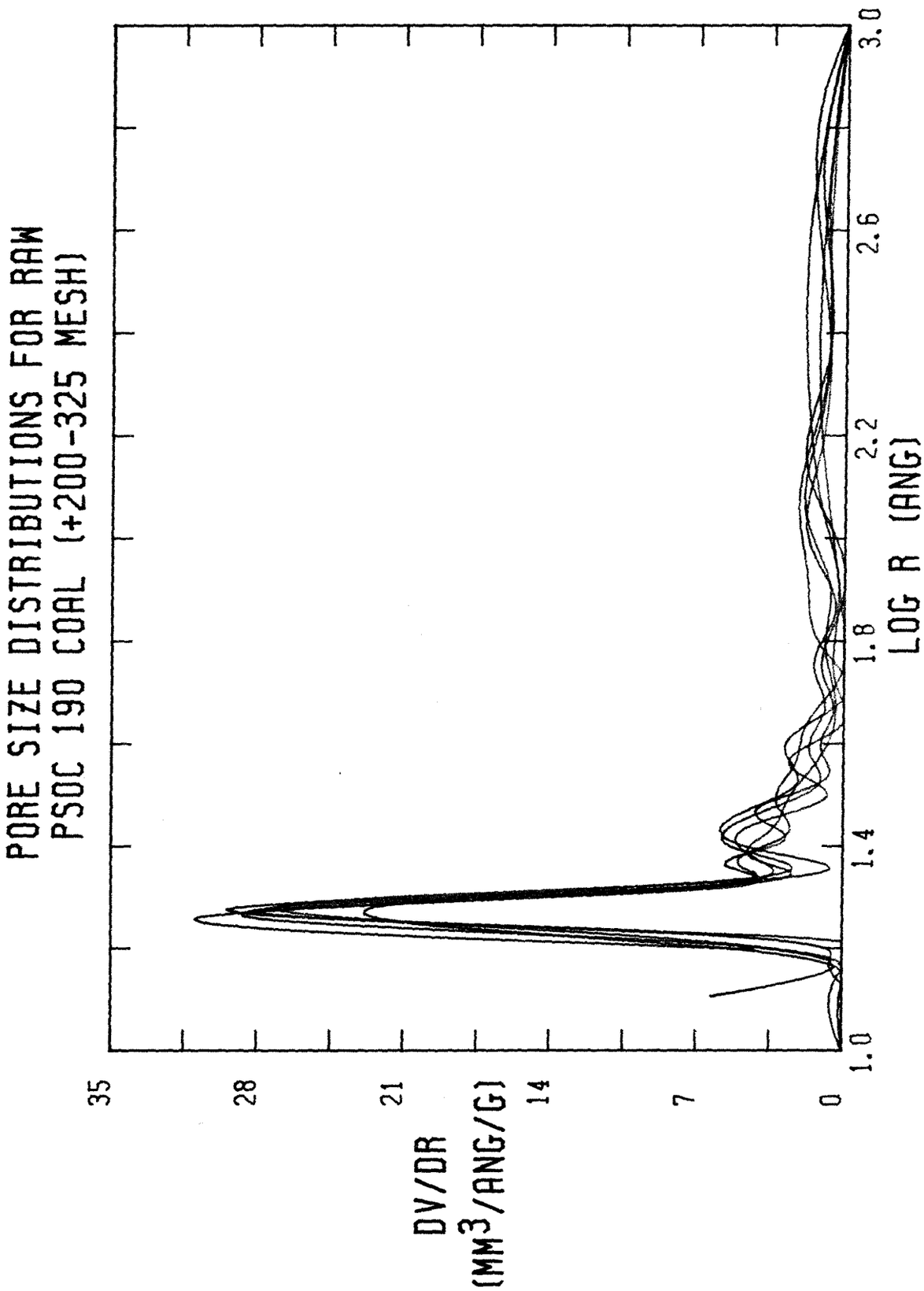
PORE SIZE DISTRIBUTIONS FOR RAW
PSOC 190 COAL (+200-325 MESH)
DV/DR
(MM3/ANG/G)
35
28
21
14
7
0
1.0
1.4
1.8
2.2
2.6
3.0
LOG R (ANG)

FIGURE 4-174

pore size distributions have one peak with a maximum at 19 Å. Furthermore, the height of the peak in each pore size distribution is relatively constant. Figure 4–175, which consists of a composite of these five pore size distributions, provides a good indication of the high degree of reproducibility in the experimental results. It is interesting to note that the wash of the PSOC 190 coal affects the pore size distribution uniformly, so that if the pore size distributions of the washed and unwashed coals are normalized, they are virtually the same. The pore size distributions of both coals have a single peak at 19 Å, which implies that the wash does not alter the pore structure, it only increases its accessibility to N_2. This conclusion is consistent with the notion that the water wash removes only soluble inorganic material from the coal particle. If this inorganic material is uniformly distributed within the void space of the particle, then its removal should lead only to an enhancement of the total pore volume without altering the pore size distribution.

Finally, it should be noted that the pore size distributions for both the washed and the raw PSOC 190 coals correspond to only about half of the total pore volume of the coal, as revealed by the isotherms. In particular, 50 ± 2 % of the total pore volume of the raw PSOC 190 resides in pores with radii less than 15 Å. On the other hand, 53 ± 1 % of the total pore volume of the washed and dried PSOC 190 is encompassed in pores with radii less than 15 Å. Thus, both coals possess a substantial amount of micropore structure before exposure to NO_2.

4.3.3.3 Changes in the Particle Structure of the Coal Treated With Nitrogen Dioxide in Water

All of the runs using H_2O as the solvent were conducted in the flow reactor. Unfortunately, it is not possible to correlate the changes in the surface area and pore volume of the coal particles with the kinetics in a quantitative manner

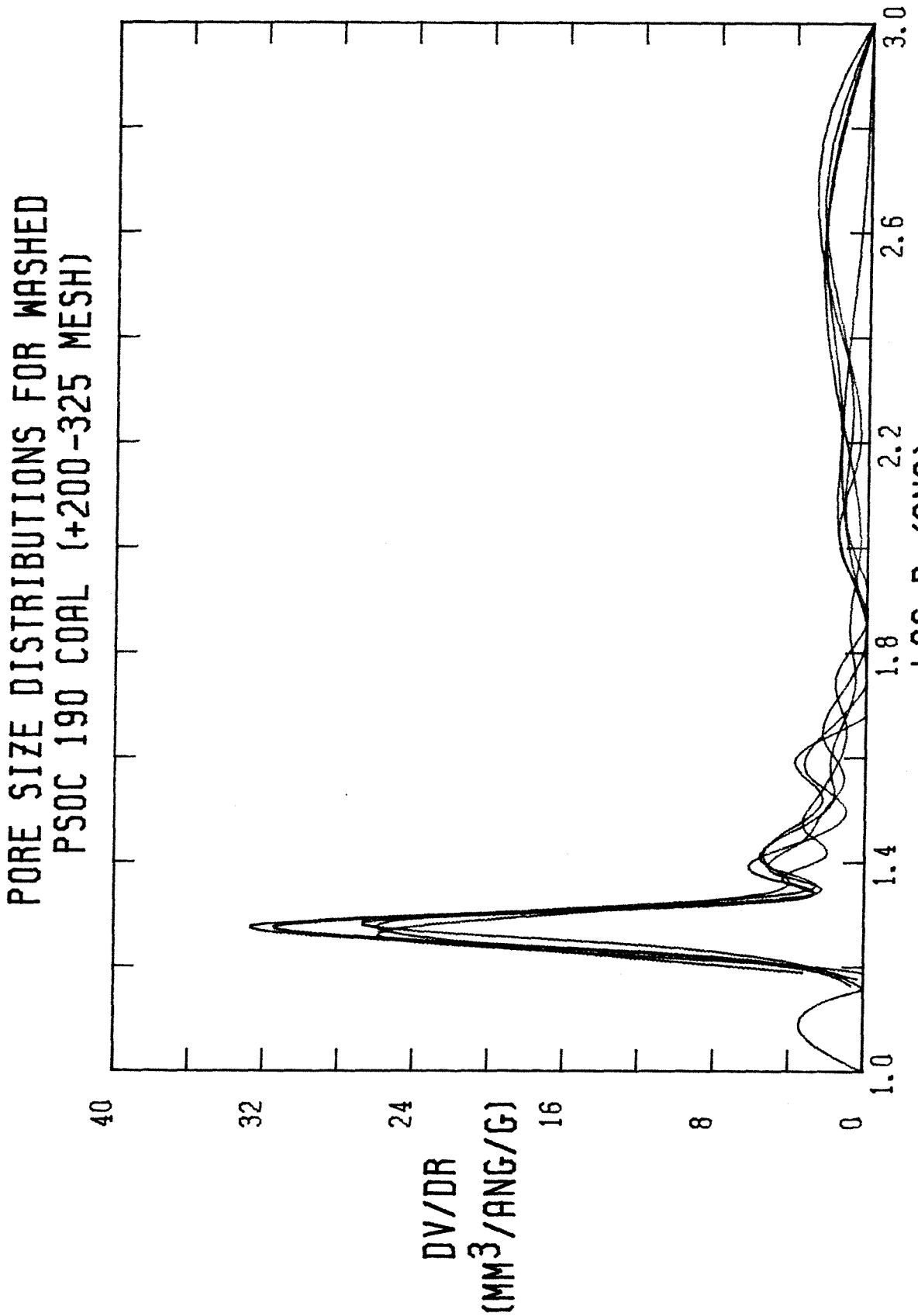
PORE SIZE DISTRIBUTIONS FOR WASHED
PSOC 190 COAL (+200-325 MESH)
DV/DR
(MM3/ANG/G)
0
8
16
24
32
40
1.0
1.4
1.8
2.2
2.6
3.0
LOG R (ANG)

FIGURE 4-175

because of the numerous reactions which take place in the NO_2/H_2O system. Nevertheless, a few qualitative conclusions can be drawn from the BET measurements. The values obtained for $S_a^{N_2}$ and V_p of the treated coals examined can be found in Table 4–5. It should be noted that Run 7 corresponds to the washed and dried PSOC 190 coal, hence there was no NO_2 exposure. No values of V_p for Runs 16 and 17 are shown because the full adsorption isotherms for these samples were not obtained. An examination of the table reveals that the trend in $S_a^{N_2}$ with exposure time and NO_2 flowrate parallels the trend in V_p. In particular, the coal from Run 8 has a value of $S_a^{N_2}$ which is only 40 % of that of the untreated coal, while the value of V_p is 47 % of that of the untreated coal. After 120 minutes of NO_2 treatment (Run 11), $S_a^{N_2}$ drops to 17 % of its initial value while V_p drops to 26 % of its initial value. Thus, both $S_a^{N_2}$ and V_p show drastic decreases upon exposure of the coal to NO_2. V_p does not decline to quite the extent that $S_a^{N_2}$ declines, however, which implies that the surface to volume ratio of the pore structure decreases upon increased exposure to NO_2. For instance, after 30 minutes of NO_2 treatment (Run 8), the $S_a^{N_2}/V_p$ ratio is only 86 % of its initial value. After 120 minutes (Run 11), the ratio drops to just 64 % of its initial value. This trend in the $S_a^{N_2}/V_p$ ratio is expected because the ratio varies as r^{-1} for cylindrical pores. Thus, if surface area is lost due to the addition of species to the surface, the loss in area should be greater than the loss in volume. Furthermore, pores with small radii may be blocked altogether due to reaction, leading to a proportionately larger decrease in $S_a^{N_2}$ than in V_p.

In the case of the PSOC 190 coal, 52 % of the N_2-determined pore volume exists in pores with radii less than 15 Å. It is interesting to note that as the exposure time increases, the amount of pore volume residing in pores with radii less than 15 Å increases slightly, being 56 % and 62 % of the total pore volume

TABLE 4-5

Nitrogen Determined Surface Area and Pore Volume of PSOC 190 Coal (+200-325 mesh) Treated with NO_2 in H_2O in the Flow Reactor at 25 C

Run #	NO_2 Exposure Time (min)	Mean NO_2 Flowrate (g NO_2/min)	$S_a^{N_2}$ (m^2/g)	V_p (cm^3/g)
7	0	0.0	58.06	0.08284
8	30	1.33	23.38	0.03857
9	60	1.24	14.04	0.02731
11	120	1.22	9.67	0.02141
16	120	0.27	11.83	-
17	120	0.48	6.94	-
18	120	1.04	5.96	0.01588
18C	-	-	4.69	0.01580

after 30 and 120 minutes of NO_2 treatment, respectively. Thus, the overall decrease in $S_a^{N_2}$ and V_p upon treatment with NO_2 seems to be drastic over the entire range of pore radii accessible to N_2, with the volume of the larger pores decreasing slightly more than the volume of the smaller pores. This latter effect can perhaps be attributed to the easier access of NO_2 to the larger pores.

The effect of the oxidative treatment on the pore structure of the coal is demonstrated in Figure 4–176, which is a composite of the pore size distribution of Runs 7, 8, 9 and 11, which correspond to NO_2-exposure times of 0, 30, 60 and 120 minutes, respectively. It should be noted that the pore size distributions were obtained by fitting the results obtained from the application of the Kelvin equation to the raw N_2 desorption data as outlined in Chapter 2 using a cubic spline curve fitting procedure. Furthermore, the distributions in this figure have been altered from those in the appendix in that the vertical scale is now log (dV/dr) rather than dV/dr, which allows the change to be seen more clearly. The maximum of the predominant peak in the distribution of the raw coal occurs at a value of r_p of 18.3 Å. After just 30 minutes of NO_2 treatment, the peak height drops to only about 30 % of that of the raw coal and the maximum is shifted slightly to a pore radius of 18.9 Å. After 60 minutes of NO_2 treatment, the peak height is only about 15 % that of the raw coal. Furthermore, the pore radius at which the maximum occurs has increased to about 19.6 Å. It is interesting to note that the peak in the distribution is now becoming indistinguishable from two other shallow peaks which occur at roughly 24 Å and 32 Å. Because the pore size distribution is essentially a numerical differentiation of the desorption branch of the isotherm, small errors in the desorption data are greatly magnified in the distribution. Consequently, the two latter peaks may just be the result of scatter in the desorption data rather than true peaks. These peaks can be conveniently referred to as noise. Therefore, the peak at

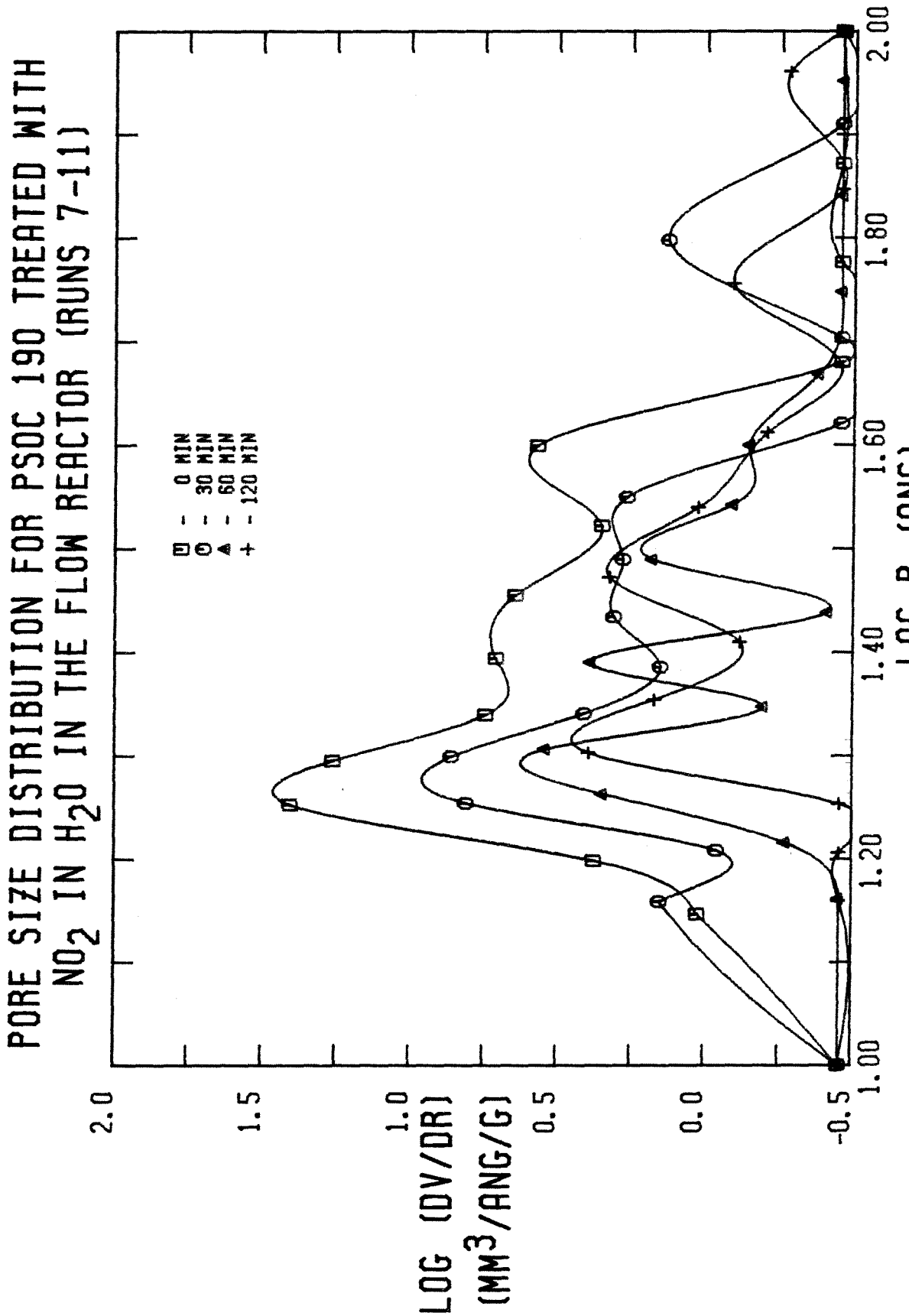
PORE SIZE DISTRIBUTION FOR PSOC 190 TREATED WITH
NO_2 IN H_2O IN THE FLOW REACTOR (RUNS 7-11)
0 MIN
30 MIN
60 MIN
120 MIN
LOG (DV/DR)
(MM3/ANG/G)
LOG R (ANG)
2.0
1.5
1.0
0.5
0.0
-0.5
1.00
1.20
1.40
1.60
1.80
2.00

FIGURE 4-176

20 Å is becoming indistinguishable from the background noise after 60 minutes of NO_2 treatment. Nevertheless, the distribution obtained for the sample after 120 minutes of NO_2 treatment shows a further decline in the peak height to about 10 % of that of the raw coal. Furthermore, the peak maximum has shifted to a pore radius of 20.7 Å. At this point, this peak is just barely discernible from the noise, however.

These observations concerning the pore size distributions demonstrate several things. Primarily, the NO_2 treatment tends to flatten the distribution so that a uniform distribution of pore sizes results. In particular, a substantial portion of the pore volume encompassed by pores with radii between 15 Å and roughly 200 Å occurs in the narrow range of 15 to 23 Å. After 120 minutes of NO_2 treatment, however, the predominance of this peak has virtually vanished. The loss of this peak is most readily explained by the pore dimensions to which it corresponds, namely a radius of 19 Å in the raw coal. In view of the trapping of substantial amounts of CCl_4 by the oxidized coal, these pores should be blocked quite easily. When the N_2 adsorption-desorption isotherm is obtained at 77°K, the CCl_4 of course solidifies and acts as an extension of the solid coal matrix. Hence, isolated void spaces in the particle, which are inaccessible to N_2 during the BET determination, may be created during the NO_2 treatment due to pore blocking.

The shift in the pore radius at which the maximum occurs can be attributed to a small degree of dilation in the remaining pore volume still accessible to N_2. Such dilation may occur as the result of either a small amount of etching of the pore walls by the NO_2-H_2O solution or the slight expansion of the pores during the treatment. In any case, the increase in radius is only 2.3 Å after 120 minutes of NO_2 exposure, which is quite modest considering the drastic decrese in surface area and pore volume.

Table 4–5 also contains the values of $S_a^{N_2}$ for Runs 16, 17 and 18. In each run, the aqueous coal slurry was exposed to NO_2 for 120 minutes at room temperature at the various NO_2 flowrates indicated. The values of $S_a^{N_2}$ indicate a dependence of the loss in surface area on the amount of NO_2 to which the coal is exposed. In particular, 80 % of the surface area is lost when the flowrate is 0.269 g NO_2/min, whereas the surface area loss is 90 % when the flowrate is 1.039 g NO_2/min. Nevertheless, the extent of the variation in $S_a^{N_2}$ with NO_2 flowrate pales when compared to the overall loss in surface area just upon exposure of the coal to NO_2. As these and the previous data indicate, the NO_2-coal reaction is extremely rapid. Consequently, most of the physical and chemical changes occur within the first 30 minutes of exposure to NO_2.

Table 4–5 also contains values of $S_a^{N_2}$ and V_p for a sample of NO_2-treated coal subsequently washed in 0.1 M Na_2CO_3 (aq) (Run 18C). The results indicate that the Na_2CO_3 (aq) wash leads to a further reduction in $S_a^{N_2}$. On the other hand, there is virtually no change in V_p. Because a substantial amount of material is exchanged with the coal during the wash, such as CCl_4 with Na^+, it is surprising that there is not a greater loss in $S_a^{N_2}$ and V_p. It should be noted, however, that the values of $S_a^{N_2}$ and V_p for the NO_2-treated coal (Run 18) are quite low to begin with, so that there is little room for a further decline in either $S_a^{N_2}$ or V_p.

Because the surface area and pore volume of the coals from Runs 16, 17 and 18 are so low, it was not possible to obtain meaningful pore size distributions for these samples. As mentioned previously in regard to Figure 4–176, once $S_a^{N_2}$ falls below about 10 m^2/g, not enough nitrogen is adsorbed to provide accurate desorption data from which an accurate pore size distribution can be obtained. In particular, it would not be possible to determine the change in the distribution peak at 18 Å with the same degree of accuracy as was possible with Runs 7,

8, 9 and 11.

4.3.3.4 Changes in the Particle Structure of Coal Treated with Nitrogen Dioxide in Carbon Tetrachloride

All of the experiments using CCl_4 as the solvent for the treatment of coal with NO_2 for which values of $S_a^{N_2}$ and V_p were obtained were conducted in the batch reactor. In particular, the coal samples from Runs 33–46 were examined using both N_2 and CO_2 as the adsorbate. Because these experiments were conducted under controlled conditions and in a solvent which did not react with NO_2, it is possible to correlate the results obtained for the surface area and pore volume with the rate data, which forms the first topic of discussion in this section. The second topic of discussion in this section concerns the change in the pore structure as evidenced by the pore size distribution.

4.3.3.4.1 Correlation of the Changes in Surface Area with the Kinetics of the Reaction of Nitrogen Dioxide with the Coal

The results of the N_2 and CO_2 adsorption studies on the coal samples generated by treatment of the washed and dried PSOC 190 (+200-325 mesh) coal with NO_2 in CCl_4 at 20°C in the batch reactor are in Table 4–6. Included in the table are the values of S_a determined from both the N_2 and CO_2 adsorption isotherms as well as the total nitrogen-determined pore volume, V_p. An examination of the table reveals that just the initial exposure of the coal to NO_2 results in virtually all of the loss in the nitrogen-determined surface area, $S_a^{N_2}$. Exposure beyond 30 minutes does not seem to alter $S_a^{N_2}$ very much. In particular, after 30 minutes, the coal has suffered a 69 % loss in $S_a^{N_2}$. After 180 minutes, the loss has increased to only 73 %. Indeed, if all of the values of $S_a^{N_2}$ of the treated coal are averaged, a value of 17.47 ± 1.10 m^2/g results for $S_a^{N_2}$, which represents a 70 % loss in the initial surface area of the coal. Again, these

TABLE 4-6

Nitrogen Determined Surface Area and Pore Volume of PSOC 190 Coal (+200-325 mesh) Treated with NO_2 in CCl_4 in the Batch Reactor at 20 C

Run #	NO_2 Exposure Time (min)	$S_a^{N_2}$ (m^2/g)	$S_a^{CO_2}$ (m^2/g)	V_p (cm^3/g)
Washed & Dried	0	58.06	165.5	0.08284
33	30	17.84	185.5	0.03808
34	60	18.02	166.8	0.03554
35	90	18.85	170.0	0.03576
36	120	17.04	187.7	0.03319
37	180	15.60	203.2	0.03270
36C	-	2.02	193.3	0.01222

results are consistent with previously discussed data which indicate that the NO_2-coal reaction is essentially complete within 30 minutes.

The results of the CO_2-determined surface area, on the other hand, are completely opposite to those of the N_2-determined surface area. Indeed, the values of $S_a^{CO_2}$ for the NO_2-treated coal are actually greater than that of the raw coal. Furthermore, the value of $S_a^{CO_2}$ for the raw coal is 2.85 times that of $S_a^{N_2}$. As mentioned previously, this phenomenon is quite common with coal, where values of $S_a^{CO_2}$ can sometimes be two orders of magnitude greater than $S_a^{N_2}$. What is interesting in this case is that $S_a^{CO_2}$ seems to increase with increasing exposure to NO_2 while $S_a^{N_2}$ decreases quite drastically. The increase in $S_a^{CO_2}$ can be attributed to the greater amount of interaction between CO_2 and the oxidized coal surface. As mentioned in Chapter 2, it is possible that CO_2 actually penetrates the solid coal matrix at 298°K, the temperature at which the CO_2-adsorption isotherm is obtained, whereas N_2 cannot penetrate the matrix at 77°K, the temperature at which the N_2 adsorption isotherm is obtained. Consequently, $S_a^{CO_2}$ probably serves more appropriately as an indication of the permeability of the coal to CO_2 in addition to the surface area of the coal.

At this point, it would be beneficial to digress for a moment and discuss the validity of the procedure used for obtaining $S_a^{CO_2}$ from the DPR plot. In particular, it is important to establish the correspondence between $S_a^{CO_2}$ determined by the BET method to $S_a^{CO_2}$ determined by the DPR method. As mentioned in Chapter 2, the volume of CO_2 adsorbed at a relative pressure, $\frac{P}{P_0}$, of 0.1 is used empirically as the monolayer capacity of the adsorbent. To determine whether this is valid, the same coal sample (Run 35) was allowed to adsorb CO_2 at both 298°K, for which the DPR method of analysis was used, and at 196°K, for which

the BET method of analysis was used. The DPR method gave a value for $S_a^{CO_2}$ of 170.0 m^2/g while the BET method gave a value of 180.6 m^2/g. These values are in very good agreement considering the difference in the relative pressure range to which they apply. Therefore, the validity of either method for obtaining values of the surface area is firmly established.

In regard to Table 4–6, it should be noted that the last entry pertains to the Na_2CO_3 (aq) washed coal from Run 36. In this case, the drop in $S_a^{N_2}$ after the wash is also quite drastic. The NO_2-treated coal retained only 29 % of its initial surface area. The washed coal, however, only retained 3 % of the initial surface area. The retention of the nitrogen-determined pore volume is 40 % and 15 % for the NO_2-treated coal and the subsequently washed coal, respectively. Although the drop in $S_a^{N_2}$ due to the Na_2CO_3 (aq) wash is greater in this case than in the case when water was the solvent, the absolute values of $S_a^{N_2}$ for the two washed coals are roughly equal (2.02 vs. 4.69 m^2/g). Rather, in the case of those experiments conducted with the CCl_4 solvent, the extent of the loss in $S_a^{N_2}$ is not as great as when H_2O was the solvent. In this case, it is obvious that the Na_2CO_3 (aq) wash leads to a substantial amount of pore blocking in the NO_2-treated coal. Furthermore, the results from the elemental analysis of the coal indicate that a substantial amount of displacement occurs during the Na_2CO_3 (aq) wash, particularly of CCl_4. Indeed, it seems reasonable to expect that if CCl_4 is effectively trapped by the oxidized coal and cannot be removed by vacuum drying at 120°C, then a more polar compound such as H_2O should be even more effectively trapped in the washed coal. Coupled with the sodium uptake by the coal, the trapping of H_2O in the coal can easily lead to a further loss in $S_a^{N_2}$ and V_p. In fact, the lower values obtained for $S_a^{N_2}$ when the coal is treated with NO_2 in H_2O than when CCl_4 is the solvent are probably the result of

the greater extent of trapping of H_2O by the oxidized coal.

In order to determine if the drastic loss in $S_a^{N_2}$ affects the kinetics of the NO_2-coal reaction, the values of $S_a^{N_2}(t)$ can be correlated with an appropriate rate of reaction. For this system, the best rate to use is the global rate of NO_2 disappearance from the NO_2/CCl_4/coal system. For Runs 33–37, these rates can be obtained by a graphical differentiation of the plot of the bulk NO_2 concentration vs. reaction time (Figure 4–8). The results are presented in Table 4–7 and Figure 4–177. Table 4–7 contains not only the absolute values of r, the global rate of NO_2 disappearance, but also the values of $\frac{r}{r_0}$, where r_0 is the initial rate, which can be compared with the values of $\frac{S_a^{N_2}}{(S_a^{N_2})_0}$, as well. Figure 4–177 illustrates this comparison graphically.

An examination of the table reveals that while $S_a^{N_2}$ is relatively constant after 30 minutes, r continues to decline. The value of r after 30 minutes is relatively small, however, compared to the initial rate, r_0, as Figure 4–177 so amply demonstrates. Indeed, the figure clearly shows that the correlation between the rate and the surface area is quite good, despite the fact that $\frac{r}{r_0}$ approaches zero asymptotically while $\frac{S_a^{N_2}}{(S_a^{N_2})_0}$ levels off at roughly 0.3. Both curves simply indicate that the reaction and loss in $S_a^{N_2}$ are essentially complete within the first 30 minutes of NO_2 exposure.

The good correlation of $\frac{r}{r_0}$ with $\frac{S_a^{N_2}}{(S_a^{N_2})_0}$ is not really surprising. As mentioned in the earlier discussion concerning the time dependence of the bulk NO_2 concentration during the reaction, it appears that NO_2 is diffusing into the solid coal matrix. Furthermore, this solid diffusion process is rate limiting during the

TABLE 4-7

Relative Surface Areas and Reaction Rates for Runs 33-37						
t(min)	$\frac{S_a^{N_2}}{(S_a^{N_2})_0}$	$r\ (\frac{\mathrm{F}}{\mathrm{min}})$	$\frac{r}{r_0}$	$1 - \frac{m_N}{m_{N0}}$	$r_N(\frac{\text{mass \%}}{\mathrm{min}})$	$\frac{r_N}{r_{N0}}$
0	1.00	0.04705	1.00	1.00	0.5271	1.00
30	0.3073	0.002154	0.04578	0.1763	0.02020	0.03832
60	0.3104	0.001131	0.02404	0.0902	0.008125	0.01542
90	0.3247	0.000914	0.01943	0.0127	0.004275	0.00811
120	0.2935	0.000619	0.01315	0.0035	0.002150	0.00408
180	0.2687	0.000256	0.00545	-	0.000075	0.00014

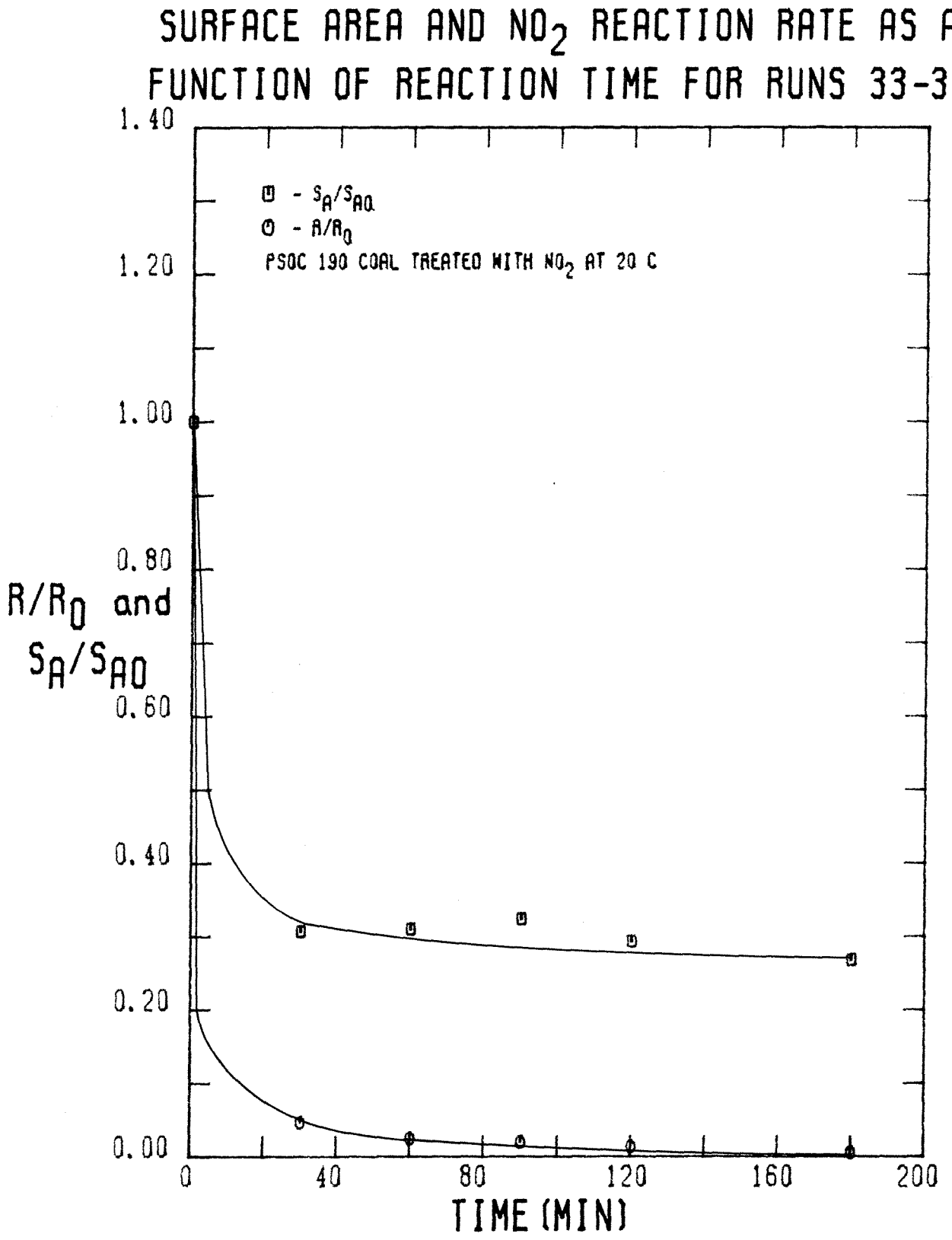
SURFACE AREA AND NO2 REACTION RATE AS A FUNCTION OF REACTION TIME FOR RUNS 33-37
□ - SA/SAO
○ - R/RO
PSOC 190 COAL TREATED WITH NO2 AT 20 C
R/RO and SA/SAO
1.40
1.20
1.00
0.80
0.60
0.40
0.20
0.00
0
40
80
120
160
200
TIME (MIN)

FIGURE 4-177

first 30 minutes of the reaction. Thus, the global rate of NO_2 disappearance is proportional to the total flux of NO_2 into the coal particle. This total flux, in turn, is proportional to the amount of surface area available to the NO_2 for diffusion into the particle. Consequently, r should be proportional to $S_a^{N_2}$, which Figure 4–177 clearly demonstrates.

A similar comparison of the change in $S_a^{N_2}$ with the rate of change in the nitrogen content of the coal during the NO_2 treatment, r_N, can be made. The results of a graphical differentiation of the curve in Figure 4–64 which pertains to the net increase in the nitrogen content of the coal, m_N, given in Table 4–7. A plot of $\frac{S_a^{N_2}}{(S_a^{N_2})_0}$ and $\frac{r_N}{(r_N)_0}$ is shown in Figure 4–178. The results are quite similar to those obtained using the global rate of NO_2 disappearance, namely a good correlation of $S_a^{N_2}$ with the rate, in this case r_N. Of course, the same explanation given for the correlation of $S_a^{N_2}$ with r applies in this instance as well.

It should be obvious that there is no correlation of $S_a^{CO_2}$ with either r or r_N, simply because $S_a^{CO_2}$ increases while the reaction rates decrease during the course of the reaction. Indeed, this fact provides further evidence that $S_a^{CO_2}$ is probably a measure of the permeability of the coal to CO_2 as well as the surface area of the coal. Apparently the permeability of the coal to CO_2 is altered by neither the NO_2 treatment nor the subsequent Na_2CO_3 (aq) wash. This latter fact is amply demonstrated by the value of $S_a^{CO_2}$ obtained for Run 36C of 193.3 m^2/g, which is essentially equal to the value obtained for Run 36 of 187.7 m^2/g. These results are in stark contrast to those obtained for $S_a^{N_2}$, which clearly show that the accessibility of the coal to N_2 after the wash is almost totally restricted. Consequently, it appears that it is better to use the nitrogen determined surface area for describing the kinetics of the NO_2-coal reaction.

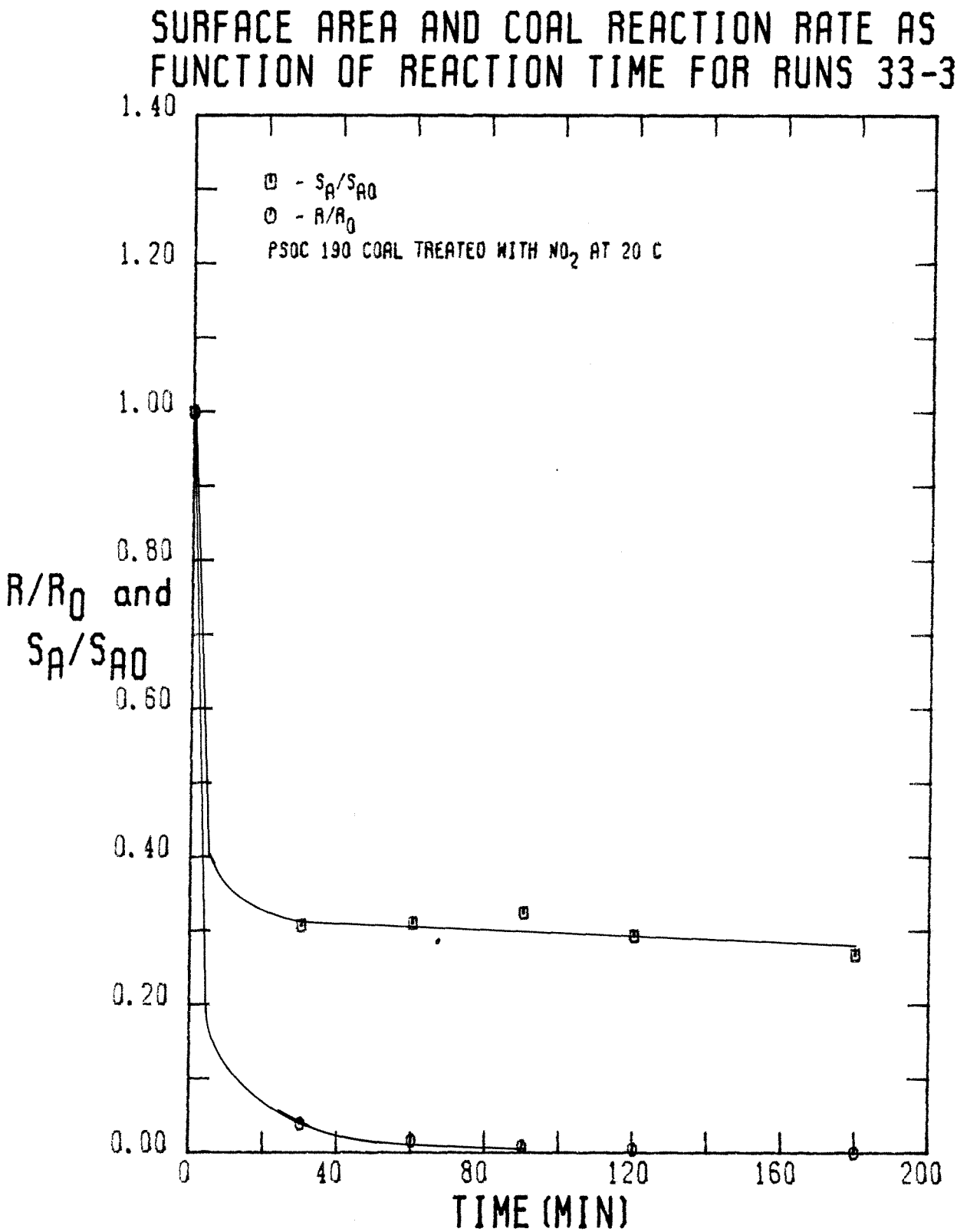
SURFACE AREA AND COAL REACTION RATE AS A FUNCTION OF REACTION TIME FOR RUNS 33-37
□ - S_A/S_{AO}
○ - R/R_0
PSOC 190 COAL TREATED WITH NO_2 AT 20 C
R/R_0 and S_A/S_{AO}
1.40
1.20
1.00
0.80
0.60
0.40
0.20
0.00
0
40
80
120
160
200
TIME (MIN)

FIGURE 4-178

Similar results were obtained when variations in $S_a^{N_2}$ and $S_a^{CO_2}$ for the PSOC 190 treated with NO_2 in CCl_4 at 0°C (Runs 42–46) in the batch reactor were examined as a function of NO_2-exposure time. The values of $S_a^{N_2}$ and $S_a^{CO_2}$, as well as V_p, for the coals from these runs are tabulated in Table 4–8. An examination of the table reveals that $S_a^{N_2}$ follows the same trend at 0°C as at 20°C, namely that virtually all of the ultimate loss in surface area occurs within the first 30 minutes. In fact, the decrease in both $S_a^{N_2}$ and V_p is slightly greater in the coals treated at 0°C than at 20°C. The most probable explanation for this behavior is that the coal surface has a higher propensity for NO_2 adsorption at the lower temperature, which would result in a slightly higher NO_2 concentration at the coal surface. Consequently, slightly more pore blocking should occur at 0°C than at 20°C. As before, the values of $S_a^{CO_2}$ tend to remain invariant or increase moderately as well, which implies that the NO_2 treatment at 0°C does not alter the permeability of the coal to CO_2.

A comparison of $\frac{S_a^{N_2}}{(S_a^{N_2})_0}$ with the relative global rate of NO_2 disappearance from the NO_2/CCl_4/coal system, $\frac{r}{r_0}$, and with the relative rate of nitrogen uptake by the coal, $\frac{r_N}{(r_N)_0}$, can be made for Runs 42–46 just as for Runs 33–37. Utilization of the same procedure yields the values tabulated in Table 4–9. It is interesting to note that the initial rate of NO_2 disappearance, r_0, is roughly 30 % higher at 0°C than at 20°C. After 30 minutes, however, the rate at 0°C becomes smaller than that at 20°C.

The correlation between $\frac{S_a^{N_2}}{(S_a^{N_2})_0}$ and $\frac{r}{r_0}$ is shown graphically in Figure 4–179. Once again, the correlation is quite good, mainly because both the reaction and

TABLE 4-8

Nitrogen Determined Surface Area and Pore Volume of PSOC 190 Coal (+200-325 mesh) Treated with NO_2 in CCl_4 in the Batch Reactor at 0 C

Run #	NO_2 Exposure Time (min)	$S_a^{N_2}$ (m^2/g)	$S_a^{CO_2}$ (m^2/g)	V_p (cm^3/g)
Washed & Dried	0	58.06	165.5	0.08284
42	30	18.39	159.8	0.03596
43	60	15.47	192.0	0.03459
44	90	16.42	179.1	0.03357
45	120	13.61	166.4	0.03136
46	180	14.84	139.0	0.03020

TABLE 4-9

Relative Surface Areas and Reaction Rates for Runs 42-46						
t(min)	$\frac{S_a^{N_2}}{(S_a^{N_2})_0}$	$r\ (\frac{\mathrm{F}}{\mathrm{min}})$	$\frac{r}{r_0}$	$1 - \frac{m_N}{m_{N0}}$	$r_N(\frac{\text{mass \%}}{\mathrm{min}})$	$\frac{r_N}{r_{N0}}$
0	1.00	0.06492	1.00	1.00	0.5700	1.00
30	0.3168	0.001935	0.0298	0.2402	0.02553	0.04479
60	0.2665	0.000802	0.0123	0.1208	0.00946	0.01660
90	0.2828	0.000444	0.0068	0.0647	0.00534	0.00936
120	0.2344	0.000280	0.0043	0.0275	0.00298	0.00522
180	0.2556	0.000164	0.0025	0.0017	0.00662	0.00116

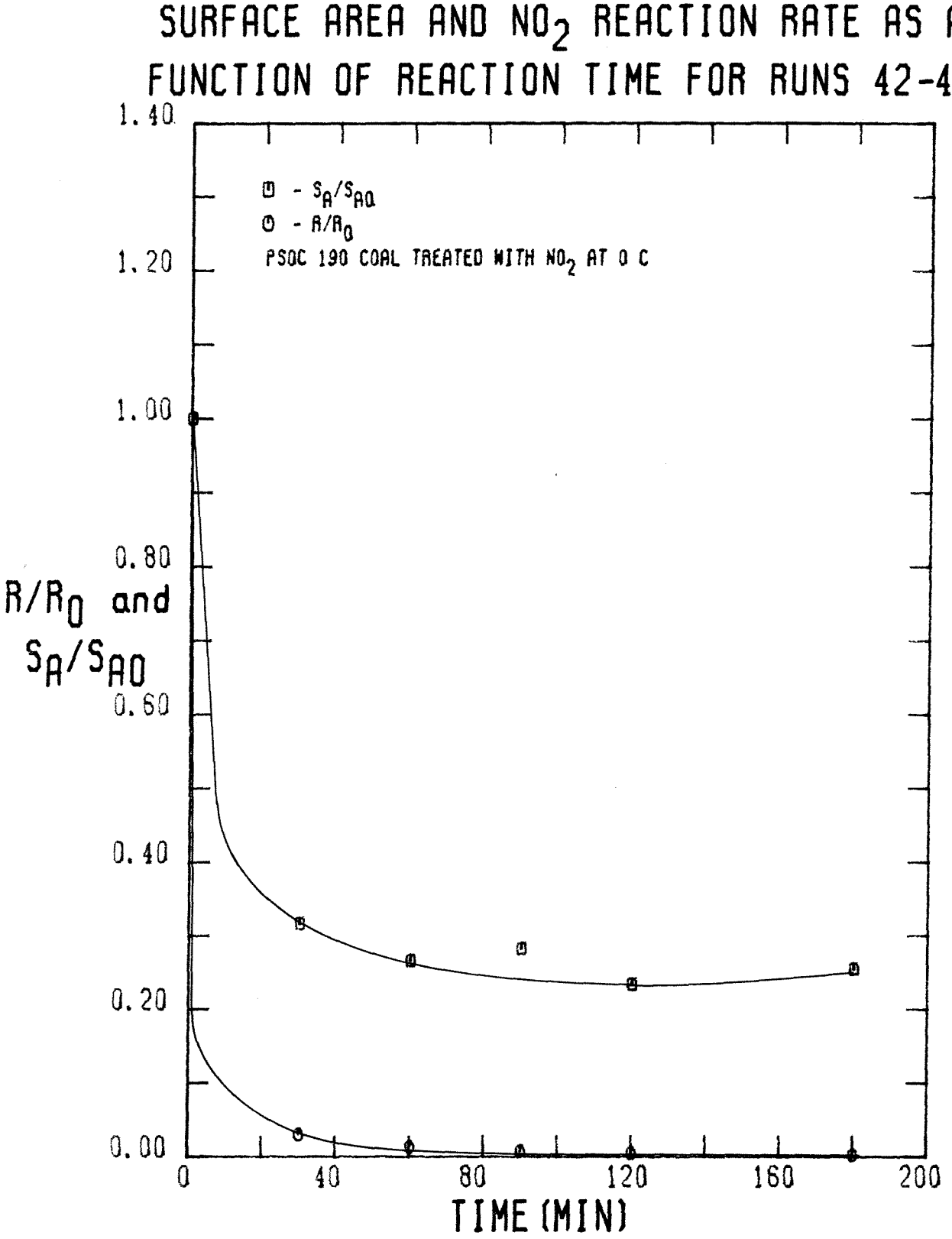
SURFACE AREA AND NO2 REACTION RATE AS A FUNCTION OF REACTION TIME FOR RUNS 42-46
□ - SA/SAO
○ - A/RO
PSOC 190 COAL TREATED WITH NO2 AT 0 C
R/RO and SA/SAO
1.40
1.20
1.00
0.80
0.60
0.40
0.20
0.00
0
40
80
120
160
200
TIME (MIN)

FIGURE 4-179

the loss in surface area are essentially complete within the initial 30 minutes of NO_2 exposure. Nevertheless, the argument invoked in the previous discussion stating that r should be proportional to $S_a^{N_2}$ because the flux of NO_2 into the solid coal matrix, which is the slow step in the overall process, is proportional to $S_a^{N_2}$, applies in this case as well. A comparison of the change in $S_a^{N_2}$ with the rate of nitrogen uptake by the coal, r_N, can be made as well for Runs 42–46. Table 4–9 contains the values of r_N obtained from the numerical differentiation of the curve in Figure 4–66 which pertains to the nitrogen content of the NO_2-treated coal. The correlation between $\frac{S_a^{N_2}}{(S_a^{N_2})_0}$ and $\frac{r_N}{(r_N)_0}$ is illustrated in Figure 4–180. Once again, the two curves display parallel behavior, which indicates that the correlation is quite good, as expected in view of the previous discussion.

The effect of the initial NO_2 concentration, $(NO_2)_0$, on the surface area and pore volume of the coal can be deduced from the results presented in Table 4–10. An examination of the table reveals a weak dependence of $S_a^{N_2}$ on $(NO_2)_0$. In particular, 120 minutes of exposure to NO_2 at the lowest concentration used results in a 61 % loss in the nitrogen-determined surface area. When $(NO_2)_0$ was at the highest concentration used, the loss in $S_a^{N_2}$ amounted to 80 %. Thus, a discernible dependence of the loss in $S_a^{N_2}$ on $(NO_2)_0$ is evident, although exposure of the coal to very small concentrations of NO_2 results in most of the nitrogen-determined surface-area loss. This conclusion is in accord with previous results, all of which indicate the facile and rapid reaction of NO_2 with the PSOC 190 coal at 20°C. The change in V_p follows that in $S_a^{N_2}$, although not as drastically. In particular, V_p drops by only 43 % when $(NO_2)_0$ = 0.1 F, but by 62 % when $(NO_2)_0$ = 1.9 F. Thus, the ratio of surface area to total pore volume decreases as $(NO_2)_0$ increases, just as it does when the exposure time increases. This effect is due to the preferential blocking of pores with small diameters.

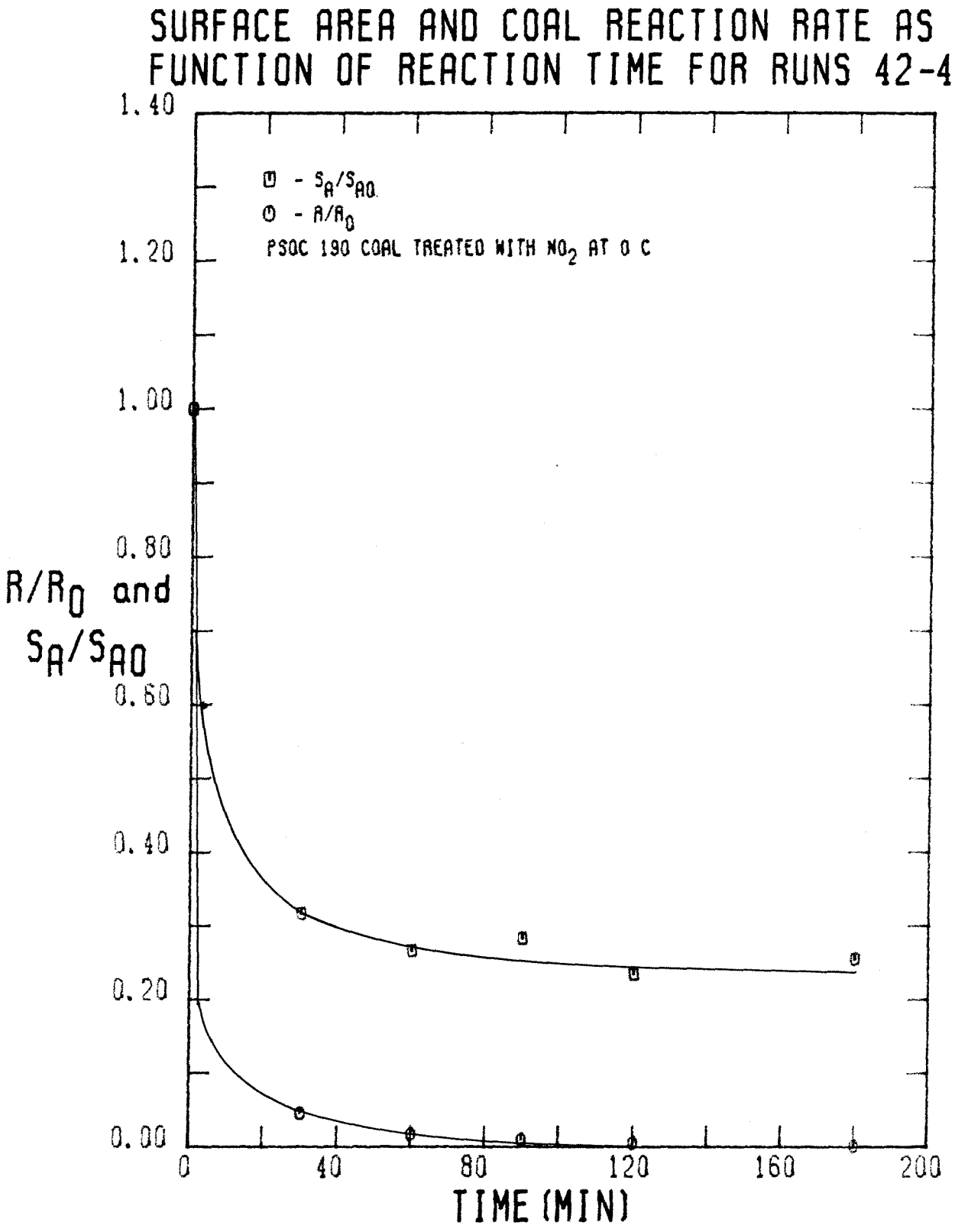
SURFACE AREA AND COAL REACTION RATE AS A FUNCTION OF REACTION TIME FOR RUNS 42-46
□ - S_A/S_{AO}
○ - R/R_0
PSOC 190 COAL TREATED WITH NO_2 AT 0 C
R/R_0 and S_A/S_{AO}
1.40
1.20
1.00
0.80
0.60
0.40
0.20
0.00
0
40
80
120
160
200
TIME (MIN)

FIGURE 4-180

TABLE 4-10

Nitrogen Determined Surface Area and Pore Volume of PSOC 190 Coal (+200-325 mesh) Treated with NO_2 in CCl_4 in the Batch Reactor at 20 C for 120 Minutes

Run #	$(NO_2)_0$ (F)	$S_a^{N_2}$ (m^2/g)	$S_a^{CO_2}$ (m^2/g)	V_p (cm^3/g)
Washed & Dried	0	58.06	165.5	0.08284
38	0.0972	22.68	180.2	0.04749
39	0.4877	18.76	170.1	0.03898
36	1.0872	17.04	187.7	0.03319
40	1.7127	14.18	192.3	0.03043
41	1.8743	11.78	158.7	0.03151

These pores contribute greatly to the total surface area but not as greatly to the total pore volume. Nevertheless, the majority of the loss in both $S_a^{N_2}$ and V_p occurs just upon exposure of the coal to NO_2, even at small concentrations.

The change in $S_a^{CO_2}$ due to the NO_2 treatment, on the other hand, is somewhat minimal and random. These values are consistent, however, with the other values of $S_a^{CO_2}$ discussed previously. Extending the previously invoked argument regarding CO_2 adsorption, the concentration of NO_2 during the treatment also does not affect the permeability of the coal to CO_2. Consequently, exposure of the coal to NO_2 does not affect the CO_2 adsorption yet adversely affects the N_2 adsorption. Because the rate data correlates quite well with $S_a^{N_2}$, but not with $S_a^{CO_2}$, nitrogen should be used as the adsorbate for acquisition of structural data for kinetic studies of the NO_2-coal reaction.

Finally, nitrogen adsorption studies were attempted with the treated PSOC 276 coal (Runs 47–52). Unfortunately, the amount of nitrogen adsorbed by these samples was too low to obtain an accurate adsorption-desorption isotherm. Nevertheless, values of $S_a^{N_2}$ and V_p were obtained for the raw PSOC 276 (Run 47) and the sample exposed to NO_2 for 180 minutes (Run 52). The values obtained are listed with the corresponding values for the treated PSOC 190 coal in Table 4–11. It should be immediately obvious that the PSOC 276 coal has an initial value of $S_a^{N_2}$ which is much smaller than that of the PSOC 190 coal. The relative change in $S_a^{N_2}$ of the PSOC 276 coal due to NO_2 treatment, however, is much smaller. In particular, whereas the PSOC 190 coal suffers a 73 % loss in $S_a^{N_2}$ after 180 minutes of NO_2 treatment, the PSOC 276 coal only suffers a 30 % loss in $S_a^{N_2}$ after 180 minutes. Of course, the PSOC 276 possesses less surface area to potentially lose in the first place, so this result is not surprising.

TABLE 4-11

Surface Area and Pore Volume of PSOC 190 and PSOC 276 Coals (+200-325 mesh) Treated with NO_2 in CCl_4 in the Batch Reactor at 20 C for 120 Minutes

Run #	Coal Type (PSOC #)	NO_2 Exposure Time (min)	$S_a^{N_2}$ (m^2/g)	$S_a^{CO_2}$ (m^2/g)	V_p (cm^3/g)
Washed & Dried	190	0	58.06	165.5	0.08284
37	190	180	15.60	203.2	0.03270
Washed & Dried	276	0	8.60	192.9	0.02091
52	276	180	6.01	143.9	0.01423

Of greater interest, however, is the effect the difference in $S_a^{N_2}$ of the two types of coal have on the global rate of NO_2 disappearance from the system and on the rate of nitrogen uptake by the coal. Table 4–12 contains the values for r and r_N of the PSOC 276 at t = 0 and t = 180 minutes. The values of r and r_N for the PSOC 276 were obtained by a graphical differentiation of the curves in Figure 4–11 and Figure 4–74, respectively. Of greatest interest are the initial rates. In the case of the global rate of NO_2 disappearance, the rate when the PSOC 276 is used is only 48 % of that when the PSOC 190 is used. The PSOC 190, however, initially has 6.8 times as much surface area as the PSOC 276. Hence, the surface area would seem to have a discernible, but seemingly mild effect on the initial rate of NO_2 disappearance from the system. Because the surface area of the PSOC 190 drops much more rapidly than that of the PSOC 276 during the initial stages of the NO_2 treatment, however, the surface areas of the two coals differ by a factor of only 3 after just 30 minutes of NO_2 exposure. Indeed, if $S_a^{N_2}$ for the PSOC 190 instantaneously drops upon exposure to NO_2, then the difference in the rates of NO_2 disappearance correlate much better with respective nitrogen-determined surface areas of the two coals. At t = 180 minutes, the rate when the PSOC 276 is used is now 84 % of that when the PSOC 190 is used, which implies that the reaction of NO_2 in both cases is nearly complete within 180 minutes.

An examination of the values of r_N reveals a similar trend as well. For instance, the initial value of r_N for the PSOC 276 coal is 53 % of that of the PSOC 190 coal, which is in good agreement with the initial values of r. The best comparison of the rates of nitrogen uptake by the two coals is provided by the ratio of their respective rate constants, because both coals have the same initial capacity for nitrogen uptake and they were treated under identical conditions. The ratio of the rate constants is 2.6, which is exactly the same as their N_2-

TABLE 4-12

Relative Surface Areas and Reaction Rates for the Treatment of PSOC 276 (+200-325 mesh) with NO_2 in CCl_4 in the Batch Reactor at 20 C

t(min)	$\frac{S_a^{N_2}}{(S_a^{N_2})_0}$	$r\ (\frac{F}{min})$	$\frac{r}{r_0}$	$r_N(\frac{mass\ \%}{min})$	$\frac{r_N}{r_{N0}}$
0	1.00	0.02243	1.00	0.2800	1.00
180	0.6988	0.000214	0.00954	0.00729	0.0260

determined surface areas at t = 180 minutes. Consequently, the proportional dependence of the rate of nitrogen uptake by the coal on $S_a^{N_2}$ is clearly established. This dependence is explained by the fact that both of these rates appear to be limited by the rate of diffusion of NO_2 into the solid coal matrix. The total rate of diffusion in turn depends upon the total accessible interfacial area between the solid coal matrix and the rest of the NO_2/CCl_4/coal system. This interfacial area seems to be well represented by the nitrogen determined surface area of the coal.

4.3.3.4.2 Changes in the Pore Size Distribution Due to Treatment of the Coal with Nitrogen Dioxide

Treatment of the coal with NO_2 results not only in a reduction in surface area and pore volume, but in the alteration of the pore size distribution as well. In particular, the exposure of the coal to NO_2 causes any predominant peaks in the distribution to become greatly diminished in magnitude, as evidenced by the previous discussion of Runs 7–11. Furthermore, the peaks may be shifted to higher or lower values of the pore radius, r_p, depending upon the predominant physical forces during the treatment. For instance, if material is etched from the pore walls, the peaks should be shifted to higher values of r_p. If material is adsorbed on the pore walls, on the other hand, the peaks could disappear entirely or show a shift to lower values of r_p.

In the case of the PSOC 190 coal, there is only one predominant peak in the distribution in the range of radii from 15 to 200 Å, which occurs at a value of r_p of 18.3 Å in the washed and dried coal. Figure 4–181 contains a composite of the pore size distributions obtained for samples of the PSOC 190 coal treated with NO_2 in CCl_4 at 20°C in the batch reactor (Runs 33–37). Once again, log (dV/dr) is plotted in the range of r_p from 10 to 1000 Å for the sake of clarity.

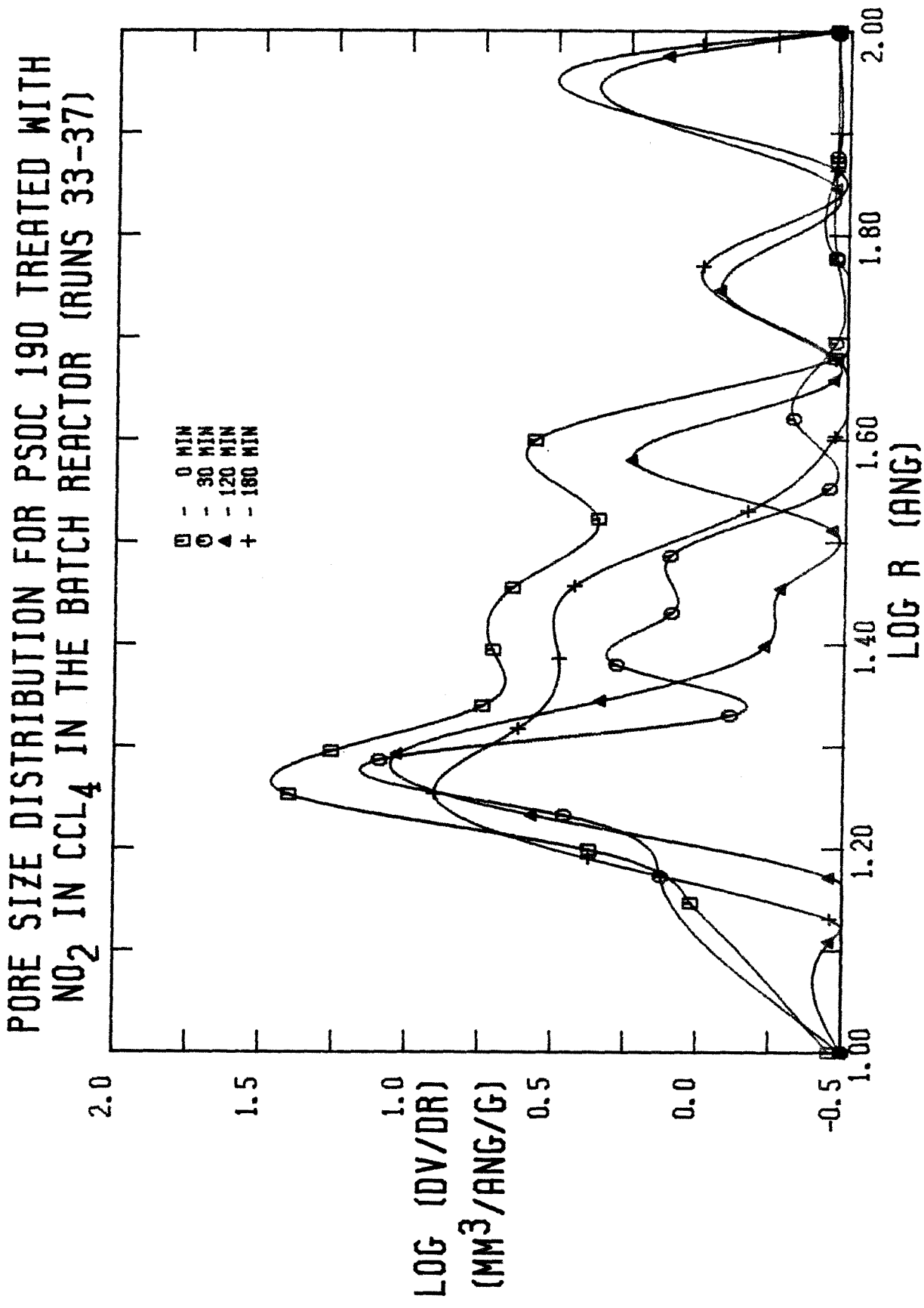
PORE SIZE DISTRIBUTION FOR PSOC 190 TREATED WITH
NO_2 IN CCL_4 IN THE BATCH REACTOR (RUNS 33-37)
0 MIN
30 MIN
120 MIN
180 MIN
LOG (DV/DR)
(MM^3/ANG/G)
2.0
1.5
1.0
0.5
0.0
-0.5
1.00
1.20
1.40
1.60
1.80
2.00
LOG R (ANG)

FIGURE 4-181

The figure shows that exposure of the coal to NO_2 results in a reduction in the main peak at 18.3 Å. In particular, after 30 minutes of NO_2 treatment, the peak height has decreased by 52 % and the position of the maximum has shifted to 18.9 Å. After 120 minutes, the peak height is 58 % less than that of the raw coal and the peak maximum has shifted further to a value of 19.4 Å. After 180 minutes, the decrease in the peak height amounts to 69 % of that of the raw coal, but the position of the maximum is now at 18.0 Å. The range of variation in the value of r_p for the peak maximum is so small, however, that it may be attributed to fluctuations in the data, rather than to some specific physical process. The decrease in peak height is due most probably, then, to pore blocking by adsorption of NO_2 and/or CCl_4. It is interesting to note that the decline in peak height is not as severe in this case as in the previous case where H_2O was used as the solvent. The difference, however, may be attributed to the fact that the concentration of the oxidizing species in the water runs was much higher than when CCl_4 was used as the solvent.

The temperature of the NO_2 treatment does not seem to affect the degree to which the pore size distribution is changed to any significant extent, as evidenced by Figure 4–182, which contains a composite of the distributions obtained from samples of PSOC 190 coal treated at 0 °C (Runs 42–46). In particular, the decline in the peak height is slightly greater at 0 °C than at 20 °C. For instance, after 30 minutes of NO_2 treatment, the peak height is 44 % of that of the untreated coal. The position of the maximum has been shifted to 19.3 Å. Interestingly, after an additional 30 minutes of NO_2 treatment, there is essentially no change in the peak height or position. After 120 minutes of NO_2 treatment, the peak height has declined to 30 % of that of the untreated coal, while the position of the maximum has shifted back to 18.5 Å. Once again, the shift in the peak position is small enough so that it can be attributed to the fluctuations

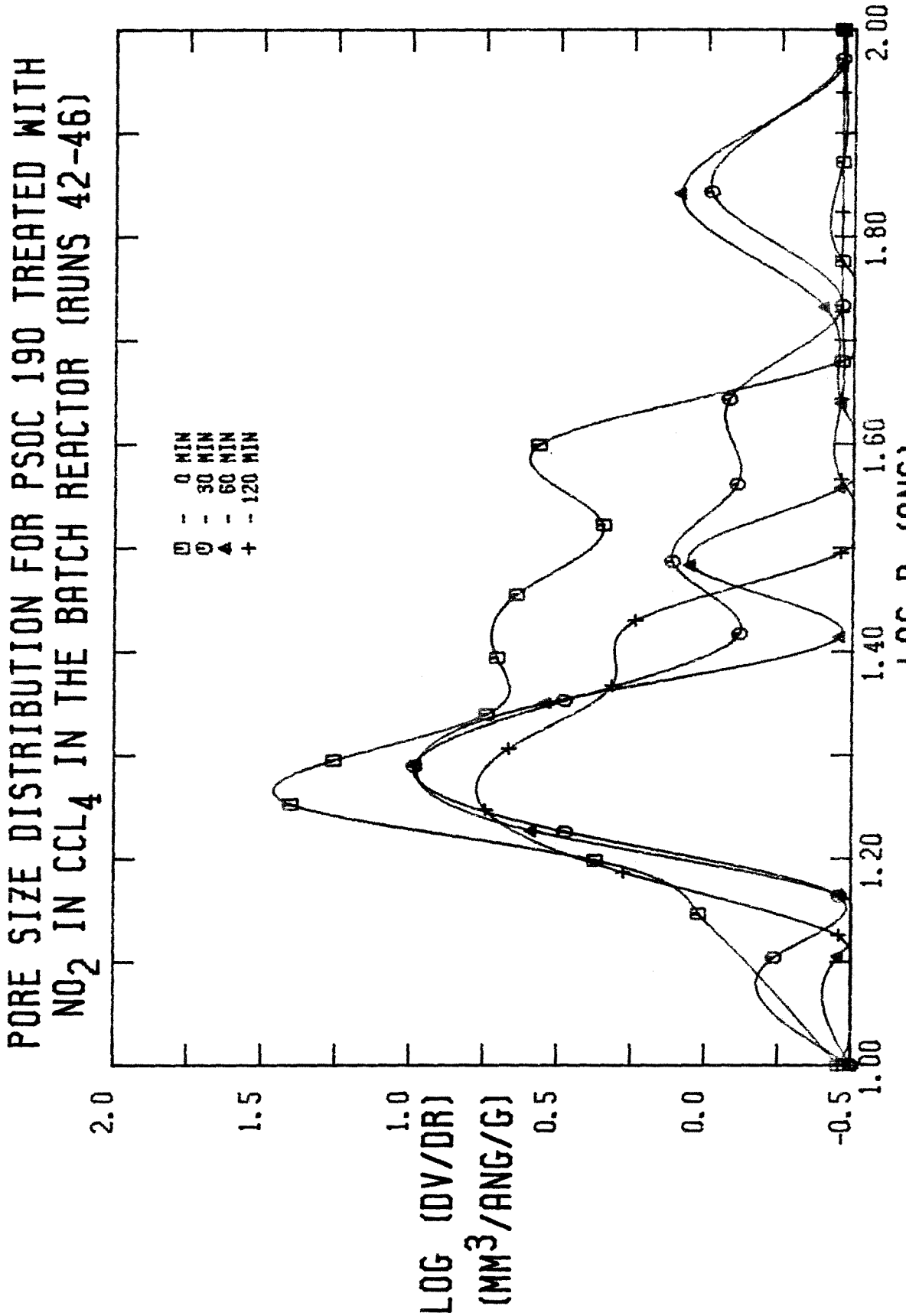
PORE SIZE DISTRIBUTION FOR PSOC 190 TREATED WITH
NO_2 IN CCL_4 IN THE BATCH REACTOR (RUNS 42-46)
0 MIN
30 MIN
60 MIN
120 MIN
LOG (DV/DR)
(MM3/ANG/G)
LOG R (ANG)
2.0
1.5
1.0
0.5
0.0
-0.5
1.00
1.20
1.40
1.60
1.80
2.00

FIGURE 4-182

in the data. Nevertheless, the data indicate that the loss in peak height is slightly greater at 0 °C than at 20 °C, which is consistent with the greater decline in $S_\alpha^{N_2}$ at 0 °C. This increase in the loss of pore volume as the temperature decreases can be accounted for by the increased adsorption of NO_2 by the coal at the lower temperature of 0 °C.

The effect of the initial NO_2 concentration, $(NO_2)_0$, on the pore size distribution is just what might be expected based on the previous discussion of this set of experiments (Runs 38–41), in which the coal was treated for 120 minutes with NO_2 at 20 °C. A composite of the pore size distributions obtained from samples of the coal from these runs is shown in Figure 4–183. An examination of the figure reveals that the height of the predominant peak at 18.3 Å decreases as $(NO_2)_0$ increases, which is expected due to the increased extent of the NO_2-coal reaction as $(NO_2)_0$ increases. In particular, the peak height declines by 38 % at the lowest initial NO_2 concentration used, namely 0.097 F. At the next highest concentration, 0.488 F, the peak height declines to only 39 % of that of the untreated coal. As $(NO_2)_0$ increases further, the rate of decline in the peak height diminishes. For instance, when $(NO_2)_0$ = 1.713 F, the peak height decreases to 28 % of that of the initially untreated coal. Hence, exposure of the coal to even small amounts of NO_2 results in a significant decrease in the height of the distribution peak. This conclusion, of course, is consistent with previously discussed data which indicate the facile and rapid attack of coal by NO_2. Finally, it should be noted that although the figure seems to indicate a shift in position of the peak maximum as $(NO_2)_0$ increases, the change is too small to be attributed to any physical process. Rather, the shift can be ascribed to the fluctuations in the adsorption-desorption data, the numerical differentiation of which yields the pore size distribution.

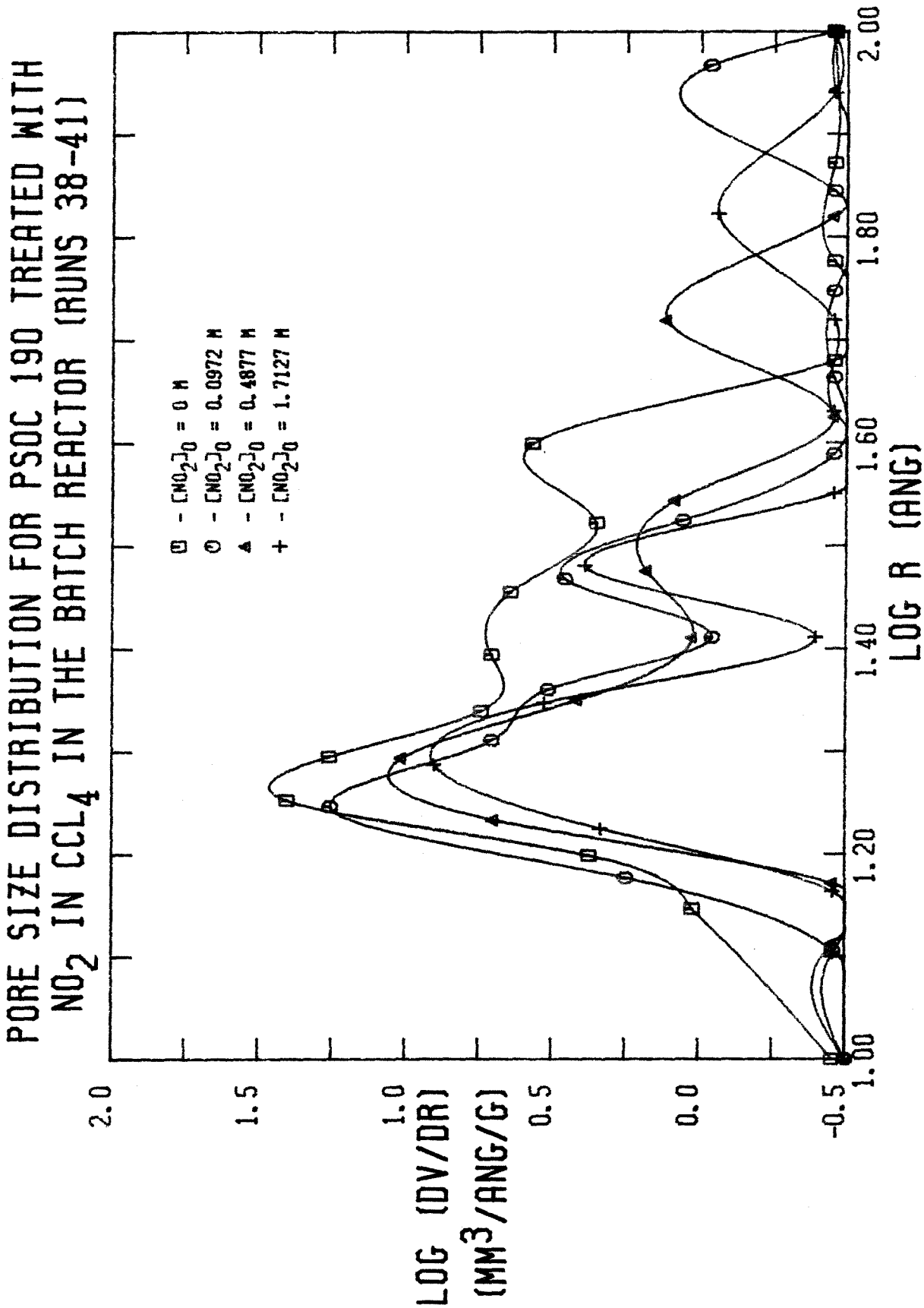
PORE SIZE DISTRIBUTION FOR PSOC 190 TREATED WITH
NO_2 IN CCL_4 IN THE BATCH REACTOR (RUNS 38-41)
□ - $[NO_2]_0$ = 0 M
○ - $[NO_2]_0$ = 0.0972 M
▲ - $[NO_2]_0$ = 0.4877 M
+ - $[NO_2]_0$ = 1.7127 M
LOG (DV/DR)
(MM^3/ANG/G)
2.0
1.5
1.0
0.5
0.0
-0.5
1.00
1.20
1.40
1.60
1.80
2.00
LOG R (ANG)

FIGURE 4-183

4.3.3.4.3 Changes in the Micropore Size Distribution Due to Treatment of the Coal with Nitrogen Dioxide

Appendix A contains the the micropore size distribution of the coals used in the CO_2 adsorption studies, namely Runs 33–46. Because the values of $S_a^{CO_2}$ did not change appreciably during the NO_2 treatment, the micropore size distributions did not change significantly either. The values of the peak height, $(\frac{dw}{dr})_{max}$, and the position of the peak maximum, r_{max}, can be found in Table 4–13. An examination of the table quickly reveals that neither the peak height nor the position of the maximum has been altered by the NO_2 treatment. These results are consistent with previously discussed data which indicate that exposure to NO_2 does not alter the adsorption of CO_2 on the coal to a discernible extent. The fact that the CO_2-determined micropore size distributions do not change despite the significant chemical alterations introduced into the coal by the NO_2 treatment provides compelling evidence which suggests that CO_2 may be an inappropriate adsorbate for determining the structural properties of the coal for use in the kinetic study of the NO_2-coal reaction.

One very interesting feature of the CO_2 adsorption is revealed by the CO_2-determined distributions, however. Recalling that N_2 should not penetrate pores with radii less than about 5 Å while CO_2 should easily penetrate 4 Å pores, it seems reasonable to expect that the large difference in $S_a^{N_2}$ and $S_a^{CO_2}$ should result in a substantial portion of the micropore size distribution being in the range of pore radii less than 5 Å. An examination of the distributions, however, reveals that virtually all of the CO_2-determined micropore volume resides in pores with radii greater than 5 Å. One of two explanations is possible for this dichotomy.

One possible explanation for the difference between the predicted and actual

TABLE 4-13

Peak Height and Position of Peak Maximum of CO_2-Determined Micropore Size Distributions		
Run #	Peak Height ($mm^3/A/g$)	Position of Peak Maximum (A)
Washed & Dried PSOC 190	215	6.76
33	235	6.58
34	211	6.56
35	215	6.57
36	239	6.62
37	261	6.70
38	226	6.55
39	215	6.58
40	244	6.62
41	201	6.57
42	200	6.48
43	245	6.65
44	226	6.58
45	211	6.56
46	174	6.49

results resides in the theory used to determine the distribution. In short, the problem is that the position of the maximum is too high. Differentiation of equation (2.4.40) reveals that the position of the maximum is proportional to $k^{\frac{1}{3}}$, where k is a function of the pore environment. Although the value used for k may be in error, it is not likely it is sufficiently in error to cause a shift in the position of the maximum so far beyond 5 Å. For instance, to shift the position of the maximum from 4.5 to 6.5 Å, k would have to be in error by a factor of 3, which is not likely.

A more plausible explanation for the dichotomy is that which has been stated before, namely that CO_2 is not just adsorbed on the surface of the coal as is N_2. Rather, the CO_2 actually penetrates into the solid coal matrix. Consequently, the values determined for $S_a^{CO_2}$ correspond not only to the surface area, but primarily to the permeability of the coal to CO_2. Hence, CO_2 should not be used as the adsorbate for the determination of the structural parameters of the coal for the kinetic study of the NO_2-coal reaction.

4.4 The Correlation of the Mathematical Model of the Reaction System with the Data

As mentioned in the introduction to this section, it would be fruitful to determine if the data can be correlated with a model which describes the various phenomena which take place in the NO_2/coal system. In particular, knowledge of the relationship between diffusion and kinetic effects is helpful in predicting the behavior of other coals when exposed to NO_2. For instance, if the global rate of the NO_2-coal reaction has a strong dependence on the specific surface area and pore volume, some coals may require longer exposure times than other coals to achieve the same extent of reaction.

Because it was possible to obtain rate constants for the rates of reaction of some of the coal species, namely H, N and O, the model can be used to obtain an estimate of the diffusion coefficient of NO_2 through the solid coal. Unfortunately, the data for the conversions of hydrogen, sulfur, nitrogen and oxygen do not fit the set of reactions proposed in section 2.5, namely

$$6\ NO_2\ (sol) + FeS_2\ (s) \overset{k_1}{\rightarrow} FeSO_4\ (s) + SO_2\ (sol) + 6\ NO\ (sol)\ , \quad (2.5.14a)$$

$$2\ NO_2\ (sol)\ +\ S_{org}\ (s)\ \overset{k_2}{\rightarrow}\ (SO_2)_{org}\ (sol)\ +\ 2\ NO\ (sol)\ , \quad (2.5.14b)$$

$$(CH_2)_{ali}(s) + 2\ NO_2(sol) \overset{k_3}{\rightarrow} (C{=}O)_{ali}(s) + H_2O(sol) + 2\ NO(sol), \quad (2.5.14c)$$

$$(CH)_{ar}\ (s)\ +\ NO_2\ (sol)\ \overset{k_4}{\rightarrow}\ (C{-}OH)_{ar}\ (s)\ +\ NO\ (sol)\ , \quad (2.5.14d)$$

$$(CH)_{ar}\ (s)\ +\ 2\ NO_2\ (sol)\ \overset{k_5}{\rightarrow} (C{-}NO_2)_{ar}\ (s)\ +\ HNO_2\ (sol). \quad (2.5.14e)$$

where "sol" implies the species is solvated, "ali" refers to aliphatic, "ar" refers to aromatic and "org" refers to organic. In particular, using the scheme outlined in section 2.5, the extent of reaction (2.5.14c) was almost always determined to be

negative. Because the hydrogen data are frequently quite scattered, the extent of reaction (2.5.14d) was also negative at times. Furthermore, it is not possible to determine the actual extent of the oxidation of sulfur from the analysis of the coal because it does not correlate at all with the residual sulfur content of the treated coal. Indeed, there is no indication that the organic sulfur reacts with NO_2 at all, because most of the desulfurization is achieved indirectly.

Nevertheless, the extent of reaction (2.5.14e) is easily determined from the nitrogen content of the treated coal as a function of NO_2-exposure time. Fortunately, it is just this reaction which will allow the determination of an estimate for the diffusion coefficient of NO_2 through the solid coal. It should be noted that although reaction (2.5.14e) is a convenient mnemonic device for discussing the uptake of nitrogen by the coal, there is no unequivocal evidence in this study which indicates that this reaction indeed occurs. In fact, it seems much more reasonable to expect that much of the nitrogen uptake by the coal is in the form of NO_2 absorbed by the solid matrix. In any case, because the rate constant for nitrogen uptake has already been determined, the value of the diffusion coefficient used in the model can be varied until the observed values of the net nitrogen mass increase match those predicted by the model as closely as possible.

4.4.1 The Determination of Important Input Parameters for the Model

As mentioned above, the value of the rate constant for the rate of nitrogen uptake by the coal has already been determined. The other important parameter which is needed for the model is the thickness of the slabs, $2L$, which comprise the solid coal in the idealized particle structure depicted in Figure 2–2. The value of $2L$ is established by the values of the specific surface area, $S_a^{N_2}$, the pore volume, V_p, and by the geometry of the particle. In this case, the

values obtained for these parameters employing nitrogen as the adsorbate are used. The value of $2L$ is determined as follows using one gram of coal as the basis:

1. The coal is assumed to have a constant density, ρ.
2. The void fraction, ε, of the coal is given by ρV_p. Hence, the solid fraction of the coal, ε_s, is given by 1-ε.
3. The particle is assumed to be a cube, so that the length of one side of the cube is $\rho^{-\frac{1}{3}}$ for one gram of coal.
4. The width of one slab, $\varepsilon_s x$, and adjacent void, εx, is x, and the particle consists of n slabs.
5. The surface area of one slab, s, is $2\rho^{-\frac{2}{3}} + 4\rho^{-\frac{1}{3}}\varepsilon_s x$.
6. The total surface area, S_a, is equal to ns; i.e., $S_a = n(2\rho^{-\frac{2}{3}} + 4\rho^{-\frac{1}{3}}\varepsilon_s x)$.
7. The total length encompassed by the n slabs and $n-1$ voids is $nx - \varepsilon x \approx nx$. This distance is also equal to $\rho^{-\frac{1}{3}}$. Hence, $x = \dfrac{\rho^{-\frac{1}{3}}}{n}$.
8. The number of slabs is given by $n = \frac{1}{2}\rho^{\frac{2}{3}}[S_a - 4\rho^{-\frac{2}{3}}\varepsilon_s]$.
9. Hence, the slab width is given by $2L = \varepsilon_s x = \dfrac{2}{\rho}[S_a - 4\rho^{-\frac{2}{3}}\varepsilon_s]^{-1}$.

For the PSOC 190 coal, the values used are $S_a^{N_2} = 58.06\ m^2/g$, $V_p = 0.08284\ cm^3/g$ and $\rho = 1.25\ g/cm^3$. These quantities yield a value of 2.474×10^{-6} cm for $2L$. For the PSOC 276 coal, the values used are $S_a^{N_2} = 8.60\ m^2/g$, $V_p = 0.02091\ cm^3/g$ and $\rho = 1.25\ g/cm^3$, which give a value of 1.889×10^{-5} for $2L$. It is interesting to note that the value of $2L$ for the PSOC 276 coal is a factor of 7.6 greater than that of the PSOC 190 coal, which is due to the smaller surface area and pore volume of the PSOC 276 coal. The other important parameters are determined directly from the data and are shown in Table 4–14. It should be

TABLE 4-14

Input Parameters for the Model			
Runs	33-37	42-46	47-52
Coal Type	PSOC 190	PSOC 190	PSOC 276
T (C)	20	0	20
$2L$ (cm)	2.474×10^{-6}	2.474×10^{-6}	1.889×10^{-5}
$(c_N^S)_0$ (mol N/cm^3)[1]	0.00348	0.00320	0.00352
c_0 (mol/cm^3)[2]	0.00100	0.00100	0.00100
k (cm^3/mol/s)	0.230	0.178	0.0867
ε' (cm^3 void volume/cm^3 total volume)	0.1	0.1	0.1

[1] Initial capacity of the coal to take up nitrogen.

[2] Bulk NO_2 concentration.

noted that three sets of runs are tested with the model, namely Runs 33–37 (PSOC 190 coal at 20°C), Runs 42–46 (PSOC 190 coal at 0°C) and Runs 47–52 (PSOC 276 coal at 20°C).

Finally, it is necessary to determine a value for ε', the solid void fraction (as opposed to ε, the particle void fraction). This value cannot be determined from the data obtained. Since only an estimate of the coefficient of diffusion of NO_2 into the solid matrix of the coal is needed, a value of 0.1 for ε' seems reasonable in view of the extent of nitrogen and oxygen uptake by the coal. Although it would be expected that ε' is a function of time if NO_2 absorption occurs (i.e., the NO_2 creates its own void space as it diffuses into the solid), a constant value of 0.1 is used for the sake of simplicity. A value for ε' is necessary so that the final NO_2 concentration in the solid coal matrix does not equal the bulk solvent NO_2 concentration, which is of course impossible.

4.4.2 Comparison of the Pseudo-Steady-State and Time-Dependent Solutions of the Modelling Equations

In order to establish the validity of the criterion in equation (2.5.11) which determines whether it is admissible to use the pseudo-steady-state approximation in the mathematical modelling of the system, the solutions obtained using the pseudo-steady-state and time-dependent equations can be compared. Using the values of 0.001 mol/cm^3, 0.0035 mol/cm^3 and 0.1 for $c_{NO_2}(t=0)$, $c_N(t=0)$ and ε', respectively, the value obtained for λ is 0.12, which is certainly not $<< 1$. Hence, the criterion predicts a significant deviation of the two solutions.

Both the pseudo-steady-state and time-dependent solutions were actually obtained for the conditions mentioned above. In both cases, the bulk NO_2 concentration was taken to be constant at 0.001 mol/cm^3. A preliminary comparison of the sets of equations used a value of 0.0001 cm for L, which is on the

order of the particle size and about 80 times larger than the value of L determined for the raw PSOC 190 coal. The pseudo-steady-state equations are the same as equations (2.5.12) and (2.5.13), except that the $\varepsilon' \frac{\partial \hat{C}}{\partial t}$ term is set equal to zero. Using the procedure outlined by Wen[6] in conjunction with the pore geometry assumed in this study, the solution is:

$$t(F) = t_c + \frac{\ln\xi(F)}{akc_0}\left[\frac{D_e}{D_e'} - 1\right] + \frac{\varphi F}{akc_0}\frac{D_e}{D_e'}\left[\frac{\varphi F}{2} - \frac{\xi'(F)}{\xi(F)}\right], \qquad (4.4.1)$$

$$z(t) = \frac{t}{t_c}\frac{\tanh(\varphi L)}{\varphi L} \quad \text{for } t \le t_c \text{, and} \qquad (4.4.2)$$

$$z(F) = \frac{F}{L} - \frac{\xi'(F)}{\varphi L \xi(F)} \quad \text{for } t \ge t_c \text{, and} \qquad (4.4.3)$$

$$\xi(x) = \cosh(\varphi x) - \tanh(\varphi L)\sinh(\varphi x), \quad \text{and}$$

$$\xi'(x) = \sinh(\varphi x) - \tanh(\varphi L)\cosh(\varphi x), \quad \text{where}$$

t = the reaction time (s),

$t_c = \frac{1}{akc_0}$ = the time at which the solid conversion at $x=0$ is unity,

a = the stoichiometric coefficient for the reaction between NO_2 and the coal, which in this case is taken as unity,

c_0 = the NO_2 concentration in the bulk solvent (mol/cm^3),

k = the reaction rate constant ($cm^3/mol/s$),

D_e = the effective diffusivity of NO_2 through the unreacted and partially reacted portion of the coal (cm^2/s),

D_e' = the effective diffusivity of NO_2 through the completely reacted portion of the coal (cm^2/s),

F = the position of the boundary between the completely reacted and partially reacted portions of the coal ($F=0$ for $0 \le t \le t_c$),

$\varphi = (\frac{akc_{X0}}{D_e})^{\frac{1}{2}}$ = a Thiele modulus (cm^{-1}),

c_{X0} = the initial solid substrate concentration (mol/cm^3),

$2L$ = the thickness of the coal slab (cm), and

$z = \frac{1}{L}\int_0^L \frac{c_X}{c_{X0}} dx$ = the solid substrate conversion.

For purposes of comparison, $D_e = D_e'$ in this study since the time-dependent equations only accommodate one solid diffusivity, namely $\hat{D}_s$. The pseudo-steady-state solution evolves in such a way that the position of the front, F, is a transcendental function of time, t. Consequently, a position for the front is chosen, which determines the time. The solid conversion, z, is also a function of F when $t \geq t_c$, as expressed by equation (4.4.3). When $t \leq t_c$, z is a function of t, as expressed by equation (4.4.2).

A graphical comparison of the solutions of the two sets of equations is provided in Figures 4–184, 4–185 and 4–186 for three different values of the diffusion coefficient, namely 10^{-9}, 10^{-10} and 10^{-11} cm^2/s. This range of values of D_e is common for the diffusion of small gas molecules in polymers.[7]

An examination of Figure 4–184 reveals that if $D_e = 10^{-9}$ cm^2/s, the pseudo-steady-state solution predicts a linear rise in z as t increases. Complete solid conversion occurs at about 84 minutes. The linear nature of the curve is due to the fact that t_c = 83.3 minutes. Hence, equation (4.4.2) applies when $t < 83.3$ minutes. An examination of equation (4.4.2) reveals that z is a linear function of t, which arises from the fact that diffusion is occurring in only one direction in rectangular coordinates. A solution of the time-dependent equations, however, yields a greatly different set of values of z, as evidenced by the upper curve in Figure 4–184. In particular, z rises much more rapidly, reaching a value of 0.84 within 17 minutes. At later times, z increases more slowly, reaching a value

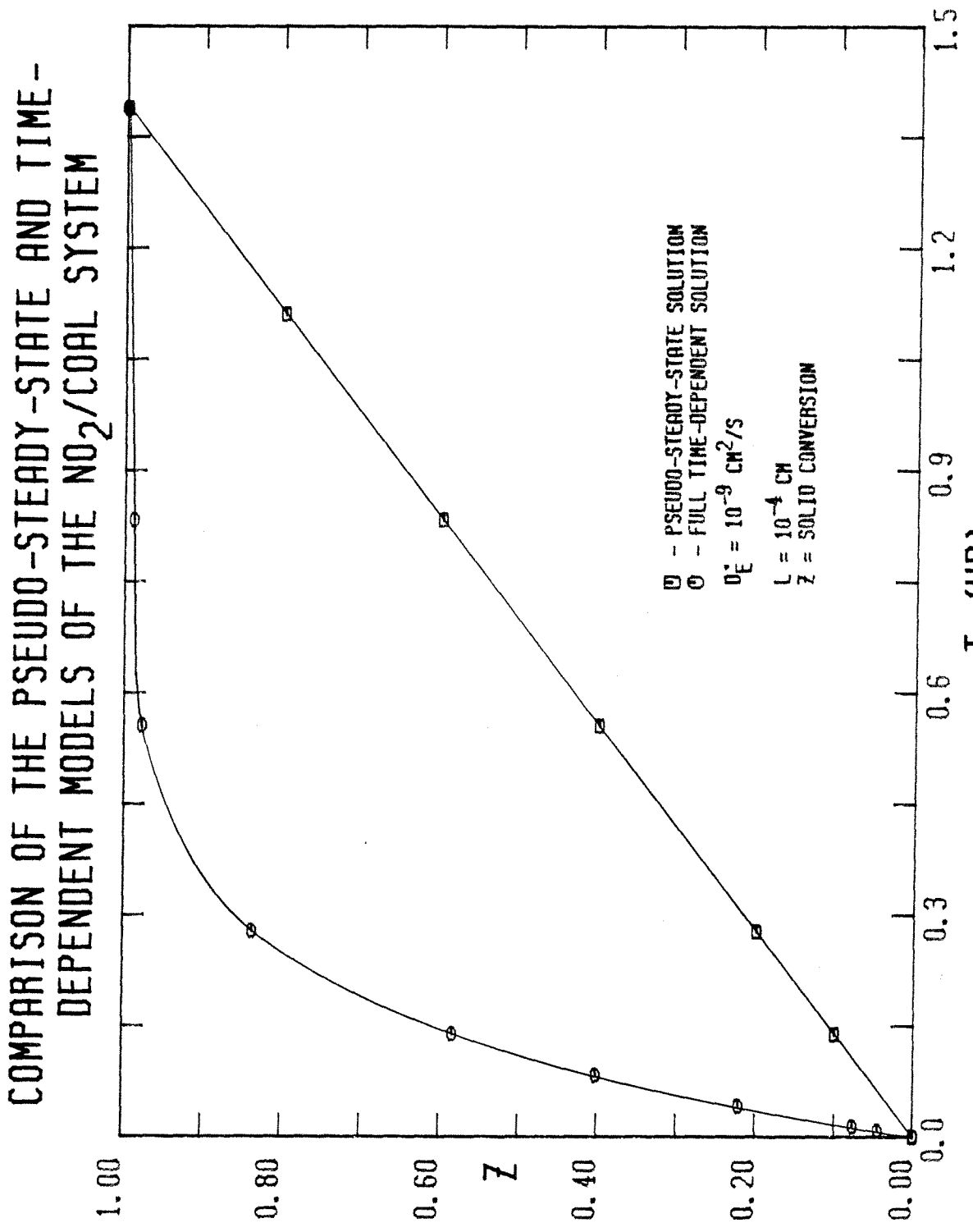
COMPARISON OF THE PSEUDO-STEADY-STATE AND TIME-DEPENDENT MODELS OF THE NO_2/COAL SYSTEM
Z
T (HR)
1.00
0.80
0.60
0.40
0.20
0.00
0.0
0.3
0.6
0.9
1.2
1.5
□ - PSEUDO-STEADY-STATE SOLUTION
○ - FULL TIME-DEPENDENT SOLUTION
$D_E' = 10^{-9}$ CM^2/S
L = 10^{-4} CM
Z = SOLID CONVERSION

FIGURE 4-184

of unity within 67 minutes. Therefore, it is obvious that the time-dependent equations must be solved under these conditions.

Figure 4–185 contains the values of z obtained from the solution of the two sets of equations with $D_e = 10^{-10}$ cm^2/s. The results are quite similar to those obtained in the previous case, although the conversion predicted by the time-dependent equations does not rise quite as rapidly as when $D_e = 10^{-9}$ cm^2/s. Hardly any change in z predicted by the pseudo-steady-state equations is discernible, however, when $D_e = 10^{-10}$ cm^2/s. In reality, however, these values are slightly lower ($\approx$ 2 %) than when $D_e = 10^{-9}$ cm^2/s. One would expect z to increase at a slower rate as D_e' decreases simply because the rate of reaction depends on c_{NO_2}. The two models predict a different degree to which z is changed by a decrease in D_e', however. In any case, the time-dependent equations must be used under these reaction conditions as well.

If D_e' is decreased further to 10^{-11} cm^2/s, the conversion predicted by the two sets of equations is that depicted by Figure 4–186. In contrast to the two previous figures, z determined by the solution of the pseudo-steady-state equations rises more rapidly than z determined by the solution of the time-dependent equations. In fact, the two curves almost coincide until t reaches about 35 minutes, at which time the two curves diverge. The conversion curve derived from the pseudo-steady-state equations continues to increase linearly until $t=t_c$=83.3 minutes, at which time z=0.818. At this point, the front between the completely reacted and unreacted zones begins to move, which results in the deviation of z from a linear dependence on t. The conversion curve derived from the time-dependent equations, on the other hand, rises much more slowly, as indicated by the lower curve in the figure. In particular, the pseudo-steady-state equations predict that the solid will have completely reacted when t = 112.5 minutes, while the time-dependent equations predict that it will take about 350

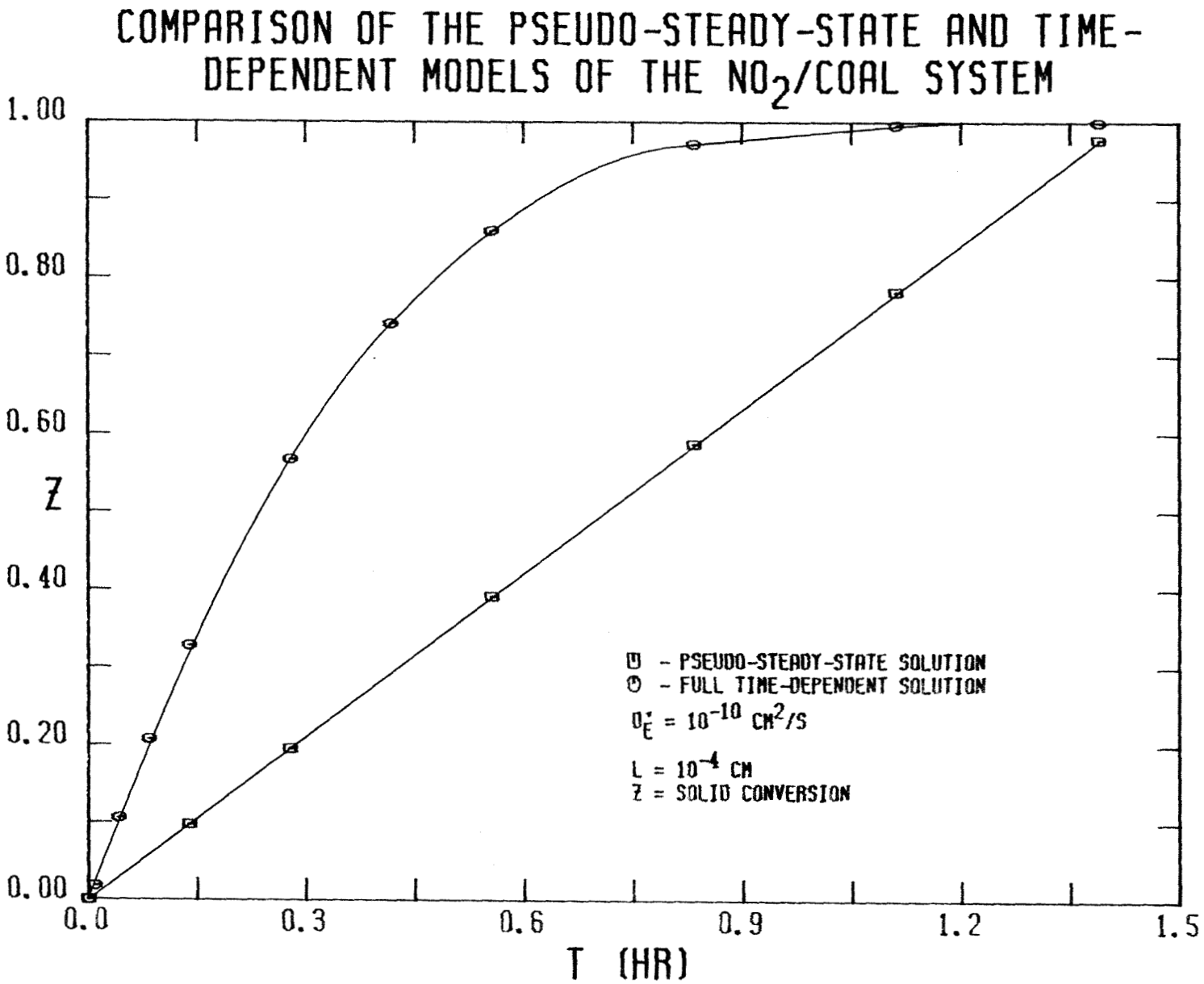
COMPARISON OF THE PSEUDO-STEADY-STATE AND TIME-DEPENDENT MODELS OF THE NO_2/COAL SYSTEM
1.00
0.80
0.60
Z
0.40
0.20
0.00
0.0
0.3
0.6
0.9
1.2
1.5
T (HR)
- PSEUDO-STEADY-STATE SOLUTION
- FULL TIME-DEPENDENT SOLUTION
$D_E^* = 10^{-10}$ CM^2/S
L = 10^{-4} CM
Z = SOLID CONVERSION

FIGURE 4-185

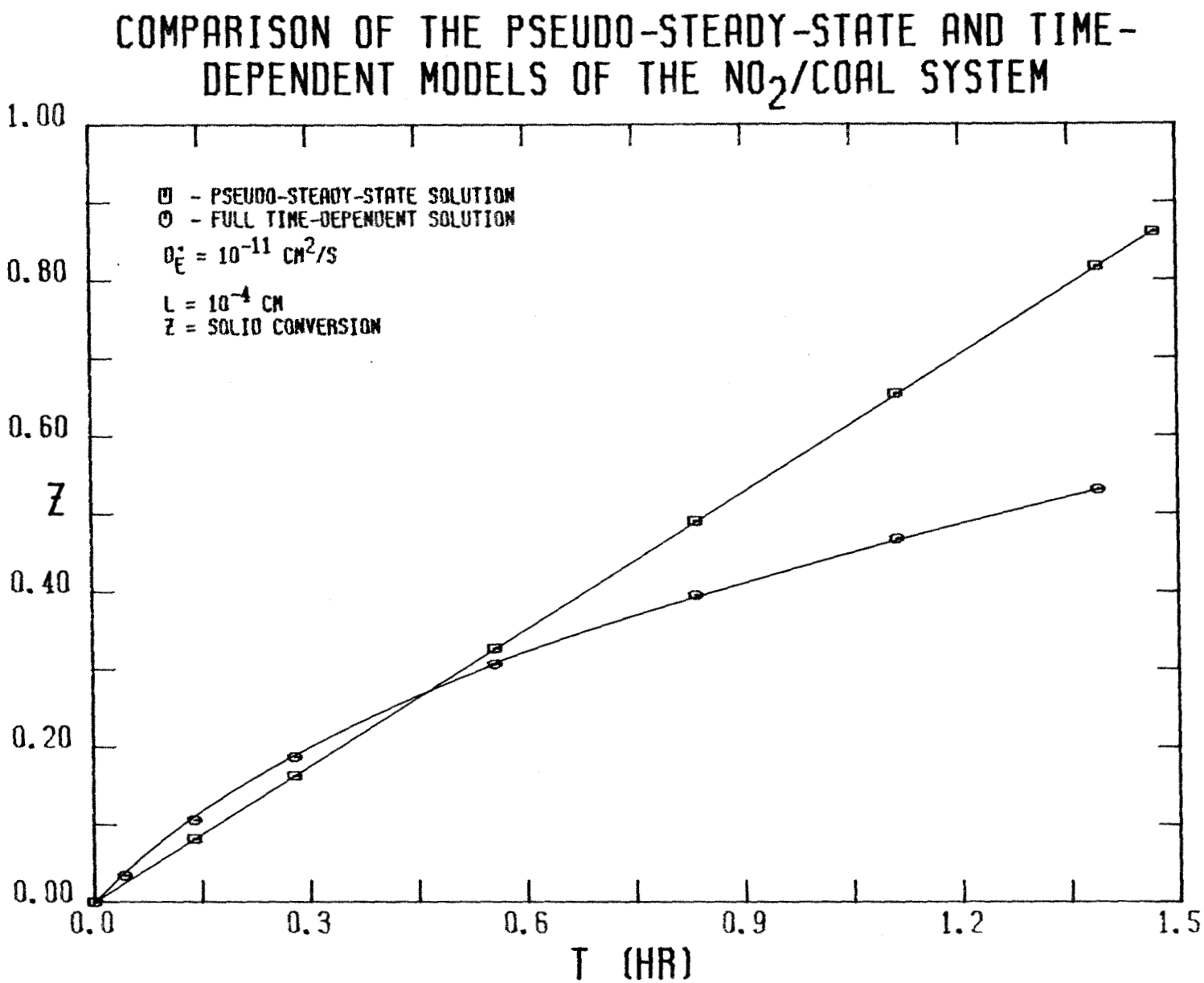
COMPARISON OF THE PSEUDO-STEADY-STATE AND TIME-DEPENDENT MODELS OF THE NO_2/COAL SYSTEM
□ - PSEUDO-STEADY-STATE SOLUTION
○ - FULL TIME-DEPENDENT SOLUTION
$D_E^* = 10^{-11}$ CM^2/S
L = 10^{-4} CM
Z = SOLID CONVERSION
Z
T (HR)
1.00
0.80
0.60
0.40
0.20
0.00
0.0
0.3
0.6
0.9
1.2
1.5

FIGURE 4-186

minutes to achieve complete conversion.

In view of the results obtained with the two sets of equations, it is obvious that the full time-dependent equations should be used for modelling the NO_2/coal system under the reaction conditions employed. It should be noted that although the value used for L in the study just discussed is about 100 times greater than the value of L determined for the PSOC 190 coal, the results obtained are still applicable because in both sets of equations, L is contained in the equations only as $\frac{D_e'}{L^2}$. Consequently, the values obtained for z with $D_e = 10^{-10}$ cm^2/s and $L = 10^{-4}$ cm are the same as those that would be obtained for z with $D_e = 10^{-14}$ cm^2/s and $L = 10^{-6}$ cm. Thus, even though the value of L used in this comparison of the pseudo-steady-state and time-dependent equations is much larger than the actual value of L which pertains to the PSOC 190 coal, the conclusion is still valid, namely the full time-dependent equations must be solved. This result is consistent, then, with the criterion established by Wen which was discussed at the beginning of this section.

4.4.3 Comparison of the Predicted Nitrogen Conversion in the Coal with the Actual Data

As mentioned previously, the actually observed data were not consistent with the set of five proposed NO_2-coal reactions. Furthermore, the data for hydrogen loss and oxygen uptake in the coal contained quite a bit of scatter. Consequently, the only data which can be compared with the model with any confidence are those of the nitrogen uptake by the coal. Since each of the proposed reactions is independent of the others except for their possible dependence on the NO_2 concentration, however, only the nitrogen uptake reaction needs to be used in the model to obtain an order of magnitude estimate for the diffusion coefficient of NO_2 in the solid coal matrix. Consequently, the nitrogen uptake data for the PSOC 190 coal treated with NO_2 in CCl_4 at 0 and 20°C as well

as that for the PSOC 276 coal treated with NO_2 in CCl_4 at 20°C are compared with the predictions of the model to arrive at an estimate for the diffusion coefficient.

The first set of reactions to be examined was that of the PSOC 190 treated with NO_2 in CCl_4 at 20°C (Runs 33–37). Using the values for the model parameters shown in Table 4–14, three different values for the diffusion coefficient, namely 10^{-14}, 10^{-15} and 10^{-16} cm^2/s, were employed in solving the model equations. The results are shown in Figure 4–187, where the nitrogen conversion in the coal, z, is displayed as a function of reaction time. The nitrogen conversion is simply the normalized nitrogen uptake by the coal. The actually observed data are also shown in the figure as the dashed curve. Examination of the figure reveals that the actual data coincide most closely with the model curve generated by using a value of 10^{-15} cm^2/s for the diffusion coefficient. Indeed, the slight difference in shape between these two curves may be due to the fact that the model assumes a constant NO_2 concentration, c_0, in the bulk CCl_4 of 1.0 F while in reality the concentration drops from 1.1 to 0.7 F during the course of the reaction. If this change in c_0 could be incorporated into the model, the shape of the predicted conversion curve would more closely resemble that obtained from the real data, mainly because as c_0 drops, the flux of NO_2 into the coal drops, which would result in less nitrogen uptake by the coal. In any event, it appears that a good estimate for the diffusion coefficient of NO_2 in the solid coal matrix as obtained by the model is 10^{-15} cm^2/s. Although this value is several orders of magnitude less than that obtained for the diffusion of gases such as N_2, O_2, CO and CO_2 in polymers (on the order of 10^{-8} to 10^{-10} cm^2/s)[7], it is not that unreasonable. After all, if there were no solid penetration, the diffusion coefficient would be zero. Hence, the value obtained indicates that penetration of the solid coal does not occur as easily as

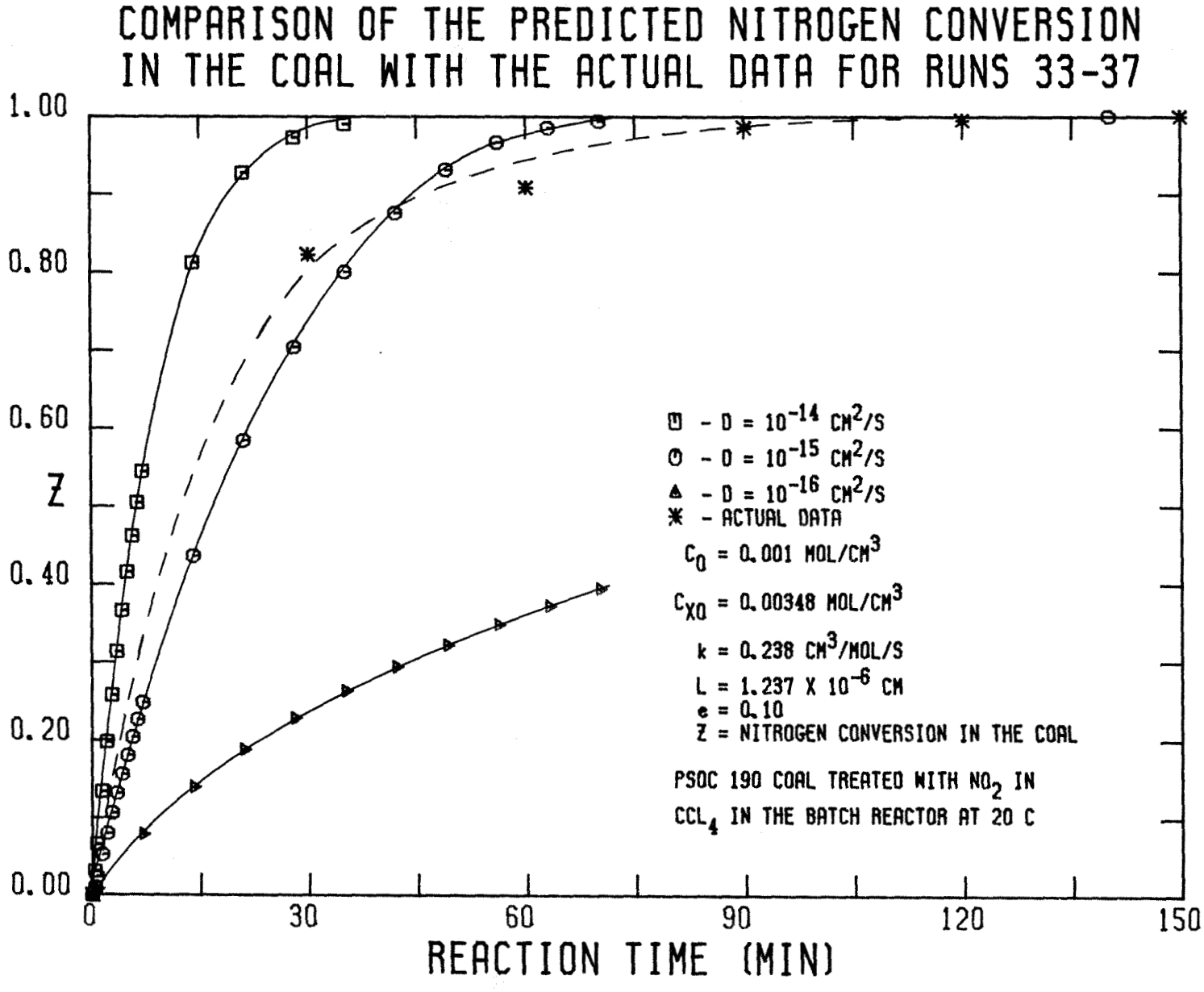
COMPARISON OF THE PREDICTED NITROGEN CONVERSION
IN THE COAL WITH THE ACTUAL DATA FOR RUNS 33-37
1.00
0.80
0.60
0.40
0.20
0.00
Z
0
30
60
90
120
150
REACTION TIME (MIN)
□ - D = 10^-14 CM^2/S
○ - D = 10^-15 CM^2/S
△ - D = 10^-16 CM^2/S
✱ - ACTUAL DATA
C0 = 0.001 MOL/CM^3
CX0 = 0.00348 MOL/CM^3
k = 0.238 CM^3/MOL/S
L = 1.237 X 10^-6 CM
e = 0.10
Z = NITROGEN CONVERSION IN THE COAL
PSOC 190 COAL TREATED WITH NO2 IN
CCL4 IN THE BATCH REACTOR AT 20 C

FIGURE 4-187

it might in a synthesized polymer. This difference in permeabilities may be attributed to two factors. First, the coal matrix may not be as flexible as that of a polymer in terms of NO_2 penetration. Secondly, the very nature of the NO_2 molecule may inhibit its ability to diffuse into coal and polymers as easily as other gases such as N_2, CO or CO_2. Consequently, a comparison of the value for the NO_2 diffusion coefficient in coal obtained in this study with those obtained for other gases in polymers may possess its own inherent faults. Indeed, a comparison of the CO_2 adsorption studies with the nitrogen uptake results indicates that CO_2 does penetrate the coal much more easily than NO_2, provided the CO_2-absorption theory previously postulated is true.

The values of the average dimensionless NO_2 concentration in the solid coal matrix, c/c_0, as predicted by the model are presented in Figure 4–188. The three curves shown correspond to the three curves in the previous figure. The values of c/c_0 were obtained by integrating the NO_2 concentration over the slab, that is:

$$\frac{c}{c_0} = \frac{1}{L}\int_0^L \frac{c(x)}{c_0}dx = \frac{1}{N}\sum_{i=1}^{N}\frac{c_i}{c_0}, \quad \text{where} \qquad (4.4.4)$$

L = the slab thickness (cm),

$\frac{c(x)}{c_0}$ = the dimensionless NO_2 concentration at x,

$\frac{c_i}{c_0}$ = the dimensionless NO_2 concentration at point i in the slab, and

N = the total number of grid points in the slab.

It is interesting to note that the range of diffusion coefficients examined with the model (10^{-14} to 10^{-16} cm^2/s) produce curves for c/c_0 which cover the spectrum from very rapid attainment of a uniform NO_2 concentration in the coal slab (10^{-14} cm^2/s) to incomplete attainment of a uniform NO_2 concentration in

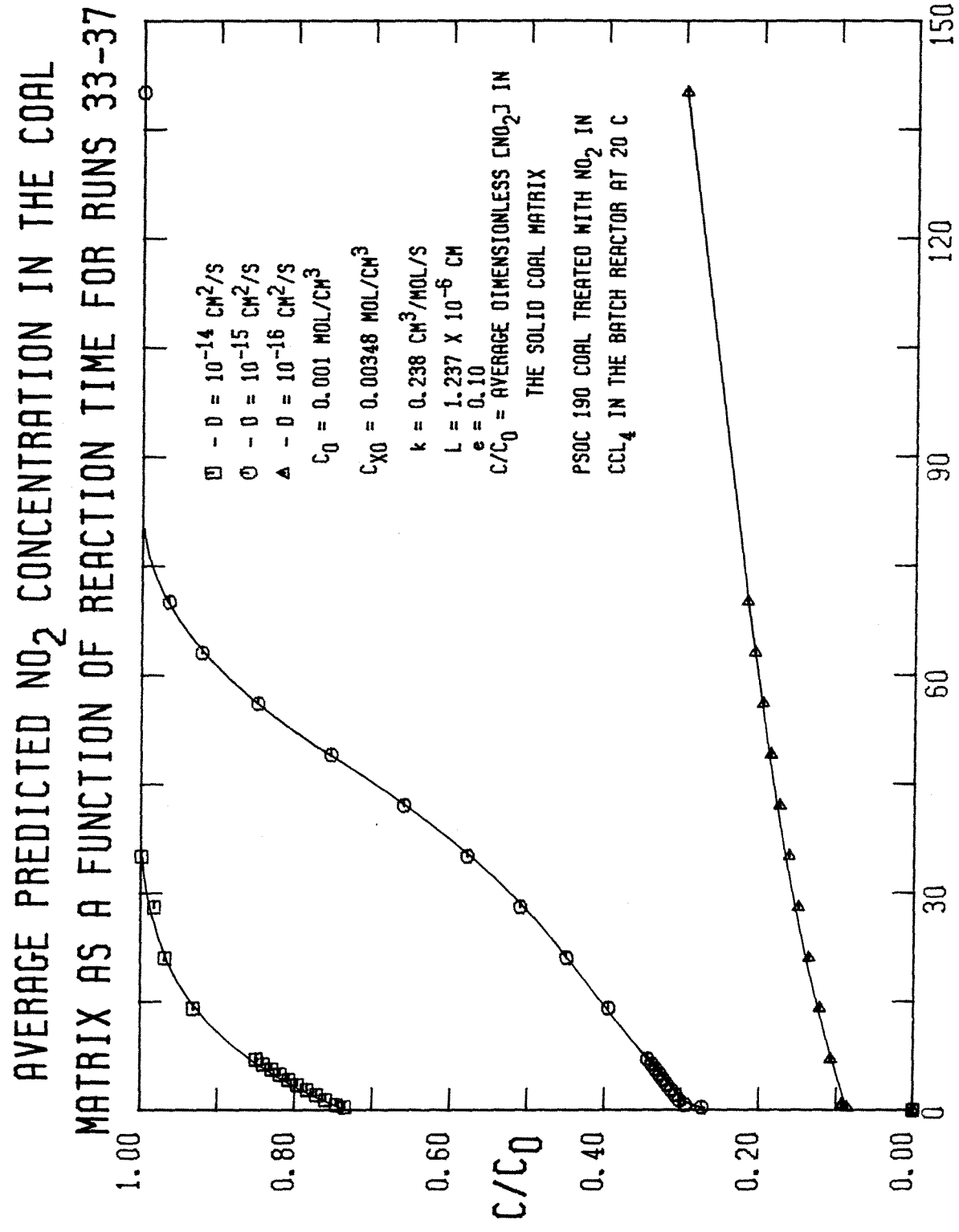
AVERAGE PREDICTED NO_2 CONCENTRATION IN THE COAL MATRIX AS A FUNCTION OF REACTION TIME FOR RUNS 33-37
□ - D = 10^{-14} CM^2/S
○ - D = 10^{-15} CM^2/S
△ - D = 10^{-16} CM^2/S
C_0 = 0.001 MOL/CM^3
C_{XO} = 0.00348 MOL/CM^3
k = 0.238 CM^3/MOL/S
L = 1.237 X 10^{-6} CM
e = 0.10
C/C_0 = AVERAGE DIMENSIONLESS [CNO_2] IN THE SOLID COAL MATRIX
PSOC 190 COAL TREATED WITH NO_2 IN CCL_4 IN THE BATCH REACTOR AT 20 C
C/C0
REACTION TIME (MIN)
1.00
0.80
0.60
0.40
0.20
0.00
0
30
60
90
120
150

FIGURE 4-188

the coal slab (10^{-16} cm^2/s) within the maximum reaction time of 180 minutes used in this study. It is also interesting to note that the middle curve, which corresponds to the value of the diffusion coefficient, D, which best matches the actual data of 10^{-15} cm^2/s, has a distinct sigmoidal shape. This shape is the result of the fact that the nitrogen conversion in the coal slab reaches unity before the NO_2 concentration in the slab reaches its maximum. As the rate of reaction decreases, then, the rate of increase in c/c_0 increases, resulting in the sigmoidal shape observed. It should be noted that the model assumes that all of the NO_2 in the coal slab relating to c/c_0 is removed by the vacuum drying so that the only nitrogen left in the coal is that which has "reacted", as indicated by z. If this is not the case, however, then the diffusion coefficient which best correlates with the data would not be altered significantly from the value of 10^{-15} cm^2/s, because the complete saturation of the coal with nitrogen represents a nitrogen concentration of 0.00348 mol/cm^3 while a value of unity for c/c_0 corresponds to a nitrogen concentration in the coal of only 0.0001 mol/cm^3 (εc_0). Hence, inclusion of c/c_0 in the total nitrogen uptake by the coal would only change the values of z shown in Figure 4–191 by about 3 %, which is well within the other errors introduced into the model by the assumptions.

The set of experiments in which the PSOC 190 coal was treated with NO_2 in CCl_4 at 0°C (Runs 42–46) was examined as well. The parameters listed in Table 4–14 which pertain to these runs were employed in the model simulation. In particular, all of the parameters were the same as in the previous set of runs, except the values of k (0.178 $cm^3/mol/s$) and c_{X0} (0.00320 mol/cm^3). The same three values of 10^{-14}, 10^{-15} and 10^{-16} cm^2/s were used for the diffusion coefficient. The results are shown in Figure 4–189, in which the normalized nitrogen uptake of the coal, z, is plotted as a function of reaction time. An examination of the figure quickly reveals that as in the previous case, the actual

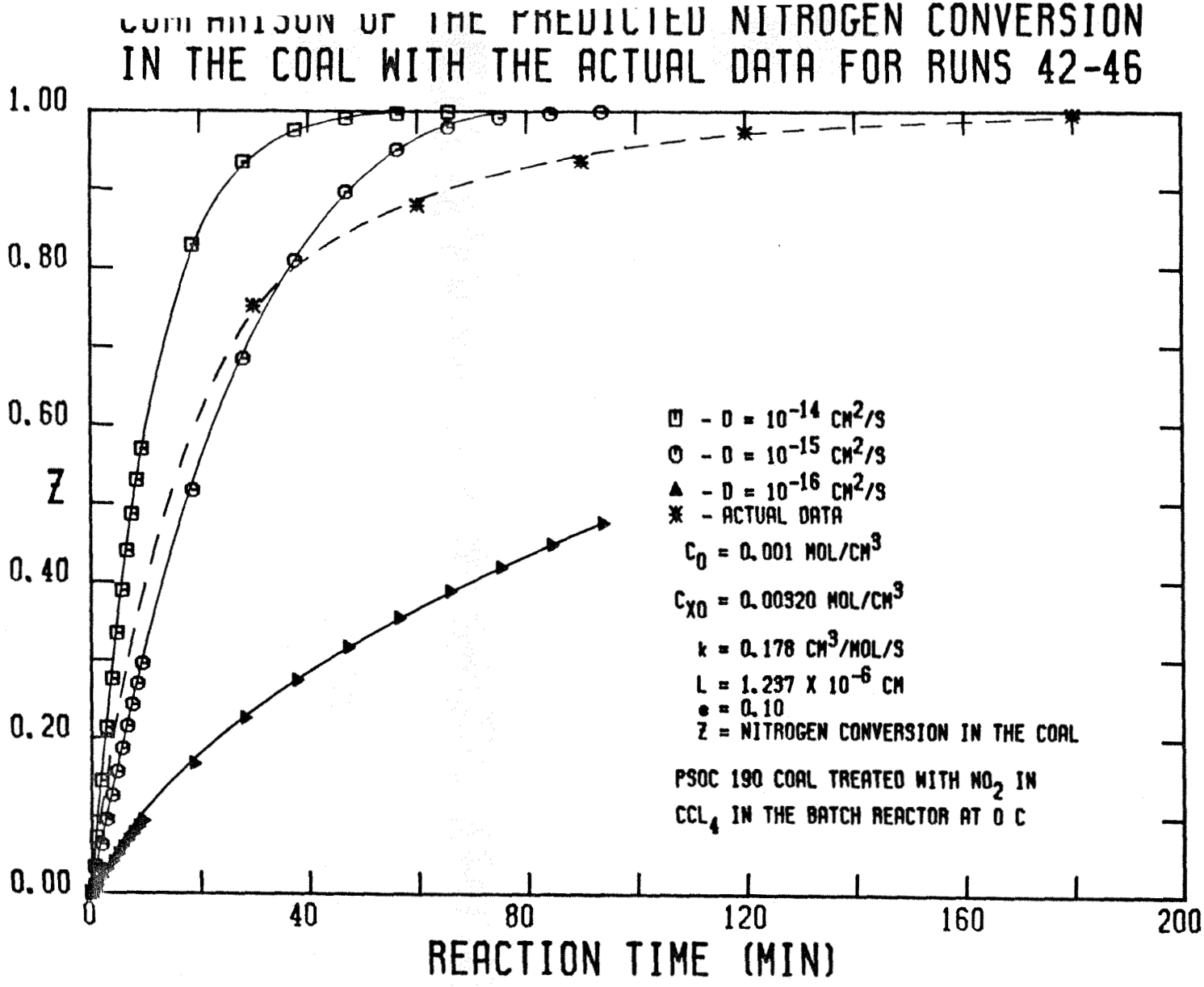
COMPARISON OF THE PREDICTED NITROGEN CONVERSION
IN THE COAL WITH THE ACTUAL DATA FOR RUNS 42-46
1.00
0.80
0.60
Z
0.40
0.20
0.00
0
40
80
120
160
200
REACTION TIME (MIN)
□ - D = 10^-14 CM^2/S
○ - D = 10^-15 CM^2/S
▲ - D = 10^-16 CM^2/S
✱ - ACTUAL DATA
C0 = 0.001 MOL/CM^3
CX0 = 0.00320 MOL/CM^3
k = 0.178 CM^3/MOL/S
L = 1.237 X 10^-6 CM
e = 0.10
Z = NITROGEN CONVERSION IN THE COAL
PSOC 190 COAL TREATED WITH NO2 IN
CCL4 IN THE BATCH REACTOR AT 0 C

FIGURE 4-189

data correlate quite well with the curve for z predicted by the model with $D = 10^{-15}$ cm^2/s. This result is not surprising because the difference in the data between the two temperatures of 0 and 20°C, while it is slight, is nevertheless accounted for by the change in the rate constants. At both temperatures, most of the reaction is complete within the first 30 minutes, which the model adequately predicts in both cases when $D \geq 10^{-15}$ cm^2/s. The same arguments presented in the previous case regarding the discrepancy in the shapes of the conversion curves of the actual data and the model prediction apply in this case as well.

The values of the average NO_2 concentration in the solid coal matrix, c/c_0, which correspond to the values of z discussed above are shown graphically in Figure 4–190. Just as in the previous case, the curve generated by the model when $D = 10^{-15}$ cm^2/s shows a sigmoidal shape. As before, this shape can be attributed to the fact that z reaches unity before c/c_0 does. Consequently, as the rate decreases as z approaches unity, c/c_0 should begin to increase at a greater rate, which leads to the sigmoidal shape observed.

It is interesting to note that at both 20 and 0°C, the diffusion coefficient seems to be pretty much the same. Even though the difference in the absolute temperature is small, the effect on the diffusion coefficient can be substantial because the coefficient of diffusion in solids generally follows an exponential dependence on the temperature:[6]

$$D = D_0 \exp\left(-\frac{E}{RT}\right), \quad \text{where} \tag{4.4.5}$$

D_0 = a pre–exponential constant (cm^2/s),

E = an activation energy for diffusion (cal/mol),

R = 1.9872 cal/mol/K, and

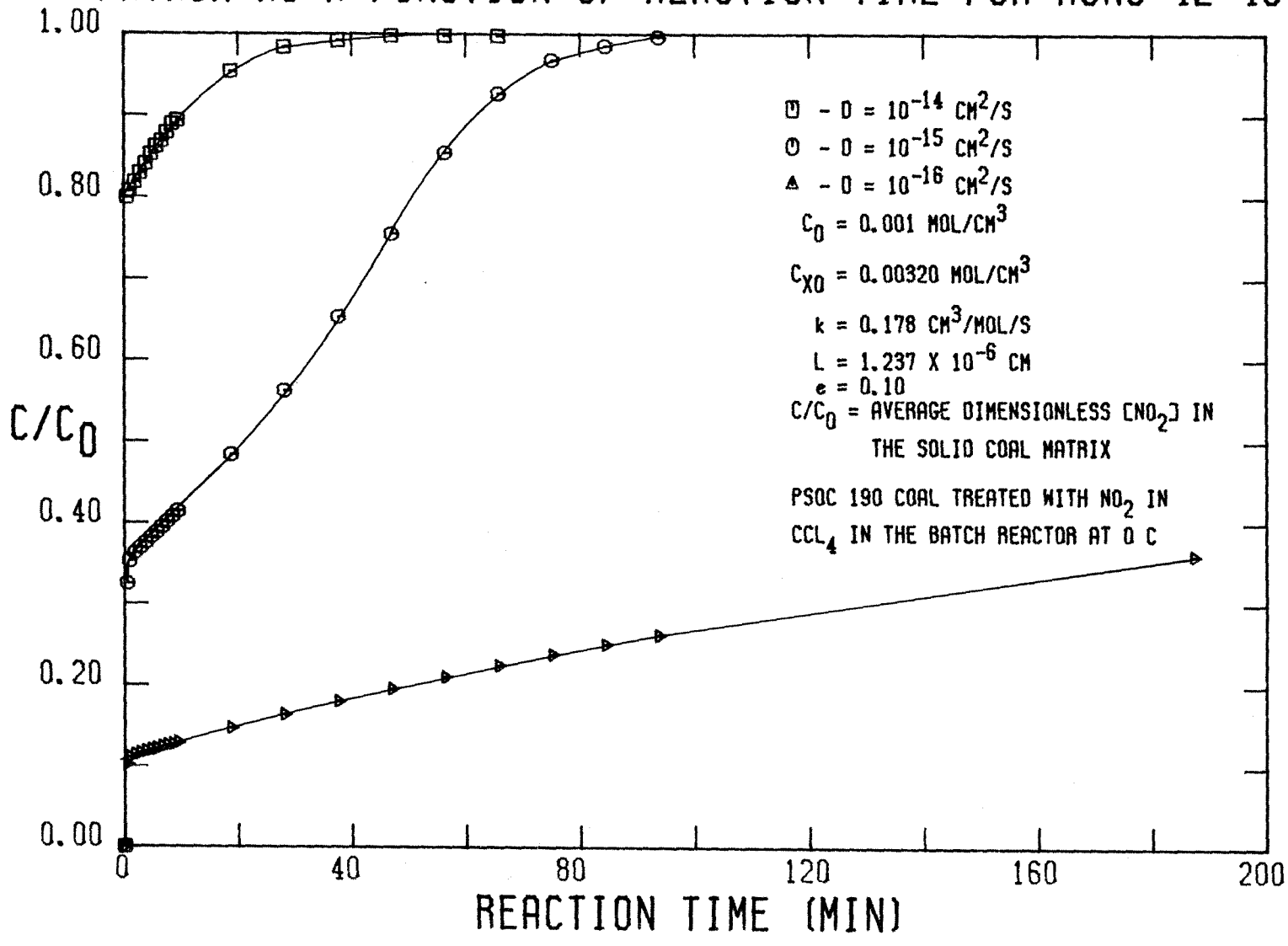
AVERAGE PREDICTED NO_2 CONCENTRATION IN THE COAL MATRIX AS A FUNCTION OF REACTION TIME FOR RUNS 42-46
1.00
0.80
0.60
0.40
0.20
0.00
C/C0
0
40
80
120
160
200
REACTION TIME (MIN)
□ - D = 10^{-14} CM^2/S
○ - D = 10^{-15} CM^2/S
△ - D = 10^{-16} CM^2/S
C_0 = 0.001 MOL/CM^3
C_{XO} = 0.00320 MOL/CM^3
k = 0.178 CM^3/MOL/S
L = 1.237 X 10^{-6} CM
e = 0.10
C/C_0 = AVERAGE DIMENSIONLESS [NO_2] IN THE SOLID COAL MATRIX
PSOC 190 COAL TREATED WITH NO_2 IN CCL_4 IN THE BATCH REACTOR AT 0 C

FIGURE 4-190

T = the temperature (K).

Therefore, unless E is rather small (< 100 cal), the change in D from 20 to 0°C can exceed several percent. For instance, if E = 1000 cal, $\frac{D^{273K}}{D^{293K}}$ = 0.88 and if E = 10,000 cal, $\frac{D^{273K}}{D^{293K}}$ = 0.28. There is no manner in which to independently estimate the activation energy for diffusion of NO_2 into the coal, however.

It should be noted, however, that a difference does exist in the values determined for k at the two temperatures. Furthermore, these rate constants correspond to the *global* rate of nitrogen uptake by the coal. Consequently, if diffusion limitations affect the global rate, these effects would be incorporated into the rate constant. Indeed, it has already been established in the earlier section concerning the nitrogen uptake by the coal that diffusion does control the overall rate of NO_2 disappearance during the first 15 to 30 minutes of the reaction, after which time the kinetics control the rate. Nevertheless, the rate of nitrogen uptake by the coal does obey first order kinetics over the entire range of reaction times with a remarkable degree of correlation. It is interesting to note that the rate constant, k, should obey an Arrhenius type of equation just like (4.4.5). Hence, if it is assumed that D is the same at both 273 and 293°K, and that k can be expressed as

$$k = k_0 \exp(-\frac{E_r}{RT}), \quad \text{where} \tag{4.4.6}$$

k_0 = a pre-exponential constant ($cm^3/mol/s$),

E_r = an activation energy for reaction (cal/mol),

R = 1.9872 cal/mol/K, and

T = the temperature (K),

then the two values of k at 273 and 293°K can be used to obtain values for k_0

and E_r. Those values are k_0 = 12.6 $cm^3/mol/s$ and E_r = 2,310 cal/mol. In fact, because k may include diffusional effects, it may be more appropriate to consider E_r as an activation energy for diffusion and reaction.

On the other hand, if it is assumed that the variation in the observed values of k are due solely to diffusional effects, then a value for the energy of activation for diffusion can be obtained. Using the theory of effectiveness factors, when diffusional resistances predominate, the rate is proportional to $\frac{1}{L}(\frac{D}{k_r})^{\frac{1}{2}}$, where L is the slab thickness and k_r is the true reaction rate constant, which is now assumed to be temperature independent. Since the rate is also proportional to k, then

$$\frac{k(T_1)}{k(T_2)} = [\frac{D(T_1)}{D(T_2)}]^{\frac{1}{2}} = [\frac{E}{R}(\frac{1}{T_2} - \frac{1}{T_1})]^{\frac{1}{2}}. \qquad (4.4.7)$$

Using this expression, a value for E of 14.2 kcal/mol is obtained. Unfortunately, it is not possible to determine the relative contributions of diffusional resistance and kinetic limitations to the overall rate. Furthermore, as the previous discussion indicates, the influence of these two factors changes during the course of the reaction. Initially, the rate of NO_2 diffusion into the solid coal matrix governs the rate while after 30 minutes, the rate of reaction governs the overall rate.

The final set of runs examined with the model concerns the PSOC 276 coal treated with NO_2 in CCl_4 at 20°C (Runs 47–52). The parameters listed in Table 4–14 which pertain to these runs were used in the simulation with one exception. Instead of using the value for k of 0.0867 $cm^3/mol/s$ listed in Table 4–14, the value listed for the rate constant for the PSOC 190 coal of 0.238 $cm^3/mol/s$ was used. Because the two coals behave in such a similar manner in all other respects, it seems reasonable to expect that they would possess the same rate

constant for nitrogen uptake. If such is the case, then the difference actually observed in the rate constants can be attributed to the difference in their respective surface areas and void fractions, which is reflected in the model as the slab thickness, L. The value of L for the PSOC 276 coal is 7.6 times that of the PSOC 190 coal. Therefore, if the difference in the rate constants is due to the difference in the pore structure, the use of the same value of k for both coals should yield the same value for the diffusion coefficient, D.

The values of z predicted by the model are shown in Figure 4–191, along with the actually observed data. The values of the average NO_2 concentration in the solid coal matrix as predicted by the model are shown in Figure 4–192. As in the previous cases, the same behavior is observed, except the values of D are greater. Referring to Figure 4–191, it can be seen that the actual data fall between the two curves corresponding to values of 10^{-13} and 10^{-14} cm^2/s for D. Thus, the value of D in the PSOC 276 coal is about 5×10^{-14} cm^2/s, which is about 50 times that of D in the PSOC 190 coal.

Nevertheless, it seems unlikely that the diffusion coefficient for two very similar coals should differ by a factor of 50. The reason that D for the PSOC 276 coal must be 50 times that of the PSOC 190 coal is that the actual conversions for the two coals are quite similar but the value of L for the PSOC 276 coal is 7.6 times that of the PSOC 190 coal. On this basis, much longer times would be needed for the PSOC 276 coal to reach the same conversion as the PSOC 190 coal if both coals had the same value of D. Consequently, it may be that the values obtained for L have no real physical significance. Indeed, the assumed pore geometry may not even apply. It should be noted that the value of L is obtained from the nitrogen adsorption results. If, on the other hand, the results of the CO_2 adsorption studies were more applicable, then the values of L for the two coals would be just about equal. In any event, more data concerning

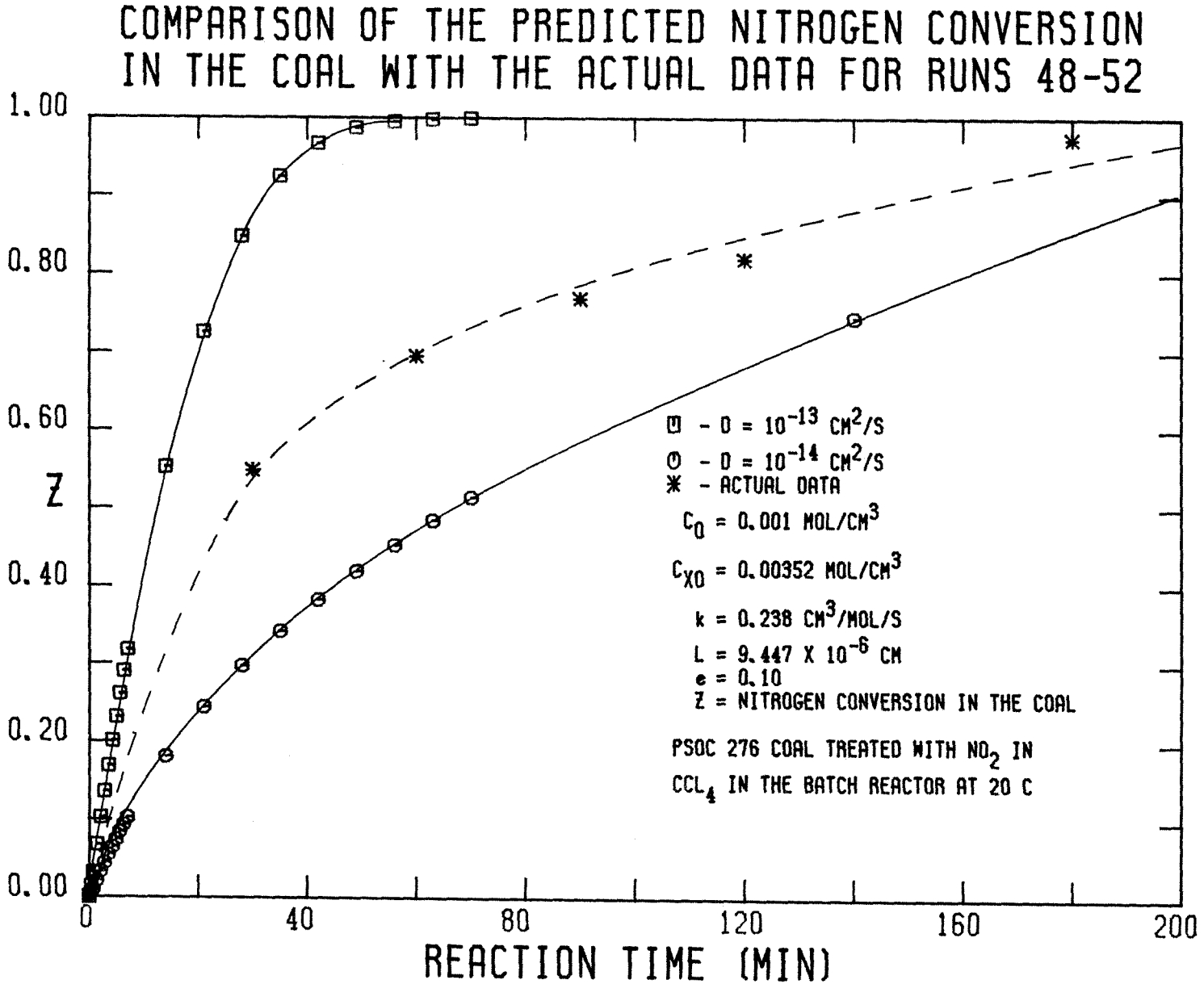
COMPARISON OF THE PREDICTED NITROGEN CONVERSION
IN THE COAL WITH THE ACTUAL DATA FOR RUNS 48-52
1.00
0.80
0.60
0.40
0.20
0.00
Z
0
40
80
120
160
200
REACTION TIME (MIN)
- D = 10^-13 CM^2/S
- D = 10^-14 CM^2/S
- ACTUAL DATA
C0 = 0.001 MOL/CM^3
CX0 = 0.00352 MOL/CM^3
k = 0.238 CM^3/MOL/S
L = 9.447 X 10^-6 CM
e = 0.10
Z = NITROGEN CONVERSION IN THE COAL
PSOC 276 COAL TREATED WITH NO2 IN
CCL4 IN THE BATCH REACTOR AT 20 C

FIGURE 4-191

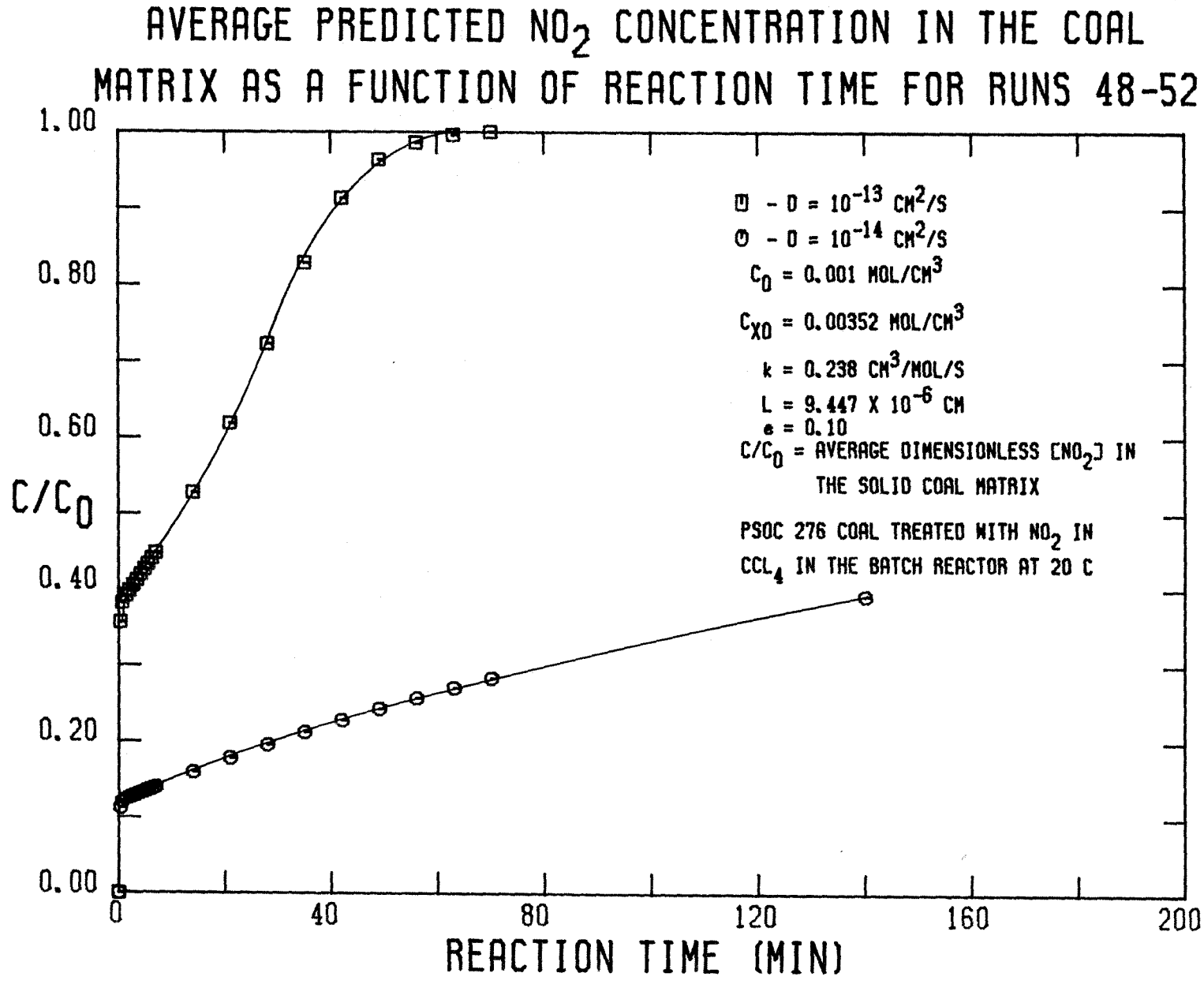
AVERAGE PREDICTED NO_2 CONCENTRATION IN THE COAL MATRIX AS A FUNCTION OF REACTION TIME FOR RUNS 48-52
1.00
0.80
0.60
0.40
0.20
0.00
C/C0
0
40
80
120
160
200
REACTION TIME (MIN)
□ - D = 10^{-13} CM^2/S
○ - D = 10^{-14} CM^2/S
C_0 = 0.001 MOL/CM^3
C_{X0} = 0.00352 MOL/CM^3
k = 0.238 CM^3/MOL/S
L = 9.447 X 10^{-6} CM
e = 0.10
C/C_0 = AVERAGE DIMENSIONLESS [NO_2] IN THE SOLID COAL MATRIX
PSOC 276 COAL TREATED WITH NO_2 IN CCL_4 IN THE BATCH REACTOR AT 20 C

FIGURE 4-192

the geometry of the pore structure of various coals are needed in order to gain confidence for either accepting the model or discarding it. Alternatively, different pore geometries can be employed by the model to determine if better agreement in the values of D for the two coals can be obtained.

References

1. Abel, E., Schmid, H., *Z. physik. Chem.*, **132,** 56, 64 (1928); **134,** 279 (1928); **136,** 135, 419, 430 (1928).

2. Chambers, F.S., Sherwood, T.K., *Ind. Eng. Chem.*, **29,** 1415 (1931); *J. Am. Chem. Soc.*, **59,** 316 (1937).

3. Denbigh, K.G., Prince, A.J., *J. Chem. Soc.*, 790 (1947).

4. Levenspiel, O., *Chemical Reaction Engineering*, Second Edition, (John Wiley and Sons, New York, New York, 1972) p. 490.

5. Anderson, R.B., et. al., *J. Phys. Chem.*, **60,** 1548 (1956).

6. Wen, C.Y., *Ind. Eng. Chem.*, **60**(9), 34 (1968).

7. Crank, J., Park, G.S., *Diffusion in Polymers*, (Academic Press, New York, New York, 1968) p. 69.

8. Barrer, R.M., *Diffusion In and Through Solids*, (Cambridge University Press, Cambridge, England, 1951) p. 283.

CHAPTER 5

Conclusions and Recommendations

The first section of this chapter summarizes the conclusions reached as a result of the discussion in the previous chapter. In particular, the significant effects on the elemental composition of the coal by the NO_2 treatment and subsequent Na_2CO_3 (aq) wash are presented, followed by a discussion of the changes in the pore structure induced by the NO_2 treatment as revealed by the N_2 and CO_2 adsorption studies. Then the salient features of the model simulation of the reaction of NO_2 with the coal are discussed. Finally, all of these results are linked together to formulate a plausible mechanism for the NO_2-coal reaction.

5.1 Conclusions

5.1.1 The Effect of the Processing on the Elemental Composition of the Coal

Exposure of the coal to NO_2 results in several changes in the elemental composition of the coal. While none of the changes are drastic, some of them possess significant ramifications, particularly in terms of the removal of SO_2 from the combustion gases of the coal. At the outset, it should be noted that the coal was slurried in a liquid phase, which served as a transport medium for the NO_2, in order to mitigate the heating value losses in the coal due to the excessive oxidation of the coal which occurs when the coal is treated with gaseous NO_2. The best liquid for the purposes of this study was determined to be CCl_4 because it did not react with either the NO_2 or the coal. Although H_2O is much cheaper and easier to handle than CCl_4, it competes with the coal for NO_2 to form HNO_3 (aq) and HNO_2 (aq), which nevertheless do attack the coal. The kinetic analysis becomes rather difficult, however. The use of aromatic solvents, such as pyridine and nitrobenzene, was found to extract significant amounts of the coal

(55 % of the PSOC 190 was extracted when treated with NO_2 in nitrobenzene at 80°C). Furthermore, these solvents were rather difficult to separate from the coal after the NO_2 treatment.

One interesting feature of the elemental analysis is that there is very little loss in carbon during the NO_2 treatment when the coal was treated with NO_2 in CCl_4 in the batch reactor at 0 and 20°C. Furthermore, the subsequent Na_2CO_3 (aq) wash results in a loss of only 3 to 7 % in the carbon content. Use of CCl_4 as the liquid phase at 25 C under much higher NO_2 concentrations (8 F vs. 1.1 F in the batch reactor), however, results in a greater carbon loss of 10 % during the NO_2 treatment and 26 % during the subsequent Na_2CO_3 (aq) wash. Consequently, it was determined that NO_2 concentrations on the order of 1 F and reaction temperatures no greater than roughly 25°C should be used in order to mitigate carbon losses.

The coal hydrogen, on the other hand, is readily attacked by NO_2. When the coal is treated with NO_2 at high concentration (8 F) at 25°C in CCl_4, 20 % of the hydrogen is rapidly lost. The subsequent Na_2CO_3 (aq) wash results in a total hydrogen loss of 27 %. Milder conditions do not alleviate the hydrogen loss. For instance, NO_2 treatment (1.1 F) at 20°C in CCl_4 in the batch reactor still results in a 22 % loss in hydrogen. The subsequent Na_2CO_3 (aq) wash does not result in any additional hydrogen loss, however. Interestingly, the same NO_2 treatment at 0°C results in only a 4 % hydrogen loss, but the wash at 25°C results in a total hydrogen loss of 16 %. It is interesting to note that the PSOC 276 coal only suffers about half the hydrogen loss of the PSOC 190 coal when treated with NO_2 at 20°C. The NO_2 treatment results in a 6 % loss and the wash yields an overall loss of 12 %. The difference in the hydrogen losses of the two coals can be attributed to their respective pore structures. The PSOC 276 coal initially has only one-sixth the surface area of the PSOC 190 coal. Although the pore volume does

not affect the amount of NO_2 which diffuses into the coal to a discernible extent, it does affect the transfer of the oxidized coal products out of the coal. In any case, about 20 % of the coal hydrogen is rapidly attacked by NO_2 under all of the reaction conditions used in this study.

The fact that the pore structure does not affect the amount of NO_2 which diffuses into the coal is supported by the nitrogen analysis of the treated coal. Under all of the conditions used in this study, the net nitrogen mass increase in the coal varied from 3.6 (g N/100 g untreated coal) at 0°C to 5.2 (g N/100 g untreated coal) at 50°C. There are several interesting features concerning the nitrogen analysis. The first feature is that both the PSOC 190 and PSOC 276 have the same ultimate net nitrogen mass increase of 3.9 (g N/100 g untreated coal), despite the difference in their pore volumes. The second feature is that the Na_2CO_3 (aq) wash, which is always conducted at 25°C for 2 hours, consistently removes between 15 and 21 % of the added nitrogen in all of the experiments conducted. These two observations imply that neither the pore structure nor the coal type influences the capacity of the coal to take up nitrogen. Rather, the coal behaves as a second phase in the NO_2/CCl_4/coal system. During the NO_2 treatment, the NO_2 seeks to establish a partition equilibrium between the coal phase and the CCl_4 phase. Indeed, the study of the effect of the initial NO_2 concentration on the nitrogen content of the coal shows that the data obey the simple expression for the partition coefficient, K, of

$$K = \frac{c_N - c_N^*}{(NO_2)}, \quad \text{where}$$

K = the partition coefficient,

c_N = the nitrogen content of the coal (mass % N),

c_N^* = the nitrogen content of the coal as $(NO_2) \rightarrow 0$ (mass % N), and

(NO_2) = the bulk NO_2 concentration in the solvent (F).

The data yield a value for c_N^* of 3.82 mass % N and a value for K of 0.814 (mass % N–l/mol) with a correlation coefficient of 0.980 at 20°C. The fact that the Na_2CO_3 (aq) wash consistently removes the same percentage of the added nitrogen just reinforces the theory of a simple equilibrium of NO_2 between the solvent and the coal.

The nitrogen data also obey simple first-order kinetics of the form:

$$-\frac{dm_N^S}{dt} = k\, m_N^S, \quad \text{where}$$

$$m_N^S = (m_{N_S})_0\,[(NO_2)] - m_N, \quad \text{where}$$

m_N^S = the concentration of available NO_2 absorption sites (mass %)

$(m_{N_S})_0\,[(NO_2)]$ = the initial number of NO_2 absorption sites in the coal, which is a function of the bulk NO_2 concentration, (NO_2),

m_N = the net nitrogen mass increase (mass %),

t = the time (min), and

k = the first order rate constant (min^{-1}).

Because the NO_2 concentration, (NO_2), does not change markedly during the course of the reaction, it is not possible to detect any dependence of the rate on (NO_2). Nevertheless, the fact that $(m_{N_S})_0$ depends on (NO_2) implies that such a dependence may exist. The following values were obtained for $(m_{N_S})_0$ and k:

	PSOC 190 Coal			PSOC 276 Coal
T (C)	0	20	50	20
$(m_{N_S})_0$ (g N/100g initial coal)	3.60	3.89	5.33	3.94
k (min^{-1})	0.0342	0.0483	0.0466	0.0183

The analysis of the coal for oxygen uptake reveals that most of the oxygen taken up by the coal during the NO_2 treatment is removed by the Na_2CO_3 (aq) wash. In particular, the NO_2 treatment results in a net oxygen increase in the coal of 12 to 18 mass percent. The Na_2CO_3 (aq) wash, however, yields an overall net oxygen increase of only 0 to 3 mass percent for the PSOC 190 coal and 7 mass percent for the PSOC 276 coal. The net increase in oxygen during the NO_2 treatment can be attributed to the uptake of nitrogen as NO_2 and the oxidation of the aliphatic hydrogen in the coal to yield ketonic and carboxylic oxygen groups. The decrease in the amount of oxygen in the coal during the Na_2CO_3 (aq) wash can be attributed to two processes. The first process is the removal of the heavily oxidized portions of the coal as water soluble compounds (humic acids). Indeed, if the coal is treated with NO_2 at 50°C, the oxidation is so extensive that virtually all of the coal forms an emulsion when mixed with 0.1 M Na_2CO_3 (aq). Hence, a certain portion of the coal is lost during the Na_2CO_3 (aq) wash. Fortunately, it is also the most heavily oxidized portion of the coal which contributes the least to the total heat content of the coal. The second process which accounts for the oxygen decrease during the wash is the uptake of sodium by the oxidized coal. In particular, it is the anionic oxygen groups in the coal which bind the sodium ions. Consequently, the oxygen which is bound to the sodium is determined as mineral matter and not organic oxygen. Therefore, the oxygen analysis of the washed coal must be treated with caution. In fact, because the oxygen content is given directly by the difference between unity and the sum of all the other elemental contents, the oxygen content may contain large relative errors. Despite this potential error, however, the oxygen analysis yields results which are consistent with the rest of the data.

The chlorine analysis of the coal after treatment with NO_2 in CCl_4 revealed some interesting results. Primarily, during the NO_2 treatment, the chlorine con-

tent rises from 0.1 mass percent to anywhere from 2.5 to 5.2 mass percent. Washing the treated coal in 0.1 M Na_2CO_3 (aq) at 25°C for 120 minutes, however, results in the reduction of the chlorine content to its original level of 0.1 mass percent. These results are easily explained. The CCl_4 is trapped in the coal particle by the polar oxygen groups introduced into the coal by the NO_2 treatment. This adsorbed CCl_4 cannot be removed by vacuum drying at 120°C for three hours. Once the treated coal is exposed to the Na_2CO_3 (aq) solution, however, the CCl_4 is easily displaced by the water and sodium ions, which have a higher affinity for the polar oxygen groups in the coal. Furthermore, the H_2O and Na^+ species are much smaller than the CCl_4 molecule, so that they should be able to penetrate any portion of the coal containing CCl_4 to displace it.

The mineral matter analysis of the coal provides corroborating evidence for the displacement of CCl_4 by sodium. In all of the runs conducted, the NO_2 treatment resulted in a slight decrease in the mineral matter content of the coal, usually less than one mass percent. The Na_2CO_3 (aq) wash, on the other hand, results in a large increase in the mineral matter content. For instance, the washed PSOC 190 coal experiences an increase from roughly 6 to 16 mass percent in the mineral matter content. The PSOC 276 coal, because it has only one-fourth the pore volume of the PSOC 190 coal, only experiences an increase in the mineral matter content from 8 to 13 mass percent. Cogent evidence for sodium uptake by the NO_2-treated coal is provided by the EDAX spectra of the ash remaining after combustion of the coal. The ash of the NO_2-treated coal contains no sodium while the ash of the subsequently washed coal contains a substantial amount of sodium. Therefore, the NO_2-treated coal behaves as an ion-exchange support. In this case, the adsorbed CCl_4 and any loosely adsorbed NO_2, as well as acidic hydrogen, are displaced by the more strongly adsorbed species in the Na_2CO_3 (aq) solution.

The uptake of sodium by the coal is the cornerstone of the ability of this processing scheme to remove SO_2 from the combustion gases of the coal. The NO_2 treatment at 0, 20 and 50°C when CCl_4 is the solvent results in the removal of only about 10 % of the sulfur from the PSOC 190 coal, which consists exclusively of organic sulfur. When water is the solvent, the sulfur removal increases to 20 %. The treatment conditions in the latter case were more severe, however, and the heating value loss was greater. The Na_2CO_3 (aq) wash of the NO_2-treated PSOC 190 increases the desulfurization to 30 %, as determined by the Bomb method. The Leco analysis, however, which determines the amount of SO_2 in the combustion gases of the coal, indicates a 97 % desulfurization when the NO_2 treatment is conducted at 20°C for 180 minutes and an 87 % desulfurization when the NO_2 treatment is conducted at 0°C. These high desulfurizations are due primarily to the trapping of SO_2 by the sodium in the coal during combustion. This conclusion is supported by the EDAX spectra, which show a predominant sulfur peak in addition to the sodium peak in the ash of the washed coals.

The PSOC 276 coal does not show as great an extent of desulfurization as the PSOC 190. The NO_2 treatment results in only a 3 % desulfurization. The Na_2CO_3 (aq) wash increases the sulfur removal to 18 % according to the Bomb analysis. The Leco analysis, however, indicates that only 40 % of the sulfur is removed from the combustion gas. There are two explanations for these observations. The sulfur in the PSOC 276 consists primarily of pyritic sulfur (66 % of the total sulfur content), which is not removed by the NO_2 treatment when CCl_4 is the solvent because once the surface of the pyrite crystals are oxidized to $FeSO_4$, no further reaction occurs. The $FeSO_4$ remains on the surface and prevents the penetration of NO_2 into the pyrite crystal. If water is the solvent, on the other hand, the $FeSO_4$ would dissolve and the pyrite crystal surface would be continually renewed until it completely reacts. Hence, most of the pyrite

remains unaltered by the NO_2 treatment and subsequent Na_2CO_3 (aq) wash. These pyrite crystals then serve as point sources of SO_2 during combustion. Because of the high concentration of SO_2 at these points, virtually all of the SO_2 escapes into the combustion gases because there is hardly any sodium at these points for trapping SO_2. This escape occurs because the sodium is uniformly dispersed throughout the coal while the SO_2 derived from the pyrite evolves at point sources. The analysis for forms of sulfur indicates the removal of only 10 % of the pyritic sulfur. Hence, the 40 % overall desulfurization translates into a 90 % removal of SO_2 derived from organic sulfur. Consequently, if the pyrite were removed by treatment with NO_2 in H_2O rather than CCl_4, where complete pyrite removal is expected, the overall desulfurization would be roughly 97 %, which compares quite well with the results obtained with the PSOC 190.

In terms of desulfurization, therefore, the results indicate that the NO_2 treatment forms an acidic and well distributed precursor in the coal, which then behaves like an ion-exchange support. Subjecting the NO_2-treated coal to a basic solution of 0.1 M Na_2CO_3 (aq) results in the uptake of sodium ions by the acidic precursor in the coal. Upon combustion of the coal, this sodium-containing precursor traps SO_2, which would otherwise escape into the combustion gases, as Na_2SO_4. The dispersion of the sodium throughout the coal is important. This dispersion is governed somewhat by the coal as evidenced by the contrasting results obtained with the two different coals. The efficiency of the sodium for trapping SO_2 in the PSOC 190 is 37 % while that in the PSOC 276 is only 18 %. The efficiency is defined simply as twice the ratio of moles of SO_2 trapped to moles of sodium in the washed coal. The efficiency is less in the PSOC 276 coal because it has a smaller pore volume than the PSOC 190. Although the pore structure does not affect the extent of the NO_2 treatment significantly, it does affect the dispersion of sodium in the coal during the wash, and hence the

amount of SO_2 trapped during combustion.

As a consequence of the formation of the acidic precursor in the coal resulting from the NO_2 treatment, a loss in the heat content of the coal occurs. The extent of this loss, however, is mitigated by conducting the NO_2 treatment under mild conditions, namely at ambient temperature and pressure using small concentrations of NO_2 (< 2 F). In particular, the NO_2 treatment results in heating value losses under 10 %. The subsequent Na_2CO_3 (aq) wash results in additional losses, but the overall loss is still only 15 % for the PSOC 190 treated at 20°C, 9 % for the PSOC 190 treated at 0°C and 9 % for the PSOC 276 treated at 20°C. By way of contrast, the PSOC 190 treated at 25°C in CCl_4 with an NO_2 concentration of 8 F experiences a 25 % loss in heating value. Most of the heating value loss can be attributed to the rapid and facile attack of NO_2 on the hydrogen in the coal. Hence, it appears that it is inevitable that a loss of 10 to 15 % in the heating value will occur when subjecting the coal to even mild oxidizing conditions.

The results of the heating value loss can be coupled with the desulfurization results in a parameter called the beneficiation coefficient, defined as:

$$B = \left[1 - \frac{(1 + f)\, c_S}{(c_S)_0} \right] \left[\frac{H_g}{(H_g)_0} \right], \quad \text{where}$$

f = the fractional mass gain of the treated coal relative to the initial mass of coal used. (If a mass loss occurs, $f = 0$),

c_S = the sulfur content of the treated coal corrected for any CCl_4 adsorption (mass %),

$(c_S)_0$ = the sulfur content of the coal before processing (mass %),

H_g = the heat content of the treated coal corrected for any mass change (Btu/lb_m of initial coal used), and

$(H_g)_0$ = the heat content of the pretreated coal before processing (Btu/lb_m coal)

Basically, B translates the desulfurization from a mass basis to an energy basis. The beneficiation coefficient, therefore, serves as an indicator of the selectivity of the process for desulfurization relative to the oxidation of the rest of the coal. In particular, the values of B obtained for the processed PSOC 190 coal in terms of SO_2 removal from the combustion gas all lie in the range from 0.80 to 0.85. A value for B of unity corresponds to complete SO_2 removal without any loss in the heating value. The value of B obtained for the PSOC 276 coal, on the other hand, is only 0.28, which is simply a reflection of the high pyrite content of the coal and the fact that the sodium uptake is not as great as that of the treated PSOC 190.

5.1.2 The Effect of the Processing on the Physical Structure of the Coal

The chemical changes which occur in the coal as the result of the NO_2 treatment and subsequent Na_2CO_3 (aq) wash are accompanied by changes in the physical structure of the coal as well. Particles of the treated coal examined with the scanning electron microscope (SEM) reveal some interesting qualitative changes in the particle structure. When the PSOC 190 coal is treated with NO_2 and washed in 0.1 M Na_2CO_3 (aq), the large amount of mineral matter initially adhering to the particle surface is removed. Furthermore, etching of the particle surface and a small amount of fissuring in the particle occur. The etching is due to the removal of the oxidized coal species from the particle surface by the Na_2CO_3 (aq) wash. The fissuring is probably caused by the penetration of the Na_2CO_3 (aq) solution into the NO_2-treated coal particles, which results in a breakdown of the internal structure of the coal matrix. The processed PSOC 276 coal, on the other hand, does not demonstrate any etching or fissuring, which is consistent with the other data which indicate that the extent of the NO_2-coal reaction is not as great in the PSOC 276 coal as in the PSOC 190 coal.

The ash remaining after combustion of the processed coal was examined with the SEM and EDAX (Energy-Dispersive Analyzer of X-Rays) as well. The ash of the NO_2-treated coal is indistinguishable from that of the untreated coal. This ash consists of very small, sharp-edged particles with average dimensions on the order of 10 μm. The ash is composed primarily of SiO_2 and Al_2O_3, with additional amounts of K_2O, CaO, TiO_2 and Fe_2O_3. The ash remaining from the combustion of the NO_2-treated coal washed in Na_2CO_3 (aq), however, consists of large, porous, globular particles with diameters on the order of 1 mm. In addition to the inorganic species mentioned above, the ash also contains very large amounts of sodium and sulfur in the form of Na_2O and Na_2SO_4. The amount of sodium and sulfur in the ash of the processed PSOC 190 is roughly twice that in the ash from

the processed PSOC 276. Furthermore, the ash was obtained by combusting the coal at both 750 and 1200°C. In both cases, the ash contained large amounts of Na_2O and Na_2SO_4, which demonstrates that the Na_2SO_4 is stable at temperatures very close to those used in commercial coal-fired utility boilers. These EDAX spectra provide unequivocal evidence that the NO_2 treatment of the coal yields an acidic and uniformly dispersed precursor which binds sodium upon exposure to an aqueous solution of Na_2CO_3. This sodium precursor then forms a flux when the coal is combusted, which explains the globular nature of the ash from the washed coal. This sodium-containing flux then traps the SO_2 generated during combustion as Na_2SO_4 in the ash.

The results of the N_2 and CO_2 adsorption studies on the treated coals show some interesting features. For instance, during the first 30 minutes of the NO_2 treatment at 20°C using CCl_4 as the solvent, the specific surface area, $S_a^{N_2}$, of the PSOC 190 coal drops 70 % from 58 m^2/g to 18 m^2/g. Washing the NO_2-treated coal in Na_2CO_3 (aq) reduces $S_a^{N_2}$ to just 2 m^2/g, which corresponds to the virtually complete blocking of the pores. The large reduction in $S_a^{N_2}$ is due to the rapid oxidation of the coal. The pore size distributions indicate that virtually all of the pores have radii less than 25 Å, which implies that little reaction in the pores is required for blockage to occur. The blockage of these pores is amply demonstrated by the change in the pore size distribution as the NO_2-exposure time increases. The peak at 19 Å rapidly disappears, which is indicative of pore closure.

The change in $S_a^{N_2}$ also correlates quite well with both the rate of NO_2 disappearance from the NO_2/CCl_4/coal system and the rate of nitrogen uptake by the coal. As has been mentioned before, it appears that the NO_2 is actually diffusing into the solid coal matrix of the coal. This solid diffusion process is rate limiting

during the first 30 minutes of the reaction. Consequently, the rate of NO_2 disappearance depends on the total flux of NO_2 into the solid coal matrix. This total flux, in turn, is proportional to the interfacial area between the solid coal matrix and the NO_2/CCl_4 solution. Consequently, the rate should be proportional to $S_a^{N_2}$, as it is. The rate of nitrogen uptake by the coal also correlates quite well with the nitrogen-determined surface area. In particular, a comparison of the first order rate constants obtained for the rate of nitrogen uptake at 20 °C by the PSOC 190 and PSOC 276 coals reveals that they differ by a factor of 2.6. Since the initial capacity of the coal which can take up nitrogen is the same for both coals, the ratio of the rate constants is also the ratio of the rates of nitrogen uptake by the two coals. The value of $S_a^{N_2}$ for the PSOC 190 coal after 180 minutes of NO_2 treatment is 15.6 m^2/g while that of the PSOC 276 coal after 180 minutes of NO_2 treatment at 20 °C is 6.0 m^2/g. Hence, the values of $S_a^{N_2}$ and k both differ by a factor of 2.6. Consequently, the rate of nitrogen uptake by the coal is proportional to the nitrogen-determined surface area.

The results of the CO_2 adsorption studies, on the other hand, are in stark contrast to those of the N_2 adsorption studies. While treatment with NO_2 causes a 70 % decrease in $S_a^{N_2}$ and the subsequent Na_2CO_3 (aq) wash results in an overall decrease of 97 % in $S_a^{N_2}$, the values of $S_a^{CO_2}$ actually increase about 10 to 20 % after the NO_2 treatment. Washing the NO_2-treated coal in Na_2CO_3 (aq) does not affect $S_a^{CO_2}$ at all. These puzzling results can be explained by the previously postulated theory of CO_2 dissolution in the solid coal matrix; that is, CO_2 penetration into the coal is not affected by the pore structure. Rather, CO_2 penetrates the solid coal in much the same manner as NO_2.

5.1.3 The Application of the Mathematical Model to the Reaction System

A mathematical model which incorporates the combined processes of diffusion and reaction of NO_2 in the solid coal matrix was developed from the experimental data. The model was applied to those experiments in which the PSOC 190 coal was treated with NO_2 in CCl_4 at 0 and 20°C. Using the assumption of a parallel slit-pore geometry, the results of the nitrogen-determined specific surface area and pore volume, and the values of the rate constants determined from the nitrogen uptake data, it was possible to estimate the coefficient of diffusion of NO_2 in the solid coal matrix.

At the outset, it was determined that the full time-dependent modelling equations must be solved in order to obtain an accurate solution. This fact was established by comparing the predicted nitrogen uptake obtained by solution of the full time-dependent equations with the predicted nitrogen uptake obtained by solution of the corresponding pseudo-steady-state equations. Under the conditions in the reaction system, it was established that the pseudo-steady-state solution deviates significantly from the solution of the full time-dependent equations. Consequently, the full time-dependent equations were used in the model simulation. It was also determined that diffusion of NO_2 in the pores was not controlling. In particular, it was established by solution of the full time-dependent equations that the NO_2 concentration in the center of the coal particle, which was assigned a radius of 50 μm, reached 96 % of the NO_2 concentration in the bulk CCl_4 within one second.

Application of the model to the actual nitrogen uptake data by the PSOC 190 coal at 20°C yields a diffusion coefficient, D, of 10^{-15} cm^2/s for NO_2 diffusion in the solid coal matrix. The same value is obtained when the data obtained at 0°C are fit to the model. Although this value of D is several orders of magnitude lower than those observed for diffusion of such gases as N_2, O_2, CO and CO_2 in

manufactured polymers, if no diffusion of NO_2 were to occur, then D would be zero. Therefore, the value obtained for D implies that NO_2 cannot diffuse into coal as easily as N_2, O_2, CO or CO_2 can diffuse in polymers. This difference may arise because either the coal itself is less susceptible to gaseous diffusion or the nature of the NO_2 molecule itself inhibits its ability to diffuse into the coal. Without any definitive information concerning the mechanism of NO_2 diffusion in the solid coal matrix, it is not possible to determine if the value of 10^{-15} cm^2/s is accurate or not. All that can be said is that the data are adequately explained on the basis of the diffusion and reaction of NO_2 in the solid coal matrix.

When the data for the nitrogen uptake by the PSOC 276 coal are fit with the model, a value of 5×10^{-14} cm^2/s is obtained for D. This value is 50 times greater than that obtained for the PSOC 190 coal. In view of the similarities in the two coals, it is hard to reconcile the large difference in the values obtained for D. The difference in the fitted values of D arises from the difference in the nitrogen-determined specific surface areas and pore volumes of the two coals, which are used to give the thickness, L, of the slabs which comprise the idealized coal particle assumed by the model. The value obtained for L for the PSOC 276 coal is 7.6 times that obtained for the PSOC 190 coal. Because the values of the nitrogen uptake by the two coals are quite similar and because L can be treated as a characteristic diffusion length, the characteristic diffusion time is given by $t = \frac{L^2}{D}$, which should be approximately the same for the two coals since they both achieve their maximum nitrogen uptakes within 120 to 180 minutes. Consequently, if the values of L differ by a factor of 7.6, then the values of D would have to differ by a factor of 58, which explains the difference in the values obtained for D. Therefore, the idealized slit-pore geometry may not correspond to the actual situation in the coal particle. There is no compelling reason, however, why the diffusion coefficients cannot differ by as large a factor as the

model predicts. In any case, the experimental data which pertain to the nitrogen uptake by both the PSOC 190 and PSOC 276 coals during treatment with NO_2 at 20°C are adequately explained on the basis of the simultaneous diffusion and reaction of NO_2 in the solid coal matrix.

5.1.4 A Plausible Mechanism Describing the Reaction of Nitrogen Dioxide with Coal

Utilizing the results of the elemental analysis, the N_2 and CO_2 adsorption studies and the mathematical modelling, it is possible to formulate a mechanism which describes the reaction of NO_2 with coal. The basic feature of this mechanism involves the formation of an acidic, uniformly distributed precursor in the coal by exposure to NO_2 under mild conditions (ambient temperature and pressure, small NO_2 concentrations). Upon exposure of the NO_2-treated coal to 0.1 M Na_2CO_3 (aq), this acidic precursor binds sodium ions in a manner analogous to an ion-exchange support. Upon combustion of the coal, the sodium-containing precursor forms a flux which traps SO_2, which would otherwise escape in the combustion gas, as Na_2SO_4 in the ash. The Na_2SO_4 containing flux is stable at 1200°C, rendering this process acceptable for the pretreatment of coal to be used in coal-fired utility boilers. A mechanism which is consistent with the findings of this thesis is:

1. Upon exposure of the coal particles (+200–325 mesh) to the solution containing NO_2 solvated in CCl_4, the NO_2 concentration in the pore structure rapidly (< 1 sec) rises to the NO_2 concentration in the bulk solvent.
2. The NO_2 reacts with the coal in various ways:
   a) The NO_2 reacts rapidly with hydrogen in the coal, which results in the formation of the acidic, well-distributed precursor, which can occur as the result of any of the following possible reactions:

$$NO_2 + > CH_2 \rightarrow > CH(OH) + NO$$

$$NO_2 + > CH(OH) \rightarrow > C{=}O + NO + H_2O$$

$$3\ NO_2 + \text{-}CH_3 \rightarrow \text{-}COOH + 3\ NO + H_2O$$

$$NO_2 + \text{-}\varphi\text{-}H \rightarrow \text{-}\varphi\text{-}OH + NO$$

where φ represents an aromatic benzene structure.

b) The NO_2 penetrates the coal surface and is absorbed by the solid coal matrix. Some removal of the water formed from the oxidation of the coal hydrogen from the solid interior must occur because up to 20 percent of the hydrogen initially in the coal is lost during the NO_2 treatment and only 2 percent is expected to reside on the particle pore-surfaces. The absorption of NO_2 accounts for the increase in the nitrogen content of the coal of several mass percent as well. Furthermore, the pore structure does not affect the extent of the uptake of nitrogen by the coal.

3. The chlorine trapped in the coal after the NO_2 treatment is due to the adsorption of CCl_4 by the acidic precursor in the form of weak inductive bonds between Cl and O, as shown in Figure 5–1. Some of the NO_2 may be adsorbed by the polar surface in an analogous manner, as illustrated in Figure 5–2.

4. Once the NO_2-treated coal is exposed to Na_2CO_3 (aq), three physical processes occur:

a) Heavily oxidized portions of the coal are leached from the coal as water soluble compounds (humic acids).

b) NO_2 diffuses back out of the coal to the extent of 20 % of the absorbed NO_2 when the wash is conducted with 0.1 M Na_2CO_3 (aq) at 25 °C for 2 hours.

c) The coal behaves like an ion-exchange support with the following reactions occurring:

i) The adsorbed CCl_4 is rapidly and quantitatively displaced from the coal. Any adsorbed NO_2 is rapidly displaced from the surface as it reacts with the Na_2CO_3 (aq):

$$2\ NO_2 + Na_2CO_3 \rightarrow NaNO_3 + NaNO_2 + CO_2$$

Adsorption of CCl_4 on the Oxidized Coal Surface

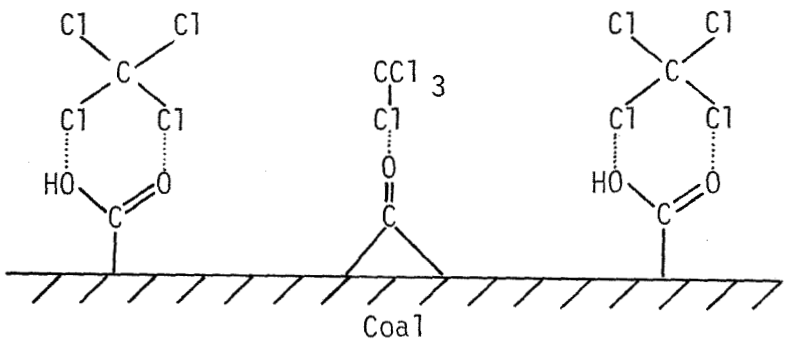

Figure 5-1

Adsorption of NO_2 on the Oxidized Coal Surface

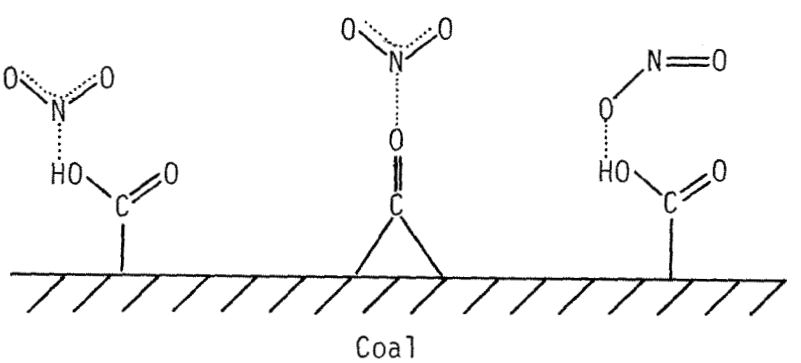

Figure 5-2

ii) The acidic hydrogen is displaced by cationic sodium:

$$> C(OH)H + \frac{1}{2}Na_2CO_3 \rightarrow > C(H)O^- Na^+ + \frac{1}{2}CO_2 + \frac{1}{2}H_2O$$

$$-COOH + \frac{1}{2}Na_2CO_3 \rightarrow -C(O)O^- Na^+ + \frac{1}{2}CO_2 + \frac{1}{2}H_2O$$

$$-\varphi-OH + \frac{1}{2}Na_2CO_3 \rightarrow -\varphi-O^- Na^+ + \frac{1}{2}CO_2 + \frac{1}{2}H_2O$$

where φ represents an aromatic benzene structure.

iii) Any NO_2, which is uniformly distributed in the coal, accessible to Na_2CO_3 (aq) would result in the formation of sodium salts of oxidized nitrogen:

$$2\,NO_2 + Na_2CO_3 \rightarrow NaNO_2 + NaNO_3 + CO_2.$$

If these salts are not completely leached out of the coal, it is possible that the $NaNO_2$ and $NaNO_3$ may be well dispersed in the pore structure of the coal, since trapping of the salts would be expected to occur primarily in the smaller pores.

5. During combustion of the coal, the well-distributed sodium containing precursor forms a flux which traps SO_2, which would otherwise escape in the combustion gas, as Na_2SO_4 in the ash.

5.1.5 Concluding Remarks

The most important feature of the entire study encompassed by this thesis is the discovery of the formation of an acidic, uniformly distributed precursor in the coal by mild oxidation with NO_2. Upon exposure of the coal to Na_2CO_3 (aq), the precursor binds sodium ions in a manner analogous to that of an ion-exchange support. Upon combustion of the coal, the sodium-containing precursor forms a flux which traps the SO_2, which would otherwise escape in the flue gas, as Na_2SO_4 in the ash. The flux has been shown to be stable with respect to SO_2 evolution at a temperature of 1200 °C for a minimum of six minutes, which is much longer than the average residence time of ash in a utility boiler of a few seconds. Consequently, this process represents a commercially viable alternative to flue gas desulfurization, provided the problem of increased NO and NO_2 emissions due to the uptake of nitrogen by the coal can be alleviated.

All other chemical desulfurization processes discussed up to this time have sought to physically remove sulfur from the coal prior to combustion in some altered form. Although many of these processes are quite good for the removal of pyritic sulfur, none of them have demonstrated any significant reduction in organic sulfur. Indeed, due to the well-dispersed nature of organic sulfur in the coal matrix, it is not possible to remove organic sulfur without drastically altering the rest of the coal, resulting in significant heating value losses. The process described in this work, however, is quite unique in that this is the first time that virtually complete removal of SO_2, which is derived exclusively from organic sulfur, from the flue gas has been demonstrated without significant heating value losses. Furthermore, in contrast to other desulfurization schemes, this process does not physically remove the organic sulfur from the coal prior to combustion. Rather, the chemical nature of the coal has been altered so that instead of evolving as SO_2, the sulfur is trapped as Na_2SO_4 by the ash upon combustion.

Due to the unique and novel aspect of the process described in this work, a patent has been filed on this chemical treatment scheme.[1]

Of all of the desulfurization work currently being conducted, perhaps that which is closest in scope to the process discussed here is that done by Freund and Lyon.[2] These researchers "mildly" oxidize the coal at 400°F to impart an ion-exchange characteristic to the coal. No heating value analyses of the oxidized coal were given in the paper, so it is not possible to comment upon the extent of the oxidation of the coal. The oxidized coal is then soaked in ammoniated calcium acetate for 48 hours and then dried, apparently through solvent evaporation without filtration or washing of the coal. Due to the large size of the $Ca(CH_3COO)_2$ molecule, it seems reasonable to expect that most of the calcium in the coal resides on the exterior particle surface with very little calcium uptake in the interior pore structure of the coal. Indeed, although the authors claim a uniform distribution of calcium in the coal, they did not prove that this is the case. In order to do so, the pore size distribution of the oxidized coal is needed in order to determine if the $Ca(CH_3COO)_2$ can penetrate into the coal pore structure.

The authors claim that if the calcium-containing coal is then burned under fuel rich conditions, the sulfur will be retained in the char as CaS. Extrapolation of their data to combustion under fuel lean conditions, as employed in the process development discussed in this work, however, indicates that no sulfur is retained by the calcium in the coal ash. Although sodium was used exclusively in the process discussed in this work, there is every reason to expect calcium to trap SO_2 during combustion just as well. The reason calcium did not trap the sulfur as $CaSO_4$ in the work conducted by Freund and Lyon is that the calcium was not well-distributed throughout the coal particle. As mentioned previously, the precursor must be in close proximity to the SO_2 as it evolves during

combustion in order to trap it as sulfate. Otherwise, the SO_2 will escape from the particle into the flue gas. It appears that this is indeed the case when the coal is treated with $Ca(CH_3COO)_2$. Therefore, the novel and unique aspect of the process discussed in this thesis for the chemical alteration of the coal under mild conditions to eliminate the evolution of SO_2 during combustion is firmly established.

5.2 Recommendations for Future Work

Although a system which successfully eliminates a substantial portion of the SO_2 emissions during coal combustion has been developed, several areas of further investigation remain.

1. An examination of other oxidants, such as air, O_2, O_3, CO_2, Cl_2, H_2O_2, $KMnO_4$, and organic peracids and peroxides, should be conducted to determine if oxidants other than NO_2 are capable of forming an acidic, uniformly distributed precursor in the coal. If other oxidants do not result in the formation of such a precursor, it may be that NO_2 possesses some unique property, such as its facile penetration into the solid coal matrix, which makes it more effective.
2. It would be desirable to establish a mechanism for NO_2 absorption by the coal. Such a study would include a comparison of the permeabilities of well-characterized polymers to NO_2 with the permeabilities of those polymers to other gases such as N_2, O_2, CO and CO_2, in order to determine if NO_2 demonstrates analogous or anamolous behavior with regard to other gases. Later on, the penetration of NO_2 in a variety of coals can be examined to determine if the NO_2 permeability correlates with any other parameters which describe the coal.
3. An identification of the type of oxygenated structures being formed in the coal upon oxidation would greatly facilitate the understanding of the nature of the acidic precursor necessary for the ultimate trapping of SO_2 during combustion. Indeed, oxidation introduces many different oxygen groups into the coal whereas only one particular group may actually be the active precursor. Hence, identification of the active precursor(s) may provide an insight into the mechanism by which the precursor traps SO_2. The types of oxygenated structures in the NO_2-treated coal may be identified by infrared

or nuclear magnetic resonance, or even wet chemical techniques which take advantage of the ion-exchange characteristics of the treated coal.[3] It would also be desirable to know if the oxygen groups are truly anionic or if some charge transfer with the aromatic structure of the coal occurs during the Na_2CO_3 (aq) wash, for instance of the quinone-hydroquinone type. This possibility can probably best be examined by using model organic compounds which best correspond to the oxygenated structures in the NO_2-treated coal.

4. The ability of metals other than sodium to bind to the precursor and subsequently trap SO_2 should be examined. In particular, calcium should be examined because it has been commercially demonstrated that $CaSO_4$ is stable in a utility boiler. Another possibility is lithium, which due to its very small size, may be able to penetrate further into the coal particle and more easily trap SO_2 during combustion. Other possibilities include potassium and any other alkali or alkaline earth metals which demonstrate any potential promise.
5. An examination of the effect of the pressure during the wash should be performed. Because this study indicates that the pore structure affects the uptake of sodium by the oxidized coal, it may be possible to dilate the pore structure somewhat by conducting the Na_2CO_3 (aq) wash at higher pressures (up to 1000 psi, for instance). Consequently, the trapping of SO_2 may be enhanced.
6. One interesting result of this study was the greatly enhanced extraction of coal by nitrobenzene when exposed to NO_2. This enhanced extraction could be examined further by investigating the extraction of other coals by the NO_2/nitrobenzene system. Additionally, the chemical nature of the extract could be examined to determine if this system can extract useful products from the coal.

7. The changes in the density of the coal during processing should be monitored to determine if significant changes occur. Such changes, if they occur, would provide an indication of the possible swelling of the coal structure due to the absorption of NO_2 or solvent by the solid coal matrix.
8. The mathematical model should be modified so that it corresponds more closely to the experimental conditions. For instance, the time dependence of the bulk NO_2 concentration should be incorporated into the model. The solid void fraction, ε', should be replaced by using a Henry's law type of relationship in which the NO_2 concentration on the CCl_4 side of the surface of the solid coal matrix is equal to a constant times the NO_2 concentration on the coal side of the surface of the solid coal matrix. Other pore geometries, such as random or cylindrical pore structures, should be investigated as well.

References

1. Kralik, J.G., Corcoran, W.H., U.S. Patent pending.

2. Freund, H., Lyon, R.K., "The Sulfur Retention of Coal Containing Calcium During Fuel Rich Combustion," presented at Western States Section/The Combustion Institute, University of Southern California, October 20-21, 1980, 25 pp.

3. Mott, R.A., *Fuel*, **29**, 53 (1950).

APPENDIX A

Results of the N_2 and CO_2 Adsorption Studies

This appendix contains both the data and the results of the N_2 and CO_2 adsorption studies made of the treated and untreated coals. The data and results are presented graphically in the order in which the experiments were conducted, and are classified by the run number. The data and the results of the study of the raw and washed and dried PSOC 190 are presented first. For each run, the data and results are presented in the following order:

1. The data are presented in the form of the N_2 adsorption-desorption isotherm.
2. If the desorption branch of the isotherm was obtained, the resulting pore size distribution is shown.
3. The data used to determine the specific surface area, $S_a^{N_2}$, are presented in the form of the BET plot, which demonstrates the degree of correlation between the data and the BET theory.
4. If the CO_2 adsorption isotherm was obtained, the data are presented in the form of the DPR plot, which demonstrates the degree of correlation between the data and the DPR theory. Also shown is the data point used for the determination of $S_a^{CO_2}$, which is taken at a relative pressure of $\frac{P}{P_0} = 0.1$. This point is delineated by the dashed lines.
5. The micropore size distribution obtained from the CO_2 adsorption data is shown.

All of the curves in these plots were generated by fitting the data points using a cubic spline technique.

The reaction conditions for the treated coals studied are:

Run #	Coal (PSOC #)	Reactor[1]	Solvent	Reaction Time (min)	T(C)	$(NO_2)_0$ (F)
1	190	F	H_2O	120	26	-
2	190	F	H_2O	120	78	-
3	190	F	Pyridine	120	26	-
4	190	F	Pyridine	120	83	-
5	190	F	Nitrobenzene	120	34	-
7	190	F	H_2O	0	25	0
8	190	F	H_2O	30	27	-
9	190	F	H_2O	60	27	-
11	190	F	H_2O	120	27	-
18	190	F	H_2O	120	24	-
33	190	B	CCl_4	30	20	1.122
34	190	B	CCl_4	60	20	1.058
35	190	B	CCl_4	90	20	1.081
36	190	B	CCl_4	120	20	1.087
37	190	B	CCl_4	180	20	1.091
38	190	B	CCl_4	120	20	0.097
39	190	B	CCl_4	120	20	0.488
40	190	B	CCl_4	120	20	1.713
41	190	B	CCl_4	120	20	1.874
42	190	B	CCl_4	30	20	0.985
43	190	B	CCl_4	60	20	1.040
44	190	B	CCl_4	90	20	1.008
45	190	B	CCl_4	120	20	1.048
46	190	B	CCl_4	180	20	1.028
47	276	B	CCl_4	0	20	0.000
52	276	B	CCl_4	180	20	1.074

[1] Refers to reactor type: F = Flow Reactor, B= Batch Reactor

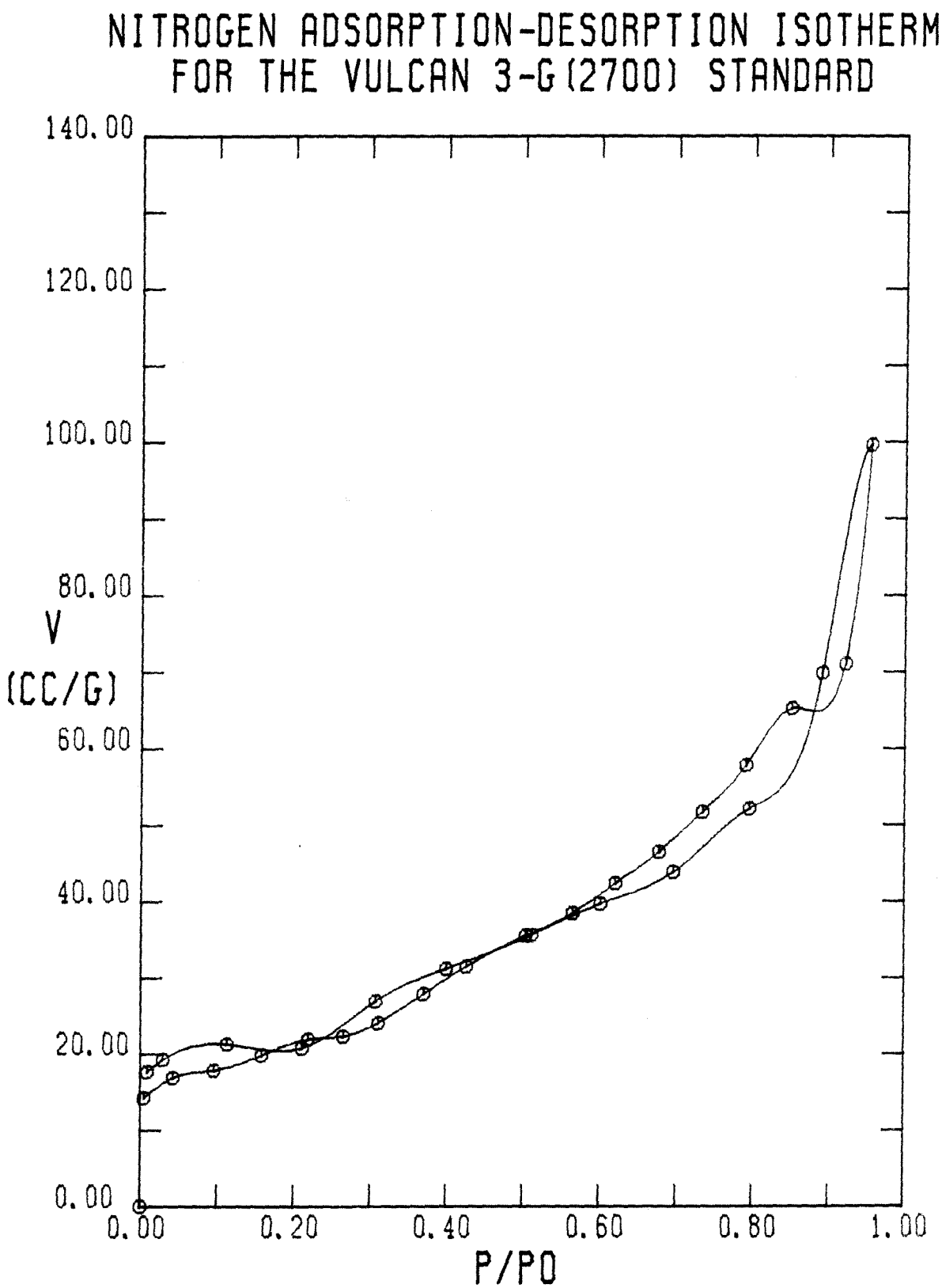
NITROGEN ADSORPTION-DESORPTION ISOTHERM
FOR THE VULCAN 3-G(2700) STANDARD
140.00
120.00
100.00
80.00
V
(CC/G)
60.00
40.00
20.00
0.00
0.00
0.20
0.40
0.60
0.80
1.00
P/PO

FIGURE A-1

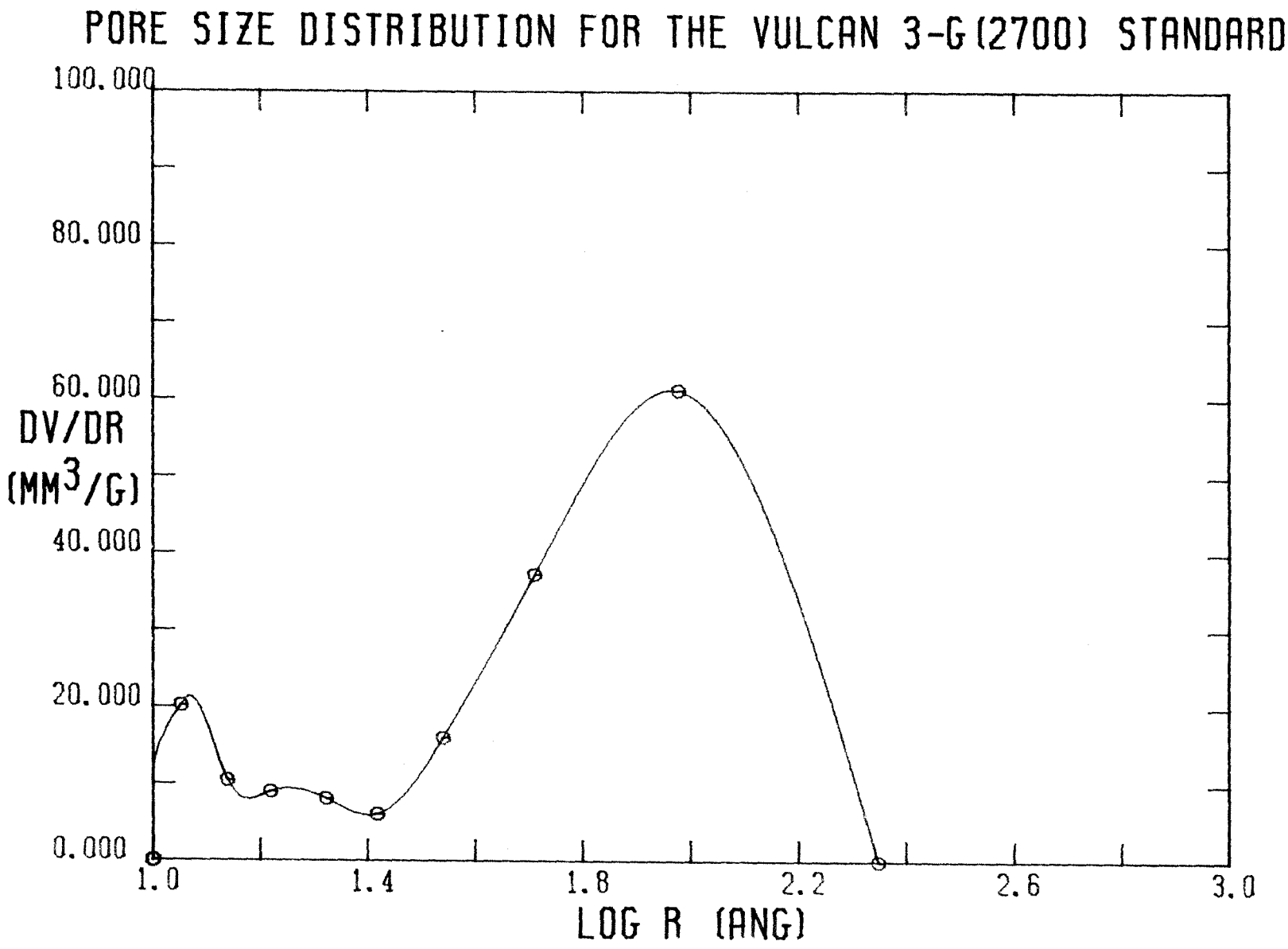
PORE SIZE DISTRIBUTION FOR THE VULCAN 3-G(2700) STANDARD
100.000
80.000
60.000
DV/DR
(MM3/G)
40.000
20.000
0.000
1.0
1.4
1.8
2.2
2.6
3.0
LOG R (ANG)

FIGURE A-2

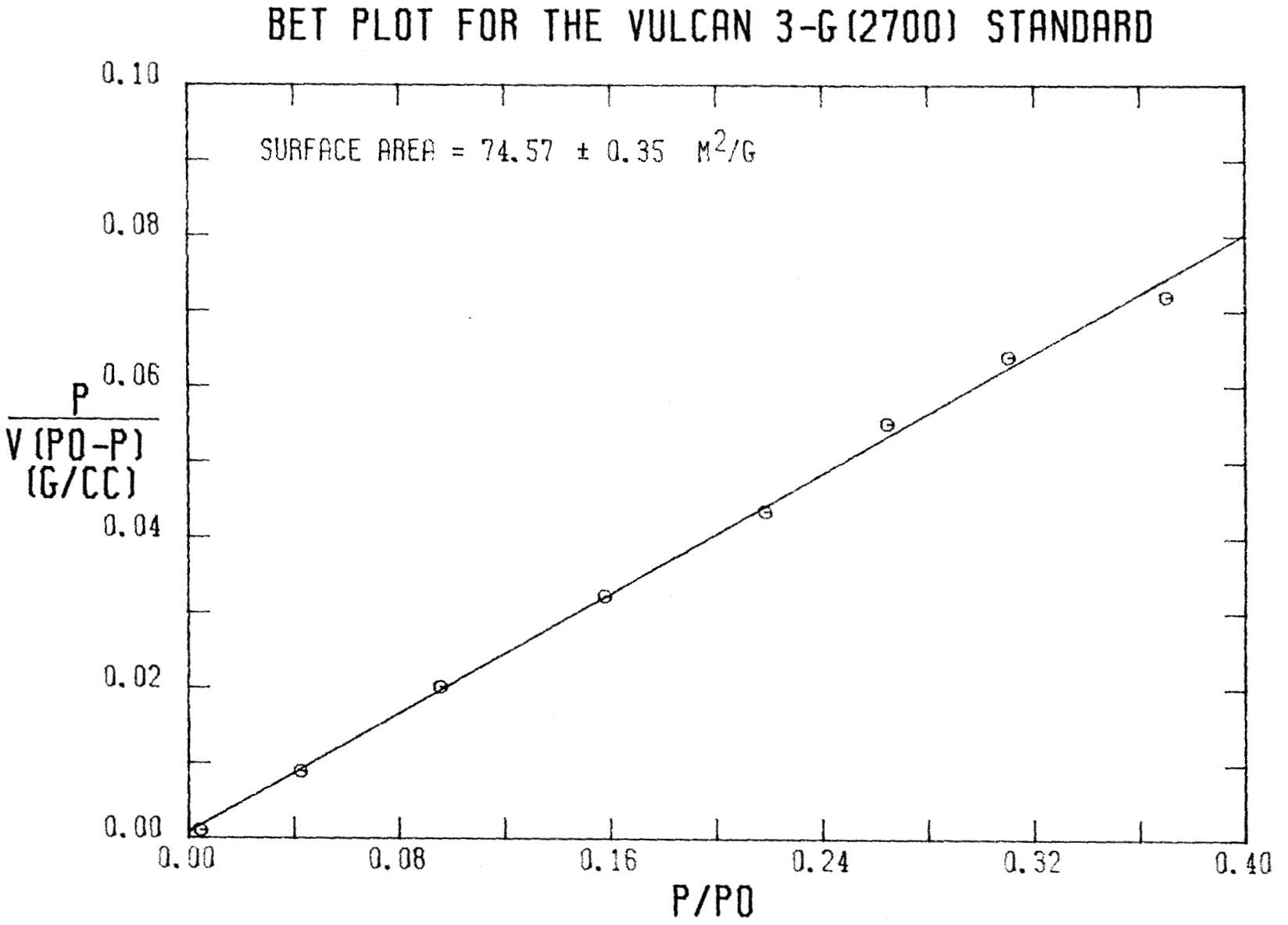
BET PLOT FOR THE VULCAN 3-G(2700) STANDARD
SURFACE AREA = 74.57 ± 0.35 M2/G
P / V(PO-P) (G/CC)
0.10
0.08
0.06
0.04
0.02
0.00
0.00
0.08
0.16
0.24
0.32
0.40
P/PO

FIGURE A-3

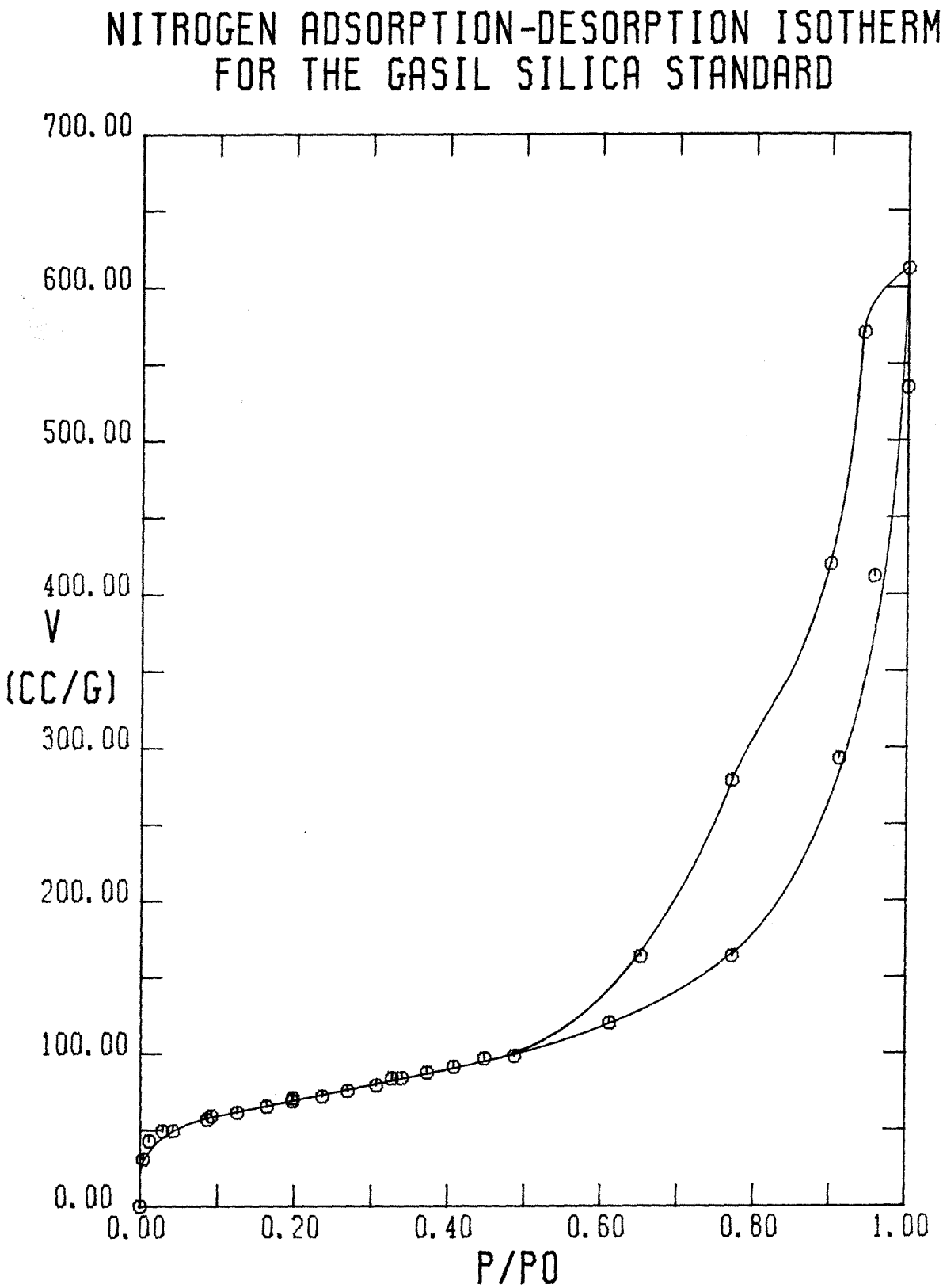
NITROGEN ADSORPTION-DESORPTION ISOTHERM
FOR THE GASIL SILICA STANDARD
700.00
600.00
500.00
400.00
V
(CC/G)
300.00
200.00
100.00
0.00
0.00
0.20
0.40
0.60
0.80
1.00
P/PO

FIGURE A-4

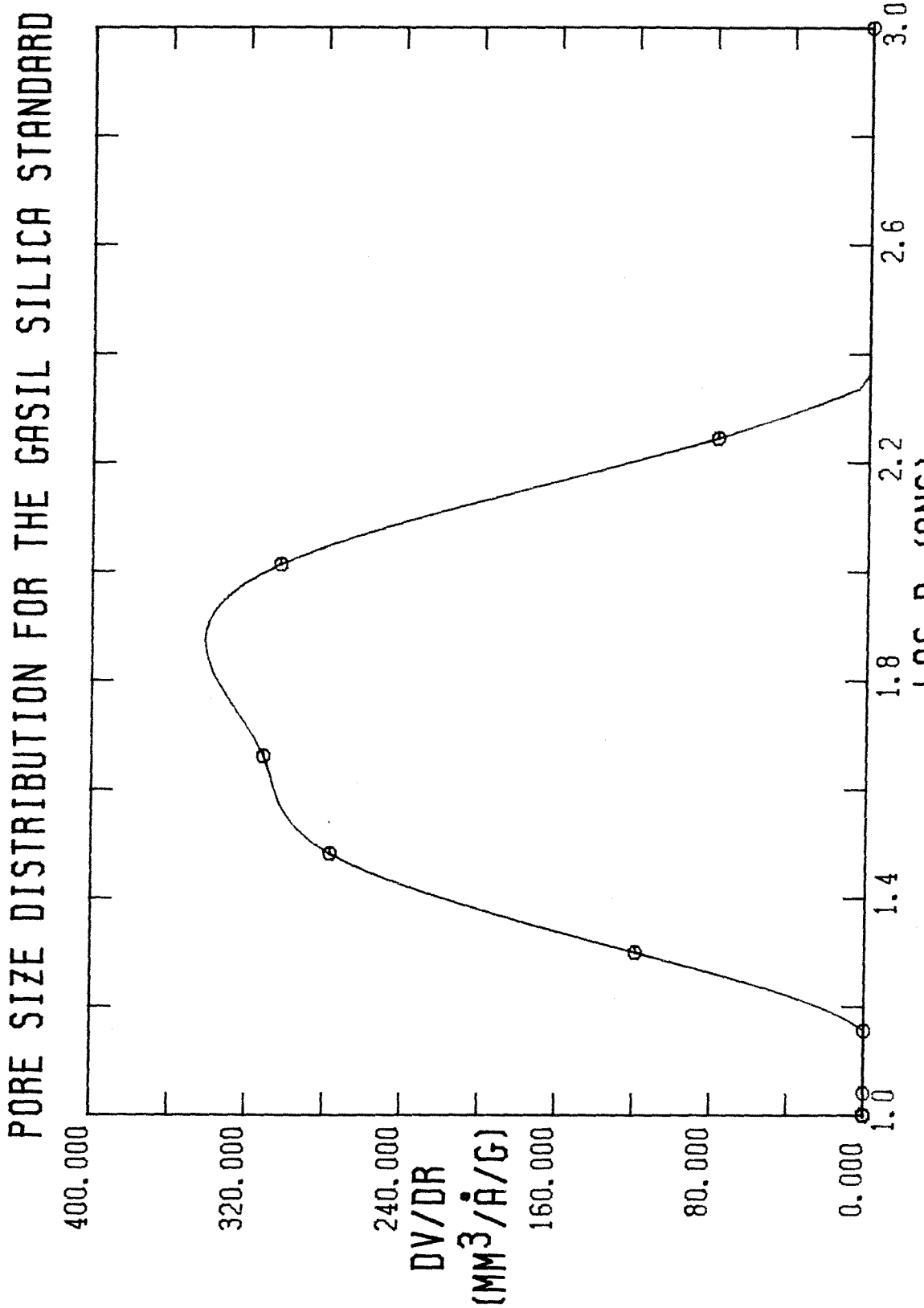
PORE SIZE DISTRIBUTION FOR THE GASIL SILICA STANDARD
400.000
320.000
240.000
160.000
80.000
0.000
DV/DR
(MM3/Å/G)
1.0
1.4
1.8
2.2
2.6
3.0
LOG R (ANG)

FIGURE A-5

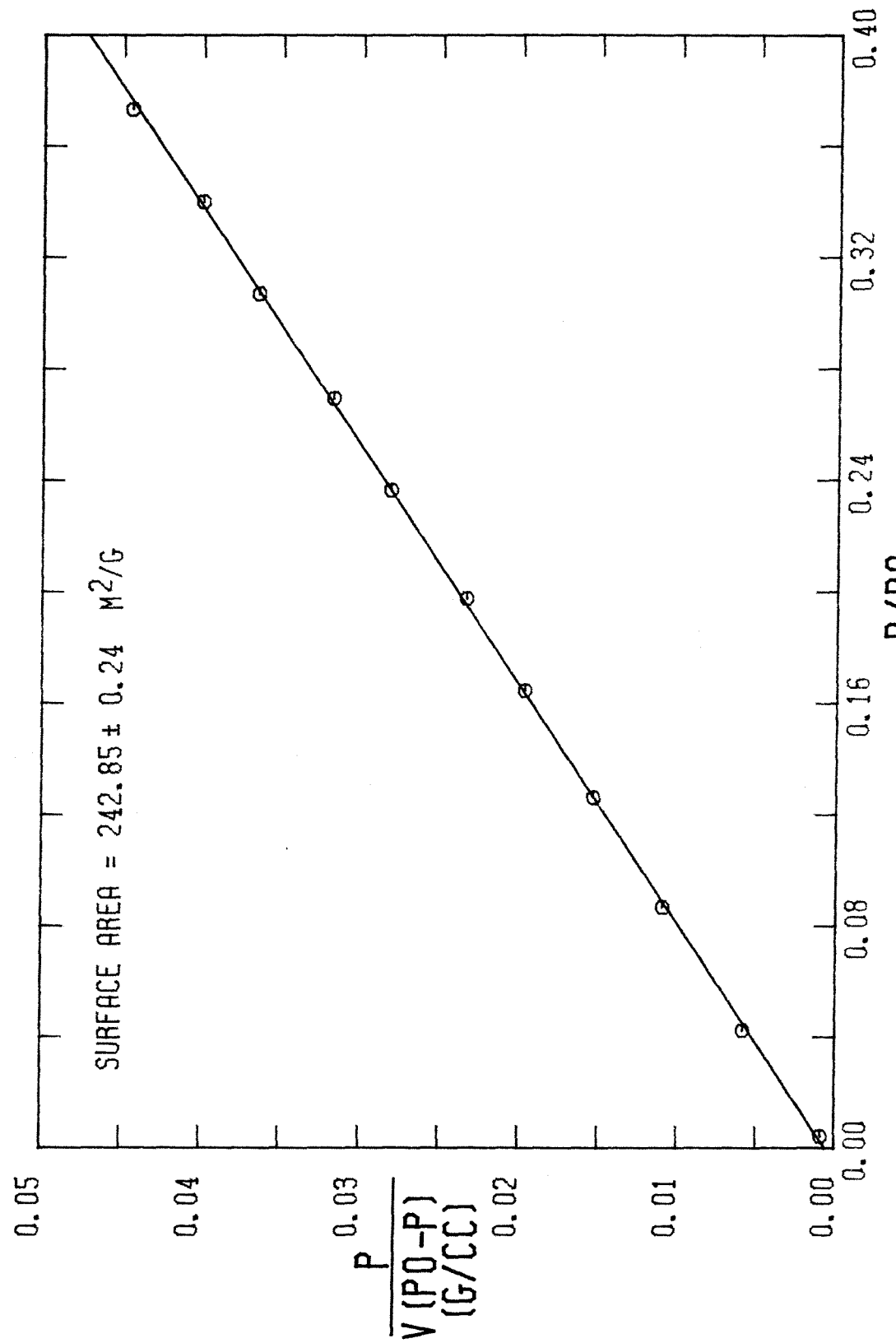
BET PLOT FOR THE GASIL SILICA STANDARD
SURFACE AREA = 242.85 ± 0.24 M2/G
P/PO
P / V(PO-P) (G/CC)
0.00
0.08
0.16
0.24
0.32
0.40
0.00
0.01
0.02
0.03
0.04
0.05

FIGURE A-6

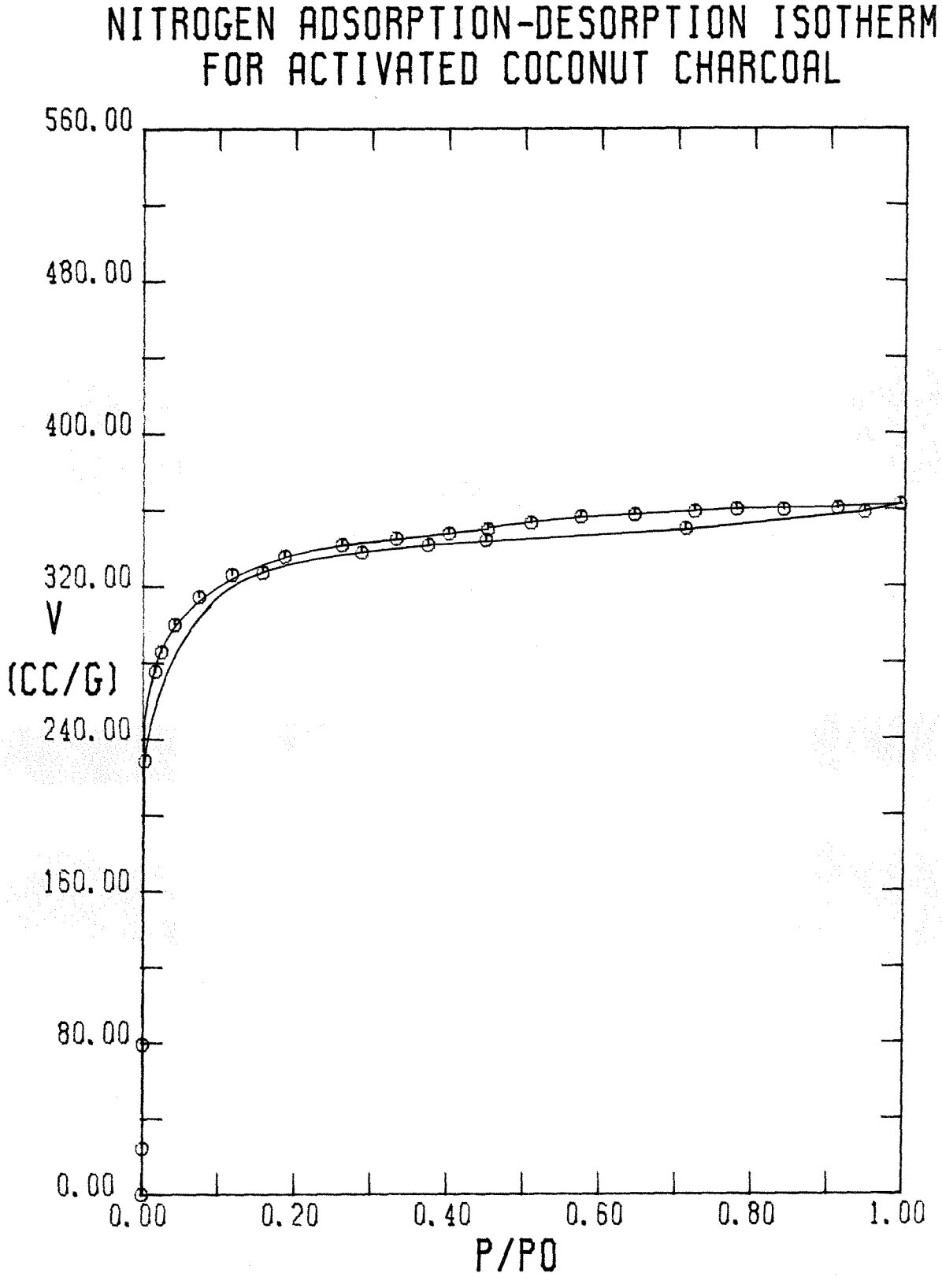
NITROGEN ADSORPTION-DESORPTION ISOTHERM
FOR ACTIVATED COCONUT CHARCOAL
560.00
480.00
400.00
320.00
V
(CC/G)
240.00
160.00
80.00
0.00
0.00
0.20
0.40
0.60
0.80
1.00
P/PO

FIGURE A-7

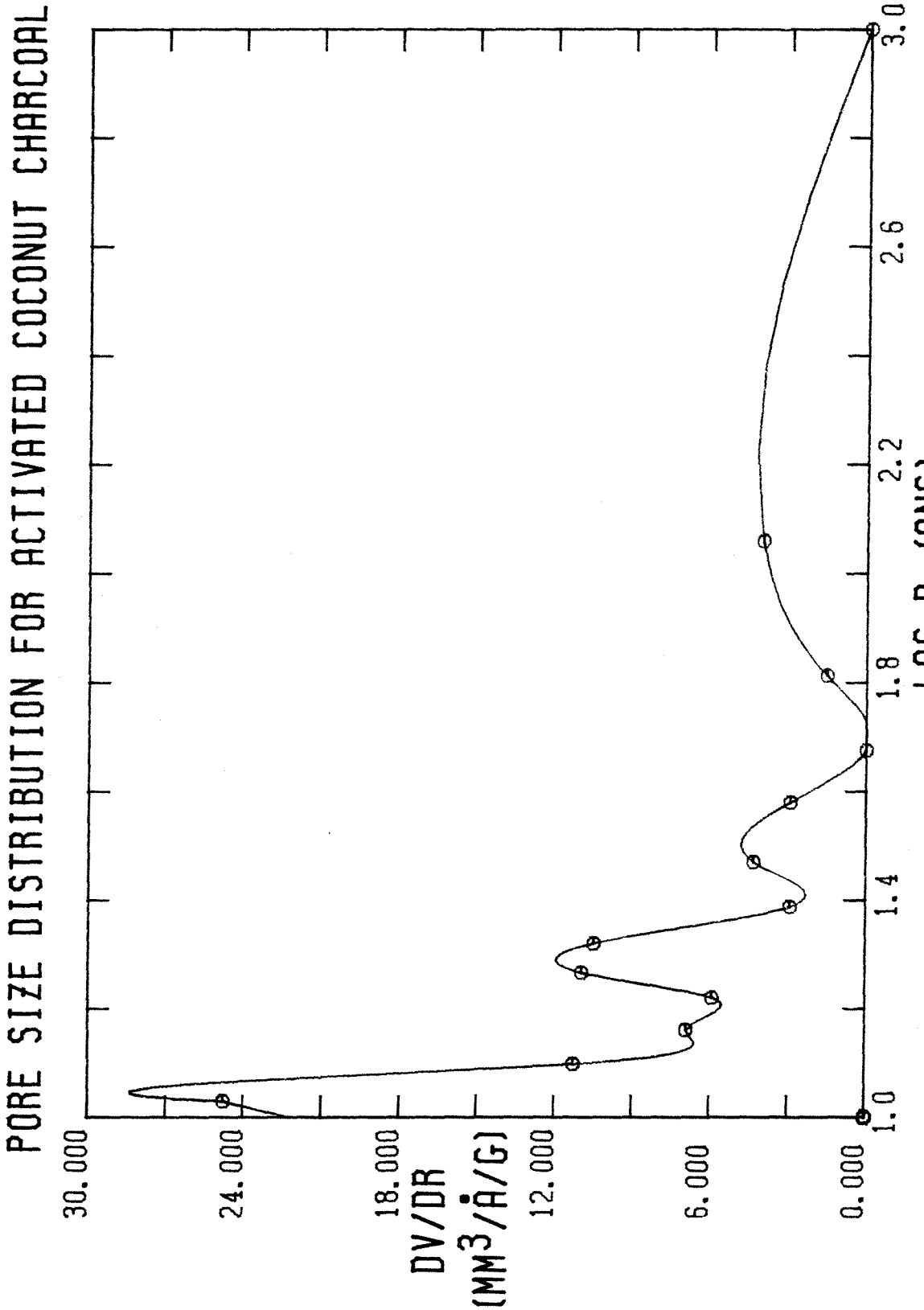
PORE SIZE DISTRIBUTION FOR ACTIVATED COCONUT CHARCOAL
30.000
24.000
18.000
12.000
6.000
0.000
DV/DR
(MM3/Å/G)
1.0
1.4
1.8
2.2
2.6
3.0
LOG R (ANG)

FIGURE A-8

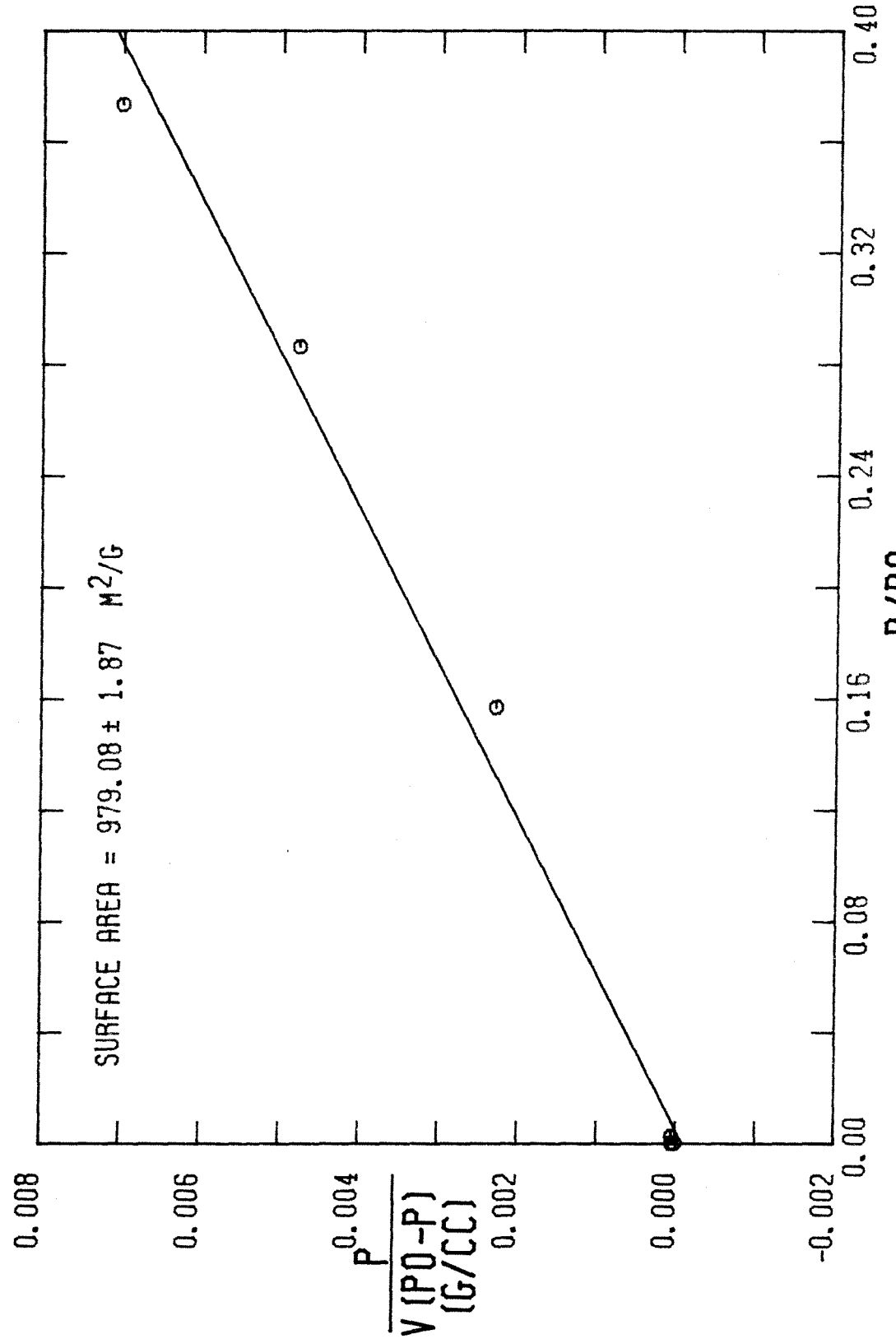
BET PLOT FOR ACTIVATED COCONUT CHARCOAL
SURFACE AREA = 979.08 ± 1.87 M2/G
P / V (PO-P) (G/CC)
P/PO
0.008
0.006
0.004
0.002
0.000
-0.002
0.00
0.08
0.16
0.24
0.32
0.40

FIGURE A-9

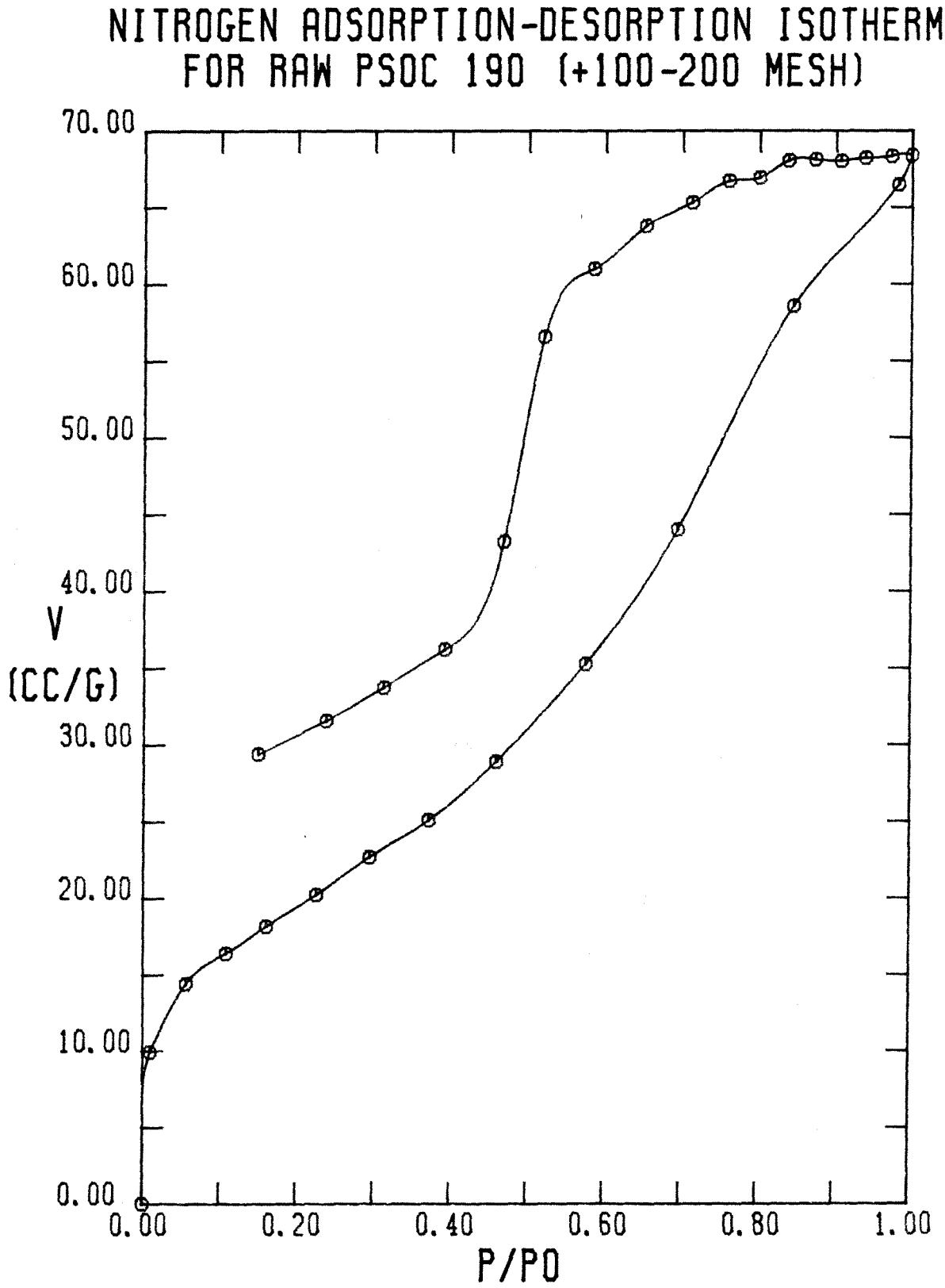
NITROGEN ADSORPTION-DESORPTION ISOTHERM
FOR RAW PSOC 190 (+100-200 MESH)
70.00
60.00
50.00
40.00
V
(CC/G)
30.00
20.00
10.00
0.00
0.00
0.20
0.40
0.60
0.80
1.00
P/PO

FIGURE A-10

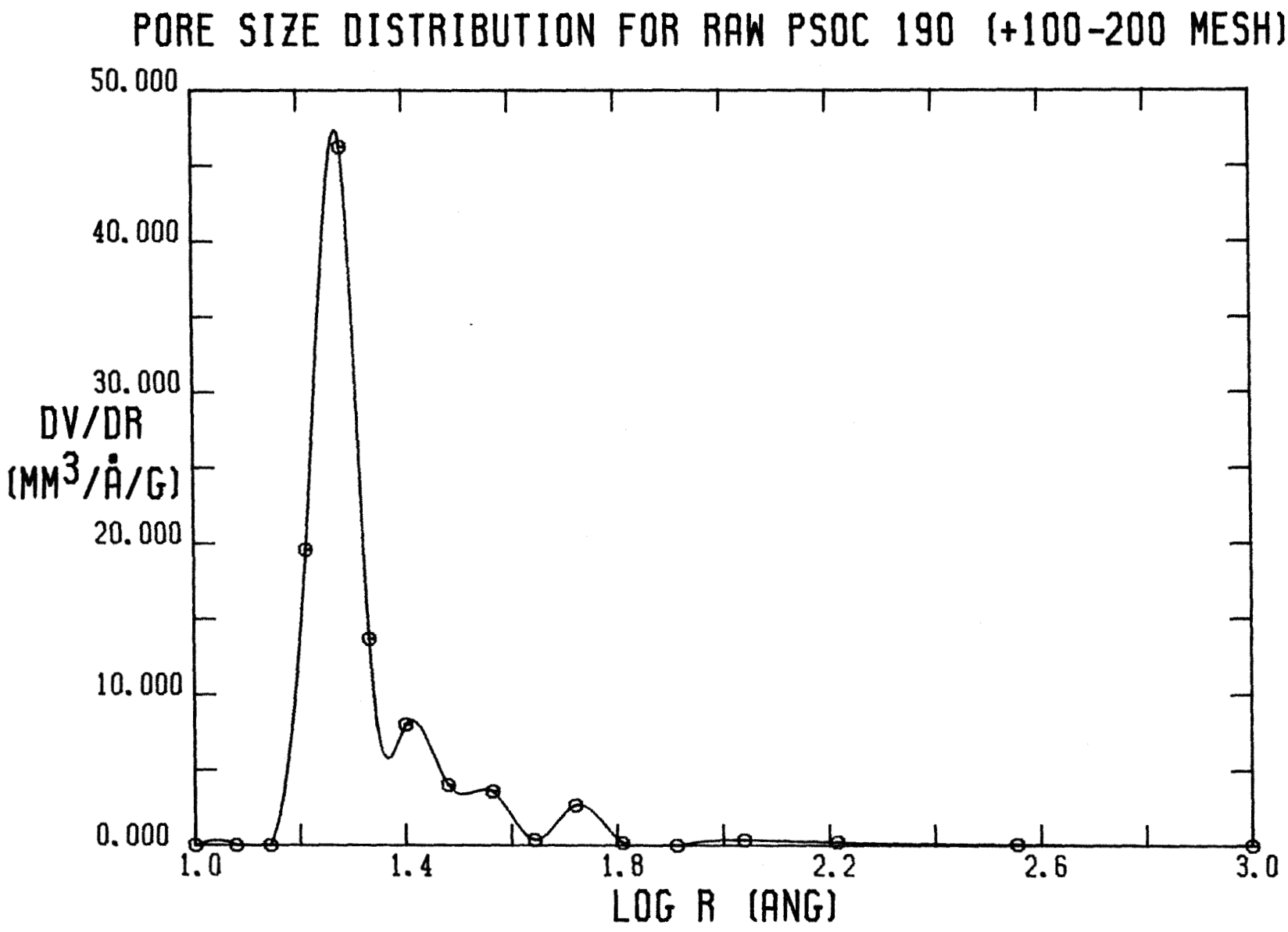
PORE SIZE DISTRIBUTION FOR RAW PSOC 190 (+100-200 MESH)
50.000
40.000
30.000
DV/DR
(MM3/Å/G)
20.000
10.000
0.000
1.0
1.4
1.8
2.2
2.6
3.0
LOG R (ANG)

FIGURE A-11

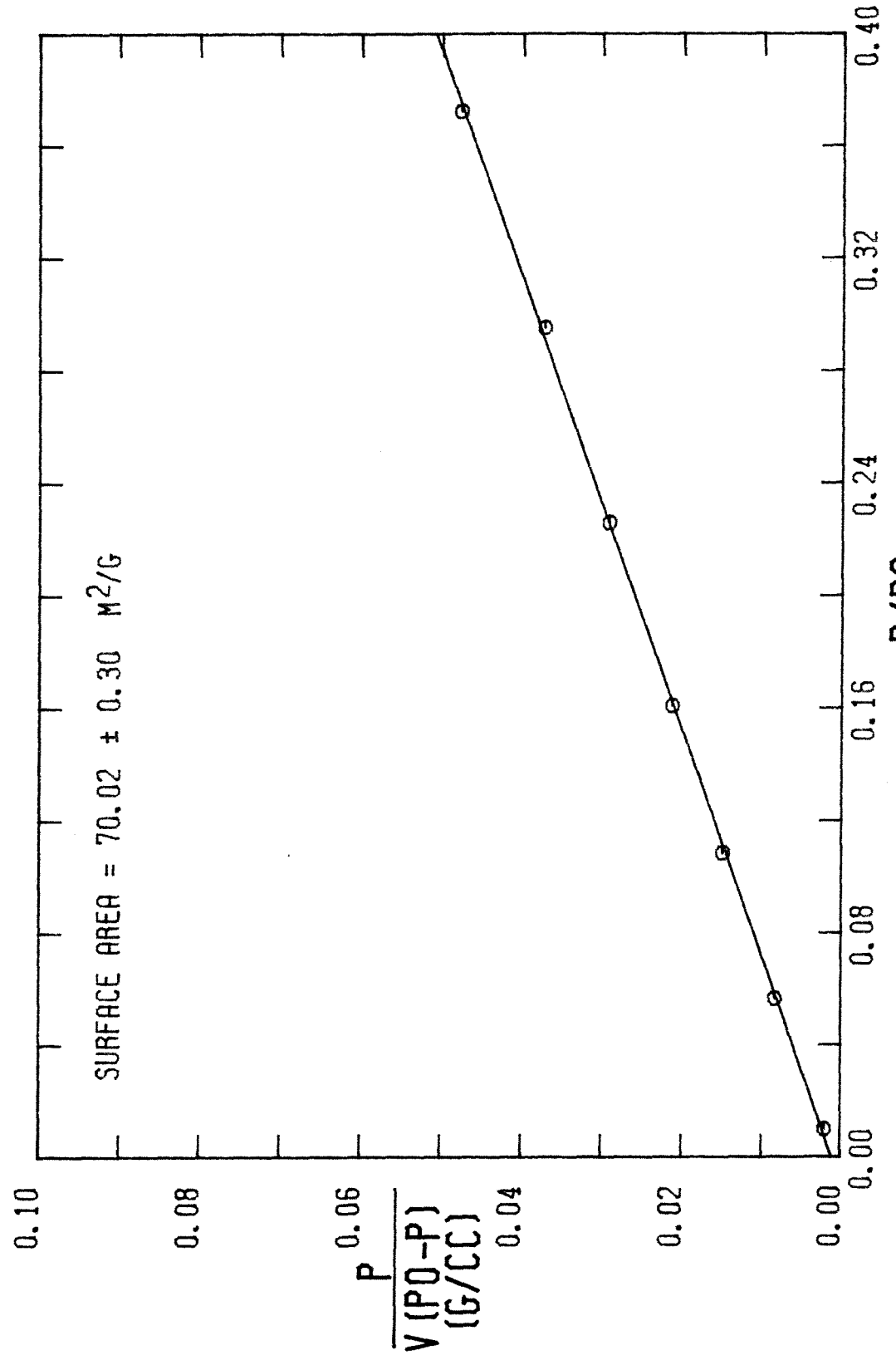
BET PLOT FOR RAW PSOC 190 (+100-200 MESH)
SURFACE AREA = 70.02 ± 0.30 M2/G
P/(V(PO-P))
(G/CC)
P/PO
0.10
0.08
0.06
0.04
0.02
0.00
0.00
0.08
0.16
0.24
0.32
0.40

FIGURE A-12

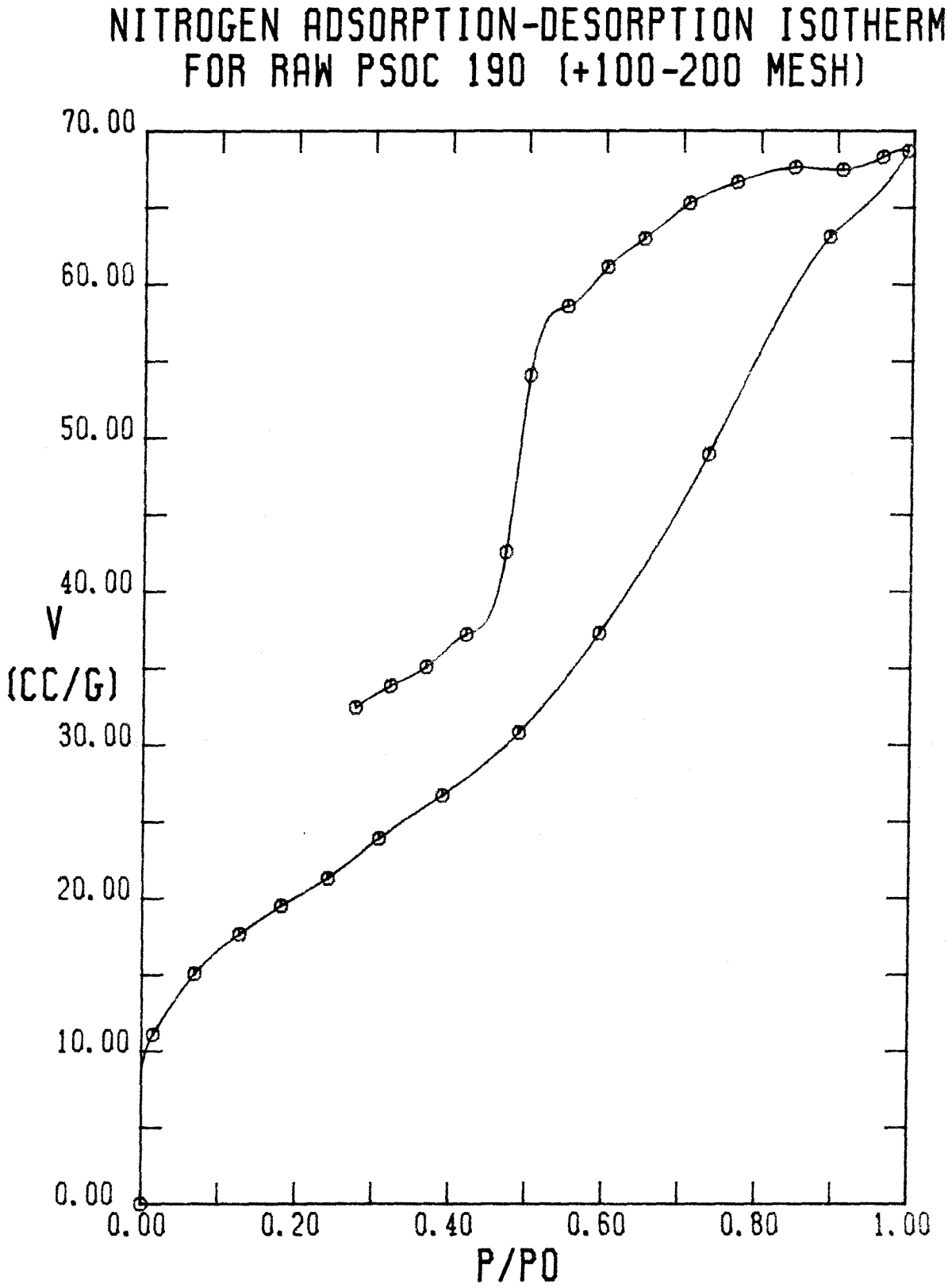
NITROGEN ADSORPTION-DESORPTION ISOTHERM
FOR RAW PSOC 190 (+100-200 MESH)
70.00
60.00
50.00
40.00
V
(CC/G)
30.00
20.00
10.00
0.00
0.00
0.20
0.40
0.60
0.80
1.00
P/PO

FIGURE A-13

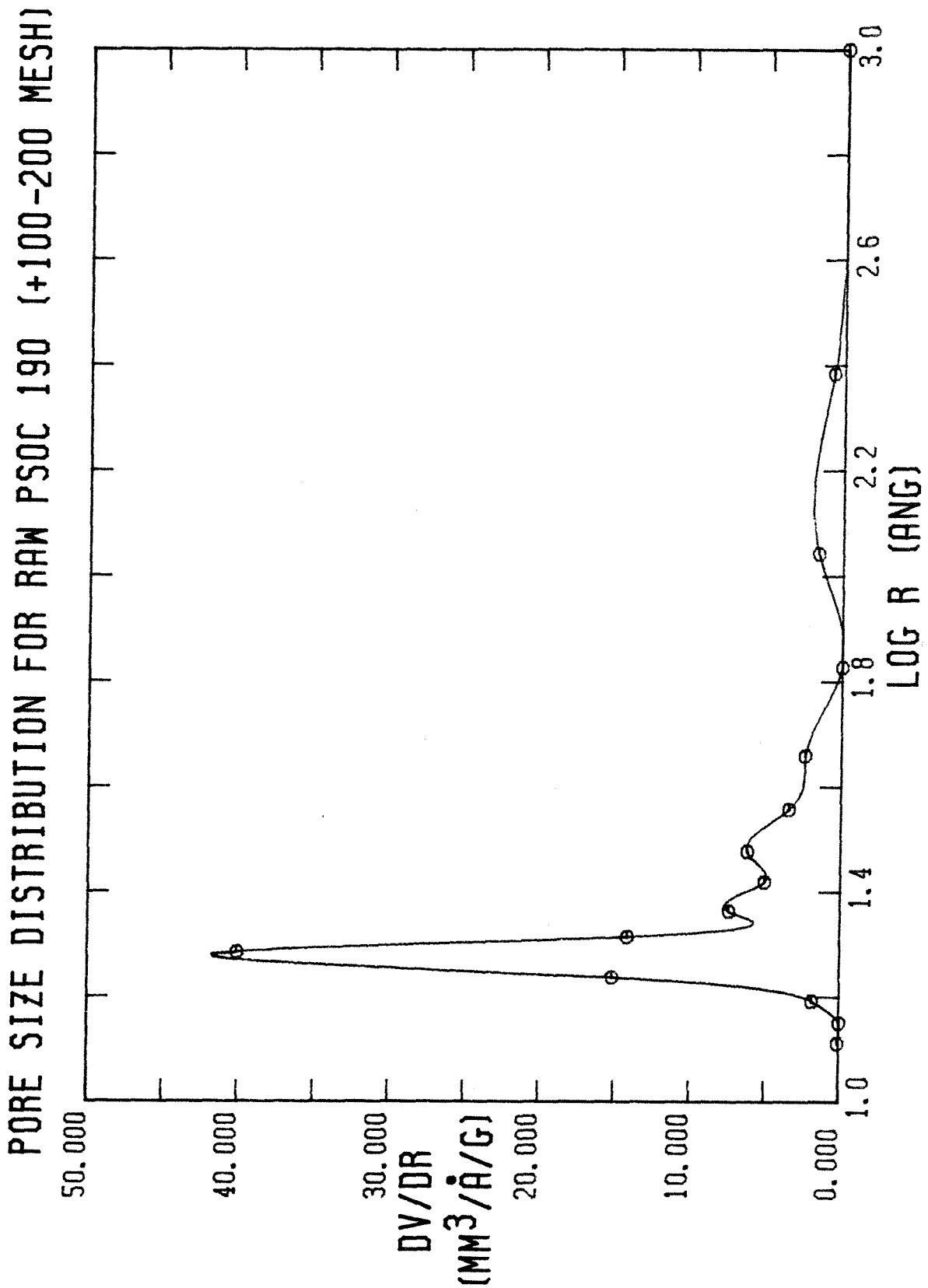
PORE SIZE DISTRIBUTION FOR RAW PSOC 190 (+100-200 MESH)
DV/DR
(MM3/Å/G)
50.000
40.000
30.000
20.000
10.000
0.000
1.0
1.4
1.8
2.2
2.6
3.0
LOG R (ANG)

FIGURE A-14

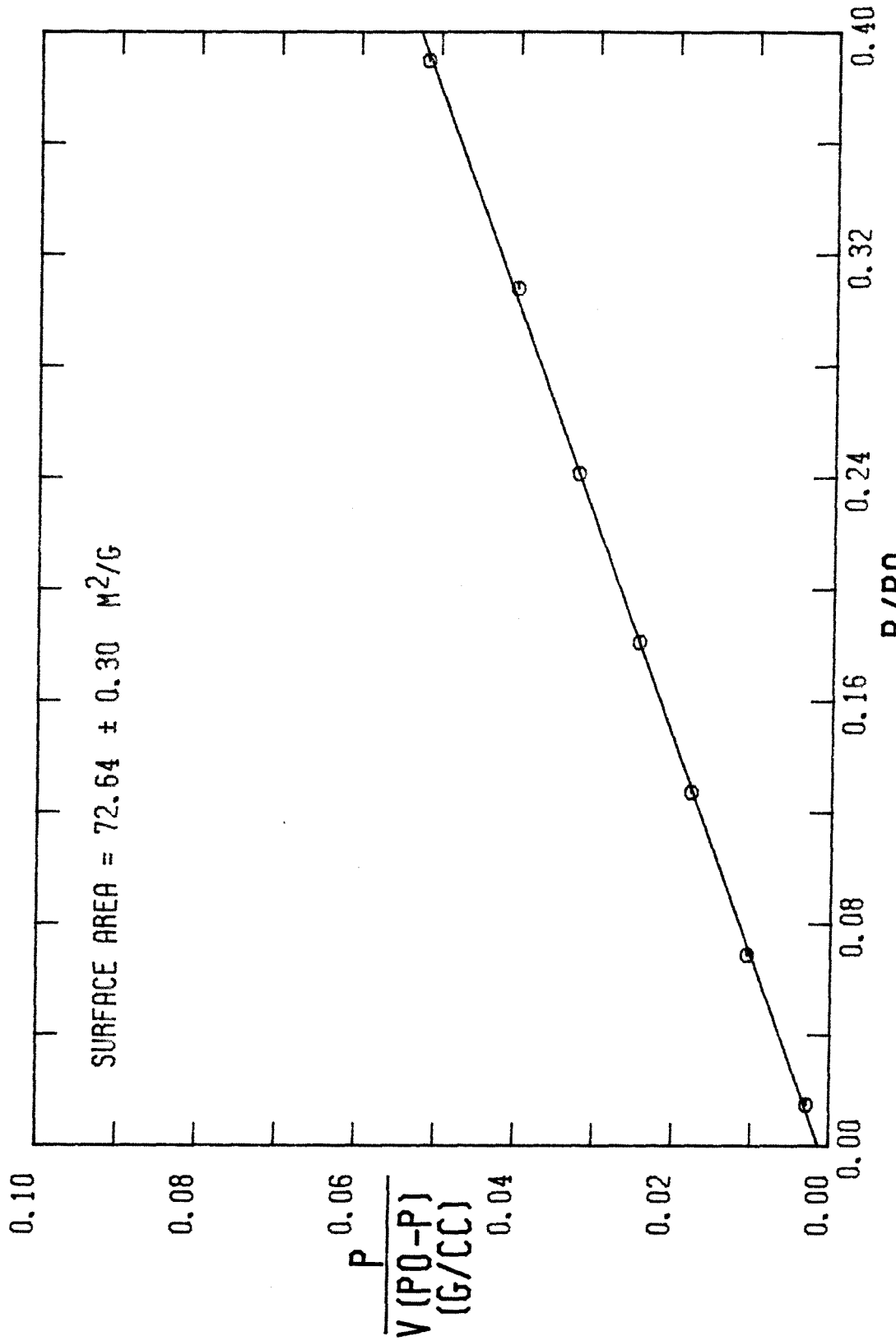
BET PLOT FOR RAW PSOC 190 (+100-200 MESH)
SURFACE AREA = 72.64 ± 0.30 M2/G
P / V(PO-P) (G/CC)
P/PO
0.00
0.02
0.04
0.06
0.08
0.10
0.00
0.08
0.16
0.24
0.32
0.40

FIGURE A-15

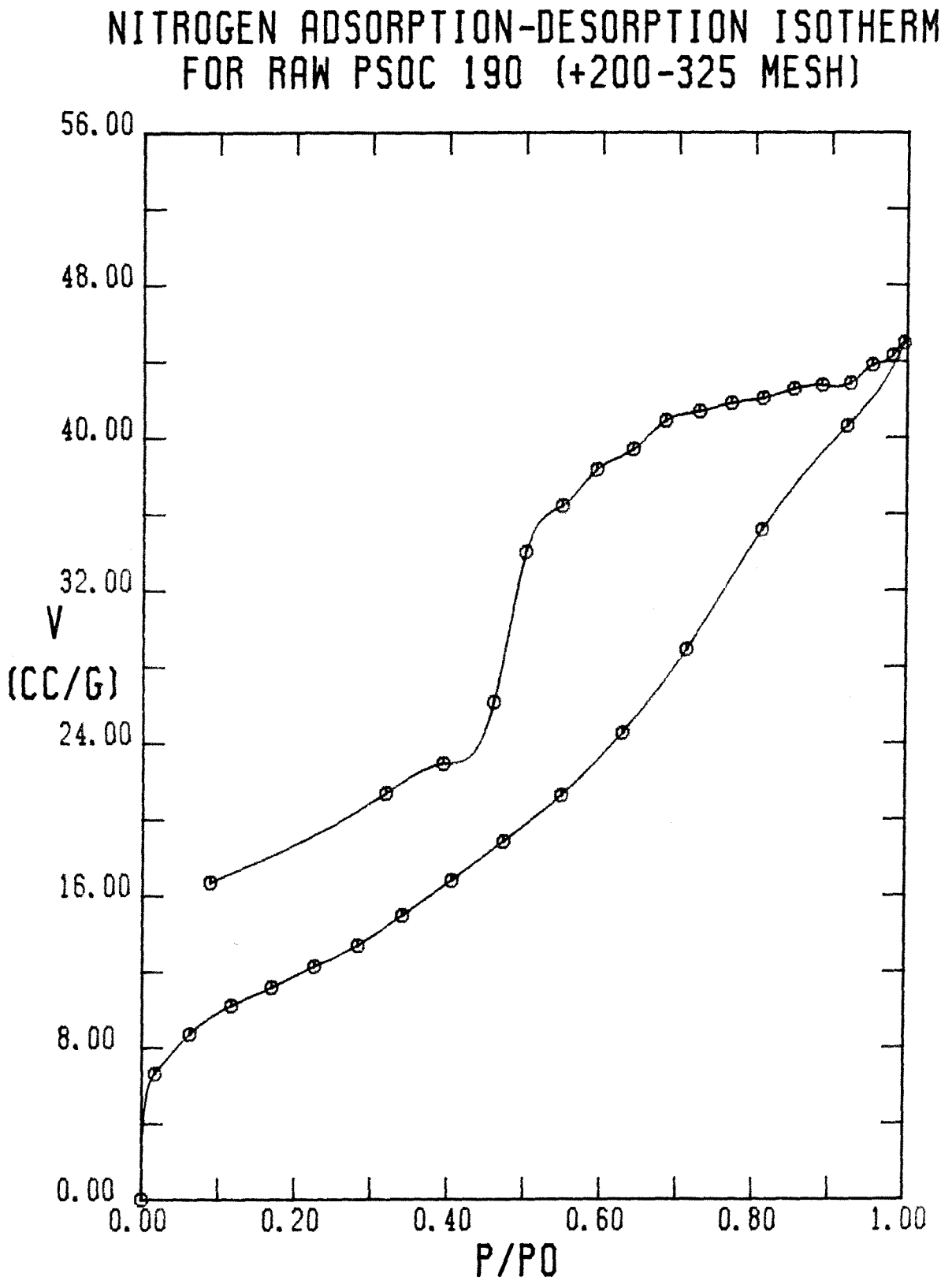
NITROGEN ADSORPTION-DESORPTION ISOTHERM
FOR RAW PSOC 190 (+200-325 MESH)
56.00
48.00
40.00
32.00
V
(CC/G)
24.00
16.00
8.00
0.00
0.00
0.20
0.40
0.60
0.80
1.00
P/PO

FIGURE A-16

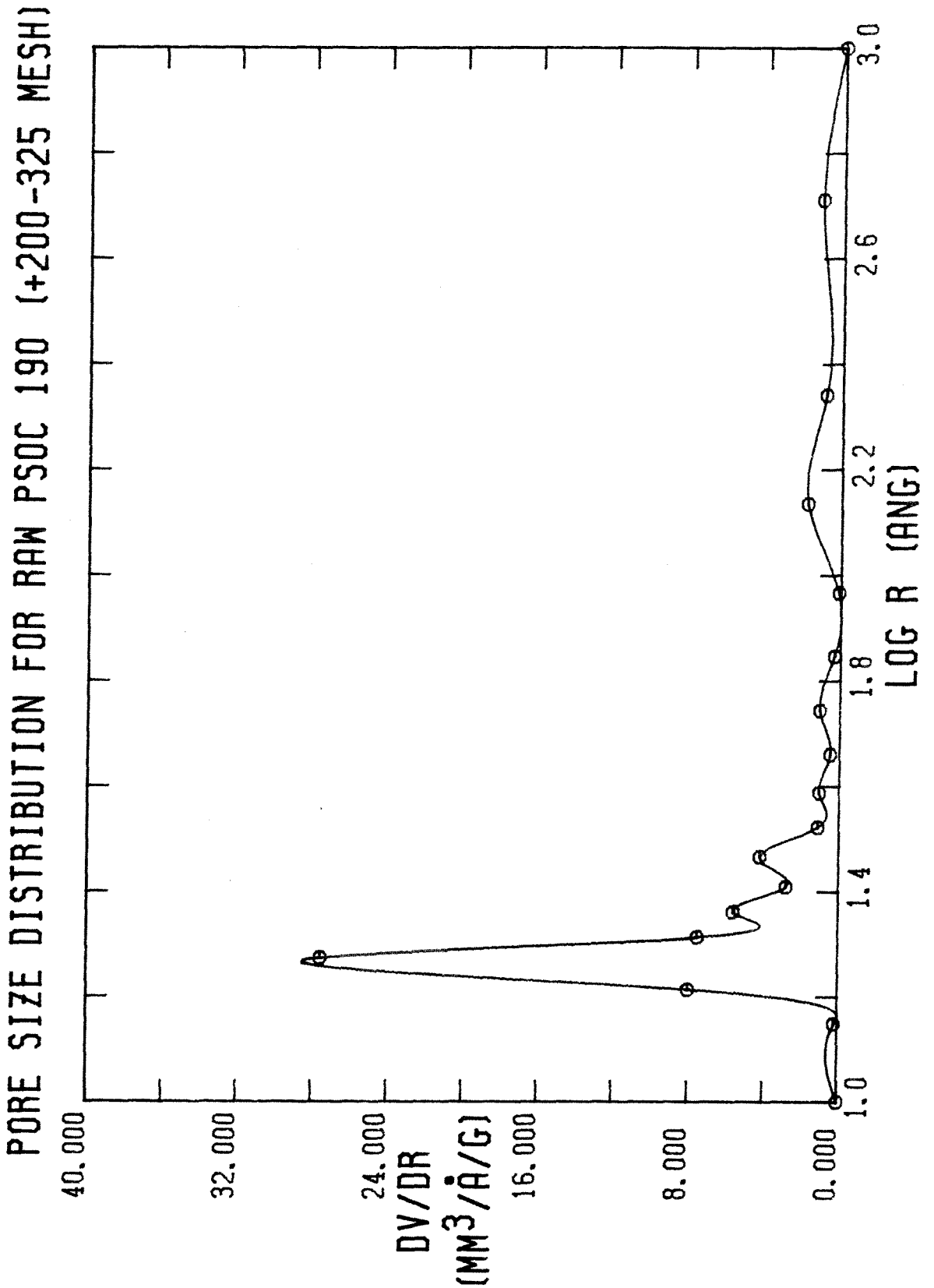
PORE SIZE DISTRIBUTION FOR RAW PSOC 190 (+200-325 MESH)
40.000
32.000
24.000
16.000
8.000
0.000
DV/DR
(MM3/Å/G)
1.0
1.4
1.8
2.2
2.6
3.0
LOG R (ANG)

FIGURE A-17

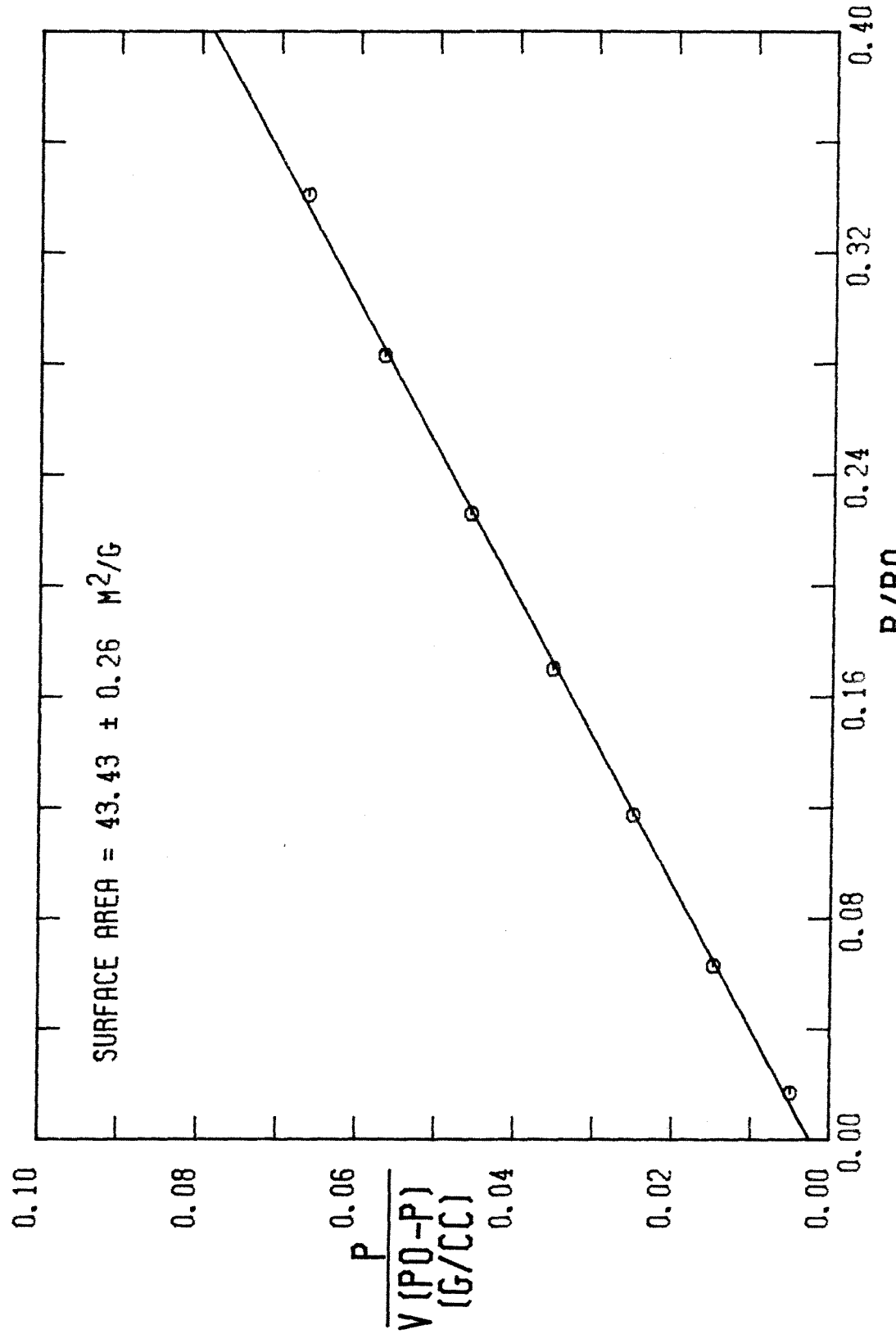
BET PLOT FOR RAW PSOC 190 (+200-325 MESH)
SURFACE AREA = 43.43 ± 0.26 M2/G
P/V(PO-P) (G/CC)
P/PO
0.00
0.02
0.04
0.06
0.08
0.10
0.00
0.08
0.16
0.24
0.32
0.40

FIGURE A-18

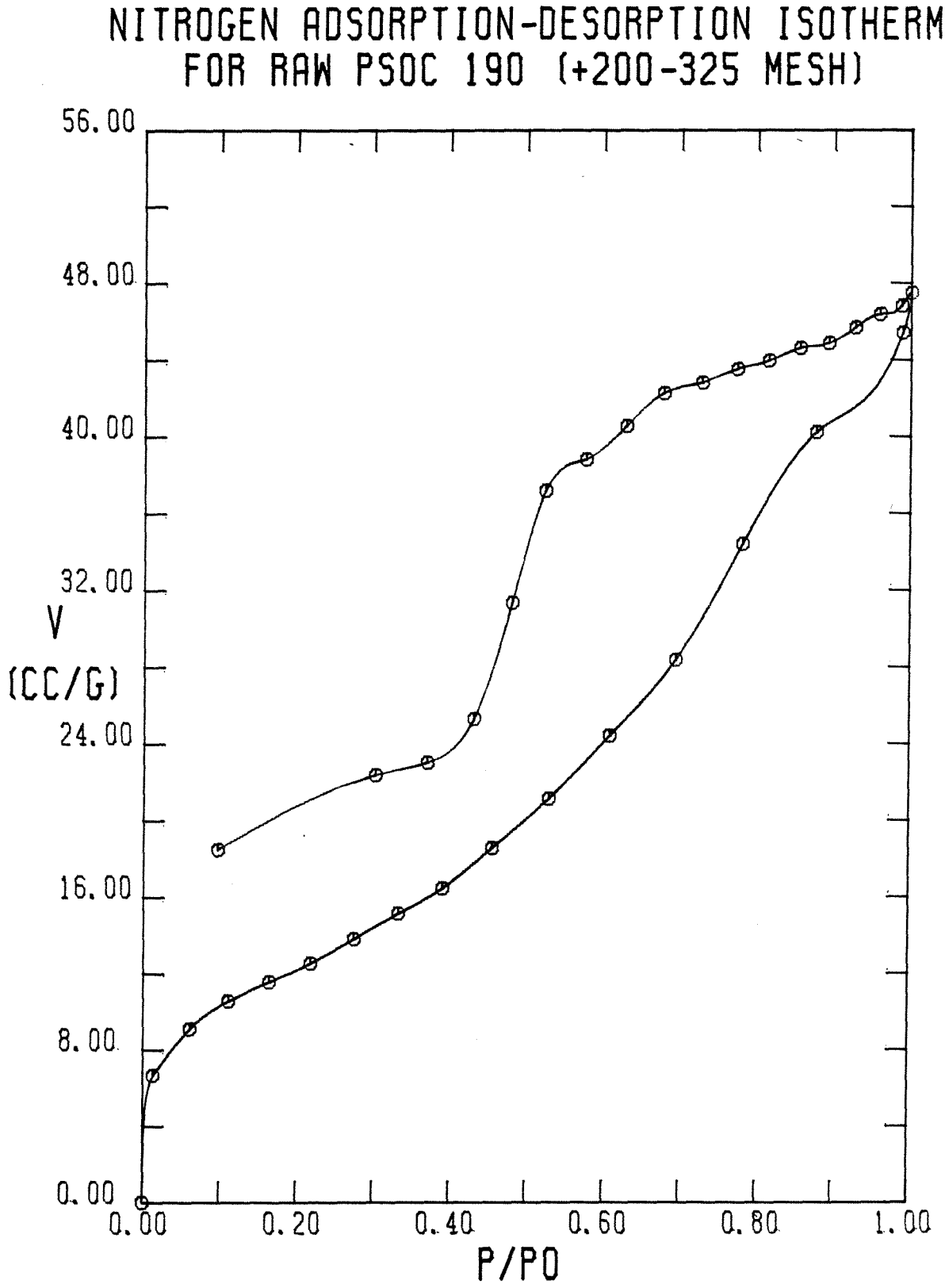
NITROGEN ADSORPTION-DESORPTION ISOTHERM
FOR RAW PSOC 190 (+200-325 MESH)
56.00
48.00
40.00
32.00
V
(CC/G)
24.00
16.00
8.00
0.00
0.00
0.20
0.40
0.60
0.80
1.00
P/PO

FIGURE A-19

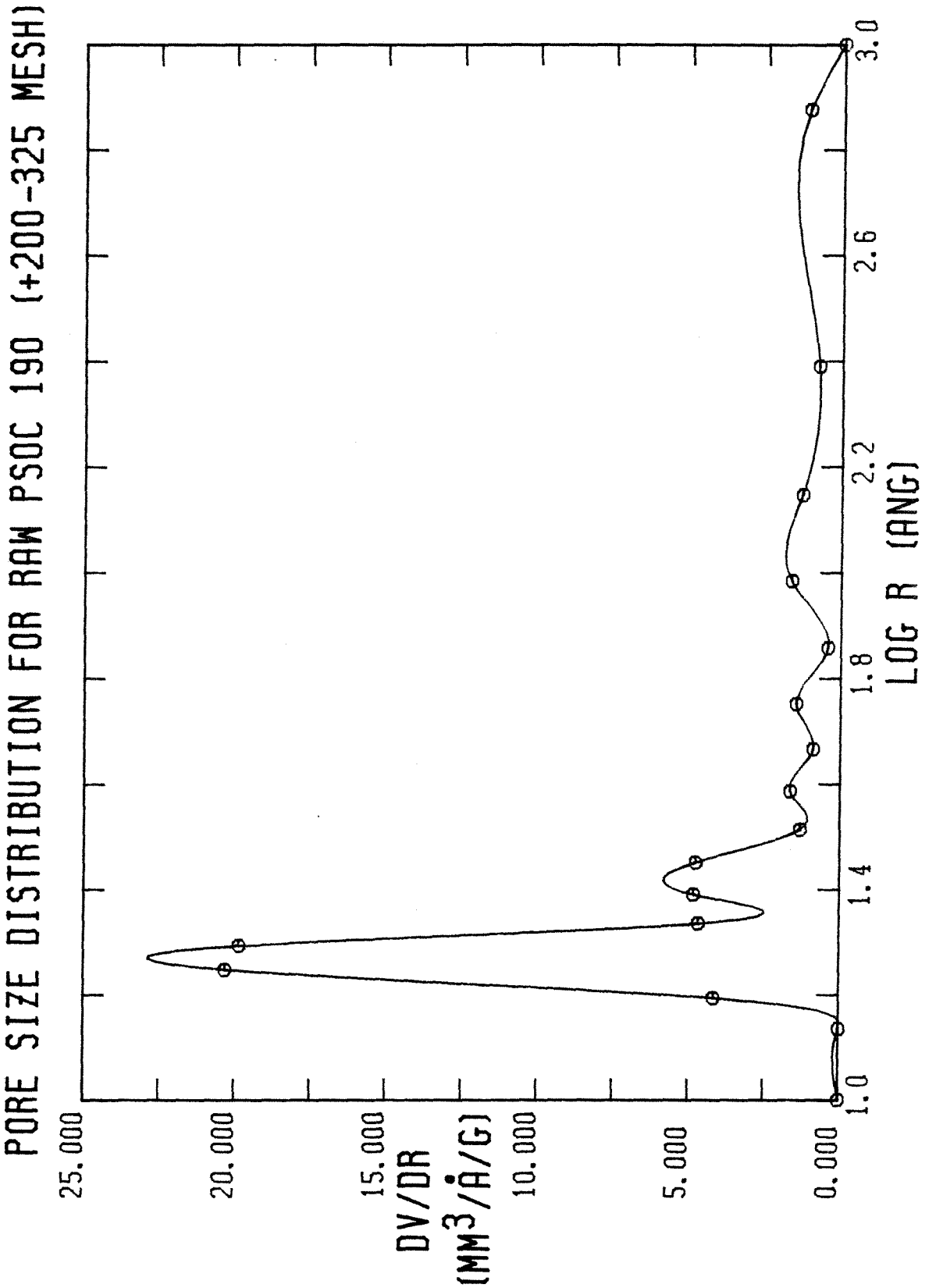
PORE SIZE DISTRIBUTION FOR RAW PSOC 190 (+200-325 MESH)
25.000
20.000
15.000
10.000
5.000
0.000
DV/DR
(MM3/Å/G)
1.0
1.4
1.8
2.2
2.6
3.0
LOG R (ANG)

FIGURE A-20

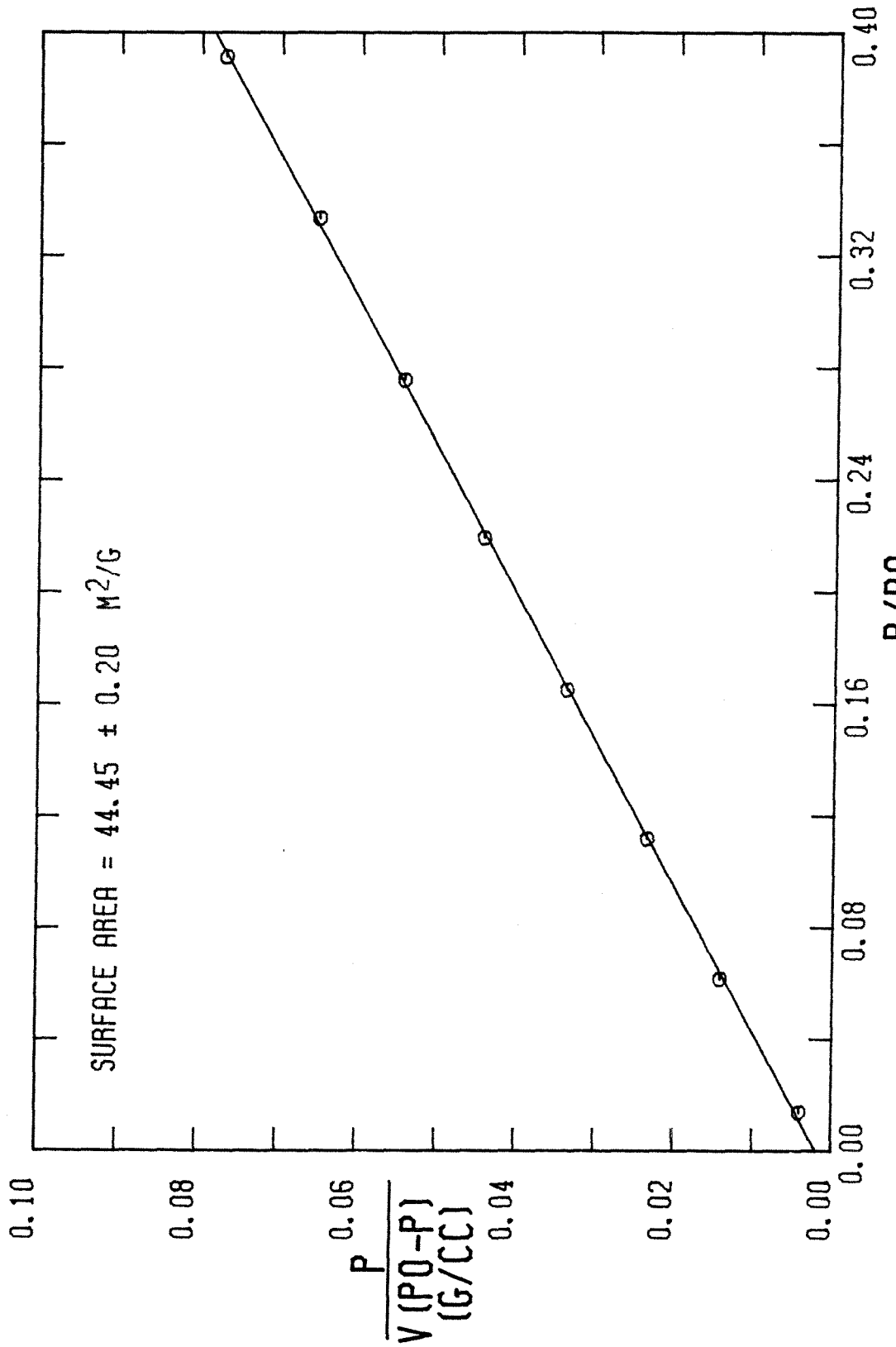
BET PLOT FOR RAW PSOC 190 (+200-325 MESH)
SURFACE AREA = 44.45 ± 0.20 M2/G
P/V(PO-P) (G/CC)
P/PO
0.00
0.02
0.04
0.06
0.08
0.10
0.00
0.08
0.16
0.24
0.32
0.40

FIGURE A-21

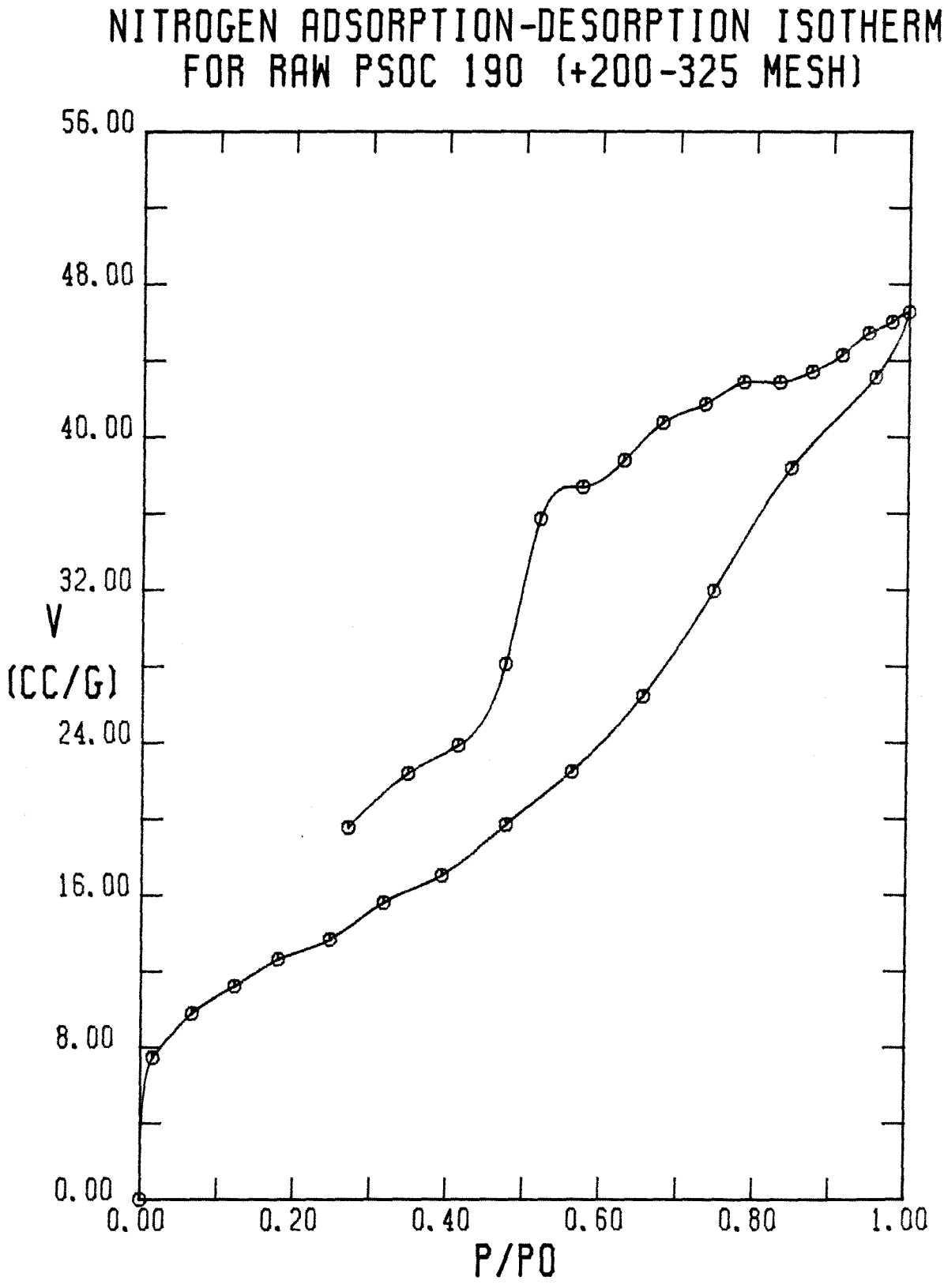
NITROGEN ADSORPTION-DESORPTION ISOTHERM
FOR RAW PSOC 190 (+200-325 MESH)
56.00
48.00
40.00
32.00
V
(CC/G)
24.00
16.00
8.00
0.00
0.00
0.20
0.40
0.60
0.80
1.00
P/PO

FIGURE A-22

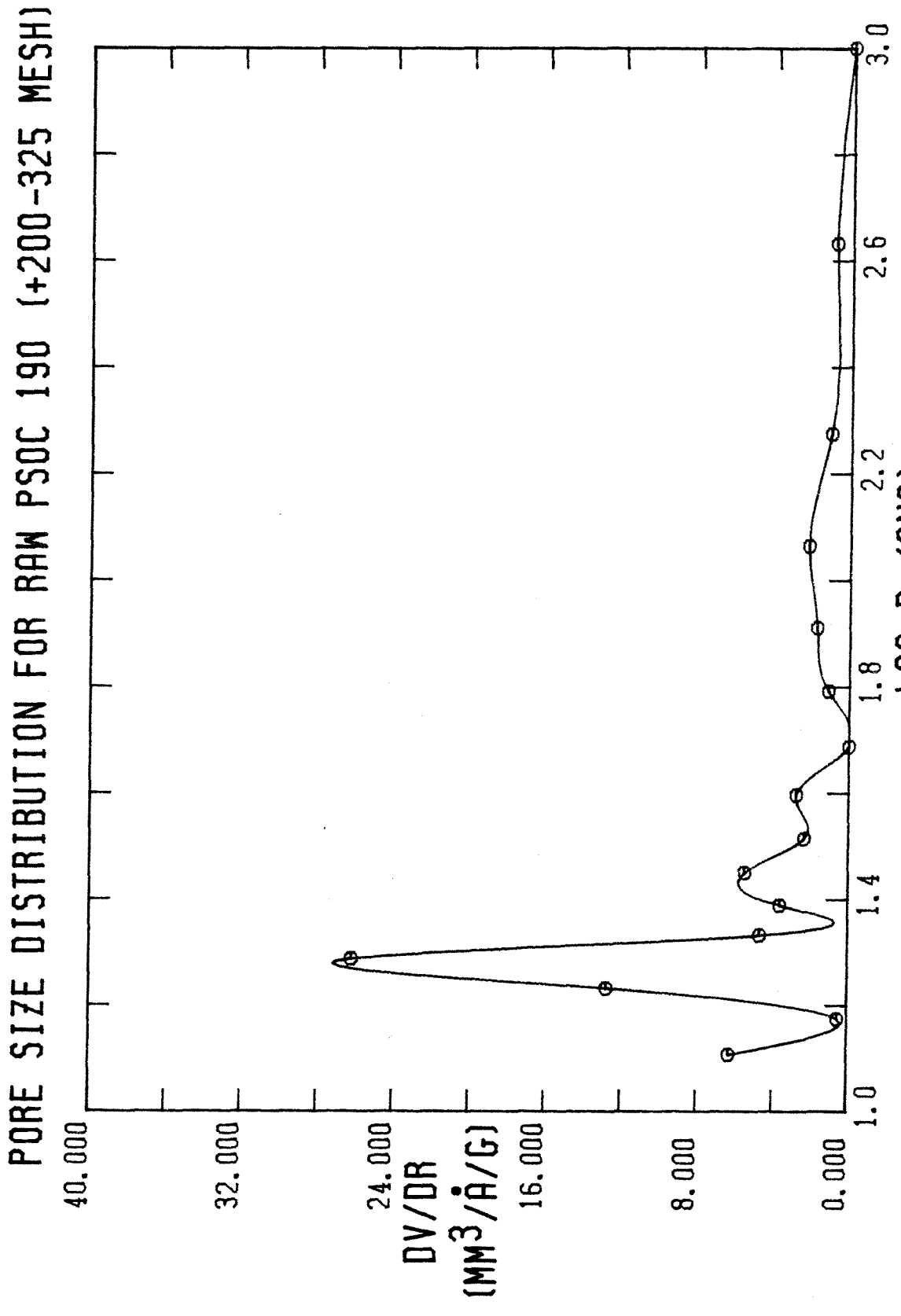
PORE SIZE DISTRIBUTION FOR RAW PSOC 190 (+200-325 MESH)
40.000
32.000
24.000
16.000
8.000
0.000
DV/DR
(MM3/Å/G)
1.0
1.4
1.8
2.2
2.6
3.0
LOG R (ANG)

FIGURE A-23

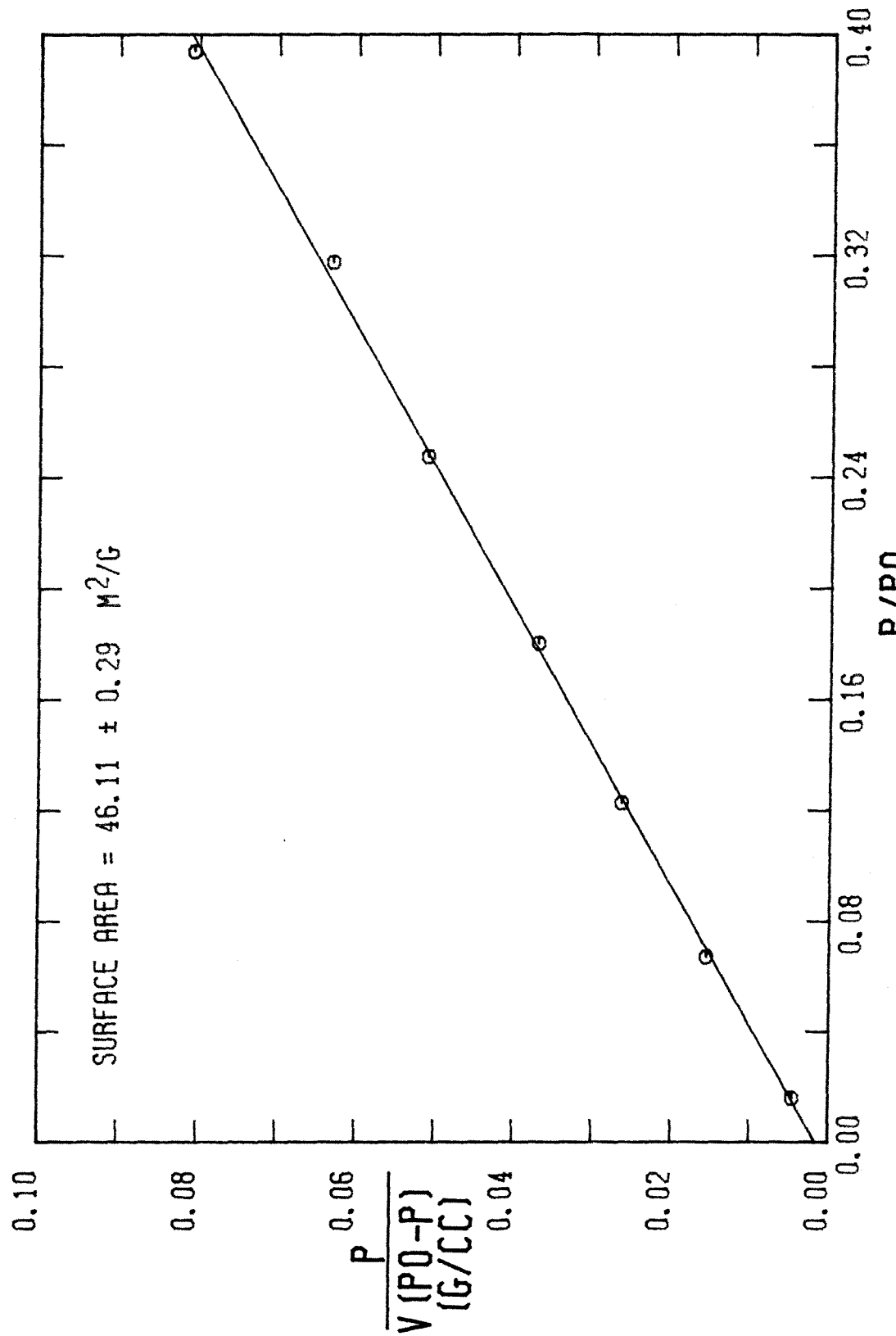
BET PLOT FOR RAW PSOC 190 (+200-325 MESH)
SURFACE AREA = 46.11 ± 0.29 M2/G
P / V(PO-P) (G/CC)
P/PO
0.10
0.08
0.06
0.04
0.02
0.00
0.00
0.08
0.16
0.24
0.32
0.40

FIGURE A-24

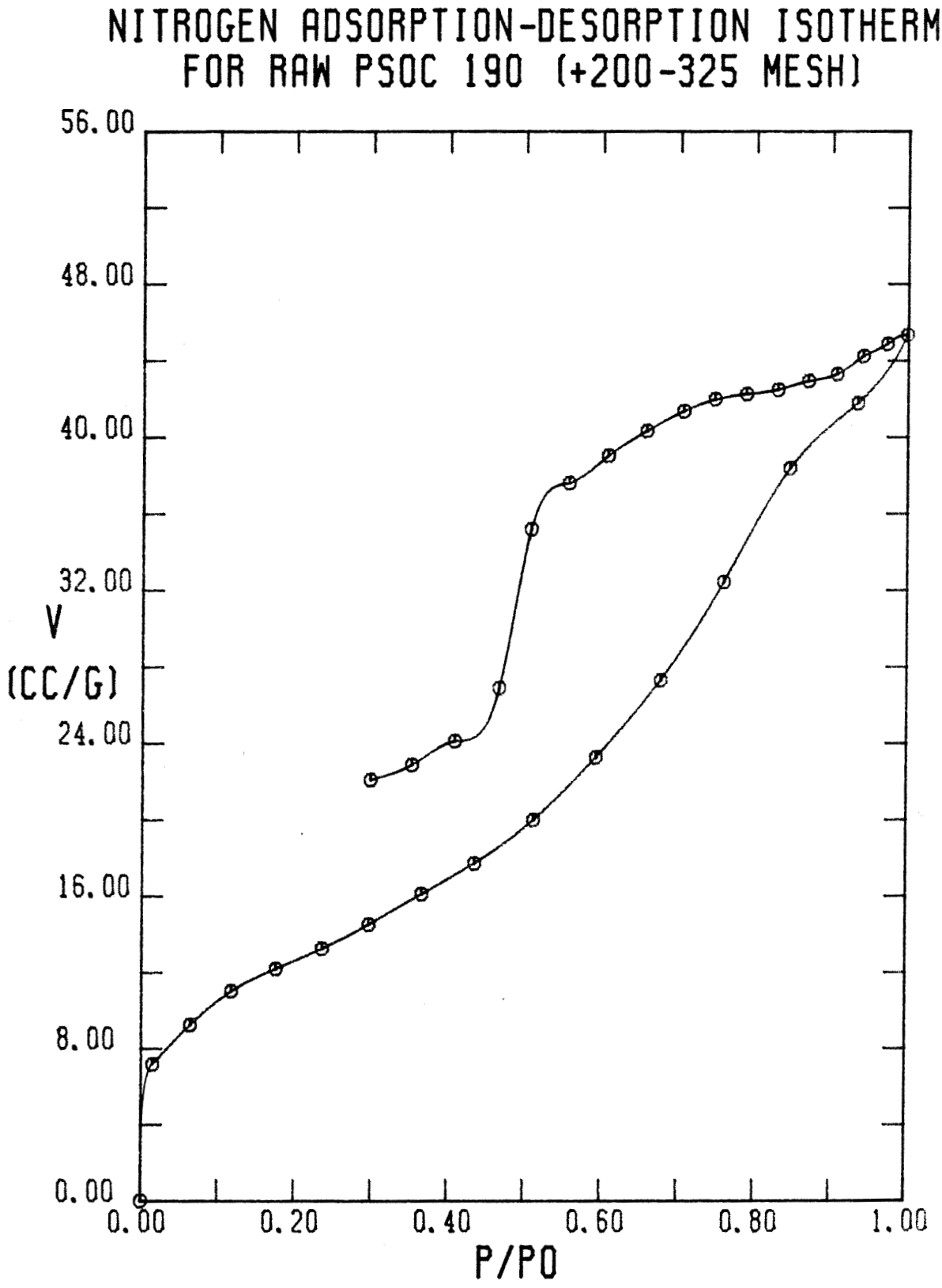
NITROGEN ADSORPTION-DESORPTION ISOTHERM
FOR RAW PSOC 190 (+200-325 MESH)
56.00
48.00
40.00
32.00
V
(CC/G)
24.00
16.00
8.00
0.00
0.00
0.20
0.40
0.60
0.80
1.00
P/PO

FIGURE A-25

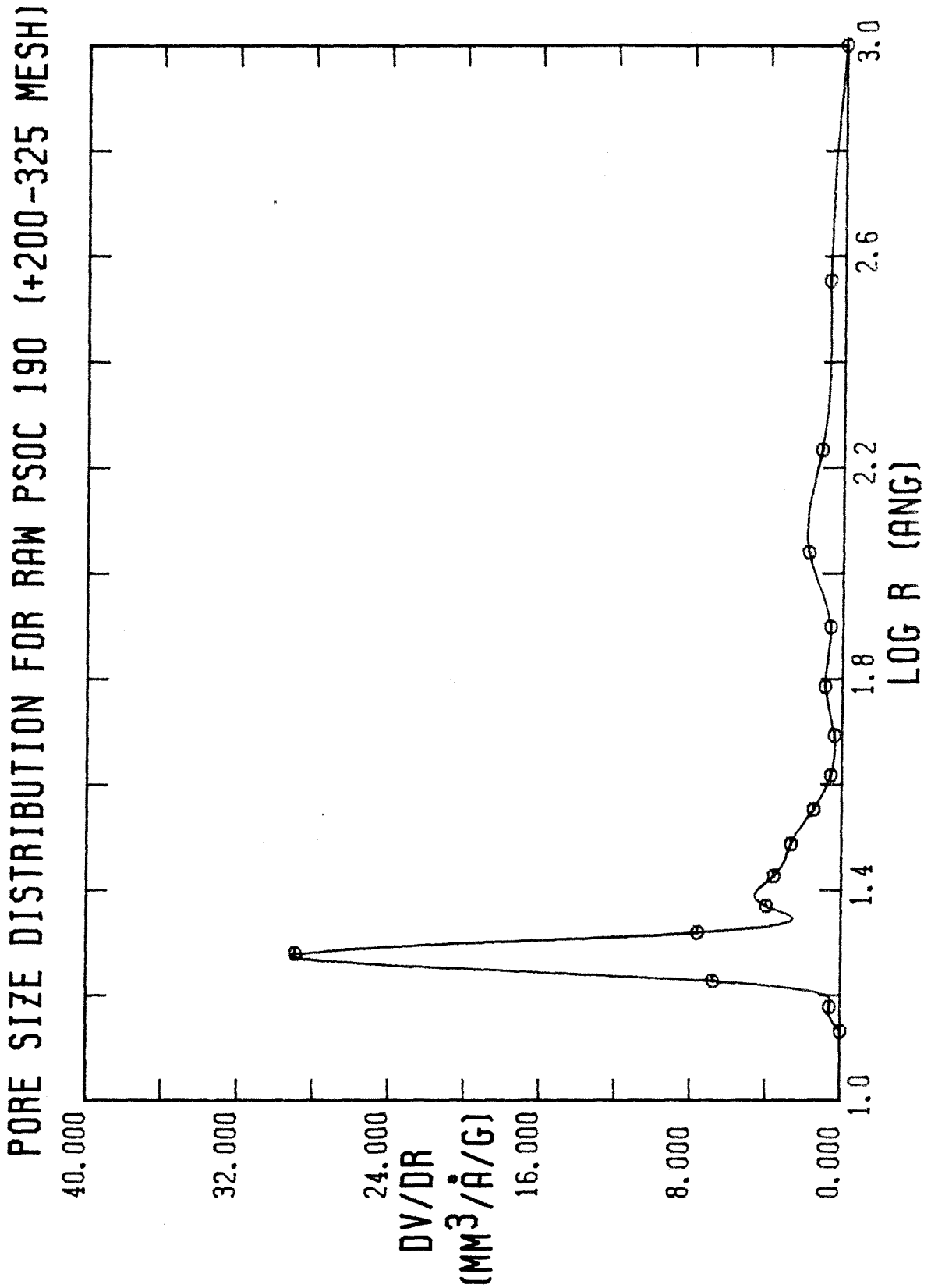
PORE SIZE DISTRIBUTION FOR RAW PSOC 190 (+200-325 MESH)
40.000
32.000
24.000
16.000
8.000
0.000
DV/DR
(MM3/Å/G)
1.0
1.4
1.8
2.2
2.6
3.0
LOG R (ANG)

FIGURE A-26

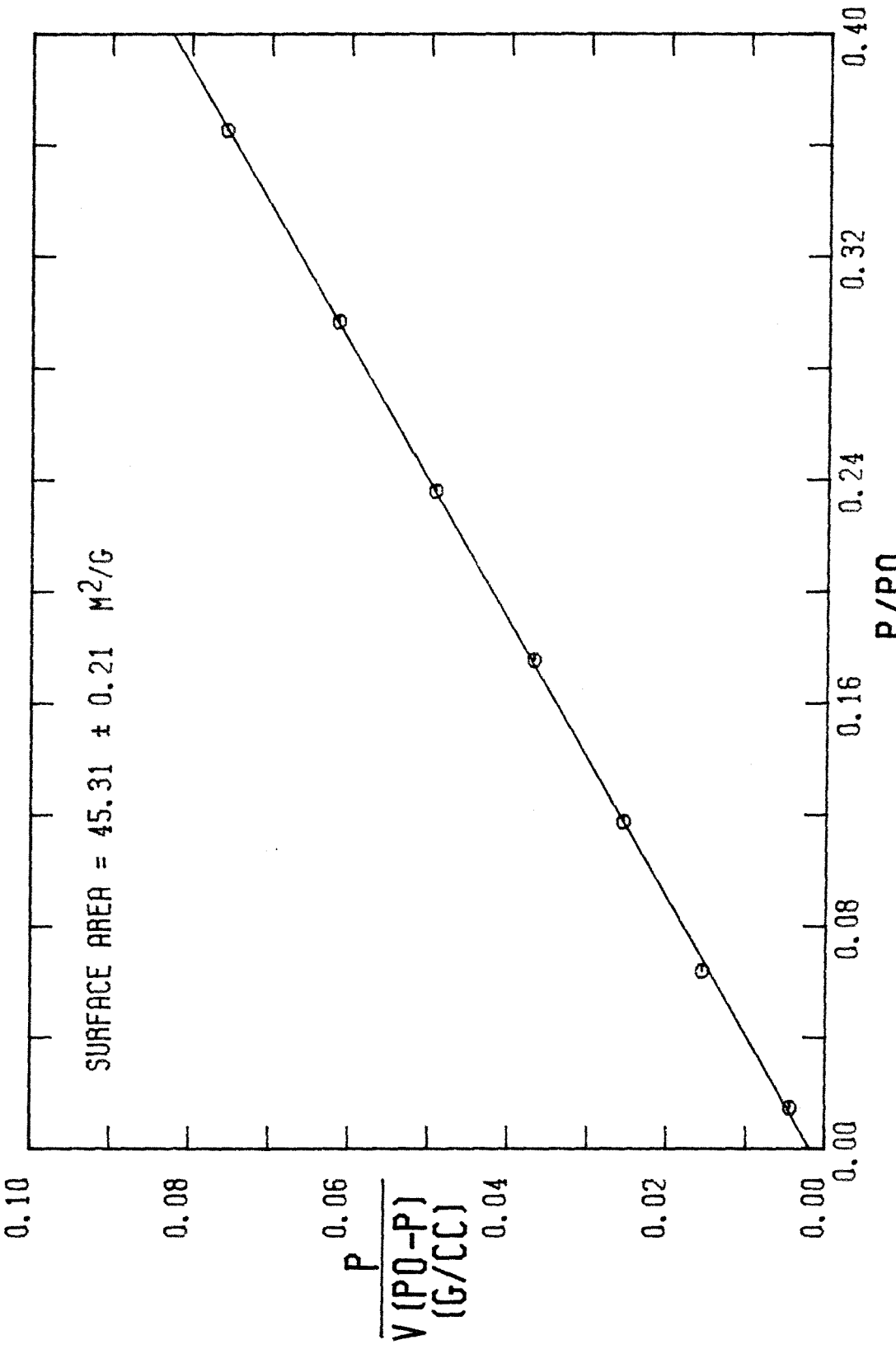
BET PLOT FOR RAW PSOC 190 (+200-325 MESH)
SURFACE AREA = 45.31 ± 0.21 M2/G
P/V(PO-P) (G/CC)
P/PO
0.00
0.02
0.04
0.06
0.08
0.10
0.00
0.08
0.16
0.24
0.32
0.40

FIGURE A-27

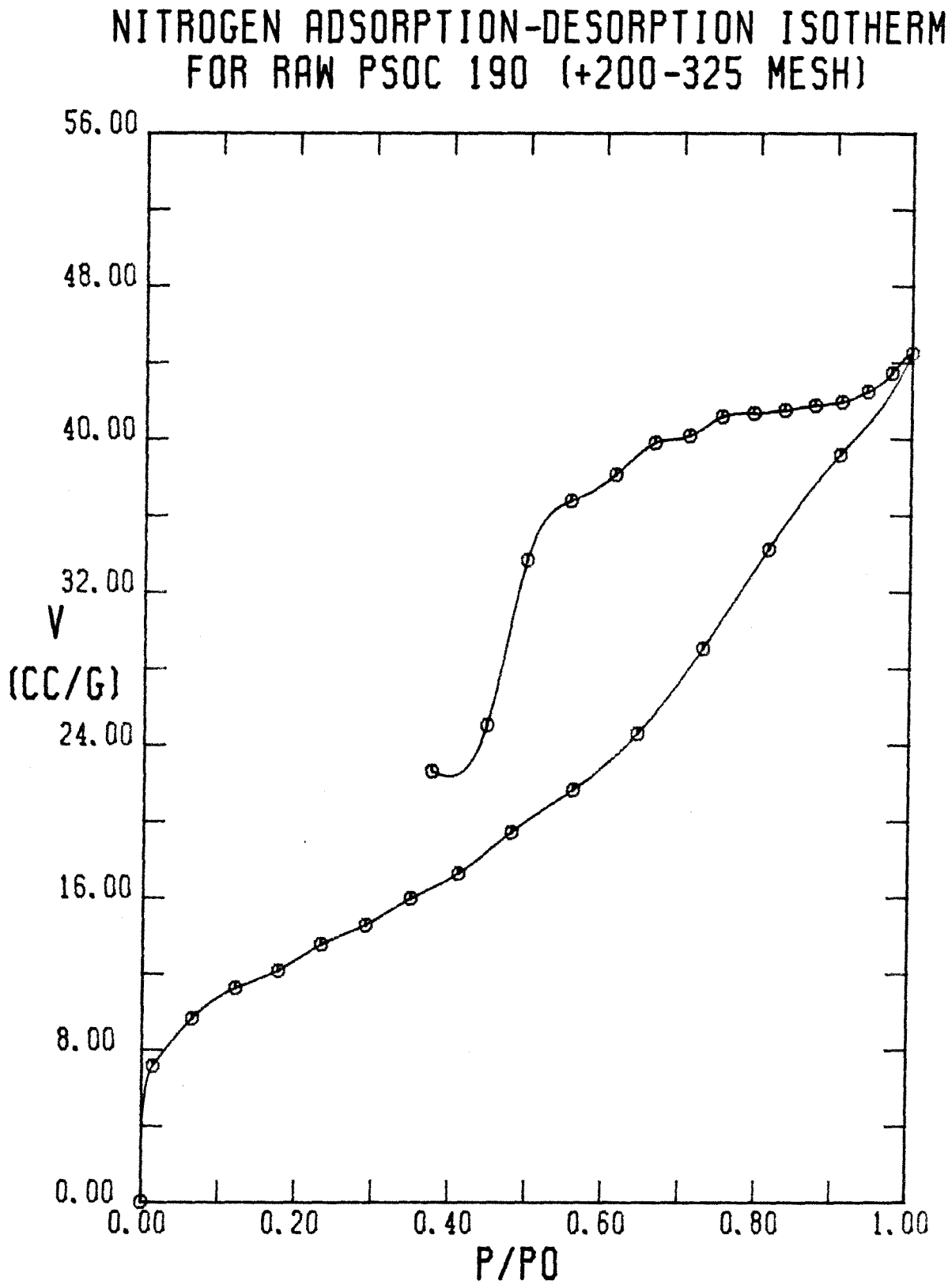
NITROGEN ADSORPTION-DESORPTION ISOTHERM
FOR RAW PSOC 190 (+200-325 MESH)
56.00
48.00
40.00
32.00
V
(CC/G)
24.00
16.00
8.00
0.00
0.00
0.20
0.40
0.60
0.80
1.00
P/PO

FIGURE A-28

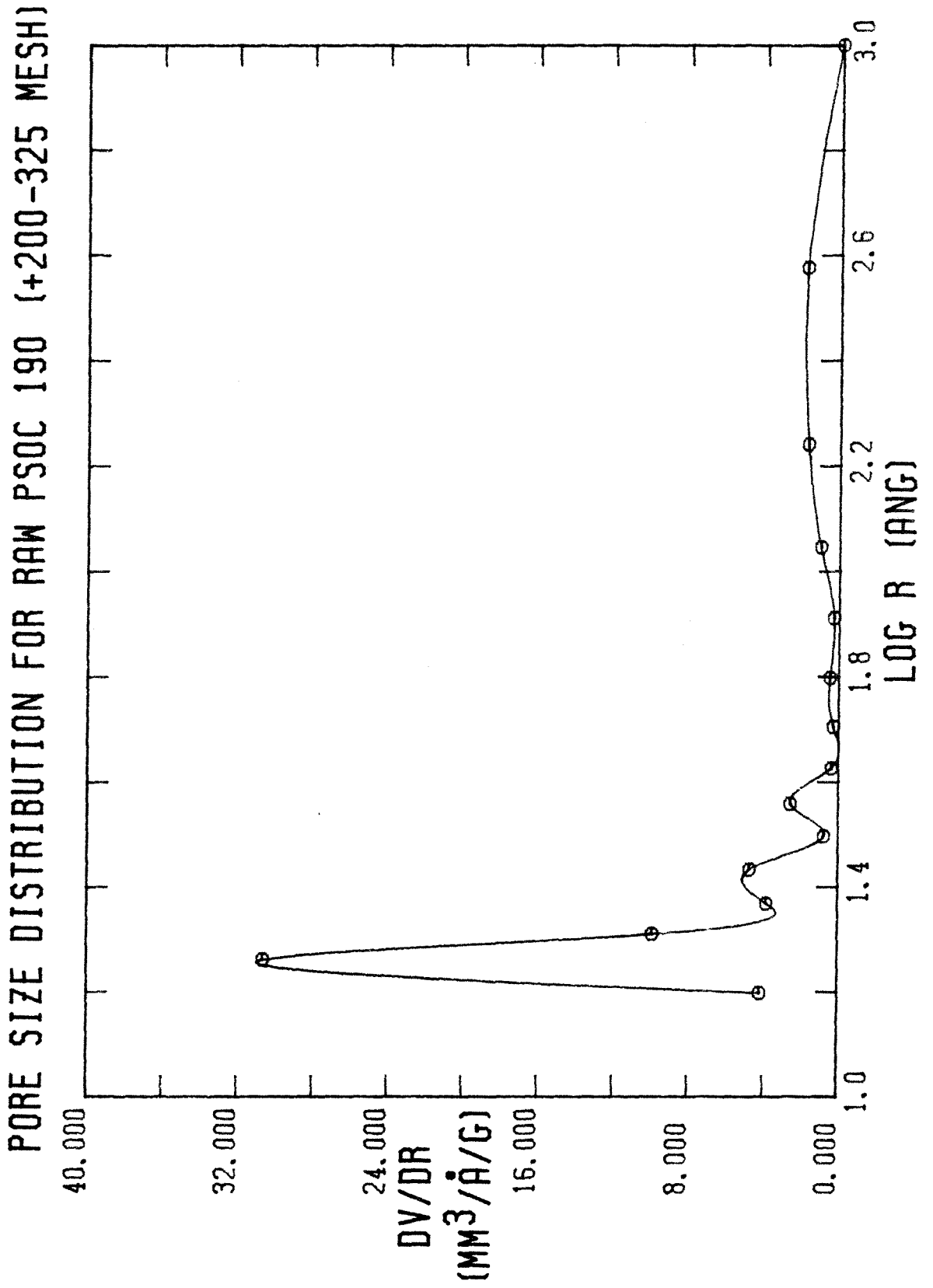
PORE SIZE DISTRIBUTION FOR RAW PSOC 190 (+200-325 MESH)
40.000
32.000
24.000
16.000
8.000
0.000
DV/DR
(MM3/Å/G)
1.0
1.4
1.8
2.2
2.6
3.0
LOG R (ANG)

FIGURE A-29

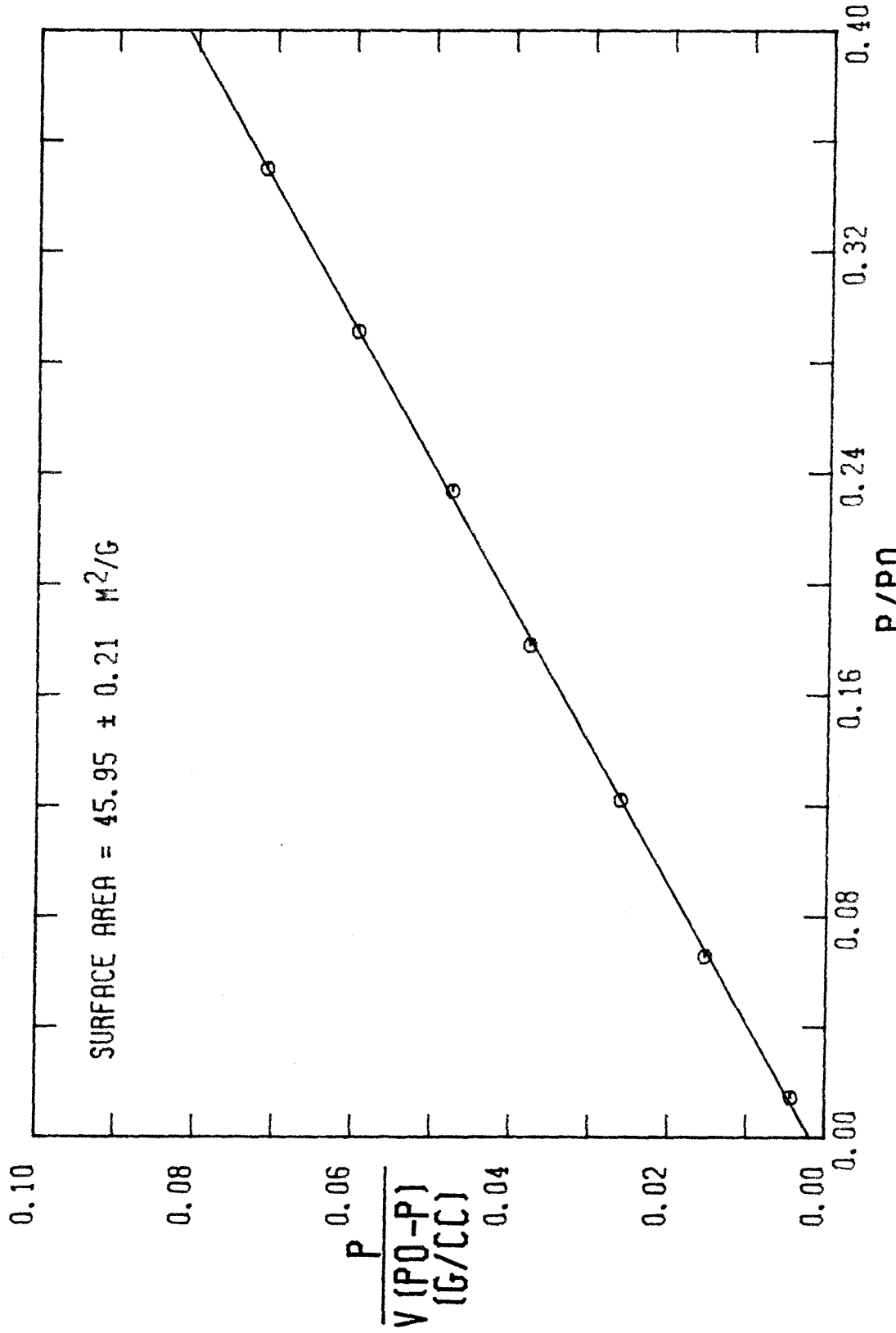
BET PLOT FOR RAW PSOC 190 (+200-325 MESH)
SURFACE AREA = 45.95 ± 0.21 M²/G
P / V(PO-P) (G/CC)
P/PO
0.10
0.08
0.06
0.04
0.02
0.00
0.00
0.08
0.16
0.24
0.32
0.40

FIGURE A-30

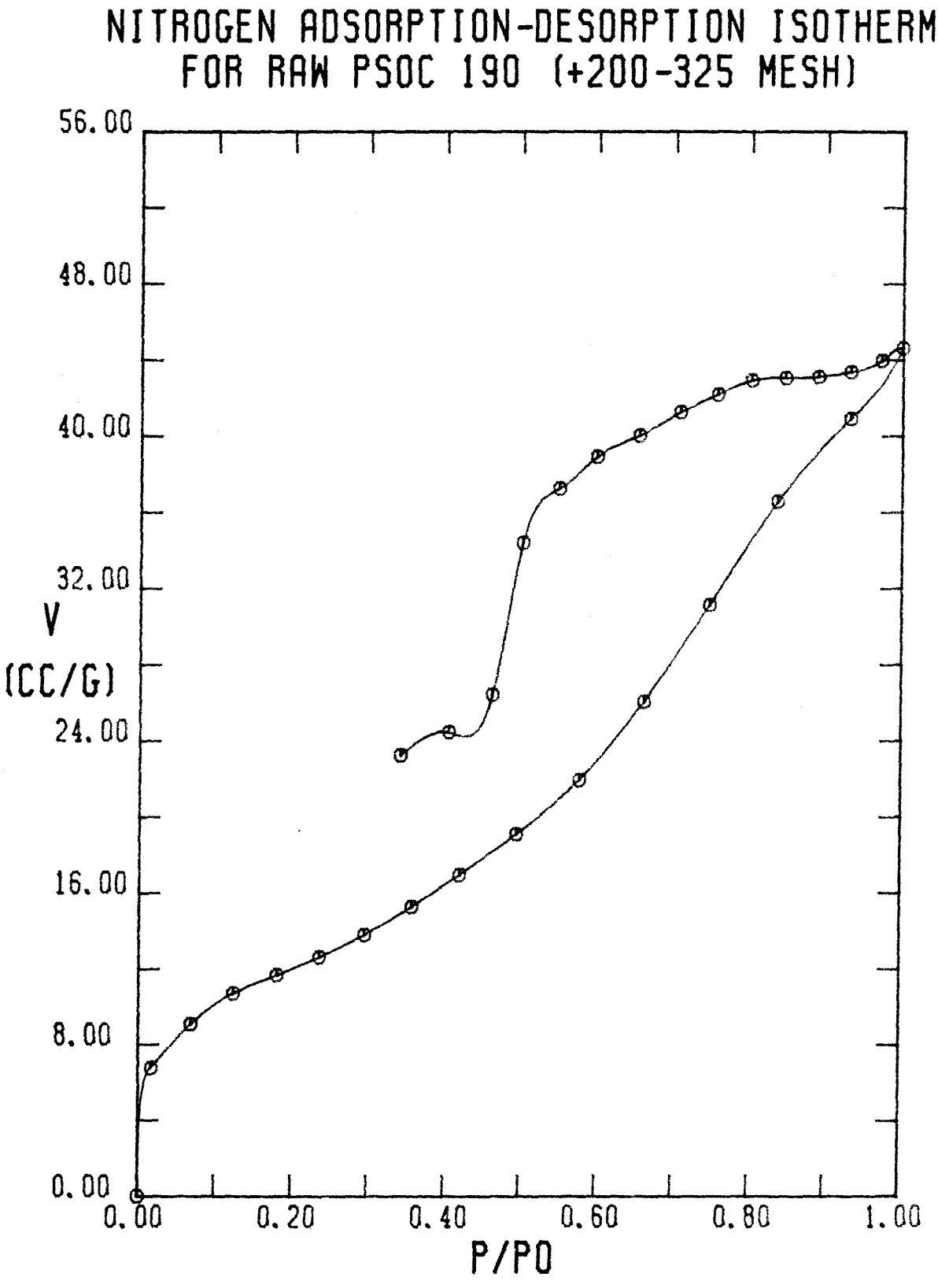
NITROGEN ADSORPTION-DESORPTION ISOTHERM
FOR RAW PSOC 190 (+200-325 MESH)
56.00
48.00
40.00
32.00
V
(CC/G)
24.00
16.00
8.00
0.00
0.00
0.20
0.40
0.60
0.80
1.00
P/PO

FIGURE A-31

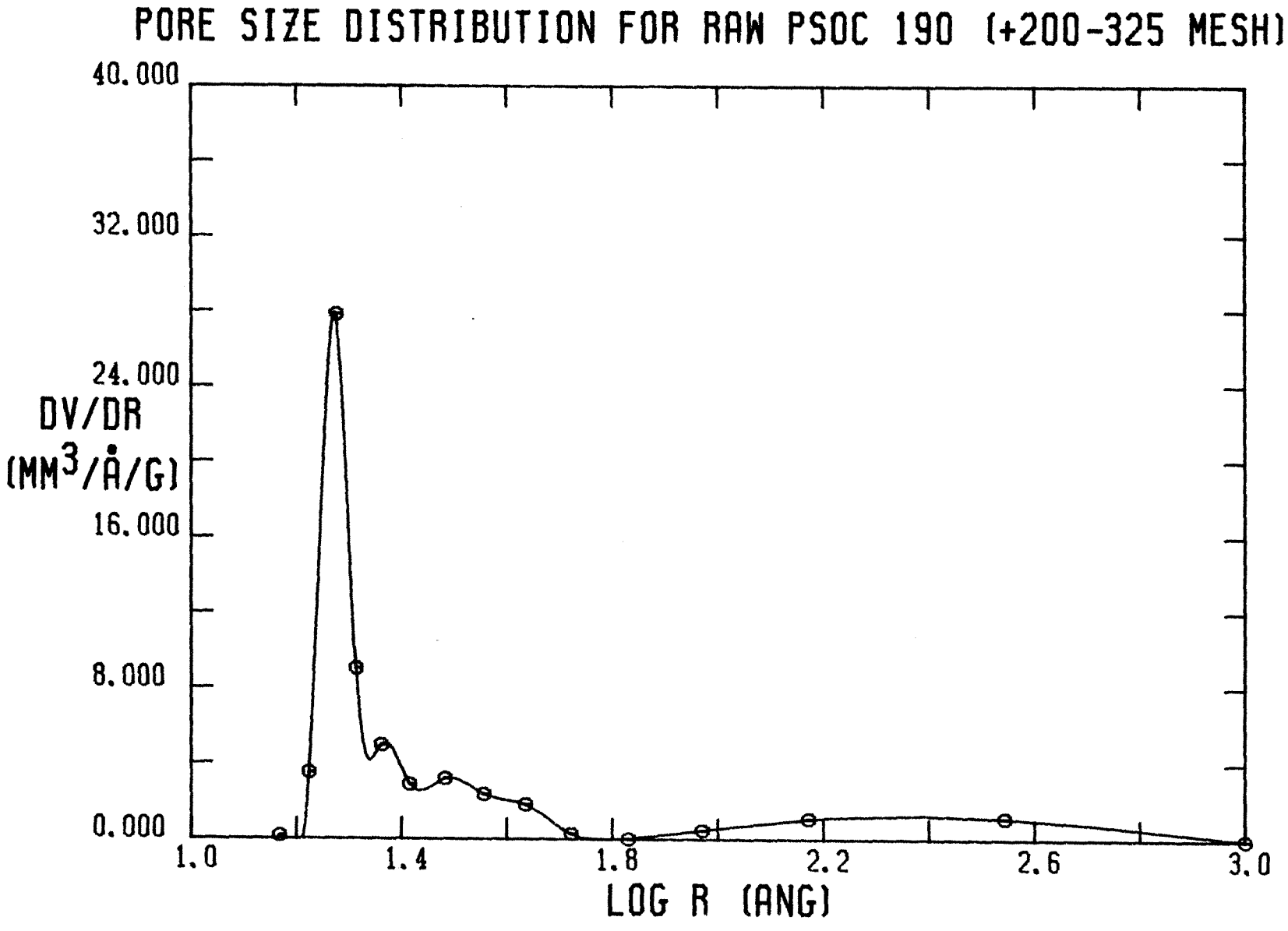
PORE SIZE DISTRIBUTION FOR RAW PSOC 190 (+200-325 MESH)
40.000
32.000
24.000
16.000
8.000
0.000
DV/DR
(MM3/Å/G)
1.0
1.4
1.8
2.2
2.6
3.0
LOG R (ANG)

FIGURE A-32

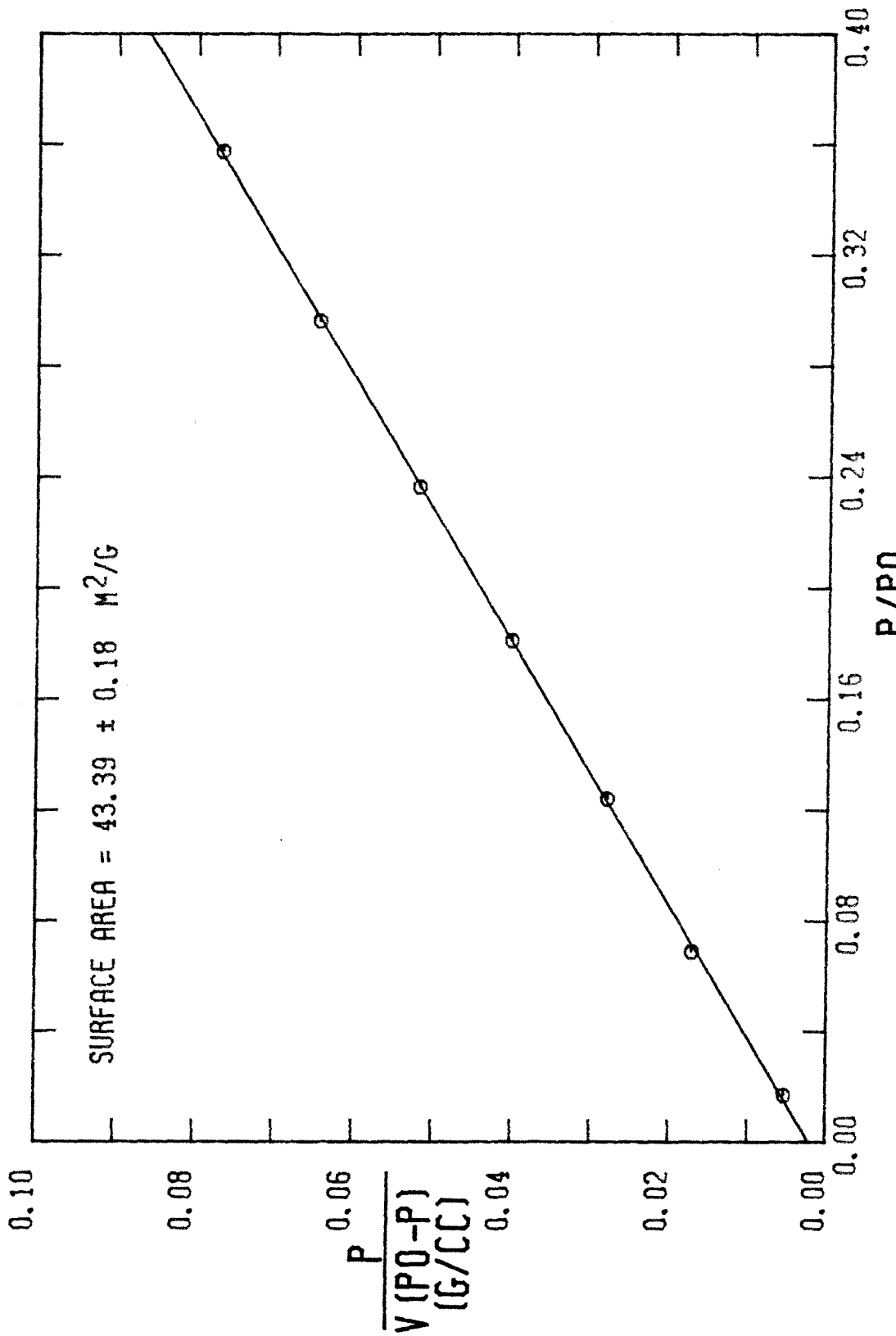
BET PLOT FOR RAW PSOC 190 (+200-325 MESH)
SURFACE AREA = 43.39 ± 0.18 M²/G
P / V (PO-P) (G/CC)
P/PO
0.10
0.08
0.06
0.04
0.02
0.00
0.00
0.08
0.16
0.24
0.32
0.40

FIGURE A-33

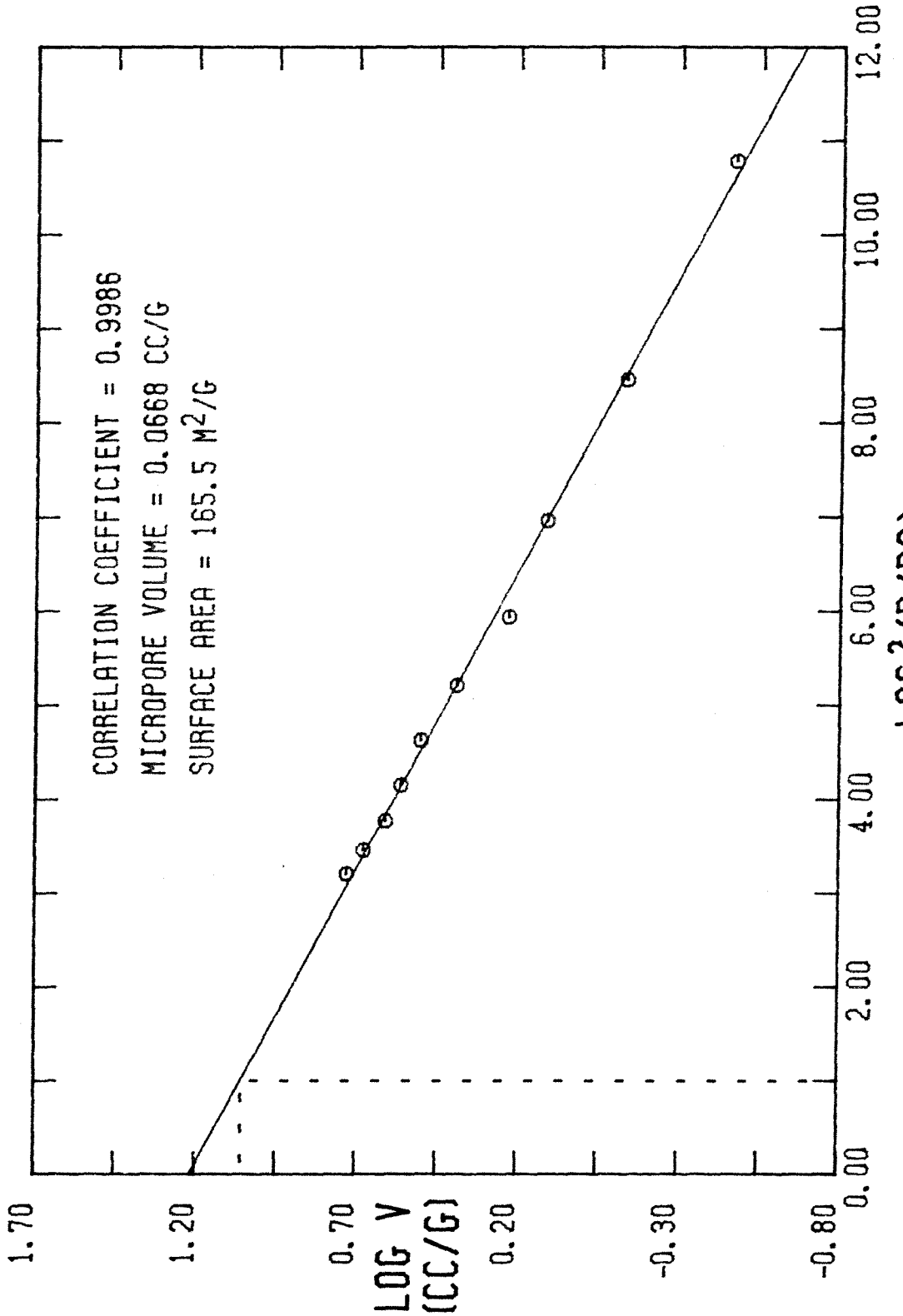
DPR PLOT FOR RAW PSOC 190 (+200-325 MESH)
CORRELATION COEFFICIENT = 0.9986
MICROPORE VOLUME = 0.0668 CC/G
SURFACE AREA = 165.5 M2/G
LOG V (CC/G)
LOG2 (P/PO)
1.70
1.20
0.70
0.20
-0.30
-0.80
0.00
2.00
4.00
6.00
8.00
10.00
12.00

FIGURE A-34

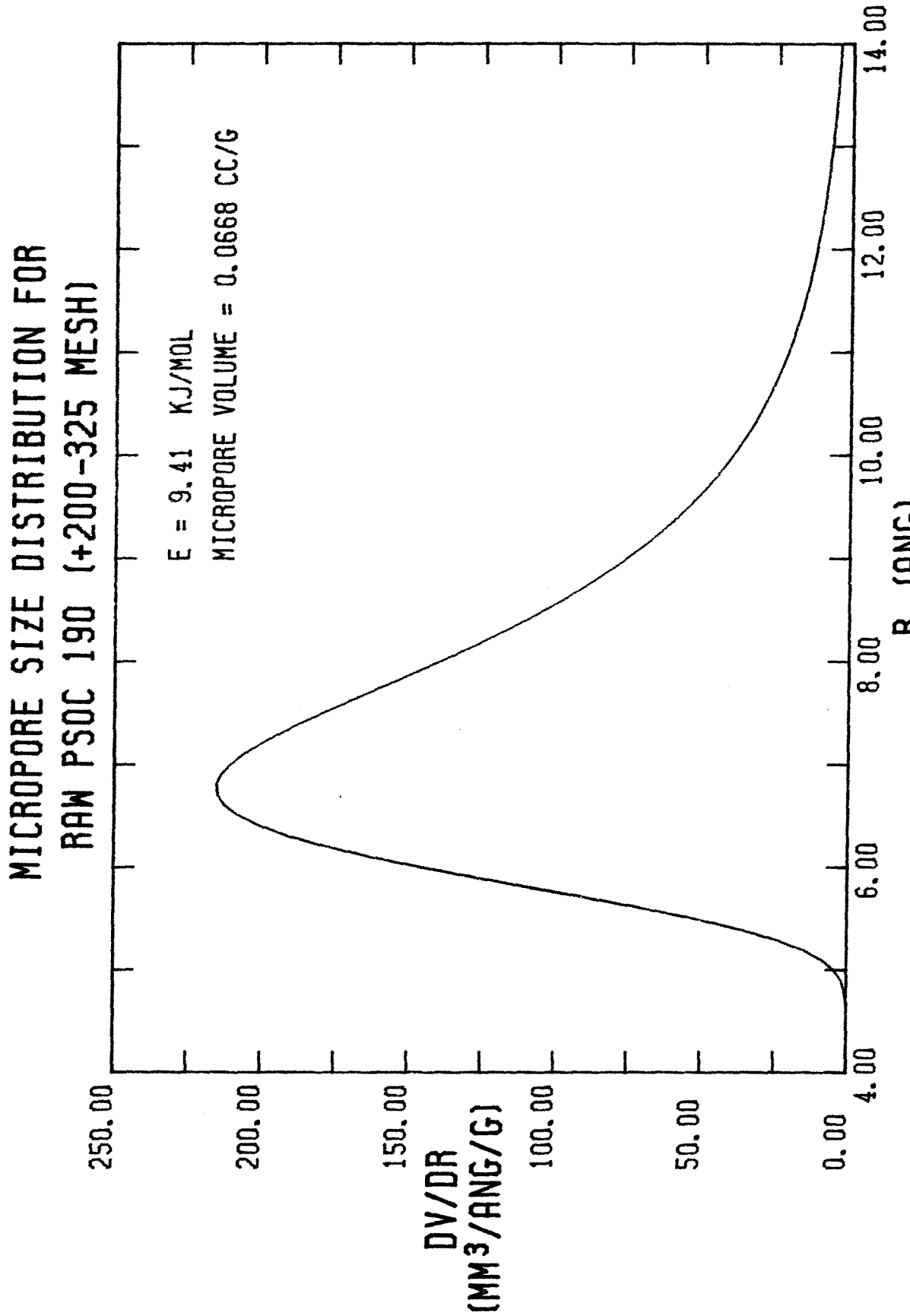
MICROPORE SIZE DISTRIBUTION FOR
RAW PSOC 190 (+200-325 MESH)
E = 9.41 KJ/MOL
MICROPORE VOLUME = 0.0668 CC/G
DV/DR
(MM³/ANG/G)
250.00
200.00
150.00
100.00
50.00
0.00
4.00
6.00
8.00
10.00
12.00
14.00
R (ANG)

FIGURE A-35

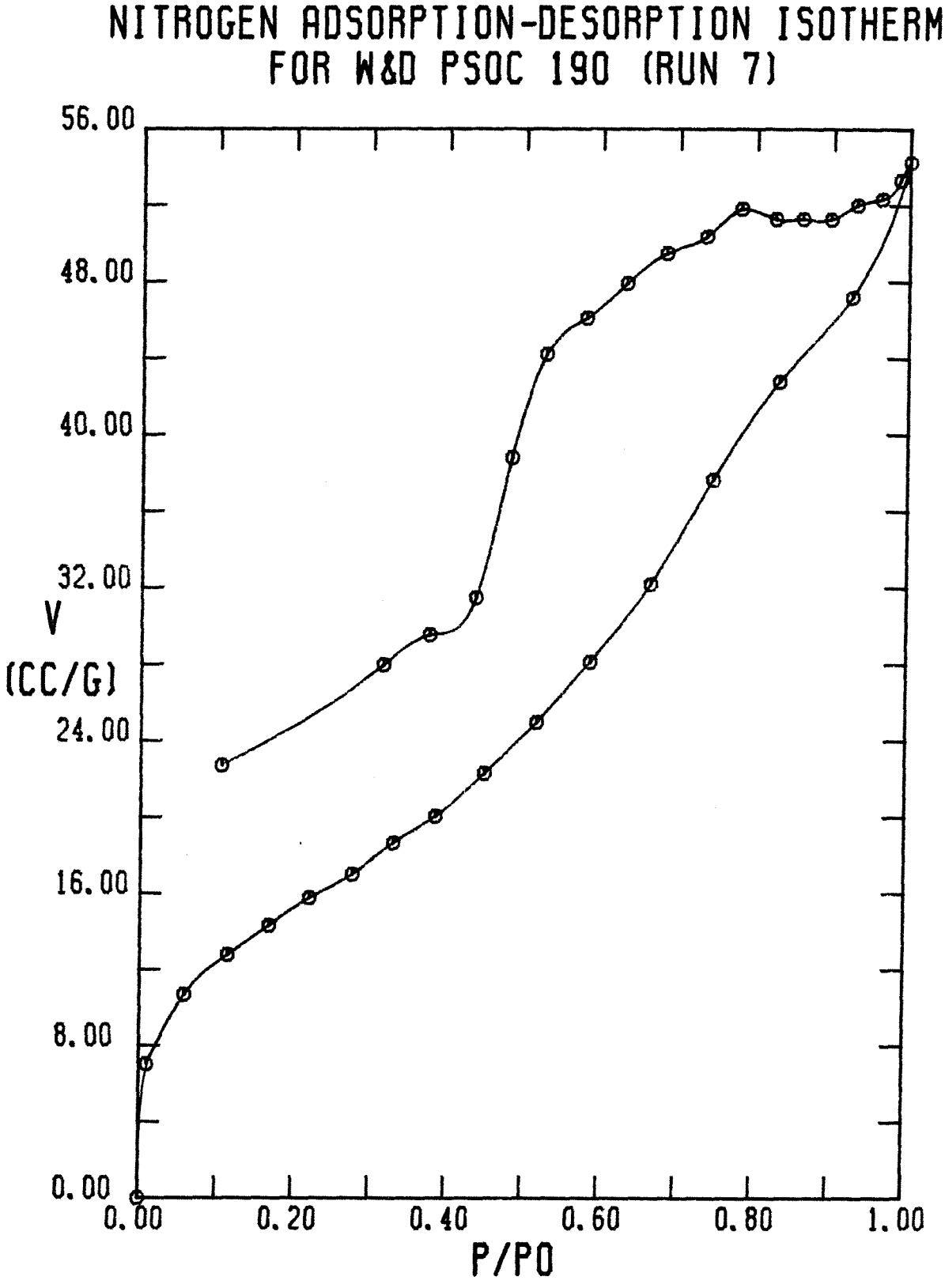
NITROGEN ADSORPTION-DESORPTION ISOTHERM
FOR W&D PSOC 190 (RUN 7)
56.00
48.00
40.00
32.00
V
(CC/G)
24.00
16.00
8.00
0.00
0.00
0.20
0.40
0.60
0.80
1.00
P/PO

FIGURE A-36

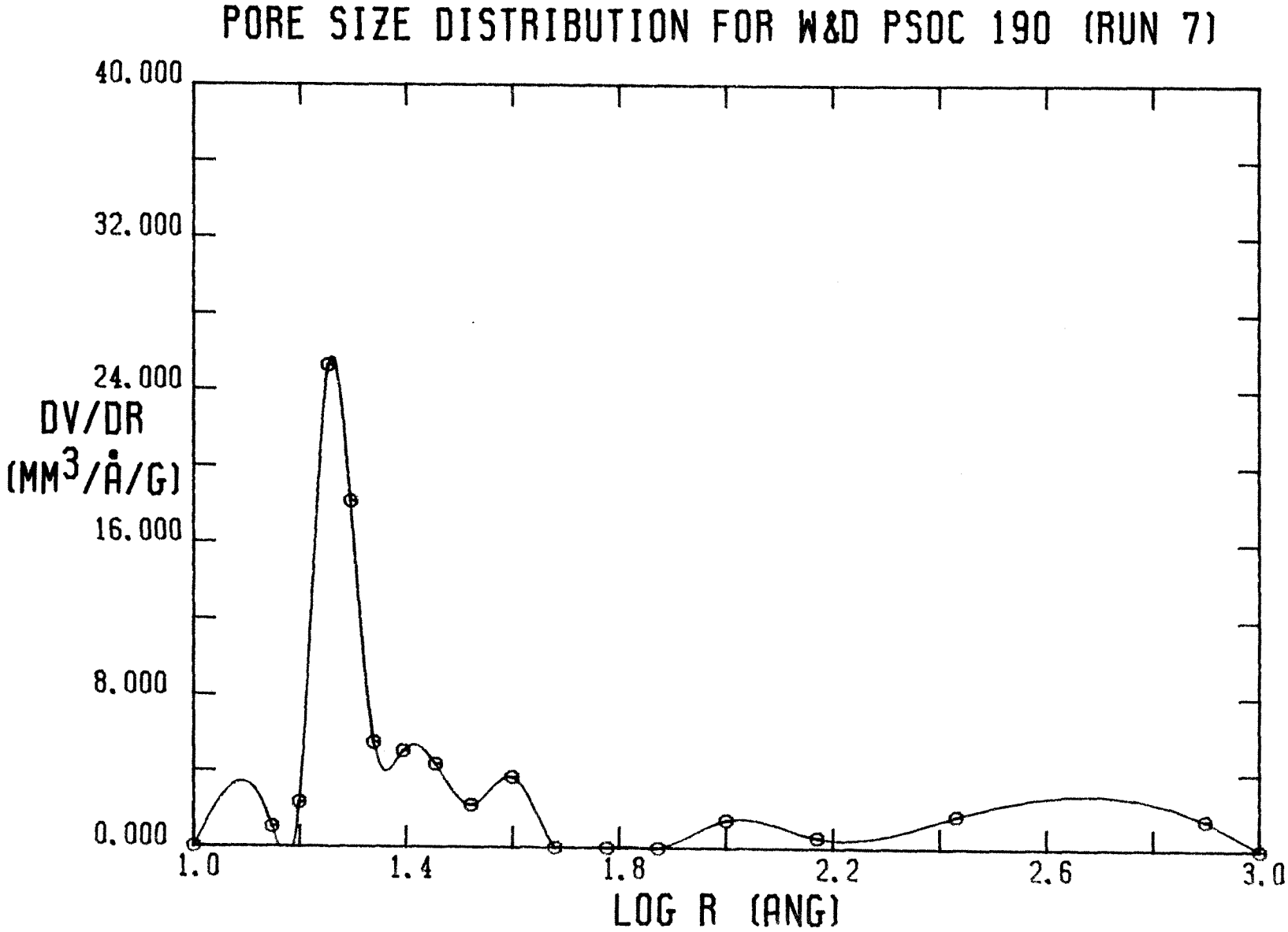
PORE SIZE DISTRIBUTION FOR W&D PSOC 190 (RUN 7)
40.000
32.000
24.000
16.000
8.000
0.000
DV/DR
(MM3/Å/G)
1.0
1.4
1.8
2.2
2.6
3.0
LOG R (ANG)

FIGURE A-37

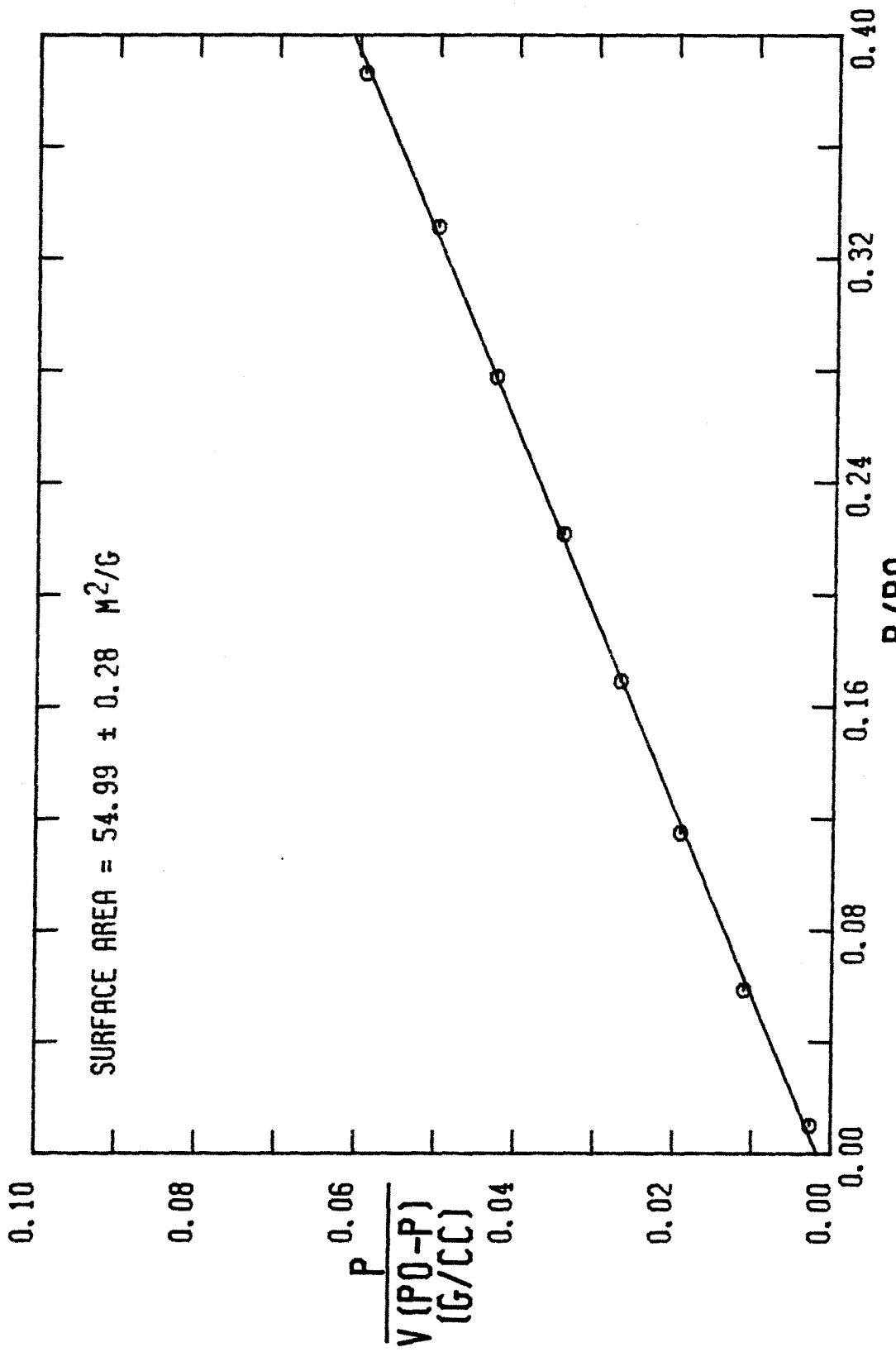
BET PLOT FOR W&D PSOC 190 (RUN 7)
SURFACE AREA = 54.99 ± 0.28 M2/G
P/PO
P / V(PO-P) (G/CC)
0.00
0.08
0.16
0.24
0.32
0.40
0.00
0.02
0.04
0.06
0.08
0.10

FIGURE A-38

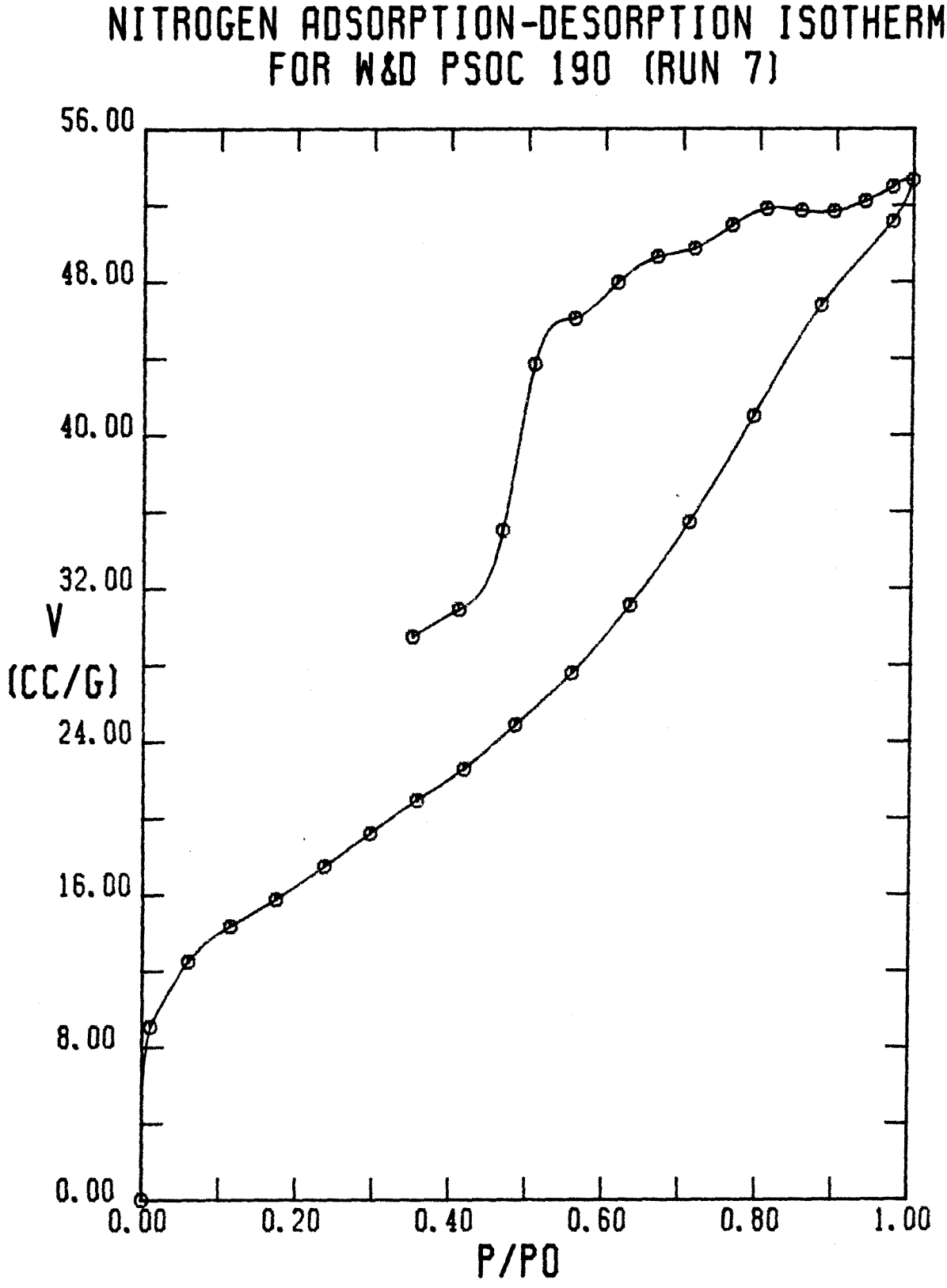
NITROGEN ADSORPTION-DESORPTION ISOTHERM
FOR W&D PSOC 190 (RUN 7)
56.00
48.00
40.00
32.00
V
(CC/G)
24.00
16.00
8.00
0.00
0.00
0.20
0.40
0.60
0.80
1.00
P/PO

FIGURE A-39

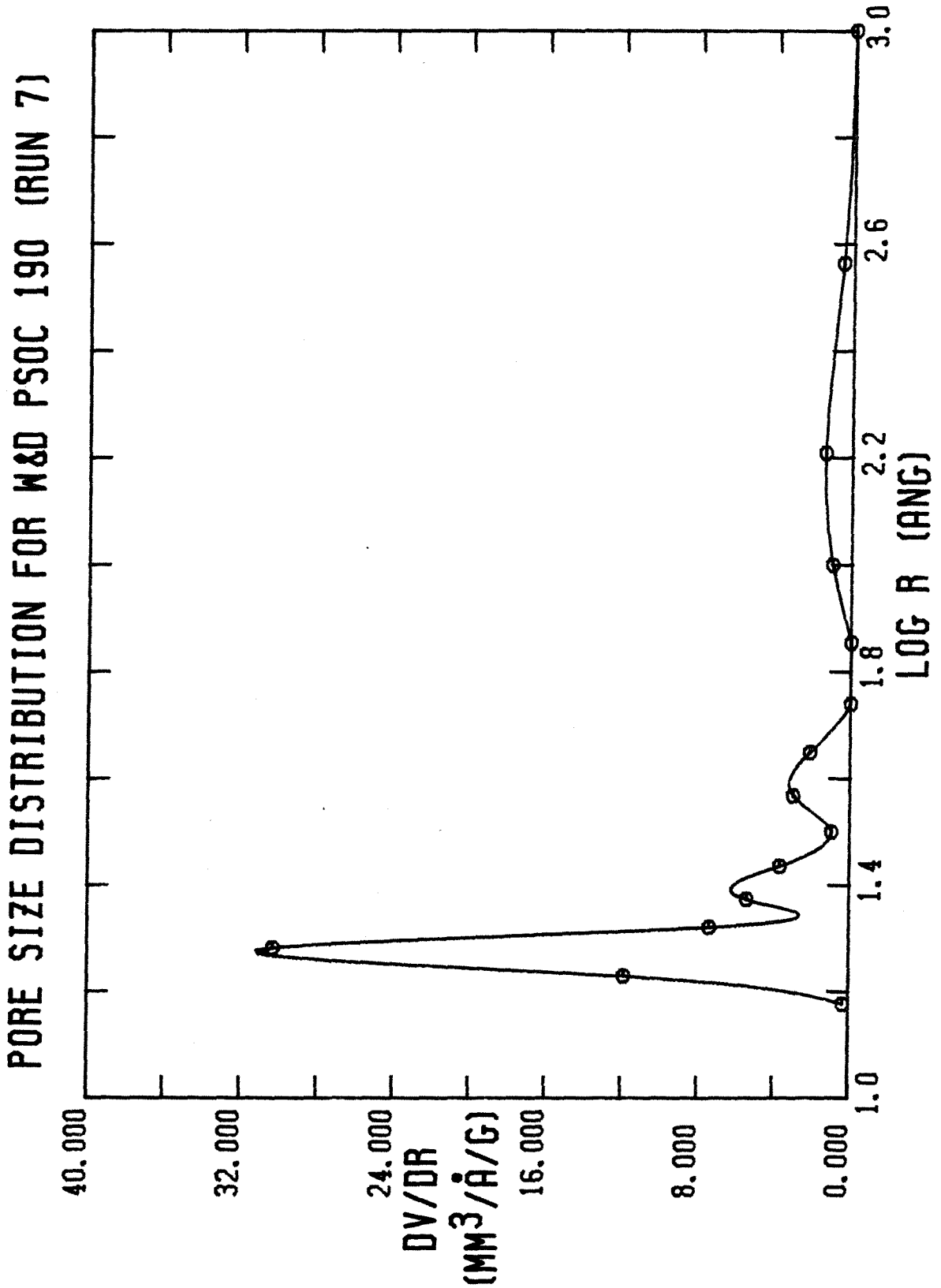
PORE SIZE DISTRIBUTION FOR W&D PSOC 190 (RUN 7)
DV/DR
(MM3/Å/G)
40.000
32.000
24.000
16.000
8.000
0.000
1.0
1.4
1.8
2.2
2.6
3.0
LOG R (ANG)

FIGURE A-40

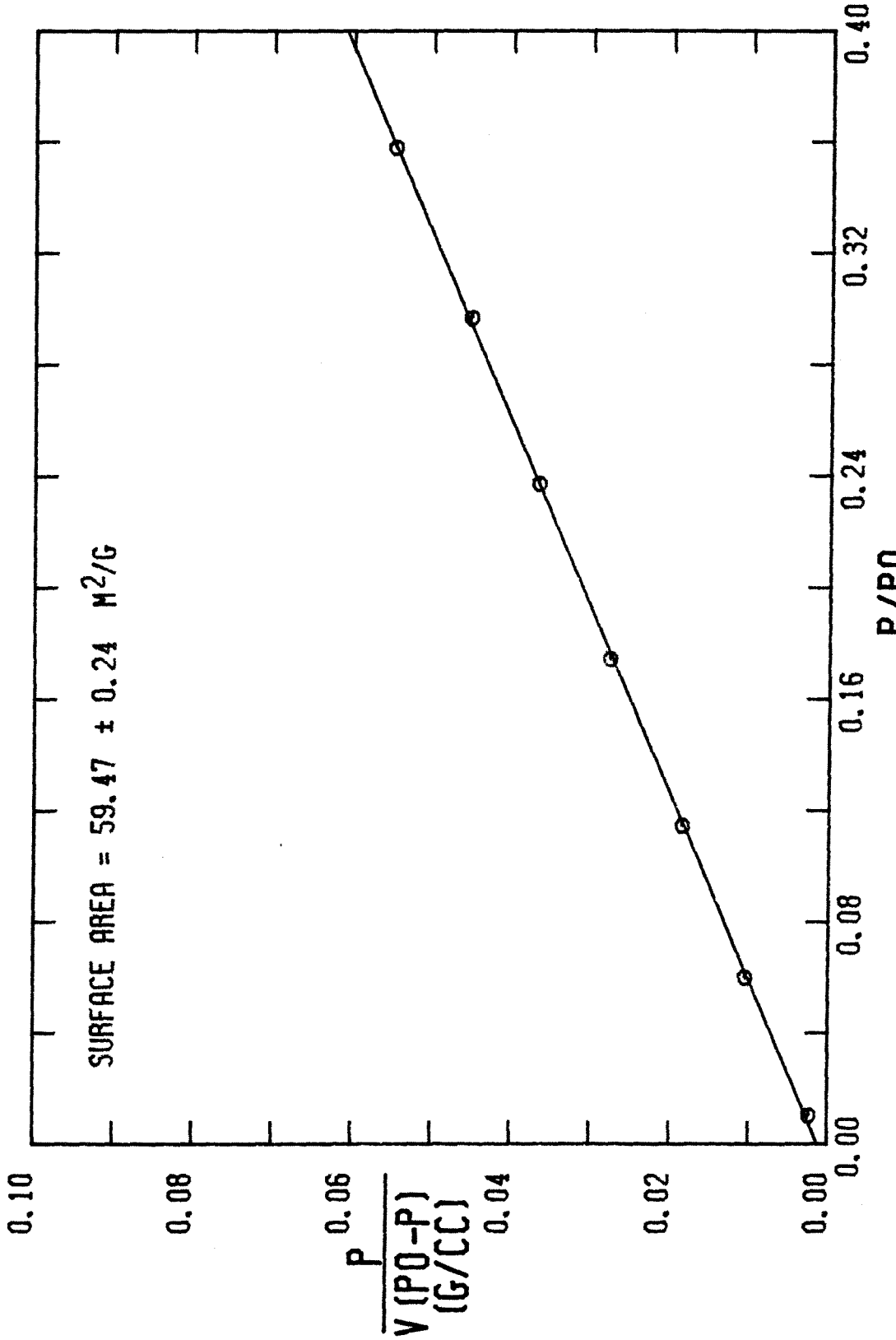
BET PLOT FOR W&D PSOC 190 (RUN 7)
SURFACE AREA = 59.47 ± 0.24 M2/G
P / V (PO-P) (G/CC)
P/PO
0.00
0.02
0.04
0.06
0.08
0.10
0.00
0.08
0.16
0.24
0.32
0.40

FIGURE A-41

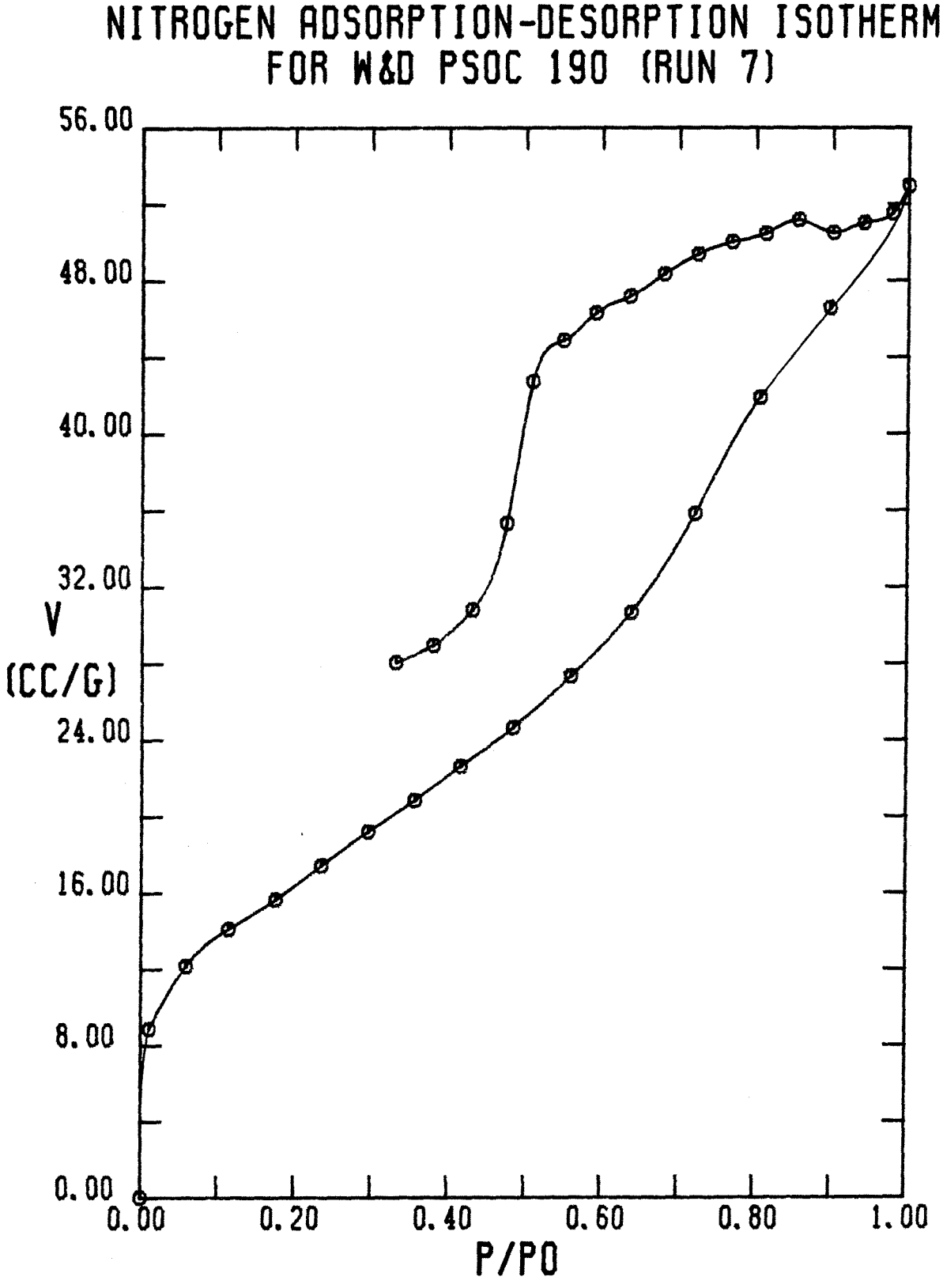
NITROGEN ADSORPTION-DESORPTION ISOTHERM
FOR W&D PSOC 190 (RUN 7)
56.00
48.00
40.00
32.00
V
(CC/G)
24.00
16.00
8.00
0.00
0.00
0.20
0.40
0.60
0.80
1.00
P/PO

FIGURE A-42

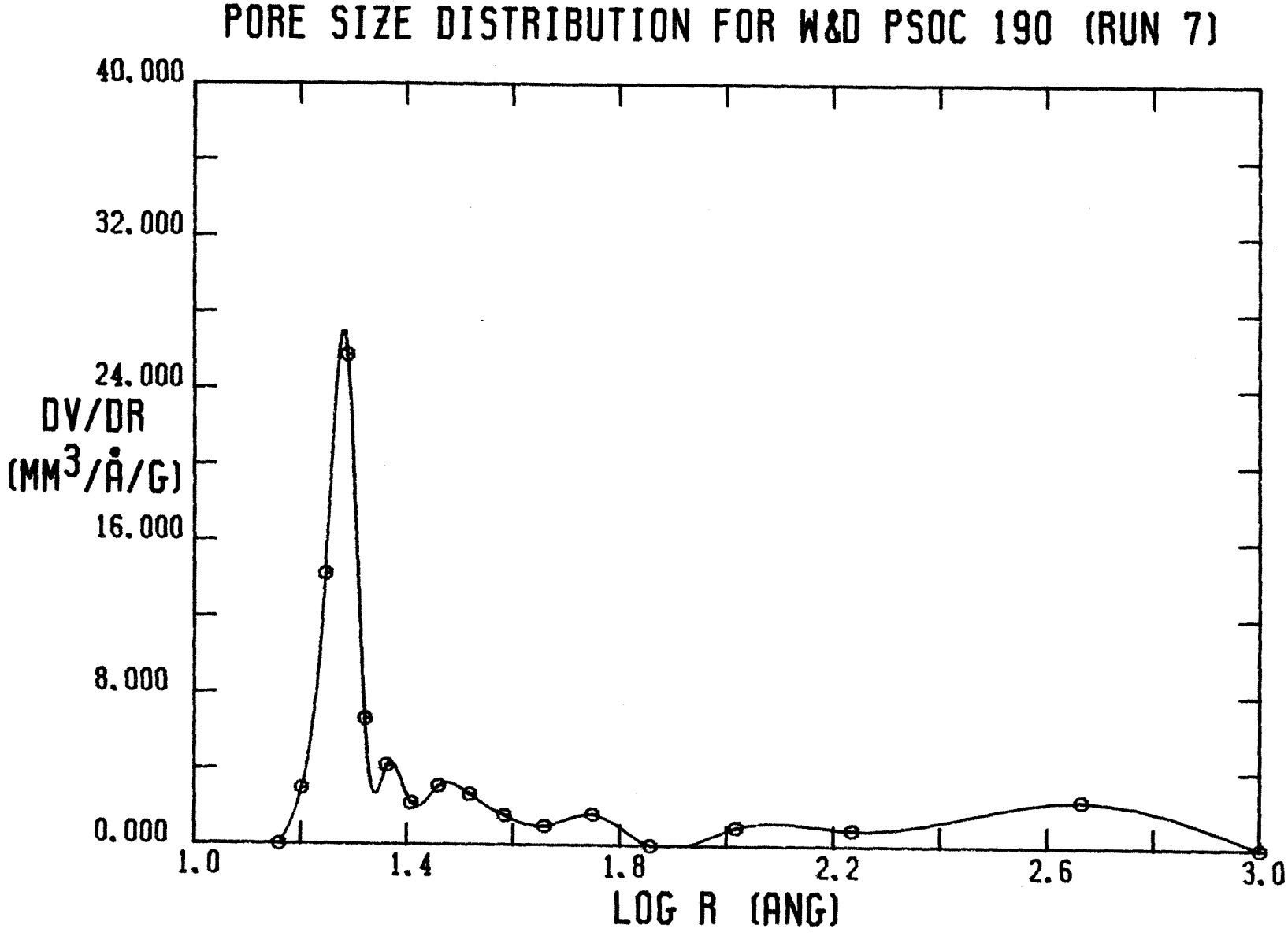
PORE SIZE DISTRIBUTION FOR W&D PSOC 190 (RUN 7)
40.000
32.000
24.000
16.000
8.000
0.000
DV/DR
(MM3/Å/G)
1.0
1.4
1.8
2.2
2.6
3.0
LOG R (ANG)

FIGURE A-43

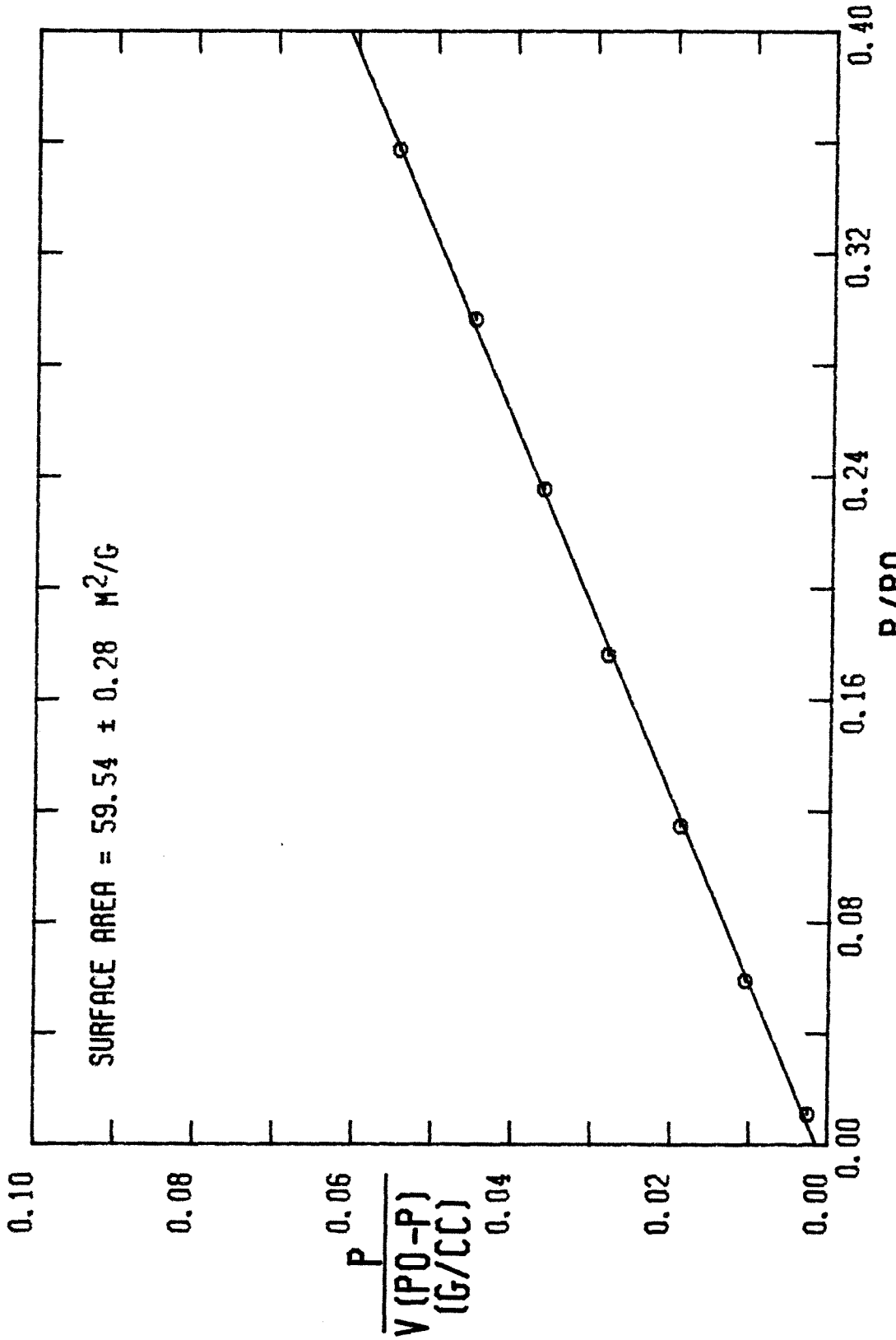
BET PLOT FOR W&D PSOC 190 (RUN 7)
SURFACE AREA = 59.54 ± 0.28 M2/G
P/PO
P / V(PO-P) (G/CC)
0.00
0.08
0.16
0.24
0.32
0.40
0.00
0.02
0.04
0.06
0.08
0.10

FIGURE A-44

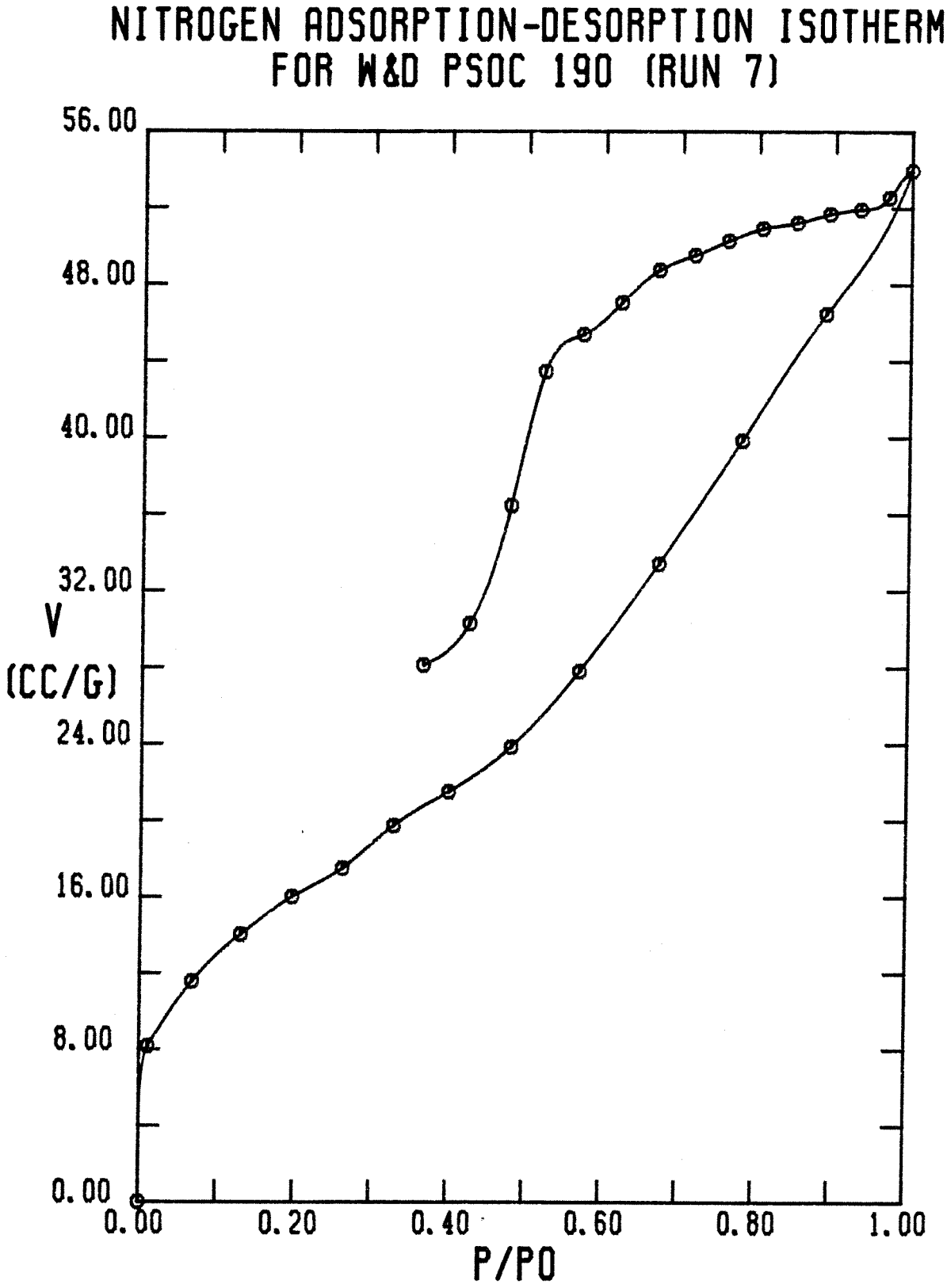
NITROGEN ADSORPTION-DESORPTION ISOTHERM
FOR W&D PSOC 190 (RUN 7)
56.00
48.00
40.00
32.00
V
(CC/G)
24.00
16.00
8.00
0.00
0.00
0.20
0.40
0.60
0.80
1.00
P/PO

FIGURE A-45

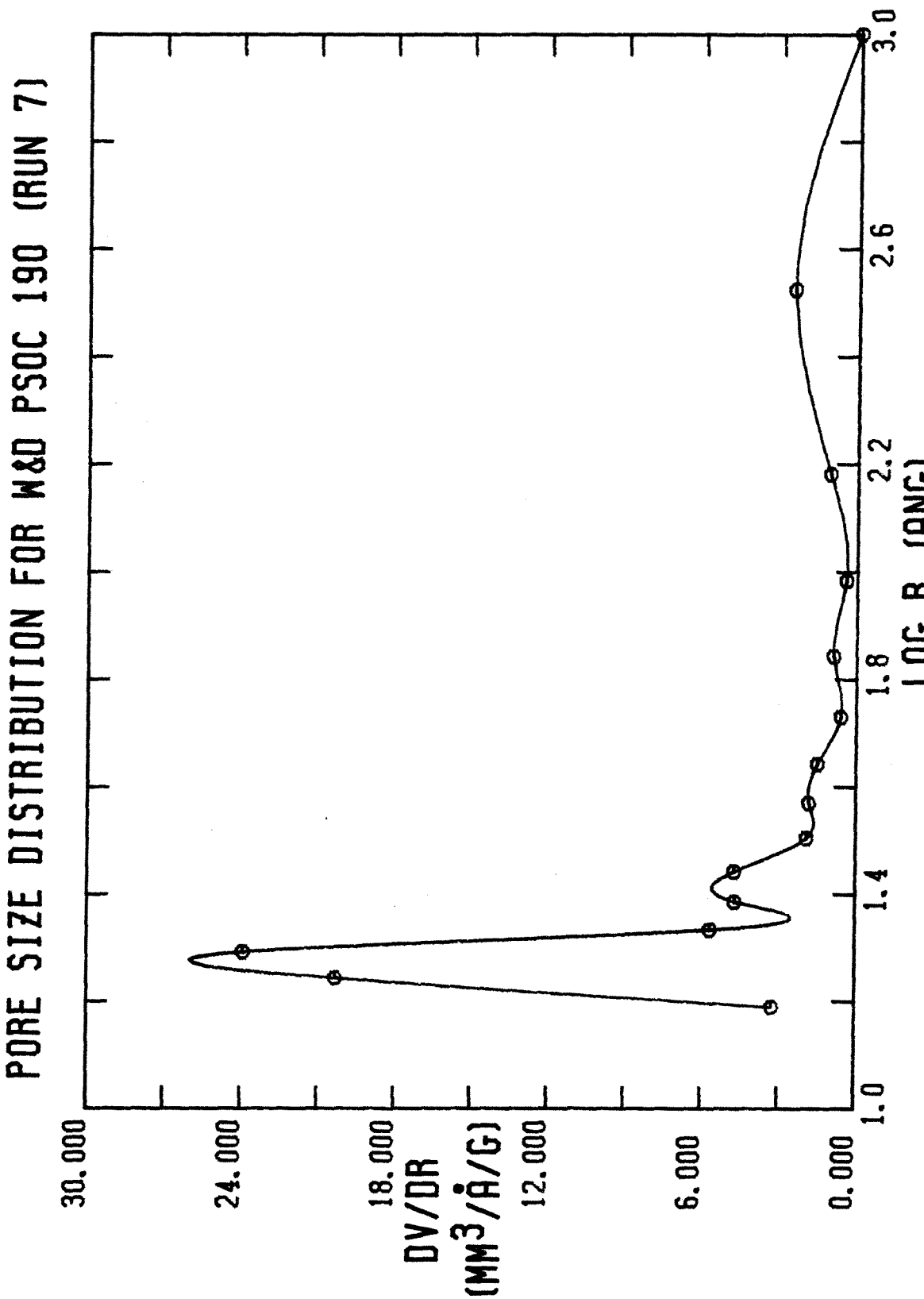
PORE SIZE DISTRIBUTION FOR W&D PSOC 190 (RUN 7)
DV/DR
(MM3/Å/G)
30.000
24.000
18.000
12.000
6.000
0.000
1.0
1.4
1.8
2.2
2.6
3.0
LOG R (ANG)

FIGURE A-46

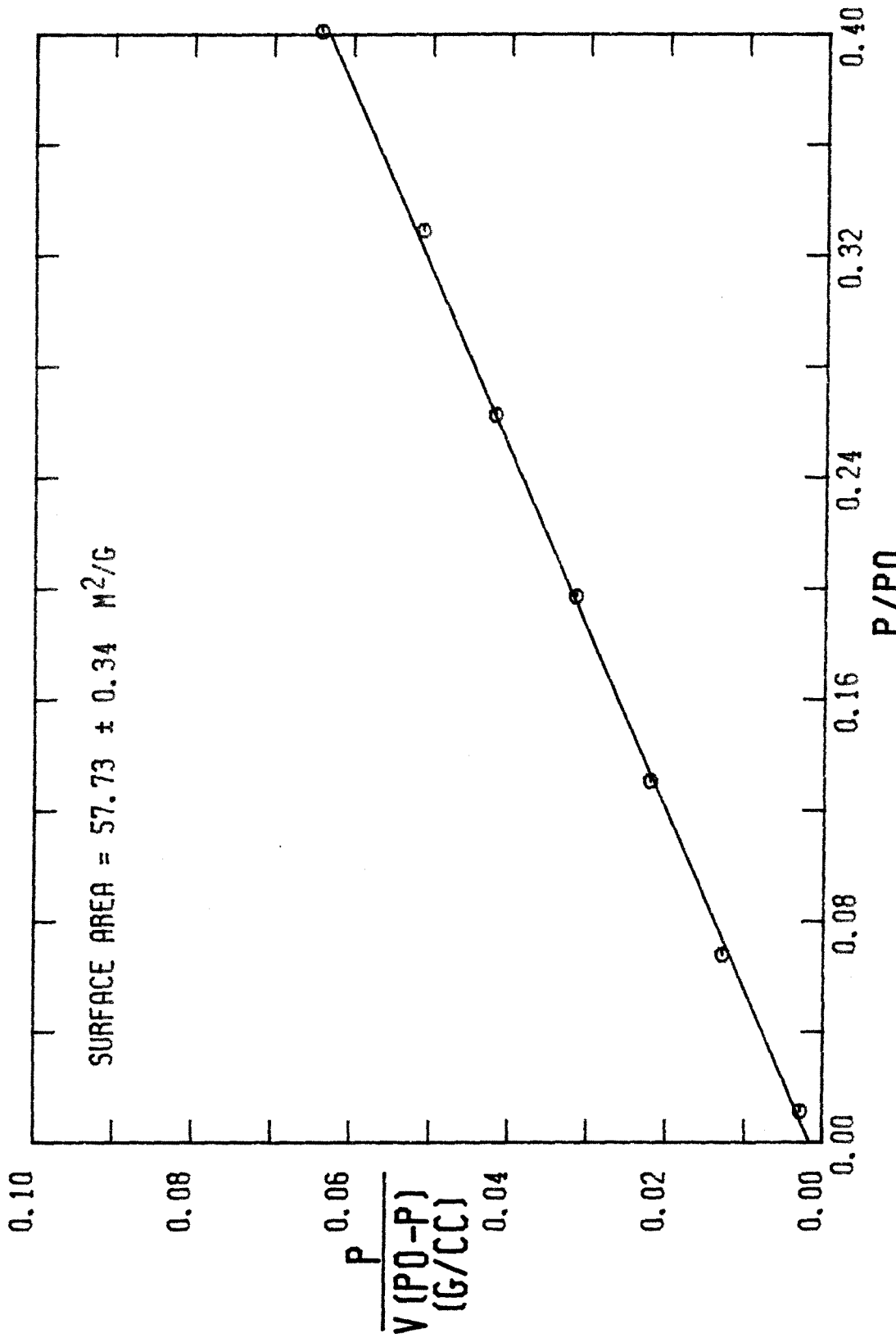
BET PLOT FOR W&D PSOC 190 (RUN 7)
SURFACE AREA = 57.73 ± 0.34 M2/G
P / V (PO-P) (G/CC)
P/PO
0.00
0.02
0.04
0.06
0.08
0.10
0.00
0.08
0.16
0.24
0.32
0.40

FIGURE A-47

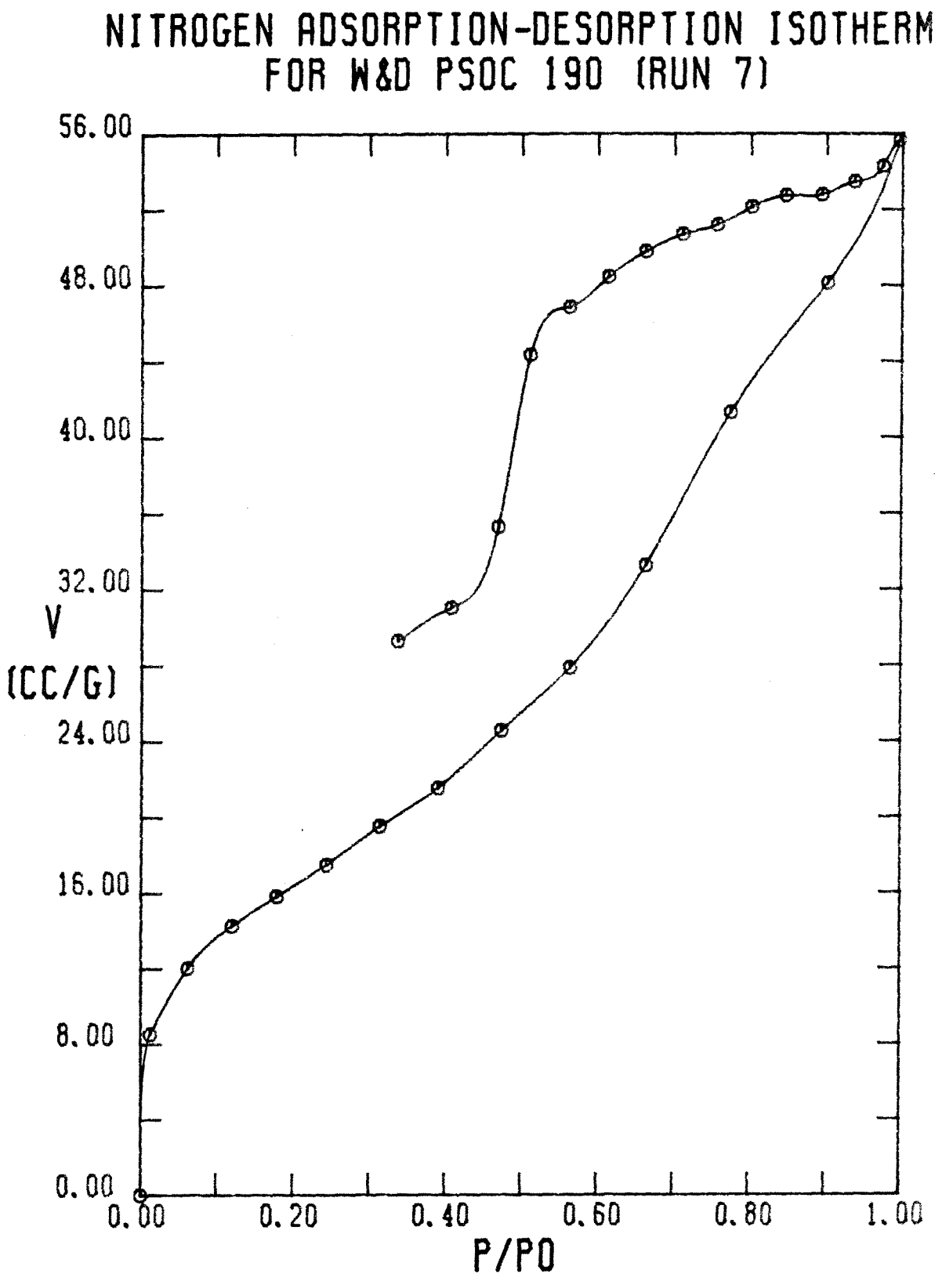
NITROGEN ADSORPTION-DESORPTION ISOTHERM
FOR W&D PSOC 190 (RUN 7)
56.00
48.00
40.00
32.00
V
(CC/G)
24.00
16.00
8.00
0.00
0.00
0.20
0.40
0.60
0.80
1.00
P/PO

FIGURE A-48

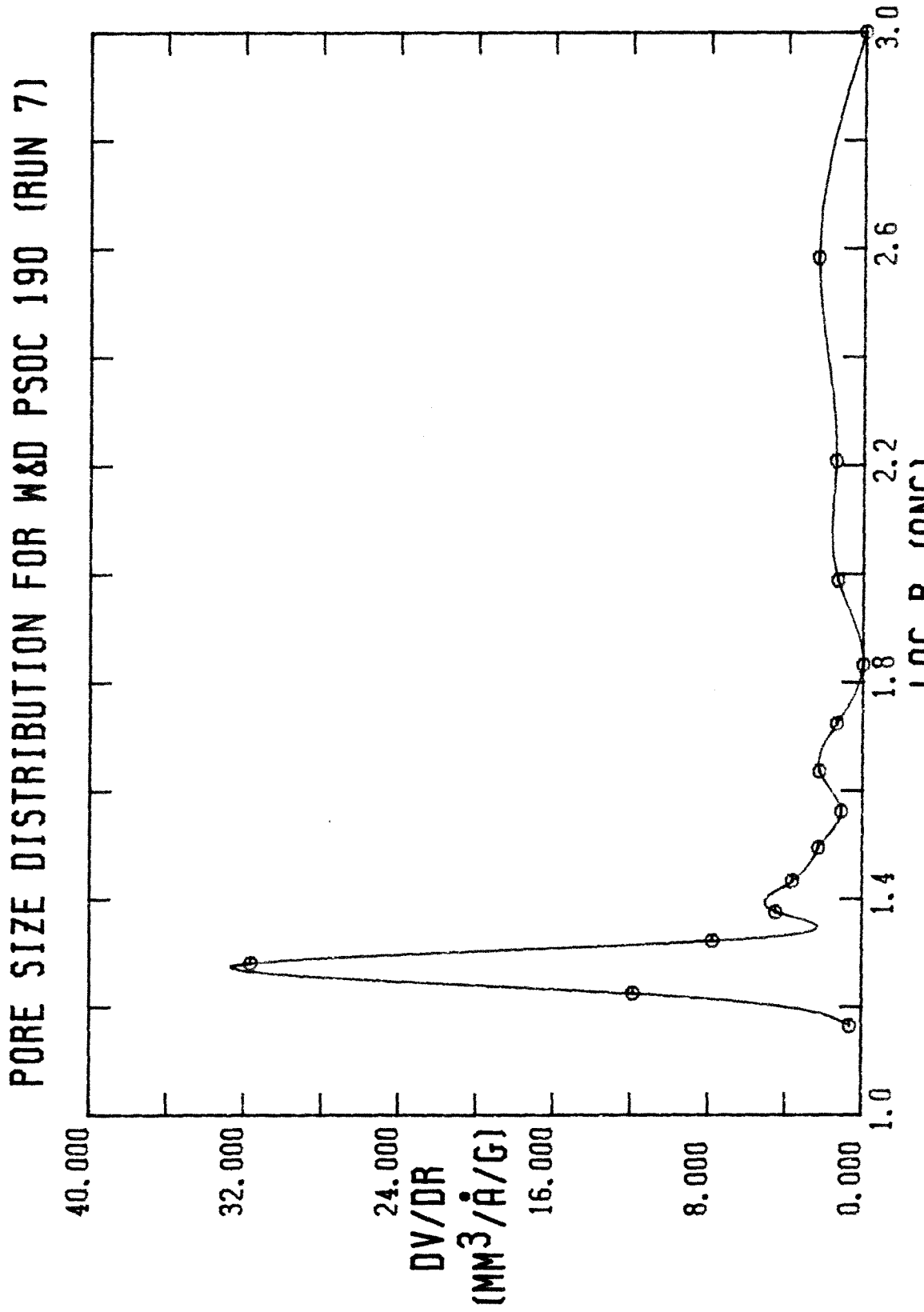
PORE SIZE DISTRIBUTION FOR W&D PSOC 190 (RUN 7)
40.000
32.000
24.000
16.000
8.000
0.000
DV/DR
(MM3/Å/G)
1.0
1.4
1.8
2.2
2.6
3.0
LOG R (ANG)

FIGURE A-49

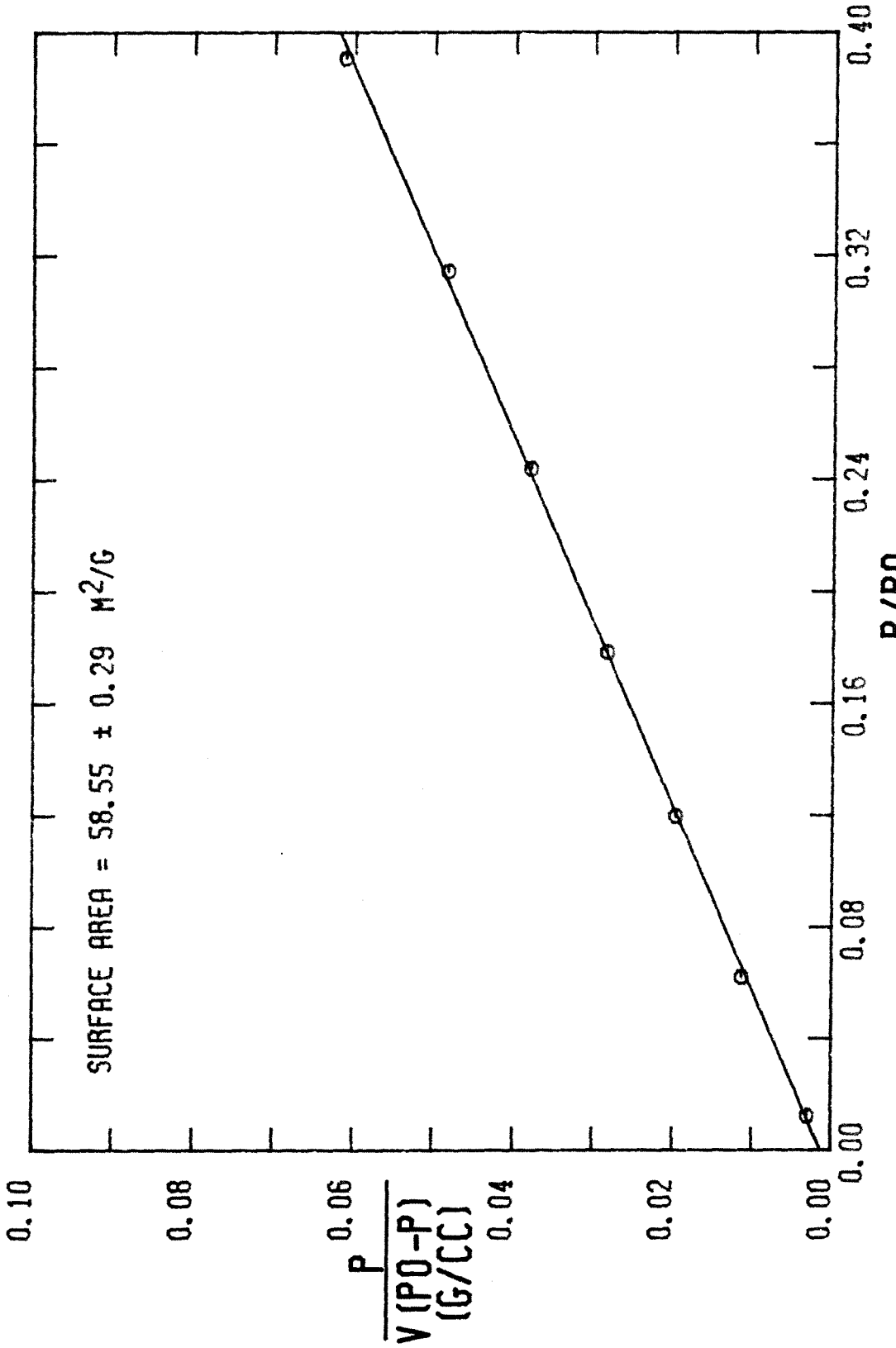
BET PLOT FOR W&D PSOC 190 (RUN 7)
SURFACE AREA = 58.55 ± 0.29 M2/G
P/PO
P / V(PO-P) (G/CC)
0.00
0.08
0.16
0.24
0.32
0.40
0.00
0.02
0.04
0.06
0.08
0.10

FIGURE A-50

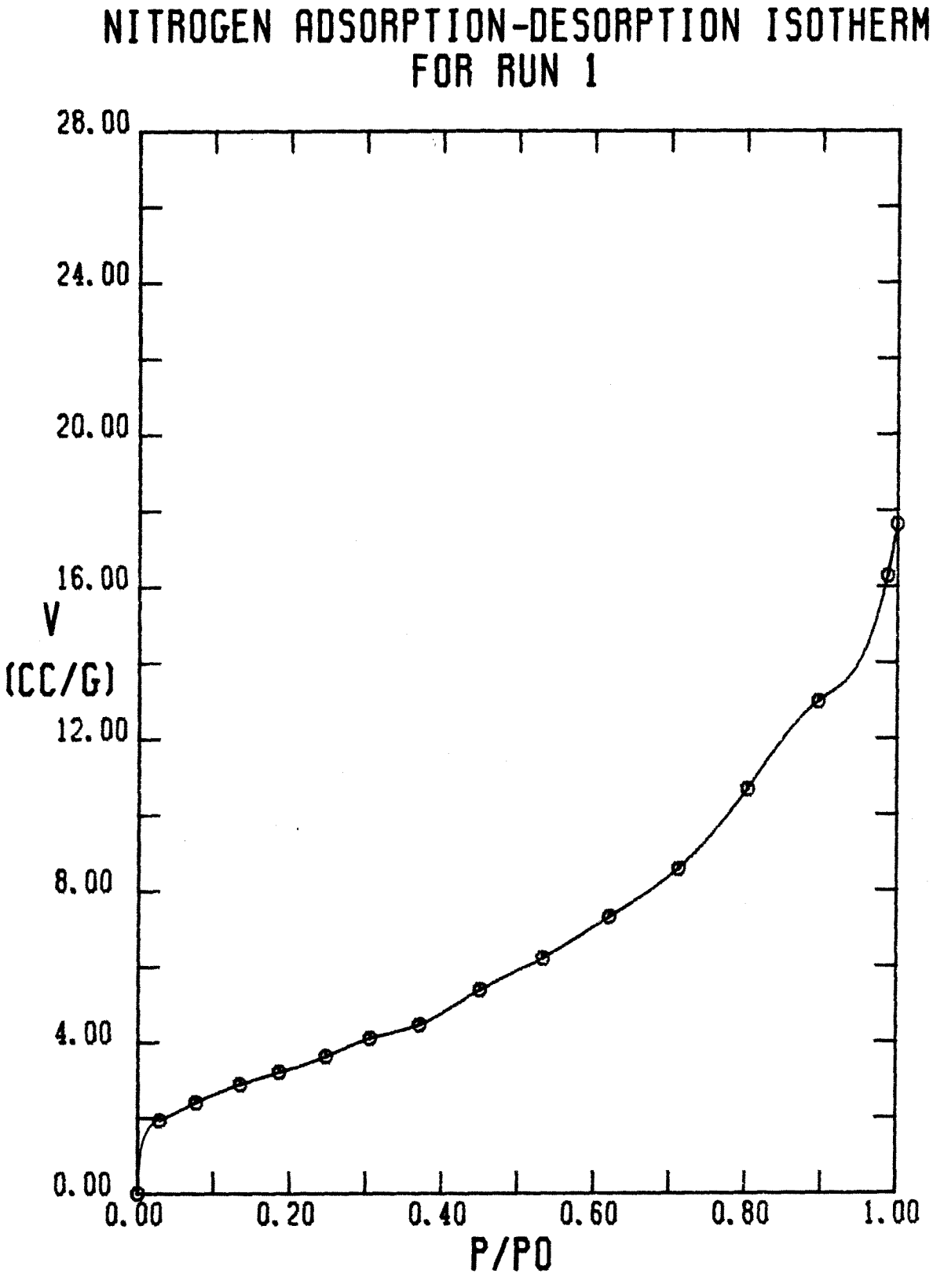
NITROGEN ADSORPTION-DESORPTION ISOTHERM
FOR RUN 1
28.00
24.00
20.00
16.00
V
(CC/G)
12.00
8.00
4.00
0.00
0.00
0.20
0.40
0.60
0.80
1.00
P/PO

FIGURE A-51

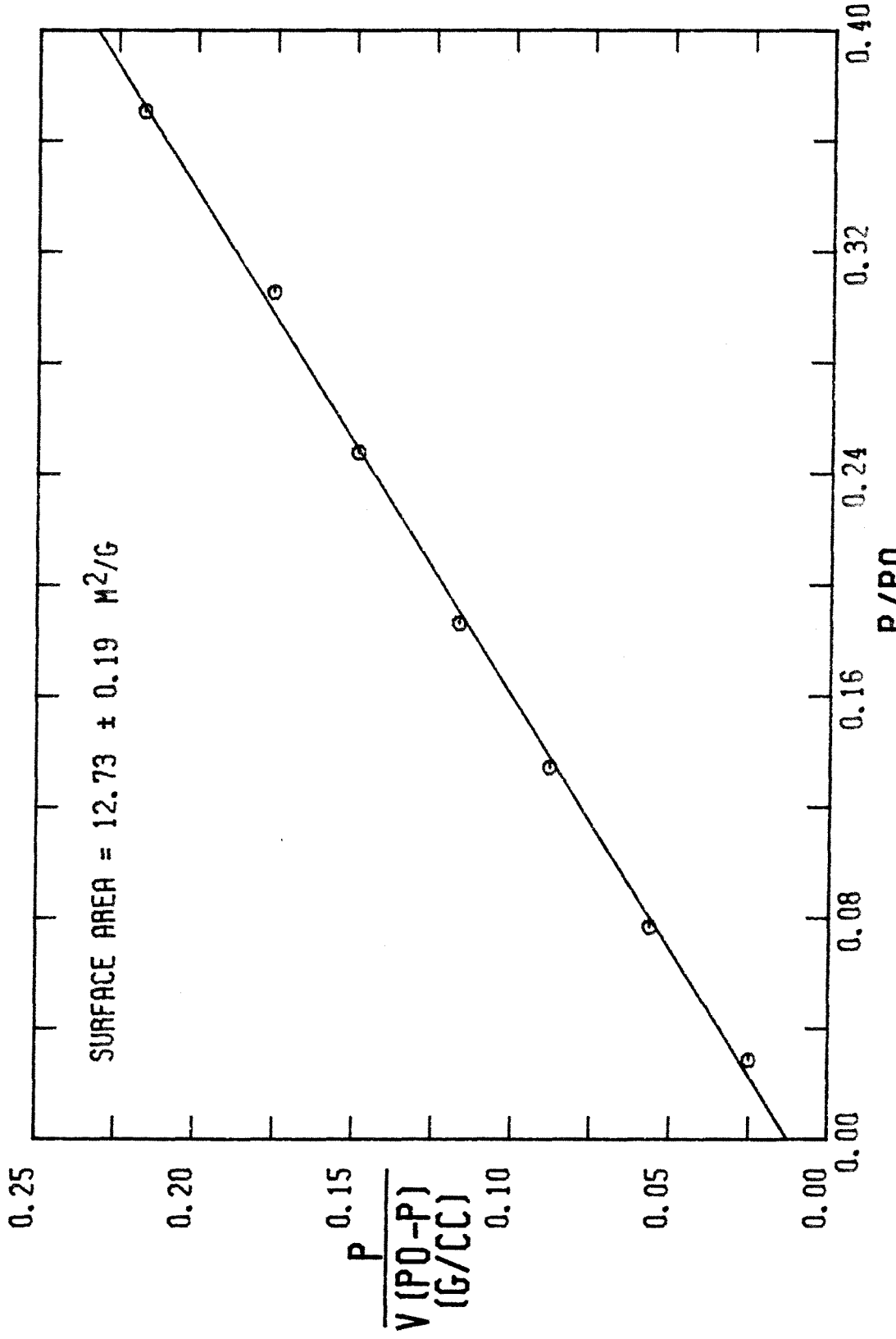
BET PLOT FOR RUN 1
SURFACE AREA = 12.73 ± 0.19 M2/G
P / V (PO-P) (G/CC)
P/PO
0.25
0.20
0.15
0.10
0.05
0.00
0.00
0.08
0.16
0.24
0.32
0.40

FIGURE A-52

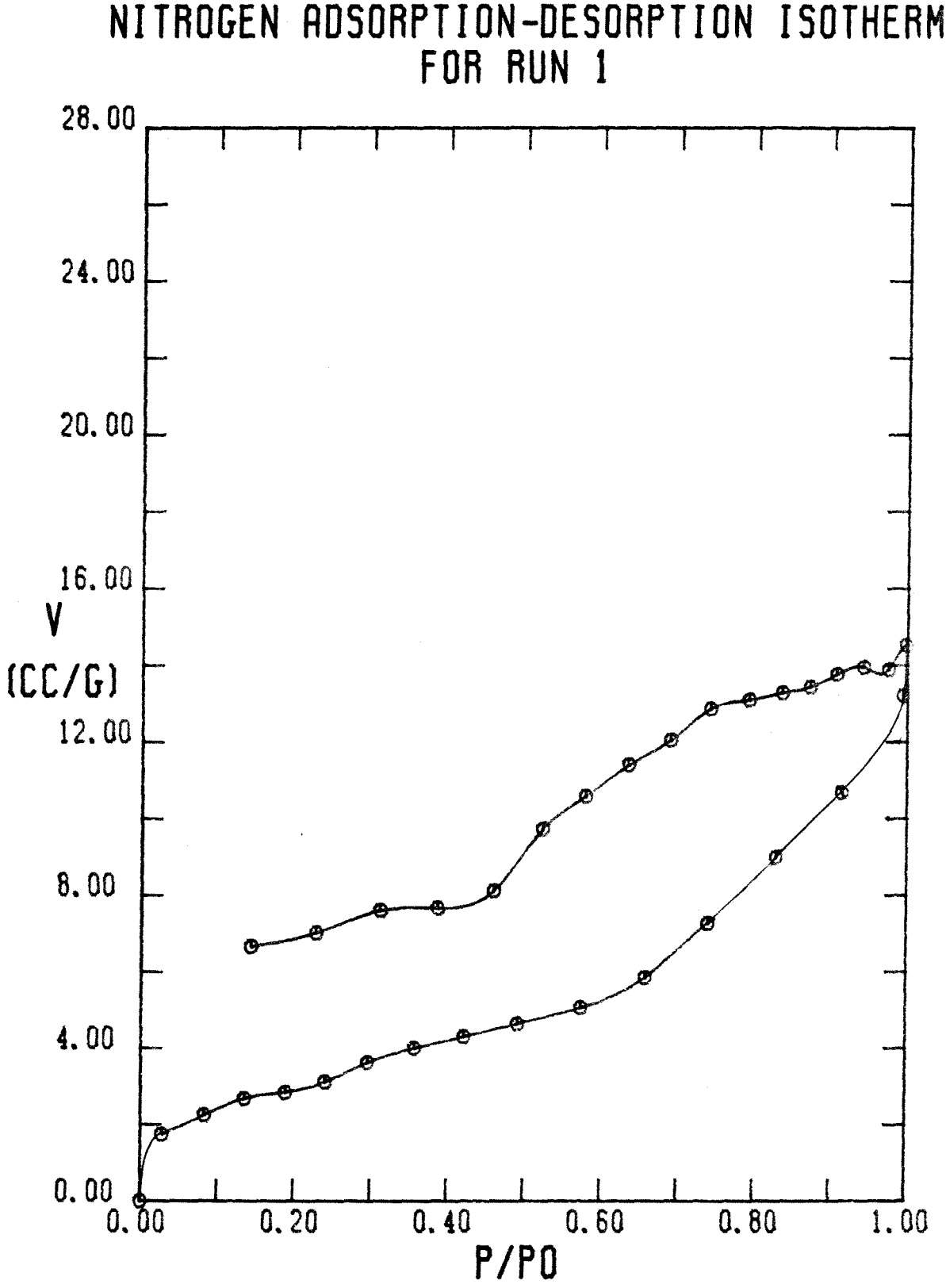
NITROGEN ADSORPTION-DESORPTION ISOTHERM
FOR RUN 1
28.00
24.00
20.00
16.00
V
(CC/G)
12.00
8.00
4.00
0.00
0.00
0.20
0.40
0.60
0.80
1.00
P/PO

FIGURE A-53

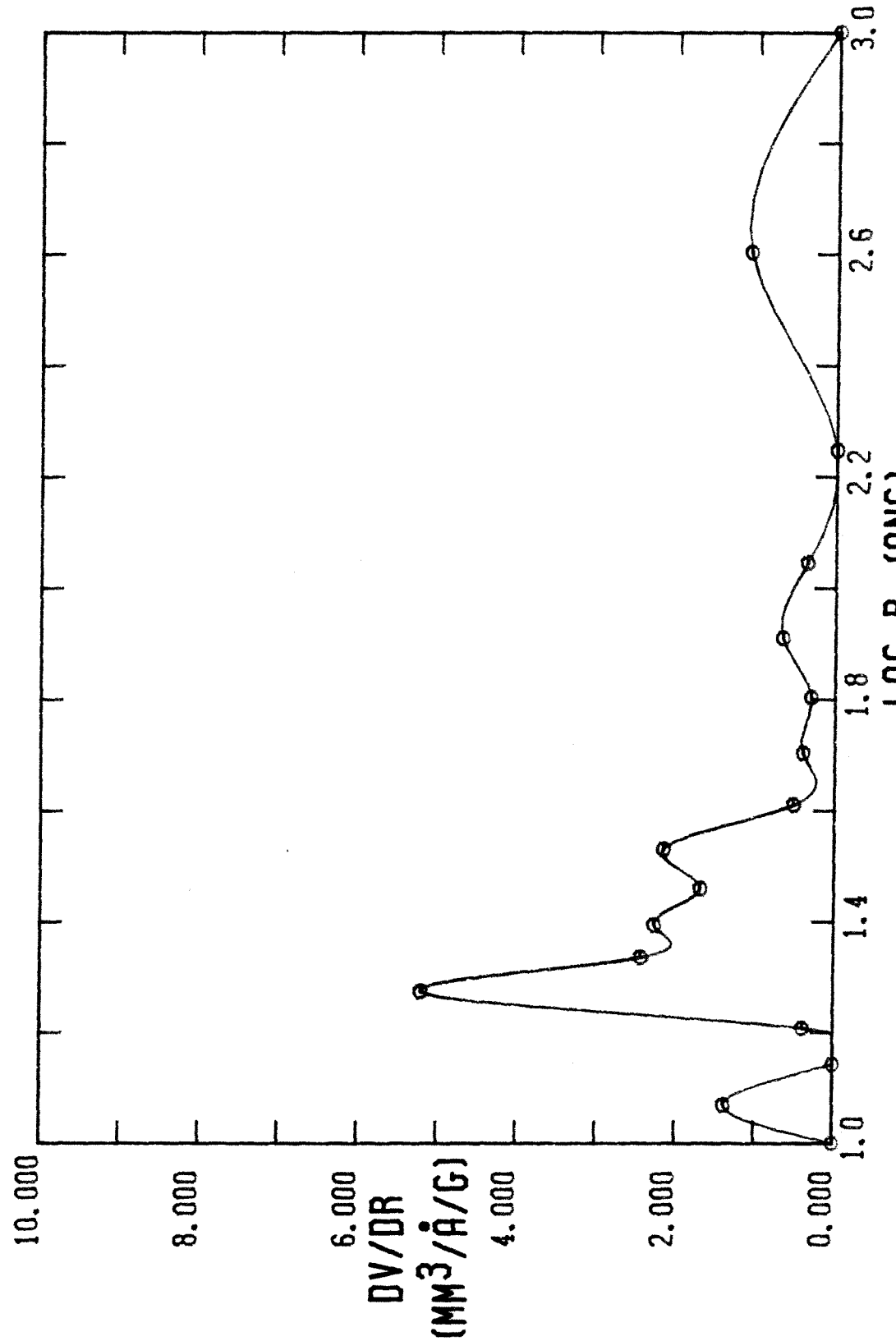
PORE SIZE DISTRIBUTION FOR RUN 1
DV/DR
(MM3/Å/G)
10.000
8.000
6.000
4.000
2.000
0.000
1.0
1.4
1.8
2.2
2.6
3.0
LOG R (ANG)

FIGURE A-54

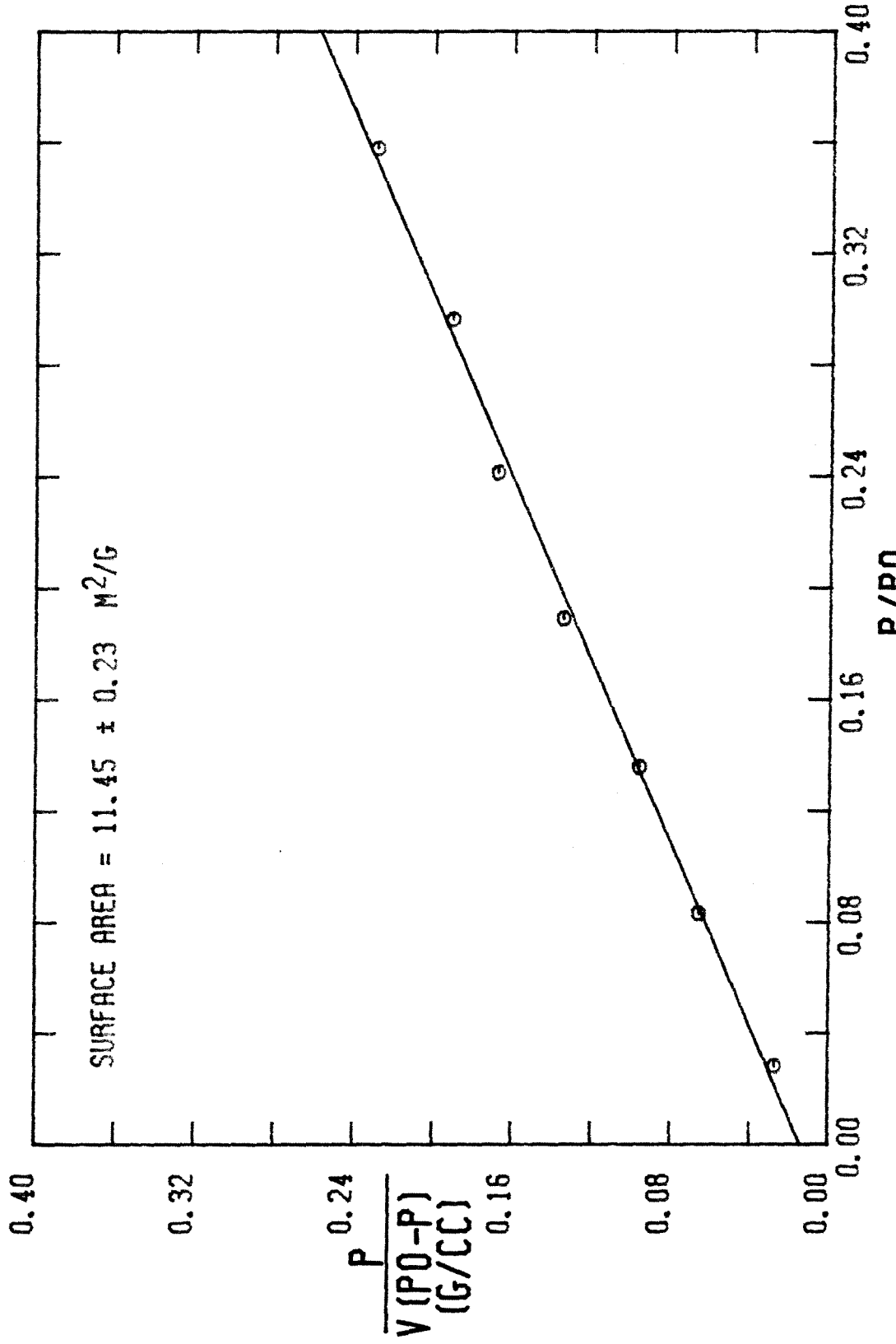
BET PLOT FOR RUN 1
SURFACE AREA = 11.45 ± 0.23 M2/G
P / V(PO-P) (G/CC)
P/PO
0.00
0.08
0.16
0.24
0.32
0.40

FIGURE A-55

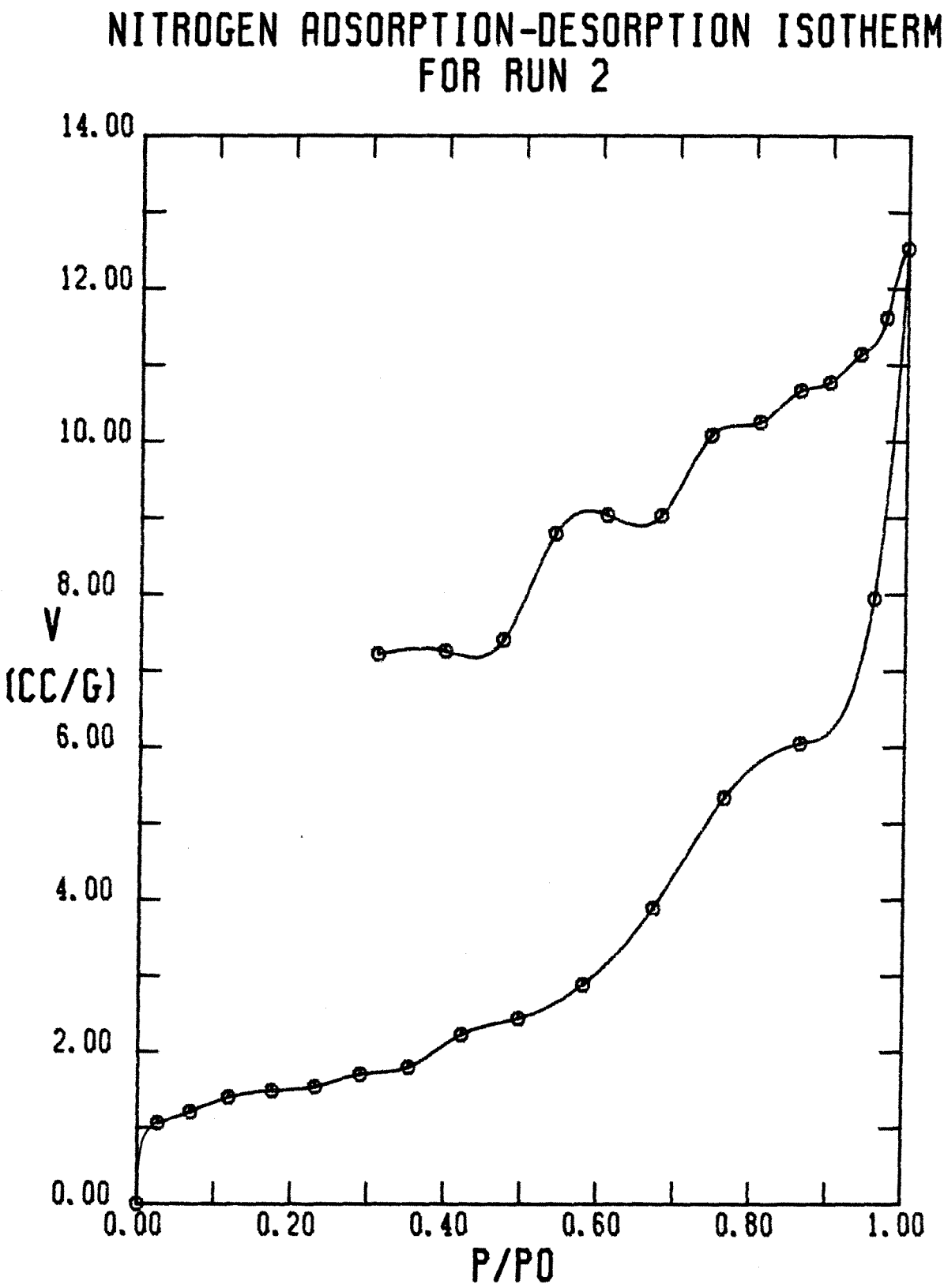
NITROGEN ADSORPTION-DESORPTION ISOTHERM
FOR RUN 2
14.00
12.00
10.00
8.00
V
(CC/G)
6.00
4.00
2.00
0.00
0.00
0.20
0.40
0.60
0.80
1.00
P/PO

FIGURE A-56

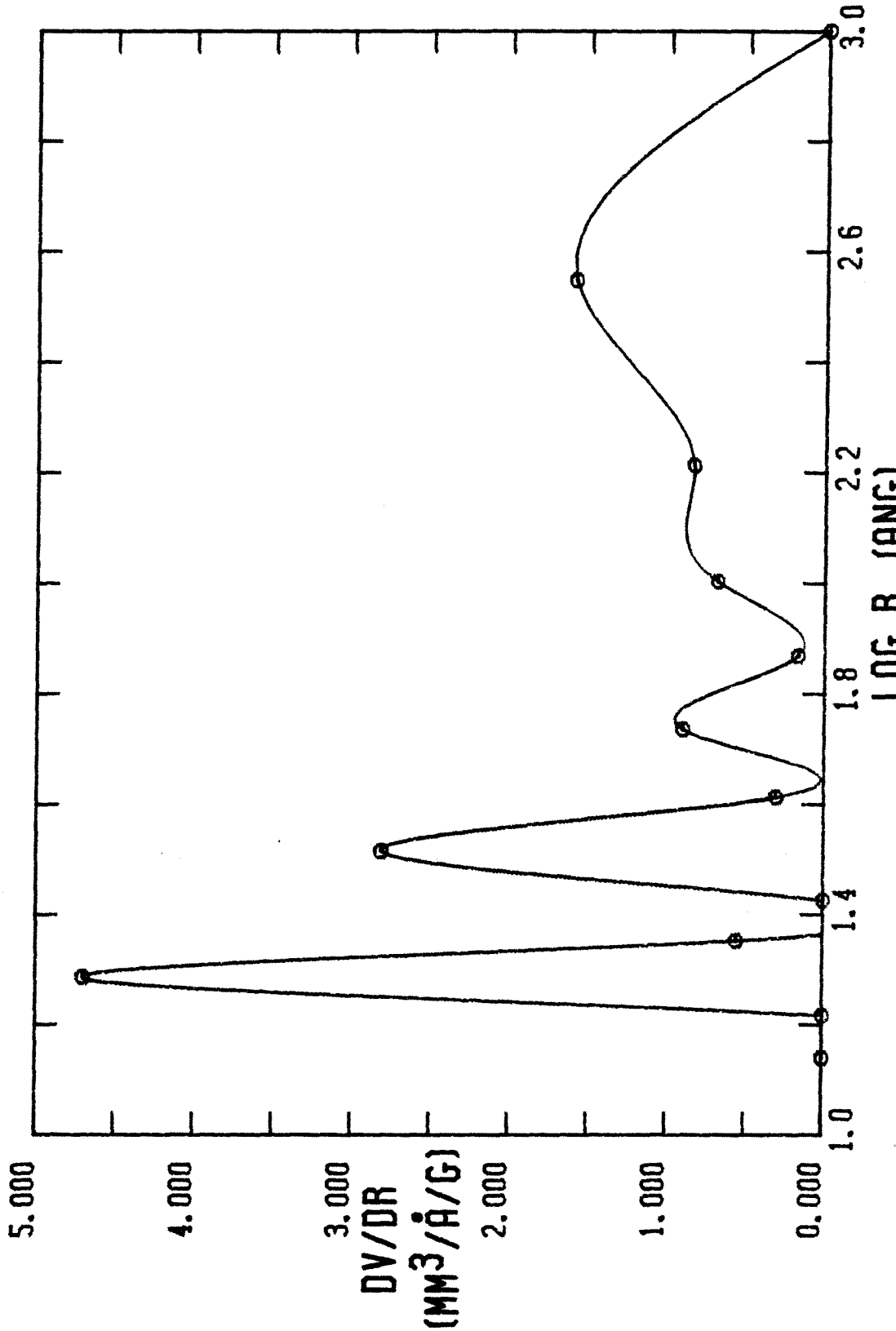
PORE SIZE DISTRIBUTION FOR RUN 2
DV/DR
(MM3/Å/G)
5.000
4.000
3.000
2.000
1.000
0.000
1.0
1.4
1.8
2.2
2.6
3.0
LOG R (ANG)

FIGURE A-57

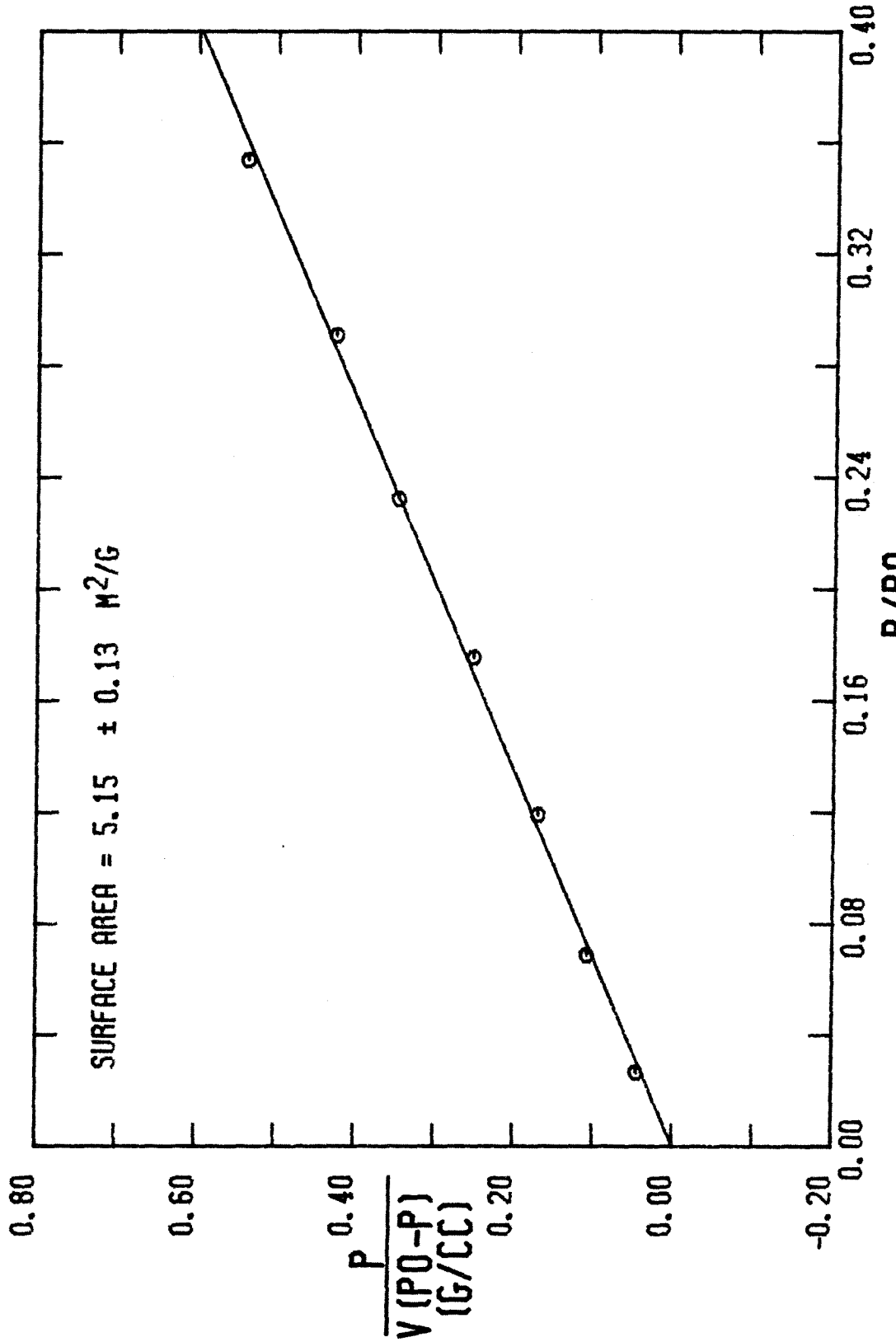
BET PLOT FOR RUN 2
SURFACE AREA = 5.15 ± 0.13 M2/G
P / V(PO-P) (G/CC)
P/PO
0.80
0.60
0.40
0.20
0.00
-0.20
0.00
0.08
0.16
0.24
0.32
0.40

FIGURE A-58

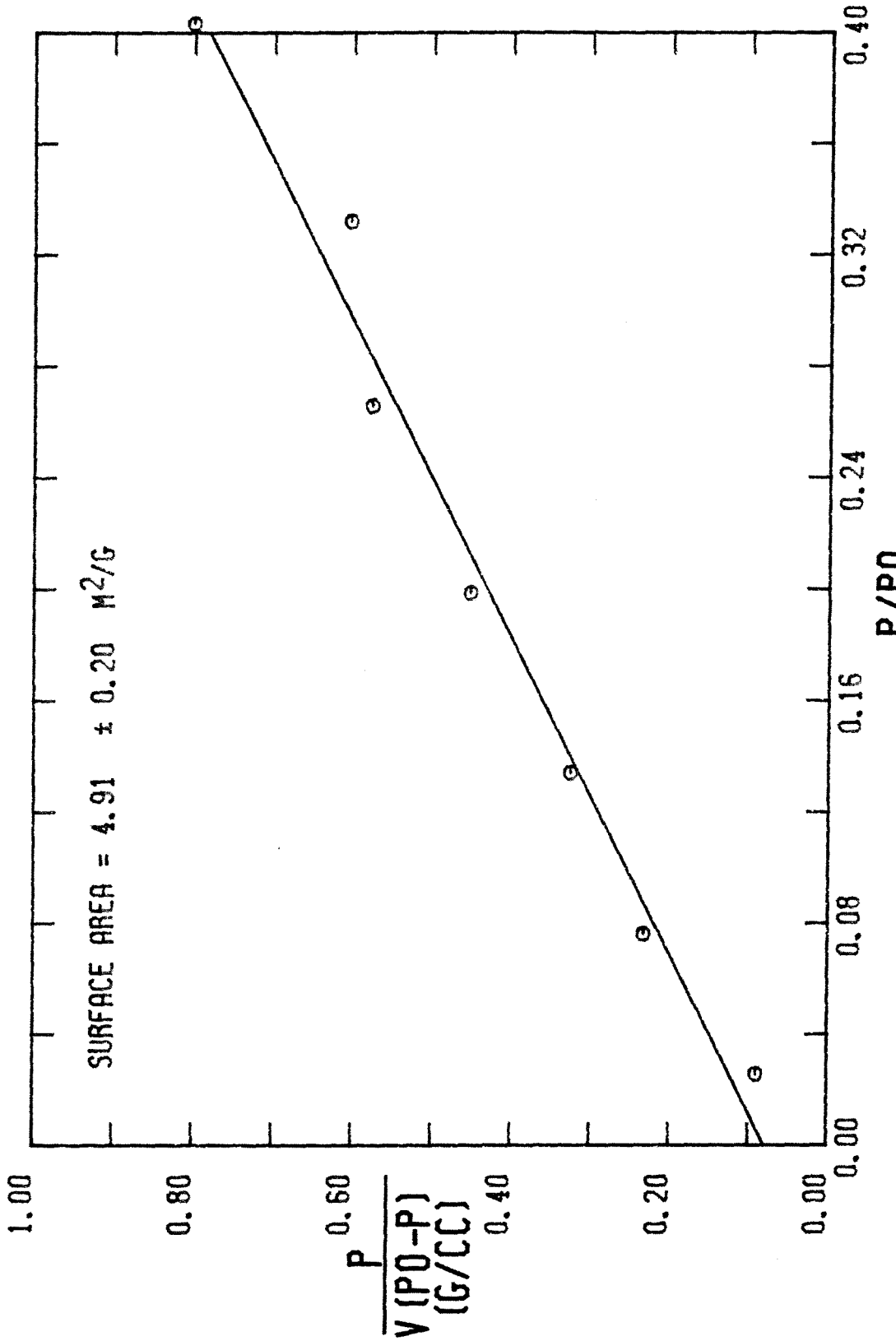
BET PLOT FOR RUN 3
SURFACE AREA = 4.91 ± 0.20 M2/G
P / V (PO-P) (G/CC)
1.00
0.80
0.60
0.40
0.20
0.00
0.00
0.08
0.16
0.24
0.32
0.40
P/PO

FIGURE A-59

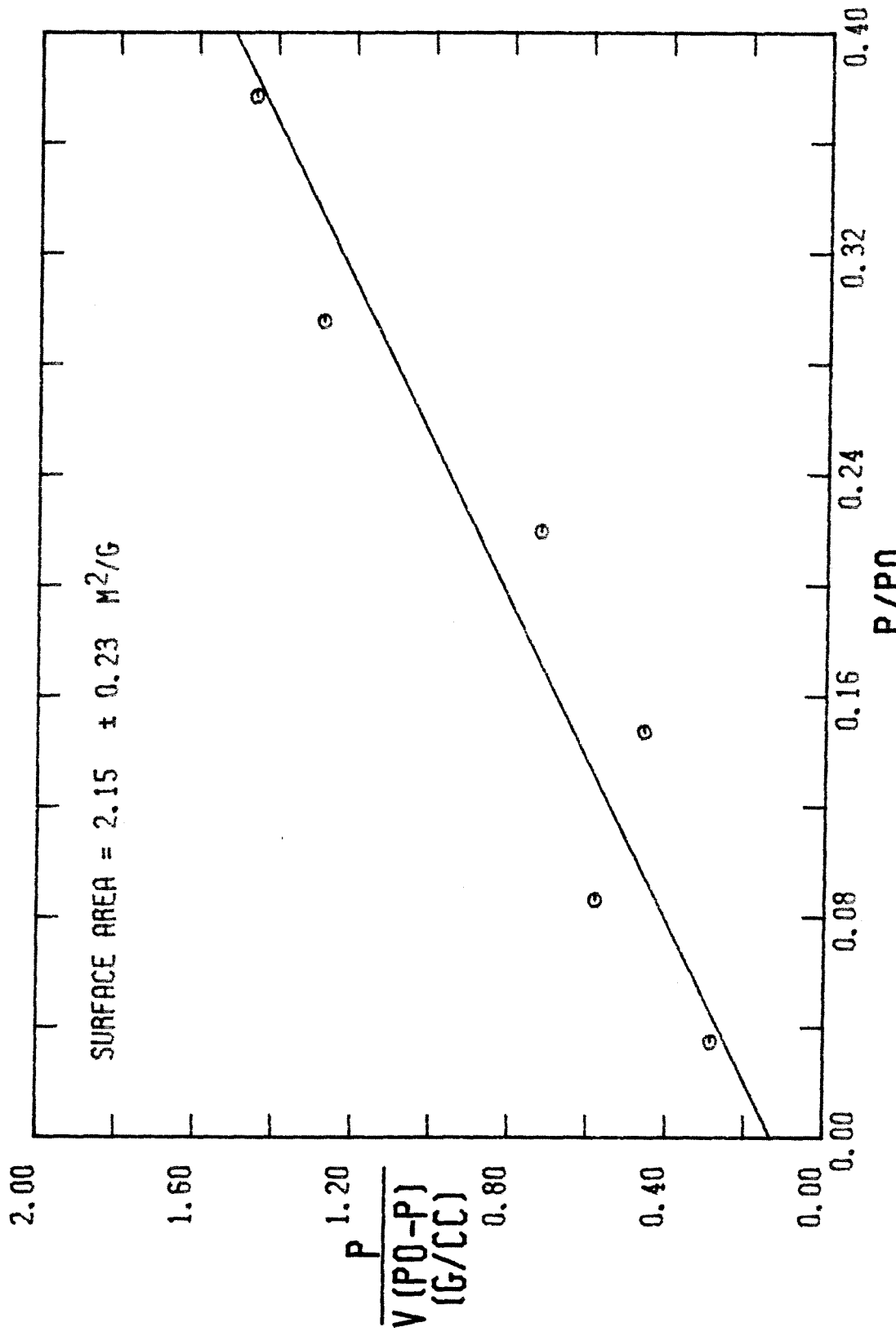
BET PLOT FOR RUN 3
SURFACE AREA = 2.15 ± 0.23 M2/G
P/V (PO-P) (G/CC)
2.00
1.60
1.20
0.80
0.40
0.00
0.00
0.08
0.16
0.24
0.32
0.40
P/PO

FIGURE A-60

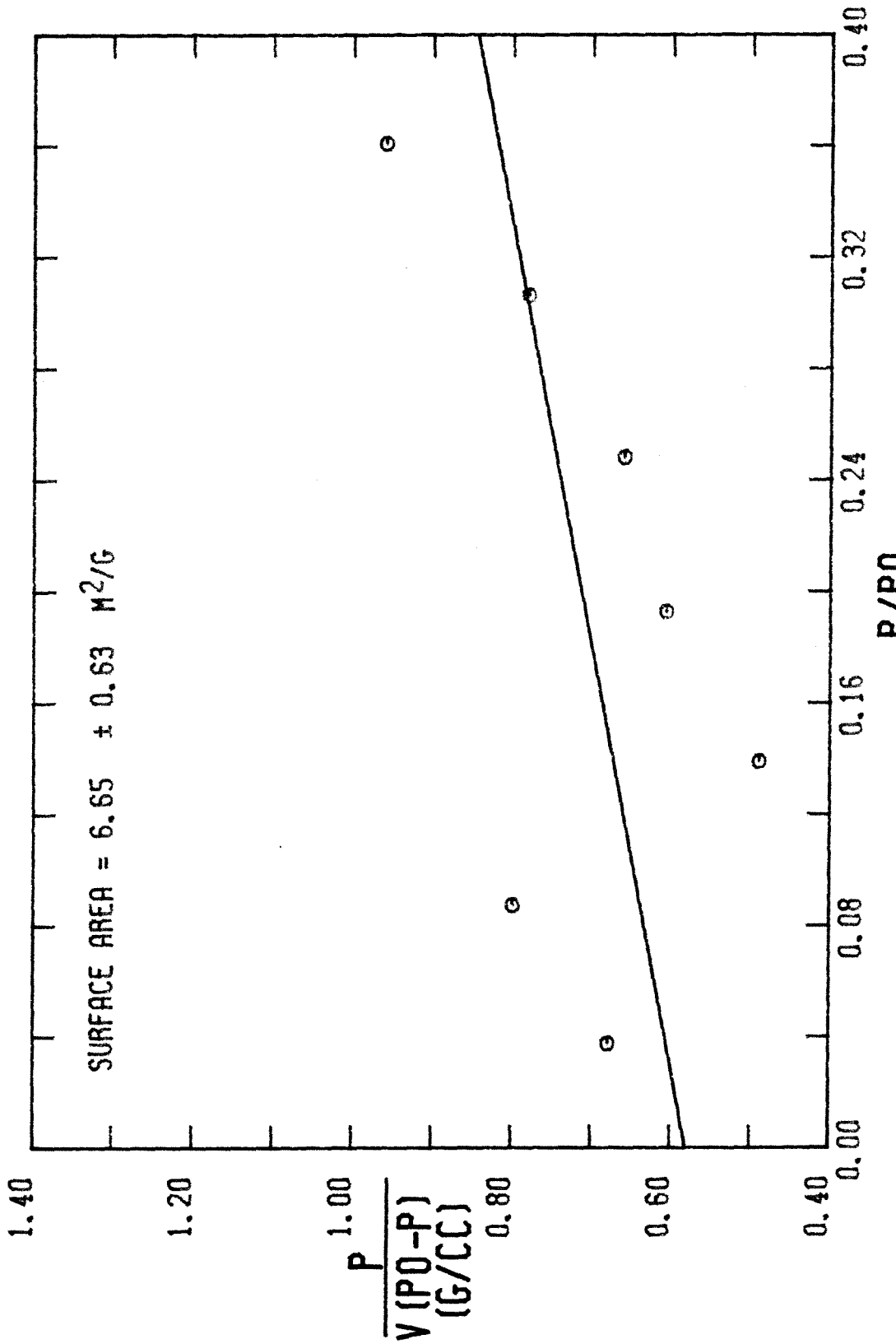
BET PLOT FOR RUN 4
SURFACE AREA = 6.65 ± 0.63 M2/G
P / V(PO-P) (G/CC)
1.40
1.20
1.00
0.80
0.60
0.40
0.00
0.08
0.16
0.24
0.32
0.40
P/PO

FIGURE A-61

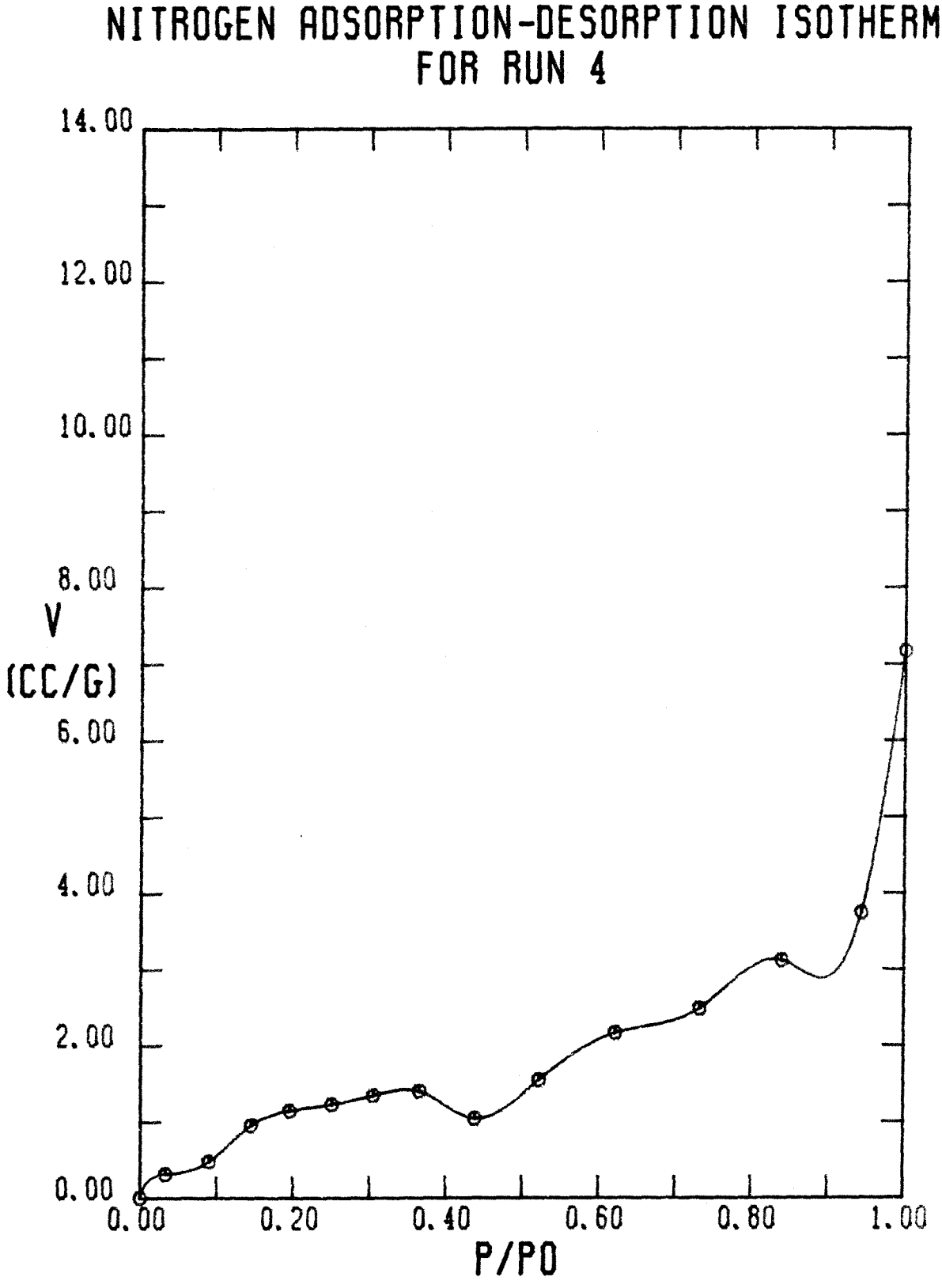
NITROGEN ADSORPTION-DESORPTION ISOTHERM
FOR RUN 4
14.00
12.00
10.00
8.00
V
(CC/G)
6.00
4.00
2.00
0.00
0.00
0.20
0.40
0.60
0.80
1.00
P/PO

FIGURE A-62

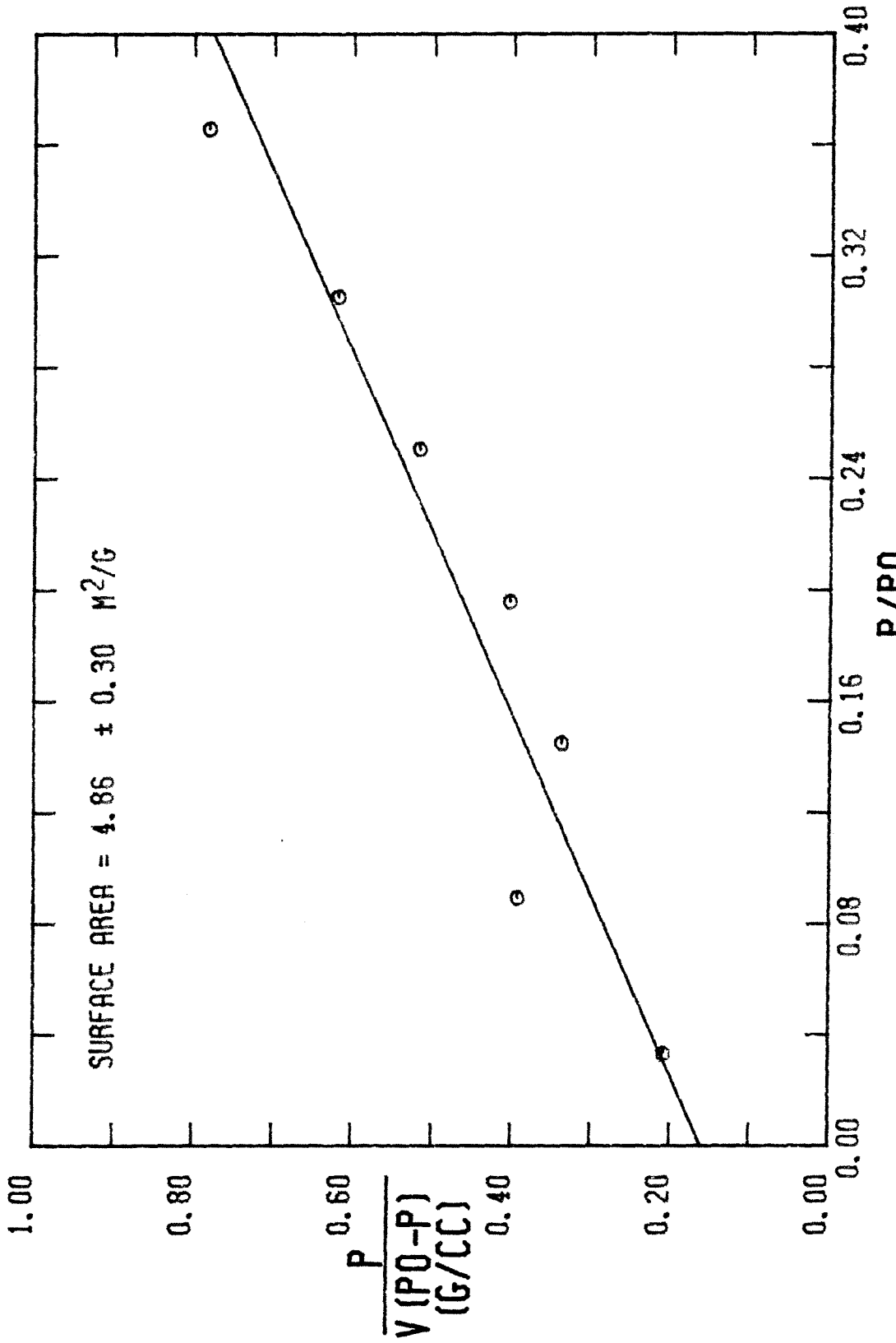
BET PLOT FOR RUN 4
SURFACE AREA = 4.86 ± 0.30 M2/G
P / V (PO-P) (G/CC)
1.00
0.80
0.60
0.40
0.20
0.00
0.00
0.08
0.16
0.24
0.32
0.40
P/PO

FIGURE A-63

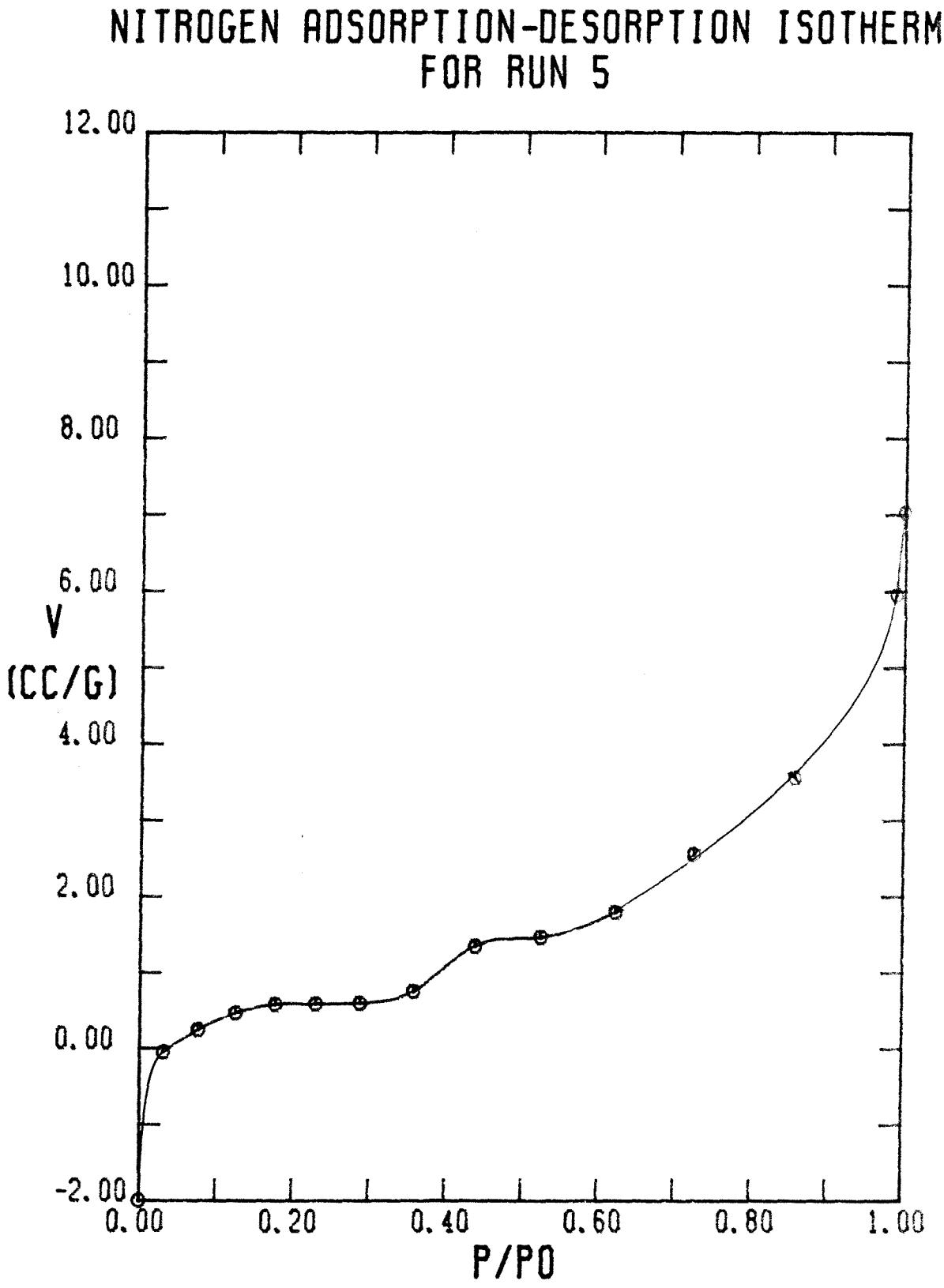
NITROGEN ADSORPTION-DESORPTION ISOTHERM
FOR RUN 5
12.00
10.00
8.00
6.00
V
(CC/G)
4.00
2.00
0.00
-2.00
0.00
0.20
0.40
0.60
0.80
1.00
P/PO

FIGURE A-64

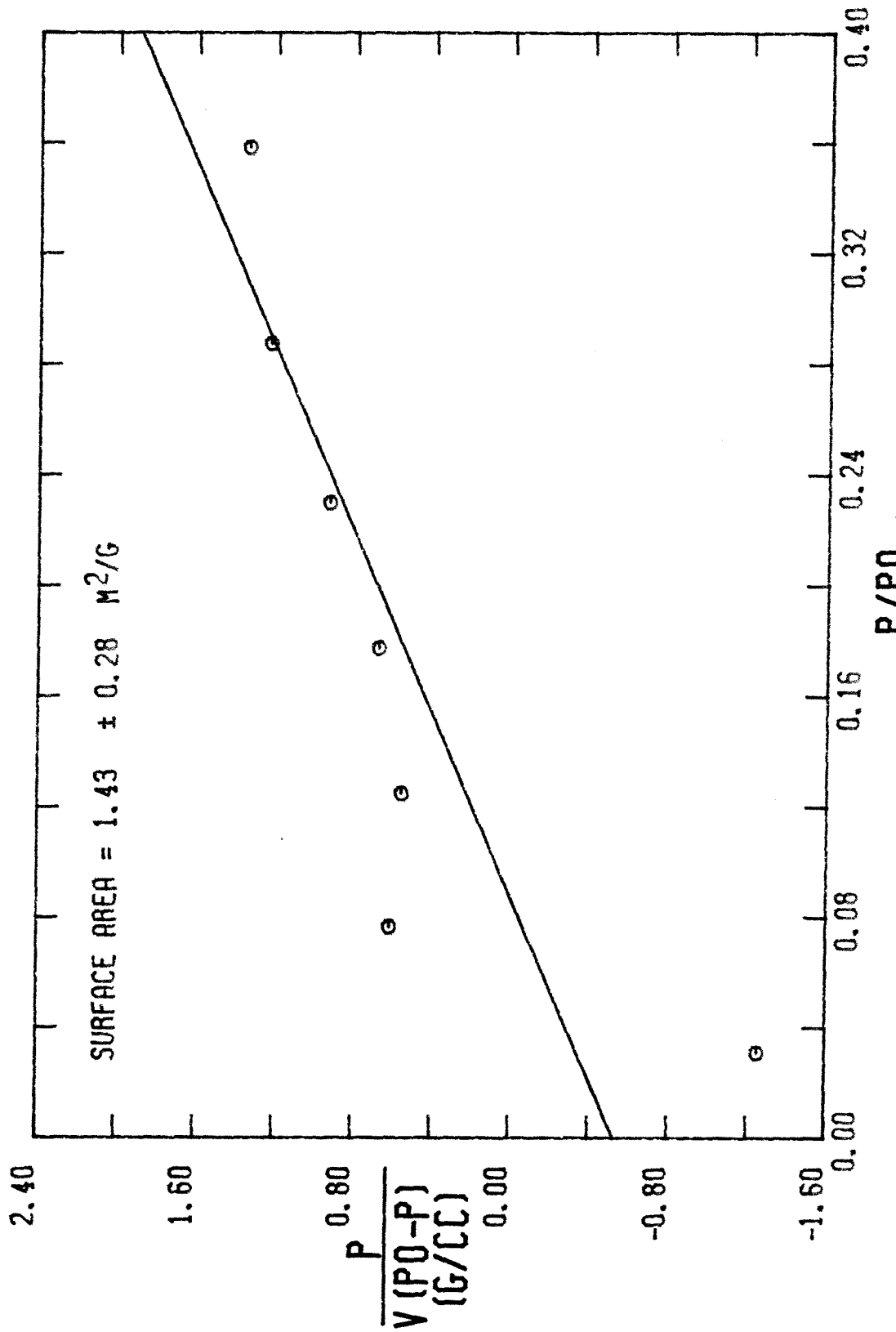
BET PLOT FOR RUN 5
SURFACE AREA = 1.43 ± 0.28 M2/G
P / V (PO-P) (G/CC)
2.40
1.60
0.80
0.00
-0.80
-1.60
0.00
0.08
0.16
0.24
0.32
0.40
P/PO

FIGURE A-65

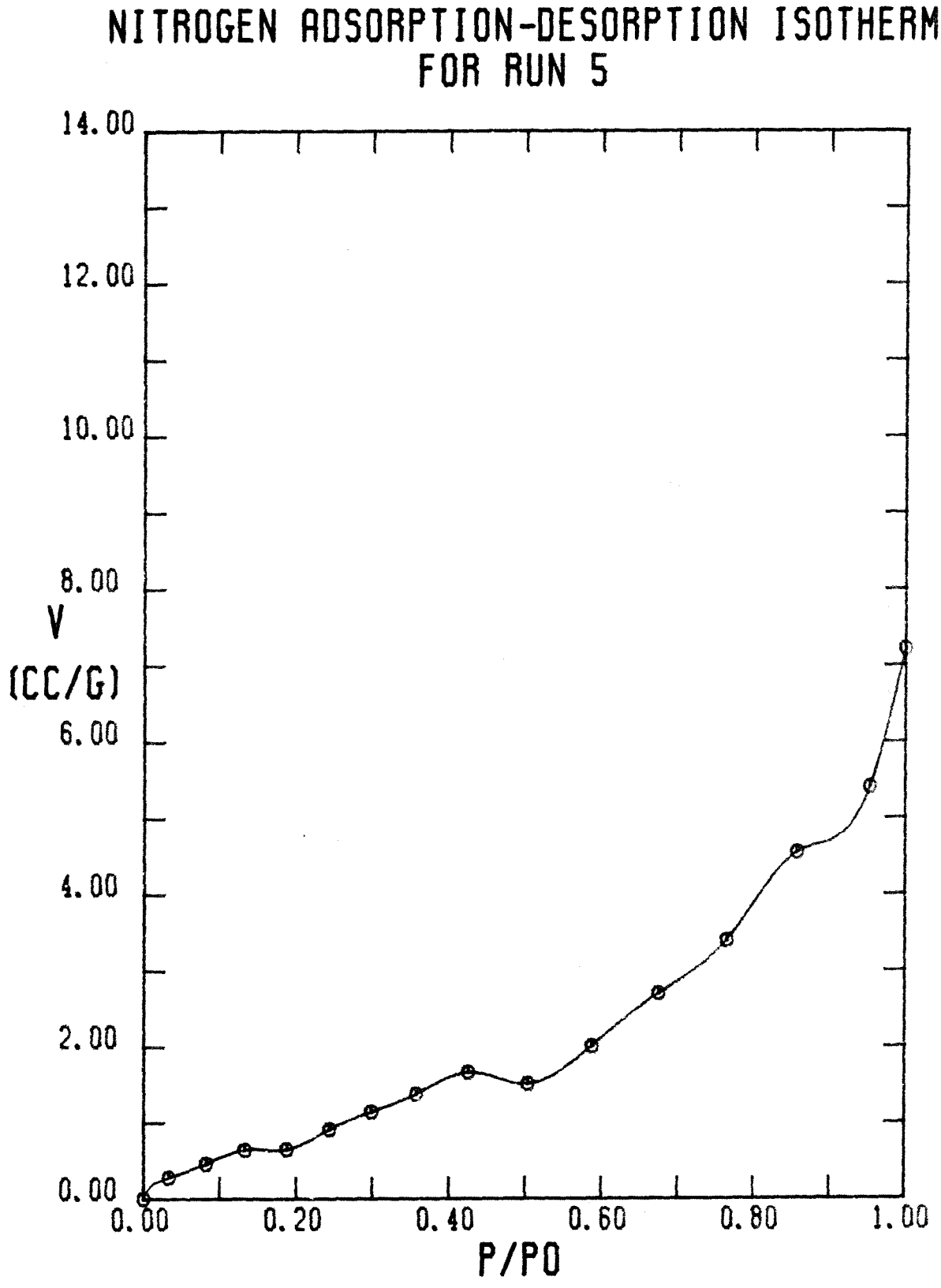
NITROGEN ADSORPTION-DESORPTION ISOTHERM
FOR RUN 5
14.00
12.00
10.00
8.00
V
(CC/G)
6.00
4.00
2.00
0.00
0.00
0.20
0.40
0.60
0.80
1.00
P/PO

FIGURE A-66

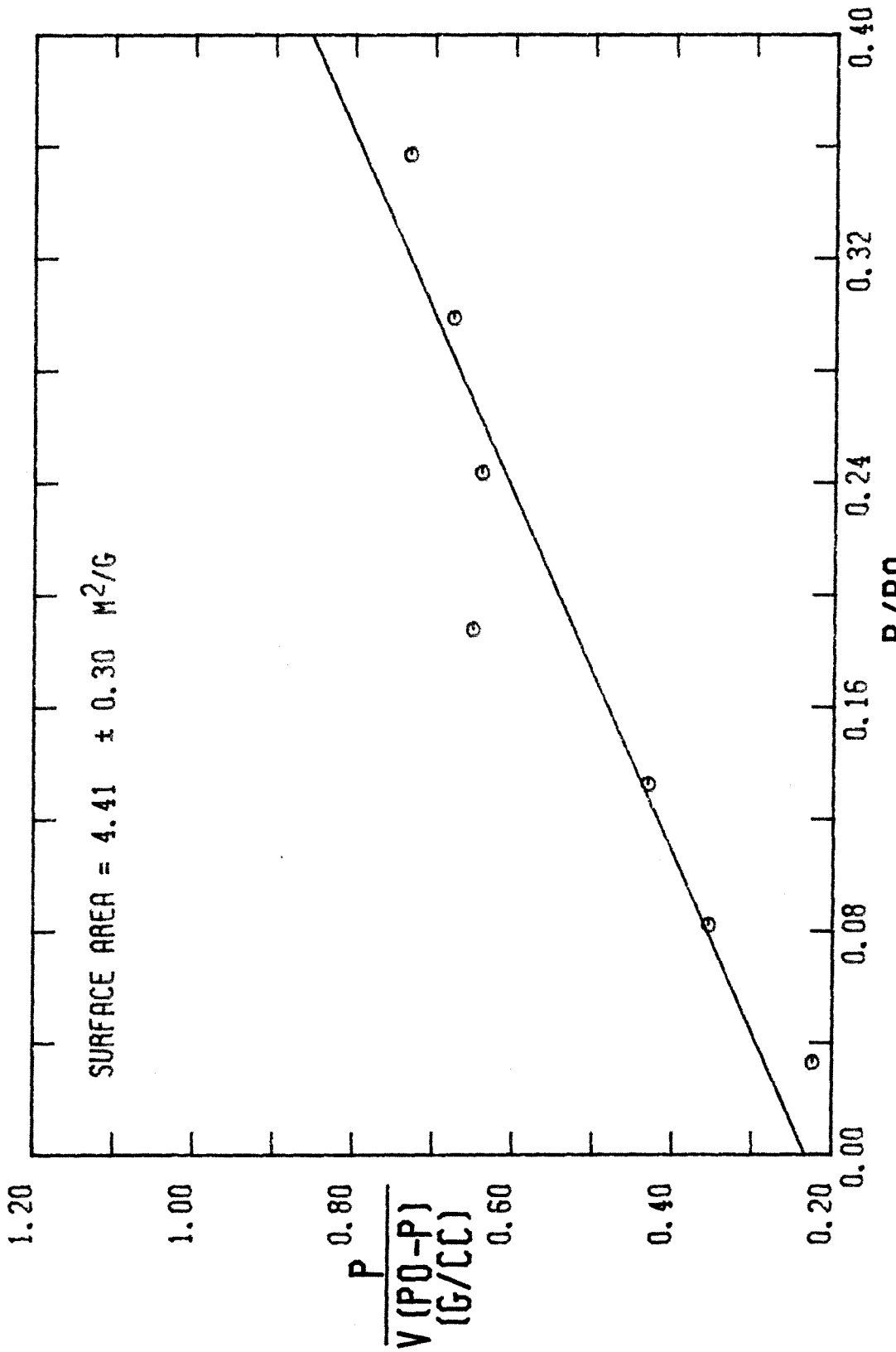
BET PLOT FOR RUN 5
SURFACE AREA = 4.41 ± 0.30 M2/G
P / V (PO-P) (G/CC)
1.20
1.00
0.80
0.60
0.40
0.20
0.00
0.08
0.16
0.24
0.32
0.40
P/PO

FIGURE A-67

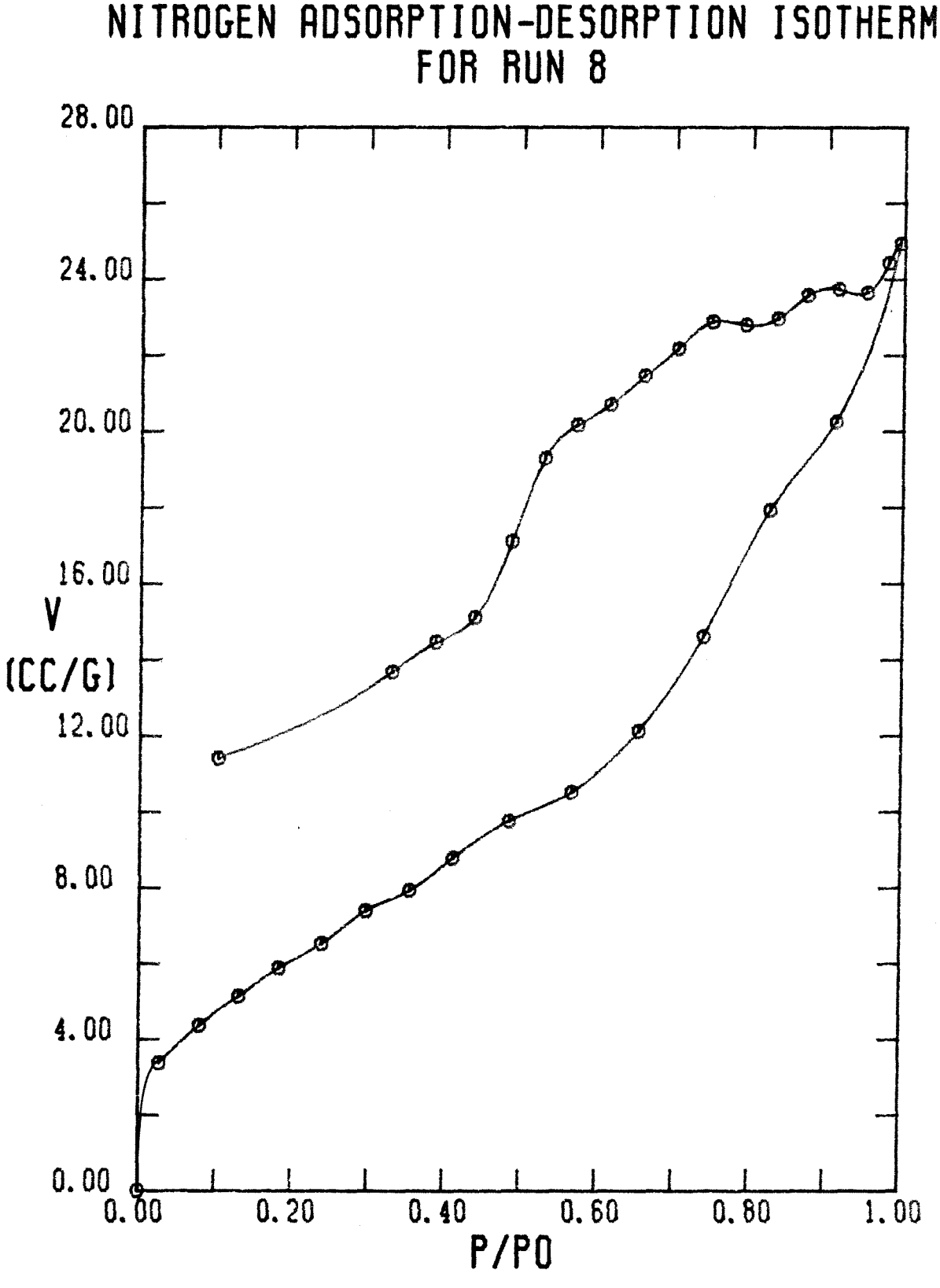
NITROGEN ADSORPTION-DESORPTION ISOTHERM
FOR RUN 8
28.00
24.00
20.00
16.00
V
(CC/G)
12.00
8.00
4.00
0.00
0.00
0.20
0.40
0.60
0.80
1.00
P/PO

FIGURA A-68

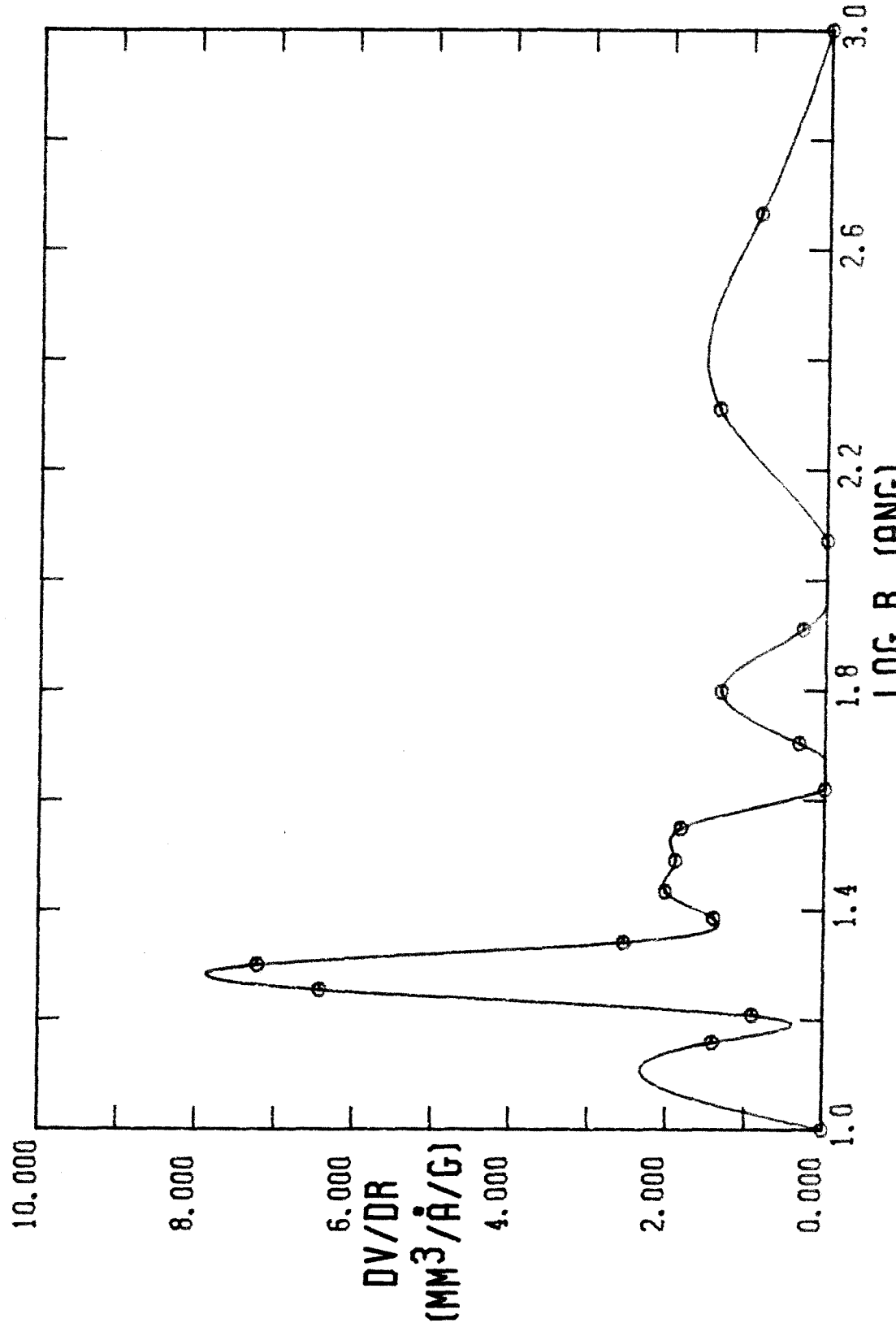
PORE SIZE DISTRIBUTION FOR RUN 8
DV/DR
(MM3/Å/G)
10.000
8.000
6.000
4.000
2.000
0.000
1.0
1.4
1.8
2.2
2.6
3.0
LOG R (ANG)

FIGURE A-69

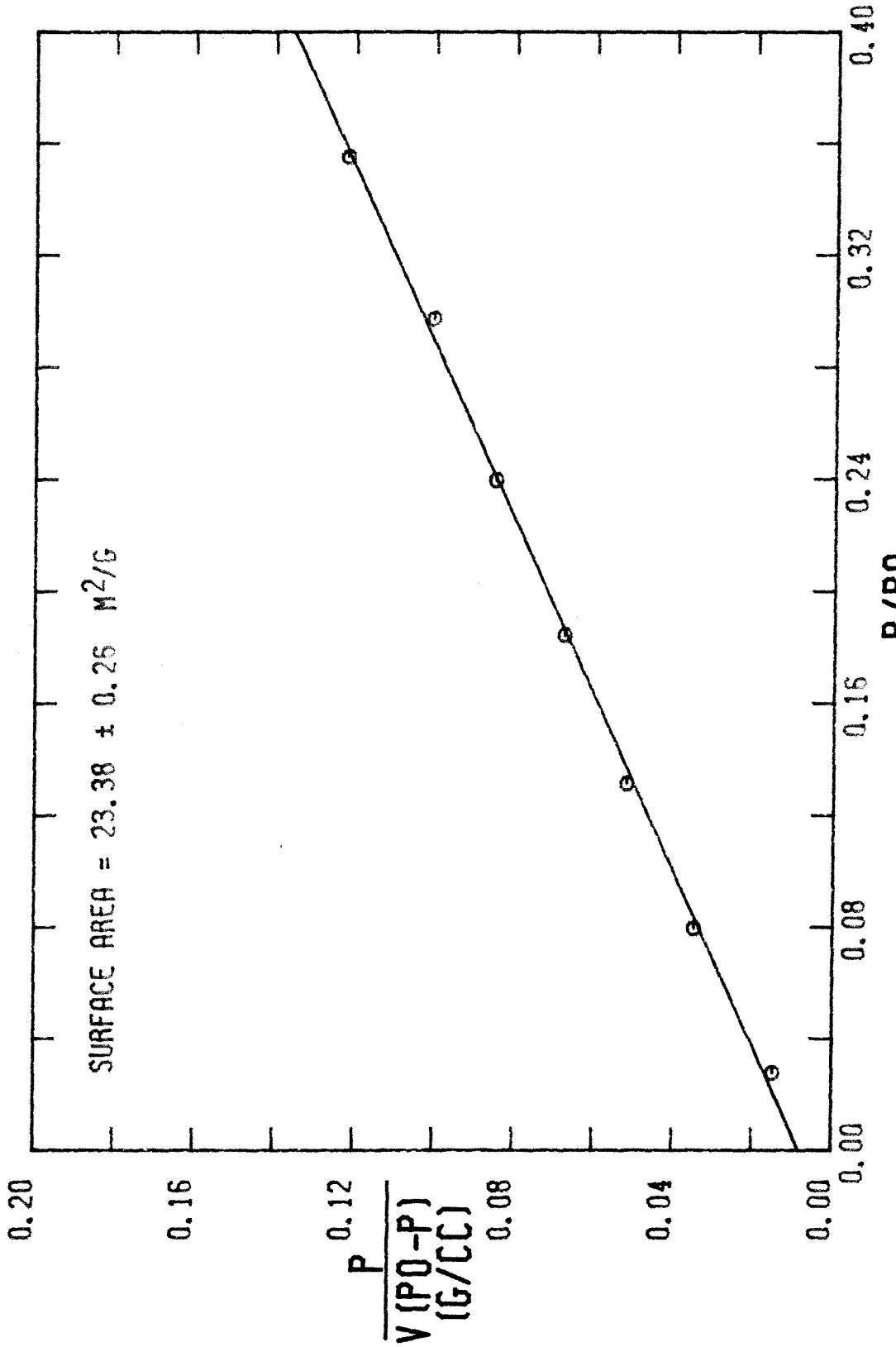
BET PLOT FOR RUN 8
SURFACE AREA = 23.38 ± 0.25 M2/G
P / V(PO-P) (G/CC)
P/PO
0.00
0.04
0.08
0.12
0.16
0.20
0.00
0.08
0.16
0.24
0.32
0.40

FIGURE A-70

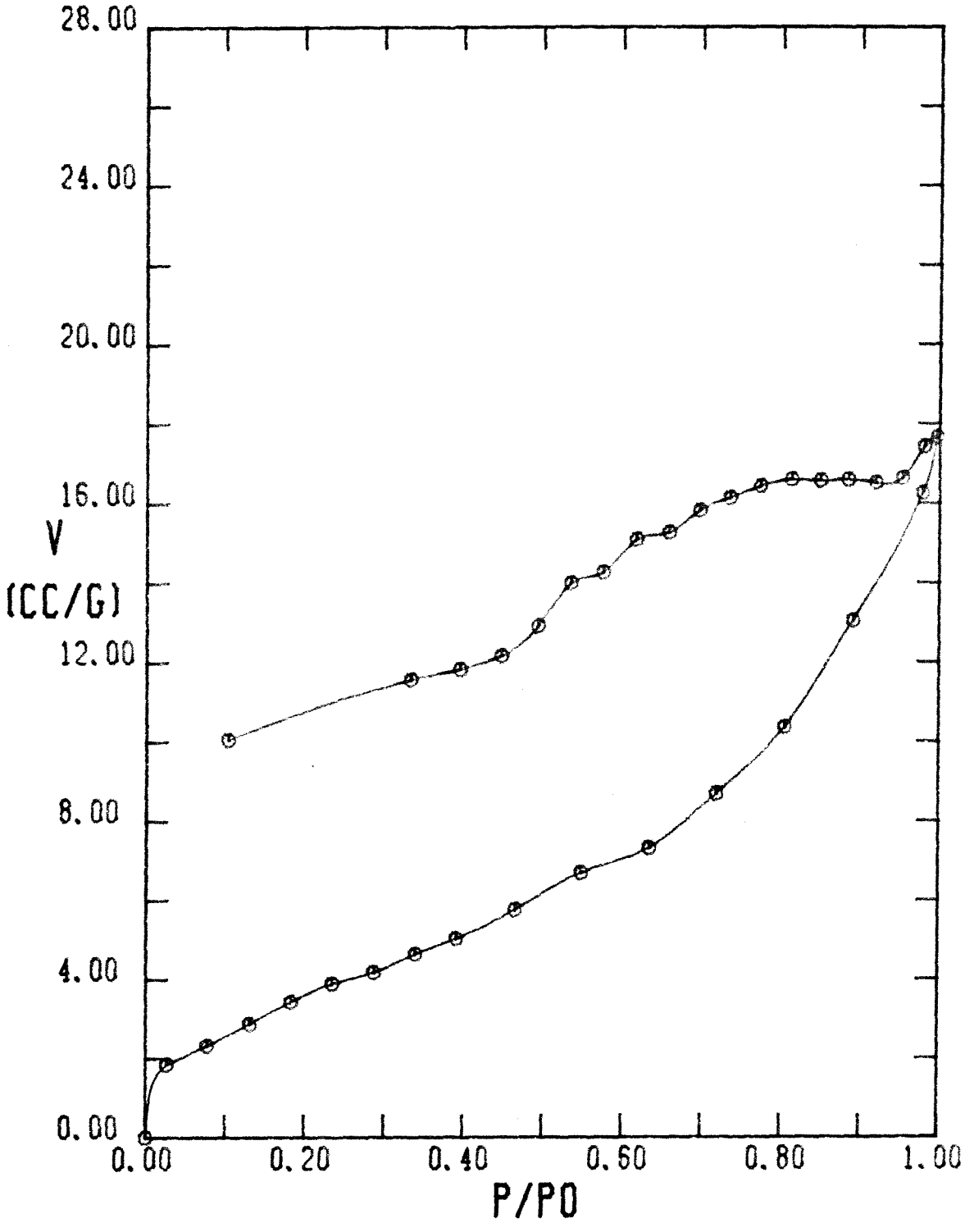
NITROGEN ADSORPTION-DESORPTION ISOTHERM
FOR RUN 9
28.00
24.00
20.00
16.00
12.00
8.00
4.00
0.00
V
(CC/G)
0.00
0.20
0.40
0.60
0.80
1.00
P/P0

FIGURE A-71

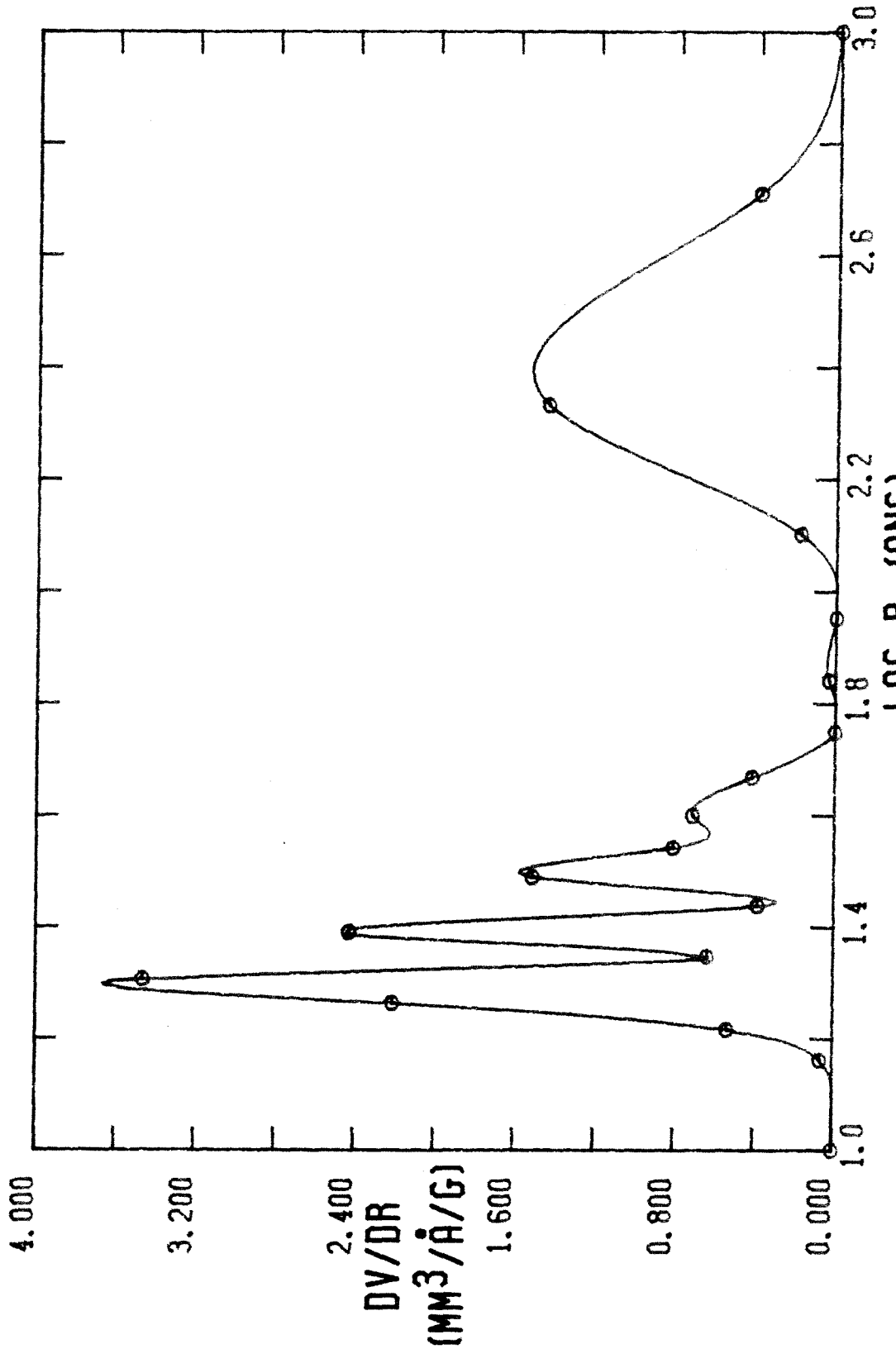
PORE SIZE DISTRIBUTION FOR RUN 9
DV/DR
(MM3/Å/G)
4.000
3.200
2.400
1.600
0.800
0.000
1.0
1.4
1.8
2.2
2.6
3.0
LOG R (ANG)

FIGURE A-72

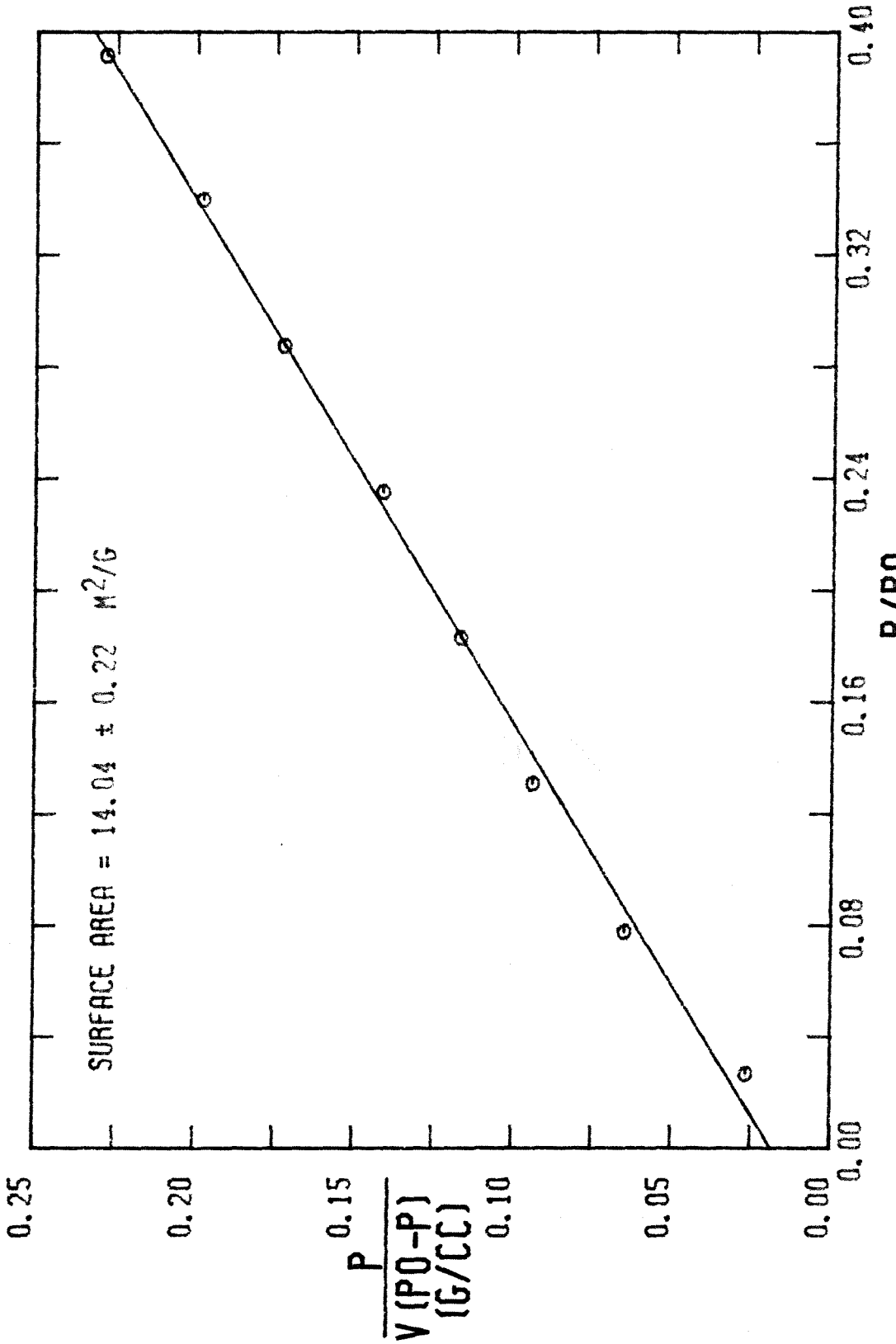
BET PLOT FOR RUN 9
SURFACE AREA = 14.04 ± 0.22 M2/G
P/PO
P / V(PO-P) (G/CC)
0.00
0.08
0.16
0.24
0.32
0.40
0.00
0.05
0.10
0.15
0.20
0.25

FIGURE A-73

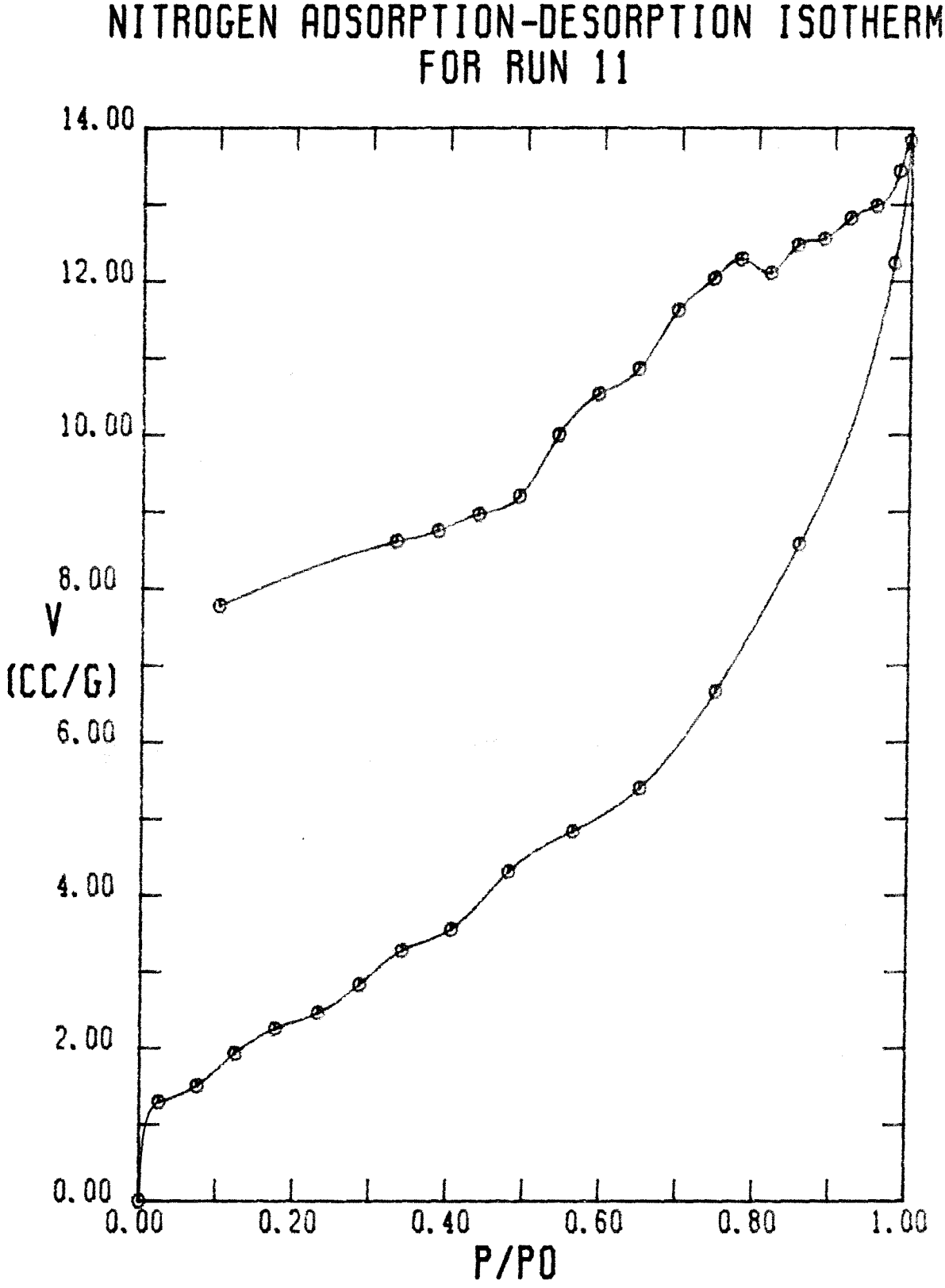
NITROGEN ADSORPTION-DESORPTION ISOTHERM
FOR RUN 11
14.00
12.00
10.00
8.00
V
(CC/G)
6.00
4.00
2.00
0.00
0.00
0.20
0.40
0.60
0.80
1.00
P/PO

FIGURE A-74

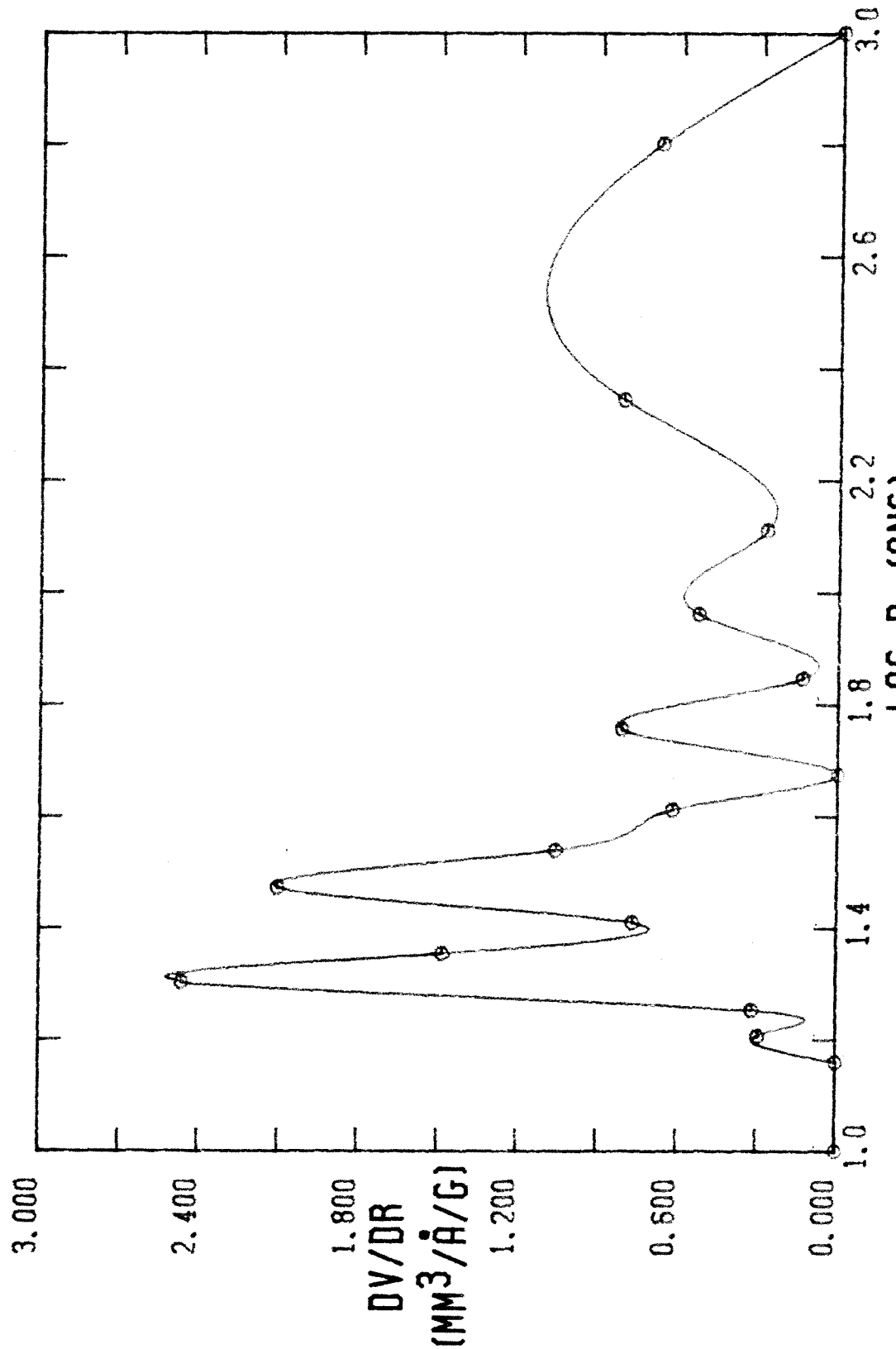
PORE SIZE DISTRIBUTION FOR RUN 11
DV/DR
(MM3/Å/G)
3.000
2.400
1.800
1.200
0.600
0.000
1.0
1.4
1.8
2.2
2.6
3.0
LOG R (ANG)

FIGURE A-75

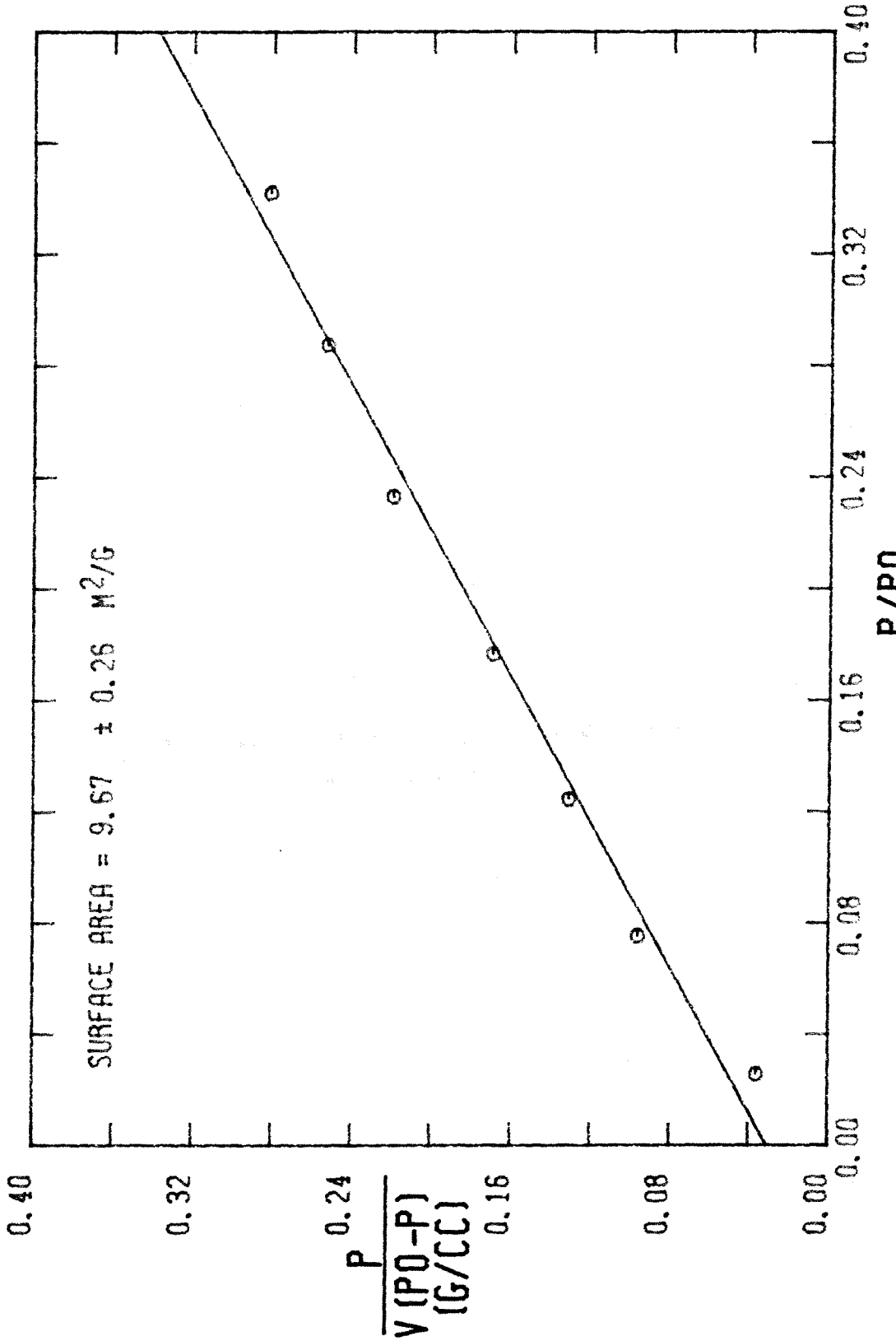
BET PLOT FOR RUN 11
SURFACE AREA = 9.67 ± 0.26 M2/G
P / V (PO-P) (G/CC)
P/PO
0.00
0.08
0.16
0.24
0.32
0.40

FIGURE A-76

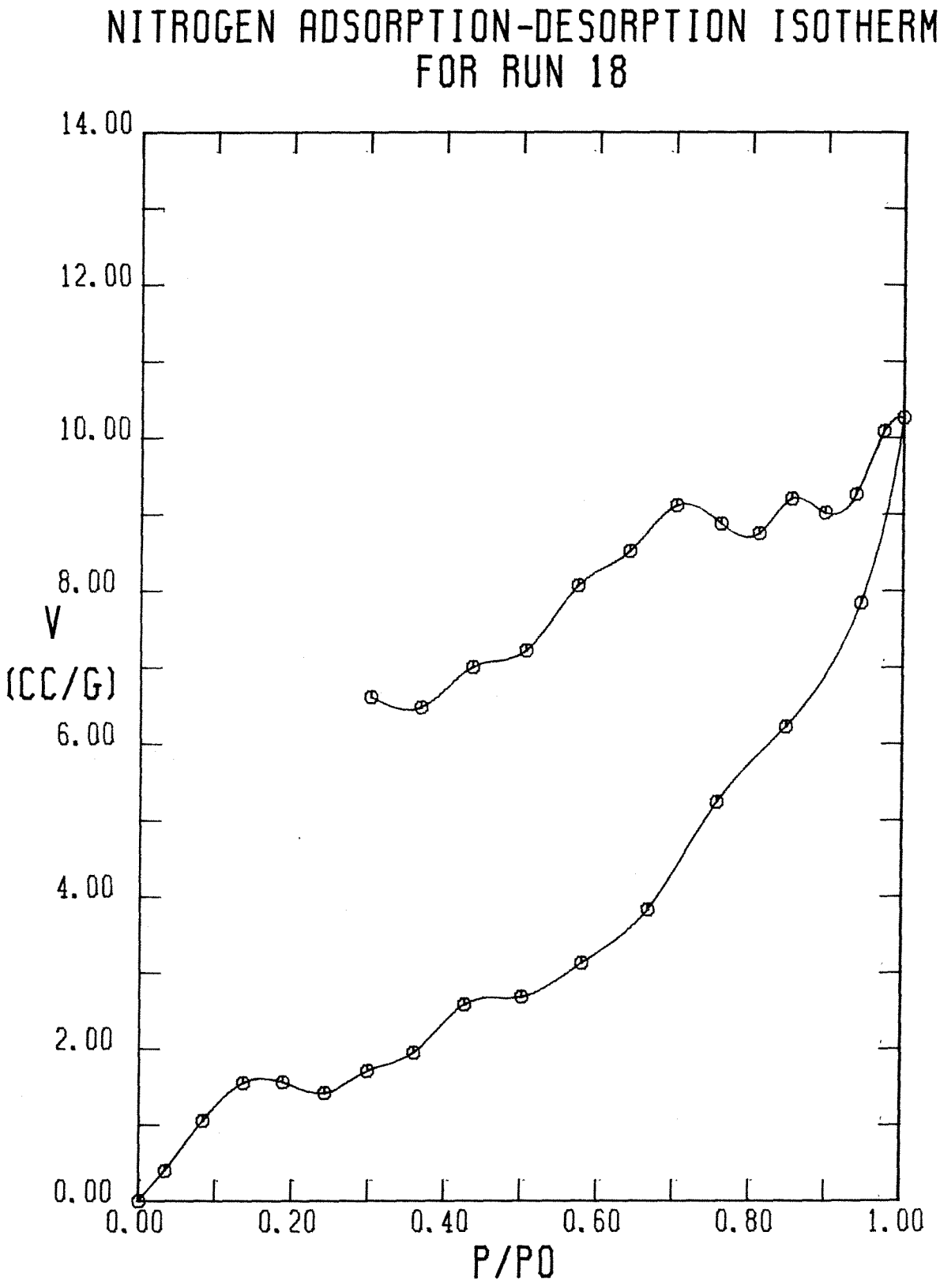
NITROGEN ADSORPTION-DESORPTION ISOTHERM
FOR RUN 18
14.00
12.00
10.00
8.00
V
(CC/G)
6.00
4.00
2.00
0.00
0.00
0.20
0.40
0.60
0.80
1.00
P/PO

FIGURE A-77

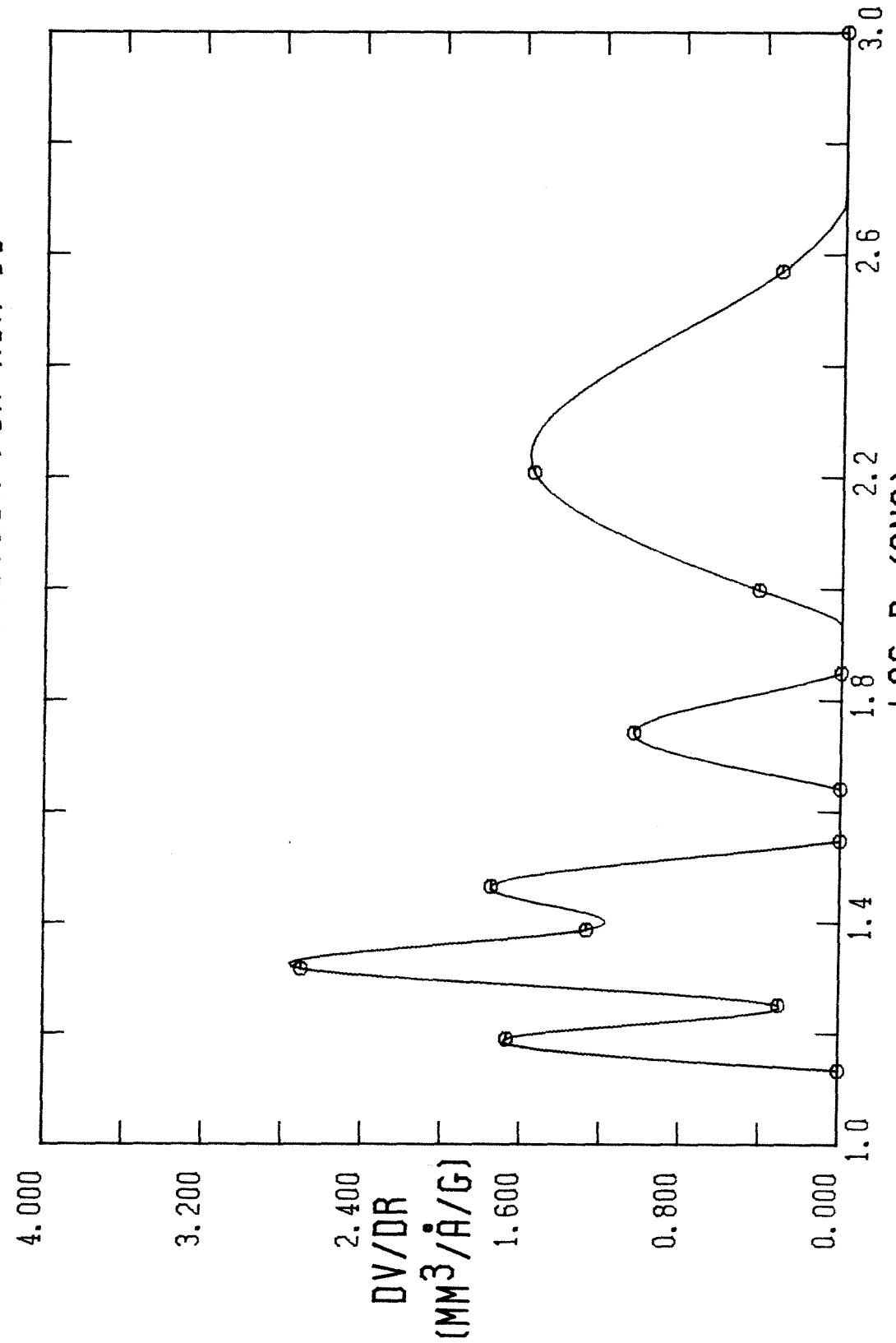
PORE SIZE DISTRIBUTION FOR RUN 18
DV/DR
(MM3/Å/G)
4.000
3.200
2.400
1.600
0.800
0.000
1.0
1.4
1.8
2.2
2.6
3.0
LOG R (ANG)

FIGURE A-78

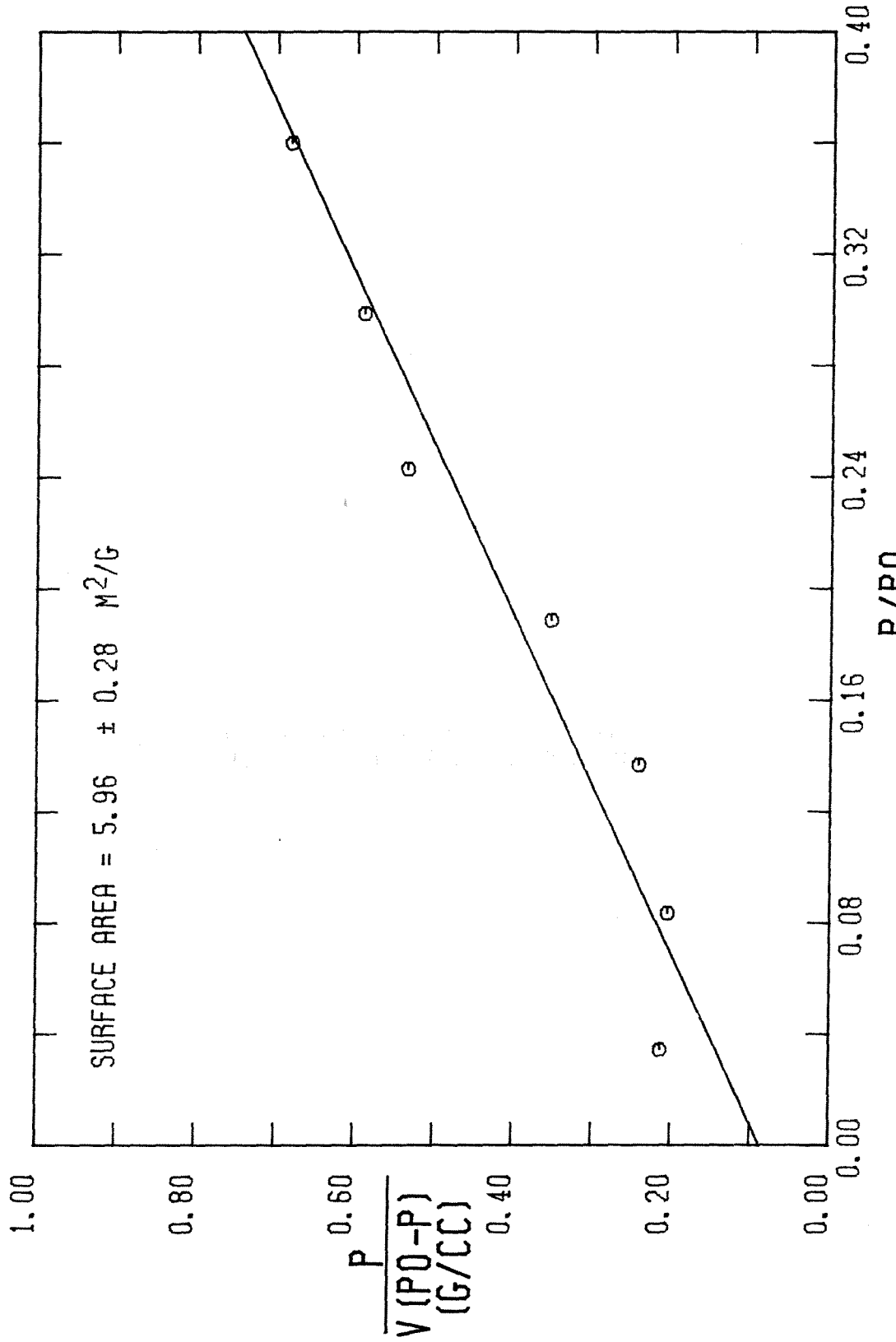
BET PLOT FOR RUN 18
SURFACE AREA = 5.96 ± 0.28 M2/G
P / V (PO-P) (G/CC)
P/PO
1.00
0.80
0.60
0.40
0.20
0.00
0.00
0.08
0.16
0.24
0.32
0.40

FIGURE A-79

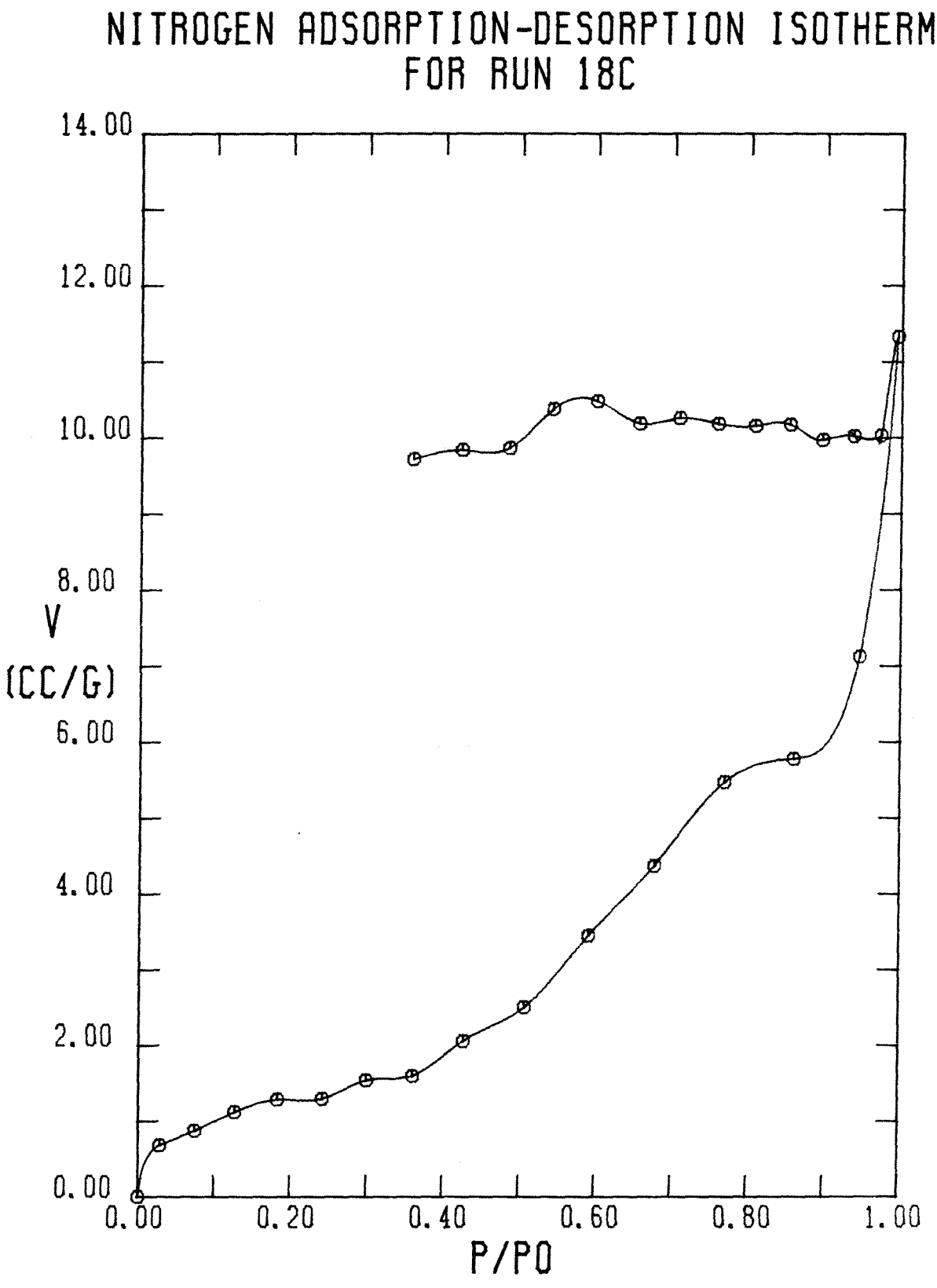
NITROGEN ADSORPTION-DESORPTION ISOTHERM
FOR RUN 18C
14.00
12.00
10.00
8.00
V
(CC/G)
6.00
4.00
2.00
0.00
0.00
0.20
0.40
0.60
0.80
1.00
P/PO

FIGURE A-80

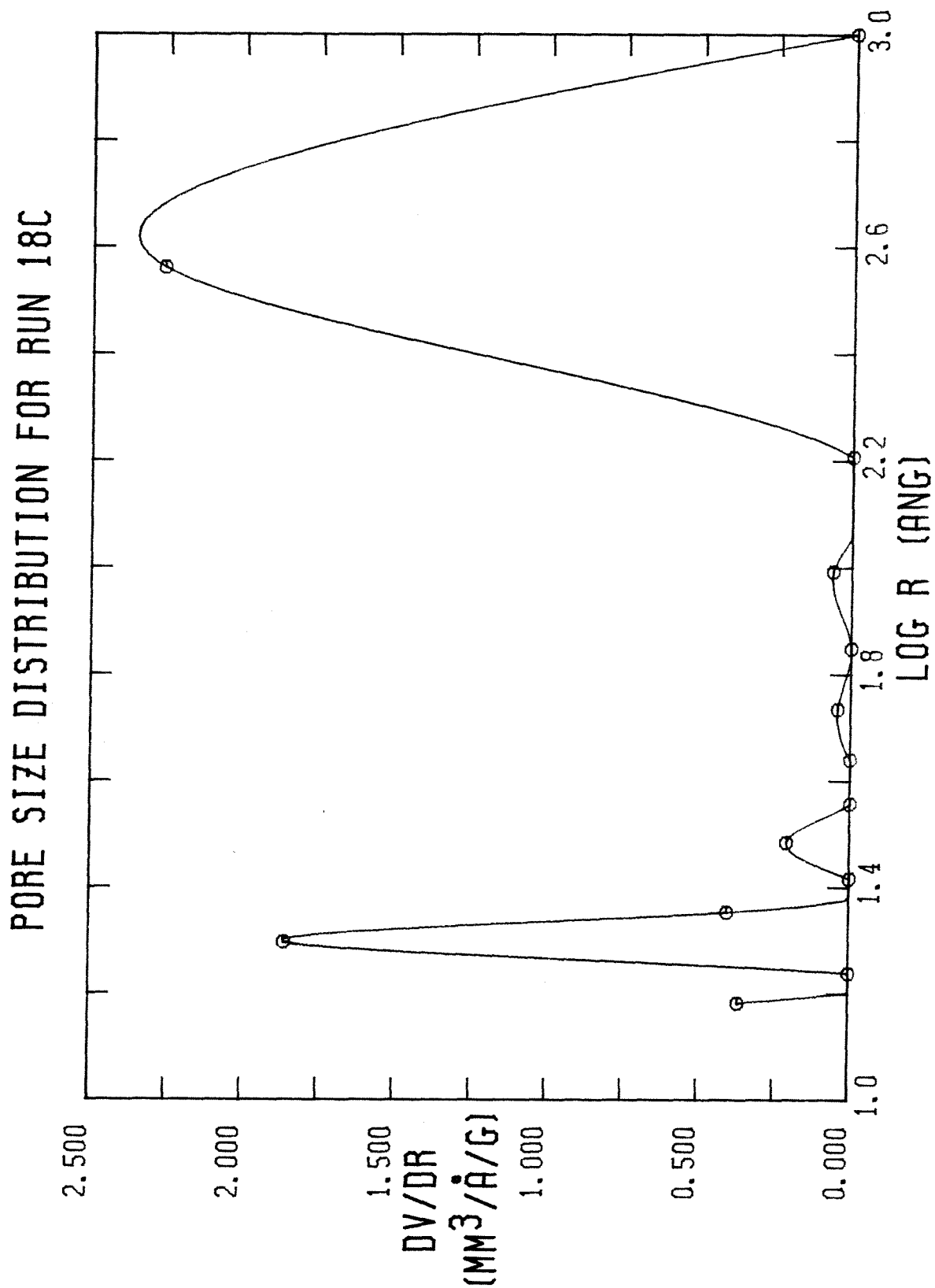
PORE SIZE DISTRIBUTION FOR RUN 18C
DV/DR
(MM3/Å/G)
2.500
2.000
1.500
1.000
0.500
0.000
1.0
1.4
1.8
2.2
2.6
3.0
LOG R (ANG)

FIGURE A-81

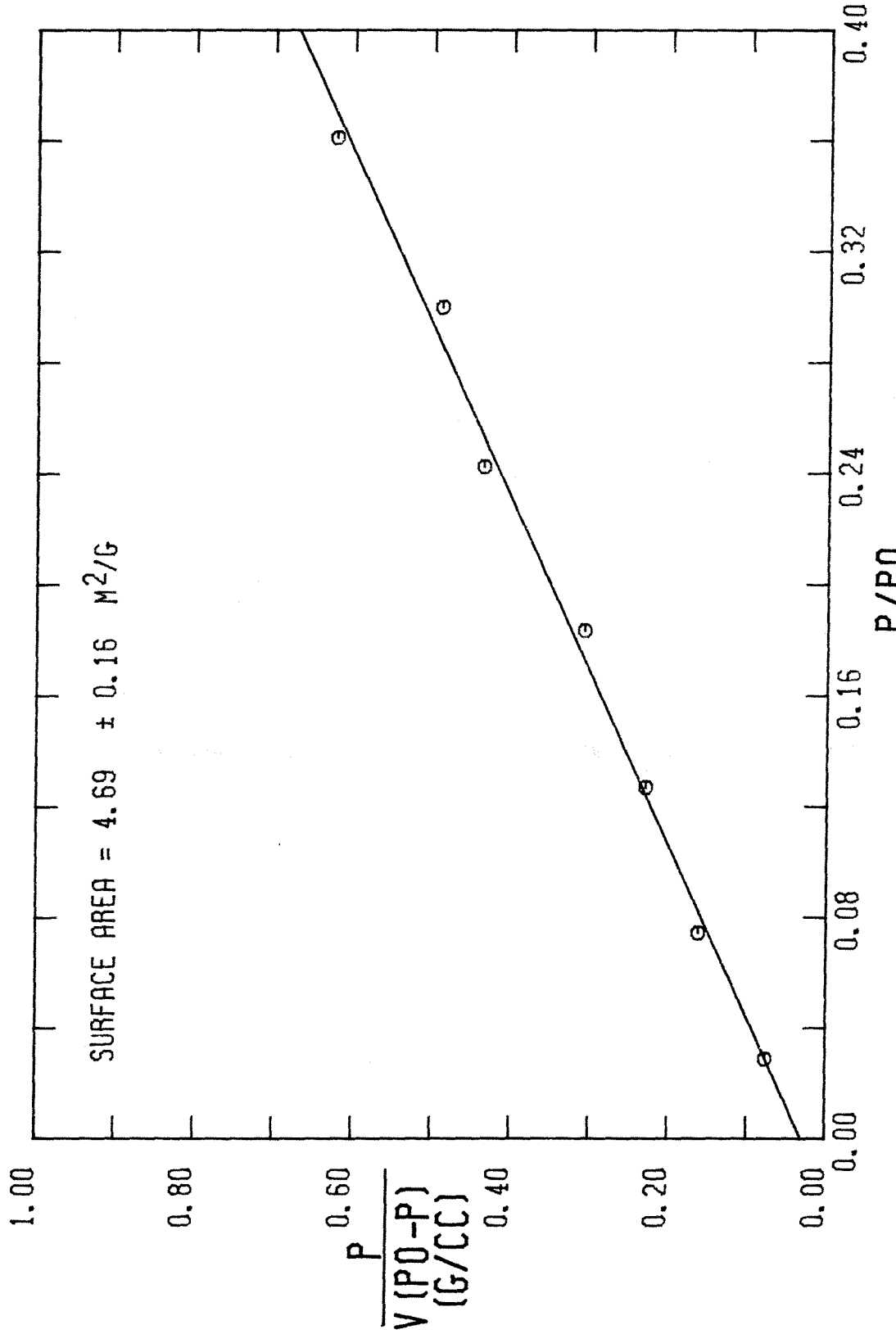
BET PLOT FOR RUN 18C
SURFACE AREA = 4.69 ± 0.16 M2/G
P / V (PO-P) (G/CC)
1.00
0.80
0.60
0.40
0.20
0.00
0.00
0.08
0.16
0.24
0.32
0.40
P/PO

FIGURE A-82

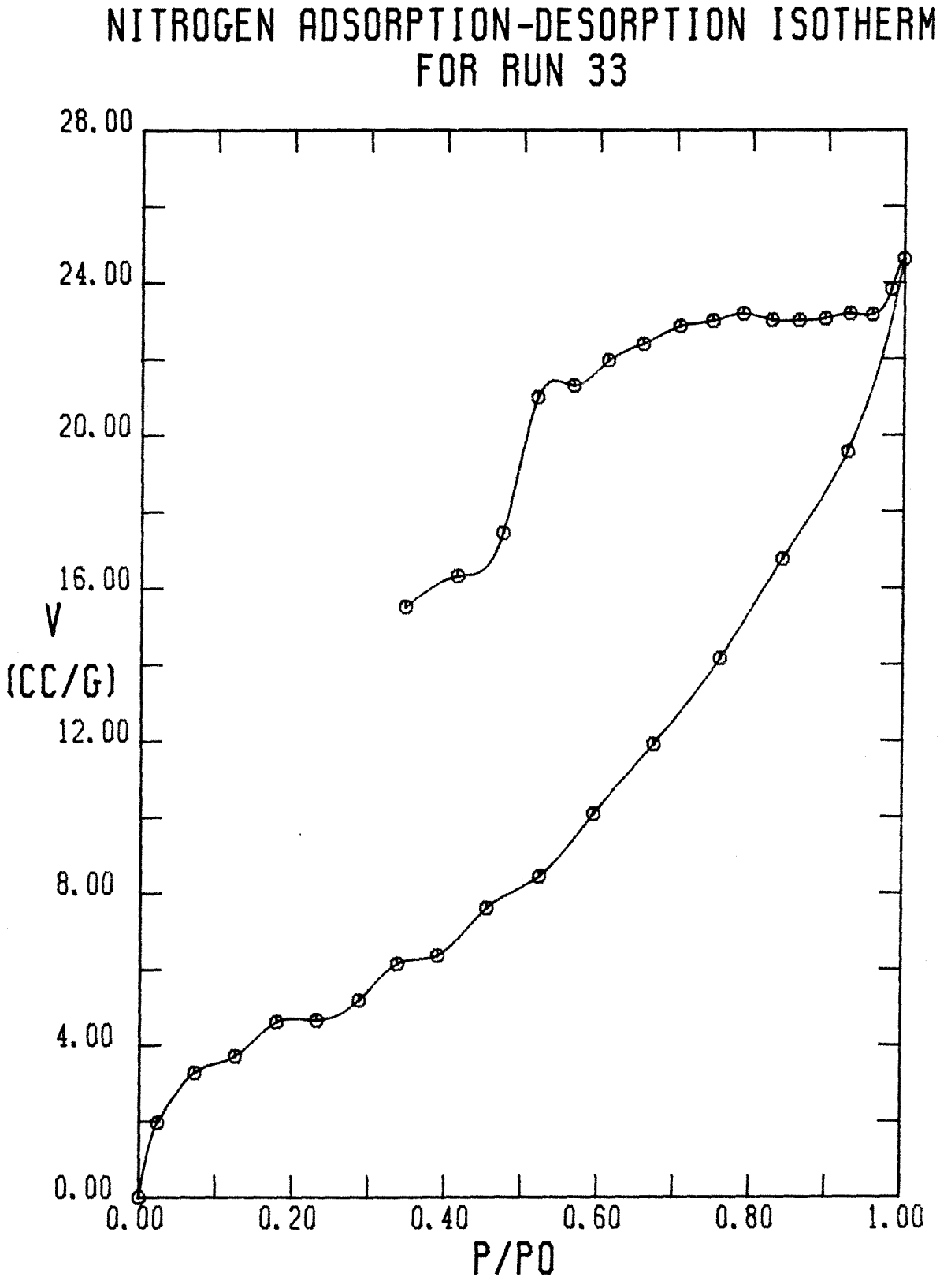
NITROGEN ADSORPTION-DESORPTION ISOTHERM
FOR RUN 33
28.00
24.00
20.00
16.00
12.00
8.00
4.00
0.00
V
(CC/G)
0.00
0.20
0.40
0.60
0.80
1.00
P/PO

FIGURE A-83

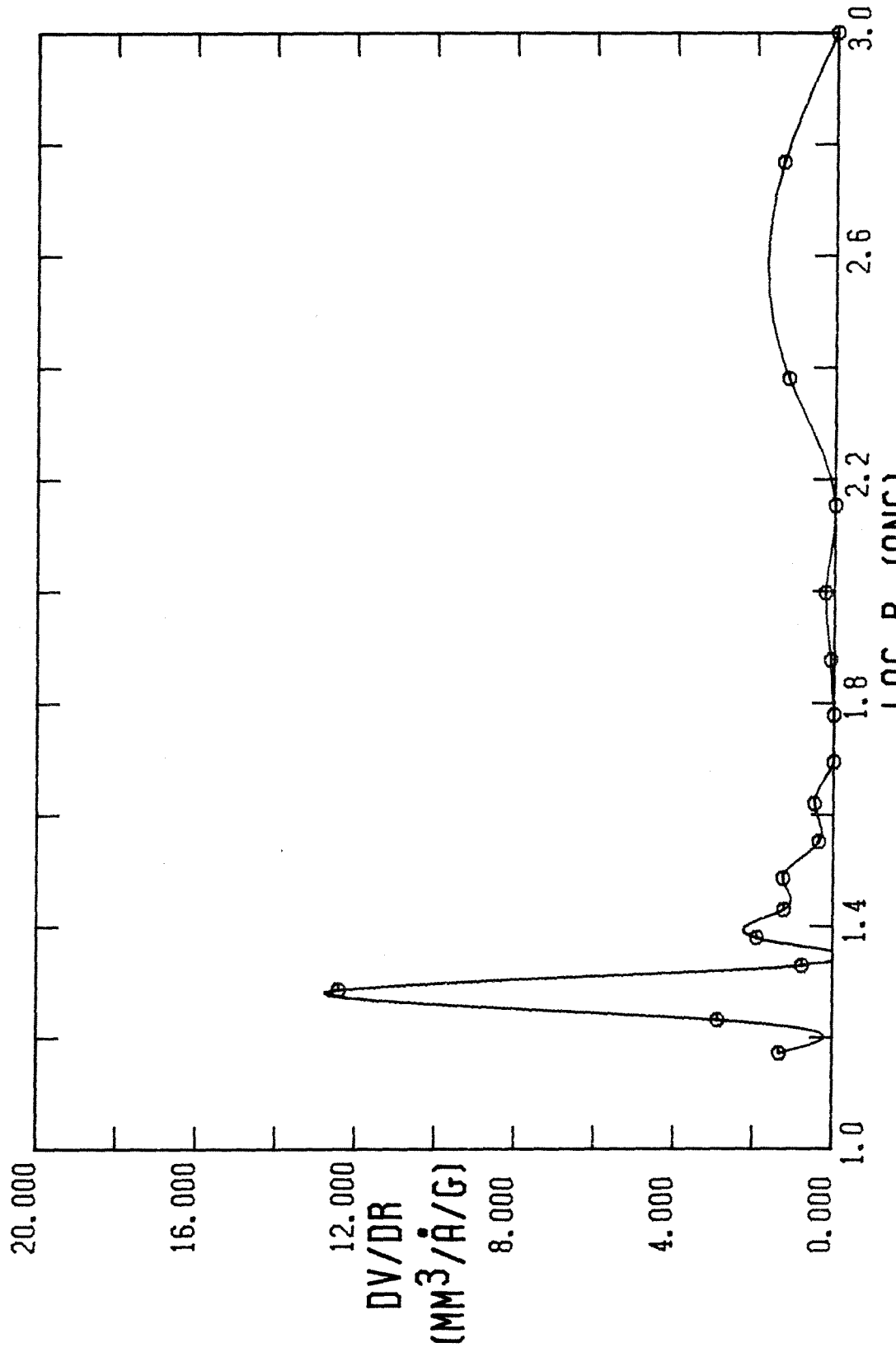
PORE SIZE DISTRIBUTION FOR RUN 33
DV/DR
(MM3/Å/G)
20.000
16.000
12.000
8.000
4.000
0.000
1.0
1.4
1.8
2.2
2.6
3.0
LOG R (ANG)

FIGURE A-84

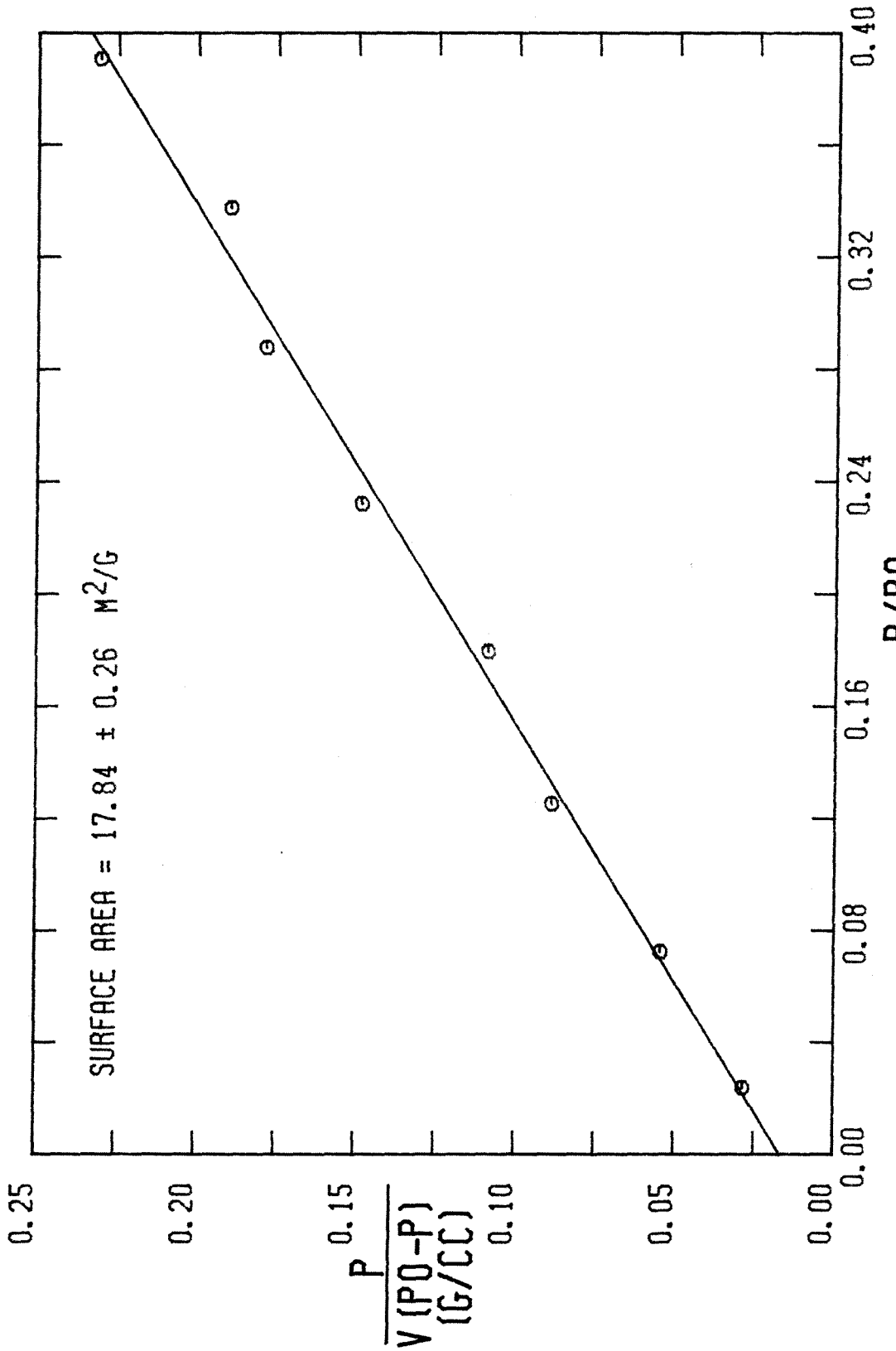
BET PLOT FOR RUN 33
SURFACE AREA = 17.84 ± 0.26 M2/G
P / V (PO-P) (G/CC)
P/PO
0.25
0.20
0.15
0.10
0.05
0.00
0.00
0.08
0.16
0.24
0.32
0.40

FIGURE A-85

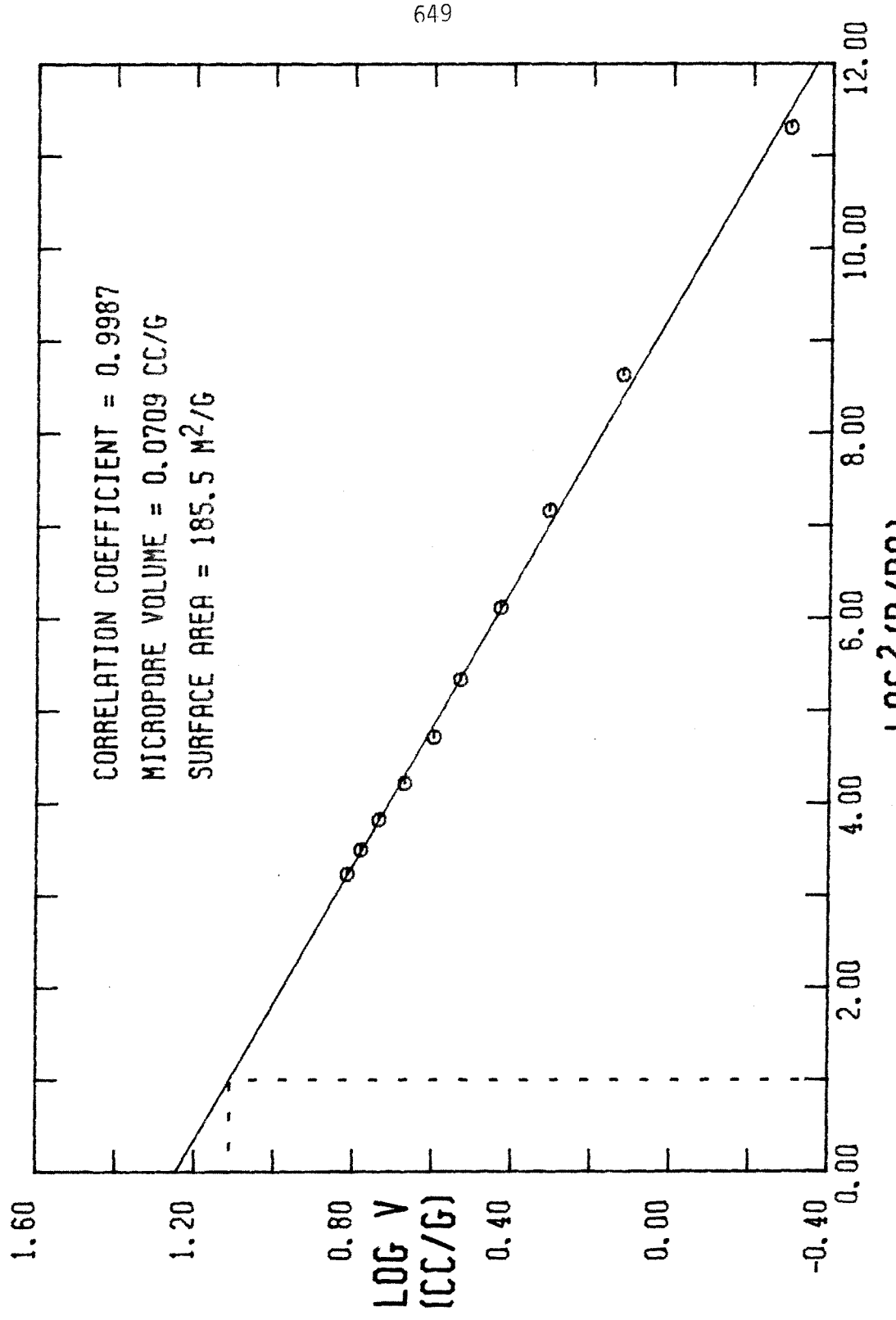
DPR PLOT FOR RUN 33
CORRELATION COEFFICIENT = 0.9987
MICROPORE VOLUME = 0.0709 CC/G
SURFACE AREA = 185.5 M2/G
LOG V (CC/G)
LOG2 (P/P0)
1.60
1.20
0.80
0.40
0.00
-0.40
0.00
2.00
4.00
6.00
8.00
10.00
12.00

FIGURE A-86

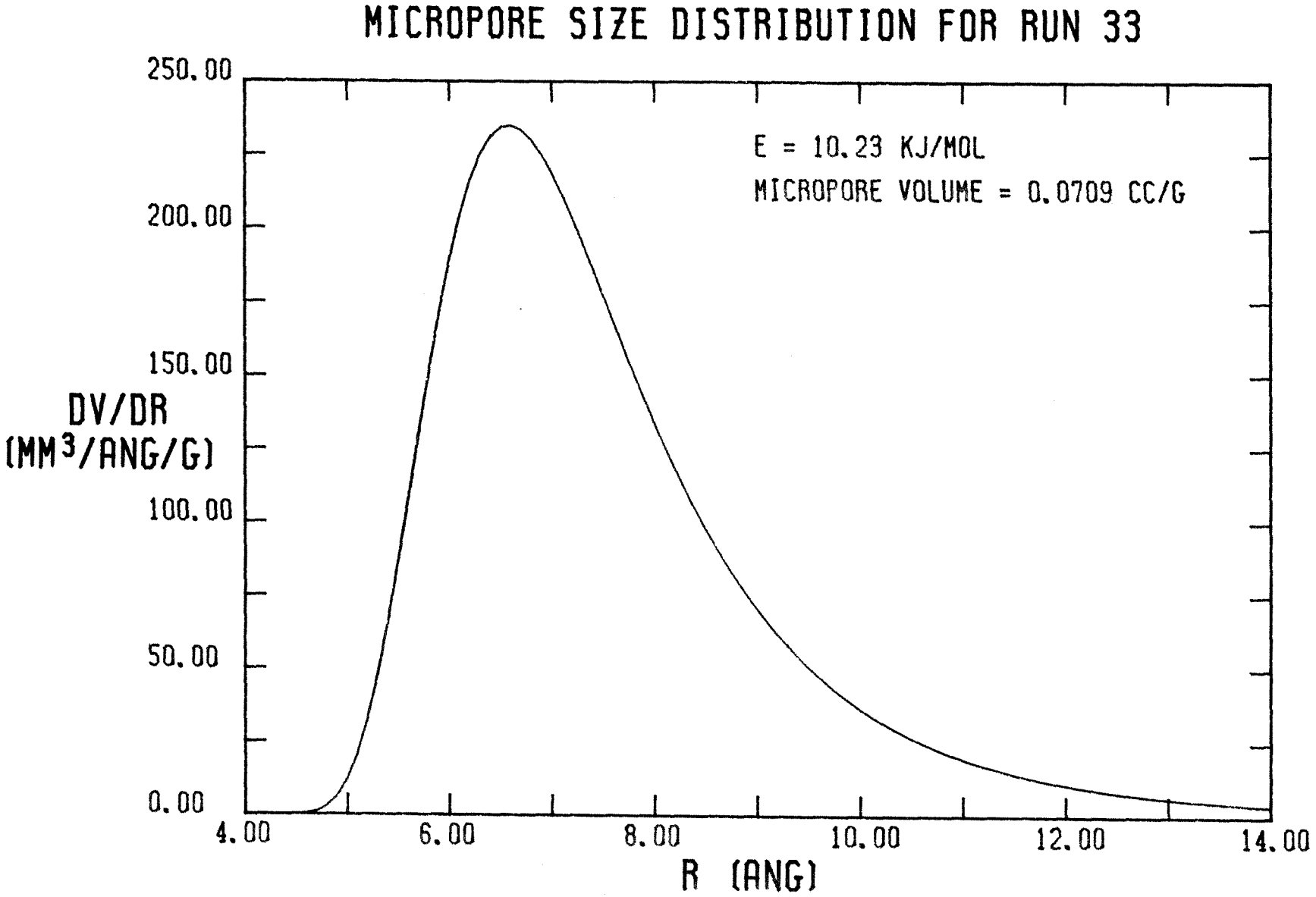
MICROPORE SIZE DISTRIBUTION FOR RUN 33
E = 10.23 KJ/MOL
MICROPORE VOLUME = 0.0709 CC/G
DV/DR
(MM3/ANG/G)
250.00
200.00
150.00
100.00
50.00
0.00
4.00
6.00
8.00
10.00
12.00
14.00
R (ANG)

FIGURE A-87

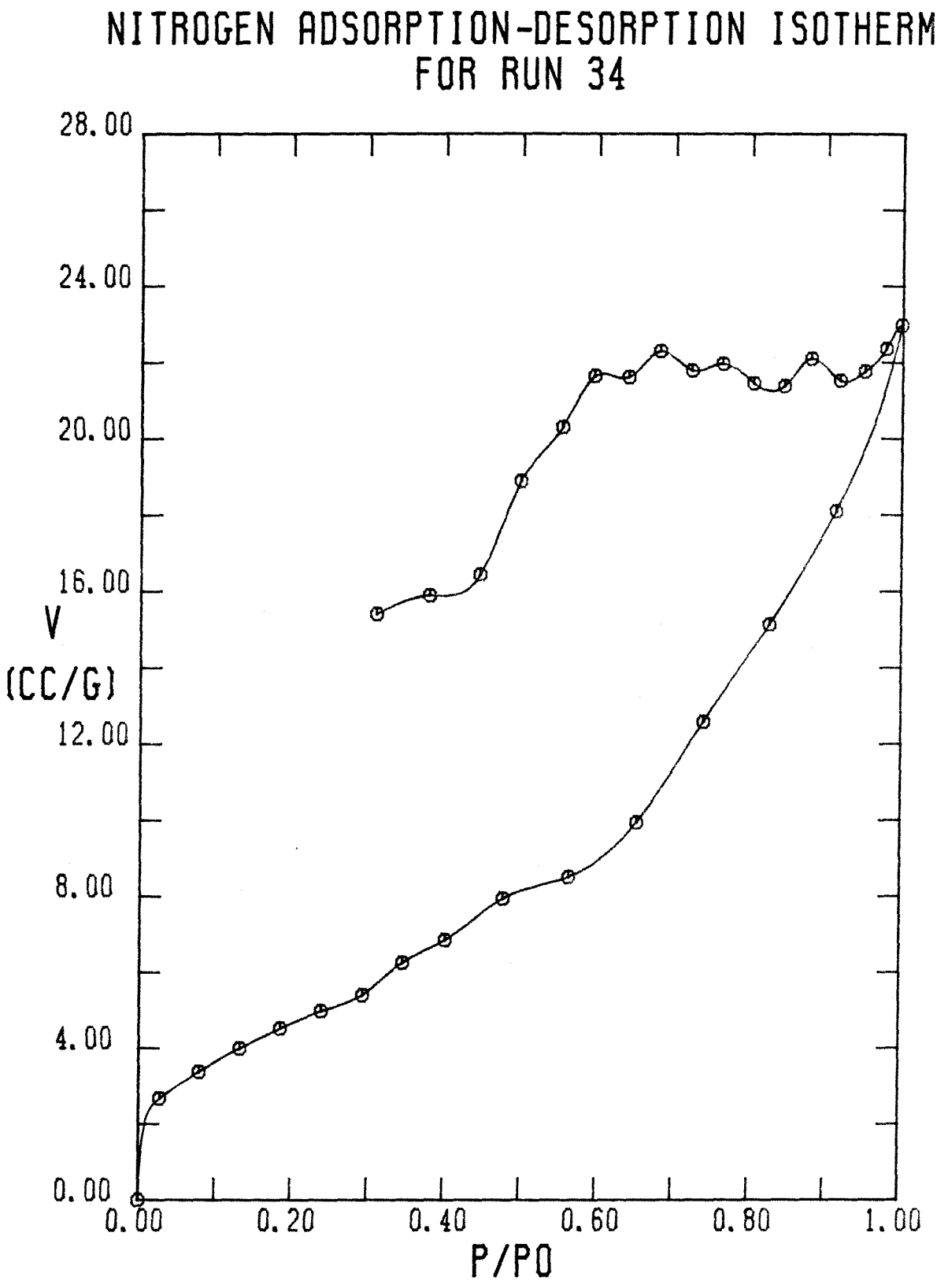
NITROGEN ADSORPTION-DESORPTION ISOTHERM
FOR RUN 34
28.00
24.00
20.00
16.00
12.00
8.00
4.00
0.00
V
(CC/G)
0.00
0.20
0.40
0.60
0.80
1.00
P/P0

FIGURE A-88

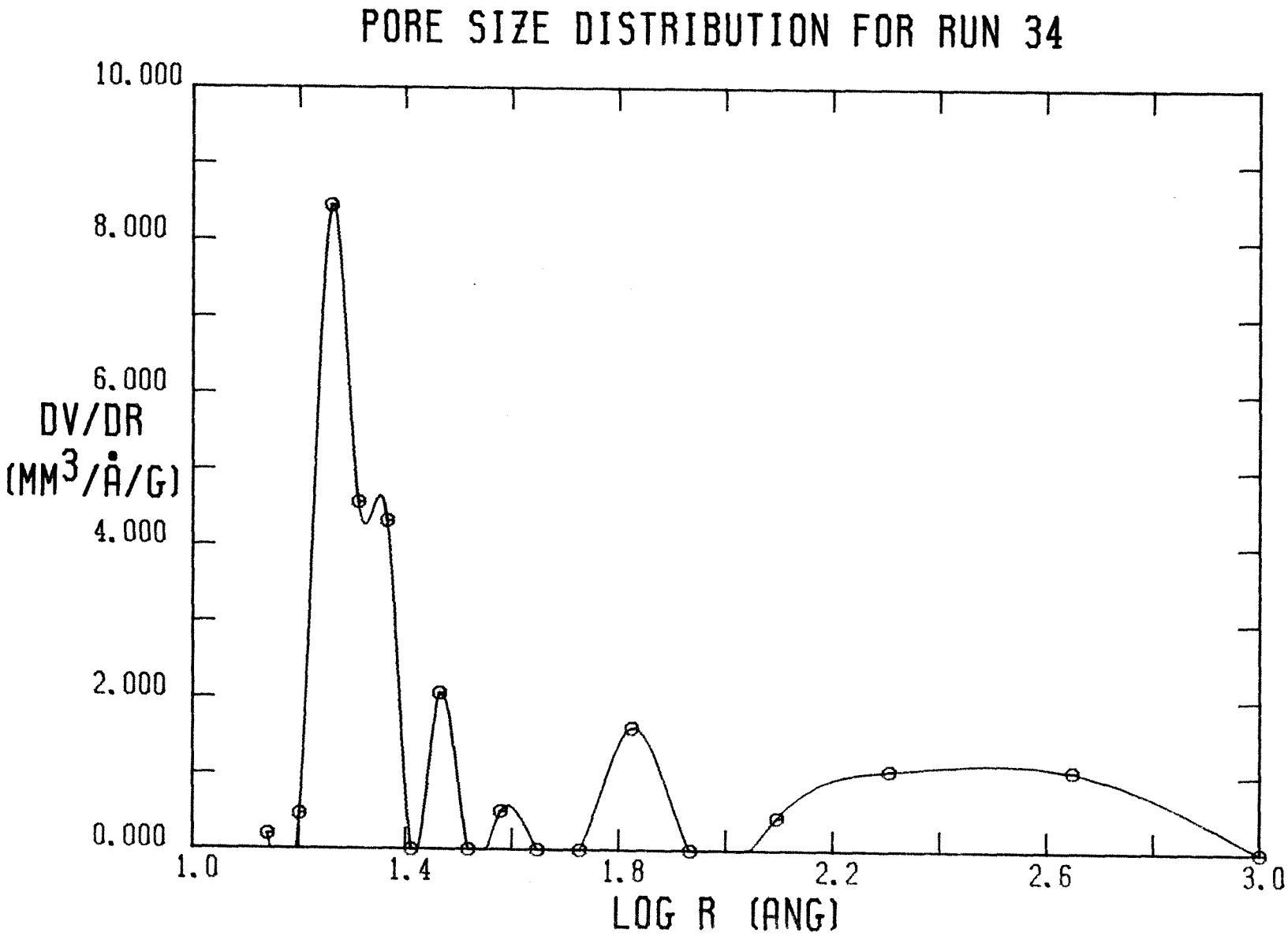
PORE SIZE DISTRIBUTION FOR RUN 34
10.000
8.000
6.000
4.000
2.000
0.000
DV/DR
(MM3/Å/G)
1.0
1.4
1.8
2.2
2.6
3.0
LOG R (ANG)

FIGURE A-89

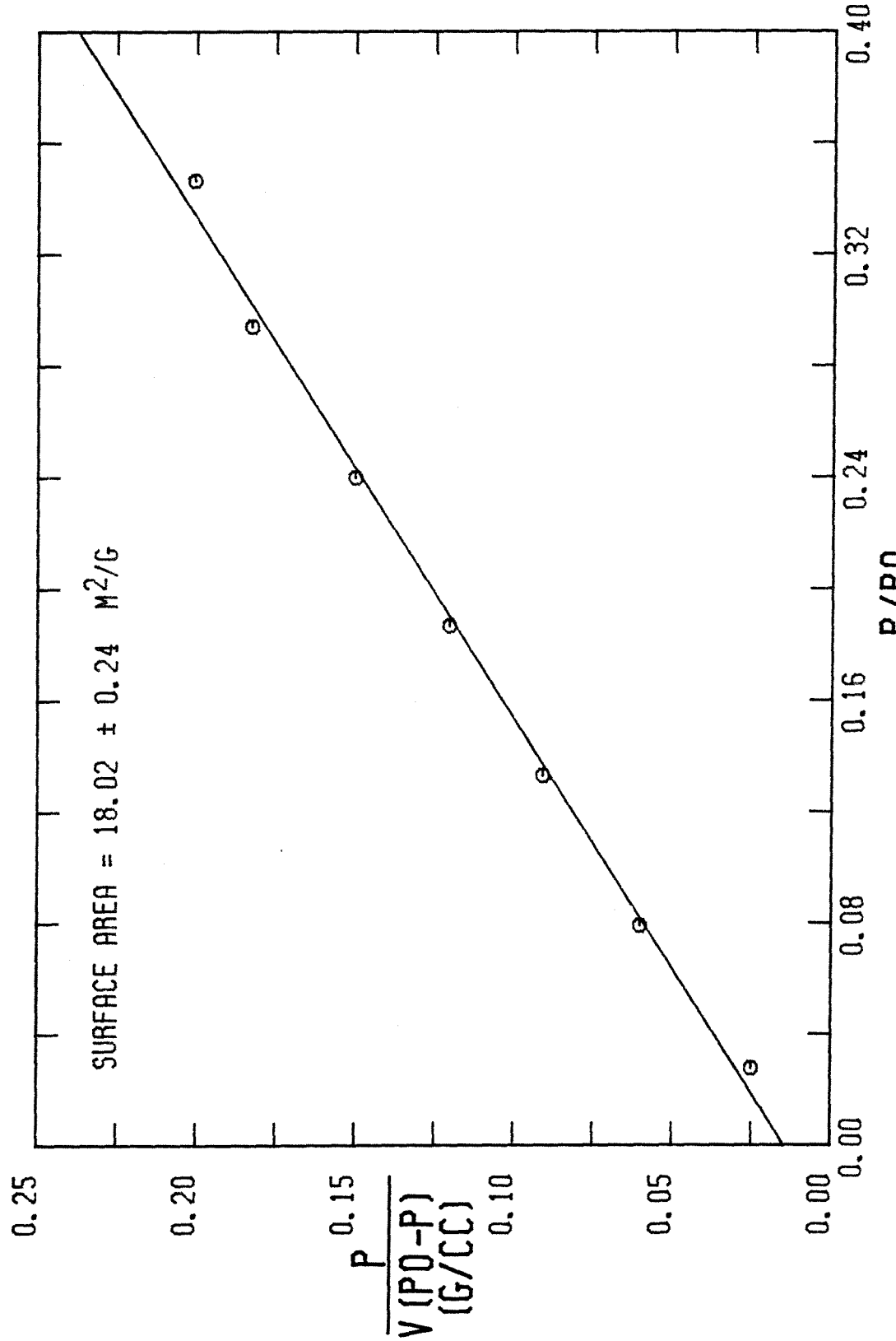
BET PLOT FOR RUN 34
SURFACE AREA = 18.02 ± 0.24 M2/G
P / V (PO-P) (G/CC)
P/PO
0.25
0.20
0.15
0.10
0.05
0.00
0.00
0.08
0.16
0.24
0.32
0.40

FIGURE A-90

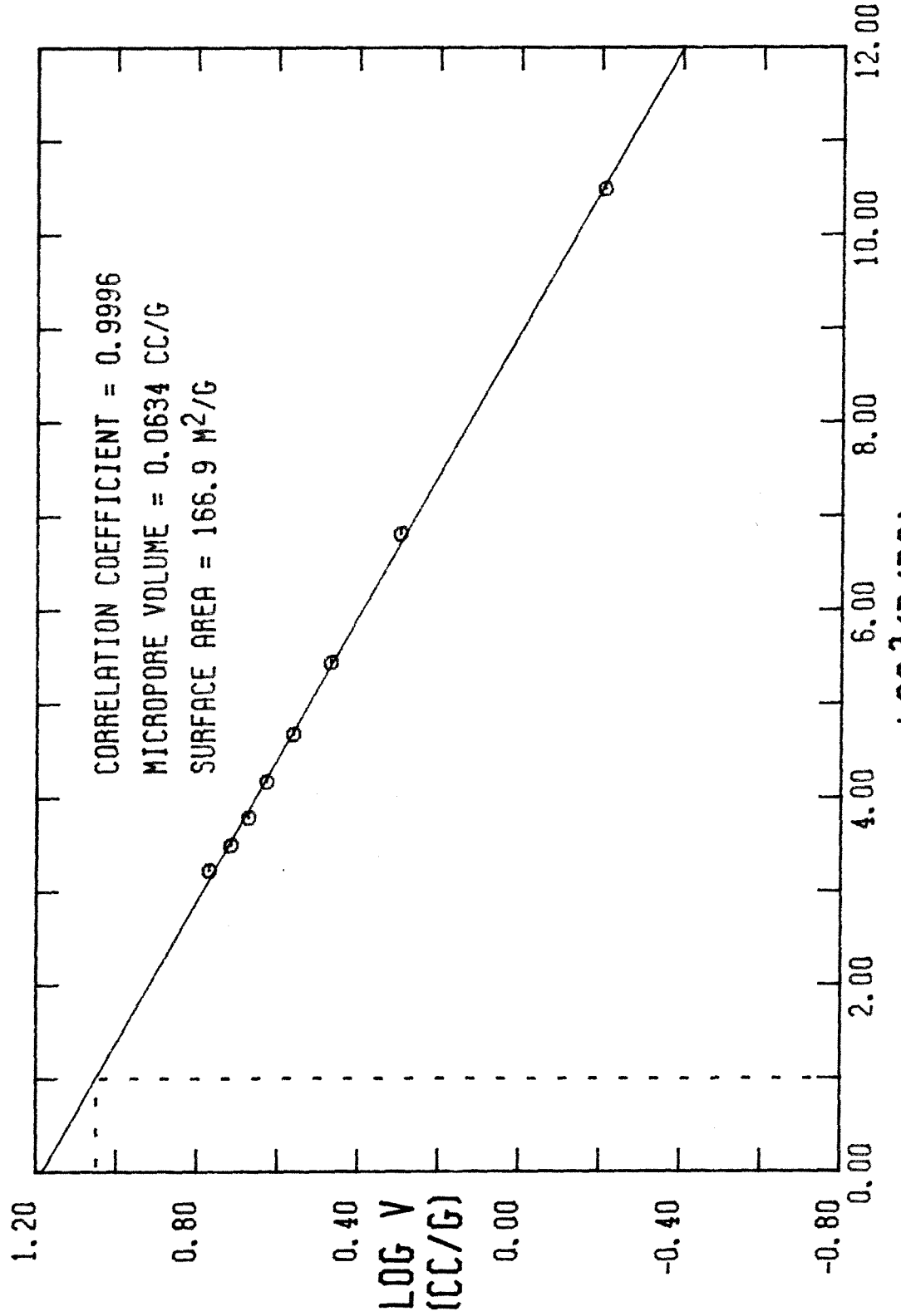
DPR PLOT FOR RUN 34
CORRELATION COEFFICIENT = 0.9996
MICROPORE VOLUME = 0.0634 CC/G
SURFACE AREA = 166.9 M2/G
LOG V (CC/G)
LOG2 (P/P0)
1.20
0.80
0.40
0.00
-0.40
-0.80
0.00
2.00
4.00
6.00
8.00
10.00
12.00

FIGURE A-91

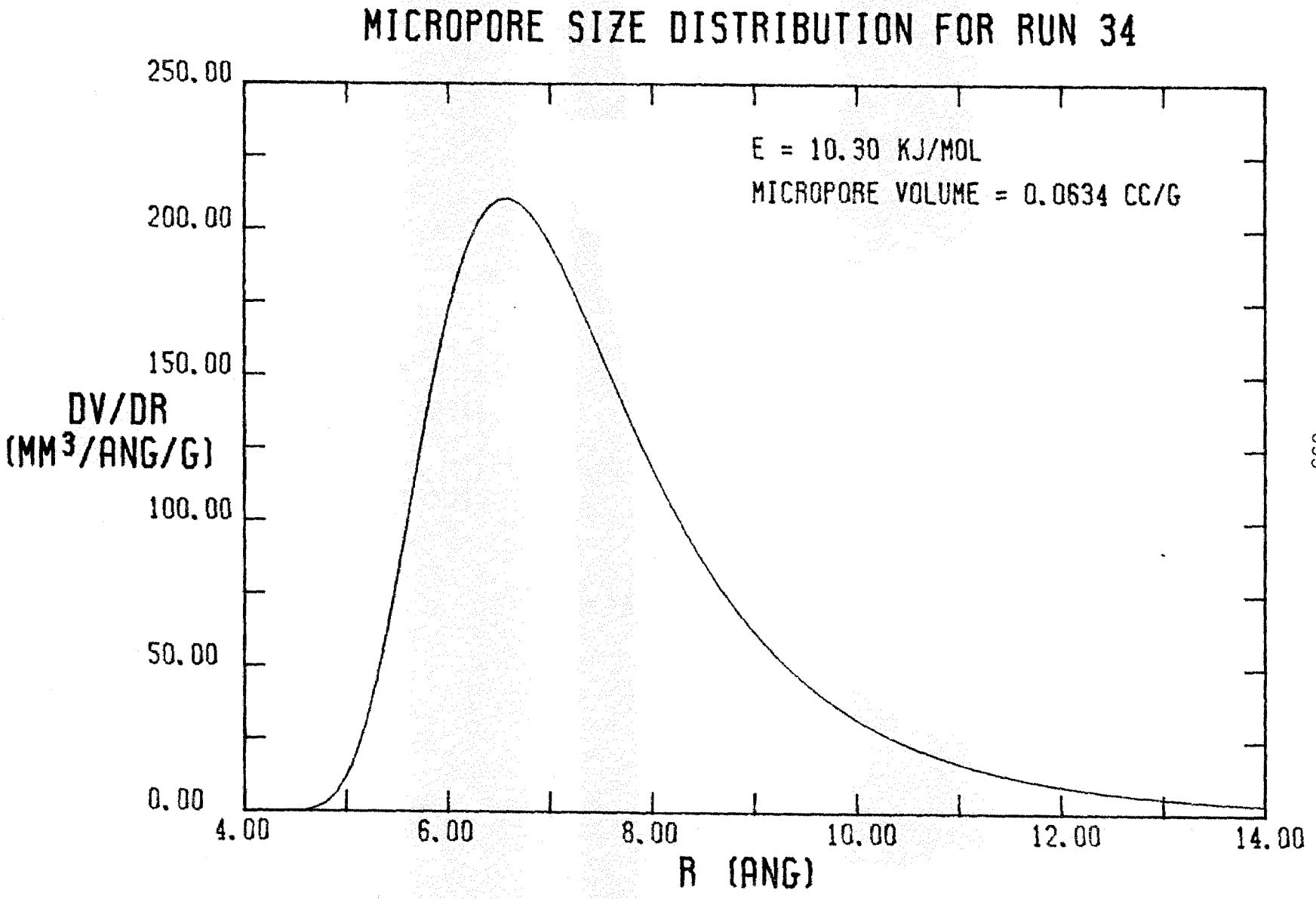
MICROPORE SIZE DISTRIBUTION FOR RUN 34
E = 10.30 KJ/MOL
MICROPORE VOLUME = 0.0634 CC/G
DV/DR
(MM3/ANG/G)
250.00
200.00
150.00
100.00
50.00
0.00
4.00
6.00
8.00
10.00
12.00
14.00
R (ANG)

FIGURE A-92

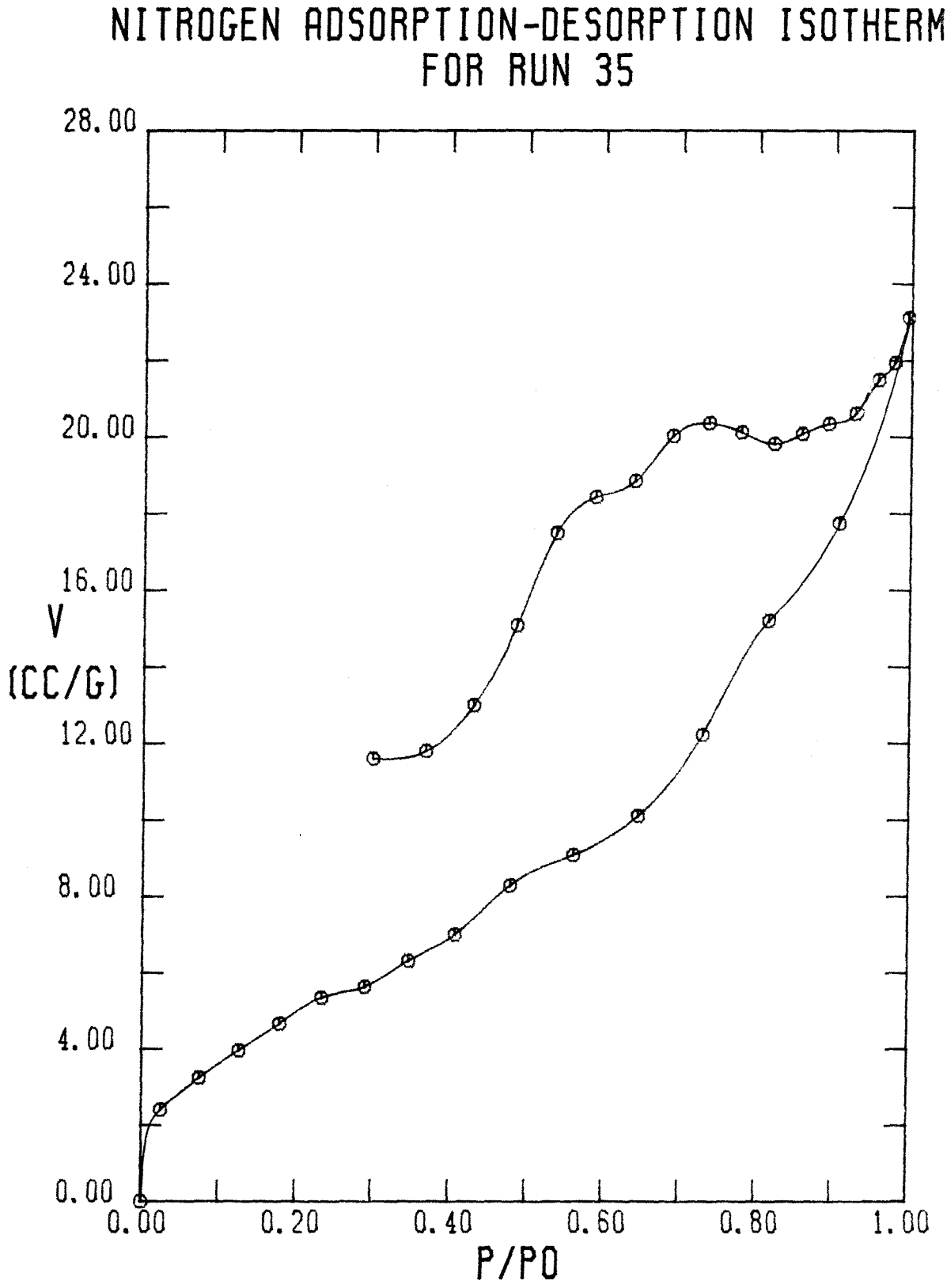
NITROGEN ADSORPTION-DESORPTION ISOTHERM
FOR RUN 35
28.00
24.00
20.00
16.00
12.00
8.00
4.00
0.00
V
(CC/G)
0.00
0.20
0.40
0.60
0.80
1.00
P/PO

FIGURE A-93

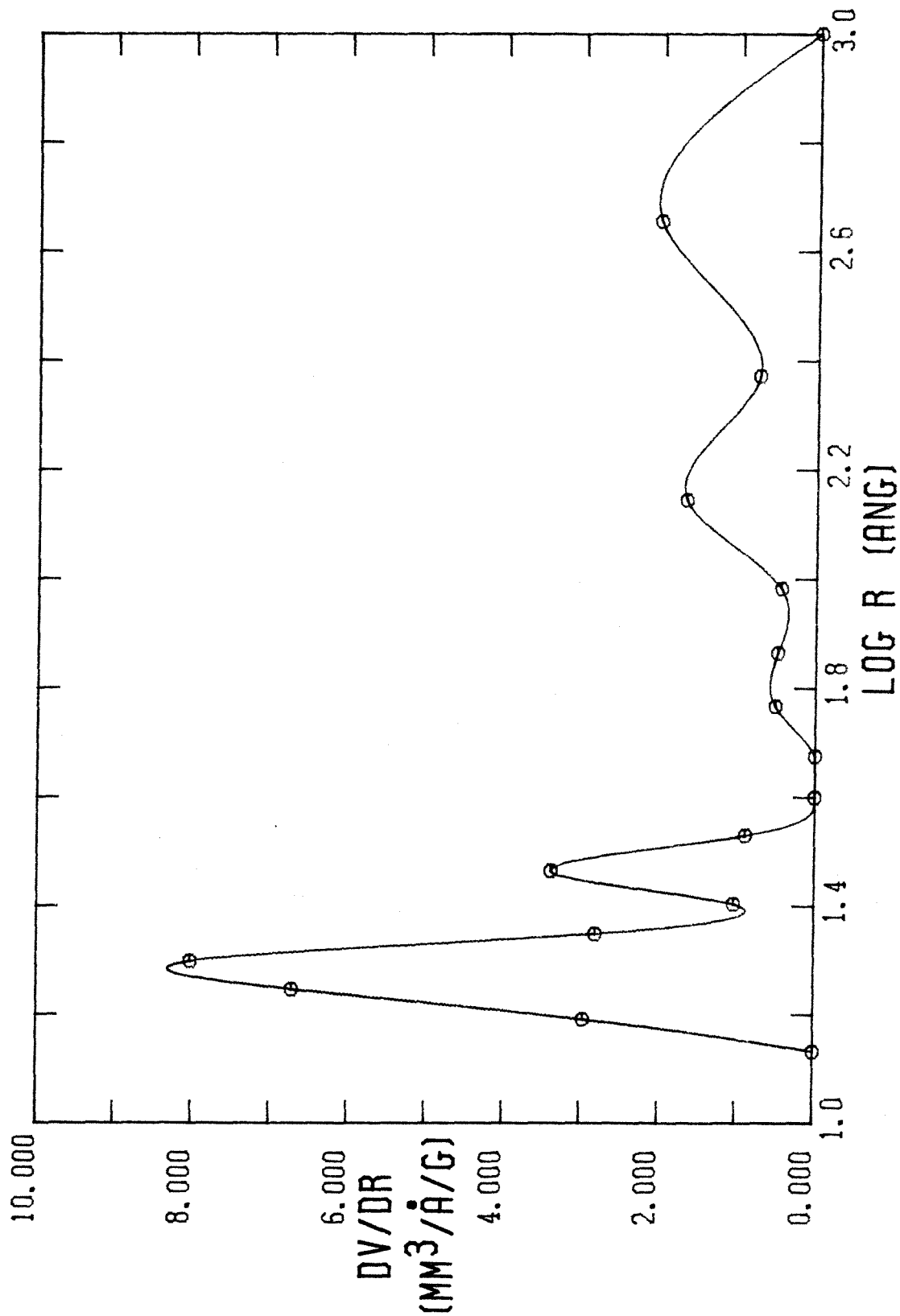
PORE SIZE DISTRIBUTION FOR RUN 35
10.000
8.000
6.000
4.000
2.000
0.000
DV/DR
(MM3/Å/G)
1.0
1.4
1.8
2.2
2.6
3.0
LOG R (ANG)

FIGURE A-94

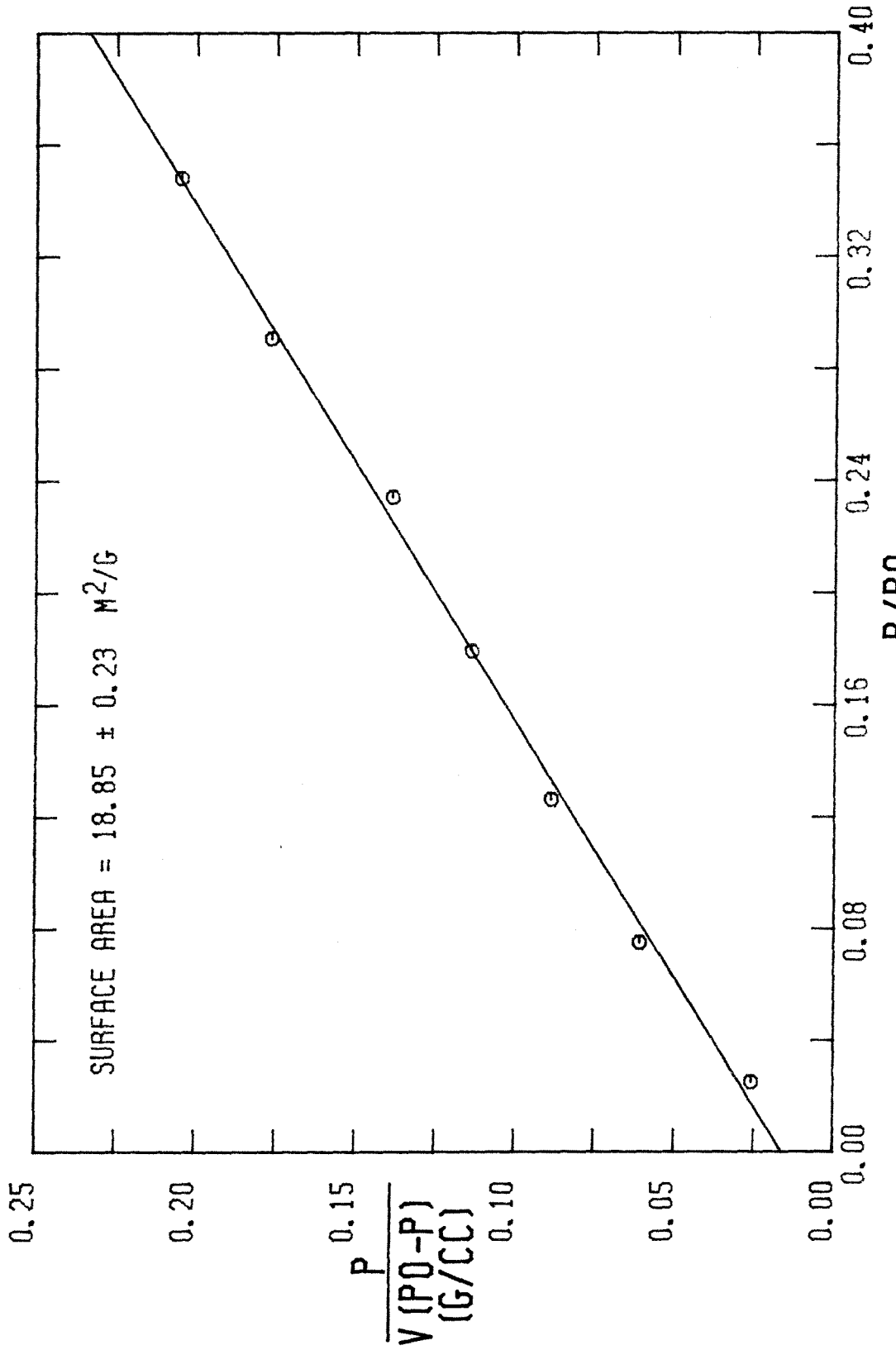
BET PLOT FOR RUN 35
SURFACE AREA = 18.85 ± 0.23 M2/G
P/PO
P / V(PO-P) (G/CC)
0.00
0.05
0.10
0.15
0.20
0.25
0.00
0.08
0.16
0.24
0.32
0.40

FIGURE A-95

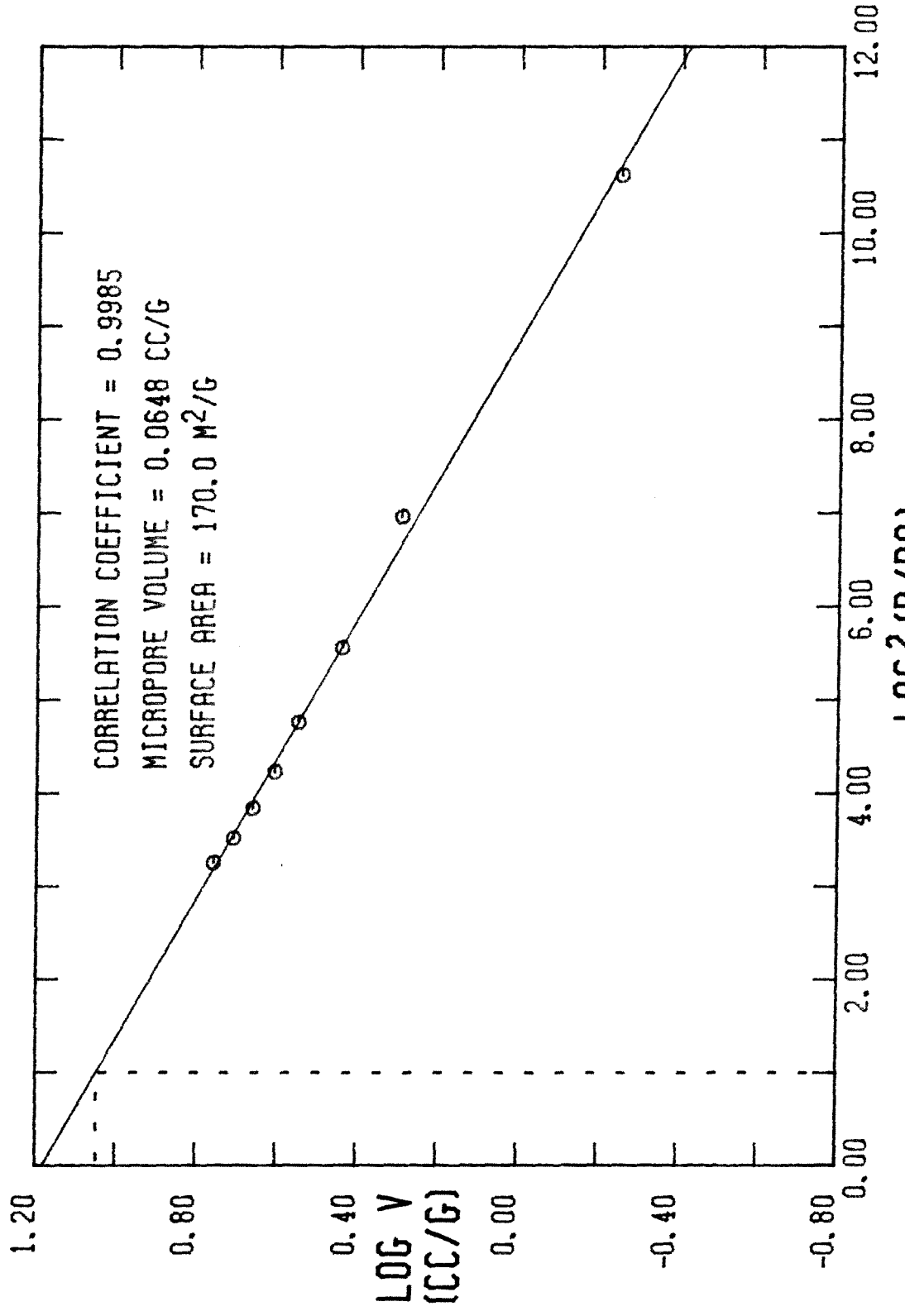
DPR PLOT FOR RUN 35
CORRELATION COEFFICIENT = 0.9985
MICROPORE VOLUME = 0.0648 CC/G
SURFACE AREA = 170.0 M2/G
LOG V (CC/G)
LOG2 (P/P0)
1.20
0.80
0.40
0.00
-0.40
-0.80
0.00
2.00
4.00
6.00
8.00
10.00
12.00

FIGURE A-96

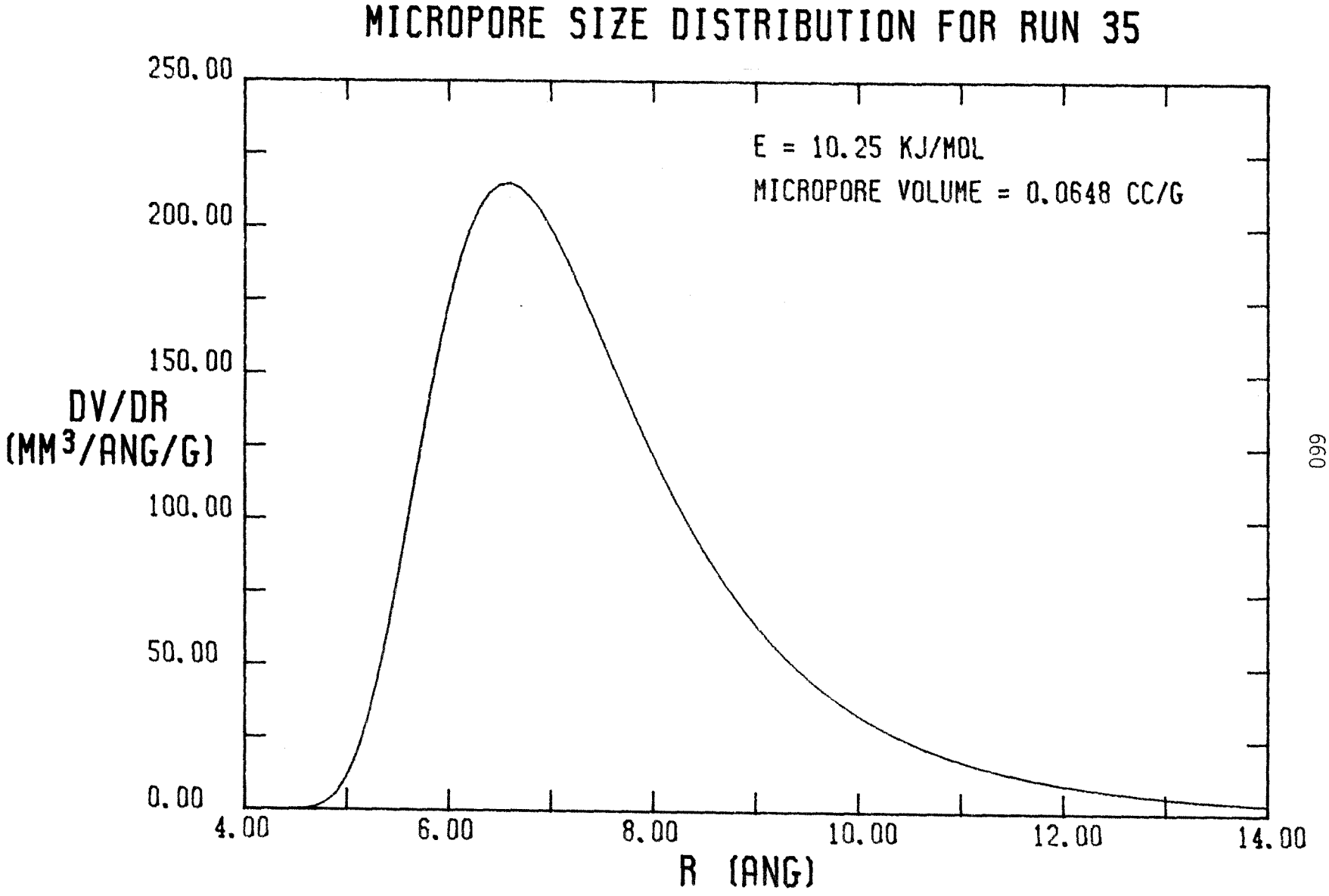
MICROPORE SIZE DISTRIBUTION FOR RUN 35
E = 10.25 KJ/MOL
MICROPORE VOLUME = 0.0648 CC/G
DV/DR
(MM3/ANG/G)
250.00
200.00
150.00
100.00
50.00
0.00
4.00
6.00
8.00
10.00
12.00
14.00
R (ANG)

FIGURE A-97

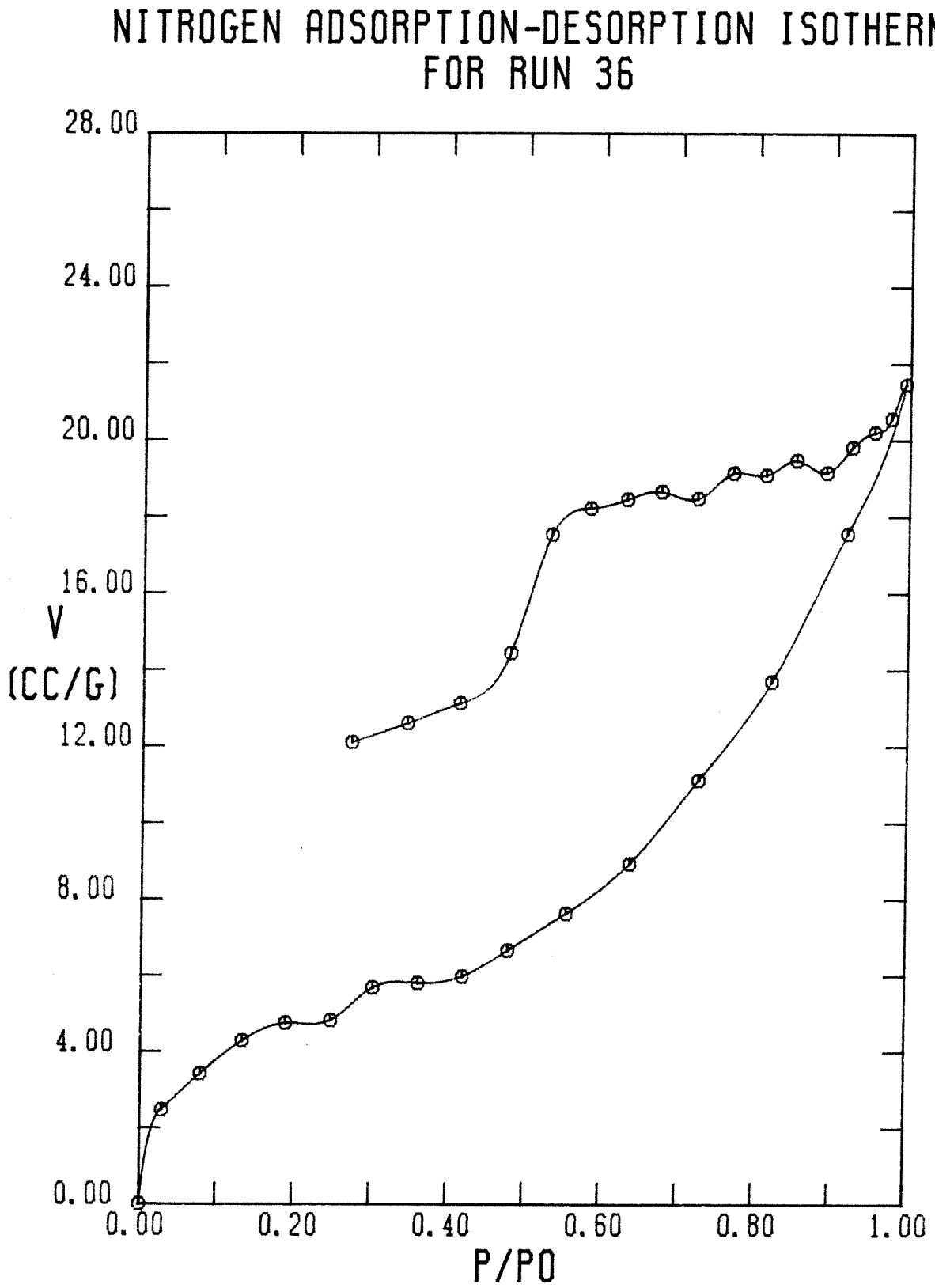
NITROGEN ADSORPTION-DESORPTION ISOTHERM
FOR RUN 36
28.00
24.00
20.00
16.00
12.00
8.00
4.00
0.00
V
(CC/G)
0.00
0.20
0.40
0.60
0.80
1.00
P/PO

FIGURE A-98

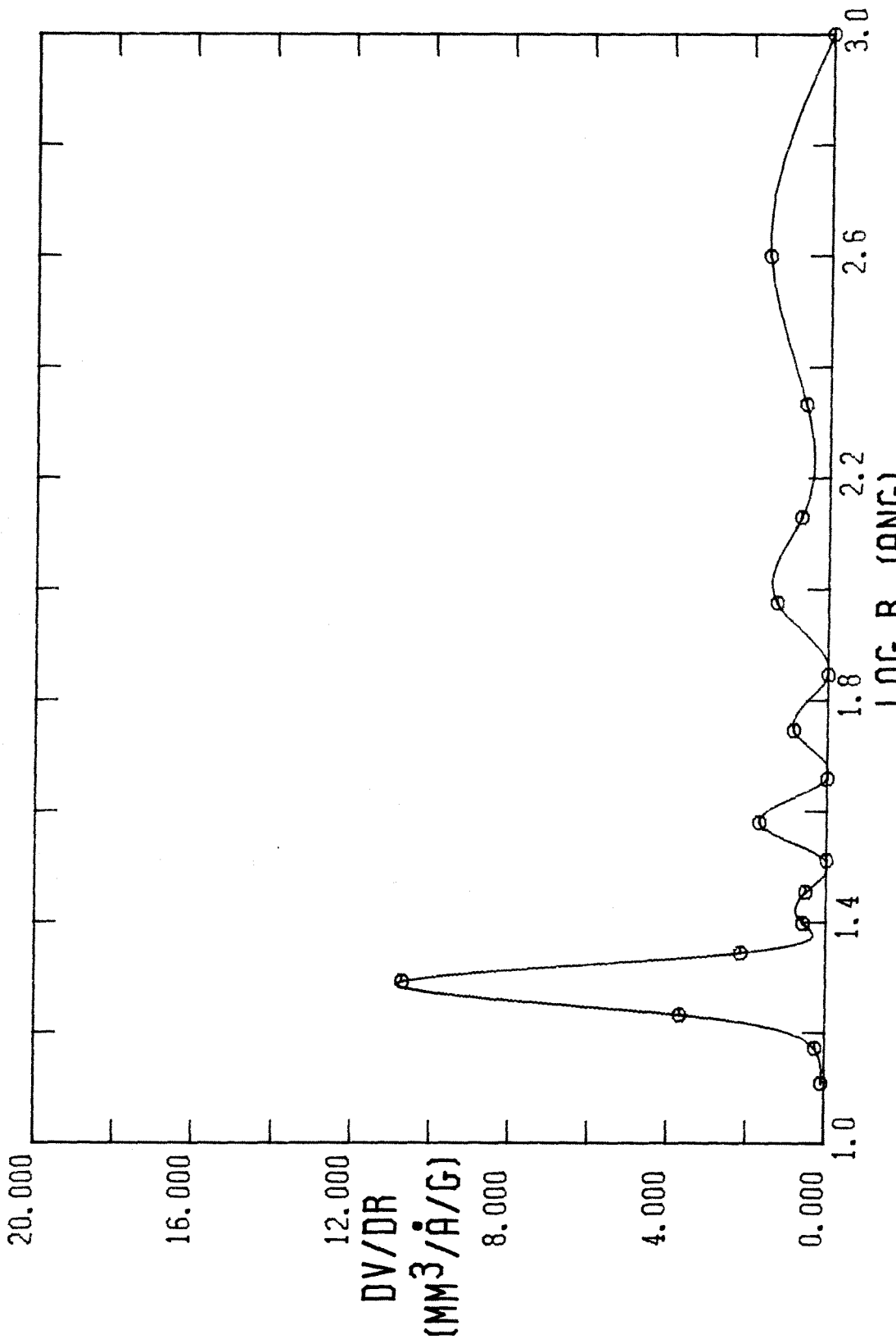
PORE SIZE DISTRIBUTION FOR RUN 36
DV/DR
(MM3/Å/G)
20.000
16.000
12.000
8.000
4.000
0.000
1.0
1.4
1.8
2.2
2.6
3.0
LOG R (ANG)

FIGURE A-99

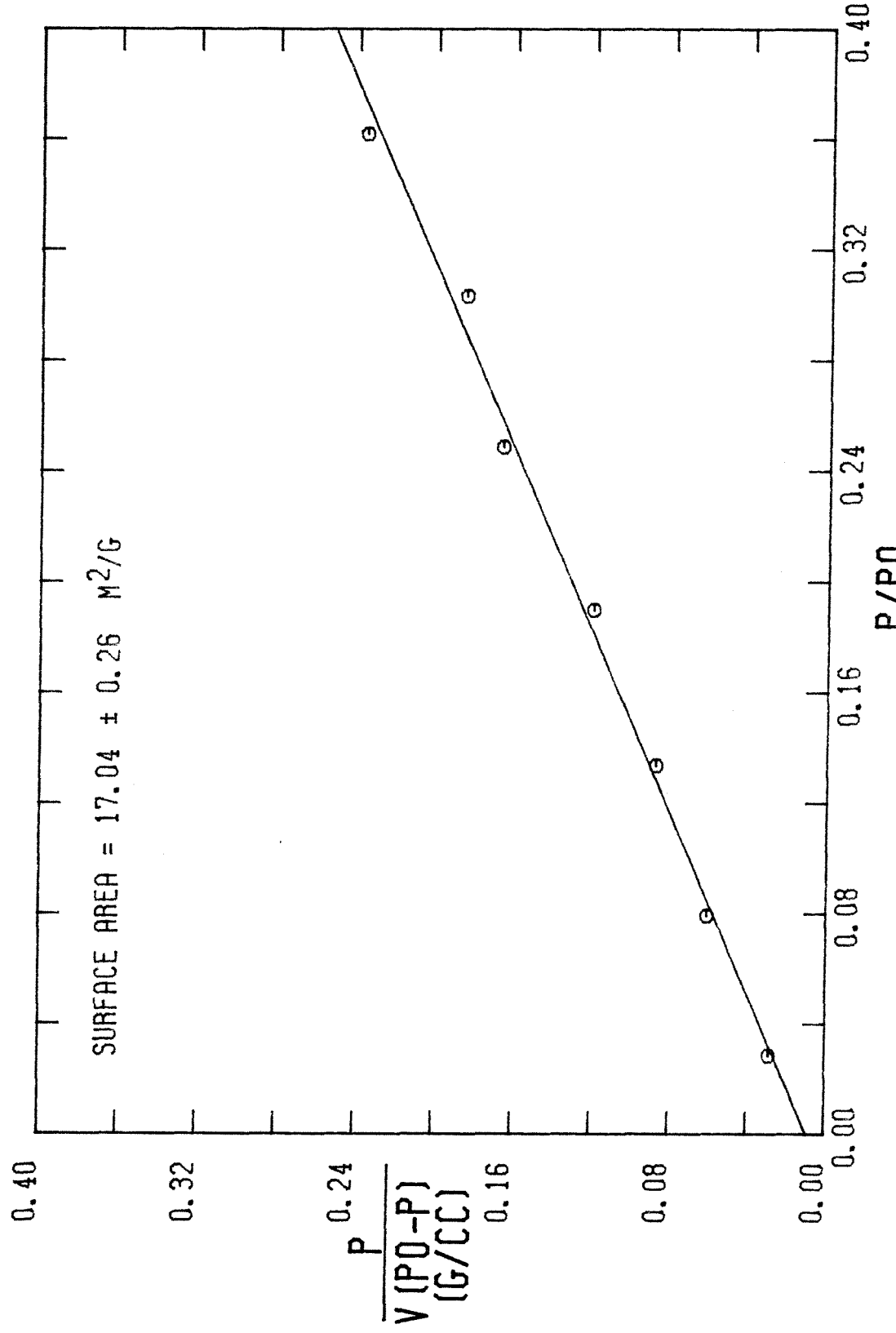
BET PLOT FOR RUN 36
SURFACE AREA = 17.04 ± 0.26 M2/G
P / V(PO-P) (G/CC)
P/PO
0.00
0.08
0.16
0.24
0.32
0.40

FIGURE A-100

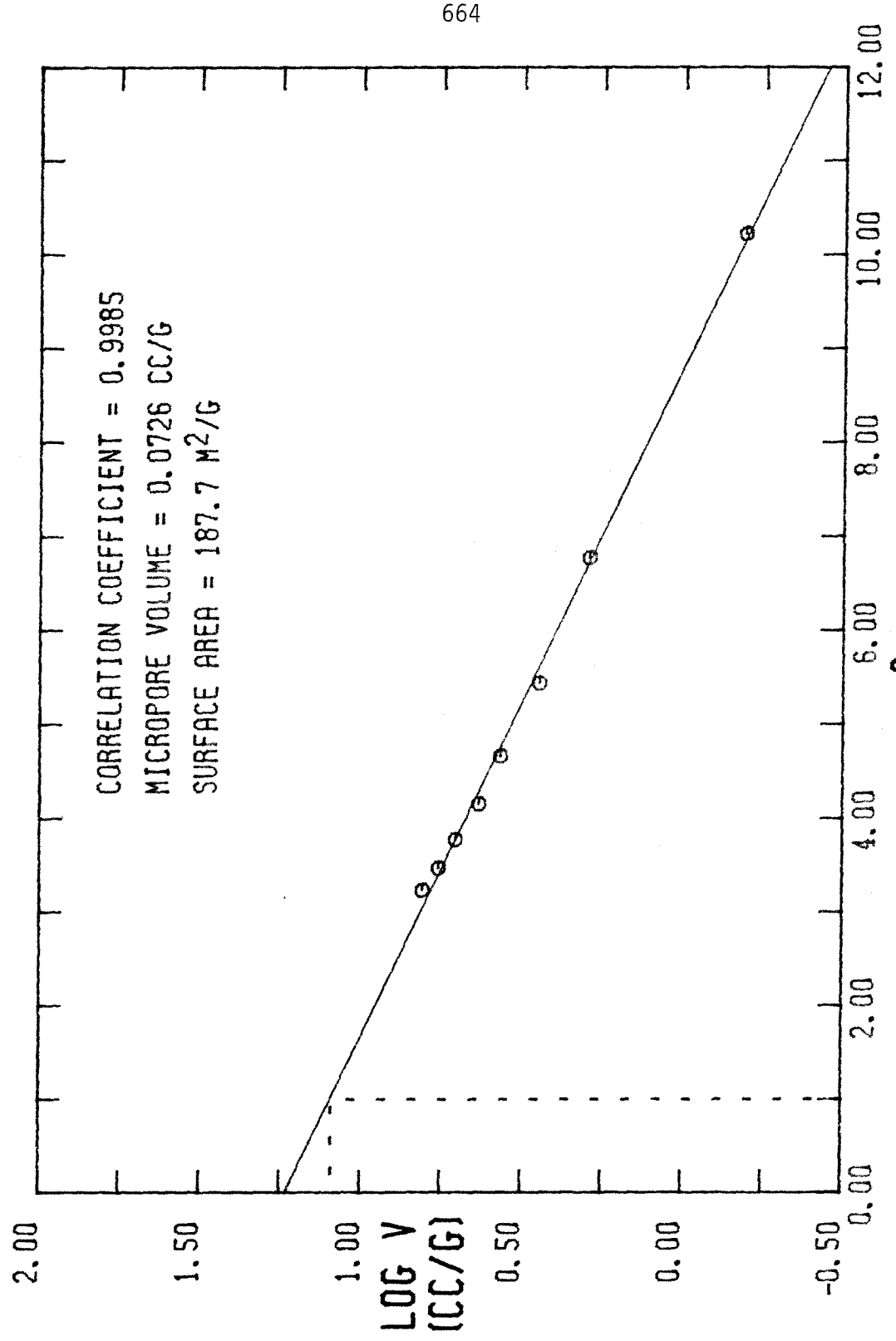
DPR PLOT FOR RUN 36
CORRELATION COEFFICIENT = 0.9985
MICROPORE VOLUME = 0.0726 CC/G
SURFACE AREA = 187.7 M2/G
LOG V (CC/G)
LOG2 (P/PO)
2.00
1.50
1.00
0.50
0.00
-0.50
0.00
2.00
4.00
6.00
8.00
10.00
12.00

FIGURE A-101

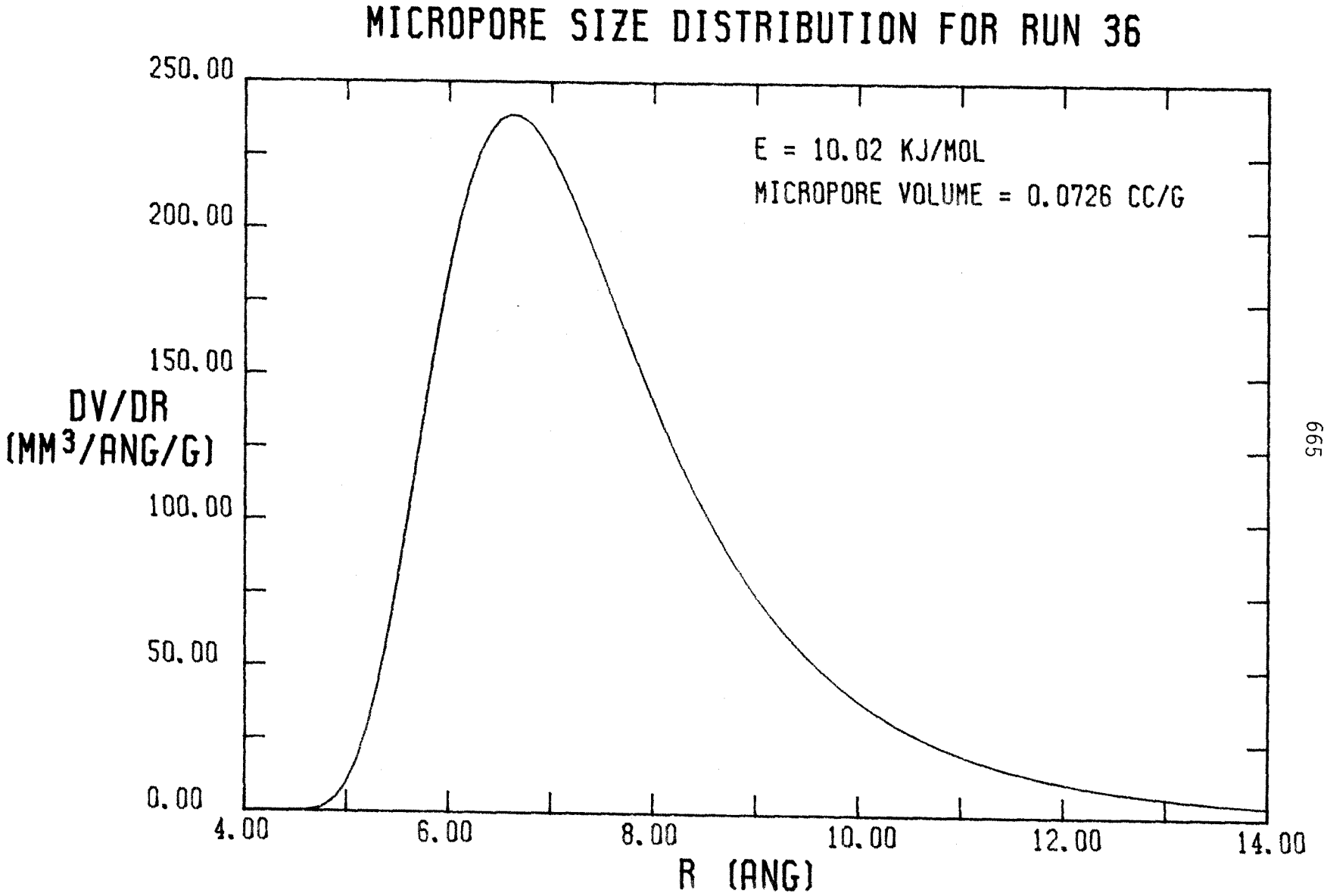
MICROPORE SIZE DISTRIBUTION FOR RUN 36
E = 10.02 KJ/MOL
MICROPORE VOLUME = 0.0726 CC/G
DV/DR
(MM3/ANG/G)
250.00
200.00
150.00
100.00
50.00
0.00
4.00
6.00
8.00
10.00
12.00
14.00
R (ANG)

FIGURE A-102

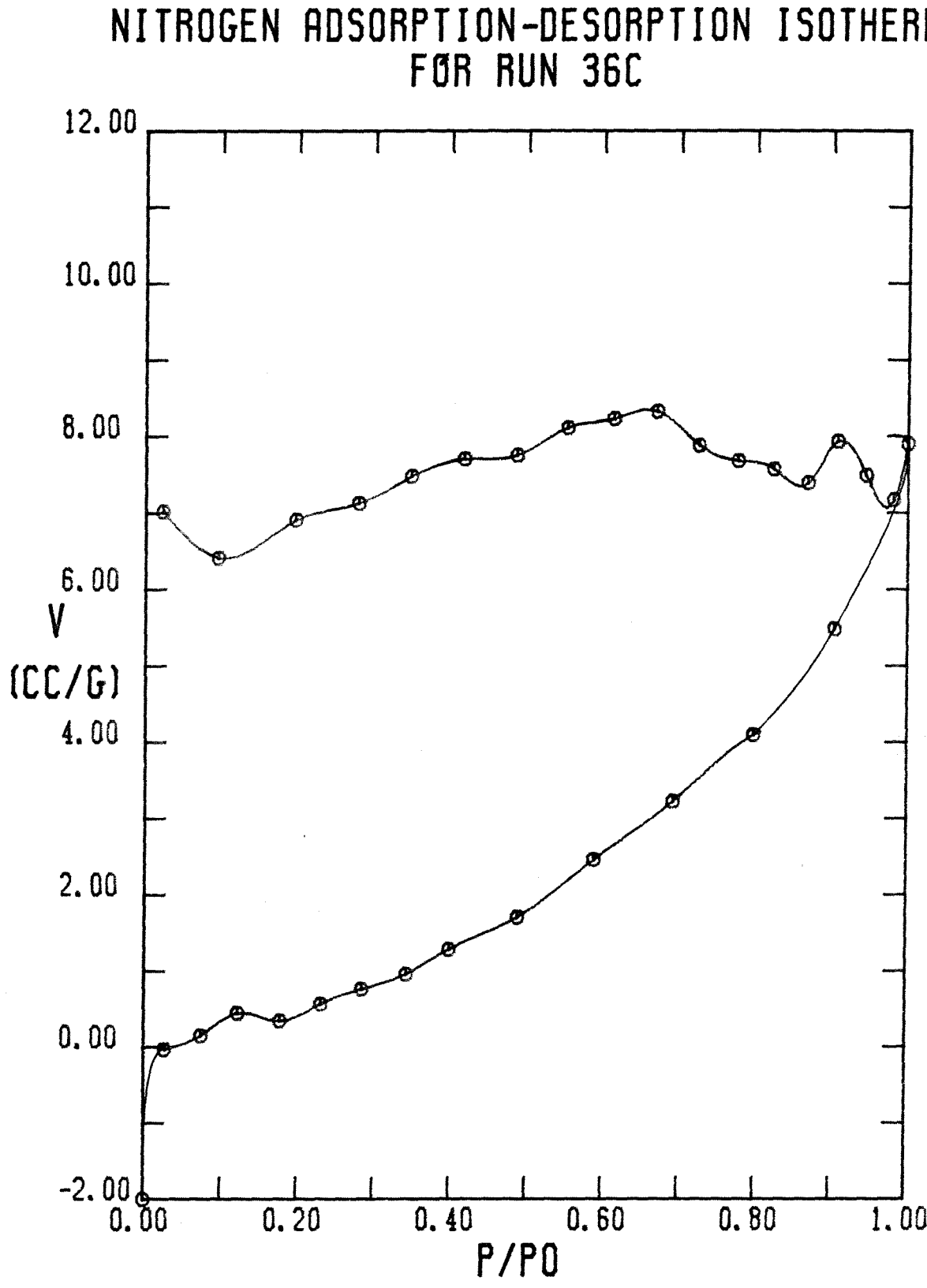
NITROGEN ADSORPTION-DESORPTION ISOTHERM
FOR RUN 36C
12.00
10.00
8.00
6.00
V
(CC/G)
4.00
2.00
0.00
-2.00
0.00
0.20
0.40
0.60
0.80
1.00
P/PO

FIGURE A-103

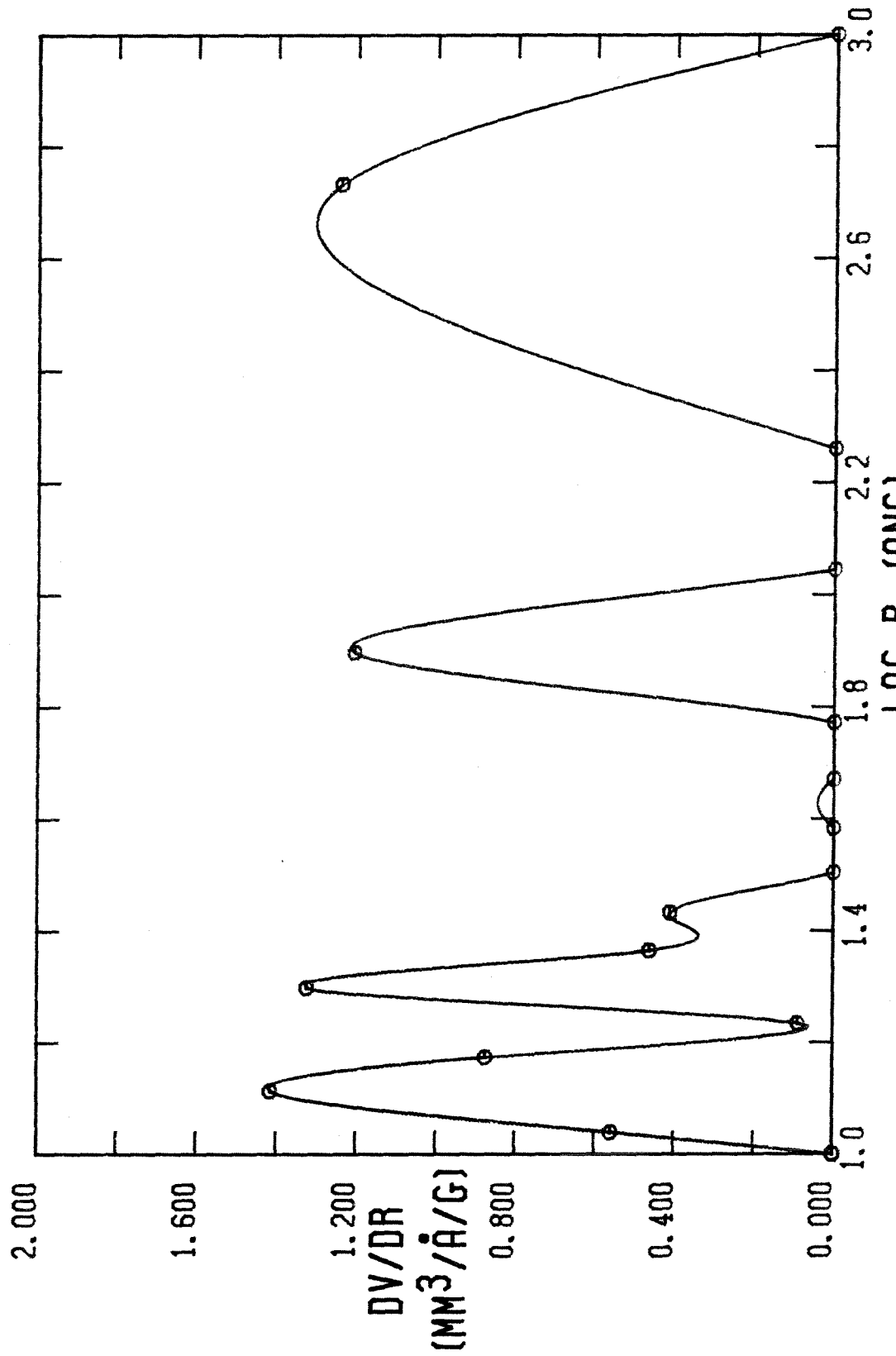
PORE SIZE DISTRIBUTION FOR RUN 36C
DV/DR
(MM3/Å/G)
2.000
1.600
1.200
0.800
0.400
0.000
1.0
1.4
1.8
2.2
2.6
3.0
LOG R (ANG)

FIGURE A-104

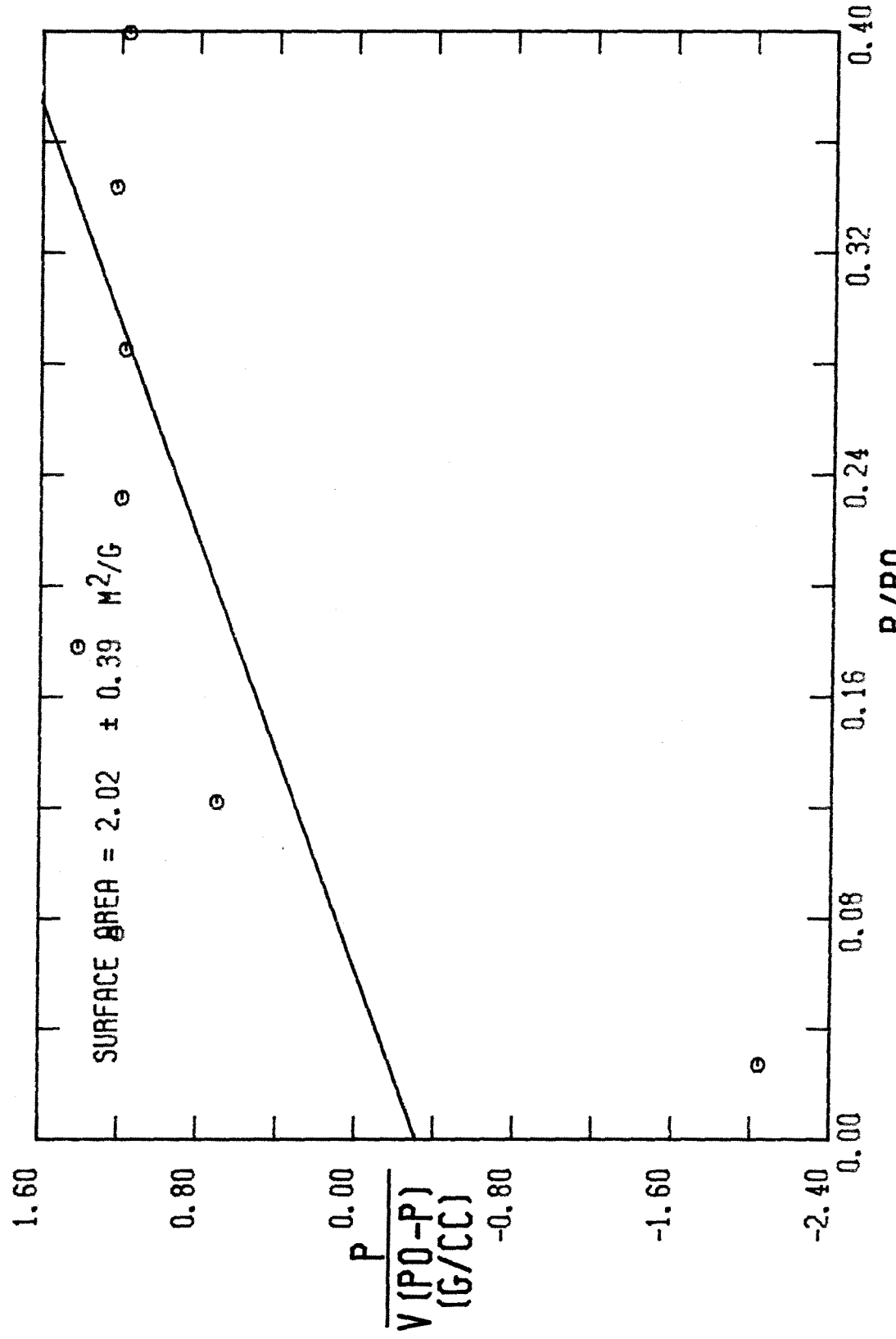
BET PLOT FOR RUN 36C
SURFACE AREA = 2.02 ± 0.39 M2/G
P/PO
P / V(PO-P) (G/CC)
0.00
0.08
0.16
0.24
0.32
0.40
1.60
0.80
0.00
-0.80
-1.60
-2.40

FIGURE A-105

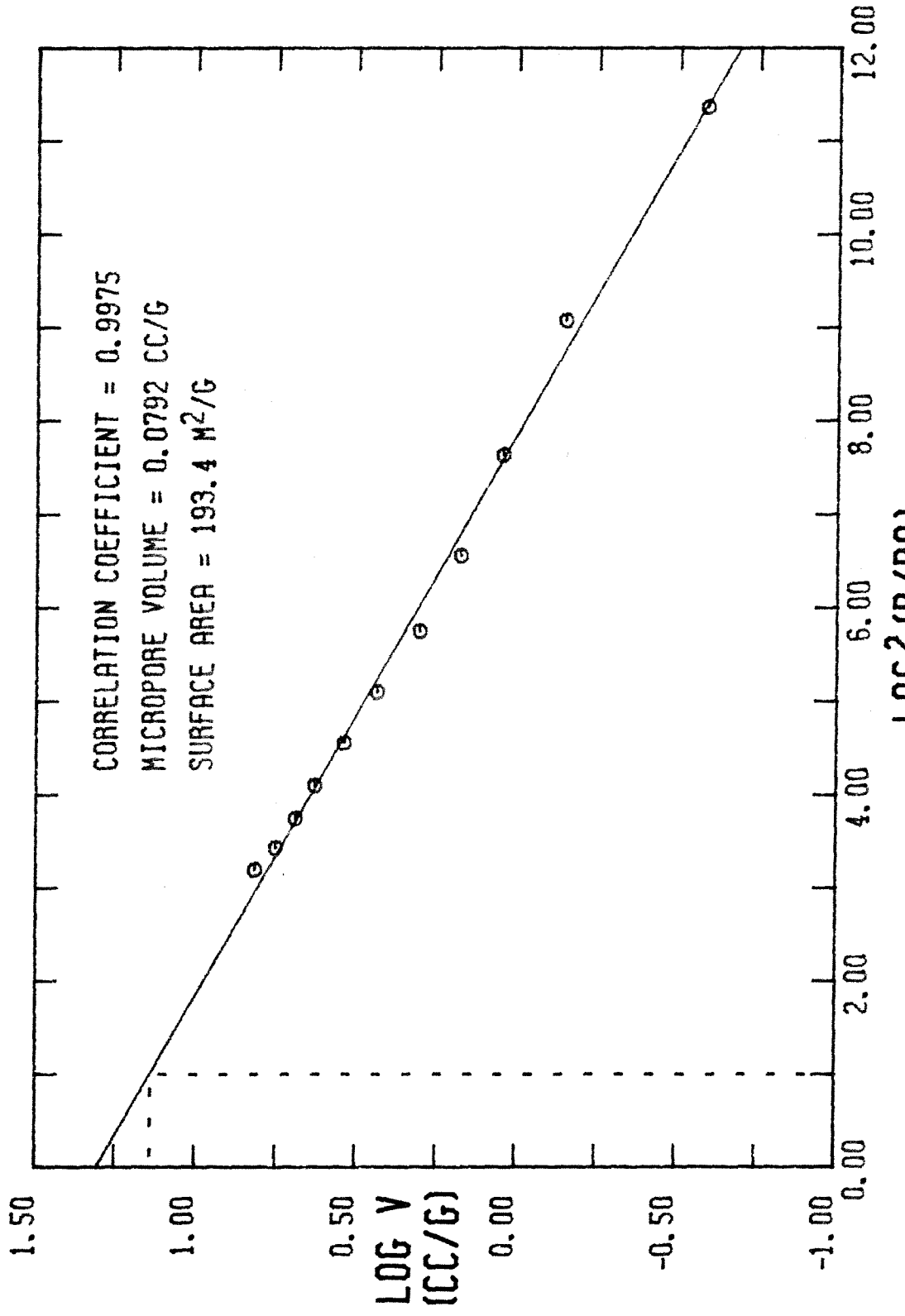
DPR PLOT FOR RUN 36C
CORRELATION COEFFICIENT = 0.9975
MICROPORE VOLUME = 0.0792 CC/G
SURFACE AREA = 193.4 M2/G
LOG V (CC/G)
LOG2 (P/PO)
1.50
1.00
0.50
0.00
-0.50
-1.00
0.00
2.00
4.00
6.00
8.00
10.00
12.00

FIGURE A-106

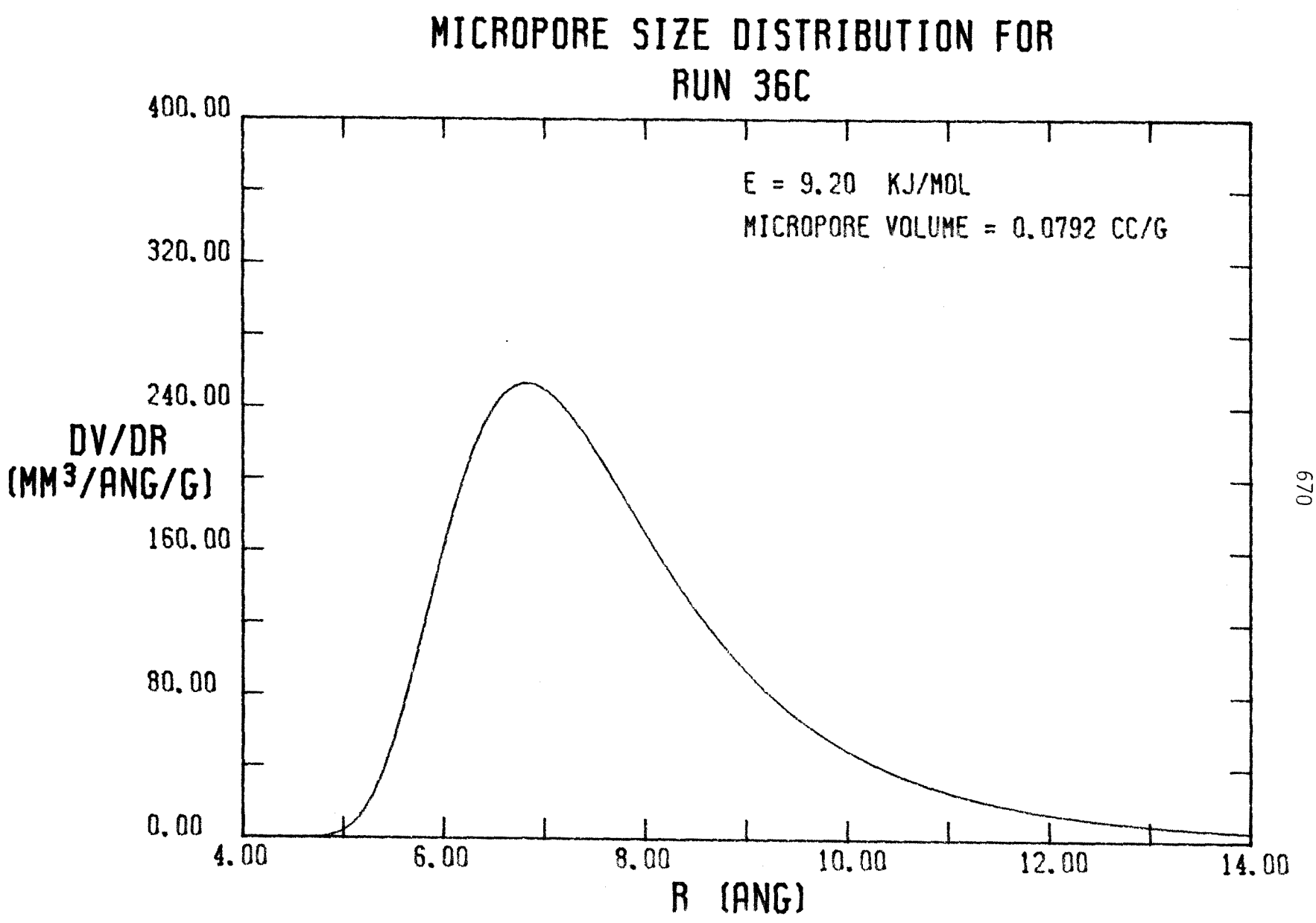
MICROPORE SIZE DISTRIBUTION FOR
RUN 36C
E = 9.20 KJ/MOL
MICROPORE VOLUME = 0.0792 CC/G
400.00
320.00
240.00
160.00
80.00
0.00
DV/DR
(MM3/ANG/G)
4.00
6.00
8.00
10.00
12.00
14.00
R (ANG)

FIGURE A-107

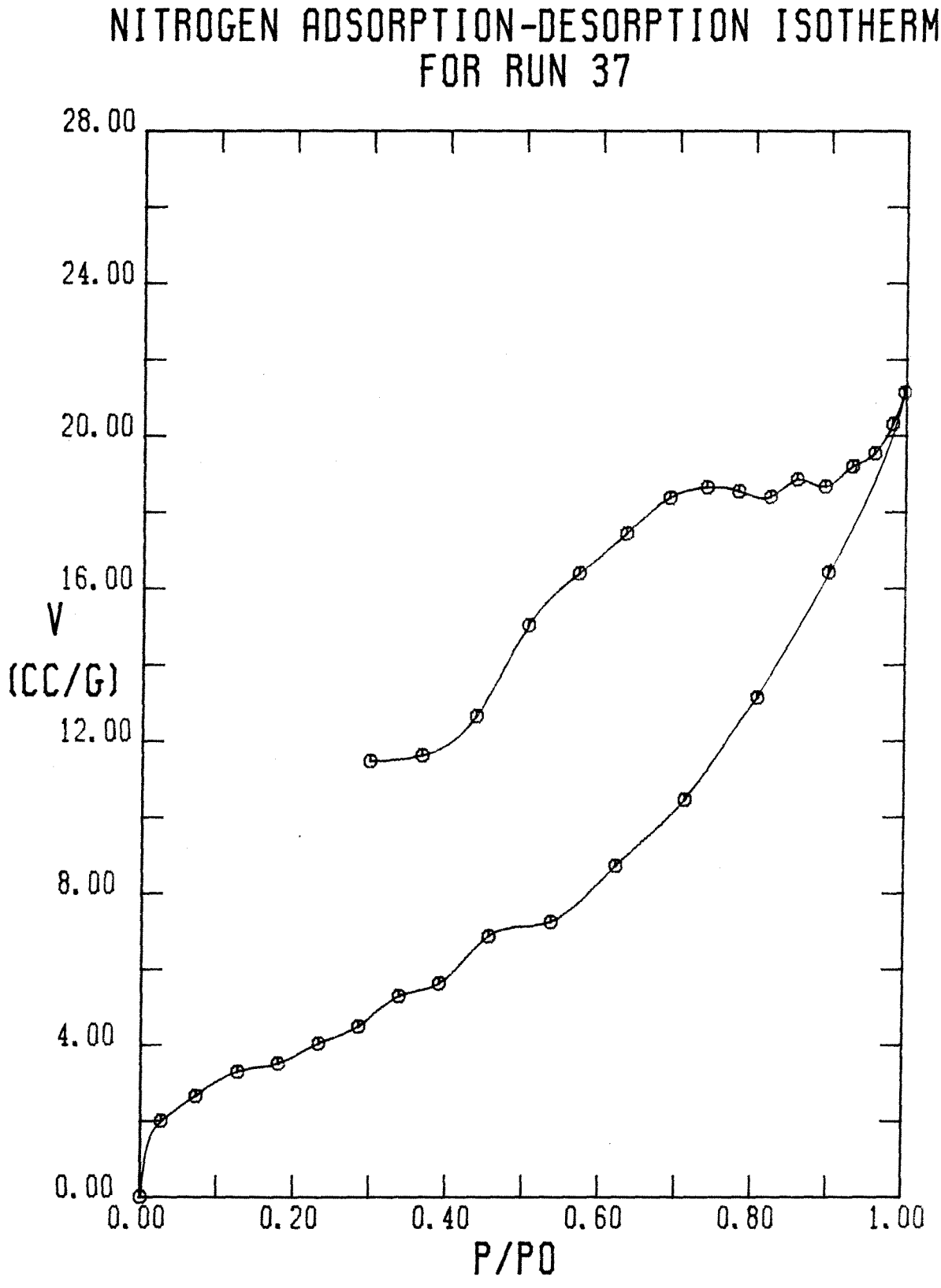
NITROGEN ADSORPTION-DESORPTION ISOTHERM
FOR RUN 37
28.00
24.00
20.00
16.00
12.00
8.00
4.00
0.00
V
(CC/G)
0.00
0.20
0.40
0.60
0.80
1.00
P/PO

FIGURE A-108

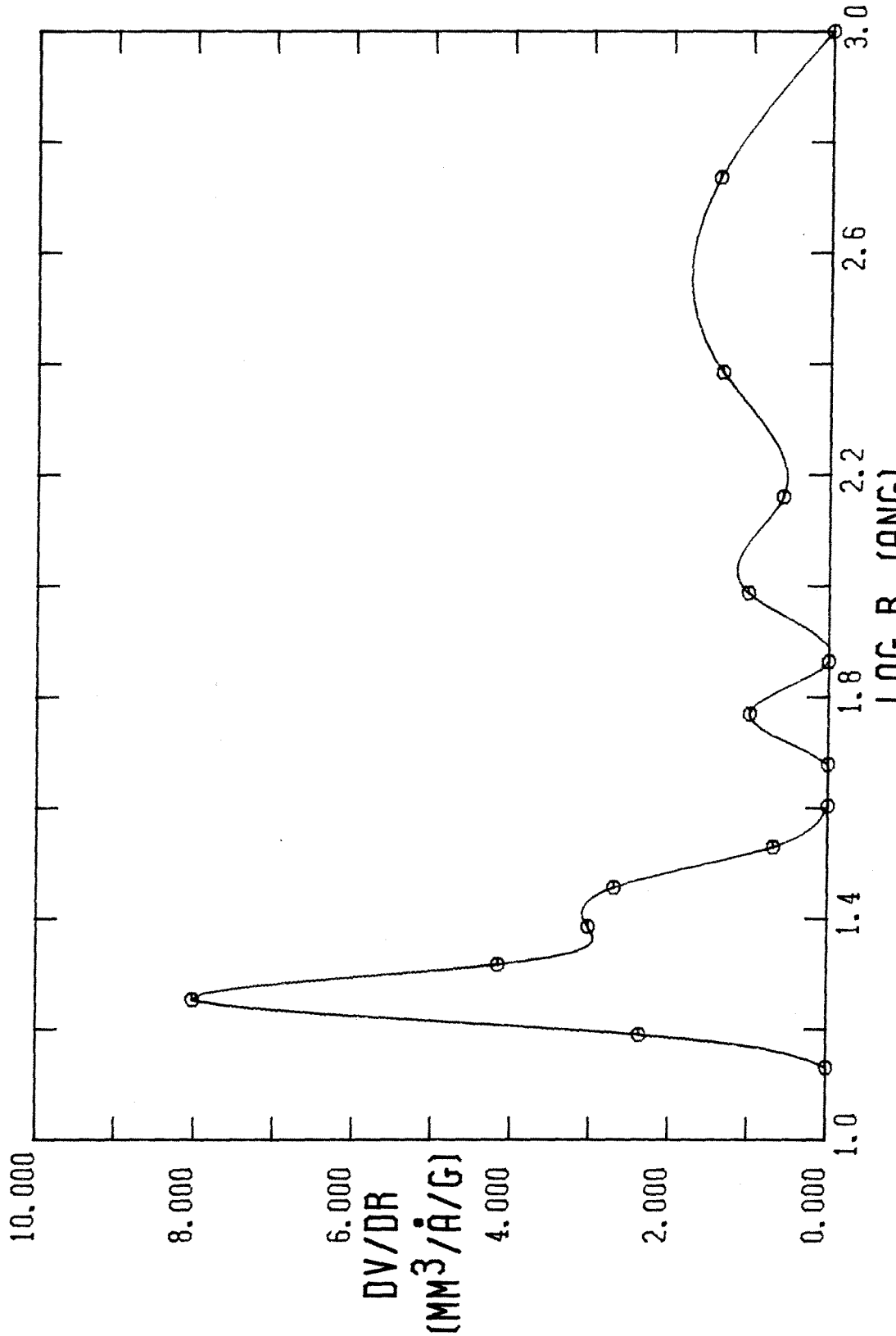
PORE SIZE DISTRIBUTION FOR RUN 37
DV/DR
(MM3/Å/G)
10.000
8.000
6.000
4.000
2.000
0.000
1.0
1.4
1.8
2.2
2.6
3.0
LOG R (ANG)

FIGURE A-109

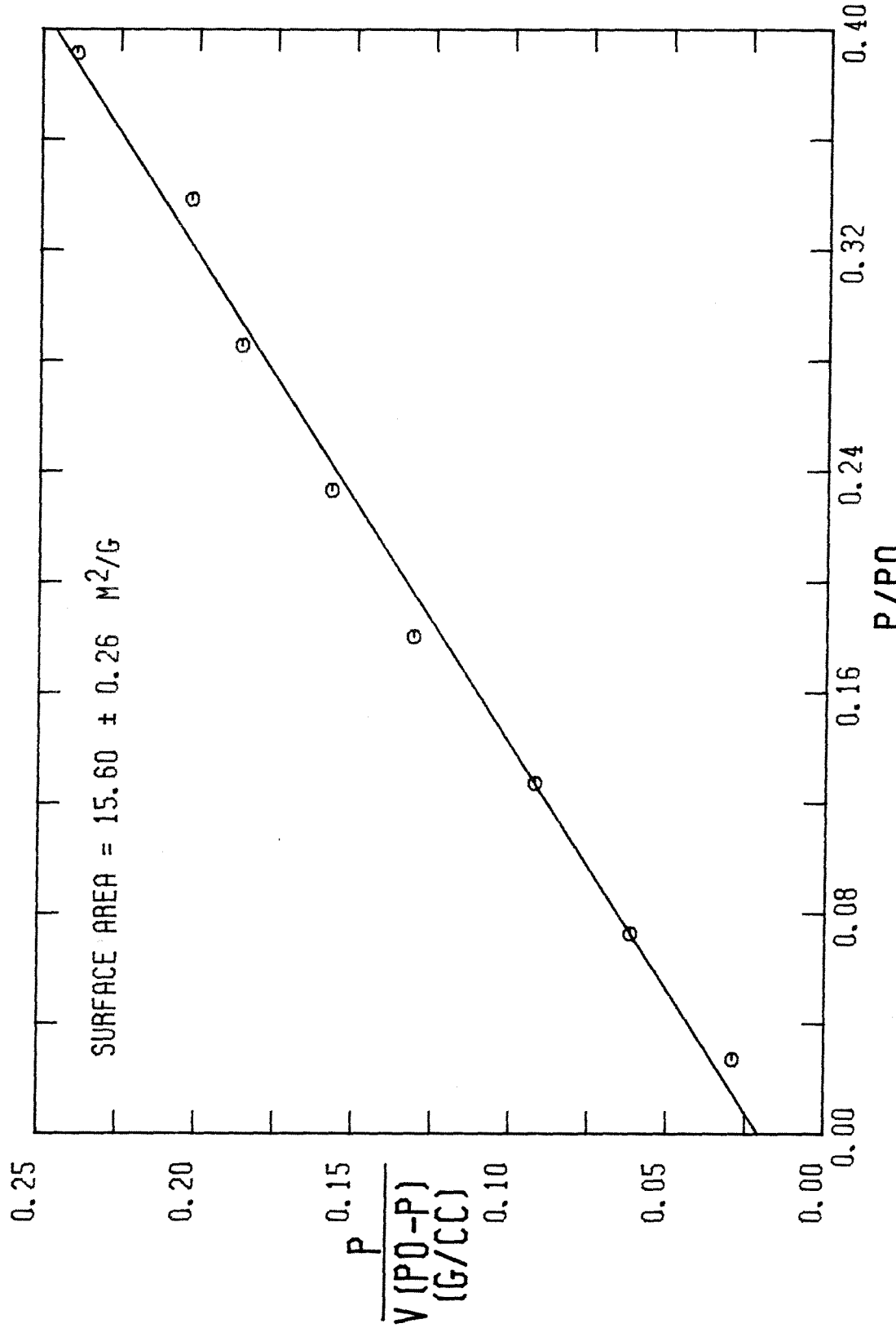
BET PLOT FOR RUN 37
SURFACE AREA = 15.60 ± 0.26 M2/G
P / V (PO-P) (G/CC)
P/PO
0.25
0.20
0.15
0.10
0.05
0.00
0.00
0.08
0.16
0.24
0.32
0.40

FIGURE A-110

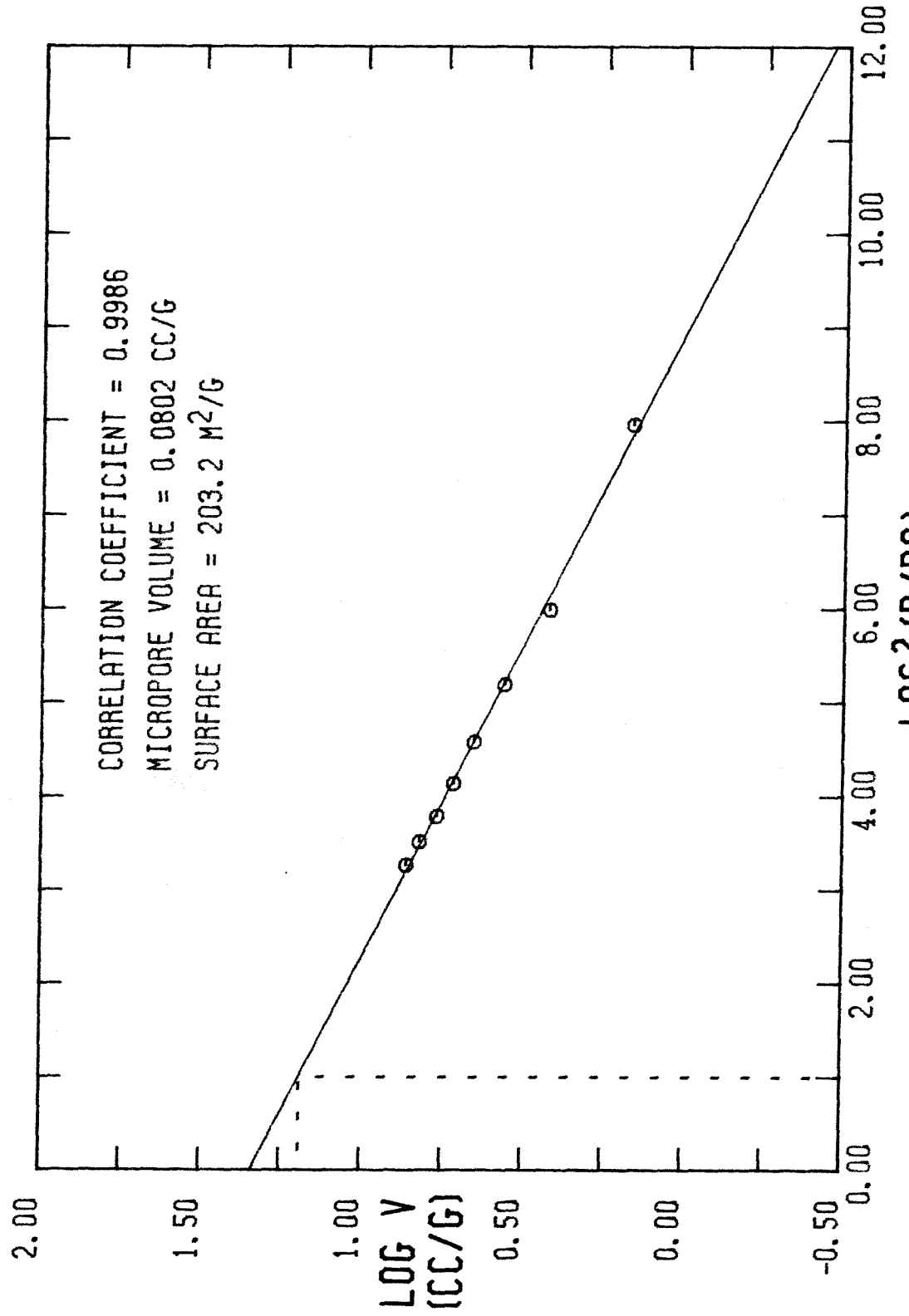
DPR PLOT FOR RUN 37
CORRELATION COEFFICIENT = 0.9986
MICROPORE VOLUME = 0.0802 CC/G
SURFACE AREA = 203.2 M2/G
LOG V (CC/G)
LOG2 (P/PO)
2.00
1.50
1.00
0.50
0.00
-0.50
0.00
2.00
4.00
6.00
8.00
10.00
12.00

FIGURE A-111

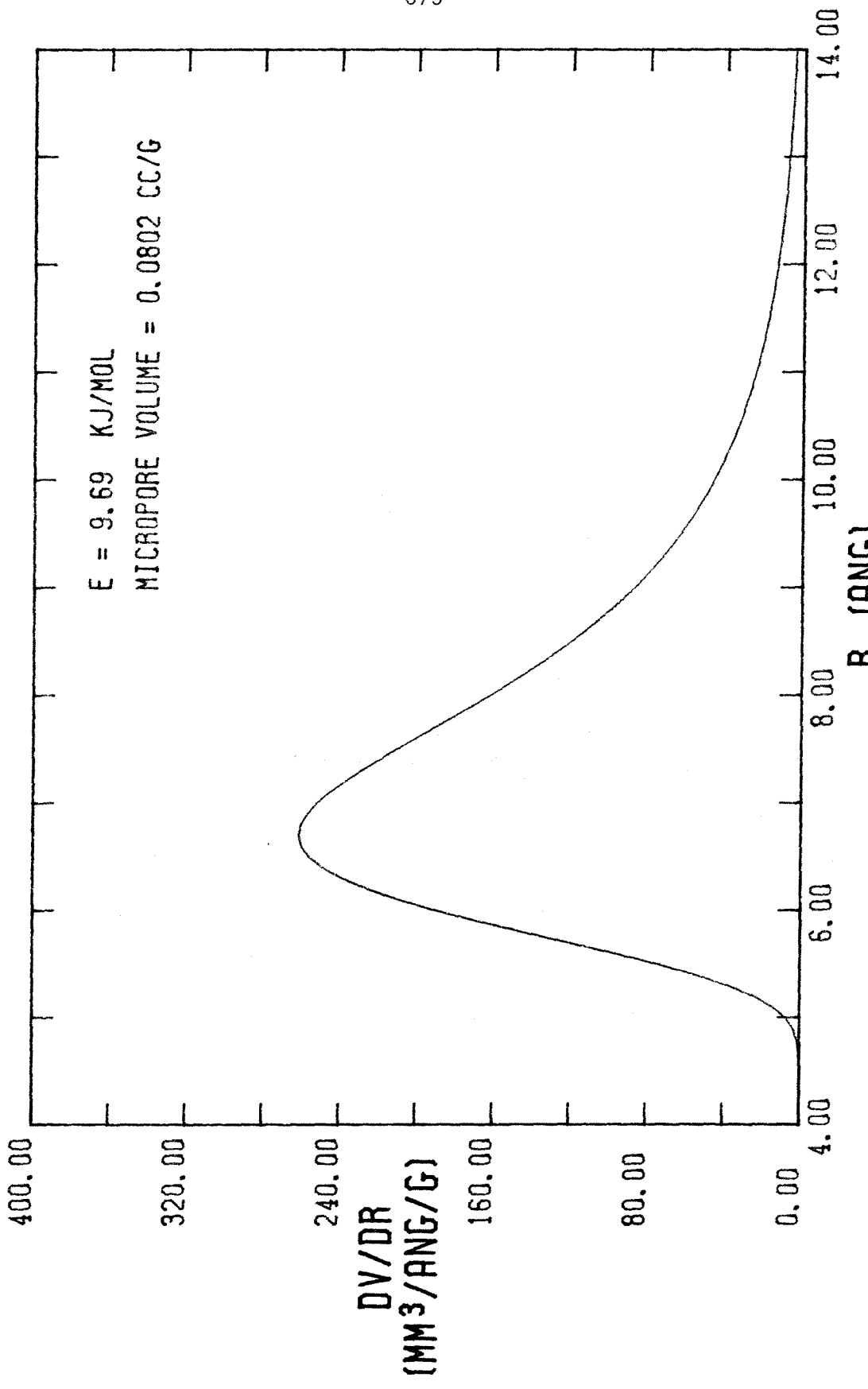
MICROPORE SIZE DISTRIBUTION FOR RUN 37
E = 9.69 KJ/MOL
MICROPORE VOLUME = 0.0802 CC/G
DV/DR
(MM3/ANG/G)
400.00
320.00
240.00
160.00
80.00
0.00
4.00
6.00
8.00
10.00
12.00
14.00
R (ANG)

FIGURE A-112

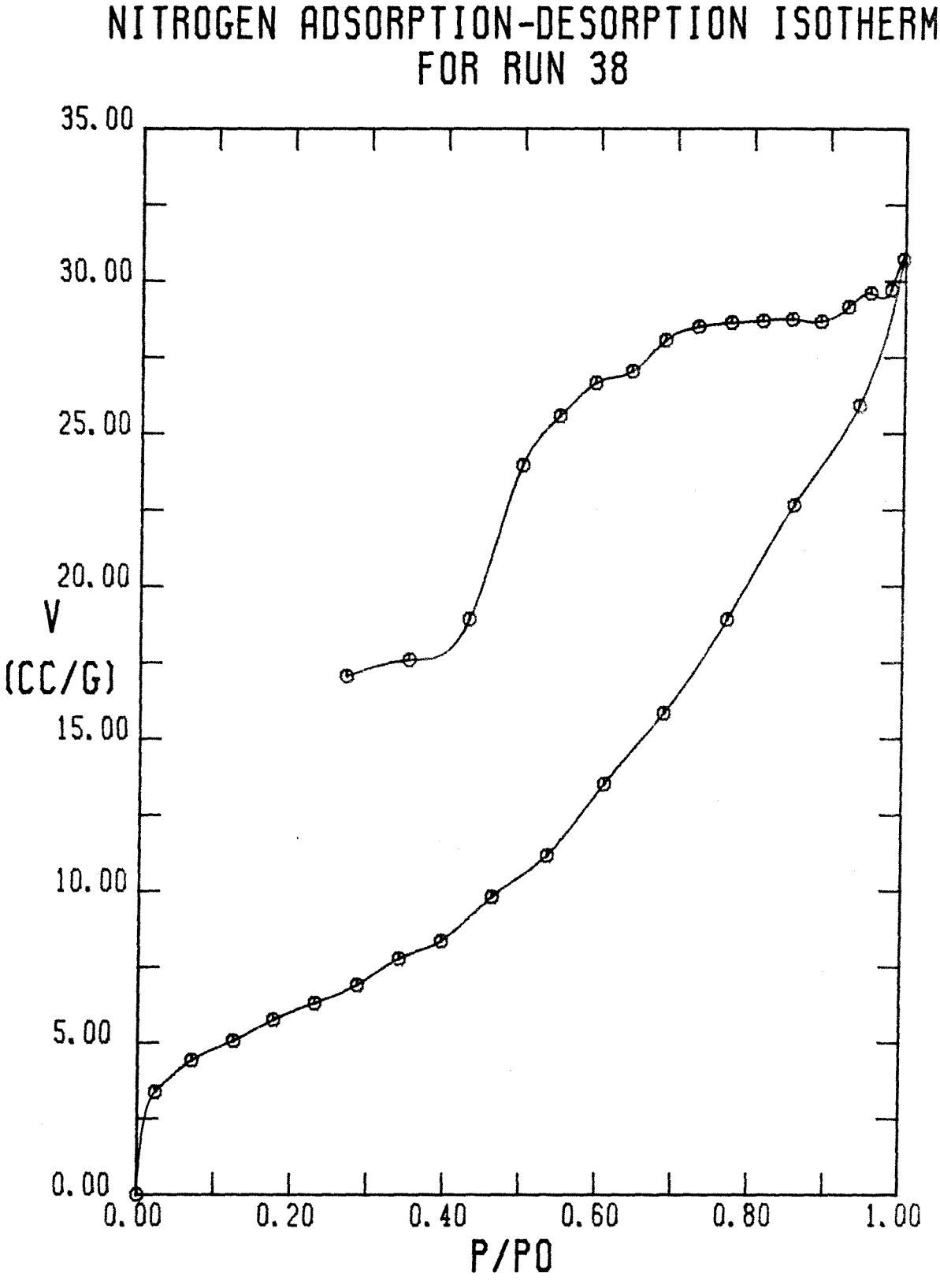
NITROGEN ADSORPTION-DESORPTION ISOTHERM
FOR RUN 38
35.00
30.00
25.00
20.00
V
(CC/G)
15.00
10.00
5.00
0.00
0.00
0.20
0.40
0.60
0.80
1.00
P/PO

FIGURE A-113

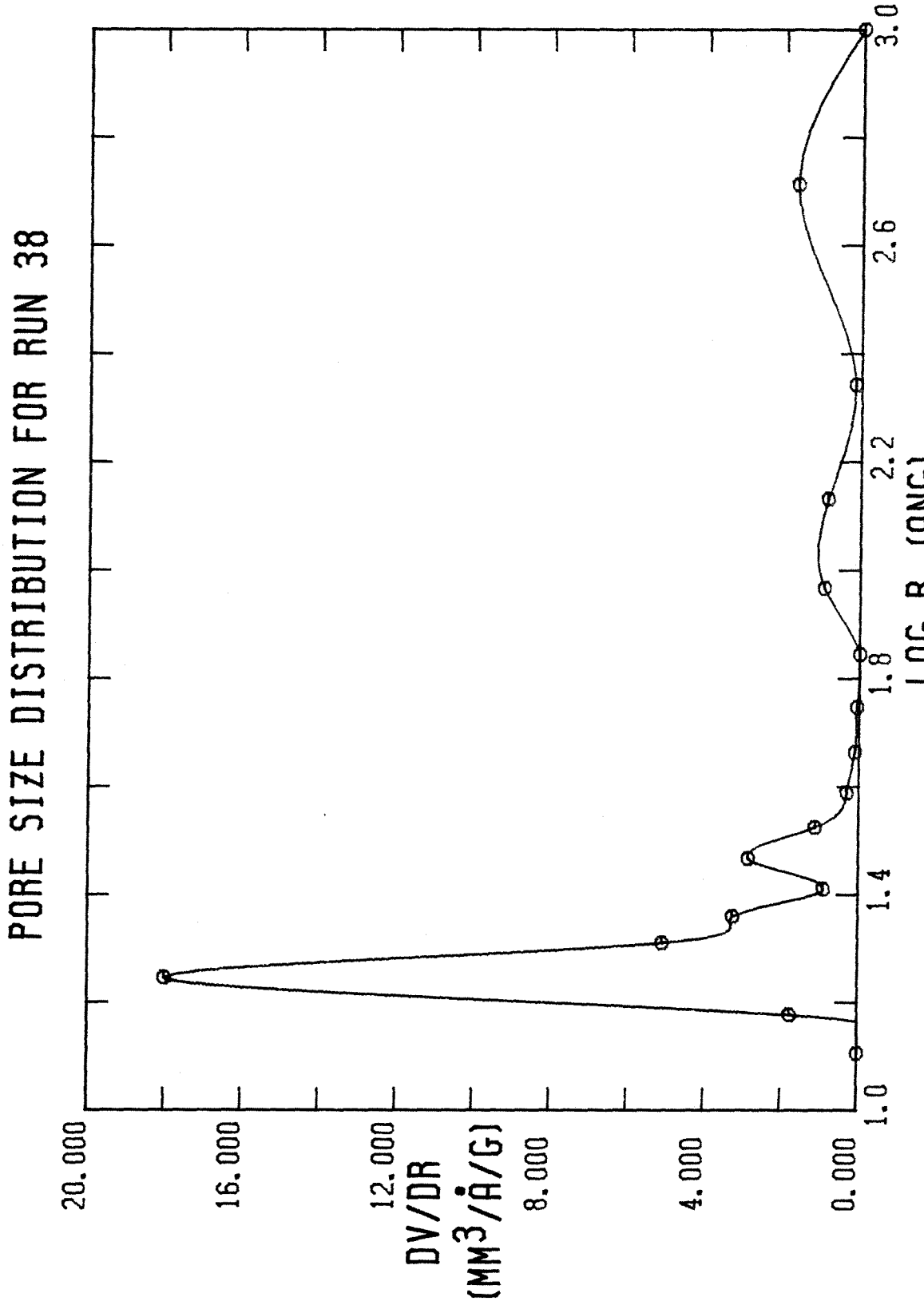
PORE SIZE DISTRIBUTION FOR RUN 38
DV/DR
(MM3/Å/G)
20.000
16.000
12.000
8.000
4.000
0.000
1.0
1.4
1.8
2.2
2.6
3.0
LOG R (ANG)

FIGURE A-114

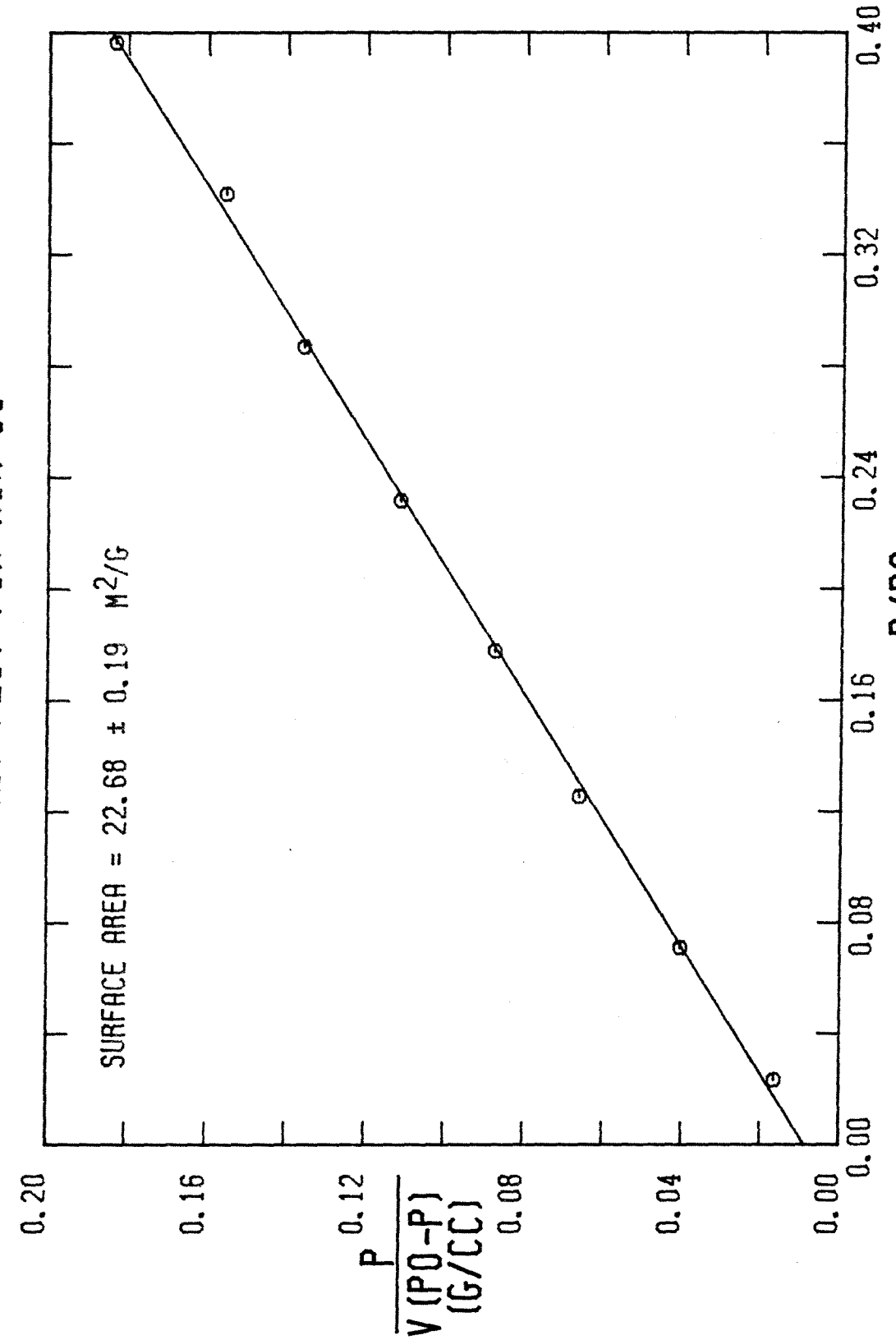
BET PLOT FOR RUN 38
SURFACE AREA = 22.68 ± 0.19 M²/G
P/V(PO-P) (G/CC)
P/PO
0.20
0.16
0.12
0.08
0.04
0.00
0.00
0.08
0.16
0.24
0.32
0.40

FIGURE A-115

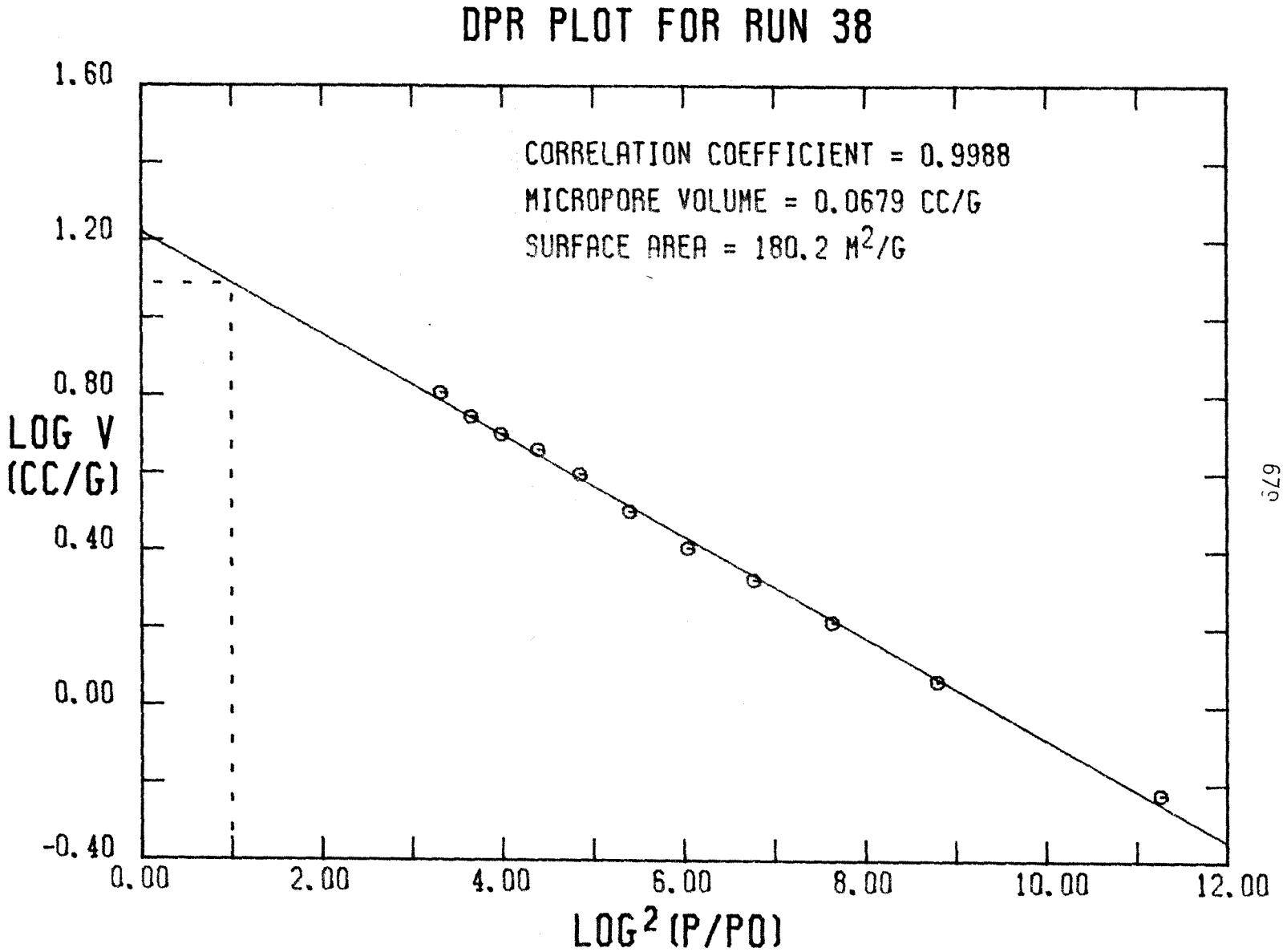
DPR PLOT FOR RUN 38
CORRELATION COEFFICIENT = 0.9988
MICROPORE VOLUME = 0.0679 CC/G
SURFACE AREA = 180.2 M2/G
1.60
1.20
0.80
0.40
0.00
-0.40
LOG V (CC/G)
0.00
2.00
4.00
6.00
8.00
10.00
12.00
LOG2 (P/PO)

FIGURE A-116

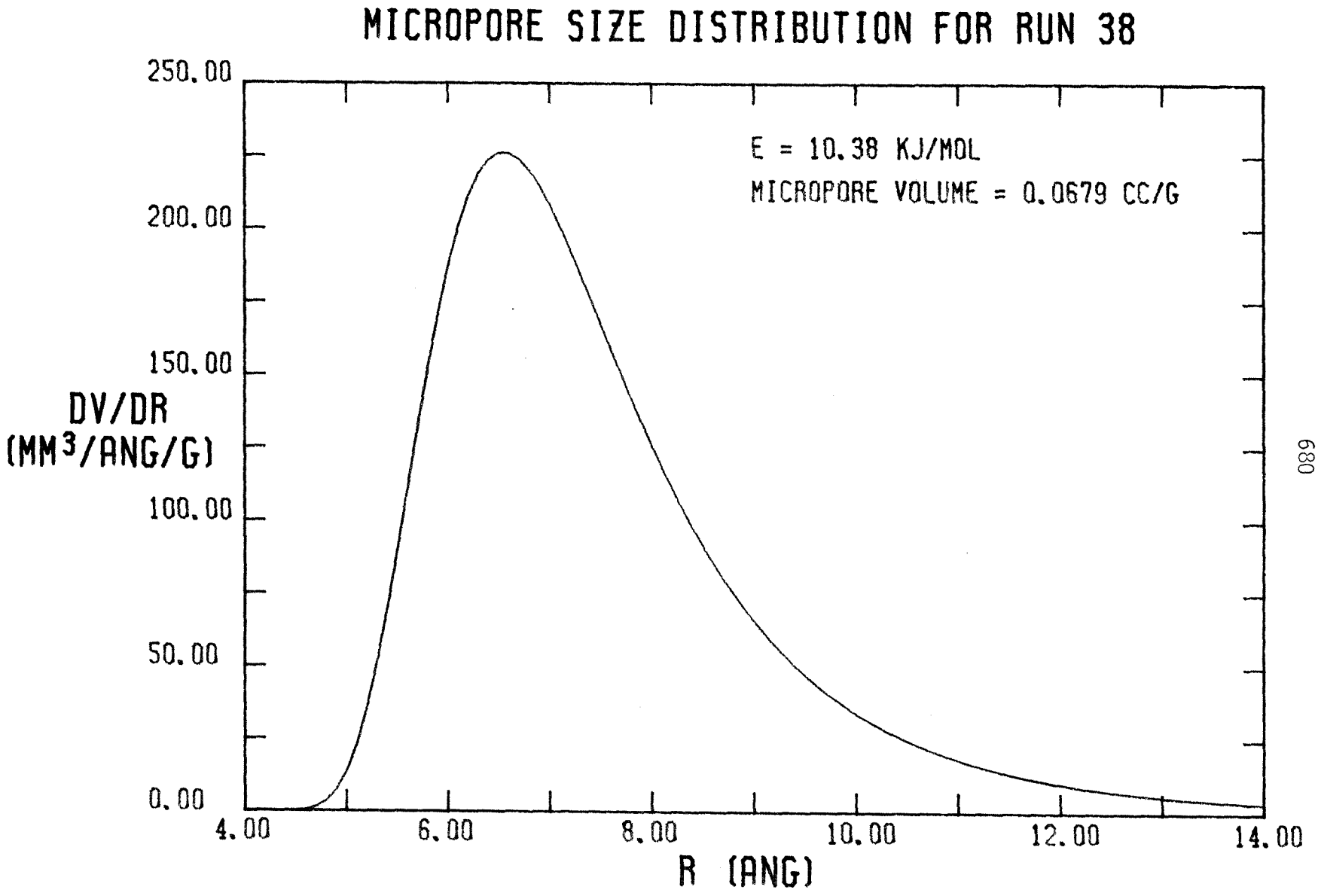
MICROPORE SIZE DISTRIBUTION FOR RUN 38
E = 10.38 KJ/MOL
MICROPORE VOLUME = 0.0679 CC/G
DV/DR
(MM3/ANG/G)
250.00
200.00
150.00
100.00
50.00
0.00
4.00
6.00
8.00
10.00
12.00
14.00
R (ANG)

FIGURE A-117

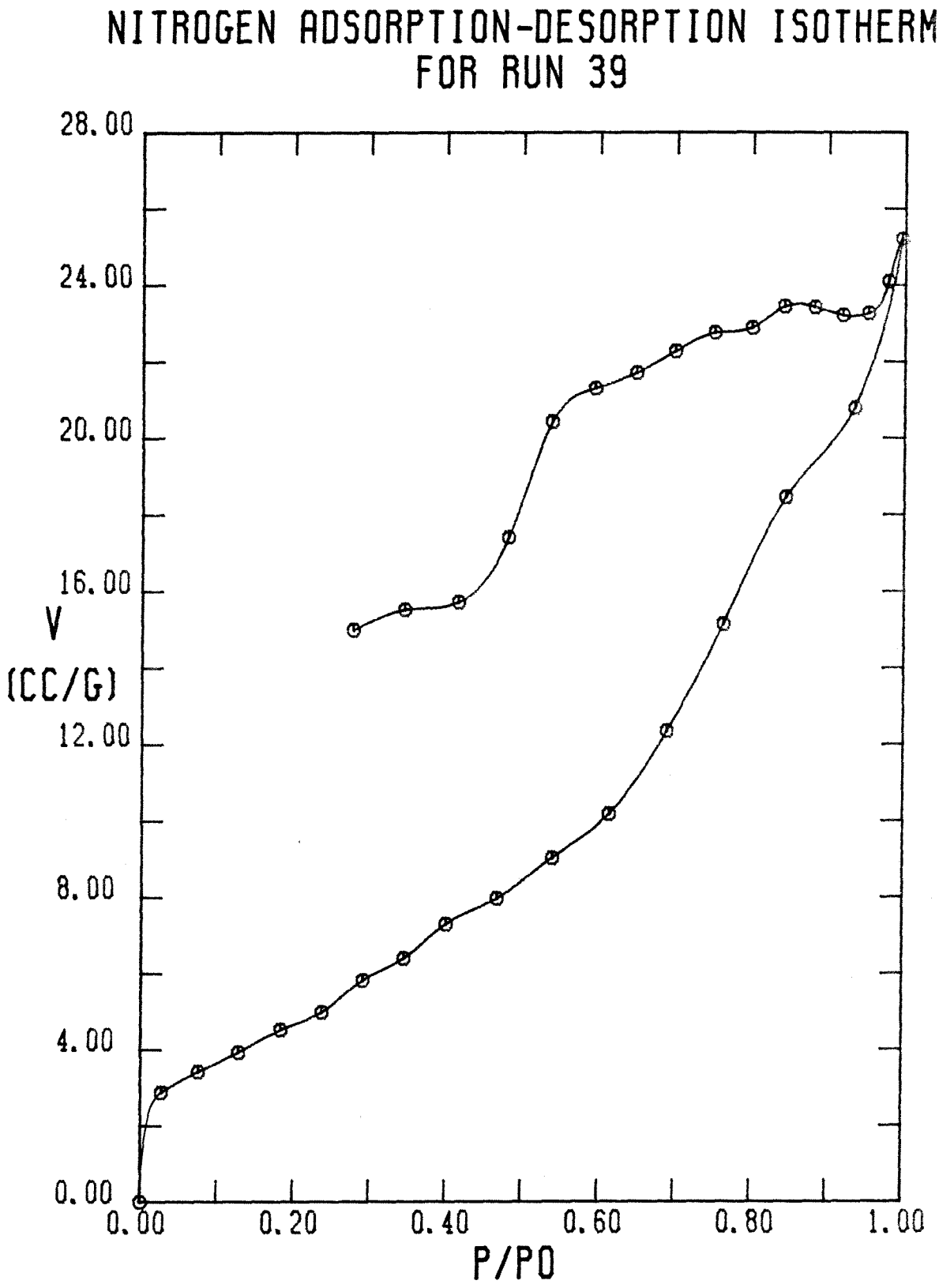
NITROGEN ADSORPTION-DESORPTION ISOTHERM
FOR RUN 39
28.00
24.00
20.00
16.00
12.00
8.00
4.00
0.00
V
(CC/G)
0.00
0.20
0.40
0.60
0.80
1.00
P/PO

FIGURE A-118

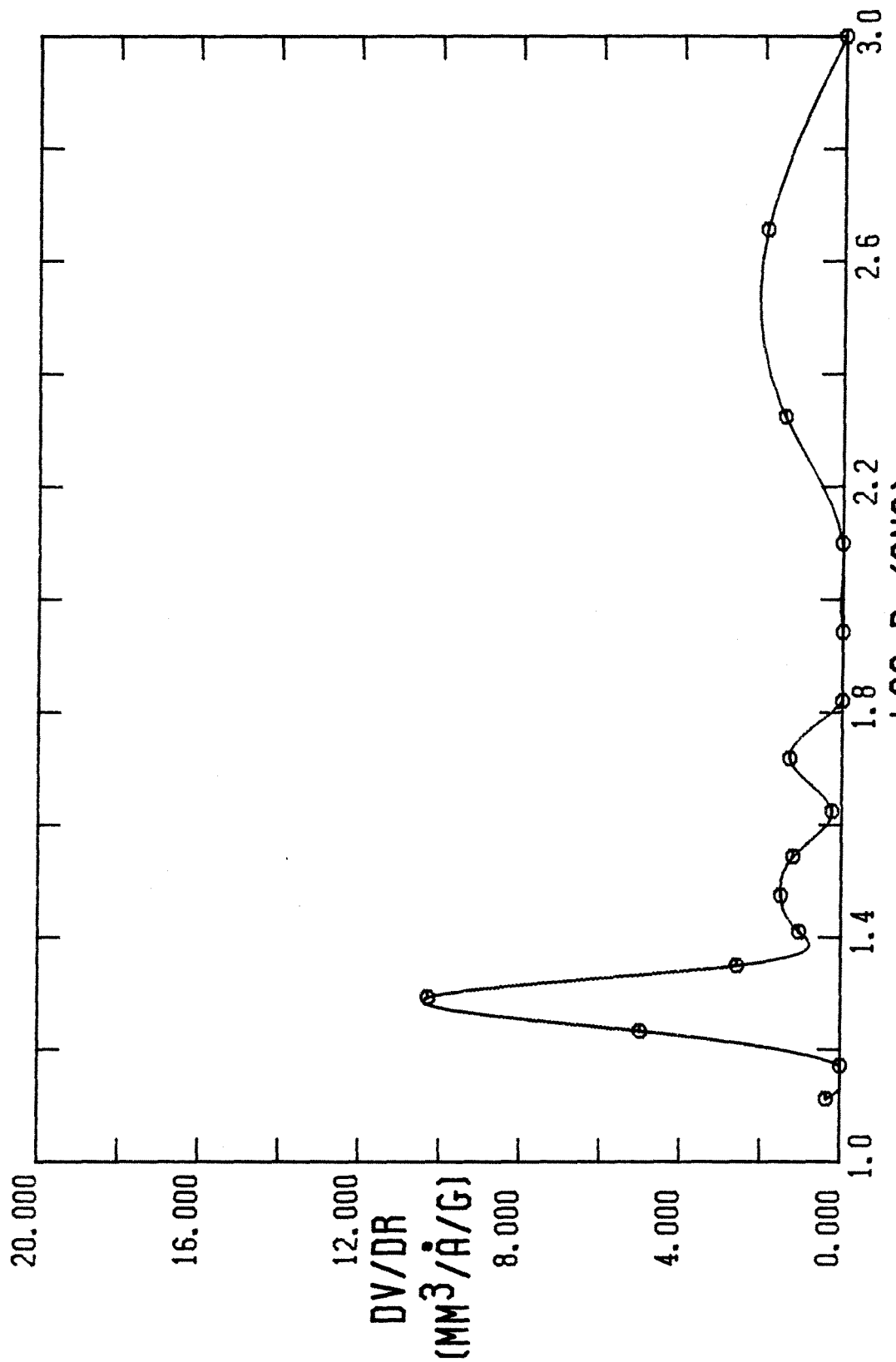
PORE SIZE DISTRIBUTION FOR RUN 39
DV/DR
(MM3/Å/G)
20.000
16.000
12.000
8.000
4.000
0.000
1.0
1.4
1.8
2.2
2.6
3.0
LOG R (ANG)

FIGURE A-119

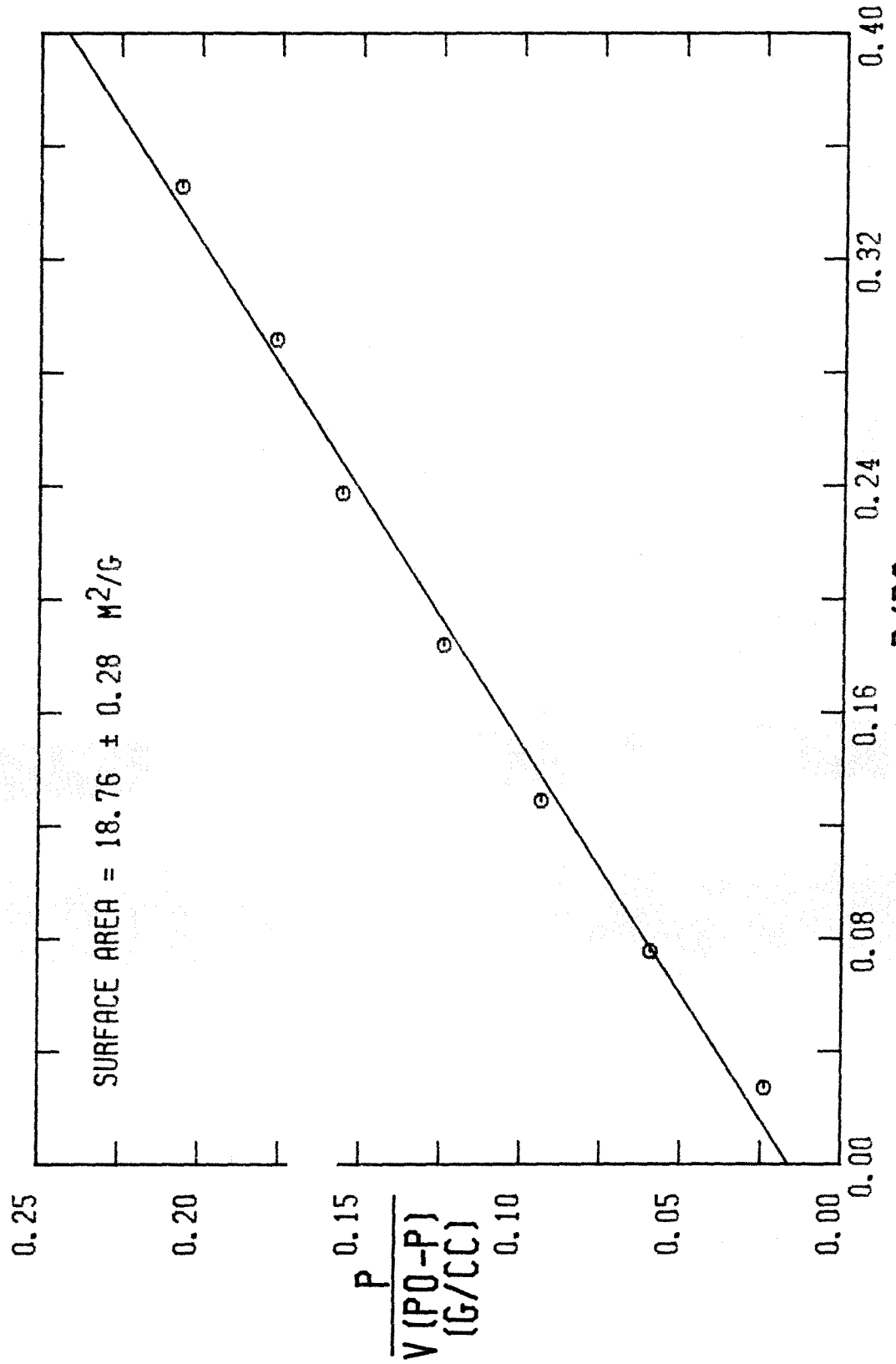
BET PLOT FOR RUN 39
SURFACE AREA = 18.76 ± 0.28 M2/G
P / V (PO-P) (G/CC)
P/PO
0.25
0.20
0.15
0.10
0.05
0.00
0.00
0.08
0.16
0.24
0.32
0.40

FIGURE A-120

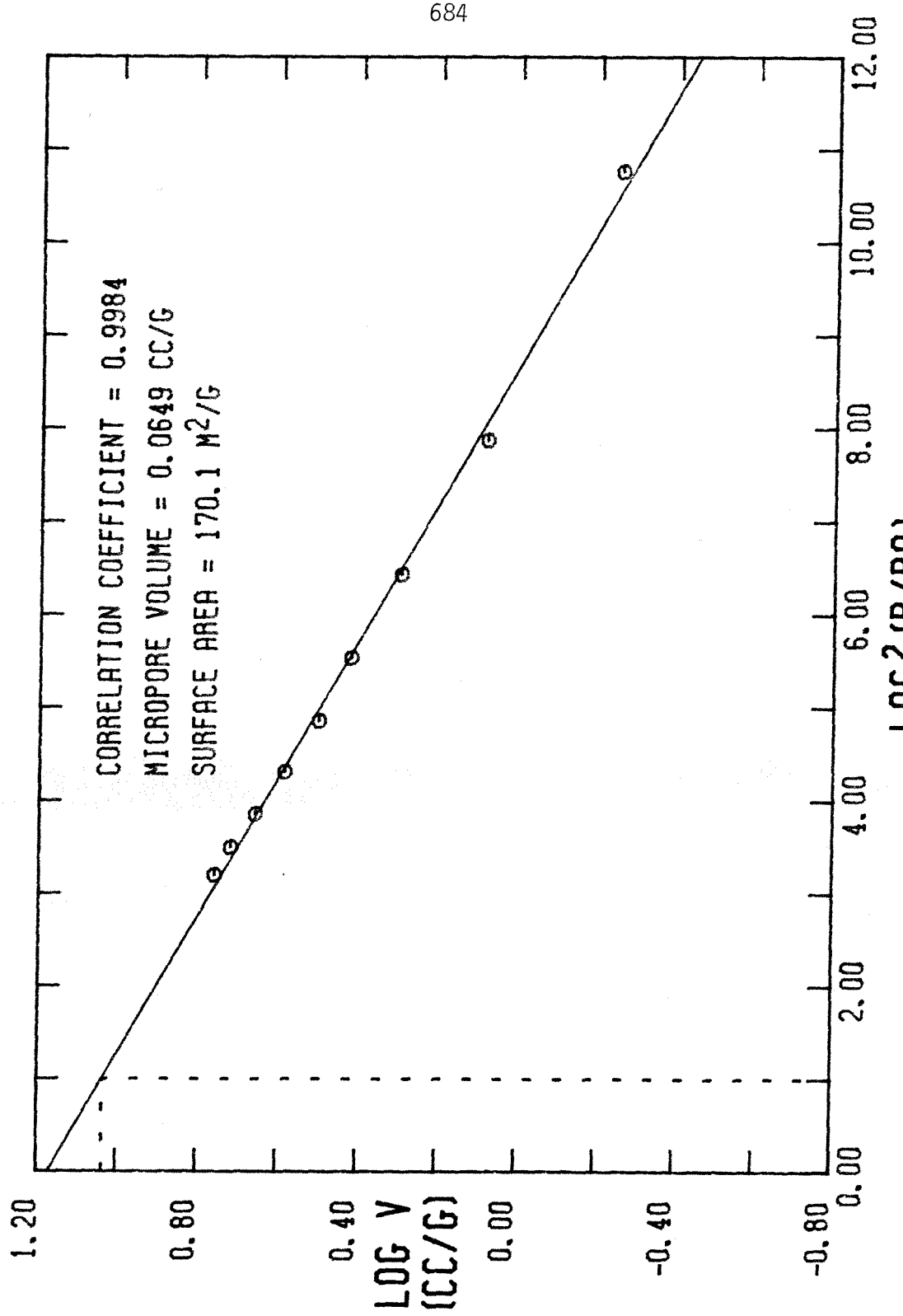
DPR PLOT FOR RUN 39
CORRELATION COEFFICIENT = 0.9984
MICROPORE VOLUME = 0.0649 CC/G
SURFACE AREA = 170.1 M2/G
LOG V (CC/G)
LOG2 (P/PO)
1.20
0.80
0.40
0.00
-0.40
-0.80
0.00
2.00
4.00
6.00
8.00
10.00
12.00

FIGURE A-121

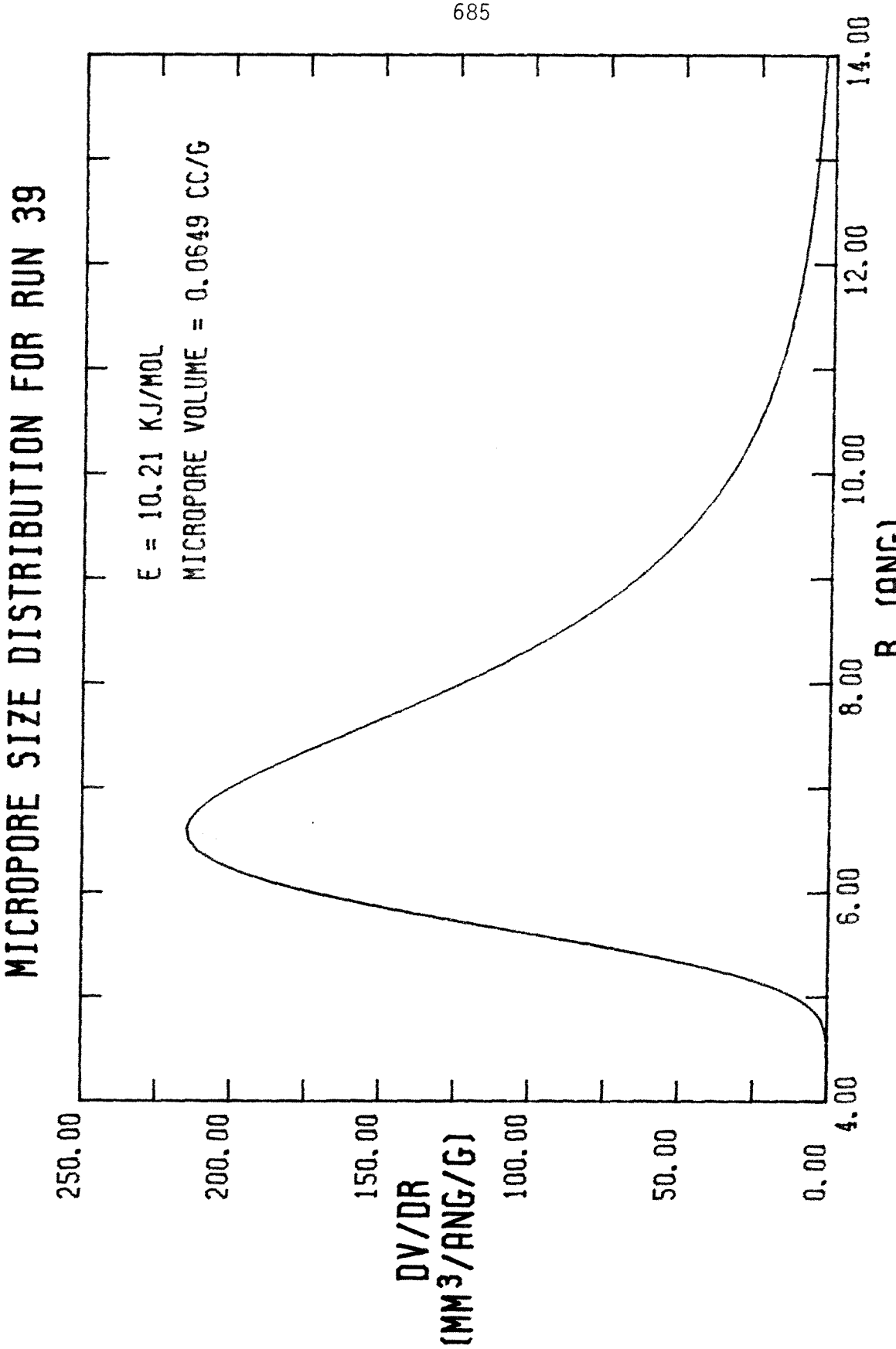
MICROPORE SIZE DISTRIBUTION FOR RUN 39
E = 10.21 KJ/MOL
MICROPORE VOLUME = 0.0649 CC/G
DV/DR (MM3/ANG/G)
R (ANG)
250.00
200.00
150.00
100.00
50.00
0.00
4.00
6.00
8.00
10.00
12.00
14.00

FIGURE A-122

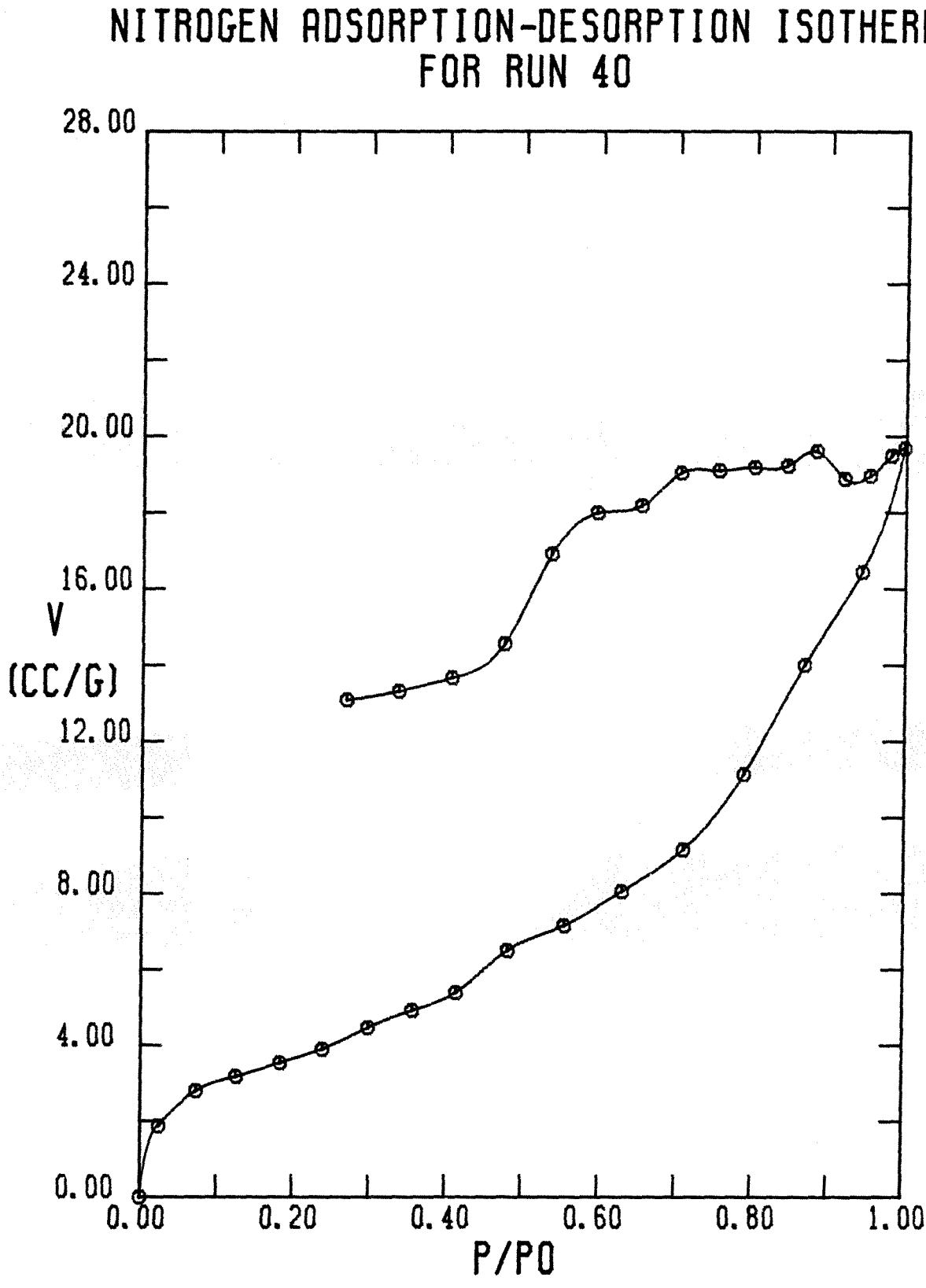
NITROGEN ADSORPTION-DESORPTION ISOTHERM
FOR RUN 40
28.00
24.00
20.00
16.00
12.00
8.00
4.00
0.00
V
(CC/G)
0.00
0.20
0.40
0.60
0.80
1.00
P/PO

FIGURE A-123

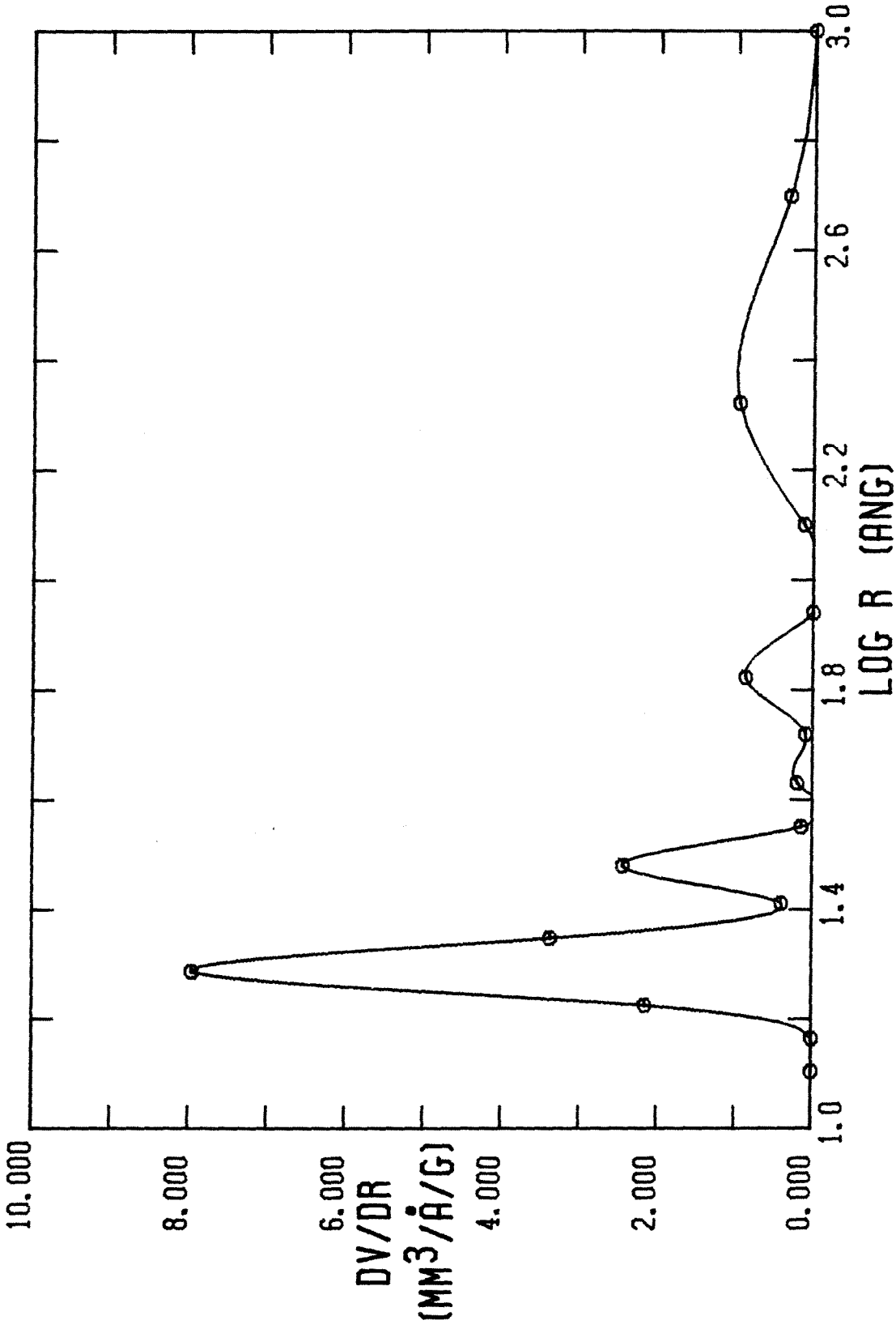
PORE SIZE DISTRIBUTION FOR RUN 40
DV/DR
(MM3/Å/G)
10.000
8.000
6.000
4.000
2.000
0.000
1.0
1.4
1.8
2.2
2.6
3.0
LOG R (ANG)

FIGURE A-124

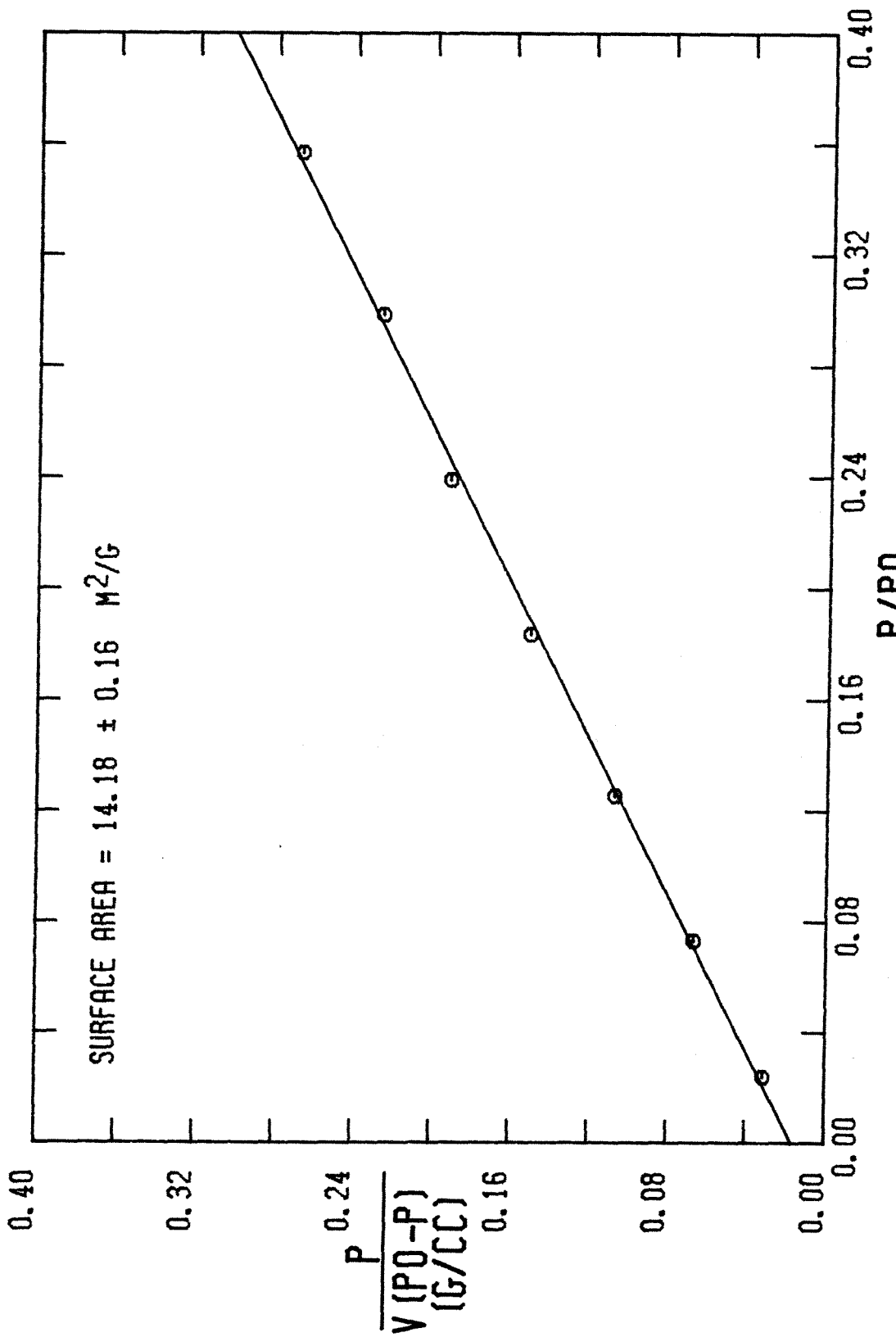
BET PLOT FOR RUN 40
SURFACE AREA = 14.18 ± 0.16 M2/G
P/PO
P / V(PO-P) (G/CC)
0.00
0.08
0.16
0.24
0.32
0.40
0.00
0.08
0.16
0.24
0.32
0.40

FIGURE A-125

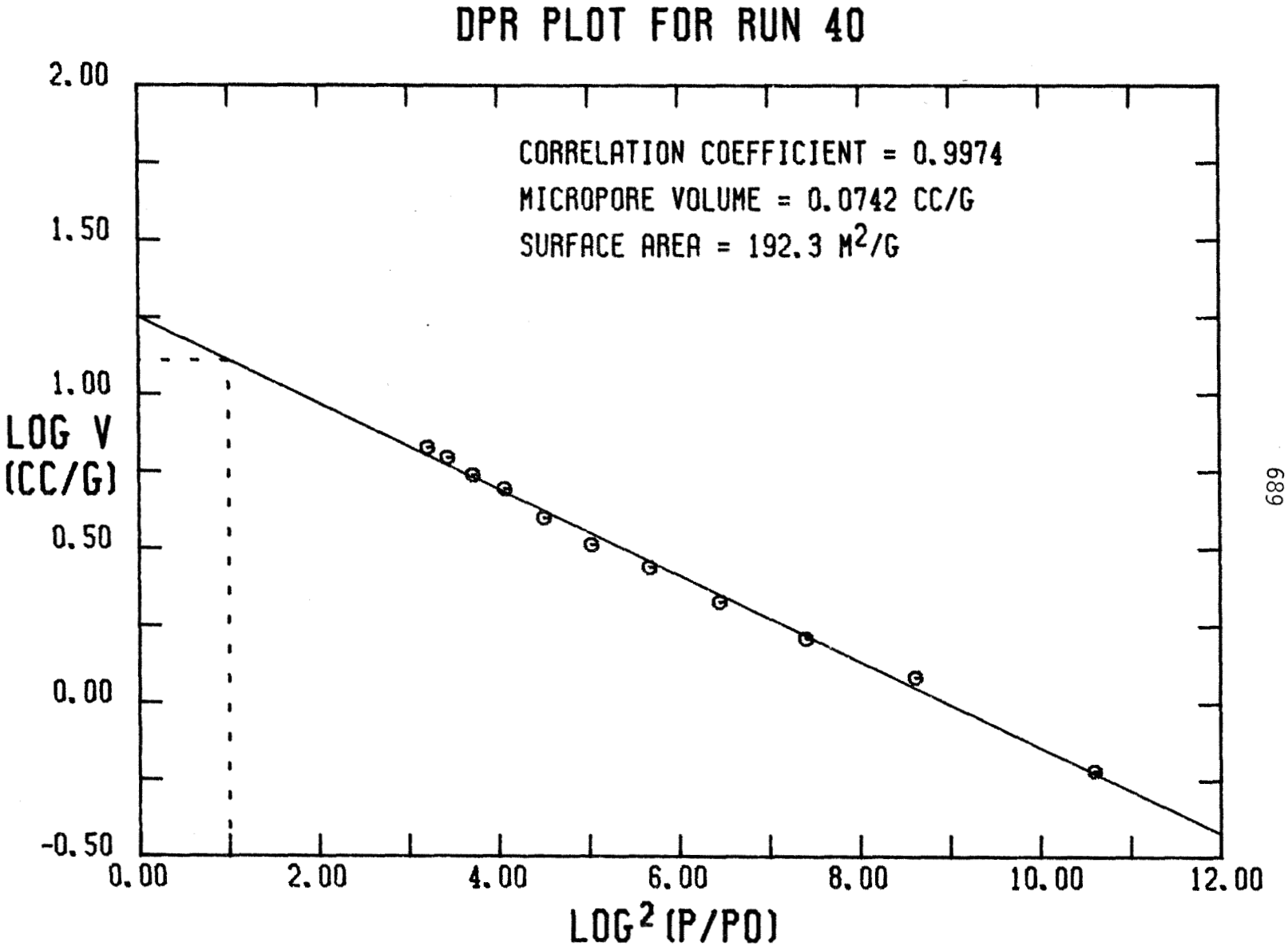
DPR PLOT FOR RUN 40
CORRELATION COEFFICIENT = 0.9974
MICROPORE VOLUME = 0.0742 CC/G
SURFACE AREA = 192.3 M2/G
LOG V (CC/G)
LOG2 (P/PO)
2.00
1.50
1.00
0.50
0.00
-0.50
0.00
2.00
4.00
6.00
8.00
10.00
12.00

FIGURE A-126

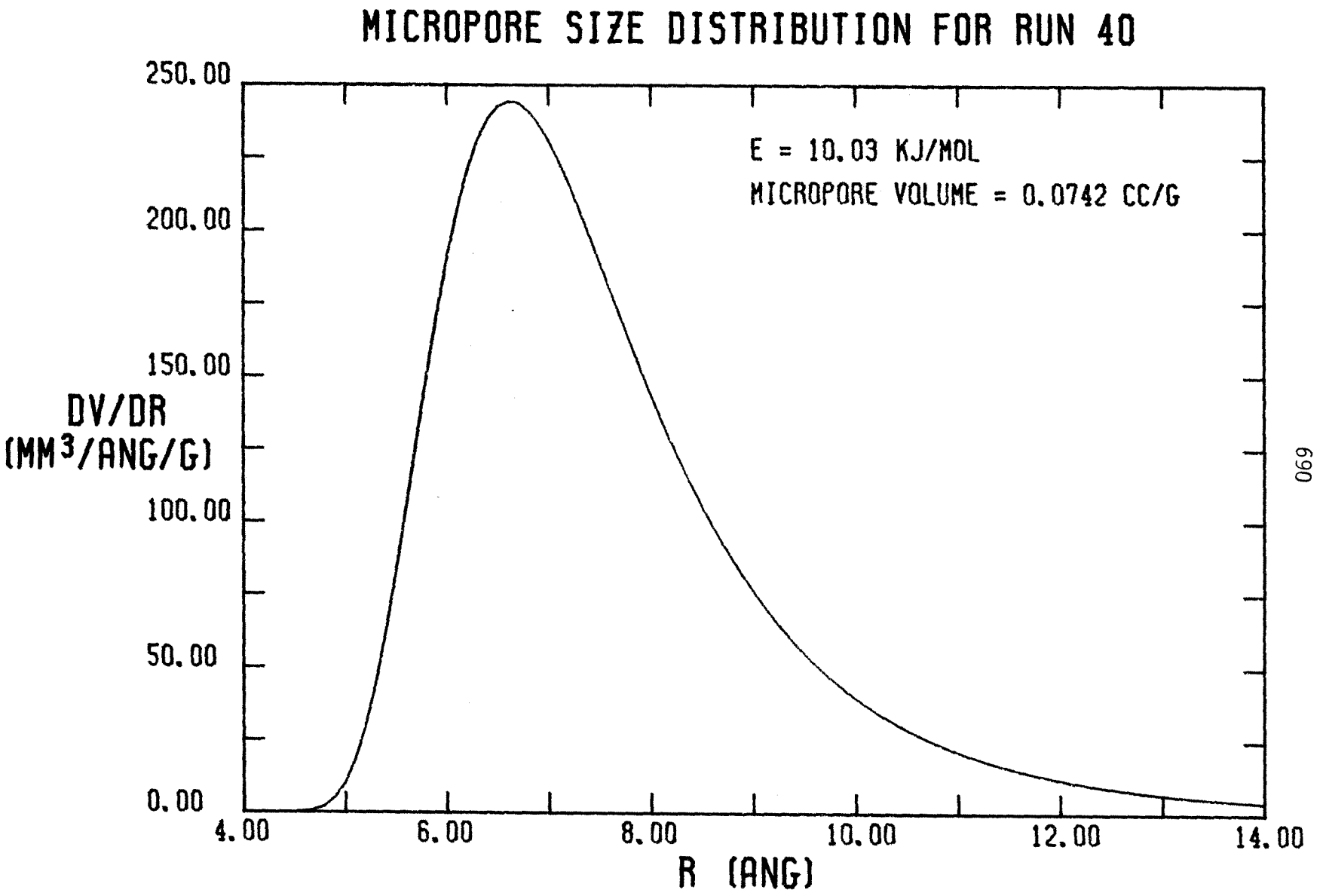
MICROPORE SIZE DISTRIBUTION FOR RUN 40
E = 10.03 KJ/MOL
MICROPORE VOLUME = 0.0742 CC/G
DV/DR
(MM3/ANG/G)
250.00
200.00
150.00
100.00
50.00
0.00
4.00
6.00
8.00
10.00
12.00
14.00
R (ANG)

FIGURE A-127

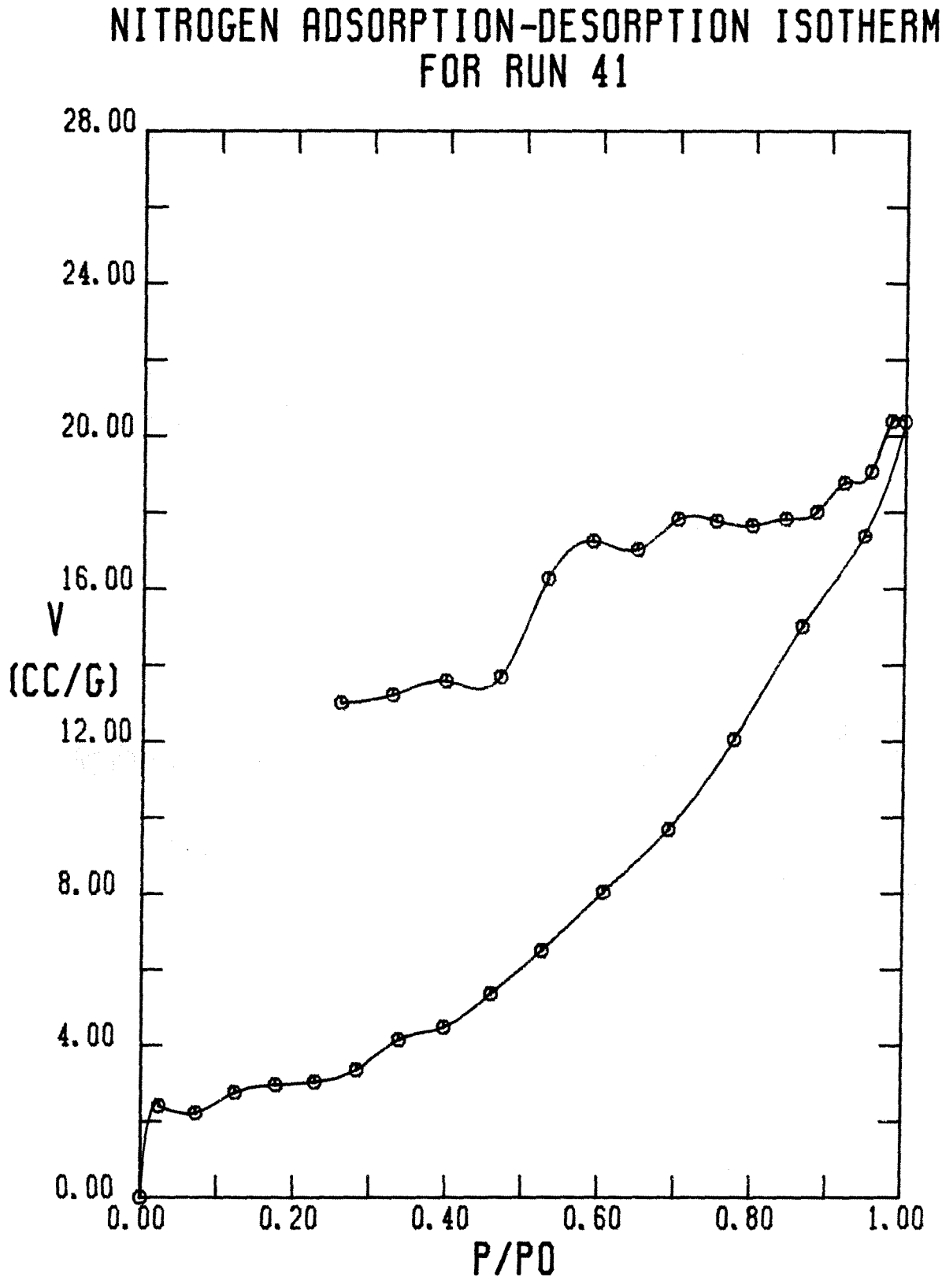
NITROGEN ADSORPTION-DESORPTION ISOTHERM
FOR RUN 41
28.00
24.00
20.00
16.00
12.00
8.00
4.00
0.00
V
(CC/G)
0.00
0.20
0.40
0.60
0.80
1.00
P/PO

FIGURE A-128

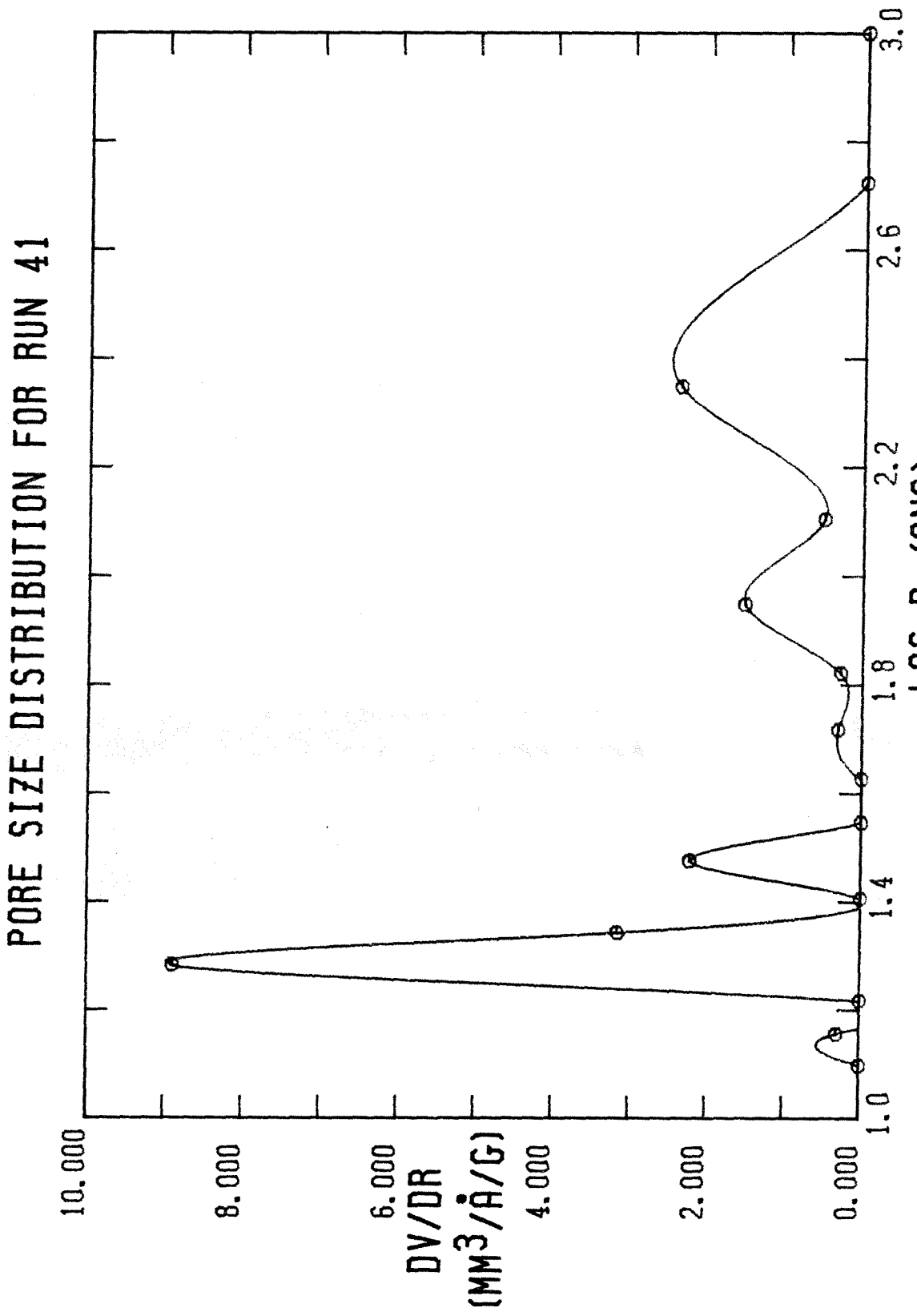
PORE SIZE DISTRIBUTION FOR RUN 41
10.000
8.000
6.000
4.000
2.000
0.000
DV/DR
(MM3/Å/G)
1.0
1.4
1.8
2.2
2.6
3.0
LOG R (ANG)

FIGURE A-129

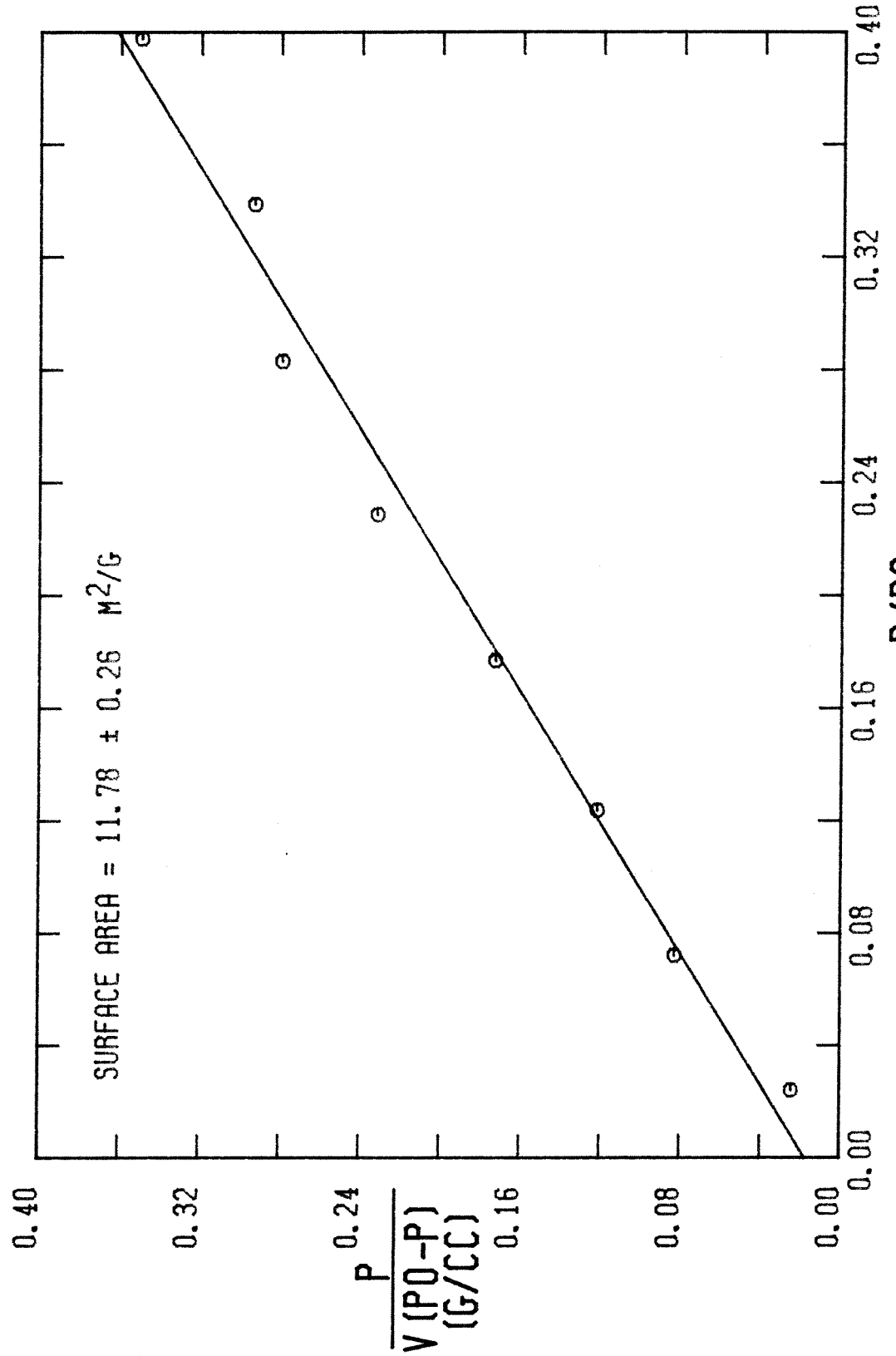
BET PLOT FOR RUN 41
SURFACE AREA = 11.78 ± 0.26 M2/G
P/PO
P / V(PO-P) (G/CC)
0.00
0.08
0.16
0.24
0.32
0.40
0.00
0.08
0.16
0.24
0.32
0.40

FIGURE A-130

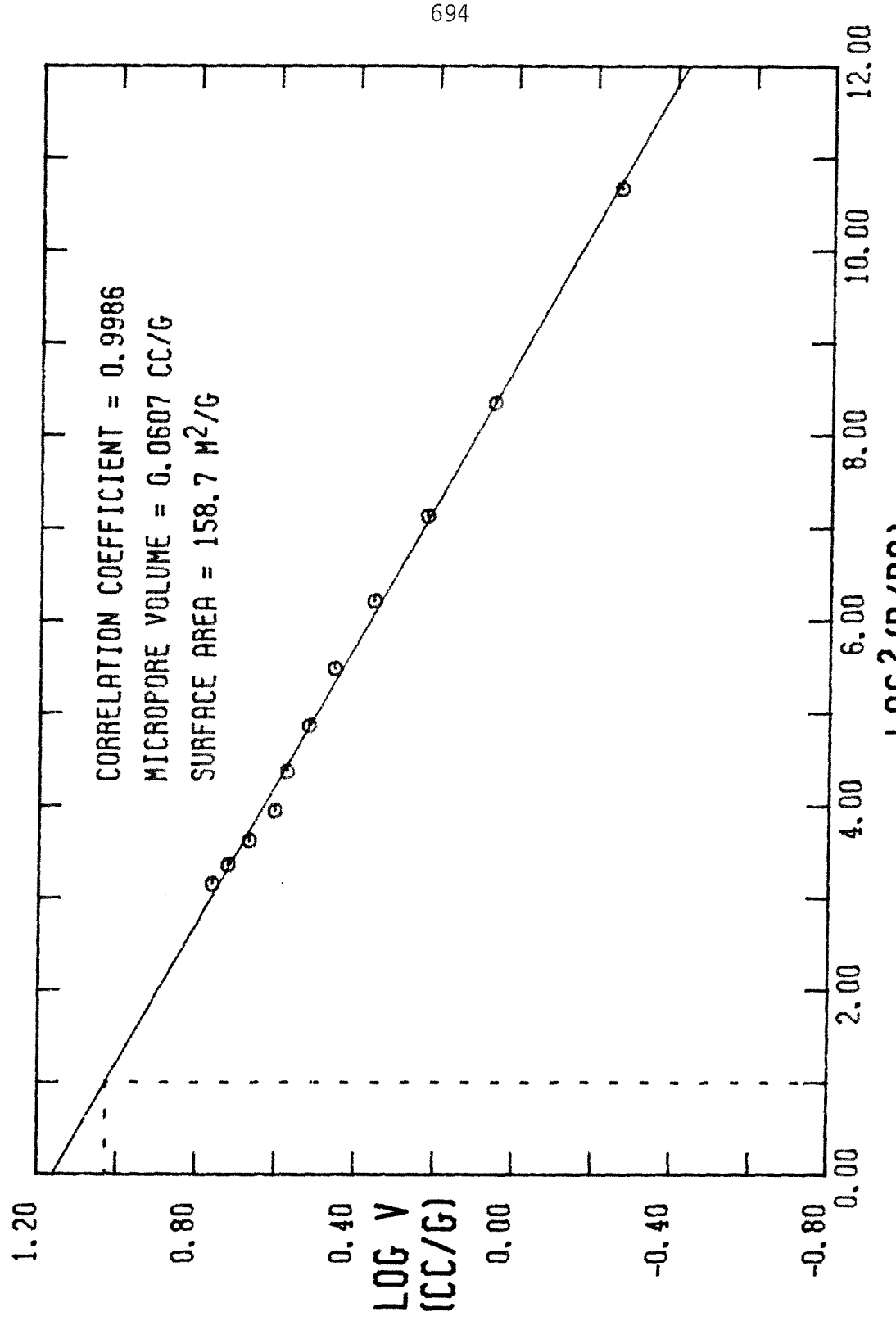
DPR PLOT FOR RUN 41
CORRELATION COEFFICIENT = 0.9986
MICROPORE VOLUME = 0.0607 CC/G
SURFACE AREA = 158.7 M2/G
LOG V (CC/G)
LOG2 (P/P0)
1.20
0.80
0.40
0.00
-0.40
-0.80
0.00
2.00
4.00
6.00
8.00
10.00
12.00

FIGURE A-131

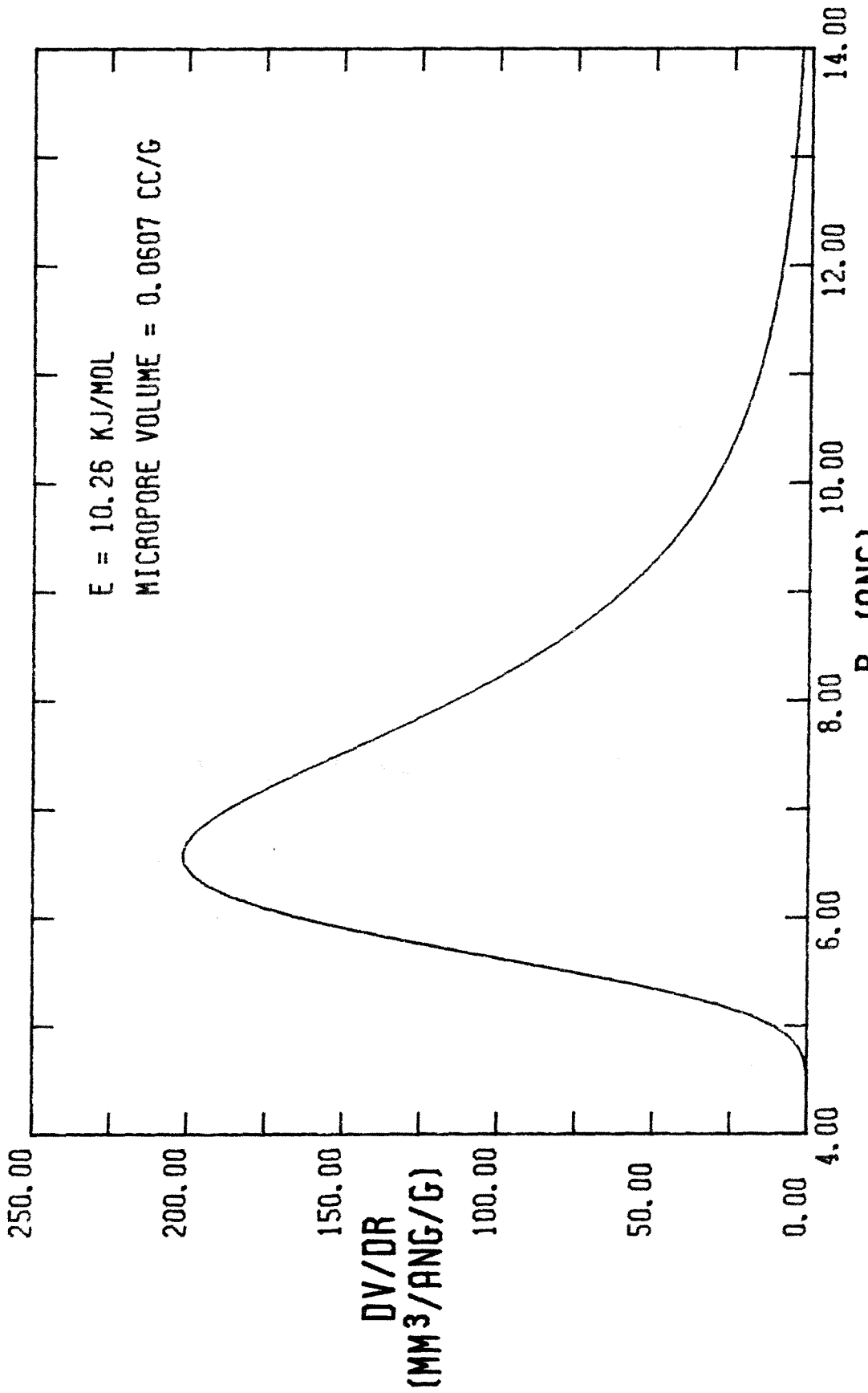
MICROPORE SIZE DISTRIBUTION FOR RUN 41
E = 10.26 KJ/MOL
MICROPORE VOLUME = 0.0607 CC/G
DV/DR
(MM3/ANG/G)
250.00
200.00
150.00
100.00
50.00
0.00
4.00
6.00
8.00
10.00
12.00
14.00
R (ANG)

FIGURE A-132

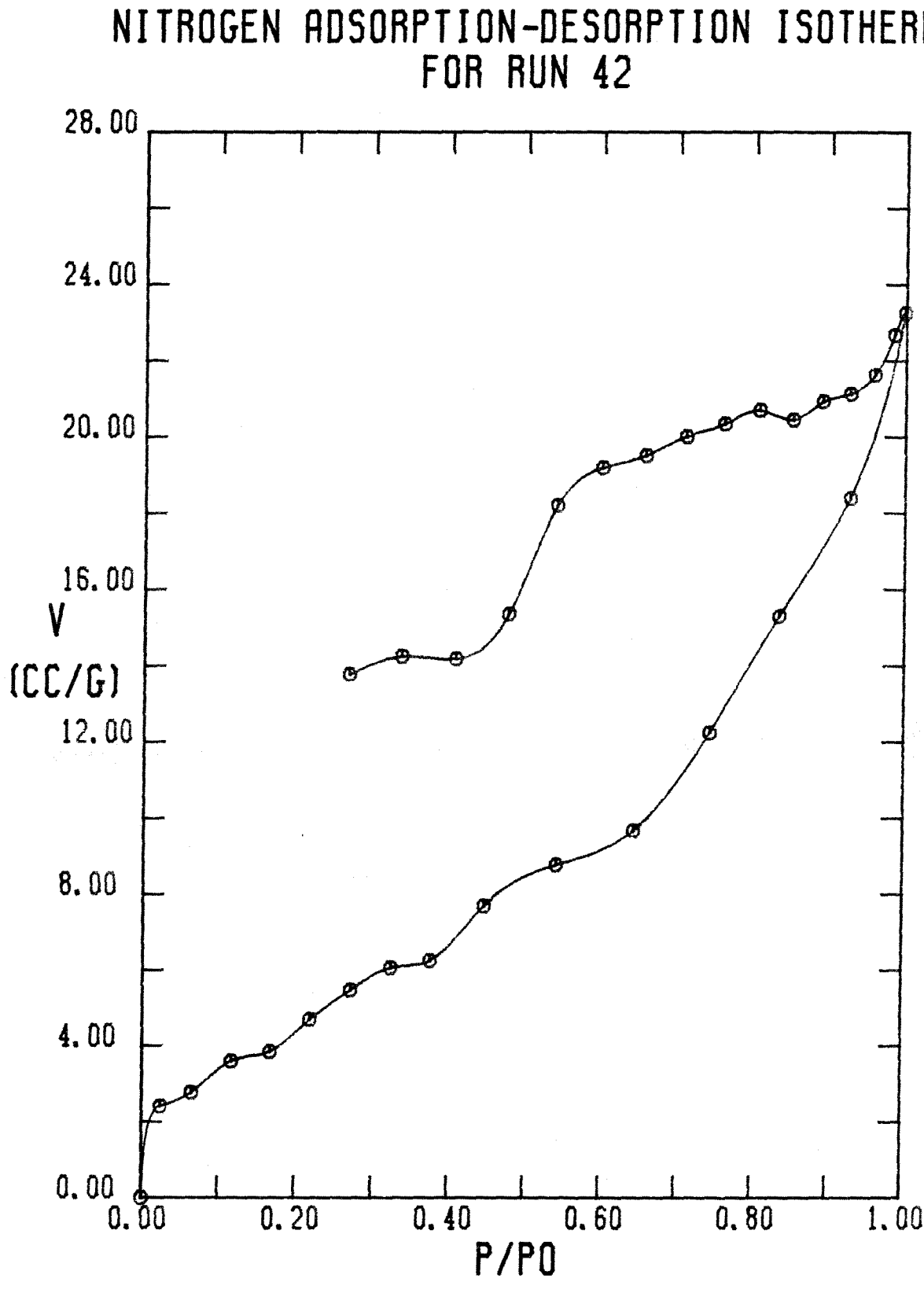
NITROGEN ADSORPTION-DESORPTION ISOTHERM
FOR RUN 42
28.00
24.00
20.00
16.00
V
(CC/G)
12.00
8.00
4.00
0.00
0.00
0.20
0.40
0.60
0.80
1.00
P/PO

FIGURE A-133

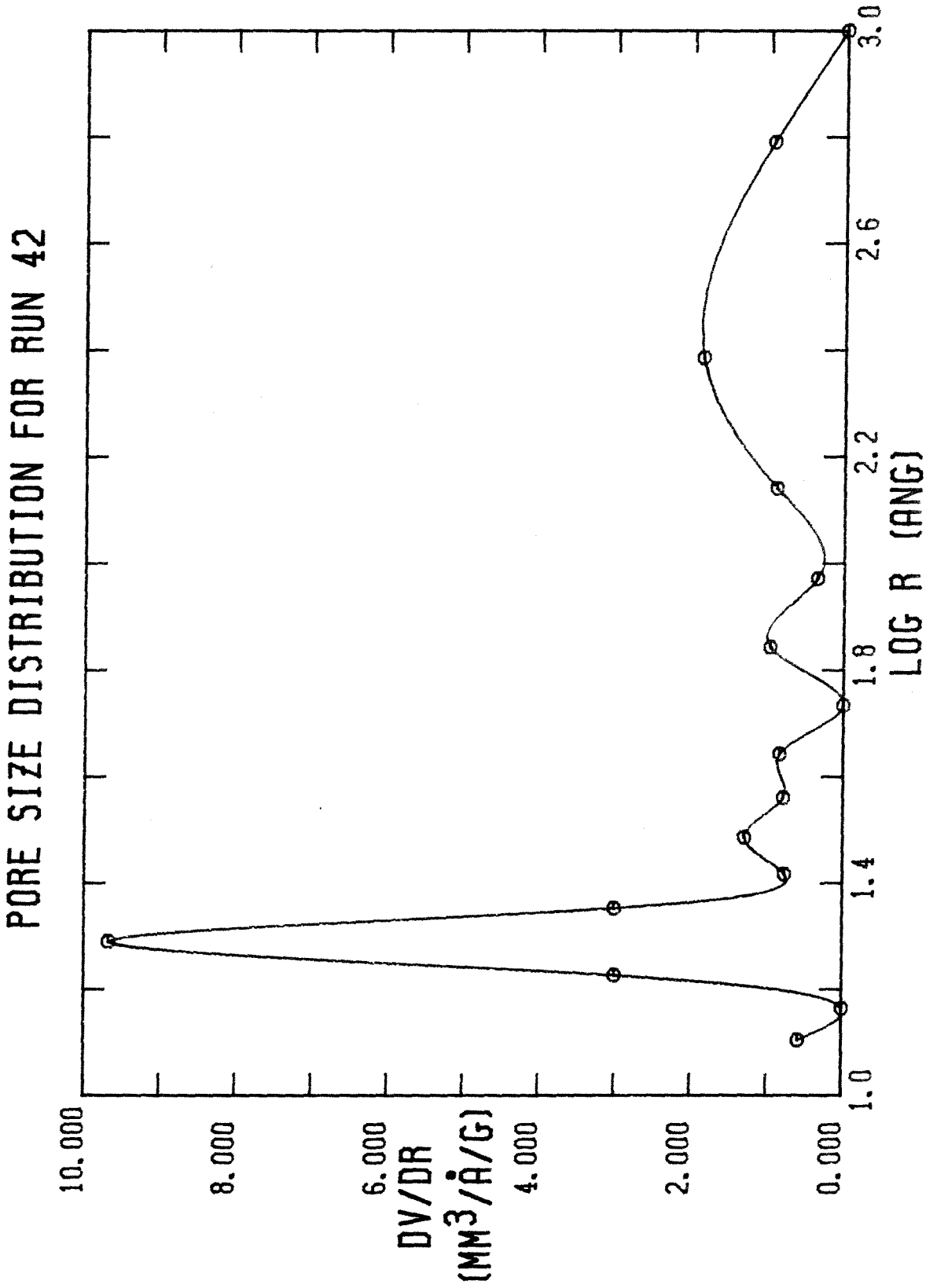
PORE SIZE DISTRIBUTION FOR RUN 42
DV/DR
(MM3/Å/G)
10.000
8.000
6.000
4.000
2.000
0.000
1.0
1.4
1.8
2.2
2.6
3.0
LOG R (ANG)

FIGURE A-134

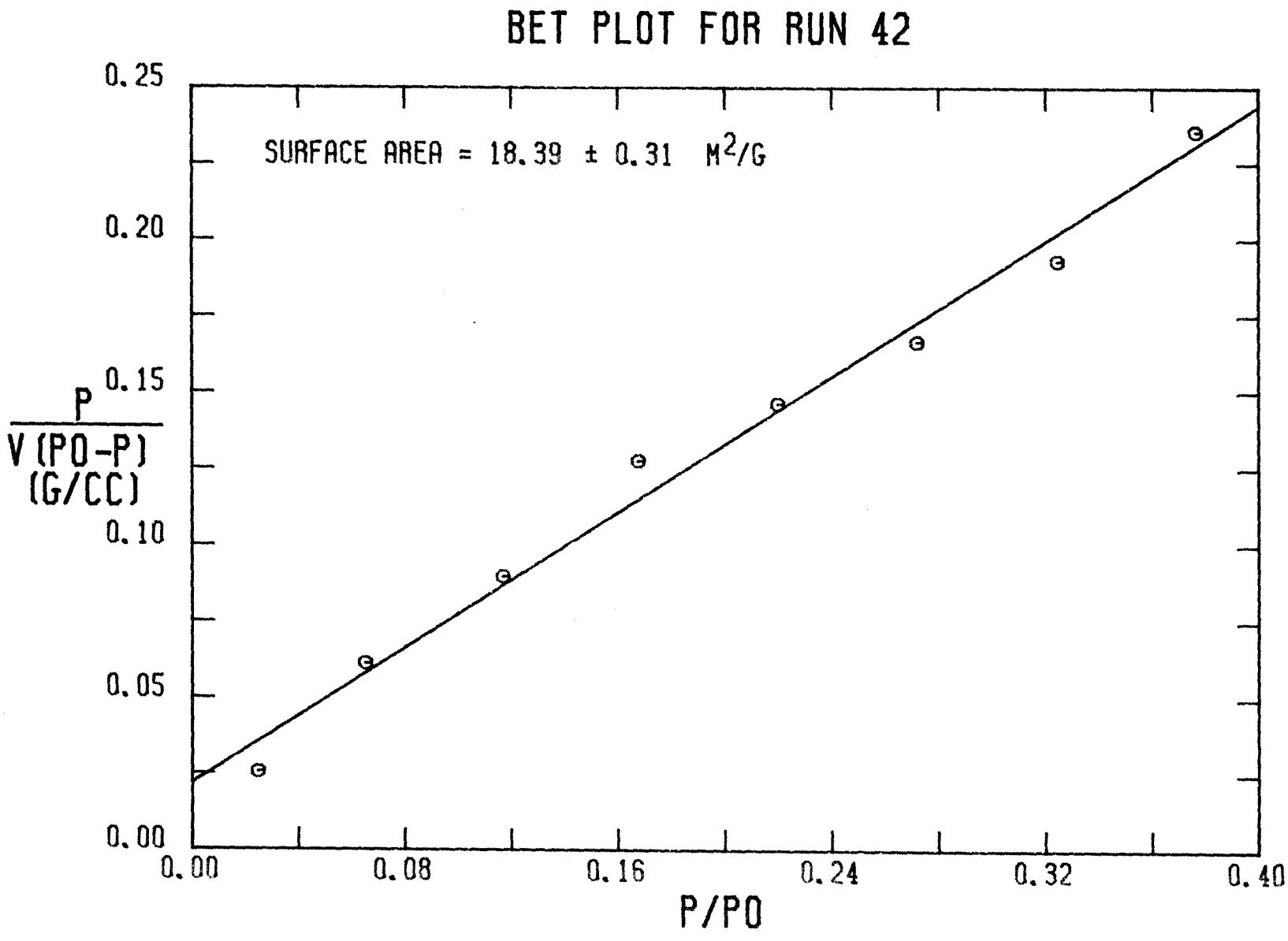
BET PLOT FOR RUN 42
SURFACE AREA = 18.39 ± 0.31 M2/G
P / V (PO-P) (G/CC)
0.25
0.20
0.15
0.10
0.05
0.00
0.00
0.08
0.16
0.24
0.32
0.40
P/PO

FIGURE A-135

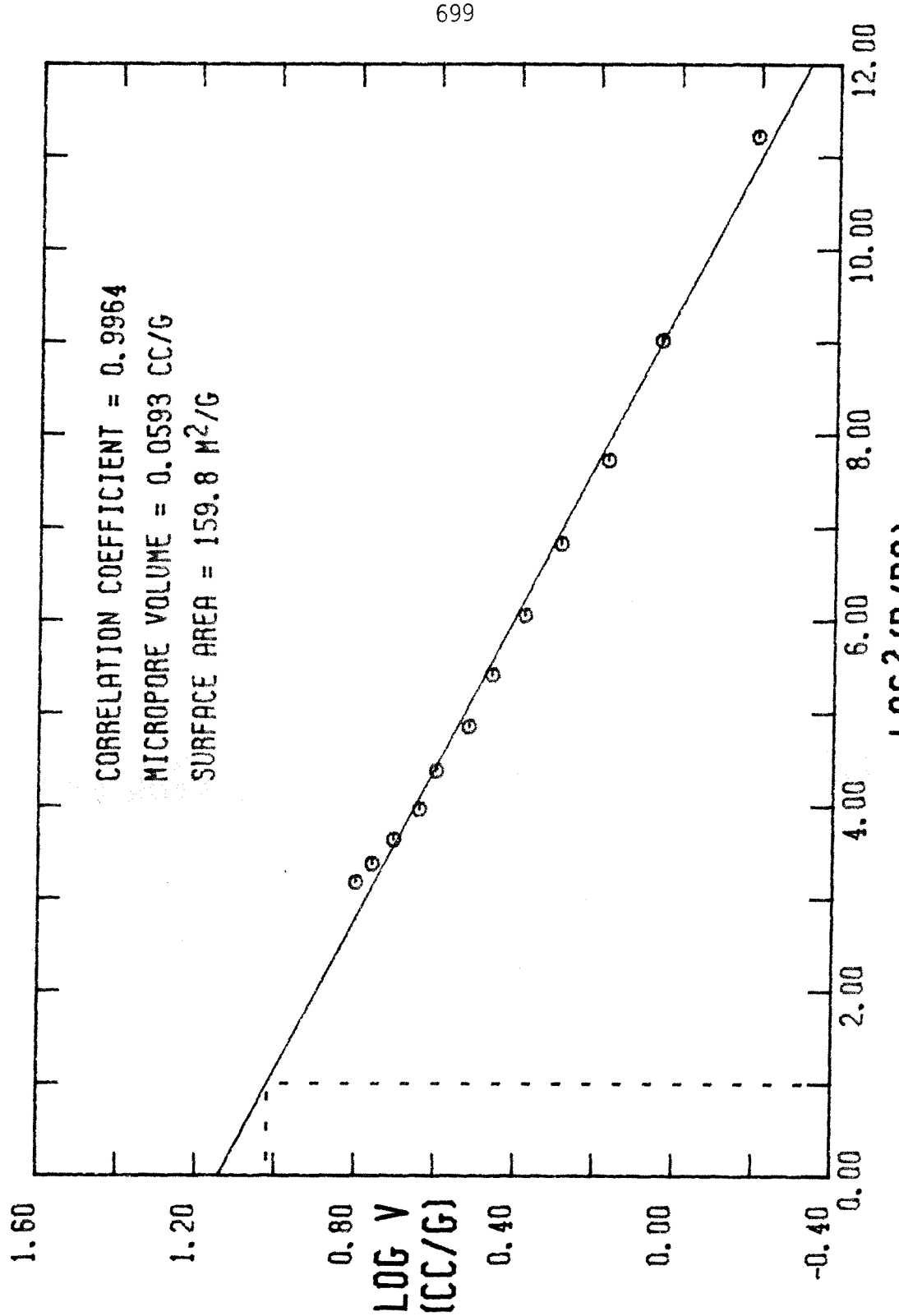
DPR PLOT FOR RUN 42
CORRELATION COEFFICIENT = 0.9964
MICROPORE VOLUME = 0.0593 CC/G
SURFACE AREA = 159.8 M2/G
LOG V (CC/G)
LOG2 (P/PO)
1.60
1.20
0.80
0.40
0.00
-0.40
0.00
2.00
4.00
6.00
8.00
10.00
12.00

FIGURE A-136

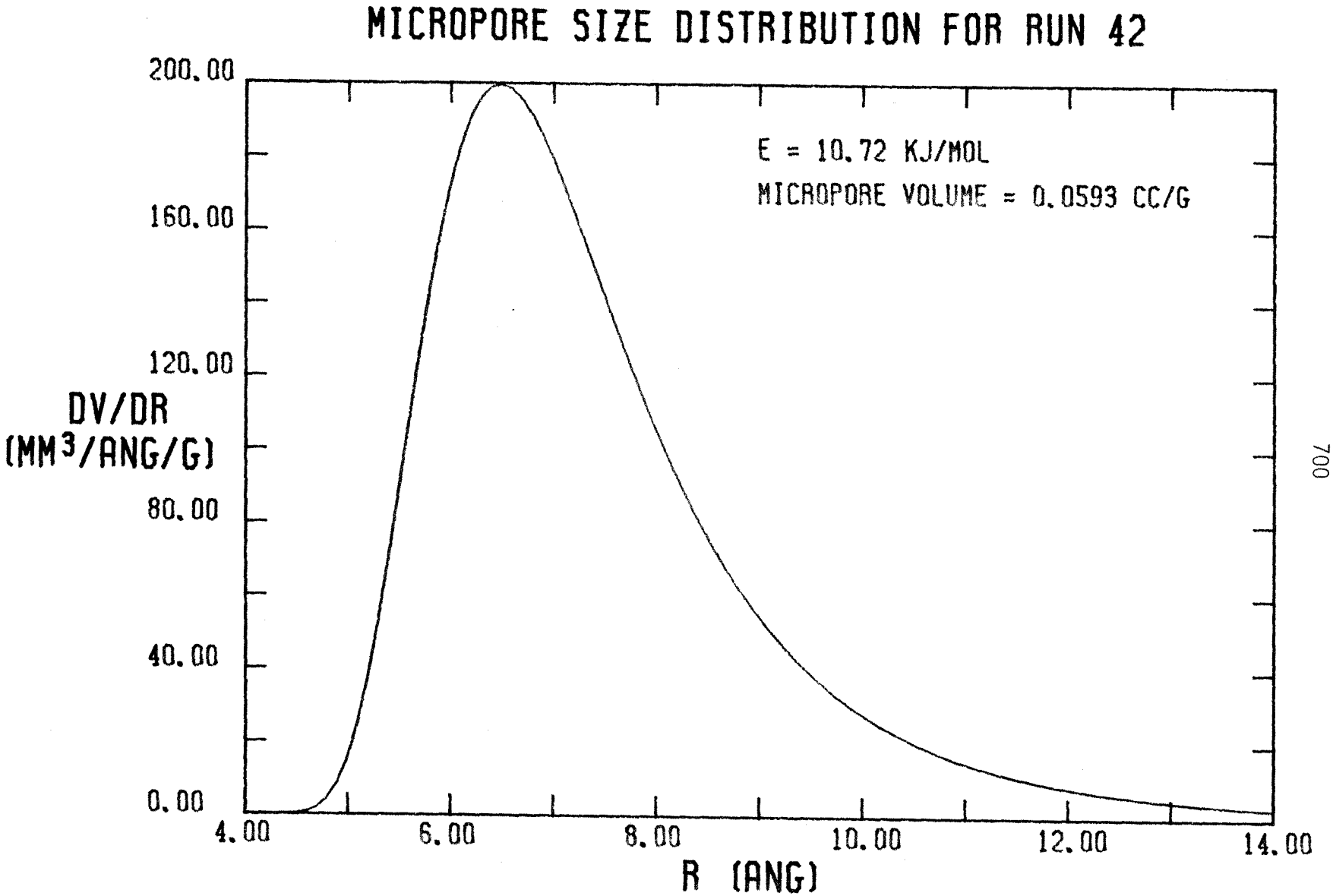
MICROPORE SIZE DISTRIBUTION FOR RUN 42
E = 10.72 KJ/MOL
MICROPORE VOLUME = 0.0593 CC/G
DV/DR
(MM3/ANG/G)
200.00
160.00
120.00
80.00
40.00
0.00
4.00
6.00
8.00
10.00
12.00
14.00
R (ANG)

FIGURE A-137

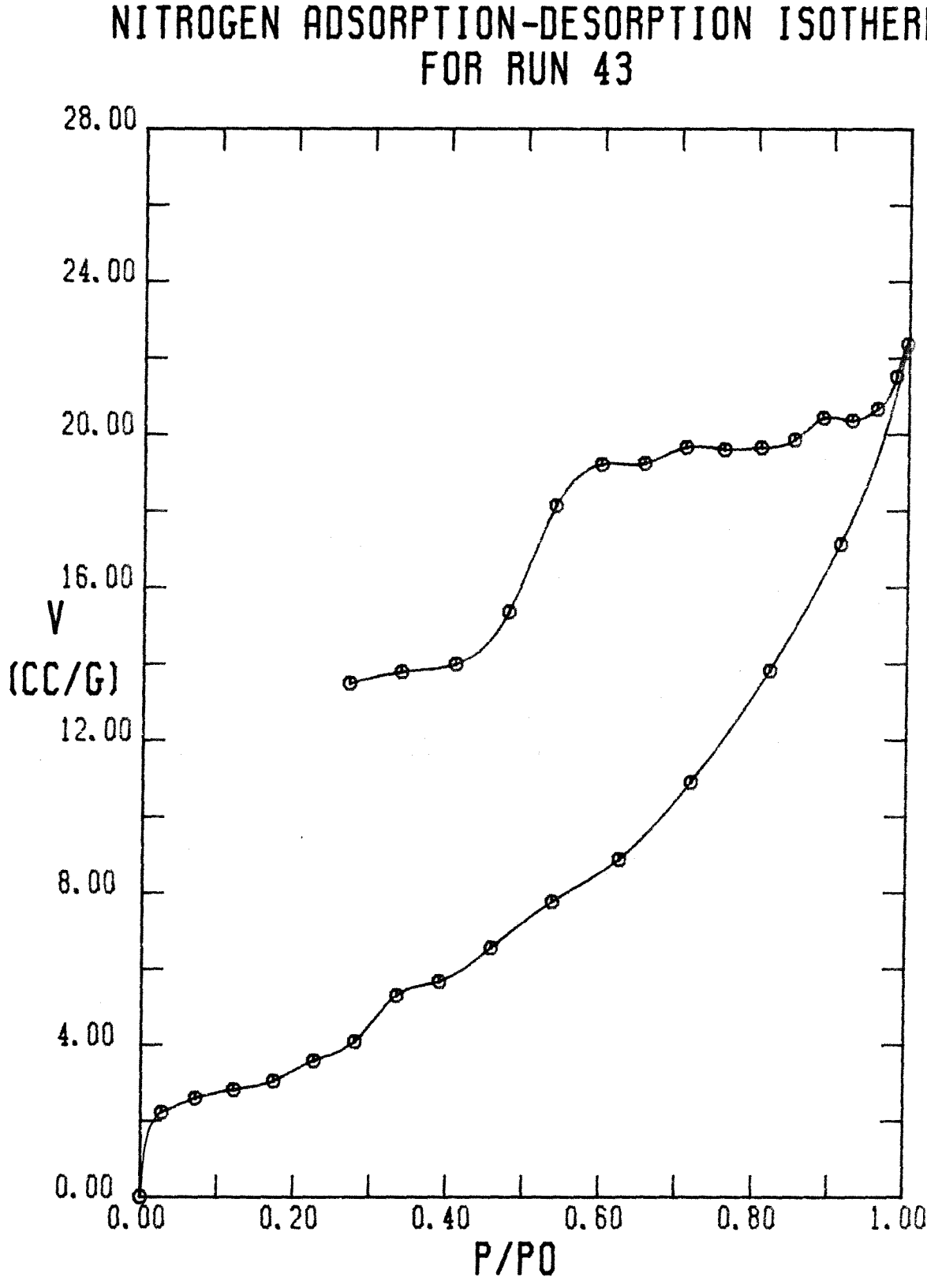
NITROGEN ADSORPTION-DESORPTION ISOTHERM
FOR RUN 43
28.00
24.00
20.00
16.00
12.00
8.00
4.00
0.00
V
(CC/G)
0.00
0.20
0.40
0.60
0.80
1.00
P/PO

FIGURE A-138

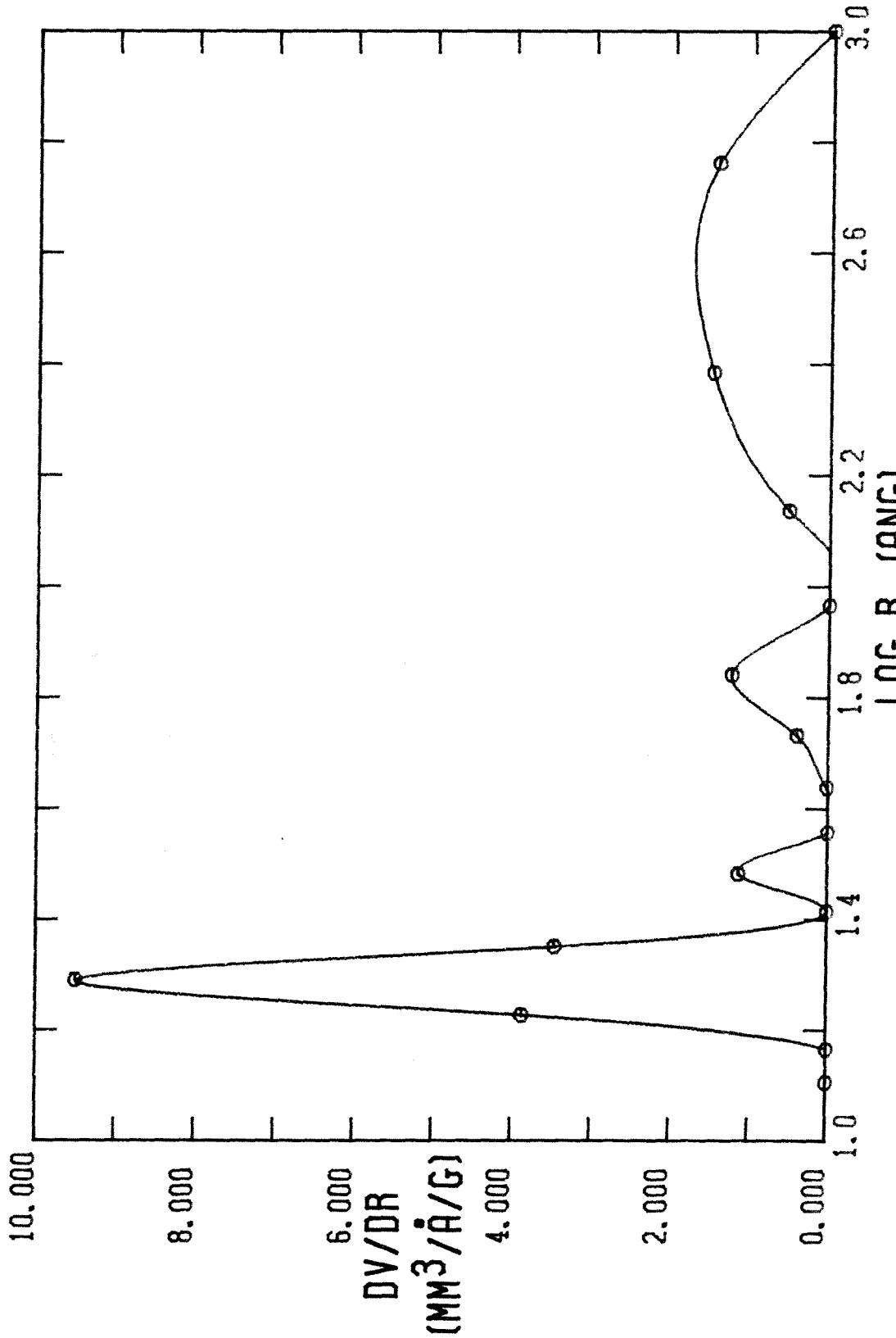
PORE SIZE DISTRIBUTION FOR RUN 43
DV/DR
(MM3/Å/G)
10.000
8.000
6.000
4.000
2.000
0.000
1.0
1.4
1.8
2.2
2.6
3.0
LOG R (ANG)

FIGURE A-139

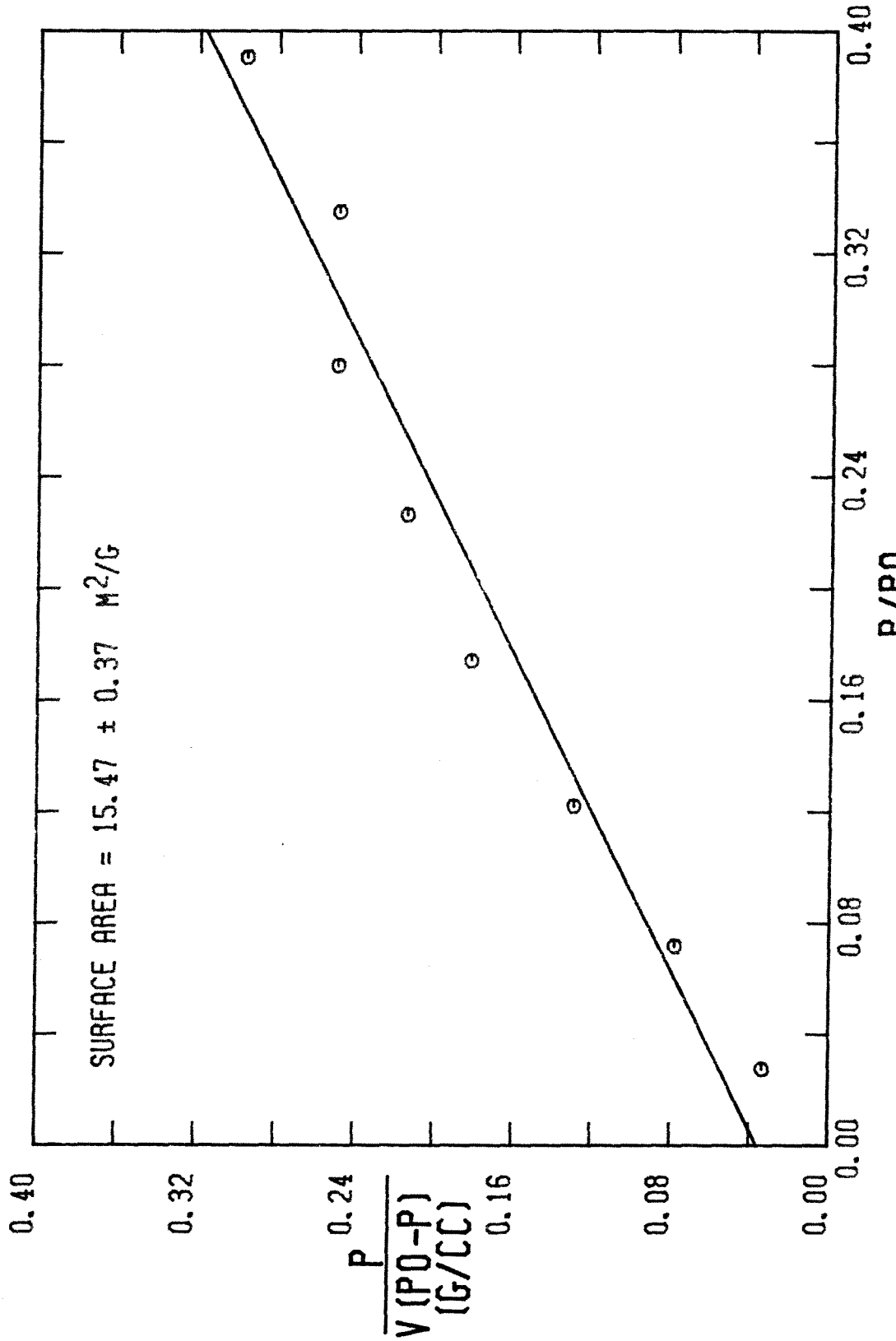
BET PLOT FOR RUN 43
SURFACE AREA = 15.47 ± 0.37 M2/G
P / V (PO-P) (G/CC)
P/PO
0.00
0.08
0.16
0.24
0.32
0.40

FIGURE A-140

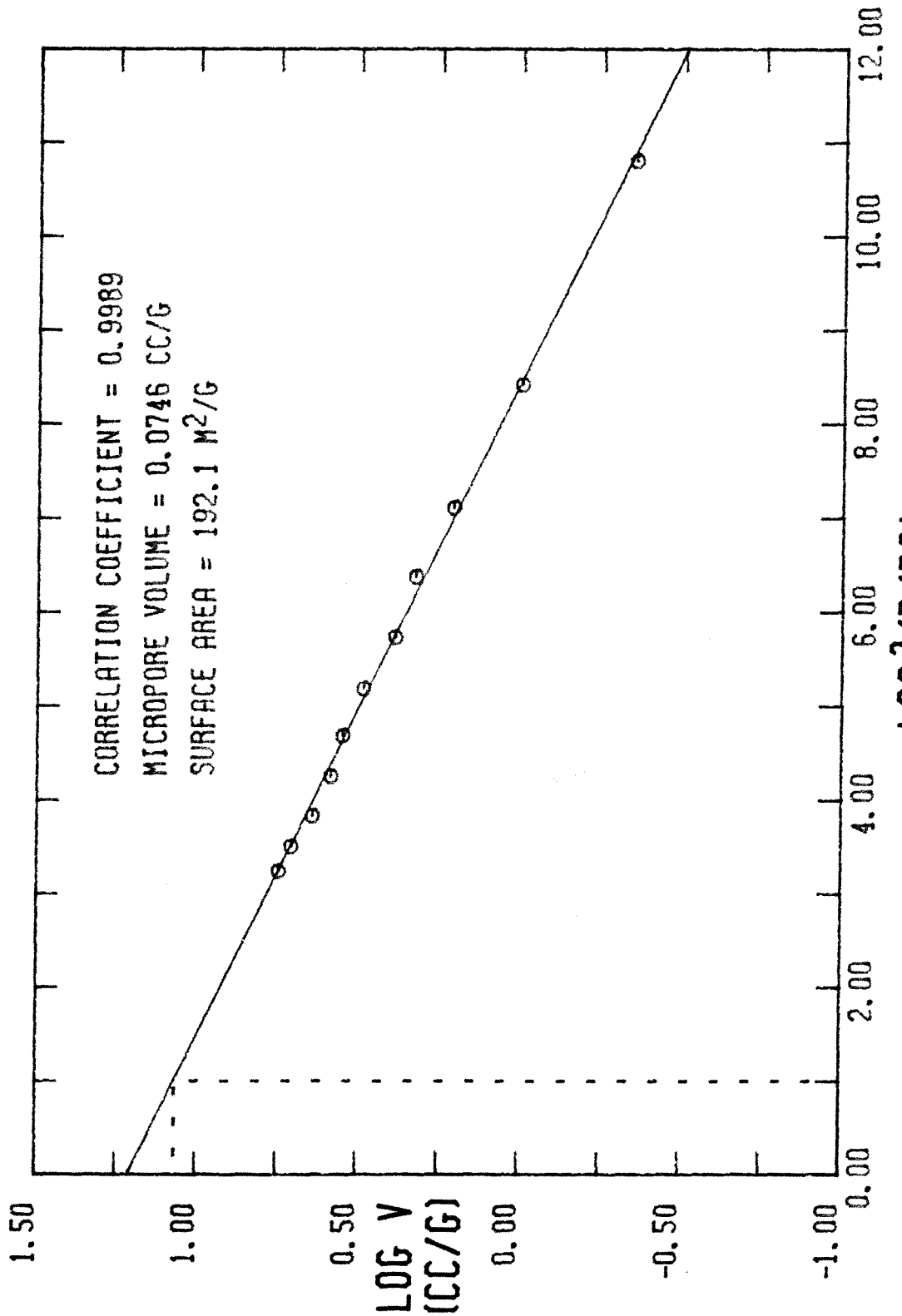
DPR PLOT FOR RUN 43
CORRELATION COEFFICIENT = 0.9989
MICROPORE VOLUME = 0.0746 CC/G
SURFACE AREA = 192.1 M2/G
LOG V (CC/G)
LOG2 (P/PO)
1.50
1.00
0.50
0.00
-0.50
-1.00
0.00
2.00
4.00
6.00
8.00
10.00
12.00

FIGURE A-141

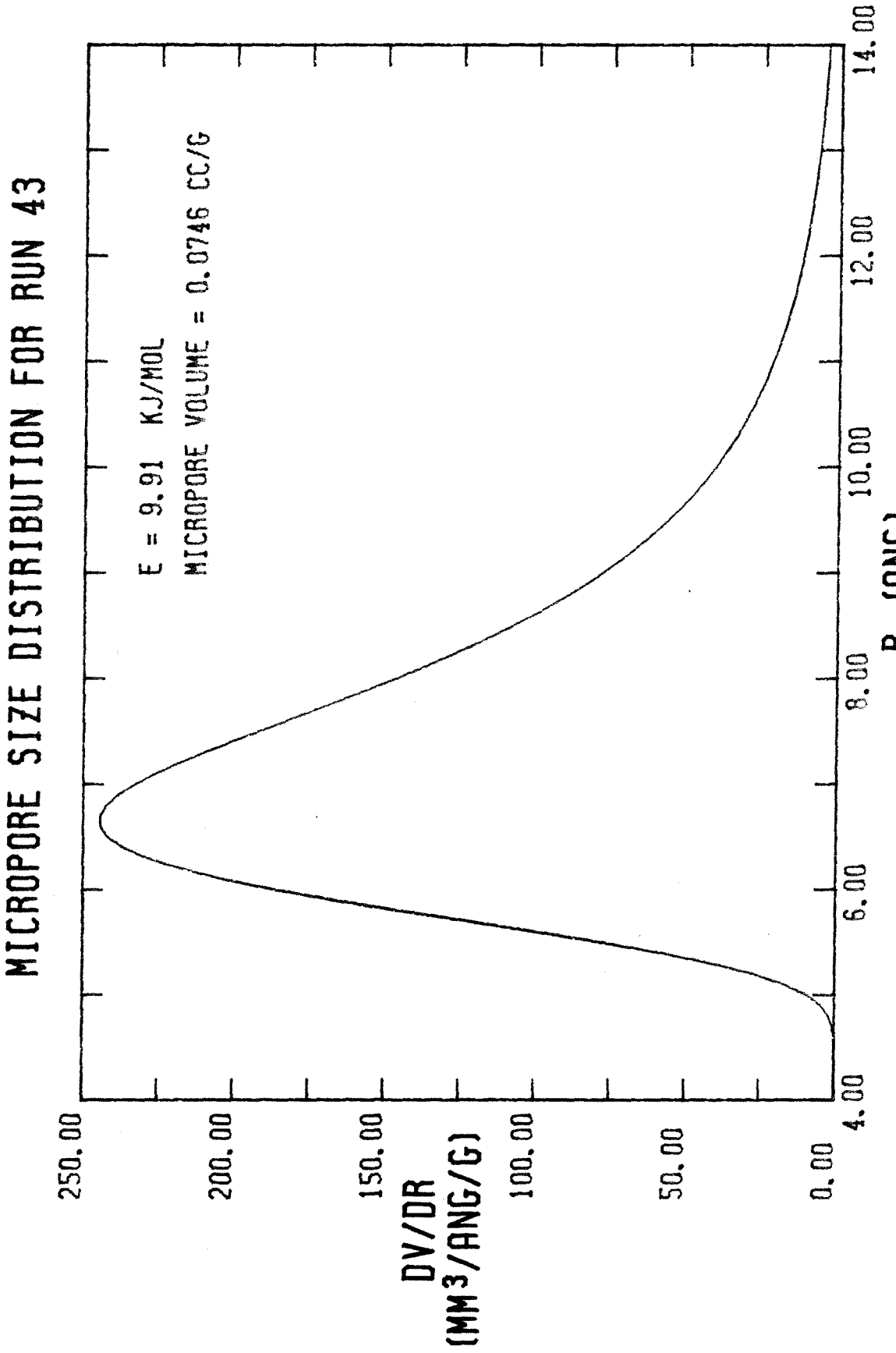
MICROPORE SIZE DISTRIBUTION FOR RUN 43
E = 9.91 KJ/MOL
MICROPORE VOLUME = 0.0746 CC/G
DV/DR
(MM3/ANG/G)
250.00
200.00
150.00
100.00
50.00
0.00
4.00
6.00
8.00
10.00
12.00
14.00
R (ANG)

FIGURE A-142

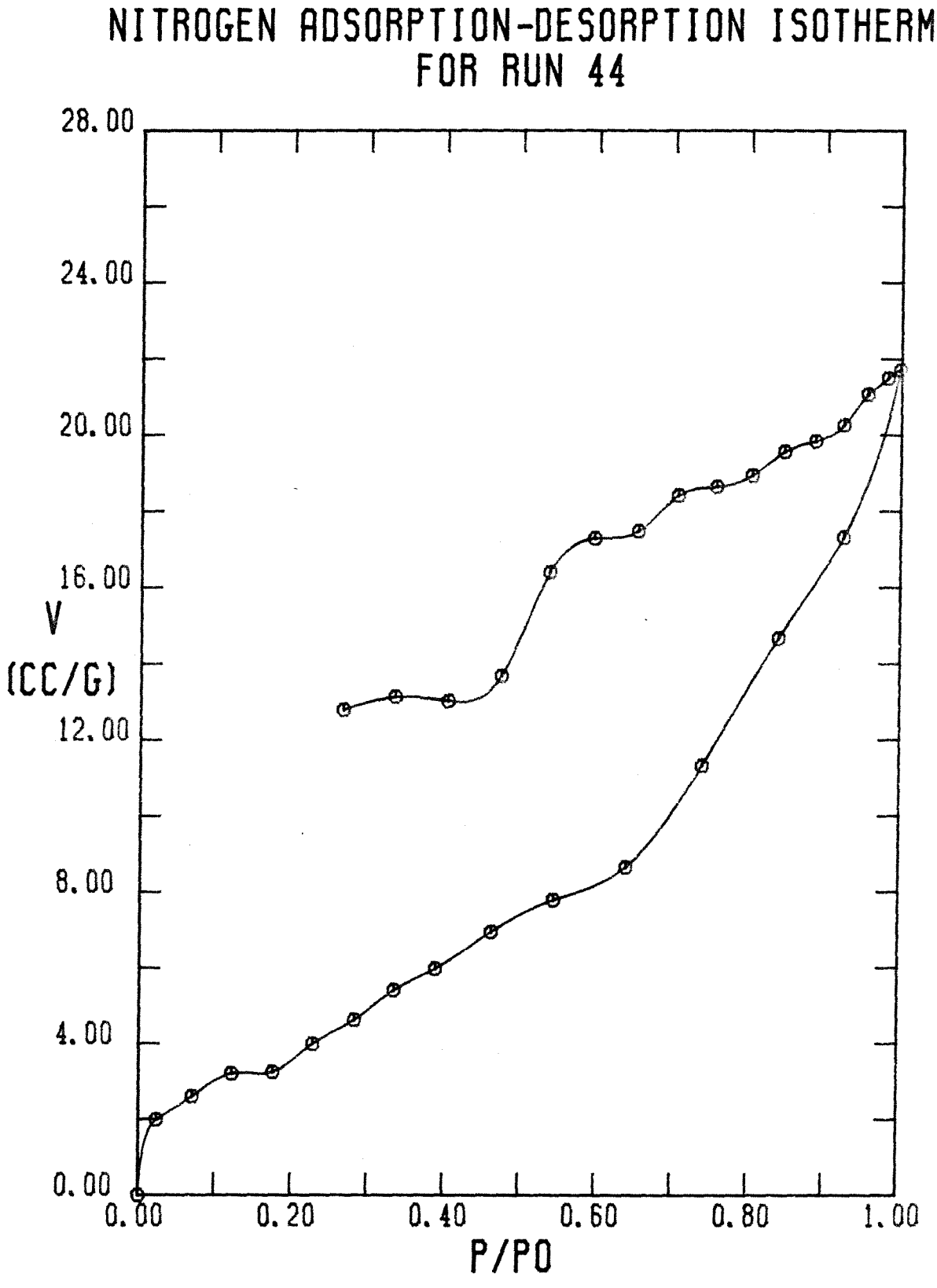
NITROGEN ADSORPTION-DESORPTION ISOTHERM
FOR RUN 44
28.00
24.00
20.00
16.00
12.00
8.00
4.00
0.00
V
(CC/G)
0.00
0.20
0.40
0.60
0.80
1.00
P/PO

FIGURE A-143

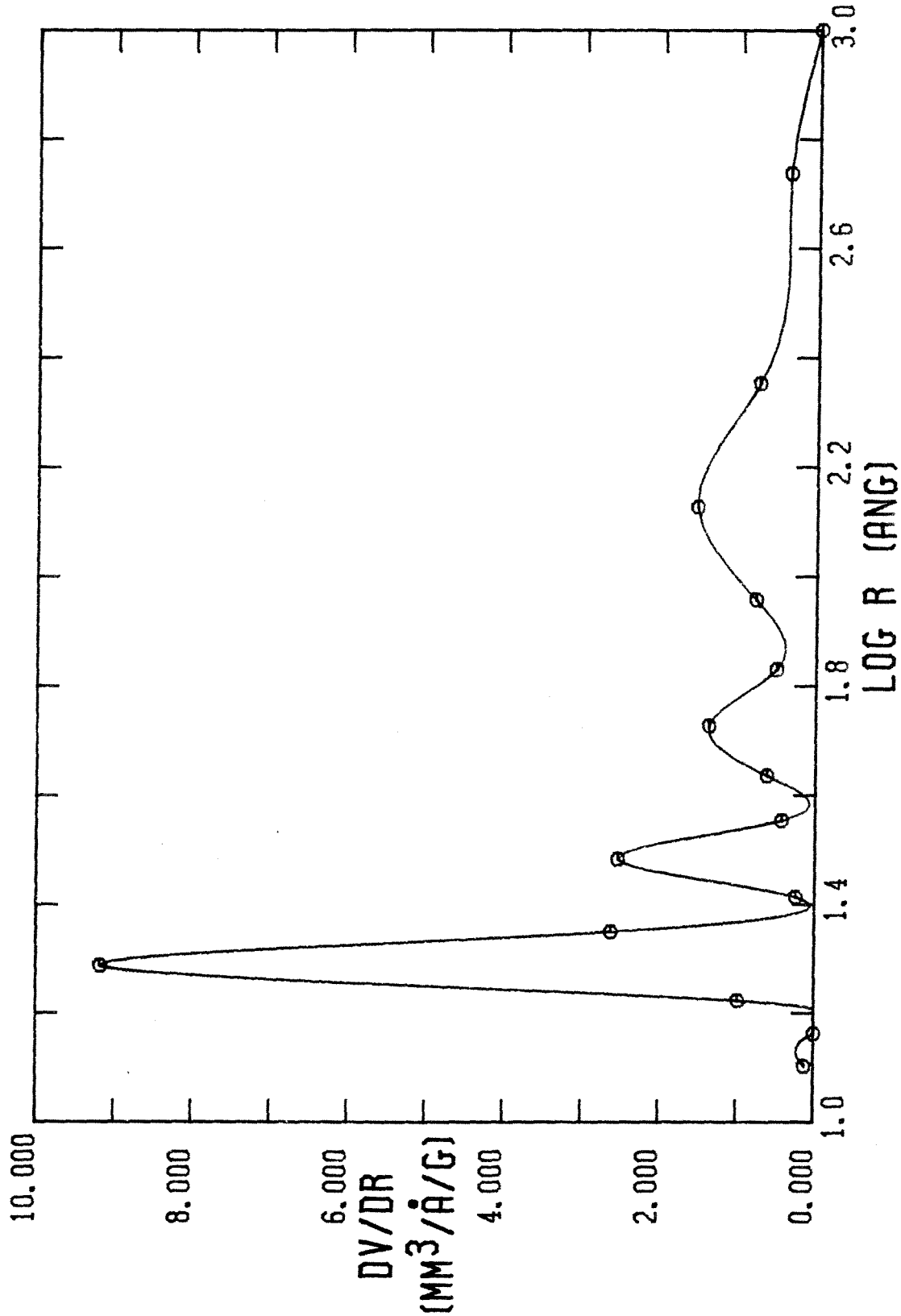
PORE SIZE DISTRIBUTION FOR RUN 44
DV/DR
(MM3/Å/G)
10.000
8.000
6.000
4.000
2.000
0.000
1.0
1.4
1.8
2.2
2.6
3.0
LOG R (ANG)

FIGURE A-144

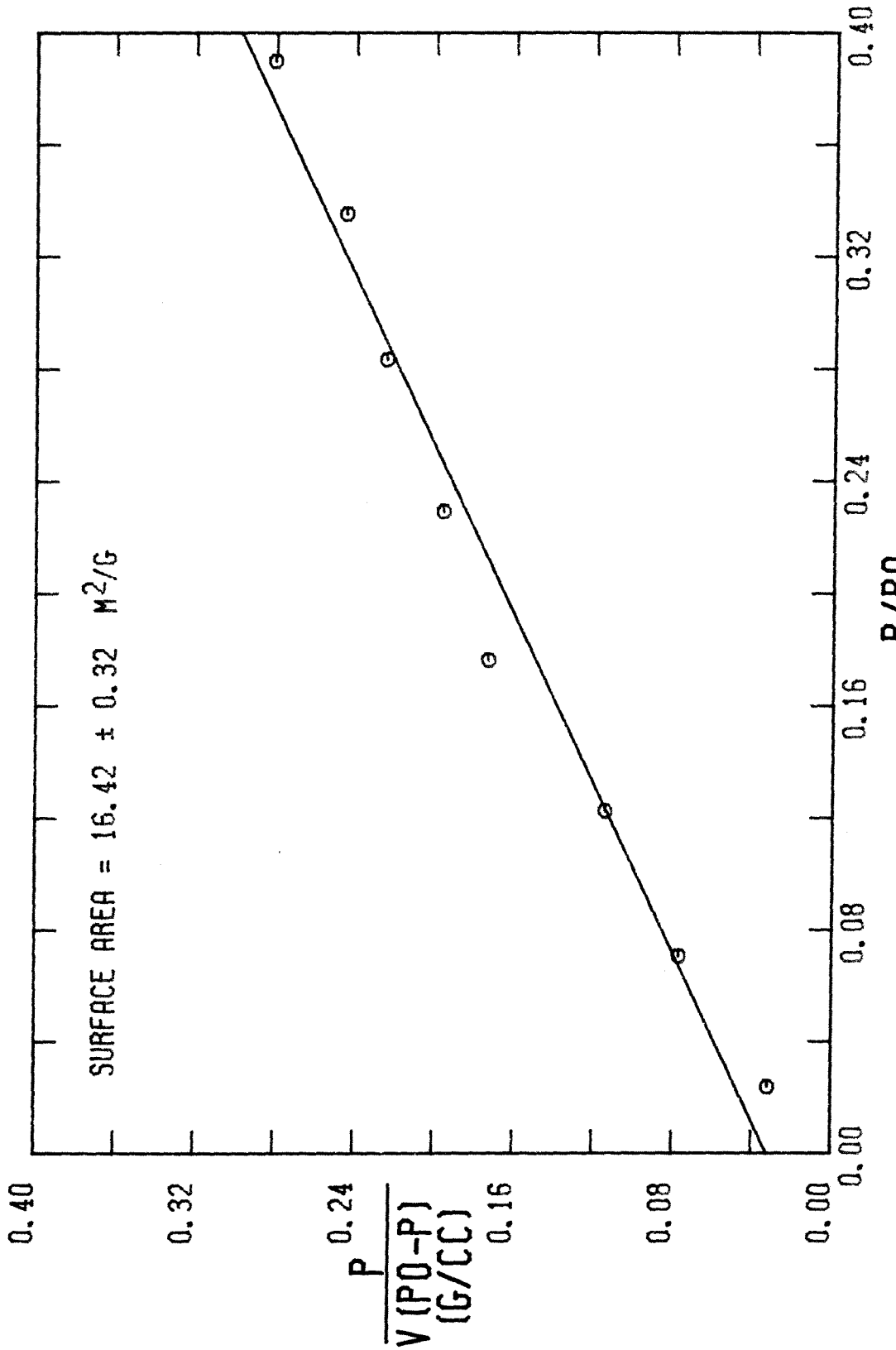
BET PLOT FOR RUN 44
SURFACE AREA = 16.42 ± 0.32 M2/G
P/PO
P / V (PO-P) (G/CC)
0.00
0.08
0.16
0.24
0.32
0.40

FIGURE A-145

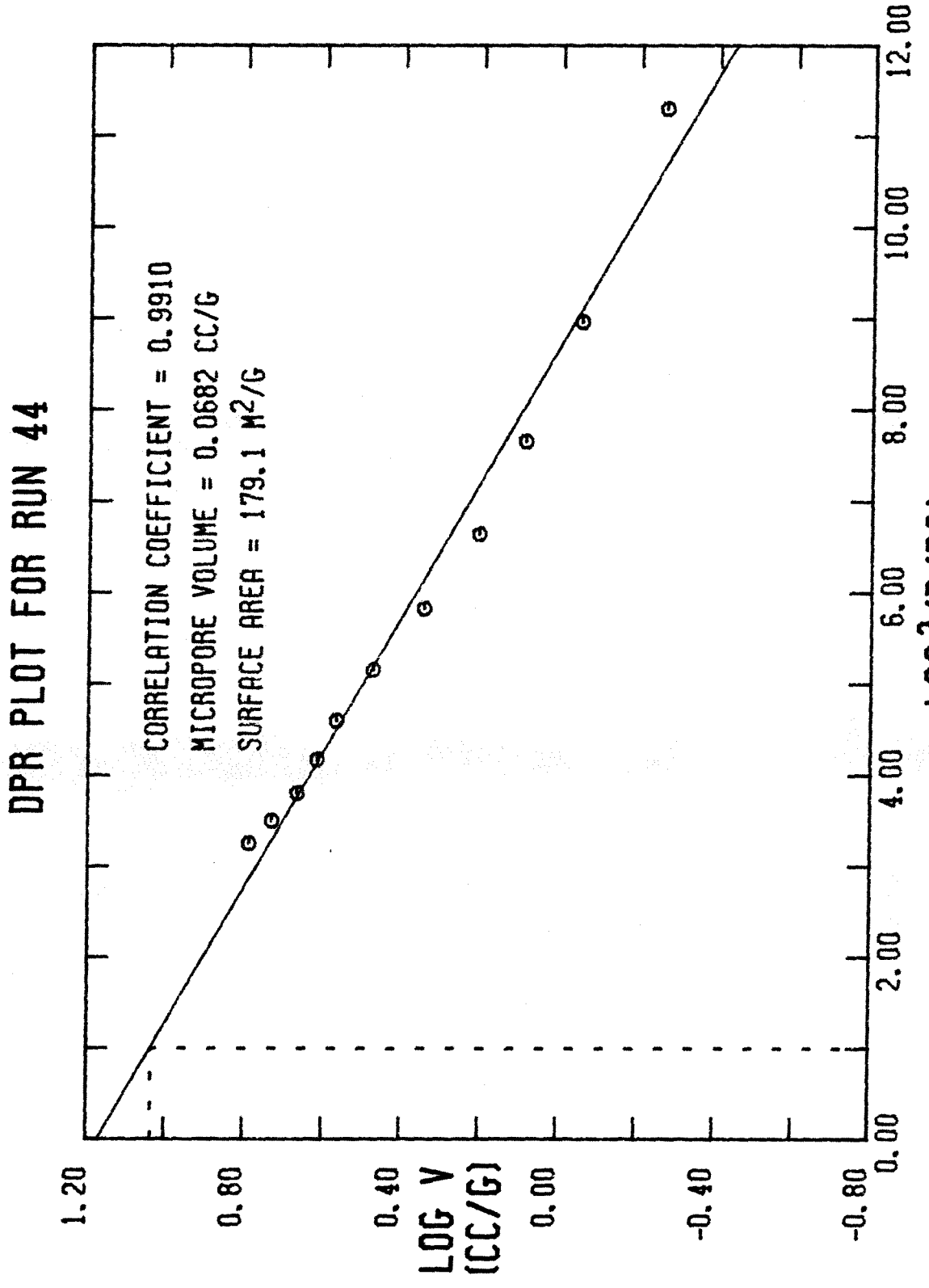
DPR PLOT FOR RUN 44
CORRELATION COEFFICIENT = 0.9910
MICROPORE VOLUME = 0.0682 CC/G
SURFACE AREA = 179.1 M2/G
LOG V (CC/G)
LOG2 (P/PO)
1.20
0.80
0.40
0.00
-0.40
-0.80
0.00
2.00
4.00
6.00
8.00
10.00
12.00

FIGURE A-146

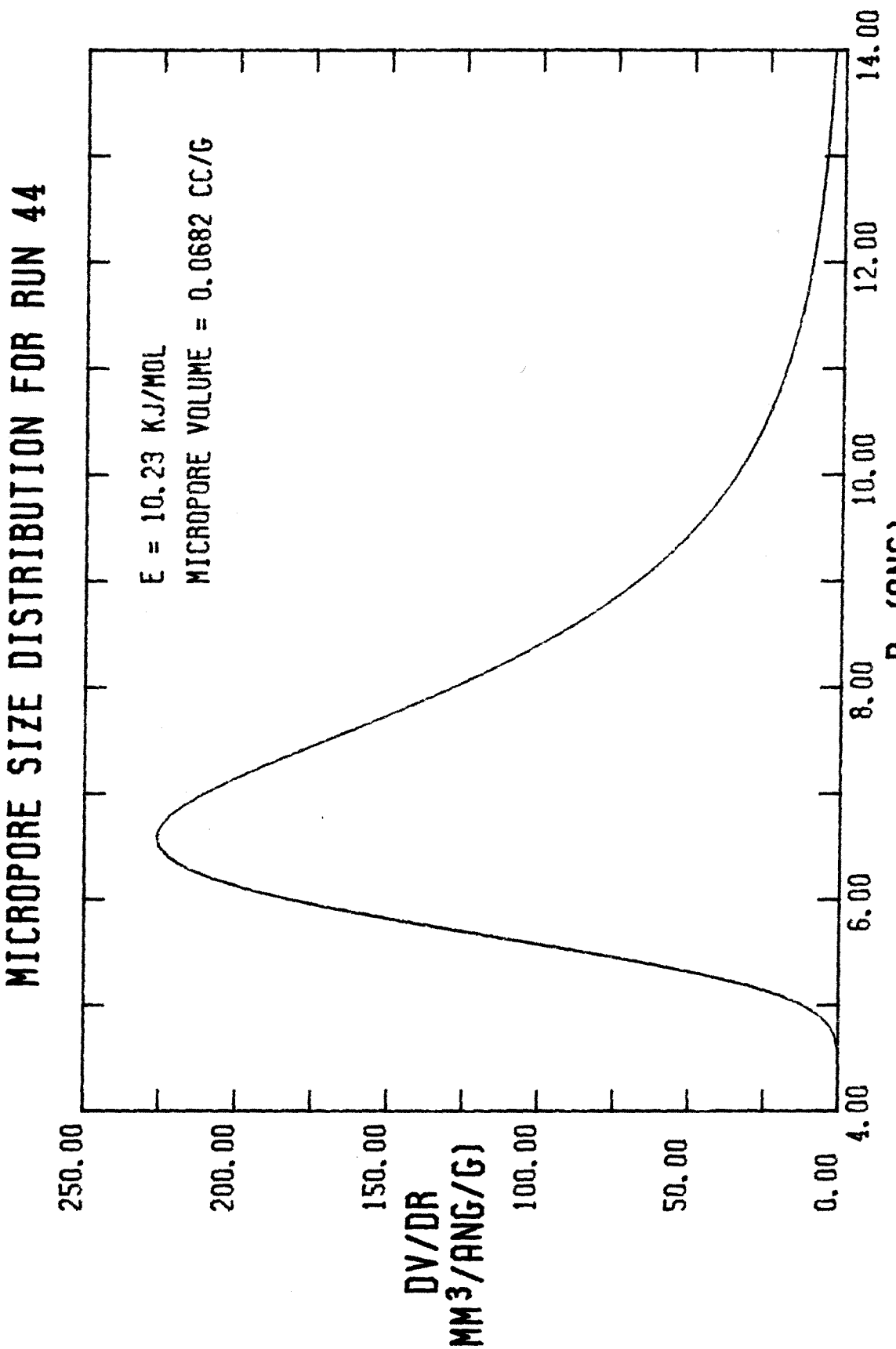
MICROPORE SIZE DISTRIBUTION FOR RUN 44
E = 10.23 KJ/MOL
MICROPORE VOLUME = 0.0682 CC/G
DV/DR
(MM3/ANG/G)
250.00
200.00
150.00
100.00
50.00
0.00
4.00
6.00
8.00
10.00
12.00
14.00
R (ANG)

FIGURE A-147

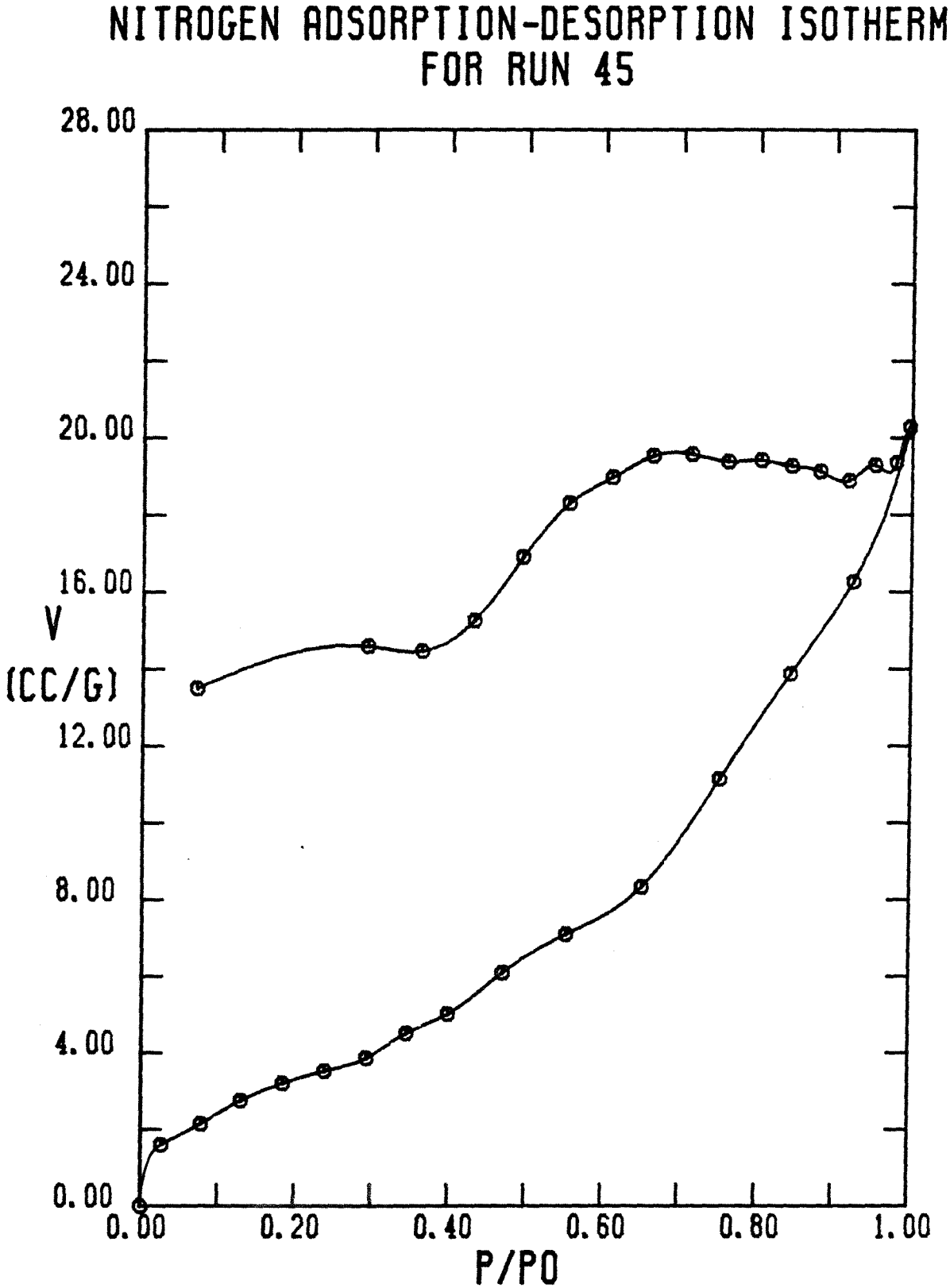
NITROGEN ADSORPTION-DESORPTION ISOTHERM
FOR RUN 45
28.00
24.00
20.00
16.00
12.00
8.00
4.00
0.00
V
(CC/G)
0.00
0.20
0.40
0.60
0.80
1.00
P/PO

FIGURE A-148

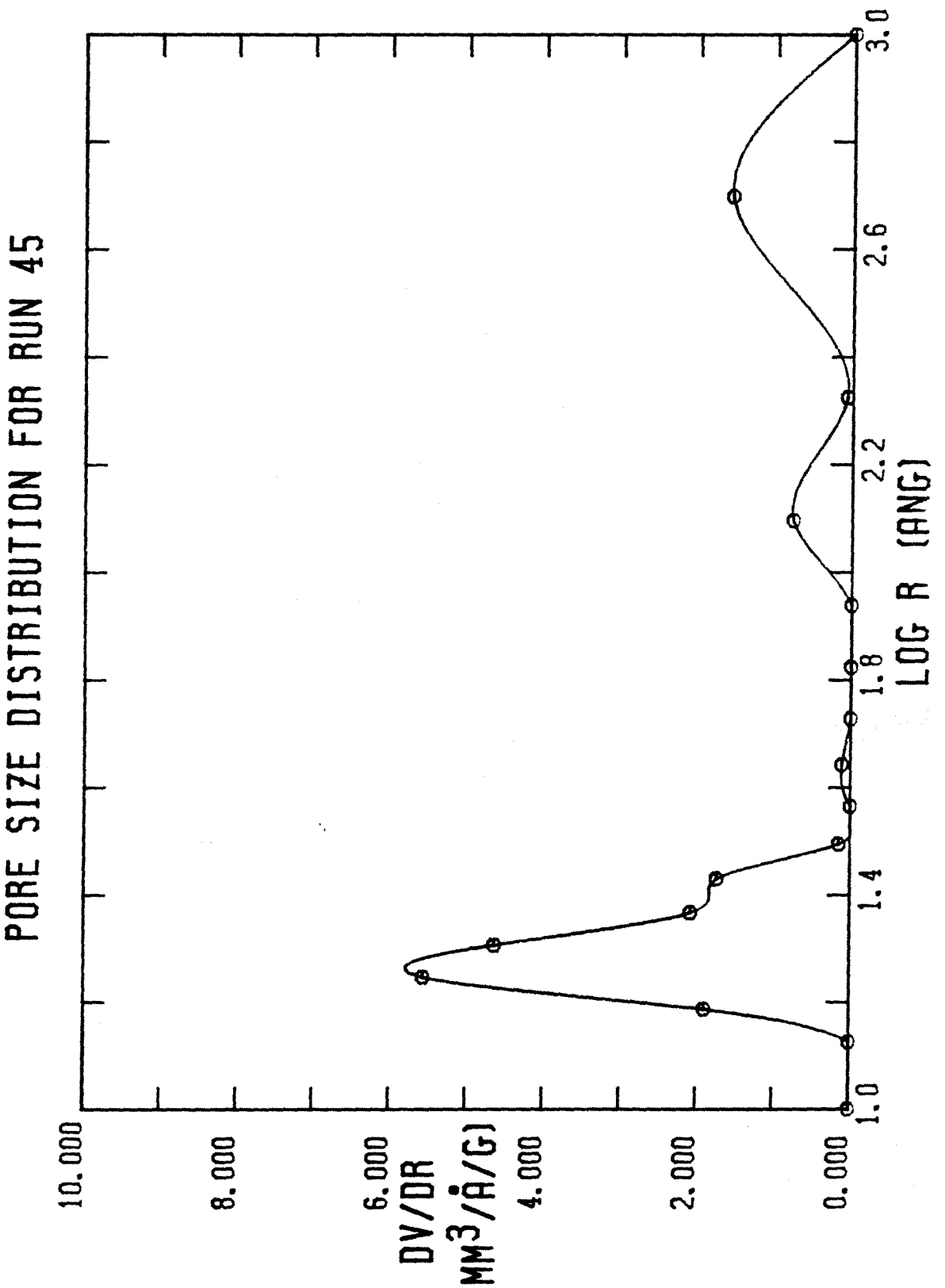
PORE SIZE DISTRIBUTION FOR RUN 45
DV/DR
(MM3/Å/G)
10.000
8.000
6.000
4.000
2.000
0.000
1.0
1.4
1.8
2.2
2.6
3.0
LOG R (ANG)

FIGURE A-149

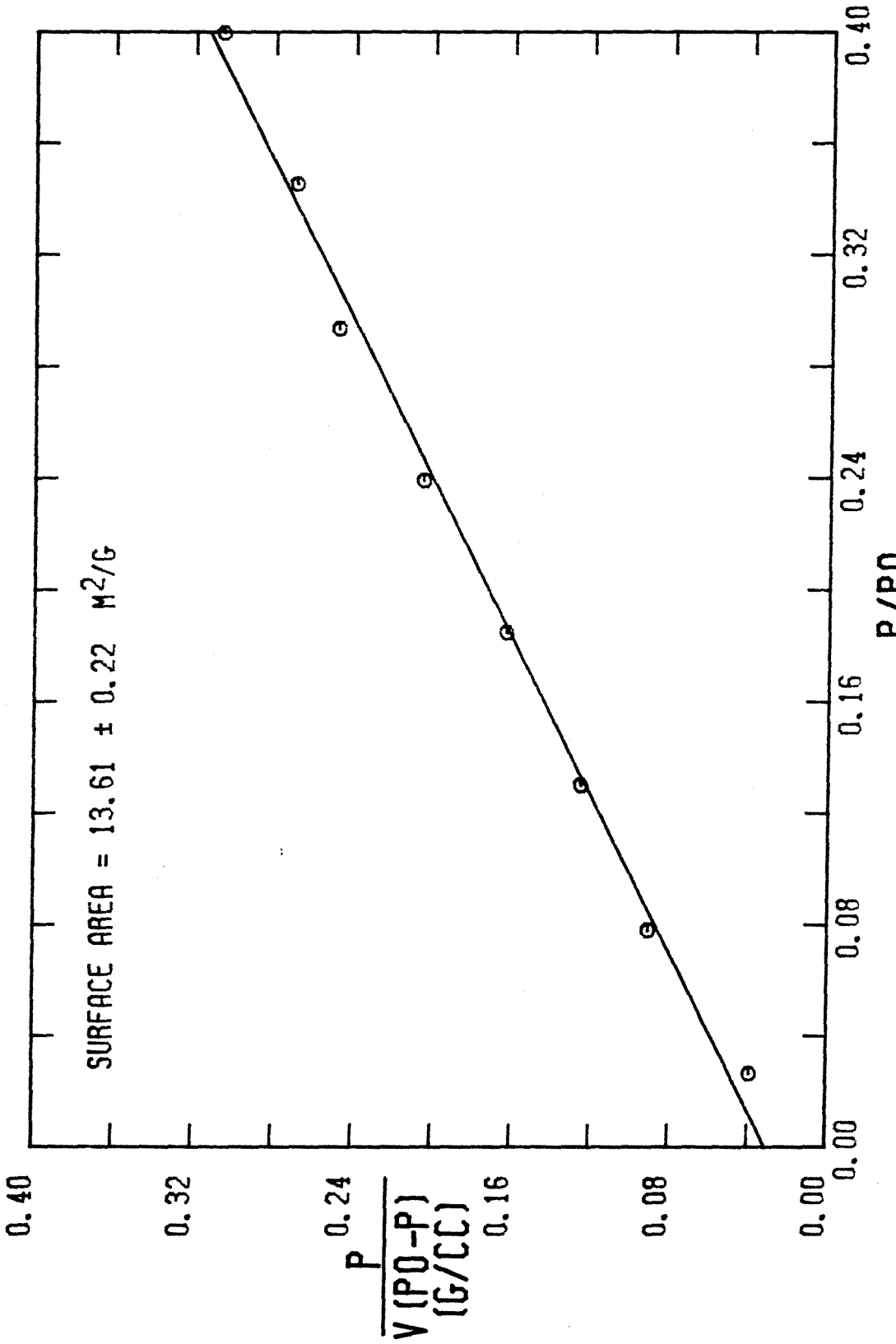
BET PLOT FOR RUN 45
SURFACE AREA = 13.61 ± 0.22 M2/G
P/PO
P / V(PO-P) (G/CC)
0.00
0.08
0.16
0.24
0.32
0.40

FIGURE A-150

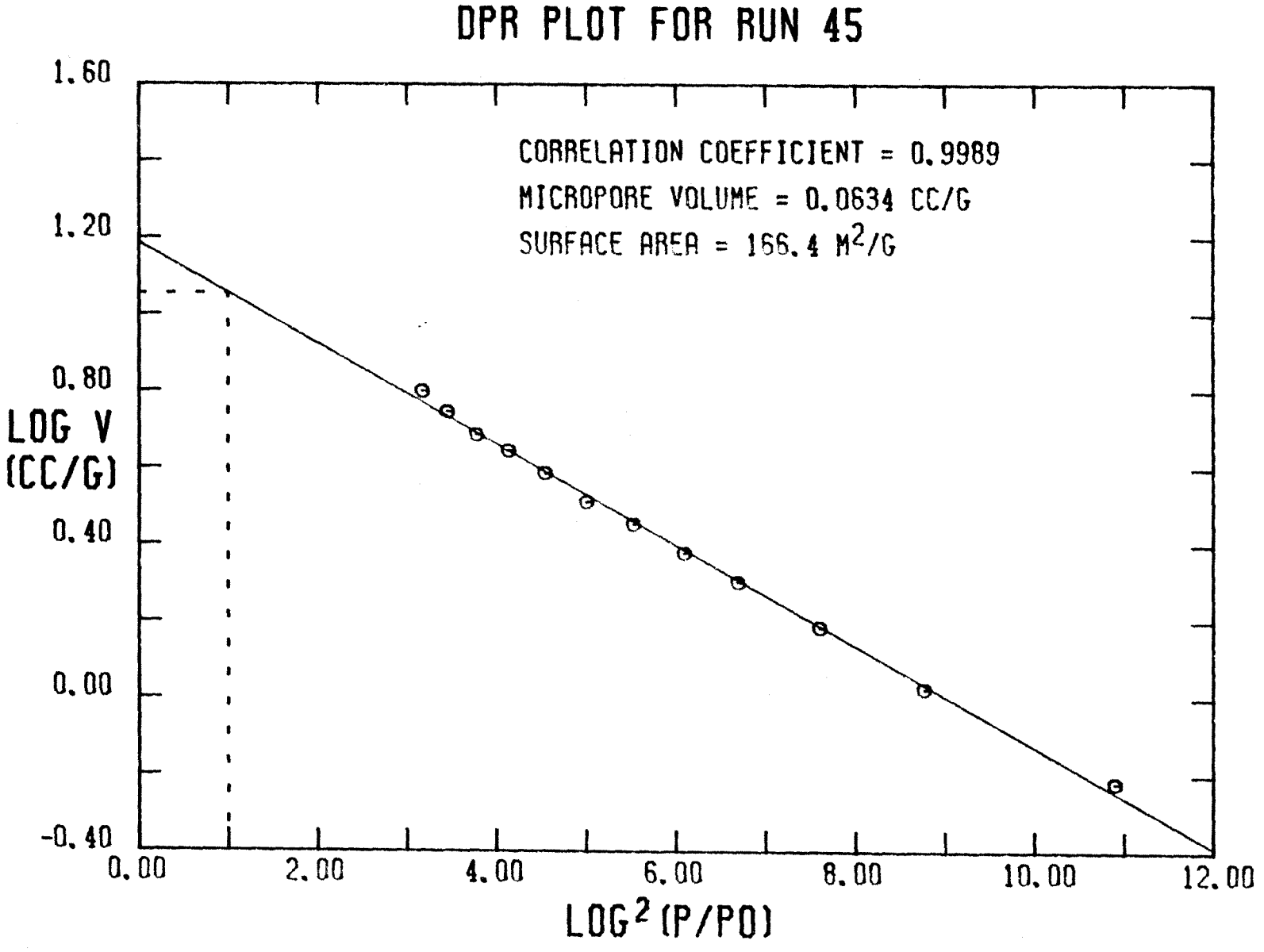
DPR PLOT FOR RUN 45
CORRELATION COEFFICIENT = 0.9989
MICROPORE VOLUME = 0.0634 CC/G
SURFACE AREA = 166.4 M2/G
1.60
1.20
0.80
0.40
0.00
-0.40
LOG V (CC/G)
0.00
2.00
4.00
6.00
8.00
10.00
12.00
LOG2 (P/PO)

FIGURE A-151

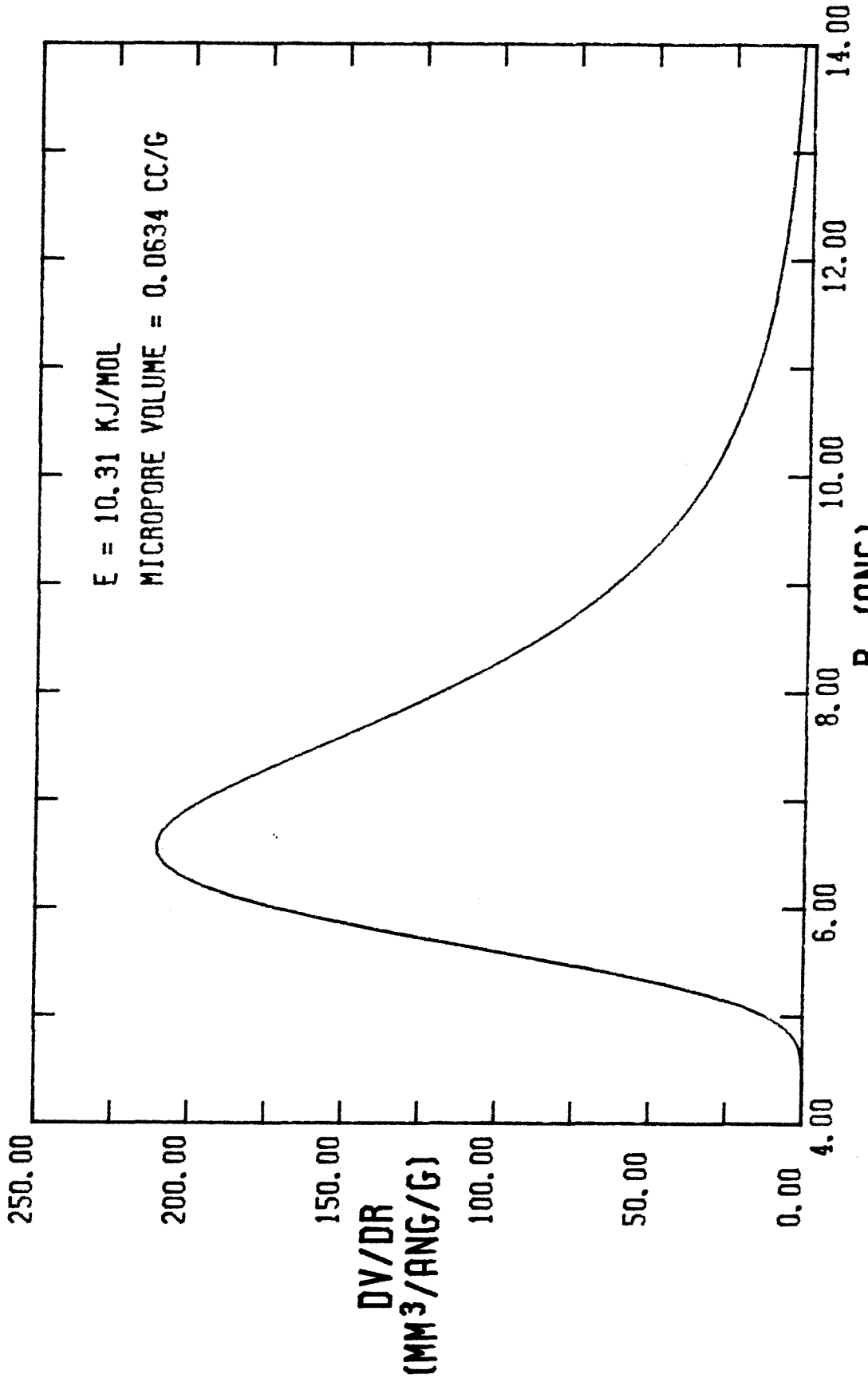
MICROPORE SIZE DISTRIBUTION FOR RUN 45
E = 10.31 KJ/MOL
MICROPORE VOLUME = 0.0634 CC/G
DV/DR
(MM3/ANG/G)
250.00
200.00
150.00
100.00
50.00
0.00
4.00
6.00
8.00
10.00
12.00
14.00
R (ANG)

FIGURE A-152

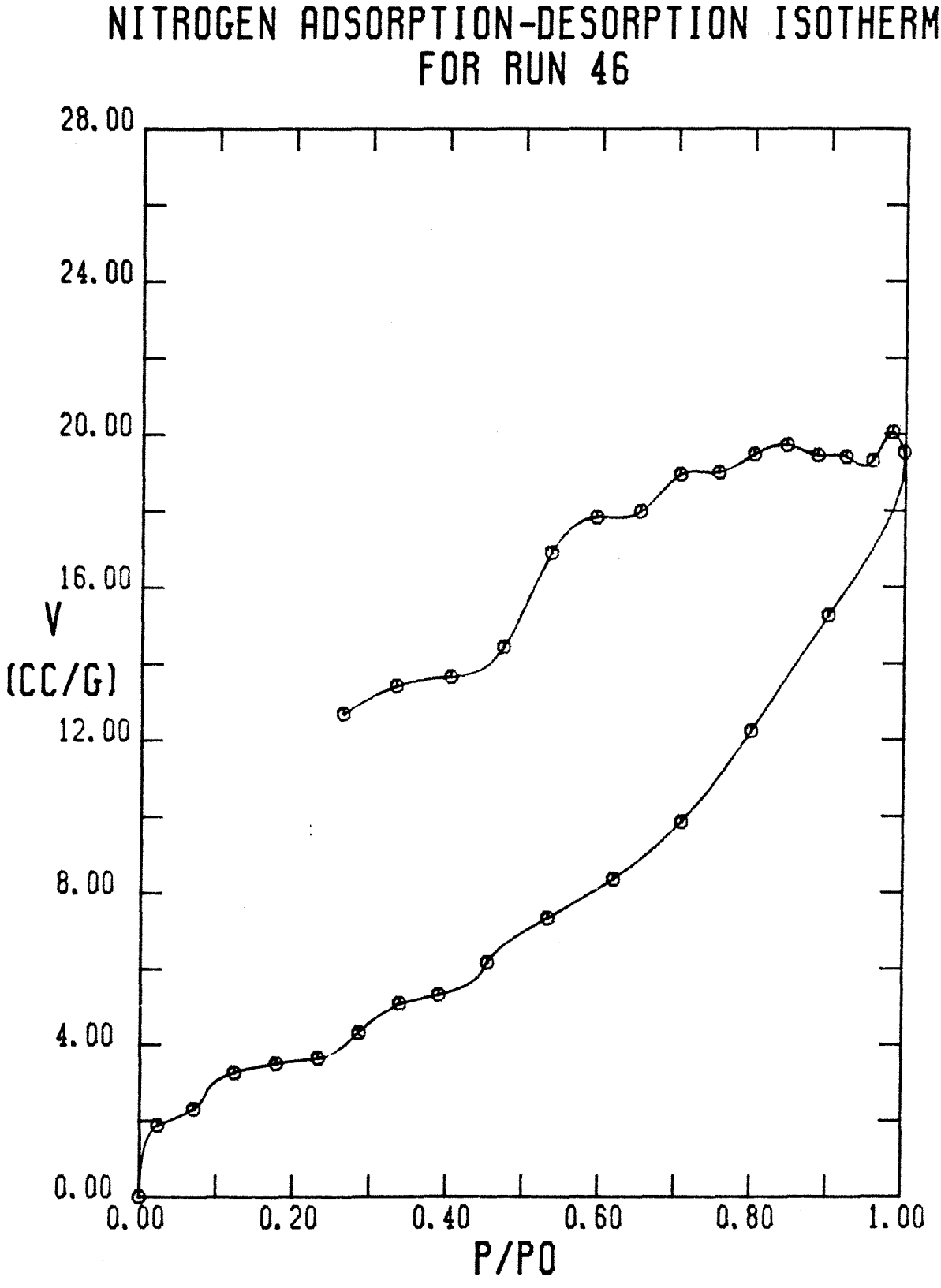
NITROGEN ADSORPTION-DESORPTION ISOTHERM
FOR RUN 46
28.00
24.00
20.00
16.00
12.00
8.00
4.00
0.00
V
(CC/G)
0.00
0.20
0.40
0.60
0.80
1.00
P/PO

FIGURE A-153

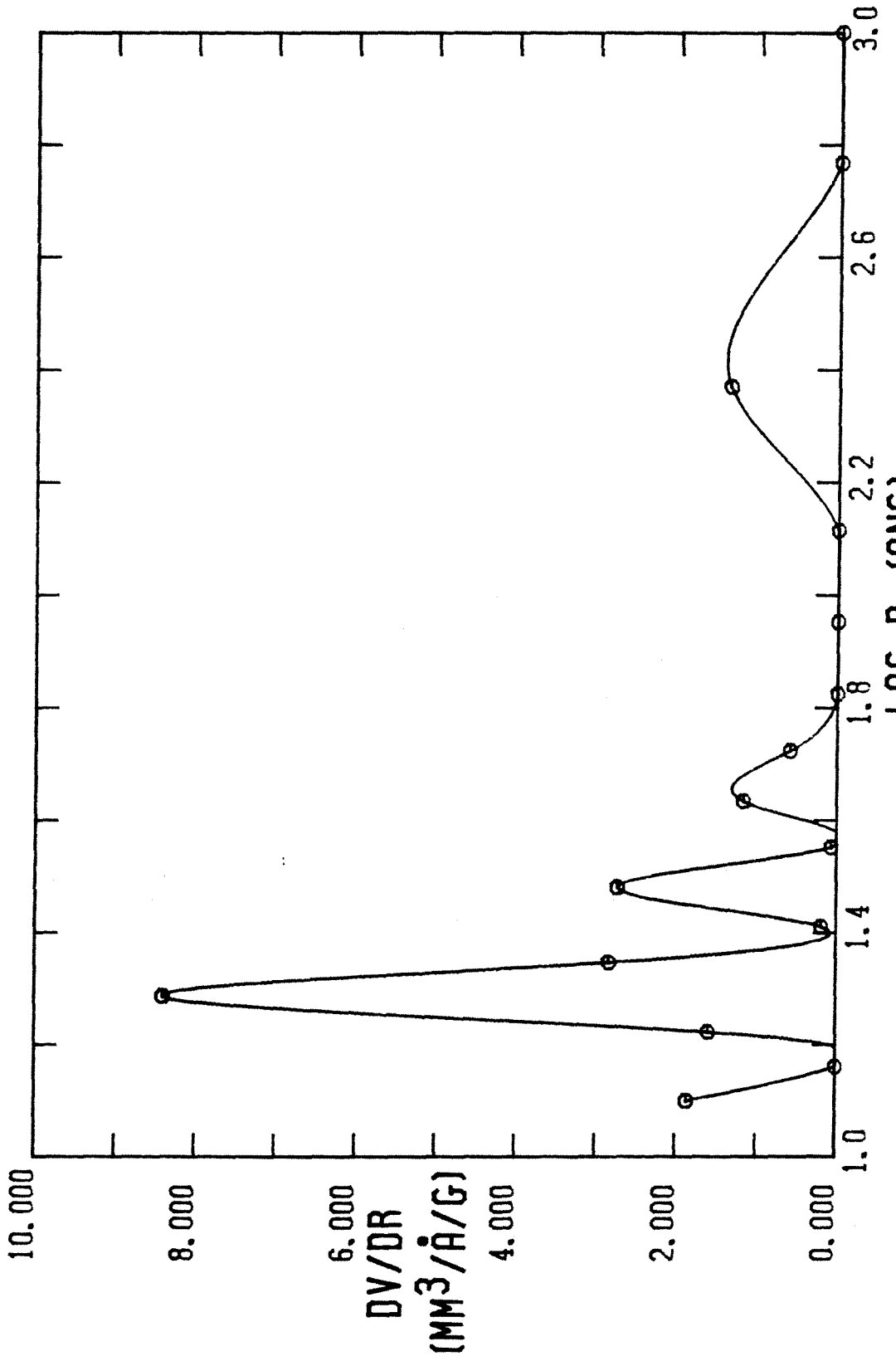
PORE SIZE DISTRIBUTION FOR RUN 46
DV/DR
(MM3/Å/G)
10.000
8.000
6.000
4.000
2.000
0.000
1.0
1.4
1.8
2.2
2.6
3.0
LOG R (ANG)

FIGURE A-154

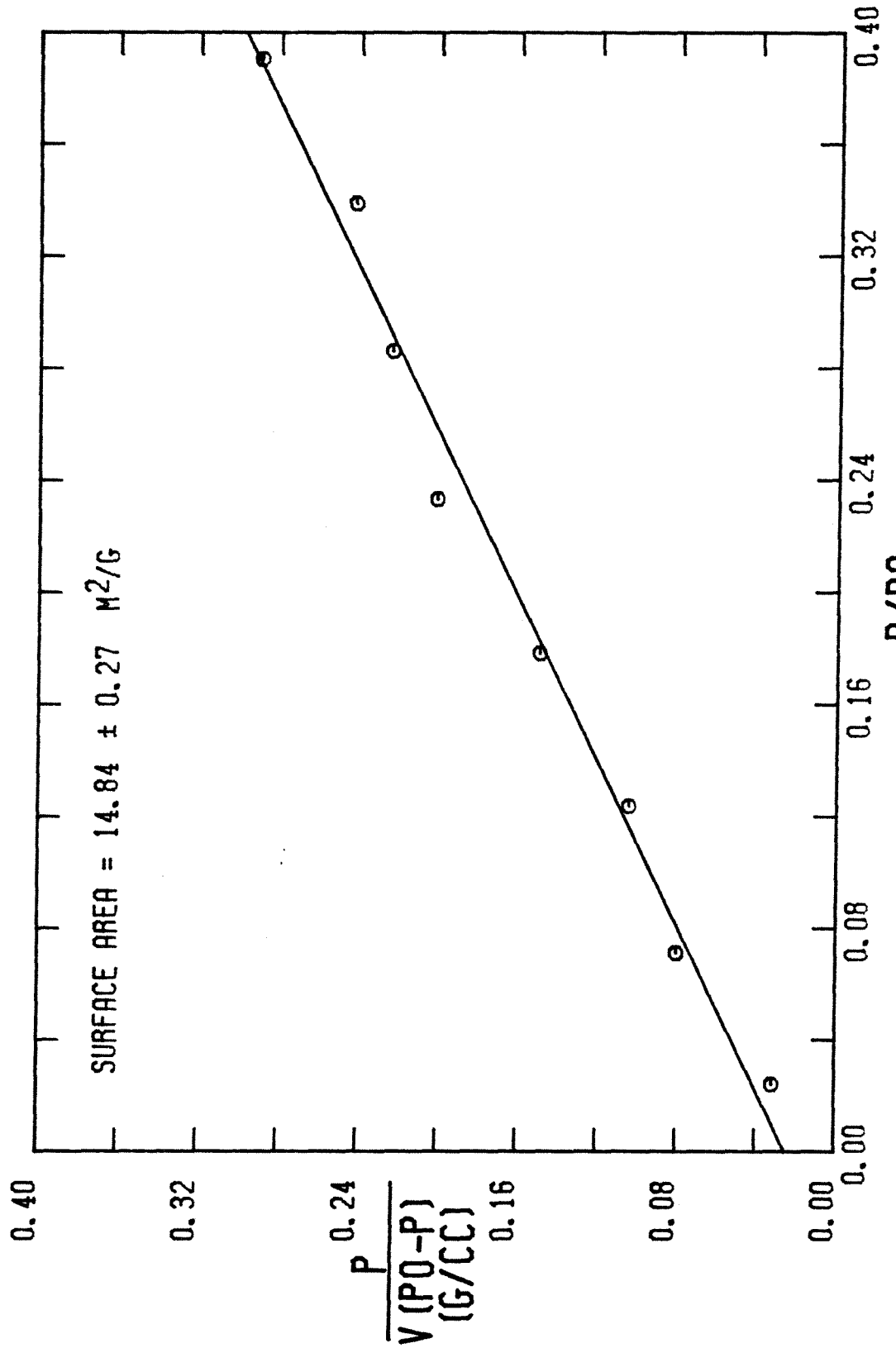
BET PLOT FOR RUN 46
SURFACE AREA = 14.84 ± 0.27 M2/G
P/PO
P / V(PO-P) (G/CC)
0.00
0.08
0.16
0.24
0.32
0.40

FIGURE A-155

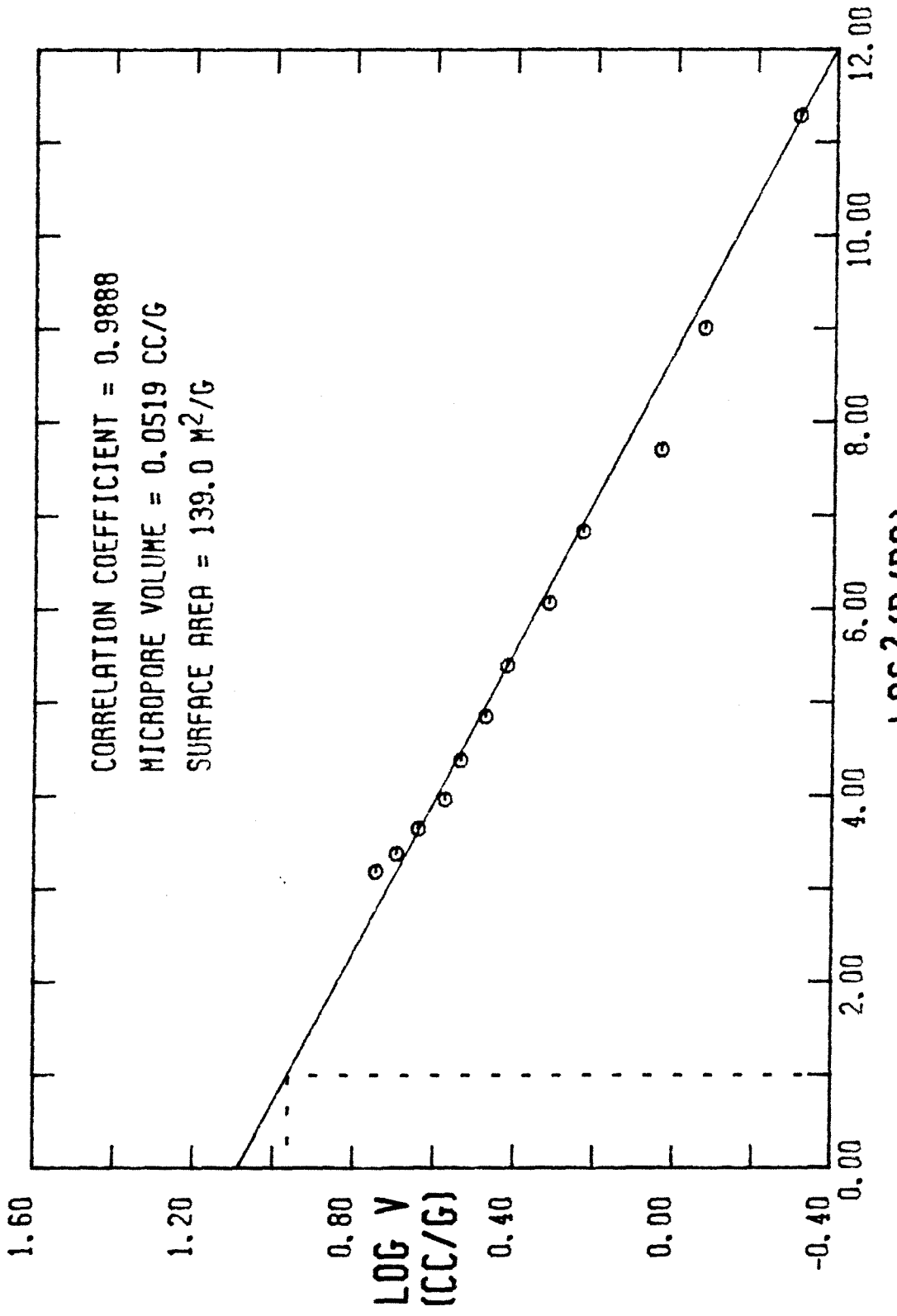
DPR PLOT FOR RUN 46
CORRELATION COEFFICIENT = 0.9888
MICROPORE VOLUME = 0.0519 CC/G
SURFACE AREA = 139.0 M2/G
LOG V (CC/G)
LOG2 (P/P0)
1.60
1.20
0.80
0.40
0.00
-0.40
0.00
2.00
4.00
6.00
8.00
10.00
12.00

FIGURE A-156

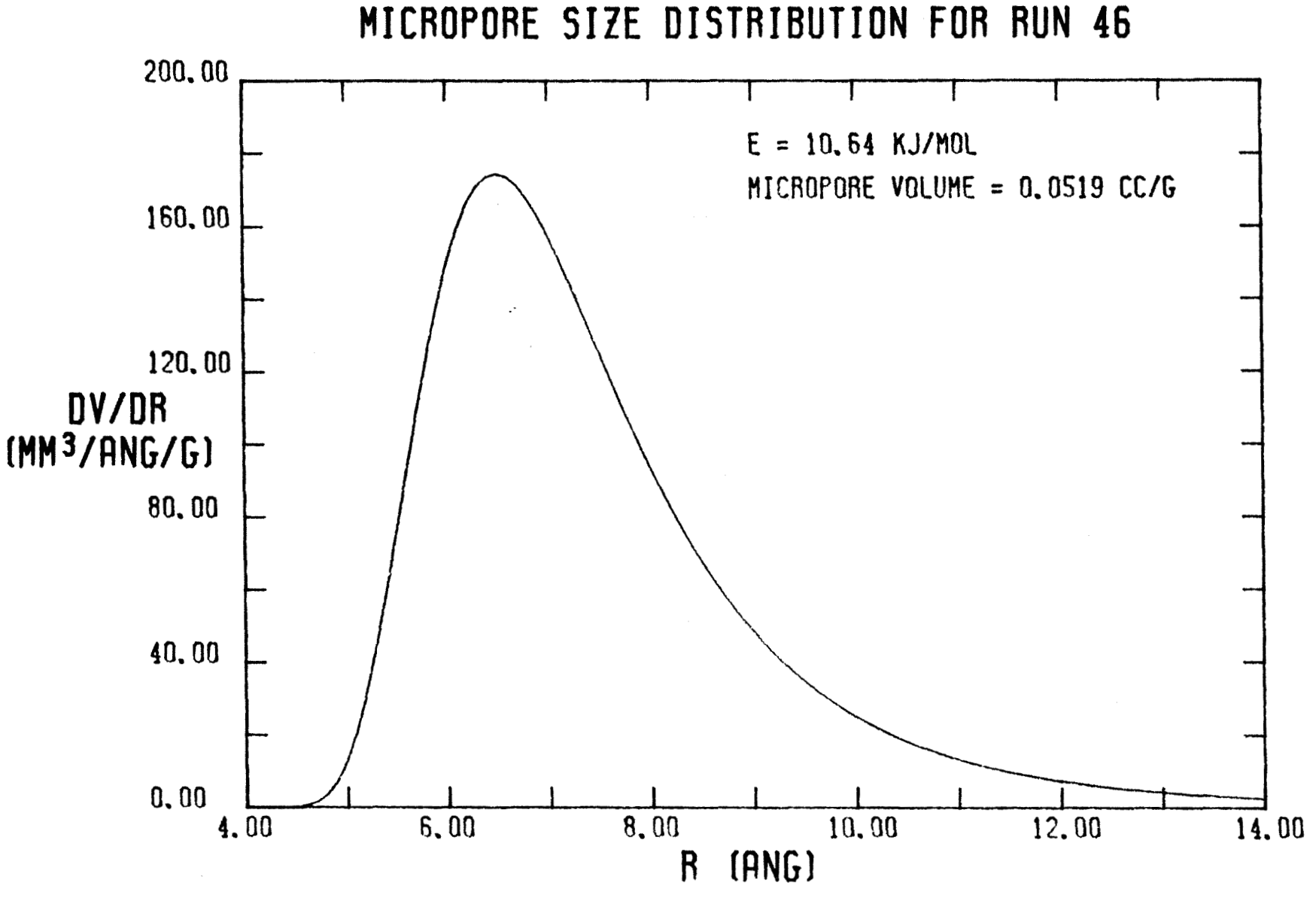
MICROPORE SIZE DISTRIBUTION FOR RUN 46
E = 10.64 KJ/MOL
MICROPORE VOLUME = 0.0519 CC/G
DV/DR
(MM3/ANG/G)
200.00
160.00
120.00
80.00
40.00
0.00
4.00
6.00
8.00
10.00
12.00
14.00
R (ANG)

FIGURE A-157

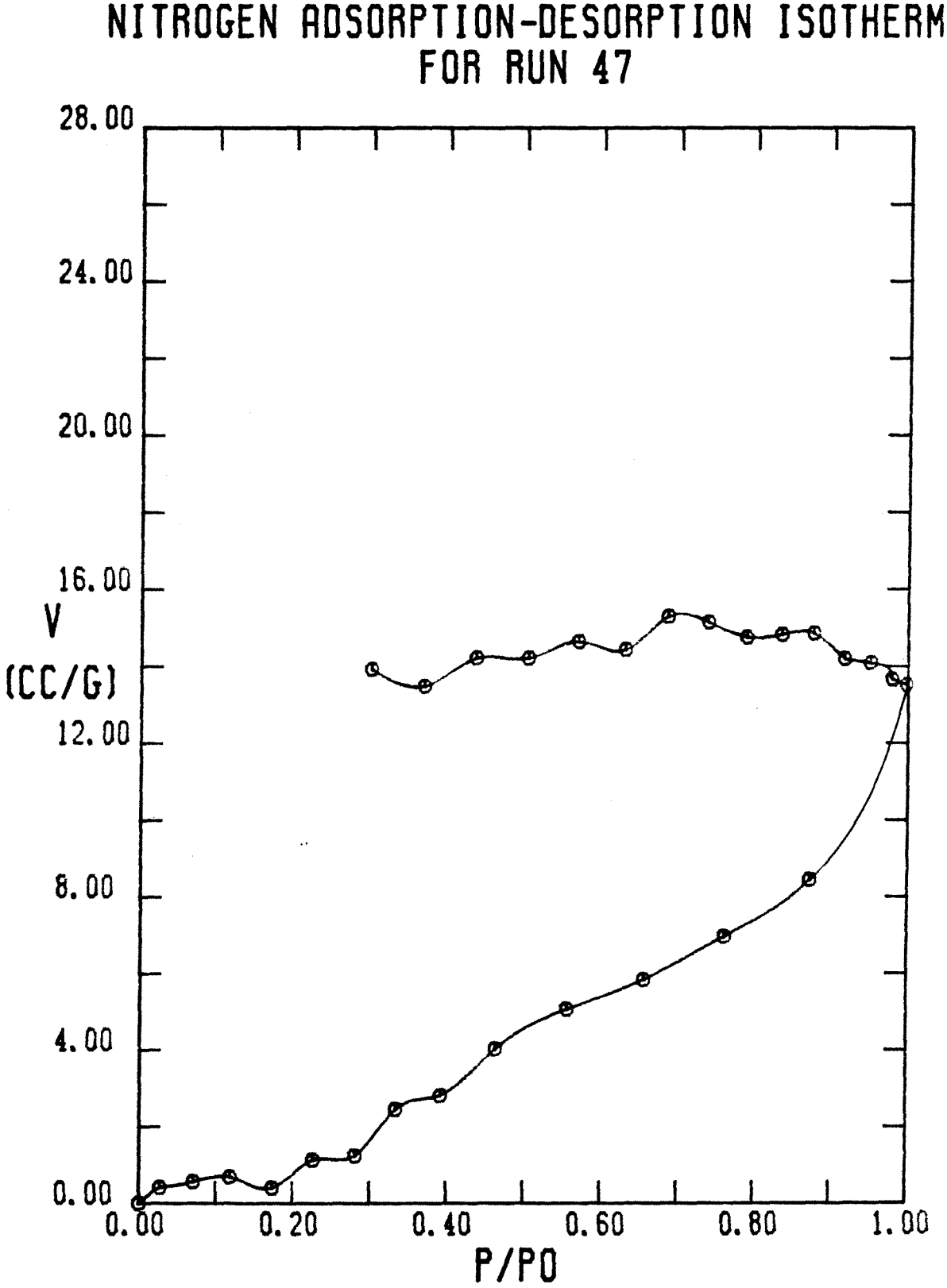
NITROGEN ADSORPTION-DESORPTION ISOTHERM
FOR RUN 47
28.00
24.00
20.00
16.00
12.00
8.00
4.00
0.00
V
(CC/G)
0.00
0.20
0.40
0.60
0.80
1.00
P/PO

FIGURE A-158

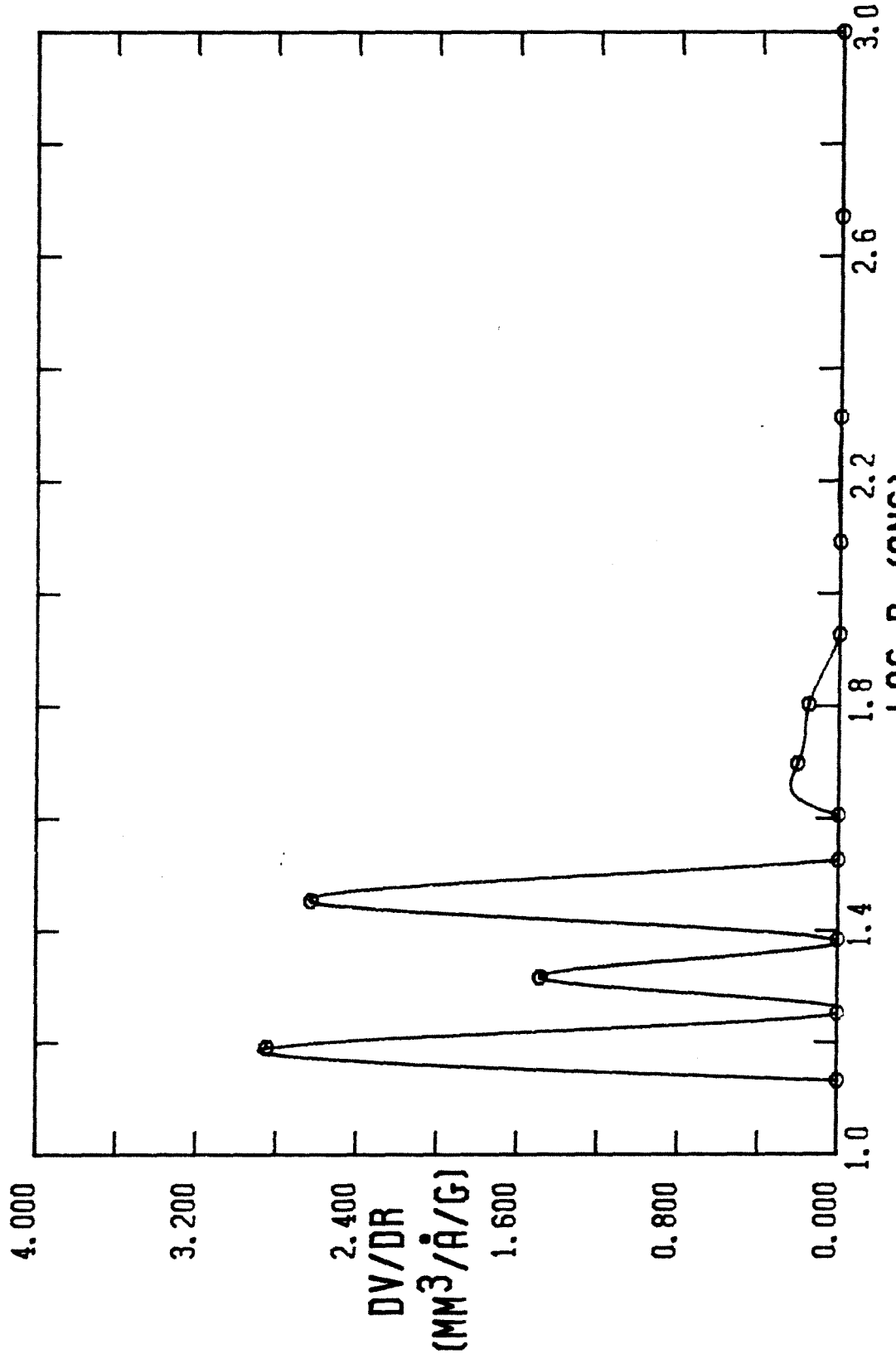
PORE SIZE DISTRIBUTION FOR RUN 47
DV/DR
(MM3/Å/G)
4.000
3.200
2.400
1.600
0.800
0.000
1.0
1.4
1.8
2.2
2.6
3.0
LOG R (ANG)

FIGURE A-159

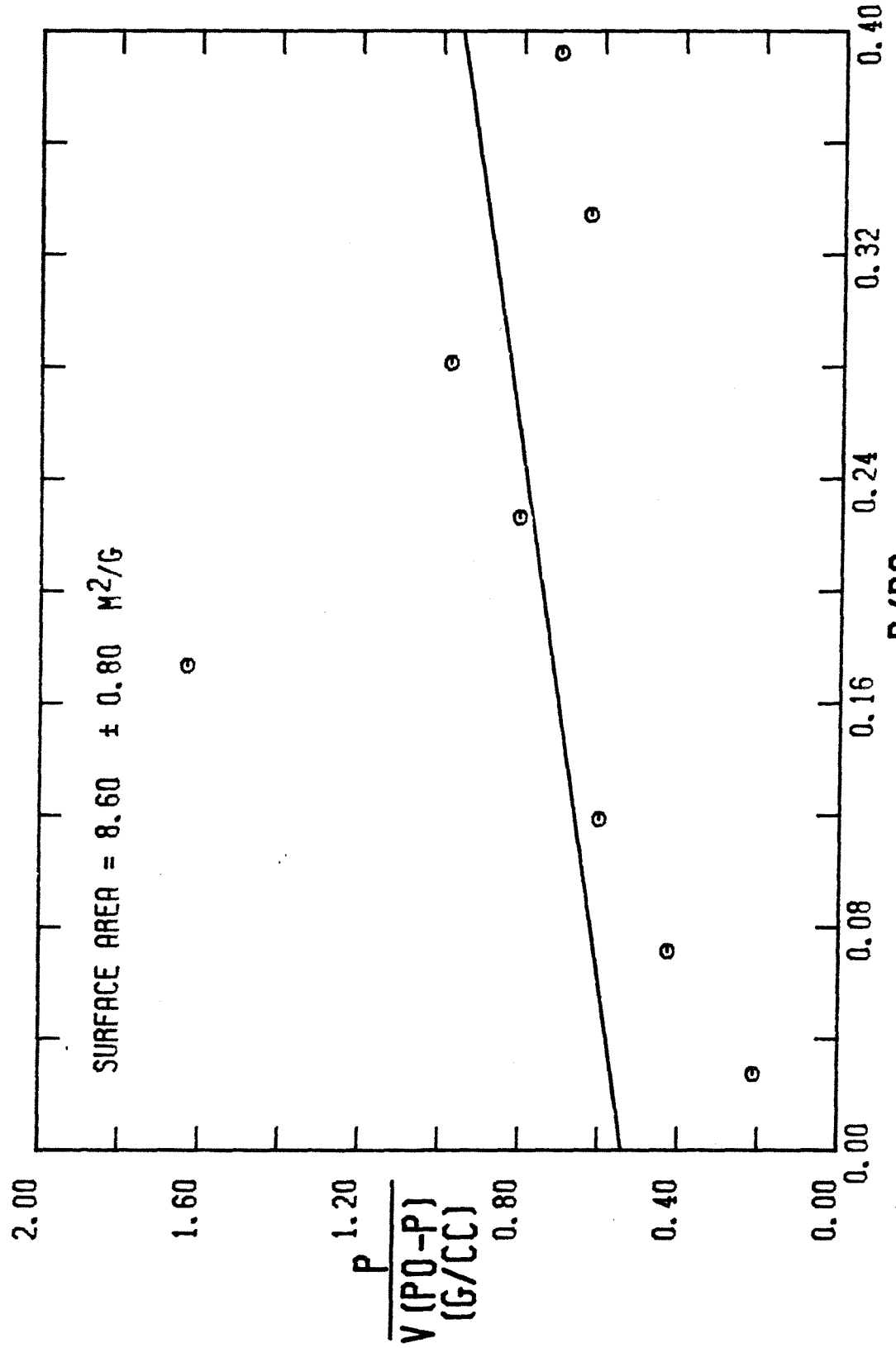
BET PLOT FOR RUN 47
SURFACE AREA = 8.60 ± 0.80 M2/G
P / V (PO-P) (G/CC)
2.00
1.60
1.20
0.80
0.40
0.00
0.00
0.08
0.16
0.24
0.32
0.40
P/PO

FIGURE A-160

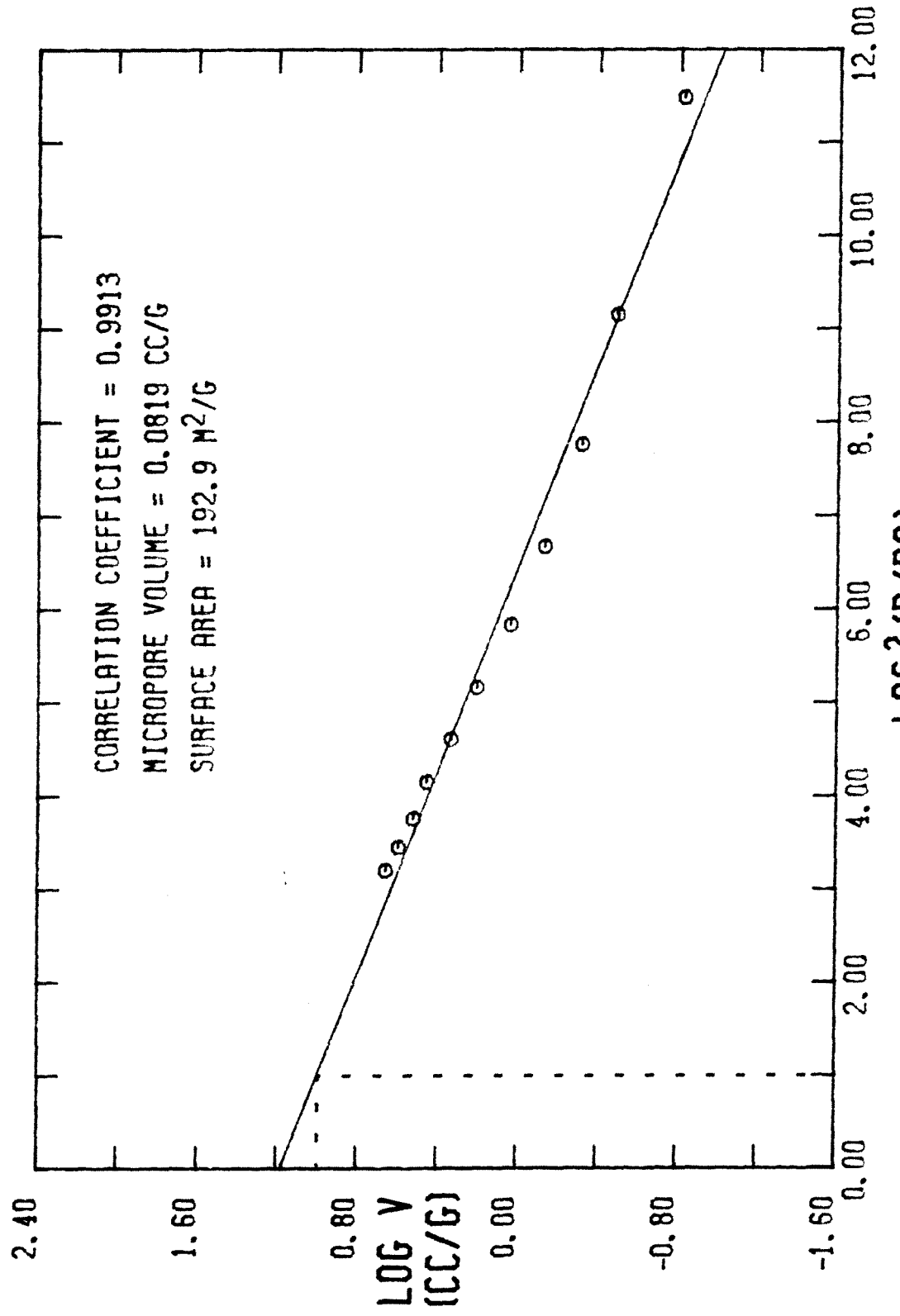
DPR PLOT FOR RUN 47
CORRELATION COEFFICIENT = 0.9913
MICROPORE VOLUME = 0.0819 CC/G
SURFACE AREA = 192.9 M2/G
LOG V (CC/G)
LOG2 (P/P0)
2.40
1.60
0.80
0.00
-0.80
-1.60
0.00
2.00
4.00
6.00
8.00
10.00
12.00

FIGURE A-161

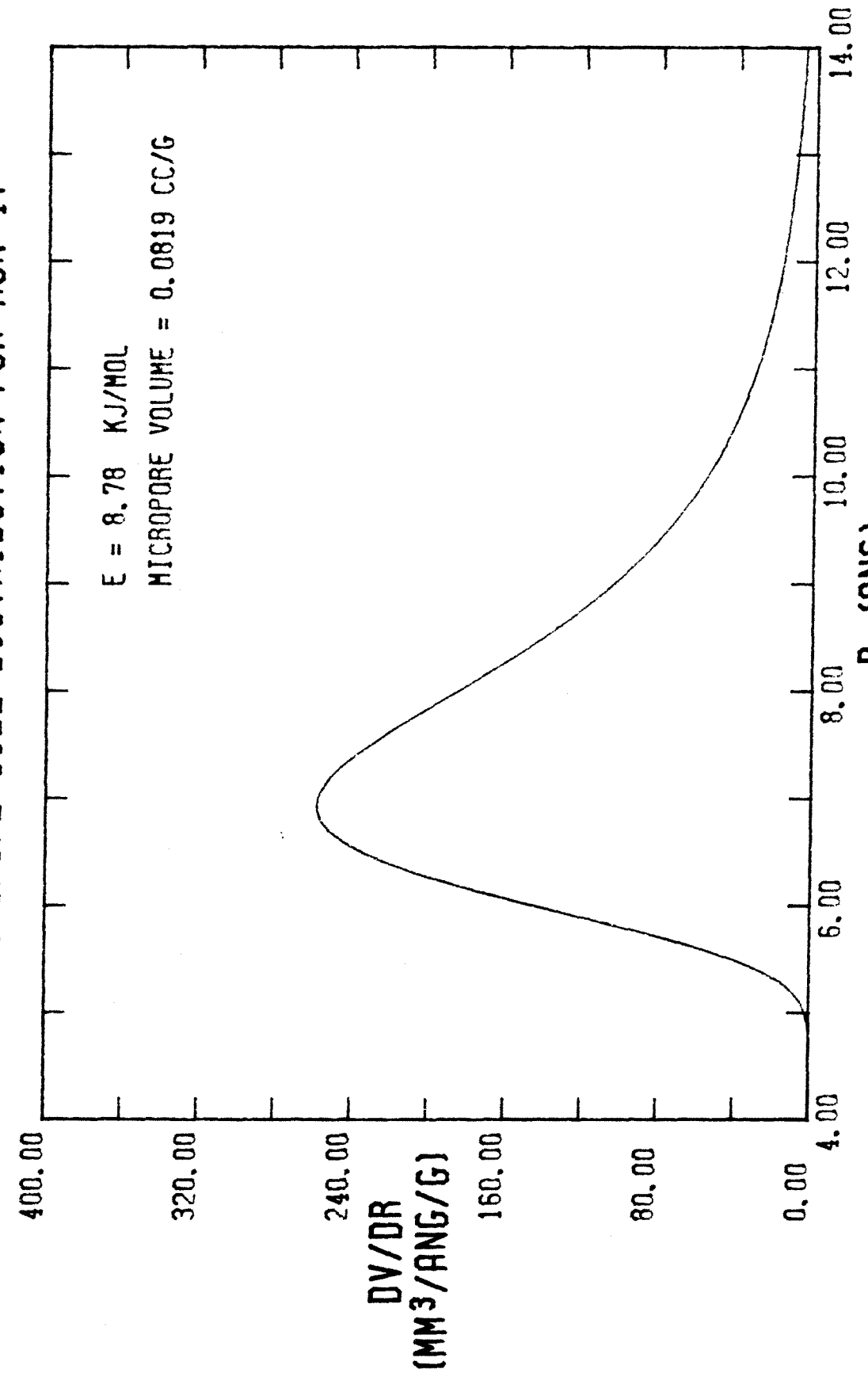
MICROPORE SIZE DISTRIBUTION FOR RUN 47
E = 8.78 KJ/MOL
MICROPORE VOLUME = 0.0819 CC/G
DV/DR (MM3/ANG/G)
400.00
320.00
240.00
160.00
80.00
0.00
4.00
6.00
8.00
10.00
12.00
14.00
R (ANG)

FIGURE A-162

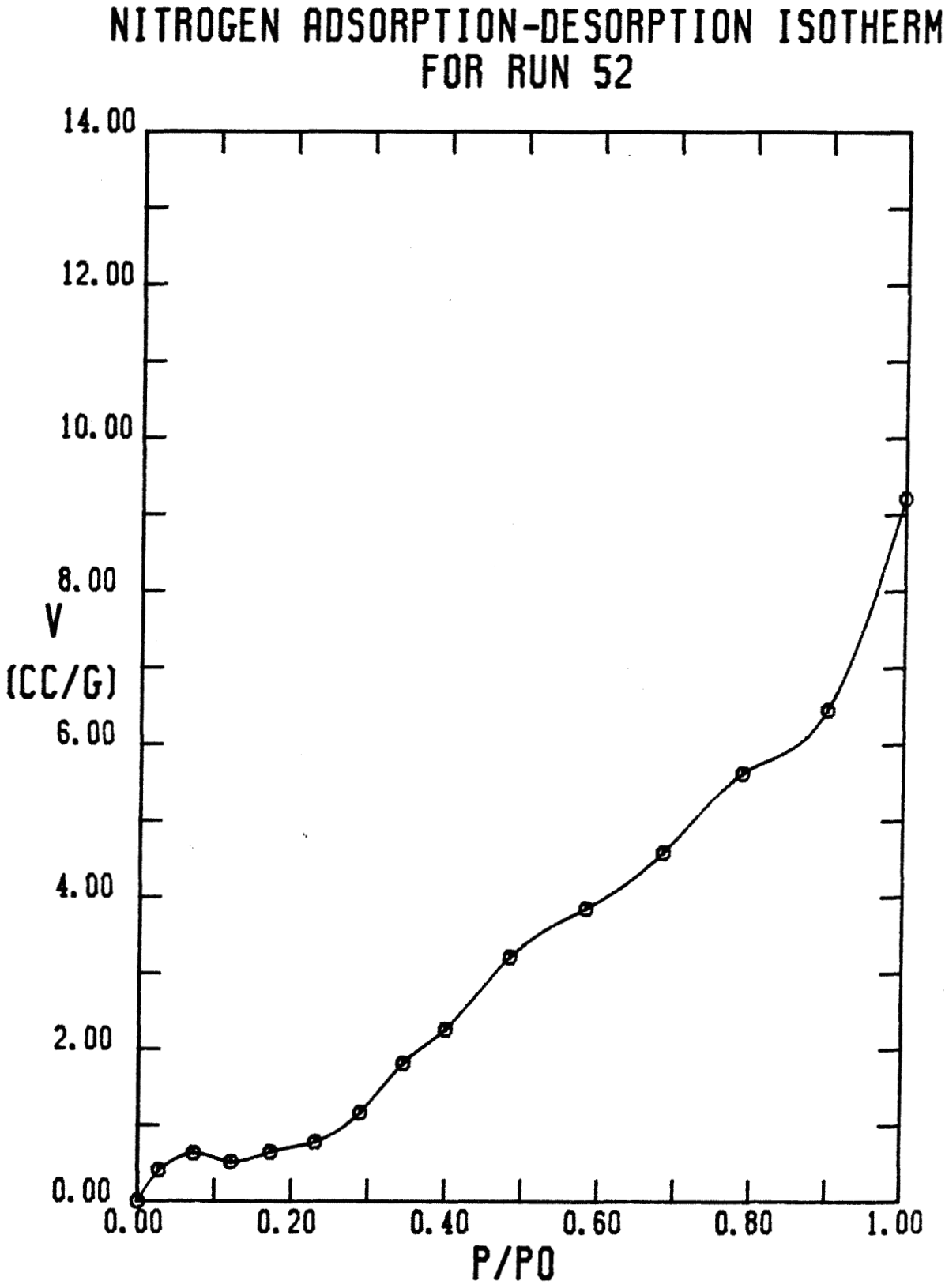
NITROGEN ADSORPTION-DESORPTION ISOTHERM
FOR RUN 52
14.00
12.00
10.00
8.00
V
(CC/G)
6.00
4.00
2.00
0.00
0.00
0.20
0.40
0.60
0.80
1.00
P/PO

FIGURE A-163

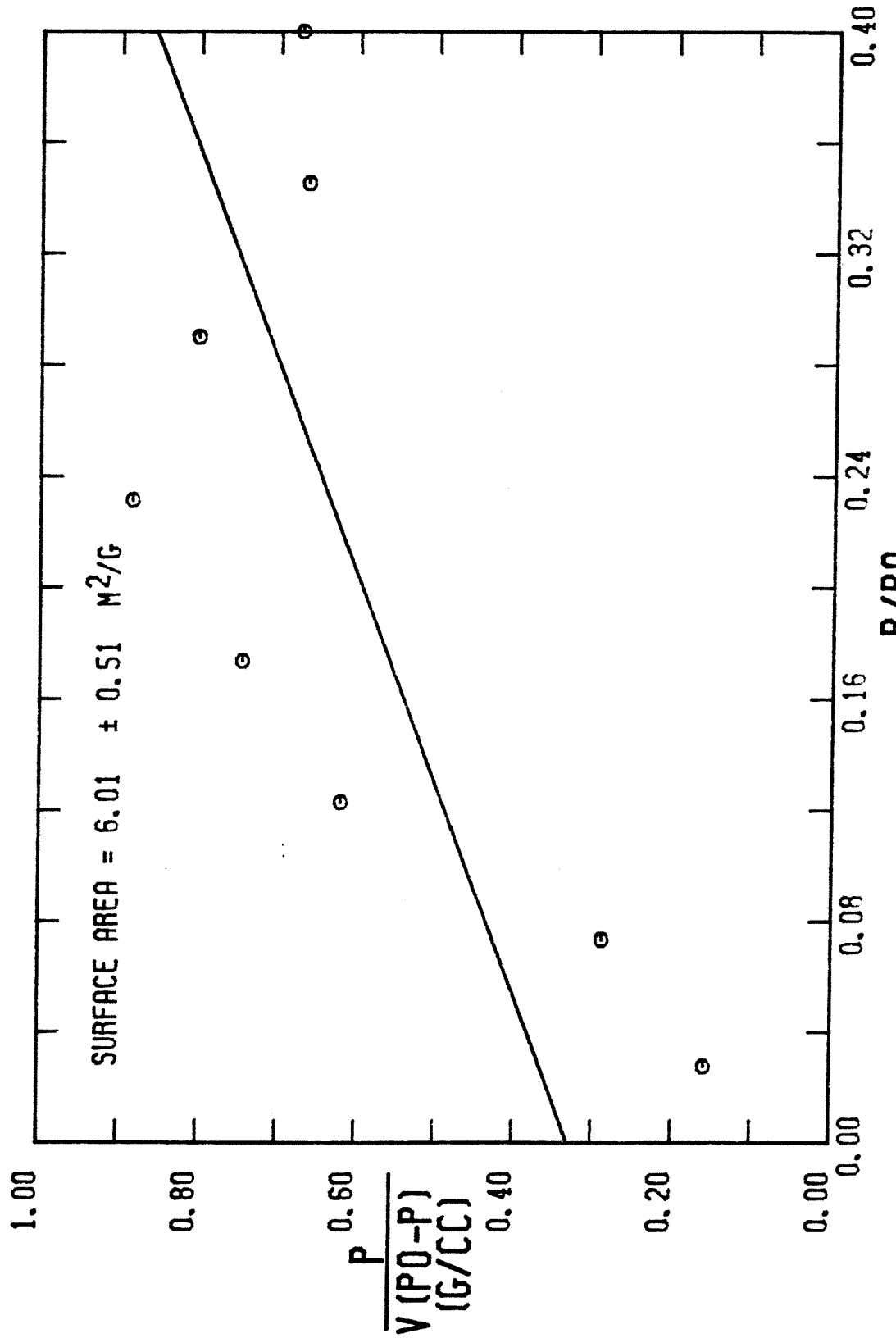
BET PLOT FOR RUN 52
SURFACE AREA = 6.01 ± 0.51 M2/G
P/PO
P / V(PO-P) (G/CC)
0.00
0.08
0.16
0.24
0.32
0.40
0.00
0.20
0.40
0.60
0.80
1.00

FIGURE A-164

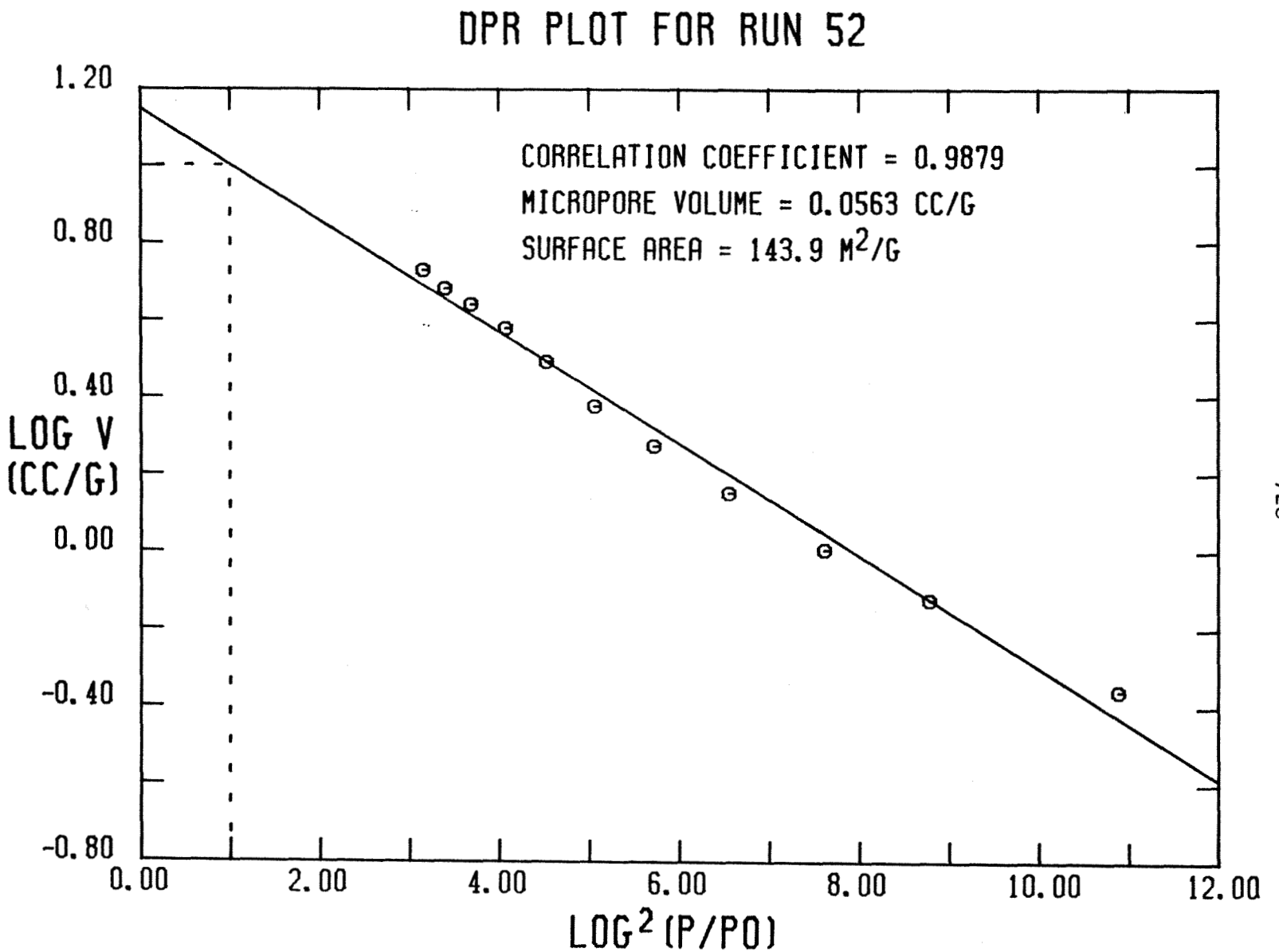
DPR PLOT FOR RUN 52
CORRELATION COEFFICIENT = 0.9879
MICROPORE VOLUME = 0.0563 CC/G
SURFACE AREA = 143.9 M2/G
1.20
0.80
0.40
0.00
-0.40
-0.80
LOG V
(CC/G)
0.00
2.00
4.00
6.00
8.00
10.00
12.00
LOG2 (P/PO)

FIGURE A-165

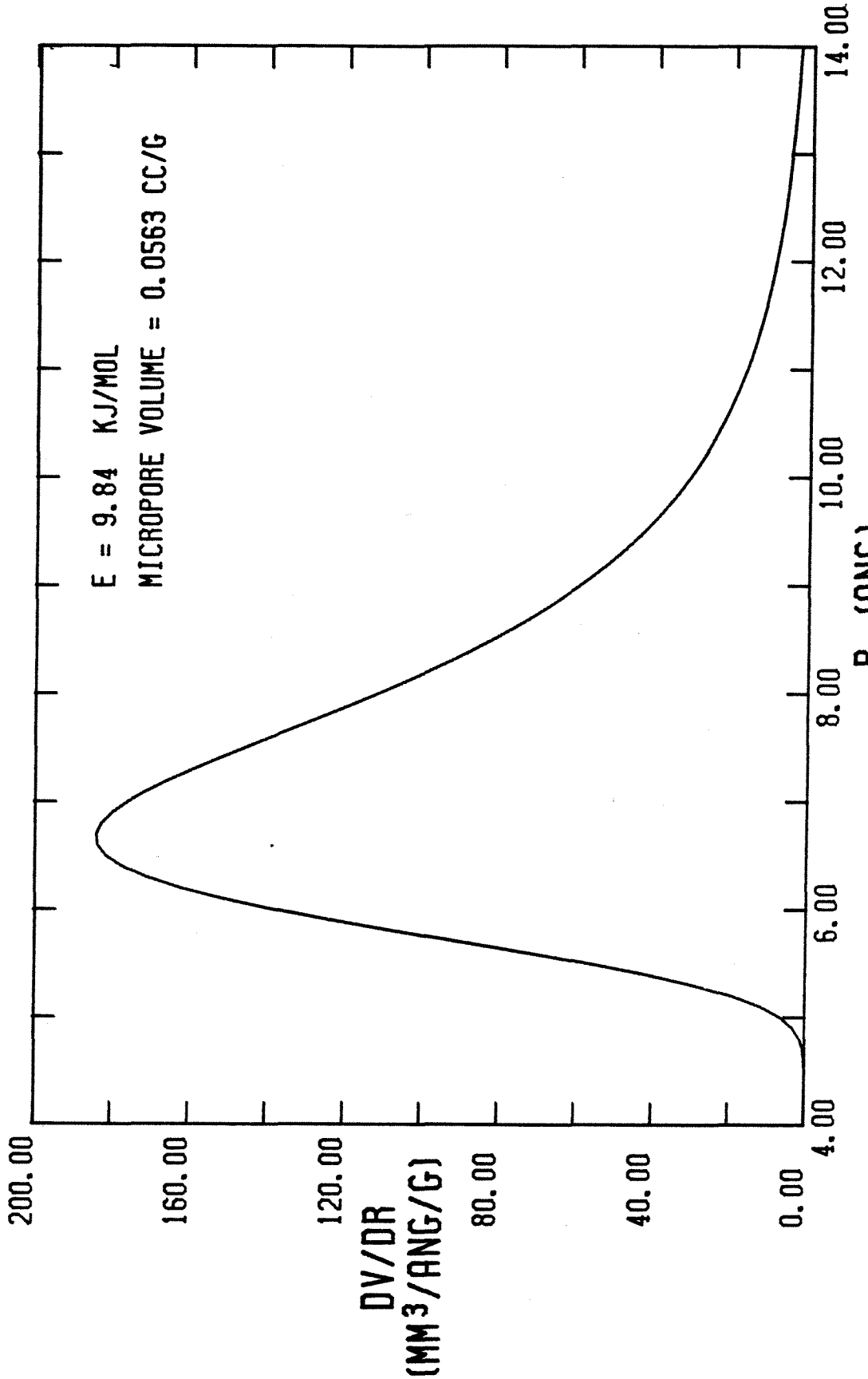
MICROPORE SIZE DISTRIBUTION FOR RUN 52
E = 9.84 KJ/MOL
MICROPORE VOLUME = 0.0563 CC/G
DV/DR
(MM3/ANG/G)
200.00
160.00
120.00
80.00
40.00
0.00
4.00
6.00
8.00
10.00
12.00
14.00
R (ANG)

FIGURE A-166